OMIKK

47

F 1103

ACADÉMIE ROUMAINE

REVUE ROUMAINE DE CHIMIE

TOME 35

N° 1

Janvier 1990

Rev. Roumaine Chim.

RRCHAX, 35, *1*, p. 1–140 (1990), Bucarest

EDITURA ACADEMIEI ROMÂNE

ACADÉMIE ROUMAINE

COMITÉ DE RÉDACTION

Rédacteur en chef:

I. G. MURGULESCU, membre de l'Académie Roumaine

Rédacteurs en chef adjoints:

A. T. BALABAN et V. EM. SAHINI, membres de l'Académie Roumaine

Collège de rédaction:

EM. BRATU, ECATERINA CIORĂNESCU NENITZESCU, P. SPACU, CR. SIMIONESCU, Gh. SUCIU, membres de l'Académie Roumaine; M. ANDRUH, M. BANCIU, M. D. GHEORGHIU, I. HAIDUC, D. I. MARCHIDAN, G. NIAC et D. SĂNDULESCU

La Revue Roumaine de Chimie paraît 10 fois par an. Toute commande de l'étranger sera adressée à ROMPRESFILATELIA — sectorul Export-Import Presă, P. O. Box 12—201, télex 10376, prsfi r 78 104 Bucarest, Calea Griviței nr. 64—66, București, Roumanie

Les manuscrits, les livres et les revues proposés en échange, ainsi que toute correspondance seront envoyés à la rédaction:

REVUE ROUMAINE DE CHIMIE
125, Calea Victoriei, 79717 Bucarest, Roumanie, téléphone 50 76 80

EDITURA ACADEMIEI ROMÂNE
125, Calea Victoriei, 79717 Bucarest, Roumanie, téléphone 50 76 80

REVUE ROUMAINE DE CHIMIE

ZÁGOS MŰSZAKI INFORMÁCIÓS TÉS KÖNYVTÁR

Tome 35, N° 1 **Janvier, 1990**

MARIUS ANDRUH, N. STĂNICĂ, AURA MEGHEA and M. BERCU, Metal complexes with 4-benzoyl-pyridine. VI. New coordination compounds of copper(II) with 4-benzoyl-pyridine . . . . 3—8
F. G. BĂNICĂ and ELENA DIACU, Catalytic hydrogen prewave in cysteine- or cystine-containing solutions. A polarographic and spectrophotometric study . . . . 9—22
P. S. MITTAL, NARINDER KUMAR and A. D. TANEJA, Spectral studies of some thiazolyl and pyrimidyl substituted thiocarbamides in different solvents . . . . 23—30
LIGIA STOICA, RODICA V. CĂTUNEANU, CORNELIA BEJAN, MARGARETA NICOLAU and V. BRETAN, Recovery of metallic ions from waste waters by flotation . . . . 31—39
CORNELIA LEONTE, AL. SZÉP, N. BÎLBĂ, C. CALISTRU, LIVIA IFRIM and GH. MIHĂILĂ, On thermal decomposition of dolomite . . . . . 41—48
S. GOCAN, LILIANA OLENIC and I. CRISTEA, Optimization of the mobile phase in thin layer chromatography for the separation of 4-benzylidene-1-pyrimidyl-5-pyrazolone dyes . . . . 49—54
S. EL-NAGDY, M. A. EL-HASHASH, A. A. AFIFY and F. EL-SHAHED, Behaviour of benzoxazinone derivatives bearing a bulky group at position-2 toward some nitrogen and carbon nucleophiles. Part 2 . . . . 55—61
ÜLKÜ OYMAN, Dehydration of some 1-(2-furyl)- and 1-(2-thienyl)-1-alkanols using cobalt (II) sulphate as catalyst . . . . 63—66
MARIA POPESCU, Study on the reaction and composition of the Hg(II) complex with diazoaminobenzene . . . . 67—76
M. FEKRY ISMAIL, FEKRIA S. SAYED, F. A. EL-BASSIOUNY and H. A. YOUNES, Reactions with N-aminophthalimide and some allied compounds . . . . 77—83
J. BRUNVOLL, R. TOŠIĆ, M. KOVAČEVIĆ, A. T. BALABAN, I. GUTMAN and S. J. CYVIN, Enumeration of catacondensed benzenoid hydrocarbons and their numbers of Kekulé structures . . . . 85—96
N. PETRESCU, MARIA PETRESCU and MIRELA BRIŢCHI, Diffusion of vanadium in iron in surface coatings and calculation of diffusion coefficients 97—103
FRANCISC A. GOTHÁRD, GHEORGHIŢA JINESCU and VICTORIA SĂVESCU, Generalized correlation for vapor pressures of organic compounds 105—109

BOOK REVIEW 111
AUTHOR INDEX . . . . 115—132
SUBJECT INDEX . . . . 133—139

| Rev. Roumaine Chim. | 35, *1*, 1—139 (1990), Bucarest

Revue Roumaine de Chimie, **35**, *1*, 3–8 (1990)

METAL COMPLEXES WITH 4-BENZOYL-PYRIDINE. VI[1]

NEW COORDINATION COMPOUNDS OF COPPER(II) WITH 4-BENZOYL-PYRIDINE

MARIUS ANDRUH[a], N. STĂNICĂ[b], AURA MEGHEA[c] and M. BERCU[d]

[a] Inorganic Chemistry Laboratory, Faculty of Chemical Technology, Polytechnic Institute of Bucharest, Dumbrava Roșie str. 23, Bucharest, Romania

[b] Center of Physical Chemistry – ICECHIM, Splaiul Independenței 202 Bucharest, Romania

[c] Chair of Applied Physical Chemistry, Faculty of Chemical Technology, Polytechnic Institute of Bucharest, Polizu str. 1, Bucharest, Romania

[d] Faculty of Physics, University of Bucharest, Romania

Received July 14, 1989

New copper (II) coordination compounds of the type $Cu(4Bz-Py)_nX_2$ (where 4Bz–Py = 4-benzoyl-pyridine and $X^- = Cl^-$, NO_3^-, n = 2, $X^- = CH_3COO^-$, n = 1) were prepared and characterized by elemental analysis, electronic, infrared and EPR spectroscopy, as well as by magnetic measurements. Chromotropic phenomena for two coordination compounds $[Cu(4Bz-Py)_2Cl_2]$ and $[Cu(4Bz-Py)_2(NO_3)_2]$, were emphasized.

1. INTRODUCTION

Following our research concerning the chemistry of coordination compounds containing 4-benzoyl-pyridine as an organic ligand,[1–5] this work is devoted to the synthesis and characterization of several copper (II) complexes of the type $Cu(4Bz\text{-}Py)_2X_2$. The literature search revealed that these coordination compounds were not isolated or characterized; there exists information regarding the formation constants for 1 : 1 adducts of heterocyclic bases, including 4-benzoyl-pyridine, with copper (II) β-diketone chelates.[6] Many coordination compounds of transition-metal ions with pyridine or its substituted derivatives exhibit thermochromic behaviour, generally due to the modification of the coordination sphere of metal ions.[7]

2. EXPERIMENTAL

The complexes were synthesized by the following general procedure: solutions containing 4-benzoyl-pyridine and copper(II) salts (chlorite, nitrate or acetate), in molar ratio 2 : 1, were mixed. The products separated from the solution as well-formed crystals or microcrystalline powder: $[Cu(4Bz-Py)_2Cl_2]$ – light blue, $[Cu(4Bz-Py)_2(NO_3)_2]$ – blue, $[Cu_2(CH_3COO)_4(4Bz-Py)_2]$ – green. The complexes were filtered off, washed with methanol and dried *in vacuo*. Dichloro(4-benzoyl-pyridine)copper(II) complex was obtained by controlled thermal decomposition of dichlorodi(4-benzoyl-pyridine)copper(II):

$$[Cu(4Bz-Py)_2Cl_2] \xrightarrow{170°C} Cu(4Bz-Py)Cl_2 + 4Bz-Py$$

(weight loss: found: 37,02%; calcd. 36,52%)
Analytical data: $[Cu(4Bz-Py)_2Cl_2]$: found: 58,1% C: 3.4% H; 5.7% N; calcd.: 57.48% C;, 3.59% H; 5.59% N; $[Cu(4Bz-Py)_2(NO_3)_2]$: found: 51.1% C; 3.1% H; 10,2% N; calcd.: 51.98% C, 3.24% H, 10.10% N; $[Cu_2(CH_3COO)_4(4BzPy)_2]$: found: 51.9% C, 4.2% H, 3.7% N; calcd. 52.60% C, 4.11% H, 3.83% N.

By heating the compound $[Cu(4Bz-Py)_2(NO_3)_2]$ at 150°C, we get the so-called "hot form", green-bluish in colour, without any mass loss. The chromotropic phenomenon is accompanied by an endothermic effect registered on the DTA curve.

The electronic spectra were recorded by diffuse reflectance technique, using MgO as a reflectance material. The magnetic measurements were performed according to Faraday's method, at room temperature using $Hg[Co(NCS)_4]$ as a standard.

The EPR spectra of the complexes, in solid state, were recorded at room temperature, on a spectrograph operating in the X band. The values of the *g* tensor were determined by means of DPPH standard.

3. RESULTS AND DISCUSSION

EPR spectra

It is well-known that, lacking the X-ray crystallographic data, the EPR spectra give the most useful information regarding the stereochemistry of copper (II) compounds. The calculated *g* factor values are presented in table 1. All the complexes under investigation, namely $[Cu(4Bz-Py)_2Cl_2]$, $[Cu(4Bz-Py)_2(NO_3)_2]$ – cold form and $[Cu(4Bz-Py)_2(NO_3)_2]$–hot form, gave anisotropic EPR spectra, with an average *g* factor value, g_0, in agreement with an orbitally non-degenerated ground state.[8]

Table 1

g factor values for some copper(II) coordination compounds investigated in this paper

Compound	g_1	$g_\perp$	g_2	$g_\parallel$	g_3	g_0^*
$[Cu(4Bz-Py)_2Cl_2]$	2 .042		2 .071		2 .236	2 .116
$[Cu[4Bz-Py)_2(NO_3)_2]$-cold		2 .081		2 .217		2 .126
$[Cu(4Bz-Py)_2(NO_3)_2]$-hot		2.062		2 .238		2 .121

* – calculated by the relations:

$$g_0 = \frac{1}{3}(g_1 + g_2 + g_3) \text{ or } g_0 = \frac{1}{3}(2g_\perp + g_\parallel)$$

The EPR spectrum of the compound $[Cu(4Bz-Py)_2Cl_2]$ (Fig. 1) is typical for a rhombic distorted symmetry, respectively an elongated octahedron along the *z* axis:. For this compound, the value of $R = (g_2 - g_1)/(g_3 - g_2)$, much lesser than unity, indicates predominantly

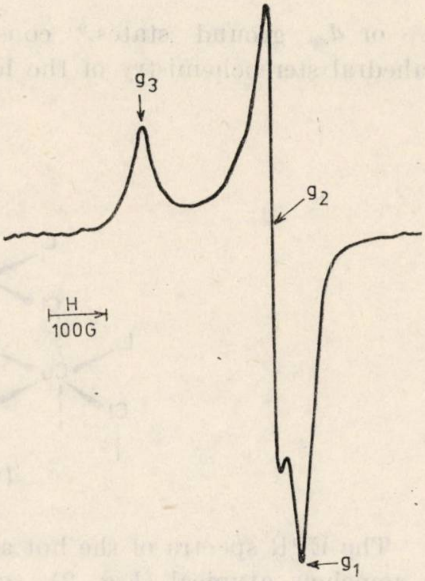

Fig.1. — The EPR spectrum of the compound $[Cu(4BZ\text{-}Py)_2Cl_2]$.

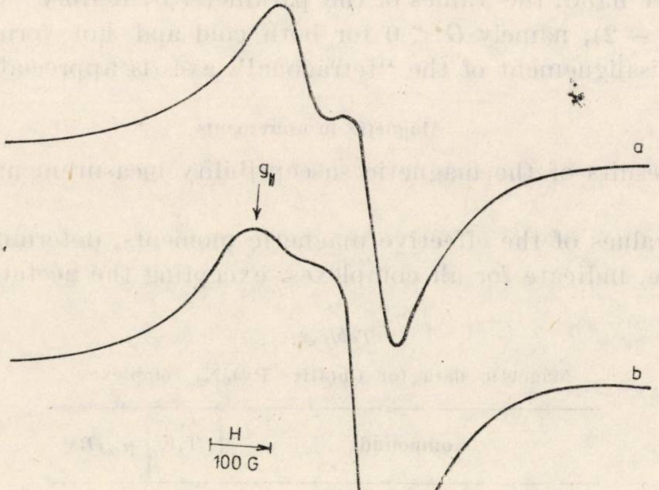

Fig. 2. — The EPR spectra of : a) $[Cu(4Bz\text{—}Py)_2(NO_3)_2]$-cold form b) the same, hot form.

$d_{x^2-y^2}$ or d_{xy} ground states,[9] consistent with the elongated rhombic octahedral stereochemistry of the local $CuCl_2N_2Cl'_2$ chromophore present.

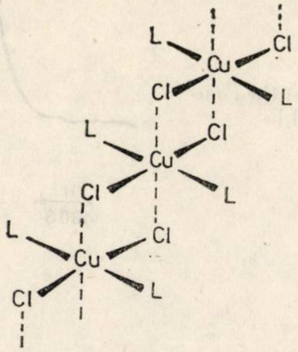

(1)

The EPR spectra of the hot and cold forms of $[Cu(4Bz\text{-}Py)_2(NO_3)_2]$ are somehow atypical (Fig. 2), suggesting an unusual stereochemistry known also for the parent compounds, hot- and cold-$[Cu(\alpha\text{-pic})_2(NO_3)_2]$.[9] On the other hand, the values of the parameter G, defined[10] by the ratio $(g_{\parallel} - 2)/(g_{\perp} - 2)$, namely $G < 0$ for both cold and hot forms, indicate that the misalignement of the "tetragonal" axes is appreciable.

Magnetic measurements

The results of the magnetic susceptibility measurements are listed in table 2.

The values of the effective magnetic moments, determined at room temperature, indicate for all complexes, excepting the acetate derivative

Table 2

Magnetic data for $Cu(4Bz-Py)_nX_2$ complexes

Compound	T,K	$\mu_{eef}BM$
$[Cu(4Bz-Py)_2Cl_2]$	290	1.88
$Cu(4Bz-Py)Cl_2$	290	1.41
$[Cu(4Bz-Py)_2(NO_3)_2]$-cold	291	1.87
$[Cu(4Bz-Py)_2(NO_3)_2]$-hot	291	1.70
$[Cu_2(CH_3COO)_4(4Bz-Py)_2]$	291	1.54

and the dichloro-mono-4-benzoyl-pyridine copper(II) complex, a normal paramagnetic behaviour. The lower μ_{eff} value for the compound $[Cu_2(CH_3COO)_4(4Bz\text{-}Py)_2]$ is in agreement with a dimeric structure, known for a long time for the copper(II) carboxylates and their adducts:

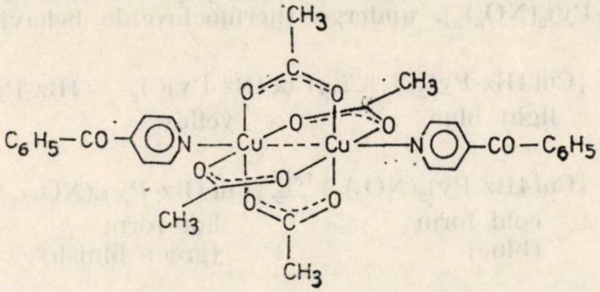

(2)

Thus, the interaction between the two copper(II) ions determines the lower value of the observed magnetic moment (1.54 BM). The subnormal magnetic moment for the complex $Cu(4Bz\text{-}Py)Cl_2$ may be explained by a superexchange mechanism between the copper(II) ions in a dimeric structure of the type:

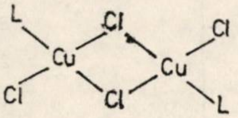

(3)

Electronic spectra. Thermochromic behaviour

The electronic spectrum of the dimer $[Cu_2(CH_3COO)_4(4Bz\text{-}Py)_2]$ is very similar to that of the classical copper(II) acetate monohydrate, exhibiting the characteristic band [12] for a dimeric structure at ~ 380 nm (Fig. 3).

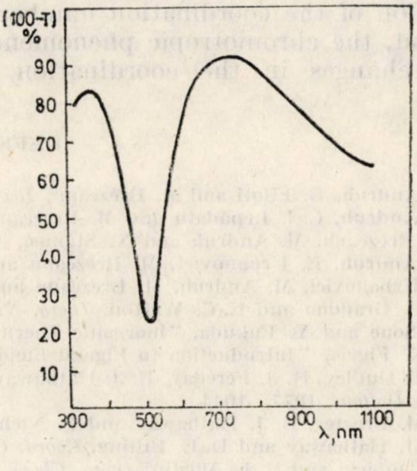

Fig. 3.— The diffuse reflectance spectrum of the compound $[Cu_2(CH_3COO)_4(4Bz-Py)_2]$.

Two of the complexes reported in this paper, namely $[Cu(4Bz\text{-}Py)_2Cl_2]$ and $[Cu(4Bz\text{-}Py)_2(NO_3)_2]$, undergo thermochromic behaviour:

$$\underset{\text{light blue}}{[Cu(4Bz\text{-}Py)_2Cl_2]} \xrightarrow{170°C} \underset{\text{yellow}}{Cu(4Bz\text{-}Py)Cl_2} + 4Bz\text{-}Py$$

$$\underset{\substack{\text{cold form}\\ \text{(blue)}}}{[Cu(4Bz\text{-}Py)_2(NO_3)_2]} \xrightarrow{150°C} \underset{\substack{\text{hot form}\\ \text{(green-bluish)}}}{[Cu(4Bz\text{-}Py)_2(NO_3)_2]}$$

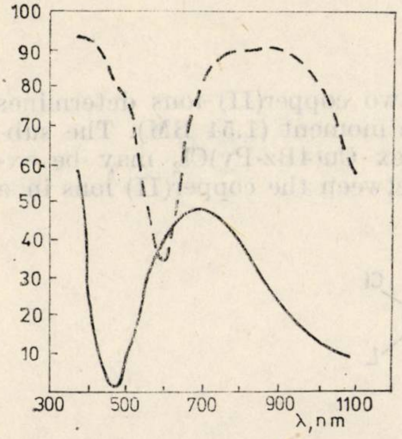

Fig. 4. — The electronic spectra of the compounds: a) $[Cu(4Bz-Py)_2Cl_2]$ (—); b) $Cu(4Bz-Py)Cl_2$ (. . .).

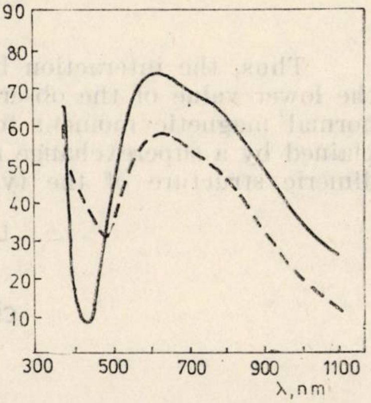

Fig. 5. — The electronic spectra of the compounds: a) $[Cu(4Bz-Py)_2(NO_3)_2]$-cold form (—); b) hot form (. . .).

The electronic spectra of the irrespective compounds are presented in figs. 4 and 5. In the first case, the thermochromism is due to the modification of the coordination number and geometry; for the second compound, the chromotropic phenomenon is associated with more complicated changes in the coordination sphere.[9]

REFERENCES

[1] M. Andruh, G. Filoti and M. Brezeanu, *Rev. Roum. Chim.*, **33**, 673 (1988).
[2] M. Andruh, C. I. Lepădatu and M. Brezeanu, *Inorg. Chim. Acta*, **131**, 159 (1987).
[3] M. Brezeanu, M. Andruh and N. Stănică, *Acta Chim. Hungarica.*, **124**, 391 (1987).
[4] M. Andruh, E. Urbanovici, M. Brezeanu and E. Segal, *Thermochim. Acta*, **95**, 257 (1985).
[5] E. Urbanovici, M. Andruh, M. Brezeanu and E. Segal, *Thermochim. Acta*, **118**, 309 (1987).
[6] D. P. Graddon and E. C. Watton, *Inorg. Nucl. Chem.*, **21**, 49 (1961).
[7] K. Sone and Y. Fukuda, "Inorganic Thermochromism", Springer., Berlin, 1987.
[8] B. N. Figgis, "Introduction to Ligand Fields", Interscience, New York, 1966 pp 296.
[9] R. T. Dudley, R. J. Fereday, B. J. Hathaway, P. G. Hodgson and P. C. Power, *J. Chem. Soc. Dalton*, **1977**, 1044.
[10] I. M. Procter, B. J. Hathaway and P. Nicholls, *J. Chem. Soc* (A), **1968**, 1678.
[11] B. J. Hathaway and D. E. Billing, *Coord. Chem. Rev.*, **5**, 143 (1970).
[12] L. Dubicki and R. L. Martin, *Inorg. Chem.*, **5**, 2203 (1966) and references therein.

Revue Roumaine de Chimie, 35, *1*, 9–22 (1990)

CATALYTIC HYDROGEN PREWAVE IN CYSTEINE- OR CYSTINE-CONTAINING SOLUTIONS. A POLAROGRAPHIC AND SPECTROPHOTOMETRIC STUDY

F. G. BĂNICĂ and ELENA DIACU

Polytechnic Institute of Bucharest, Department of Analytical Chemistry, Spl. Independenţei No. 313, Bucharest, Romania

Received February 11, 1989

The catalytic hydrogen prewave (CHP) was studied in a broader pH-range than previously by DC and AC polarography. It was found out that the CHP occurs at pH between 5 and 8, the maximum intensity being observed at pH of about 6.5. The electrochemical and spectrophotometric data show the importance of the complex NiL (L^{2-} = fully dissociated cysteine). The reduction of this species produces the transient zero-valent nickel complex involved in the catalytic hydrogen evolution. In the presence of cystine, the actual ligand-catalyst is cysteine generated by the reduction of disulphide. Consequently, the half-wave potential and the apparent transfer coefficient have the same values in the presence of both cysteine or cystine. Minor differences in the intensity of the catalytic current are due to the peculiarities of the reaction routes leading to the complex NiL in cysteine- or cystine-containing systems.

INTRODUCTION

During the polarographic investigation of selenocysteine in the presence of nickel ion, a new wave of catalytic hydrogen evolution was discovered.[1,2] This wave occurs at pH about 6 and its half-wave potential is located between – 1.1 and –1.2 V vs. SCE. Since the catalytic wave precedes the diffusion wave of hydronium, it was termed "catalytic hydrogen prewave" (CHP). Subsequently, it was shown that the CHP also appears in the presence of cysteine [3,4] or cysteinyl-dipeptides [5] and analogous processes occur if nickel is replaced by cobalt.[6] The main characteristics of the CHP may be resumed as follows: (1) it has the normal shape of the irreversible wave, in contrast to the Brdička wave, which is maximum-shaped; [7] (2) the half-wave potential of the CHP shows a much more important decrease of the hydrogen overvoltage as compared to the Brdička wave; (3) the hydrogen evolution is much less intensive than in the case of the Brdička wave and no hydrogen bubbles can be observed by microscope. However, the limiting current can be higher than the diffusion current of any species, except hydronium.[1] (4) A rate-determining proton transfer step was evidenced by the study of the isotope effect [8] and by cyclic voltammetry on a hanging mercury drop electrode.[9]

There are several evidences of the participation of nickel complexes in low oxidation state in the electrode process.[1,4] Complexes of this kind seem to be also involved in some enzymatic reactions, as for example hydrogen evolution in the presence of hydrogenase [10,11] or carbon dioxide reduction by the carbon monoxide dehydrogenase.[12,13] The presence of sulphur in the coordination sphere of nickel has been ascertained at least for hydrogenase from *Desulfovibrio gigas*.[14] In this connection, the conclusions resulted from the study of hydrogen evolution catalysed by nickel-cysteine complexes may be useful in understanding the enzymatic processes involving nickel centers.

This paper completes the previous results concerning the CHP in the nickel-cysteine system with new data on the occurrence of this wave in the presence of cystine. Since the acetate buffer previously used is not suitable at pH > 6.5, another buffer system was selected, namely the phosphate-acetate buffer. Therefore, it was also necessary to perform a systematic investigation of the CHP produced by cysteine in this buffer. Thus, it was possible to compare the results obtained in the presence of cysteine or cystine in a large pH-range. The experimental techniques used were direct- and alternating current polarography and ultraviolet absorption spectrometry.

EXPERIMENTAL PART

Cysteine hydrochloride, cystine (Merck), cobalt-free nickel chloride (Riedel de Haën) and the other reagents were of p.a. degree.

Conventional polarographic equipment supplied by Laboratorny Přistroje (Czechoslovakia) was used to record DC polarograms. AC polarographic studies were carried out by means of the non-phase sensitive Radelkis OH 105 polarograph (Hungary), at 60 Hz and 20 mV r.m.s. The characteristics of the dropping mercury electrode were : drop-time, 5.69 s, flow-rate, 1.40 mg/s in 0.1 M sodium acetate at 0V vs. SCE and 64 cm mercury column height. The three-electrode cell (with a platinum plate as auxilliary- and a SCE as reference electrode was thermostated at 25 ± 0.1°C. Argon was bubbled through the test-solution for 10 minutes prior to each run. The pH was measured by a glass electrode combined with the Radelkis OP 208 digital pH-meter and calibrated according to NBS recommendations. UV spectra were recorded by a SPECORD UV-VIS spectrophotometer (Carl Zeiss, Jena). Data processing was carried out by a desk-top computer (Tektronix 31).

EXPERIMENTAL RESULTS

1. The characteristics of the buffer system

Since the electrode process giving the CHP consists in the hydrogen evolution, it is very important to use well-buffered solutions. Otherwise, the local modifications of pH near the electrode surface make difficult the interpretation of the experimental data.

Due to the characteristics of the CHP, the buffer system must fulfil several conditions. It must be able to adjust the pH near neutrality without noticeable modifications of the buffer capacity. The composition of the buffer system must enable a satisfactory separation of the CHP from the nickel diffusion wave. To this end, the ionic strength must be low in order to avoid the displacement of the nickel diffusion wave towards the range of more negative potentials. Additionally, the strong complexing compounds must be absent due to the unfavourable effects on the half-wave potential of the nickel wave and the interference in the complex equilibria involving the catalytically-active complex. The absence of strongly adsorbable compounds is another important requirement.

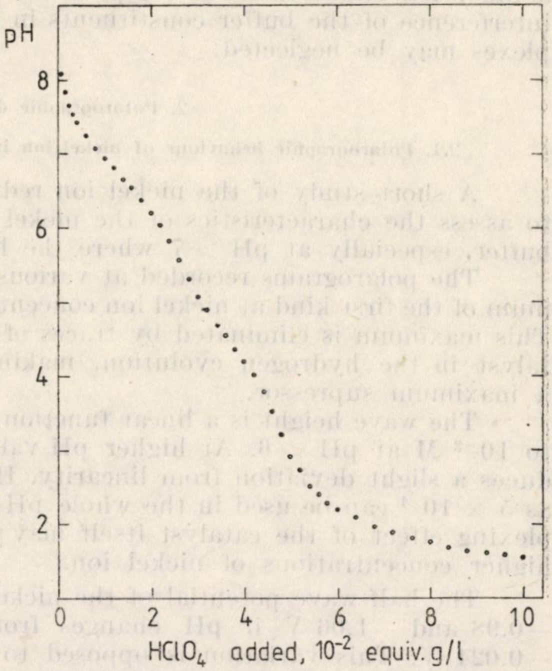

Fig. 1. — Neutralization curve of the buffer system containing sodium acetate and di-sodium hydrogen phosphate (0.024 M both).

The zwitterionic buffers[15] seem to fulfil most of these conditions except the last one. Among the usual buffers, the phosphate buffer appears to be the most suitable. However, the lowest limit of the pH range of this buffer is too high for our purposes. This drawback was corrected by addition of acetate and finally, the most suitable buffer system was found to be composed of Na_2HPO_4 and CH_3COONa (0.024 M both). The pH-value was adjusted by proper addition of perchloric acid and was checked by glass electrode. A typical neutralization curve of this buffer is shown in Fig. 1.

The phosphate-acetate buffer permits the variation of pH between 2.5 and 7.5 with minor changes of the buffer capacity. The ionic strength varies with the pH thus modifying the structure of the double layer. However, the CHP occurs on the negative side of the electrocapillary curve, where the structure of the double layer is mainly determined by the cations of the supporting electrolyte. Since the concentration of the sodium ion is constant and the contribution of other cations (e.g. H_3O^+) is negligible, the structure of the double-layer can be considered as independent of pH, at least in the potential range characteristic for the CHP.

The complexing properties of the buffer system are very slight. A survey of equilibrium data for the nickel-acetate complex[16] shows that the 1 : 1 complex has a stability constant of about 10, whereas no evidence for the formation of a nickel-phosphate complex was found. The complex $[Ni(HPO_4)]$ is more stable ($\log \beta = 2.08$) but even this complex is much less stable than the complexes with cysteine.[17] Consequently, the interference of the buffer constituents in the formation of cysteine complexes may be neglected.

2. Polarographic data

2.1. Polarographic behaviour of nickel ion in the phosphate-acetate buffer

A short study of the nickel ion reduction was performed in order to assess the characteristics of the nickel diffusion wave in the selected buffer, especially at pH > 7 where the hydrolysis can occur.

The polarograms recorded at various pH-values show a little maximum of the first kind at nickel ion concentration higher than 6×10^{-4} M. This maximum is eliminated by traces of organic compound used as catalyst in the hydrogen evolution, making unnecessary the addition of a maximum supressor.

The wave height is a linear function on the nickel concentration up to 10^{-3} M at pH < 6. At higher pH-values the partial hydrolysis produces a slight deviation from linearity. However, concentrations as high as 5×10^{-4} can be used in the whole pH-range of the buffer. The complexing effect of the catalyst itself may prevent the hydrolysis even at higher concentrations of nickel ion.

The half-wave potential of the nickel wave varies linearly between -0.98 and -1.06 V if pH changes from 4 to 7.5, the slope being -0.024 V. This variation is opposed to those observed in unbuffered media.[18] Taking into account the half-wave potential determined in absence of complexants (-1.1 V[19]), it follows that in the phosphate-acetate buffer the nickel ion is mainly present as an aquo-complex. The slight variation of the half-wave potential with the pH may be due to the displacement of the complexing equilibria involving acetate or phosphate ions.

In conclusion, the phosphate-acetate buffer is suitable for the study of electrode processes involving the nickel ion in low concentrations.

2.2. The main characteristics of the CHP in cysteine- or cystine-containing phosphate-acetate buffer

Several polarograms characteristic for the systems here studied are presented in Fig. 2. Curve 1 corresponds to the reduction of cystine (5×10^{-5} M) at pH 6.50, the two waves of disulphide reduction being clearly developed. The effects of nickel ion are illustrated by curve 2 which displays the following new features:

1. the depression of the first disulphide wave, probably due to the inhibition produced by the nickel-cystine complex;
2. the appearance of the maximum-shaped catalytic nickel prewave (CNP) with the maximum located at -0.69 V;
3. the nickel diffusion wave at about -1.1 V;
4. the CHP with $E_{1/2} = -1.25$ V.

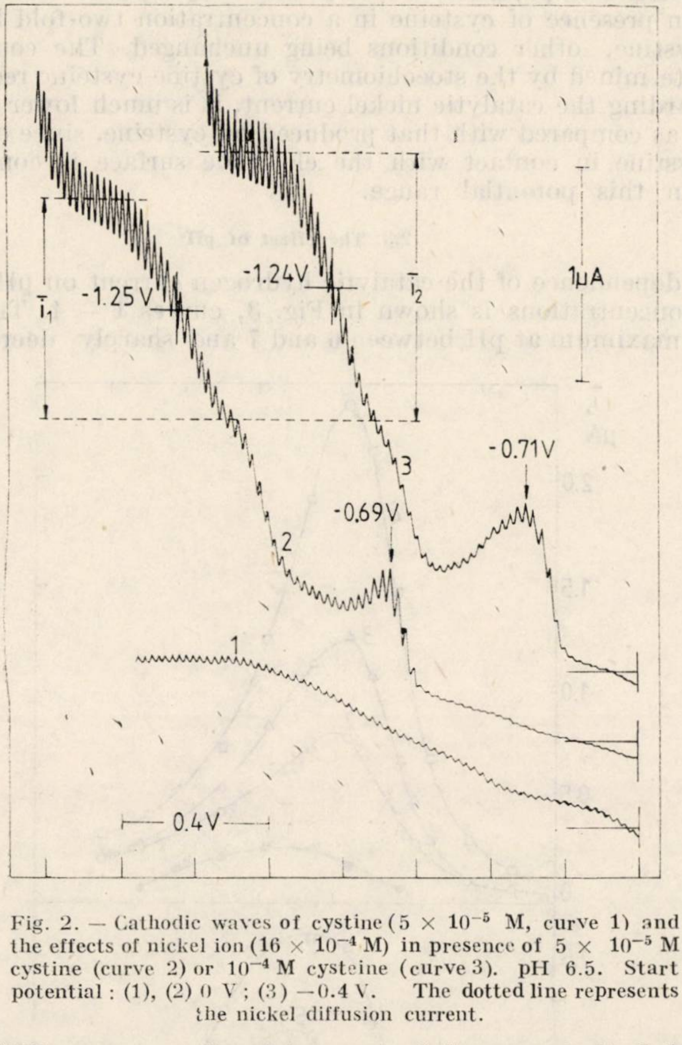

Fig. 2. — Cathodic waves of cystine (5×10^{-5} M, curve 1) and the effects of nickel ion (16×10^{-4} M) in presence of 5×10^{-5} M cystine (curve 2) or 10^{-4} M cysteine (curve 3). pH 6.5. Start potential : (1), (2) 0 V ; (3) −0.4 V. The dotted line represents the nickel diffusion current.

The CNP occurs on the rising part of the second disulphide wave. Conversely, the CHP is located in the range of the diffusion current of disulphide. Therefore, near the electrode surface, cystine is totally converted into cysteine in the range of the CHP, but the conversion is partial at the potentials of the CNP.

For comparison, curve 3 in Fig. 2 was recorded in the presence of cysteine in a concentration two-fold higher than that of cystine. The catalytic waves on the curves 2 and 3 in Fig. 2 have nearly identical half-wave potentials but slightly different values of the limiting currents. In a semi-logarithmic representation, both waves give straight lines with the slopes corresponding to $\alpha n = 0.56$.

In order to compare the catalytic effects, it is useful to introduce the ratio $\bar{i}_1/\bar{i}_2^{\mathrm{I}}$ where $\bar{i}$ represents the mean limiting catalytic hydrogen current recorded in presence of cystine and $\bar{i}_2$ is the same limiting current recorded in presence of cysteine in a concentration two-fold higher than that of cystine, other conditions being unchanged. The concentrations ratio is determined by the stoechiometry of cystine-cysteine redox system.

Regarding the catalytic nickel current, it is much lower in presence of cystine as compared with that produced by cysteine, since only a fraction of cystine in contact with the electrode surface is converted into cysteine in this potential range.

2.3. The effect of pH

The dependence of the catalytic hydrogen current on pH at various cysteine concentrations is shown in Fig. 3, curves 1 — 4. The catalytic current is maximum at pH between 6 and 7 and sharply decreases when

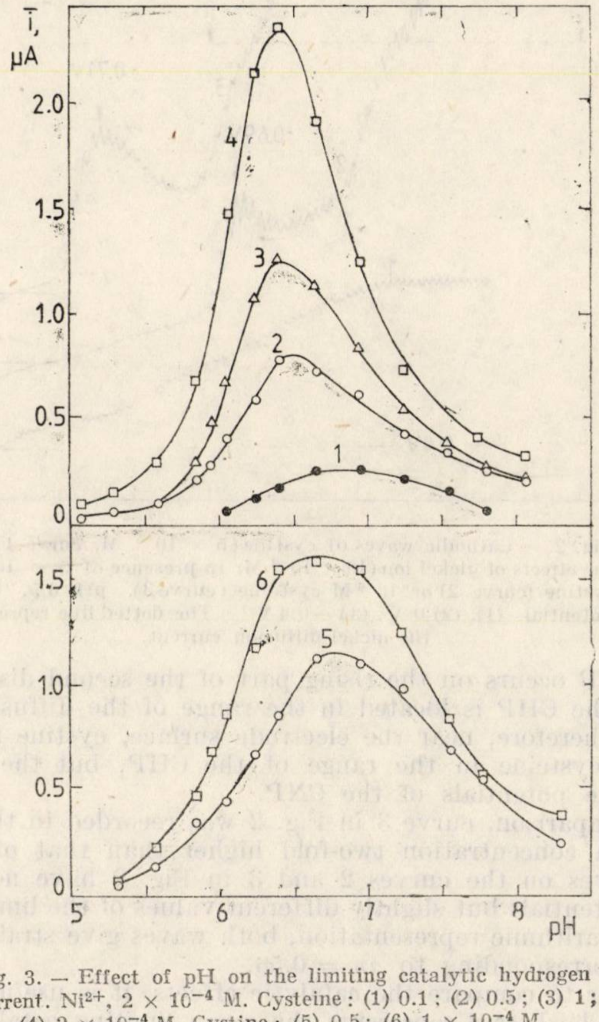

Fig. 3. — Effect of pH on the limiting catalytic hydrogen current. Ni^{2+}, 2×10^{-4} M. Cysteine: (1) 0.1; (2) 0.5; (3) 1; (4) 2×10^{-4} M. Cystine: (5) 0.5; (6) 1×10^{-4} M.

the pH varies towards higher or lower values. The position of the maximum is slightly displaced towards lower pH-values when the cysteine concentration increases. The approximate limits of the pH-range characteristic for the CHP are 5 and 8; these limits are dependent on the concentration of cysteine. At pH > 7.5 the Brdička wave tends to obscure the CHP.

In the case of cystine, the effect of pH is analogous (Fig. 3, curves 5, 6), but the maximum is located at slightly lower pH-values as compared with cysteine. The $\bar{i}_1/\bar{i}_2$ ratio is smaller than 1 at pH < 6.8 but it is higher than 1 at upper pH-values.

The effects of pH on the half-wave potential and on the steepnes of the wave are negligible.

Taking into account the effect of pH, further experiments were performed at pH 6.5, i.e. in the range of the maximum catalytic current.

2.4. The effect of cysteine or cystine concentration

As is shown in Fig. 4, the ratio $\bar{i}_1/\bar{i}_2$ is less than 1 in the whole concentration range but the deviation from unity is moderate. Studies at higher concentration as shown in Fig. 4 are hindered by the interference of the Brdička wave. The initial parts of the curves in Fig. 4 are linear, but a slight deflection appears at higher concentrations.

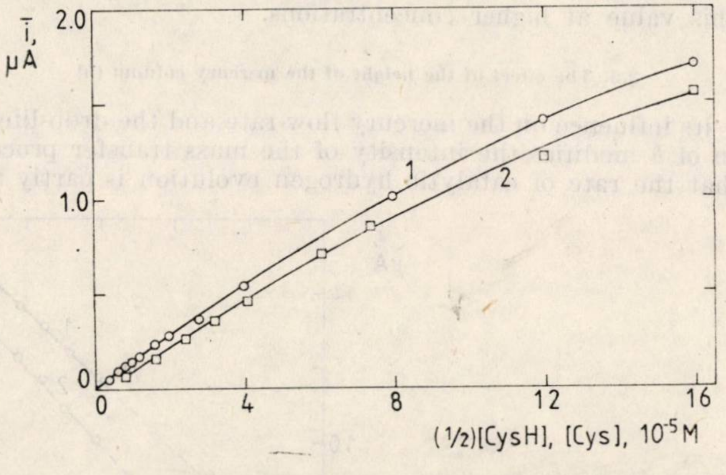

Fig. 4. — Effect of cysteine, CysH (1) or cystine, Cys (2) concentration. pH 6.5; Ni^{2+}, 2×10^{-4} M.

2.5. The effect of nickel ion concentration

The catalytic hydrogen current is a non-linear function of the nickel ion concentration at constant pH and cysteine or cystine concentration (Fig. 5). Although the nickel ion is in excess as compared to cysteine or cystine, the height of the CHP is very sensitive to nickel additions, denoting the low degree of complexation.

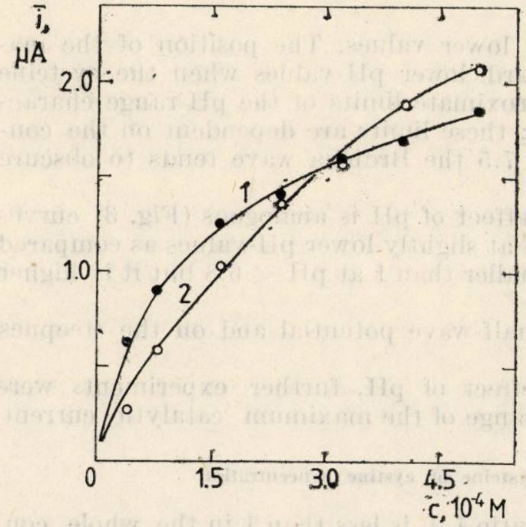

Fig. 5. — Influence of nickel ion concentration. pH 6.5. (1) cysteine 10^{-4} M; (2) cystine, 5×10^{-5} M.

The $\bar{i}_1/\bar{i}_2$ ratio is also a function of the nickel ion concentration. Its value is less than 1 at nickel concentration below 3×10^{-4} M but overcomes this value at higher concentrations.

2.6. The effect of the height of the mercury column (h)

By its influence on the mercury flow-rate and the drop-life time, the variation of h modifies the intensity of the mass transfer process. Fig. 6 shows that the rate of catalytic hydrogen evolution is partly influenced

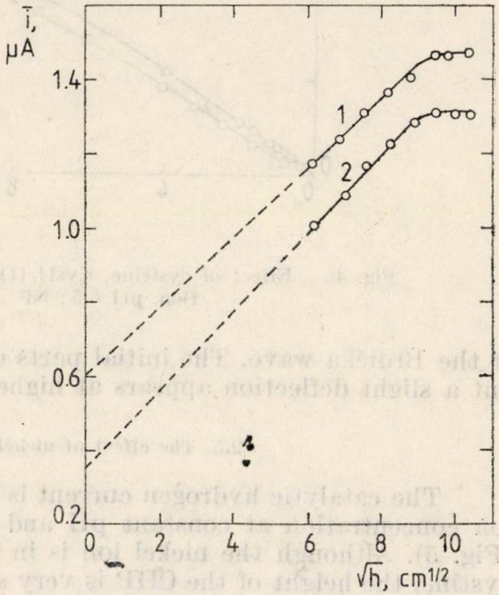

Fig. 6. — Effect of the height of the mercury column. pH 6.5; Ni^{2+}, 2×10^{-4} M. (1) cysteine 10^{-4} M; (2) cystine 5×10^{-5} M.

by the mass transfer both in the case of cysteine (curve 1) or cystine (curve 2) if $h^{1/2} < 9\ \mathrm{cm}^{1/2}$. At higher values, the catalytic current becomes independent of h, showing a behaviour typical for the limiting currents controlled by a chemical reaction. The transition from a partial diffusional to a kinetic character is rather sharp. The curves in Fig. 6 are almost parallel, denoting the same kind of mass transfer influence in presence of both cysteine or cystine.

2.7. Studies by alternating current polarography

Since the electrode processes in the nickel-cystine system are complicated by the reduction of disulphide bond, the AC determinations were performed in presence of cysteine.

Typical results are shown in Fig. 7. According to the electrode processes occurring in this system, the potential scale was divided in five regions denoted by roman figures.

Curve 1 in Fig. 7 was recorded in phosphate-acetate buffer containing 2×10^{-4} M $NiCl_2$. Except the region III, where the irreversible reduction of the nickel ion produces a very slight maximum, this curve is identical with that obtained in presence of the buffer alone.

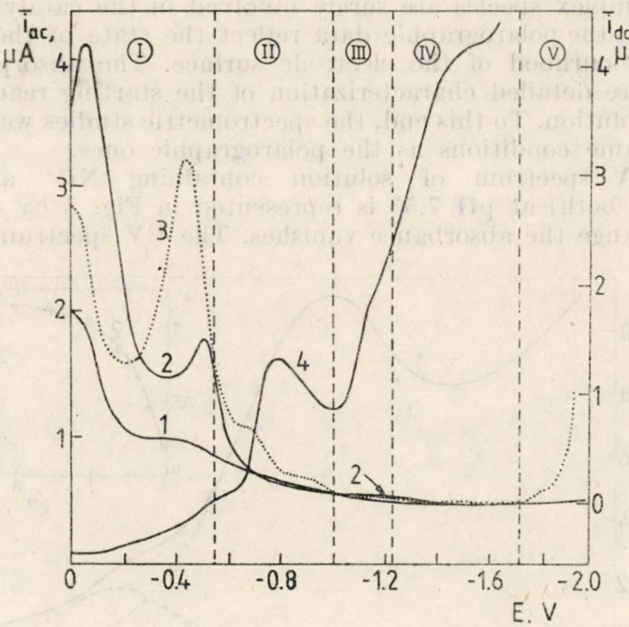

Fig. 7. — AC (curves 1—3) and DC (curve 4) polarograms. pH 6.5. (1) Ni^{2+} 2×10^{-4} M; (2) cysteine 10^{-4} M; (3), (4) Ni^{2+} and cysteine respectively as (1) and (2).

Curve 2 is the AC polarogram of cysteine in the same buffer. There are not evidences of the adsorption of cysteine at potentials more negative than −0.7 V, in agreement with the electrocapillary data.[4]

Curves 3 (AC) and 4 (DC) were recorded in the same solution which contains both cysteine and the nickel ion. In the region IV, where the CHP occurs (curve 4) the AC polarogram (curve 3) is identical with the background (curve 1) proving the strong irreversibility of the CHP and the absence of any noticeable adsorption in this potential range. The increase of the AC current in the region I may be related to the formation of a strongly adsorbable nickel-cysteine complex which induces a tensammetric component in the peak on curve 3 at about −0.4 V.

In the range of the CNP (II), curve 3 displays two maxima. Taking into account the location of the second maximum at the limit of the adsorption range, it may be of tensammetric character. The first maximum, corresponding to the rising part of the CNP is a faradaic one.

Finally, the small shoulder in the region V is related to the Brdička-type catalytic hydrogen evolution, since an analogous feature has been noticed in ammonia buffer containing cobalt ion.[20]

3. UV spectrometry

The complex species are surely involved in the catalytic hydrogen evolution, but the polarographic data reflect the state of these reactants in the neighbourhood of the electrode surface. The absorption spectra permit a more detailed characterization of the starting reactants in the bulk of the solution. To this end, the spectrometric studies were performed under the same conditions as the polarographic ones.

The UV spectrum of solution containing Ni^{2+} and cysteine (2×10^{-3} M both) at pH 7.53 is represented in Fig. 8 by curve 1. In the visible range the absorbance vanishes. The UV spectrum was deconvoluted assuming that the absorption band is described by the Gauss function:

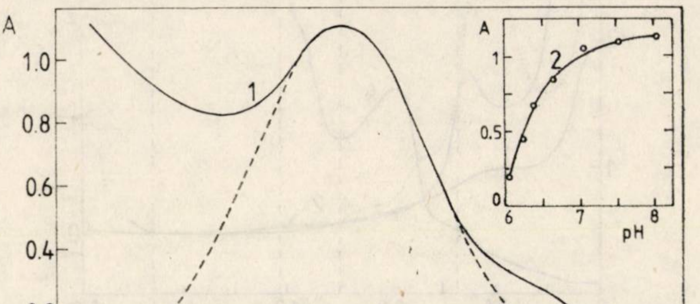

Fig. 8. — UV spectrum of nickel-cysteine complexes as recorded (1) and after deconvolution (dotted lines). Curve 2 : effect of pH on the maximum absorbance of the first band (3.685×10^4 cm^{-1}).

$$A = A_m \exp\{-[(\nu - \nu_m)/\vartheta]^2\}$$

where A is the absorbance, ν is the wavenumber (in cm^{-1}), A_m is the maximum absorbance (at the wavenumber ν_m) and $\vartheta = (\Delta\nu_{1/2})/2(\ln 2)^{1/2}$ $\Delta\nu_{1/2}$ being the width of the band for $A = A_m/2$. The absorbance instead of the absorption coefficient was used because the concentration of the absorbing species is not known. The individual absorption bands resulted by deconvolution are represented in Fig. 8 by dotted lines. The parameters of the bands are given in the Table for two pH values.

The parameters of the absorption bands of the solution containing nickel and cysteine (2×10^{-4} M both)

	First band		Second band	
pH	6.23	7.53	6.23	7.53
ν_m, 10^4 cm^{-1}	3.685	3.675	3.145	3.126
A_m	0.441	1.110	0.071	0.164
$\Delta\nu_{1/2}$, 10^3 cm^{-1}	5.486	5.438	2.843	3.202
$A_{m,1}/A_{m,2}$	2.517		2.319	

Fig. 8. shows that in the range of its maximum the first band is not interfered by the second one. Therefore, the maximum absorbance can be read directly on the spectrum. The intensity of the first band may be estimated if it is assumed that the absorbing species is a 1 : 1 nickel-cysteine complex in the same concentration as cysteine. Thus the lower limit of the absorption coefficient was found to be about 2500 $mole^{-1}$ dm^3 cm^{-1}. The actual value may be much higher, taking into account the previous assumptions.

The maximum absorbance of the first band increases with the pH and levels off at pH > 7 (Fig. 8, curve 2). Conversely, ν_m and $\Delta\nu_{1/2}$ are not dependent on pH (see the Table). Therefore, the properties of the absorbing site are not influenced by pH, although the concentration changes.

The second band shows an analogous dependence on pH. However, the ratio of the heights of the bands is not influenced by pH within the limits of the experimental errors (see the Table). This observation, as well as the absence of an isobestic point permits to assign both bands to the same complex species.

UV absorption bands with the same characteristics as above were recorded in 0.1 M ammonia buffer. However, these bands are less intensive than in phosphate-acetate buffer since ammonia strongly competes cysteine in the complex equilibria. On the other hand, the invariance of the maximum wavenumbers point to the absence of ammonia from the coordination sphere. The characteristics of the bands are also the same in deuterium oxide solutions.

DISCUSSION

Our studies showed that the upper limit of the pH-range favourable for the occurrence of the CHP is about 8. This result was obtained by means of the phosphate-acetate instead of the acetate buffer previously employed. It is important to note that the main kinetic parameters of the CHP, i.e. the half-wave potential and the apparent transfer coefficient do not change by the modification of the buffer. Therefore, the participation of buffer components in the complex equilibria is very low and they do not seem to be included in the composition of complex species responsible for the catalytic hydrogen evolution. Additionally, the limiting current of the CHP is only slightly dependent on the composition of the buffer, as long as the buffer itself has poor complexing properties. Some minor variations are rather due to the differences in both proton-donor concentrations or ionic strength than to kinetic factors as the rate of the proton-transfer reaction. Consequently, the data in this paper may be compared with those previously published [1-8] despite the difference in the composition of the supporting electrolyte.

The occurrence of the CHP in a limited pH-range centered at about 6.5 can be related to the complex equilibria involving cysteine and the nickel ion. It was already shown [17] that the following complexes may form with maximum probability at medium pH-values: NiL, $Ni_2L_3^{2-}$, and $Ni_3L_4^{2-}$ (where L^{2-} represents the fully dissociated cysteine molecule). The complex NiL_2 forms in a high degree at $pH > 6$ and its concentration levels off at $pH > 8$. The complex equilibria are, therefore, rather complicated, but the selection of the species involved in the hydrogen evolution can be made taking into account the following remarks:

1. The distribution curves in [17] were represented for concentrations 10—100 times higher than those suitable for the polarographic study of the CHP. But at very low concentrations of cysteine and nickel ion the formation of polynuclear complexes is less probable, as is also suggested by the formation curves.[17]

2. The CHP occurs not only only in the presence of cysteine or selenocysteine, but it is also produced by several cysteinyl-dipeptides, including cysteinyl-glycine.[5] However, this last compound can form with the nickel ion two complexes only, formulated as NiA and NiA_2[21] (no mention is made of the degree of protonation of the ligand A). In agreement with the polarographic data,[5] the spectroscopic results [21] show that the cysteine residue is involved in metal-ion binding. Therefore, a complex of the same kind is responsible for the catalytic hydrogen evolution, both in the case of cysteine or cysteinyl-glycine and this complex cannot be a polynuclear species.

3. A Job-type plot of the catalytic hydrogen current as a function of the cysteine molar fraction shows a maximum at about 0.5.[4] Although the linear correlation between the catalytic hydrogen current and the concentration of the complex involved in the electrode process is not yet firmly substantiated, this observation points to the implication of a 1 : 1 nickel-cysteine complex.

There are, therefore, sufficient evidences which support the participation of a complex of the NiL type in the electrode process giving the CHP. The occurrence of the CHP is thus confined to the pH-range favourable for the formation of this complex. The effect of cysteine concentration is also in agreement with a reaction order equal to 1. A complex with an analogous composition is involved in the catalytic reduction of nickel ion produced by cysteinyl-dipeptides.[22]

The same reason explains the low intensity of the CHP as compared to the Brdička wave. The latter is probably due to a higher complex (e.g. NiL_2) which forms in alkaline media and is more stable than the species NiL.[17, 18]

The UV absorption bands and the CHP behave differently when the pH increase: the absorption increases and levels off at $pH > 7$, whereas the catalytic current decreases at $pH > 8$. Both variables are connected with the concentration of complexes. The absorption bands are of charge-transfer type and the composition of the complex influences the absorptivity, but not the energy of the transition.[21] The degree of formation of the complexes increases with the rise of pH, giving the absorbance variation shown in Fig. 8. Conversely, the CHP is strongly dependent on the concentration of the species NiL, proving to be a selective tool for the study of this kind of complex of nickel with cysteine or related compounds.

If cysteine is replaced by cystine, the complex equilibria are totally different, as concerns the bulk of the solution. A nickel-cystine complex with the formula $[Ni(C_6H_{10}N_2O_4S_2)]H_2O$ has been isolated [23] but, more recently, a polymeric structure was assigned to this complex in solid state,[24] cystine molecules forming bridges between two adjacent nickel ions. This structure explains the high surface activity of the complex, as is proved by the inhibition of the first disulphide wave in the presence of nickel ion.

The CHP is located in the range of the limiting current of the second disulphide wave. Consequently, the actual ligand involved in the catalytic hydrogen evolution is cysteine. This is why the half-wave potential and the apparent transfer coefficient are almost insensitive to the change of cysteine by cystine. In the nickel-cystine system, the complex NiL can form by two ways:

1. the reduction of free cystine, followed by the reaction of cysteine thus formed with nickel ion. The reaction rate of complex formation is rather high (1.5×10^4 M^{-1} s^{-1} [25]) and no kinetic control is introduced by this tep.

2. The reduction of cystine in the nickel-cystine complex followed by the rearrangement of the coordination sphere to give the species NiL.

These processes occur inside the diffusion layer, where the concentration of nickel ion is lower than in the bulk of the solution. Consequently, the formation of the complex NiL by the first pathway occurs in less favourable conditions as compared to the cysteine-containing solution. This is why, in many instances, the ratio $\bar{i}_1/\bar{i}_2$ is less than 1. However, if the nickel-cystine complex forms in higher concentrations (e.g. at high pH or nickel concentration), the second pathway becomes important. Thus, the concentration of the species NiL becomes higher and, therefore, the hydrogen evolution is more intensive than in presence of cysteine.

The reduction of the complex NiL produces the actual complex-catalyst containing zero-valent nickel, which is involved in the reaction mechanism previously formulated.[1, 4] As proved by AC data, the electrode process is strongly irreversible and does not involve adsorbed species (at least at cysteine concentration $< 10^{-4}$ M). At higher mercury-flow rate, the process has a kinetic character, as also happens under the conditions of linear-sweep voltammetry on the hanging mercury drop electrode.[9] In agreement with the isotope effect,[8] the rate-determining step under these conditions is the protonation of the zero-valent nickel complex.

In conclusion, the CHP shows the same kinetic characteristics either cysteine is present in solution or is generated during the reduction of cystine on the dropping mercury electrode. Some minor differences regarding the intensity of the catalytic current are due to the different pathways leading to the species NiL, which is involved in the electrode process. This statement may be extended to cysteine derivatives and justifies the comparison of data obtained in systems containing either the reduced or the oxidized form of the ligand-catalyst.

REFERENCES

[1] A. Călușaru and V. Voicu, *Experientia*, **29**, 140 (1973).
[2] A. Călușaru and V. Voicu, *J. Electroanalyt. Chem.*, **43**, 257 (1973).
[3] A. Călușaru and F. G. Bănică, *J. Electroanalyt. Chem.*, **47**, 190, 554 (1973).
[4] F. G. Bănică and A. Călușaru, *J. Electroanalyt. Chem.*, **145**, 389 (1983).
[5] F. G. Bănică, *J. Electroanalyt. Chem.*, **171**, 351 (1984).
[6] A. Călușaru and F. G. Bănică, *J. Electroanalyt. Chem.*, **55**, 157 (1974).
[7] A. Călușaru, *J. Electroanalyt. Chem.*, **15**, 269 (1967).
[8] F. G. Bănică and A. Călușaru, *J. Electroanalyt. Chem.*, **158**, 47 (1983).
[9] F. G. Bănică, E. Diacu and C. Luca, *Bull. Soc. Chim. belges*, **96**, 485 (1987).
[10] J. J. G. Moura, M. Teixeira, I. Moura and A. V. Xavier, *J. Molec. Catal.*, **23**, 303 (1984).
[11] I. Okura, *Coord. Chem. Rev.*, **68**, 53 (1985).
[12] S. W. Ragsdale, H. G. Wood and W. E. Antholine, *Proc. Nat. Acad. Sci. U.S.A.*, **82**, 6811 (1985).
[13] M. Aresta, E. Quaranta, I. Tommasi, *J. Chem. Soc., Chem. Commun.*, **1988**, 450.
[14] R. A. Scott, S. A. Walin, M. Czechowski, D. V. Der Vartanian, J. Le Gall, H. D. Peck, Jr. and I. Moura, *J. Amer. Chem. Soc.*, **106**, 6864 (1984).
[15] N. E. Good, G. D. Winget, W. Winter, T. N. Connoly, S. Izawa and R. M. M. Singh, *Biochemistry*, 5, 467 (1966).
[16] L. G. Sillen, R. E. Martell, Stability Constants of Metal-Ion Complexes, The Chemical Society, London, 1964, 1971.
[17] D. D. Perrin and I. G. Sayce, *J. Chem. Soc. (A)* **1968**, 53.
[18] V. N. Pavlov and V. V. Bondar, *Uspekhi Khim.*, **42**, 988 (1973).
[19] A. A. Vlček, "Tables of Half-wave Potentials", Academia, Prague, 1956.
[20] M. Shinagawa, H. Nezu, H. Sunahara, F. Nakashima, H. Okoshita and T. Yamada, "Advances in Polarography" (I. S. Longmuir, ed.), Pergamon Press, 1960, p. 1142.
[21] H. Kozlowski, B. Decock-Le Révérend, D. Ficheux, C. Loucheux and I. Sovago, *J. Inorg. Biochem.*, **29**, 187 (1987).
[22] F. G. Bănică, *Talanta*, **32**, 1145 (1985).
[23] R. Rây and A. Bhaduri, *J. Indian. Chem. Soc.*, **27**, 297 (1950).
[24] M. Marc and A. Ungureanu, *Rev. Roumaine Chim.*, **26**, 587 (1981).
[25] G. Davies, K. Kustin and R. F. Pasternak, *Trans. Faraday Soc.*, **64**, 1006 (1968).

Revue Roumaine de Chimie, **35**, *1*, 23–30 (1990)

SPECTRAL STUDIES OF SOME THIAZOLYL AND PYRIMIDYL SUBSTITUTED THIOCARBAMIDES IN DIFFERENT SOLVENTS

P. S. MITTAL[a], NARINDER KUMAR[a] and A. D. TANEJA[b]

[a] D. N. College, Hisar – 125001, India
[b] Biochemist Cotton, H.A.U., Hisar, India

Received September 21, 1987

Some thiazolyl and pyrimidyl substituted thiocarbamides have been examined in ultraviolet region in a series of solvents covering a broad polarity range i.e., from benzene (Z, 54.0) to ethylene glycol (Z, 85.1). Transition energies were calculated and plotted against Z-values, a new empirical measurement of solvent polarity. A linear relationship was observed. Solvent sensitivities of these ligands have been calculated.

Thiazolyl and pyrimidyl substituted thiocarbamides constitute an important class of compounds because of their increasing utility in everyday life. Some work has been reported on their preparation, ionisation constants and antifungal activity etc.[1-3] Survey of literature reveals that a little work has been reported on the spectral studies of these thiocarbamides. The purpose of the present paper is to study the effect of solvents of different solvent polarities on the electronic transitions of some thiazolyl and pyrimidyl substituted thiocarbamides.

EXPERIMENTAL

The compounds selected for the present study N-methyl-N′-(2-thiozolyl) thiocarbamide, (MTTuH); N-allyl-N′-(2-thiazolyl)-thiocarbamide, (ATTuH); N-methyl-N′-(5-nitro-2-thiazolyl)-thiocarbamide, (MNTTuH), N-allyl-N′-(5-nitro-2-thiazolyl)-thiocarbamide, (ANTTuH), N-phenyl-N′-2-(pyrimidyl)-thiocarbamide, (PPmTuH); N-methyl-N′-2-(pyrimidyl)-thiocarbamide, (MPmTuH); -N-ally-N′-2-(pyrimidyl)-thiocarbamide, (APmTuH); N-phenyl-N′-2-(4-hydroxy-6-methyl pyrimidyl)-thiocarbamide, (PHMPmTuH); N-methyl-N′-2-(4-hydroxy-6-methyl pyrimidyl)-thiocarbamide, (MHMPmTuH); and N-allyl-N′-2-(4-hydroxy-6-methyl pyrimidyl)-thiocarbamide, (AHMPmTuH) were synthesized as described earlier [4,5]. All the solvents used were of either BDH Analar quality or E Merck GR quality. Freshly distilled solvents[6] were used in all the experiments and the solutions were prepared immediately before used. The absorbance measurements were made at 30 ± 0.1°C with a UV-VIS spectrophotometer model PMQ-3 using 1 cm matched quartz cells equipped with thermoplates to stabilize the temperature. The results are reported in Tables 1 and 2.

RESULTS AND DISCUSSION

It is evident from Table 1 that thiazolyl substituted thiocarbamides show three intense absorption peaks in the range 195–215 nm, 245–275 nm and 280–310 nm or 350–400 nm. These peaks have been assig-

Table 1

UV Spectral data of thiazolyl substituted thiocarbamides in various solvents

Solvent	MTTuH		ATTuH		MNTTuH		ANTTuH	
	λ_{max}	E_{max}	λ_{max}	E_{max}	λ_{max}	E_{max}	λ_{max}	E_{max}
Dioxane	206	9760	205	9257	207	9416	203	9016
(Diox)	255	13861	255	13743	247	13616	247	13804
	302	22732	300	22937	360	28471	360	26316
Benzene	206	9690	205	9161	207	9301	205	9163
(Bz)	258	13556	257	13291	248	13431	259	13762
	301	22361	301	22422	354	28022	356	26322
Carbon tetrachloride	205	9729	202	9142	203	9221	202	9602
(CT)	259	13161	256	13431	245	13422	256	13721
	300	22432	302	22231	350	27763	352	26802
Chloroform	204	9657	203	9081	208	9161	204	9191
(CF)	258	13261	258	13247	249	13417	258	13262
	301	22161	302	22041	352	27701	355	26116
Acetic acid	201	9107	201	8651	203	8923	205	8821
(AcOH)	251	12631	255	11961	250	11962	253	12241
	296	21207	294	21090	355	25027	360	26521
Dichloro methane	200	9431	200	8741	205	8761	200	8901
(DM)	251	12281	254	12261	248	12527	255	12471
	292	21423	290	21424	355	25727	363	25321
Dichloro ethane	198	9651	199	8661	202	8962	204	8816
(DE)	252	12431	252	11961	252	12263	257	12816
	294	20761	293	21862	361	26861	365	25763
X n-butyl alcohol	203	9531	202	8961	208	8861	205	9023
(n-BuOH)	256	12902	257	13963	252	12941	264	13046
	294	21931	295	22052	364	27122	365	24916
n-Propyl alcohol	205	9631	206	8764	205	9663	205	8981
(n−PrOH)	258	12806	256	13282	255	12782	257	12816
	293	21452	293	21792	365	26964	365	24860
Ethyl alcohol	204	9562	203	8862	204	8816	205	8916
(EtOH)	259	12942	261	13261	253	12623	259	12602
	296	21571	294	21922	368	26916	365	24722
Methyl alcohol	205	9461	205	8790	205	8616	203	8814
(MeOH)	260	12446	262	12990	254	12416	262	12516
	297	21371	295	21461	370	26516	361	24616
Acetonitrile	203	9763	201	9161	205	9116	205	8961
(AN)	262	13400	266	12416	253	13220	253	13116
	294	22421	296	22924	370	27916	372	24961
Ethylene glycol	202	9876	202	9140	203	8861	200	8880
(EG)	253	11521	254	12421	243	12516	253	12221
	288	21729	287	22816	374	25416	370	25116
Pyridine	205	9142	207	8321	208	9220	207	8261
(Py)	—	—	—	—	—	—	—	—
	304	21431	305	20422	370	24516	370	24490
Dimethyl formamide	203	8231	201	8116	210	8290	202	8192
(DMF)	267	12451	267	12651	262	12542	261	13542
	297	22067	298	21009	370	24042	370	24521
Dimethyl sulphoxide	208	9046	210	9056	212	9042	205	9061
(DMSO)	270	11352	270	11421	260	11961	262	12421
	302	22406	302	21423	376	26516	374	26111
Formamide	205	9021	204	3036	210	8916	200	9011
(FA)	270	12652	270	12731	258	10916	260	11521
	298	21953	297	21427	371	24165	372	23220

Table 2

UV Spectral data of pyrimidyl substituted thiocarbamides in various solvents

Solvent	MPmTuH		PPMTuH		APmTuH		MHMPmTuH	
	λ_{max}	E_{max}	λ_{max}	E_{max}	λ_{max}	E_{max}	λ_{max}	E_{max}
Diox	203	10662	202	11916	201	11816	203	12019
	236	18146	236	19723	236	19922	243	20621
	283	23761	283	24719	283	26268	285	25402
Bz	206	10416	204	11462	204	11522	206	11661
	238	17916	240	19663	241	19641	246	20554
	282	23918	283	24663	284	26116	280	25116
CT	202	10266	203	11462	202	11522	203	11916
	236	17922	235	19263	235	19716	246	20423
	284	23593	285	24427	286	25516	285	25093
CF	205	10180	204	10917	204	11417	204	11819
	237	17616	239	19160	240	19620	246	20223
	282	23116	284	24110	285	25120	280	24852
ACOH	201	9431	202	9512	203	10127	200	11423
	235	17222	236	18616	237	18927	245	18762
	280	22116	282	21416	283	21516	285	22462
DM	201	10761	202	10862	203	11022	200	12417
	239	18222	240	18810	241	19216	243	20922
	287	22427	286	22516	286	23420	285	24827
DE	200	9962	201	10641	202	10822	200	12521
	241	17823	242	18516	243	18823	239	20622
	281	21890	280	22116	281	23216	285	24327
n-BuOH	204	10147	202	10522	199	10923	205	11521
	235	18023	235	19116	236	19821	235	20617
	296	22510	297	23610	297	25016	283	25116
n-ProH	208	10009	207	10216	203	10820	205	11427
	236	17614	238	18861	239	19420	237	20222
	297	22423	298	23521	300	24822	284	24622
EtoH	205	9745	204	9817	205	10620	205	10810
	235	17310	236	18720	237	19294	238	19916
	295	22212	295	23420	296	24697	285	24310
MeoH	205	9681	204	9719	204	10410	200	10690
	236	16941	237	18421	236	18971	240	19961
	290	21961	289	23016	289	24420	286	24110
AN	204	9916	201	9947	202	11491	207	11317
	238	18221	239	19810	239	19816	240	20110
	291	22862	292	25527	293	24610	286	25220
EG	201	9762	200	10621	201	9876	203	10110
	234	18416	236	20116	236	18916	242	19616
	296	23660	297	24490	298	23216	288	24317
Py	204	8961	202	9327	205	10916	208	9317
	—	—	—	—	—	—	—	—
	300	20620	301	20616	302	19216	307	21110
DMF	200	9620	201	9819	202	9614	202	9714
	257	19216	258	18971	258	18110	255	20816
	295	21621	296	22119	297	23993	288	26916
DMSO	202	9410	201	9777	202	9441	202	9271
	264	20310	241	19949	246	20661	250	21710
	295	22516	297	24410	298	25420	286	25867
FA	200	9267	203	9461	204	9416	203	9620
	240	19116	265	18993	260	19421	255	18961
	295	22230	294	23116	296	24916	286	26119

Table 2 (continued)

Solvent	PHMPmTuH		AHMPmTuH	
	λ_{max}	E_{max}	λ_{max}	E_{max}
Diox	203	11820	204	12026
	242	20486	244	21221
	285	21516	284	27119
Bz	206	11710	206	11911
	245	20210	247	20920
	286	26201	282	26749
CT	204	11423	203	11871
	242	19816	243	20770
	285	26610	286	26371
CF	205	11110	205	11671
	247	19616	248	20717
	282	25816	282	26216
AcOH	200	12316	203	12521
	245	19761	246	19916
	286	25810	286	26620
DM	201	12417	201	12716
	242	21666	244	21961
	285	25110	285	25620
DE	200	12516	201	12661
	238	21216	245	21210
	284	25310	284	25327
n-BuOH	201	11116	202	12819
	236	19961	236	20360
	284	26320	282	26216
n-PrOH	204	10917	203	12510
	238	19521	238	19716
	285	25712	283	25710
EtOH	204	10760	202	12229
	239	19116	240	19409
	286	25460	284	25220
MeOH	201	10416	201	11920
	241	18880	241	19110
	287	24950	285	24716
AN	206	11116	205	9920
	240	19910	240	20317
	286	26662	286	25616
EG	202	9827	202	10315
	242	18316	242	20617
	287	25116	268	25327
Py	207	10361	207	9110
	—	—	—	—
	—	—	—	—
	308	21716	308	22310
DMF	201	10068	202	10320
	256	19527	257	19326
	287	24521	288	25871
DMSO	201	9910	202	9813
	250	18416	250	19509
	286	22320	286	24210
FA	202	9520	201	9617
	254	18320	255	19210
	288	22160	286	25910

ned to : (i) high energy thiazolyl Π → Π* transitions, (ii) thiocarbonyl Π → Π* and (iii) thiazolyl Π → Π* transitions.[7, 8] The pyrimidyl substituted thiocarbamides show three intense peaks in the region of 195—215 nm, 235—255 nm and 275—310 nm. These peaks have been assigned to : (i) Π → Π* high energy pyrimidyl transition, (ii) thiocarbonyl Π → Π* transition and (iii) Π → Π* pyrimidyl transition respectively.

High Energy Π → Π* transitions

In case of thiazolyl substituted thiocarbamides, high energy Π → Π* transitions are observed in the region 195—215 nm. In the same region high energy Π → Π* pyrimidyl transitions are observed in case of pyri-

Table 3

Solvent sensitivity of thiazolyl substituted and pyrimidyl substituted thiocarbamides

Compound	Thiocarbonyl Π→Π* transition			Thiazolyl Π→Π* + Nitro thiazolyl Π→Π*			High energy thiazolyl Π→Π* transition		
		$E_T = mz + b$		ΔE_T^*	$E_T = mz + b$		ΔE_T^*	$E_T = mz + b$	
	ΔE_T^* (kcal/ /mole)	m	$m \times \Delta z$** (kcal/ /mole)	(kcal/ /mole)	m	$m \times \Delta z$** (kcal/ /mole)	(kcal/ /mole)	m	$m \times \Delta z$** (kcal/ /mole)
MTTuH	2.79	0.087	2.77	4.29	0.142	4.41	2.75	0.093	2.89
ATTuH	1.31	0.053	1.65	4.63	0.154	4.78	2.07	0.051	1.58
MNTTuH	2.27	0.074	2.30	−4.32	−0.138	−4.29	2.72	0.087	2.70
ANTTuH	2.62	0.083	2.58	−3.03	−0.092	−2.86	3.49	0.116	3.60
	Thiocarbonyl Π→Π* transition			Pyrimidyl Π→Π* transition			High energy pyrimidyl transition		
		$E_T = mz + b$			$E_T = mz + b$			$E_T = mz + b$	
	ΔE_T^* (kcal/ /mole)	m	$m \times \Delta z$** (kcal/ /mole)	ΔE_T^* (kcal/ /mole)	m	$m \times \Delta z$** (kcal/ /mole)	E_T^* (kcal/ /mole)	m	$m \times \Delta z$** (kcal/ /mole)
MPmTuH	2.04	0.086	2.67	−4.80	−0.152	−4.72	3.44	0.109	3.39
PPmTuH	2.02	0.081	2.51	−4.76	−0.156	−4.85	2.81	0.086	2.67
APmTuH	2.51	0.090	2.79	−4.72	−0.149	−4.63	2.09	0.069	2.14
MHMPmTuH	1.93	0.052	1.61	−2.83	−0.094	−2.93	1.95	0.061	1.89
PHMPmTuH	1.36	0.062	1.92	−1.08	−0.056	−1.74	2.75	0.088	2.73
AHMPmTuH	2.40	0.087	2.70	−2.11	−0.069	−2.14	2.53	0.079	2.45

* Defined as the difference between ethylene glycol and benzene transition energy

** These values should be compared with those in column ΔE_T of the same table.

midyl substituted thiocarbamides. These transitions have moderate intensities ($E_{\max} = 5000-15000$) and moderate oscillator strength. The plots of Z vs E_T are amenable to a reasonable least square fit. The deviations in certain cases like acetonitrile, dichloramethane, formamide etc. can be explained by considering the charge transfer interactions between the thiazolyl group or pyrimidyl group and the solvent. The solvent sensitivities obtained as the difference between the transition energies in ethylene glycol and benzene are given in Table 3 and the solvent sensitivity values as obtained from the regression line are also given in the same Table. The dipole moment of the excited state of these compounds produced by $\Pi \rightarrow \Pi^*$ high energy thiazolyl or $\Pi \rightarrow \Pi^*$ high energy pyrimidyl transitions have been calculated and the values are : 5.26 D for MTTuH, 4.71 D for ATTuH, 5.40 D for MNTTuH, 5—05 D for ANTTuH, 4.69 D for MPmTuH, 4.99 D for PPmTuH, 4.14 D for APmTuH, 4.23 D for MHMPmTuH, 4.94 D for PHMPmTuH and 4.76 D for AHMPmTuH.

Thiocarbonyl $\Pi \rightarrow \Pi^*$ transitions

The thiocarbonyl $\Pi \rightarrow \Pi^*$ transitions fall in the region of 245—275nm in case of thiazolyl substituted thiocarbamides and 235—250 nm in case of pyrimidyl substituted thiocarbamides. In this case also blue shifts are found as one goes from dioxane to acetonitrile. This band appears to be mixed with some other transitions, probably $n \rightarrow \Pi^*$ transitions overlapping with it. The plots of Z vs. $E\ '$ are drawn and it gives a scatter diagram from which the best straight line was obtained by least square fit. Deviation from the regression line in case of dimethyl formamide can be explained by considering the charge transfer interactions between the thiocarbonyl group and the solvent. The deviation in case of acetonitrile may be due to the presence of polarised Π-bond in the solvent molecules which enables the easy acceptance of electrons from sulphur of thiocarbonyl group resulting in the formation of complex[9]. The solvent sensitivities measured as the difference in the excitation energies in ethylene glycol and benzene are presented in Table 3. The solvent sensitivity can also be evaluated from the slope of regression line. The solvent sensitivities obtained from least square fit show a marked difference from the previous values. This is attributed to the $Z-E$ correlation, being only approximate in nature in case of bulky molecules. The solvent sensitivities of these transitions vary between 1.31—2.79 and 1.36—2.50 in case of thiazolyl substituted thiocarbamides and pyrimidyl substituted thiocarbamides respectively. In case of thiazolyl substituted thiocarbamides, MTTuH has the highest solvent sensitivity whereas ATTuH has the lowestone. In pyrimidyl substituted thiocarbamides, APmTuH has the highest and MHMPmTuH has the lowest solvent sensitivity. The difference in the solvent sensitivity values is due to the increasing and decreasing electron density of ground state and the excited state of the compounds. The absorption maxima is shifted to longer wavelength with increasing polarity and hence, in such cases, the solvent sensitivity will decrease.

Thiazolyl $\Pi \rightarrow \Pi^*$ and pyrimidyl $\Pi \rightarrow \Pi^*$ transitions

Thiazolyl $\Pi \rightarrow \Pi^*$ transitions occur in the region of 280−310 nm in case of MTTuH and ATTuH whereas in case of MNTTuH and ANTTuH these transitions occur in the region of 350-400nm. The pyrimidy $\Pi \rightarrow \Pi^*$ transitions occur in the region of 275−310 nm. In compounds MPmTuH, PPmTuH, APmTuH, MHMPmTuH, PHMPmTuH, AHMPmTuH, MNTTuH and ANTTuH red shift is observed on going from benzene to ethylene glycol. Absorption maxima of MNTTuH and ANTTuH occur at longer wavelengths in comparison to other substituted thiocarbamides. The large difference in the position of λ max is due to the fact that the $\Pi \rightarrow \Pi^*$ transitions of nitro group get superimposed with the transitions of thiazolyl group, and the presence of nitro group in thiazolyl ring shifts the position of thiazolyl the $\Pi \rightarrow \Pi^*$ transitions from 280−310 nm to 350−400 nm. The presence of nitro group at 5-position imparts some sort of extended conjugation in the molecule which imparts stability to the molecule. The transition energies of these substituted thiocarbamides are plotted against the Z-value. The correlation between Z and E_T gives a scatter diagram for which the best straight line was obtained by a least square fit. The deviations in cases of DMF, DMSO and FA are attributed to the charge transfer interaction between pyrimidyl ring and the solvent in case of pyrimidyl thiocarbamides whereas in case of thiazolyl thiocarbamides it may be due to charge transfer interaction between thiazolyl ring and carbonyl groups respectively. The small shifts in other solvents are consistent with the expected trend from the solvent effect on the spectrum of the single species having an excited state which is more polar than the ground state[10,11]. The transitions in DMSO, DMF and FA require lesser energy than predicted by the plot of E_T vs Z_T value. Carbonyl oxygen and sulphur in these solvents act as good donor and from charge transfer complexes with thiones. A high value of transition energy in AN may be due to the presence of polarised $\Pi \rightarrow \Pi^*$ bonds which enable easy acceptance of electrons from the sulphur of enethiolate ion by forming a complex.[9] Since the molecules are bulky, it is difficult to achieve a fruitful relationship between Z and E_T because it is a well-known fact that as the solute molecules increase in size, the correlation becomes less precise due to the specific solute-solvent interactions, self association and distortion of cybotactic region[9].

Negative values of the slope and hence E_T (Table 2) in case of MNTTuH, ANTTuH, MPmTuH, PPmTuH, APmTuH, MHMPmTuH, PHMPmTuH and AHMPmTuH indicate that the solvent sensitivity of these compounds is very small in ethylene glycol. The λ max of these compounds is shifted to longer wavelengths in ethylene glycol as compared to benzene. The E_T of these compounds in ethylene glycol is much smalter as compared to benzene. This may be attributed to intermolecuar hydrogen bonding which imparts stability and hence more solubility of these compounds in ethylene glycol. The UV-spectral data permit an estimation of hydrogen bonding as suggested by Kosower.[9]

REFERENCES

[1] B. Dash and S. K. Mahapatra, J. *Indian Chem. Soc.*, **50,** 738(1973).

[2] O. P. Khurana, J. S. Tyagi and A. D. Taneja, *J. Chinese Chem. Soc.*, **29,** 185 (1982).

[3] J. D. Gauba, A. D. Taneja and J. S. Tyagi, *Indian J. Chem.*, **24**A, 138 (1985).

[4] P. S. Mittal, J. S. Tyagi, N. Kumarand A. D. Taneja, *J. Indian Chem. Soc.* (Communicated).

[5] N. Kumar, P. S. Mittal, A. D. Taneja and V. P. Kudesia, *Indian J. Chem.* (Communicated).

[6] A. I. Vogel, Practical Organic chemistry", III Edition, Longmans London (1962).

[7] J. D. Gauba, Spectroscopic and Thermodynamic Studies on Some Substituted Thiazolyl – Thioureas", Ph. D. Thesis, Meerut University, Meerut (1982).

[8] J. R. Dyer, "Applications of Absorption Spectra of Organic Compounds", Prentice-Hall of India Ltd., New Delhi (1971).

[9] E. M. Kosower, *J. Amer. Chem. Soc.*, **80,** 3267 (1958).

[10] C. N. R. Rao, Ultra-violet and Visible Spectroscopy, Chemical Applications", 2nd Ed. Butter-worths, London (1967).

[11] C. N. R. Rao and A. Balasubramanian, *Chem. and Ind.*, **1960** (1025).

Revue Roumaine de Chimie, 35, *1*, 31–39 (1990)

RECOVERY OF METALLIC IONS FROM WASTE WATERS BY FLOTATION

LIGIA STOICA[a], RODICA V. CĂTUNEANU[a], CORNELIA BEJAN[a],
MARGARETA NICOLAU[b] and V. BRETAN[c]

[a] Bucharest Polytechnic Institute – Department of Inorganic Chemistry and Inorganic Technology, Bucharest, Romania
[b] I.C.P.E.A.R. – Bucharest, Romania
[c] C. M. Baia Mare, Romania

Received October 2, 1987

Waste waters resulting from metallic octoate industry contain Co(II) in quantities varying from 50–5000 mg/L, determining metal losses that require recovery technologies. The present paper studies the possibility of separating insoluble hydroxospecies produced by Co(II) at $pH > 8$ treated with NaOH by flotation with dissolved air, using as a collector reactive 2-ethyl sodium hexanoate (solution 30% in 2-ethylhexanoic acid). The selection of the collector is determined by the experimental results concerning surface tension and electrokinetic potential. The optimum flotation pH, the collector colligend rate, the necessary air and the possibility of recovering Co(II) from foam have been established. Separation efficiency is high (> 98%).

As a consequence of chemical technology diversification, waste waters contain a large number of soluble and insoluble impurifying agents, of ionomolecular and colloidal size representing a danger both for the industrial equipment and the environment.

Under these conditions, although the classical technologies solve the problem of purification, the resulting large amounts of mud require storing and processing places. To avoid these disadvantages, new and more efficient purifying technologies for recovering separate components from the aqueous phase have been developed.

Promising results have been obtained by applying *flotation*, a procedure belonging to the group of separation methods by means of adsorptive bubbles.[1–4]

FLOTATION consists in :

— The distribution of the component to be separated between the aqueous phase and the gaseous phase at the interface of microdispersed bubbles forming the foam.

The required concentration of an impurifying agent in the aqueous phase is obtained :

— either by the effect of its own density, which is inferior to that of the liquid ;

— or by the apparent density effect obtained artificially by fixing the gas bubbles on particles in suspension or emulsion being attracted to the surface by the bubbles.

The phases of waste water flotation are the following :

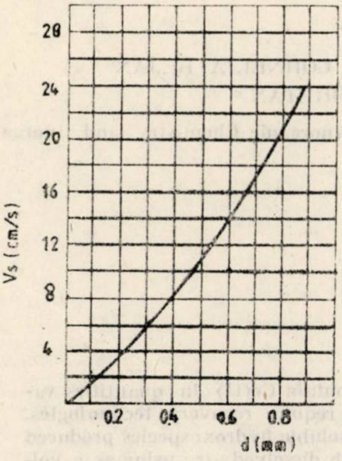

Fig. 1. — Ascensional rate dependence of diameter bubbles.

— the liquid phase, represented by water resulting from different industries, containing dissolved species of ionomolecular or colloidal dimensions.

In the presence of inorganic impurities the ions may be aquo compounds or polynuclear species. An important characteristic of the liquid phase is surface tension (σ) influencing bubble size foam formation and bubble to particle adhesion.

— the solid phase represented by particles having colloidal or quasicolloidal dimensions of $\Phi < 2.5$ g cm^{-3} densities and high flotability.

— the gaseous phase — consisting of a system of microbubbles dispersed in the liquid phase. The gas bubbles adhere to the surface of solid particles forming aggregates of low density, concentrating at the surface in a thick foam.

During flotation the system bubble-particle must be stable. The bubble-particle adhesion depends on the properties of the surface in contact, and on the bubble size. A study of the dependence of the velocity in the upward direction on the bubble diameter (Fig. 1) shows a direct proportionality between the two parameters. Surface properties, surface energy, and electric phenomena, determined by the very structure and properties of water, contribute to the formation of the mobile bubble — particle system.

To modify the surface characteristic of the particles interacting with the microdispersed bubbles, a polyelectrolyte system is introduced — the collector.

The gas bubbles can be generated by dispersion (flotation by dispersed gas), by expanding pressurized water (dissolved air flotation) or by electrolysis (electroflotation).

Dissolved air flotation has the advantage of forming small bubbles (Φ 30—180 μ) at the expansion moment. Such bubbles can also penetrate inside particles with spongy structure (e.g. hydroxides), into which bubbles generated by dispersion could not penetrate.

The separation method of precipitate flotation for the concentration range 10^{-2}—10^{-6} mol/L is superior to other separation methods being simple and economical ; it can be applied to a wide range of inorganic and organic impurifying agents of ionomolecular and colloidal dimensions.

The paper studies the recovery separation conditions of Co(II) in waste waters yielded by the production of cobalt II octoate.

The presence of Co(II) in an amount over 1 g/L made it necessary to recover and reintroduce it in the production cycle.

The classical purifying method using $Ca(OH)_2$ or Na_2CO_3 for precipitating Co(II) as hydroxides or carbonates, introduces an additional step, i.e. separating Co(II)—Ca(II).

EXPERIMENTAL

A synthetical solution in the range 50—5000 mg Co(II)/L [as $Co(NO_3)_2$] and waste waters have been studied, using as a precipitating reactive NaOH 6 n and as a collector reactive 2-Na ethyl hexanoate in 2 ethyl hexanoic acid.

We used:

- — a flotation device with dissolved air (Fig. 2)
- — a pH-meter MV—85 with glass electrode and calomel for pH control.
- — spectrophotometer VSU—2G—Karl Zeiss Jena to determine Co(II) before and after flotation
- — stalagmometer to determine surface tension.
- — an apparatus to determine the electrokinetic potential.

Air flotation methodology was presented in a previous paper. The separation efficiency of Co(II) is established by spectrophotometric method using α-nitrozo R and is calculated by the relation below:

$$R\% = \left(1 - \frac{C_t}{C_0}\right)100$$

Where: C_t = Co(II) concentration after flotation C_0 = Co(II) concentration in the initial sample.

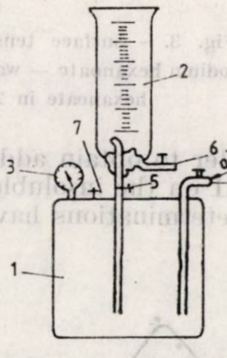

Fig. 2. — Flotation apparatus: 1 — pressure container; 2 — flotation cell; 3 — manometer; 4 — compressed air introduction; 5 — valve to introduce pressurized water in the flotation cell; 6 — sample collection of separation control; 7 — safety valve.

To establish the optimum efficient separation conditions of the Co(II) ion, the following parameters have been studied:

- — collector selection;
- — flotation optimum pH;
- — collector — Colligend ratio;
- — metallic ion concentration;
- — necesary air.

RESULTS AND COMMENTS

Collector selection

Collectors are surface-active agents of heteropolar structure forming by polar groups insoluble complexes of ion — pair type or coordination with ionic or molecular species that can be extracted by flotation.

By nonpolar groups, the collectors are fixed on gas bubbles concentrating in the foam.

The behaviour as a collector reactive of the system 2 ethyl sodium hexanoate — acid 2 ethyl hexanoic (II) is proved by the curve characteristic $\sigma = f(c)$ in Fig. 3, confirming the surface-active qualities superior to the 2 ethyl sodium hexanoate-water system(I).

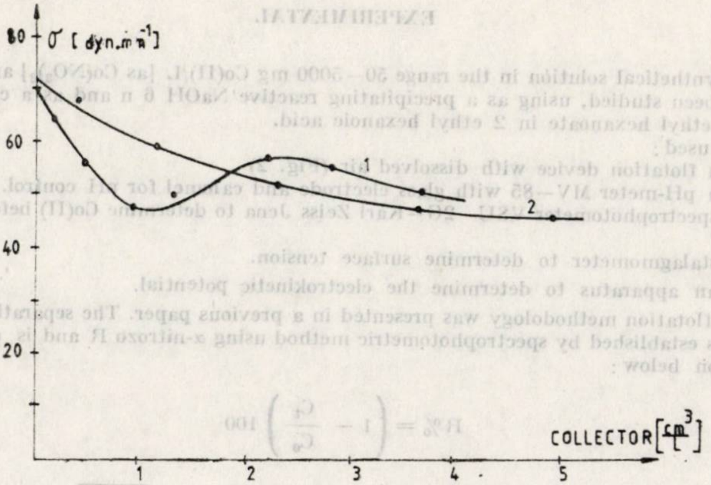

Fig. 3. — Surface tension determination ; System I — 2 — ethyl sodium hexanoate — water (curve 1) ; System II — 2 — ethyl sodium hexanoate in 2 — ethyl hexanoic acid (curve 2).

In order to obtain additional information concerning the influence of system II on the insoluble species of Co(II) at pH > 8, electrokinetic potential determinations have been carried out by macroelectrophoresis (Fig. 4.).

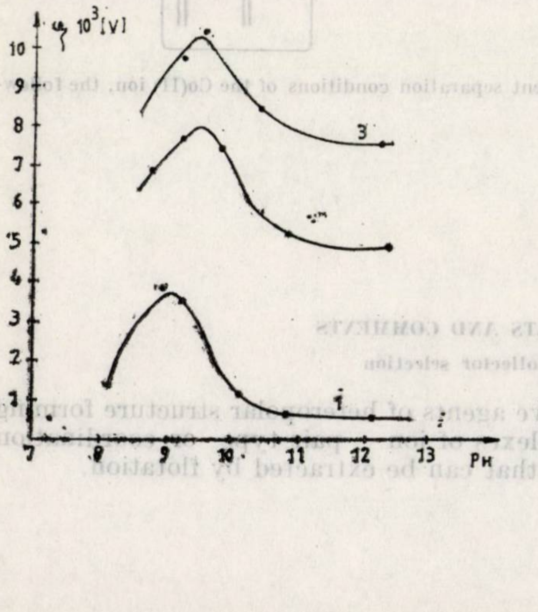

Fig. 4. — Electrokinetic potential determination : 1 — Auxiliary liquid — distilled water ; 2 — Auxiliary liquid — waste water + collector ; 3 — Filtered auxilliary liquid without collector.

A decrease electrokinetic potential of the insoluble species in the presence of system II to values lower than 5 mV, recommends system II as a collector reactor to separate cobalt insoluble species by flotation.

Flotation optimum pH

As illustrated in literature, the pH range in flotation separation of precipitates is the optimum in the range of complete insoluble species precipitation.[6-8]

For the concentration range 50—5000 mg Co(II)/L the optimum flotation pH of the hydroxo species formed in the presence of NaOH as a precipitating reactive and of 2 ethyl sodium hexanoate in acid —2 ethyl hexanoic as collector, ranges between 8.5—9.5 (Table 1).

Table 1

Establishment of the optimum pH flotation (Co = 500 mg/L)

Precipitant reactive		Collector		PH flotation	Sample after flotation		Volume foam after 10 min.	R %
cm/^{3}L	g/L	cm^3/V$_{pr}$	cm^3/L		pH after flotation	C_t mg/L	cm^3	
76	1.8	0.5	1.6	8	8.2	50	80	90
8	1.92	0.5	1.6	8.5	8.3	25	75	95
8,6	2.1	0.5	1.6	8.7	8.3	10	70	98
10	2.4	0.5	1.6	9.2	8.5	10	65	98
10,6	2.5	0.5	1.6	9.5	9	10	50	98
11	2.64	0.5	1.6	9.8	9.3	20	60	96

Although high efficiencies are obtained at pH > 9.5, exceeding this value is not economical.

Collector — colligend rates

Using a solution of Co(II) of 500 mg/L, the efficiency of flotation separation has been studied for various ratios collector Co(II).

The results are presented in Fig. 5.

The separation efficiency R $> 95\%$ at the molar ratio collector Co(II) is 0.15 (RCOONa) : 1.

Metallic ion concentration

To investigate the possibility of separating Co(II) by insoluble species flotation at the optimum pH at the best collector-colligend rates, experiments have been made on synthetic solutions of concentrations 50—5000 mg Co(II)/L.

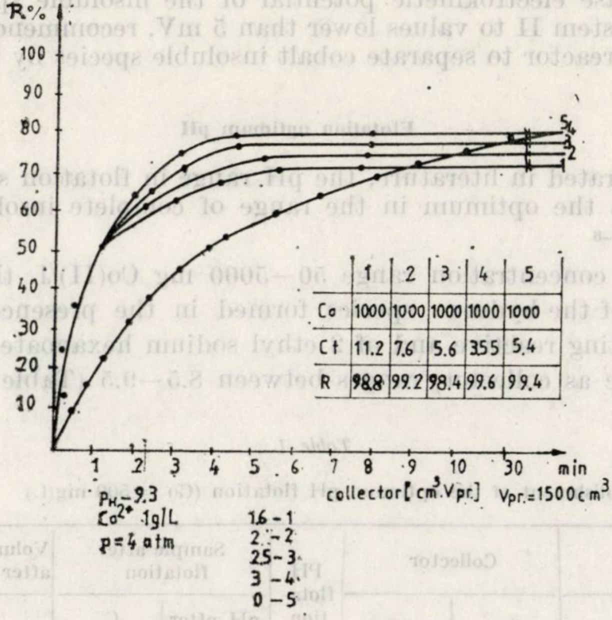

Fig. 5. — Collector — colligend rate determination.

The experimental results presented in Table 2 show that in order to maintain maximum separation efficiency at high concentration of Co(II), the ratio V : V pressurized water has to be considered; it must favour flotation and not sedimentation.

Table 2

Metallic ion concentration

Co mg/L	Precipitant reactive NaOH		Collector		pH flotation	Sample after flotation		R%
	cm^3/L	g/L	cm^3/V$_{pr}$	cm^3/L		after flotation	C$_t$ mg/L	
50	6.6	1.6	0.2	0.7	9.3	8.8	0.35	99.3
500	9.4	2.4	0.3	1	9.5	9	20	96
1000	11.4	2.74	0.5	1.7	9.2	9.3	20	98
3000	29.7	7.13	1.5	5	9.3	9	100	96.7
3000	36.3	8.7	30	7	9.3	9.1	125	95.8
5000	46.2	11	—	8.3	9.3	9.0	200	96

Necessary air

According to the Henry-Dalton law, a quantity of air proportional to the equilibrium pressure of air in contact with water can be dissolved in water, and the proportionality constant is dependent on temperature.[4]

The air quantity liberated at air saturated water expansion at pressure $p > 1$ atm. is equal, at the most, to the difference between the saturation concentrations at the two pressures.

To establish the necessary air for insoluble species flotation of Co(II) at the optimum pH and the optimum collector ratio : Co(II) the pressurizing time has been selected to obtain a working pressure ensuring separation maximum efficiency and a small volume of foam.

The experimental results are shown in Figs. 6 and 7.

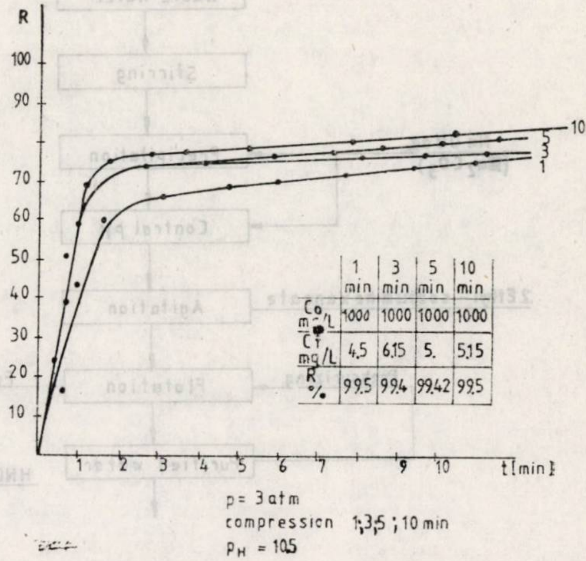

	1 min	3 min	5 min	10 min
Co mg/L	1000	1000	1000	1000
Cf mg/L	4.5	6.15	5.	5.15
R %	99.5	99.4	99.42	99.5

Fig. 6. — Optimum time of pressurizing air determination at $p = 4$ atm and pH = 10.5.

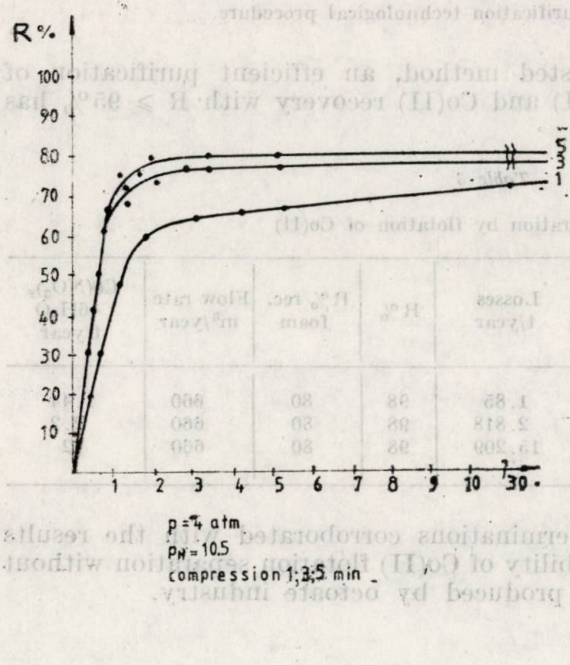

Fig. 7. — Optimum time of pressurizing air determination at $p = 3$ atm. and pH = 10.5.

Increasing the pressurizing time over 3 minutes does not determine essential improvement of the separation efficiency value.

On the basis of the results obtained from the study on synthetic solutions, and on waste waters, a recovery technological procedure has been suggested to recover Co(II)existing in waste waters as $Co(NO_3)_2$ aq. (Fig. 8).

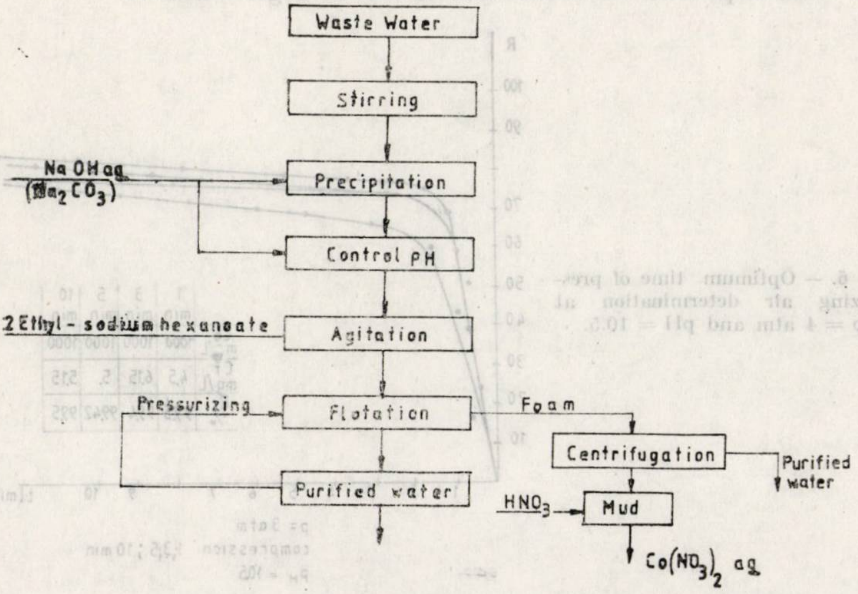
Waste Water
Stirring
Na OH aq
(Na_2CO_3)
Precipitation
Control pH
2 Ethyl - sodium hexanoate
Agitation
Pressurizing
Flotation
Foam
Centrifugation
Purified water
HNO_3
Mud
Purified water
$Co(NO_3)_2$ aq

Fig. 8. — Flotation purification technological procedure.

By applying the suggested method, an efficient purification of waste waters containing Co(II) and Co(II) recovery with R ⩾ 95% has been obtained (Table 3).

Table 3

Efficiency separation by flotation of Co(II)

Sample	Caracteristics			Losses t/year	R %	R % rec. foam	Flow rate m^3/year	$Co(NO_3)_2 \cdot 6H_2O$ t/year
	pH	C_0 mg/L	dyn. cm^{-1}					
1	7.1	500	71	1.85	98	80	660	1.44
2	7	1100	67.6	2.818	98	80	660	2.2
3	6.8	4120	56.1	15.209	98	80	660	12

The surface tension determinations corroborated with the results given in Fig. 2 show the possibility of Co(II) flotation separation without collector, from waste waters produced by octoate industry.

REFERENCES

[1] R. Lemlich, "Adsorptive Bubble Separation Techniques", Academic Press, New York—London, 1972.

[2] R. Lewandowschi, Cebedeau—Becerwa no. 407, p. 321—323, 1977.

[3] F. Sebba, "Ion Flotation", Elsevier, Amsterdam, New York, London 1963.

[4] Ian Leja, "Surface Chemistry of Froth Flotation", Interscience New York, 1983.

[5] J. Melloitte, *J. Colloid Interface Sci.*, **57**, 94 (1976).

[6] E. J. Mahne, A. T. Pinfold, *Chemistry and industry*, **253**, (1966).

[7] R. E. Baarson and C. L. Ray, "Hydrometallurgy", Gordon and Breach Sci. Publ., New York London 1964.

[8] I. Pushcarev, *J. Prikl. Him.*, **33**, 81 (1966).

Revue Roumaine de Chimie, 35, *1*, 41–48 (1990)

ON THERMAL DECOMPOSITION OF DOLOMITE

CORNELIA LEONTE, AL. SZÉP, N. BÎLBĂ, C. CALISTRU, LIVIA IFRIM
and GH. MIHĂILĂ
Department of Chemical Technology, Polytechnic Institute,
Splai Bahlui 71, Iaşi, Romania

Received June 25, 1988
Revised December 1988

The present paper deals with a study on the dolomite thermal decomposition in order to elaborate the macrokinetic mechanism of the process. The experiments were carried out using both big and micronic granules. The dolomite granules with 20 — 60 mm in diameter were decomposed under isothermal conditions and the micronic ones by thermal differential analysis technique. Composition of the solid reaction products were determined by both X-ray diffraction and chemical analysis. Depending on the ratio between heat transfer and heat consumption rates, three macrokinetical mechanisms have been found.

INTRODUCTION

Obtention of dolomite lime with such a quality to satisfy the requirements of the magnesium compounds manufacture with rational material and energetical consumptions, requires firstly a chemical engineering investigation of the dolomite thermal decomposition process. This investigation establishes the mechanism of transformation, mass and heat transfer, whose basis, the macrokinetical mechanism can be elaborated and, therefore, the parameters controlling the rate of the industrial process.[1]

The literature [2–5] reports certain aspects on thermal decomposition of the ground dolomite, carried out by thermal analysis, that allowed to find the temperature ranges in which the thermal decomposition takes place and the influence of crystallinity and impurities of raw dolomite on these ranges. Also, a series of kinetical equations for the real process description are reported.[6–9] Taking into account these data and performing the investigation in a larger temperature range, with several granule size from different dolomite deposits, we obtained enough data to elaborate the possible macrokinetic mechanisms of the dolomite thermal decomposition. The dolomite samples with the granule size ranging from 0.1 to 60 mm have been decomposed in both isothermal and nonisothermal regime in the temperature range of 373–1323 K at different heating rates.

EXPERIMENTAL

The behaviour of the raw dolomite samples, under heating, was investigated by two groups of experiments. In the first group, the study had in view the behaviour of four varieties of fine ground raw dolomite, $0.1 < d < 0.5$ mm, under variable heat supply, using the differential thermal analysis (DTA) technique. In the second group, the decomposition of the dolomite samples, shaped in spherical granules, $20 < d < 60$ mm, dried and weighted beforehand, entered, on special supports, in an electric muffle furnace, close by the thermocouple, so that the heat supply to be uniformly realized on the entire outer surface of the granule. After certain periods of time, the samples were taken out, cooled in an inert atmosphere and weighted again, followed by their division into parallel sections. From the distinct zones of the sections obtained, small amounts of solid were taken out, ground and analysed by X-ray diffraction in order to determine the content of magnesium oxide and calcium oxide, using raw dolomite and pure carbonates as reference material.

RESULTS AND DISCUSSION

The DTA data for different varieties of raw dolomite are in good agreement with the data reported in literature, making more clearly that the thermal decomposition of dolomite takes place in two steps, namely

$$CaMg(CO_3)_2 \rightleftharpoons CaCO_3 + MgO + CO_2 \qquad (1)$$

$$CaCO_3 \rightleftharpoons CaO + CO_2 \qquad (2)$$

The thermograms presented in figure 1 point out the fact that, depending on the heating rate and granule size, the two processes can be superimposed, so that reaction (2) starts before the end of reaction (1). In the case of big granules of dolomite, the loss in weight is practically

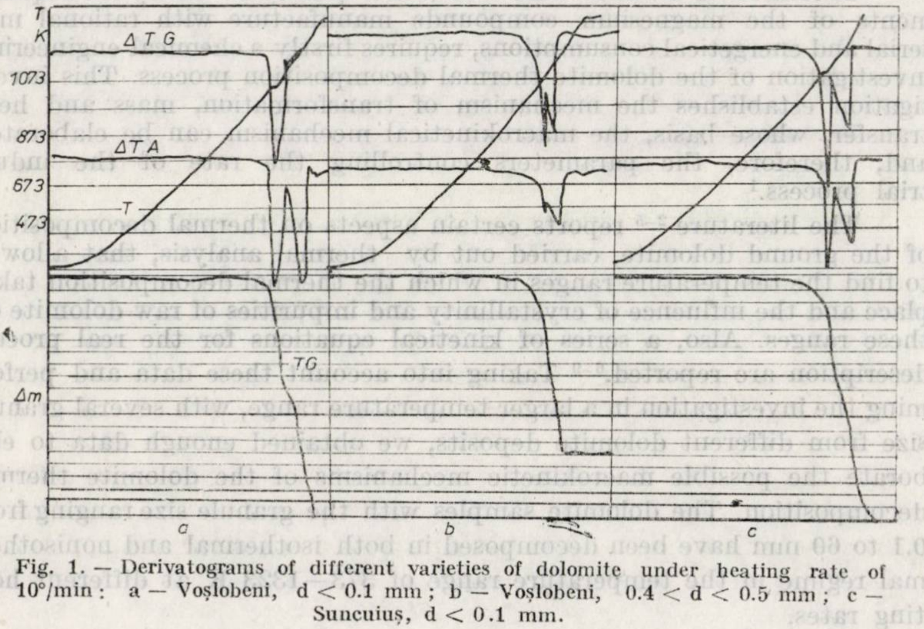

Fig. 1. — Derivatograms of different varieties of dolomite under heating rate of 10°/min: a — Voşlobeni, $d < 0.1$ mm; b — Voşlobeni, $0.4 < d < 0.5$ mm; c — Suncuiuş, $d < 0.1$ mm.

continuous and, in the case of small ones, it is not. Also, it can be seen that the temperature of decomposition beginning, as well as the temperatures corresponding to the maximum rates of reactions (1) and (2) do modify with the nature of the initial dolomite investigated, being specific for each dolomite variety. This conclusion is well proved by the data summarized in table 1, proper for several varieties of dolomite in Romania.

Table 1

Dissociation temperature of the investigated dolomites

Dolomite of :	Temperature, K		
	Beginning	Maximum rate of the step :	
		(1)	(2)
Voșlobeni	898	1073	1201
	898	1073	1218
	903	1080	1193
	863	1080	1091
	843	1083	1193
Buru	763	1080	1177
Suncuiuș	903	1003	1093
Bratca	773	1086	1185

Based on the thermograms shape, two possible decomposition mechanisms have been elaborated (Fig. 2 and Fig. 3). The mechanisms were presented as a form of succession of the mass transfer and mass transformation as well as a succession of the heat transfer and heat consumption, according to the two steps of the entire process. Thus, for low heating rates, the macroscopic processes succeed to each other, rigorously in time, as can be seen in figure 2 and, for high heating rates, the two processes are partially superimposed, as can be seen in figure 3.

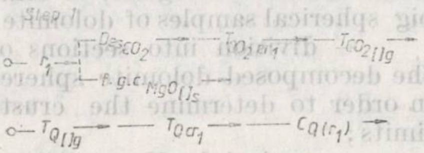
Step 1
r_1
Des_{CO_2}
$T_{CO_2 cr_1}$
$T_{CO_2[]g}$
f. g. c. $MgO_{[]s}$
$T_{Q[]g}$
T_{Qcr_1}
$C_{Q(r_1)}$
Step 2
r_2
Des_{CO_2}
$T_{CO_2 cr_2}$
$T_{CO_2[]g}$
f g c $CaO_{[]s}$
$T_{Q[]g}$
$T_{Q cr_2}$
$C_{Q(r_2)}$

Fig. 2. — The structure of mass and heat processes for small granules under slow heating.

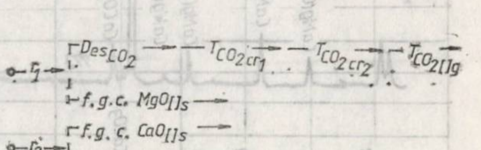
r_1
Des_{CO_2}
$T_{CO_2 cr_1}$
$T_{CO_2 cr_2}$
$T_{CO_2[]g}$
f. g. c. $MgO_{[]s}$
f. g. c. $CaO_{[]s}$
r_2
Des_{CO_2}
$T_{CO_2 cr_2}$
$T_{CO_2[]g}$
$T_{Q[]g}$
T_{Qcr_2}
$C_{Q(r_2)}$
v_1
$T_{Q cr_1}$
$C_{Q(r_1)}$
v_2

Fig. 3. — The structure of mass and heat processes for big granules under fast heating.

Depending on the ratio between the heat transfer and heat consumption rates, the specific decomposition mechanisms can be established. Thus, if V_1 is the rate of heat consumption due to the reaction (2) and V_2 is the heat transfer rate through crust 1 and heat consumption due to the reaction (1), figure 3, three distinct cases can be evidenced.

If $V_1 \gg V_2$, i.e. for temperatures much higher than the $CaCO_3$ dissociation one, the two processes are superimposed and the thermal decomposition takes place according to the reactions reported by Baikov [1], namely

$$nCaMg(CO_3)_2 = nCaCO_3yMgCO_3 + (n-y)MgO + (n-y)CO_2 \qquad (3)$$

$$nCaCO_3yMgCO_3 = nCaO + yMgO + (n+y)CO_2 \qquad (4)$$

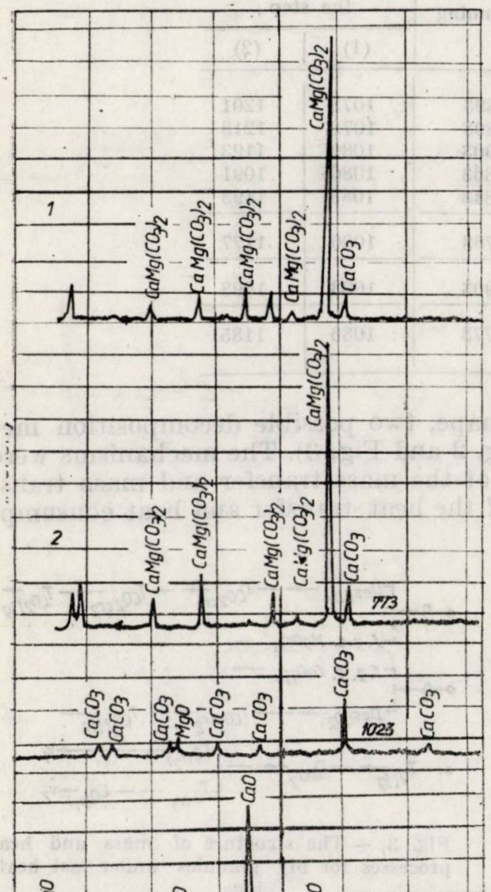

Fig. 4. — X-ray diffraction patterns of dolomite granules with d=20 mm, calcined at different temperatures in comparison with the uncalcined one : 1 — uncalcined ; 2 — calcined at 773, 1023 and 1323 K.

If $V_1 \simeq V_2$, the process develops according to the mechanism presented in figure 3, appearing two crusts, the crust 1 made up of magnesium oxide and calcium carbonate, $[CaCO_3+MgO+A'']_{cr.1}$ and the crust 2 made up of dolomite lime, $[CaO + MgO + A'']_{cr.2}$.

If $V_1 \ll V_2$, reaction (2) does not take place practically, the crust 2 disappears and the mechanism is that presented in figure 2, step 1.

To verify the macrokinetical mechanisms mentioned above, the following experiments have been carried out :

— thermal decomposition, under isothermal regime, of some big spherical samples of dolomite ;

— division into sections of the decomposed dolomite spheres in order to determine the crusts limits ;

— analysis by X-ray diffraction of the solid zones evidenced.

The X-ray diffraction patterns of the dolomite granules with 20 mm in diameter, uncalcined and calcined for three hours at 773, 1023 and 1323 are set out in figure 4. As shown in figure 4, the dolomite calcined at 1023 K contains in the whole volume only MgO and $CaCO_3$ and that calcined at 1323 K contains only MgO and CaO, i.e. the products of reactions (1) and (2).

To evidence the two distinct crusts in the case of heat transfer rate that does not ensure the temperature necessary to the calcium carbonate decomposition, spherical granules of dolomite with 50 mm in diameter, have been calcined at 1073 K for 25 minutes, followed by X-ray diffraction analysis of the outer zone and of the unreacted core. The diffraction patterns are represented in figure 5. As it can be seen in figure 5, the two zones differ from one another by composition : the outer zone, crust 1, contains MgO and $CaCO_3$ and only traces of undecomposed dolomite, while the core contains only undecomposed dolomite.

Further on, the dolomite granules with 60 mm in diameter have been calcined at 1323 K for 45 minutes. After their division into sections, three zones, visible with even naked eyes, can be seen. The X-ray diffraction patterns of the three zones are set out in figure 6. The outer zone, crust 2, is made up of $CaCO_3$, the intermediate zone, crust 1, contains MgO, $CaCO_3$ and only traces of CaO, and the granule core contains mainly undecomposed dolomite and the reaction (1) products, i.e. MgO and $CaCO_3$.

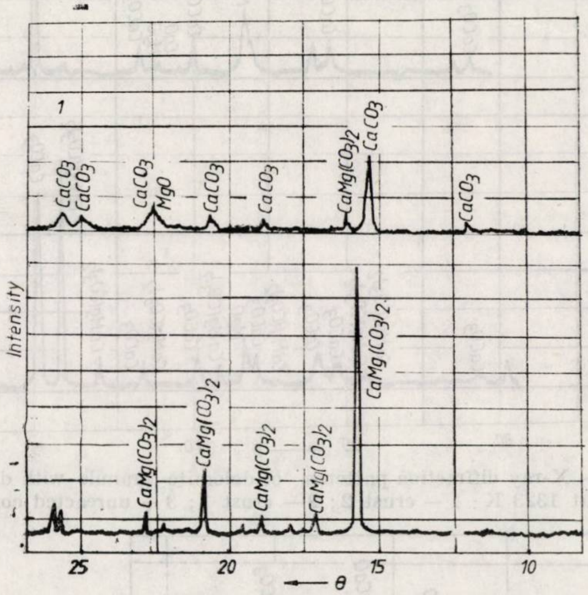

Fig. 5. — X-ray diffraction pattern of calcined dolomite granule with d = 50 mm at 1073 K : 1 — crust 1 ; 2 — unreacted core.

Coexistence of $CaCO_3$, MgO and CaO in the outer zone, crust 2, as well as of MgO and $CaCO_3$ in core, pointed out by X-ray diffraction patterns in figure 7, shows that the decomposition does not take place strictly on a surface, as some authors reported,[5] but in a relatively narrow zone.

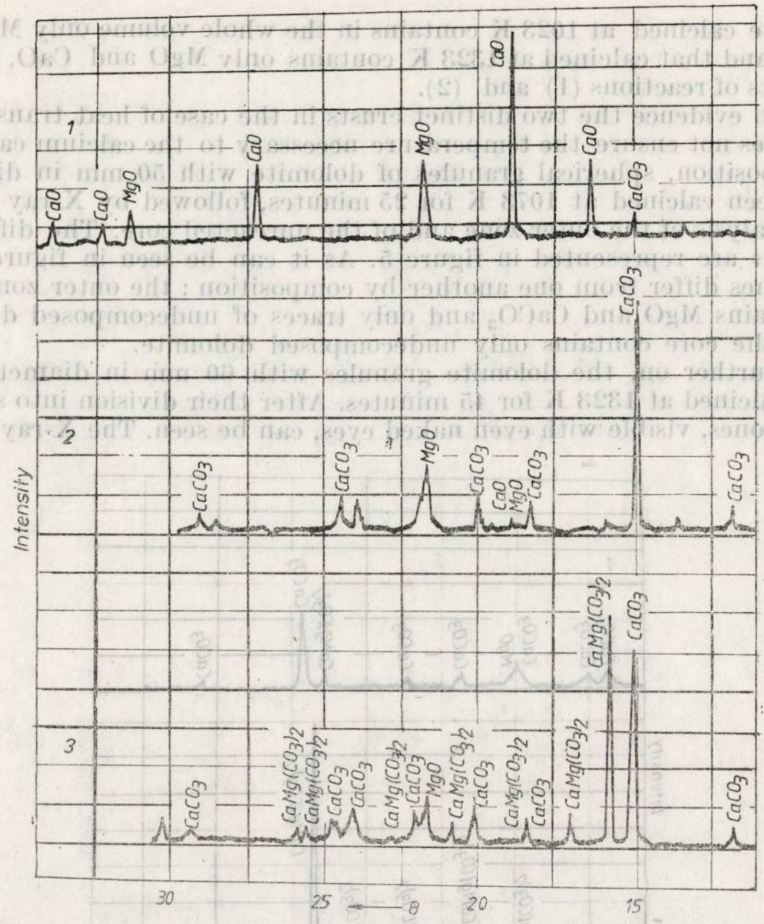

Fig. 6. — X-ray diffraction patterns of dolomite granule with d = 60 mm at 1323 K : 1 — crust 2 ; 2 — crust 1 ; 3 — unreacted core.

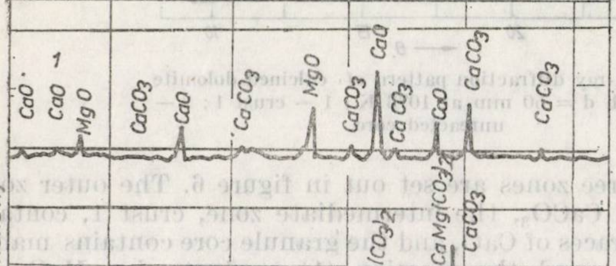

Fig. 7. — X-ray diffraction patterns of calcined high crystallinity granule with d = 40 mm at 1173 K for 25 minutes : 1 — crust ; 2 — unreacted core.

The three zones, namely crust 2, crust 1 and core were evidenced also by hydration of the semispheres obtained by division into sections of the calcined dolomite granules. After hydration, in the sectioned granules appeared two concentric cracks that mark the limits between the crust 2, crust 1 and core. Based on these determinations, two ideal models of decomposition, set out in figure 8, were elaborated, models in good agreement with the macrokinetic mechanism of the process. In the first case, there appear only two zones, figure 8.a. and, in the second one, there appear three zones, figure 8.b.

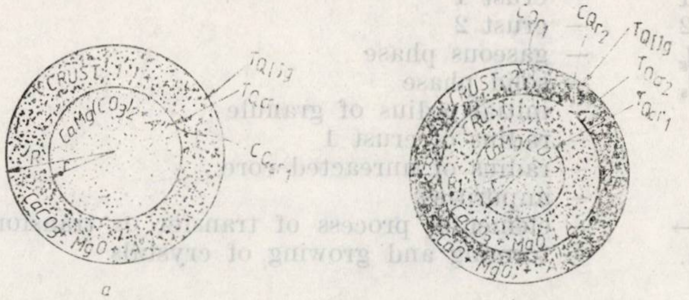

Fig. 8.—Geometrical model of the dolomite granule under calcination at $T_{[\ ]g} < T_{\mathrm{dis \cdot CaCO_3}}$ (a) and $T_{[\ ]g} > T_{\mathrm{dis \cdot CaCO_3}}$ (b)

CONCLUSIONS

From the experimental results presented above, the following conclusions may be drawn:

1. Investigation of the thermal decomposition of several dolomite varieties in both big and micronic granules, under isothermal and non-isothermal conditions, allowed to find the proper macrokinetical mechanisms of the process, depending on the ratio between heat transfer and heat consumption rates.

2. At lower temperatures, $T_{[\ ]g} < T_{\mathrm{dis \cdot CaCO_3}}$, the thermal decomposition of dolomite takes place according to the mechanism presented in figure 2 and geometrical model 8.a.

3. At higher temperatures, $T_{[\ ]g} > T_{\mathrm{dis \cdot CaCO_3}}$, and heat transfer rates comparable to heat consumption rates due to the reactions (1) and (2), the process is described by the mechanism presented in figure 3 and geometrical model 8.b.

4. The experiments carried out with dolomite granules, close in diameter to the industrially employed ones, are very useful for the macrokinetical description of the real dolomite decomposition process.

NOMENCLATURE

$r_{1,2}$ — chemical reaction (1) or (2)
Des — desorption
T_{CO_2}, T_Q — CO_2 transfer or heat transfer
$C_{Q(r_{1,2})}$ — heat consumption in the reaction (1) and (2)
cr. 1 — crust 1
cr. 2 — crust 2
$[\ ]_g$ — gaseous phase
$[\ ]_s$ — solid phase
R — initial radius of granule
R_2 — radius of crust 1
r — radius of unreacted core
A″ — impurities
— → — elemental process of transfer or transformation
f.g.c. — forming and growing of crystals

REFERENCES

[1] C. Calistru and C. Leonte, "Tehnologia substanţelor anorganice", Ed. didactică şi pedagogică Bucharest, 1972.
[2] S. T. Rostovtiev, "Teoria proceselor metalurgice", Ed. tehnică, Bucharest, 1959, p. 61.
[3] E. K. Beliaiev, V. M. Pomenko and E. M. Panasenko, *Vopr. Khim. i Khim. Technol.*, **53**, 91 (1978).
[4] I. Paulik, F. Paulik and E. Wiczarek, *Termochimica Acta*, **38**, 165 (1980).
[5] * * * *Zement Kalk Gips*, **32**, 390 (1979).
[6] A. Pop, Doctoral Thesis, "Gh. Asachi" Polytechnic Institute, Iaşi, 1983.
[7] V. H. Gropianov, B. A. Soboleva and E. A. Cachonova, *Phosphornaya Prom.-st*, **1978**, no. 6, 52 *(Chem. Abstr.*, **91**, 1979, 7049 k).
[8] M. Hints, *Rev. Chim. (Bucureşti)*, **29**, 84 (1979).
[9] C. Leonte, Al. Szép, C. Calistru and L. Ifrim, *Rev. Chim. (Bucureşti)*, **34**, 894 (1983).

Revue Roumaine de Chimie, 35, *1*, 49–54 (1990)

OPTIMIZATION OF THE MOBILE PHASE IN THIN LAYER CHROMATOGRAPHY FOR THE SEPARATION OF 4-BENZYLIDENE-1-PYRIMIDYL-5-PYRAZOLONE DYES

S. GOCAN *, LILIANA OLENIC and I. CRISTEA
Chemistry Department, University of Cluj-Napoca, 3400 Cluj-Napoca, Romania

Received November 21, 1988

Using a method based on the classification of solvents into eight groups according to their specific interactions, we succeeded in finding, by a small number of experiments, several optimum eluent systems for the separation of some 4-benzylidene-1-pyrimidyl-5-pyrazolone synthetic dyes.

INTRODUCTION

In order to achieve a successful chromatographic separation, a series of factors should be considered, among which the most important one is the choice of the stationary and the mobile phase according to the nature of the components to be separated.

The selection of the stationary phase is less complicated because the number of such phases is more reduced. By establishing the elementary separation mechanism, a decision taken in direct correlation with the components nature, a restriction of some adsorbent types has been made. In order to give accurate results, reproducible in other laboratories, a characterization of the adsorbent within the thin layer, from the point of view of its adsorption properties, namely the level of activity of the silica gel thin layer α and $p = V_a W / V_M$ is necessary. Here V_a is the volume of the mobile adsorbed phase in the monomolecular layer per mass unit of the adsorbent and W/V_M is the ratio between the adsorbent and the mobile phase.[1]

In choosing the mobile phase we have considered Snyder's [2,3] papers where the solvents are classified into eight groups according to the interactions which they can produce. Generally speaking, in the selection of binary and ternary systems, it is advisable to choose the solvent from different groups so that the interactions can be various, a better selectivity being thus achieved. Experimentally, Nyiredy et al.[4–7] have arrived at a system of selection of the solvents known as the "Prisma" model.

---

* To whom correspondence should be addressed

One can moderate polarities with hexane or petroleum ether whose strength P' is considered zero. As to mixtures of solvents, the strength is calculated from the sum of the strengths of the solvents multiplied by the corresponding volume fraction.[2,3]

The separations were evaluated according to a criterion suggested by Gocan and Liteanu.[8]

EXPERIMENTAL

Chromatographic thin layer silica gel plates produced by the Chemistry Institute in Cluj-Napoca were used. The solvents were produced by "Reactivul" Bucharest.

The developments were carried out in saturated chromatographic chambers. The samples to be analysed were a series of synthetic dyes (4-benzylidene-1-pyrimidyl-5-pyrazolones)[9] dissolved in chloroform. The values ($\alpha = 0.53$ and $p = -1.62$) were determined with test dyes (*p*-aminoazobenzene, Sudan red and Sudan yellow) using benzene as eluent.[10]

RESULTS AND CONCLUSIONS

In order to find some eluents which could give best selectivities in the separation by thin layer chromatography of the 4-benzylidene-1-pyrimidyl-5-pyrazolone dyes, several solvents from different groups were chosen. The results obtained with these solvents are given in Table 1 and

Table 1

The hR_f and I_p values of some 4-benzylidene-1-pyrimidyl-5-pyrazolone synthesis dyes versus those of the eluent strength

Eluent	P'	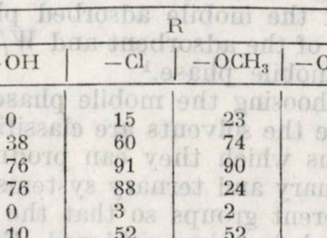				I_p
		R				
		$-OH$	$-Cl$	$-OCH_3$	$-OC_2H_5$	
Ethyl ether (I)	2.8	0	15	23	28	13.2
Isopropanol (II)	3.9	38	60	74	78	5.6
THF (III)	4.0	76	91	90	92	14.2
Acetic acid (IV)	6.0	76	88	24	48	3.3
Methylene chloride (V)	3.1	0	3	2	3	19.1
Ethyl acetate (VI)	4.4	10	52	52	64	8.1
Methyl ethyl ketone (VI)	4.7	48	88	88	91	10.1
Dioxane (VI)	4.8	77	95	95	95	13.7
Acetone (VI)	5.1	68	89	88	88	12.5
Benzene (VII)	2.7	0	0	0	0	20.0
Chloroform (VIII)	4.1	0	5	2	2	18.7

Table 4. The Roman figures point to the group to which they belong while P' stands for the solvent strength. The solvents with the best selectivities were thus chosen. Then, with these solvents we formed a number of binary, ternary and quaternary eluent systems. The results are given in Tables 2, 3, 5 and 6.

Table 2

The hR_f and I_p values of some 4-benzylidene-1-pyrimidyl-5-pyrazolone synthetic dyes versus those of the eluent strength for the binary eluent systems

Eluent	P'	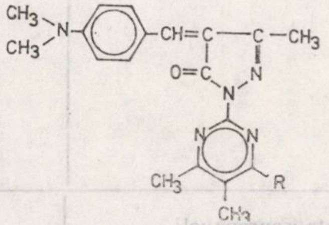 R				I_p
		$-$OH	$-$Cl	$-$OCH$_3$	$-$OC$_2$H$_5$	
Ethyl acetate/ acetic acid (9 :1)	4.6	35	78	66	73	6.1
Ethyl acetate/isopropanol (9 :1)	4.4	23	68	70	78	7.4
Ethyl acetate/isobutanol (3 :7)	4.3	37	76	82	85	7.6
(5 :5)	4.2	37	68	76	81	6.2
THF/petroleum ether (9 :1)	3.6	59	85	86	90	10.6
(8 :2)	3.2	59	86	84	90	10.5
(7 :3)	2.8	39	78	72	82	7.0
(6 :4)	2.4	20	64	66	73	6.1
(5 :5)	2.0	7	40	44	53	8.5
Isopropanol/ethyl ether (2 :8)	3.0	4	73	83	84	12.5
(1.5 :8.5)	2.8	0	56	71	74	10.0
(1 :9)	2.9	0	62	74	78	11.2
(0.5 :9.5)	2.8	0	50	63	68	9.3

Analysing the results from Tables 1—3 we came to the conclusion that the best results were obtained with the following solvents : acetic acid ($I_p = 3.3$), isopropanol ($I_p = 5.6$) and ethyl acetate ($I_p = 8.1$) (Table 1). From these results we chose the solvents with the best selectivities and we formed with them a number of binary eluent systems. The results are given in table 2. The same very good results were obtained with ternary and quaternary eluent systems and they are given in Table 3.

Table 3

The hR_f and I_p values of some 4-benzylidene-1-pyrimidyl-5-pyrazolone synthetic dyes versus those of the eluent strength for the ternary and quaternary eluent systems

Eluent		P'	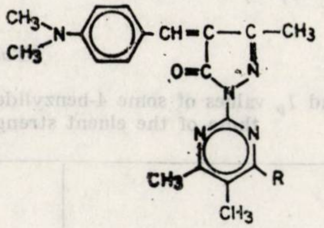				I_p
			R				
			$-OH$	$-Cl$	$-OCH_3$	$-OC_2H_5$	
Ethyl acetate/isopropanol/ethyl ether	(1 : 1 : 1)	3.7	41	80	85	89	8.3
	(8 : 1 : 1)	4.2	22	77	78	79	9.9
	(1 : 8 : 1)	3.8	32	73	82	83	7.3
	(1 : 1 : 8)	3.1	4	60	81	82	9.8
	(6 : 2 : 2)	4.0	36	81	83	87	8.8
	(2 : 6 : 2)	3.8	39	75	81	83	7.6
	(2 : 2 : 6)	3.3	32	84	90	92	9.6
Acetic acid/isopropanol/ethyl acetate	(1 : 1 : 1)	4.7	64	85	66	72	10.4
	(8 : 1 : 1)	5.6	73	88	36	47	15.8
	(1 : 8 : 1)	4.2	48	77	78	81	8.7
	(1 : 1 : 8)	4.5	39	88	68	74	7.4
Acetic acid/isopropanol/ethyl acetate/petroleum ether	(1.66 : 1.66 : 1.66 : 5)	2.4	19	74	18	31	7.1
	(4 : 0.5 : 0.5 : 5)	2.8	43	86	0	7	8.3
	(0.5 : 4 : 0.5 : 5)	2.1	16	69	72	81	8.7
	(0.5 : 0.5 : 4 : 5)	2.3	0	40	24	37	10.9

Following the same method we tried the separation of another number of dyes and the results are given in Tables 4—6.

To conclude, we succeeded with this method in rather a short time and by a small number of experiments in obtaining some eluent systems which were suitable for the study of the chromatographic behaviour of some 4-benzylidene-1-pyrimidyl-5-pyrazolone synthetic dyes. The thin layer chromatography is a very suitable method for the study of the separation and the characterization of the purity of the dyes and offers a large amount of information. Using this method we found some eluent mixtures which have a good selectivity within this class of dyes.

Table 4

The hR_f and I_p values of some 4-benzylidene-1-pyrimidyl-5-pyrazolone synthetic dyes versus those of the eluent strength

Eluent		P′	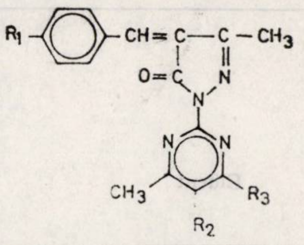				I_p
			R_1 R_2 R_3	$\mathrm{Me_2N}$— H— HO—	$\mathrm{Me_2N}$— $\mathrm{H_3C}$— HO—	$\mathrm{H_3CO}$— $\mathrm{H_3C}$— HO—	
Ethyl ether	(I)	2.8		0	0	0	25
Isopropanol	(II)	3.9		20	38	28	12.6
THF	(III)	4.0		65	76	84	13.4
Acetic acid	(IV)	6.0		63	76	85	12.7
Methylene chloride	(V)	3.1		0	0	0	25
Ethyl acetate	(VI)	4.4		5	10	20	18.8
Methyl ethyl ketone	(VI)	4.7		42	48	64	8.4
Dioxane	(VI)	4.8		70	77	86	15.1
Acetone	(VI)	5.1		57	68	77	11.1
Benzene	(VII)	2.7		0	0	0	25
Chloroform	(VIII)	4.1		0	0	0	25

Table 5

The hR_f and I_p values of some 4-benzylidene-1-pyrimidyl-5-pyrazolone synthetic dyes versus those of the eluent strength for the binary eluent systems

Eluent		P′	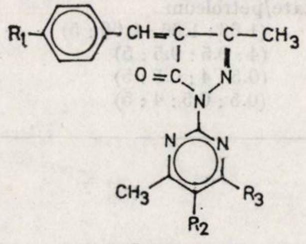				I_p
			R_1 R_2 R_3	$\mathrm{Me_2N}$— H— HO—	$\mathrm{Me_2N}$— $\mathrm{H_3C}$— HO—	$\mathrm{H_3CO}$— $\mathrm{H_3C}$— HO—	
THF/petroleum ether	(9 : 1)	3.6		44	59	71	7.3
	(9 : 2)	3.2		45	59	79	6.8
	(7 : 3)	2.8		34	39	61	7.7
	(6 : 4)	2.4		13	20	42	11.7
	(5 : 5)	2.0		4	7	10	21.7
Isopropanol/ethyl ether	(2 : 8)	3.0		2	4	0	23.7
Ethyl acetate/acetic acid	(9 : 1)	4.6		22	35	54	7.2
Ethyl acetate/isopropanol	(9 : 1)	4.4		15	23	38	12.4
Ethyl acetate/isobutanol	(3 : 7)	4.3		28	37	52	8.6
	(5 : 5)	4.2		24	37	50	8.7

Table 6

The hR_f and I_p values of some 4-benzylidene-1-pyrimidyl-5-pyrazolone synthetic dyes versus those of the eluent strength for the ternary and quaternary eluent systems

Eluent		P′	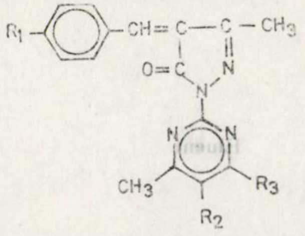				I_p
			R_1 R_2 R_3	Me_2N- $H-$ $HO-$	Me_2N- H_3C- $HO-$	H_3CO- H_3C- $HO-$	
Ethyl acetate/isopropanol/ ethyl ether	(1 : 1 : 1)	3.7		32	41	57	7.7
	(8 : 1 : 1)	4.2		23	22	45	11.2
	(1 : 8 : 1)	3.8		34	32	37	12.7
	(1 : 1 : 8)	3.1		3	4	14	24.3
	(6 : 2 : 2)	4.0		35	36	59	8.8
	(2 : 6 : 2)	3.8		40	39	58	9.6
	(2 : 2 : 6)	3.3		27	32	42	12.0
Acetic acid/isopropanol/ ethyl acetate	(1 : 1 : 1)	4.7		70	64	82	14.3
	(8 : 1 : 1)	5.6		77	73	87	16.8
	(1 : 8 : 1)	4.2		55	48	73	10 1
	(1 : 1 : 8)	4.5		43	39	70	8.2
Acetic acid/isopropanol/ ethyl acetate/petroleum ether	(1.66 : 1.66 : 1.66 : 5)	2.4		26	19	70	7.9
	(4 : 0.5 : 0.5 : 5)	2.8		43	43	85	9.6
	(0.5 : 4 : 0.5 : 5)	2.1		12	16	60	10.0
	(0.5 : 0.5 : 4 : 5)	2.3		0	0	26	17.4

REFERENCES

[1] L. R. Snyder, "Principles of Adsorption Chromatography", Marcel Dekker, New York, 1968.

[2] L. R. Snyder, *J. Chromatogr.*, **92**, 223 (1974).

[3] L. R. Snyder, *J. Chromatogr. Sci.*, **16**, 223 (1978).

[4] Sz. Nyiredy, B. Meier, C.A.J. Erdelmeier and O. Sticher, *J. High Resolut. Chromatogr. and Chromatogr. Commun.*, **8**, 186 (1985).

[5] Sz. Nyiredy, C.A.J. Erdelmeier, B. Meier and O. Sticher, in E. Tyihák (Editor), "Proceeding on TLC with Special Emphasis on OPLC", Labor MIM Company, Budapest, 1986, p. 222.

[6] Sz. Nyiredy, C.A.J. Erdelmeier, B. Meier and O. Sticher, *GIT Suppl. Chromatogr.*, **4**, 24 (1985).

[7] K. Dallenbach-Toelke, Sz. Nyiredy, B. Meier and O. Sticher, *J. Chromatogr.*, **365**, 63 (1986).

[8] S. Gocan and V. Liteanu, *Stud. Univ. Babeş-Bolyai, Chemia*, **33** (2) 82 (1988).

[9] G. Vernin, "La France et ses Parfums", No. 64, p. 205.

[10] I. Cristea, *Stud. Univ. Babeş-Bolyai, Chemia*, **33**, 2, 60 (1988).

Revue Roumaine de Chimie, 35, 1, 55–61 (1990)

BEHAVIOUR OF BENZOXAZINONE DERIVATIVES BEARING A BULKY GROUP AT POSITION-2 TOWARD SOME NITROGEN AND CARBON NUCLEOPHILES.

PART 2

S. EL-NAGDY, M. A. EL-HASHASH, A. A. AFIFY and F. EL-SHAHED

Chemistry Department, Faculty of Science, Ain Shams University,
Abbassia, Cairo, Egypt

Received August 28, 1987

A number of 2-(substituted)-4H-3,1-benzoxazin-4-ones (I*a-c*) were prepared by treatment of anthranilic acid with 2-phenyl-4-arylidene-5(4)-oxazolones. Treatment of 2-(benzamido-*p*-methoxystyryl)-4H-3,1-benzoxazin-4-one (I*a*) with NH_2OH, gave the 2-(substituted)-3-hydroxy-4-quinazolone (II). Acylation and/or benzoylation of II gave the corresponding 3N-(acetoxy or benzoxy)-4-quinazolone derivatives (III*a* and *b*). Compounds (I*a* or *b*) react with ethyl acetoacetate, ethyl cyanoacetate and/or diethyl malonate to yield the same product 2-(substituted)-3-carboxy (or carbethoxy)-1,4-quinolinones (IV*a* or *b*). Benzoxazone (I*c*) reacts with NaN_3 to yield 1-(2′-carboxy phenyl)-2-(α-*o*-chlorobenzamido-*p*-methoxystyryl) tetrazole (V). Benzoxazones (I*a* or *b*) react with Grignard reagents, namely, methylmagnesium iodide, benzylmagnesium chloride and/or α-naphthylmagnesium bromide to give the corresponding alkyl/or aryl-*o*-(α-benzamido substituted styryl) formamido-phenyl ketone (VI*a-e*). However, I*a* reacts under Friedel-Crafts conditions with indole, pyrazole and pyrazolone derivatives to afford the corresponding ketones (VII) and (VIII*a-d*). Compound I*a* undergoes Diels-Alder reaction with maleic anhydride or diethyl maleate to give the adducts (IX) and (X) respectively. Hydrolysis of X with alcoholic NaOH (10%) solution gave (IX), while the reaction of X with hydrazine hydrate and/or aniline gave the corresponding quinazolin-4-one derivatives (XI) and (XII) respectively.

It is noteworthy to mention here some reactions of the 2-(substituted)-4H-3,1-benzoxazin-4-ones (I*a-c*) bearing bulky substituents in position-2. Recently, it has been reported [1] that 2-substituted benzoxazones reacted with hydroxylamine hydrochloride in presence of pyridine to give 2-substituted-3-hydroxy-4-quinazolones. Similarly, the author investigated the reaction of $NH_2OH(HCl)$ with 2-(benzamido-*p*-methoxystyryl)-4H-3,1-benzoxazin-4-one (I*a*), in the presence of sodium acetate in boiling methanol to give 2-(substituted)-3-hydroxy-4-quinazolone (II).

The IR spectrum of II showed bands at 1685, 1650 cm^{-1} (quinazolone and amido $>$C=O), 3220 (amido NH) and 3450 cm^{-1} (OH group).

The acylation of 2-(substituted)-3-hydroxy-4-quinazolone (II) with excess of Ac_2O and/or PhCOCl, gave 2-(substituted)-3-acetoxy (or benzoxy) quinazolones (III*a* or *b*). Their infrared spectra exhibit bands characteristic for $>$C=O (ester) at 1740–1735, C=C and/or C=N at 1605–1595 cm^{-1} while lacked the bands correlated with OH group.

It has been also reported [2] that 2-phenyl-3,1-benzoxazone reacted with ethyl acetoacetate, ethyl cyanoacetate and diethyl malonate to give N-(*o*-ethoxycarbonyl acetyl phenyl) benzamide.

In the present investigation, it has been found that the reaction of I*a* or *b* with ethyl acetoacetate, ethyl cyanoacetate and/or diethyl malonate, yielded the same products, namely, 2-(substituted)-3-carboxy (or carbethoxy)-1,4-quinolinones derivatives (IV*a* or *b*) depending on the time factor of the reaction. These results could be explained by the opening of heterocyclic ring of benzoxazones (I*a* and *b*), with the carbanion of active methylene group, followed by ring closure accompanied by deacetylation or elimination of carbethoxy or cyano groups.

The structure of IV*a* was substantiated on the basis of analytical data (cf. Table 1) and IR spectrum which showed the bands correlated with ν_{CO} (ester and amido group) at 1762, 1647; ν_{NH} (amido) at 3230 $cm^{-}{}_{1}$, respectively. Compound IV*b* exhibits the stretching frequencies characteristic of carboxylic, amido and NH and/or OH groups at 1690, 1650, 3410—3260 cm^{-1} respectively.

Benzoxazone (I*c*) reacted with NaN_3 in boiling acetic acid to yield 1-(2′-carboxyphenyl)-2-(α-*o*-chlorobenzamido-*p*-methoxystyryl) tetrazole (V). The IR spectrum of (V) was shown to be consistent with the proposed structure exhibiting strong bands at 1690, 1650 (broad ν_{CO} of carboxylic and amido), 3400—3265 (ν_{OH} and/or ν_{NH}) and 1030 cm^{-2} attributable to tetrazole nucleus.

The ^1H-NMR spectrum of V (δ; $CDCl_3$/TFA) showed from low to high field the following signals at δ 6.8—7.8 (*m*, 13*H*, Ar-*H* and olefinic) and 3.85 (*s*, 3*H*, Ar-OCH_3) p.p.m.

It was previously stated [3] that 2-substituted-3,1-4H-benzoxazones reacted with Grignard reagents *via* normal addition with ring fission to give diaryl-*o*-(substituted amido) phenyl carbinol. In the present investigation, the authors extended these reactions to include the reaction of I*a* or *b* with methylmagnesium iodide, benzylmagnesium chloride and/or α-naphthylmagnesium bromide to give the corresponding *o*-amidophenyl alkyl (or aryl) ketones (VI*a-e*). The structures of VI were proved on the basis of their analytical data (cf. Table 1), and infrared spectra, which showed bands at 1670—1640 cm^{-1} (ν_{CO} of ketonic and amido group).

The $_1H$-NMR spectrum of VI*b* (δ; DMSO) showed signals at 10.15 (broad, protons of amide), 6.9—7.7 (*m*, 18*H*, Ar-*H*), 6.27 (*s*, 1*H*, olefinic), 3.75 (*s*, 2*H*, COCH_2-Ar) and 3.25 (*s*, 3*H*, —OCH_3), the ^1H-NMR spectrum of VI*a* (δ; $CDCl_3$ + TFA) showed signals at 6.8—7.8 (*m*, 1,4*H*, Ar-*H* and olefinici) 3.8 (*s*, 3*H*, Ar-COCH_3) and 2.9 (*s*, 3*H*, —OCH_3) p.p.m.

It was reported [3] that 2-substituted-4H-3,1-benzoxazones reacted with hydrocarbons in presence of anhydrous $AlCl_3$ under the Friedel-Crafts conditions to give 2-aryl(alkyl)imido-(substituted)-benzophenones. Now, the authors extended some of these reactions of 2-(benzamido-*p*-methoxystyryl)-4H-3,1-benzoxazin-4-one (I_a) with indole; 3,5-dimethyl pyrazole; 3-methyl-5-pyrazolone; 1-*p*-nitrophenyl-3-methyl-5-pyrazolone and/or 1-*p*-nitrophenyl-3,5-dimethyl pyrazole in the presence of anhydrous $AlCl_3$ and dry benzene under the Friedel-Crafts conditions and obtained the corresponding *o*-substituted phenyl-3-indolyl ketone (VII)

Table 1

Characterisation and physical data of compounds (II–XII)

Compound	M.P. °C colour	Solvent	Yield (%)	Molecular formula	Analysis % Found / Calcd C	H	N
II	233 yellow	M,	70	$C_{24}H_{19}N_3O_4$	69.3 69.73	4.8 4.60	10.5 10.16
III*a*	207 brown	A,	65	$C_{26}H_{21}N_3O_5$	68.1 68.57	4.2 4.61	8.9 9.23
III*b*	248 pale yellow	A,	65	$C_{31}H_{23}N_3O_5$	72.1 71.95	4.3 4.44	8.4 8.12
IV*a*	212 yellow	M,	70	$C_{28}H_{24}N_2O_5$	71.4 71.79	4.9 5.12	6.1 5.98
IV*b*	189 colourless	M,	75	$C_{25}H_{17}N_3O_6$	65.6 65.93	4.1 3.73	9.1 9.23
V	122 yellow	B,	65	$C_{24}H_{18}N_5O_4Cl$	60.3 60.56	3.9 3.78	14.2 14.72
VI*a*	200 pale yellow	B,	65	$C_{25}H_{22}N_2O_4$	72.8 72.4	5.4 5.3	6.3 6.76
VI*b*	161 colourless	B,	60	$C_{31}H_{26}N_2O_4$	76.1 75.91	5.6 5.30	6.1 5.71
VI*c*	187 yellow	B,	60	$C_{30}H_{23}N_3O_5$	71.1 71.28	4.2 4.55	8.1 8.31
VI*d*	122 decomp. 165 yellow	B,	55	$C_{34}H_{26}N_2O_4$	77.2 77.56	5.1 4.94	4.9 5.32
VI*e*	210 yellow	B,	55	$C_{33}H_{23}N_3O_5$	73.4 73.5	4.5 4.2	8.1 7.76
VII	>270 yellow	A,	70	$C_{32}H_{25}N_3O_4$	74.1 74.56	4.6 4.85	7.8 8.15
VIII*a*	249 yellow	A,	70	$C_{29}H_{26}N_4O_4$	69.9 70.4	4.9 5.2	10.8 11.3
VIII*b*	>270 pale yellow	A,	70	$C_{28}H_{24}N_4O_5$	68.1 67.74	4.6 4.83	11.4 11.29
VIII*c*	219 brown	A,	70	$C_{34}H_{27}N_5O_7$	66.0 66.12	4.7 4.37	10.9 11.34
VIII*d*	254 yellow	A,	75	$C_{35}H_{29}N_5O_6$	68.1 68.2	4.9 4.7	11.6 11.38
IX	250 yellow	B,	50	$C_{28}H_{24}N_2O_9$	63.15 62.8	4.51 4.7	5.26 5.6
X	237 brown	X,	50	$C_{32}H_{30}N_2O_8$	67.36 67.1	5.26 5.00	4.91 5.10
XI	>270 yellow	E,	60	$C_{28}H_{24}N_5O_4$	67.9 68.01	5.1 4.85	13.7 14.17
XII	>270 pale yellow	E,	60	$C_{40}H_{30}N_4O_5$	74.9 74.30	4.5 4.64	8.3 8.66

A = Acetic acid, B = Benzene, E = Ethanol, M = Methanol, X = Xylene

and/or *o*-substituted phenyl 4-(3,4-dihydro substituted) pyrazolyl ketones (VII*a-d*).

The structures of VII and VIII*a-d* were confirmed from their analytical data (cf. Table 1), and IR spectra which showed characteristic bands of $\rangle C=O$ (ketonic and pyrazolones groups at **1685–1660, 1695–1670** and (NH) at 3197–3240 cm^{-1}).

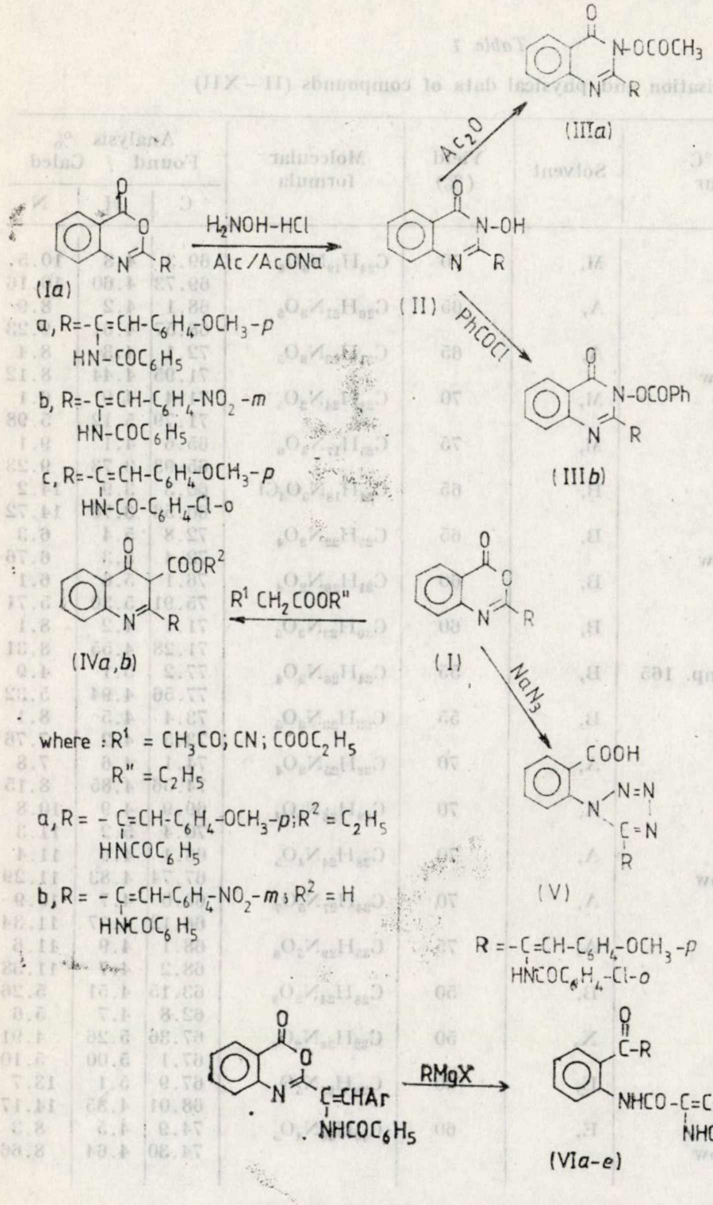
(IIIa)
N-OCOCH3
Ac2O
(Ia)
H2NOH-HCl
Alc/AcONa
N-OH
(II)
PhCOCl
N-OCOPh
(IIIb)
COOR2
R1 CH2COOR"
(IVa,b)
(I)
NaN3
COOH
N=N
C=N
(V)
RMgX
C=CHAr
NHCOC6H5
C-R
NHCO-C=CH-Ar
NHCOC6H5
(VIa-e)

a, R= $-\underset{\text{HN-COC}_6\text{H}_5}{\text{C}}=\text{CH-C}_6\text{H}_4\text{-OCH}_3\text{-}p$

b, R= $-\underset{\text{HN-COC}_6\text{H}_5}{\text{C}}=\text{CH-C}_6\text{H}_4\text{-NO}_2\text{-}m$

c, R= $-\underset{\text{HN-CO-C}_6\text{H}_4\text{-Cl-o}}{\text{C}}=\text{CH-C}_6\text{H}_4\text{-OCH}_3\text{-}p$

where : $R^1 = CH_3CO; CN; COOC_2H_5$

$R'' = C_2H_5$

a, R = $-\underset{\text{HNCOC}_6\text{H}_5}{\text{C}}=\text{CH-C}_6\text{H}_4\text{-OCH}_3\text{-}p$; $R^2 = C_2H_5$

b, R = $-\underset{\text{HNCOC}_6\text{H}_5}{\text{C}}=\text{CH-C}_6\text{H}_4\text{-NO}_2\text{-}m$; $R^2 = H$

R = $-\underset{\text{HNCOC}_6\text{H}_4\text{-Cl-}o}{\text{C}}=\text{CH-C}_6\text{H}_4\text{-OCH}_3\text{-}p$

where: R		Ar
a,	CH_3	C_6H_4-OCH_3-p
b,	$C_6H_5CH_2$	C_6H_4-OCH_3-p
c,	$C_6H_5CH_2$	C_6H_4-NO_2-m
d,	$C_{10}H_7$-1	C_6H_4-OCH_3-p
e,	$C_{10}H_7$-1	C_6H_4-NO_2-m

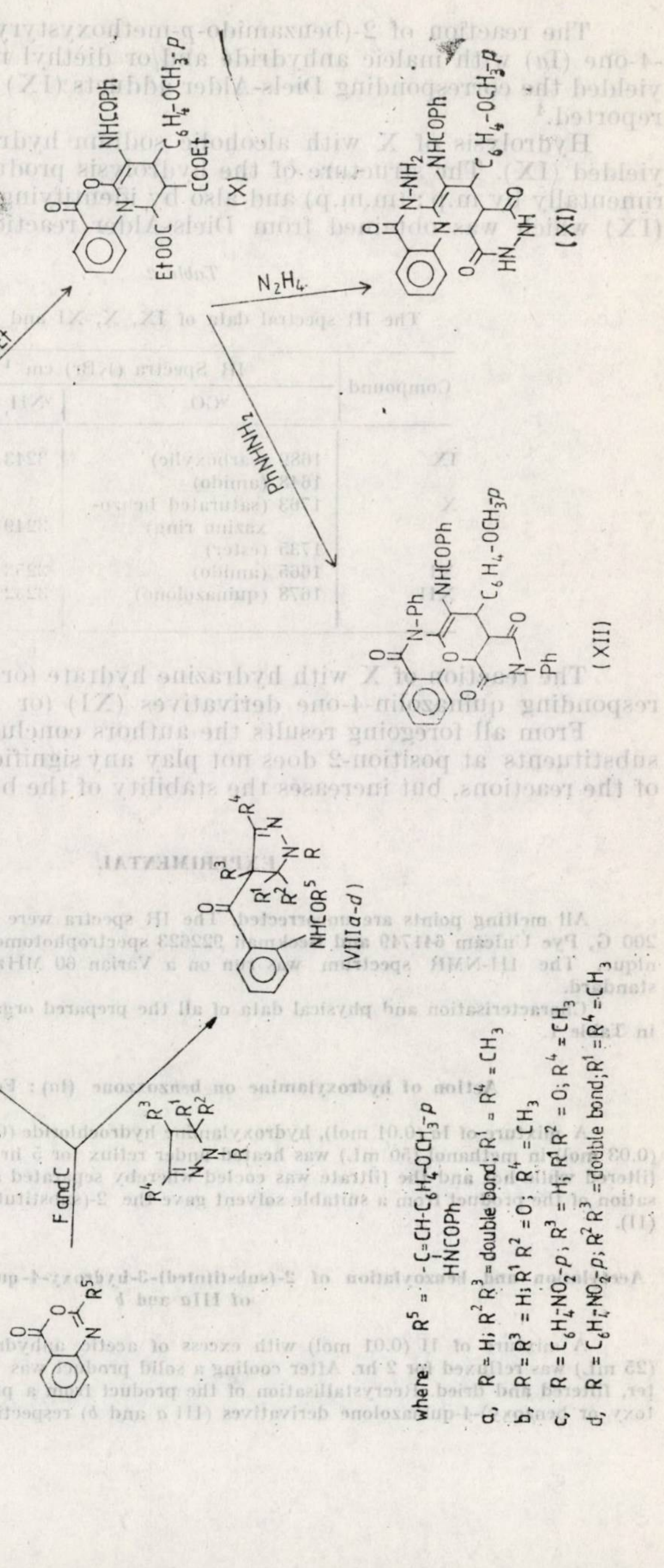
(IX)
(X)
(XI)
(XII)
(VII)
(VIIIa-d)
D and A
F and C
N_2H_4
PhNHNH$_2$
where: R^5 = -C=CH-C$_6$H$_4$-OCH$_3$-p, HNCOPh
a, R = H; R^2 R^3 = double bond R^1 = R^4 = CH$_3$
b, R = R^3 = H; R^1 R^2 = O; R^4 = CH$_3$
c, R = C$_6$H$_4$-NO$_2$-p; R^3 = H; R^1 R^2 = O; R^4 = CH$_3$
d, R = C$_6$H$_4$-NO$_2$-p; R^2 R^3 = double bond; R^1 = R^4 = CH$_3$

The reaction of 2-(benzamido-*p*-methoxystyryl)-4H-3,1-benzoxazin-4-one (I*a*) with maleic anhydride and/or diethyl maleate in dry xylene yielded the corresponding Diels-Alder adducts (IX) and (X) as previously reported.[4]

Hydrolysis of X with alcoholic sodium hydroxide (10%) solution yielded (IX). The structure of the hydrolysis product was verified experimentally by m.p; (m.m.p) and also by identifying its IR spectrum with (IX) which was obtained from Diels-Alder reaction.

Table 2

The IR spectral data of IX, X, XI and XII

Compound	IR Spectra (KBr) cm^{-1}		
	$^{\nu}CO$	$^{\nu}NH$	$^{\nu}OH$
IX	1689 (carboxylic) 1648 (amido)	3243	3314
X	1763 (saturated benzoxazino ring) 1735 (ester)	3249	
XI	1665 (amido)	3253	
XII	1678 (quinazolono)	3252	

The reaction of X with hydrazine hydrate (or aniline) gave the corresponding quinazolin-4-one derivatives (XI) (or XII).

From all foregoing results the authors concluded that the bulky of substituents at position-2 does not play any significant role in the course of the reactions, but increases the stability of the benzoxazinone nucleus.

EXPERIMENTAL

All melting points are uncorrected. The IR spectra were measured on a Unicam SP 200 G, Pye Unicam 641749 and Beckman 922623 spectrophotometers using KBr wafer technique. The 1H-NMR spectrum was run on a Varian 60 MHz using TMS as an internal standard.

Characterisation and physical data of all the prepared organic compounds are grouped in Table 1.

Action of hydroxylamine on benzoxzone (I*a*); Formation of II

A mixture of I*a* (0.01 mol), hydroxylamine hydrochloride (0.03 mol) and sodium acetate (0.03 mol) in methanol (50 mL) was heated under reflux for 5 hr. The reaction mixture was filtered while hot and the filtrate was cocled whereby separated a solid product. Recrystallisation of the product from a suitable solvent gave the 2-(substituted)-3-hydroxy-4-quinazolone (II).

Acetylation and benzoylation of 2-(substituted)-3-hydroxy-4-quinazolone (II). Formation of III*a* and *b*

A mixture of II (0.01 mol) with excess of acetic anhydride and/or benzoyl chloride (25 mL) was refluxed for 2 hr. After cooling a solid product was separated, washed with water, filtered and dried. Recrystallisation of the product from a proper solvent gave 3N-(acetoxy or benzoxy)-4-quinazolone derivatives (III *a* and *b*) respectively.

Action of active methylene compounds on benzoxazones (I*a* and *b*) : Formation of IV*a* and *b*

A solution of I*a* or *b* (0.01 mol) and active methylene compound (ethyl acetoacetate, ethyl cyanoacetate or diethyl malonate) (0.03 mol) in pyridine (50 mL) was heated under reflux for 12 hr. The reaction mixture was cooled, washed with dilute HCl and filtered. The separated solid was recrystallised from a suitable solvent to give 2-(substituted) 3-carboxy (or carbethoxy)-1,4-quinolinones (IV*a* and *b*).

Action of sodium azide on benzoxazone (I*c*) : Formation of tetrazole (V)

A mixture of benzoxazone (I*c*) (0.01 mol) and sodium azide (0.015 mol) in boiling acetic acid (50 mL) was refluxed for 3 hr. Upon concentration the reaction mixture separated a solid product, which was filtered and dried. Recrystallisation of the solid product from an appropriate solvent gave the tetrazole derivative (V).

Action of Grignard reagents on benzoxazones (I*a* or *b*) : Formation of VI*a-e*

An ethereal solution of methylmagnesium iodide, benzylmagnesium chloride and/or α-naphthylmagnesium bromide (0.03 mol) was added portionwise to a solution of benzoxazones (I*a* or *b*) (0.01 mol) in dry tetrahydrofuran (100 mL). The reacticn mixture was refluxed for 5 hr on a water bath, then left overnight at room temperature. The reaction mixture was worked-up as usual and the ethereal extracts were distilled under reduced pressure to give a viscous oil which was triturated with light petrol to give a solid product. Recrystallisation of the solid product from a proper solvent gave the corresponding alkyl (or aryl)-*o*-(α-benzamido substituted styryl) formamido phenyl ketone (VI*a-e*).

Friedel Crafts reaction with benzoxazone (I*a*). Formation of VII and VIII*a-d*

To a solution of I*a* (0.01 mol) in dry benzene (50 mL) and indole, 3,5-dimethyl pyrazole, 3-methyl-5-pyrazolone, 1-*p*-nitrophenyl-3-methyl-5-pyrazolone and/or 1-*p*-nitrophenyl-3,5-dimethyl pyrazole (0.01 mol) anhydrous $AlCl_3$ (0.04 mol) was added portionwise with stirring for 30 min. The stirring was continued for an additional 10 hr. at room temperature. The reaction mixture was then poured on ice-cold HCl. The organic layer was separated, washed with water and the excess solvent was distilled under reduced pressure. The solid obtained was recrystallised from a proper solvent to give (VII) and (VIII*a-d*) respectively.

Diels-Alder reaction of (I*a*)

A mixture of benzoxazone (I*a*) (0.01 mol), maleic anhydride (or diethyl maleate) (0.01 mol) and dry xylene (50 mL) was heated under reflux for 20 hr. The reaction mixture was filtered while hot, the filtrate was concentrated and cooled. The separated solid was recrystallised from a suitable solvent to give the Diels-Alder adduct (IX) (or X).

Action of hydrazine hydrate (or aniline) on (X) : Formation of (XI) (or XII)

A solution of X (0.01 mol) and hydrazine hydrate (or aniline) (0.03 mol) in ethanol (30 mL) was refluxed for 4 hr. The solid product obtained was recrystallised from a proper solvent to give XI (or XII).

REFERENCES

[1] M. A. El-Hashash, A. M. Kaddah, M. El-Kady and I. Ammar, *Pakistan J. Sci. Ind. Res.*, **25**, 104 (1982).

[2] A. Sammour, A. F. M. Fahmy and M. Mahmoud, *Indian J. Chem.*, **11**, 222 (1973).

[3] M. A. El-Hashash, and M. A. Sayed, *Egypt. J. Chem.*, **21**, 115 (1980).

[4] A. Sammour, T. Zimaity and M. Anwar Abdo, *Egypt. J. Chem.*, **16**, 215 (1973).

Revue Roumaine de Chimie, **35**, *1*, 63–66 (1990)

DEHYDRATION OF SOME 1-(2-FURYL)- AND 1-(2-THIENYL)-1-ALKANOLS USING COBALT(II) SULPHATE AS CATALYST

ÜLKÜ OYMAN

Department of Chemistry, Faculty of Science and Letters, Technical University of Istanbul Turkey

Received April 11, 1989

Dehydration reactions of some 1-(2-furyl) — and 1-(2-thienyl)-1-alkanols are investigated by using cobalt (II) sulphate as heterogeneous catalyst. During the reaction, a mixture of dehydration and dehydrogenation products is obtained from the furyl alkanols, but only dehydration products from the thienyl alkanols.

The dehydration of alcohols to alkenes has been performed by many methods in homogeneous and heterogeneous media.[1-4] As solid catalyst for dehydration, metal oxides have been used mostly.[5-9] The usage of metal(II) sulphates as catalysts has not been much applied yet and the results are very limited in this area.[10-15] Particularly, only one study was made in 1982 [16] by using anhydrous cobalt(II) sulphate as solid catalyst.

According to some investigators,[17,18] hydrate form of a salt structure of the solid catalyst gives better result than anhydrous form of the salt. In this study, therefore, $CoSO_4 \cdot H_2O$ has been selected for dehydration of the secondary alcohols containing furan and thiophen rings.

The procedure involves the treatment of the neat alcohol with solid catalyst at 160°C for 3 hours under diminished pressure (10 mm Hg).

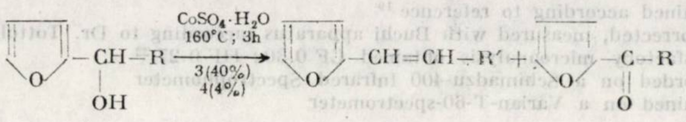

1 3 4

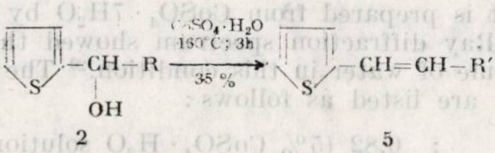

2 5

a : $C_{18}H_{37}$ d : $C_{15}H_{31}$

R = b : $C_{17}H_{35}$ e : $C_{14}H_{29}$

c : $C_{16}H_{33}$ f : $C_{13}H_{27}$

In these conditions, a mixture of alkenes and ketones was formed from 1-(2-furyl)-1-alkanols; the expected alkenes were obtained with 40% efficiency from the corresponding 1-(2-furyl)-1-alkanols. 1-(2--Thienyl)-1-alkanols gave a simple dehydration reaction with about 35% yield without any dehydrogenation product.

The properties of used 1-(2-furyl)-1- and 1-(2-thienyl)-1-alkanols are given in Table 1.

Table 1

The properties of used akanols **1,2**

Alkanols[a]	R	mp [°C][b]	Molecular Formula[c]	IR (KBr) [cm^{-1}][d]	^1H NMR ($CDCl_3$) [ppm][e]
1a	$C_{18}H_{37}-$	64–65	$C_{23}H_{42}O_2$	3300, 2800, 1610, 1560, 1470, 1200 910, 720,	0.95 (t, 3H); 1.25 (s, 34H) 1.92 (s, 1H); 4.58 (m, 1H); 6.25 (m, 1H); 6.60 (m, 1H) 7.20 (m, 1H).
1b	$C_{16}H_{33}-$	58–60	$C_{21}H_{38}O_2$	3300, 2800, 1610, 1470, 1240, 910, 720	0.97 (t, 3H); 1.25 (s, 30H) 1.95 (s, 1H); 4.50 (m, 1H) 6.25 (m, 1H); 6.60 (m, 1H) 7.20 (m, 1H)
1c	$C_{14}H_{29}-$	53.8–54.3	$C_{19}H_{34}O_2$	3300, 2850, 1590, 1470, 1240, 910, 720	0.97 (t, 3H); 1.25 (s, 26H) 1.78 (s, 1H); 4.50 (m, 1H) 6.25 (m, 1H); 6.60 (m, 1H) 7.20 (m, 1H)
2a	$C_{18}H_{37}-$	53–55	$C_{23}H_{42}OS$	3300, 2900, 1460, 1240, 1000, 930, 690	0.95 (t, 3H); 1.40 (s, 34H) 2.75 (s, 1H); 4.95 (m, 1H) 6.80 (m, 1H); 6.90 (m, 1H) 7.20 (m, 1H)
2b	$C_{17}H_{35}-$	48–50	$C_{22}H_{40}OS$	3300, 2900, 1460, 1240, 1000 930, 690	0.92 (t, 3H); 1.40 (s, 32H) 2.76 (s, 1H); 4.95 (m, 1H) 6.98 (m, 1H) 7,20 (m, 1H)ü

[a] Obtained according to reference [19]
[b] Uncorrected, measured with Buchi apparatus (according to Dr. Tottoli)
[c] Satisfactory microanalysis obtained CF 0.30; HF 0.27 [22]
[d] Recorded on a Schimadzu-400 Infrared Spectrophometer
[e] Obtained on a Varian-T-60-spectrometer

The catalyst is prepared from $CoSO_4 \cdot 7H_2O$ by heating at 220°C for 8 hours.[16] X-Ray diffraction spectrum showed that the compound retains one molecule of water in this condition.[20] The properties of the prepared catalyst are listed as follows:

pH : 6.82 (5% $CoSO_4 \cdot H_2O$ solution)
Water content : 10.40 (% per molecule)
Surface area : 930 m^2/g (measured by pentane absorption at room temperature)
Particle size : 1–100μ (determined with standard sieves)

The dehydration reactions have occurred as stereoselective. The alkenes obtained are only of *trans* form.

EXPERIMENTAL

The dehydration reaction is carried out in a 50 mL round bottom flask which is connected to another 50 mL round-bottom flask with an H bridgehead. A thermometer is attached to the first tip of the H bridgehead. The second tip of the H bridgehead has a finger-type water condenser and a vacuum connection.

The neat alcohol (1 mole) and powdered $CoSO_4 \cdot H_2O$ (1 mole) are mixed well and poured into the first flask. The flask is heated in an oil bath up to 145—150°C, under diminished pressure (10 mm Hg). The vacuum tap is closed and the pump is removed. The temperature rises to 160°C and the reaction mixture is heated for a further 3 hours. Then the mixture is cooled and extracted with ether (50 mL). The etheral solution is dried over sodium sulphate and evaporated under diminished pressure. The products obtained are purified by fractional crystallisation or distillation. UV spectrograms are recorded on a Varian-635-Tection spectrometer. IR and ^{1}H-NMR spectra are obtained with the instruments shown in Table 1. Micro analysis are done with a Heraeus-Microstandard instrument.

The following compounds were obtained :

a) From-1-(2-furyl)-1-nonadecanol : (1a)

2-Furylnonadecanone (4a) ;
yield : 8% ; mp : 52—53°C (heptane) ;
$C_{23}H_{40}O_2$ calc. C 79.31 ; H 9.19 ; found C 79.18 ; H 9.70%
UV (CH_2Cl_2) : : 240, 270 nm
IR (KBr) : 2900, 2850, 1700, 1460, 940, 710
^{1}H-NMR ($CDCl_3$) : 0.97 (t, 3H), 1.45 (s, 32H), 2.38 (m, 2H), 6.10 (m, 1H), 6.50 (m, 1H), 7.22 ppm (m, 1H)

1-(2-Furyl)-1-nonadecene) (3b) ;
Yield : 41% ; m.p.: 42—43°C (acetone and heptane)
$C_{23}H_{40}O$ calc : C 83.13; H 12.40; found C 82.54; H 11.93%
UV(CH_2Cl_2) : 240, 282 nm
IR KBr) : 2900, 2850, 2915, 1465, 960, 720 cm^{-1}
^{1}H-NMR($CDCl_3$) : 0.98 (t, 3H), 1.45 (s, 32H), 2.40 (m, allylic H), 5.0 (m, olefinic H), 6.22 (m, 1H), 6.65 (m, 1H) 7.22 ppm (m, 1H)

From 1-(2-furyl)-1-heptadecanol (1 c) ;

2-Furylheptadecanone (4b) ;
Yield 5% ; mp : 47—51°C (acetone heptane)
$C_{21}H_{36}O_2$ calc C 78.75; H 11.25; found C 78.13; H 11.20%
UV(CH_2Cl_2) : 240, 270 nm
IR(KBr) : 2900, 2850, 1700, 1460, 900, 715 cm^{-1}
^{1}H-NMR($CDCl_3$) : 0.97 (t, 3H), 1.25 (s, 28H), 2.30 (m, 2H), 6.20 (m, 1H), 6.45 (m, 1H), 7.38 ppm (m, 1H)

1-(2-Furyl)-1-heptadecene (3c) ;
Yield : 38, mp : 38—40°C (acetone)
$C_{21}H_{36}O$ calc. C 82.89; H 11.84; found C 82.59; H 10.89%
UV(CH_2Cl_2) : 235, 282 nm
IR KBr) : 2900, 2850, 1470, 1005, 960, 720 cm^{-1}
^{1}H-NMR($CDCl_3$) : 0.98 (t, 3H), 1.40 (s, 28H), 5.0 (m, olefinic H) 6.20 (m, 1H), 6.55 (m, 1H), 7.22 ppm (m, 1H).

From 1-(2-furyl)-1-pentadecanol (1 d) ;

1-Furylpentadecanone (4 d) ;
Yield : 4% ; bp : 170—190°C/5 mm Hg
$C_{19}H_{32}O_2$ calc. C 78.08; H 10.95; found C 78.13; H11.20%
UV(CH_2Cl_2) : 230, 268 nm
IR ($CHCl_3$) : 2950, 2850, 1725, 1465, 1080, 910, 720 cm^{-1}
^{1}H-NMR($CDCl_3$) : 0.98 (t, 3H), 1.32 (s, 24 H), 2.15 (m, 2H), 6.20 (m, 1H), 6.35 (m, 1H), 7.25 ppm (m, 1H)

1-(2-Furyl)-1-pentadecene (3 f) ;
Yield : 37 % bp : 145—170°C/5 mm Hg
$C_{19}H_{32}O$ calc. C 82.60 ; H 11.59 ; found C 81.98 ; H11.45 %
UV(CH_2Cl_2) : 230, 282 nm
IR ($CHCl_3$) : 2900, 2850, 1675, 1460, 1080, 960, 720 cm^{-1}
^1H NMR($CDCl_3$) : 0.96 (t, 3H), 1.25 (s, 24 H),
2.09 (m, allylic H), 6.02 (m, olefinic H)
6.22 (m, 1H), 6.55 (m, 1H), 7.25 ppm (m, 1H)

From 1-(2-thienyl)-1-nonadecanol (2a) ;
1-(2-Thienyl)-1-nonadecene : (5b)
Yield : 27 % ; mp : 31—33°C (acetone)
$C_{23}H_{40}OS$ calc C 79.31 ; H 11.49 ; found C 79.33 ; H 10.68 %
UV(CH_2Cl_2) : 282, 230 nm
IR KBr) : 2915, 2850, 1460, 1220, 960, 690 cm^{-1}
^2H-NMR($CDCl_3$) : 0.98 (t, 3H), 1.40 (s, 32H),
2.40 (m, allylic H) 6.60 (m, 1H),
6.90 (m, 1H), 7.38 ppm (m, 1H)

From 1-(2-thienyl)-1-Octadecanol (2b) ;
1-(2-Thienyl)-1-octadecene (5c) ;
Yield : 43 % ; mp : 28—31°C (acetone)
$C_{22}H_{32}S$ calc C 79.04 ; H 11.37 ; found C 78.36 ; H 11.40 %
UV(CH_2Cl_2) : 279, 230 nm
IR KBr) : 2940, 2850, 1460, 1380, 960, 695 cm^{-1}
^1H-NMR($CDCl_3$) : 0.92 (t, 3H), 1.40 (s, 30H),
2.43 (m, allylic H) 6.45 (m, 1H),
6.90 (m, 1H), 7.18 ppm (m, 1H)

ACKNOWLEDGMENTS : I thank Dr. H. Özbal for NMR data, Dr. S. Öksüz for UV spectral data and Dr. I. Kumbasar for X-Ray spectral data.

REFERENCES

[1] H. Williams, *J. R. Saunders and F. E. Antony*, "Mechanism of Elimination Reactions" Wiley-Interscience, New York, 1973.
[2] D. V. Bantrop, "Elimination Reactions", Elsevier, Amsterdam, 1963.
[3] S. G. Solomon, "Organic Chemistry", Wiley-Interscience, New York, 1980.
[4] H. Knozinger "The Chemistry of Hydroxyl Group" Part 2 (Patai, S.) Interscience, New York, 1971, p. 641.
[5] M. E. "Catalysis" Vol. III, Emment, Ed. Reinhold New York, 93, (1960).
[6] H. Pines and Y. Manassen, *Adv. Catal.*, **16**, 49 (1966).
[7] V. N. Ipatieff "Catalytic Reactions at High Pressure and Temperatures", Mc Millan Co., New York, 60—120 (1936).
[8] Z. G. Szabo, *J. Catal.*, **6**, 458 (1966).
[9] G. M. Schwab and Schwab-Agallidis, *J. Amer. Chem. Soc.* **71**, 1806, (1949).
[10] F. K. Signaio and P. L. Cramer, *J. Amer. Chem. Soc.*, **55**, 3326, (1933).
[11] C. C. Price and J. V. Karabinos, *J. Amer. Chem. Soc.*, **62**, 1159 (1940).
[12] F. C. Whitmore and E. Rohrman *J. Amer. Chem. Soc.*, **63**, 2033 (1941).
[13] M. V. Schlatter, *J. Amer. Chem. Soc.*, **76**, 4952 (1954).
[14] G. W. Francis and J. F. Berg, *Acta Chem. Scand.*, B 31 721 (1977).
[15] R. V. Hoffmann, R. D. Bishop, P. M. Fitch and R. C. Hardenstein, *J. Org. Chem.* **45**, 917, 1980.
[16] R. Özkan, Thesis, Faculty of Science, University of Atatürk, 1982.
[17] L. A. Munro, and W. R. Horn, *Can. J. Research*, **12**, 707 (1935).
[18] J. H. De Boer, *Industrie Chim. Belge*, **21**, 1159 (1956)
[19] F. L. Breusch, Ü. Oyman, *Revue de la'Faculte des Sciences de L'Universite d'Istanbul*, **CXXX** 103 (1966).
[20] Powder Diffraction File Sets (11—15), Inorganic, Joint Committe on Powder Diffraction on Standards U.S.A. (1972).
[21] A. D. Cross and R. A. Jones, "An Introduction to Practical Infra-Red Spectroscopy", Butterworth, (1969).
[22] R. M. Silverstein, G. C. Basler and T. C. Morril, "Spectroscopic Identification of Organic Compounds", John Wiley Sons Inc., 1974.
[23] J. W. Robinson, (Ed), "CRC Handbook of Spectroscopy", Vol. II, CRC Press (1974).

Revue Roumaine de Chimie, 35, 1, 67–76 (1990)

STUDY ON THE REACTION AND COMPOSITION OF THE Hg(II) COMPLEX WITH DIAZOAMINOBENZENE

MARIA POPESCU
Institute of Construction Bucharest, Bd. Lacul Tei No. 124 code 72302, Romania

Received February 11, 1988

Hg(II) forms with diazoaminobenzene a stable monomer complex with the formula

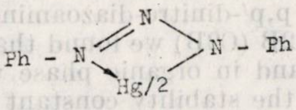

which enables the extractive photometric and gravimetric determination of Hg(II) in a medium of pH = 5.5–11. The extraction constants and the solubility products of the mercury complex in several solvents as well as the main X-ray diffraction lines of the reagent and the complex are presented.

The triazenic compounds containing in their molecule the —N=N—NH— diazoamino group proved to be very selective to Hg(II), forming stable complex combinations. The hydroxytriazenic compounds are analytical reagents for the determination of Mg(II), Zn(II), Cd(II), Cu(I, II), Ni(II), Mn(II), Pb(II), Fe(II, III), Sn(II, IV), Hg(II), Pd(II), Ti(IV), V(IV).[1-3] The selectivity increases very much for the triazenic compounds without hydroxyl groups and they form complexes with a number of ions : Cd(II), Hg(II), Hg_2(II), Pd(II), Ag(I), Cu(II), Ni(II).[4-10] At a pH = 6–11, diazoaminobenzene forms with Hg(II) and Hg_2(II) stable complexes that may be extracted from organic solvents and with Ag(I) it forms a partially extractable complex. Ag(I) precipitated under the form of AgCl does not interfere up to a Ag(I)/Hg(II) ratio = 500. Due to its particular selectivity, the reagent could be used for the Hg(II) determination in waste water rich in acetaldehyde, in industrial caustic soda and in waste water from sodium chloride electrolysis [11, 12] in ores and rocks containing HgS.[13]

The structures of these compounds is much discussed ; the literature classifies them in type I,[14-18] type II,[19] or type III, [20] with monomer structure, dimer structure [18] or polymer structure.[15]

Various formulas of the complexes depending on the anion to which Hg(II) is linked, namely : chloride, bromide, nitrate or acetate are given in the literature. [19]

The present paper studies the type of complex formed between diazoaminobenzene as a reagent and Hg(II) at a neutral and basic pH.

From the triazenic compounds studied, we selected this reagent because the complex formed with Hg(II) has a higher solubility in organic solvents, therefore, the reagent enabled the determination of its molecular weight and the H-NMR analysis.

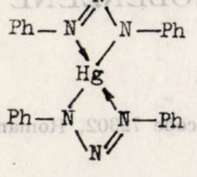

I

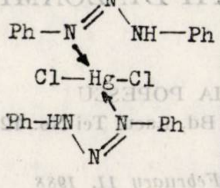

II

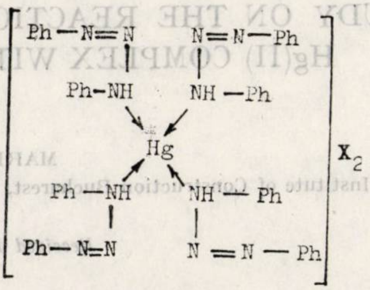

III

From the spectrophotometric studies carried out by us[6] with five triazenic reagents such as: diazoaminobenzene (DAB), p-nitro-diazoaminobenzene (NDAB), p,p'-dinitro-diazoaminobenzene (DNDAB), Cadion A (CA) and Cadion 2B (C2B) we found that Hg(II) forms complexes both in aqueous phase and in organic phase with the Hg(II)/R combination ratio of 1:2 and the stability constant of 10^{10} order.

In this paper we present a number of arguments supporting the formation of complex Hg-DAB of type I, with monomer structure in pH ranges of 5.5—11, a structure independent of the nature of anion linked to mercury.

EXPERIMENTAL

Reagents and Instrumentation

Solutions of $HgCl_2$ and $Hg(NO_3)_2$ with titre of 100 ppm were freshly prepared from a stock solution having a concentration of 1000 ppm.

In the radiometric measurements a ^{203}Hg acetate solution, with specific activity $\lambda_s =$ 95.7 mCi/g and with titre of 186 ppm, was used.

Solution of reagent with a concentration of 0.05% in EtOH, buffer solution of 2M potassium acetate and a solution of Na and K tartrate 20% for complexing some easily hydrolysable ions at the working pH were employed.

The visible absorption spectra were recorded with a SPECORD UV-VIS Carl Zeiss Jena spectrophotometer and those in IR with a Perkin Elmer 621 spectrophotometer. The molecular weight of the Hg(II) complex was determined with a Knauer Dampfdruck osmometer and the H-NMR spectra were carried out in d_6-DMSO solution using a VARIAN A-60 A instrument.

The derivatograms were obtained with a derivatograph type 2895 F. Paulik-J. Paulik-L. Erdey system and the radiometric measurements were carried out with an impulse counter NP-40 made in Czechoslovakia.

The X-ray diffraction determinations were effected with a generator TUR-M62 fitted with a diffractometer MZG-3 and a proportional counter.

The experimental conditions

The determinations were carried out at a pH of the aqueous phase of 6.5 obtained with 2M potassium acetate using the mercury under the form of nitrate, chloride, acetate and the reagent dissolved in EtOH, the complex that was formed being extracted in an aromatic solvent.

The reagent absorbs at 354.6 nm, the complex at 326.6 nm, the measurements were carried out at 410 nm wavelength where the reagent absorption is negligible.

Influence of extraction solvent

For determining the influence of the extraction solvent, the following organic solvents were used: benzene, toluene, p-xylene, chloroform, carbon tetrachloride, nitrobenzene and carbon sulphide. The experimental results prove that the complex is well extracted in the above-mentioned solvents (Table 1). The distribution ratio (D) of Hg(II) between the aqueous and organic phase was determined with ^{203}Hg and then it was used in the computation of the extraction constants. [21] The relatively low value of the distribution ratio may be due to the disproportion of Hg(II) at a neutral pH and the formation of hydrocomplexes.

Table 1

Values of extraction distribution ratios and the extraction constants of Hg(II)-DAB in various solvents

No.	Solvent	$[HA]^* \times \times 10^{+4}$	D	E%	log K	log K (graph)
1	C_6H_6	3.1 0.93 0.31	59.33 4.16 0.39	98.35 80.63 28.45	−4.21 −4.31 −4.38	−4.1
2	$C_6H_5-CH_3$	3.1	103.08	99.04	−3.96	
3	$pC_6H_4-(CH_3)_2$	3.1	81.82	98.79	−4.07	
4	$C_6H_5-NO_2$	3.1	60.88	98.38	−4.20	
5	CCl_4	3.1	87.95	98.87	−4.04	
6	$CHCl_3$	3.1	0.08	7.42	−7.08	
7	CS_2	3.1	79.20	98.75	−4.08	

* HA = DAB

Fig. 1 illustrates the variation lgD depending on the reagent concentration. From the slope of the linear section the Hg/R combination ratio of 1:2 was determined and from the intersection of the line with the ordinate, the benzene extraction constant shown in Table 1 was determined.

The stability constant of the complex extracted in benzene using the Job method for non-isomolar solutions [22] for $[Hg] = 5 \times 10^{-5}$ and $[R] = 10^{-4}$ and $[R] = 2 \times 10^{-4}$ was determined (Figs. 2, 3).

The data presented in Table 2 show that the complex is stable having a stability constant of 10^{10} order.

Study of the percentage extraction variation of ^{203}Hg complex in C_6H_6 (Fig. 4) depending on the quantity of reagent, shows that it is sufficient to have three times more reagent than the stoichiometric quantity necessary to the quantitative formation of the complex. The solubility product of the complex was determined using ^{203}Hg. The ^{203}Hg complex was obtained using an excess of ^{203}Hg acetate, then the excess was quantitatively removed by washing it with water and it was radiometrically checked. Then, 2 mL of the respective solvent and an ex-

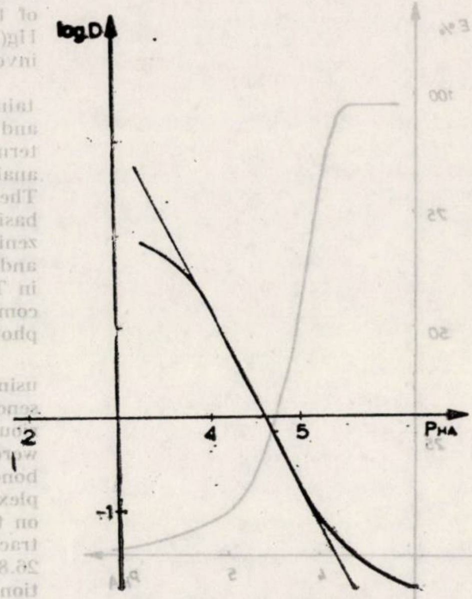

Fig. 1. — Variation of distribution ratio with the reagent concentration.

cess of complex under solid state were introduced in 3 mL test tubes fitted with stopper. The test tubes were mechanically stirred for half an hour, then centrifugated and introduced into a thermostat at 25°C.

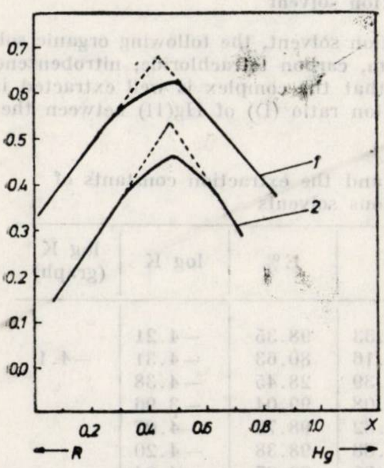

Fig. 2. — Job's curves obtained in benzene phase for :
[Hg] = 5 × 10^{-5} ; [R] = 10^{-4}
1. $\nu = 25 \times 10^3$ cm^{-1}
2. $\nu = 24 \times 10^3$ cm^{-1}.

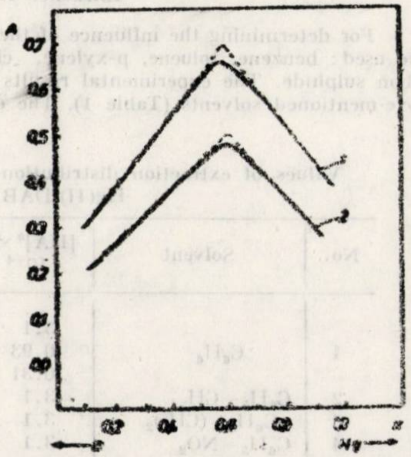

Fig. 3. — Job's curves obtained in benzene phase for :
[Hg] = 5 × 10^{-5} ; [R] = 2 × 10^{-4}
1. $\upsilon = 24 \times 10^1$ cm^{-1}
2. $\upsilon = 24.5 \times 10^1$ cm^{-1}.

We had in view that all the test tubes should contain an excess of undissolved complex. Samples of 1 mL were taken from each test tube and the activity was measured. The solubility products of the complex in H_2O, CH_3OH, C_2H_5OH, C_3H_7OH, $(CH_3)_2CO$, $C_2H_5COCH_3$ and $CHCl_3$ (Table 3), could be determined on the basis of the solution activity. The low solubility of Hg(II) complex limits very much the possibility to investigate its structure.

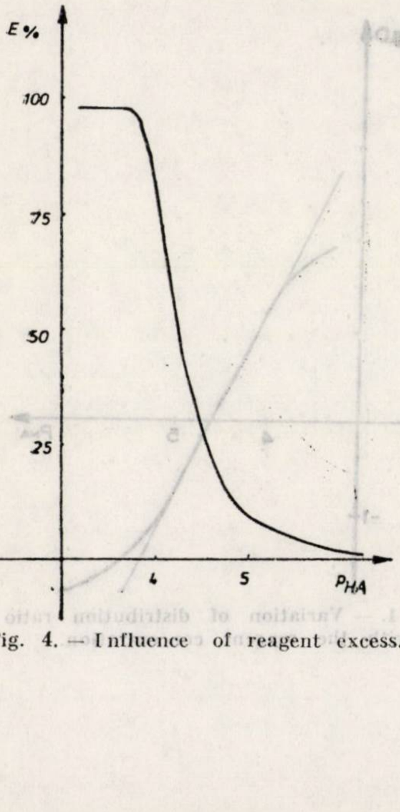

Fig. 4. — Influence of reagent excess.

Hg(II) complexes in solid phase were obtained from diazoaminobenzene dissolved in EtOH and $HgCl_2$, $Hg(NO_3)_2$ and they were used in the determination of the molecular weight, elementary analysis, IR spectra, H-NMR and X-ray spectra. The values of the molecular weight obtained on the basis of the osmotic pressure variation of the benzenic solution of the complex obtained from DAB and $HgCl_2$ and the elementary analysis are shown in Table 4 where the monomer structure of the complex is given. The Hg percentage was spectrophotometrically determined with dithizon.

The mercury complexes were synthesized using $HgCl_2$, $Hg(NO_3)_2$ and $Hg(NO_3)_2$ in the presence of Cl^- ions because we tried to clarify various hypotheses on the complex structure. We were especially interested in the existence of Hg-Cl bond and N-H bond in the molecule of the complex. Following the influence of Cl^- concentration on the distribution ratio we found a maximum extraction in benzene (Fig. 5) at a $Cl^-/Hg(II)$ ratio of 26.8 followed by a marked decrease of the distribution ratio which may be due to the formation of non-extractable and anionic Hg chlorocomplexes which did not react with the reagent. The visible spectra were traced in toluene for the Hg(II) complexes obtained from $Hg(NO_3)_2$, $Hg(NO_3)_2$ in the presence of Cl^- ions at a $Cl^-/Hg(II)$ ratio of 26.8, from $HgCl_2$ and $Hg_2(NO_3)_2$. In order to obtain in solution the stable $Hg_2(II)$ ion, a solution of $Hg(NO_3)_2$ was used in the presence of metallic Hg, where the $Hg_2(II)/Hg(II)$ ratio is 88.[23]

Table 2

Experimental data and stability constant values of the complex in benzene phase

[Hg(II)]	ρ	x_{max}	K	K_m
5×10^{-5}	2	0.54	1.9×10^{10}	
5×10^{-5}	4	0.40	2.25×10^{10}	2.07×10^{10}

Table 3

Solubility products of Hg(II) complex in various organic solvents

Solvent	H_2O	CH_3OH	C_2H_5-OH	C_3H_7OH	CH_3COCH_3	$CH_3COC_2H_5$	$CHCl_3$
p^{25}_{s}	7.68×10^{-18}	1.27×10^{-12}	6.26×10^{-13}	1.09×10^{-13}	6.81×10^{-11}	7.06×10^{-11}	2.04×10^{-16}

Table 4

Elementary analysis and molecular weight of Hg(II) complex

C% theo.	C% exp.	H% theo.	H% exp.	Hg% theo.	Hg% exp.	M theo.	M exp.	Formula
48.56	47.36 48.22	3.37	3.58 3.43	33.78	33.20 33.90	593	610 630	$C_{24}H_{20}N_6Hg$

Fig. 6 shows that the position of the isosbestic point is not clear for the spectra obtained with $Hg(NO_3)_2$ which probably is disproportioned in neutral medium unlike those obtained with $HgCl_2$ (Fig. 8) and with $Hg(NO_3)_2$ in the presence of Cl^- at a $Cl^-/Hg(II)$ ratio of 26.8 (Fig. 9). The position of the isosbestic points for the Hg(II) complexes obtained with $HgCl_2$ and $Hg_2(NO_3)_2$ (Fig. 7) is at $\upsilon = 26.8 \times 10^3$ cm^{-1} and 26.7×10^3 cm^{-1}, respectively, and for the complex obtained with $Hg(NO_3)_2$ in the presence of Cl^- is at $\upsilon = 26.75 \times 10^3$ cm^{-1}. In the presence of Cl^-, the mercury from the nitrate may pass in $HgCl_2$ which is a little dissociated and does not disproportionate like the mercury nitrate and acetate; this increases the distribution ratio until the whole mercury passes in $HgCl_2$ (at a ratio corresponding to the maximum illustrated in Fig. 5). The spectra were recorded with a low speed of the wavelength increase.

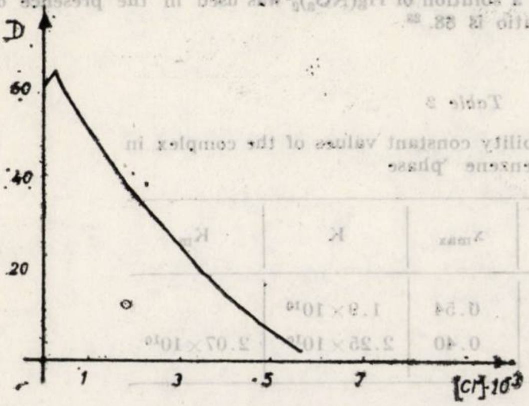

Fig. 5. — Influence of Cl^- concentration on the distribution ratio of ^{203}Hg between the aqueous and benzene phase.

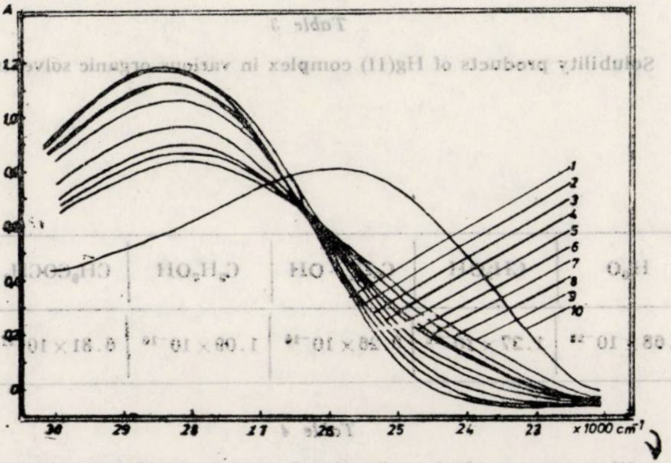

Fig. 6. — Absorption spectra for solutions of 7.24×10^{-5} M diazoaminobenzene in benzene containing $Hg(NO_3)_2$ in the following concentrations: (1) 0; (2) 1.42×10^{-6} M; (3) 2.84×10^{-6} M; (10) Hg(II) excess.

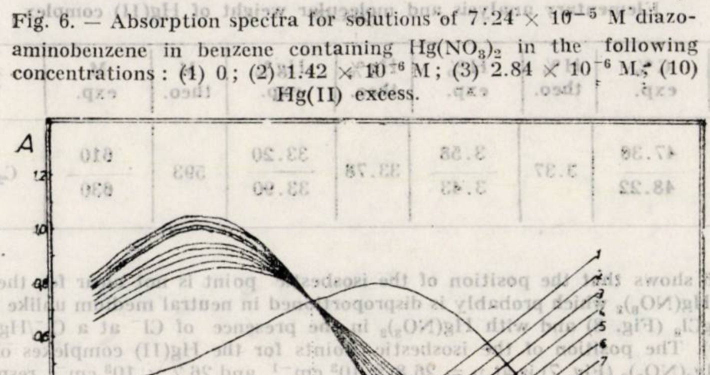

Fig. 7. — Absorption spectra for solutions of 6.33×10^{-5} M diazoaminobenzene in benzene containing $Hg_2(NO_3)_2$ in the following concentrations: (1) 0; (2) 1.245×10^{-6} M; (3) 2.49×10^{-6} M; (10) $Hg_2(II)$ excess.

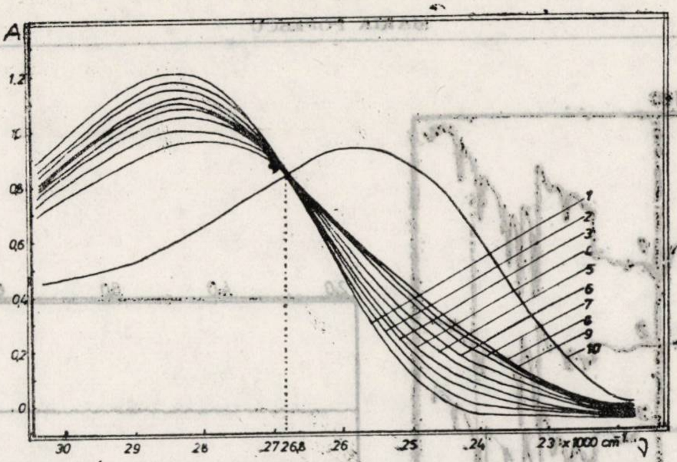

Fig. 8. — Absorption spectra for solutions of 7.24×10^{-5} M diazoaminobenzene in benzene containing $HgCl_2$ in the following concentrations: (1) 0; (2) 1.42×10^{-6} M; (3) 2.48×10^{-6} M; (10) Hg(II) excess.

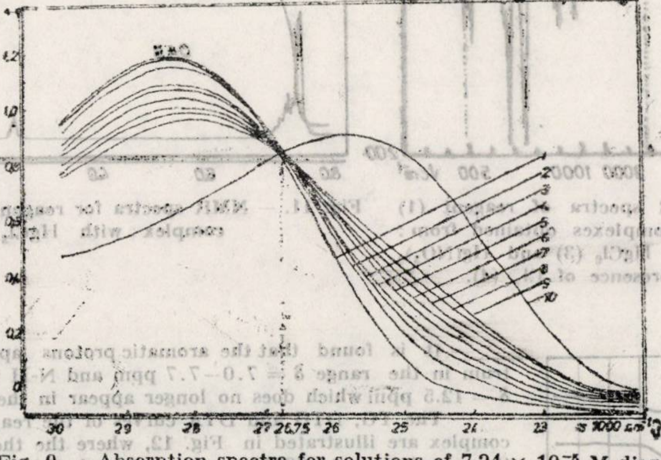

Fig. 9. — Absorption spectra for solutions of 7.24×10^{-5} M diazoaminobenzene in benzene containing $Hg(NO_3)_2$ in the presence of Cl^-, Hg(II) being in the following concentrations: (1) 0; (2) 1.42×10^{-6} M; (3) 2.84×10^{-6} M; (10) Hg(II) excess.

Fig. 10 illustrates the IR specra of the same Hg(II) complexes and of the reagent and it is found that the characteristic vibrations of N-H bond at 1520 cm^{-1} and 3185 cm^{-1} [14,24–26] in the reagent, disappear in all the Hg(II) complexes; the characteristic vibrations of C_2H_5—N = are shifting from 1235 cm^{-1} and 1320 cm^{-1} for the reagent to 1210 cm^{-1} and 1275 cm^{-1}, respectively, for the complex.[14] The characteristic vibration of N-Hg bond is given in literature[25] between 400 and 700 cm^{-1} but in the complexes synthesized by us we have found that the vibration of N-Hg bond appears at 480 cm^{-1} and a widening of the band between 1295 and 1345 cm^{-1} [14] also takes place. The vibrations at 360 cm^{-1} and 413 cm^{-1}, which are characteristic for $HgCl_2$ do not appear in the IR spectrum of the Hg(II) complexes.[27]

Fig. 11 shows the NMR spectra of the reagent and the Hg(II) complex obtained with $HgCl_2$ dissolved in d_6-DMSO.

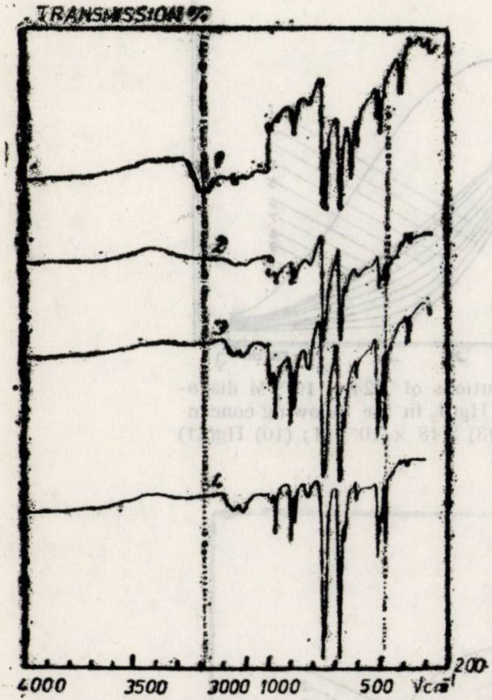

Fig. 10. — IR spectra of reagent (1) and Hg(II) complexes obtained from: $Hg(NO_3)_2$ (2); $HgCl_2$ (3) and $Hg(NO_3)_2$ in the presence of Cl^- (4).

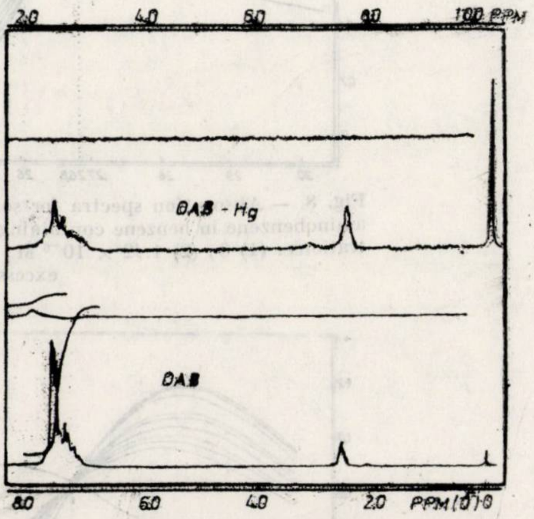

Fig. 11. — NMR spectra for reagent (DAB) and complex with $HgCl_2$.

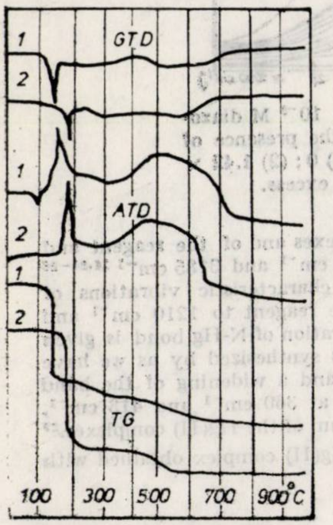

Fig. 12. — Derivatograms of reagent (1) and complex (2).

It is found that the aromatic protons appear in the spectrum in the range $\delta = 7.0-7.7$ ppm and N-H in the reagent at $\delta = 12.5$ ppm which does no longer appear in the Hg(II) complex.

The TG, DTG and DTA curves of the reagent and Hg(II) complex are illustrated in Fig. 12, where the thermal stability of the complex up to 200°C may be inferred, this allowing the use of the reagent in the gravimetric determination of Hg(II) in rocks and ores.[13] The reagent and the complex are decomposed explosively by heating at 155° and 200°C, respectively, when the reagent loses 55.3% of the mass and the complex 72%. These data were used to establish the Hg/R combination ratio of 1 : 2.

Table 5 shows the most important lines of the X-ray diffraction spectra obtained under the following experimental conditions: CuK α radiation, Ni filtre and the impulse scale of $t.8 \times 10^5$ imp/min.

From the X-ray diffraction spectra, the interplan distances "d" and the intensities of the most significant diffraction lines that appeared in the spectrum, were calculated. Examination of the table shows that the conversion of the reagent in the Hg complex is quantitative.

In the case of two lines of the reagent (9.1 Å and 4.56 Å) we could not determine exactly their intensities because the reagent consists of very well moulded crystals (plates), this determining their preferential orientation.

Table 5

Main diffraction lines for diazoaminobenzene (DAB), its Hg(II) complex (DAB Hg) and $HgCl_2$

DAB		DAB-Hg		$HgCl_2$ (ASTM 4—331)	
d Å	Iobs	d Å	Iobs	d Å	Iobs
		16.2	46		
		9.4	39		
9.1	100	8.11	100		
7.7	26				
6.57	29	6.15	29		
5.63	83				
5.19	28	5.03	20		
5.01	45	4.72	25		
4.56	100	4.54	8		
				4.35	100
				4.10	38
4.02	21	4.08	8		
3.83	45	3.89	15		
3.58	41	3.80	44		
		3.556	8		
		3.501	8		
3.416	72				
3.388	69	3.367	12	3.383	31
3.314	10			3.188	11
		3.166	18		
		3.097	15		
3.076	47			3.033	21
3.035	100			2.986	48
2.976	60	2.913	12		
2.820	19				
2.777	14				
		2.782	19	2.707	36
		2.401	8	2.420	14
2.277	10				
2.252	9			2.132	9
2.079	10			2.065	13
2.016	16			2.004	16
1.997	10			1.940	11
1.857	9			1.902	8

CONCLUSIONS

1. The complex formed between diazoaminobenzene and Hg(II) corresponds to type I having a monomer structure within 5.5—11 pH range.

2. For various studies and for the complex synthesis we recommend the use of Hg(II) under the form of $HgCl_2$ because it is negligibly disproportioned as compared to mercury nitrate and acetate.

At a neutral pH the $HgCl_2$ solution is stable for a longer period and it not necessary to prepare it daily.

REFERENCES

[1] V. Ja. Pochinok and M. S. Marenets, *Ukrain. Khim. Zhur*, **19**, 179 (1953).

[2] C. N. Sogani and S. C. Bhattacharyya, *J. Indian Chem. Soc.*, **36**, 563 (1959), *Chem. Abstr.*, **54**, 22143g (1960).

[3] I. P. Khazova, *Izv. Vysshikh, Uchbn. Zavedenii Khim. i Khim. Tekhnol.*, **6**, 218(1963), *Chem. Abstr.*, **59**, 8114a (1963).

[4] P. Chavanne and C. Geronimi, *Analyt. Chem. Acta*, **19**, 442 (1958).

[5] Nai-K'Nei Ch'Én, Wei-Kang Chiao and Shang Ihsüch Pao, 155 (1958), *Chem. Abstr.*, **53**, 14834a (1959).

[6] Gr. Popa, F. A. Dăneţ and M. Popescu, *Talanta*, **25**, 546 (1978).

[7] M. Popescu and F. A. Dăneţ, *Rev. Roumaine Chim.*, **28**, 65 (1983).

[8] A. F. Dăneţ and M. Popescu, *Rev. Chim.* (Bucureşti), **31**, 5, 480 (1980).

[9] M. Popescu and D. Crişan, *Rev. Roumaine Chim.*, **25**, 1187 (1980).

[10] M. Popescu and D. Todor, *Rev. Chim.* (Bucureşti), **29**, 10, 987 (1978).

[11] Gr. Popa, M. Popescu and A. Dăneţ, *Rev. Roumaine Chim.*, **25**, 1427 (1980).

[12] A. F. Dăneţ, M. Popescu and O. Maior, *Rev. Chim.* (Bucureşti), **30**, 583 (1979).

[13] M. Popescu and D. Todor, *Rev. Chim.* (Bucureşti), **29**, 1182 (1978).

[14] T. V. Ershova, E. G. Rukhadze and A. P. Terent'ev, *Zhur. Obshchei. Khim.*, **39**, 59 (1969).

[15] C. M. Harris, F. B. Hoskins and R. L. Martin, *J. Chem. Soc.*, 3729 (1959).

[16] A. P. Terent'ev, T. V. Ershova and E. G. Rukhadze, *Anal. Chim. Acta*, **40**, 93 (1968).

[17] A. P. Terent'ev, T. V. Ershova and E. G. Rukhadze, *Zhur. Obshchei. Khim.* **36**, 1046 (1966).

[18] C. M. Harris and R. L. Martin, *Pr. Chem. Soc.*, 259 (1958).

[19] C. M. Knowles and G. W. Watt, *J. Amer. Chem. Soc.*, **64**, 935 (1942).

[20] P. Mandal, *Science a Cultura*, **6**, 59 (1940).

[21] Jiri Stary, K. Kratzer, *Anal. Chim. Acta*, **40**, 93 (1968).

[22] P. Job, *Ann. Chem.*, **9**, 113 (1929).

[23] B. Latimer, *Ochislitelnye sostoiania elementov i ih potentsialy v vodnyh rastvorah*, M.I.L., 1954.

[24] K. Nakamoto, "Infrared spectra of Inorganic and Coordinative compounds", New York, Wiley, (1963).

[25] K. Brodersen and H. J. Becher, *Chem. Ber.*, **89**, 1487 (1956).

[26] D. Hadzi, *J. Jan. Spectrosc. Lett.* **1**, 139 (1968).

[27] W. Klemperer and L. Lindeman, *J. Chem. Phys.*, **25**, 397 (1956).

Revue Roumaine de Chimie, 35, 1, 77–83 (1990)

REACTIONS WITH N-AMINOPHTHALIMIDE AND SOME ALLIED COMPOUNDS

M. FEKRY ISMAIL, *FEKRIA S. SAYED, F. A. EL-BASSIOUNY and H. A. YOUNES
Chemistry Department, Faculty of Science, Ain Shams University Abbassia, Cairo, A.R. Egypt

Received August 15, 1987

N-Aminophthalimide (1) reacted as a normal amino compound with phenylisocyanate and benzoylisothiocyanate, to give the urea and thiourea derivatives (2) and (3) respectively. It reacted also with succinic and homophthalic anhydrides via ring opening to give the corresponding acidic products (4) and (5). The condensation of (1) with 2,4-dihydroxybenzaldehyde, isatin and N-acetylisatin gave the phthalimide derivatives (6*a* and 7*b*). The reaction of the latter compounds with amines was investigated and a mechanism for this reaction was suggested. p-Benzoquinone reacted with (1) via 1,4-addition to give N-(2,4-dihydroxyphenylamino) phthalimide (13).

N-Substituted phthalimides have been reported to exhibit antibacterial,[1] antifungal,[2] anthelmintic [3] antitumour [4–6] local anesthetic,[7] diuretic,[8] adrenolytic[9] and schistosomicidal [10] properties.

N-Aminophthalimide represents an easily-available starting material for the synthesis of some N-substituted phthalimides.[11, 12] This is shown by its reaction with reagents that are known to react readily with amino groups. Thus, when N-aminophthalimide **(1)** was allowed to react with phenylisocyanate and benzoyl-isothiocyanate it behaved as a normal amino compound giving the urea and thiourea derivatives **(2)** and **(3)** respectively.

The structures of **(2)** and **(3)** were confirmed by analytical data (1 : 1) and by showing the characteristic C=N, carbonyl and NH stretching frequencies in their infrared spectra.

N-Aminophthalimide reacted normally with succinic anhydride via ring opening of the anhydride ring giving N-(3-carboxy-propionamido)phthalimide **(4)**. The reaction of N-aminophthalimide with homophthalic anhydride proceeded similarly yielding N-*o*-carboxyphenylacetylaminophthalimide **(5)**.

The structures assigned for these products were substantiated, other than from analytical data, from a study of their infrared spectra which show $\nu_{=CN}$ and the carbonyl stretching frequencies of both cyclic imides and carboxylic acids. They show, in addition, broad absorptions at the 3μ region characteristic of polymeric ν_{OH} of carboxylic acids. The acidic nature of these compounds was shown by their ready solubility in aqueous sodium carbonate solutions and reprecipitation by the addition of mineral acids. The product of reaction of homophthalic anhydride with N-aminophthalimide was suggested to be formed by the nucleophilic attack of the amino compound on the carbonyl group (b) attached to the saturated carbon atom, since the other carbonyl group (a) is conjugated

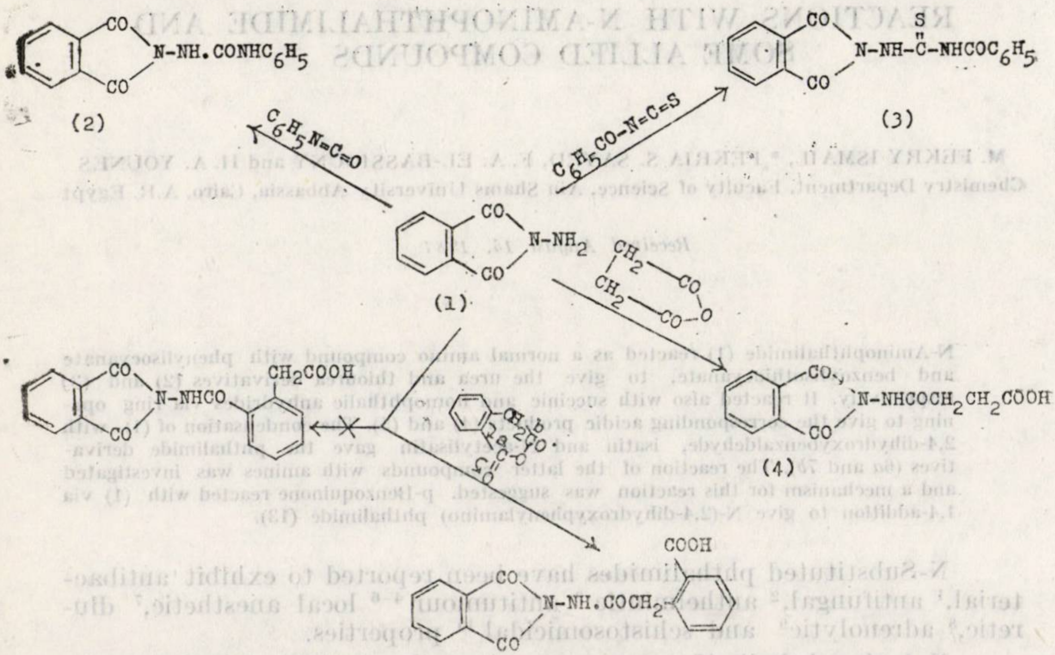

with the aryl group, thus resulting in the decrease of its nucleophilicity and consequently the carbonyl (b) becomes more susceptible to attack by nucleophilic reagents.

The reactivity of N-aminophthalimide towards condensation with aldehydes was further investigated by its reaction with the deactivated 2,4-dihydroxybenzaldehyde, whereupon, N-2,4-dihydroxyphenylmethyleneaminophthalimide (**6a**) was formed in moderate yield.

The interesting pharmacological properties of both phthalimide [1–10] and 3-substituted-imino-2-indolinone moieties [13,14] led us to synthesize compounds incorporating both moieties for the sake of getting compounds of marked biological effect. This was accomplished by allowing N-aminophthalimide to react with isatin and N-acetylisatin. The reaction proceeded smoothly to give the desired compounds (**7a** and **b**). The structures of the phthalimide derivatives (**6** and **7**) were confirmed by (i) analytical data (ii) their infrared spectra are closely similar to that of previously prepared related compounds.[11,12] They show the carbonyl stretching frequencies of phthalimide derivatives. Compounds **7a** and **b** show, in addition the amide carbonyl stretching frequencies of indolinones. The ν_{NH} of indolinones was identified in **7a** at 3280 cm^{-1} (cf. Table).

N-Arylmethyleneaminophthalimides are known to undergo cleavage under the influence of some Grignard reagents.[10,11] This behaviour tempt-

Table

Physical data of compounds (6), (7), (9) and (10)

Compound	M. p. °C	Yield (%)	Solvent	Molecular formula	Analysis (%) Fd/calc.			IR (cm^{-1})		
					C	H	N	νNH	νC=N	νC=O
6a	230–32	65	ethanol	$C_{15}H_{10}N_2O_4$	64.40 63.83	4.10 3.60	9.60 9.90	—	1610	1720, 1785
7a	260–62	70	ethanol	$C_{16}H_9N_3O_3$	65.20 65.98	2.90 3.09	14.20 14.43	3280	1600	1725, 17,40, 1785
7b	194–96	60	ethanol	$C_{18}H_{11}N_3O_4$	64.40 64.86	3.90 3.30		—	1600	1635, 1750, 1770
9a	177–79	60	ethanol	$C_{20}H_{21}N_3O_4$	65.10 65.39	6.10 5.72	12.00 11.44	3190	1610	1650
9b	210–11	75	benzene-ethanol	$C_{21}H_{23}N_3O_3$	68.80 69.04	6.30 6.30		3200	1600	
9c	202–204	75	benzene-ethanol	$C_{20}H_{21}N_3O_4$	65.20 65.39	5.40 5.72	11.40 11.44	3200	1605	1660
10a	220–21	70	ethanol	$C_{21}H_{20}N_4O_3$	67.20 67.02	5.40 5.32	15.00 14.89	3180, 3280	1610	1675, 1720
10b	232–34	70	ethanol	$C_{20}H_{18}N_4O_4$	63.50 63.50	4.70 4.76	14.30 14.81	3225	1620	1685, 1710

ed us to investigate the reaction of phthalimide derivatives (**6a** and **7a**) with amines. It was found that these compounds underwent complete cleavage under the influence of benzylamine to give N,N′-dibenzylphthalimide (**8**). The structure of this compound was confirmed by its identity with an authentic sample prepared by the action of benzylamine on N-aminophthalimide.[11] The reaction apparently proceeded by nucleophilic attack on both carbonyl groups. However, the reaction of **6** and **7a** wiith secondary amines, namely, piperidine and morpholine proceeded differently by nucleophilic attack on only one of the carbonyl groups to give **9** and **10**, respectively.

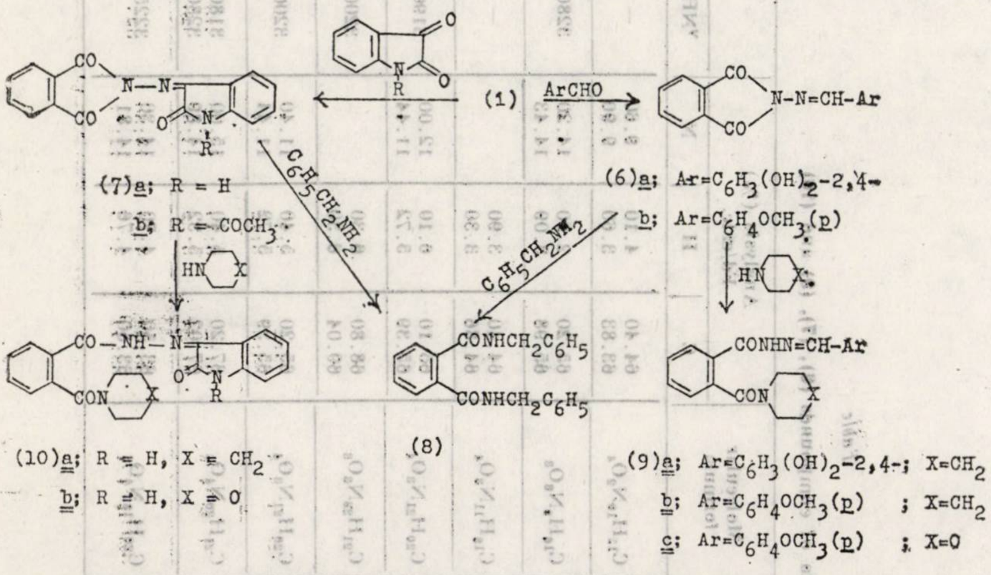
(1)
ArCHO
$C_6H_5CH_2NH_2$
$C_6H_5CH_2NH_2$
HN X
CONHCH$_2$C$_6$H$_5$
CONHCH$_2$C$_6$H$_5$
CONHN=CH-Ar
N-N=CH-Ar
(7)a; R = H
b; R = COCH$_3$
(6)a; Ar=C$_6$H$_3$(OH)$_2$-2,4-
b; Ar=C$_6$H$_4$OCH$_3$(p)
(10)a; R = H, X = CH$_2$
b; R = H, X = O
(8)
(9)a; Ar=C$_6$H$_3$(OH)$_2$-2,4-; X=CH$_2$
b; Ar=C$_6$H$_4$OCH$_3$(p) ; X=CH$_2$
c; Ar=C$_6$H$_4$OCH$_3$(p) ; X=O

A probable mechanism for these reactions is outlined as follows:

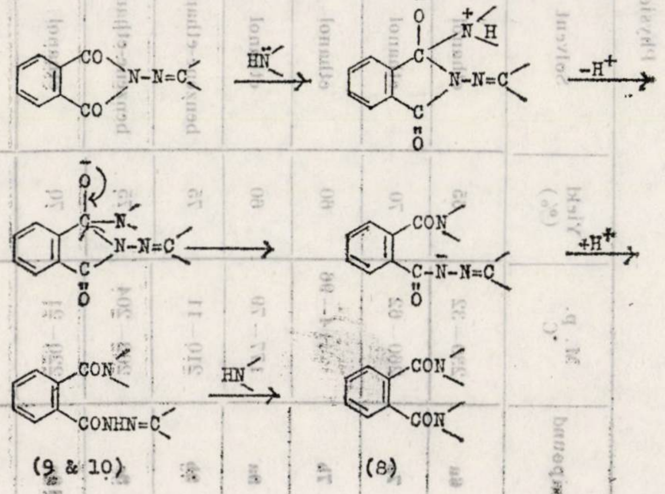
HN
-H$^+$
+H$^+$
HN
(9 & 10)
(8)

The proposed mechanism was verified by allowing **9b** to react with benzylamine, under similar conditions to those followed in the reaction of this amine with **6a** and **7a**, whereupon the expected N,N′-dibenzylphthalamide **(8)** was obtained in good yield, in addition to the corresponding azine **(11)**.

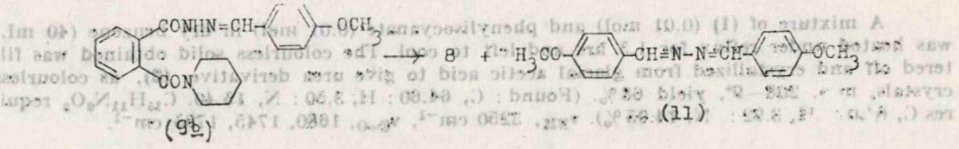

The structures of **9** and **10** were established from analytical data and a study of their infrared spectra which show NH and carbonyl stretching frequencies of amides (Table). The structure was further confirmed by the fact that these compounds are converted back to their starting materials **(6** and **7)** under the influence of dil. HCl in a reaction involving the extrusion of the amine part.

The reaction of N-aminophthalimide with *p*-benzoquinone is of interest since such reaction may proceed by nucleophilic attack on the carbonyl group of the quinone, to give the condensation product **(12)**, or by 1,4-addition to give N-(2,4-dihydroxyphenylamino)phthalimide **(13)**. However the addition product **(13)** was the sole product of the above reaction as shown by analytical data and the fact that its infrared spectrum shows sharp NH and OH stretching frequencies in addition to the carbonyl stretching frequencies of imides. The presence of phenolic OH groups in the product was shown by the dark reddish violet colour formed when its alcoholic solution was treated with ferric chloride solution, and its ready solubility in aqueous sodium hydroxide solution.

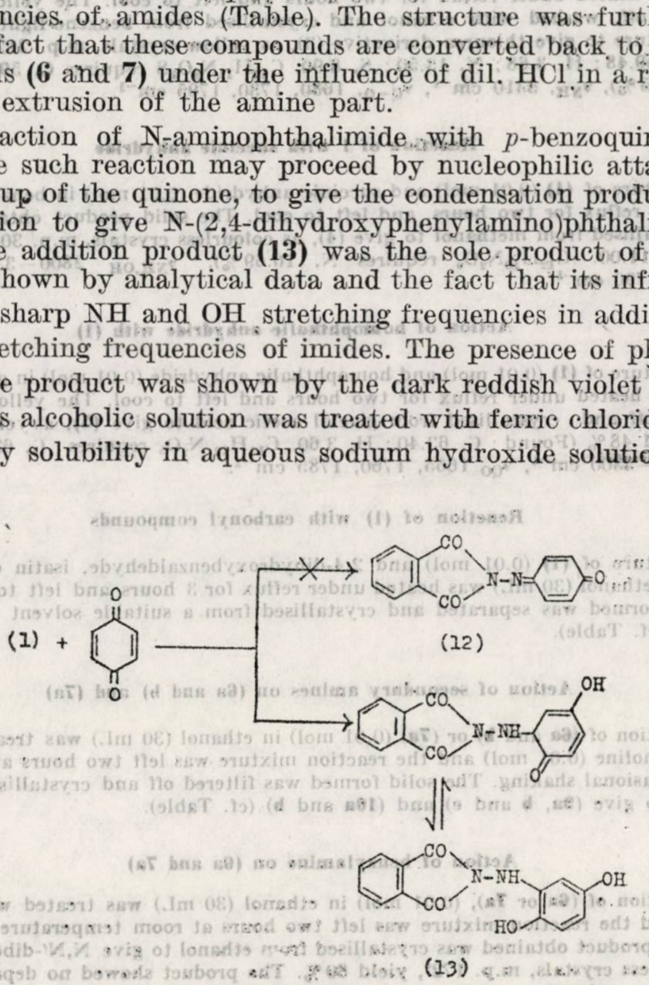

EXPERIMENTAL

Melting points are uncorrected. IR spectra in KBr were recorded on a Pye-Unicam Sp 1200 spectrophotometer.

Reaction of (1) with phenylisocyanate

A mixture of **(1)** (0.01 mol) and phenylisocyanate (0.01 mol) in dry benzene (40 mL) was heated under reflux for 1.5 hrs and left to cool. The colourless solid obtained was filtered off and crystallized from glacial acetic acid to give urea derivative **(2)**, as colourless crystals, m.p. 208–9°, yield 68%. (Found : C, 64.60 ; H, 3.50 ; N, 15.40. $C_{15}H_{11}N_3O_3$ requires C, 6[illegible] ; H, 3.92 ; N, 14.95%). ν_{NH}, 3250 cm^{-1}, $\nu_{C=O}$, 1680, 1745, 1795 cm^{-1}.

Reaction of (1) with benzoylisothiocyanate

A mixture of **(1)** (0.005 mol) and benzoylisothiocyanate (0.005 mol) in dry acetone (30 mL) was heated under reflux for two hours and left to cool. The yellow solid obtained was filtered off, washed with ethanol and crystallised from benzene-light petroleum (b.p. 60–80°) mixture to give thiourea derivative (3), as yellow crystals, m.p. 212–3°, yield 82%. (Found : C, 59.48 ; H, 3.68 ; N, 13.50 ; S, 8.90. $C_{16}H_{11}N_3O_3S$ requires C, 59.08 ; H, 3.38 ; N, 12.92 ; S, 9.85%), ν_{NH}, 3310 cm^{-1}, $\nu_{C=O}$, 1680, 1730, 1795 cm^{-1}.

Reaction of 1 with succinic anhydride

A mixture of **(1)** (0.01 mol) and succinic anhydride (0.01 mol) in benzene (30 mL) was heated under reflux for two hours, and left to cool. The solid product obtained was filtered off and crystallised from methanol to give (4), as colourless crystals, m.p. 306–7°, yield 32% (Found : N, 11.00. $C_{12}H_{10}N_2O_5$ requires N, 10.69%). $\nu_{NH,OH}$ 2800–3300 cm^{-1}, $\nu_{C=O}$ 1665, 1750, 1790 cm^{-1}.

Action of homophthalic anhydride with (1)

A mixture of **(1)** (0.01 mol) and homophthalic anhydride (0.01 mol) in glacial acetic acid (25 mL) was heated under reflux for two hours and left to cool. The yellow solid obtained was filtered off and crystallised from glacial acetic acid to give **(5)**, as yellow needles, m.p. 301–2°, yield 48% (Found : C, 63.40 ; H, 3.60. $C_{17}H_{12}N_2O_5$ requires C, 62.96 ; H, 3.70%), $\nu_{NH,OH}$ 2800–3300 cm^{-1}, ν_{CO} 1665, 1760, 1785 cm^{-1}.

Reaction of (1) with carbonyl compounds

A mixture of **(1)** (0.01 mol) and 2,4-dihydroxybenzaldehyde, isatin or N-acetylisatin (0.01 mol) in ethanol (30 mL) was heated under reflux for 3 hours and left to cool. The crystalline solid formed was separated and crystallised from a suitable solvent to give (**6a**) and (**7a** and **b**) (cf. Table).

Action of secondary amines on (6a and b) and (7a)

A solution of (**6a** and **b**) or (**7a**) (0.01 mol) in ethanol (30 mL) was treated with piperidine or morpholine (0.01 mol) and the reaction mixture was left two hours at room temperature with occasional shaking. The solid formed was filtered off and crystallised from a suitable solvent to give (**9a**, **b** and **c**) and (**10a** and **b**) (cf. Table).

Action of benzylamine on (6a and 7a)

A solution of (**6a** or **7a**), (0.01 mol) in ethanol (30 mL) was treated with benzylamine (0.02 mol) and the reaction mixture was left two hours at room temperature with occasional shaking. The product obtained was crystallised from ethanol to give N,N′-dibenzylphthalimide (**8**), as colourless crystals, m.p. 172°, yield 80%. The product showed no depression when admixed with an authentic sample prepared by the action of benzylamine on N-aminophthalimide (**1**).[11]

Action of benzylamine on (9b)

A solution of (**9b**) (0.01 mol) in ethanol (30 mL) was treated with benzylamine (0.02 mol) and the reaction mixture was left two hours at room temperature with occasional shaking. The solid formed was filtered off and crystallised from ethanol to give (**8**), as colourless crystals, m.p. 172°, yield 75%. The product showed no depression when admixed with an authentic sample prepared by the action of benzylamine on N-aminophthalimide (**1**). The mother liquor was concentrated to give a yellow solid which was crystallised from ethanol to give the corresponding azine (**11**) as yellow crystals. The product showed no depression when admixed with an authentic sample.

Action of dil. hydrochloric acid on (9 and 10)

A suspension of the solid compound (**9**) (0.5 g) in dil. hydrochloric acid (10 mL) was left at room temperature for 4 hours with occasional shaking. The coloured solid formed in each case was filtered off and crystallised from ethanol to give the corresponding N-arylmethyleneaminophthalimides (**6**) as shown by m.p. and m.m.p. experiments; when compounds (**10a** and **b**) were treated similarly, they gave (**7a**) in excellent yields.

Reaction of (1) with benzoquinone

A mixture of (**1**) (0.01 mol) and benzoquinone (0.01 mol) in ethanol (30 mL) was heated under reflux for 4 hours. The red solid formed after cooling was filtered off and crystallised from acetic acid to give (**13**) as red crystals, m.p. $>$ 300°, yield 70%. (Found : N 10.8. $C_{14}H_{10}N_2O_4$ requires N, 10.3 %), νNH,OH 3265 cm^{-1}, $\nu_{C=O}$ 173 , 1785 cm^{-1}.

REFERENCES

[1] E. Profft, H. Teubner and W. Weuffen, *Arch. Exp. Veterinaermed.*, **21**, 225 (1967).

[2] O. T. Săvulescu, V. Barbu and V. Tudoescu, *Phytopathol. Z.*, **59**, 129 (1967).

[3] W. Weuffen, *Arch. Exp. Veterinaermed.*, **22**, 127 (1968).

[4] H. Mueckter, E. Frankus and E. More, 5th Int. Congr., Chemotherap., **2**, 267 (1967).

[5] W. H. Finley and W. C. Carlson, *Albama J. Med. Sci.*, **1**, 252 (1964).

[6] H. Mueckter, E. Frankus, E. More, W. E. Kolmer and M. Staemmler, *Z. Krebsforsch*, **69**, 60 (1967).

[7] M. B. Moore and R. T. Rapala, *J. Amer. Chem. Soc.*, **68**, 1957 (1946).

[8] MRS. E. J. Cornish, G. E. Lee and W. R. Wragg, *J. Pharm. Pharmacol.*, **18**, 65 (1966).

[9] J. Porszaz and K. Nador, *Arzneimittel — Forsch.*, **6**, 695 (1956).

[10] R. F. Collins, M. Davis, N. D. Edge, J. Hill, H. W. Reading and E. R. Turnbull, *Brit. J. Pharmacol.*, **14**, 467 (1959).

[11] M. F. Ismail and N. G. Kandil, *Ind. J. Chem.*, **21**, 462 (1982).

[12] M. F. Ismail, E. A. El-Bassiuny, E. I. Enayat, A. M. Kaddah and H. A. Younes, *J. Prakt. Chem.*, **327**, 176 (1985).

[13] R. Agarwal, S. Misra, R. K. Satsangi and S. S. Tiwari, *Arch. Pharmazie*, **1981** (314).

[14] R. Agarwal, R. K. Satsangi and S. S. Tiwari, *Ind. J. Chem.*, **20 B**, 1099 (1981).

Revue Roumaine de Chimie, **35**, *1*, 85–96 (1990)

ENUMERATION OF CATACONDENSED BENZENOID HYDROCARBONS AND THEIR NUMBERS OF KEKULÉ STRUCTURES *

J. BRUNVOLL,[a] R. TOŠIĆ[b], M. KOVAČEVIĆ,[b] A.T. BALABAN,[c] I. GUTMAN[a,d]
and S. J. CYVIN[a]

[a]Division of Physical Chemistry, The University of Trondheim, N-7034 Trondheim-NTH, Norway

[b]Institute of Mathematics, Faculty of Science, University of Novi Sad, YU-21000 Novi Sad, Yugoslavia

[c]The Polytechnic, Organic Chemistry Department, R-77206 Bucharest, Romania

[d]On leave from : Faculty of Science, University of Kragujevac, YU-34000 Kragujevac, Yugoslavia

Received November 14, 1988

The enumeration data for unbranched catafusenes are extended to systems with 20 hexagons ($h = 20$) in general (all symmetries), and to $h = 30$ for the mirror- and centro-symmetrical systems. Curves for the distribution of K (the number of Kekulé structures), as produced by computer programming, are given for unbranched and branched catafusenes with $7 \leqslant h \leqslant 12$.

INTRODUCTION

The early enumeration of catacondensed benzenoid systems (*alias* catacondensed benzenoids *alias* catafusenes)[2–4] were taken up, after some years with apparently no activity in this research field, by extensive studies with the aid of modern computers.[5–10] These papers are quoted, along with supplements, in a recent consolidated report.[11] The most recent contribution to the topic, with special emphasis on the enumeration of branched catacondensed benzenoids, was published by some of the present authors.[1]

Kekulé structures in benzenoid systems and, in particular, their numbers have been extensively studied in the recent years.[12] Although an easy method for the calculation of the number of Kekulé structures in both unbranched and branched catacondensed benzenoids is long

---

[*] Part VI of the series "Distribution of K, the Number of Kekulé Structures, in Benzenoid Hydrocarbons". For Part V, see reference 1.

known,[13] there still remain many unsolved problems in this field. For instance, it is not known which catacondensed benzenoid systems (with a given number h of hexagons) have maximum number of Kekulé structures. The solution of this problem is known only for $h \leqslant 12$, and was obtained from a systematic computer search.[2] Unbranched catacondensed systems with maximum Kekulé structure counts were recognized some time ago.[14] Nevertheless, the closely related task, namely the finding of unbranched catacondensed systems with h hexagons, k kinks and maximum number of Kekulé structures, has found its solution quite recently.[15,16]

The present work consists of two parts, both containing substantial supplements to a previous paper.[1] Firstly, the results of some enumerations of unbranched catafusenes are reported. Secondly, the distributions of K (the number of Kekulé structures) for unbranched and branched catafusenes at given h values are illustrated.

DEFINITIONS

An unbranched catacondensed benzenoid (catafusene) is a planar system of identical regular hexagons in a single chain, where the hexagons may have the following modes for $h > 1$. Two terminal hexagons (mode L_1) are always present; in addition there may be linearly annelated (mode L_2) and/or angularly annelated (A_2) hexagons. The system is a branched catafusene if it possesses one or more branching hexagons (mode A_3), but otherwise there should not be any hexagon in a mode different from L_1, L_2 and A_2.

A (non-planar) helicenic quasi-benzenoid has overlapping edges. Also these systems may be classified among unbranched and branched catafusenes.

ENUMERATION OF UNBRANCHED CATAFUSENES

The numbers of catafusenes for $h \geqslant 12$ are found elsewhere,[1] where the benzenoids and helicenic systems are listed separately. Numbers up to $h = 20$ for the unbranched catacondensed benzenoids are also available.[11] They are reproduced in table 1, where the data are supplemented by the corresponding numbers (in parentheses) for the helicenic quasi-benzenoids.

The systems are classified as:

a acenes (linear); D_{6h} for $h = 1$, otherwise D_{2h}

m mirror-symmetrical; C_{2v}

c centrosymmetrical; C_{2h}

u unsymmetrical; C_s

In total:

$$a + m + c + u = N_{ub} \tag{1}$$

where the classification symbols are used for the numbers themselves and as such are functions of h. Let the numbers of helicenic systems be marked by an asterisk, viz. a^*, m^*, c^*, u^* and N^*_{ub}. Furthermore, we write for the numbers of benzenoid and helicenic systems at a given h added together:

$$a' = a \ (a^* = 0), \qquad m' = m + m^*, \tag{2}$$

$$c' = c + c^*, \qquad u' = u + u^*, \qquad N'_{ub} = N_{ub} + N^*_{ub}$$

Table 1

Numbers of unbranched catafusenes; helicenic systems in parentheses

h	a	$m(m^*)$	$c\ (c^*)$	$u\ (u^*)$	Total $N_{ub}(N^*_{ub})$
1	1	0	0	0	1
2	1	0	0	0	1
3	1	1	0	0	2
4	1	1	1	1	4
5	1	4	1	4	10
6	1	3 (1)	4	16	24 (1)
7	1	12 (1)	4	50 (2)	67 (3)
8	1	10 (3)	13	158 (11)	182 (14)
9	1	34 (6)	13	472 (48)	520 (54)
10	1	28 (12)	39 (1)	1406 (194)	1474 (207)
11	1	97 (24)	39 (1)	4111 (729)	4248 (754)
12	1	81 (40)	116 (5)	11998 (2643)	12196 (2688)
13	1	271 (93)	115 (6)	34781 (9263)	35168 (9362)
14	1	226 (138)	339 (25)	100660 (31836)	101226 (31999)
15	1	764 (329)	336 (28)	290464 (107388)	291565 (107745)
16	1	638 (455)	988 (105)	837137 (357512)	838764 (358072)
17	1	2141 (1139)	977 (116)	2408914 (1176126)	2412033 (1177381)
18	1	1787 (1493)	2866 (414)	6925100 (3833300)	6929754 (3835207)
19	1	6025 (3816)	2832 (448)	19888057 (12390423)	19896915 (12394687)
20	1	5030 (4811)	8298 (1543)	57071610 (39773671)	57084939 (39780025)

The explicit formulas for a', m', c', u' and N'_{ub} are known.[1,2] They are obtained from the simple recurrence properties [2]

$$a'(h + 1) = a'(h); \qquad h = 1, 2, 3, \ \ldots . \tag{3a}$$

$$m'(h + 2) = 3m'(h) + 1; \qquad h = 1, 2, 3, \ \ldots \tag{4a}$$

$$c'(h + 2) = 3c'(h) + 1; \qquad h = 2, 3, 4, \ \ldots \tag{5a}$$

together with

$$a' + m' + c' + u' = N'_{ub} \tag{6}$$

and

$$a' + 2(m' + c') + 4u' = 3^{h-2} \tag{7}$$

The last formula was obtained from a combinatorial reasoning for a numerical (three-digit) notation for the unbranched catafusenes.[2]

If we add the numbers (3)—(5) we may refer to the result as the number of symmetrical, unbranched catafusenes. Let it be denoted

$$s' = a' + m' + c' \tag{8}$$

Since $a'(h) = 1$ for all h we may modify eqns. (3a)-(5a) into :

$$a'(h+2) = a'(h); \qquad h = 1, 2, 3, \ldots \tag{3b}$$

$$m'(h+2) = 3m'(h) + a'(h); \quad h = 1, 2, 3, \ldots \tag{4b}$$

$$c'(h+2) = 3c'(h) + a'(h); \quad h = 2, 3, 4, \ldots \tag{5b}$$

On adding these three equations we arrive at

$$a'(h+2) + m'(h+2) + c'(h+2) = 3[a'(h) + m'(h) + c'(h)] \tag{9}$$

and consequently, by virtue of (8):

$$s'(h+2) = 3s'(h); \qquad h = 2, 3, 4, \ldots \tag{10}$$

Gutman[17] pointed out that the numbers N'_{ub} follow the third-order recurrence relation :

$$N'_{ub}(h+6) = 13\ N_{ub}^{\prime b}\ (h+4) - 39\, N'_{ub}\ (h+2) + 27\, N'_{ub}\,(h); \quad h = 2, 3, 4, \ldots \tag{11}$$

We find that the same form is obeyed by the u' numbers, viz.

$$u'(h+6) = 13u'(h+4) - 39u'(h+2) + 27u'(h); \; h = 1, 2, 3, \ldots \tag{12}$$

With the aid of the above formulas and the known initial conditions it is now easy to list and check the numerical values of a', m', c', s', u' and $N'_{ub} = s' + u'$. The values were used in practice when producing the (parenthesized) numbers $m^* = m' - m$, $c^* = c' - c$, ..., etc. in table 1.

A new, efficient computer program was written for the enumeration of mirror-symmetrical and centrosymmetrical benzenoids, viz. m and c, respectively. The results for $21 \leqslant h \leqslant 30$ (in continuation of table 1) are entered into table 2, together with the corresponding numbers derived for the helicenic systems.

Table 2

Numbers of some symmetrical unbranched catafusenes; helicenic systems in parentheses

h	m (m^*)	c (c^*)
21	16924 (12600)	8185 (1656)
22	14116 (15408)	23969 (5555)
23	47623 (40950)	23623 (5901)
24	39727 (48846)	69109 (19464)
25	133934 (131786)	68057 (20516)
26	111655 (154065)	198995 (66725)
27	377003 (420158)	195806 (69914)
28	314297 (482864)	572216 (224945)
29	1061064 (1330420)	562675 (234486)
30	884199 (1507285)	1642975 (748509)

One can note the following approximate relationships:

$$m(2h-1)/m(2h) \approx 1.2 \tag{13}$$

$$c(2h)/c(2h+1) \approx 1.02 \tag{14}$$

DISTRIBUTIONS OF K

A distribution of K, the number of Kekulé structures, for a class of benzenoids, gives information on the numbers of systems with different K numbers at a given h, the number of hexagons.[1,18-20]

Especially for the branched catafusenes the distributions of K for $h = 6$, 7 and 8 were presented in diagrams,[1] but the data were produced by computer programming for h values up to 12.

We have now computerized also the drawing of diagrams for K distributions. Figures 1–6 show these distributions for the branched (bottom diagrams) as well as unbranched catafusenes (top diagrams) for $h = 7-12$.

In spite of many irregularities the diagrams display some characteristic features, which are strikingly different for the branched and unbranched systems. The curves for branched catafusenes tend to assume a roughly Gaussian shape, but with the maximum clearly shifted towards larger K than the mid-point between $K_{\min}$ and $K_{\max}$. The curves for unbranched catafusenes, on the other hand, have a tendency, apart from violent oscillations, to increase steadily from the start and maintain at high values through the last part (largest K). However, the curves drop down to zero at irregular intervals throughout the range of K value. The occurrence of a gap with zero values near the end of the curves seems to be a characteristic feature.

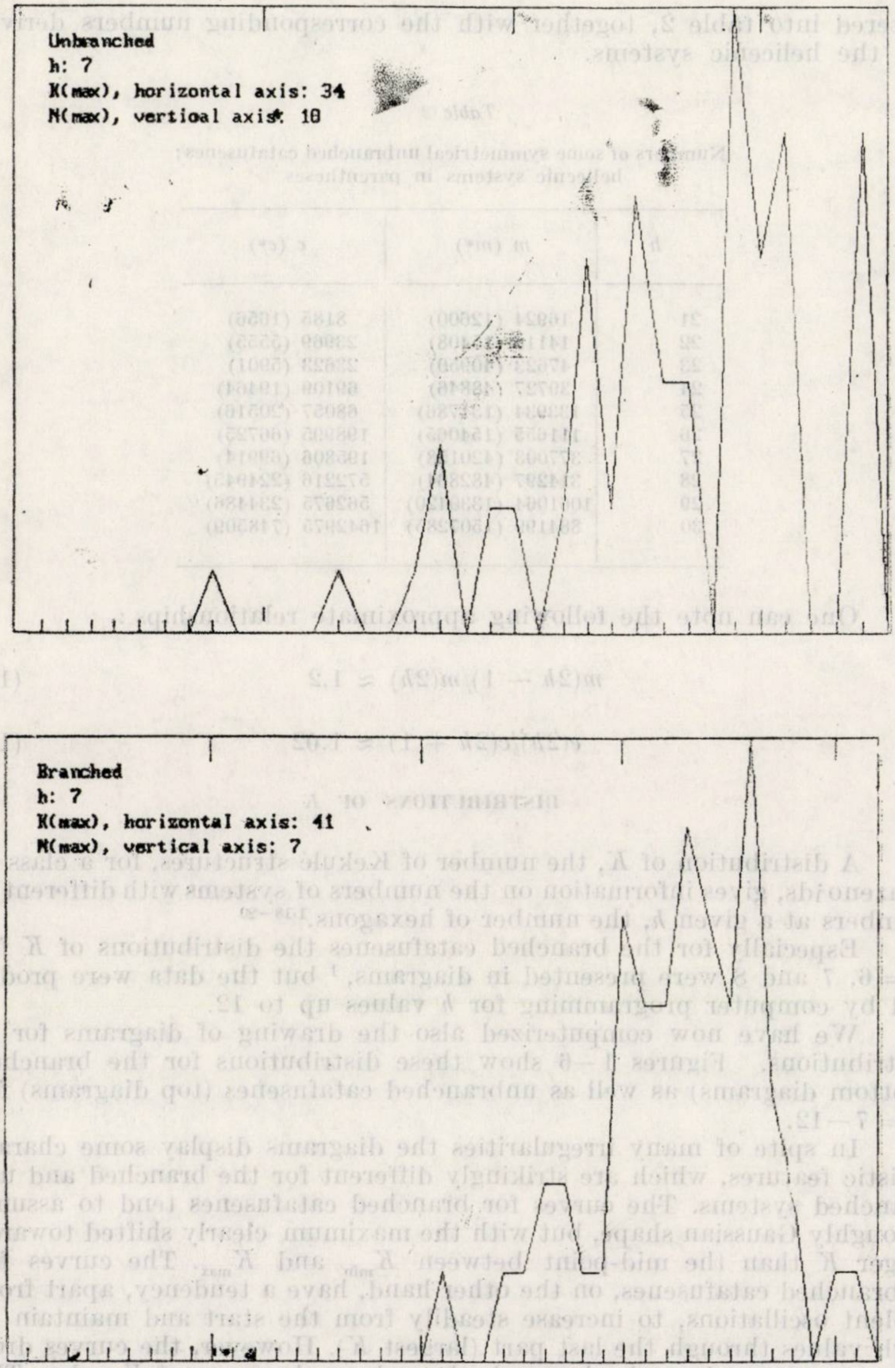

Fig. 1. — Distribution of *K*, the number of Kekulé structures, for unbranched (top) and branched (bottom) catafusenes at *h* (the number of hexagons) = 7.

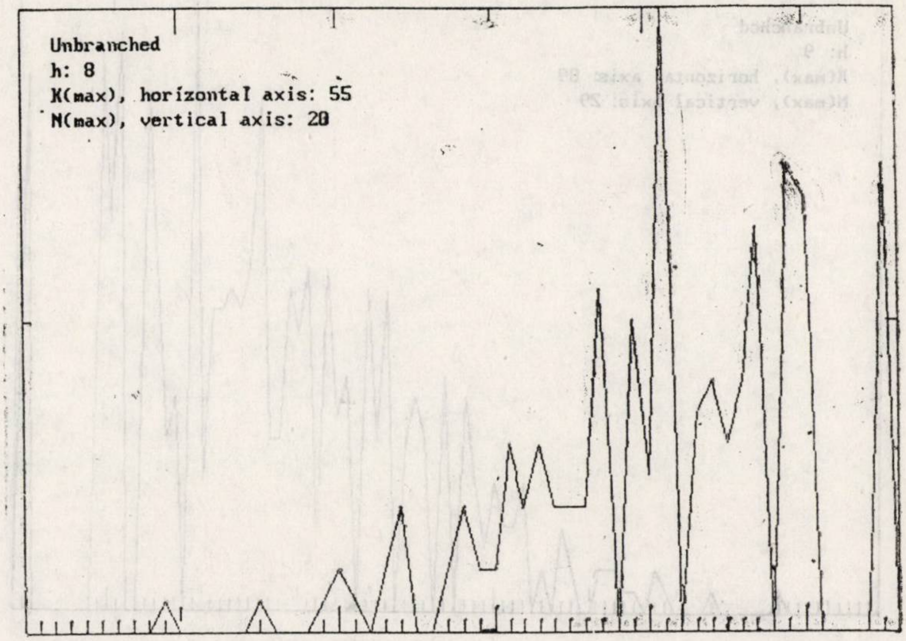

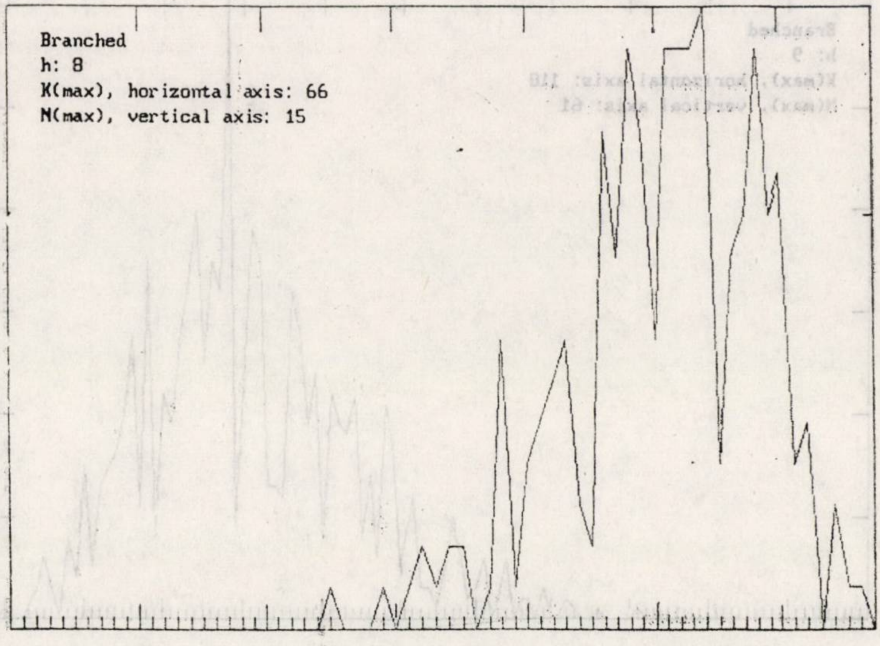

Fig. 2. — As Fig. 1 at $h = 8$.

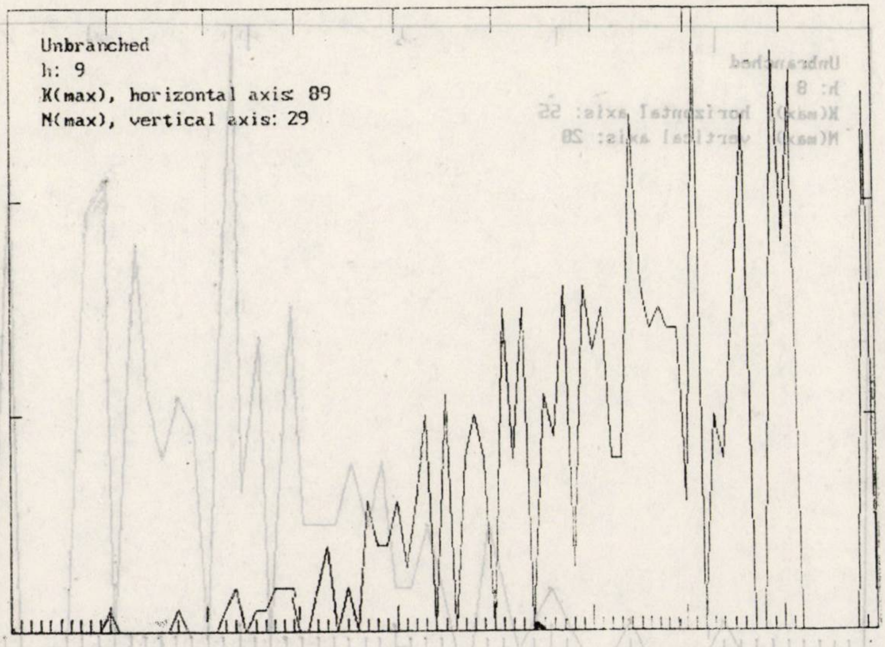

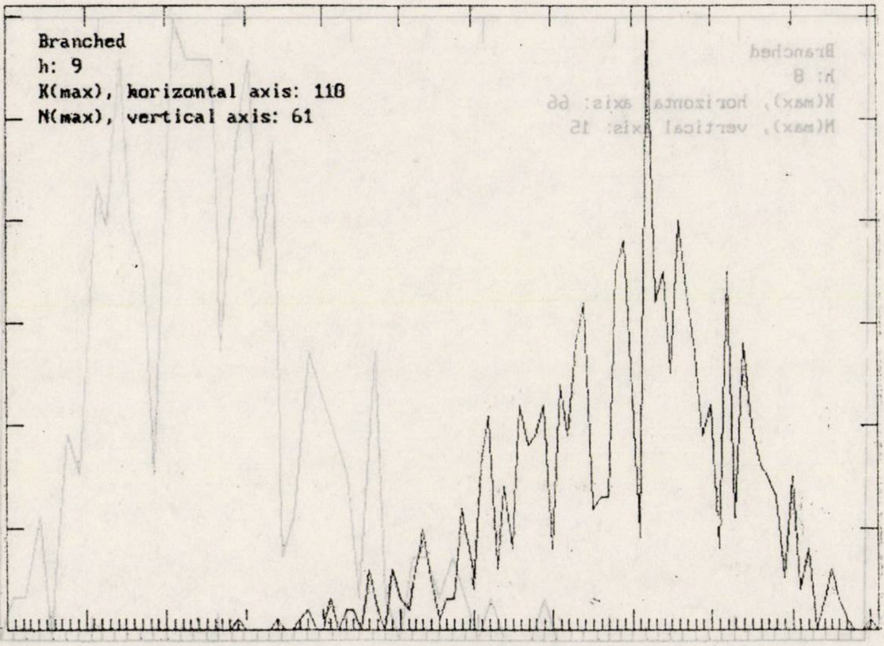

Fig. 3. — As Fig. 1 at $h = 9$.

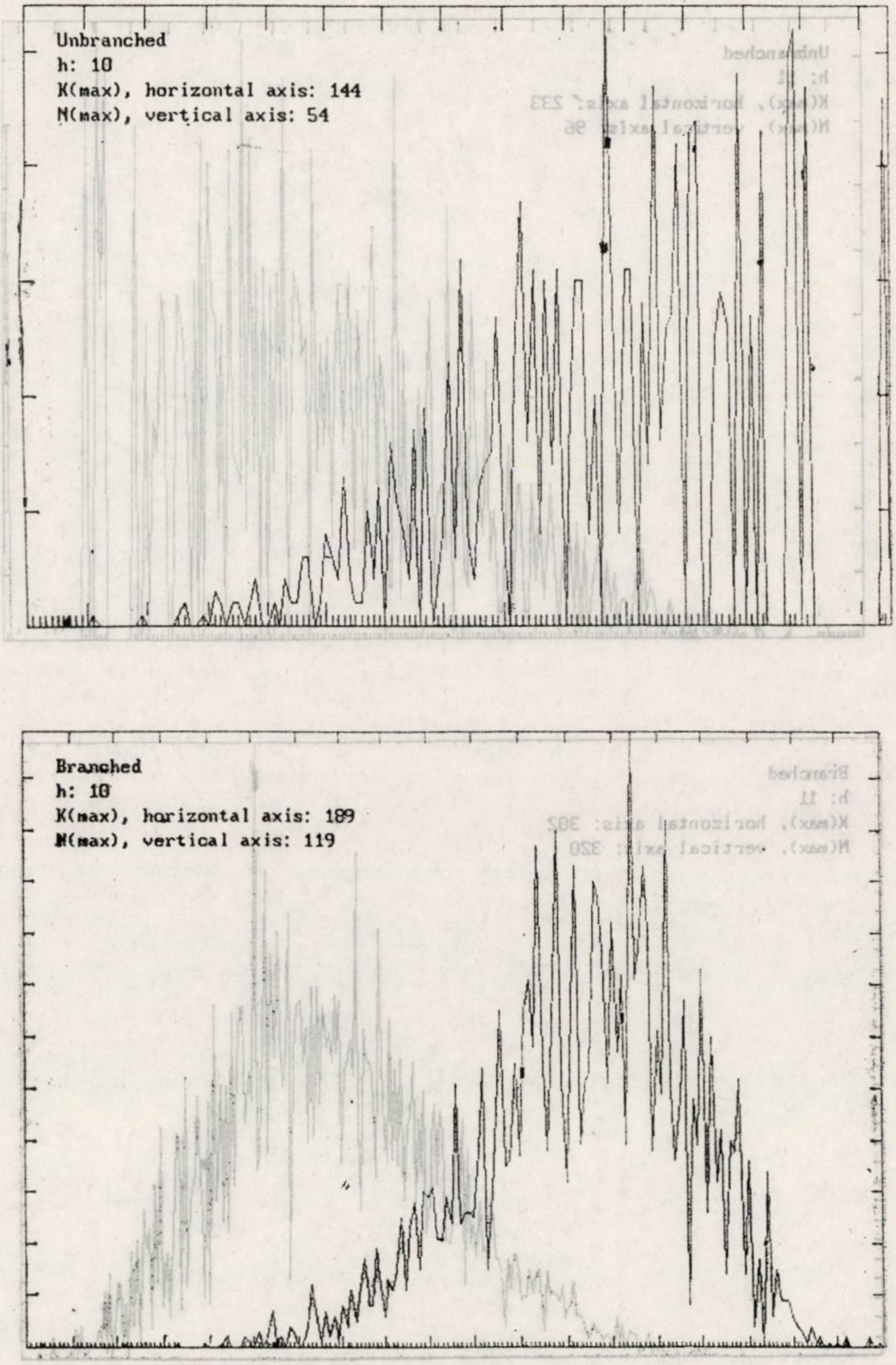

Fig. 4. — As Fig. 1 at $h = 10$.

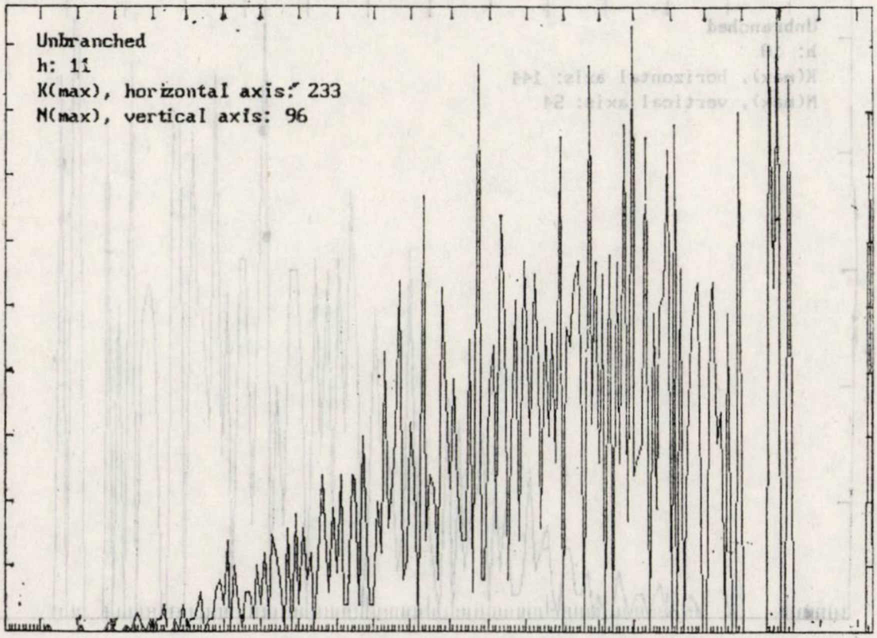

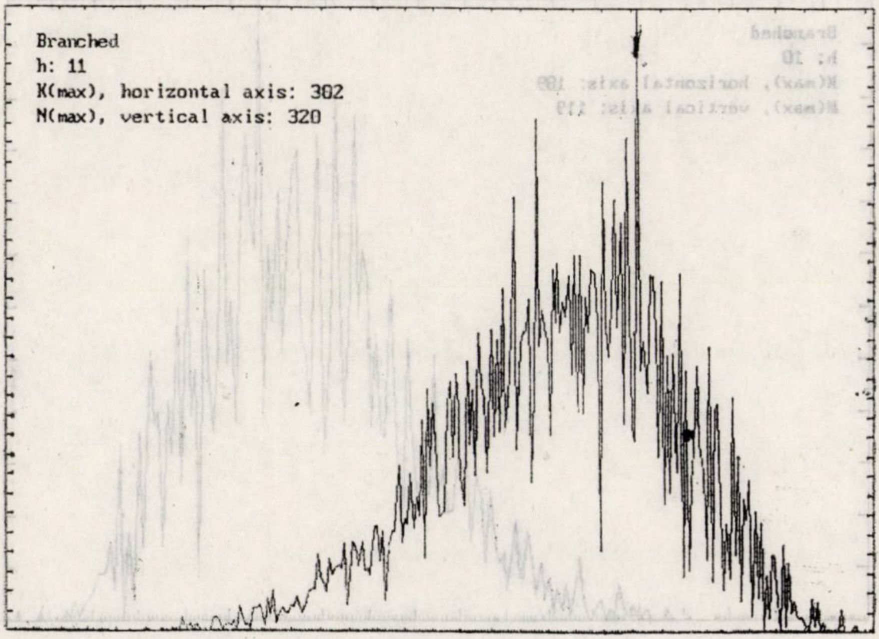

Fig. 5. — As Fig. 1 at $h = 11$.

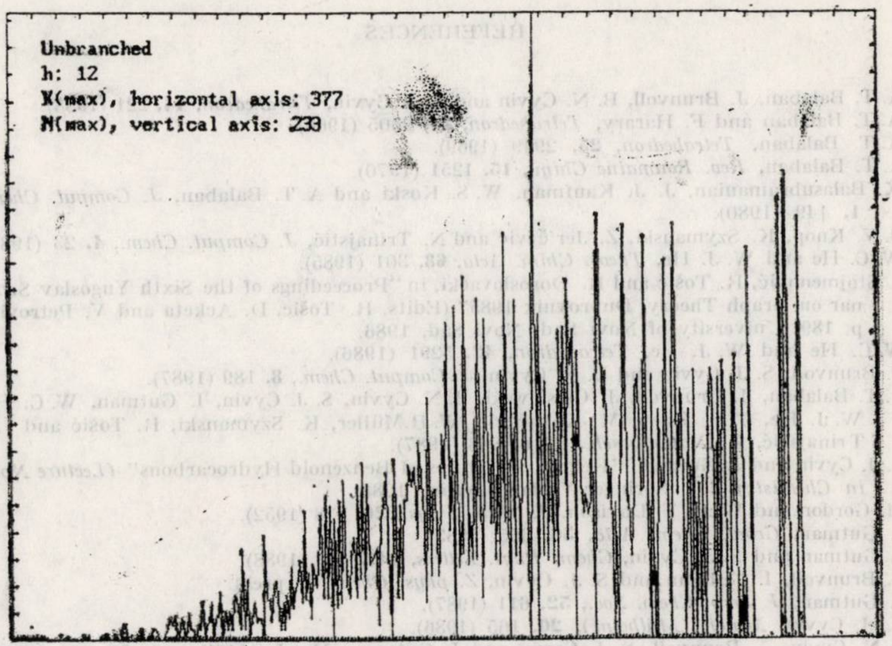

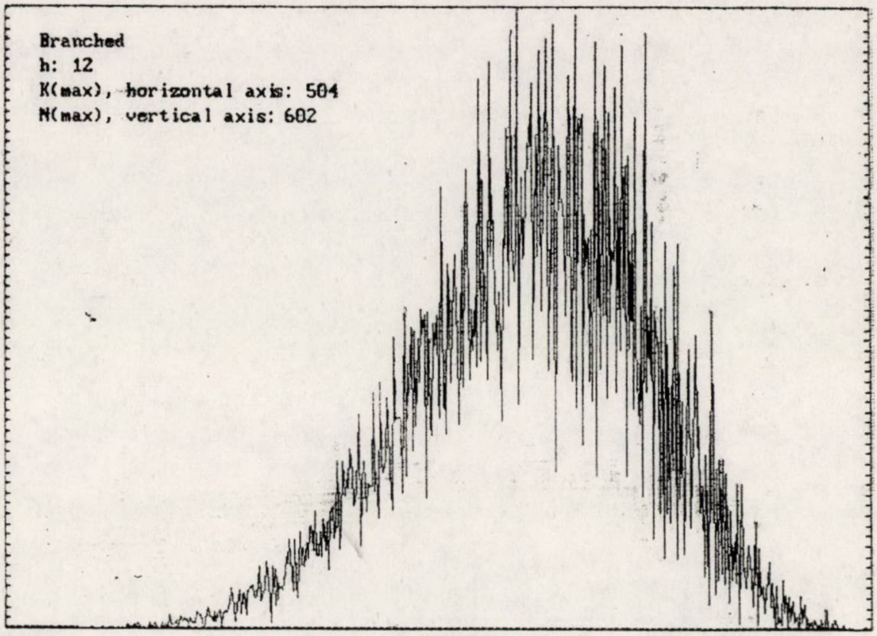

Fig. 6. — As Fig. 1 at $h = 12$.

REFERENCES

[1] A. T. Balaban, J. Brunvoll, B. N. Cyvin and S. J. Cyvin, *Tetrahedron*, **44**, 221 (1988).
[2] A. T. Balaban and F. Harary, *Tetrahedron*, **24**, 2505 (1968).
[3] A. T. Balaban, *Tetrahedron*, **25**, 2949 (1969).
[4] A. T. Balaban, *Rev. Roumaine Chim.*, **15**, 1251 (1970).
[5] K. Balasubramanian, J. J. Kaufman, W. S. Koski and A. T. Balaban, *J. Comput. Chem.*, **1**, 149 (1980).
[6] J. V. Knop, K. Szymanski, Ž. Jeričević and N. Trinajstić, *J. Comput. Chem.*, **4**, 23 (1983).
[7] W. C. He and W. J. He, *Theor. Chim. Acta*, **68**, 301 (1985).
[8] I. Stojmenović, R. Tošić and R. Doroslovački, in "Proceedings of the Sixth Yugoslav Seminar on Graph Theory, Dubrovnik 1985" (Edits. R. Tošic, D. Acketa and V. Petrović), p. 189; University of Novi Sad, Novi Sad, 1986.
[9] W. C. He and W. J. He, *Tetrahedron*, **42**, 5291 (1986).
[10] J. Brunvoll, S. J. Cyvin and B. N. Cyvin, *J. Comput. Chem.*, **8**, 189 (1987).
[11] A. T. Balaban, J. Brunvoll, J. Cioslowski, B. N. Cyvin, S. J. Cyvin, I. Gutman, W. C. He, W. J. He, J. V. Knop, M Kovačević, W. R.Müller, K. Szymanski, R. Tošić and N. Trinajstić, *Z. Naturforsch.*, **42 a**, 863 (1987).
[12] S. J. Cyvin and I. Gutman, "Kekulé Structures of Benzenoid Hydrocarbons" *(Lecture Notes in Chemistry* 46), Springer-Verlag, Berlin, 1988.
[13] M. Gordon and W. H. T. Davison, *J. Chem. Phys.*, **20**, 428 (1952).
[14] I. Gutman, *Croat. Chem. Acta*, **56**, 365 (1983).
[15] I. Gutman and S. J. Cyvin, *Chem. Phys. Letters*, **147**, 121 (1988).
[16] J. Brunvoll, I. Gutman and S. J. Cyvin, *Z. phys. Chem.*, in press.
[17] I. Gutman, *J. Serb. Chem. Soc.*, **52**, 611 (1987).
[18] S. J. Cyvin, *Match (Mülheim)*, **20**, 165 (1986).
[19] B. N. Cyvin, J. Brunvoll, S. J. Cyvin and I. Gutman, *Match (Mülheim)*, **21**, 301 (1986).
[20] S. J. Cyvin, J. Brunvoll and B. N. Cyvin, *Z. Naturforsch.*, **41a**, 1429 (1986).

Revue Roumaine de Chimie, **35**, *1*, 97—103 (1990)

DIFFUSION OF VANADIUM IN IRON IN SURFACE COATINGS AND CALCULATION OF DIFFUSION COEFFICIENTS

N. PETRESCU[a], MARIA PETRESCU[a] and MIRELA BRIŢCHI[b]
[a] **Polytechnic Institute of Bucharest, Faculty of Metallurgy, Spl. Independenţei 313, Romania**
[b] Physical Chemistry Center, ICECHIM, Spl. Independenţei 202, Bucharest 77208, Romania

Received February 28, 1989

The diffusion of vanadium in Armco iron has been investigated by tracing the penetration curve using the microprobe quantitative point analysis across the diffusion layers obtained by pack cementation in a powder mixture comprising ferro-vanadium, NH_4Cl and Al_2O_3. The diffusion layers have been studied by optical microscopy, electronic microprobe analysis and microhardness determinations. The penetration curves of the diffusing element traced by using microprobe quantitative point analysis allowed the calculation of the interdiffusion coefficients in the V-Fe system. Both Boltzmann-Matano and modified Grube methods have been used for deriving the diffusion coefficients. In applying the Boltzmann-Matano method a graphical determination and a computer program have been used to calculate the diffusion coefficients. The interdiffusion coefficients in the V-Fe system determined at 1100°C were composition dependent, in a range of values 1.5×10^{-9}/s (for $N_v = 0.326$) to 5.65×10^{-9} cm²/s (for $N_v = 0.021$).

Metallic diffusion coatings stand as a convenient manner for surface alloying resulting in protective layers strongly bonded to the support material. Such diffusion coatings are highly superior in chemical resistance and mechanical properties, as compared to the uncoated material. Moreover diffusion coatings offer an experimental basis for calculating diffusion coefficients in metallic systems.

The paper presents the experimental results on the diffusion of vanadium in iron carried out by pack cementation of pure iron samples in ferro-vanadium powders.

EXPERIMENTAL

The Fe-V diffusion couple was set up by reducing the vanadium from its chloride at the surface of an Armco iron sample packed up in a powder mixture comprising ferro-vanadium and NH_4Cl. The conditions for the thermochemical treatment and the composition of the powder mixture are given in table 1. The principles of the metal diffusion coating process were dealt with in a previous paper. [1]

The iron samples (pure Armco iron with carbon content ~0.006 w%) were packed up in the powder mixture in refractory steel boxes tightly sealed with a mixture of kaolin 70%, Al_2O_3 20%, Na_2SiO_3solution 10%. The boxes were slowly heated in an electrical furnace, from 20° to 500°C, then heated at the treatment temperature and held for a definite time.

Table 1

Powder mixture composition and conditions of thermochemical treatment

Composition of the powder mixture, %			Temp. (°C)	Time (hours)
Ferro-vanadium (80% V; <0.012% C; 0.25—0.50 mm) %	Al_2O_3 %	NH_4CL %		
78	20	2	1100	10

The diffusion layer was analyzed by optical and electron microscopy, by microprobe quantitative determination of the chemical composition and by microhardness measurements.

The thickness of the diffusion layers vanadized for 10 hours at 1100°C was about 370 μm (Fig. 1a). The microhardness measurements in the diffusion layer presented values, between 110 and 56 HV, with a continuous decrease from the outer surface to the inner interface (Fig. 1b). This type of hardness decrease is characteristic for a solid solution. This conclusion is supported by the decreasing vanadium concentration in the diffusion layer pointed out by the X ray intensity profile of $V_{K\alpha}$ recorded in the microprobe image (Fig. 1c).

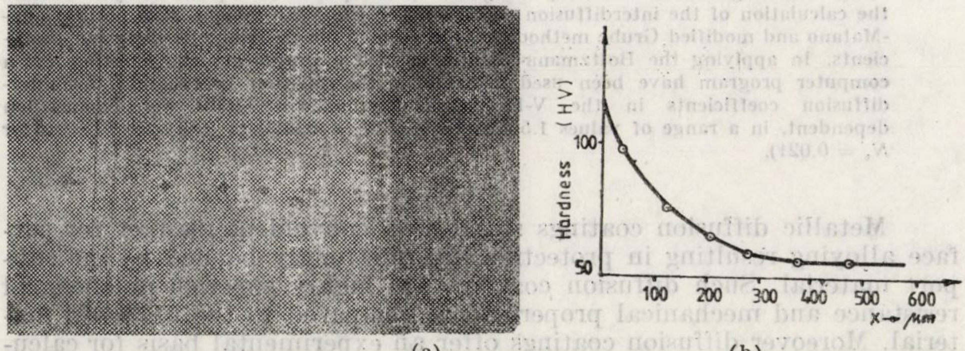

(a) (b)

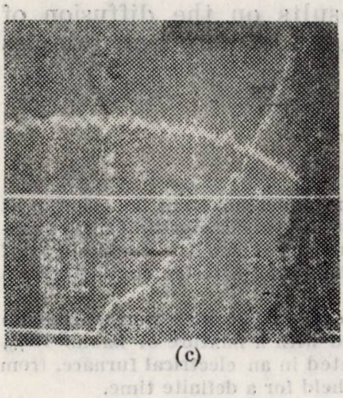

(c)

Fig. 1. — Diffusion layer on Armco iron obtained by diffusion of vanadium 10 hours at 1100°C.
1a) optical micrograph 100 :1 with microhardness identations;
1b) microhardness variation across the layer width;
1c) microprobe composition image 150 : 1 (reduced to 1/2 in photo); superimposed are the X ray intensity profiles for V_{K_α} and Fe_{K_α} across the layer width.

The interdiffusion coefficients in the Fe-V system have been derived from the experimental data by means of the Boltzmann-Matano method and by means of the modified Grube method[2] These methods relevant to diffusion in binary systems require the concentration profile of the diffusing element traced across the diffusion layer. The penetration profile of vanadium has been established in our research through microprobe analysis. The concentrations of vanadium and iron have been determined in different points across the layer thickness, by counting the pulses of $V_{K\alpha}$ and $Fe_{K\alpha}$ characteristic X-rays, in comparison with a standard sample of pure V and pure Fe. The ratio of X-ray intensity in the sample and in the standard represents the relative concentration of the diffusing element in the analyzed point in the diffusion layer. The relative concentrations have been subjected to a computer program (in FORTRAN) for correcting the atomic number effect, for self-absorption and for fluorescence. The corrected relative concentrations have been transformed into molar fraction of V and Fe. The data thus obtained are given in table 2.

Table 2

Molar fractions of vanadium and iron *versus* the depth in the diffusion layer.

No.	Depth from surface $x \cdot 10^2$(cm)	N_V	N_{Fe}
1	0.060	0.311	0.689
2	0.400	0.242	0.758
3	0.733	0.196	0.804
4	1.066	0.146	0.854
5	1.400	0.115	0.885
6	1.733	0.090	0.910
7	2.066	0.070	0.930
8	2.400	0.055	0.945
9	2.733	0.041	0.959
10	3.066	0.033	0.967
11	3.400	0.023	0.977
12	3.733	0.011	0.989
13	4.066	0.00015	0.99975

N_V şi N_{Fe} ar molar fractions of V and Fe

The penetration curve of vanadium in the diffusion layer is represented in fig. 2.

The limit of the γ solid solution (FCC crystal lattice) at 1100°C in the Fe-V system has been established at $N_V = 0.018$ molar fraction through examination of the vanadium penetration curve. This figure has been derived as the coordinate of the point of low vanadium concentration in the penetration curve, assuming that the sudden decrease is to be ascribed to passing in the α solid solution (BCC crystal lattice). The value of the limit of the γ domain in the Fe-V phase equilibrium diagram differs according to different authors : Hansen[3] gives a value $N_V = 0.0164$, while Müller[4] gives $N_V = 0.0208$. Our value stands between these two figures, so that we have used it ($N_V = 0.018$) in calculating the interdiffusion coefficients through the Matano-Boltzmann method.

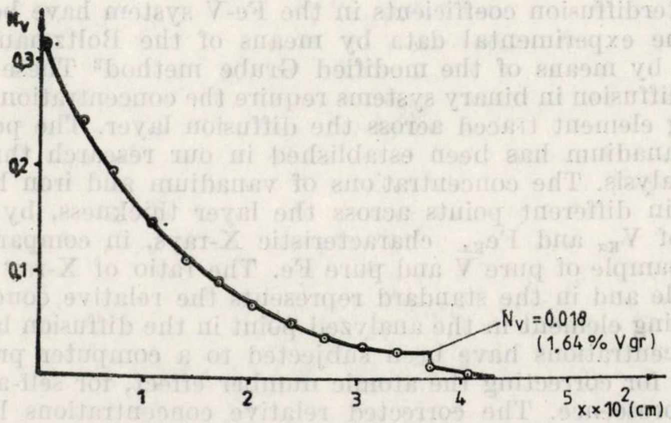

Fig. 2. — The penetration curve of vanadium in Armco iron for a diffusion time 10 hours at 1100°C (vanadium concentration values determined by microprobe quantitative point analysis).

Determination of the interdiffusion coefficients by the Matano-Boltzmann method

The Matano-Boltzmann method allows the interdiffusion coefficients to be calculated in metallic diffusion couples where the two diffusing elements migrate at different rates[5]. The basic equation is:

$$\widetilde{D}_{A-B} = -\frac{1}{2t}\left(\frac{dx}{dN_A}\right)\int_{0}^{N_A} x \cdot dN_A \qquad (1)$$

where: t is the diffusion time; dx/dN_A is the inverse of the tangent at the penetration curve in point of concentration N_A; $\int_0^{N_A} x \cdot dN_A$ is the area of the surface under the penetration curve starting from point N_A.

To solve equation (1) one has to localize the Matano plane. This plane is the initial surface through which the number of element A atoms passing in one direction is equal to the number of element B atoms passing in the opposite direction. In a binary diffusion couple, where the two component elements have different diffusion rates the original surface moves a distance x_M from its initial position. This displacement, x_M, of the original surface can be determined from measuring the sample size before and after diffusion.

The interdiffusion coefficients calculated by the Matano-Boltzmann method from our experimental data are given in table 3.

The main source of errors in the interdiffusion coefficients derived by the Matano-Boltzmann method lies in the establishment of the position of the tangents. To minimize this source of errors a computer program has been written in FORTRAN for tracing the best penetration

Table 3

The interdiffusion coefficients, $\widetilde{D}$, in the Fe-V system graphically derived through the Boltzmann-Matano method

No.	N_V	N_{Fe}	$x \cdot 10^2$ (cm)	$-\frac{dx}{dN_V} 10^2$	$\int_0^{N_V} x dN_V \cdot 10^2$	$\widetilde{D} \cdot 10^9$ (cm²/s)	$\lg\widetilde{D} \cdot 10^9$
1	0.327	0.673	0.000	0.040	0.268	1.49	0.173
2	0.300	0.700	0.110	0.040	0.285	1.58	0.199
3	0.280	0.720	0.200	0.040	0.289	1.61	0.207
4	0.260	0.740	0.300	0.050	0.293	2.03	0.307
5	0.250	0.750	0.360	0.060	0.294	2.45	0.389
6	0.220	0.780	0.550	0.064	0.292	2.59	0.413
7	0.200	0.800	0.690	0.074	0.288	2.96	0.471
8	0.180	0.820	0.840	0.080	0.282	3.13	0.495
9	0.160	0.840	0.990	0.080	0.272	3.02	0.480
10	0.140	0.860	1.150	0.083	0.259	3.00	0.477
11	0.120	0.880	1.355	0.110	0.243	3.71	0.569
12	0.100	0.900	1.580	0.100	0.223	3.09	0.490
13	0.080	0.920	1.890	0.173	0.197	4.73	0.675
14	0.060	0.940	2.300	0.222	0.164	5.04	0.702
15	0.040	0.960	2.780	0.267	0.122	4.51	0.654
16	0.032	0.968	3.066	0.350	0.104	5.04	0.702

Note : — diffusion time $t = 36000$ s ; $1/2t = 1.389 \times 10^{-9}$ s^{-1} ;
— Matano plane at $x_M = 0.00437$ cm.

curve through the experimental points and for calculating the tangents. The computer program makes use of a polynomial equation of superior order equal to the number of experimental points. This computer program allows the penetration curve to be traced with minimizing the experimental errors, an accurate calculation of the tangents and of the areas, and finally the deriving of the interdiffusion coefficients. The interdiffusion coefficients in the Fe-V system derived by means of this computer program are listed in table 4.

Figures 3a and 3b present the dependence of the interdiffusion coefficient in the Fe-V system versus iron concentration, as obtained by a graphical establishment of the tangents and areas (Fig. 3a) in comparison with the computer program derivation (Fig. 3b). It is obvious that the computer derived values of the diffusion coefficients fit better on the curve than the values obtained by graphical operation.

Figure 3 points to a continuous increase of the interdiffusion coefficient as the iron content increases (or as the vanadium content decreases) in the Fe-V system. For the experimental conditions used (diffusion time 10 hours, temperature 1100°C) the values of the interdiffusion coefficients in the Fe-V system vary from 1.5×10^{-9} to 5.65×10^{-9} cm²/s (Table 4). These values are about one order of magnitude larger than the values derived by the Grube method[4] in which a constancy of the interdiffusion coefficient in the whole concentration range was assumed. In this form the Grube method is of poor precision, as it takes into account only the extreme values of the vanadium concentration in the diffusion layer.

Table 4

The interdiffusion coefficients $\widetilde{D}$, in the Fe-V system determined through a computer program

No.	N_V	N_{Fe}	$\widetilde{D} \cdot 10^9$ (cm²/s)	$\lg\widetilde{D} \cdot 10^9$	No.	N_V	N_{Fe}	$\widetilde{D} \cdot 10^9$ (cm²/s)	$\lg\widetilde{D} \cdot 10^9$
1	0.326	0.674	1.51	0.179	27	0.171	0.829	3.20	0.505
2	0.320	0.680	1.57	0.196	28	0.165	0.835	3.27	0.515
3	0.314	0.686	1.63	0.212	29	0.159	0.841	3.35	0.525
4	0.308	0.692	1.68	0.225	30	0.153	0.847	3.43	0.535
5	0.302	0.698	1.75	0.243	31	0.147	0.853	3.52	0.546
6	0.296	0.704	1.81	0.258	32	0.140	0.860	3.60	0.556
7	0.290	0.710	1.87	0.272	33	0.135	0.865	3.69	0.567
8	0.284	0.716	1.93	0.286	34	0.129	0.871	3.78	0.577
9	0.278	0.722	1.99	0.300	35	0.127	0.877	3.88	0.589
10	0.272	0.728	2.06	0.314	36	0.117	0.883	3.98	0.599
11	0.266	0.734	2.13	0.328	37	0.111	0.889	4.08	0.617
12	0.260	0.740	2.19	0.340	38	0.105	0.895	4.18	0.621
13	0.254	0.746	2.26	0.354	39	0.099	0.901	4.28	0.631
14	0.248	0.752	2.32	0.365	40	0.093	0.907	4.39	0.642
15	0.242	0.758	2.39	0.378	41	0.087	0.913	4.49	0.652
16	0.237	0.763	2.45	0.389	42	0.081	0.919	4.59	0.661
17	0.231	0.769	2.51	0.400	43	0.075	0.925	4.69	0.671
18	0.225	0.775	2.58	0.411	44	0.069	0.931	4.78	0.680
19	0.219	0.781	2.64	0.422	45	0.063	0.937	4.86	0.687
20	0.213	0.787	2.71	0.433	46	0.057	0.943	4.94	0.694
21	0.207	0.793	2.78	0.444	47	0.051	0.949	4.98	0.697
22	0.200	0.800	2.84	0.453	48	0.045	0.955	5.03	0.701
23	0.195	0.805	2.92	0.465	49	0.039	0.961	5.03	0.701
24	0.189	0.811	2.98	0.474	50	0.033	0.967	5.02	0.701
25	0.183	0.817	3.05	0.484	51	0.027	0.973	5.04	0.702
26	0.177	0.823	3.12	0.494	52	0.021	0.979	5.65	0.752

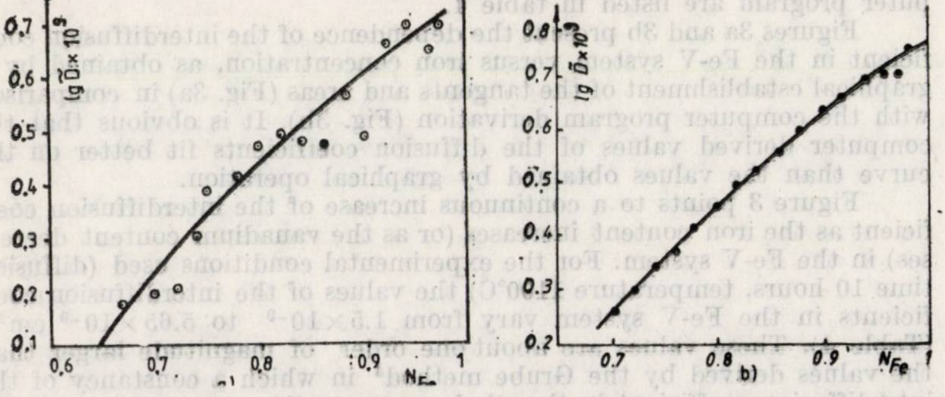

Fig. 3. — Interdiffusion coefficients versus iron concentration in the V-Fe system at 1100°C (semi-logarithmic scale)

a) values derived graphically by the Boltzmann-Matano method;

b) values obtained by means of the computer program.

The Grube method can be applied in a modified manner if a large number of concentration determinations across the diffusion layer width are available, as was the case in our work.

Determination of the interdiffusion coefficients by a modified Grube method

The solution of the second Fick's law for a semi-infinite diffusion system is:

$$\frac{C_s - C_x}{C_s - C_0} = \mathrm{erf}\left[\frac{x}{2(\tilde{D}t)^{1/2}}\right] \tag{2}$$

where: C_s is the concentration at the interface; C_x is the concentration at depth x; C_0 is the initial concentration at zero diffusion time; x is the location (depth) of the point of concentration C_x on the penetration curve; $\tilde{D}$ is the interdiffusion coefficient; t is the diffusion time.

The general form of the Gauss error function is:

$$\mathrm{erf}(z) = \frac{2}{\pi^{1/2}}\int_0^z e^{-y^2}\cdot \mathrm{d}y \tag{3}$$

The numerical computed values are available in tabular form. The equation can be applied in a system where the interdiffusion coefficient is concentration dependent, if one divides the penetration curve in small enough regions, so that the interdiffusion coefficient can be taken as constant. This way one gets a series of values for $\tilde{D}$, each of them representative for the narrow concentration range used for its derivation.

We applied the modified Grube method by introducing in eq. (2) our experimental data on vanadium concentration across the diffusion layer. The values of the interdiffusion coefficient in the Fe-V system at 1100°C obtained by the modified Grube method were close to those obtained by the Matano-Boltzmann method.

REFERENCES

[1] Suzana Gâdea, N. Petrescu, Maria Petrescu and Mirela Brițchi, *Metalurgia*, **38**, 549 (1986).

[2] Giles F. Carter, *J. Less-Common Metals*, **37**, 189 (1974).

[3] Hansen M. and Anderko K., "Constitution of Binary Alloys" New York, Mc Graw-Hill Book Comp., 1958.

[4] H. Müller, *HTM*, **28**, 247 (1973).

[5] Chassin C. and Hilly G., "Metallurie d'aliages metalliques", Paris DUNOD, p. 96, 1973.

The Grube method can be applied in a modified manner if a large number of concentration determinations across the diffusion layer width are available, as was the case in our work.

Determination of the interdiffusion coefficients by a modified Grube method

The solution of the second Fick's law for a semi-infinite diffusion system is:

$$\frac{C_x - C_s}{C_s - C_0} = \operatorname{erf}\left[\frac{x}{2(\bar{D}t)^{1/2}}\right] \qquad (2)$$

where: C_s is the concentration at the interface; C_x is the concentration at depth x; C_0 is the initial concentration at zero diffusion time; x is the location (depth) of the point of concentration C_x on the penetration curve; $\bar{D}$ is the interdiffusion coefficient; t is the diffusion time.

The general form of the Gauss error function is:

$$\operatorname{erf}(z) = \frac{2}{\pi^{1/2}} \int_0^z e^{-y^2}\, dy \qquad (3)$$

The numerical computed values are available in tabular form. The equation can be applied in a system where the interdiffusion coefficient is concentration dependent, if one divides the penetration curve in small enough regions, so that the interdiffusion coefficient can be taken as constant. This way one gets a series of values for $\bar{D}$, each of them representative for the narrow concentration range used for its derivation.

We applied the modified Grube method by introducing in eq. (2) our experimental data on vanadium concentration across the diffusion layer. The values of the interdiffusion coefficient in the Fe-V system at 1100°C obtained by the modified Grube method were close to those obtained by the Matano-Boltzmann method.

REFERENCES

[1] Suzana Gâdea, N. Petrescu, Maria Petrescu and Mirela Britchi, *Metalurgia*, 38, 549 (1986).
[2] Giles F. Carter, *J. Less-Common Metals*, 37, 180 (1974).
[3] Hansen M. and Anderko K., "Constitution of Binary Alloys" New York, Mc Graw-Hill Book Comp., 1958.
[4] H. Müller, *NTM*, 28, 247 (1973).
[5] Chassin C. and Hilly G., "Metallurie d'alliages metalliques", Paris DUNOD, p. 96, 1973.

Revue Roumaine de Chimie, 35, *1*, 105–109 (1990)

GENERALIZED CORRELATION FOR VAPOR PRESSURES OF ORGANIC COMPOUNDS*

FRANCISC A. GOTHÁRD,[a] ** GHEORGHIȚA JINESCU[b] and VICTORIA SĂVESCU[c]
[a]Romanian Institute for Research, Design and Development for Oil Refineries, Ploiești
[b]Polytechnic Institute, Bucharest, Romania
[c]Research Center for Chemical Fertilizers, Craiova, Romania

Received August 18, 1989

The correlation given by Lee and Kessler (1975) for the temperature dependence of saturated vapor pressures of nonpolar compounds was extended in order to be used also for polar or associative substances by including an additional term with three adjustable parameters. The predicting performances of the new correlation are compared with those of the Antoine equation, in temperature ranges where the use of this equation is recommended, on various reference data sets and organic compounds including hydrocarbons, alcohols, aldehydes, ketones, acids, esters. In most cases the use of the new correlation improves significantly the result of the data reduction.

INTRODUCTION

Accurate prediction of saturated vapor pressures of pure components is required in all computations related to thermodynamic analysis or reduction of binary or multicomponent liquid-vapor equilibrium data.[1] Although many correlations were proposed to describe the temperature dependence of saturated vapor pressures, especially for organic compounds,[2] in most of recent papers the equation given 100 years ago by Antoine [3]

$$\lg P^s = A - \frac{B}{C + t} \tag{1}$$

is still considered, containing three adjustable parameters A, B and C. This correlation is a very suitable one in temperature ranges as wide as 50 K. For larger temperature ranges, various other correlations are recommended, and especially the equations based on the principle of corresponding states are suitable, e.g. the correlation given by Lee and Kessler [4] for nonpolar compounds:

$$\ln(P^s/P_c) = f^{(0)}_{\mathrm{TR}} + \omega \cdot f^{(1)}_{\mathrm{TR}} \tag{2}$$

where $f^{(0)}_{\mathrm{TR}}$ and $f^{(1)}_{\mathrm{TR}}$ are empirical functions of the reduced temperature T/T_c given in tabular form or as equations as in the extensive compilation published by Ambrose [5]:

---

* Communication at the 3rd National Congress of Chemistry, Bucharest, September 1988.

** Deceased on July 18, 1989

$$f_{Tr}^{(0)} = 5.92714 - 6.09648/\mathrm{Tr} - 1.28862 \cdot \ln \mathrm{Tr} + 0.169347 \cdot \mathrm{Tr}^6 \quad (3)$$

$$f_{Tr}^{(1)} = 15.2518 - 15.6875/\mathrm{Tr} - 13.4723 \cdot \ln \mathrm{Tr} + 0.43577 \cdot \mathrm{Tr}^2 \quad (4)$$

In this contribution the extension of this correlation to polar and associative compounds is attempted.

METHOD

In a first attempt the extension of equations (2)—(4) for predicting saturated vapor pressures of polar and associative organic compounds, was made by including in equation (2) and additional term to give

$$\ln(P^s/P_c) = f_{Tr}^{(0)} + \omega \cdot f_{Tr}^{(1)} + f_{Tr}^{(2)} \quad (5)$$

where, for the function $f_{Tr}^{(2)}$ the following three-parameter equation was selected:

$$f_{Tr}^{(2)} = a + b \cdot \mathrm{Tr}^{-n} \quad (6)$$

In this contribution the predicting performances of the equations (5)—(6) are compared with the results of the reductions of saturated vapor pressures using the Antoine equation (1) in temperature ranges where the Antoine equation is recommended for predicting vapor pressures of pure organic compounds. In this order, selected vapor pressures from the compilation of Boublík et al.[6] were considered.

RESULTS

The results of the reduction of the reference data to the parameters in equations (5)—(6) are given in table 1 together with the deviations of the predicted vapour pressures using the Antoine equation (1) with constants given in the compilation of Boublík et al.[6] All reducing parameters were considered from the data bank included in the treatise of Reid et al.,[19] and reproduced also in the table.

For 252 data points belonging to 19 data sets, the new correlation leads to r.m.s. of 0.78 Torr, whilst the use of the Antoine equation to 0.89 Torr. The largest deviations are, in the case of the data for acetaldehyde, 4.88 Torr for the Antoine equation, 4.28 Torr for the new correlation (5)—(6). In 14 from the 19 data sets the new correlation improves the prediction of the saturated vapor pressures.

CONCLUSIONS

1. The correlation given by Lee and Kessler,[4] based on the principle of the corresponding states with three parameters for predicting saturated vapor pressures of pure organic nonpolar compounds, may be extended

Table 1

The results of the reduction of reference vapor pressure data for pure organic compounds to the parameters in equations (5)–(6) compared with the results given [6] using the Antoine equation

Compounds	No. of data	Temperature range, K	Reference from [6]	Reducing parameters			The constants in the Antoine equation (1) for P^s /Torr, t/°C			R.m.s. deviation, P^s, Torr	The constants in equation (6),			R.m.s. deviation, P^s, Torr
				T_c K	P_c Ata	ω —	A	B	C		a	b	n	
n-Pentane	9	286–310	7	469.6	33.3	0.251	6.84471	1060.793	231.541	0.82	0.00057	−1.00957	−8.0	0.54
n-Hexane	16	286–343	7	507.4	29.3	0.296	6.88555	1175.817	224.867	0.24	−0.11547	0.03536	2.0	0.22
n-Heptane	20	299–372	7	540.2	27.0	0.351	6.90253	1267.828	216.823	0.09	−0.18226	0.07134	1.65	0.15
Cyclohexane	17	294–355	7	553.4	40.2	0.213	6.84941	1206.001	223.148	0.32	0.00188	−0.31323	−6.0	0.32
Methanol	17	288–357	8	512.6	79.9	0.559	8.08097	1582.271	239.726	0.18	−0.19818	0.01269	5.7	0.46
Ethanol	8	273–352	9	516.2	63.2	0.635	8.16556	1624.08	228.993	0.33	−0.14129	0.00294	6.8	0.41
2-Propanol	19	325–362	8	508.3	47.0	0.248	7.74021	1359.517	197.527	0.07	1.12963	−1.03248	2.03	0.05
Isobutyl alcohol	17	353–389	10	547.7	42.4	0.588	7.29491	1230.81	170.947	0.06	0.37157	−0.02324	5.0	0.03
n-Butanol	16	362–399	10	562.9	43.6	0.590	7.36366	1305.198	173.427	0.08	0.30886	−0.02521	4.6	0.05
Acetaldehyde	10	273–308	11	461.15	51.4	0.275	8.00558	1600.017	291.809	4.88	−0.04749	0.000018	16.0	4.28
Isobutyraldehyde	10	286–336	12	513.0	41.0	0.35	6.73513	1053.178	209.134	0.41	4.620804	−4.97344	−0.2	0.37
Acetone	8	310–329	13	508.1	46.4	0.24	7.15857	1231.232	231.76	0.12	−0.112423	0.16048	4.0	0.10
Methyl-ethyl-ketone	17	316–361	14	535.6	41.0	0.329	7.06356	1261.339	221.969	0.30	−0.109752	0.016294	3.8	0.25
Formic acid	5	310–374	15	580.0	84.06	0.7396	7.58178	1699.173	260.714	1.18	−1.4593	0.7469	2.45	1.07
Propionic acid	6	330–413	15	612.0	53.0	0.536	7.71423	1733.418	217.724	1.64	−0.1479	0.0049	6.5	1.60
Butyric acid	8	363–400	15	628.0	52.0	0.67	7.7399	1764.68	199.892	0.87	−0.2113	0.01496	4.5	0.82
Ethyl formiate	13	277–327	17	508.0	46.8	0.283	7.00902	1123.943	218.247	0.25	−0.02147	−0.037	3.4	0.26

Table 1 (continued)

Ethyl acetate	16	289–349	18	523.2	37.9	0.363	7.10179	1244.451	217.831	0.70	−0.20379	0.10303	1.0	0.14
Acrylic acid	6	293–343	20	615.0	56.0	0.56	5.65204	648.629	154.683	10.2	−0.81602	1.0930	2.0	6.49
1,1,2-Trichloroethane	5	323–386	15	602.0	41.0	0.22	6.95185	1314.410	209.197	0.06	0.0550	−0.023703	3.75	0.09
Chloromethane	10	183–249	21	416.3	65.9	0.156	6.9876	899.739	242.921	0.19	0.05928	−0.5844	−4.5	0.09
Pyridine	5	340–426	22	620.0	55.6	0.24	7.04115	1373.799	214.979	0.15	0.042135	−0.1255	−1.2	0.26
Propionitrile	5	308–370	15	564.4	41.3	0.318	6.83945	1221.99	211.240	2.98	−0.218954	0.0658	2.5	1.74
Propylene	12	165–225	20	365.0	45.6	0.148	6.82359	786.532	247.243	0.25	0.093346	−0.3398	−2.95	0.14
1,3-Butadiene	12	197–271	24	425.0	42.7	0.195	6.85364	933.586	239.511	0.30	0.49458	−0.63559	−0.50	0.84
n-Butane	11	195–272	25	425.2	37.5	0.193	6.82485	943.453	239.711	0.70	0.02785	−0.1665	−2.0	0.64
Cyclopentane	11	288–323	7	511.6	44.5	0.192	6.90325	1132.868	232.375	0.05	0.41403	−0.4993	−0.25	0.04
1-Pentanol	19	347–429	26	586.0	38.0	0.58	7.18246	1287.625	161.330	0.91	−0.1546	−0.01296	6.0	0.45
Carbon tetrachloride	7	292–350	27	556.4	45.0	0.194	6.92180	1235.172	228.937	0.5	−0.23608	0.177837	0.5	0.43
Carbonylsulphide	14	161–223	28	373.0	58.0	0.099	6.90723	804.480	250.00	0.05	−0.013585	−0.00044	8.5	0.09
1,2-Dichlorobenzene	6	403–454	29	697.3	40.5	0.272	7.14378	1704.488	219.416	0.18	−0.041941	0.000057	1.0	0.17
1,3-Dichlorobenzene	6	363–446	15	684.0	38.0	0.260	7.04012	1607.051	213.378	0.24	0.079845	−0.094576	0.5	0.20
1,4-Dichlorobenzene	8	367–447	29	685.0	39.0	0.270	7.02075	1590.883	210.226	0.25	−0.0447717	−0.000061	7.0	0.27
Phenol	6	380–454	15	694.2	60.5	0.440	7.13301	1516.790	174.954	0.10	−0.013254	−1.210882	7.0	0.30

to polar and associative substances by including an additional term to give $\ln(P^s/P_c) = f_{\mathrm{TR}}^{(0)} + \omega f_{\mathrm{TR}}^{(1)} + f_{\mathrm{TR}}^{(2)}$, where $f_{\mathrm{TR}}^{(2)} = a + b \cdot \mathrm{Tr}^{-n}$ and a, b and n are three adjustable parameters.

2. The use of the new correlation improves in many cases the prediction of the saturated vapor pressures even in comparison with the Antoine equation in temperature ranges up to 50 K where this later equation is almost exclusively considered in processing liquid-vapor equilibrium data.

3. The results obtained promoted the extension of the research to large data sets and various other forms of the additional term $f_{\mathrm{TR}}^{(1)}$ with performances to be presented in additional papers.

ACKNOWLEDGMENTS. The authors wish to express grateful thanks to Ion Burlacu and Mihaela Ionescu from the Chemical Works Borzești, as well as to Mihaela Alexe from the Romanian Institute for Research, Design and Development for Oil Refineries in Ploiești for their helpful assistance in programming and computations.

REFERENCES

[1] H. C. Van Ness, S. M. Byer and R. E. Gibbs, *A. I. Ch. E. J.*, **19**, 238 (1971).

[2] F. A. Gothard, G. Jinescu and V. Săvescu, "100 Years of Antoine Equation", The 13rd Romanian Symposium on Fluid Phase Equilibria, Bucharest, June 1988.

[3] A. Antoine, *Compt. rend.*, **107**, 681, 836, 1143 (1888).

[4] B. I. Lee and M. G. Kessler, *J. Amer. Inst. Chem. Engrs.*, **21**, 510 (1975).

[5] D. Ambrose, "Equations for the Correlation and Estimation of Vapour Pressures", NPL Repost CHEM 114, August 1980.

[6] F. Boublik, V. Fried and E. Hála, "The Vapour Pressures of Pure Substances", Elsevier, Amsterdam, 1973.

[7] C. J. Willingham, W. J. Taylor, J. M. Pignocco and F. D. Rossini, *J. Res. Nat. Bur. Stand.*, **35**, 219 (1945).

[8] D. Ambrose and C. H. S. Sparke, *J. Chem. Thermodyn*, **2**, 6316 (1970).

[9] C. B. Kretschmer and R. I. Wiebe, *J. Amer. Chem. Soc.*, **71**, 1793 (1949).

[10] D. P. Biddiscombe, *J. Chem. Soc.*, 1965 (1954).

[11] K. F.Coles and F. Popper, *Ind. Eng. Chem.*, **42**, 1434 (1950).

[12] M. Separkova, S. Paulech and J. Dykyj, *Chem. Zvesti*, **13**, 313 (1959).

[13] I. Brownm and E. I. Smith, *Austral. J. Chem.*, **10**, 423 (1957).

[14] R. R. Collerson et al., *J. Chem. Soc.*, 1965 (3097).

[15] R. R. Dreisbach and S. A. Shrader, *Ind. Eng. Chem.*, **41**, 2879 (1949).

[16] A. E. Potter and H. L. F. Ritter, *J. Phys. Chem.*, **58**, 1040 (1954).

[17] I. Mertl and J. Polak, VZCHR-UTZCHT, Praque, 1964.

[18] I. Mertl and J. Polak, *Coll. Czeh. Chem. Comm.*, **30**, 3526 (1965).

[19] R. C. Reid, J. M. Prausnitz and T. K. Sherwood, "The Properties of Gases and Liquids" 3rd Ed., McGraw-Hill, New York — Tokyo, 1977.

[20] A. N. Gubkov, N. A. Fermor and N. I. Smirnov, *Zhur. priklad.* Khim., **87**, 2204 (1964).

[21] J. Beermans and J. C. Jungers, *Bull. Soc. chim. belges*, **66**, 238 (1947).

[22] J. P. McCullogh et al., *J. Amer. Chem. Soc.*, **79**, 4289 (1957).

[23] T. M. Powell and W. F. Giauque, *J. Amer. Chem. Soc.*, **61**, 2366 (1939).

[24] G. B. Heisig, *J. Amer. Chem. Soc.*, **55**, 2304 (1933).

[25] J. G. Aston and G. H. Messerly, *J. Amer. Chem. Soc.*, **62**, 1917 (1940).

[26] D. Ambrose and C. H. S. Sparke, *J. Chem. Thermodynamics*, **2**, 631 (1970).

[27] D. L. Hildebrand and R. A. McDonald, *J. Phys. Chem.*, **63**, 1521 (1959).

[28] J. D. Kemp and W. F. Giauque, *J. Amer. Chem. Soc.*, **99**, 79 (1937).

[29] R. A. McDonald, S. A. Shrader and D. R. Stull, *J. Chem. Eng. Data*, **4**, 311 (1959).

to point and associated with zero [illegible], including all additional terms to give [illegible] $= k_1^{(0)} + \omega k_1^{(1)} + k_2$, where [illegible] are three adjustable parameters.

2. The use of the new correlation improves [illegible] the prediction of the calculated vapor pressures even in comparison with the Antoine equation in temperature ranges up to 30 [illegible] where this equation is almost exclusively considered in engineering liquid–vapor equilibrium sets.

3. The results obtained, provided the [illegible] of the research to large data sets and various other forms of the additional term [illegible] with performances [illegible] in additional systems.

ACKNOWLEDGMENTS. The authors wish to express [illegible] thanks to [illegible] from the Chemical Works [illegible], as well as [illegible] from the [illegible] Institute for Research, Design and Development for Oil Refineries, in Ploiești, for their help and assistance in programming and computations.

REFERENCES

[1] [illegible] Van Ness, S. [illegible] and R. C. Smith, [illegible] 18, [illegible]
[2] [illegible] "The Theory of [illegible]," [illegible] Symposium on Fluid Phase Equilibria, [illegible]
[3] [illegible] 107, 851, [illegible] (1953).
[4] B. [illegible] and [illegible], J. [illegible] 25, [illegible]
[5] [illegible] "Equations for the [illegible] and [illegible] of [illegible] Pressures," [illegible] Report [illegible], August [illegible]
[6] [illegible] and [illegible] "The Vapour Pressures [illegible]" [illegible] Amsterdam, [illegible]
[7] [illegible] Taylor, [illegible] and [illegible], J. [illegible]
[8] D. Ambrose and [illegible] Sparks, J. Chem. Thermodyn. [illegible]
[9] [illegible] and [illegible], J. [illegible] 73, [illegible]
[10] [illegible], [illegible] 1653 (1956).
[11] [illegible] and [illegible], [illegible] Eng. Chem., 12, [illegible]
[12] [illegible] Phys. [illegible]
[13] [illegible], J. [illegible] 10, 422 [illegible]
[14] [illegible] et al., [illegible]
[15] [illegible] and [illegible] Shreve, [illegible] Eng. Chem., [illegible] 2859 [illegible]
[16] [illegible] and [illegible], [illegible] Phys. Chem., 58, [illegible]
[17] [illegible] and [illegible], [illegible]
[18] [illegible] and [illegible], [illegible] 46, [illegible]
[19] R. C. Reid, J. [illegible] Prausnitz and T. K. Sherwood, "The Properties of Gases and Liquids," 3rd Ed., McGraw-Hill, New York — Toronto, 1977.
[20] A. [illegible], [illegible] and [illegible], [illegible] 67, 2314 [illegible]
[21] [illegible] and [illegible], [illegible]
[22] [illegible] et al., J. [illegible] Chem. Soc., 78, [illegible]
[23] T. M. [illegible] and W. E. [illegible], J. Amer. Chem. Soc., [illegible]
[24] [illegible], J. Amer. Chem. Soc., 56, 2308 [illegible]
[25] [illegible] and G. H. [illegible], J. Amer. Chem. Soc., 52, [illegible]
[26] [illegible] and [illegible], J. Chem. Thermodynamics, 2, [illegible]
[27] [illegible] Hildebrand and [illegible], J. Phys. Chem., [illegible]
[28] [illegible] and [illegible], J. Amer. Chem. Soc., [illegible]
[29] H. A. McDonough [illegible] and [illegible] Stull, J. Chem. [illegible]

Revue Roumaine de Chimie, 35, 1, 111 (1990)

BOOK REVIEW

A. Krief, L. Hevesi, "Organoselenium Chemistry I — Functional Group Transformations", Springer Verlag, Berlin, 1988. 220 pp, hard-cover, 186 DM, ISBN 3-540-18629-8.

Professors Alain Krief and Laszlo Hevesi from the University of Namur, Belgium, are well known for their work in organiselenium chemistry. In a joint effort, they offer this volume which is to be the first in a two-volume series covering their field of interest. In this first volume, syntheses using selenium reagents are comprehensively reviewed. Only those reactions are described which do not involve the isolation of the selenium-containing intermediate and are thus "one-step" procedures for various functional group transformations. A future second volume will describe more than one-step transformations which involve the isolation (and purification) of stable organoselenium intermediates, as well as a detailed review of the methods of preparation for the various selenium reagents.

After an introduction which stresses the fact that the safety precautions taken when working with organoselenium compounds are by no means harsher than the usual measures, taken in a chemical laboratory (work in a well-ventilated hood and destruction of wastes) each of the ten other chapters reviews reactions involving a particular type of selenium-based ragent. The order of chapters, i.e. of reagents, is that of increasing order of the oxidation level around the selenium atom. The longest chapter, (9 with 65 pp.) is as expected the one covering oxidations with selenium dioxide, the most popular selenium-based reagent. Other chapters cover the following reagents : H_2Se and RSeH or ArSeH (chapter 2, 32 pp.) ; benzeneseleninic anhydride $(PhSeO)_2O$, BSA and related reagents (chapter 6 with 26 pp.) ; metallic or amorphous selenium (chapter 3 with 12 pages) ; selenoxides and related species R_2SeO (chapter 4 with 10 pages). The remining chapters are shorter and describe the use of selenenyl halides e.g. PhSeCl (chapter 5), benzeneseleninyl halides e.g. PhSeOCl (chapter 7), perseleninic acids $RSeO_3H$ (chapter 8), imidoselenium compounds, e.g. $RN{=}Se{=}NR$ (chapter 10), and of selenium oxychloride $SeOCl_2$ and selenium tetrachloride $SeCl_4$ (chapter 11).

Within each chapter specific transformations are discussed separately allowing an easy and critical evaluation of the scope and limitations of the selenium reagent. Numerous examples, including natural products are given in the professionally drawn schemes. There are over 260 schemes with an average of about four examples per scheme covering the literature cited in the 600 references. Both the fine artwork, as well as the vast amount of information processed and assembled, account for the relatively high price. An excellent subject index (over 1600 entries) and a detailed Table of contents make an easy access to this information.

As stated in the foreword, organoselenium chemistry has evolved from an exotic area of chemistry practised by a few specialist, becoming a dynamic research field with a well-established methodology and with a pallette of reagents capable of performing specific transformations, often under mild conditions. The book is highly recommended to synthetic organic researchers. They can benefit of a critical evaluation for a specific transformation *via* an organoselenium intermediate.

T.-S. Balaban
Centre of Organic Chemistry
Bucharest

[illegible]

A. Krief, L. Hevesi, Organoselenium Chemistry I — Functional Group Transformations, Springer-Verlag, Berlin, 1988, 2[illegible] pp hard cover, DM [illegible], ISBN [illegible]

Professors Alain Krief and Laszlo Hevesi [illegible] well known for [illegible] in organoselenium [illegible] author which [illegible] to be the first in a two-volume series [illegible] first volume, synthesis [illegible] reactions are described which do [illegible] the [illegible] "one-step" procedures for various functional group transformations [illegible] and [illegible] of stable organoselenium [illegible] as well as a [illegible] of the methods of preparation for the various selenium reagents.

After an introduction which stresses the [illegible] working with organoselenium compounds [illegible] each of the ten chapters [illegible] reactions involving [illegible] The order of chapters [illegible] around the [illegible] oxidations with [illegible] the most popular selenium-based reagents [illegible] covers the following reagents [illegible] selenious anhydride (H_2SeO_3), [illegible] of [illegible] chapter 4 [illegible] (chapter 5), [illegible] and of [illegible] (SeO_2) and [illegible]

Within each chapter [illegible] and critical evaluation of the scope and limitations of the [illegible] ples, including [illegible] products, are [illegible] with an average of about [illegible] the [illegible] references [illegible] used and assembled [illegible] for the [illegible] and a detailed table of contents make [illegible]

As stated in the [illegible], organoselenium chemistry [illegible] chemistry practised [illegible] methodology and [illegible] tions, often under mild conditions. The book is highly recommended [illegible] searchers [illegible] intermediate.

[illegible]
Centre of Organic Chemistry
Bucharest

The Editorial Board of Revue Roumaine de Chimie apologizes for the fact that, in 1989, the Author and Subject Indexes did not appear, as usual, in the last issue of 1989 but are included with the first issue of 1990.

As a result of the pressure put on the Editorial Board, the 1989 first issues have been published — contrary to the previous 40-year editorial practice of our journal — as a homage to the pseudoscientist (Elena Ceaușescu) who was an impostor in the Roumanian culture and science.

In fact, in recent years, several issues in this journal include various articles abusively signed by her without having made any real contribution. Therefore the present Indexes do not contain her name.

The Editorial Board also recommends that the pages preceding the Table of Contents in the first "homage" issues of 1989 be removed from each issue.

The Editorial Board of Revue Roumaine de Chimie apologizes for the fact that, in 1989, the Author and Subject Indexes did not appear as usual in the last issue of 1989 but are included with the first issue in 1990.

As a result of the pressure put on the Editorial Board, the 1989 first issues have been published — contrary to the previous 40-year editorial practice of our journal — as a homage to the pseudo-scientist Elena Ceausescu who was an impostor in the Roumanian culture and science.

In fact, in recent years, several issues in this journal include various articles abusively signed by her without having made any real contribution. Therefore the present indexes do not contain her name.

The Editorial Board also recommends that the pages preceding the Table of Contents in the first "homage" issues of 1989 be removed from each issue.

Revue Roumaine de Chimie, **35**, *1*, 115–132 (1990)

INDEX DES AUTEURS

ABABI V., voir VASILE A. 1601
AELENEI N., voir BELDIE C. 445
AGARWALA B. V., voir SINGH H. R. 2021
AGEEV V. P., voir PROKHOROV A. M.. 235
AGRAWAL G.L. and KU. SHAMI JHA, Oxidation of ethylene glycol with pyridinium chlorochromate. A kinetic approach 1769
AIRINEI A., voir SPIRATOS M. 1413
ALBAIU D., voir BANCIU M. 7
ALBU B., voir POPESCU G. 577
ALDICA GH., voir OSICEANU P. 1541
ALEXANDRESCU R., voir URSU I. 667
ALEXANDROAEI M., voir BOLD A. 59
ALEXANDROAEI M., voir BOLD A. 1699
ANDREI A., voir LUCA C. 197
ANDRONESCU E., voir TEOREANU I. 869
ANDRUH MARIUS, O. D. CHIRICA and M. BREZEANU, Angular overlap model (AOM) calculations for the coordination compounds with macrocyclic ligands. II. AOM parameters for nickel (LI) coordination compounds with saturated macrocyclic ligands 111
ANDRUH M., voir BANCIU A.C. 1711
ANDRUH M., voir CIMPOEŞU F. 2013
ANGELESCU EMILIAN, G. MUSCĂ, G. POP, EC. POP, D. SMOLEANU and G. POGONARU, Conversion of C_2-C_4 alkenes into gasolines by using ZSM-5 zeolites catalysts. 25
ANSARI EL., voir BADRAN MM. 2093
ANTONESCU L., voir S. NEAGOE 845
APATEANU L., voir V. BRANZOI 937
APATEANU L., voir G. STERNBERG 1281
APATEANU L., voir V. BRANZOI 1457
APATEANU L., voir S. STERNBERG 1581
ARVAY G. Z., voir RAZUS A. 1397
ATTIA I., voir NAGDY EL S. 1979
AVRAM M., voir GHEORGHIU MIRCEA 1931
AVRAM R. and DUMITRU SAVU, Relationship between structure and effect of some organic compounds containing sulphur on steel corrosion inhibition process in acid medium 35
AVRAMESCU F., voir NICOLESCU I.V. 1047

BABICH S. A., voir BRUMA M. 1313
BADAU E., voir NEAGOE S. 1867
BADAU E., voir NEAGOE S. 2029
BADAWY D.S., voir HABIB O.M.O. 1949
BADEA I., voir VLADESCU L. 895
BADRAN M. M., S. EL-MELIGIE and A. K. EL-ANSARI, Synthesis and cardiotonic properties of 6-(3-pyridyl)nicotinonitrile derivatives 2093
BAIULESCU G. E., voir TODOR D. N. 877
BAKHMUTOV V. I., voir KALININ V. N. 503
BALABAN T. ALEXANDRU and TEODOR-SILVIU BALABAN, Pyrylium salts formed by diacylation of olefins. Part XXIV. Synthesis of *meta*-terphenyl deri-

vatives and heterocyclic analogs *via* bis-pyrylium salts obtained by bis-diacetylation of *meta*-diisopropenylbenzene 41
BALABAN T. A., voir STANESCU M. 617
BALABAN A. T., voir GHEORGHIU D. MIRCEA 1005
BALABAN T. A., voir BOLOGA U. 1131
BALABAN T. A., voir UNCUTA C. 1425
BALABAN T. A., voir HERDAN J. 1515
BALABAN T. A., Chemical graphs. Part 42. Valence isomers of bis-homoannulenes 1745
BALABAN T. A., voir STANCIUC G. 1895
BALABAN T. S., voir BALABAN T. A. 41
BALABAN T. S., voir UNCUTA C. 1425
BALABAN T.-S., E. COSTACHE and A. PETRIDE, Nitration of 2,6-dimethyl-4-phenylpyrylium sulfoacetate 1449
BALINT I., voir VASS M.. 683
BALTA PETRU and M. BIALE, Redox behaviour of 3d ions in oxide glasses . . . 1301
BANCHOV I., voir STEFANOVA 331
BANCIU A. C., Bis(3-carbethoxy-1,5-di-*o*-anisyl-formasyl)Ni(II). A new unusual pentacoordinate formazane complex 921
BANCIU A. C., S. PLOSTINARU, M. ANDRUH, L. PATRON and A. CONTESCU, Oxidation of cumene with molecular oxygen in presence of Co(II) acetyl-acetonate complexes heterogenized on silane modified silica 1711
BANCIU A. C., Electronic transitions in the square-planar Rh(PPh)3SnCl$_3$ complex (PPh$_3$ = triphenylphosphine) 1857
BANCIU MIRCEA, voir STANESCU M. 617
BANCIU M. D., C. HADA, D. ALBAIU and C. DRAGHICI, The physico-chemical characterization of Z-4b,10b-dihydrochrysene 1907
BANCIU M., D. M. D. STANESCU and F. CHIRALEU, Heterocycles with annelated dibenzocycloalkane skeletons. III. Pyrazoles with dibenzo-barrelene and dibenzohommobarrelene skeletons 1921
BARTHA C., voir LAUDONIU D. 191
BARTHA E., voir RAZUS A. 1263
BARTHA E., voir RAZUS A. 1397
BARTHA E., voir RAZUS A. 2075
BASSIOUNY EL F. A., voir NAGDY EL. S. 1979
BASSIOUNY F. A. EL, voir MAHMOUD M. R 1973
BĂRBOIU V., voir BELDIE C. 51
BĂRBOIU V., voir SIMIONESCU I. C. 317
BECHERESCU D., voir IVAN E. 797
BELDIE C., GH. NEMTOI, Em. DUMITRIU and V. BARBOIU, The behaviour of diethyl maleate vinyl acetate copolymers in solution 51
BELDIE C., I. GROSU, M. BOURCEANU and G. BOURCEANU, Periodically driven Briggs Rauscher reaction 725
BELDIE C., N. AELENEI, ANA ONU, GH. NEMTOI, F. SANDESCU, Termochemical aspects of the reaction between aliphatic alcohols and POCl$_3$. 445
BELOMOINA N. M., voir BRUMA M. 1313
BELOMOINA N. M., voir BRUMA M. 1467
BERDAN IOAN and O. COSTINOAIA, Study of Ni(II) hydroxylamine reaction system (in French) 1307
BIALE M., voir BALTA P. 1301
BILBA N., voir DUMITRIU E. 983
BLAU B., voir EPPERLEIN J. 1835
BOBROV A. J., voir ZACHINYAEV Y.A.V. 901
BOGHINA C. M., C. I. CINCU, N. N. MARINESCU, M. M. MARINESCU, M. V. DIMONIE and D. S. VASILESCU, Radical polymerization of acrylamide in homogeneous and heterogeneous systems. I. Solutions properties of acrylamide in water 933
BOHL M., voir GERGEN I 995
A. BOLD, A. POPA, A. VASILE, M. CRUCEANU, Ev. POPOVICI and M. ALEXANDROAEI, Zeolite molecular sieves as stationary phase in thin layer chromatography. V. On migration mechanism 59

A. BOLD, A. VASILE, A. POPA, M. CRUCEANU, EV. POPOVICI and M. ALEXANDROAEI, Ion-exchange with transitions, metals on highly silicious zeolites of ZSM-5 type. Behaviour of Ah(I) and Cu(II) . . . 1699
BOLOGA URSULA, A. SCHIKETANZ, C. MUSAT, D. VILCICA, C. DRAGHICI, M.D. GHEORGHIU and A.T.BALABAN, Synthesis and stereochemistry of 3,5-dialkyl-2-furyl-*p*-substituted-styryl ketones (furanic analogues of chalcone) . . . 1131
BONCIOCAT N., voir STERNBERG S. . . . 1627
BOTAR A., voir MARCU GH. . . . 207
BOURCEANU G., voir BELDIE C. . . . 725
BOURCEANU M., voir BELDIE C. . . . 725
BOZESANU M., voir IONESCU N. I. . . . 779
BOZGA GRIGORE, CR. TSAKIRIS and ALEX. ISOPESCU, Studies of the thermal regime influence on the ethylene yield in naphthapyrolysis process . . . 1139
BOZGA G., voir GH. MARIA . . . 1377
BÖSECKE P., voir STRIBECK N. . . . 635
BRANZOI V., S. STERNBERG and LILIANA APATEANU, Polarization behaviour of lead in sulphuric acid solution containing ammonium dichromate additions . . . 937
BRANZOI V., voir STERNBERG S. . . . 1281
BRANZOI V., S. STERNBERG and LILIANA APATEANU, Polarization behaviour on limited potential ranges of the $Pb/H_2SO_4 + Na_2SO_4$ system. . . . 1457
BRANZOI V., voir STERNBERG S. . . . 1581
BREZEANU M., voir ANDRUH M. . . . 917
BRIE MARIA and I. A. SILBERG, Derivatives of 1,2-pyrazoles. I. Synthesis and IR-spectra of some new 3-methyl-5-aryl-1,2-pyrazoles . . . 733
BRIE MARIA, I. A. SILBERG and N. PALIBRODA, Derivatives of 1,2-pyrazoles. II. The influence of alkaline media on the reaction of 1,3-dicarbonyl compounds with hydrazine . . . 945
BRIE M., N. PALIBRODA and I. A. SILBERG, Derivatives of pyrazoles. III. Mass spectra of 2-methyl-5-substituted-phenyl-pyrazoles . . . 2067
BRUMA M., I. SAVA, C. HAMCIUC, C. I. SIMIONESCU, N. M. BELOMOINA, S. A. BABICH, E. S. KRONGAUZ and V. V. KORSHAK, Synthesis of new polymers containing phenylquinoxaline units . . . 1313
BRUMA M., I. SAVA, C. HAMCIUC, I. SIMIONESCU, N. M. BELOMOINA, E. S. KRONGAUZ and V. V. KORSHAK, Polyphenylquinoxaline-ester-imides. . . . 1467
BUGARU E., voir VOLINTIRU T.. . . . 1101
BUJENITA P., voir VOLINTIRU T. . . . 1101
BUJGOI C. GH., World-wide and national concerns and tendencies regarding the turning to account of non-ferrous metals from low grade raw materials . . . 65
BULACOVSKI V., voir MIHAILESCU C. . . . 1535
BULATOV A. B., Hydrogenation of aromatic nitro compounds in the presence of dye-containing catalysts . . . 1149
BUTUCEA A., A. SARBU, C. SP. GEORGESCU, A. IONESCU and I. DEACONESCU, The evaluation and significance of kinetic parameters k_i and k_t in the emulsion polymerization of vinyl chloride. . . . 1155

CACHAU, R. E., E. OTTAVIANELLI and E. A. CASTRO, Improved two parameteromega technique. IX. On the use of the ITOOT/RF on the study of excited states (in Spanish) . . . 1645
CARAGHEORGHEOPOL A., voir STANCIUC G. . . . 1895
CARP E., voir LEONTE C. . . . 1241
CARP N. voir GOSA K. . . . 1203
CARPOV A., voir POINESCU C.IG . . . 1061
CĂLDARARU H., voir STANCIUC G. . . . 1895
CĂLUȘARU A., Catalytic cobalt and hydrogen discharge in the Co(II)-2-mercaptobenzothiazole-ammonia buffer . . . 1473
CĂLUSARU A., Why life can be only a carbon chemistry . . . 1787
CĂPROIU M. T., voir STANCIUC G. . . . 1895

CECAL ALEX. and G. I. CIUCHI, Radiochemical method for determination of solubility of some hard soluble compounds (in German) 953

CERCASOV C., voir NEAGOE S. 845

CHALAYA S. N., voir KHARCHENKO V. G. 503

CHEN H. D., voir SHUN GU QI 165

CHIARIZIA R., voir PERESCU N. 1651

CHICINAS I., voir JUMATE N. 1369

CHIFU E., I. STAN, M. SALAJAN and E. GAVRILA, Surface mobility of surfactant solutions. XIII. Influence of the magnetic field 79

CHIFU E., voir STAN I. 603

CHIPER S., voir SEVER S. 297

CHIPER S., voir VLADESCU L.. 1287

CHIRALEU F., voir GHENCIULESCU A. 477

CHIRALEU F., voir DRAGUTAN V.. 759

CHIRALEU F., voir ENESCU L. 765

CHIRALEU F., voir ENESCU L. 989

CHIRALEU F., voir UNCUTA C. 1425

CHIRALEU F. voir BANCIU M. 1921

CHIRIAC A., voir SIMIONESCU I. C. 597

CHIRIAC A., voir SIMIONESCU I. C. 1573

CHIRIAC A., voir MONTSENIGOS A. 2101

CHIRICA O. D., voir ANDRUH M. 917

CHRISTOVA M., D. PANAYOTOV and D. MEKHANDJIEV, Neutralization of nitrogen oxides on CuO and Co_3O_4 catalysts and $Cu_xCO_{3-x}O_4$ spinels (in Russian) 517

CIMPOESU F., M. FERBINTEANU and M. ANDRUH, On the electronic structure of μ_3-exo-trinuclear chromium acetate in the frame of the overlap model. 2013

CINCU C. I., voir BOGHINA C. M. 933

CIOBANU S., voir LAUDONIU D. 2 10

CIORANESCU ECATERINA, ANCA VOICU and M. ELIAN, Carbonium ion reactions. XIX. The solvolysis of 5-(1′, 1′-dimethylethyl)-5-hydroxy-5H-dibenzo-[*a*, *d*]-cycloheptene and some related compounds. An uncommon neopentyl rearrangement 87

CIUBOTARIU D., voir MONTSENIGOS 2101

CIUCAU I. and C. LUCA, Permethylated dextran as stationary phase in gas chromatography 1829

CIUREANU M., J. HERDAN and ALEXANDRU T. BALABAN, Electrochemical oxidation of N-(nitro-substituted phenyl)-4-amino-2,6-dibutyl-phenols by cyclic voltammetry 739

CIUREANU M., M. CONSTANTINESCU and A. MEGHEA, Cyclic voltammetry study of 2-aminoanthraquinone 1491

COCHECI V., E. GERASIMOU, C. CSUNDERLIK, L. COTARCĂ and A. NOVAC, Ozone oxidation of alkylamines in aqueous solution. I. Rate constants of ozone reactions with primary, secondary and tertiary amines 749

COCHECI V., GH. PETCA and E. GLÜCK, Studies concerning calcium carbonate scales formation and its prevention. I. Kinetics of calcium carbonate precipitation from hyperthermal water 1681

COCIRLA I., L. TATARU, M. VATA, I. MAZILU, L. WAGNER, D. SCUTARU and C. PETRESCU, Study on the reactivity of some AS naphthols possessing benzimidazolonic rest 1945

COMAN C., voir TARANU I. 1593

COMANITA E., voir SIMIONESCU I. C. 317

CONDEIU C., voir DRAGUTAN V. 977

CONSTANTIN B., voir TUDOSE R. Z.. 1081

CORCIOVEI M., M. DIMONIE, D. BARB, M. CHIPARA and T. SARBU, ESR studies on $AlCl_3$ catalytic systems 1117

CONSTANTINESCU C., voir VASILIU-OPREA Cl. 883

CONSTANTINESCU D., voir STERNBERG S. 623

CONSTANTINESCU D., D. JINGA, A. ANDREI, I. V. COTÂRȚĂ, The structural characterization of manganese dioxide obtained by anodic oxidation 1499

CONSTANTINESCU T., voir STANCIUC G. 1895

CONSTANTINESCU T., voir LUCA C. 2093

CONSTANTINESCU M., voir ZUCA S. 1439

CONSTANTINESCU S., voir TEOREANU I. 869

CONȚESCU A., voir SPACU P. 323

CONȚESCU A., voir SPACU P. 1275

CONȚESCU A., voir OSICEANU P. 1541

CONȚESCU A., voir A. C. BANCIU 1711

CORDOS E., voir DARVASI E. 961

CORNEA F., A. CIOBANU, I. BACIU, O. MAIOR and A. A. EL BAHNASAWY, Synthesis of some new heterocyclic derivatives of di- and tetrahydroquinozaline 103

CORNEA F., voir ZALARU F.. 1107

COSEAC T., voir SEGAL E. 287

COSTACHE E., voir BALABAN T. S. 1449

COSTINOAIA O., voir BERDAN I. 1307

COTÂRȚĂ ADINA, voir STERNBERG S. 623

COTÂRȚĂ ADINA, voir STERNBERG S. 1627

COUTURE AXEL, A. LABLACHE-COMBIER, A. POLLET, and HARRY OFENBERG, Photoreactivity of 2,3-diphenylbenzo[b]furan derivatives 2087

CRISTEA I., voir SORAN S. 1509

CRISTEA L., voir OSICEANU P. 1541

CRISTESCU C. and ST. TOMAS, AS-triazine derivatives with potential therapeutic action. XXIII. Synthesis of 4-thioxo-5(chlorobenzyl)-thio-6-azauracil derivatives and their nucleosides 1321

CRISTIANI C., voir LAUDONIU D. 119

CRISAN D., voir SPACU P. 323

CRISAN M., voir ZAHARESCU M. 703

CRUCEANU M., voir BODD A. 59

CRUCEANU M., voir BODD A. 1699

CRUCEANU M., voir VASILE A. 1601

CSUMA A., voir LUCA C. 2039

CUCU O., voir MOGA N. 1995

CURRAN A. KEVEN, J. O. PETERSON and EM. MERDINGER, Progress in hemodialysis 111

DARVASI E., H. MIOSCU, A. MORARU, C. OANCEA and E. CORDOS, Microprocessor operating scanning UV—VIS monochromate 961

DATSKO YA. TATIANA and V. I. ZELENTSOV, The role of electrolytic gases in the electrochemical stabilization of aluminium hydroxide (in Russian) 1163

DAUDEL RAYMOND, Electronic structure of molecules. Applications in physics, chemistry and biology (in French) 115

DAVID V., voir TODOR D. N. 877

DĂNEȚ A., voir LUCA C. 1849

DEACONESCU I., voir BUTUCEA A. 1155

DEAKY A., T. SIMANDAN, N. MIRICA, S. DRAGOS and M. D MEDELEANU, Hydroquinone electrosynthesis from phenol 1169

DIMONIE M., V. FIEROIU, G. HUBCA, V. GRUBER, E. G. BADEA, M. VLADULESCU, A. VERESTOI, H. IOVU and I. VASILE, Aspects concerning the polymerization of isoprene with lanthanide-based catalysts 5

DIMONIE M., A. CORNILESCU, V. DRAGUTAN , E. NICOLESCU, S. COCA, L. POPESCU, M. CUZMICI, C. OPRESCU, M. TEODORESCU, GH. HUBCA, R. GEORGESCU, A. VASILESCU and M. CHIPARA, Aspects on the stereochemistry and mechanism of ring-opening polymerization of ring-opening polymerization of cyclo-olefins 907

DIMONIE M., A. CORNILESCU, V. DRAGUTAN, E. NICOLESCU, S. COCA, M. CUZMICI, V. APOSTOL, R. MUNTEANU, R. DROSSESCU, A. VASILESCU

and M. TEODORESCU, Influence of activator in the catalytic systems of ring-opening polymerization of cyclopentene . . . 1293
DIMONIE M. V., voir BOGHINA C. M. . . . 933
DINULESCU I. G., voir A. GHENCIULESCU . . . 477
DINULESCU I. G., voir ENESCU L. . . . 765
DINULESCU I. G., voir ENESCU L. . . . 989
DIUDEA V. MIRCEA and I. SILAGHI-DUMITRESCU, Molecular topology. I. Valence group electronegativity as a vertex discriminator . . . 1175
DIXIT RANJANA and BHAGWAN S. GARG, Stabilities of bivalent metal complexes with benzoyl-2-hidroxy-4-metoxy-3-methyl acetophenone (BHMMA). . . 1705
DONESCU A., J. WEINBERG and V. EM. SAHINI, Solute-solvent interactions in carbenicillin solubility processes . . . 453
DONESCU D., voir GOSA K. . . . 1203
DRAGOS S., voir DEAKY A. . . . 1169
DRAGANOIU M., voir STERNBERG S. . . . 859
DRAGANOIU M. and S. STERNBERG, The mean activity coefficient of $ZnSO_4$ and $CuSO_4$ in the electrolyte solutions $ZnSO_4 + LiSO_4 + H_2O$ and $CuSO_4 + Li_2SO_4 + H_2O$ . . . 967
DRAGHICI C., voir BOLOGA U. . . . 1131
DRAGHICI C., voir GHEORGHIU D. MIRCEA . . . 1341
DRAGHICI C., voir BANCIU M. . . . 1907
DRAGUTAN I., voir DRAGUTAN V. . . . 759
DRAGUTAN I., voir DRAGUTAN V. . . . 977
DRAGUTAN V., I. DRAGUTAN, F. CHIRALEU and A.M. GLATZ, Friedel-Crafts chemistry of unsaturated alicyclic systems. III. Friedel-Crafts reaction of unsaturated alicyclic acids in the presence of various Lewis acids . . . 759
DRAGUTAN V., I. DRAGUTAN, C. CONDEIU and A. M. GLATZ, Friedel-Crafts chemistry of unsaturated alicyclic systems. IV. Effect of the catalytic system in Friedel-Crafts reaction of unsaturated esters . . . 977
DRONDINA V. R., voir MATVEEVICH V. A. . . . 831
DUMITRASCU FLOREA and D. RAILEANU, Rearrangement of 4-alkyl-3-(*o*-carboxylphenyl) sydnones to 1-acyl-1,2-dihydro-3*H*-indazol-3-ones . . . 1183
DUMITRIU EM., voir BELDIE C. . . . 51
DUMITRIU EM., N. BILBA, V. HULEA and SP. OPREA, Selective alkylation of toluene on ZSM-5 zeolites . . . 983
DUMITRIU EM., V. HULEA, M. STOICA and SP. OPREA, Kinetic study of the maltodextrine hydrolysis catalyzed by immobilized glucoamylase . . . 1195

ELIAN M., voir GHEORGHIU D. MIRCEA . . .
ELIAN M., voir GHEORGHIU D. MIRCEA . . . 1341
EL-RAHMAN A.H.A., voir HABIB O.M.O. . . . 1949
ENESCU L., voir GHENCIULESCU A. . . . 477
ENESCU LUCIAN, A. GHENCIULESCU, F. CHIRALEU and I. G. DINULESCU, Facile synthesis of 9-substituted exo-benzocyclo-butenonorbornenes . . . 765
ENESCU L., A. GHENCIULESCU, F. CHIRALEU and I.G. DINULESCU, Reaction of ketones with benzocyclobuteno-norbornenic skeleton in the presence of dimethyloxosulfonium methylide . . . 989
EPPERLEIN J., B. BLAU and U. SCHIERIG, UV-VIS-spectral behaviour of arylazo-compound. III. Solvent effects on the visible absorption band of 4-amino-substituted azobenzenes . . . 1835

FEDIN E. I., voir KRAVTSOV D. I. . . . 807
FENESAN I., voir MURESAN V. . . . 1761
FENESAN M., voir VLASSA M. . . . 1611
FEROIU V. and DAN GEANA, Prediction of vapour-liquid equilibria at low pressure by a general equation of state . . . 1329
V. FIEROIU, V. DRAGUTAN, E. SIMIONESCU, E. GRUBER, C. PIROJOC, C. ION and VIORICA APOSTOL, Mechanism and stereochemistry of 1,3-butadiene polymerization in the presence of modified $TiCl_4 - TIBA - I_2$ catalyst . . . 15
FILOTI, voir NICOLESCU I.V. . . . 1047
FINTA Z., voir STAN I. . . . 603
FLONDOR A., voir MAXIM S. . . . 1389

FLORSECU MIHAIL, Biotechnologies in the chemical industry 459
FOURAR M., voir TUDOSE R.Z. 1081
FUSULAN L., voir GOSA K. 1203
FÜLOP J., voir MARCU GH. 1029

GARG S. B., voir DIXIT R. 1705
GAUST M., voir S. STERNBERG 1581
GAVRILA E., voir STAN I. 603
GAINAR I., voir VILCU R. 697
GANESCU I., J. ZSAKÓ, CS. VÁRHELYI and E. PÁLI, Study on the tetranitroplatinites (II) and hexanitro-platinites (IV) 771
GEANA D., voir O. IULIAN 1209
GEANA D., voir LANDAUER O. 1529
GENDY A. M., voir SALEM A. I. M. 1963
GEORGESCU S. C., voir BUTUCEA A. 1155
GEORGESCU M., voir TEOREANU I. 649
GERGEN I., M. BOHL, Z. SIMON and H. SIMON, Structure-activity relations for steroids by the MTD method. Superposition procedure for molecules with different condensed cycles 995
GHATTAS A. G. ABDEL-BAHID, M. ABDEL-RAHMAN T. EL-WASSIMY and G. A. EL-SARAT, Benzofurans. Part III. Synthesis and antifungal activity of some new Mannich bases and sulphides derived from (1,3,4-thiadiazolyl)-and (1,2,4-triazolyl)-benzofurans.. 1987
GHENCIULESCU A., L. ENESCU, F. CHIRALEU and I. G. DINULESCU, Reaction of endo- and exo-benzocyclo-butenenorboran-7-one with dimethyloxosulfonium methylide 477
GHENCIULESCU A., voir L. ENESCU. 765
GHENCIULESCU A., voir L. ENESCU 989
GHEORGHIU D. MIRCEA, ANGELA POPESCU and GH. SURPATEANU, ^{1}H-NMR spectra of 5,9-methano-5H-benzo[3,4]cyclobuta[1,2]-cycloheptene derivatives. . 481
GHEORGHIU D. MIRCEA, A. SCHIKETANZ, A. NECULA and ALEX. T. BALABAN Carbon-13 nuclear magnetic resonance assignments of the saturated segment from 1,2,3,4-tetrahydrophenanthrene by means of ^{13}C and ^{2}H labelling 1005
GHEORGHIU D. MIRCEA voir BOLOGA U. 1131
GHEORGHIU D. MIRCEA, voir RAZUS A. 1263
GHEORGHIU D. MIRCEA, voir RAZUS A. 1397
GHEORGHIU D. MIRCEA, voir RAZUS A. 2075
GHEORGHIU D., C. DRAGHICI, L. PARVULESCU and M. ELIAN, Nuclear magnetic resonance investigations of small rings. 6. The stereochemistry of cycloaddition of *t*-butylcyanoketone to norbornene derivatives. A multicenter approach for establishing the configuration with the aid of Europium shift reagent of some polycyclic α-*t*-butyl-α-cyanocyclobutanones 1341
GHEORGHIU D., voir HERDAN J. 1515
GHEORGHIU D. and ANGELA POPESCU, Nuclear magnetic resonance of small rings. 8. ^{13}C-NMR spectra of 8-substituted, 5,9-methano-5H-benzo [3,4]cyclobuta [1,2] cycloheptenes 1779
GHEORGHIU D. MIRCEA, E. OLTEANU, L. STANESCU, M. AVRAM and GH. SURPATEANU, The synthesis of benzonorbornane, *exo*-benzocyclobutano- and *endo*-benzocyclobutanonorbornanes annelated with *exo*-cyclobutene ring *via* Shechter reaction 1931
P. GHIOCA, H. PAVEN, G. BANICA, E. BUZDUGAN, L. CERCHEZ, R. STANCU, ANCA ION and D. MARDARE, Thermoplastic plastomer/elastomer systems. Mechanical properties of the compounds of polyolefins and thermoplastic elastomer block-copolymers (in French) 711
GHINAC A. I., voir ZACHINYAEV V. YA 901
GHINAC A. I., voir SEROVA I. 1075
GIRGIS M. MAHER and ZARIF H. KHALIL, Charge-transfer complexes of hydroxy styryl cyanine dyes and their analogues with nicotine. Structure-activity relationship studies 1721
GIURGINCA M., voir G. IVAN 1017
GIURGINCA M., voir G. IVAN 1351

GLATZ A. M., voir DRAGUTAN V. 759
GLATZ A. M., voir DRAGUTAN V. 977
GOCAN S., L. OLENIC and I. CRISTEA, The optimization of eluent systems for separation by thin layer chromatography of some 1-(2-pyrimidyl)-3-methyl-5-pyrazolone derivatives 1509
GOLOVCHENCO L. S., voir KRAVTSOV D. I. 807
GOSA KR., D. DONESCU, N. CARP and L. FUSULAN, Interactions between emulsifiers utilized in polymerization of vinyl acetate 1203
GRECU M. N., voir HERDAN J. 1515
GREINER W., voir IVASCU M. 143
GRIGORIU C., voir URSU I. 667
GROSU I., voir BELDIE C. 725
GUARDIA T. C., voir HERNANDEZ E. J. 1637
GUTU ANTONINA and M. VASS, Work function and electron impact desorption studies on CO/W adsorption states. 1843

HAAS A., Recent developments in perfluoroorgano chemistry of selenium in various oxidation states 121
HABIB O. M. O., A. H. ABD EL-RAHMAN and D. S. BADAWY, Synthesis and reactions of some new benzofurano-(3,2-c)pyrazol-3-one and benzofurano (3,2-c) isoxazo-3-one derivatives of expected biological activity 1949
HADA CATALINA, voir BANCIU MIRCEA 1907
HAFEZ ABDEL A. A., voir YANNY SABET AMAL 1775
HAIDUC I., voir SILAGHI-DUMITRESCU L. 305
HAMCIUC C., voir BRUMA M. 1313
HAMCIUC C., voir BRUMA M. 1467
HAMED E. A., voir SAAD E. F., ... 1753
HANDREA M., voir NEGOIU D. 1245
HERDAN M. JEAN, N. NEGOITA, M. N. GRECU, M. D. GHEORGHIU and A. T. BALABAN, Synthesis and ESR spectra of persistent azoxyls. III. Dialkyl 3,5-di-t-butyl-4-hydroxy-benzylphosphonates and their corresponding azoxyles. . . 1515
HERNANDEZ, E. J., QUERO J. L. VILCHEZ and CARRILLO T. GUARDIA, Study of pyrazinhydroxamic acid reduction on a mercury electrode. 1637
HOURANI E., voir IVASCU M. 143
HULEA V., voir DUMITRIU E. 983
HULEA V., voir DUMITRIU E. 1195

IANCU I. A., voir RAZUS A. 1397
IONESCU A., voir BUTUCEA A. 1155
IONESCU-BUJOR I., voir LECA M. 811
IONESCU D., voir ZALARU F. 1107
IONESCU GH., ANA ONU and V. NAGACEVSCHI, Determination of some liquid-vapour equilibrium data for acetone (1)-chloroform (2)-nonideal solution. . . 1009
IONESCU M., Polymers of permanently antistatic ε-caprolactam (in French) . . . 129
IONESCU N. I., M. BOZESANU and I. IOSIF, The influence of propylene on the mechanism of homogeneous pyrolysis of n-heptene. 779
IONESCU S. G., voir POPA N. 1561
IONNALAGADDA S. B., voir SHIUNDU P. M. 1661
IORDACHE O., GHEORGHITA JINESCU, D. LAVRIC and V. LAVRIC, Kinetic theory of gas-liquid dispersions 785
IOSIF I., voir N. I. IONESCU 779
ISOPESCU A., voir BOZGA G.. 1139
ISOPESCU A., voir GH. MARIA 1377
ITUL D., voir MARCU GH. 1029
IULIAN O., O. LANDAUER, D. GEANA and C. MATEESCU, The study of the vapor-liquid equilibrium in the dioxane-water system 1209
IULIAN O., voir O. LANDAUER 1529
IVAN E. and D. BECHERESCU, Ceramic pigments in the TiO_2-BaO-M_xO_y system 797
IVAN G., voir VOLINTIRU T. 1101
IVAN G., E. TAVARU, M. GIURGINCA and D. N. NICOLESCU, Crosslinking of brominated butyl rubber by means of aromatic diamines 1017

IVAN G. and M. GIURGINCA, The effect of several hindered amine light stabilizers (HALS) in oxidative degradation of rubber compounds 1351
IVANCIUC O., Design on topological indices. 1. Definition of a vertex topological index in the case of 4-trees 1361
IVASCU I., voir IVASCU M. 143
IVASCU M., D. N. POENARU, I. IVASCU, E. HOURANI and W. GREINER, Vibration energy of new kinds of radioactivities 143
IVASCU M., voir NICOLESCU I. V. 1047

JAQUHARI R., General study of the benzylation of functionalized aromatic hydrocarbons catalyzed by ruthenium complexes (in French) 1733
JINESCU GHEORGHITA and V. LAVRIC, Mass transfer in an air-lift, biological reactor. Part I. An experimental study 149
JINESCU GHEORGHITA voir O. IORDACHE 785
JINESCU GHEORGHITA and ALEX. STEFAN, A study at the isothermal flow instability of polymeric fluids 1217
JINESCU V. VALERIU, A fundamental property of matter. Part II 161
JINESCU V. VALERIU, The high degree generality of the principle of critical energy 491
JITARU M., voir ONICIU L. 537
JUMATE N. and I. CHICINAS, High voltage plasma applied to determine boron and silicon in superallied metallic powder 1369

KALININ V. N., MOISEEV S. K., V. I. BAKHMUTOV and N. I. UDALOV, Synthesis of 6,7-benzomorphanes using arenetricarbonylchromium complexes (in Russian) 503
KEZDI M., voir VLASSA M. 1611
KHACHATRYAN L. A., voir MANTASHYAN 821
KHALIL Z., voir GIRGIS M. 1721
KHARCHENKO V. G. and S. N. CHALAYA, Nucleophilic and electrophilic reactions of 1,5-diketones (in Russian) 509
KHARLAMOV V. V., voir MINACHEV KH. M. 527
KIRIYAC L. G., voir VATAMAN I. I. 689
KNOR Z. and J. SOTOLA, New application of field emission techniques (FEM and FIM) to the study of catalytic systems 1373
KOCHETKOV N. K., Synthesis ways of the o-antigenic polysaccharides 1225
KONOV V. I., voir PROKHOROV 235
KONOV V. I., voir URSU I. 667
KOPANSKAYA L. S., voir I. I. VATAMAN 689
KOPTYUG V. A., Dependence of substituent electronic effects in π-systems on the character of molecular orbitals 169
KORSHAC V. V., voir BRUMA M 1313
KORSHAC V. V. voir BRUM M. 1661
KÖKLÜ ÜNEL and TÜLAY ORKUN, Lead, chromium and barium in Turkish printing inks and colored newspapers 1677
KRAVTSOV D. I., V. M. PACHEVSKAYA, L. S. GOLOVCHENCO, B. A. KVASOV and E. I. FEDIN, Substituent effect on ^{19}F chemical shifts in 2-halo- and 2,6-dihalo-4-fluorophenols and amizoles (in Russian) 708
KRONGAUZ E. S., voir BRUMA M. 1313
KRONGAUZ E. S., voir BRUMA M. 1467
KUANG R. Z., voir SHUN-QI GU 1565
KUMANOVA B. and L. PETROVA, Study on the monoalkylsulphosuccinate structure by mass spectroscopy 1523
KURUNCZI L., voir VILCEANU R.A. 377
KVASOV B. A., voir D. I. KRAVTSOV 807

LANDAUER O., voir IULIAN O. 1209
LANDAUER ORTANSA, OLGA IULIAN, CORNELIA MATEESCU and DAN GEANA, The study of the vapor-liquid equilibria in the system dimethylsulfoxide-water. I. Experimental data 1529

LAUDONIU D., S. CIOBANU, M. SCARLETE, C. BARTHA, V. VANCA, D. VASILIU, V. NINULESCU and G. CRISTIANI, Decreased thermo-dynamical activity of oxygen in silicon single crystals grown by Czochrolski method 191
LAVRIC D. voir IORDACHE O. 785
LAVRIC V., voir JINESCU GHEORGHITA 149
LAVRIC V., voir IORDACHE O. 785
LECA M., voir VILCU R. 387
LECA M., voir TRANDAFIR V. 661
LECA M., M. OLTEANU and INGRID IONESCU-BUJOR, Interpolymer complexes formed by carboxylic polyacids with quaternary ammonium polysalts 811
LEONTE CANDIANO and E. CARP, An extension of the Koch-Haaf reaction N-acylglycines from N-hydroxymethylamines and -imides 1241
LUCA C., A. ANDREI and G. SEMENESCU, Considerations concerning oxide/metal/electrolyte system in non-equilibrium regime 197
LUCA C., A. DĂNEŢ and CORNEL RADU, Mercury determination in water and atmosphere at concentrations lower than parts per billion 1849
LUCA C., LUCIA MUTIHAC, T. CONSTANTINESCU and ANA CSUMA, The active transport of amino-acids through liquid membranes by macrocyclic carriers and pHgradient 2039
LUCA N., voir POPESCU G. 577
LUCA N., voir NECHIFOR GH. 2047

MAHMOUD M. R., voir NAGDY EL. S. 1979
MAHMOUD M. R., S. EL-NAGDY and F. A. EL-BASSIOUNY, The condensation of some aromatic aldehydes and ketones with dimethyl homophthalate 1973
MAIOR O., voir NEGOIU D. 1245
MAJA M., voir PAVLOV D. 551
MANDACHE S., voir OSICEANU P. 1541
MANDRAVEL C., voir TRANDAFIR 661
MANTASHYAN A. A., L. A. KHACHATRYAN and A. A. SUKIASYAN, The study of chain gas phase reactions of hydrocarbon-oxygen mixtures conversion in laser irradiation conditions (in Russian) 821
MARCU GH., M. RUSU and A. BOTAR, Unsaturated heteropolytungstates with Th(IV) centrali ion 207
MARCU GH., CS. VÁRHELYI, J. FÜLÖP and DANA ITUL, New cobalt chelates with ethylenediimino-bis-benzoyl-acetone 1029
MARIA CRISTINA, voir GH. MARIA 1377
MARIA GHEORGHE, Cr. TSAKIRIS, CRISTINA MARIA, ALEXANDRU ISOPESCU and GRIGORE BOGZA, An adapted model to predict operating conditions for a radiant furnace thermal cracking reactor 1377
MARINESCU M. M., voir BOGHINA C. M. 933
MARINESCU N. N., voir BOGHINA C. M. 933
MATEESCU C., voir IULIAN O. 1209
MATEESCU C., voir LANDAUER O. 1529
MATVEEVICH A. VERA, A. M. ROMANOV, R. V. DRONDINA, V. N. SHAFRANSKI and V. P. MOTSPAN, Investigation of aluminium hydroxyfluoride complexes composition as a result of natural waters defluorination (in Russian) 831
MAXIM STELIANA and A. FLONDOR, New crosslinked functionalized acrylic copolymers for biotechnological applications 1389
MEDELEANU M., voir DEAKY A. 1169
MEGEED MOHAMED F. ABDEL and MOHAMED A. H. SALEH, Synthesis and reactions of D-glucosyl derivatives of 2-aryl-4(3H)-quinazolinones and their thione derivatives 1957
MEGHEA A., voir ZALARU F. 1107
MELIGIE EL. S., voir BADRAN M. M. 2093
MERCHES M., voir PINCOVSKI E. 1055
MIHAILESCU CAMELIA, V. BULACOVSKI and C. SIMIONESCU, Phase transfer free radical reactions. II. Polymerization of acrylonitrile 1535
MIHAILESCU I. N., voir PROKHOROV A. M. 235
MIHAILESCU I. N., voir URSU I. 667

MINACHEV KH. M. and V. V. KHARLAMOV, Oxidative acetoxylation of hydrocarbons over metal-containing catalysts (in Russian) 527

MIOSCU H., voir DARVASI E. 961

MIRICA N., voir DEAKY A. 1169

MISHRA S. K. A. P. MISHRA and K. L. YADAVA, Study of mixed ligand complexes of Hg(II), Be(II) and Cu(II) by paper electrophoresis (M-nitrilotriacetate-adenine systems) 1877

MISHRA A. P., voir S. K. MISHRA 1877

MOGA N., O. CUCU, A. PANESCU and M. POPESCU, Considerations on the synthesis and properties of usual surfactant-free acrylic dispersions 1995

MOHARRAM M. A., voir YANNY SABET A. 1775

MOISEEV S. K., voir KALININ V. N. 503

MONAKHOV B., voir PAVLOV D. 551

MONTSENIGOS A., D. CIUBOTARIU, A. CHIRIAC and Z. SIMON, Alpha adrenergic clonidine derivatives, Qsar by MTD for multiconformational molecules. . . 2101

MORARU A., voir DARVASI E. 961

MORJAN I., voir URSU I. 667

MOSTAFA M. R., H. M. ABU EL-NADER and G. M. ABU EL-REASH, Effect of acetophenone benzoyl hydrazone derivatives as corrosion inhibitors for the dissolution of aluminium in HCl solution 839

MOTSPAN P. V., voir MATVEEVICH V. A. 831

MURESAN V., I. FENESAN and L. PASKUCZ, 2-Arylthio-5-methyl-2-thiono-1,2,3-di-oxaphospholanes. 1761

MUSCA G., voir ANGELESCU E. 25

MUSAT C., voir BOLOGA U. 1131

MUTIHAC LUCIA, voir LUCA C. 2039

NADER EL ABU H. M., voir MOSTAFA M. R 839

NAGACEVSCHI V., voir IONESCU GH. 1009

NAGDY S. EL., voir MAHMOUD M. R. 1973

NAGDY S. EL., voir SALEH A. J. M. 1957

NAGDY S. EL, F. A. EL-BASSIOUNY, I. ATTIA and M. R. MAHMOUD, Studies on the condensation of 1,3 diaryl-propen-1-one with ethyl cyanoacetate. . . . 1979

NEAGOE S., L. ANTONESCU, V. NEAGOE, D. NEGOIU and C. CERCASOV, Transition metal complexes with thioamides 845

NEAGOE S., D. NEGOIU, V. NEAGOE, M. NEGOIU and E. BADAU, Pd(II) complex compounds with tioethers. II. Pd(II) compounds of bis-(benzyl-thio-p-phenyl)ethers 1867

NEAGOE S., D. NEGOIU, V. NEAGOE, M. NEGOIU and E. BADAU, Pd(II) complex compounds with thioether. III. Pd(II) compounds of bis-(benzylthio-*p*-phenyl) sulphides 2029

NEAGOE VIORICA, voir NEAGOE S. 845

NEAGOE VIORICA, voir NEAGOE S. 1867

NEAGOE VIORICA, voir NEAGOE S. 2029

NEAMTU I., voir SIMIONESCU C. 597

NEAMTU I., voir SIMIONESCU C. 1573

NECHIFOR M., voir NECHIFOR GH. 2047

NECHIFOR GH., N. LUCA, G. POPESCU and M. NECHIFOR, Preparation of membranes by immersion-precipitation method 2047

NECHIFOR GH., voir POPESCU G. 577

NECULA A., voir M. D. GHEORGHIU 1005

NEDYALKOVA T., voir PETROVA L. 561

NEGOITA N., voir HERDAN M. J. 1515

NEGOIU D., voir NEAGOE S. 845

NEGOIU D., voir NEAGOE S. 1867

NEGOIU D., voir NEAGOE S. 2029

NEGOIU D., M. HANDREA, M. NEGOIU and O. MAIOR, Complex compounds of divalent manganese 1245

NEGOIU MARIA, voir S. NEAGOE 845

NEGOIU MARIA, voir D. NEGOIU 1245

NEGOIU MARIA, voir S. NEAGOE . . . 1867
NEGOIU MARIA, voir S. NEAGOE . . . 2029
NEGULESCU L., Considerations on the chemical regime maintenance in a water cooling system (in German) . . . 1037
NEMES M., voir TARANU I. . . . 1593
NEMTOI GH., voir BELDIE C. . . . 59
NEMTOI GH., voir BELDIE C. . . . 445
NENNO V. E., voir STURZA A. R. . . . 351
NICOLESCU D. N., voir IVAN G. . . . 1017
NICOLESCU I. V., GH. NEDELCU, R. MANAILA, M. IVASCU, FL. AVRAMESCU, V. SPANU and FILOTI, Phase composition and structure in Fe-Mg-O catalysts for oxydehydrogenation of n-butenes to butadiene . . . 1047
NINULESCU V., voir LAUDONIU D. . . . 191

OANCEA C., voir DARVASI E. . . . 961
OLEINIKOVA G., voir SEROVA I. . . . 1075
OLENIC L., voir GOCAN S. . . . 1509
OLTEANU BUJOR, Achievements and expectations in crude oil processing . . . 215
OLTEANU E., voir GHEORGHIU MIRCEA . . . 1931
OLTEANU M., voir LECA M. . . . 811
ONCESCU TATIANA, voir POSTOLACHE C. . . . 581
ONICIU L., MARIA JITARU and I. A. SILBERG, Mediated electrocatalysis. I. General aspects . . . 537
ONU A., voir BELDIE C. . . . 445
ONU A., voir IONESCU GH. . . . 1009
OPREA S., voir DUMITRIU E. . . . 983
OPREA S., voir DUMITRIU E. . . . 1195
ORKUN TULAY, KÖKLÜ ÜNEL . . . 1677
OSICEANU P., L. PATRON, S. PLOSTINARU, A. CONTESCU, L. CRISTEA, M. VASS, GH. ALDICA, S. MANDACHE, P. PAUSESCU and M. PETRASCU, Electrical and magnetic propierts of high$-T_c$ superconductors (Y,Tm)—Ba—Cu oxides . . . 1541

PACHEVSKAYA V. M., voir KRAVTSOV D. I. . . . 87
PALAFOX M. ALCOLEA, Torsional and inversion potential function of amino group (in Spanish) . . . 1667
PALI E., voir GANESCU I. . . . 771
PALIBRODA N., voir BRIE M. . . . 945
PALIBRODA N., voir BRIE M. . . . 2067
PANESCU A., voir MOGA N. . . . 1995
PASKUCZ L., voir MURESAN V. . . . 1761
PARVULESCU L., voir GHEORGHIU M. . . . 1341
PATRON L., voir SPACU P. . . . 323
PATRON L., voir SPACU P. . . . 1275
PATRON L., voir OSICEANU P. . . . 1541
PATRON L., voir A. C. BANCIU . . . 1711
PAUSESCU P., voir OSICEANU P. . . . 1541
PAVLOV D., B. MONAKHOV, M. MAJA and N. PENAZZI, Sn-free effect at the positive lead acid battery plotes . . . 551
PENAZZI N., voir PAVLOV D. . . . 551
PERESCU NISTOR and RENATO CHIARIZIA, Extraction of europium (III) from nitric and perchloric media by neutral bifunctional carbamoylmethylene-phosphonates . . . 1651
PERISANU ST., voir VILCU R. . . . 697
PETRASCU M., voir OSICEANU P. . . . 1541
PETRIDE H. and D. RAILEANU, Mesoionic oxazolones. III. Planar and nonplanar acylated compounds . . . 1251
PETRIDE A., voir UNCUTA C., . . . 1425
PETRIDE A., voir BALABAN T.S. . . . 1449
PETRIDE H., Pyridinium ylides. Hindered rotation about the $N^+(sp^2)\,C^-\,(sp)^2$ bond . . . 2057
PETROV YU. N., voir URSU I. . . . 667
PETROV I., voir STEFANOVA R. . . . 331
PETROVA L., voir KUMANOVA B. . . . 1523

PETROVA L., J. STOIANOVA, TS. NEDYALKOVA and E. TORBOVA, Purification of the air from styrene in production of glass reinforced resin by chemical methods (in Russian) . . . 561
PETRUS O., voir TUDOSE R.Z. . . . 1081
PINCOVSCHI E., M. MERCHES and KIM CHOL SIK, Synthesis and characterization of ZSM-5 zeolites . . . 1055
PÎRLOG C., voir ZAHARESCU M. . . . 703
PLATE N. A. and YU. P. YAMPOLSKY, Some problems of polymer membranes for gas separation . . . 1545
PLOSTINARU S., voir OSICEANU P. . . . 1541
PLOSTINARU S., voir SPACU P. . . . 323
PLOSTINARU S., voir SPACU P. . . . 1275
POENARU D. N., voir IVASCU M. . . . 143
POGONARU G., voir ANGELESCU E., . . . 25
POINESCU IG. G. and A. CARPOV, Relationships between crosslinked copolymer synthesis and their features . . . 1061
POLIZZI S., voir STRIBECK N.. . . . 635
POP E., voir ANGELESCU E. . . . 25
POP G., voir ANGELESCU E.. . . . 25
POPA A., voir BOLD A. . . . 59
POPA A. A., voir SIMIONESCU C. . . . 317
POPA A., voir BOLD A. . . . 1699
POPA C., voir SAHINI V. E. . . . 253

POPA M., voir C. VASILIU OPREA . . . 365
POPA N. and S. G. IONESCU, Kinetics of iodine sonolytic generation in potassium iodide aqueous solutions . . . 1561
POPA V., voir VASS M. . . . 683
POPESCU ANGELA, voir MIRCEA D. GHEORGHIU . . . 481
POPESCU ANGELA, voir MIRCEA D. GHEORGHIU . . . 1779
POPESCU CRISAN and E. SEGAL, On the temperature integral used in nonisothermal kinetics . . . 567
POPESCU DUMITRU-SILVIU, voir SERBANSEVER . . . 297
POPESCU GEORGETA, GH. NECHIFOR, BUJOR ALBU and N. LUCA, Microporous polyethersulphone membranes . . . 577
POPESCU G., voir NECHIFOR GH. . . . 2047
POPESCU M., voir MOGA N. . . . 1995
POPOVICI EV., voir BOLD A. . . . 59
POPOVICI EV., voir BOLD A. . . . 1699
POPOVSKII V. V., Main problems in the field of ecologic catalysis (in Russian). . . 855
POSTOLACHE CARMEN and T. ONCESCU, Kinetics of hemoglobin and casein hydrolysis catalyzed by alcolase . . . 581
PROKHOROV A. M., V. I. KONOV, V. P. AGEEV, I. URSU and I. N. MIHAILESCU, Surface structuring by UV-laser irradiation in a gaseous atmosphere 235
PROKHOROV A. M., voir URSU I. . . . 667
PURI A. M., voir TEOREANU I. . . . 357

RADU C., voir LUCA C. . . . 1849
RAILEANU D., voir DUMITRASCU F. . . . 1183
RAILEANU D., voir PETRIDE H. . . . 1251
RAZUS C. ALEXANDRU, M. D. GHEORGHIU and E. BARTHA, Solvolyses in substituted cyclopropylcarbinylic systems. 5. Behaviours of spiro-cyclopropane-indanic alcohols . . . 1263
RAZUS C. AL., M. D. GHEORGHIU, ZS. G. ARVAY, A. I. IANCU and E. BARTHA, Solvolyses in substituted cyclopropylcarbinylic systems. 6. Solvolysis of spiro(acenapthene-1,1′-cyclo-propan)-2-ol . . . 1397
RAZUS C. AL., M. D. GHEORGHIU and E. BARTHA, Solvolyses in substituted cyclopropylcarbinylic systems. Part 7. Solvolysis of spiro [2.4] heptan-4-ol. . . 2075
REASH EL ABU G. M., voir MOSTAFA M. R. . . . 839
RIMAN JOSEF, Contribution of the Czechoslovak Academy of Sciences to the development of the modern Czechoslovak biotechnologies. . . . 247
ROMANOV A. M., voir MATVEEVICH V. A. . . . 831

ROMANOV A. M., voir STURZA A. R. 351
ROSCA S., voir STERNBERG S. 337
RUSAN V., voir SIMIONESCU C. I. 597
RUSAN V., voir SIMIONESCU C. I. 1573
RUSU M., voir MARCU GH. 207
RUSSU V. G., voir VATAMAN I. I 689

SAAD E. F. and E. A. HAMED, Addition compounds of isolated, fused and isolated-fused aromatic systems with 2,4,6-trinitrophenol. A spectroscopic study. . . . 1753
SAHINI MARINA, voir M. ZAHARESCU 703
SAHINI V. E., and CRISTINA POP, A molecular orbital approach to some radiogenetic mechanisms 253
SAHINI V. EM., voir DONESCU A. 453
SALEH A.H.M., voir MAHOMED F. ABDEL MEGEED. 1957
SALEM A. I. MONEER, A. M. EL-GENDY and S. I. EL-NAGDY, Behaviour of 4-(4'-bromo-3'-methyl)phenyl-1(2H)-phthalazionone towards some nucleophiles and electrophiles 1963
SAVA G., voir SANDULESCU D. 259
SAVA I., voir BRUMA M. 1467
SAVU D., voir AVRAM R. 35
SALAGEANU I. and E. SEGAL, Building-up and testing a catalytic stirred flow-reactor 1569
SANDESCU F., voir BELDIE C.. 445
SANDULESCU D. and GABRIELA SAVA, Thermodynamics of irreversible processes on electroosmosis of aqueous electrolyte and nonelectrolyte solutions. . 259
SĂRGHIE and CATINCA SIMION, Kinetics of the back-extraction of iron β-diketonates 1405
SCÂRLETE M., voir LAUDONIU D. 191
SCHIERIG U., voir J. EPPERLEIN 1835
SCHIKETANZ A., voir U. BOLOGA 1131
SCHIKETANZ A., voir M. D. GHEORGHIU 1005
SCHROTH WERNER, New aspects in the chemistry of pyrylium salts : changes due to dialkylamino substituents 271
SDRULA S., M. PIRLOG, L. FIERASCU, A.-M. HINTZ, L. CORNEA, N. LUCACIU and M. PATRU, Polyesters for polyurethanes. Triethanolamine based polyesters 437
SEGAL E. and T. COSEAC, Basic versatile program for nonisothermal kinetics. . . 287
SEGAL E., voir CRIŞAN POPESCU 567
SEGAL E., voir VLAD O. M.
SEGAL E., voir SALAGEANU I. 1563
SEMENESCU G., voir LUCA C. 197
SEROVA IRINA, G. OLEINIKOVA and A. I. GHINAC, Investigation of the processes of the oleandomycin phosphate inactivation (in Russian) 1075
SHAFRANSKI V. N., voir MATVEEVICH 831
SHAMI KU JHA, voir AGRAWAL G. L. 1769
SHIUNDU P. M. and S. B. JONNALAGADDA, A novel spectrophotometric method for determination of peroxydisulphate ion using *o*-dianisidine-S_2O^8 Cu(II) reaction 1661
QI-SHUN GU, H. D. CHEN and R. Z. KUANG, Rare earth perovskite catalysts for control of automatice pollutants 1565
SIK O. K., voir PINCOVSKI E. 1055
SILAGHI-DUMITRESCU I., voir SILAGHI D. L. 305
SILAGHI-DUMITRESCU I, voir DIUDEA V. M. 1175
SILAGHI-DUMITRESCU LUMINIŢA, I. SILAGHI-DUMITRESCU and IONEL HAIDUC, The sulfotropic molecular rearrangement of tetraorganodiarsine disulfides 505
SILBERG I. A., voir ONICIU L. 537
SILBERG I. A., voir BRIE M. 733
SILBERG I. A., voir BRIE M. 945
SILBERG I. A., voir BRIE M. 111
SILING S. A., Synthesis and research of polymers based on nitriles of polycarboxilic acids and on diamines (in Russian). 585
SIMION CATINCA, voir SĂRGHIE I. 1405

SIMIONESCU I. CRISTOFOR, A. A. POPA, E. COMANITA and VIRGIL BARBOIU, Azoamide derivatives obtained from ethyl phenylazocarboxylate. . . 317

SIMIONESCU I. CR., A. CHIRIAC, I. NEAMTU and V. RUSAN, Adhesive emulsions. 4. Synthesis of the vinyl acetate/methyl methacrylate/acrylamide in the absence of emulgators 597

SIMIONESCU I. CR., voir BRUMA M. 1467

SIMIONESCU I. CR., voir MIHAILESCU C. 1535

SIMIONESCU I. CR., A. CHIRIAC, I. NEAMTU and V. RUSAN, Adhesive emulsions 5. On some acrylic and methacrylic copolymers. 1573

SIMON H., voir GERGEN I. 995

SIMON ZENO, voir VALCEANU R. 377

SIMON ZENO, voir I. GERGEN I. 995

SINGH H. R., and B. V. AGARWALA, Bipositive metal complexes of nicotinic acid hydrazone derived from hydroxybenzaldehyde 2021

SINGH H. and S. P. S. TOMAR, Micellar behaviour of calcium and magnesium soaps of higher fatty acids in dilute aqueous solutions at different temperatures . . 1691

SÎRBU A., voir BUTUCEA A. 1155

SMELOV V. A., voir I. I. VATAMAN. 689

SMOLEANU D., voir ANGELESCU E. 25

SOTOLA Y., voir KNOR Z. 1373

SOACU P., S. PLOSTINARU, L. PATRON, A. CONTESCU, D. CRISAN and N. STANICA, Rare earth mixed oxides with transition metals. II. Mixed oxides with Fe(III) having a perovskite and garnet structure 323

SPACU P., L. PATRON, S. PLOSTINARU, A. CONTESCU and. N. STANICA, Coordination compounds as raw materials for mixed oxides. V. Mixed coordination compounds of lanthanides and Co(II), Ni(II) or Fe(III) with gluconic acid . . . 1275

SPANU V., voir NICOLESCU I. V. 1047

SPIRATOS M., A. AIRINEI, N. STANICA, N. VOICULESCU and G. I. RUSU, Coordination polymers. VIII. Chelate polymers of 2,4-dihydroxyacetophenone. 1413

STAN I., E. CHIFU, Z. FINTA and E. GAVRILA, Marangoni translation motion of a free drop initially at rest 603

STANCIUC G., MIRON-TEODOR CAPROIU, H. CALDARARU, A. CARAGHEORGHEOPOL, T. CONSTANTINESCU and A. T. BALABAN, Factors affecting stability and equilibria of free radicals. XVI. Preparation and ESR spectra of capto-dative-N-alkoxy-dinitrophenylaminyls 1895

STANESCU MICHAELA, M. BANCIU and ALEXANDRU T. BALABAN, 1-Oxonia and 1-aza analogues of triptycene 617

STANESCU D. M., voir BANCIU M. 1921

STANESCU LIGIA, voir MIRCEA D. GHEORGHIU 1931

STANICA N., voir P. SPACU 323

STANICA N., voir P. SPACU 1275

STANICA N., voir SPIRATOS M. 1413

STEFANOVA R., I. BANCHOV and I. PETROVA, On the structure of the disodium *p*-isononylphenylethoxysulphosuccinate 331

STERNBERG S., M. UNGUREANU and S. ROSCA, Electrochemical oxidation of carboxilic acids. I. Electrode processes in the electrochemical oxidation of 3-phenylpropionic acid 337

STERNBERG S., I. V. COTÂRȚĂ and D. CONSTANTINESCU, Oscillating phenomena during anodic polarization of sulphur containing nickel electrodes. 623

STERNBERG S. and M. DRAGANOIU, The mean activity coefficient of $CuSO_4$ and excess functions in the aqueous electrolyte systems: $CuSO_4 + Na_2SO_4 + H_2O$; $CuSO_4 + K_2SO_4 + H_2O$ and $CuSO_4 + ZnSO_4 + H_2O$. 859

STERNBERG S., voir V. BRANZOI 937

STERNBERG S., voir DRAGANOIU M. 967

STERNBERG S., voir V. BRANZOI 1457

STERNBERG S., V. BRANZOI and L. APATEANU, Contribution to the calculation of E—I curves for electrode processes with insoluble films formation. I. The influence of the potential sweep rate on the Pb/Pb^{2+} electrode process, in sulphur acid solutions 1281

STERNBERG S., L. APATEANU, V. BRANZOI and M. GAUST, Contribution to the calculation of E—I curves for electrode processes with insoluble films formation. II. Computation model of the E—I curves, at the Pb/Pb^{2+} electrode process, in

sulphuric acid solutions 1581
STERNBERG S., N. BONCIOCAT, A. COTÂRŢĂ and T. VISAN, Electrode processes with interfacial generation of the electrochemical active species. II. 1627
STOIANOVA J., voir PETROVA L. 561
STOICA M., voir DUMITRIU E. 1195
STRIBECK N., S. POLIZZI, P. BÖSECKE and H. G. ZACHMANN, Investigations of strained S—B—S block copolymers with dilute elastic networks 635
STURZA A. RODICA, V. E. NENNO and A. M. ROMANOV, About the electrochemical durability of dioxide manganese anodes obtained by electric spark method (in Russian) 351
SUKIASYAN A. A., voir MANTASHYAN A. A. 821
SURPATEANU GH., voir M. D. GHEORGHIU 481
SURPATEANU GH., voir M. D. GHEORGHIU 1931
SYAMAL A., Studies on biguanide derivatives. Copper (II) complexes with ethylenedibiguanide, trimethylenedibiguanide, *meta*-phenylenedibiguanide, piperazinedibiguanide and phenylbiguanide 1887
SERBAN SEVER, STELUTA CHIPER and SILVIU-DUMITRU POPESCU, Determination of $Cu^{2+} \cdot Pd^{22}$ and Zn^{22} by differential-pulse polarography 297
SIMANDAN T., voir DEAKY A. 1169
STEFAN A., voir JINESCU G. 1217

TARASZEWSKA J., Complexation of isomeric chloronitrobenzenes by β-cyclodextrin in the presence of ethanol 1419
TAVARU E., voir IVAN G. 1017
TANASE A., voir TODOR D. N.. 877
TEOREANU I. and ANNEMARIE PURI, Formation and stability of $3(CaO \cdot Al_2O_3) \cdot BaSO_4$ (in German) 357
TEOREANU I. and MARIA GEORGESCU, Hydratation processes in the $3CaO \cdot SiO_2$ $-3(CaO \cdot Al_2O_3)CaSO_4 - H_2O$ system (in French) 649
TEOREANU I., EC. ANDRONESCU and S. CONSTANTINESCU, Compatibility relations in the $Li_2O—BaO—SiO_2$ system 869
TODOR D. N., A. TANASE, V. DAVID and G. E. BAIULESCU, Thermo-analytical study of the complexes of palladium with α, α′-dipyridyl, *p*-nitrosodimethylaneline and *p*-nitrosodiphenylamine 877
TOMAR S. P. S., voir H. SINGH 1691
TOMAS ST., voir CRISTESCU C. 1321
TORBOVA E., voir L. PETROVA 561
TRANDAFIR V.,M. LECA and C. MANDRAVEL,Characterization of complexes formed by chromium basic salts, with natural and synthetic tanning polyphenols 661
TSAKIRIS C., voir GH. MARIA. 1377
TSAKIRIS C., voir BOGZA G. 1139
TUDOSE R. Z., M. FOURAR, O. PETRUS and B. CONSTANTIN, Study of the performance of a new type of vibration extraction apparatus. I. Hydrodynamic characteristics of the apparatus (in French). 1081
TARANU I., I. COMAN, M. NEMES and C. COMAN, The electrode surface — a decisive factor in electrochemical oxidation of benzene to *p*-benzoquinone in undivided cells 1593

UDALOV N. I., voir KALININ V. N. 503
UNCUTA C., T.—S. BALABAN, A. PETRIDE, F. CHIRALEU and A. T. BALABAN, Reaction of pyrylium salts with nucleophiles. XXII. Regioselectivity (formation of aniline derivatives from primary amines and non-symmetrically substituted pyrylium salts) and chemoselectivity (pyridinium vs. aniline formation) 1425
UNGUREANU M., voir STERNBERG S. 337
URSU I., voir PROKHOROV A. M. 235
URSU I., R. ALEXANDRESCU, I. MORJAN, I. N. MIHAILESCU, C. GRIGORIU, A. M. PROKHOROV, V. I. KONOV and YU. N. PETROV, Prospects for IR laser applications in chemical technology 667

VANCA V., voir D. LAUDONIU . . . 191
VARHELYI CS., voir GANESCU I. . . . 171
VARHELYI CS., voir GH. MARCU . . . 1029
VASILE AURELIA, voir A. BOLD . . . 59
VASILE AURELIA, M. CRUCEANU and V. ABABI, Contributions to the interpretation of experimental adsorption isotherms of water on highly silicious zeolites ZSM-5 . . . 1601
VASILE AURELIA, voir A. BOLD . . . 1699
VASILESCU MARILENA, Quenching of fluoranthene fluorescence by amines. . . . 1819
VASILESCU D. S., voir BOGHINA C. M. . . . 933
VASILIU-OPREA CLEOPATRA and MARCEL POPA, Tensile creep of monofilaments based on acrylonitril-vinyl acetate-α-methyle styrene ternary copolymer (in German). . . . 365
VASILIU-OPREA CLEOPATRA, AL. C. CONSTANTINESCU and S. DUMITRIU, Study of thermal complexing of microcrystalline celluloses with transition metals . . . 883
VASILIU D., voir LAUDONIU D. . . . 191
VASS M. I., I. BALINT and V. POPA, Methane oxidation on supported palladium catalysts . . . 683
VASS M., voir OSICEANU P. . . . 1541
VASS M., voir GUTU A. . . . 1843
VATAMAN I. I., L. S. KOPANSKAYA, I.G. KIRIYAC, V. A. SMELOV and V. G. RUSSU, The polarography determination of lead and tin in alloys (in Russian) 689
VALCEANU RADU, ZENO SIMON and LUDOVIC KURUNCZI, Quantum chemical calculations for dipole moments of phosphorous compounds . . . 377
VILCHEZ J. L. Q, voir HERNANDEZ E. J. . . . 1637
VILCICA D., voir BOLOGA U. . . . 1131
VILCU RODICA and MINODORA LECA, Thermodynamic characterization of polymers by chromatography with gas mobile phase . . . 387
VILCU RODICA, I. GAINAR, ST. PERISANU and GH. ANITESCU, Vapour pressures of *cis*- and *trans*-2-butenes . . . 697
VLAD M. O. and E. SEGAL, Chemical systems with uncertain parameters. The method of integral equations . . . 1095
VLASSA M., MARIA KEZDI and MARIA FENESAN, Preparation of n-alkylphthalamides of Ce(IV) with sulphanilic acid. . . . 1611
VLADESCU LUMINITA and IRINEL BADEA, Analytical applications of a few azopyrazolonic derivatives, I. Spectrometric determination of iron (III) with an azopyrazolonic derivative of anthranilic acid . . . 895
VLADESCU LUMINITA and STELUTA CHIPER, Combined ion exchange spectrometric study of the Ce(IV)-sulphanilic acid system. II. Spectrometric determination of sulphanilic acid. . . . 1287
VOLINTIRU T., G. IVAN, ELENA BUGARU and PAULA BUJENITA, Vulcanization of acrylonitrile-butadiene rubber with alkylphenol formaldehyde resin. . 1101

WANG YUAN X., voir YANG WAN L. . . . 377
WEINBERG J., voir DONESCU A. . . . 453

YADAVA K. L., voir MISHRA S. K. . . . 1877
YAMPOLSKY IM. P., voir PLATE N. A. . . . 1545
LIAN-WAN YANG and XIU-YUAN WANG, Studies on the hydrocarbon production by immobilized *Botryococcus braunii* cells . . . 397
YANNY AMAL SABET, ALI ALI ABEL-HAFEZ and AHMED MOHAMED MOHARRAM, Synthesis of some new 7-substituted aminimethyl-8-hydroxy-quinoline-5-substituted sulphonamides for biological interest . . . 1775
YATSIMIRSKII, K. B., Application of macrocyclic compounds for biosynthesis modelling (in Russian) . . . 403

ZACHINYAEV YA. V., A. I. BOBROV and A. I. GHINAC, 13-Dipolar cycloaddition reactions of nitril-imines with potassium salts of ethynylthio (seleno) lates (in Russian) 901
ZACHMANN H. G., voir STRIBECK N. 635
ZAHARESCU MARIA, C. PIRLOG, M. CRISAN and MARINA SAHINI, Structural characterization of vitreous SiO_2 made from gels 703
ZAKHAROVA A. INESSA, Some aspects of biocoordination chemistry of palladium and platinum compounds 1615
ZALARU FLORICA, F. CORNEA, A. MEGHEA and D. IONESCU, Coordination compounds of $CuBr_2$ with some triazenoimidazole derivatives 1107
ZELENTSOV V. I., voir DATSKO YU. T. 1163
ZHAVORONKOV N. M., Chemical technology as science and subject (in Russian) 409
ZSAKO J., voir GANESCU I. 771
ZUCA STEFANIA and MARIELA CONSTANTINESCU, On the complex ions in molten $TlCl-CdCl_2$ system 1439

Revue Roumaine de Chimie, **35**, *1*, 133–139 (1990)

INDEX DES SUJETS

Achievements and expectations in crude oil processing — B. OLTEANU 215
Activator in the catalytic systems of ring-opening polymerization of cyclopentene — M. DIMONIE, A. CORNILESCU, V. DRĂGUŢAN, E. NICOLESCU, S. COCA, M. CUZMICI, V. APOSTOL, R. MUNTEANU, R. GROSESCU, A. VASILESCU and M. TEODORESCU 1293
Active transport of amino acids through ligand membranes by macrocyclic carriers and pH gradient — C. LUCA, L. MUTIHAC, T. CONSTANTINESCU and ANA CSUMA 2039
Activity coefficient of $ZnSO_4$ and $CuSO_4$ in the electrolyte solutions — M. DRAGANOIU and S. STERNBERG 967
Addition compounds of isolated, fused and isolated-fused aromatic systems with 2,4,6-trinitrofenol. A spectroscopic study — E. F. SAAD and E. A. HAMED.. . . 1753
Adhesive emulsions. 4. Synthesis of the vinyl acetate/methyl methacrylate/acrylamide — C. SIMIONESCU, A. CHIRIAC, V. RUSAN and I. NEAMTU. 597
Adhesive emulsions. 5. On some acrylic and methacrylic copolymers — C. I. SIMIONESCU, AURICA CHIRIAC, IORDANA NEAMTU and V. RUSAN 1573
Alpha adrenergic clonidine derivatives. Qsar by MTD for multiconformational molecules. A. MONTSENIGOS, D. CIUBOTARIU, A. CHIRIAC and Z. SIMON 2101
Aminoanthraquinone (cyclic voltametry). M. CIUREANU, M. CONSTANTINESCU and A. MEGHEA.. 1491
An adapted model to predict operating conditions for a radiant furnace—thermal craching reactor GH. MARIA, C. TSAKIRIS, C. MARIA, A. ISOPESCU and G. BOZGA 1377
Analytical applications of a few azopyrazolonic derivatives. I. Spectrometric determination of iron(III) with an azopyrazolonic derivative of anthranilic acid. LUMINIŢA VLĂDESCU and IRINEL BADEA. 895
Angular overlap model (AOM) calculations for the coordination compounds with macrocyclic ligands. II. AOM parameters for nickel (II). M. ANDRUH, O. D. CHIRICA and M. BREZEANU 917
Application of macrocyclic compounds for biosynthesis modelling (in Russian). K.B. YATSIMIRSKII 403
2-Arylthio-5-methyl-2-thiono-1,3,2-dioxaphospholanes. V. MURESAN, I. FENESAN and L. PASKUCZ 1761
As-triazine derivatives with potential therapeutic action. XXIII. Synthesis of 4-thioxo-5(chlorobenzyl)thio-6-azauracil derivatives and their nucleosides. C. CRISTESCU and ST. TOMAS 1321
Aspects concerning the polymerization of isoprene with lanthanide based catalysts. M. DIMONIE, V. FIEROIU, G. HUBCA, V. GRUBER, E. G. BADEA, M. VLADULESCU, A. VERESTOI, H. IOVU and IOANA VASILE 5
Aspects on the stereochemistry and mechanism of ring-opening polymerization of cycloolefines chemistry and mechanism. M. DIMONIE, A. CORNILESCU, V. DRAGUŢAN, E. NICOLESCU, S. COCA, L. POPESCU, M. CUZMICI, C. OPRESCU, M. TEODORESCU, GH. HUBCA, R. GROSESCU, A. VASILESCU and M. CHIPARĂ 907
Azoamide derivatives obtained from ethyl phenylazocarboxylate. C. SIMIONESCU, A.A. POPA, E. COMANITA and V. BARBOIU 317

Basic versatile program for nonisothermal kinetics — E. SEGAL and T. COSEAC 287
Benzofurans. III. ABDEL BAHID, A. G. GHATTAS 1987
Biguanide derivatives. A. SYAMAL 1887
Biotechnologies in the chemical industry. M. FLORESCU. 459

Bipositive metal complexes of nicotinic acid hydrazone derived from hydroxybenzaldehyde H. R. SINGH and B. V. AGARWALA 2021

Bis(3-carbethoxy-1,5-di-*o*-anisylformasyl)Ni(II). A new unusual pentacoordinate formazane complex. A. C. BANCIU 921

1,3-Butadiene polymerization in the presence of modified $TiCl_4$-TIBA-I_2 catalyst. Mechanism and stereochemistry of — V. FIEROIU, V. DRĂGUŢAN, E. SIMIONESCU, E. GRUBER, C. PIROJOC, C. ION and V.APOSTOL 15

Carbon chemistry. A. CALUSARU 1787

Carbon 13 nuclear magnetic resonance assignments of the saturated segment from 1,2,3,4-tetrahydrophenanthrene by means of ^{13}C and ^2H labelling. M. D. GHEORGHIU, A. SCHIKETANZ, A. NECULA and A. T. BALABAN 1005

Catalytic cobalt and hydrogen discharge in the Co(II)-2-mercaptobenzo-thiazole-ammonia buffer. A. CALUSARU 1473

Ceramic pigments in the TiO_2-BaO-M_xO_y system. E. IVAN and D. BECHERESCU . . . 797

Characterization of complexes formed by chromium basic salts with natural and synthetic tanning polyphenols. V. TRANDAFIR, M. LECA and C. MANDRAVEL 661

Charge-transfer complexes of hydroxy styryl cyanine dyes and their analogues with nicotine. M. GIRGIS and Z. KHALIL 1721

Chemical graphs. Part 42. Valence isomers of bis-homoannulenes. A. T. BALABAN. . 1745

Chemical systems with uncertain parameters. The method of integral equations. M. O. VLAD and E. SEGAL. 1095

Cobalt chelates with ethylenediimino-bis-benzoyl-acetone. C. H. MARCU, CS. VARHELYI 1029

Coefficient activity of $CuSO_4$ · S. STERNBERG and M. DRAGANOIU. 859

Combined ion exchange spectrometric study of the Ce(IV) — sulphanilic acid system. II. Spectrometric determination of sulphanilic acid. L. VLADESCU and S. CHIPER 1287

Compatibility relations in the Si_2O-BaO-SiO_2 system. I. TEOREANU, L. ANDRONESCU and S. CONSTANTINESCU 869

Complexation of isomeric chloronitrobenzenes by β-cyclodextrin in the presence of ethanol. J. TARASZEWSKA. 1419

Complex compounds of divalent manganesse. D. NEGOIU, M. HANDREA, M. NEGOIU and O. MAIOR 1245

Complex ions in molten TlCl-$CdCl_2$ system. S. ZUCA and M. CONSTANTINESCU 1439

Contribution to the calculation of E — I curves for electrode processes. S. STERNBERG, L. APATEANU, V. BRANZOI 1281

Contribution to the calculation of E — I curves for electrode processes with insoluble films formation. II. Computation model of the E — I curves, at the Pb/Pb^{2+} electrode process, in sulphuric acid solutions. S. STERNBERG, L. APATEANU, V. BRANZOI and M. GAUST 1581

Considerations concerning oxide/metal/electrolyte system in non-equilibrium regime. C. LUCA, A. ANDREI and G. SEMENESCU. 197

Contributions to the interpretation of experimental adsorption isothermes of water on highly silicious zeolites ZSM-5. A. VASILE, M. CRUCEANU and V. ABABI 1601

Considerations on the chemical regime maintenance in a water colling system. L. NEGULESCU 1037

Considerations on the synthesis and properties of usual surfactant-free acrylic dispersions. N. MOGA, O. CUCU, M. POPESCU 1995

Conversion of $C_3 - C_4$ alkenes into gasolines by using ZSM-5 zeolites catalyst E. ANGELESCU, G. MUSCA, G. POP, E. POP, D. SMOLEANU and G. POGONARU 25

Coordination compounds of $CuBr_2$ with some triazenoimidazole derivatives. F. ZALARU, F. CORNEA, A. MEGHEA and D. IONESCU. 1107

Coordination compounds as raw materials for mixed oxides. V. P. SPACU, L. PATRON, S. PLOSTINARU, A. CONTESCU and N. STANICA 1275

Coordination polymers. VIII. M. SPIRATOS, A. AIRINEI, N. STANICA, N. VOICULESCU and C. I. RUSU 1413

Critical energy. The high degree generality of the principle. V. V. JINESCU. 491

Crosslinking of brominated butyl rubber by means of aromatic diamines. G. IVAN, E. TAVARU, M. GIURGINCA and D. N. NICOLESCU 1017

Decreased thermodynamical activity of oxygen in silicon single crystals grown by Czochrolski method. D. LAUDONIU, S. CIOBANU, A. MANEA, M. SCARLETE, C. BARTHA, V. VANCA, D. VASILIU, V. NINULESCU and G. CRISTIANI 191
Determination of Cu^{2+}, Pd^{22} and Zn^{22} by differential pulse polarography. S. SEVER, S. CHIPER and S. D. POPESCU 297
Determination of some liquid-vapour equilibrium data for acetone (1)-chloroform (2)-nonideal solution. GH. IONESCU, A. ONU and V. NAGACEVSCHI 1009
3,5-Dialkyl-2-furyl *p*-substituted-styryl ketones Synthesis and stereochemistry of — . U. BOLOGA, A. SCHIKETANZ, C. MUSAT, D. VILCICA, C. DRAGHICI, M. D. GHEORGHIU and A. T. BALABAN 1131
Diethyl maleate vinyl acetate copolymers in solutions. C. BELDIE, GH. NEMTOI, EM. DUMITRIU and V. BARBOIU 51

Electrochemical oxidation of carboxilic acids. I. Electrode processes in the electrochemical oxidation of 3-phenylpropionic acid. S. STERNBERG, M. UNGUREANU and S. ROSCA 337
Electrode processes with interfacial generation of the electrochemical active spaces II. S. STERNBERG, N. BONCIOCAT, ADINA COTARTA and T. VISAN . . . 1627
Electrical and magnetic properties of high — T_c superconductors (Y, Tm)-Ba-Cu oxides. P. OSICEANU, L. PATRON, S. PLOSTINARU, A. CONTESCU, L. CRISTEA, M. VASS, GH. ALDICA, S. MANDACHE, P. PAUSESCU and M. PETRASCU 1541

Electrolytic gases in the electrochemical stabilization of aluminium hydroxide, T. Ya. DATSKO and V. I. ZELENTSOV 1163
Electronic structure of molecules. Applications in physics chemistry and biology. R. DAUDEL 115
Electronic transitions in the square planar $Rh(PPh_3)SnCl_3$complex. A. C. BANCIU 1857
Emulsion polymerization of vinyl chloride (kinetic parameters k_i and k_t) A. BUTUCEA, A. SIRBU, C. S. GEORGESCU, A. IONESCU and I. DEACONESCU . . . 1155
Ethylene yield in naphtha pyrolysis process. Study of the thermal regime. G. BOZGA, C. TSAKIRIS, A. ISOPESCU 1139
Extraction of europium (III) from nitric and perchloric media by neutral bifunctional carbamoylmethylenephosphonates. NISTOR PERESCU and RENATO CHIARIZIA 1651

Factors affecting stability and equilibria of free radicals. XVI. G. STANCIUC, M.T. CAPROIU, H. CALDARARU, A. CARAGHEORGHEOPOL, T. CONSTANTINESCU and A.T. BALABAN 1895
Friedel-Crafts chemistry of unsaturated alicyclic systems. III. Friedel-Crafts reaction of unsaturated alicyclic acids in the presence of various Lewis acids. V. DRAGUTAN, I. DRAGUTAN, F. CHIRALEU and A.M. GLATZ 759
Friedel-Crafts chemistry of unsaturated alicyclic systems. IV. Effect of the catalytic system in Friedel-Crafts reaction of unsaturated esters V. DRAGUTAN, I. DRAGUTAN, C. CONDEIU and A.M. GLATZ 977

Heterocycles with annelated dibenzocycloalkene skeletons. M.D. BANCIU, M. D. STANESCU and F. CHIRALEU 1921
High voltage plasma applied to determine boron and silicon in superallied metallic powder. N. JUMATE and I. CHICINAS 1369
Hoch-Haaf reaction. N-acyl-glycines from N-hydroxymethyl-amides and -imides. An extension of — C. LEONTE and E. CARP 1241

^{1}H-NMR spectra of 5,9 methano-5H-benzo[3,4]cyclobuta[1,2]-cycloheptene derivatives. M. GHEORGHIU, ANGELA POPESCU and GH. SURPATEANU 481
Hydratation processes in the $3CaO.SiO_2$-3 $(CaO.Al_2O_3)CaSO_4$-H_2O system (in French). I. TEOREANU and MARIA GEORGESCU 649
Hydrogenation of aromatic nitro compounds. A. V. BULATOV 1149
Hydroquinone electrosynthesis from phenol. A. DEAKY, T. SIMANDAN, N. MIRICA, S. DRAGOS and M. MEDELEANU 1169

Interpolymer complexes formed by carboxylic polyacids with quaternary ammonium polysalts. M. LECA, M. OLTEANU and I. IONESCU-BUJOR 811
Investigation of the processes of the oleandomycin phosphate inactivation (in Russian). I. SEROVA, G. OLEINIKOVA and A. I. GHINAC 1075
Isoprene (polymerization with lanthanide based catalysts). M. DIMONIE, V. FIEROIU, G. HUBCA, V. GRUBER, E. G. BADEA, M. VLĂDULESCU, A. VERESTOI, H. IOVU and I. VASILE 5
Isothermal flow instability of polymeric fluids. G. JINESCU and A. STEFAN . . . 1217
Ketones with benzocyclobutano-norbornenic skelaton in the presence of dimethyloxosulphonium methylide. I. ENESCU, A. GHENCIULESCU, F.CHIRALEU . . 989
Kinetic study of the maltodextrine hydrolysis catalysed by immobilised glucoamylase. E. DUMITRIU, V. HULEA, M. STOICA and SP. OPREA 1195
Kinetics of the back-extraction of iron β-diketonates. I. SÂRGHIE and CATINCA SIMION 1405
Kinetics of hemoglobin and casein hydrolysis catalysed alcalase. C. POSTOLACHE and T. ONCESCU 581
Kinetics of iodine. N. POPA and S. G. IONESCU 1561
Kinetic theory of gas-liquid dispersions. O. IORDACHE, GHEORGHITA JINESCU D. LAVRIC and V. LAVRIC. 785

Marangoni translation motion of a free drop initially at rest. I. STAN, E. CHIFU, E. GAVRILA 603
Mass transfer in an air-lift biological reactor. I. GHEORGHITA JINESCU and V. LAVRIC 149
Mediated electrocatalysis. General aspects. L. ONICIU, M. JITARU and I. A. SILBERG 537
Membranes by immersion-precipitation method. GH. NECHIFOR, N. LUCA, G. POPESCU and M. NECHIFOR 2047
Mercury determination in water and atmosphere at concentrations lower than parts per billion. C. LUCA, A. DANET and C. RADU 1849
Mesoionic oxazolones. III. M. PETRIDE and D. RAILEANU 1251
Methane oxidation on supported palladium catalysts. M. I. VASS, I. BALINT and V. POPA 683
Microporous polyethers membranes. G. POPESCU, GH. NECHIFOR, B. ALBU. . . 577
Microprocessor operated scanning UV-VIS monochromator. E. DARVASI, N. MIOSCU, A. MORARU, C. OANCEA and E. CORDOS 961
Molecular topology. I. Valence group electronegativity as a vertex discriminator. MIRCEA DIUDEA and ION SILAGHI DUMITRESCU 1175

Nitration of 2,6-dimethyl-4-phenylpyrylium sulfoacetate. T. S. BALABAN, E. COSTACHE and A. PETRIDE 1449
N-(nitro-substituted phenyl(-4-amino-2,6-dibutyl-phenols by cyclic voltammetry Electrochemical oxidation of — M. CIUREAN, J. HERDAN and A. T. BALABAN 739
Neutralization of nitrogen oxides on CuO and Co_3O_4 catalysts. M. CHRISTOVA, D. PANAYOTOV. 517
Ni(II)-hydroxylamine reaction system (in French). I. BERDAN and O. COSTINOAIA 1307
Nuclear magnetic resonance investigations. M. D. GHEORGHIU, C. DRAGHICI, L. PARVULESCU and M. ELIAN 1341
Nuclear magnetic resonance of small rings. 8. ^{13}C-NMR spectra of 8-substituted 5,9 methano-5H-benzo[3,4]cyclobuta[1,2]cycloheptenes. M. D. GHEORGHIU and A. POPESCU 1779
Nucleophilic and electrophilic reactions of 1,5 diketones V. G. KHARCHENKO and S. N. CHALAYA 509

Optimization of eluent synthesis for separation by thin layer chromatography of some 1-(2-pyrimidyl)-3-methyl-5-pyrazolone derivatives. S. GOCAN, L. OLENIC and I. CRISTEA 1509
Oscillating phenomena during anodic polarization of sulphur containing nickel electrodes. S. STERNBERG, I. V. COTARTA and D. CONSTANTINESCU. 623
Oxidation of ethylene glycol with pyridinium chlorochromate. G. L. AGRAWAL and KU SHAMI JHA 1769
Oxidation of cumene with molecular oxygen in presence of Co(II) acetylacetonate complexes. A. C. BANCIU, S. PLOSTINARU, M. ANDRUH, L. PATRON and A. CONTESCU 1711

μ_3-oxo-trinuclear chromium acetate in the frame of the angular overlap model. Electronic structure of — F. CIMPOESU, M. FIERBINTEANU and M. ANDRUH 2013
Oxidative acetoxylation of hydrocarbons over metal-containing catalysts. (in Russian). KH. M. MINACHEV and V. V. KHARLAMOV 527
1-Oxonia and 1-aza analogues of triptycene. M. STANESCU, M. BANCIU and A. T. BALABAN 617

Periodically driven Briggs-Rauscher reaction. C. BELDIE, I. GROSU, M.BOURCEANU, and G. BOURCEANU 725
Permethylated dextran as stationary phase in gas chromatography. I. CIUCANU and C. LUCA 1829
Pd(II) complex compounds with tioethers. S. NEAGOE, D. NEGOIU, V. NEAGOE, M. NEGOIU 2029
Phase composition and structure in Fe-Mg-O catalysts for oxydehydrogenation of n-butenes to butadiene. I. V. NICOLESCU, GH. NEDELCU, R. MĂNĂILĂ, M. IVASCU, F. AVRAMESCU, V. SPĂNU and G. FILOTI 1047
Phase transfer free radical reactions. II. Polymerization of acrylonitrile. C. MIHAILESCU V. BULACOVSKI and CR. SIMIONESCU 1535
Polarization behaviour of lead in sulfuric acid solution containing ammonium. V. BRANZOI, S. STERNBERG and L. APATEANU 937
Polarization behaviour on limited potential ranges of the $Pb/H_2SO_4+Na_2SO_4$ system. V. BRANZOI, S. STERNBERG and L. APATEANU 1457
Polarography determination of lead and tin in alloys. I. I. VATAMAN, L. S. KOPANSKAYA, L. G. KIRIYAC, Y. A. SMELOV and V. G. RUSSU. . . 689
Polyesters for polyurethanes triethanolamine based polyesters. C. SDRULA, M. PÎRLOG, L. FIERĂSCU, A. M. HINTZ, L. CORNEA, N. LUCACIU and M. PĂTRU 437
Polymers of permanently antistatic ε-caprolactam (in French) M. IONESCU. . . . 129
Polymers containing phenylquinoxaline units. M. BRUMA, I. SAVA, C. HAMCIUC, C. I. SIMIONESCU, N. M. BELOMOINA, S. A. BABICH, E. S. KRONGANZ and V. V. KORSHAK 1313
Polyphenylquinoxaline-ester-imides. M. BRUMA, I. SAVA, C. HAMCIUC. 1467
Prediction of vapour-liquid equilibria at low pressure by a general equation. V. FEROIU and D. GEANA 1329
Preparation of n-alkylphthalimides of Ce(IV) with sulphanilic acid M. VLASSA, M. KEZDI and M. FENESAN 1607
Property of matter. II. V. JINESCU 161
Prospects for IR laser applications in chemical technology. I. URSU, R. ALEXANDRESCU, I. MORJAN, I. N. MIHAILESCU, C. GRIGORIU, A. M. PROKHOROV, V. I. KONOV and YU. N. PETROV. 667
1,2 Pyrazoles, Derivatives of—I. M. BRIE, I. A. SILBERG 733
1,2 Pyrazoles, Derivatives of — II. M. BRIE, I. A. SILBERG and N. PALIBRODA 945
1,2 Pyrazoles, Derivatives of — III. M. BRIE, M. PALIBRODA and I. A. SILBERG 2067
Pyridinium ylides Hindered rotation about the $N^+(sp^2)-C^-(sp^2)$ bond. H. PETRIDE 2057
Pyrylium salts : changes due to dialkylamino substituents. New aspects in the chemistry of W. SCHROTH 271
Pyrylium salts formed by diacylation of olefins. Part XXIV. Synthesis of *meta*-terphenyl derivatives and heterocyclic analogs *via* bis-pyrylium salts obtained by bis-diacetylation of *meta*-diisopropenylbenzene A. T. BALABAN and T. S. BALABAN 41

Quantum chemical calculations for dipole moments of phosphorus compounds. R. VALCEANU, ZENO SIMON and L. KURUNCZI 377
Quenching of fluoranthene fluorescence by amines. M. VASILESCU 1819

Radical polymerization of acrylamide in homogeneous and heterogeneous systems. C. M. BOGHINA, C. I. CINCU, N. N. MARINESCU, M. M. MARINESCU, M. V. DIMONIE and D. S. VASILESCU 933
Radiochemical method for determination of solubility. A. CECAL and GRETY-IRINA CIUCHI 953
Rare earth mixed oxides with transition metals. II. P. SPACU, S. PLOSTINARU, L. PATRON, A. CONTESCU, D. CRISAN and N. STANICA. 323
Reaction of *endo*- and *exo*-benzocyclobutenonorbornan-7-one with dimethyloxosulfonium

methylide. A. GHENCIULESCU, L. ENESCU, F. CHIRALEU and I. G. DINULESCU . . . 477

Reaction of pyrylium salts with nucleophiles. XXII. Regioselectivity formation of aniline derivatives from primary amines and non-symmetrically substituted pyrylium salts and chemoselectivity pyridinium as aniline formation. C. UNCUTA, T.S. BALABAN, A. PETRIDE, F. CHIRALEU and A. T. BALABAN . . . 1425

Rearrangement of 4-alkyl-3-(*o*-carboxyphenyl)sydnones to 1-acyl-1,2 dihydro-3*H*-indazol-3-ones. FL. DUMITRESCU and DAN RAILEANU . . . 1183

Recent developments in perfluoroorgano chemistry of selenium in various oxidation states. A. HAAS . . . 121

Redox behaviour of 3d ions in oxide glasses. P. BALTA and M. BIALE . . . 1301

Relationship between structure and effect of some organic compounds containing sulphur on steel corrosion inhibition process in acid medium R. AVRAM and D.SAVU . . . 35

Selective alkylation of toluene on ZSM-5 zeolites. E. DUMITRIU, N. BILBA, V. HULEA and S. OPREA . . . 983

Sn-free effect at the positive lead acid battery plates. D. PAVLOV, B. MONAKHOV, M. MAJA and N. PENAZZI . . . 551

Solute-solvent interactions in carbenicillin solubility processes. A. DONESCU, J. WEINBERG and V. EM. SAHINI . . . 453

Solvolysis of 5-(1′, 1′-dimethylethyl)-5-hydroxy-5*H*-dibenzo[a,d]-cycloheptene and some related compounds. E. CIORANESCU, A. VOICU and M. ELIAN . . . 87

Solvolyses in substituted cyclopropylcarbinylic systems. 5,6,7. A. RAZUS, M. D. GHEORGHIU, E. BARTHA . . . 1263, 1397, 2075

Stabilities of bivalent metal complexes with benzoyl-2-hydroxy-4-metoxy-3-methyl acetophenone. R. DIXIT and BHAGWAN S. GARG . . . 1705

Stereochemistry and mechanism of ring-opening polymerization of cycloolephins. Chemistry and mechanism. M. DIMONIE, A. CORNILESCU, V. DRAGUTAN, E. NICOLESCU, S. COCA, L. POPESCU, M. CUZMICI, C. OPRESCU, M. TEODORESCU, GH. HUBCA, R. GROSESCU, A. VASILESCU and M. CHIPARĂ . . . 907

Structural characterization of vitreous SiO_2 made from gels. M. ZAHARESCU, C. PIRLOG, M. CRISAN and M. SAHINI . . . 703

Structure activity relations for steroids by the MTD method. I. GERGEN, M. BOHL, H. SIMON and Z. SIMON . . . 995

Study on the monoalkylsulphosuccinate structure of mass spectroscopy. B. KUMANOVA and L. PETROVA . . . 1523

Study of the performance of a new type of vibration extraction apparatus. I. R. Z. TUDOSE, M. FOURAR, O. PETRUS and B. CONSTANTIN . . . 1081

Study of pyrazinhydroxamic acid reduction on a mercury electrode H. E. J. ALONSO, QUERO J. L. VILCHEZ and C. T. GUARDIA . . . 1637

Study of thermal complexing of microcrystalline celluloses with transition metals. CLEOPATRA VASILIU-OPREA, A. C. CONSTANTINESCU and S. DUMITRIU . . . 895

Study on the tetranitroplatinites (II) and hexanitro-platinates(IV) I. GANESCU, J. ZSAKÓ, CS. VÁRHELYI and E. PÁLL . . . 771

Study of the vapor-liquid equilibrium in the dioxane-water system. O. IULIAN, O. LANDAUER, D. GEANA and C. MATEESCU . . . 1209

Substituent effect on ^{19}F chemical shifts in 2-halo- and 2,6-dihalo-4-fluorophenols and anisoles (in Russian). D. I. KRAVTSOV, V. M. PACHEVSKAYA, L.S. GOLOVCHENKO, B. A. KVASOV and E. I. FEDIN . . . 807

Sulfotropic molecular rearrangement of tetraorganodiarsine disulfides L. S. DUMITRESCU and I. HAIDUC . . . 305

Surface mobility of surfactant solutions. XIII. E. CHIFU, I. STAN, M. SALAJAN and E. GAVRILA . . . 79

Surface structuring by UV-laser irradiation in a gaseous atmosphere. A. M. PROKHOROV, V. I. KONOV and I. N. MIHAILESCU . . . 235

Synthesis of 6,7-benzomorphanes using arenetricarbonylchromium complexes (in Russian). V. N. KALININ, S. K. MOISEEV, V. I. BARHMUTOV and M. I. UDALOV . . . 503

Synthesis of benzonorbornane exo-benzocyclobutano and endo-benzocyclobutanonorbornanes. M. D. GHEORGHIU, E. OLTEANU, L. STANESCU, M. AVRAM and GH. SURPATEANU . . . 1931

Synthesis and cardiotonic properties of 6-(3-pyridyl)nicotinonitrile derivatives. M. M. BADRAN, S. El MELIGIE and A. K. El-ANSARI 2093

Synthesis and ESR spectra of persistent aroxyls. III. Dialkyl 3,5-di-t-butyl-4-hydroxybenzylphosphonates and their corresponding aroxyls. J. HERDAN, N. NEGOIȚĂ, M. N. GRECU, M. D. GHEORGHIU and A. T. BALABAN 1515

Synthesis and reactions of D-glucosyl derivatives of 2-aryl-4(3H)-quinazolinones and their thione derivatives. M. F. ABDEL MEGEED and M. A. H. SALEH . . 1957

Synthesis and reactions of some new benzofurano(3,2-c)pyrazol-3-one. O.M.O. HABIB, A. H. ABD EL-RAHMAN and D. S. BADAWY. 1949

Synthesis of 9-substituted *exo*-benzocyclobutenonorbornenes. L. ENESCU, A. GHENCIULESCU, F. CHIRALEU and ILIE G. DINULESCU. 765

Synthesis ways of the o-antigenic polysaccharides. N. K. KOCHETKOV 1225

Unsaturated heteropolytungstates with Th(IV) central ion. GH. MARCU, M. RUSU and A. BOTAR 207

UV-VIS spectral behaviour of arylazo-compound. III. Solvent effect on the visible absorption band of 4-amino-substituted azobenzenes. J. EPPERLEIN, B. BLAU and U. SCHIERIG 1835

Vapor-liquid equilibria in the system dimethylsulfoxide-water I. O. LANDAUER, O. IULIAN, C. MATEESCU and D. GEANA 1529

Vapour pressures of *cis*- and *trans*-2-butenes. RODICA VILCU, I. GAINAR, ST. PERISANU and GH. ANITESCU 697

Vibration energy of new kinds of radioactivities. M. IVASCU, D. N. POENARU, I. IVASCU, E. HOURANI and W. GREINER 143

Vulcanization of acrylonitrile-butadiene rubber with alkylphenol formaldehyde resin. T. VOLINTIRU, G. IVAN, E. BUGARU and P. BUJENITA. 1101

Work function and electron impact desorption studies on Co/W adsorption A. GUTU and M. VASS 1843

Z-4b, 10b-dihydrochrysene (the physico-chemical characterization of). M. BANCIU, C. HADA, D. ALBAIU and C. DRAGHICI 1907

Zeolite molecular sieves as stationary phase in thin layer chromatography. V. On migration mechanism A. BOLD, A. POPA, A. VASILE, M. CRUCEANU, EV. POPOVICI, and M. ALEXANDROAEI 59

Zeolites (silicious) of ZSM-5 type. Ion exchange with transition metals. A. BOLD, A. VASILE, A. POPA, M. CRUCEANU, EV. POPOVICI and M. ALEXANDROAEI 1699

ZSM-5 zeolites (synthesis and characterization). E. PINCOVSCHI, M. MERCHES and KIM CHOL SIK 1055

ORSZÁGOS MŰSZAKI DOKUMENTÁCIÓS [illegible]

NOTE POUR LES AUTEURS

La Revue Roumaine de Chimie publie des articles en anglais, français, russe, allemand ou espagnol. Les auteurs sont priés d'envoyer des articles et des comptes rendus inédits.

Les manuscrits seront dactylographiés à double interligne. La bibliographie, les tableaux et la légende des figures seront placés après le texte.

Si l'article fait partie d'une série numérotée, la partie précédente sera donnée comme première reference.

Chaque article sera précédé d'un résumé comprenant quinze lignes au maximum.

Les références bibliographiques dans le texte seront faites par des exposants sans parenthèses et paraîtront à la fin de l'ouvrage.

Les publications périodiques mentionnées dans la bibliographie seront présentées suivant les prescriptions internationales : le nom de l'auteur précédé de l'initiale du prénom, le titre du périodique abrégé conformément à «Chemical Abstracts» et souligné par une ligne, le numéro du tome indiqué par des chiffres arabes et souligné par deux lignes, suivi de la première page de l'article : à la fin, l'année de la parution sera placée entre parenthèses. Le numéro de la revue ne sera pas indiqué si les pages du volume sont numérotées consécutivement.

Les textes des livres ou traités inclueront : le nom des auteurs, précédé de l'initiale du prénom, le titre du livre entre guillemets et sans être souligné, le numéro du tome précédé par l'abréviation «vol. » (ou «Bd »), le numéro de l'édition, les éditions (the publisher), la localité de la parution du livre, l'année de la parution et la page de la référence précédée(s) par l'abréviation «p » (ou «S »).

Les brevets seront indiqués comme suit : l'auteur ou la firme, le pays et le numéro du brevet, la date de la revue (*Chem. Abstr.*). Par ex. : M. Jones (to Union Carbide Co.) Brit. Pat. 610 238, 2 Sept. 1959 : cf. *Chem. Abstr.*, 54, 12808 (1960).

Si la référence n'a pas été lue en original, on indiquera aussi la revue de références consultée.

Les diagrammes seront tracés à l'encre de Chine sur papier calque. Les tableaux et les figures (en nombre strictement nécessaire), ainsi que les courbes dans les figures seront numérotés par des chiffres arabes. Leur explication sera donnée dans la légende des figures. Prière de ne pas inscrire les mêmes données dans les tableaux et les figures. Chaque tableau aura un titre. On indiquera dans le texte la place approximative des tableaux et des figures. Les formules chimiques seront incluses dans le texte ; en outre, elle seront transcrites sur papier calque, à l'encre de Chine.

Les auteurs sont priés d'indiquer les caractères italiques (en soulignant les lettres au crayon), ainsi que tout autre caractère spécial : les préfixes *ortho*, *méta*, *para*, *cis*, *trans*, etc. seront soulignés pour indiquer leurs caractères italiques, et ne seront jamais écrits avec des majuscules.

Aucune correction à la main ne sera admise sur le manuscrit. Les corrections seront frappées à la machine. Les lettres grecques ou d'autres symboles spéciaux seront insérés à la main à l'encre clairement.

Le manuscrit sera signé par l'auteur.

Le titre courant aura 50 lettres au maximum.

L'entière responsabilité du contenu des articles appartient aux auteurs.

Sur demande on peut obtenir une note plus complète.

PRINTED IN ROMANIA

TRAVAUX PARUS AUX ÉDITIONS DE L’ACADÉMIE ROUMAINE

I. G. MURGULESCU, **Introducere în chimia fizică, vol. I. 1. Atomi, molecule, legătură chimică,** 1976, 560 p.

I. G. MURGULESCU, V. EM. SAHINI, **Introducere în chimia fizică, Vol. I. 2. Structura şi proprietăţile moleculelor,** 1979, 604 p.

I. G. MURGULESCU, E. SEGAL, **Introducere în chimia fizică, Vol. II. 1. Teoria molecular-cinetică a materiei,** 1979, 1036 p.

I. G. MURGULESCU, TATIANA ONCESCU, E. SEGAL, **Introducere în chimia fizică, Vol. II. 2. Cinetică chimică şi cataliză,** 1981, 1024 p.

I. G. MURGULESCU, J. PĂUN, **Introducere în chimia fizică, Vol. I. 3. Nucleul atomic, reacţii nucleare, particule elementare,** 1982, 606 p.

I. G. MURGULESCU, RODICA VÎLCU, **Introducere în chimia fizică. Vol. III. Termodinamica chimică,** 1982, 624 p.

I. G. MURGULESCU, O. M. RADOVICI, **Introducere în chimia fizică, Vol. VI. Electrochimica,** 1986, 410 p.

C. SIMIONESCU, V. GORDUZA, **Implicaţiile bioenergetice ale coloranţilor,** 1988, 207 p.

R. VÎLCU, M. LECA, **Termodinamica polimerilor prin cromatografie de gaze,** 1987, 238 p.

I. ZUGRĂVESCU, M. PETROVANU, **Cicloadiţii 3 + 2 dipolare,** 1987, 446 p.

RAUL MIHAIL, ION GROZEANU, **Estimarea secvenţială aplicată sistemelor chimice,** 1986, 406 p.

M. BREZEANU, I. PATRON, M. ANDRUH, **Combinaţii complexe polinucleare şi aplicaţiile lor,** 1986, 244 p.

A. T. BALABAN et al., **Labelled Compounds and Radiopharmaceuticals Applied in Nuclear Medicine,** coédition avec John Wiley and Sons, 1986, 742 p.

D. PURDELA, **Nomenclatura chimiei organice — IUPAC,** 1986, 451 p.

PETRU BUDRUGEAC, **Probleme de chimie,** 1986, 280 p.

T. ONCESCU, S. G. IONESCU, **Conversie fotochimică şi stocare de energie,** 1985, 272 p.

V. DRĂGUŢAN, A. T. BALABAN, M. DIMONIE, **Olefin Metathesis and Ring-Opening Polymerization of Cyclo-Olefins,** coédition avec John Wiley and Sons, 1985, 544 p.

C. LITEANU, I. RÎCĂ, **Optimizarea proceselor analitice,** 1985, 360 p.

N. PERESCU, **Chimia extracţiei cu solvenţi şi aplicaţii,** 1985, 212 p.

ISSN 0035 — 3930

I.P. Universul c. 1655

43 426

Lei 40

F 1103

ACADÉMIE ROUMAINE

REVUE ROUMAINE DE CHIMIE

TOME 35
N° 3
Mars 1990

Rev. Roumaine Chim.

RRCHAX 35, *3*, p. 277–488 (1990), Bucarest

EDITURA ACADEMIEI ROMÂNE

ACADÉMIE ROUMAINE

COMITÉ DE RÉDACTION

Rédacteur en chef :

I. G. MURGULESCU, membre de l'Académie Roumanie

Rédacteurs en chef adjoints :

A. T. BALABAN et V. EM. SAHINI, membres de l'Académie Roumaine

Collège de rédaction :

EM. BRATU, ECATERINA CIORĂNESCU-NENITZESCU, CR. SIMIONESCU, P. SPACU, membres de l'Académie Roumaine, M. ANDRUH, M. BANCIU, M. D. GHEORGHIU., I. HAIDUC, D. MARCHIDAN, G. NIAC et D. SĂNDULESCU

La Revue Roumaine de Chimie paraît 10 fois par an. Toute commande de l'étranger sera adressée à « ROMPRESFILATELIA » — sectorul Export-Import Presă, P.O. Box 12—201, télex 10376 prsfi r 78104 Calea Griviței nr. 64—66, Bucuresti, Roumanie.

Les manuscrits, les livres et les revues proposés en échange, ainsi que toute correspondance seront envoyés à la rédaction :

REVUE ROUMAINE DE CHIMIE

125, Calea Victoriei, 79717 Bucarest, Roumanie, téléphone 50 76 80

EDITURA ACADEMIEI ROMÂNE
125, Calea Victoriei 79717, Bucarest, Roumanie, téléphone 50 76 80

REVUE ROUMAINE DE CHIMIE

ORSZÁGOS MŰSZAKI INFORMÁCIÓS KÖZPONT ÉS KÖNYVTÁR 1883

Tome 35, Nº 3 **Mars, 1990**

Dr. MIHAI ELIAN (1937–1988) 279–280

MIHAI ELIAN, Conformational preferences in substituted 5*H*-dibenzo [*a*, *d*]-cycloheptenes : the influence of a carbon-bonded substituent in position 5 . . 281–297

MIHAI ELIAN, CĂLIN DELEANU and SORIN ROȘCA, From camphor to bis[3-(trifluoroacetyl)camphorato] barium(II) in a one step synthesis . . 299–303

ROALD HOFFMANN, Creation and discovery 305–308

MIRCEA D. BANCIU, MIHAI ELIAN, ANCA BANCIU, CONSTANTIN DRĂGHICI, LIGIA STĂNESCU, PHAN LE THUY and ECATERINA CIORĂNESCU, Carbonium ion reactions. XX. Synthesis and acetolysis of 8-chloromethyl-dibenzo [b, d]bicyclo [5.1.0]octa-2,4-diene 309–322

CORNELIA UNCUȚA, FILIP CHIRALEU, MIRCEA D. GHEORGHIU and ALEXANDRU T. BALABAN,Reactions of pyrylium salts with nucleophiles. XV. Stereoisomers of polyarylpyridinium salts and their interconversion 323–338

MIRCEA D. GHEORGHIU, IOSIF SCHIKETANZ, ANA SCHIKETANZ and ALEXANDRU T. BALABAN, ^{13}C–NMR spectral assignments for 2,5-diarylthiazoles 339–343

IOSIF SCHIKETANZ, ANDREI ȘTEFĂNESCU, MIRCEA D. GHEORGHIU, ANA SCHIKETANZ and ALEXANDRU T. BALABAN, Aminoketone, oxazole and thiazole syntheses. Part XII. 2,5-diarythiazoles from thioazlactones and aromatic hydrocarbons 345–348

CĂLIN DELEANU and ALEXANDRU T. BALABAN, Chemical graphs. Part 53. Benzo- and polybenzo-derivatives of valence isomers of [12] annulene . . . 349–391

CLAUDIU SUPURAN, MARIUS ANDRUH and IOAN PUȘCAȘ, Carbonic anhydrase inhibitors. I. Metal complexes of sulfonamides : a novel class of carbonic anhydrase inhibitors 393–397

CLAUDIU SUPURAN, ALEXANDRU T. BALABAN, MIRCEA D. GHEORGHIU, ANA SCHIKETANZ, ANTONIE DINCULESCU and IOAN PUȘCAȘ, Carbonic anhydrase inhibitors. II. Membrane-impermeable derivatives of 1, 3, 4-thiadiazole-2-sulfonamide 399–405

JEAN M. HERDAN, VASILE DINOIU, AURELIA MEGHEA, MIRCEA D. GHEORGHIU, ANA SCHIKETANZ, MARIA GIURGINCA and ALEXANDRU T. BALABAN, Synthesis and EPR spectra of persistent aroxyls. IV. *Ortho*, *ortho'*-disubstituted phenols possessing in the *para*-position a 2-bonded-1,3-dicarbonylic (or a functionally related) group 407–414

Rev. Roumaine Chim. 35, *3*, 277–488 (1990), Bucarest

ANCA MARTON, URSULA BOLOGA, TEODOR-SILVIU BALABAN, MIRCEA D. GEORGHIU and ALEXANDRU T. BALABAN, ^{1}H–NMR assignments for 2,4-diaryl-pyrylium salts and -pyridines having fused 5- or 6-membered saturated rings bridging 5,6-positions 415–419

DANIELA CARMEN ONICIU, NICOLAE NEGOIȚĂ, MARILENA MORJAN, MIRCEA D. GHEORGHIU and ALEXANDRU T. BALABAN, Synthesis of substituted benzoins and the corresponding bis-1,2-enedithiol complexes of nickel, platinum, and palladium 421–426

MIRCEA D. GHEORGHIU, LUMINITZA PĂRVULESCU, K. M. TURDIBEKOV and YU. T. STRUCHKOV, Crystal and molecular structure of the 2-t-butyl-2-cyanocyclobutanones resulted from the cycloaddition of Moore's ketene to *endo*- and *exo*-benzocyclobutanonorbornenes 427–435

IOANA ȘARAMET, CONSTANTIN DRĂGHICI and MIRCEA D. BANCIU, Interactions of substituted five-membered heteroaromatic compounds with electron acceptors. II. Interaction of 2-*p*-bromophenylsulphonylphenyl-5-ethylamino-1,3,4-thiadiazole with tetracyanoethene 437–444

ALEXANDRU C. RĂZUȘ, FILIP CHIRALEU and ADRIAN I. IANCU, Solvolyses in substituted cyclopropylcarbinylic systems. 8. Solvolyses of 2-aryl-1-cyclopropylethanols and their 3,5-dinitrobenzoates 445–452

V. DRĂGUȚAN, ILEANA DRĂGUȚAN, C. CONDEIU and ALICE-MARIE GLATZ, Friedel-Crafts chemistry in alicyclic systems. V. Reaction of cyclohexylidene- and 1-cyclohexenylacetic acids with benzene in the presence of AlCl$_3$, CH$_3$NO$_2$ as the catalyst 453–457

DAN RĂILEANU and HORIA PETRIDE, Mesoionic oxazolones. IV. Protonation of planar and nonplanar acylated compounds 459–466

CONSTANTIN LUCA, LUCIA MUTIHAC and TITUS CONSTANTINESCU, Separation of amino acids by liquid membranes with macrocyclic carriers 467–473

IOAN SILAGHI-DUMITRESCU and IONEL HAIDUC, The electronic structure of [H$_3$SiNSiH$_3$]$^-$ anion. A simple molecular orbital treatment 475–484

BOOK REVIEWS 485–487

Revue Roumaine de Chimie, 35, 3, 279—280 (1990)

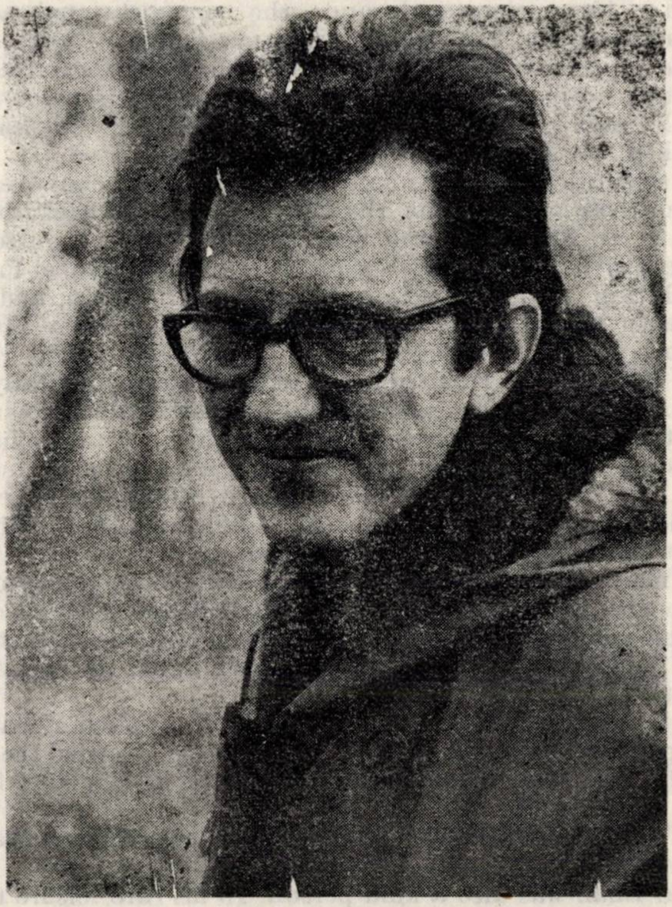

Dr. MIHAI ELIAN

(1937—1988)

Dr. Mihai Elian (1937—1988) was born in Bucharest on May 19, 1937. After graduating from the Chemistry Department of the Bucharest Polytechnic in 1959, he got his Ph. D. degree in organic chemistry in 1973 with Professors C. D. Nenitzescu and Ecaterina Ciorănescu-Nenitzescu. After spending two years as chemical engineer in a rubber factory, he was invited in 1961 by Prof. Nenitzescu to join the Institute of Organic Chemistry of the Romanian Academy, which later became the Centre of Organic Chemistry under the Ministry of Chemistry. Here he worked until his very last day and here he became in 1975 head of section. At the Centre of Organic Chemistry, he supervised a group of coworkers on physical methods and a group of synthetic organic chemists.

Both his scientifical and the organizational achievements were remarkable. His knowledge of organic, inorganic and physical chemistry was impressive. He had an unusual ability to penetrate any domains of chemistry, no matter how far they were from his previous scientific interest. Therefore, colleagues and friends were always asking for his advice, which he gladly provided and he never failed.

His scientific profile resulted from his own exceptional native resources and those provided by the fine educational background due to Professors C. D. Nenitzescu and Ecaterina Ciorănescu-Nenitzescu, as well as to the decisive moments with Prof. E. O. Fischer (Nobel Prize 1974) in Munich during 1967—68 with a Humboldt fellowship, and with Prof. R. Hoffmann (Nobel Prize 1981) at Cornell University, Ithaca, New York with a Fulbright fellowship during 1973—1974. The collaboration with Prof. R. Hoffmann resulted in one of the most scientifically productive periods from his career. The isolobal analogy, now evidently a basic concept of chemistry, along with other joint discoveries, were published in top journals such as *Journal of American Chemical Society* and *Inorganic Chemistry*. The *Science Citation Index* indicated that this latter paper has been cited in over 505 publications (R. Hoffmann and M. Elian, *Citation Classic*, in *Current Contents*, **44**, 18 (1988).

His main research interests were in carbonium ion reactions, organometallic chemistry, applications of physical methods to organic chemistry, and computational chemistry. He published about 60 papers in chemistry journals in Romania as well as abroad. He is also author of six patents.

In the last years he became involved in applied research projects concerning the chemical industry. In 1978 he was awarded the "N. Teclu" prize of the Academy of the Socialist Republic of Romania for his work on liquid crystals.

In the last 15 years he was associate lecturer at the Bucharest Polytechnic Institute.

Mihai Elian was also a kind person. In his rare leisure time, he was fond of reading novels (in Romanian, English. French or German), he enjoyed good music and diving into the Black Sea as well as camping in the Carpathian mountains.

His keen intelligence, devotion to science and personal kindness will never be forgotten.

Revue Roumaine de Chimie, 35, 3, 281–297 (1990)

CONFORMATIONAL PREFERENCES IN SUBSTITUTED 5*H*-DIBENZO[*a*, *d*]-CYCLOHEPTENES : THE INFLUENCE OF A CARBON-BONDED SUBSTITUENT IN POSITION 5

MIHAI ELIAN *

Centre of Organic Chemistry — ICECHIM, 202 B, Splaiul Independenţei, 77208
Bucharest, Romania

Received September 29, 1989

^{1}H—NMR studies of some 5*H*-dibenzo[*a*, *d*]cycloheptanes substituted in position 5 show an axial preference if the substituent is bonded to the seven-membered ring through a carbon atom. This preference can be explained in terms of steric interactions. Energy diagrams are suggested for such compounds.

INTRODUCTION

Chemical Aspects

The solvolytic interconversion of substituted 5*H*-dibenzo[*a*, *d*]cycloheptenes (**1**) and 5,6-dihydrodibenzo[*a*, *e*]cyclooctenes (**2**) as well as the transannular involvement of the double bond from the seven-membered ring of **1** in the formation of the bicyclic compounds **3**, **4** and **5** raised the question of conformational preferences of the substituent in position 5 of the compounds **1**.[1]

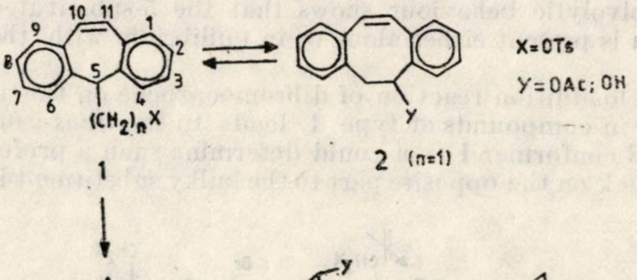

---

* The present paper is based on a chapter from M. Elian's Ph. D. thesis, and was translated posthumously.

In the solvolysis of the tosylate **1** (n = 1, X = OTs) the steric requirements for the formation of a nonclassic ion (**1** — π), formed by the transannular double bond participation, or of a phenonium ion (**1**— **Φ**), forerunners of the bicyclic compounds **3** and **4**, or respectively ring-enlarged isomer **2**, are fulfilled only for the axial conformer of **1**.

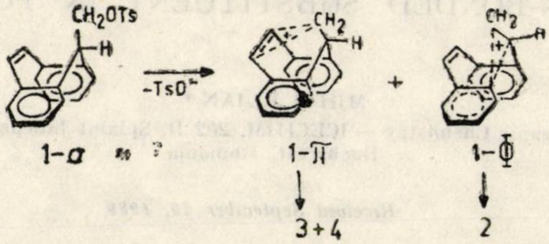

In the case of the superior homolog of **1** (n = 2), owing to the length of the side-chain, the transannular involvement of the double bond (**1′** — — π) becomes prevalent.

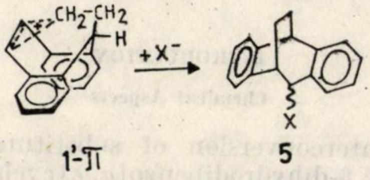

This solvolytic behaviour shows that the 5-substituted axial conformer **1** — **a** is present either alone or in quilibrium with the equatorial conformer.

The cycloaddition reaction of dibromocarbene on the transannular double bond in compounds of type **1** leads to the *trans*-isomer **6**[2,3] and only an axial conformer **1** — **a** could determine such a preferential electrophilic attack on the opposite part to the bulky substituent in position 5.

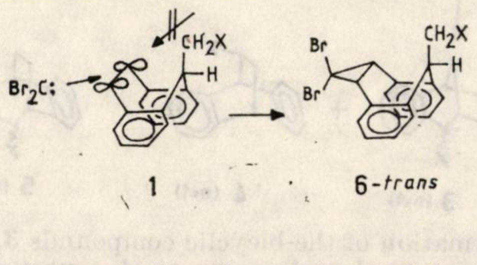

Owing to the above-mentioned experimental facts, it became interesting to carry out ^{1}H—NMR studies on the conformational equilibrium of substituted 5*H*-dibenzo]*a*,*d*] cycloheptenes (**1**) in order to establish the conformational preferences for various substituents.

Energetic Aspects

Examination of the steric model of 5*H*-dibenzo[*a*, *d*]cycloheptene (**7**) shows that the molecule cannot be planar. The two conformers **7a** and **7b** which can result through inversion of the seven-membered ring are, in this case, identical.

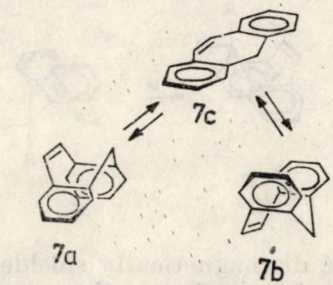

The inversion barrier of **7** determined using dynamic NMR spectroscopy is 9.1 kcal/mol[4]. As in the planar transition state **7c**, involved in the ring inversion, there are important steric strains, this value of the inversion barrier is relatively small and could be explained by the gain of resonance energy of the *cis*-stilbene type.

The literature data[4,5] show that the activation energy for the inversion of the ring can be increased by introducing a bulky substituent in positions 5 or 10 owing to the interactions between the substituent and the hydrogen atoms from the vicinal positions (H_A and H_B in the representatin **8**).

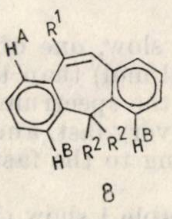

8

In Table 1 some data of free energies of activation for the ring inversion (ΔC_{inv}, kcal/mol) and collapse temperatures (t_c, °C) for 5-or 10-substituted 5*H*-dibenzo[*a*, *d*] cycloheptenes (**8**) are collected.

Table 1

Free activation energies for the ring inversion and the collapse temperatures for 5- or 10-substituted 5*H*-dibenzo [*a*, *d*]cycloheptenes (8)

R_1	R_2	ΔG_{inv} (kcal/mol)	t_c (°C)	Ref.
H	H	9.1	−90	4
$C(CH_3)_2OH$	H	17.1−17.5	44−67	4
H	OCH_3	14.9	29	5

If the substituent is bulky enough, the conformational equilibrium in compounds of type **9** can be evidenced using dynamic NMR spectroscopy; an equatorial substituent linked in position 5 is almost on the line where the planes of both aromatic rings intersect and it is expected to be deshielded due to the ring current[6], while an axial substituent in

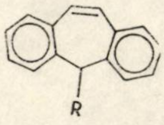

9

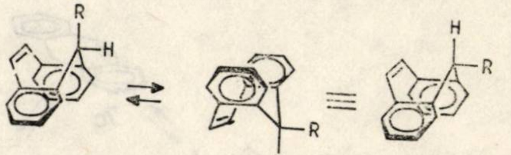

9-a

9-e

the same position is to be diamagnetically shielded by the transannular double bond.[7] In the following section of this paper, this is the very key to discriminate axial and equatorial conformers in the ^1H-NMR spectrum of the mixture.

RESULTS

Conformational Analysis of 5-Methyl-5H-dibenzo[a, d]cycloheptene

The ^1H-NMR spectra of some compounds of type **1** ($X = Cl$, Br, OH, OAc) at variable temperatures (−60 to +40°) are simple spectra, they do not depend on temperature and may be rationalized in one of the following two ways:

i) The ring inversion is slow, one of the conformers is much more stable (at least with 2−3 kcal/mol) than the other, which exists in a too small ratio to be detected in the spectrum.

ii) The ring inversion is very fast, and even at −60° only the mediated spectrum is observed owing to the fast equilibration of the two conformers.

The data presented in Table 1 show that on passing from the unsubstituted hydrocarbon **7** to the derivative **8** ($R_1 = H$, $R_2 = OCH_3$) the activation energy for inversion (ΔG_{inv}) rises with about 6 kcal/mol. It may be supposed that for the investigated compounds (**1**) the activation energy for inversion is sufficiently high so that even at room temperature the inversion is slow.

In order to make an unequivocal choice between the above two hypotheses it became necessary to study a compound of type **9** carrying a small substituent, so that it should be possible to detect both conformers in the NMR spectrum if the inversion is slow.

For this purpose 5-methyl-5*H*-dibenzo[*a*, *d*]cycloheptene (**9**; $R = CH_3$) was chosen and ^1H-NMR spectra were recorded at temperatures ranging from −60 to +100° (Fig. 1). The mediated spectrum recorded at 100° (Fig. 1c) presents a doublet at 1.50 ppm corresponding to the CH_3 group and a quartet at 3.79 ppm corresponding to the adjacent CH group. At low temperatures (−20 to −60°), in the NMR spectra the signals corresponding to both conformers (**9 — a** and **9 — e**) are well resolved. In Fig. 1a can be seen two doublets at 1.31 and 1.86 ppm corresponding to the axial and equatorial CH_3 groups and two quartets at 3.47 and 4.19 ppm corresponding to the axial and equatorial CH groups. One can also see the splitting of the signal corresponding to the olefinic protons.

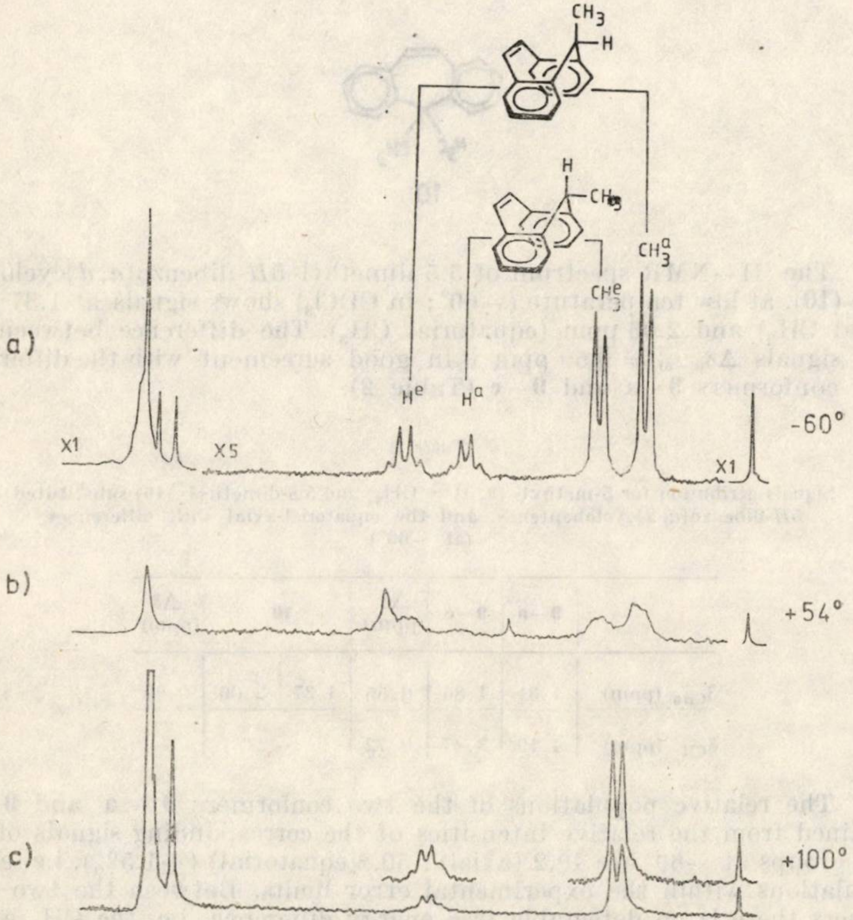

Fig. 1. — ^1H—NMR spectrum of 5-methyl-5*H*-dibenzo [*a*, *d*]cycloheptene (9 ; R = CH_3) at variable temperatures : a) —60°, b) 54°, c) 100° ; (a, b in $CDCl_3$; c in C_2Cl_4).

In the conformer **9 — a**, the signal of the axial CH_3 group appears at higher field values (shielding produced by the double bond) than the equatorial CH_3 group from the conformer **9 — e**. The signal of the equatorial hydrogen atom from the conformer **9 — a** (deshielded by the ring current) appears at lower field values than the signal of the axial hydrogen atom from the conformer **9 — e** (shielded by the double bond. The assignment of signals is shown in Fig. 1a and Table 2. Additional proofs have been obtained from spin decoupling experiments. Thus on irradiation of the doublet from $\delta = 1.31$ ppm, the quartet from $\delta = 4.19$ ppm (CH^e) collapses into a singlet, whereas irradiation of the doublet from $\delta = 1.86$ ppm results in the collapse of the quartet from $\delta = 3.47$ ppm into a singlet (CH^a).

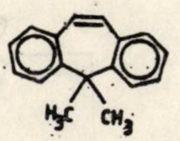

10

The ^1H—NMR spectrum of 5.5-dimethyl- 5*H*-dibenzo[*a*, *d*]cycloheptene (**10**), at low temperature (—60°; in $CDCl_3$) shows signals at 1.37 ppm (axial CH_3) and 2.06 ppm (equatorial CH_3). The difference between the two signals $\Delta\delta_{(e-a)} = 0.69$ ppm is in good agreement with the difference for conformers **9**—**a** and **9**—**e** (Table 2).

Table 2

Signals atribution for 5-methyl- (**9**, $R = CH_3$) and 5,5-dimethyl- (**10**) substituted 5*H*-dibenzo[*a*, *d*]cycloheptenes, and the equatorial-axial shift differences (at —60°)

	9—a	**9—e**	$\Delta\delta$ (ppm)	**10**		$\Delta\delta$ (ppm)
δ_{CH_3} (ppm)	1.31	1.86	0.55	1.37	2.06	0.69
δ_{CH} (ppm)	4.19	3.47	0.72	—		—

The relative populations of the two conformers **9** — **a** and **9** — **e** obtained from the relative intensities of the corresponding signals of the CH_3 groups at —60° are 49.2 (axial) : 50.8(equatorial) (±1.5%), i.e. equal populations within the experimental error limits. Between the two conformers there is no detectable free energy difference, i.e. the CH_3 group has no conformational preference.

The Conformations of Some 5H-Dibenzo[a, d]cycloheptenes. Substituted in Position 5 with CH_2X Groups

The temperature dependence of the ^1H—NMR spectra of the 5-methyl substituted hydrocarbon **9** ($R = CH_3$) and 5,5-dimethyl substituted **10** (Fig. 1 and Table 2) shows that a substituent having the volume of the CH_3 group rises enough the inversion energy barrier in dibenzocycloheptenes (**9**) so that the inversion becomes sufficiently slow to permit the

Table 3

Calculated and experimental chemical shifts for CH_2X and CH groups in compounds 9

R	Experimental chemical shifts[a]		K_X[8] (ppm)	Calculated chemical shifts		Error[b] for δ_{CH_2}
	δ_{CH_2}(ppm)	δ_{CH}(ppm)		δ_{CH_2}(ppm)	δ_{CH^a}(ppm)	
CH_2OH	CH_2^a : 3.72 CH_2^e : (4.57)	CH^e : 4.15 CH^a : (3.42)	2.56	3.87 4.42	— 3.43	0.15 (0.15)
CH_2Br	CH_2^a : 3.61 CH_2^e : ( )[c]	CH^e : 4.28 CH^a : ( )	2.33	3.64 4.19	— 3.56	0.04 ( )
CH_2OCH_3	CH_2^a : 3.62 CH_2^e : (4.42)	CH^e : 4.26 CH^a : ( )	2.36	67·8 4.22	— 3.54	0.05 (0.20)
CH_2OCHO	CH_2^a : 4.39 CH_2^e : (5.23)	CH^e : 4.39 CH^a : (3.67)	3.13	4.44 4.99	— 3.67	0.05 (0.24)
CH_2NH_2	CH_2^a : 2.96 CH_2 : ( )[d]	CH^e : 3.93 CH^a : ( )	1.57	2.88 3.43	— 3.21	0.08 ( )
CH_2CN	CH_2^a : 2.76 CH_2 : ( )[d]	CH^e : 4.37 CH^a : ( )	1.70	3.01 3.56	— 3.65	0.25 ( )
CH_2COOH	CH_2^a : 2.74 CH_2^e : (3.41)	CH^e : 4.52 CH^a : (3.83)	1.55	2.86 3.41	— 3.80	0.12 (0.00)
CH_2COOEt	CH_2^a : 2.63 CH_2^e : (3.32)	CH^e : 4.50 CH^a : ( )	—	2.86 3.41	— 2.69	0.23 (0.09)
CH_2CH_2OH	CH_2^a :1.95 CH_2 : (2.76)	CH^e : 4.21 CH^a : ( )	—	—	—	—

---

[a] All spectra were recorded in $CDCl_3$, the values enclosed in brackets refer to the less stable conformer.

[b] $|(\delta_{CH_2})^{stable}_{exp.} - (\delta_{CH_2^a})_{calcd.}|$: in brackets, $|(\delta_{CH_2})^{less\ stable}_{exp.} - (\delta_{CH_2})_{calcd.}|$

[c] Under the signal of the major conformer (at 4.28 ppm) one can see a weaker signal which could belong to the minor conformer, but the precise chemical shift cannot be determined owing to the signals superposition.

[d] The available sample amounts were too small to allow good quality spectra at high amplification.

[e] The value for the K_X constant is that for the NR_2 group.[8]

detection of both conformers in the ^1H-NMR spectrum at temperatures lower than 60°. For a bulkier substituent, such as a CH_2X ($X \neq H$) group. the inversion barrier must be higher. It is possible that the ^1H-NMR spectra of compounds **1** at 40° correspond to a slow equilibrium in which one of the conformers prevails, according to hypothesis ***i*** (vide supra).

Using some substituent constants K_X,[8] it was possible to calculate the effect of the substitution of a hydrogen atom from the CH_3 group by another atom or group of atoms X, on the ^1H-NMR signal of that group. Thus, starting from the chemical shifts of the signals of the axial CH_3 ($\delta = 1.31$ ppm) and equatorial CH_3 groups ($\delta = 1.86$ ppm) corresponding to the conformers **9** – **a** and **9** – **e** respectively ($R = CH_3$), was calculated the effect of the substituent X (δ_{CH_2}) using K_X constants, in the relation :

$$\delta_{CH_2} = \delta_{CH_3} + K_X \text{ (ppm)}$$

The chemical shifts of the axial CH group from the less stable conformers (**9** – **e**) were also calculated using the relation :

$$\delta_{CH^a} = \delta_{CH^e} - 0.72 \text{ (ppm)}$$

where δ_{CHe} is the experimentally determined chemical shift for the stable conformer (**9** – **a**) and 0.72 is the shift difference between the axial and the equatorial signals in the compound **9** ($R = CH_3$) ; $\Delta\delta = \delta_{CH^e} - \delta_{CH^a} = 0.72$ (Table 2). The calculated chemical shifts δ_{CH_2} and δ_{CH} are presented in Table 3, together with the experimental values and the substituent constants (K_X) for variously substituted dibenzocycloheptenes (**9** ; $R = CH_2X$).

As it can be seen from Table 3, the calculated values for the $\delta_{CH_2^a}$ are, in all cases, in very good agreement with the experimental ones.

The differences of experimental chemical shifts between the two conformers **9** – **a** and **9** – **e** ($\delta^e - \delta^a$; ppm) for the substituent R and the CH group are presented in Table 4.

Some of the spectra above described in which the less stable conformer signals are evident, are presented in Figures 2–4. In every case the signals of the groups CH and CH_2 appear as an AB_2 spectrum in which the H_A proton appears in the region $\delta = 4.0-4.5$ ppm ; the position of the H_B protons from the CH_2X group varies in a larger region depending on the nature of the X substituent. A second AB_2 spectrum can be detected in the ^1H-NMR spectrum of the alcohol **9** ($R = CH_2OH$) on the flanks of the first AB_2 spectrum recorded at high apmlification (Fig. 2).

Table 4

Experimental chemical shift differences between the equatorial and axial conformers of **9**, for the R and CH groups.

R	$\delta^e - \delta^a$ (ppm)	
	CH_2X	CH
CH_3	0.55	0.72
CH_2OH	0.85	0.73
CH_2OCH_3	0.80	—
CH_2OCHO	0.84	0.72
CH_2COOH	0.67	0.69
CH_2COOEt	0.69	—
CH_2CH_2OH	0.72	—

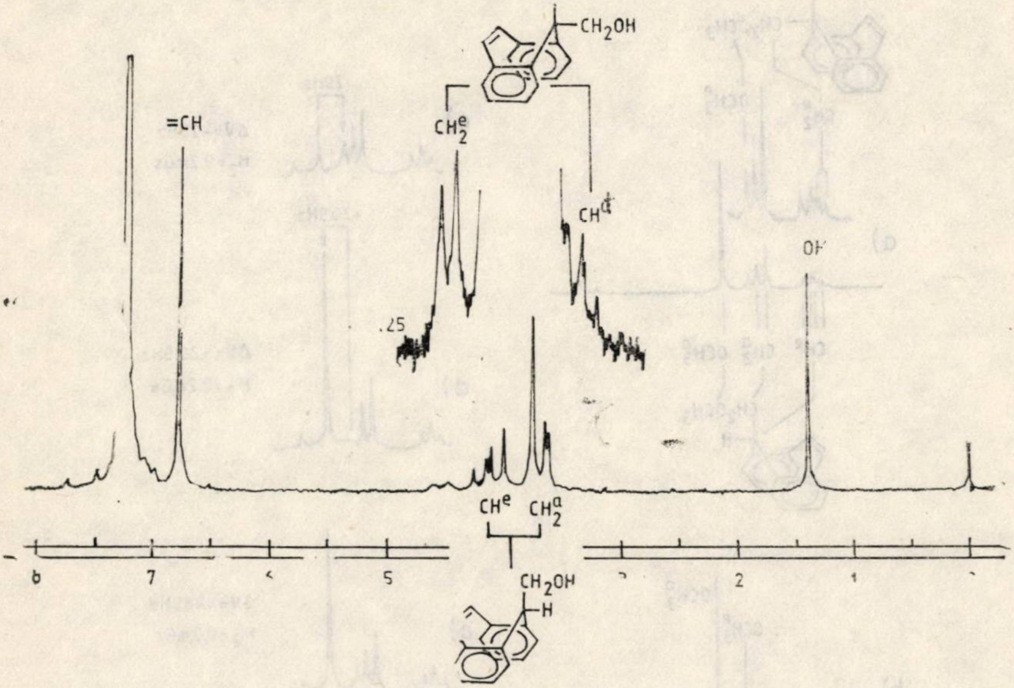

Fig. 2. — ^{1}H—NMR spectrum of 5-hydroxymethyl-5*H*-dibenzo[*a*,*d*]-cycloheptene (**9**; R = = CH_2OH) in $CDCl_3$.

In the ^{1}H—NMR spectrum of the ether **9** (R = CH_2OCH_3), in addition to the signals corresponding to the axial conformer (**9** — *a*) at δ=4.26 (4 lines ; CH), 3.62 (CH_2) and 3.12 ppm (OCH_3), the weaker signals of the CH_2 and OCH_3 groups from the equatorial conformer (**9** — **e**) can be distinguished at δ = 4.42 and 3.45 ppm respectively (Fig. 3a). In the ^{1}H—NMR spectrum recorded in acetone-d_6 (Fig. 3b) the only signal which can be distinguished from the equatorial conformer is that of the OCH_3 group, the signal of the CH_2^e group being hidden under the more intense quartet centered at 4.2 ppm.

An interesting case is that of the acid **9** (R = CH_2COOH) for which the equatorial : axial ratio exhibits an appreciable dependence on the solvent polarity, owing probably to solvation effects. Thus, the signals of conformer **9** — **e** can hardly be distinguished in the NMR spectrum recorded in $CDCl_3$ (Fig. 4a), but they become easily observable in the spectrum recorded in pyridine-d_5 (Fig. 4c) and dimethylsulfoxide-d_6 (Fig. 4d). The equatorial : axial ratio ranges from 15 : 85 in $CDCl_3$ to 27 : 73 in dimethylsulfoxide-d_6 (Fig. 4a—d).

An independent proof of the fact that the weak signals in the NMR spectra of compounds **9** (Fig. 2—4) correspond to a minor conformer in equilibrium with a major one, was obtained using the double-resonance technique.

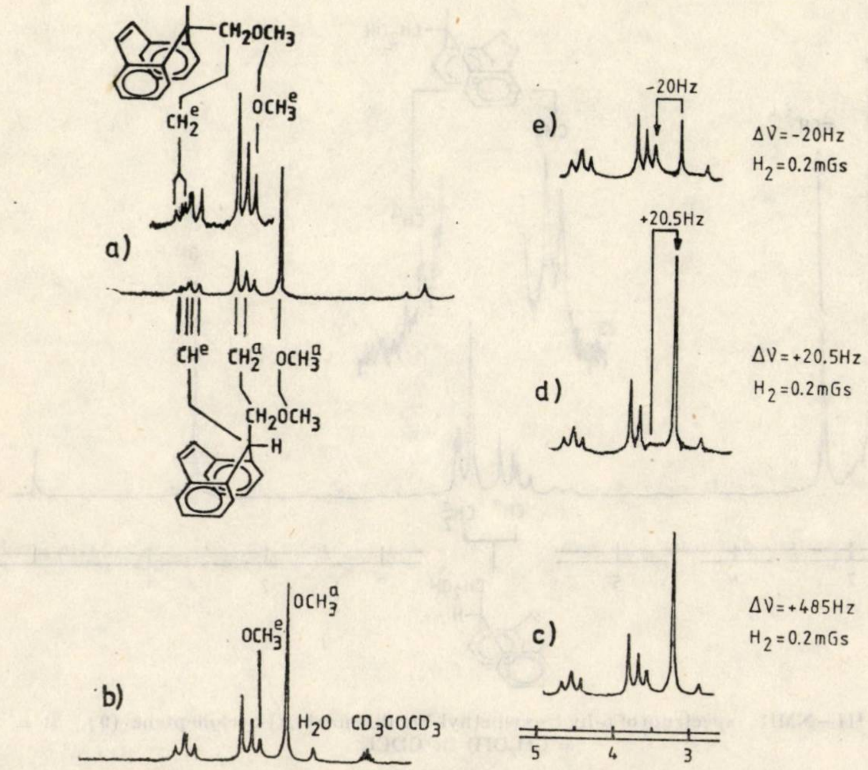

Fig. 3. —^{1}H—NMR spectrum of 5-methoxymethyl-5*H*-dibenzo [*a,d*] cycloheptene (**9**; R = CH_2OCH_3) in different solvents : a) $CDCl_3$, b) acetone-d_6, and the less stable conformer (equatorial CH_2OCH_3 group in **9**-*e*) by double-resonance experiments c) — e), $\Delta\upsilon$ represents the frequency difference between the observation field (H_1) and the irradiation field (H_2), solvent : acetone-d_6.

The double-resonance phenomenon, discovered by Forsén and Hoffman,[9] can be described as an ecited state transfer. If the exchange rate is higher than the relaxation rate, when a hydrogen atom from one conformer is irradiated with a secondary field, the intensity of the signal of the same category of protons in the other conformer will be weaker than in the absence of the secondary field. For the case of the conformational equilibrium $\mathbf{9} - \mathrm{a} \rightleftarrows \mathbf{9} - \mathrm{e}$ the situation is presented in the following scheme :

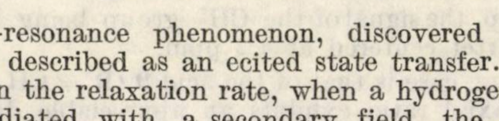

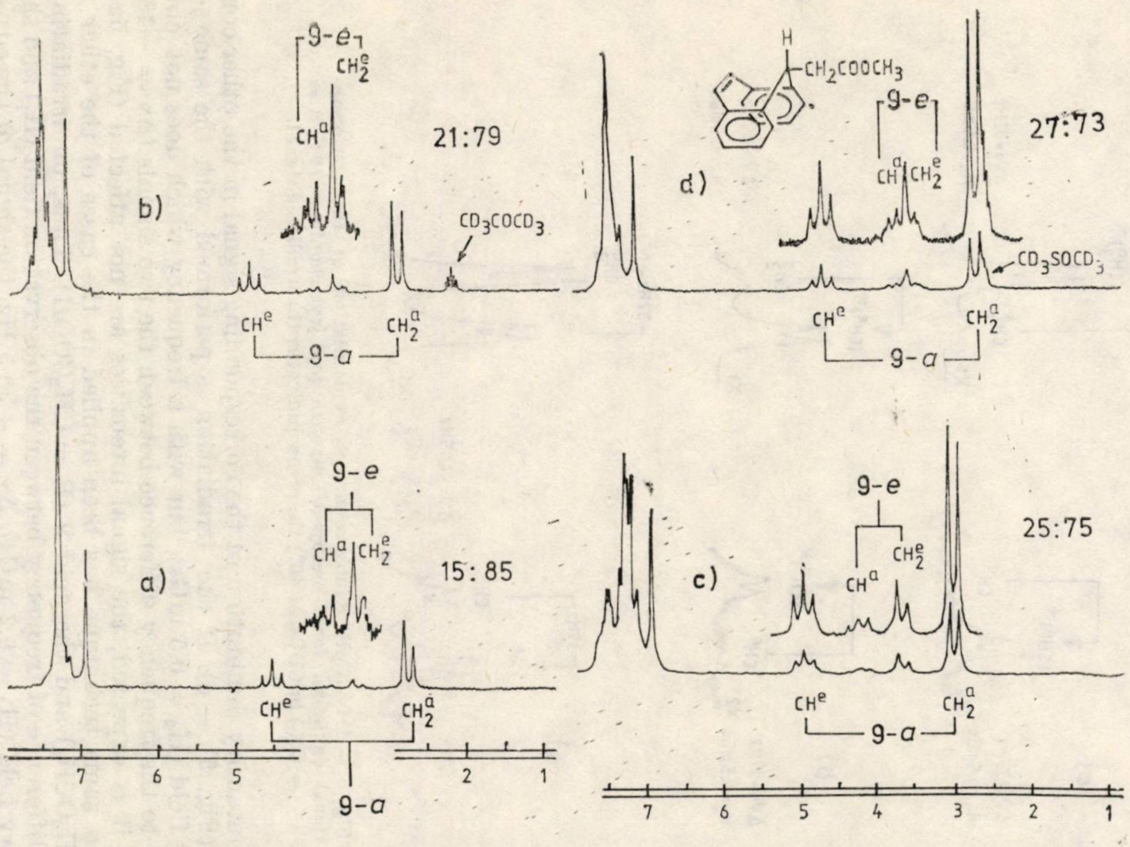

Fig. 4. — ^{1}H—NMR spectra of 5-carboxymethyl-5*H*-dibenzo[*α*, *d*]-cyclohepene (**9**: R = CH_2COOH) in different solvents, a) $CDCl_3$, b) acetone-d_6, c) pyridine-d_5, and d) dimethylsulfoxide-d_6. In the right-hand side of every spectrum, the equatorial versus axial conformer ratio is shown.

For the hydrocarbon **9** (R = CH_3), the results of the double-resonance are presented in Fig. 5. Thus, irradiation of one of the groups CH or CH_3 from one of the two conformers **9 — a** or **9 — e** results in a spectacular intensity diminution of the corresponding signal in the other conformer (Fig. 5b — c). If the irradiation is performed with the same secondary field (H_2 = 0.5 mGs), but with a frequency which does not correspond to the frequency difference between the two signals ($\Delta\nu = -485$ Hz), as it is expected, the signal intensities are not affected (Fig. 5a).

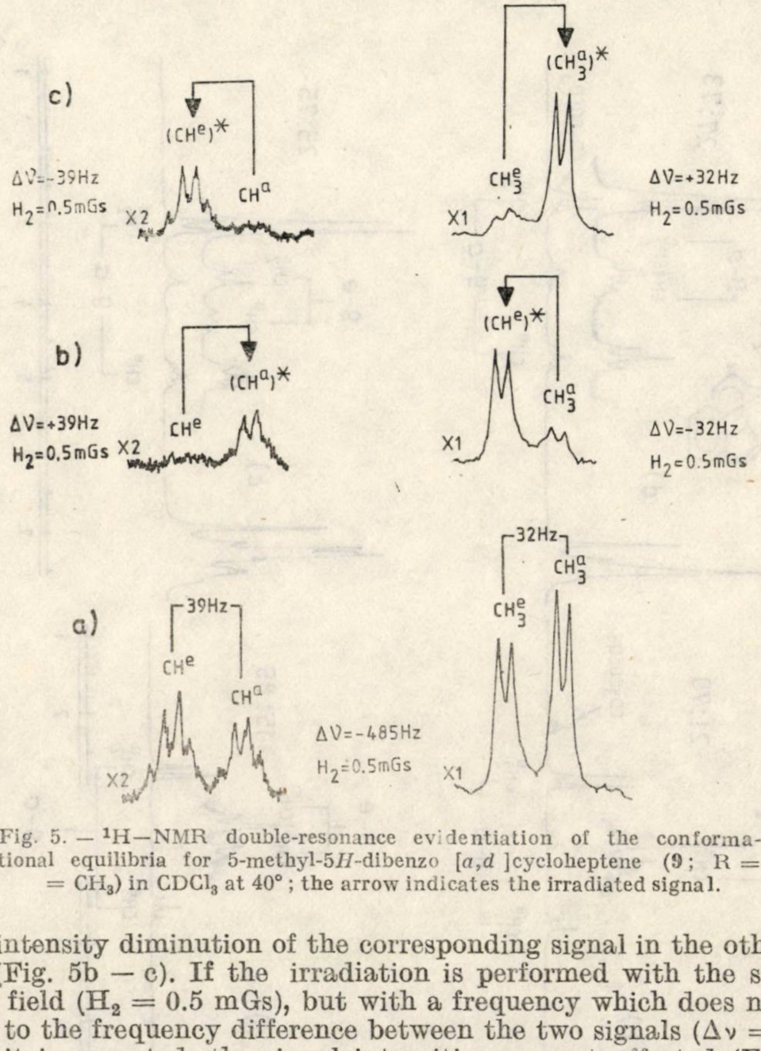

Fig. 5. — ^1H—NMR double-resonance evidentiation of the conformational equilibria for 5-methyl-5*H*-dibenzo [*a,d*]cycloheptene (**9**; R = CH_3) in $CDCl_3$ at 40° ; the arrow indicates the irradiated signal.

The same technique has been applied in the cases of the ether **9** (R = CH_2OCH_3) and the acid **9** (R = CH_2COOH). Thus, on irradiation with a difference of frequency between the observation field (H_1) and the secondary field (H_2 = 0.2 mGs), $\Delta\nu = +20.5$ Hz, the signal of the equatorial OCH_3 group disappeared completely (Fig. 3d) whereas on irradiation with a frequency difference $\Delta\nu = -20$ Hz, the signal intensity corresponding to the axial OCH_3 group diminished very much (Fig. 3e). Similar experiments were performed with the acid **9** (R = CH_2COOH). In this case, the irradiation with a frequency $\Delta\nu = +46$ Hz results in diminution of signal intensities for the CH^e and CH_2^e groups whereas the irradiation with $\Delta\nu = -46$ Hz results in disappearance of the signal corresponding to CH^a group and in an appreciable decrease of the signal intensity for the CH_2^a group.

The results of the double-resonance experiments may be considered as a direct proof for the fact that the weak signals in the ^1H-NMR spectra of the compounds **9** ($R = CH_2X$) correspond indeed to the minor conformer (**9** — **e**) from the equilibrium **9** — **a** $\rightleftarrows$ **9** — **e**.

Conformational Energies for Differently Substituted 5H-Dibenzo [a,d] cycloheptenes

The free energy differences between conformers can be calculated analogously to a chemical reaction,[10] i.e. for the equilibrium :

$$\mathbf{9} - \mathbf{a} \overset{K}{\rightleftarrows} \mathbf{9} - \mathbf{e}$$

the well-known relation $\Delta G = -RT\ln K$ can be used, where ΔG represents the free energy difference between the axial (**9** — **a**) and equatoria

Table 5

Conformational energies for different substituents in 5*H*-dibenzo[*a*, *d*]cycloheptenes (**9**)

R	Solvent	p_a	p_e	T(K)	ΔG conf (Kcal/mol)[a]
CH_2OCHO	$CDCl_3$	93	7	313	1.61
CH_2Br	$CDCl_3$	91	9	313	1.44
CH_2OH	$CDCl_3$	89	11	313	1.28
CH_2NH_2	$CDCl_3$	86	14	313	1.13
CH_2CH_2OH	$CDCl_3$	85	15	313	1.08
CH_2OCH_3m	$CDCl_3$	84	16	313	1.03
	acetone-d_6	81	19	313	0.90
CH_2COOH	$CDCl_3$	85	15	313	1.08
	acetone-d_6	79	21	313	0.82
	pyridine-d_5	75	25	313	0.68
	dimethyl-sulfoxide-d_6	73	27	313	0.62
CH_3	$CDCl_3$	49.2	50.8	213	max. −0.01

[a] $\Delta G_{conf} = \Delta G_e - \Delta G_a$; $\Delta G_{conf} > 0$, the axial conformer is the more stable one; $\Delta G_{conf} < 0$, the equatorial conformer is the more stable one.

9 — e) conformers, and K is the equilibrium constant as the ratio of the populations corresponding to the two conformers p_e and p_a ($K = p_e/p_a$), and it is equal with the integrated intensity ratio for the signals in the

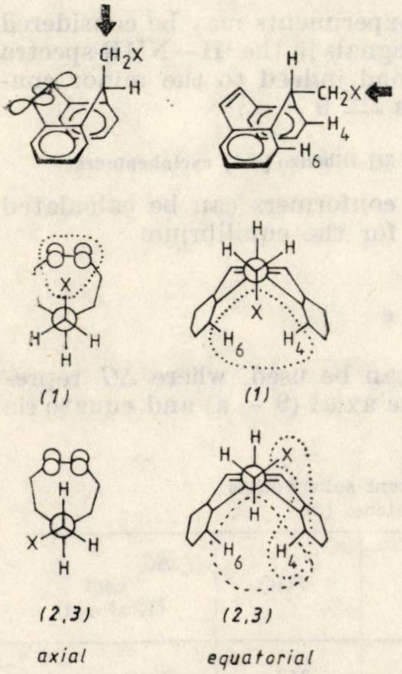

Fig. 6. — Important steric interactions in different rotamers corresponding to axial and equatorial conformers of compounds **9**. The regions where important steric strains appear are marked by dotted lines. The thick arrows indicate the direction from which it should be looked at the upper side formulas in order to construct the Newman projections from the 2nd and 3rd lines.

spectrum determined at a temperature at which the conformational equilibration is slow.

The ΔG values for the equilibrium **9 — a**$\rightleftarrows$**9 — e** represent just the conformational energies for the substituents[11] in 5*H*-dibenzo[*a*, *d*] cycloheptenes. Conformational energies for some substituents are presented in Table 5. A remarkable conformational energy dependence on the solvent in the case of the CH_2COOH group can be seen. A similar dependence in the case of some polar groups substituted on cyclohexanes was previously reported.[11]

As it can be seen from Table 5, the volume of the CH_3 group seems to be insufficient to determine a conformational preference for this type of compounds ($p_a \approx p_e$). When the substituent volume is increased (by substituting a hydrogen atom in it with an X group) a conformational preference of the substituent apperas toward the axial conformation for which the steric strains between non-bonded atoms are smaller.

For compunds of type **9** ($R = CH_2X$), the regions where appreciable steric strains may appear are marked in Fig. 6 by dotted lines. Thus, the strongest interactions of the CH_2X substituent appear between the X group and the transannular carbon atoms C_{10} and C_{11} of the double bond in the axial conformer, or between the X group and the hydrogen atoms H_4 and H_6 from the aromatic rings in the equatorial conformer of **9**. In the equatorial conformer, there are also important steric strains between the hydrogen atoms from the CH_2X group and the hydrogen atoms H_4 and H_6. From the three possible rotamers in each conformation (*1*), (*2*) and (*3*), there will be preferred those with less steric strains (*2*) and (*3*).

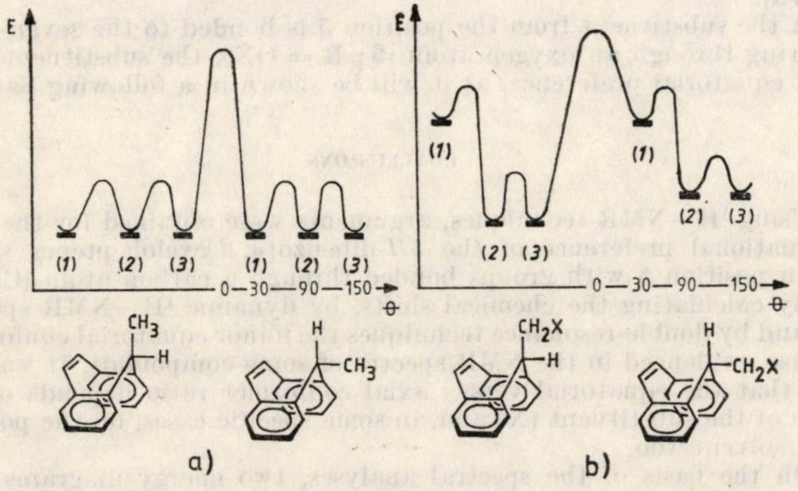

Fig. 7. — Energy diagrams for different conformations in compounds of type **9**; a) R = CH_3, b) R = CH_2X, E stands for *energy* and θ stands for the *rotational angle* of the CH_3, respectively CH_2X group.

For the compound **9** (R = CH_3), the experimental data (equal populations for axial and equatorial conformers) indicate that the steric strains must be equal. The corresponding energy diagram is presented in Fig. 7 a. On the left-hand side of Fig. 7a are shown the energy levels for the three staggered rotamers (which are identical) for the axial conformer, and on the right-hand side are shown the energy levels for the three staggered rotamers (*1*), (*2*) and (*3*), corresponding to the equatorial conformer (which are also identical). The rotamers are separated by rotation energy barriers having the same magnitude as in the case of *n*-butane [12] (aprox. 3—5 kcal/mol). All six rotamers from both conformations have been drawn on the same energy level, according with the experimental data regarding the populations. The three rotamers of the axial conformer are separated from the rotamers of the equatorial conformer by a much higher energy barrier necessary for the inversion of the seven-membered ring.

In the case of the compounds of type **9** (R = CH_2X) the energy diagram is presented in Fig. 7b. For these compounds, the rotamer (*1*) is strongly destabilized in both conformers **9** — **a** and **9** — **e** owing to the larger volume of the X group; for these compounds, (*2*) and (*3*) are the only populated rotamers. In the case of the equatorial conformer, the examination of the steric models (Fig. 6) shows that in rotamers (*2*) and (*2*), there are important steric strains between the X group and the hydrogen atoms H_4, H_6 and carbon atoms C_4, C_6 in **9**. On the contrary, in the case of the axial conformer, the steric strains between the X group and any other atom in the molecule are less important. Consequently, the axial rotamers (*2*) and (*3*) for CH_2X group remain approximately at the same energy level as in case of the axial CH_3 group; on the other hand, the equatorial rotamers (*2*) and (*3*) for CH_2X group occupy a higher level, leading to an axial conformational preference of the CH_2X substituent (Fig. 7b).

If the substituent from the position 5 is bonded to the seven-membered ring through an oxygen atom (**9**; R = OX), the substituent exhibits an equatorial preference, as it will be shown in a following paper.[13]

CONCLUSIONS

Using ^1H-NMR techniques, arguments were obtained for the axial conformational preference of the 5*H*-dibenzo[*a, d*]cycloheptenes substituted in position 5 with groups bonded through a carbon atom (CH_2X).

By calculating the chemical shifts, by dynamic ^1H-NMR spectroscopy and by double-resonance techniques the minor equatorial conformers were also evidenced in the NMR spectra of some compounds. It was also shown that the equatorial versus axial conformer ratio depends on the volume of the substituent (X) and, in some specific cases, on the polarity of the solvent too.

On the basis of the spectral analyses, two energy diagrams were proposed for the conformers of the compounds **9** ($R = CH_3$) and **9** ($R = CH_2X$). It was suggested that the axial preference of the substituent in this type of compounds is dictated by non-bounding interactions of the Van der Waals type.

EXPERIMENTAL

The NMR spectra were recorded at 60 MHz with a VARIAN A–60A spectrometer. The chemical shifts were reported as δ values in ppm, using TMS as internal standard. The coupling constants are reported in Hz. The solvents for spectra recorded at normal temperature are those indicated in each experiment, and they are commercially available solvents stored on sodium carbonate.

The temperature control for the variable temperature spectra was performed with a V–4341/V–6057 device (Varian Assoc.). The solvents used in these experiments were : $CDCl_3$ for temperatures ranging from -60 to $+60°$ and tetrachloroethene and hexachlorobutadiene for temperatures over 60°. The temperature was recorded immediately before and after the spectrum recording, using a sample of methanol for temperatures ranging from -60 to $+40°$ and ethyleneglycol for temperatures over $+40°$. The temperature differences so determined were less than 1°.

The concentration determinations were performed by recording 6–20 signal integrations. The conformational energies were calculated using an average value of the integrated signals which included only those values with a deviation less than $\pm 2\%$ from the averaged value of all integrals.

The double-resonance experiments were performed using a V6058A decoupling device (Varian Assoc.). In every case the experiment began by applying a frequency equal to the difference which was read on the recorded spectrum, then this frequency was modified in the limit of ± 5 Hz in order to obtain the maximum effect. When the double-resonance technique was applied for evidencing the less stable conformer, a levelling effect was observed for some values of the secondary field intensity (H_2). In order to obtain good quality spectra, relatively small field intensities were applied. In such cases the secondary field intensity (H_2) applied was 0.2–0.5 mGs, and in decoupling experiments it was 2–6 mGs.

REFERENCES

[1] E. Ciorănescu, A. Bucur, M. Elian, M. Banciu, M. Voicu and C. D. Nenitzescu, *Tetrahedron Lett.*, **1964**, 3835 ; E. Ciorănescu, A. Bucur, M. Elian and C. D. Nenitzescu, *Rev. Roumaine Chim.*, **10**, 149 (1965) ; E. Ciorănescu, A. Bucur, M. Elian, M. Banciu, M. Voicu and C. D. Nenitzescu, *ibid.*, **10**, 161 (1965) ; E. Ciorănescu, A. Bucur, F. Badea, M. Renţea and C. D. Nenitzescu, *Tetrahedron Lett.*, **1969**, 1867 ; E. Ciorănescu, M. Banciu, R. Jelescu, M. Renţea M. Elian and C. D. Nenitzescu, *ibid.*, **1969**, 1871 ; E. Ciorănescu, M. Banciu, M. Elian, A. Bucur and C. D. Nenitzescu, *Liebigs Ann. Chem.*, **739**, 121 (1970) ; E. Ciorănescu, A. Bucur, M. Banciu, F. Badea, M. Elian and C. D. Nenitzescu, *Rev. Roumaine Chim.*, **16**, 1555 (1971) : M. Stănescu, M. Elian and E. Ciorănescu, *ibid.*, **31**, 1001 (1986) ; M. Stănescu, M. Elian and E. Ciorănescu, *ibid.*, **32**, 969 (1987) ; E. Ciorănescu, A. Voicu and M. Elian, *ibid.*, **34**, 87 (1989).

[2] M. Elian, Ph. D. Thesis, Centre of Organic Chemistry, Bucharest, 1973.

[3] A. Banciu, M. Elian, A. Bucur, D. Georgescu, E. Ciorănescu and C. D. Nenitzescu, *Rev. Roumaine Chim.*, **19**, 213 (1974).

[4] M. Nógradi, W. D. Ollis and I. O. Sutherland, *Chem. Commun.*, **1970**, 158.

[5] W. Tochtermann, G. Schnabel and A. Mannschreck, *Liebigs Ann. Chem.*, **705**, 169 (1967).

[6] C. E. Johnson and F. A. Bovey, *J. Chem. Phys.*, **29**, 1012 (1958).

[7] L. M. Jackman and S. Sternhell, "Applications of NMR Spectroscopy in Organic Chemistry", Pergamon Press, Oxford, 2nd edition, 1969, p. 83.

[8] J. N. Shoolery, "Technical Information Bulletin", **2**, No. 3, Varian Assoc., Palo Alto ; quoted in : R. M. Silverstein and G. C. Bassler, "Spectrometric Identification of Organic Compounds", Wiley, New York, 1964.

[9] S. Forsén and R. A. Hoffman, *Acta Chim. Scand.*, **17**, 1787 (1963) ; *J. Chem. Phys.*, **39**, 2892 1963) ; *ibid.*, **40**, 1189 (1964).

[10] E. L. Eliel, N. L. Allinger, S. J. Angyal and G. A. Morrison, "Conformational Analysis", Interscience, New York, 1967 ; E. L. Eliel, "Stereochemistry of Carbon Compounds", McGraw-Hill, New York, 1962.

[11] J. A. Hirsch, "Table of Conformational Energies", in : "Topics in Stereochemistry", vol. **1**, p. 199, Eds. N. L. Allinger and E. L. Eliel, Interscience, New York, 1967.

[12] K. S. Pitzer, *J. Chem. Phys.*, **8**, 711 (1940) ; **12**, 310 (1944).

[13] M. Elian and A. Voicu, *Rev. Roumaine Chim.*, to be published.

Revue Roumaine de Chimie, **35**, *3*, 299–303 (1990)

FROM CAMPHOR TO BIS[3-(TRIFLUOROACETYL)-CAMPHORATO[BARIUM(II) IN A ONE STEP SYNTHESIS

MIHAI ELIAN,[a] CĂLIN DELEANU[b] and SORIN ROȘCA[b]

[a]Centre of Organic Chemistry, Splaiul Independenței 202 B, 77208 Bucharest, Romania
[b]Polytechnic Institute, Organic Chemistry Department, Splaiul Independenței 313, 76206 Bucharest, Romania

Received October 15, 1989

The title compound has been synthesized starting from natural camphor and ethyl trifluoroacetate, followed by direct complexation of the formed β-diketone in the reaction mixture with barium ions. The case of a chiral hindered amide for which the two enantiomers have been evidenced in the ^{1}H-NMR spectrum, using a chiral lanthanide shift reagent derived from the barium complex, is also presented.

Lately, the use of chiral shift reagents in the study of optic active compounds has become a routine practice.

One of the most used types of chiral shift reagents (maybe the most used) is the class of β-diketonates having a comphor skeleton (**1**).

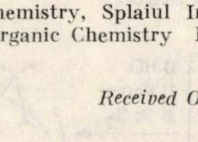

M = Eu, Pr, Yb, Sm, Dy, Ho.

R = t-Bu, CF_3, C_3F_7.

1

There are four major advantages which led to the high popularity of this class of reagents : (i) the relatively large induced shifts, even for compounds of weak basicity ;[1] (ii) the ready availability of the starting material (the natural optical active camphor) ; (iii) the relatively simple synthesis ; and (iv) a good solubility in the common solvents used in the NMR spectroscopy.

The early syntheses of these reagents included as an intermediate step the isolation of the β-diketones of the type **2**, followed by their reaction with a lanthanide salt in basic medium.[2] The disadvantages of these syntheses are the difficult purification of the β-diketone and the requirement of well definite pH in the next. step. Traces of unreacted camphor (or another presursor of the β-diketone) which may contaminate the reagents **1** affect their use as shift reagents in the NMR spectroscopy. These disadvantages were surpassed by Schurig, [3] who used an artifice consisting in the trapping of the β-diketone **2** as barium salt (**3**), directly from the reaction mixture of a Grignard reaction type between 3-bromocamphor and ethyl trifluoroacetate.[4] The barium salt **3** is insoluble in ether,[3] and this fact allows its easy purification from the unreacted camphor. The shift reagents **1** were synthesized by the fast exchange reaction between the Ba^{2+} ions and those of the needed lanthanide (M^{3+}) in an almost quantitative yield.[5]

In the present paper we report a new synthesis of the barium salt **3** by the β-diketone trapping from an ester condensation reaction type between camphor-(**4**) and ethyl trifluoroacetate.

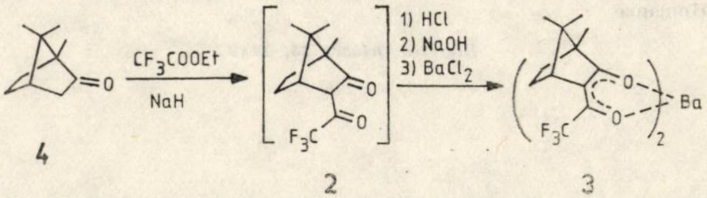

The advantage of this method is the shortening of the synthetic route of the reagents **1** by eliminating the bromination step.

The condensation reaction was carried in diglyme. After the unreacted hydride destruction with concentrated hydrochloric acid and alkalinization with sodium hydroxide, the barium salt **3** was precipitated directly from the reaction mixture with a barium chloride solution, without any separation of the formed phases. After ethanol extraction, the barium salt **3** was converted, without any further purification, into the chiral shift reagents **1** ($R = CF_3$; M = Pr, Eu) following Schurig's method.[5]

In the following we shall discuss the signals resolution in the ^1H-NMR spectrum for enantiomers of the aromatic amide **5**, using the chiral shift reagent $Eu(facam)_3$ (**1**; M = Eu, $R = CF_3$) which was synthesized according to the above-described method.

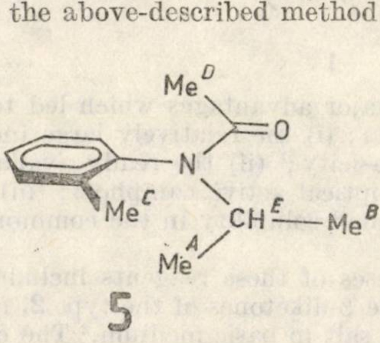

5

The *N*-(2-methylphenyl)-*N*-*i*-propylacetamide (**5**) represents a case of atropoisomerism caused by frozen internal rotation around $N-C_{Arom}$ bond. Owing to the frozen rotation, this molecule which is not planar, becomes chiral (if the aryl group is unsymmetrically substituted) and the two methyl groups (A and B) from the i-propyl residue become magne-

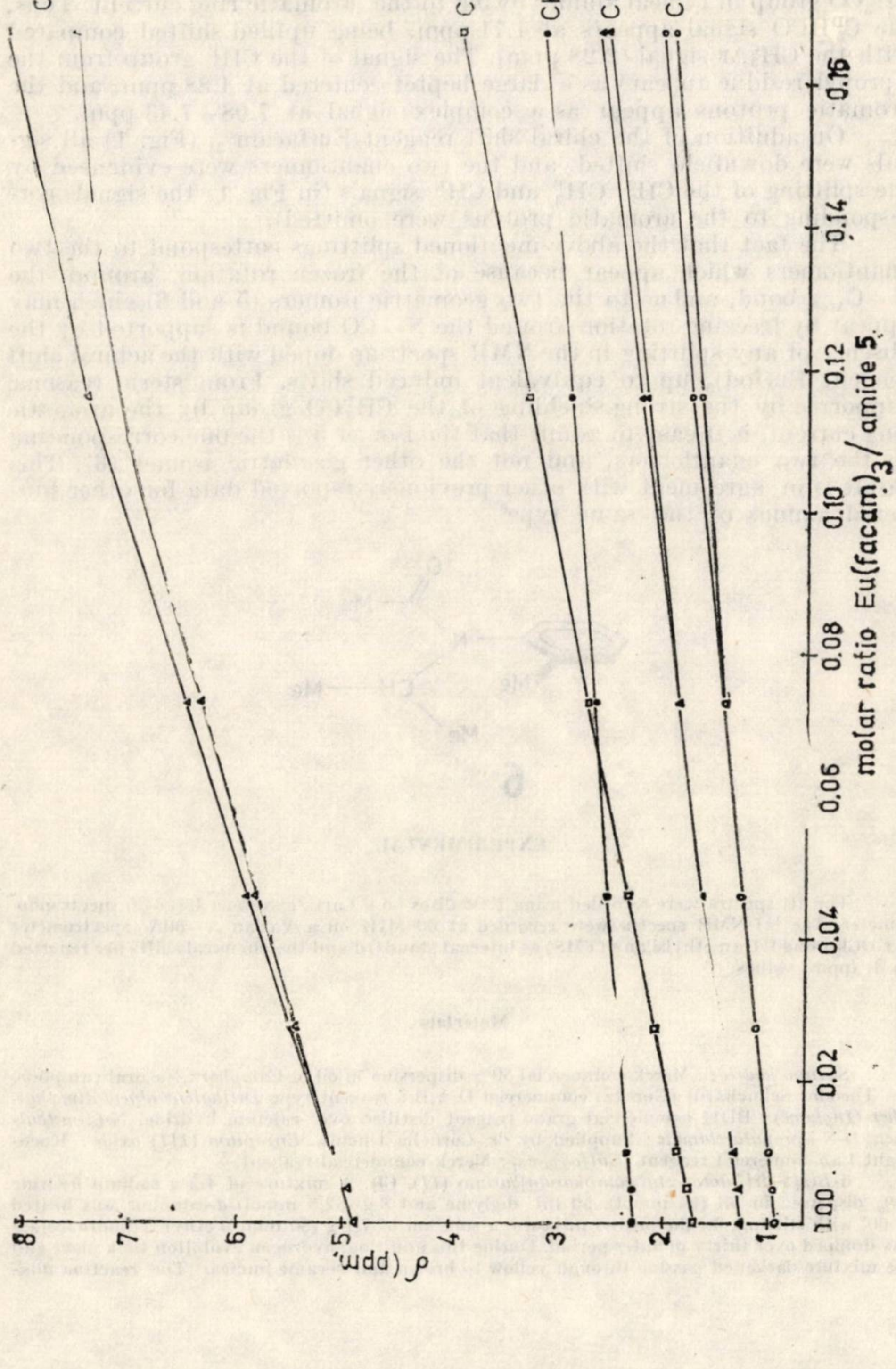

Fig. 1. — The effect of the progressive addition of Eu(facam)$_3$ on the spectrum of the amide 5.

tically unequivalent (doublets centered at 0.95 and 1.26 ppm). It is worth mentioning that the signal of the CH_3^DCO group is more shielded than the CH_3CO group in typical amides owing to the aromatic ring current. Thus, the CH_3^DCO signal appears at 1.71 ppm, being upfiled shifted compared with the CH_3^CAr signal (2.28 ppm). The signal of the CH^E group from the *i*-propyl residue appears as a large heptet centered at 4.88 ppm, and the aromatic protons appear as a complex signal at 7.08–7.43 ppm.

On addition of the chiral shift reagent Eu(facam)$_3$, (Fig. 1) all signals were downfield shifted, and the two enantiomers were evidenced by the splitting of the CH_3^A, CH_3^B and CH^E signals (in Fig. 1, the signals corresponding to the aromatic protons were omitted).

The fact that the above-mentioned splittings cottespond to the two enantiomers which appear because of the frozen rotation around the $N-C_{Arom}$ bond, and no to the two geometric isomers (**5** and **6**) which may appear by freezing rotation around the N–CO bound is supported by the absence of any splitting in the NMR spectrum doped with the achiral shift reagent Eu(fod)$_3$ up to equivalent induced shifts. From steric reasons, supported by the strong shielding of the CH_3^DCO group by the aromatic ring current, it is easy to admit that the isomer **5** is the one corresponding to the two enantiomers, and not the other geometric isomer (**6**). This result is in agreement with other previously reported data for other hindered amides of the same type[6].

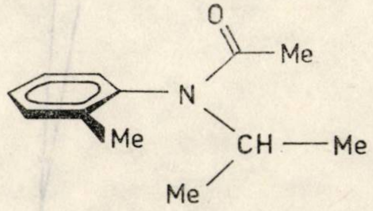

6

EXPERIMENTAL

The IR spectra were recorded using KBr discs on a Carl Zeiss-Jena UR–20 spectrophotometer. The ^1H-NMR spectra were recorded at 60 MHz on a Varian A–60A spectrometer in $CDCl_3$ using tetramethylsilane (TMS) as internal standard and the chemical shifts are reported as δ, (ppm) values.

Materials

Sodium hydride : Merck commercial 50% dispersion in oil. d-*Camphor* : Natural camphor, Dr. Theodor Schuchardt (Gorlitz) commercial D.A.B.6 reagent type *Diethylene glycol dimethylether (Diglyme)* : BDH commercial grade reagent distilled over calcium hydride. N-*(2-methylphenyl)*-N-i-*propylacetamide* : Supplied by dr. Cornelia Uncuţa. *Europium (III) oxide* : Koch-Light Lab. comercial reagent. *Eu(fod)*$_3$-*d*$_{27}$: Merck commercial reagent.

d-*Bis[3-(trifluoroacetyl)camphorato]barium (II)*, (**3**). A mixture of 4.5 g sodium hydride 50% dispersed in oil (94 mmol), 50 mL diglyme and 8 g (52,6 mmol) *d*-camphor was heated to 60° with stirring. In the heated mixture, a solution of 7.1 g (50 mmol) ethyl trifluoroacetate was dropped over thirty minutes period. During this addition, hydrogen evolution took place and the mixture darkened passing through yellow to brown and became unclear. The reaction mixture was heated at 80° with stirring for one and a half hour, when it became reddish, after which it was cooled at room temperature. Concentrated hydrochloric acid was dropped. When the entire unreacted hydride was destroyed, the reaction mixture became instantaneously clear and yellow, and at the bottom remained a fine, white precipitate of sodium chloride. This mixture was poured into 50 mL water and then a solution of 15% sodium hydroxide was added till the pH became strongly basic. The two phases which formed were treated without separation, with a solution of 7 g barium chloride in 20 mL water, when a white precipitate formed on shaking. The precipitate was separated by suction and washed with diethyl ether and cool water. The precipitate was air dried and extracted with ethanol, after the distillation of the ethanol, the barium salt **3** was obtained as a white amorphous solid. Yield 6.5 g (41%). Uncorrected m.p. 279–280° (Lit. [3] 285°). *Anal.* Calcd. for $C_{24}H_{28}O_4F_6Ba$: C, 45.64, H, 4.44, Ba, 21.71%. Found : C, 46.19, H, 5.32, Ba, 20.08%. *IR-spectrum* (KBr, cm^{-1}) : 465 w, 495 m, 510 m, 530 m, 557 m, 597 m, 645 m, 685 m, 720 m, 740 m, 810 s, 815 (sh), 855 w, 925 m, 1010 w, 1050 s, 1080 s, 1110 s, 1135 vs, 1145 (sh), 1180–1200 vs, 1220 vs, 1265 vs, 1290 s, 1325 s, 1370 m, 1385 m, 1415 s, 1450 m, 1545 vs, 1645 vs, 2875 m, 2930 (sh) and 2960 s,

Europium (III) nitrate. The nitrate was obtained by dissolving europium oxide in concentrated nitric acid, followed by the acid evaporation. The operation was repeated for three times. The remained solid was dissolved in water followed by the water evaporation. The washing operation was also repeated for three times.

Ethyl trifluoroacetate. The ester was synthesized by continuous distillation of a mixture of trifluoroacetic acid (20 mL, 0.27 mol), ethanol (60 mL, 1.03 mol) and sulphuric acid (0.6 mL), according to Henne's method[7].

d-*Tris[3-(trifluoroacetyl) camphorato] europium (III)*, (**1**; M=Eu, R=CF_3), (*Eu(facam$_3$)*) was synthesized by the exchange reaction between the barium salt **3** and europium nitrate, according to Schurig's method. [5]

REFERENCES

[1] A mixture of reagents 1 and Ag(fod) was successfully used for shifting resonances of aromatic compounds, olefins, phosphines and halogenated compounds : T.J. Wenzel, T. C. Bettes, J. E. Sadlowski and R. E. Sievers, *J. Amer. Chem. Soc.*, **102**, 5903 (1980), T. J. Wenzel and R. E. Sievers, *Anal. Chem.*, **53**, 393 (1981).

[2] G. M. Whitesides and D. W. Lewis, *J. Amer, Chem. Soc.*, **92**, 6979 (1970), H. L. Goering, J.N. Eikenberry and G. S. Koermer, *J. Amer. Chem. Soc.*, **93**, 5913 (1971).

[3] V. Schuring, *Inorg. Chem.*, **11**, 736 (1972).

[4] B. Feibush, C. S. Springer Jr. and R. E. Sievers, Abstrracts, 158-th National Meeting of the A. C. S., New York, Sept. 1969, No. INoR66 — quoted in ref. [5]

[5] V. Schurig, *Tetrahedron Letters*, **1972**, 3297.

[6] T. H. Siddal, III and W. E. Stewart, *J. Phys. Chem.*, **73**, 40 (1969), T. H. Siddal, III, *J. Org. Chem.*, 31, 3719 (1966), T. H. Siddal, III and C. A. Phohaska, *J. Amer. Chem. Soc.*, **88**, 1172 (1966), W. E. Stewart and T. H. Siddal, III, *Chem. Rev.*, **1970**, 517.

[7] A. L. Henne, M. S. Newman, L. L. Quill and R. A. Staniforth, *J. Amer. Chem. Soc.*, **69**, 1819 (1947).

Revue Roumaine de Chimie, 35, 3, 305–308 (1990)

CREATION AND DISCOVERY

ROALD HOFFMANN
Cornell University, Department of Chemistry, Baker Laboratory, Ithaca, N. Y. 14853, U.S.A

Received November 24, 1989

In describing what they do, scientists have by and large bought the metaphor of discovery, and artists that of creation. The cliche "uncovering the secrets of nature" has set, like good cement, in our minds. But I think that the metaphor of discovery is effective in describing only part of the activity of scientists, a smaller piece still of the work of chemists. There are historical, psychological and sociological reasons for the ready acceptance of the metaphor, and these need to be brought out.

History and psychology : The rise of modern science in Europe coincided with the age of geographical exploration. Men set foot on distant shores, explored *terra incognita*. Even in our century, a man I was named after first sailed the Northwest passage, and reached the South Pole. Voyages of discovery, maps filled in, those are powerful images indeed. So is penetration into a royal tomb full of glistening gold vessels. It's no surprise that these metaphors were and are accepted by scientists as appropriate descriptors of their generally laboratory-bound activity. Is there some vicarious sharing of imagined adventures at work here?

Philosophy : The French rationalist tradition, and the systematization of astronomy and physics before the other siences, have left science with a reductionist philosophy at its core. There is supposed to exist a logical hierarchy of the sciences, and understanding is to be defined solely as vertical understanding, reduction to the more basic science. The more mathematical, the better. So biological phenomena are to be explained by chemistry, chemistry by physics, etc. The logic of a reductionist philosophy fits the discovery metaphor — one digs deeper and discovers the truth.

But reductionism is only one face of understanding. We have been made not only to disassemble, disconnect and analyze, but also to build. There is no more stringent test of passive understanding than active creation. Perhaps "test" is not the word here, for building or creation differ inherently from reductionist analysis. I want to claim a greater role in science for the forward, constructive mode.[1]

This paper is dedicated to the memory of my friend, Mihai Elian. Reprinted from *American Scientist* with permission.

Sociology : Those philosophers of science who started out as practicing scientists have generally, I believe, come from physics and mathematics. The education of professional philosophers is likely to favor the same fields ; there is a special role, quite understandably, for logic in philosophy. No wonder that the prevailing ideology of reasoning in the underlying scientific areas of expertise of philosophers of science has been extended by them, unrealistically I believe, to all science.

What is strange is that chemists should accept the metaphor of discovery. Chemistry is the science of molecules (up to a hundred years ago one would have said "substances" or "compounds") and their transformations. Some of the molecules are indeed *there*, just waiting to be known by us. "Konwn" in their static properties — what atoms are in them, how these are connected up, the shapes of molecules, their splendid colors. And in their dynamic characteristics — the molecules' internal motions, their reactivity. The molecules are those of the earth for instance simple water and complex malachite. Or of life — pretty simple cholesterol, more complicated hemoglobin. The discovery paradigm certainly applied to the study of these molecules.

But so many more molecules of chemistry are made by us, in the laboratory. We're awfully prolific — a registry of known, well-characterized compounds numbers now near ten million. These were not on earth before. It is true that their constitution follows underlying rules, and if chemist A had not made such-and-such a molecule on a certain day, then it is likely to have been synthesized a few days or decades later by chemist B. But the human being, a chemist, chooses the molecule to be made and a distinct way to make it [2]. It's not that different from the artist, who constrained by the physics of pigment and canvas, shaped by his or her training, nevertheless creates the new.

¶ Even when one is operating clearly in the discovery mode in chemistry, elucidating the structure or dynamics of a known, naturally-occurring molecule, one usually has to intervene with created molecules. I recently heard a beautiful lecture by Alan Battersby, an outstanding British organic chemist. It dealt with biosynthesis of uroporphyrinogen-III. Sven in the trade, the name of this molecule is abbreviated as uro'gen-III. It's not a glamorous molecule, but it should be. For from this precursor plants make chlorophyll, the basis of all photosynthetic activity. All cells use another uro'gen-III derivative in cytochromes for electron transport. And the crucial iron-containing oxygen carrier piece of hemoglobin derives from this small disc-shaped molecule.

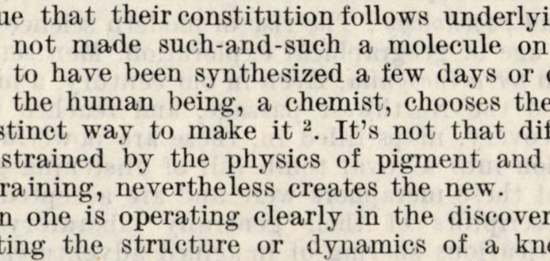

Uro'gen-III, pictured above is made from four rings, called pyrroles, themselves tied into a larger ring.

Note the markers A and P in each ring. They're in the same order as lone goes around the ring (from around 10 o'clock). Except for the last set, which are "reversed". So the markers read A, P, A, P, A, P, P, A.

How this natural molecule is assembled, within us, is clearly a discovery question. In fact the four pyrrole rings are connected up, with the aid of an enzyme, into a chain, then cyclized. But the last ring is first put in ,,incorrectly", i.e. with the order of the A, P labels the same as in the other rings, A. P, A, P, A, P, A, P. Then, in a fantastic separate reaction sequence, just that last ring, with its attached labels, is flipped into position.

This incredible but true story was deduced by Battersby and co-workers using a sequence of synthetic molecules, not natural ones. [3] Each was designed to model some critical waypoint molecule in the living system. Each synthetic hypothetical intermediate was subjected to conditions resembling physiological ones, eventually tracing out the sequence of the natural processes. Using molecules we've made, we've learned how nature builds a molecule that makes life possible.

The synthesis of molecules puts chemistry very close to the arts. We create the objects that we or others then study or appreciate. 4 That's exactly what writers, composers, visual artists, working within their areas, working perphaps closer to the soul, do. I believe that, in fact, this creative capacity is exceptionally strong in chemistry. Mathematicians also study the objects of their own creation, but those objects, not to take anything away form their uniqueness, are mental concepts rather than real structures. Some branches of engineering are actually close to chemistry in this matter of synthesis. Perhaps this is a factor in the kinship the chemist-narrator feels for the builder Faussone, who is the main character of Primo Levi's novel *The Monkey's Wrench.* [5]

In the building of theories and hypotheses, even more than in synthesis, the act is a creative one. One has to imagine, to conjure up a model that fits often irregular observations.[6] There are rules; the model should be consistent with previously received reliable knowledge. There are hints of what to do; one sees what was done in related problems. But what one seeks is an explanation which was not there before, a connection between two worlds. Often, actually, it's a metaphor that is the clue "Two interacting systems, hmm..., let's model then with resonating pair of harmonic oscillaters, or... a barrier penetration problem".[7] The world out there is moderately chaotic, friglitening???? the parts we do not understand. We want to see a pattern in it. We're clever, we ,,connoisseurs of chaos", so we find/create one.

Had more philosophers of science been trained in chemistry, I'm sure we would have a very different paradigm of sciencce before us.

Is art all creation? I dont' think so. It is in substantial measure discovery — of the deep truths of what is also around us, often overlapping, but more often reaching outside the set of problems that science has set for itself to try to understand. Art aspires to discover, explore, unravel — whatever metaphor you please — the nonunique, chanced, irreductible world within us.

REFERENCES

[1] For a relevant debate on reductionism see S. Weinberg, *Nature*, **330**, 433 (1987) ; *Ibid.* **331**, 475 (1988) ; E. Mayr, *Nature*, **331**, 475 (1988).

[2] See in this context G. Stent, *Scientific American* **227**, December, 84 (1972) ; G. Stent, *Engineering and Science (Cal. Inst. Technol.)* Sept. 1985, p. 9 (1985).

[3] For leading references to the beautiful chemistry discussed so cursorily here see A .R. Battersby and E. McDonald, *Accounts Chem. Res.* **12**, 14 (1979) ; A. R. Battersby, *Pure Appl Chem.* **61**, 337 (1989).

[4] Often quoted here is M. Berthelot : *Chimie Organique Fondée sur la Synthese*, Tome 2, Mallet-Bachelier, Paris 1860 (1988), See also J. — P. Malrieu. *L'Actualité Chimique*, No. 3, p. IX (1987) ; A. F. Bochkov and A. V. Smit, *Organicheskii Sintez*, **1987**, Nauka, Moscow.

[5] Primo Levi, *The Monkey's Wrench*, 1986. Simon & Schuster, published originally as *La Chiave a Stella*, 1978. Giulio Einaudi editore s.p.a., Torino.

[6] Baruch S. Blumberg has stressed the role of fantasy in model building, in an interesting recent article : *Amer. Med. Writers Assoc J.*, **4**, 2 (1989).

[7] For a discussion of metaphor in science see various articles, especially that by R. R. Hoffman, in *The Ubiquity of Metaphor*, ed. R. Dirvan and W. Paprotte, 1985. John Benjamin, Amsterdam.

Revue Roumaine de Chimie, **35**, *3*, 309–322 (1990)

CARBONIUM ION REACTIONS. XX [1]

SYNTHESIS AND ACETOLYSIS OF 8-CHLOROMETHYL-DIBENZO-[b, d]BICYCLO[5.1.0]OCTA-2,4-DIENE [2]

MIRCEA D. BANCIU,[a] MIHAI ELIAN[b], ANCA BANCIU,[b]
CONSTANTIN DRĂGHICI,[b] LIGIA STĂNESCU,[b] PHAN LE THUY[a]
and ECATERINA CIORĂNESCU[a,b]

[a]Organic Chemistry Department, The Polytechnic — TCH, Spl. Independenţei 313, 76206 Bucharest, Romania

[b]Centre of Organic Chemistry — Spl. Independenţei 202B, 78100 Bucharest, Romania

Received October 23, 1989

The title chloroderivative **6** including a cyclopropylcarbinyl moiety was obtained from the known 5H-dibenzo[*a,c*]cycloheptene (**7**) by carbethoxycarbene addition, followed by $LiAlH_4$ reduction of stereoisomeric esters **8** and subsequent treatment of alcohols **9** with *p*-toluenesulfonyl chloride or thionyl chloride. Acetolysis of exo-**6** (in presence or in absence of NaOAc) afforded rearranged products containing a vinyl substitutent : chloride **12** and acetate **10** with seven-membered central ring and chloride **11** with six-membered central ring ; along with them the unstable conjugated diene **13** seems to be formed. The reaction mechanism is discussed pointing the importance of covalent return phenomena. A parallel of solvolytic behaviour of **6** with related previously studied cyclopropylcarbinyl systems **1** and **2** is also presented.

INTRODUCTION

In preceding papers we described the rearrangements of polycyclic cyclopropylcarbinyl systems **1** [3] and **2**. [4] Acetolysis of tosylate **1** (X = = OTs) proceeded with cyclopropyl-participation affording [3] the rearranged benzylic acetate **3** and homobenzylic acetate **4** as main reaction products. On the other hand, treatment of the alcohol **2** (X = OH) with *p*-toluenesulfonic acid in benzene conducted to a rearranged tosylate **5**, very probably *via* a concerted pathway.

Due to the continuous interest aroused by cyclopropylcarbinyl rearrangements, [5] the investigation of the solvolytic behaviour of a dibenzobicyclic derivative **6**, closely related with **1** and **2**, seemed interesting.

In this paper we describe the synthesis and solvolysis of chloroderivative **6**.

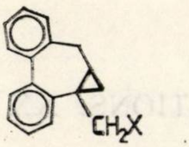

1 (X = OTs)

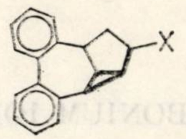

2 (X=OH)

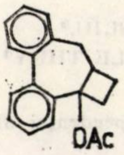

3

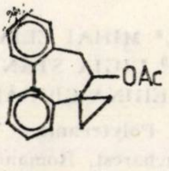

4

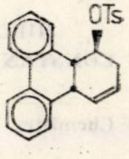

5

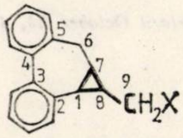

6 (X=Cl)

RESULTS

Synthesis

The synthesis of dibenzo[*b*, *d*]bicyclo[5.1.0]octa-2,4-diene skeleton was achieved through carbethoxycarbene addition to the known[6] 5H-dibenzo[*a*, *c*]cycloheptene (**7**). The reaction was performed with ethyl diazoacetate either at 130–140° in the presence of powdered copper or at room temperature under UV-irradiation. From the reaction mixture an esteric fraction was separated in about 70% yield by column chromatography. The IR spectrum of this fraction presented a $\nu_{C=O}$ absorption at 1720 cm^{-1} in agreement with an esteric group conjugated with a cyclopropanic ring. The ^{1}H–NMR signals of the carbethoxy group were doubled suggesting the existence of two isomers of **8**. The v.p.c.-analysis confirmed the presence of two compounds in a 3 : 1 ratio.

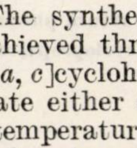

7

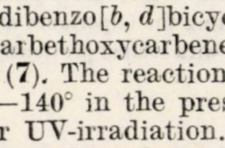

8

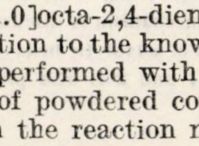

9

The reaction of ethyl diazoacetate with **7** could lead to four isomeric esters **8** (two *exo* and two *endo*), each of them possessing two conformations interconvertible by rotation around the biphenylic central bond (only one of these conformations is presented in formulas of **8**-*exo* and **8**-endo).

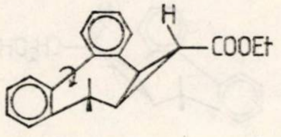

8-exo-A

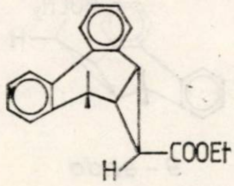

8-exo-B

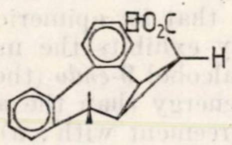

8-endo-A

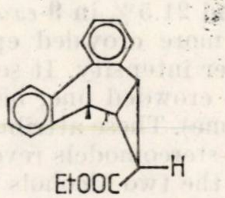

8-endo-B

Assuming, as in other related cases,[7] that the barrier of ring inversion is small, such individual conformers cannot be isolated. Moreover, inspection of Dreiding stereomodels indicates that **8**-*exo*-A and **8**-*exo*-B (each in one of its conformations), and similarly **8**-*endo*-A and **8**-*endo*-B, are enantiomers; it results that the actual composition of the addition product includes only two racemic isomers: one *exo* (**8**-*exo*) and one *endo* (**8**-*endo*).

The ^1H-NMR spectrum of the esteric fraction presents the signals of the five aliphatic ring protons betwen $\delta = 1.5-3.2$ ppm; due to its complexity this signal could not be resolved. However, the duplication of signals for C_2H_5 protons is informative concerning the configuration: the signals of lower intensity, belonging to the minor isomer, are shielded by 0.1 ppm in comparison with the corresponding signals of the major isomer. Examination of the Dreiding stereomodels of **8** reveals that both **8**-*endo*-A and **8**-*endo*-B could present a shielding of the C_2H_5 protons through magnetic anisotropy of an aromatic ring. Thus the minor isomer of **8** possesses the *endo*-configuration whereas the major one the *exo*-configuration. These attributions are in agreement with the known[8] *exo*-stereoselectivity in reactions of ethyldiazoacetate with olefins.

The $LiAlH_4$-reduction of the esteric fraction (**8**-*exo* + **8**-*endo*) afforded in quantitative yield a 3 : 1 mixture (v.p.c. analysis) of the corresponding alcohols **9**. The individual isomers **9**-*endo* and **9**-*exo* were separated by preparative v.p.c. As in the case of the corresponding esters, the ^1H-NMR signals of cyclopropanic protons ($\delta = 1.1-2$ ppm) are very complex in both isomers and could not be resolved even in the presence of $Eu(fod)_3$ as shift reagent.

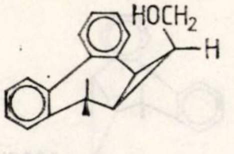

9 - endo

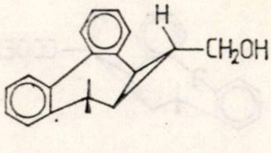

9 - exo

The mass spectra of isomeric alcohols **9**-*exo* and **9**-*endo* (see Experimental) are practically identical concerning the m/z values but differ in peak intensities. The base peak is in both cases the ion $M^+ - H_2O$ with m/z = 218, while the parent ion M^+ at m/z = 236 has intensity 8.7% in **9**-*endo* and 21.5% in **9**-*exo*. It is known that for epimeric pairs of alcohols the more crowded epimer generally exhibits the molecular ion (M^+) of lower intensity. It seems that the alcohol **9**-*endo* (the minor one) is the more crowded one, being richer in energy than the alcohol **9**-*exo* (the major one). These attributions are in agreement with : a) the analysis of Dreiding stereomodels revealing the crowding of **9**-*endo* and b) the occurrence of the two alcohols **9** (*endo*/*exo*) in the same ratio as the isomers of the starting esteric mixture (**8**).

The attempted synthesis of a tosylate starting from the alcoholic mixture **9** failed. Treatment of this mixture **9** (*exo* + *endo*) with *p*-toluenesulfochloride in pyridine afforded a solid whose IR, ^1H-NMR spectral data and elemental analysis (see Experimental) are in agreement with the structure of 8-chloromethyl-dibenzo[*b*, *d*]bicyclo[5.1.0]octa-2,4-diene (**6**).

Very probably the corresponding tosylate is formed in the first stage of the reaction but subsequently this compound is converted into **6**. Similar conversions of primary alcohols into the corresponding chlorides (by reaction with PyH^+Cl^- at room temperature) are known. [10]

The same chloroderivative **6** was obtained on treatment of the alcoholic mixture **9** (*exo* + *endo*) with thionyl chloride in pyridine. The ^1H-NMR spectrum of **6** (see Experimental) indicates the existence of a single compound, corresponding to the major alcoholic isomer (namely **9**-*exo*). It seems that the chloroderivative corresponding to the minor isomer (**9**-*endo*) is lost during work-up and recrystallization.

Acetolysis of chloroderivative exo-6

The acetolysis of chloroderivative **6** follows a first-order kinetics, indicating a rate constant of $k_{110^\circ} = 9.4 \times 10^{-5}\ s^{-1}$.

The analytical acetolyses of exo-**6** were performed in unbuffered and in NaOAc-buffered media at different temperatures and reaction times. After the usual work-up (see Experimental) the reaction mixtures were v.p.c.-analysed. The reactions at 90° were chosen to describe most explicitly the evolution of the acetolyses (reaction at 60° was found to be very sluggish whereas that at 110° was too fast). The distribution of the reaction products for acetolyses of exo-**6** at 90° is presented in fig. 1.

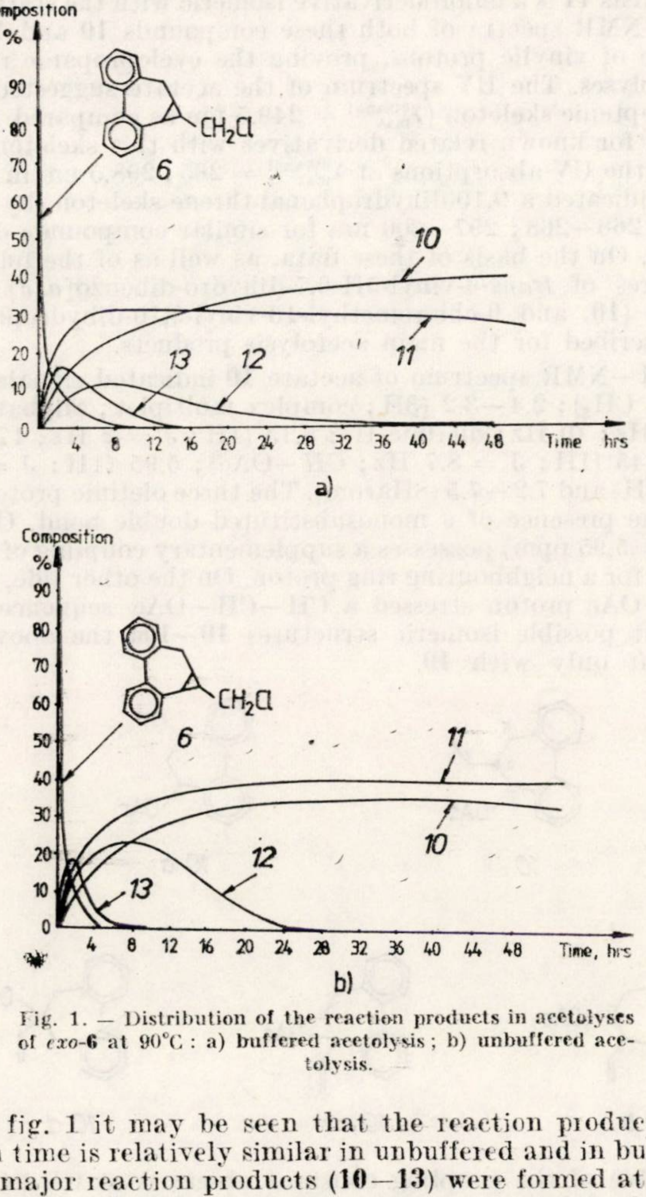

a)

b)

Fig. 1. — Distribution of the reaction products in acetolyses of *exo*-**6** at 90°C : a) buffered acetolysis ; b) unbuffered acetolysis.

From fig. 1 it may be seen that the reaction products and their evolution in time is relatively similar in unbuffered and in buffered acetolyses ; four major reaction products (**10**—**13**) were formed at the expense of chloroderivative **6**. Numerous minor components (up to 3 — 4 % each) were not included in fig. 1. Whereas compounds **12** and **13** disappear (rapidly in unbuffered acetolysis and more slowly in unbuffered one) the products **10** and **11** increase in first stages of the reaction remaining further practically unmodified.

The compounds **10** and **11** could be separated by preparative v.p.c. of products obtained from preparative acetolyses of **6**. The IR spectra and elemental analyses of these compounds have shown that **10** is an acetate whereas **11** is a chloroderivative isomeric with the starting chloride **6**. The ^1H-NMR spectra of both these compounds **10** and **11** indicated the presence of vinylic protons, proving the cyclopropanic ring opening during solvolyses. The UV spectrum of the acetate suggested a dibenzo-[*a*, *c*]cycloheptenic skeleton ($\lambda_{max}^{ethanol} = 249.5$ nm as compared to $\lambda_{max}^{ethanol} = 248.5$ nm for known related derivatives with this skeleton[11]). On the other hand, the UV-absorptions at $\lambda_{max}^{ethanol} = 265$; 298.5 nm in the chloroderivative indicated a 9,10-dihydrophenanthrene skeleton (by comparison with $\lambda_{max} = 266-268$; 297–300 nm for similar compounds described in literature[11]). On the basis of these data, as well as of the following ones the structures of *trans*-6-vinyl-5H-6,7-dihydro-dibenzo[*a*, *c*]cyclohepten-7-yl acetate (**10**) and 9-chloromethyl-10-vinyl-9,10-dihydrophenanthrene (**11**) were ascribed for the main acetolysis products.

The ^1H-NMR spectrum of acetate **10** indicated signals at ($\delta_{ppm}^{CCl_4}$): 1.97 (3H; s, CH_3); 2.4–3.2 (3H; complex multiplet; aliphatic H); 5.10 (1H; J = 2Hz; 10 Hz; olefinic H); 5.15 (1H; J = 2 Hz; 17.5 Hz; olefinic H); 5.45 (1H; J = 8.7 Hz; C*H*–OAc); 5.95 (1H; J = 8 Hz; 10 Hz; olefinic H) and 7.2–7.5 (8Harom). The three olefinic protons strongly suggested the presence of a monosubstituted double bond. One of these protons ($\delta = 5.95$ ppm) possesses a supplementary coupling of 8 Hz which is indicative for a neighbouring ring proton. On the other side, the doublet of the C*H*–OAc proton stressed a CH–CH–OAc sequence. From the five different possible isomeric structures **10**–**10d** the above data are in agreement only with **10**.

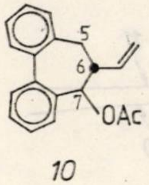

10

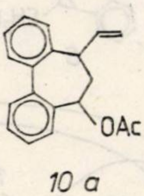

10 a

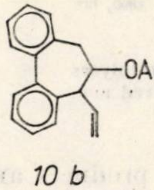

10 b

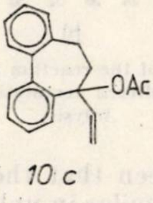

10 c

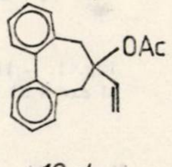

10 d

The value of the coupling constant observed at C*H*–OAc proton (J = 8.7 Hz) is of the same magnitude with coupling constants observed[12] at some conformationally fixed dibenzo[*a*, *c*]cycloheptenic derivatives with *trans*-isomerism ($J_{H-H}^{trans} = 8-10$ Hz ; $J_{H-H}^{cis} = 3-5$ Hz). Consequently, in the acetate **10** the vinyl and acetoxy groups are situated in a *trans* relationship.

The ^1H-NMR spectrum of the chloroderivative **11** presents signals at ($\delta^{CCl_4}_{ppm}$): 3.35 (1H; multiplet); 3.8–4.1 (3H; complex multiplet; aliphatic H); 5.20 (1H; J = 2.5 Hz; 9 Hz; olefinic H); 5.30 (1H; J = = 2.5 Hz; 17.5 Hz; olefinic H); 5.95 (1H; J = 8.5 Hz; 9 Hz; 17.5 Hz; olefinic H); 7.35 (6Harom); 7.8–8.0 (2Harom). This spectrum agrees well with the 9,10-dihydrophenanthrenic skeleton (suggested by UV spectra) through a more deshielded position of two aromatic protons ($\delta = 7.8-8.0$ ppm) characteristic for such systems. The existence of three olefinic protons, indicating a monosubstituted double bond as well as the absence of some characteristic signals for CH_3 group, reduces the number of the possible structures to the following five (**11**–**11d**).

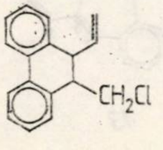

11

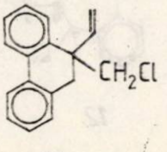

11 a

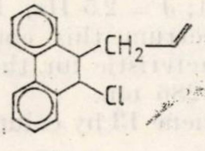

11 b

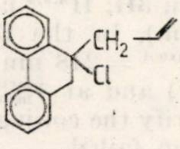

11 c

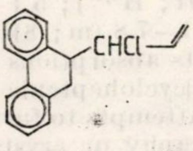

11 d

The structures **11a**–**11c** could be eliminated on the basis of coupling constants observed for olefinic protons, which show a supplementary coupling with *one* proton, denoting a $CH_2 = CH-CH$ sequence. The structure **11d** could be discarded on the basis of the observed chemical shifts: in compounds which contain (as in **11d**) a CH_2-group in the six-membered central ring [11c] the signals of this group appear at about $\delta =$ = 3 ppm, a value which differs considerably from the observed one ($\delta =$ = 3.8–4.1 ppm). Nevertheless, the observed δ value is normal for a CH_2 group carring an electron-withdrawing substituent such as the chlorine atom. It follows that the structure of the chloroderivative is undoubtfully **11**.

The third reaction product, **12**, could be isolated through liquid chromatography on neutral alumina from the reaction mixture of an unbuffered acetolysis of *exo*-**6** performed at 90° for 7.5 hrs. The UV spectrum suggests a seven-membered central ring by the absorption of $\lambda^{methanol}_{max} = 247$ nm. The ^1H-NMR spectrum presents the following signals; ($\delta^{CCl_4}_{ppm}$): 2.3–3.4 (m; 3H; $H^{5,5'}$, H^6); 4.60 (d; 1H; H^7; J = 9 Hz); 5.10 (dd; 1H; H^9: J = 2; 10 Hz): 5.15 (dd; 1H; $H^{9'}$; J = 2; 18 Hz); 5.95 (m; 1H; H^8; J = 18; 10; 8 Hz); and 7.1–8 (m; 8Harom). This spectrum agrees well with that of acetate **10** excepting the doublet of H^7 at 4.6 ppm (instead that of 5.45 ppm) which is characteristic for an

$\mathrm{Ar-C}H\mathrm{(Cl)-CH}\langle$ sequence. The coupling constants of $J = 9$ Hz for this doublet indicated again the *trans*-relationship between the vinyl- and chlorine substituents in **12**. The IR data are also in agreement with the structure of *trans*-6-vinyl-5H-6,7-dihydro-dibenzo[*a*,*c*]cyclohepten-7-yl-chloride (**12**).

The fourth acetolysis product, **13**, was isolated from the reaction product of a preparative buffered acetolysis of *exo*-**6** at 90° for 2.5 hrs. Column chromatography on alumina afforded small amounts of a colourless thick oily product whose ^1H-NMR data are in agreement with the structure of 6-vinyl-5H-dibenzo[*a*, *c*]cycloheptene (**13**): $\delta_{ppm}^{CCl_4} = 2.4-3.4$ (m; 2H; $H^{5,5'}$); 5.1–6.0 (m; 3H; $H^{8,9,9'}$); 6.55 (t; $J = 2.5$ Hz; 1 H; H^7) and 7.1–7.8 (m; 8H; Harom). In the UV spectrum this component presents absorptions at $\lambda_{max}^{methanol} = 248$ nm (characteristic for the dibenzo[*a*, *c*]cycloheptenic moiety) and at $\lambda_{max}^{methanol} = 286$ nm.

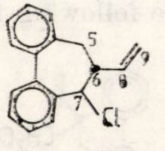

12

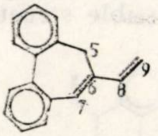

13

Attempts to further purify the conjugated diene **13** by column chromatography or crystallization failed.

DISCUSSION

The relatively large rate constant of acetolysis of *exo*-**6** is associated with the cyclopropylcarbinyl moiety. The reaction products result by cyclopropanic ring opening in the starting material. Ionisation of a chlorine anion in **6** affords an unstable cyclopropylcarbinyl cation **14**. This cation could easily undergo cyclopropanic ring opening in two related ways (*a* and *b*, Scheme 1). Thus two isomeric homoallylic cations **15** and **16** could appear, most probably as ion pairs with chloride anions. The main difference between these cations resides in the benzylic structure of **15** and the homobenzylic one of **16**. The stable benzylic-homoallylic ion **15** could afford by covalent return the benzylic chloride (**12**) which was isolated at short reaction time. It may be mentioned here that covalent returns are well-known phenomena in solvolyses of cyclopropylcarbinyl derivatives.[13]

At longer reaction time, the chloride **12** disappears being converted (mainly) into the stable benzylic acetate **10**. A proton loss in **15** affords the diene **13**. On the other hand, the homobenzylic cation **16** could easily afford a phenonium ion **17**. Indeed, the Dreiding stereomodels indicate excellent steric conditions for generation of **17** from **16**. A covalent return

Scheme 1

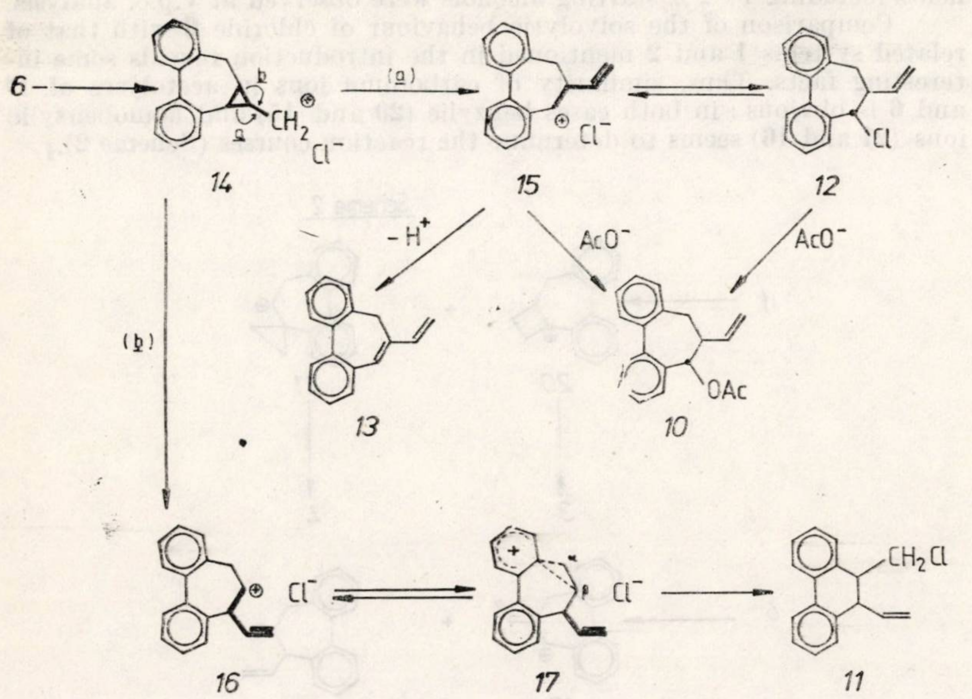

within 17+Cl− ion pairs affords, by attack of chlorine in α-position, the covalent ring-contracted product **11**. The primary chloride **11** being much less reactive than **6** or **12** could be isolated even after 48 hrs at 90°C.

In connection with the phenonium ions in this series it should be added here that an ion **18**, isomeric with **17** might be also formed from **16**; geometric requirements for its formation are also fulfilled as Dreiding models showed. However, this ion **18** seems to be defavoured by the +E effect of the vinyl substituent which decreases the positive charge of the cation. Consequently, a rearranged chloride **19** which should result from **18** was not observed among the major products of acetolysis. Thus, the most favoured reaction route of cation **16** seems to remain its easy conversion to phenonium ion **17** affording finally the stable rearranged chloride **11**.

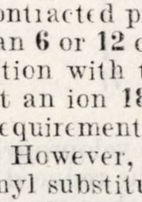

18

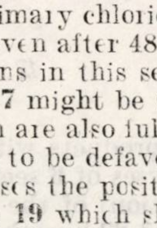

19

Attempts to gain further information concerning the cationic reactions of system **6** by treating the alcohols **9**-*exo* or **9**-*endo* with *p*-toluensulphonic acid in benzene failed : even after 2 hrs at 80 °C, 13 minor components including 1–2% starting alcohols were observed at v.p.c. analysis.

Comparison of the solvolytic behaviour of chloride **6** with that of related systems **1** and **2** mentioned in the introduction reveals some interesting facts. Thus, similarity of carbonium ions in acetolyses of **1**[3] and **6** is obvious : in both cases benzylic (**20** and **15**) and homobenzylic ions (**21** and **16**) seems to determine the reaction courses (Scheme 2).

Scheme 2

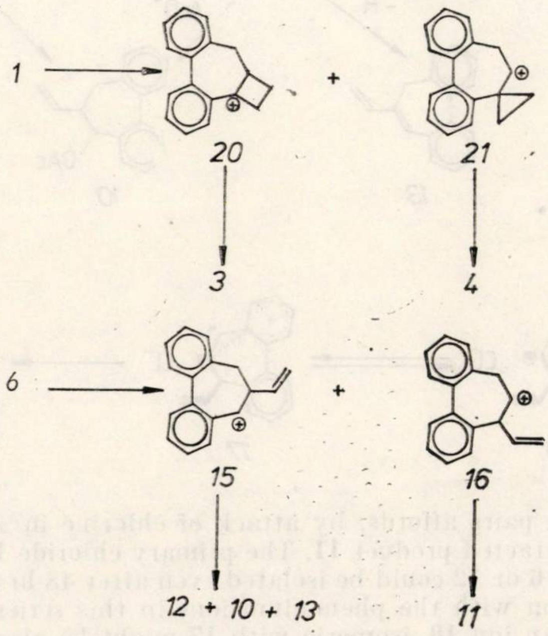

The lack of products with cyclobutyl- or cyclopropyl moieties (like **3** and **4**) in solvolyses of **6** seems to be due to the reduced stability (thus to difficult formation) of the corresponding carbonium ions **22**, **23** and **24** : whereas **22** and **23** lose the benzylic character the ion **24** loses an important part of biphenylic conjugation due to its eight-membered central ring.

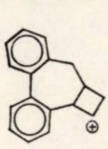
22

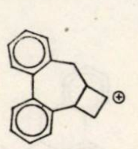
23

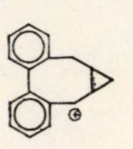
24

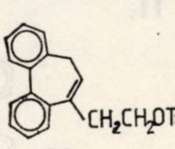

25

Formation of rearranged homoallylic products such as **12** by covalent return finds analogy in acetolyses of tosylate **1**[3] where a homoallylic tosylate **25** was also isolated.

On the other hand, the formation of **11** from **6** by ring contraction is perfectly analogous to the occurrence of six-membered product **5** during the acid-catalyzed reaction of bridged cyclopropyl-carbinyl alcohol **2**.[4]

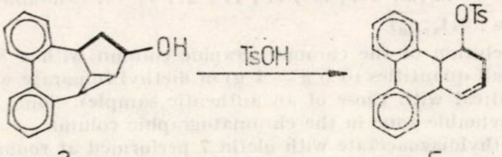

2 5

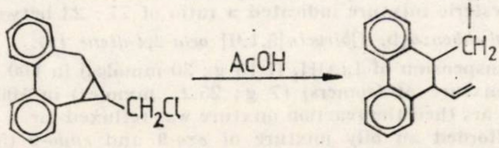

6 11

In conclusion, it was proved that acetolysis of chloride **6** proceeds with rearrangements to vinyl derivatives possessing six- and seven-membered central ring. Covalent return phenomena were suggested conducting to a relatively unstable seven-membered chloride **12** and a stable six-membered chloride **11**. The intermediacy of bifunctional cations (benzylic-homoallylic and homoallylic-phenonium) was postulated and some parallelism with the related systems **1** and **2** was observed.

EXPERIMENTAL

The melting points are uncorrected. IR spectra were registered on a UR 20 C. Zeiss Jena double beam spectrometer, UV spectra on a SPECORD UV—VIS C. Zeiss spectrometer, ^{1}H—NMR spectra on a VARIAN A60—A spectrometer (TMS as internal standard) and mass spectra on a Du Pont DP—101 GC/MS apparatus.

V.p.c. analyses were performed on a Carlo Erba 2450 apparatus with a SE 30 methylsilicone polymer column (10% on silanized Chromosorb W, 60—80 mesh, 1.5 m long, 2 mm diameter) at 180° with a nitrogen flow-rate 30 mL/min. V.p.c. separation of alcohols **9** was realized on a Carlo Erba model GV gas chromatograph using a SE 30 methyl silicone polymer column (20% on silanized Chromosorb W, 30—60 mesh, 3 m long, 6 mm internal diameter) at 180° with a hydrogen flow-rate of 180 mL/min. V.p.c. separations of acetolysis products were performed on the same apparatus using a QF$_1$ silicone column (20% on Anaprep, 30—60 mesh, 2 m long, 10 mm internal diameter) at 200° with hydrogen flow-rate 350 mL/min.

8-Ethoxycarbonyl-dibenzo[b,d]*bicyclo*[5.1.0]*octa-2-4-diene* (**8**)

a) A mixture of 5H-dibenzo[*a,c*]cycloheptene (**7**)^6 (8 g; 41.5 mmoles) and powdered cooper (0.6 g; 9.4 mg-atoms) was heated at 130° in argon atmosphere. Freshly synthesized ethyl diazoacetate (7.2 g; 62 mmoles) was dropped over this mixture during three hours with a vigorous stirring. The reaction mixture was heated at 140° for one hour. After cooling the reaction mixture was diluted with ethyl ether and the organic layer was separated. Evaporation of the solvent afforded an oily brown residue which was chromatographed on a neutral alumina column. On elution with petroleum ether (b. p. 30—50°C) unreacted alkene **7** was separated (2.4 g) and utilized in another run. On further elution with a 9 : 1 petroleum ether : ethyl ether mixture the ester **8** was obtained (5.65 g; 70% — calculated on the converted alkene **7**) as a yellow oil with pleasant smell. The v.p.c. analysis indicated the presence of two isomers *(exo-**8*** and *endo-**8***) in 75 : 25 ratio.

IR spectrum of **8**(as isomeric mixture), CS_2; CCl_4; cm^{-1}: 745s, 755vs, 785vs, 1155vs, 1428m, 1468m, 1720vs, 2937w, 2981m, 3018w and 3067m.

^1H-NMR spectrum of **8** (as isomeric mixture), CCl_4; δ_{ppm}: 1 .23 (doubled t; 3H; CH_2-CH_3; J = 7 Hz); 1 .5—3 .2 (m, 5H; H^1; H^7, H^8, $2H^6$); 4 .15 (doubled q; 2H; CH_2-CH_3; J = 7Hz): 7 .2—7 .8 (m; $8H_{arom}$).

Continuing the elution of the chromatographic column with a 8 : 2 petroleum ether; ethyl ether mixture small quantities (0 .5 g — 1 g) of diethyl fumarate were obtained (IR- and ^1H-NMR spectra identical with those of an authentic sample). Some brown polymeric material remains as an uneluable zone in the chromatographic column.

b) Reaction of ethyldiazoacetate with olefin **7** performed at room temperature without solvent by irradiation with a medium pressure Hg—UV lamp (Rasotherm filter) afforded, after 60 hrs a crude reaction mixture which was subsequently chromatographed through a neutral alumina column. Elution with petroleum ether afforded an esteric fraction (**8**-*exo* + **8**-*endo*) in 15% yield. The IR- and ^1H-NMR spectra were similar to those from procedure a). V.p.c. analysis of the esteric mixture indicated a ratio of 77 : 23 between the two isomers.

8-Hydroxymethyl-dibenzo[b, d]*bicyclo*[5.1.0] *octa-2,4-diene* (*9*).

Over a stirred suspension of $LiAlH_4$ (1.15 g; 30 mmoles) in 100 mL anhydrous ether a solution of ester **8** (mixture of isomers) (7 g; 25.2 mmoles) in 100 mL anhydrous ether was dropped during 24 hrs then the reaction mixture was refluxed for 5 hrs and left overnight. The usual work-up afforded an oily mixture of *exo*-**9** and *endo*-**9** (5 g; 84%). The v.p.c. analysis indicated two components in 75 : 25 ratio. The pure alcohols *exo*-**9** (major component) and *endo*-**9** (minor component) were separated by preparative v.p.c.

exo-*8-Hydroxymethyl-dibenzo*[b, d]*bicyclo*[5.1.0]*octa-2,4-diene*, *(exo-**9**)*, colourless thick oil:

IR spectrum (CCl_4; cm^{-1}): 1016s, 1036s, 1428m, 1442m, 1481m, 2868m, 2920m, 2946m, 3016m, 3046m and 3625m.

^1H-NMR spectrum (CCl_4: δ_{ppm}): 1.0—3.2 (m, 6H, H^1, H^7, H^8, $2H_6$, OH); 3.55 (m; 2H; CH_2); 7.1—7.5 (m; $8H_{arom}$).

Mass spectrum (m/z; %int.) 63(4 .5); 83(3 .9); 88(3 .1); 89(4 .6); 95(12 .2); 96(4 .3); 101(10 .7); 107(7.7); 108(13 .3); 109(7 .3); 115(3 .2); 139(3 .3); 151(3 .5); 152(8 .1); 163(5 .0); 164(4 .3); 165(29 .5); 166(6 .1); 176(9 .1); 177(6 .4); 178(27 .6); 179(13 .9); 188(3 .9); 189(25 .6); 190(14.2); 191(32.6); 192(23.5); 193(4.1); 200(3 .7); 201(7 .7); 202(43 .4); 203(71 .1); 204(16 .9); 205(23.9);206(5.7); 213(4 .5); 215(25.9); 216(13 .3); 217(56 .2); 218(100; M^+-H_2O); 219(21 .1); 234(6.0); 236(21 .5; M^+); 237(3 .6; $M^+ + 1$); 238(0 .1; $M^+ + 2$).

endo-*8-Hydroxymethyl-dibenzo*[b, d]*bicyclo*[5.1.0]*octa-2,4,diene* *(endo **9**)* colourless crystals with m.p. 104—107°.

IR spectrum (CCl_4; cm^{-1}): 1020s, 1432w, 1472w, 2856w, 2888w, 2929m, 3017m' 3068m and 3626m.

^1H-NMR spectrum (CCl_4; δ_{ppm}): 0.98—3.0 (m, 4H; H^1 H^7; H^8, OH); 2.52 (dd; 1H; H^6; J = 13; 9Hz); 2.87 (dd, 1H; $H^{6'}$; J = 13; 6 Hz); 3.58 (dd; 1H from CH_2O); J = 12; 8 Hz); 3.93 (dd; 1H from CH_2O; J = 12; 6.5 Hz); 7.1—7.5 (m; $8H_{arom}$).

Mass spectrum (m/z; %int); 51(3.2); 63(4.0); 76(4.3); 82(3.4); 83(4.0); 88(4.5); 89(4.7); 94(10.2); 95(6.5); 96(4.3); 101(13.9); 107(3.7); 108(16.2) 109(9.9); 115(3.3); 152(5.7); 165(22.1); 176(5.3); 177(3.1); 178(17.9); 179(5.9); 189(21.3); 190(9.4); 191(24.2); 192(13.2); 201(5.3); 202(40.1); 203(69.2); 204(13.5); 205(14.5); 213(3.7); 215(28.0); 216(12.3); 217(57.4); 218(100; M^+-H_2O); 219(17.9); 234(4.2); 236(8.7; M^+); 237(0.9, $M^+ + 1$); 238(0.1; $M^+ + 2$).

exo,*8-Chloromethyl-dibenzo*[b, d]*bicyclo*[5.1.0]*octa-2,4-diene (exo-**6**)*

a) *From the alcoholic mixture (**9**-exo/**9**-endo) with p-toluene-sulfochloride.* Over an ice-cooled solution of isomeric alcoholic mixture (**9**-*exo*/**9**-*endo*) (2.5 g; 10 mmoles) in 20 mL anhydrous pyridine, *p*-toluenesulfochloride (2.2 g; 11 mmoles) was addes in small portions. After 30 min. the separation of crystals of pyridine hydrochloride is visible but after 2—3 hrs these crystals disappeared. The reaction mixture was kept 24 hrs at 0°C then poured in 50 mL cold water. The organic product was extracted with ethyl ether (3×35 mL) and the combined organic layers were washed with water, dil. HCl and again with water until pH 7. The neutral solution was dried, filtered and evaporated *in vacuo* affording an oily product which soon crystallised (1.05 g; 40%). After rapid recrystallization from ethanol the chloroderivative **6**-*exo*, a white solid, indicated m.p. 102–104°C. Found: C, 80.28; H, 6.26; Cl, 14.38. Calculated for $C_{17}H_{15}Cl$: C, 80.10; H, 5.90; Cl, 14.00%.

IR spectrum (CS_2; CCl_4; cm^{-1}): 699w, 751vs, 1441m, 1483m, 2855w, 2921m, 2950m, 3018m and 3066m.

^1H-NMR spectrum ($CDCl_3$; δ_{ppm}): 1.2–2.1 (m; 3H; H^1, H^7, H^8); 2.3 (dd; 1H; H^6; $J_{6,6'} = 12.5$; $J_{6,7} = 11$ Hz); 3.06 (dd; 1H; $H^{6'}$, $J_{6',6} = 12.5$; $J_{6',7} = 5$ Hz); 3.4 (dd; 1H; one H from CH_2Cl; $J_{gem} = 12$; $J_{9,8} = 8.5$ Hz); 3.8 (dd; one H from CH_2Cl; $J_{gem} = 12$; $J_{9',8} = 6.5$ Hz); 7.18–7.8 (m; $8H_{arom}$).

b) *From the alcoholic mixture* (**9**-*exo*/**9**-*endo*) *with* $SOCl_2$. Over an ice-cooled solution of isomeric alcoholic mixture (**9**-*exo*/**9**-*endo*) (2.2 g; 9,3 mmoles) in 5 mL anhydrous pyridine and 5 mL anhydrous benzene, 1 mL $SOCl_2$ (1.64 g; 13,8 mmoles) was added. An exothermal reaction accompanied by formation of solid pyridine hydrochloride was immediately visible. The reaction was kept 1 hr at room temperature then heated at 75°C for 1 hr. The reaction mixture was decomposed with cold water (10 mL) and the organic products were ether-extracted. The ethereal solution was washed with water, dil. HCl, again with water until pH 7, then dried and evaporated. The solid residue (1 g; 42%) afforded after recrystallization from ethanol white crystals of **6**-*exo*, m. p. 102–104°C, identical (IR- and ^1H-NMR spectra) with the product obtained by the method a).

Acetolyses of chloride exo-**6**

a) *Analytical acetolyses*. A solution of chloride *exo*-**6** (0.2 g; 0.79 mmoles) in 30 mL anhydrous acetic acid without or respectively with added anhydrous sodium acetate (67 mg; 0.82 mmoles) was heated with stirring on an oil bath at 90°C. From time to time samples of 2 mL from reaction mixture were taken out, diluted with 10 mL water, neutralized with solid Na_2CO_3 and thoroughly ether-extracted. After drying and evaporation of the solvent at room temperature the residual oily products were v.p.c. analyzed. The results of v.p.c. analyses for a buffered and an unbuffered acetolysis of **6** are presented graphically in fig. 1. Minor components (up to 3–4% each) were not included in fig. 1.

b) *Preparative acetolyses of* **6**. A solution of chloride *exo*-**6** (0.75 g; 2.95 mmoles) in 75 mL anhydrous acetic acid was heated at 90° for 48 hrs. After cooling at room temperature the reaction mixture was poured in 150 mL cold water and neutralized by slow addition of solid Na_2CO_3. The alkaline solution was thoroughly ether-extracted; the ethereal extracts were washed with water up to pH 7 then evaporated *in vacuo* at room temperature. The oily residue (0.8 g; 95% calculated as acetate **10**) was subjected to preparative v.p.c. Two major components of the reaction mixture, **10** and **11**, could be separated in high purity (checked by v.p.c.):

trans-*6-Vinyl-5H-6,7-dihydro-dibenzo*[a, c] *cyclohepten-7-yl-acetate* (**10**) colourless thick oil.

IR spectrum (CS_2; cm^{-1}): 738m, 752vs, 760s, 786vs, 918s, 994m, 1040s, 1230vs, 1745vs, 2857w, 2920w, 2945w, 2978w, 3026w and 3068m.

^1H-NMR and UV-data, see text.

9-Chloromethyl-10-vinyl-9,10-dihydrophenanthrene (**11**) thick oil. Found: C, 80.28; H, 6.23; Cl, 12.82%. Calculated for $C_{17}H_{15}Cl$ C, 80.15; H, 5.93; Cl, 13.92%.

IR spectrum (CS_2; cm^{-1}): 737vs, 755vs, 767vs, 788vs, 920s, 994w, 2858w, 2918w, 2951w, 2976w, 3028w and 3066m.

^1H-NMR- and UV data, see text.

Mass spectrum (m/z); %int.): 89(4.1); 95(8.1); 101(9.4); 102(6.2); 108(5.6); 109(6.3); 152(5.0); 165(12.7); 176(6.4); 177(5.6); 178(22.9); 179(6.7); 189(13.1); 190(11.5); 191(13.9); 192(3.0); 201(5.3); 202(24.8); 203(30.2); 204(15.6); 205(100; M^+-CH_2Cl); 206(17.2); 215(6.7); 217(7.2); 218(9.6); 219(6.1); 254(52.1; M^+); 255(9.9; $M^+ + 1$); 256(16.8; $M^+ + 2$).

The third product of acetolysis, namely trans-*6-vinyl-5H-6,7-dihydro-dibenzo*[a, c]-*cyclohepten-7-yl chloride* (**12**) was isolated by column chromatography on neutral alumina (Pechiney) of a reaction product from an unbuffered acetolysis of *exo*-**6** conducted at 90° for 7.5 hrs (reaction time at which **12** reaches a maximum, see fig. 1). Elution with petroleum ether (b.p. 30–60°C) afforded in first eluates the colourless oily product **12** (about 15% yield).

IR spectrum (CS_2; CCl_4; cm^{-1}): 745s, 761vs, 784s, 791s, 925s, 996m, 1450m, 1478m, 1636w, 2860w, 2928w, 2941m, 3028m and 3068m.

^1H-NMR- and UV data, see text.

The fourth reaction product, *6-vinyl-5H-dibenzo*[a, c]*cycloheptene* (**13**), was isolated by column chromatography on neutral alumina (Pechiney) of a reaction mixture obtained from a buffered acetolysis of *exo*-**6** conducted at 90° for 2.5 hrs (time interval at which **13** reaches a maximum, see fig. 1). Elution with petroleum ether (b.p. 30–60°C) afforded, after two fractions containing **12**, other two fractions containing **13** (about 5%) as a colourless, thick oil;

^{1}H—NMR- and UV data — see text.

Kinetic determinations

The kinetic determinations in acetolysis of *exo*-**6** were performed titrimetrically. The formed HCl was determined, after addition of a known excess of 0.05 M NaOAc solution (in acetic acid), through titration with 0.05M $HClO_4$ in acetic acid solution using crystal violet as indicator. Concentration of *exo*-**6** was 7.8×10^{-3} M.

ACKNOWLEDGEMENTS. The authors express their thanks to dr. M. Gheorghiu for registration of mass spectra.

REFERENCES

[1] Part XIX : E. Ciorănescu, A Voicu and M. Elian, *Rev. Roumaine Chim.*, **34**, 87 (1989).

[2] See preliminary note : M. Banciu, M. Elian, Phan Le Thuy, L. Stănescu and E. Ciorănescu, *Bull. Inst. Polytechn. "Gh. Gh. Dej" — Bucharest*, **XLIII** (4), 97 (1981).

[3] E. Dragu, M. Banciu, C. Drăghici, M. Elian and E. Ciorănescu, *Rev. Roumaine Chim.*, **21**, 1497 (1976).

[4] M. Banciu, Phan Le Thuy, M. Elian, C. Drăghici and E. Ciorănescu, *Rev. Roumaine Chim.*, **26**, 1115 (1981).

[5] a) H. G. Richey, in "Carbonium Ions", vol. 3, G. A. Olah and P.v.R. Schleyer (editors), J. Wiley, Interscience, New York, 1972, p. 1201 ; b) K. B. Wiberg, B. A. Hess and A. J. Ashe, *ibid.*, p. 1295 ; c) P. Vogel, "Carbocation Chemistry", Elsevier, New York, 1985 ; d) J. S. Staral and J. D. Roberts, *J. Amer. Chem. Soc.*, **100**, 8018 (1978) ; e) M. Saunders and H. U. Siehl, *J. Amer. Chem. Soc.*, **102**, 6868 (1980) ; f) W. J. Brittian, M. E. Squillacote and J. D. Robert, *J. Amer. Chem. Soc.*, **106**, 7280 (1984) ; g) J. C. Schultz, F. A. Houle and J. L. Beauchamp, *J. Amer. Chem. Soc.*, **106**, 7336 (1984) ; h) M. J. S. Dewar and C. H. Reynolds, *J. Amer. Chem. Soc.*, **106**, 6388 (1984) ; i) D. Cremer, E. Kraka, T. S. Lee and R.F.W. Bader, *J. Amer. Chem. Soc.*, **105**, 5069 (1983) ; j) M. L. McKee, *J. Phys. Chem.*, **90**, 4908 (1986).

[6] H. Lettré, *Angew. Chem.*, **59**, 219 (1947) ; b) J. W. Cook, G. T. Dickson and J. D. Loudon, *J. Chem. Soc.*, **1947**, 746.

[7] F. Bell, *J. Chem. Soc.*, **1952**, 1527 ; D. C. Iffland and H. Siegel, *J. Amer. Chem. Soc.*, **80**, 1947 (1958) ; A. C. Cope and R. D. Smith, *J. Amer. Chem. Soc.*, **78**, 1012 (1956).

[8] R. A. Moss, "Steric Selectivity in the Addition of Carbenes to Olefins", in "Selective Organic Transformations", B. S. Thyagarayan (editor), vol. 1, Wiley, Interscience, New York, 1970, p. 35.

[9] a) K. Bieman and J. Seibl, *J. Amer. Chem. Soc.*, **81**, 3149 (1959) ; b) K. Bieman, "Mass Spectrometry", McGraw-Hill Book, New York, 1962, p. 142 ; c) E. Ciorănescu, M. Banciu, R. Jelescu, M. Rentzea, M. Elian and C. D. Nenitzescu, *Rev. Roumaine Chim.*, **14**, 911 (1969).

[10] R. T. Blickenstoff and F. C. Chang, *J. Amer. Chem. Soc.*, **80**, 2726 (1958).

[11] a) G. H. Beaven, G. R. Bird, D. M. Hall, E. A. Johnson, J. E. Ladbury M. S. Lesslie and E. E. Turner, *J. Chem. Soc.*, **1955**, 2708 ; b) E. Ciorănescu, M. Banciu, M. Elian, A. Bucur and C. D. Nenitzescu, *Liebigs Annal. Chem.*, **739**, 121 (1970) ; c) M. Banciu, Phan Le Thuy and L. Stănescu, *Rev. Roumaine Chim.*, **24**, 957 (1979).

[12] M. Elian, Ph. Dr. Thesis, Centre of Organic Chemistry, ICECHIM — Bucharest, 1973.

[13] M. C. Caserio, W. H. Graham and J. D. Roberts, *Tetrahedron*, **11**, 171 (1960).

Revue Roumaine de Chimie, **35**, *3*, 323–338 (1990)

REACTIONS OF PYRYLIUM SALTS WITH NUCLEOPHILES. XV[1]

STEREOISOMERS OF POLYARYLPYRIDINIUM SALTS AND THEIR INTERCONVERSION*, **

CORNELIA UNCUŢA,[a] FILIP CHIRALEU,[a] MIRCEA D. GHEORGHIU[b] and ALEXANDRU T. BALABAN[b]
[a]Centre of Organic Chemistry, Spl. Independenţei 202 B, 78100 Bucharest, Romania
[b]Polytechnic Institute, Organic Chemistry Department, Spl. Independenţei 313, 77206 Bucharest, Romania

Received September 16, 1989

From 2-aryl-4,6-dimethyl- or 2,6-diaryl-4-methylpyrylium salts (the aryl groups are phenyl, *o*-chlorophenyl or *o*-tolyl) and *o*, *m*, *p*-anisidines or -toluidines, pyridinium salts **3a–j** and **4a–g** were prepared. The ^{1}H–NMR spectra of the pyridinium salts having two or three adjacent *o*- or *m*-substituted aryl rings present evidence for the existence of stereoisomerism based on hindered rotation. Assignments were made on the basis of shifts induced by Eu(fod)$_3$ and of the relative peak intensities; there are two diastereoisomers, both chiral, for each such 1,2-diarylpyridinium salts, and three diastereoisomers (one chiral, two achiral) for the 1,2,6-triarylpyridinium salts. By DNMR it wasfound that the interconversion barrier $\Delta G^{\neq}$ for the 1,2-diarylpyridinium compounds is 21–22 kcal/mol.

LITERATURE DATA ON STEREOISOMERISM OF POLYARYLBENZENES AND HETEROCYCLIC ANALOGUES

Both static and dynamic stereochemistry of polyaryl systems advanced during the last years. [2] The stereoisomerism arising from hindered rotation about the bonds between a central ring (*C*-ring) and substituted peripheral rings (*P*-ring) lacking local C_2 symmetry was thoroughly investigated by Gust and coworkers beginning with 1977, for hexaarylbenzenes, [3] pentaarylbenzenes,[4] pentaarylpyridines [5] and pentaarylpyrroles. [6]

Isomer enumeration takes into account a geometry of the ground state with peripheral rings perpendicular to the central ring and simple symmetry criteria for ascribing chirality. Actually, this is an ideal geometry, which cannot be distinguished experimentally at present from a geometry with peripheral rings twisted with a certain dihedral angle and flipping easily around the bond joining them to the central ring.

---

* Dedicated to the memory of Mihai Elian.

** Presented in part at the 4th IUPAC International Conference on Organic Synthesis, Moscow, 1986.

An isomerization mode (denoted by M_1) [3] involving uncorrelated rotation of one P-ring at a time by ~ 180° was found satisfactory for explaining the interconversion of isomers in all above systems. Diastereoisomerisations were experimentally observed either by DNMR or by classical kinetic methods for long-lived diastereoisomers which could be separated (generally by chromatographic methods).

Pertinent information about the mode of internal rotation responsible for the interconversion of rotamers was obtained from examination of 1-(2-methoxyphenyl)-2-(2-methylphenyl)-3,6-bis(3-methylphenyl)-4,5-diphenylbenzene. [3b] Two dynamic processes were observed:

1) a low-temperature process (30—35 °C) freezing the rotation of *m*-Me bearing rings, with an activation energy of 17.7 kcal/mol; at the upper limit of this range, two residual diastereoisomers exist, with *o*-substituents in *cis* or *trans* relative position, which can be separated by column chromatography on silicagel;

2) a high-temperature process (up to 150 °C), interconverting the residual *cis*, *trans* isomers, with an activation energy of 32.6 kcal/mol.

These experimental data may be explained by an M_1 rearrangement mode, wherein only one aryl ring at a time rotates with about 180°. Any other rearrangement mode among those theoretically possible for the hexaphenylbenzene skeleton does not fit the experimental data.

Among the factors influencing the magnitude of the rotational barriers, the steric requirements of substituents in *ortho* positions of the rotating rings were found to be important. Conversely, the size of the substituents in *meta* positions makes only a small contribution to the magnitude of the barrier. The rotational barrier of two adjacent phenyl rings possessing an *o*-methyl group in hexaarylbenzenes has been shown to be ca. 38 kcal/mol, whereas with a neighbouring *m*-methyl or -methoxy group the value is ca. 16 kcal/mol.

Buttressing effects of substituents X in any position on the central ring are operating in the conformational dynamics of polyarylbenzenes. [4] The steric interaction is of "side by side" type, similar to that observed between 1,3-axial groups in cyclohexanes, as indicated by the linear correlation between the magnitude of the rotational barrier and the "*A* value" of the substituent X. An interesting suggestion was made to use this linear relationship for calculating "*A* values" for substituents lacking such values from equilibrium data of substituted cyclohexanes. For instance, using this relationship, it appears that the lone pair on nitrogen has a smaller steric requirement than a hydrogen atom. [5]

The size of the central ring was found to be of major importance for the rotational barriers of the peripheral rings. Compared to hexaarylbenzenes, pentaarylpyrroles have lower rotational barriers with ~18 kcal/mol. Most of this difference may be associated to the larger angle between adjacent rings (approximately 126° instead of 120°), but some other factors such as bond lengths, ring deformability, etc. are also operating. [6]

Rotational barriers for simpler polyaryl systems such as 2,2″-dimethyl-*o*-terphenyls,[7] methyl-substitued quinquiphenyl hydrocarbons, [8] and *peri*-arylnaphthalenes [9] were determined.

In these simple models, an attempt was made to ascribe ^1H-NMR signals to individual isomers. The *cis*, *trans* isomers of 1,8-di-*o*-tolylnaphthalene, separated by column chromatography, presented different ^1H-NMR patterns for the aromatic hydrogens in the *o*-tolyl substituents, along with the expected different chemical shifts for the *o*-methyl groups. From the analysis of these NMR patterns, the upfield *o*-Me signal was assigned to the *trans* isomer, and the downfield *o*-Me signal to the *cis* isomer.[9]

The *cis*, *trans* isomers of 1,2-di-*o*-tolylbenzene, with an interconversion barrier $\Delta G^{\neq}_{T_c} = 14.8$ kcal/mol ($T_c = 9$ °C), were assigned the following chemical shift values for the *o*-methyl signals : $\delta = 2.1$ ppm for the *cis*-isomer, and $\delta = 2.0$ ppm for the *trans*-isomer,[7] taking into account the previously mentioned assignment.[9]

Conformational studies of 1,2-diaryl-and 1,2-hetarylbenzenes whose (het)aryl groups had *meta*-substituents revealed rotational barriers of ~ 10 kcal/mol for 1,2-di-*m*-tolylbenzene and unsuccessful attempts to determine the low intramolecular rotational barriers of 1,2-bis(6-methylpyridyl-2)benzene.[10]

Assigning the structure to individual isomers for polyaryl-compounds presenting more than two diastereoisomers is a difficult task. It was successfully solved for hexakis(2-methyl/methoxy/phenyl)- and hexakis-(3-methyl/methoxy/phenyl)benzenes as will be presented in detail below.

For *ortho*-substituted systems, the study of rotational isomerism in hexakis(2-methoxyphenyl)benzene and hexakis(2-methylphenyl)benzene revealed high rotational barriers (> 30 kcal/mol).[11] From the nine theoretically predicted rotamers (seven achiral and one *d*, *l* pair), seven have been separated by preparative HPLC on silica. A global assignment of the ^1H-NMR patterns to these individual isomers was made, according to the following route :[11]

a) the pattern expected for each rotamer in the methoxy (methyl) region was easily deduced from symmetry considerations, resulting in four pairwise interchangeable assignments (obviously, the *d*, *l* pair has a single NMR pattern) ; this leads to $2^4 = 16$ global assignments to the eight predicted rotamers ;

b) the next step involved a comparison between experimental equilibrium populations of isomers and theoretically predicted populations of rotamers. The equilibrium model takes into account for each rotamer the free enthalpy contribution associated with its rotational symmetry, the mixing entropy of the pair of enantiomeric rotamers, and the free enthalpy contribution associated with interactions within each pair of *P*-rings in an *ortho* position on the *C* ring for relative *cis*, *trans* position of the substituents. A satisfactory fit between experimental and theoretical isomer population values was obtained for two global assignments which could be interchanged assuming *cis* interactions as being either repulsive or attractive. The incremental free enthalpy contributions ΔG^{cis}, ΔG^{trans} are supposed to be rotamer independent ; for the repulsive or attractive interaction between neighbouring *o*-methoxy groups, the difference $\Delta G^{cis} - \Delta G^{trans}$ was found to be $+ 0.4$ and -0.4 kcal/mol, respectively, while the corresponding values for neighbouring *o*-methyl groups are $+(-)$ 0.84 kcal/mol ;

c) the final choice between these two global assignments succeeded for hexakis(2-methoxyphenyl)benzene using chromatographic data. The capacity factors were correlated in a Hammett-like equation with a factor accounting for the substituent distribution on both faces of the *C*-ring. The calculated capacity factors gave a satisfactory fit with the experimental values only for the one global assignment assuming ***repulsive cis***-interactions. For hexakis(2-methylphenyl)-benzene, both global assignments gave satisfactory fit with calculated capacity, without allowing a definite choice.

For *meta*-substituted systems, the stereochemistry of hexakis(3-methoxyphenyl)benzene and hexakis(3-methylphenyl)benzene was investigated.[12] A rotational barrier of ~ 15.6 kcal/mol was found, in satisfactory agreement with 16.4 kcal/mol reported [3a] for 1,2-bis(3-methylphenyl)-3,4,5,6-tetraphenylbenzene. This is a confirmation of the fact that the rotational barrier does not depend on the nature of the substituent în *meta* position and is basically determined by the interaction between the hydrogen atoms in *ortho* positions on neighbouring aryl rings.

The ^1H-NMR patterns at 270 and 500 MHz of the methoxy (methyl) groups and of the aromatic proton in position 5 present peculiar features with could not be explained by either preferential isomerism (most unlikely, if compared to the *o*-substituted analogues) or by a residual isomerism (under any mode of internal rotation), even taking into account accidental isochronism. To explain the experimental data, a chemical shift model was derived based on the hypothesis that the *meta* substituents do not disturb the geometry of the hexaphenylbenzene skeleton nor the statistical population of the isomers. The through-space influence of the substituents, such as magnetic anisotropy and electric field effects, are supposed to affect the chemical shift of a certain probe group. Only the incremental contribution of *meta*-substituents on *P*-rings in the *o*-position to the one bearing the probe was found to be significant. The probabilities for a given probe to have both its neighbouring *meta* substituents in ***cis*** position (***cis — cis*** interaction), to have one in ***cis*** and the other in ***trans*** position (***cis — trans*** interaction) and to have both substituents in ***trans*** position (***trans — trans*** interaction) are 1/4, 2/4 and 1/4, respectively, explaining the observed NMR pattern.

As a concluding remark regarding these literature data, rotamer interconversion in polyaryl compounds can be successfully explained using the M_1 isomerization mode. However, the static stereochemistry of these systems is straightforward only in enumeration of isomers. Assigning experimental data (such as NMR spectra) to individual isomers is rather tedious and the procedures used for it still escape generalization.

PREPARATION OF DI- AND TRIARYLPYRIDINIUM SALTS

Pyridinium perchlorates **3** and **4** with two or three adjacent aryl substituents, one of which is linked to the nitrogen heteroatom, were prepared from alkyl-substituted 2-aryl- or 2,6-diarylpyrylium salts (**1** and **2**, respectively) and substituted anilines (*o*, *m*, *p*-toluidines and -anisidines). Tables 1 and 4 will present all the structures thus obtained with their notation.

The reaction was effected by heating a mixture of pyrylium perchlorate with excess of substituted aniline (1 : 3 molar ratio) dissolved in isopropanol or ethanol, at the reflux of the solvent. The pyridinium perchlorates precipitated from the solution on cooling. The crude products were recrystallized from isopropanol or acetic acid/ethyl ether (see Experimental part). The salts presented definite melting points, and had satisfactory solubility in $CDCl_3$ for ^1H-NMR spectra with $Eu(fod)_3$.

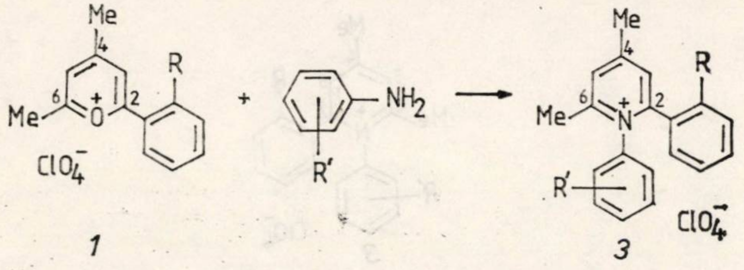

R= H, Cl, Me R'= o-, m-, p-Me ; o-, m-, p- OMe

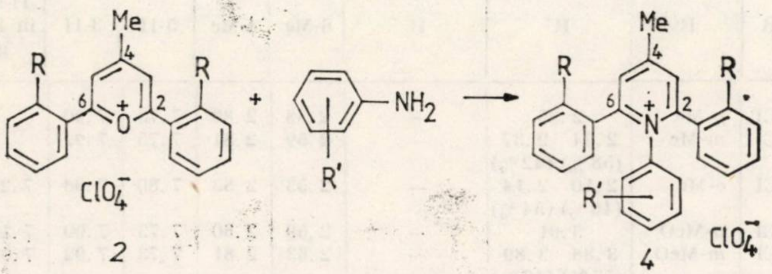

R= H, Me R'= H, o-, m-, p-OMe

STEREOISOMERS OF 1,2-DIARYLPYRIDINIUM SALTS

In Table 1 are displayed the ^1H-NMR data of the 1,2-diaryl-pyridinium perchlorates **3** prepared from R'-substituted anilines and 2-aryl-4,6-dimethylpyrylium perchlorates, where the aryl is an *o*-chlorophenyl or an *o*-tolyl group, and the R' substituents are *o*, *m*, *p*-methyl or -methoxy.

The following discussion focuses on the signals corresponding to R, R' substituents of adjacent phenyl rings. As illustrated in scheme 1, two diastereomeric *cis*, *trans* structures (**A**, **B**) can be written for pyridinium cations possessing an *ortho*-R' substituent (the same holds true for a *meta*-R' substituent), but only one structure for the *para*-R' substituted cation **C**. * Both **A** and **B** are chiral. The R (R') groups in *cis*, *trans* diaste-

---

* We use capital letters **A** — **F** for conformers of systems **3** and **4**. Small letters **a** — **j** denote different constitutions due to different substituents. In all schemes and formulas henceforth, all rings are aromatic.

Table 1

^{1}H—NMR Data for 1,2-diaryl-4,6-dimethylpyridinium perchlorates **3** in trifluoroacetic acid (TFA) unless otherwise stated. All peaks are singlets except those with an asterisk which are multiplets. Figures in brackets indicate populations of diastereoisomers

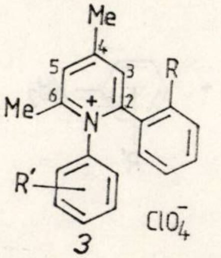

3

Structure			Chemical shifts (δ, ppm)						
Comp.	R	R′	R′	R	6-Me	4-Me	5-H	3-H	H-aromatic in 1-2-diaryl groups
3a	Cl	*p*-Me	2.35	—	2.58	2.80	7.73	7.90	7.30
3b	Cl	*m*-Me	2.34 2.37 (58%) (42%)	—	2.59	2.81	7.75	7.92	7.34
3e	Cl	*o*-Me	2.10 2.14 (46%) (54%)	—	2.53	2.83	7.80	7.98	7.25—7.38*
3d	Cl	*p*-MeO	3.91	—	2.59	2.80	7.73	7.90	7.12—7.33*
3e	Cl	*m*-MeO	3.88 3.89 (57%) (43%)	—	2.63	2.81	7.73	7.92	7.02—7.35*
3f	Cl	*o*-MeO	3.76 3.93 (27%) (73%)	—	2.53	2.79	7.73	7.93	7.00—7.48*
3g	Me	*p*-MeO	3.92	2.19	2.58	2.79	7.73	7.87	7.10—7.21*
3h	Me	*m*-MeO	3.88 3.92 (52%) (48%)	2.19 2.25 (52%) (48%)	2.62	2.81	7.74	7.89	6.87—7.23*
3i	Me	*o*-MeO	3.81 3.98 (40%) (60%)	2.25	2.55	2.82	7.79	7.95	7.08—7.27*
	,,	,,[a]	3.73 3.90 (40%) (60%)	2.15 2.18 (40%) (60%)	2.48	2.76	7.65	7.83	6.90—7.32*
3j	H	*o*-MeO	3.87	—	2.52	2.78	7.76	7.83	6.95—7.32*

[a] In $CDCl_3$ + TFA.

reomers **A**, **B**, which are diastereotopic by external comparison, are expected to be anisochronous in the NMR spectra.

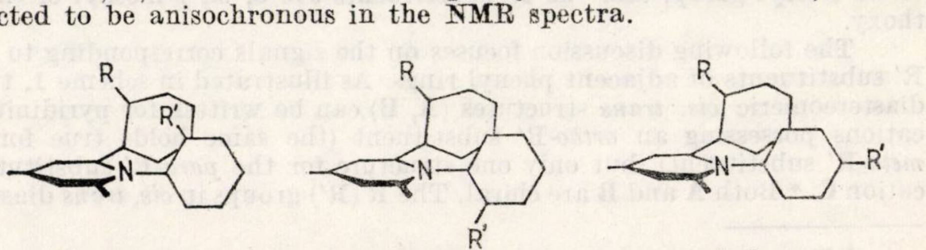

cis(A) trans(B) (C)

Scheme 1. — Structures of compounds 3.

The data in Table 1 entirely support this picture. Indeed, compounds **3a**, **3d** and **3g** with *p*-R′ substituents present one signal for R′ = Me or MeO groups, while compounds **3b**, **3e**, **3h** and **3c**, **3f**, **3i** with *m*- and *o*-R′ substituents, respectively, exhibit two signals for R′ = Me or MeO groups as well as two signals for R = Me groups (in **3h** and **3i**). The signals of R = Me group in compound **3i** are accidentally isochronous in TFA but become anisochronous in $CDCl_3$ + TFA. Compound **3j** with an unsubstituted 2-phenyl ring was included in Table 1 as reference for the position of the methoxy signal.

The proportions of the two *cis*, *trans*-diastereoisomers, indicated in brackets in Table 1, are those calculated from the height of the individual peaks for the diastereotopic R, R′ groups.

The *cis-trans* diastereoisomerization of 1,2-diaryl-substituted pyridinium cations was investigated by DNMR. Variable temperature ^1H—NMR spectra were recorded for compounds **3f** and **3i** using DMSO-d_6 as solvent. Chemical shift differences ($\Delta\nu$), isomer populations (p_a, p_b), coalescence temperature (T_c) and activation free energies ($\Delta G^{\neq}_{T_c}$) are presented in Table 2. Owing to the different solvents, isomer populations differ quantitatively (but not qualitatively, i.e. major/minor isomers) in Tables 1 and 2. The same is true for Tables 1 and 3. Approximate equations for exchange between two unequally populated singlets were used for calculation[13] of $\Delta G^{\neq}_{T_c}$ values at the coalescence temperature.

Table 2

Free energies of aetivation for 1,2-diaryl-substituted pyridinium cations **3**
(solvent : DMSO-d_6)

Compd.	$\Delta\nu$ (Hz)	p_a^*	p_b	T_c (°C)	$\Delta G^{\neq}_{T_c}(a \rightarrow b)$	$\Delta G^{\neq}_{T_c}(b \rightarrow a)$
3f	8.75	0.60	0.40	133±2	22.0±0.3	21.7±0.2
3i	11.0	0.53	0.47	125±2	21.1±0.3	21.0±0.2

* downfield signal.

On recording the ^1H—NMR spectra of the pyridinium perchlorate **3i** in the presence of $Eu(fod)_3$ using $CDCl_3$ as solvent, a complete separation of the signals belonging to the two isomeric species was achieved, except for the aromatic protons (see Fig. 1). As the mixture consisted of unequal amounts of isomers, the signals belonging to each isomer could be easily recognized.

The induced shift values $\Delta\delta$ are very small, the largest values observed being only 30—40 Hz at a value of 0.8 of the molar ratio ρ between LSR and pyridinium salt. However, the $\Delta\delta$ vs. ρ curves present a fairly linear portion in the range $\rho = 0.1—0.5$, allowing the calculation of molar induced shift (MIS) values. Table 3 presents the MIS values for the two diastereoisomers of pyridinium perchlorate **3i** denoted for the moment as major and minor isomers (55 % and 45% in the mixture).

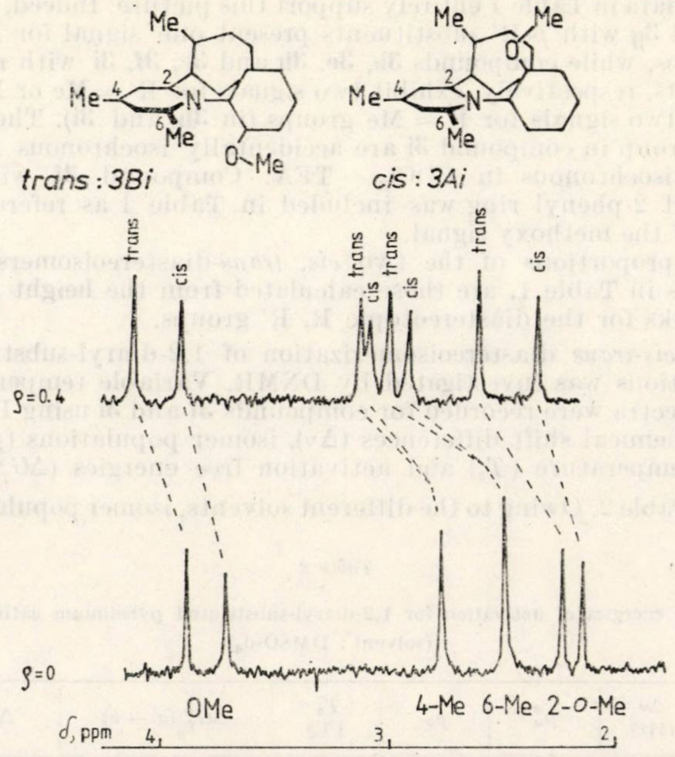

Fig. 1. — The ^1H—NMR spectrum of the pyridinium perchlorate **3i** *(cis + trans)* in $CDCl_3$ (bottom), and the spectrum of the same probe with added $Eu(fod)_3$ at molar ratio (LSR/3i) : ρ = 0.4 (top).

Table 3

Molar induced shift (MIS) values (ppm) of the methyl protons in *cis, trans*-diastereoisomers of the pyridinium perchlorate 3i in $CDCl_3$

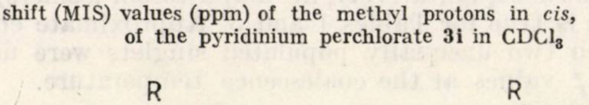

cis : 3Ai trans : 3Bi

Group / Isomer 3i	R′ (OMe)	R (Me)	MIS difference ΔMIS (R − R′)	6-Me	4-Me
major (55%)	0.48	0.77	+0.29	1.02	0.76
minor (45%)	0.44	0.41	−0.03	0.89	0.66

The data in Table 3 were used for attempting the assignment of the signals to individual isomers. Indeed, in the minor isomer **3i**, the *o*-methoxy and *o*-methyl groups present fairly similar MIS values, suggesting spatial proximity relative to the plane of the pyridinium ring. On the other hand, in the major isomer significantly different MIS values were observed for the same groups.

The complexation ability of pyridinium salts with various shift reagents was reported in the literature. [14,15] It seems to be firmly established by now [15] that the anion mediates the association of the LSR with the organic cation. The complexation site of the pyridinium cation is most probably located in the proximity of the positive nitrogen leading to maximal deshielding in the α-positions of the pyridinium ring. Ion pair complexes of this type result in induced shifts that are primarily dipolar in origin with no significant contact contribution, enabling calculation of the geometry of the organic cations.

Three of the MIS values in Table 3 for R, R′ groups are in the range 0.4—0.5 ppm, whereas the fourth one is almost twice as large. In can be assumed that the *trans*-isomer forms complexes with almost equal likelihood on both faces of the pyridinium ring, while the *cis*-isomer would be expected to lead to a preference for complexation on the less hindered face, devoid of R, R′-substituents. As a consequence, it would be expected to obtain for the *cis*-isomer two small MIS values corresponding to large distances separating the methyl groups and the europium atom on different sides, while for the *trans*-isomer only one such MIS is expected, with the other MIS value being considerably larger.

According to these observations, the major isomer is assigned ***trans*** conformation (structure **3Bi**) and the minor isomer is the *cis* conformation (structure **3Ai**). The lower amount of the *cis*-isomer can be rationalized on the basis of its higher energy due to steric hindrance.

Our results seem to fit the previously mentioned representation for the interaction between LSR and pyridinium cations. It is obvious that the oxygen atom in a methoxy group is not able to compete with the anion for the LSR. Indeed, the methoxy group protons in **3i** present smaller induced shifts relative to all methyl groups listed in Table 3; on the other hand, larger induced shifts are observed for α-methyl protons. Therefore, it seems reasonable to assume that in our case an ion pair complex mechanism operates. The steric congestion at the pyridinium nitrogen explains the poor complexation ability of these cations with the LSR, and most probably plays an important role in the orientation of the principal magnetic axis of the paramagnetic atom.

Taking into account the previous assignments, one may infer the effect of the *o*-methyl substituent on the chemical shift of the *o*-methoxy group (see Table 1). In compound **3j** possessing in the 2-position an unsubstituted phenyl ring and therefore devoid of stereoisomers, the methoxy group singlet appears at 3.87 ppm (in TFA). Comparing this value with the chemical shifts of the methoxy groups in *cis*-**3i** and *trans*-**3i** in the same solvent, an upfield shift of 0.06 ppm for the *cis*-**3i** and a downfield shift of 0.11 ppm for the *trans*-**3i** is observed. This effect will be taken into account for assigning conformations in 1,2,6-triarylpyridinium cations.

Reasoning on the same line, the 1,2,6-triaryl-substituted pyridinium cations **4**, with 2,6-aryls being *o*-tolyl groups and possessing an *ortho*-R′ substituent (R′ = OMe) in the 1-aryl group, may exist as three stereoisomers denoted by **D**, **E**, **F** in the scheme 2 (again the picture is the same for a cation with a *meta*-R′ substituted 1-aryl group); **D** and **F** are achiral, **E** is chiral. The notation *cis-cis*, etc. indicates relative stereochemistry for the pair 1,2-Ar_2 followed by the pair 1,6-Ar_2.

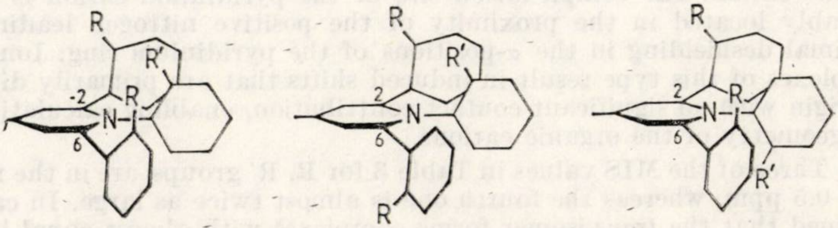

cis, cis (D) *cis, trans (E)* *trans, trans (F)*

Scheme 2. — Stereoisomers of compounds **4**.

Should R′ become a hydrogen atom or a *para*-substituent, structures **D** and **F** would become degenerate and then only two stereoisomers may exist, namely **D** ≡ **F** (*cis*) and **E** (*trans*) involving the conformations of 2,6-Ar_2 groups. From symmetry considerations, R groups are enantiotopic in **D** and **F**, but diastereotopic in **E** for R′ ≠ H; for R′ = H, R groups are enantiotopic in **D** (≡ **F**) but equivalent (homotopic) in **E**.

Table 4 presents the ^1H-NMR data for the 1,2,6-triarylpyridinium cations which were investigated; compounds **4a**, **4b** and **4c**, which are not expected to exhibit diastereoisomerism, are included as reference.

Compound **4d** (N-phenyl-2,6-di-*o*-tolylpyridinium perchlorate) presents two singlets for the *o*-methyl groups, indicating two stereoisomers in unequal amounts (60 : 40). Recording the spectra of **4d** in the presence of $Eu(fod)_3$ gave additional proof for the existence of two diastereoisomers; the signal of the 4-Me substituent was split into two singlets indicating the same proportion of the isomers as above. The MIS values for methyl groups in **4d** are presented in Table 5; the isomers are denoted as major (60%) and minor (40%).

An attempt was made to differentiate the isomers by using a chiral shift reagent instead of $Eu(fod)_3$ (*cis*-**4d** is achiral, but since *trans*-**4d** is chiral, a diastereomeric complexation interaction was expected). Unfortunately, no complexation at all of **4d** with $Eu(hfcamph)_3$ occurred.

Compound **4e** with a *para*-substituted 1-aryl group should present similar stereochemical characteristics as **4d**, but in this case only one signal was observed for *o*-methyl groups (in $CDCl_3$ + TFA), obviously due to accidental isochronism.

Compounds **4f** and **4g**, with *m*-methoxy and *o*-methoxy substituents in the central (1-aryl) ring, presented ^1H-NMR signals in accordance

Table 4

^{1}H–NMR Data for 1,2,6-triarylpyridinium perchlorates **4**. All peaks are singlets except those marked with an asterisk which are multiplets. Figures in brackets indicate populations of diastereoisomers

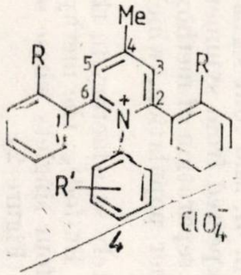

4

Comp.	R	R′	Solv.	R	R′	4-Me	3,5 - H_2	H-aromatic in 1, 2, 6-aryl groups
4a	H	*p*-MeO	TFA	—	3.79	2.86	7.95	6.67–7.36*
4b	H	*m*-MeO	TFA	—	3.69	2.86	7.93	6.83–7.33*
4e	H	*o*-MeO	TFA	—	3.68	2.87	7.94	6.70–7.37*
4d	Me	H	$CDCl_3$	2.22; 2.28 (60%) (40%)	—	2.86	7.83	7.18*
4e	Me	*p*-MeO	$CDCl_3$ + TFA	2.19	3.62	2.83	7.83	7.23*
4f	Me	*m*-MeO	$CDCl_3$	2.22; 2.24; 2.27; 2.34	3.57 3.60 3.63 (24%) (38%) (38%)	2.82	7.78	7.17*
4g	Me	*o*-MeO	$CDCl_3$	2.23; 2.25; 2.31; 2.39	3.54 3.68 3.84 (35%) (43%) (22%)	2.79 2.84 2.90 (35%) (43%) (22%)	7.71; 7.77; 7.83	7.12*
			CD_2Cl_2	2.20; 2.27; 2.32	3.48 3.61 3.78 (25%) (45%) (30%)	2.77 2.79 2.82	7.71; 7.76; 7.77	7.12*
			TFA	2.28; 2.38	3.58 3.71 3.88 (30%) (45%) (25%)	2.85	7.88	7.15*

Table 5

MIS Values (ppm) for the methyl protons in diastereoisomers of **4d**

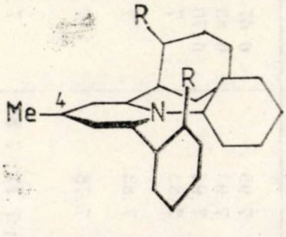

cis - 4d

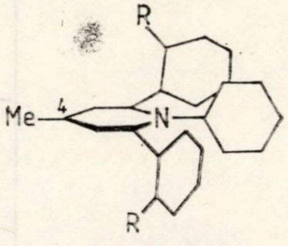

trans - 4d

4d Isomer \ Group	R (Me)	4-Me
major (60%)	0.45	0.76
minor (40%)	0.67	0.80

with the existence of three diastereoisomers, namely three signals for the methoxy group in both **4f** and **4g**, three signals for the 4-Me group in **4g** (in $CDCl_3$ and CD_2Cl_2) and a broad singlet in **4f**, and four signals for the methyl groups of *o*-tolyl substituents (as expected from symmetry considerations) in both **4f** and **4g** (in $CDCl_3$). The separation of methoxy signals was sufficiently large to measure the isomer population, which is indicated in brackets in Table 4.

The signal separation became completely satisfactory in the spectra of **4g** recorded in CD_2Cl_2 in the presence of $Eu(fod)_3$; the methyl protons in 2,6-*o*-tolyl groups present the expected four singlets whose separation was sufficient for intensity measurements (Figure 2).

The assignment of the signals to diastereoisomers of **4g** is straightforward based on the following data : the highest intensity methoxy signal in CD_2Cl_2 at $\delta = 3.61$ ppm belongs to neither the *cis*, *cis* nor the *trans*, *trans* isomer, since these last isomers are expected to give one signal of double intensity for the two isochronous methyl groups, and no such signal appears in the methyl groups region. Consequently, the methoxy signal at $\delta = 3.61$ ppm along with the corresponding two singlets of equal intensity at $\delta = 2.20$ and $\delta = 2.32$ ppm were assigned to the *cis*, *trans* isomer.

The assignment of the remaining signals to *cis*, *cis* and *trans*, *trans* isomers takes into account the previously mentioned effect of the methyl group on the methoxy singlet for *cis* and *trans* relative position. The downfield-shifted methoxy signal at $\delta = 3.78$ and the signal of double intensity at $\delta = 2.27$ were attributed to the *trans*, *trans* isomer **F**; the remaining upfield shifted methoxy signal at $\delta = 3.48$ and the signal at $\delta = 2.20$ were attributed to the *cis*, *cis* isomer **D**.

The experimental chemical shifts of methoxy groups in **4g D**, **E**, and **F** measured in TFA (see Table 4) are in good agreement with calculated values starting from the chemical shift of the probe methoxy group in 1-*o*-anisyl-1,2-diphenylpyridinium cation **4c** (3.68 ppm in TFA) and using the previously determined increments for an *o*-methyl group in *cis*-posi-

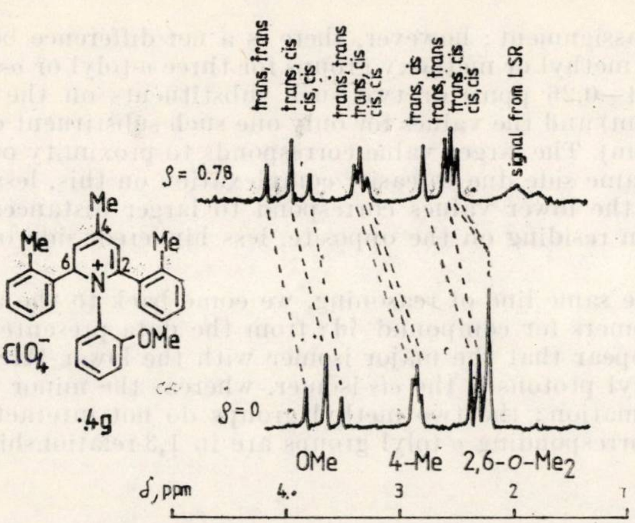

Fig. 2. — The ^1H-NMR spectrum of pyridinium perchlorate **4g** (*cis, cis* **D** + *cis, trans* **E** + *trans, trans* **F**) in CD_2Cl_2(bottom) and the spectrum of the same probe with added $Eu(fod)_3$ at molar ratio (LSR/**4g**) : ρ = 0.78 (top).

tion (Δδ = − 0.06 ppm) and in *trans*-position (Δδ = + 0.11 ppm) in the adjacent 2- and 6-*o*-tolyl rings. This is demonstrated by the data presented in Table 6.

Table 6

Experimental and calculated chemical shifts (δ, ppm) of methoxy protons in stereoisomers of **4gD**, **E**, and **F** in TFA

Stereoisomer	*cis-cis*	*trans-trans*	*cis-trans*
Experimental	3.58	3.88	3.71
Calculated	3.68−2×0.06=3.56	3.68+2×0.11=3.90	3.68−0.06+0.11=3.73

In scheme 3 are given the MIS values for the methyl groups in stereoisomers of **4g**. The values are too small to be significant as reliable

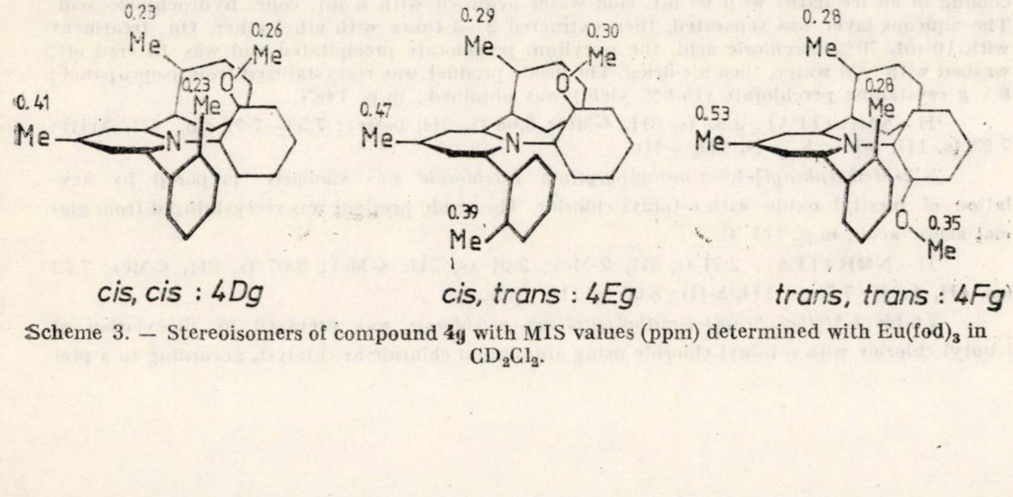

cis, cis : 4Dg *cis, trans* : 4Eg *trans, trans* : 4Fg

Scheme 3. — Stereoisomers of compound **4g** with MIS values (ppm) determined with $Eu(fod)_3$ in CD_2Cl_2.

proof for the assignment; however, there is a net difference between the MIS values of methyl or methoxy groups for three *o*-tolyl or *o*-anisyl substituents (0.23—0.26 ppm) or two such substituents on the same side (0.28—0.30 ppm) and the values for only one such substituent on one side (0.35—0.39 ppm). The larger value corresponds to proximity of europium atom on the same side due to easier complexation on this, less hindered, side, whereas the lower values correspond to larger distances from the europium atom residing on the opposite, less hindered, side of the pyridinium ring.

Using the same line of reasoning, we come back to the assignment of diastereoisomers for compound **4d**; from the data presented in Table 5, it would appear that the major isomer with the lower MIS value for the *ortho*-methyl protons is the *cis*-isomer, whereas the minor isomer has a *trans*-conformation; the two methyl groups do not interact sterically because the corresponding *o*-tolyl groups are in 1,3-relationship.

EXPERIMENTAL PART

^{1}H—NMR Spectra were recorded with 60 MHz Varian A-60 A and Varian EM-360L instruments. The variable temperature ^{1}H—NMR spectra were recorded using the variable temperature unit of the Varian A-60 A instrument. For temperature determinations, the temperature-dependent chemical shift differences of protons in ethyleneglycol were used; the precision in temperature determination was estimated as ± 2°.

The ^{1}H—NMR chemical shifts of the 1,2-di- and 1,2,6-triarylpyridinium salts **3** and **4** are presented in Tables 1 and 4, respectively. All new compounds gave satisfactory elemental analysis (% N).

Melting points were determined in open capillary tubes.

Pyrylium salts

2-[2-*Chlorophenyl*]-4,6-*dimethylpyrylium perchlorate*: 16.2 g (0.121 mole) anhydrous aluminum chloride was added under stirring and with external cooling to 53 g (0.303 mole) *o*-chlorobenzoyl chloride, then 12 g (0.122 mole) mesityl oxide was added dropwise maintaining the temperature at 22—25°C. Stirring was continued for two hours at room temperature, then the mixture was left overnight. The mixture was heated under stirring at 50—60° for one hour, cooled to room temperature, diluted with 50 mL ethyl ether and decomposed (with external cooling in an ice bath) with 60 mL cold water acidified with 5 mL conc. hydrochloric acid. The aqueous layer was separated, then extracted 2—3 times with ethyl ether. On treatment with 10 mL 70% perchloric acid, the pyrylium perchlorate precipitated and was filtered off, washed with cold water, then air-dried. The crude product was recrystallized from isopropanol; 6.1 g crystalline perchlorate (15.8% yield) was obtained; m.p. 148°C.

^{1}H—NMR (TFA): 2.92 (s, 3H, 4-Me); 3.08 (s, 3H, 6-Me); 7.53—7.72 (m, 4H, ArH); 7.93 (s, 1H, 5-H); 8.35 (s, 1H, 3-H).

2-[2-*Methylphenyl*]-4,6-*dimethylpyrylium perchlorate* was similarly prepared by acylation of mesityl oxide with *o*-toluyl chloride. The crude product was recrystallized from glacial acetic acid; m.p. 161 °C.

^{1}H—NMR (TFA): 2.71 (s, 3H, 2-Me); 2.91 (s, 3H, 4-Me); 3.07 (s, 3H, 6-Me); 7.53 (m, 4H, ArH); 7.75 (s, 1H, 5-H); 8.03 (s, 1H, 3-H).

2,6-bis[2-*Methylphenyl*]-4-*methylpyrylium perchlorate* was prepared by diacylation of *t*-butyl chloride with *o*-toluyl chloride using aluminium chloride as catalyst, according to a previously described procedure.[16] The crude product was recrystallized from glacial acetic acid; m.p. 177—178° (decomp.).

^1H—NMR (TFA): 2.68 (s, 6H, 2-Me in 2,6-Ar_2); 3.03 (s, 3H, 4-Me); 7.68 (m, 8H, ArH); 8.22 (s, 2H, 3,5-H_2).

Pyridinium salts

Pyridinium salts were prepared according to the following general procedure: to the suspension of pyrylium salt in isopropanol, an excess of aromatic amine was added (1 : 3 molar ratio); a deep-red colour developed instantly. The mixture was heated at the gentle reflux of the solvent for 2—3 hours when the colour of the solution turned into dark brown. The pyridinium salt precipitated on cooling, was filtered off and purified by recrystallization from appropriate solvents (to be indicated below). The pyridinium salts prepared from 4-methyl-2,6-diphenylpyrylium perchlorate required longer reaction time (10—12 hours).

2-[2-*Chlorophenyl*]-1-[4-*methylphenyl*]-4,6-*dimethylpyridinium perchlorate* **3a**, m.p. 206° (from isopropanol).

2-[2-*Chlorophenyl*]-1-[3-*methylphenyl*]-4,6-*dimethylpyridinium perchlorate* **3b**, m.p. 202—203° (from isopropanol).

2-[2-*Chlorophenyl*]-1-[2-*methylphenyl*]-4,6-*dimethylpyridinium perchlorate* **3c**, m.p. 240—241° (from isopropanol).

2-[2-*Chlorophenyl*]-1-[4-*methoxyphenyl*]-4,6-*dimethylpyridinium perchlorate* **3d**, m.p. 215° (decomp.) (from isopropanol).

2-[2-*Chlorophenyl*]-1-[3-*methoxyphenyl*]-4,6-*dimethylpyridinium perchlorate* **3e**, m.p. 209° (decomp). (from isopropanol).

2-[2-*Chlorophenyl*]-1-[2-*methoxyphenyl*]-4,6-*dimethylpyridinium perchlorate* **3f**, m.p. 215—216° (decomp.) (from isopropanol).

1-[4-*Methoxyphenyl*]-2-[2-*methylphenyl*]-4,6-*dimethylpyridinium perchlorate* **3g**, m.p. 208° (from isopropanol).

1-[3-*Methoxyphenyl*]-2-[2-*methylphenyl*]-4,6-*dimethylpyridinium perchlorate* **3h**, m.p. 198° (from isopropanol).

1-[2-*Methoxyphenyl*]-2-[2-*methylphenyl*]-4,6-*dimethylpyridinium perchlorate* **3i**, m.p. 238° (decomp.) (from isopropanol).

1-[2-*Methoxyphenyl*]-4,6-*dimethyl*-2-*phenylpyridinium perchlorate* **3j**, m.p. 179 (from isopropanol).

1-[4-*Methoxyphenyl*]-4-*methyl*-2,6-*diphenylpyridinium perchlorate* **4a**, m.p. 228 (from glacial acetic acid).

1-[3-*Methoxyphenyl*]-4-*methyl*-2,6-*diphenylpyridinium perchlorate* **4b**, m. p. 216—217° (from glacial acetic acid/ether).

1-[2-*Methoxyphenyl*]-4-*methyl*-2,6-*diphenylpyridinium perchlorate* **4c**, m.p. 272—273° (decomp.) (from glacial acetic acid then from isopropanol).

2,6-*bis*-[2-*Methylphenyl*]-4-*methyl*-1-*phenylpyridinium perchlorate* **4d**, m.p. 249—250° (decomp.) (from glacial acetic acid, then from isopropanol/ether).

1-[4-*Methoxyphenyl*]-2,6-*bis*[2-*methylphenyl*]-4-*methylpyridinium perchlorate* **4e**, m.p. 280° (decomp.) (from glacial acetic acid, then isopropanol/ether).

1-[3-*Methoxyphenyl*]-2,6-*bis*[2-*methylphenyl*]-4-*methylpyridinium perchlorate* **4f**, m.p. 187° (from isopropanol).

1-[2-*Methoxyphenyl*]-2,6-*bis*[2-*methylphenyl*]-4-*methylpyridinium perchlorate* **4g**, m.p. 229° (decomp.) (from glacial acetic acid, then from isopropanol).

REFERENCES

[1] Preceding part: *Rev. Roum. Chim.*, **25**, 1505 (1980). Parts XVI—XXII have already appeared: *ibid*, **28**, 699 (1983); **31**, 37 (1986); **32**, 155 (1987); **33**, 377 (1988); **33**, **717** (1988) and **34**, 1425 (1989).

[2] R. Willem, M. Gielen, C. Hoogzand and H. Pepermans, "The Internal Rotation Dynamics of Polyaryl Compounds in Solution" in "Advances in Dynamic Stereochemistry", vol. 1, p. 207—285, (M. Gielen, editor), Freund Publishing House, Ltd., 1985, London.

[3] a) D. Gust, *J. Amer. Chem. Soc.*, **99**, 6980 (1977); b) D. Gust and A. Patton, *J. Amer. Chem. Soc.*, **100**, 8175 (1978).

[4] A. Patton, J. Wang Dirks and D. Gust, *J. Org. Chem.*, **44**, 4749 (1979).

[5] D. Gust and M. W. Fagan, *J. Org. Chem.*, **45**, 2511 (1980).

[6] M. W. Fagan and D. Gust, *J. Org. Chem.*, **46**, 1499 (1981).

[7] R. H. Mitchell and J. S. H. Yan, *Can. J. Chem.*, **58**, 2584 (1980).

[8] E. Hammerschmidt and F. Vögtle, *Chem. Ber.*, **113**, 1121 (1980).

[9] R. L. Clough and J. D. Roberts, *J. Org. Chem.*, **43**, 1328 (1978); R. L. Clough and J. D. Roberts, *J. Amer. Chem. Soc.*, **98**, 1018 (1976).

[10] G. R. Newkome, J. M. Roper and J. M. Robinson, *J. Org. Chem.*, **45**, 4380 (1980).

[11] H. Pepermans, R. Willem, M. Gielen and C. Hoogzand, *J. Org. Chem.*, **51**, 301 (1986).

[12] H. Pepermans, R. Willem, M. Gielen and C. Hoogzand, *Magn. Res. Chem.*, **26**, 311 (1988).

[13] J. Sandström, "Dynamic NMR Spectroscopy", Academic Press, London, 1982.

[14] A. T. Balaban, *Tetrahedron Lett.*, **1978**, 5055.

[15] R. L. Bassfield, *J. Amer. Chem. Soc.*, **105**, 4168 (1983).

[16] A. T. Balaban, M. Gavăt, P. T. Frangopol, M. Mocanu and C. D. Nenitzescu, *Rev. Roum. Chim.*, **9**, 79 (1964).

Revue Roumaine de Chimie, 35, 3, 339–343 (1990)

^{13}C–NMR SPECTRAL ASSIGNMENTS FOR 2,5-DIARYLTHIAZOLES *

MIRCEA D. GHEORGHIU, IOSIF SCHIKETANZ, ANA SCHIKETANZ and
ALEXANDRU T. BALABAN

Polytechnic Institute, Department of Organic Chemistry, Splaiul Independenței 313, 77206
Bucharest, Romania

Received November 29, 1989

Six 2,5-diarylthiazoles with phenyl, 4-tolyl, 3,4-dimethylphenyl and 4-fluorophenyl groups were investigated by ^{13}C–NMR spectroscopy. Assignments were performed on the basis of incremental methods, coupling constants, and comparison with literature data for ^{13}C–NMR spectra and calculated electron densities.

INTRODUCTION

Several 2,5-diarylthiazoles were obtained in our laboratory by two different synthetic approaches :[1,2] their ^{1}H–NMR, IR and UV spectra confirmed the structure. The ^{13}C–NMR spectra, on the other hand, raised interesting problems of assignment. The present paper reports the experimental ^{13}C–NMR data and presents a tentative assignment of the observed signals to the carbon atoms according to their structure. The numbering which will be used in the present paper is shown in formula I.

I

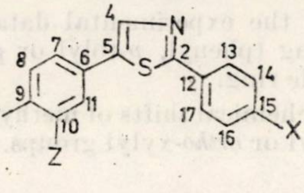

Six 2,5-diaryloxazoles were synthesized and examined by ^{13}C–NMR spectroscopy, in $CDCl_3$: their structures are presented in Table 1, and the abbreviations indicate the 2- and the 5-aryl group (in this order) according to the following key : P = phenyl, T = *p*-tolyl, X = 3,4-xylyl, F = *p*-fluorophenyl.

---

* Dedicated to the memory of Mihai Elian.

Table 1

Structure of 2,5-diaryloxazoles

Compound	2-Aryl	5-Aryl
PP	Phenyl	Phenyl
PT	Phenyl	*p*-Tolyl
PX	Phenyl	3,4-Dimethylphenyl
TT	*p*-Tolyl	*p*-Tolyl
TX	*p*-Tolyl	3,4-Dimethylphenyl
FT	*p*-Fluorophenyl	*p*-Tolyl

The spectral assignments are based upon :

(i) literature data for the unsubstituted thiazole ;

(ii) data for alkyl-substituted thiazoles ;

(iii) increments for methyl groups attached to aromatic nuclei :

(iv) modelling incrementally the 5-aryl — C—5 — C—4 sequence with a styrenic system : the 2-aryl group is modelled incrementally by a toluene system. We prefer increments according to Levy et al., [2] rather than those reported by Pretsch et al. [4] ;

(v) comparison between chemical shifts of structurally related compounds differing in the degree of methyl substitution :

(vi) carbon-fluorine coupling constants.

The basic tenet was the assumption that for identical substitution patterns of 5-Ar or 2-Ar groups, the corresponding chemical shifts remain practically uncharged.

EXPERIMENTAL RESULTS

Table 2 presents the experimental data for aromatic carbon atoms in the 5-aryl ring (phenyl, *p*-tolyl or *o*-xylyl) and in the 4 and 5 positions of the thiazole ring ; incrementally calculated data for the corresponding styrene moiety confirm the assignment.

Table 3 contains the experimental data for the aromatic carbon atoms in the 2-aryl ring (phenyl, *p*-tolyl or *p*-fluorophenyl) and in the 2-position of the thiazole ring.

Table 4 gives the chemical shifts of methyl carbons in the compounds which contain *para*-tolyl or *ortho*-xylyl groups.

DISCUSSION OF THE RESULTS

1. Quaternary carbon atoms

The carbon atoms which are the most deshielded are two quaternary atoms : C—2 in the thiazole nucleus, and its adjacent C—12 atom in the 2-Ar group. Whereas in the unsubstituted thiazole C—2 resonates at $\delta = 152.7$ or 153.4 ppm, the C—2 atom in 2,5-diarylthiazoles has

Table 2

Chemical shifts (ppm) of carbon atoms from the 5-aryl groups and thiazolic C—4 and C—5 atoms[a]

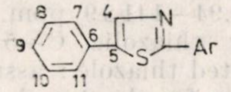

Compound Carbon	PP	PT	TT	FT[b]	PX	TX
C—4	139.23	138.70	138.59	138.73	138.70	138.72
C—5	129.73	128.55	128.71	128.47	129.03	129.10
C—6	138.78	133.76	131.20	130.15	133.94	131.28
C—7	126.68	126.53	126.51	126.56	124.14	124.10
C—8	129.09	129.75	129.74	129.81	130.33	130.30
C—9	128.98	138.27	138.16	138.36	137.00	136.93
C—10	Like C—8	Like C—8	Like C—8	Like C—8	137.31	137.41
C—11	Like C—7	Like C—7	Like C—7	Like C—7	127.89	127.85

[a] Abbreviations for compounds as in Table 1.

[b] Coupling constants for compound FT: see text.

Table 3

Chemical shifts (ppm) for carbon atoms in the 2-aryl groups and for the adjacent thiazolic C—2 atom

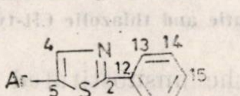

Compound Atom	PP	PT	PX	TT	TX	FT
C—2	166.17	166.62	166.48	166.87	166.78	165.34
C—12	141.19	139.44	139.61	140.09	140.04	139.52
C—13, 17	126.39	126.31	126.35	126.26	126.27	128.25
C—14, 16	128.96	128.92	128.92	129.61	129.62	116.07
C—15	129.98	129.84	129.80	138.92	139.07	164.14

Table 4

Chemical shifts (ppm) of carbon atoms in methyl groups of thiazoles I

Compound Methyl	PT	PX	TT	TX	FT
X	—	—	21.38	21.39	—
Y	2.19	19.50[a]	21.20	19.51[b]	21.24
Z	—	19.74[a]	—	19.75[b]	—

[a,b] — Interchange possible

$\delta = 166.17-166.87$ ppm (hence the aryl group deshields this carbon atom by 13—14 ppm, whereas the same aryl group in styrene deshields the adjacent olefinic carbon by a decrement of 12.5 ppm, the agreement between these two values is satisfactory). The adjacent aromatic C—12 atom resonates at $\delta = 139.94-141.19$ ppm.

The other quaternary thiazolic C—5 atom has $\delta = 118.6$ or 119.7 ppm in the unsubstituted thiazole : assuming an equal deshielding caused by the 5-aryl group as for the 2-aryl substituent, one obtains for C—5 in 2,5-diarylthiazoles $\delta = 128.55-129.73$.

The quaternary carbon atom C—6 bonded to the 5-position of the thiazole ring appears to resonate in the range 131.20—133.76 ppm, in agreement with the calculated value from the styrene model, which reproduces satisfactorily the chemical shifts of aromatic carbon atoms in the 5-aryl ring.

For C—9 in the *p*-tolyl compounds (PT and TT) the incrementally calculated value is 138.9 ppm, while the experimental data are 138.27 and 138.16 ppm, very close to one another. The same C—9 atom in the *o*-xylyl compounds (PX and TX) has a calculated value of 137.6 ppm, whereas the experimental data are 136.9—137.0 ppm : in these compounds, there is yet another quaternary atom, C—10, for which the calculated chemical shift is 138.3 and the experiemntal value is 137.3 ppm.

For the quaternary C—15 atom in the *p*-tolyl compounds TT and TX, the assigned chemical shitfs are 138.92 and 139.07 ppm, respectively.

2. Aromatic and thiazolic CH-type carbons

The C—4 atom in the unsubstituted thiazole ring resonates at $\delta = 143.7$ or 143.6 ppm. The C—4 atom in 2,5-diarylthiazoles (doublet in off-resonance experiments) appears at 138.52—139.23 ppm, i.e. wit at shielding of about 2 ppm, due to the 2-aryl group. A shielding is also observed for the β-carbon atom in styrene, but this shielding is much more pronounced than for the 2,5-diarylthiazoles.

It can be observed from Tables 2 and 3 that the chemical shifts of aromatic CH-type carbon atoms for the 2- and 5-aryl groups are remarkably constant for each substitution pattern.

3. Methyl carbon atoms

The assignments of methyl chemical shifts (Table 4) reveal that the X-type methyl (*p*-tolyl as 2-aryl group) is more deshielded than the Y-type (*p*-tolyl as the 5-aryl group), obviously because of the lower electron density in position 2 than in position 5 of the thiazole nucleus (formula I).

This is in agreement with theoretical calculations, and with ^{1}H—NMR data : in CCl_4 or in C_6D_6, H—2 resonates at 8.7 ppm while H—5 appears at 7.2 ppm.

Methyl groups in *ortho*-xylyl substituents are more shielded than in *p*-tolyl substituents, but the discrimination between the 3- and 4-methyl groups (Y vs. Z) of *o*-xylyl substituents is ambiguous.

4. Carbon—fluorine coupling constants

Compound FT has for the 2-aryl group $^{13}C-^{19}F$ coupling constants which characterize the carbon atoms of the fluorine-containing ring :the values of these coupling constants (in Hz) are compared with the values of the corresponding data (in brackets) for 4-(2,6-di-t-butyl-4H-pyran-4-ylidene)-1-(4-fluorophenyl)-2-butene-1-one : $J_{F,C-4} = 249.9$ (252.7) : $J_{F,C-3} = 21.8$ (21.6) : $J_{FC-2} = 9.4$ (8.9). These doublet splittings in the ^{13}C—NMR spectra bring further confirmation to the above assignments because they help in pinning up the corresponding 2-*p*-fluorophenyl carbon atoms : the strong deshielding of the carbon atom bonded to fluorine and the pronounced shielding of the adjacent carbon atoms are in agreement with incrementally calculated data using the *p*-fluorotoluene model.

EXPERIMENTAL PART

^{13}C—NMR spectra were recorded in $CDCl_3$ in vials with 5 or 10 mm diameter using a Varian FT80A instrument : pulse width 12—15 μs, spectral window 4000 Hz, 16384 data points, acquisition time 2.047 s. For observing quaternary carbon atoms, chromium(III) acetylacetonate was added in several instances.

The preparation of 2,5-diarylthiazoles was described earlier.[1,2]

REFERENCES

[4] I. Schiketanz, A. Ştefănescu, M. C. Balaban, A. Schiketanz, M. D. Gheorghiu and A. T. Balaban, *Rev. Roum. Chim.*, **32**, 1175 (1987).

[2] A. Schiketanz, A Ştefănescu, M. D. Gheorghiu, I. Schiketanz and A. T. Balaban, *Rev. Roum. Chim.* **35**, 345 (1990).

[3] G. C. Levy, R. L. Lichter and G. L. Nelson, "Carbon-13 Nuclear Magnetic Resonance Spectroscopy", Wiley, New York, 1980, pp. 82, 112.

[1] E. Pretsch, J. Seibl, W. Simon and T. Clerc, "Tabellen zur Strukturaufklärung organischer Verbindungen", Springer-Verlag, Berlin, 1981, p. C—120.

[5] R. Garnier, R. Faure, A. Babadjamian and E. J. Vincent, *Bull. Soc. Chim. France, 3,* 1040 (1972).

[6] J. V. Metzger and E. J. Vincent, in "Thiazole and Its Derivatives", Part 1 (ed. J. V. Metzger), Wiley-Interscience, New York, 1979, p. 26, 67.

[7] A. T. Balaban, M. Fahmy, M. D. Gheorghiu and V. Wray, *Liebigs Ann. Chem.*, 1807 (1983).

Revue Roumaine de Chimie, 35, 3, 345—348 (1990)

AMINOKETONE, OXAZOLE AND THIAZOLE SYNTHESES. Part XII[1]

2,5-DIARYTHIAZOLES FROM THIOAZLACTONES AND AROMATIC HYDROCARBONS *

IOSIF SCHIKETANZ, ANDREI ŞTEFĂNESCU, MIRCEA D. GHEORGHIU,
ANA SCHIKETANZ and ALEXANDRU T. BALABAN
Polytechnic Institute, Department of Organic Chemistry,
Splaiul Independenţei 313, 77206 Bucharest, Romania

Received November 2, 1989

p-Substituted hippuric acids (with fluoro or methyl groups) were thionated, cyclized to thioazlactones and reacted with aromatic hydrocarbons (benzene, toluene, *ortho*-xylene) in the presence of aluminium chloride yielding 2,5-diarylthiazoles. Their ^1H—NMR and UV spectra are reported.

In previous parts of this series[1-3] we have reported that azlactones **1** substitute electrophilically aromatic compounds ArH under Friedel—Crafts conditions affording α-acylaminoketones **2** which can be cyclized to aryl-substituted oxazoles **3** or (in the presence of thionating agents) thiazoles **4**, cf Scheme 1, where R was an aromatic group (phenyl or substituted phenyl [1,2]) or a styryl group originating from a cinnamoyl residue. [3]

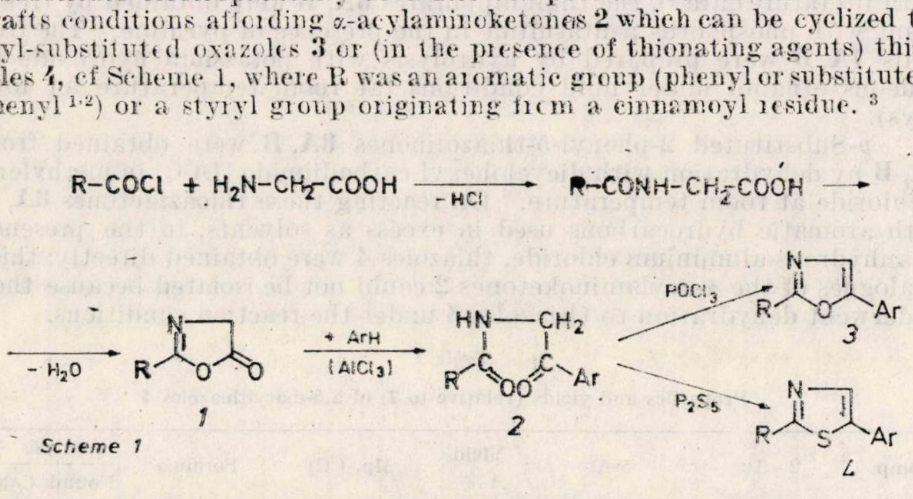

Scheme 1

An alternative approach for obtaining thiazoles *via* such electrophilic substitutions involves the preparation of thioazlactones and their reaction with aromatic compounds (Scheme 2).

---

* Dedicated to the memory of Mihai Elian.

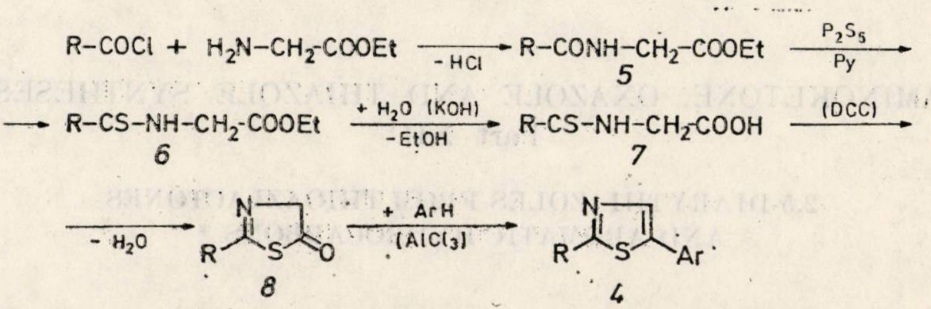

Scheme 2

A, $R = p\text{-}MeC_6H_4$
B, $R = p\text{-}FC_6H_4$

a, Ar = Ph
b, $Ar = p\text{-}MeC_6H_4$
c, $Ar = 3,4\text{-}Me_2C_6H_4$

In Part XI [1] we presented reactions involving the former approach, in which R was *p*-fluorophenyl, as well as the latter approach in which R was phenyl.

In the present paper, continuing these investigations, we report the results for the synthesis of thiazoles **4** involving the latter approach when R is *p*-tolyl (**A**) or *p*-fluorophenyl (**B**), and when the aromatic substrates ArH are benzene (**a**), toluene (**b**) and *ortho*-xylene (**c**). Thus we present an alternative synthesis of the 2-(*p*-fluorophenyl)-5-aryl-substituted thiazoles **4B**, as well as the preparation of new 2-(*p*-tolyl)-5-aryl-substituted thiazoles **4A**.

From the *p*-substituted ethyl hippurates **5A, B** (prepared in analogy with literature data [4]), the thionhippurates **6A, B** were obtained by treatment with phosphorus pentasulfide in the presence of pyridine. The free acids **7A, B** were prepared by hydrolysis with potassium hydroxide in aqueous ethanol under mild conditions (at room temperature for four days).

p-Substituted 2-phenyl-5-thiazolinones **8A, B** were obtained from **7A, B** by dehydration with dicyclohexyl-carbodiimide (DCC) in methylene dichloride at room temperature. [6] On reacting these thioazlactones **8A, B** with aromatic hydrocarbons used in excess as solvents, in the presence of anhydrous aluminium chloride, thiazoles **4** were obtained directly; thioanalogues of the α-acylaminoketones **2** could not be isolated because they underwent dehydration to thiazoles **4** under the reaction conditions.

Table 1

Properties and yields (relative to **7**) of 2,5-diarylthiazoles **4**

Comp.	2 – R	5-Ar	Yield (%)	Mp. (°C)	Formula	Analysis %	
						Found	Calc.
4Aa	$p\text{-}MeC_6H_4$	Ph	32	120	$C_{16}H_{13}NS$	5.48	5.57
4Ab	$p\text{-}MeC_6H_4$	$p\text{-}MeC_6H_4$	83	146	$C_{17}H_{15}NS$	5.09	5.28
4Ac	$p\text{-}MeC_6H_4$	$3,4\text{-}Me_2C_6H_3$	72	128–130	$C_{18}H_{16}NS$	5.11	5.01
4Bb	$p\text{-}FC_6H_4$	$p\text{-}MeC_6H_4$	82	130 (lit. [1]130)	$C_{16}H_{12}FNS$	5.08	5.20
4Bc	$p\text{-}FC_6H_4$	$3.4\text{-}Me_2C_6H_3$	70	95 (lit. [1]97)	$C_{17}H_{14}FNS$	4.85	4.94

Table 2

^{1}H—NMR chemical shifts (singlets unless otherwise stated, δ, ppm) of 2,5-diarylthiazoles **4**

Comp.	Solvent	Methyl	Thiazole (4-H)	Aromatic protons
4Aa	$CDCl_3$	2.36 (3H)	7.80 (1H)	7.13—8.03 (m, 9H)
4Ab	$CDCl_3$	2.36 (6H)	7.87 (1H)	7.37^a (d, 2H, 5-Ar), 7.77^a (d, 2H, 2-R), 7.00—7.23 (m, 4H)
4Ac	$CDCl_3$	2.27 (6H) 2.37 (3H)	7.87 (1H)	7.77 (d, 2H, 2-R), 7.00—8.37 (m, 5H)
4Bb	$(D_3C)_2CO$	2.33 (3H)	8.00 (1H)	6.9—7.6 (m, 6H : 2-R, 2,6-H_2 and 5-Ar), 7.89 (2H, dd, 2-R, 3,5-H) ^{b}
4Bc	$(D_3C)_2CO$	2.23 (6H)	8.00 (1H)	6.8—7.5 (m, 5H : 2-R, 2,6-H and 5-Ar), 7.9 (2H, dd, 2-R, 3,5-H_2)^b

Coupling constants : $^aJ_{H-H} = 8$Hz $^bJ_{H-H} = J_{H-F} = 9$Hz

Properties and yields of thiazoles **4** are presented in Table 1, ^{1}H—NMR spectra in Table 2, and UV absorption spectra in Table 3.

The ^{1}H—NMR spectra (Table 2) present for the thiazole ring proton (in position 4) signals at $\delta = 7.8—7.9$ for compounds **4A** in $CDCl_3$, and at $\delta = 8.0$ for the less soluble compounds **4B** in acetone-d_6. In all cases, the methyl protons appear at $\delta = 2.2—2.4$ but overlaps occur.

The electronic absorption band around 330 nm presents a slight bathochromic shift relatively to 2,5-diphenylthiazole, whose maximum in ethanol appears at 322 nm ($\varepsilon = 24500$).[7-9]

Table 3

Electronic absorption bands of 2,5-diarylthiazoles 4 in methanol

Comp.	λ_{max} (nm)	ε_{max}
4Ab	331	27100
4Ac	332	24400
4Bb	328	23700
4Bc	329.5	26800

EXPERIMENTAL PART

^{1}H—NMR spectra were recorded with a Varian EM 360 L instrument, IR spectra with a Jena UR — 20, and UV spectra with a Jena Specord spectrophotometer.

Ethyl p-*methylhippurate* (**5A**) mp. 70—71 (from ligroin, lit.[10]mp 71) was prepared in 90% yield from *p*-toluyl chloride and ethyl aminoacetate hydrochloride (1.1 : 1 moles) under reflux in benzene until the evolution of hydrogen chloride ceased. *Methyl 4-fluorohippurate*, mp. 114 , was obtained similarly, and had the following ^{1}H—NMR data in $CDCl_3$ (δ, ppm) : 3.73(3H, s, CH_3) ; 4.15(2H, d, CH_2, $J = 5$Hz), 7.00 (2H, dd, 3,5-H_2, $J_{H-F} = 9$Hz, $J_{H-H} = 9$ Hz), 7.20 (1 H, NH), 7.73 (2 H, dd 2,6-H_2, $J_{H-F} = 6$Hz, $J_{H-H} = 9$Hz) ; the *ethyl 4-fluorohippurate*, **5B**, mp. 100 (from benzene—hexane 60 : 40) was obtained similarly in 93% yield and had in $CDCl_3$ $\delta = 1.33$(3H, t, Et—CH_3, $J = 7$ Hz), 4.10(2H, d, NCH_2, $J = 5$Hz), 4.12 (2H, q, Et—CH_2, $J = 7$ Hz), 7.03 (2H, dd, 3,5-H_2, $J_{F-H} = J_{H-H} = 9$ Hz) ; 7.80 (2H, dd, 2,6-H_2, $J_{F-H} = 5$ Hz, $J_{H-H} = 9$ Hz), 7.30 (1H, NH).

IR (CCl_4) : 3280 (NH), 1735 (CO), 1665 cm^{-1}(CONH).

These hippurates were converted into the corresponding *thionohippuric derivatives* in two steps, by thionation with phosphorus pentasulfide (0.7 moles per mole of ester) in pyridine according to literature data ,[5] followed by hydrolysis of the ester group (4 days at room temperature with excess of an ethanolic 15% solution of potassium hydroxide). The *ethyl 4-methyl-*

thionohippurate **6A**, mp. 88 (from hexane) has strong IR bands at 3380, 1740, 1500, 1370, 1210 and 1020 cm^{-1} and ^{1}H–NMR peaks ($CDCl_3$) : 1.37 (3H, t, Et–CH_3, J = 7 Hz), 2.37 (3H, s, Me), 4.30 (2H, q, Et–CH_2, J = 7 Hz), 4.50 (2H, d, CH_2–N, J = 5 Hz), 7.20 (2H, d, 3,5-H_2, J = 9 Hz), 7.76 (2H, d, 2,6-H_2, J = 9 Hz), and 8.13 (1H, NH, broad). *Ethyl 4-fluoro-thionohippurate* **6B** mp. 72 from benzene–hexane (10 : 90) has analogous ^{1}H–NMR data (except for the aromatic protons which couple with the fluoro substituent) : 1.33 (3H, t, Et–CH_3, J = 7Hz), 4.20(2H, q, Et–CH_2, J = 7 Hz), 4.33(2H, d, CH_2, J = 5 Hz), 6.93 (2H, dd, 3,5-H_2, $J_{H-H} = J_{H-F}$ = 9 Hz), 7.73 (2H, dd, 2,6-H_2, J_{H-H} = 9 Hz, J_{H-F}=6 Hz), 8.07 (1H, NH, broad).

After hydrolysis (31 % yield relative to **5B**), the *4-fluoro-thionohippuric acid* **7B**, mp, 166 (from water) has in the IR spectrum the NH stretching band at 3270 cm^{-1} and the carbonyl stretching at 1700 cm^{-1}, and the following ^{1}H–NMR data (in DMSO-d_6) :δ = 4.33 ,2H, d, CH_2), 7.30(2H, dd, 3,5-H_2, $J_{H-H}=J_{H-F}$=9 Hz, 7.93 (2H, dd, 2,6-H_2, J_{H-H} = 9 Hz, J_{H-F}= = 6 Hz), 10.50 ppm (1H, t, NH).

The 4-methyl-thionohippuric acid **7A** (yield 43 % relative to **5A**), mp. 178° (from water) had IR bands (KBr pellet) at 3280 (NH) and 1700 (C = O) cm^{-1}. ^{1}H–NMR (DMSO-d_6) : 2.34 (3H, s, CH_3), 4.43 (2H, d, CH_2, J = 5 Hz), 7.36(2H, d, 3,5-H_2, J = 9 Hz), 7.83 (2H, d, 2,6-H_2, J = 9 Hz), 10.30 ppm (1H, t, NH, J = 5 Hz).

2-*(4-Fluorophenyl)-thiazolin-5-one* (**8B**), mp. 96° (from n-hexane) was obtained by adding the acid **7B** portionwise to a stirred mixture of an equimolar amount of DCC in methylene chloride at room temperature and perfecting the reaction for 15 minutes. IR (CCl_4) : 1730 (C =O) 1590 cm^{-1}. ^{1}H–NMR (CCl_4) : δ = 4.73 (2H, s, CH_2), 7.07(2H, dd, 3,5-H_2, $J_{F-H} = J_{H-H}$ = = 9 Hz), 7.80 (2H, dd, 2,6-H_2, J_{F-H} = 5 Hz, J_{H-H} = 9 Hz).

2-*(4-Methylphenyl)-thiazolin-5-one* (**8A**), mp. 82–4° (from petroleum ether) was prepared analogously. ^{1}H–NMR(CCl_4), δ = 2.40 (3H, s, CH_3), 4.70 (2H, s, CH_2), 7.16 (2H, d, 3,5-H_2, J_{H-H} = 9 Hz), 7.66 (2H, d, 2,6-H_2, J_{H-H} = 9 Hz).

2,5-*Diarylthiazoles* **4** were prepared from the above thiazolinones (1 mole) in aromatic hydrocarbons (⩾ 10 moles) and anhydrous aluminium chloride (3 moles) at room temperature overnight ; the products were recrystallized from ethanol or hexane. Results are presented in Tables 1–3.

REFERENCES

[1] Part XI, I. Schiketanz, A. Ştefănescu, M. C. Balaban, A. Schiketanz, M. D. Gheorghiu, and A. T. Balaban, *Rev. Roum. Chim.*, **32**, 1175 (1987).

[2] M. C. Balaban, I. Schiketanz, A. T. Balaban, A. Schiketanz and M. D. Gheorghiu, *Rev. Roum. Chim.*, **32**, 957 (1987).

[3] I. Schiketanz, A. Schiketanz, M. D. Gheorghiu and A. T. Balaban, *Rev. Roum. Chim.*, **30**, 977 (1985).

[4] H. Franzen, *Ber. dtsch. chem. Ges.*, **42**, 2465 (1909).

[5] H. Muxfeld, J. Behling, G. Grethe and W. Rogalski, *J. Am. Chem. Soc.*, **89**, 4991 (1967).

[6] G. C. Barrett, *J. Chem. Soc. (C)*, 1380 (1971).

[7] R. Arnaud, M. Gelus, J. C. Malet and J. M. Bouvier, *Bull. Soc. Chim. France*, **9**, 2357 (1966).

[8] J. A. Aune, H. J. M. Dou and J. Crousier, in "Thiazole and its Derivatives", Part 1 (ed. J. V. Metzger), Wiley-Interscience, New York, 1979, p. 352.

[9] V. N. Kerr, F. N. Hayes, D. G. Ott and E. Hansbury, *J. Org. Chem.*, **24**, 1861 (1959).

[10] A. Klages and O. Haack, *Ber dtsch. chem. Ges.*, **36**, 1648 (1903).

Revue Roumaine de Chimie, 35, 3, 349–391 (1990)

CHEMICAL GRAPHS. Part 53[1]

BENZO- AND POLYBENZO-DERIVATIVES OF VALENCE ISOMERS OF [12]ANNULENE *

CĂLIN DELEANU and ALEXANDRU T. BALABAN
Polytechnic Institute, Chair of Organic Chemistry, Splaiul Independenţei 313, 77206 Bucharest, Romania

Received October 15, 1989

Formulas of all possible topologically planar, non-*ortho*-quinonoid benzo- and polybenzo-derivatives of valence isomers of [12]annulene are presented neglecting stereoisomerism. A literature survey of known compounds indicates that most of the compounds presented in this overview have yet to be prepared because they are still unknown.

INTRODUCTION

In a previous paper of this series,[2] in a review[3] and in a book[4] the problem of finding all possible formulas for benzo-derivatives of valence isomers of [n]annulenes was discussed in detail for n ⩽ 10. Graph-theoretical procedures were applied for finding valence isomers of [n]annulenes,[5,6] and then the problem of benzoannelation was attacked, neglecting stereoisomerism.[2]

We simplified the enumeration problem of generating and counting annulene valence isomers corresponding mathematically to cubic multigraphs, i.e. graphs in which each vertex has degree three (a double bond being counted twice in the degree) by neglecting the non-planar graphs; topologically planar graphs, the only ones to be counted, can be drawn on a plane without intersecting lines (of course, molecules represented by planar graphs have a tridimensional geometry).

The graph-theoretical literature on counting cubic graphs was reviewed in a recent paper [5] in which a computer program was used for counting cubic graphs with n ⩽ 12 (without generating the structures).

In the present paper we extend the above procedure for generating and counting valence isomers of benzo[12]annulenes. ** In order to simplify the problem further, we shall not consider *ortho*-quinonoid structures, which are expected to be less stable than the isomeric compounds which are discussed in the present paper.

---

* Dedicated to the memory of Mihai Elian.

** As in previous papers[2–4] we consider only benzo-derivatives of valence isomers of [12]annulene (and not the much larger set of valence isomers of benzo[12] annulene), and we shall call the former compounds for brevity benzo- or polybenzo-$(CH)_{12}$ valence isomers.

Since the number of valence isomers of [14]annulene is quite large,[8] we restrict ourselves to systems which may still be handled without a computer.

MONO- AND POLYBENZO-$(CH)_{12}$ VALENCE ISOMERS

For monobenzo-$(CH)_{12}$ valence isomers, we start from the table of planar valence isomers of [12]annulene[9,10] having a single double bond, and annelate it with a benzenoid ring. This leads to a one-to-one (1—1) correspondence between the above $(CH)_{12}$ valence isomers and the corresponding benzo-derivatives which have no remaining double bond.

For monobenzo-$(CH)_{12}$ valence isomers which have 1—5 olefinic bonds we benzo-annelate all non-equivalent valence isomers with $\beta = 2-6$ double bonds at each non-equivalent double bond. Since we exclude *ortho*-quinonoid systems, it does not matter if the double bonds are or are not conjugated (if *ortho*-quinonoid systems had been included, they would have been derived from conjugated systems).

For di- and polybenzo-$(CH)_{12}$ valence isomers, we proceed similarly. There is always a 1—1 correspondence between the number of $(CH)_{12}$ valence isomers with β double bonds and the number of β-benzo-$(CH)_{12}$ valence isomers.

It is interesting to compare the numbers of $(CH)_{12}$ valence isomers * (Table 1) with those of the benzoderivatives (lower part of Table 2). It can be seen that there is complete coincidence of the rows with $\beta = 1-6$ from Table 1 with the upper rows (having the corresponding β-values) for $n = 12$ in Table 2. The lower rows in Table 2 have always higher en-

Table 1

Numbers of planar valence isomers of [**12**]annulene according the numbers β of double bonds and t of 3-membered circuits

β \ t	0	1	2	3	4	5	6	Total
0	2	2	9	7	9	2	1	32
1	4	13	26	19	11	2	—	75
2	15	30	42	17	8	—	—	112
3	21	30	26	7	2	—	—	86
4	18	14	8	1	—	—	—	41
5	6	3	1	—	—	—	—	10
6	1	—	—	—	—	—	—	1
Grand total								357

---

* One error should be corrected in ref.[9] (Fig. 2 on p. 687): the structure labelled as 2—4—0—1 should actually be 2—3—0—2; therefore one structure should be moved from the column with $t = 4$ to that with $t = 3$; this correction changes the entries 16 and 9 with $\beta = 2$ of Table 7 in ref.[8] into 17 and 8 of the present Table 1.

Table 2

Numbers of non-orthoquinonoid benzo- and polybenzo-derivatives of planar valence isomers $(CH)_n$ with β-double bonds and t threemembered circuits. The number of benzo-fused rings is denoted by B.

n	B	1							2						3						4					5				6		Grand Total
	β \ t	0	1	2	3	4	5	Total	0	1	2	3	4	Total	0	1	2	3	4	Total	0	1	2	3	Total	0	1	2	Total	0	Total	
4	1	—	—	—	—	—	—	0	—	—	—	—	—	0																		
	2	1	—	—	—	—	—	1	1	—	—	—	—	1																		
	Total	1	0	0	0	0	0	**1**	1	0	0	0	0	0						—					—				—		—	**2**
6	1	—	—	1	—	—	—	1	—	—	—	—	—	1	—	—	—	—	—	0												
	2	1	—	1	—	—	—	2	1	—	1	—	—	2	—	—	—	—	—	0												
	3	1	—	—	—	—	—	1	1	—	—	—	—	1	1	—	—	—	—	1												
	Total	2	0	2	0	0	0	**4**	2	0	1	0	0	**3**	1	0	0	0	0	**1**					—				—		—	**8**
8	1	—	1	2	1	—	—	4	—	—	—	—	—	0	—	—	—	—	—	0	—	—	—	—	0							
	2	2	1	3	—	—	—	6	2	1	2	—	—	5	—	—	—	—	—	0	—	—	—	—	0							
	3	3	2	2	—	—	—	7	3	2	2	—	—	7	2	1	1	—	—	4	—	—	—	—	0							
	4	1	—	—	—	—	—	1	2	—	—	—	—	2	1	—	—	—	—	1	1	—	—	—	1							
	Total	6	4	7	1	0	0	**18**	7	3	4	0	0	**14**	3	1	1	0	0	**5**	1	0	0	0	**1**				—		—	**38**
10	1	1	3	7	3	2	—	16	—	—	—	—	—	0	—	—	—	—	—	0	—	—	—	—	0	—	—	—	0			
	2	5	10	12	4	1	—	32	4	6	9	1	1	21	—	—	—	—	—	0	—	—	—	—	0	—	—	—	0			
	3	11	11	9	1	—	—	32	11	11	9	1	—	32	6	5	4	1	—	16	—	—	—	—	0	—	—	—	0			
	4	7	6	2	—	—	—	15	12	8	4	—	—	24	7	6	2	—	—	15	4	2	1	—	7	—	—	—	0			
	5	1	—	—	—	—	—	1	2	—	—	—	—	2	2	—	—	—	—	2	1	—	—	—	1	1	—	—	1			
	Total	25	30	30	8	3	0	**96**	29	25	22	2	1	**79**	15	11	6	1	0	**33**	5	2	1	0	**8**	1	0	0	**1**		—	**217**
12	1	4	13	26	19	11	2	75	—	—	—	—	—	0	—	—	—	—	—	0	—	—	—	—	0	—	—	—	0	—	0	
	2	19	54	66	30	11	—	180	15	30	42	17	8	112	—	—	—	—	—	0	—	—	—	—	0	—	—	—	0	—	0	
	3	47	75	60	18	4	—	204	47	75	60	18	4	204	21	30	26	7	2	86	—	—	—	—	0	—	—	—	0	—	0	
	4	42	44	22	3	—	—	111	66	63	34	4	—	167	42	44	22	3	—	111	18	14	8	1	41	—	—	—	0	—	0	
	5	16	11	3	—	—	—	30	29	20	6	—	—	55	29	20	6	—	—	55	16	11	3	—	30	6	3	1	10	—	0	
	6	1	—	—	—	—	—	1	3	—	—	—	—	3	3	—	—	—	—	3	3	—	—	—	3	1	—	—	1	1	1	
	Total	129	197	177	70	26	2	**601**	160	188	142	39	12	**541**	95	94	54	10	2	**255**	37	25	11	1	**74**	7	3	1	**11**	1	**1**	**1483**

tries than the corresponding ones in Table 1 with n = 12 and the same couple of β and t values, because one and the same valence isomer of [12]annulene gives rise to more than one benzoderivative when it has nonequivalent double bonds.

Table 2 also contains data for the numbers of previously obtained[2–4] benzo-$(CH)_n$ valence isomers with n = 4, 6, 8 and 10.

Structures of mono- and polybenzo-$(CH)_{12}$ valence isomers are presented in Tables 3–8. All structures are drawn so as to emphasize the topological planarity (no crossing lines). Stereoisomerism is neglected, therefore the actual numbers of isomers are larger than those indicated in Table 2. Though molecules corresponding to separable graphs * can be obtained fairly easily, they are less prone to interconversions into other valence isomers by thermal or photochemical pathways or reactions catalyzed by transition metal ions or complexes. [10,11]

KNOWN MONOBENZODERIVATIVES OF VALENCE ISOMERS OF [12]ANNULENE

Benzo[12]*annulene; (Benzocyclododecene); (Benzocyclododeca-1,3,5,7,9,11-hexaene)* is still unknown, but some theoretical considerations-appeared, suc has studies concerning its paratropicity,[74] prediction of the chemical shift in the ¹H-NMR using HMO theory, [75] or its resonance energy. [76] Subsequent structures are presented in Table 9 (p. 379).

1-(Cyclohepta-2,4,6-trien-1-yl)indene; (benzodihydrosesquifulvalene); (**1**) was obtained by Prinzbach et al. [12] in 1966 from tropylium bromide and indenylmagnesium bromide. Benzodihydrosesquifulvalene (**1**) is a liquid (b.p. 110–112° at 0.05 Torr) with characteristic IR and ¹H–NMR spectra. [12] Its dehydrogenation with chloranil affords benzosesquifulvalene (**28**), which is stable only in solution. [12]

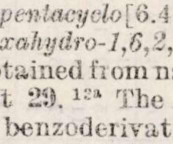
28

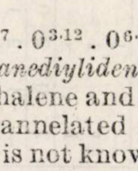

29

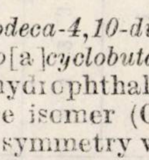
30

Benzo[*d*]*pentacyclo*[6.4.0.$0^{2,7}$.$0^{3,12}$.$0^{6,9}$] *dodeca-4,10-diene; (1,2,2a, 5,6,10b-Hexahydro-1,6,2,5-ethanediylidene-benzo*[a]*cyclobuta*[c]*cyclooctene);* (**2**) was obtained from naphthalene and 1,2-dihydrophthalic anhydride via the adduct **29**. [13a] The non-annelated valence isomer $(CH)_{12}$ corresponding to the benzoderivative **2** is not known; its symmetry was analyzed in a recent paper. [13b] Complexation of **2** with bis(bicyclo[2.2.1]heptadienyl)rhodium followed by reaction with triphenyl phosphite led to **3**. [13a]

---

* Separable graphs are those graphs which become disconnected by deleting a single line (edge).

Table 3

Graphs of benzo-$(CH)_{12}$ valence isomers.

t	β=1
0	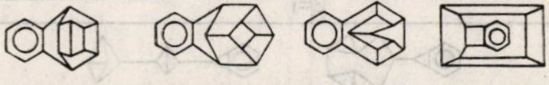
1	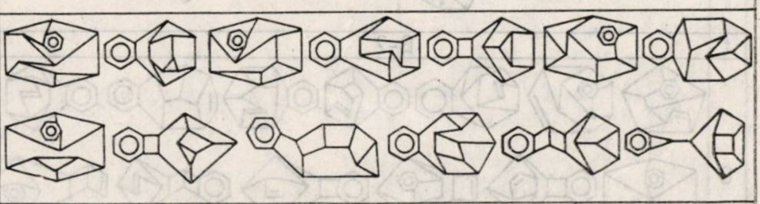
2	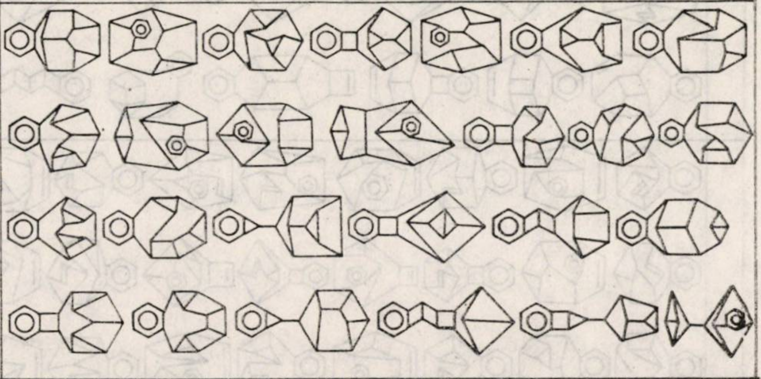
3	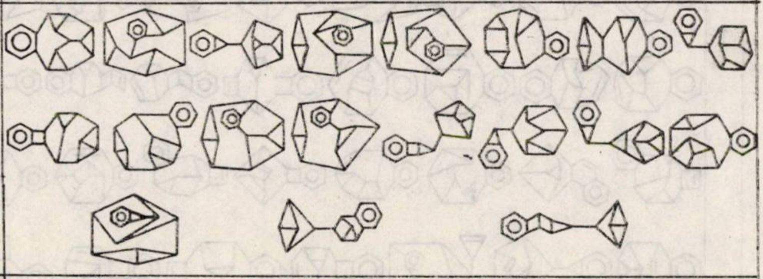
4	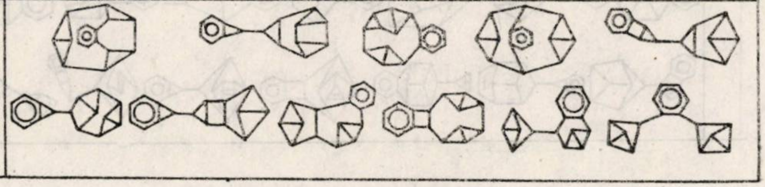

Table 3 (Continued)

t	β=1
5	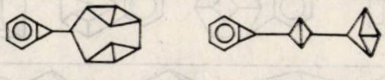
t	β=2
0	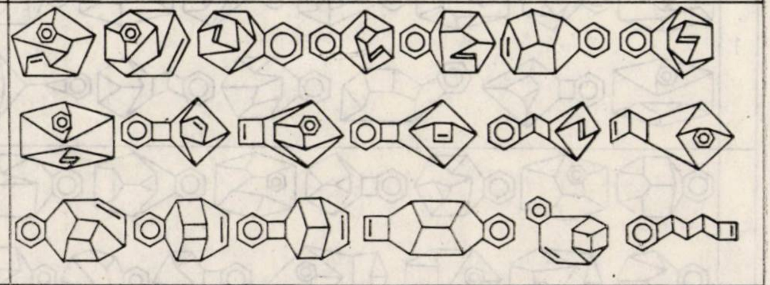
1	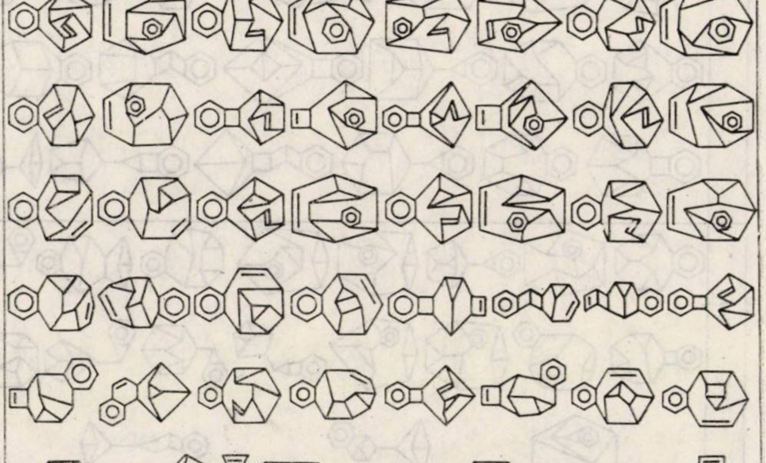

Table 3 (Continued)

t	β=2
2	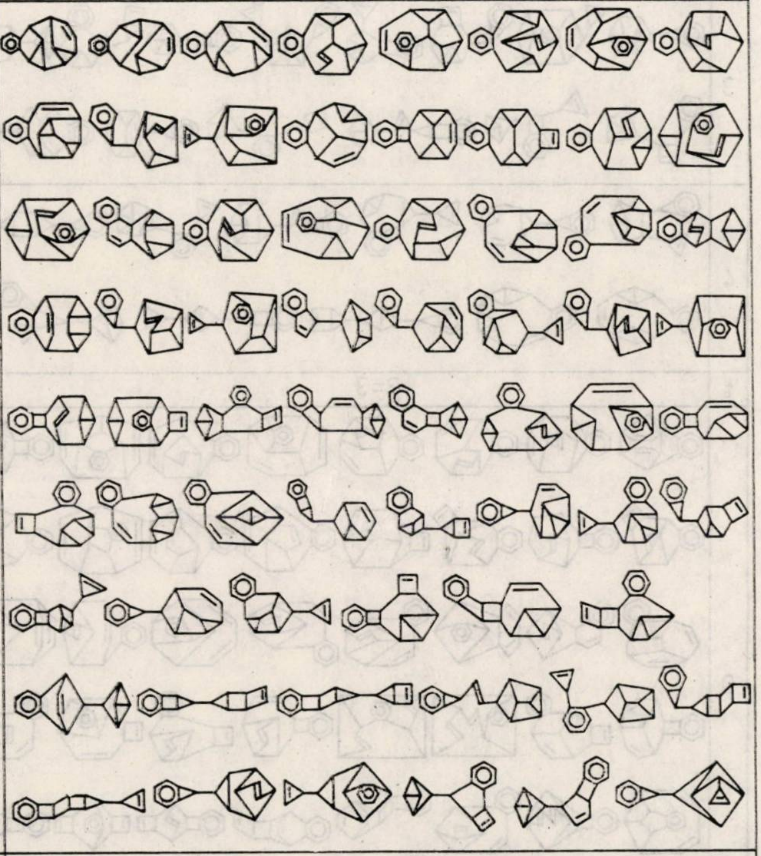
3	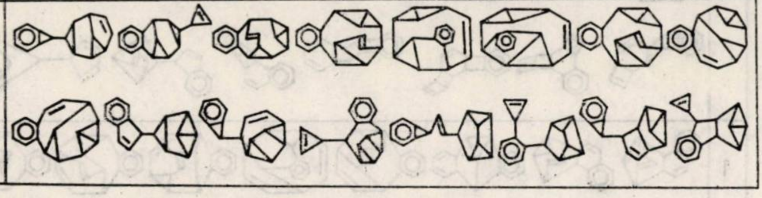

Table 3 (Continued)

t	β=2
3	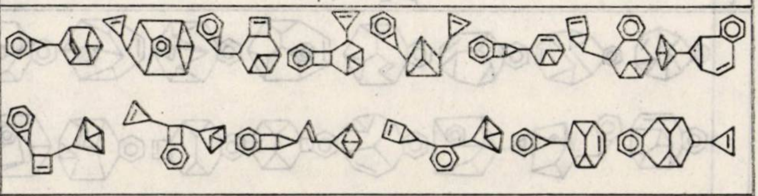
4	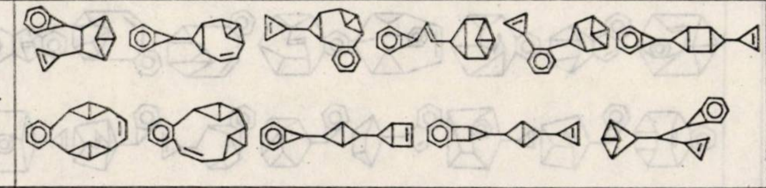
t	β=3
0	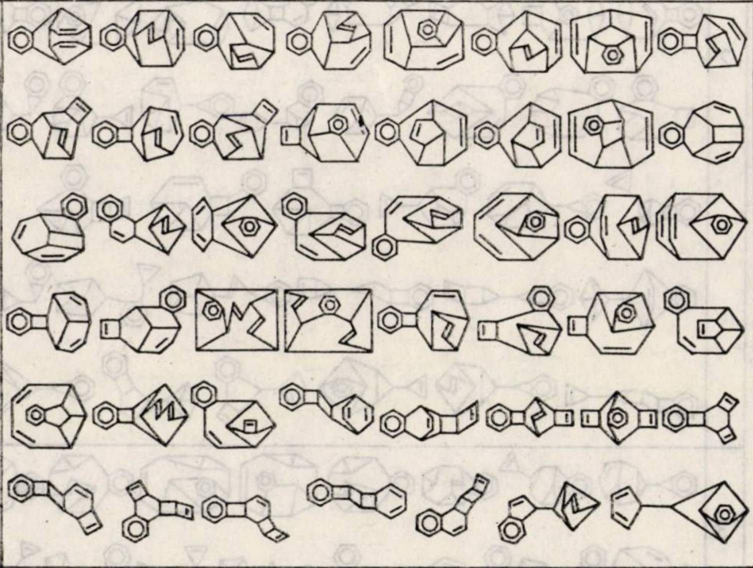
1	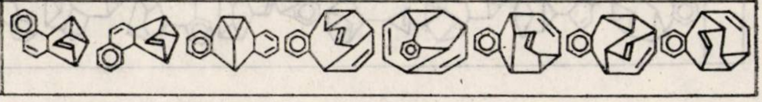

Table 3 (Continued)

t	β=3
1	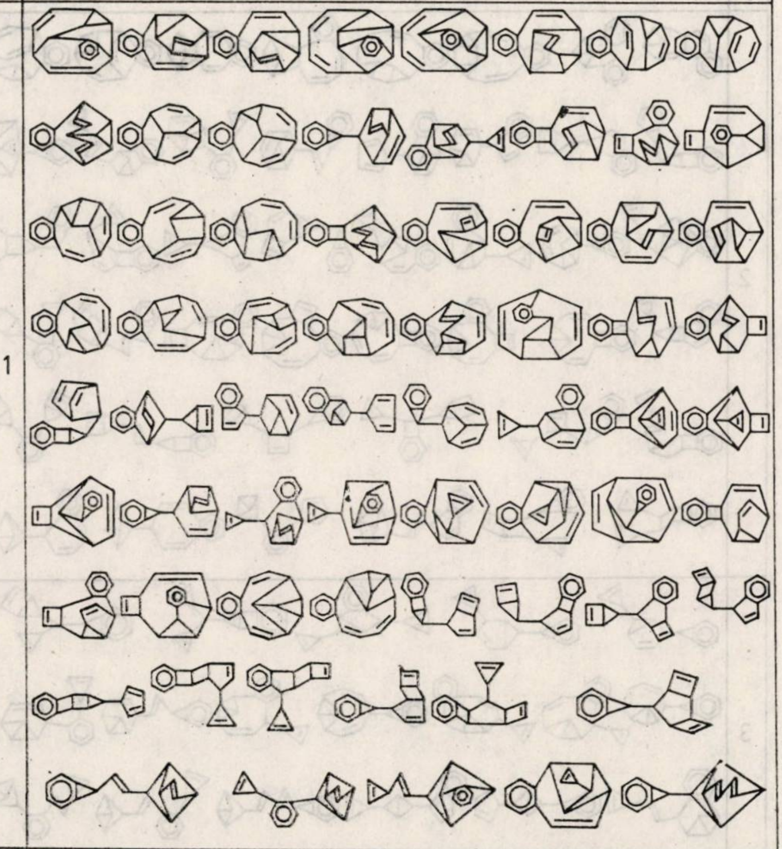
2	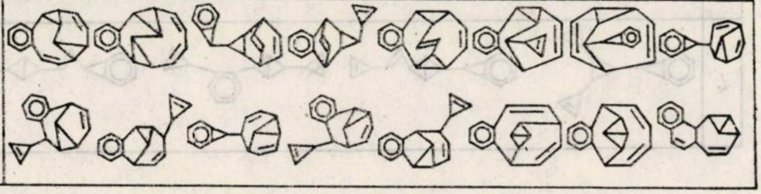

Table 3 (Continued)

t	β=3
2	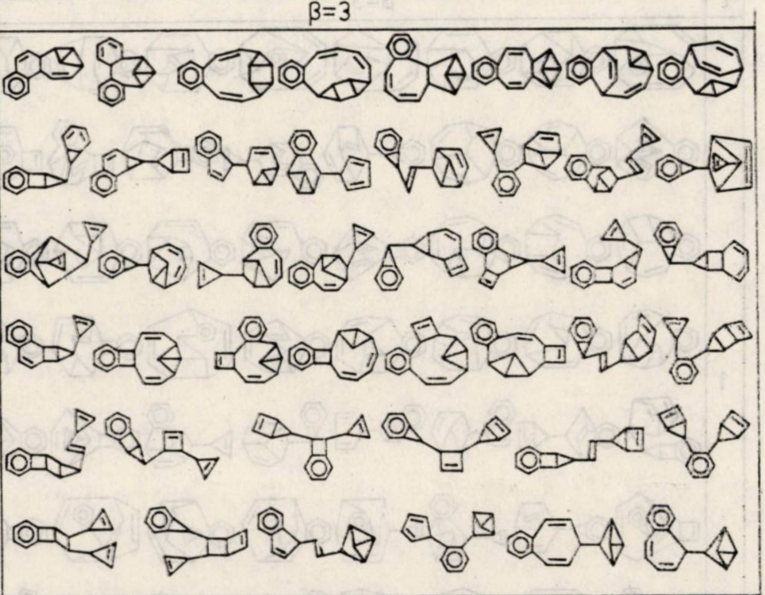
3	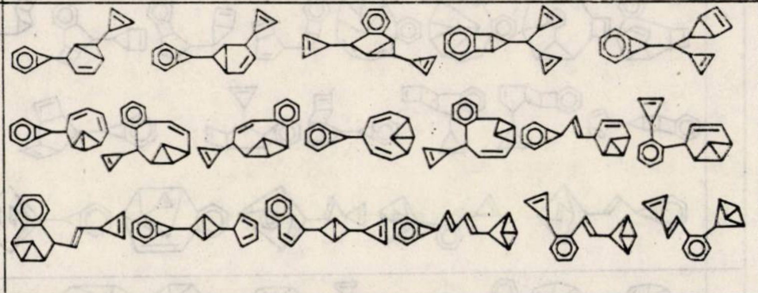
4	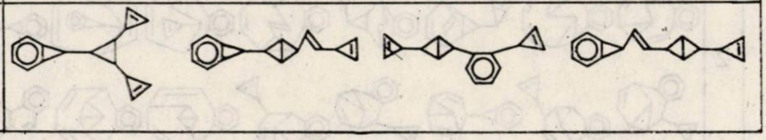

Table 3 (Continued)

t	β=4
0	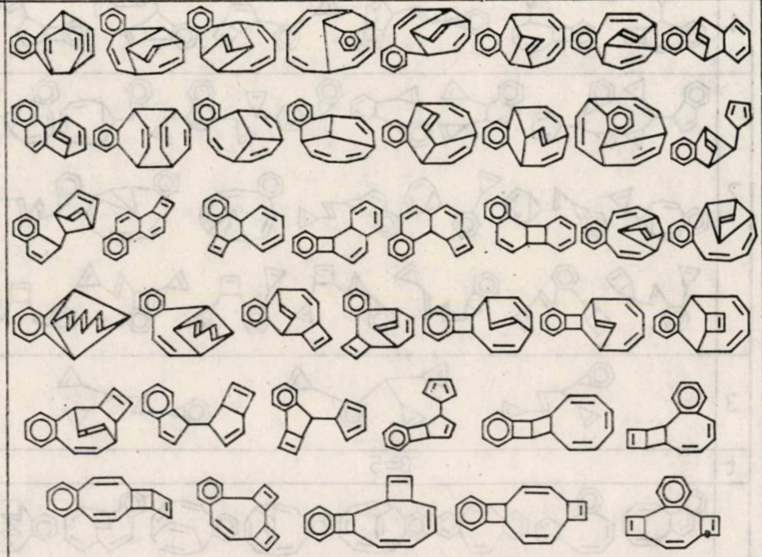
1	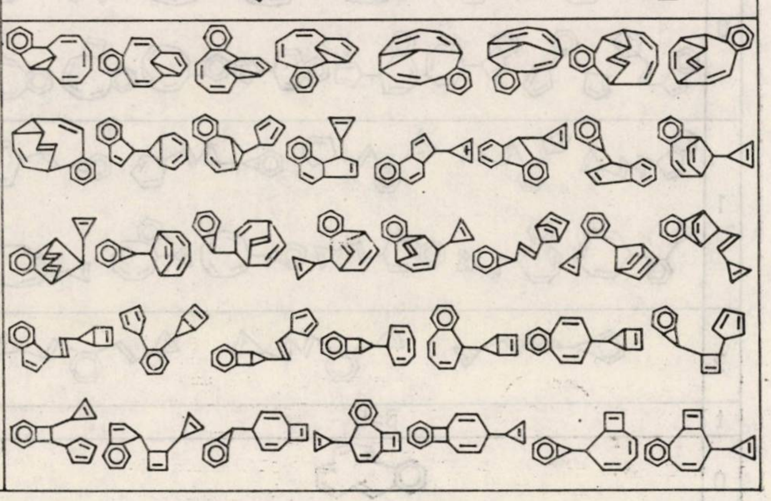

Table 3 (Continued)

t	β=4
1	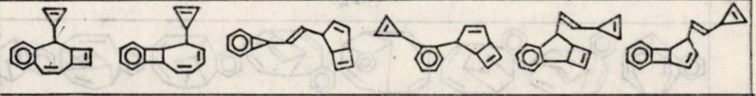
2	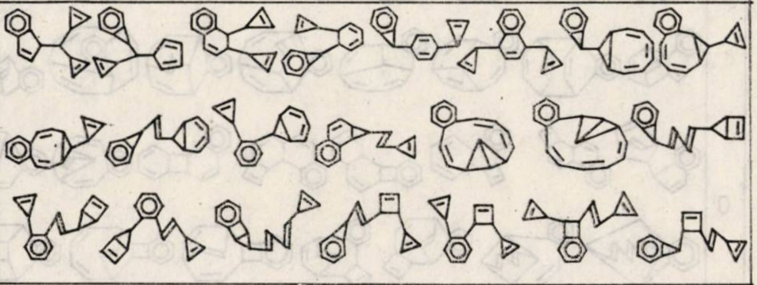
3	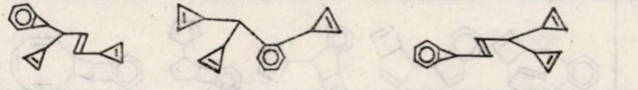
t	β=5
0	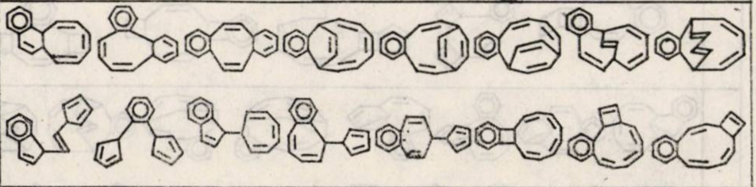
1	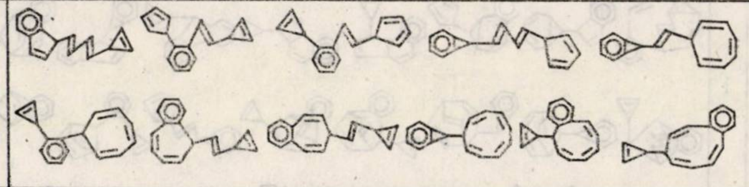
2	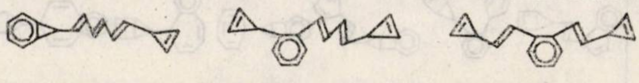
t	β=6
0	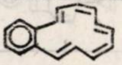

Table 4

Graphs of dibenzo-$(CH)_{12}$ valence isomers

t	β=2
0	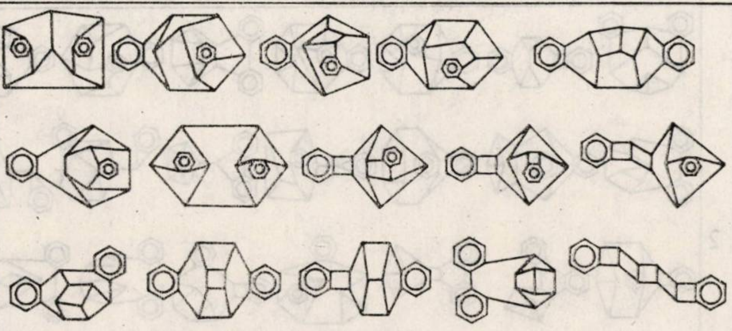
1	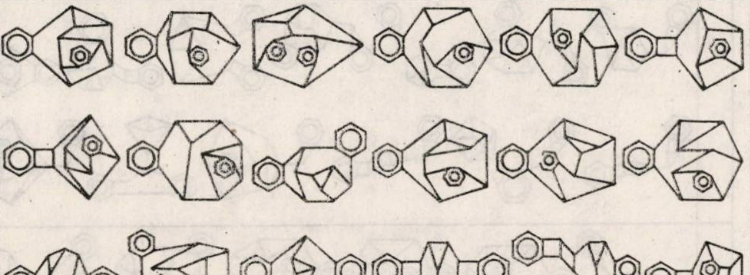
2	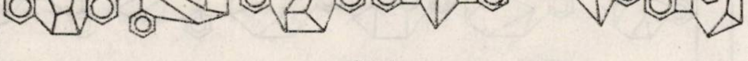

Table 4 (Continued)

t	β=2
2	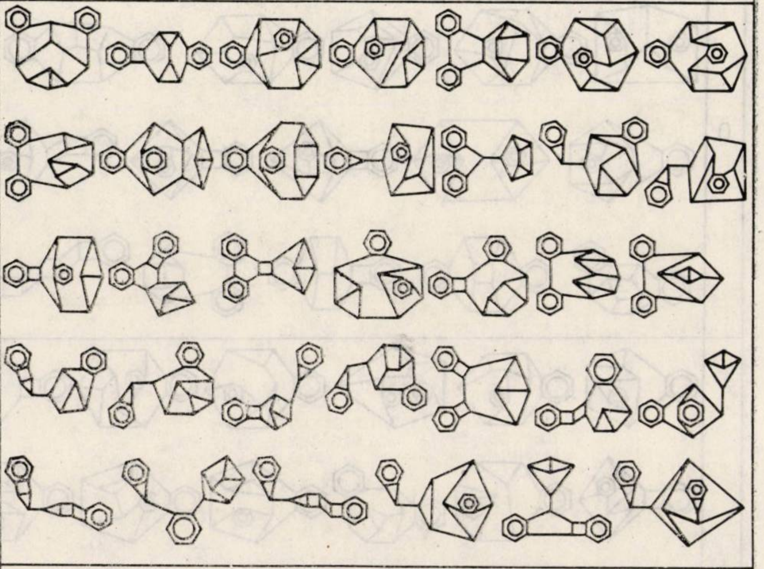
3	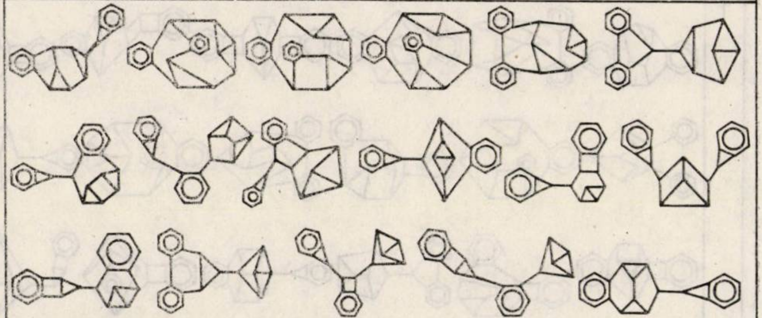
4	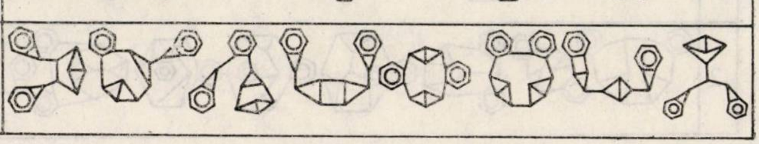

Table 4 (Continued)

t	β=3
0	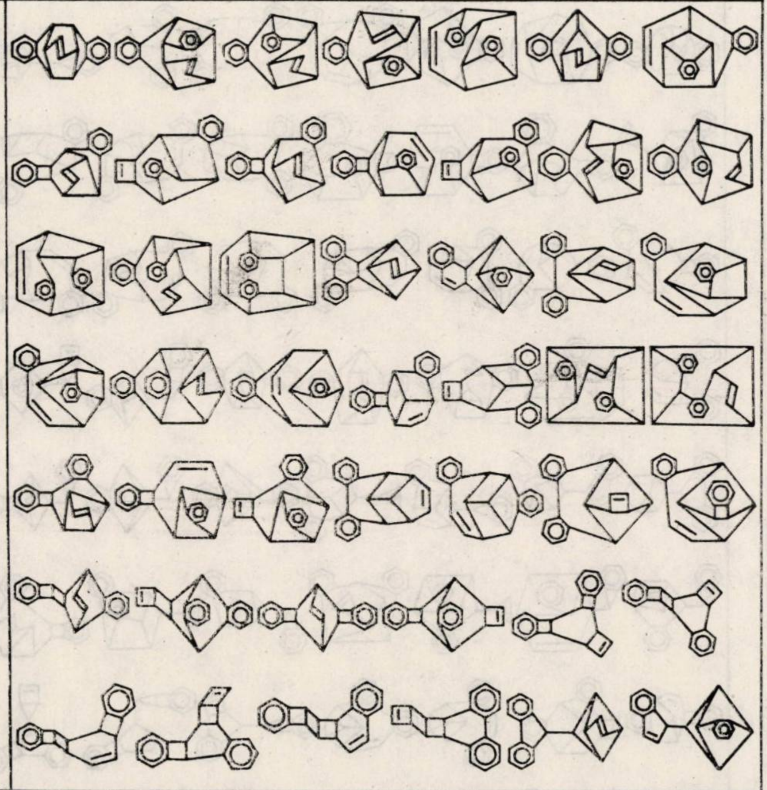
1	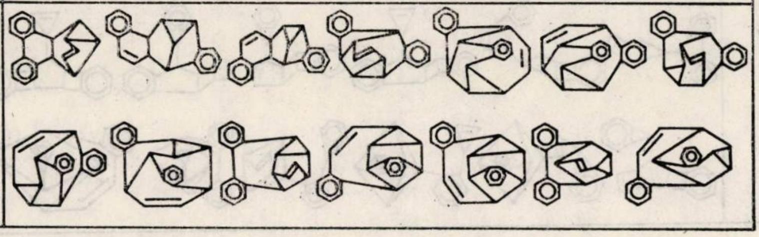

Table 4 (Continued)

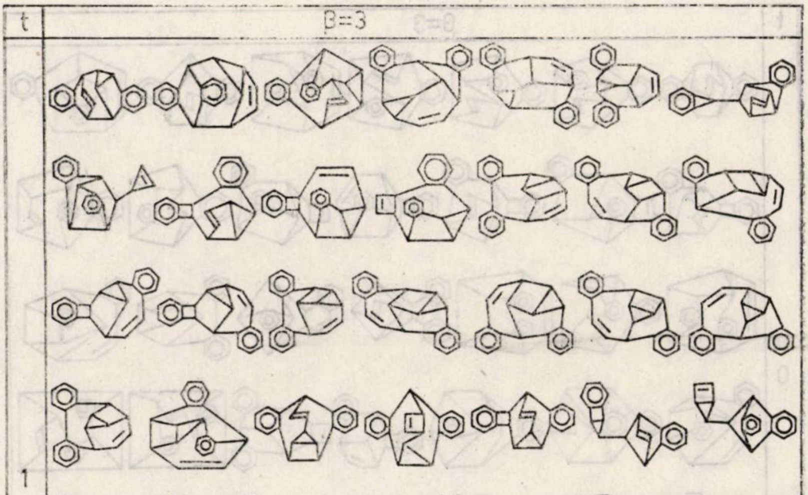

Table 4 (Continued)

t	β=3
2	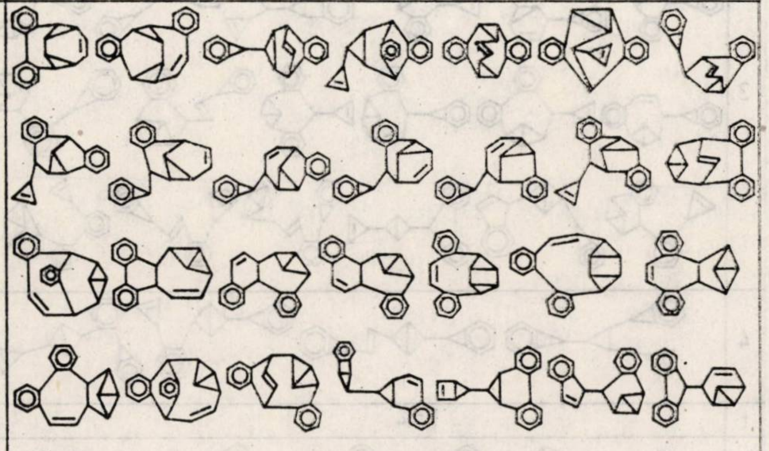

Table 4 (Continued)

t	β=3
3	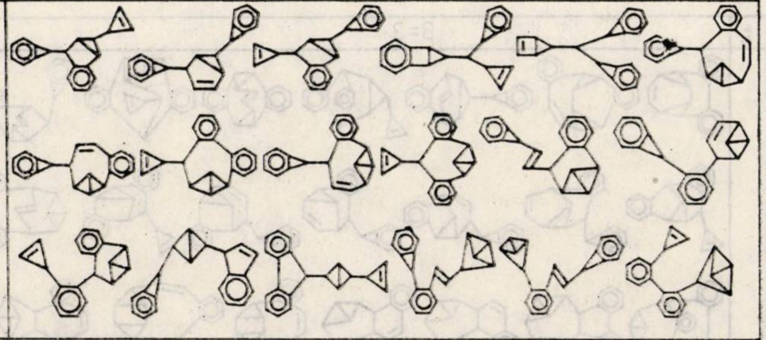
4	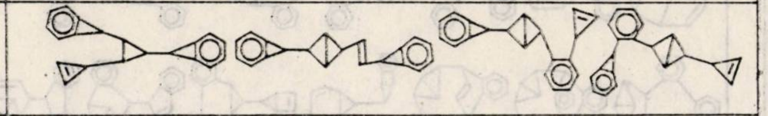
t	**β=4**
0	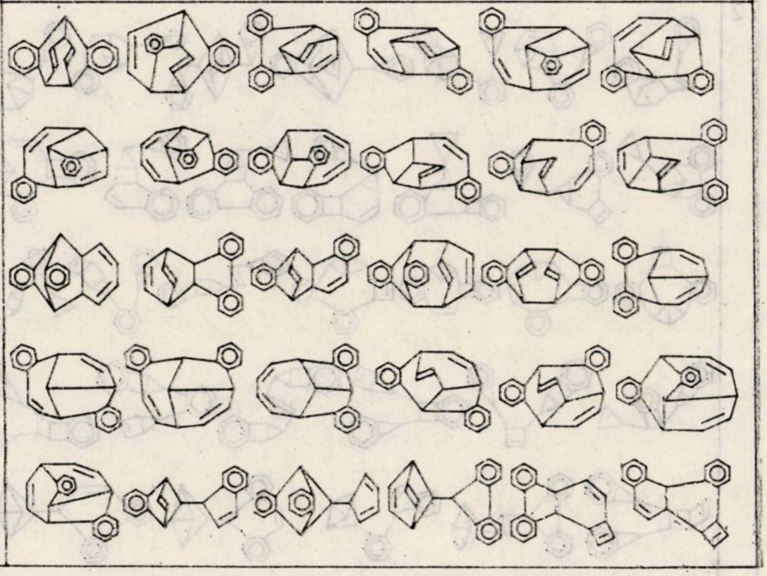

Table 4 (Continued)

t	β=4
0	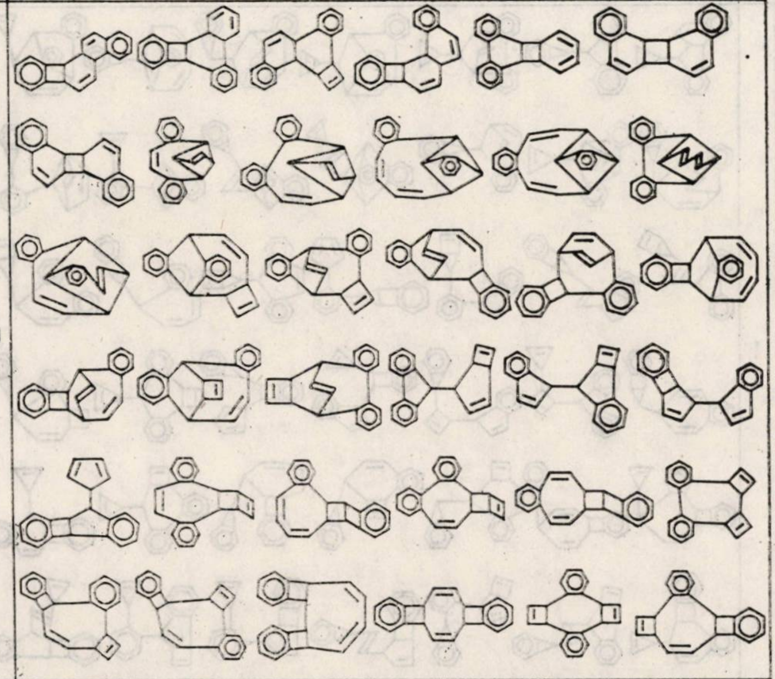
1	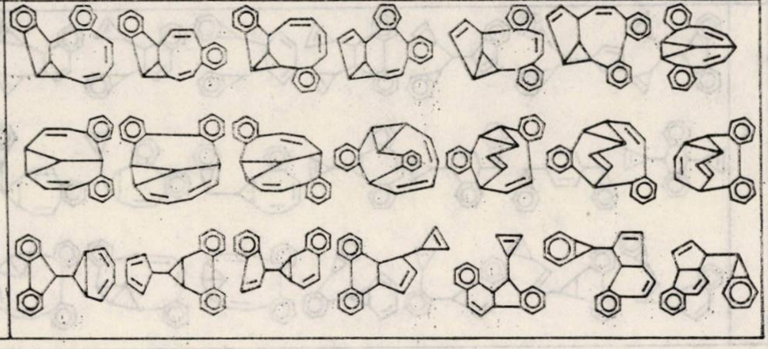

Table 4 (Continued)

t	β=4
1	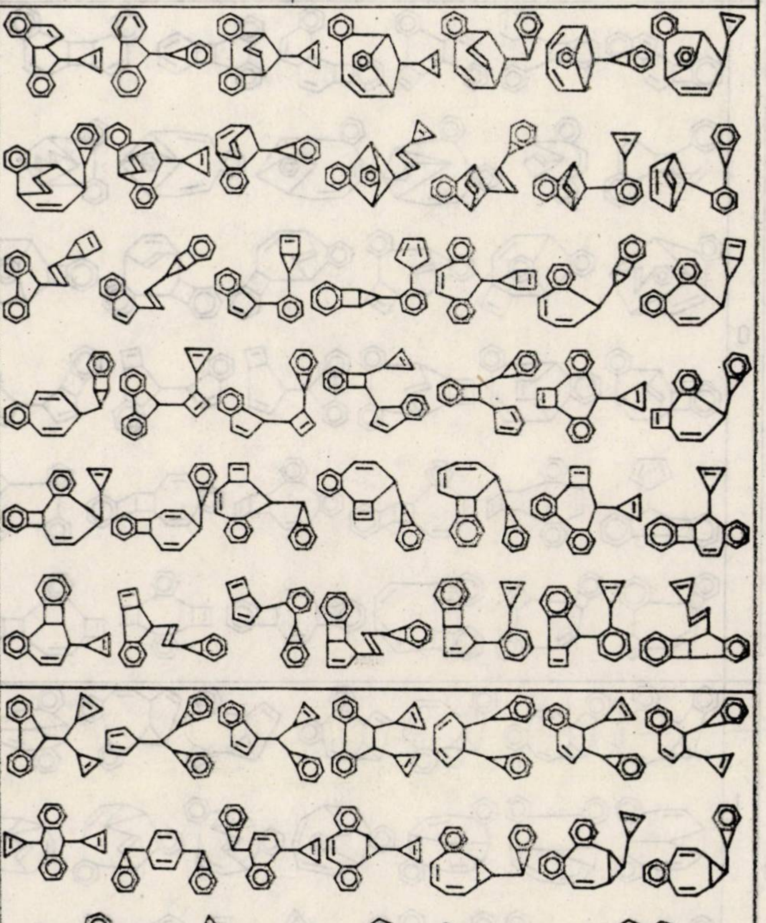
2	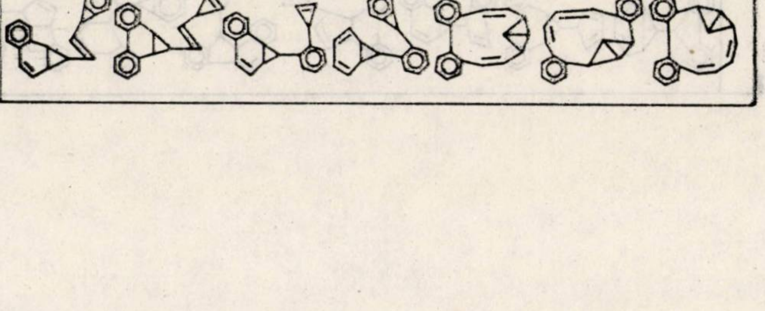

Table 4 (Continued)

t	β=4
2	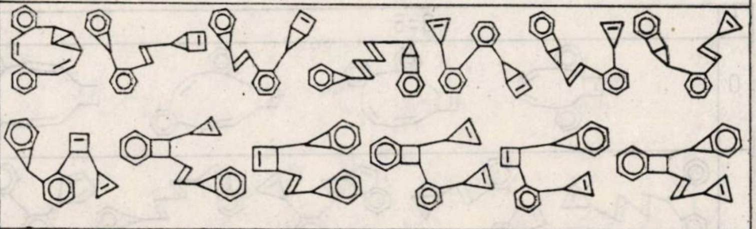
3	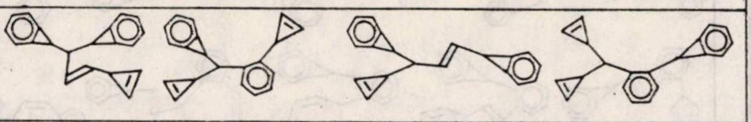
t	β=5
0	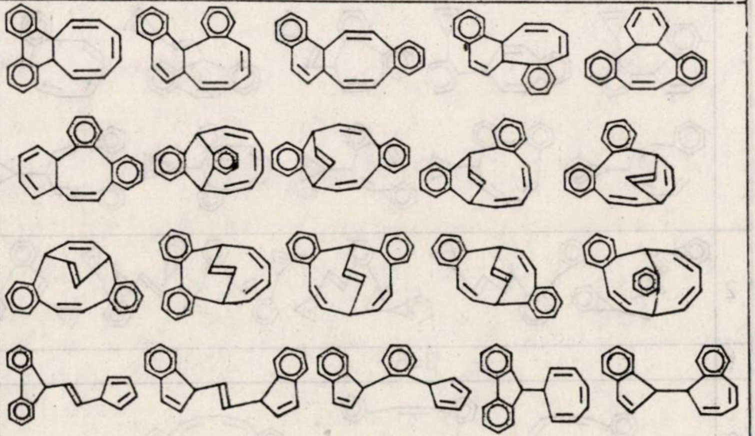

Table 4 (Continued)

t	β=5
0	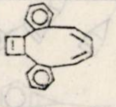 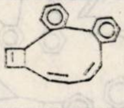 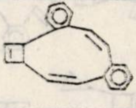 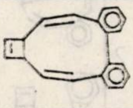
1	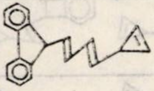 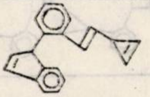 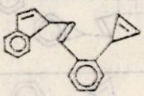 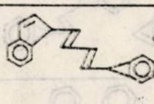 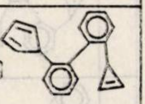 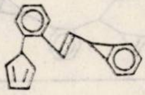 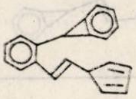 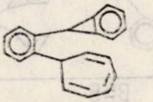 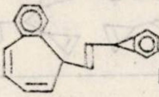 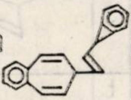 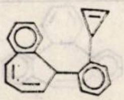 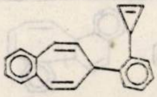 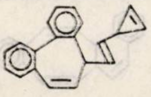 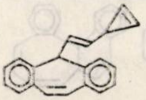 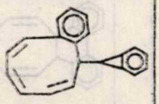 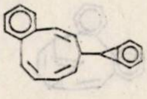 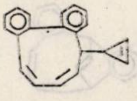 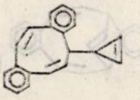 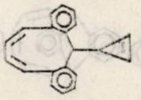 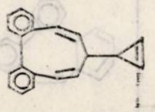
2	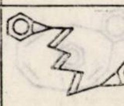 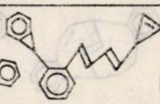 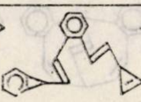 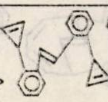 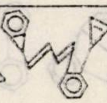 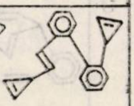
t	**β=6**
0	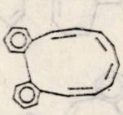 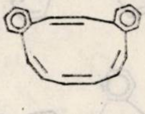 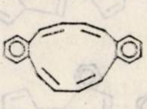

Table 5

Graphs of tribenzo-$(CH)_{12}$ valence isomers.

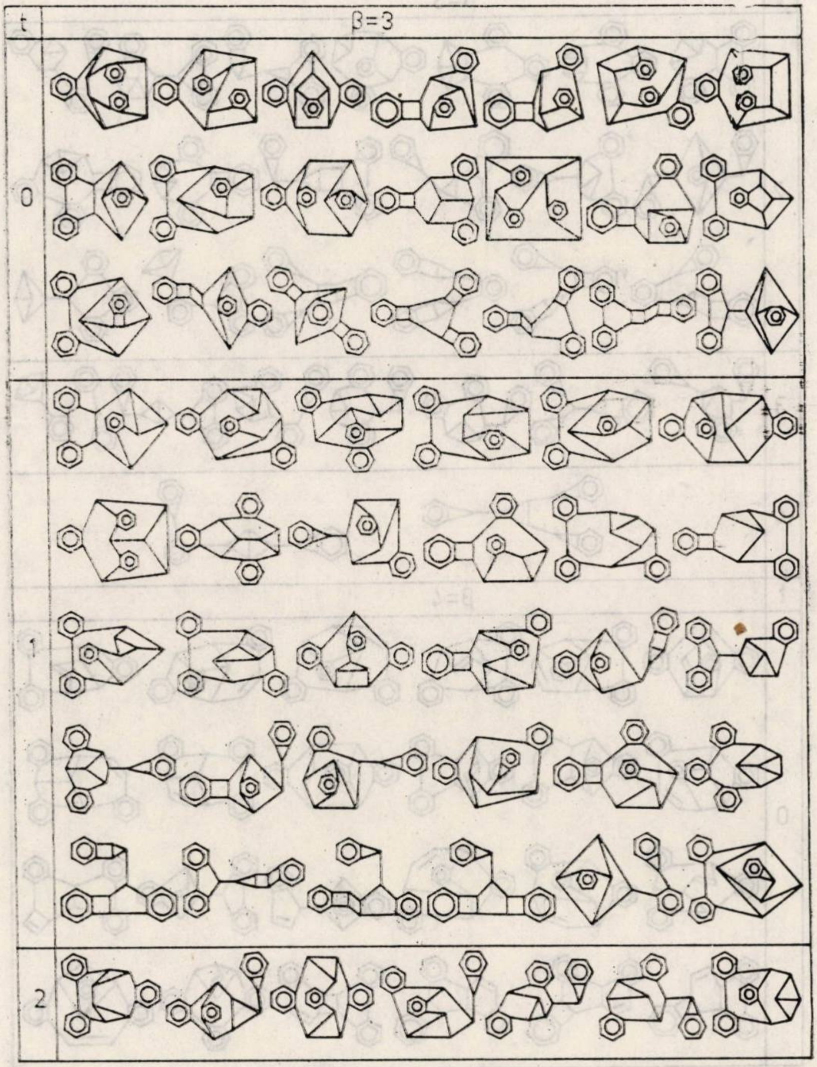

Table 5 **(Continued)**

t	β=3
2	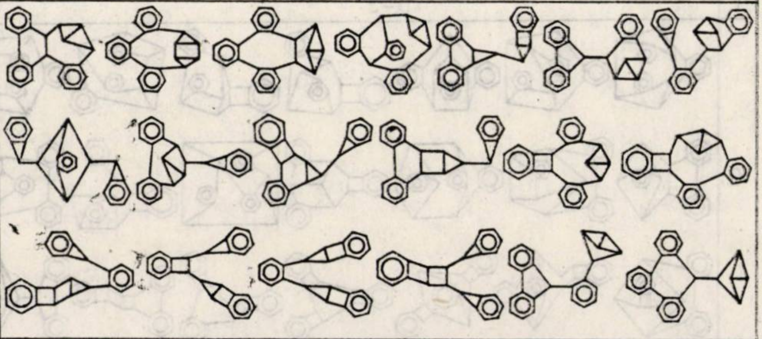
3	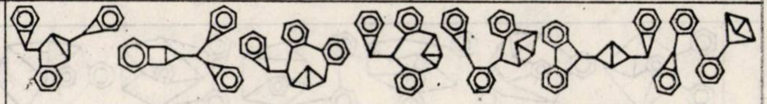
4	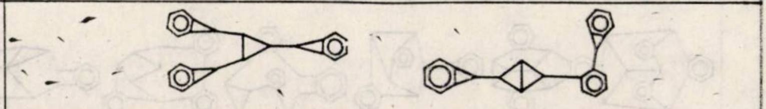
t	**β=4**
0	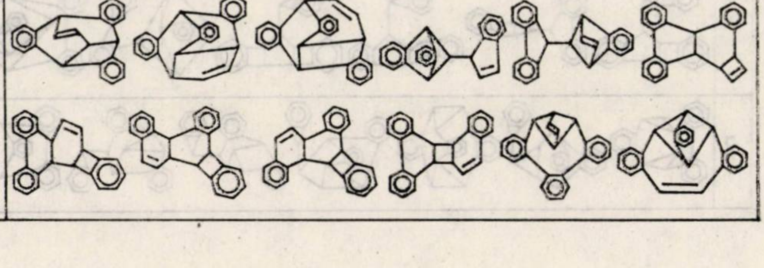

Table 5 (Continued)

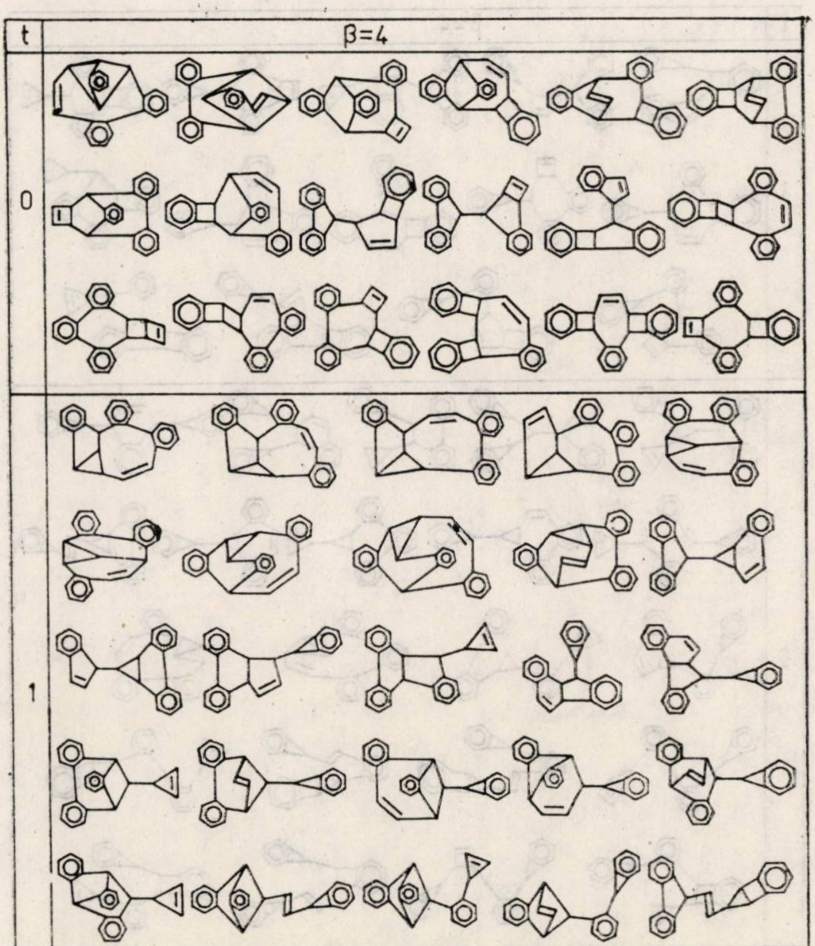

Table 5 (Continued)

t	β=4
1	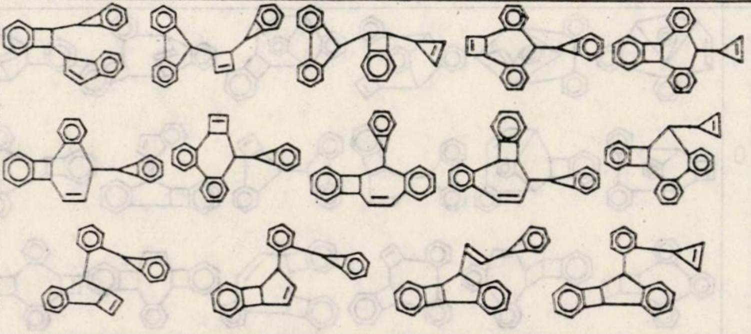
2	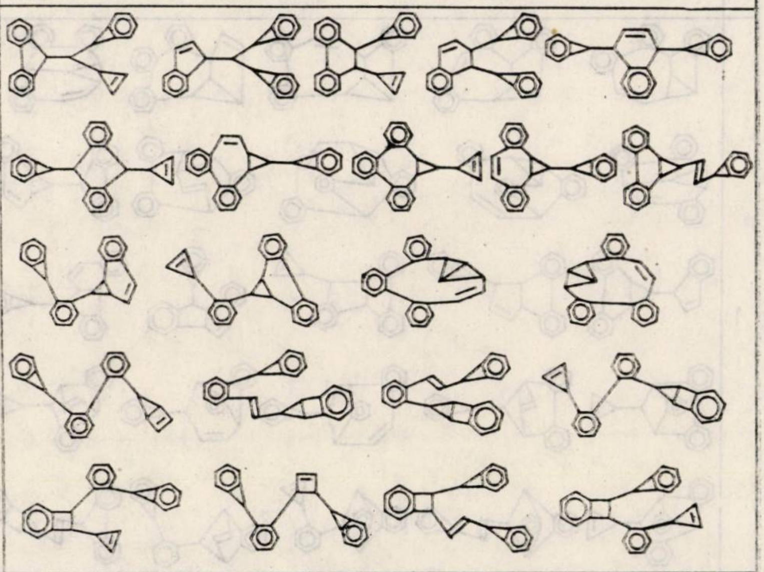
3	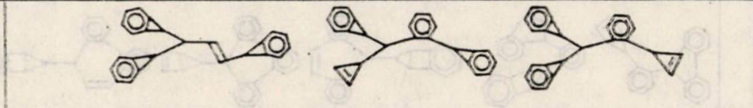

Table 5 (Continued)

t	β=5
0	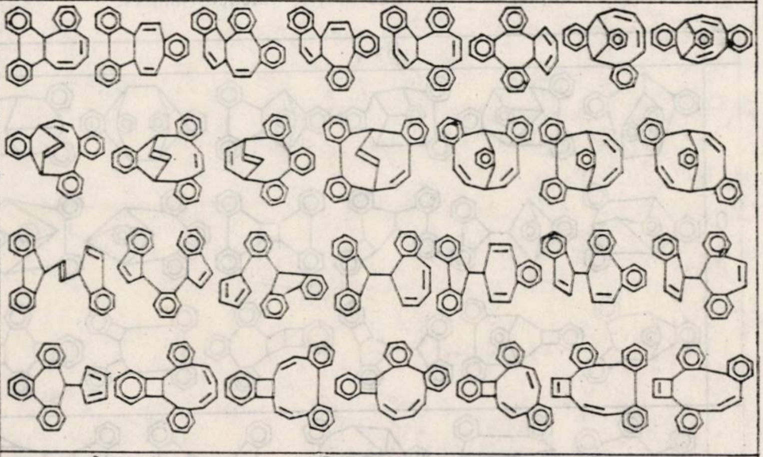
1	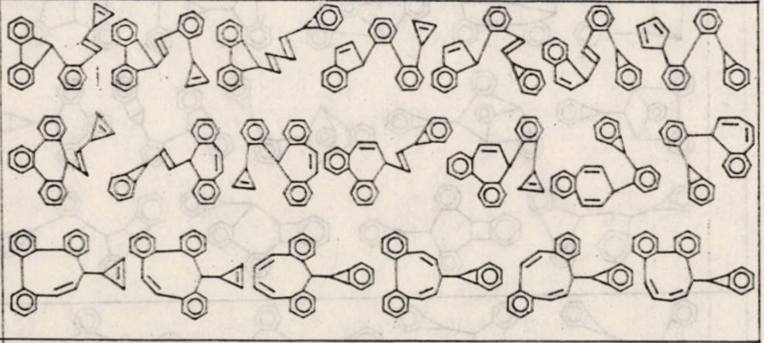
2	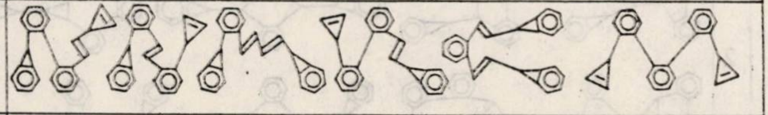
t	β=6
0	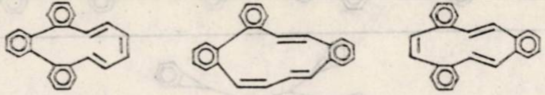

Table 6

Graphs of tetrabenzo-$(CH)_{12}$ valence isomers.

t	$\beta=4$
0	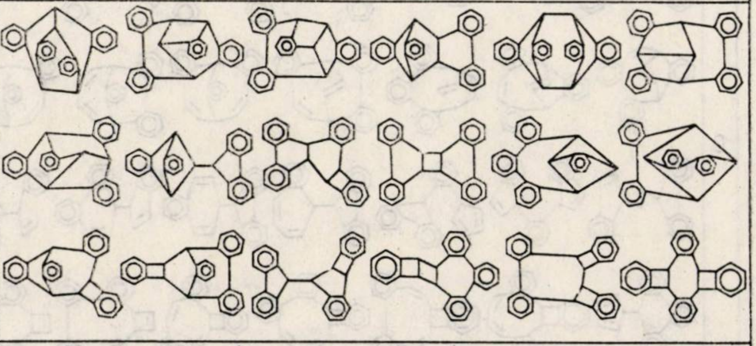
1	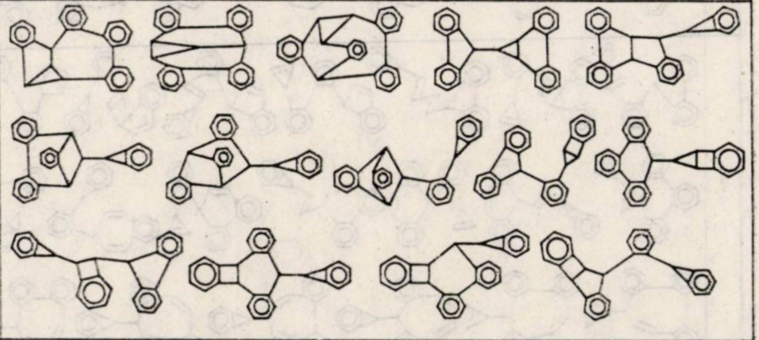
2	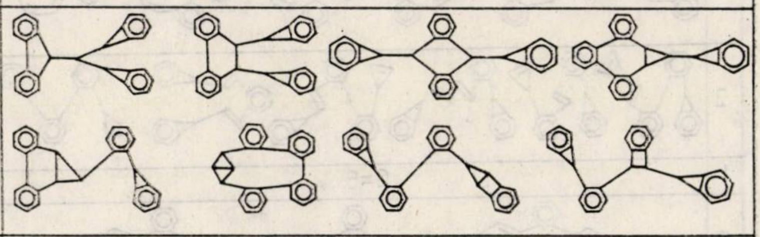
3	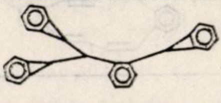

Table 6 (Continued)

t	β=5
0	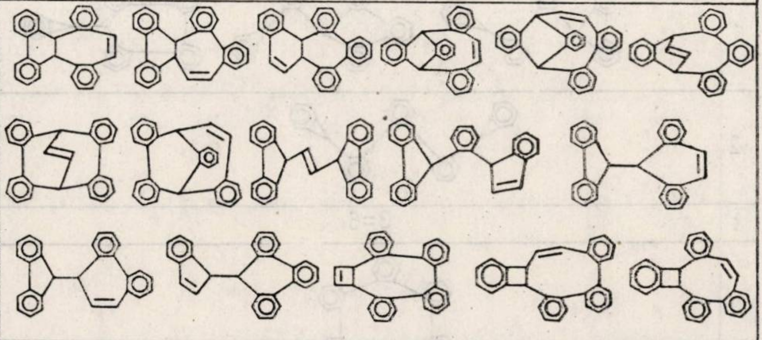
1	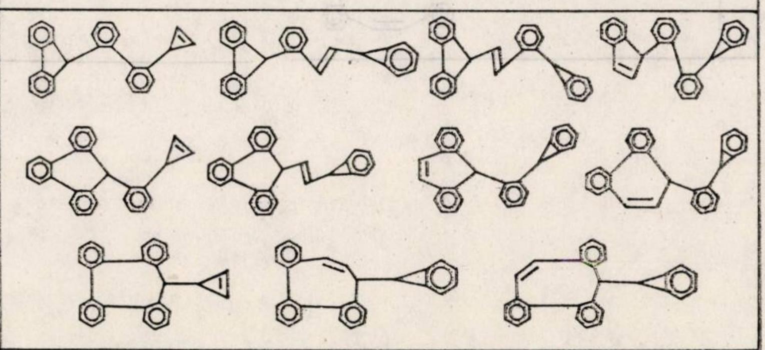
2	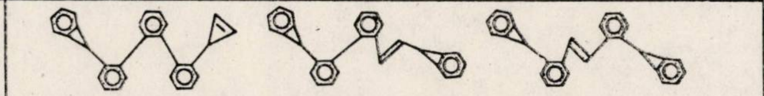
t	β=6
0	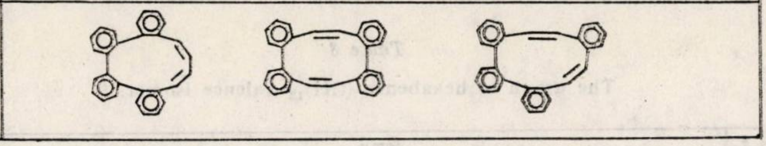

Table 7

Graphs of pentabenzo-$(CH)_{12}$ valence isomers.

t	β=5
0	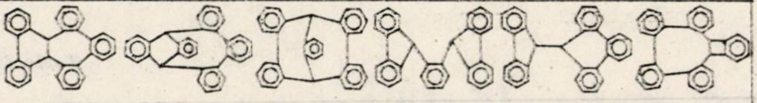
1	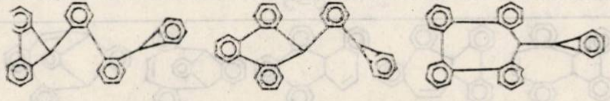
2	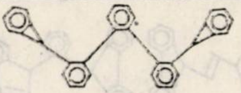
t	β=6
0	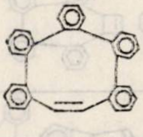

Table 8

The graph of hexabenzo-$(CH)_{12}$ valence isomer.

t	β=6
0	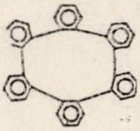

Table 9

Known monobenzoderivatives of valence isomers of [12]annulene (first denomination is according to the IUPAC, the other ones according to *Chem. Abstr.*, etc.)

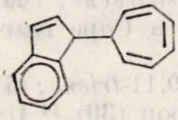 1	1-(Cyclohepta-2,4,6-trien-1-yl)indene or : Benzodihydrosesquifulvalene	1966 Prinzbach et al.[12]
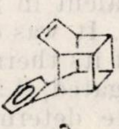 2	Benzo[*d*]pentacyclo[6.4.0.$0^{2,7}$.$0^{3,12}$.$0^{6,9}$]-dodeca-4,10-diene or : 1,2,2a,5,6,10b-Hexahydro-1,6,2,5-ethanediylidenebenzo[*a*]cyclobuta[*c*]cyclooctene	1979 Kwok et al.[13a]
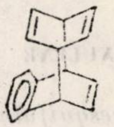 3	Benzo[*c*]tricyclo[4.2.2.$2^{2,5}$]dodeca-3,7,9,11-tetraene or : 5,6,9,10-Tetrahydro-5,10 : 6,9-diethenobenzocyclooctene	1979 Kwok et al.[13a]
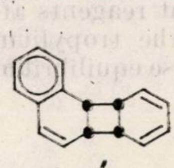 4	*cis, syn, cis*-Benzo[*c*]tricyclo[6.4.0.$0^{2,7}$]-dodeca-3,5,9,11-tetraene or : 6a,6b,10a,10b-Tetrahydrobenzo[*a*]-biphenylene	1980 Grimme and Koser[14]
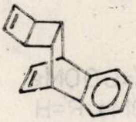 5	*cis, anti, cis*-Benzo[*i*]tetracyclo-[6.2.2.$0^{2,7}$.$0^{3,6}$]dodeca-4,9,11-triene	1980 Grimme and Koser[14]
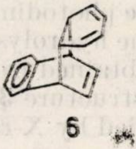 6	Benzo[*i*]tricyclo[6.2.2.$0^{2,7}$]dodeca-3,5,9,11-tetraene or : 4a,9,9a,10-Tetrahydro-9,10-ethenoanthracene	1980 Grimme and Koser[14]

Benzo[c]*tricyclo*[*4.2.2.2* ^{2,5}] *dodeca-3,7,9,11-tetraene; (5,6,9,10-Tetrahydro-5,10 : 6,9-diethenobenzocyclooctene)*; (**3**) is formally a [2+2] cycloadduct of benzene with naphthalene and has no known non-annelated correspondent. It was obtained from the benzoderivative **2** via its rhodium complex. [13a] Thermally **2** affords **4**. [13a]

cis, syn, cis-*Benzo*[c]*tricyclo*[6.4.0.0 ^{2,7}]*dodeca-3,5,9,11-tetraene; (6a, 6b, 10a, 10b-Tetrahydrobenzo*[a]*biphenylene;* (**4**) results by a Cope rearrangement of **3**. [13a]

cis, anti, cis-*Benzo*[i]*tetracyclo*[*6.2.2.0* ^{2,7}. 0^{3,6}]*dodeca*-4,9,11-*triene;* (**5**) has been obtained from *anti*-benzo Nenitzescu's hydrocarbon (**30**). [14] Its iron-carbonyl complex is also known. [14]

Benzo[i]*tricyclo*[*6.2.2.0* ^{2,7}]*dodeca-3,5,9,11-tetraene; (4a,9,9a,10-Tetrahydro-9,10-ethenoanthracene)*; (**6**) can be formally considered as a Diels-Alder adduct of naphthalene and benzene. It has no equivalent in the non-annelated series of the valence isomers of [12]annulene. It was obtained from the ironcarbonyl complex of **5**. [14] The kinetics of its thermal decomposition at 0° to naphthalene and benzene was investigated, [14] and the activation parameters for the [4+2] cycloreversion were determined, [15] a synchronous mechanism being proposed. [15] The 1,3-dienic structure of **6** explains the ready cycloaddition at −30° with 4-ethyl-1,2,4-triazolinedione. [14]

KNOWN DIBENZODERIVATIVES OF VALENCE ISOMERS OF [12]ANNULENE

9-(Cyclohepta-2,4,6-trien-1-yl)fluorene; (Dibenzodihydrosesquifulvalene); (**8**) results on treatment of fluorenyl-sodium with tropylium bromide. [16] Compound **8** is a solid with m.p. 108—109° and characteristic **UV**, IR and NMR spectra. [16] Its dehydrogenation using different reagents affords dibenzosesquifulvalene (**31**). [16] The fluoroborate of the tropylium derivative **32** was obtained starting from **8**, [16] and the acid-base equilibrium **32** ⇄ **31** was studied. [16]

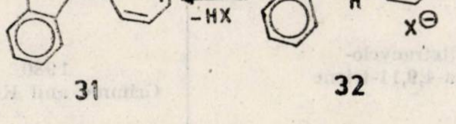

31

32

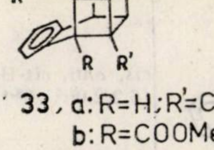

33, a: R=H; R'=COOMe
b: R=COOMe; R'=H

Dibenzo[d, j]*pentacyclo*[*6.4.0.0* ^{2,7}. *0* ^{3,12} · *0*^{6,9}]*dodeca-4,10-diene; (1,2, 2a,7,8,12b-Hexahydro-1,8,2,7-ethanediylidenedibenzo* [a,e]*cyclobuta*[c]*cyclooctene)*; (**9**) was obtained [17] from the early known naphthalenic photodimer **33** [18] on removal of carbomethoxy group by sequential alkaline hydrolysis, brominative decarboxylation and debromination; [17] **9** was obtained from another valence isomer **10**, on irradiation in acetone. [17] The structure **33a** (in agreement with UV, ^{1}H—NMR and MS data [18]) was certified by X-ray

Table 10

Known dibenzoderivatives of valence isomers of [12]annulene (first denomination is according to the IUPAC, the other ones according to *Chem. Abstr.*, etc.)

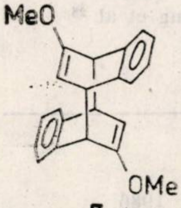 7	*anti*-Dibenzo[*c*, *g*]tricyclo[4.2.2.2^{2,5}]dodeca-3,7,9,11-tetraene or : *anti*-5,6,11,12-Tetrahydro-5,12 : 6,11-diethenodibenzo[*a*, *e*]cyclooctene or : *trans*-1,4 : 1′,4′-dinaphthalene	1963 Bradshaw and Hammond[22]
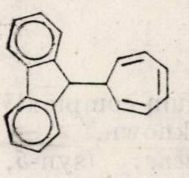 8	9-(Cyclohepta-2,4,6-trien-1-yl)fluorene or : Dibenzodihydrosesquifulvalene	1966 Prinzbach et al.[16]
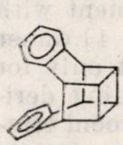 9	Dibenzo[*d*, *j*]pentacyclo[6.4.0.0^{2,7}.0^{3,12}.0^{6,9}]-dodeca-4-10-diene or : 1,2,2a,7,8,12b-Hexahydro-1,8,2,7-ethanediylidenedibenzo[*a*, *e*]cyclobuta[*c*]-cyclooctene	1981 Tobe et al.[17]
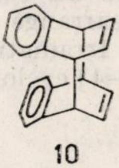 10	*syn*-Dibenzo[*c*, *g*]tricyclo[4.2.2.2^{2,5}]dodeca-3,7,9,11-tetraene or : *syn*-5,6,11,12-Tetrahydro-5,12 : 6,11-diethenodibenzo[*a*, *e*]cyclooctene or : *syn*-1,4 : 1′,4′-Dinaphthalene	1981 Tobe et al.[17]
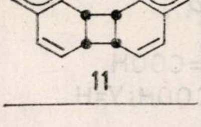 11	*cis*, *syn*, *cis*-Dibenzo[*c*, *k*]tricyclo-[6.4.0.0^{2,7}]dodeca-3,5,9,11-tetraene or : 6a,6b,12b,12c-Tetrahydrodibenzo[*a*, *i*]-bipenylene	1981 Tobe et al.[17]
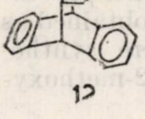 12	Dibenzo[*i*, *l*]tricyclo[6.2.2.0^{2,7}]dodeca-3,5,9,11-tetraene or : 4a,9,9a,10-Tetrahydro-9,10[1′, 2′]-benzenoanthracene	1982 Yang et al.[25]

Table 10 (Continued)

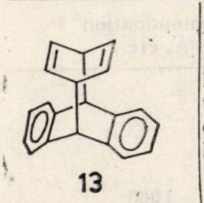 **13**	Dibenzo[*c, m*]tricyclo[4.2.2.2^{2,5}]dodeca-3,7,9,11-tetraene or : 9,10,11,14-Tetrahydro-9,10[1′, 4′]-benzenoanthracene	1982 Yang et al. [25]
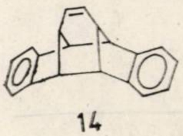 **14**	Dibenzo[*b, f*]tetracyclo[6.4.0.0^{4,12} . 0^{5,9}]-dodeca-2,6,10-triene or : 5, 6, 11, 12-Tetrahydro-5,12,6,11-[2]-butene[1,4]diylidenedibenzo[*a, e*]cyclooctene	1986 Prinzbach and co-workers [29]

analysis. [19] The valence isomerisation of **9** to **10** via a rhodium complex[17] and the thermal valence isomerisation of **33b** to **34**, [18] are known.

syn-*Dibenzo*[c, g]*tricyclo*[*4.2.2.2* ^{2,5}]*dodeca-3,7,9,*11-*tetraene;* (syn-*5, 6,11,12-Tetrahydro-5,12 : 6,11-diethenodibenzo*[a, e]*cyclooctene);* (syn-*1,4 : 1′,4′-dinaphthalene);* (**10**) is unknown as non-benzoannelated compound, and it was obtained from the rhodium complex of **9** on treatment with triphenylphosphite. [17] Compound **10** can be considered as [4+4] dimer of naphthalene and the dimerization was early performed, but only for the case of 2-substituted naphthalenes, leading to the corresponding derivatives **35**. [20,21] The *cis*-type naphthalenic dimer **10** affords at room temperature a Cope rearrangement, giving rise to another valence isomer **11**. [17] The remarkably low activation energy for this rearrangement is most probably due to the removal of repulsive interactions in the boat-shaped transition state. The **35b** derivative was shown to rearrange on heating to the valence isomeric derivative derived from **11**. [21] Irradiation of **10** in acetone gave a 2 : 1 mixture of naphthalene (the [4+4] cycloreversion product) and the [2+2] cycloadduct **9**. [17]

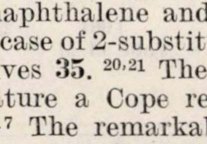

34, R=COOMe

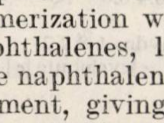

35, a: R=CN
b: R=OMe

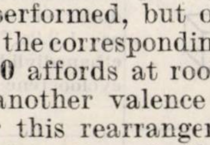

36, a: X=Y=COOH
b: X=COOH; Y=H

anti-*Dibenzo*[c, g]*tricyclo*[*4.2.2.2* ^{2,5}] *dodeca-3,7,9,11-tetraene;* (*5,6,11, 12-Tetrahydro-5,12 : 6,11-diethenodibenzo*[a, e]*cyclooctene);* (anti-*p,p′-dinaphthalene);* (**7**) is known only as derivatives, and it was first obtained as dimethoxy derivative. [22] Later other similar derivatives where synthetised.[23,24] Heating of **7** produces decomposition to monomeric 2-methoxyanphthalene. [22]

cis, syn, cis-*Dibenzo*[c, k]*tricyclo*[*6.4.0.0* ^{2,7}] *dodeca-3,5,9,11-tetraene; (6a,6b, 12b, 12c-Tetrahydrodibenzo* [a, i]*-biphenylene)*; (**11**) results at room temperature in a very low activation energy Cope rearrangement of **10.**[17] Derivative **34** was previously obtained on heating of the corresponding derivative **33a.**[18] Derivative **34** undergoes thermal or photochemical decomposition to dimethyl naphthalene-1,8-dicarboxylate. [18]

Dibenzo[i, l]*tricyclo*[*6.2.2.0* ^{2,7}]*dodeca-3,5,9,11-tetraene; (4a,9,9a,10-Tetrahydro-9,10*[*1',2'*]*benzenoanthracene)*; (**12**) which can be considered as [$4\pi_s + 2\pi_s$] cyclodimer of anthracene and benzene was synthetised in a photocycloaddition of substituted 1,3-cyclohexadiene to anthracene, followed by conversion of a 1,3-dioxolane moiety into a double bond, by base-induced fragmentation.[25] Thermally allowed concerted cycloreversion led to anthracene and benzene. [25,26] The same products of decomposition were obtained on irradiation of **12.** [26] The entropy of activation in the thermal dissociation of **12** is negative, [26] but photolysis at 0° yielded excited anthracene in a low but appreci able efficiency. [25,26] Activation parameters were determined for the [4+2] cycloreversion of **12.** [27]

Dibenzo[c, m]*tricyclo*[*4.2.2.2* ^{2,5}]*dodeca-3,7,9,11-tetraene; (9,10,11,14-Tetrahydro-9,10*[1', 4']*-benzenoanthracene)*; (**13**), which can be considered as [$4\pi_s + 4\pi_s$] cyclodimer of anthracene and benzene, results in the photocycloaddition of substituted 1,3-cyclohexadienes to anthracene, together with **12.** [25] Both thermal and photochemical cycloreversions of **13** led to benzene and anthracene, as in the case of the compound **12.** [25,26] Kinetic data clearly indicated that the thermal cycloreversion of **13** is a stepwise process. [25] In spite of favorable kinetic and thermodynamic reported parameters, the thermal dissociation is not chemiluminescent. [26] The quantum yield of anthracene fluorescence showed that the photochemical conversion of excited **13** to excited anthracene is a highly efficient process. [25,26] These data clearly demonstrate orbital symmetry control of both the ground-and excited-state reactions. Although the thermolysis of the parent hyrocarbon **13** was not detectably chemiluminescent, thermolyses of those derivatives bearing an electron-withdrawing carboxyl function at the bridgehead positions (**36**) are chemiluminescent. [28] Neither **13** nor **12** have an equivalent in the non-benzoannelated series of valence isomers of [12]annulene.

Dibenzo[b, f]*tetracyclo*[*6.4.0.0* ^{4,12}. *0* ^{5,9}]*dodeca-2,6,10-triene*; (*5,6,11,12-Tetrahydro-5,12,6,11-*[2]*butene-*[*1,4*]*-diylidenedibenzo*[a,e]*cyclooctene)*; (**14**) has no equivalent in the non-benzoannelated series and its existance was reported, [29] without any information concerning its synthesis. Irradiation of **14**, 48 hours at 20° afforded 10% phenanthrene and benzene. [29]

KNOWN TRIBENZODERIVATIVES OF VALENCE ISOMERS OF [12]ANNULENE

E,E,E-Tribenzo[a, e, i][12]*annulene;* (trans, trans, trans-*Tribenzo* [a, e, i]*cyclododecene)*; (**15**) was first obtained by Staab et al. [31,32] in a Wittig reaction of *o*-phthaldialdehyde with the ylide of 2,2'-bis(bromomethyl)-*trans*-stilbene. Alternative syntheses consist in a bromination/ /dehydrobromination sequence [37] applied to hexahydrotribenzo[*a*, *e*, *i*]-[12]annulene [30] and a triple Wittig reaction involving the ylide of *o*-bro-

Table 11

Known tribenzoderivatives of valence isomers of [12]annulene (first denomination is according to the IUPAC, the other ones according to *Chem. Abstr.*, etc.)

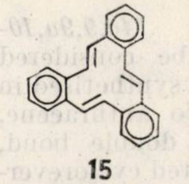 **15**	E,E,E-Tribenzo[*a, e, i*][12]annulene or : *trans, trans, trans*-Tribenzo[*a, e, i*]-cyclododecene or : *trans, trans, trans*-Tribenzo[*a, e, i*]-cyclododeca-1,3,5,7,9,11-hexaene	1966 Staab et al. [31]
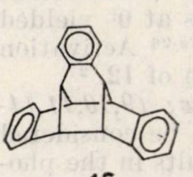 **16**	Tribenzo[*b, f, j*]tetracyclo$[6.4.0.0^{4,12}.0^{5,9}]$-dodeca-2,6,10-triene	1966 Staab et al. [31]
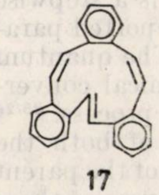 **17**	Z,Z,E-Tribenzo[*a, e, i*][12]annulene or : *cis, cis, trans*-Tribenzo[*a, e, i*]cyclododecene or : *cis, cis, trans*-Tribenzo[*a, e, i*]cyclododeca-1,3,5,7,9,11-hexaene	1971 Staab et al. [32]
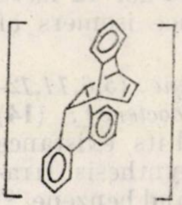 **18**	Tribenzo[*c, e, i*]tricyclo$[6.2.2.0^{2,7}]$-cyclododeca-3,5,9-triene or : 9,10,13,14-Tetrahydro-9,14-ethenobenzo-[*b*]triphenylene	1977 Ciorănescu and co-workers [37]
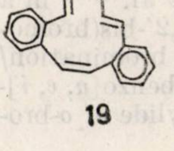 **19**	Z,E,E-Tribenzo[*a, e, i*][12]annulene or : *cis, trans, trans*-Tribenzo[*a, e, i*]-cyclododecene or : *cis, trans, trans*-Tribenzo[*a, e, i*]-cyclododeca 1,3,5,7,9,11-hexaene	1977 Ciorănescu and co-workers [38]

momethylbenzaldehyde. [33] Formation of traces of **15** during the electrochemical reduction of 1,2-bis(dibromomethyl)benzene was also mentioned. [34] The *trans*, *trans*, *trans*-isomer **15** is a colorless solid (m.p. 219—220°), whose spectral data [32] (IR absorptions at 966 and 978 cm^{-1}, UV absorption at 267 nm, and ^{1}H—NMR singlet at 7.13 ppm for definic protons) prove the nonplanarity of the molecule, i.e. the reduced conjugation between double bonds and benzenic rings. The ^{1}H—NMR spectrum is in agreement with a rapid interconversion of two conformations, exchanging internal ring protons with the external ones. It seems that the ring inversion barrier is sufficiently low, since no temperature dependence of this NMR spectrum is observed. In neither of the two conformations can the conjugation exceed the steric effects opposing the planarity. The ESR spectrum of radical anions of **15** was investigated [35] and compared with that of stilbene. [36] Concerning the chemical behavior of **15**, the hydrogenation of olefinic double bonds, [31,32] the significant thermal stability [37] and the photochemical valence isomerization into **16** [37] proceeding probably via the elusive *cis,trans,trans*-isomer **19**, may be mentioned.

Z,Z,E-Tribenzo[a, e, i][*12*]*annulene;* (cis, cis, trans-*Tribenzo* [a, e, i]-*cyclododecene);* (**17**) was obtained on hydrogenation of hexahydrotribenzo-[12]annulene. [32] Its ^{1}H—NMR data ($\delta = 6.45$ ppm for *trans*-vinylic H, and 6.9 ppm for *cis*-vinylic H) support the proposed nonplanar structure. [32]

Z,E,E-Tribenzo[a, e, i][12]*annulene;* (cis, trans, trans-*Tribenzo*[a,e,i]-*cyclododecene);* (**19**) could not be isolated, but it was suggested to appear as reactive intermediate in the photochemical rearrangement of **15**. [37]

Tribenzo[b, f, j]*tetracyclo*[*6.4.0.0* ^{4,12}. *0*^{5,9}]*dodeca-2,6,10-triene;* (**16**) has no equivalent in the non-benzoannelated series and it was obtained along with **15** from the above-mentioned Wittig reaction between the ylide of 2,2′-bis(bromomethyl)-*trans*-stilbene and *o*-phthaldialdehyde. [31,32] UV irradiation of **15** also affords **16**. [37] Compound **16** is a solid with m.p. 252°. Its photolysis affords phenanthrene and naphthalene, possibly via the nonisolable isomer **18**. [37]

Tribenzo[c, e, i]*tricyclo*[6.2.2.0 ^{2,7}]*cyclododeca-3,5,9-triene;* (*9,10,13,14-Tetrahydro-9,14-ethenobenzo*[b]*triphenylene);* (**18**) has no equivalent in the non-benzoannelated series, and also it was not isolated, but it was proposed as intermediate in the photochemical dissociation of **16** to phenanthrene in a [4+2] retrodiene reaction involving a $[\sigma^2 + \sigma^2]$ mechanism. [37]

KNOWN TETRABENZODERIVATIVES OF VALENCE ISOMERS OF [12]ANNULENE

Z,Z-Tetrabenzo[a, c, g, i][12]*annulene;* (cis, cis-*Tetrabenzo*-[a, c, g,i] *cyclododecene);* (**21**) was first obtained in 1955 by Wittig et al. [38] in the **21a** conformation, together with the *cis*, *trans*-isomer **23**. The multistep synthesis involved the Hofmann degradation of **37**. An alternative synthesis performed by Sondheimer and co-workers [39,40] consists in a Wittig reaction of diphenic dialdehyde with the ylide of 2,2′-bis(bromomethyl)-biphenyl and produced **21a** together with **24**. The same Wittig type reaction performed by Staab et al. [41] yielded only traces of tetrabenzo[12]annulenes, whereas the very same reaction was first employed by Bergman [42,43,44] who obtained two other diastereoisomers **23** and **24**, but no **21a**. Wittig

Table 12

Known tetrabenzoderivatives of valence isomers of [12]annulene (first denomination is according to the IUPAC, the other ones according to *Chem. Abstr.*, etc.)

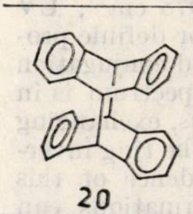 20	Tetrabenzo[*c*, *g*, *j*, *m*]tricyclo$[4.2.2.2^{2,5}]$dodeca-3,7,9,11-tetraene or : 5,6,11,12-Tetrahydro-5,12[1′,2′] : 6,11 [1′,2′]-dibenzenodibenzo[*a*, *e*]cyclooctene or : *meso*-coupled anthracene or : 9,10-dianthracene	1867 Fritzsche[53]
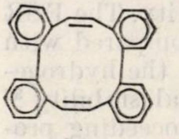 21	Z,Z-Tetrabenzo[*a*, *c*, *g*, *i*][12]annulene or : *cis*, *cis*-Tetrabenzo[*a*, *c*, *g*, *i*]cyclododecene or : *cis*, *cis*-Tetrabenzo[*a*, *c*, *g*, *i*]cyclododeca-1,3,5,7,9,11-hexaene	1955 Wittig et al.[38]
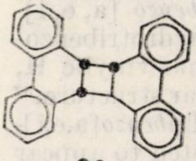 22	*cis*, *syn*, *trans*-Tetrabenzo[*c*, *e*, *i*, *k*]tricyclo-$[6.4.0.0^{2,7}]$dodeca-3,5,9,11-tetraene or : *cis*, *syn*, *trans*-6a, 6b, 12b, 12c-Tetrahydrotetrabenzo[*a*, *c*, *g*, *i*]biphenylene	1955 Wittig et al.[38]
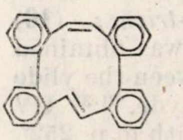 23	E,Z-Tetrabenzo[*a*, *c*, *g*, *i*] [12] annulene or : *cis*, *trans*-Tetrabenzo[*a*, *c*, *g*, *i*]cyclododecene or : *cis*, *trans*-Tetrabenzo[*a*, *c*, *g*, *i*]cyclododeca-1,3,5,7,9,11-hexaene	1955 Wittig et al.[38] 1965 Bergmann[42]
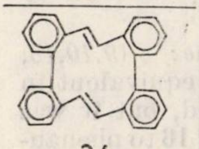 24	E,E-Tetrabenzo[*a*, *c*, *g*, *i*][12] annulene or : *trans*, *trans*-Tetrabenzo[*a*, *c*, *g*, *i*]-cyclododecene or *trans*, *trans*-Tetrabenzo[*a*, *c*, *g*, *i*]-cyclododeca-1,3,5,7,9,11-hexaene	1965 Bergman[42,44]
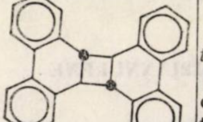 25	*trans*, *anti*, *trans*-Tetrabenzo[*c*,*e*,*i*,*k*]tricyclo-$[6.4.0.0^{2,7}]$dodeca-3,5,9,11-tetraene or : *trans*, *anti*, *trans*-6a,6b,12b,12c-Tetrahydro-tetrabenzo [*a*, *c*, *g*, *i*]biphenylene	1975 Wittig and Skipka[47]
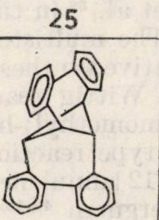 26	Tetrabenzo[*c*,*e*,*i*,*k*]tricyclo$[5.5.0.0^{2,8}]$dodeca-3,5,9,11-tetraene or : 6,7-Dihydro-6,5,7-([1,2]benzeno[1,2]-benzenometheno)-5*H*-dibenzo[*a*, *c*]cycloheptene	1975 Wittig and Skipka[47]

and Skipka showed [47] that the dehydration of the diols **38** affords **21a** or **24** depending on reaction conditions. **21a** was stereoselectively obtained from the corresponding disulfone in a Ramberg-Bäcklund reaction. [46] The formation of **21a** was also reported at the UV irradiation of **23**. [47] The **21a** isomer is a solid with reported uncorrected m.p. 297–298°, [38] 296–297°, [3,940] corrected m.p. 306°, [45] and it was characterized by its IR spectra, [38,48] UV spectra, [38,45] and ^{1}H–NMR spectra. [45] The X-ray analyses [49] show that the double bonds are parallel, at a distance of 3.396 Å, the symmetry of the molecule is approximately C_{2h}, and the C_{12}-ring has a crown shape similar to hexaphenylene. The product of UV irradiation of **21a** is 2 mol of phenanthrene [49] owing to the large distance between the two double bonds which makes impossible the [2+2] cycloaddition. Phenanthrene is also the thermal reaction product of **21a**. [47] Another *cis*, *cis*-isomer with conformation **21b** was suggested to appear too in the **38a**, **b** dehydration [45] but it was later corrected by Bestmann [46] to be tetrahydrophenanthrenofluoranthrene.

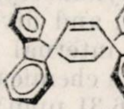
21a

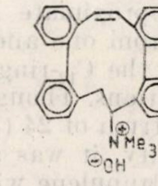

37

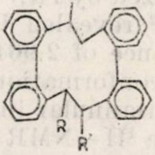

38, a: R=OH; R'=H
b: R=H; R'=OH

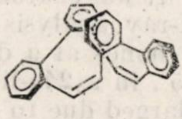
21b

E,Z-Tetrabenzo[a, c, g, i][12]*annulene;* (cis, trans-*Tetrabenzo*[a, c, g, i] *cyclododecene);* (**23**) was first obtained by Wittig et al. in 1955, in the above described reaction, together with the *cis*, *cis*-isomer **21**. [38] But at that time the structure of **23** was wrongly assigned as *trans*, *trans* (**24**). Later, Bergmann obtained **23** together with **24** in the Wittig reaction type of diphenic dialdehyde with the ylide from 2,2′-bis(bromomethyl)-biphenyl. [42,43,44,50] In 1973, Sondheimer and co-workers [39] repeated the initial synthesis of Wittig, [38] showing that the real structure for this isomer is *cis*, *trans* (**23**), and not (**24**). The *cis*, *trans*-isomer (**23**) is a solid with reported m.p. 163–164°, [38,39,43] 160–163°, [50] and characteristic IR, [38,48] UV, [38,45] and ^{1}H–NMR[45] data. The X-ray analysis [48] of **23** shows that it has the conformation **23a**, with double bonds diverging by 50.5°. Transannular interactions between the double bonds, distanced by about 3.086 Å, led to the enlargement of all angles from the C_{12}-ring. **23** was thermally converted into **22**. [38,47] The UV irradiation of **23** produced **21** along with phenanthrene. [47]

E,E-Tetrabenzo[a, c, g, i][12]*annulene;* (trans, trans-*Tetrabenzo*[a, c, g, i]*cyclododocene);* (**24**). In 1965, Bergmann performing a Wittig reaction of diphenic dialdehyde with the ylide from 2,2′-bis(bromomethyl)biphenyl obtained either a single reaction product with undetermined structure, [42] or two products, [43,44,50] one of them being **24**, the other one **23**, as shown above. The same Wittig reaction conducted by Staab et al. [41] produced only traces of tetrabenzo[12]annulenes, whereas Sondheimer and co-workers [39,40] obtained **24** together with **21**. More recently, **24** was obtained through a Horner-Emmons cyclization of *o,o'*-diphenyldialdehyde.[51] **24** also results from the dehydration of **38a, b** in proper reaction conditions.[45] Stereoselectively, **24** was obtained[46] in the Ramberg-Bäcklund reaction

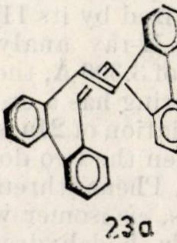
23a

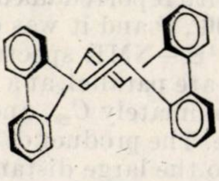
24a

of the corresponding disulfone. The *trans, trans*-isomer (**24**) is a solid with uncorrected m.p. > 300°,[43] 312°,[50] 302–303°,[39,40] and corrected m.p. 301°.[45] It was characterized by IR,[38,48] UV,[38,45] and ^1H-NMR[45] spectra. The X-ray analysis[50,52] revealed its approximate D_2 symmetry, with double bonds at a distance of 2.964 Å from one another, and diverging by 33.5°, in a **24a**-like conformation. In the C_{12}-ring the internal angles are enlarged due to transannular interactions. Though the chemical shift of vinylic protons in the ^1H-NMR spectrum of **24** ($\delta = 6.31$ ppm) could be considered as a proof for paratropicity, it was argued[50] that such data are not conclusive since **24** is a [12]annulene with strong deviations from coplanarity and important double bond localization. The thermal reaction of **24** produces the valence isomer **26**,[47] whereas the UV irradiation affords **25**.[47]

Tetrabenzo[c, g, j, m]*tricyclo*[4.2.2.2 ^{2,5}]*dodeca-3,7,9,11-tetraene, (5,6, 11,12-Tetrahydro-5,12*[*1',2'*] : 6,11[*1'',2''*]*-dibenzenodibenzo*[a, e]*cyclooctene)* (meso-*coupled anthracene); (9,10-dianthracene);* (**20**) is the most investigated derivative among those presented in this paper in spite of the fact that the corresponding non-benzoannelated compound is still unknown. Its first synthesis consists in the photochemical dimerization of anthracene and was done by Fritzsche in 1867.[53] Later it was thoroughly studied and applied to numerous substituted derivatives.[54] The same dimer results as an important byproduct in different photochemical reactions involving anthracene.[55] The [4+4] cycloaddition leading to **20** takes place not only in various solvents, but also in solid phase or in Vycor glass having absorbed anthracene, and it may be sensitized by biacetyl. Also anthracene when refluxed with palladium diacetyl in glacial acetic acid gave **20** together with 9,9'-bianthranyl and anthraquinone.[56] The structure of **20** was confirmed through electron diffraction studies[57] and X-ray analysis.[58] The UV spectrum[59] ($\lambda_{max} = 217.5$ nm) resembles that of 9,10-dihydroanthracene. Both heating or UV irradiation of **20** produce cycloreversion to anthracene.[60,61,62] Many other derivatives of **20** have been studied.[54,63]

cis, syn, trans-*Tetrabenzo*[*c*, e, i, k]*tricyclo*[6.4.0.0 ^{2,7}]*-dodeca-*3,5,9,11-*tetraene;* (cis, syn, trans-*6a, 6b, 12b, 12c-Tetrahydrotetrabenzo*[a, c, g, i]*-biphenylene);* (**22**) was obtained on thermolysis of **23**.[38,47] An alternative synthesis consists in the Hofmann degradation of the quaternary ammonium salt **37**.[38] The solid compound **22** (m.p. 236°) affords phenanthrene on heating.[47]

trans, anti, trans-*Tetrabenzo*[c ,e, i, k]*tricyclo*[*6.4.0.0* ^{2,7}]-*dodeca-3,5,9,11-tetraene*; (trans, anti, trans-*6a, 6b, 12b, 12c-Tetrahydrotetrabenzo*[a, c, g, i] *biphenylene)*; (**25**) results on photolysis of **24**. [47] Heating of **25** produces, as in the case of **22**, cycloreversion to two phenanthrene molecules. [47]

Tetrabenzo[c, e, i, k]*tricyclo*[5.5.0.0 ^{2,8}]*dodeca*-3,5,9,11-*tetraene*; (6,7-*Dihydro*-6,5,7-[1,2]*benzeno*[1,2]*benzenometheno)-5H-dibenzo*[a, c]*cycloheptene)*; (**26**) was obtained by heating **24**. [47] Photoelectron spectroscopy, [64,65] polarized electronic absorption spectroscopy in stretched polymer sheets [65] and semiempirical theoretical methods [65] have been applied to investigate the valence electronic structure of **26**.

KNOWN HEXABENZODERIVATIVES OF VALENCE ISOMERS OF [12]ANNULENE

Hexabenzo[a,c,e,g,i,k][12]*annulene*; (*Hexabenzo*[a,c,e,g,i,k]*cyclododecene)*; (o-*Hexaphenylene)*; (**27**). The two atropisomers of **27**, namely **27a** and **27b** were obtained together in 1957 by Wittig and Lehmann [66] in the reaction of 2,2′-dilithiumbiphenyl with $CoCl_2$. At that time the structure of the isomer **27b** was wrongly assigned as *o*-octaphenylene. Formation of **27b** was also observed in the reaction of *o*-dilithiumbenzene with Ni^{2+}, Ag^{+}, Ti^{2+} and Co^{2+} halides, [67,68] or of dilithiumbiphenyl with $FeCl_3$. [69] An improved synthesis of **27a** consists in treatment of dilithiumbiphenyl with $CrCl_3$, followed by reaction of the intermediately formed complex with transition metal halides. [70] Ten years after the first synthesis, it was shown that **27a** and **27b** are isomers [69,71] (same molecular peak m/z = 456), and moreover, they are atropisomers of *o*-hexaphenylene. [70] Both isomers present IR absorptions at 750 cm^{-1} (*o*-disubstituted phenyl). [70] The screw shaped isomer **27a** with D_2 symmetry absorbs in UV at 218, 237 and 260 nm whereas the centrosymmetric isomer **27b** absorbs at 214 nm (steric inhibition of conjugation). [70] The mass spectra of **27a** and **27b** differ appreciably, **27b** being more stable than **27a** under electron impact. [70] The ^1H-NMR spectrum indicates for **27b** an AA′BB′ pattern whereas for

Table 13

Known hexabenzoderivatives of valence isomers of [12]annulene

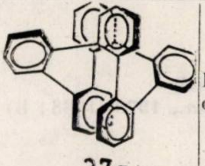 27a	Hexabenzo[*a*, *e*, *e*, *g*, *i*, *k*][12]annulene or : Hexabenzo.[*a*, *c*, *e*, *g*, *i*, *k*]cyclododecene	1957 Wittig and Lehmann [66]
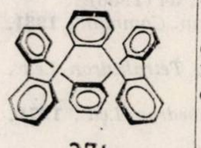 27b	or : Hexabenzo [*a*, *c*, *e*, *g*, *i*, *k*]cyclododeca-1,3,5,7,9,11-hexaene or : *o*-Hexaphenylene	1957 Wittig and Lehmann [66] 1967 Wittig and Klar [69]

27a, beside the AA'BB' spectrum of two benzenic rings, an ABCD spectrum for the remaining four rings was observed. [72] The X-ray investigations confirm the structures **27a** and **27b**, suggesting for **27a** [60] an arrangement of two units of terphenyl, whereas for **27b** [73] a centrosymmetric structure was observed with a twist angle between benzenic rings of 77°. The enantiomers of **27a** were separated. [70] The thermal stability of both isomers was revealed : pyrolysis at 470°, proceeding with partial conversion, affords triphenylene and derivatives. [70] No interconversion (internal rotation) of **27a** and **27b** was observed in these conditions.

REFERENCES

[1] A. T. Balaban, preceding part : *Rev. Roum. Chim.*, **34**, 1745 (1989) — to be corrected as Part 52; Part 51, A. T. Balaban and C. Artemi, *Polycyclic AromaticCompounds*, **1**, 171 (1990); Part 50, A. T. Balaban, *Math. Chem.* **24**, 29 (1989).

[2] A. T. Balaban, *Rev. Roum. Chim.*, **19**, 1185 (1974).

[3] M. Banciu and A. T. Balaban, *Chim. Scripta*, **22**, 188 (1983).

[4] A. T. Balaban, M. Banciu and V. Ciorba, "Annulenes, Benzo, Hetero, Homo-Derivatives and Their Valence Isomers", CRC Press, Boca Raton, Florida, 1987.

[5] A. T. Balaban, *Rev. Roum. Chim.*, **11**, 1097 (1966) ; erratum, *ibid.*, **12**, No. 1, last page (1967).

[6] A. T. Balaban, *Rev. Roum. Chim.*, **21**, 1083 (1976).

[7] A. T. Balaban, R. Vancea, I. Motoc and S. Holban, *J. Chem. Inf. Comput. Sci.*, **26**, 72 (1986).

[8] A. T. Balaban and C. Deleanu, *Rev. Roum. Chim.*, **32**, 271 (1987).

[9] A. T. Balaban, *Rev. Roum. Chim.*, **17**, 865 (1972).

[10] M. Banciu, C. Popa and A. T. Balaban, *Chem. Scripta*, **24**, 28 (1984).

[11] A. T. Balaban and M. Banciu, *J. Chem. Educ.*, **61**, 766 (1984).

[12] H. Prinzbach, D. Seip and G. Englert, *Liebigs Ann. Chem.*, **698**, 57 (1966).

[13] a) T. -M. Kwok, K. Sprinivasachar and N. C. C. Yang, *Chem. Commun.*, **1979**, 1038 ; b) A. T. Balaban, *Rev. Roum. Chim.*, **31**, 695 (1986).

[14] W. Grimme and H. G. Koser, *Angew. Chem.*, **92**, 307 (1980).

[15] A. Bertsch and G. Reinhardt, *Angew. Chem.*, **98**, 361 (1986).

[16] H. Prinzbach, D. Seip, L. Knothe and W. Faisst, *Liebigs Ann. Chem.*, **698**, 34 (1966).

[17] Y. Tobe, F. Hirata, K. Nishida, H. Fujita, K. Kimura and Y. Odaira, *Chem. Commun.*, **1981**, 786.

[18] P. J. Collin, D. B. Roberts, G. Sugowdz, D. Wells and W. H. F. Sasse, *Tetrahedron Lett.*, **1972**, 321.

[19] C. Kowala, G. Sugowdz, W. H. F. Sasse and J. A. Wunderlich, *Tetrahedron Lett.*, **1972**, 4721.

[20] T. W. Mattingly Jr., J. E. Lancaster and A. Zweig, *Chem. Commun.*, **1971**, 595.

[21] T. Teitei, D. Wells and W. H. F. Sasse, *Tetrahedron Lett.*, **1974**, 367.

[22] J. S. Brandshaw and G. S. Hammond, *J. Amer. Chem. Soc.*, **85**, 3953 (1963).

[23] J. S. Bradshaw, N. B. Nielson and D. P. Rees, *J. Org. Chem.*, **33**, 259 (1968).

[24] P. J. Collin, G. Sugowdz, T. Teitei, D. Wells and W. H. F. Sasse, *Aust. J. Chem.*, **27**, 227 (1974).

[25] N. C. C. Yang, M. -J. Chem, P. Chen and T. K. Mak, *J. Amer. Chem. Soc.*, **104**, 853 (1982).

[26] N. C. C. Yang, M. -J. Chen and P. Chen, *J. Amer. Chem. Soc.*, **106**, 7310 (1984).

[27] A. Bertsch and G. Reinhardt, *Angew. Chem.*, **98**, 361 (1986).

[28] N. C. C. Yang and X. Q. Yang, *J. Amer. Chem. Soc.*, **109**, 3804 (1987).

[29] G. Sedelmeier, W. D. Fessner, C. Grund, P. R. Spurr, H. Fritz, and H. Prinzbach, *Tetrahedron Lett.*, **1986**, 1277.

[30] E. Müller and G. Röscheisen, *Chem. Ber.*, **90**, 543 (1957).

[31] H. A. Staab, F. Graf and B. Junge, *Tetrahedron Lett.*, **1966**, 743.

[32] H. A. Staab, F. Graf, K. Doerner and A. Nissen, *Chem. Ber.*, **104**, 1159 (1971).

[33] J. Castells and M. Morreno-Manas, *Ann. Quim.*, **68**, 193 (1972).

[34] L. Rampazzo, A. Inesi and R. M. Bettolo, *J. Electroanal. Chem. Interfacial Electrochem.*, **83**, 341 (1977).

[35] H. Brunner, K. H. Hausser, M. Rawitscher and H. A., Staab, *Tetrahedron Lett.*, **1966**, 2775.

[36] C. S. Johnson and R. Chang, *J. Chem. Phys.*, **43**, 3183 (1965).

[37] M. W. Tausch, M. Elian, A. Bucur and E. Ciorănescu, *Chem. Ber.*, **110**, 1744 (1977).

[38] G. Wittig, G. Koenig and K. Klauss, *Liebigs Ann. Chem.*, **593**, 127 (1955).

[39] K. Grohmann, P. D. Howes, R. H. Mitchell, A. Monahan and F. Sondheimer, *J. Org. Chem.*, **38**, 808 (1973).

[40] R. H. Mitchell and F. Sondheimer; Footnote 6, *Tetrahedron Lett.*, **1968**, 2873.

[41] H. A. Staab, E. Wehinger and W. Thorwart, *Chem. Ber.*, **105**, 2290 (1972).

[42] E. D. Bergmann, *Bull. Soc. Chim. France*, **1965**, 2681.

[43] E. D. Bergmann; unpublished data, quoted in *Liebigs Ann. Chem.*, 59 (1973).

[44] E. D. Bergmann, I. Agranat and M. Kraus, *Isr. J. Chem.*, **3**, 48 (1965).

[45] G. Wittig and G. Skipka, *Liebigs Ann. Chem.*, 59 (1973).

[46] H. J. Bestmann and W. Schaper, *Tetrahedron Lett.*, **1975**, 3511.

[47] G. Wittig and G. Skipka, *Liebigs Ann. Chem.*, 1157 (1975).

[48] H. Irngartinger, *Chem. Ber.*, **105**, 2068 (1972).

[49] H. Irngartinger, *Chem. Ber.*, **106**, 2786 (1973).

[50] I. Agranat, M. A. Kraus, E. D. Bergmann, P. J. Roberts and O. Kennard, *Tetrahedron Lett.*, **1973**, 1265.

[51] I. Agranat, M. Rabinovitz and W. -C. Shaw, *J. Org. Chem.*, **44**, 1936 (1979).

[52] a) H. Irngartinger, *Chem. Ber.*, **106**, 2796 (1973); b) P. J. Roberts and O. Kennard, *J. Chem. Soc. Perkin 2*, **1973**, 1984.

[53] J. Fritzsche, *J. Prakt. Chem.*, **101**, 333 (1867).

[54] a) E. Leppin, in: "Houben-Weyl, Methoden der Organischen Chemie", Vol. IV/5a, Georg Thieme Verlag, Stuttgart, 1975, 478; b) F. D. Greene, S. L. Misrock and J. R. Wolfe Jr., *J. Amer. Chem. Soc.*, **77**, 3852 (1955); c) D. E. Applequist, R. L. Little, E. C. Friedrich and R. E. Wall, *J. Amer. Chem. Soc.*, **81**, 452 (1959); d) G. Kaupp, *Chimia*, **25**, 230 (1971); e) I. L. Aptekar and A. E. Galashin, *Pis'ma Zh. Eksp. Theor. Fiz.*, **28**, 421 (1978); f) D. E. Applequist and R. Searle, *J. Amer. Chem. Soc.*, **86**, 1389 (1964).

[55] a) T. Sasaki, K. Kanematsu, I. Ando and O. Yamashita, *J. Amer. Chem. Soc.*, **98**, 2686 (1976); b) T. Sasaki, K. Kanematsu and K. Hayakawa, *J. Amer. Chem. Soc.*, **95**, 5632 (1973); c) J. Saltiel, R. Dabestani, S. K. Schanze, D. Trojan, E. D. Townsend and L. V. Goedken, *J. Amer. Chem. Soc.*, **108**, 2674 (1986); d) N. Toshima, T. Sugano and H. Hirai, *Can. J. Chem.*, **62**, 2047 (1984).

[56] P. L. Majumder and M. Joardar, *Indian J. Chem. Sect. B*, **22B**, 1191 (1983).

[57] J. Hengstenberg and J. Palacios, *An. Real. Soc. Espan. Fis. Quim. (Madrid)*, **30**, 5 (1932).

[58] W. R. Orndorf and F. K. Cameron, *Am. Chem. J.*, **17**, 658 (1895).

[59] C. A. Coulson, L. E. Orgel, W. Taylor and J. Weiss, *J. Chem. Soc.*, **1955**, 2961.

[60] G. Kaupp, *Chimia*, **25**, 230 (1971).

[61] A. R. Barber, P. De Mayo and K. Okada, *Chem. Commun.*, **1982**, 1073.

[62] A. R. Barber, P. De Mayo, K. Okada and K. S. Wong, *J. Amer. Chem. Soc.*, **104**, 4995 (1982).

[63] a) L. Burnelle, J. Lahiri and R. Detrano, *Tetrahedron*, **24**, 3517 (1968); C. R. Theocharis and W. Jones, *Chem. Commun.*, **1984**, 369; c) N. M. Weinshenker and F. D. Greene, *J. Amer. Chem. Soc.*, **90**, 506 (1968); d) R. L. Vivattene, F. D. Greene, L. D. Cheung, R. Majeste and L. M. Trefonas, *J. Amer. Chem. Soc.*, **96**, 4342 (1974); e) J. Masnovi and J. K. Kochi, *J. Amer. Chem. Soc.*, **107**, 6781 (1985).

[64] R. Gleiter, R. Haider, J. Spanget-Larsen and P. Bischof, *Tetrahedron Lett.*, **1983**, 1149.

[65] J. Spanget-larsen, R. Gleiter and R. Haider, *Helv. Chim. Acta*, **66**, 1441 (1983).

[66] G. Witting and G. Lehmann, *Chem. Ber.*, **90**, 875 (1957).

[67] G. Wittig and F. Bickelhaupt, *Chem. Ber.*, **91**, 883 (1958).

[68] H. J. S. Winkler and G. Wittig, *J. Org. Chem.*, **28**, 1733 (1963).

[69] G. Wittig and G. Klar, *Liebigs Ann. Chem.*, **704**, 91 (1967).

[70] G. Wittig and K. -D. Rümpler, *Liebigs Ann. Chem.*, **751**, 1 (1971).

[71] H. A. Staab and C. Wünsche, *Chem. Ber.*, **101**, 887 (1968).

[72] L. Ernst and A. Mannschreck, *Org. Magn. Reson.*, **5**, 125 (1973).

[73] H. Irngartinger, *Isr. J. Chem.*, **10**, 635 (1972).

[74] H. A. Staab, U. E. Meissner and F. Diederich, *Koen Yoshishu-Hibenzenkei Hokozoku Kagaku Toronkai [oybi] kozo Yuki Kagaku Toronkay, 12th* **1979**, 3—I—3—IV, 4 Shinsku Daigaku Rigakubu: Matsumoto, Japan; cf. *Chem. Abstr.*, **93**, 25647 (1980).

[76] H. Ugler and Ege, *Tetrahedron*, **32**, 1789 (1976).

[75] A. B. Hess Jr., L. J. Schaad and I. Agranat, *J. Amer. Chem. Soc.*, **100**, 5268 (1978).

[36] C. S. Johnson and B. Chang, *J. Chem. Phys.*, **43**, 3183 (1965).
[37] M. W. Dausch, M. Ellam, A. Euber and E. Cioranescu, *Chem. Ber.*, **110**, 1744 (1977).
[38] G. Wittig, G. Koenig and K. Klaus, *Liebigs Ann. Chem.*, **593**, 127 (1955).
[39] K. Grohmann, P. D. Howes, R. H. Mitchell, A. Monahan and F. Sondheimer, *J. Org. Chem.*, **38**, 808 (1973).
[40] R. H. Mitchell and F. Sondheimer, Footnote 6, *Tetrahedron Lett.*, **1968**, 2873.
[41] H. A. Staab, E. Wehinger and W. Thorwart, *Chem. Ber.*, **105**, 2290 (1972).
[42] E. D. Bergmann, *Bull. Soc. Chim. France*, **1965**, 2681.
[43] E. D. Bergmann, unpublished data, quoted in *Liebigs Ann. Chem.*, 59 (1973).
[44] E. D. Bergmann, I. Agranat and M. Kraus, *Isr. J. Chem.*, **A 48** (1965).
[45] G. Wittig and G. Skipka, *Liebigs Ann. Chem.*, 59 (1973).
[46] H. J. Bestmann and W. Schaper, *Tetrahedron Lett.*, **1975**, 3511.
[47] G. Wittig and G. Skipka, *Liebigs Ann. Chem.*, 1157 (1973).
[48] H. Irngartinger, *Chem. Ber.*, **105**, 2068 (1972).
[49] H. Irngartinger, *Chem. Ber.*, **106**, 2796 (1973).
[50] I. Agranat, M. A. Kraus, E. D. Bergmann, P. J. Roberts and O. Kennard, *Tetrahedron Lett.*, **1973**, 1265.
[51] I. Agranat, M. Rabinovitz and W.-C. Shaw, *J. Org. Chem.*, **44**, 1936 (1979).
[52] a) H. Irngartinger, *Chem. Ber.*, **106**, 2796 (1973); b) P. J. Roberts and O. Kennard, *J. Chem. Soc. Perkin 2*, **1973**, 1984.
[53] J. Fritzsche, *J. Prakt. Chem.*, **101**, 333 (1867).
[54] a) E. Zbiral, in: "Houben-Weyl, Methoden der Organischen Chemie", Vol. IV/5a, Georg Thieme Verlag, Stuttgart, 1975, 475; b) E. D. Greene, S. L. Misrock and J. R. Wolfe Jr., *J. Amer. Chem. Soc.*, **77**, 3852 (1955); c) D. E. Applequist, R. L. Litle, E. C. Friedrich and R. E. Wall, *J. Amer. Chem. Soc.*, **81**, 452 (1959); d) G. Kaupp, *Chimia*, **25**, 230 (1971); e) I. L. Aptekar and A. S. Cherkasov, *Pis'ma Zh. Eksp. Teor. Fiz.*, **28**, 437 (1978); f) D. E. Applequist and R. Searle, *J. Amer. Chem. Soc.*, **86**, 1389 (1964).
[55] a) T. Sasaki, K. Kanematsu, I. Ando and O. Yamashita, *J. Amer. Chem. Soc.*, **98**, 2686 (1976); b) T. Sasaki, K. Kanematsu and K. Hayakawa, *J. Amer. Chem. Soc.*, **95**, 5632 (1973); c) J. Saltiel, R. Dabestani, S. K. Schanze, D. Trojan, D. E. Townsend and L. V. Goedken, *J. Amer. Chem. Soc.*, **108**, 2674 (1986); d) N. Fukuma, T. Sugano and H. Hirai, *Can. J. Chem.*, **62**, 2047 (1984).
[56] P. L. Majumder and M. Joardar, *Indian J. Chem.*, Sect. B, **22B**, 1191 (1983).
[57] J. Hengstenberg and J. Palacios, *An. Real Soc. Espan. Fis. Quim.* (Madrid), **30**, 5 (1932).
[58] W. R. Orndorff and F. K. Cameron, *Am. Chem. J.*, **17**, 658 (1895).
[59] C. A. Coulson, L. E. Orgel, W. Taylor and J. Weiss, *J. Chem. Soc.*, **1955**, 2961.
[60] G. Kaupp, *Chimia*, **25**, 230 (1971).
[61] A. R. Barber, P. De Mayo and K. Okada, *Chem. Commun.*, **1982**, 1073.
[62] A. R. Barber, P. De Mayo, K. Okada and K. S. Wong, *J. Amer. Chem. Soc.*, **104**, 4995 (1982).
[63] a) L. Barbella, J. Lambi and E. Dutrano, *Tetrahedron*, **24**, 3517 (1968); c. R. Theocharis and W. Jones, *Chem. Commun.*, **1984**, 369; c) N. M. Weinshenker and F. D. Greene, *J. Amer. Chem. Soc.*, **90**, 506 (1968); d) R. L. Vivattene, F. D. Greene, L. D. Cheung, R. Majeste and L. M. Trefonas, *J. Amer. Chem. Soc.*, **96**, 4342 (1974); e) J. Masnovi and J. K. Kochi, *J. Amer. Chem. Soc.*, **107**, 6781 (1985).
[64] R. Gleiter, R. Haider, J. Spanget-Larsen and P. Bischof, *Tetrahedron Lett.*, **1983**, 1149.
[65] J. Spanget-Larsen, R. Gleiter and R. Haider, *Helv. Chim. Acta*, **66**, 1441 (1983).
[66] G. Wittig and G. Lehmann, *Chem. Ber.*, **90**, 875 (1957).
[67] G. Wittig and F. Bickelhaupt, *Chem. Ber.*, **91**, 883 (1958).
[68] H. J. S. Winkler and G. Wittig, *J. Org. Chem.*, **28**, 1733 (1963).
[69] G. Wittig and G. Klar, *Liebigs Ann. Chem.*, **704**, 91 (1967).
[70] G. Wittig and K.-D. Rümpler, *Liebigs Ann. Chem.*, **751**, 1 (1971).
[71] H. A. Staab and C. Wünsche, *Chem. Ber.*, **101**, 887 (1968).
[72] L. Ernst and A. Mannschreck, *Org. Magn. Reson.*, **5**, 125 (1973).
[73] H. Irngartinger, *Isr. J. Chem.*, **10**, 635 (1972).
[74] H. A. Staab, U. E. Meissner and J. Dieterich, *Koen Yoshishu Hibenzenkei Hokozoku Kagaku Toronkai* [*and*] *Kozo Yuki Kagaku Toronkai*, 12th 1979, 3–1, 3–17, 4 Shinsho Daigaku Rigakubu Matsumoto, Japan; cf. *Chem. Abstr.*, **93**, 25647 (1980).
[75] R. Gleiter and Kaw, *Tetrahedron*, **32**, 1789 (1976).
[76] A. B. Hess Jr., L. J. Schaad and I. Agranat, *J. Amer. Chem. Soc.*, **100**, 5268 (1978).

Revue Roumaine de Chimie, 35, 3, 393–397 (1990)

CARBONIC ANHYDRASE INHIBITORS. I

METAL COMPLEXES OF SULFONAMIDES: A NOVEL CLASS OF CARBONIC ANHYDRASE INHIBITORS *

CLAUDIU SUPURAN[a,***], MARIUS ANDRUH[b,**] and IOAN PUȘCAȘ[a]
[a]Șimleu Silvaniei Hospital, G. Coșbuc 29A, 4775 Șimleu Silvaniei, Romania
[b]Inorganic Chemistry Laboratory, Faculty of Chemical Technology, Polytechnic Institute of Bucharest, Dumbrava Roșie 23, Bucharest, Romania

Received November 10, 1989

Coordination compounds of Zn(II), Cu(II) and Ni(II) with acetazolamide (AAZ) and ethoxzolamide (EZA) were synthesized. The new complexes were characterized by means of elemental chemical analysis, infrared and UV–VIS spectroscopy as well as by thermal analysis. Their inhibitory activity towards carbonic anhydrase (CA) was tested. All these complexes are highly active as enzyme inhibitors.

1. INTRODUCTION

The inhibition of carbonic anhydrase (CA) is responsible for a variety of physiological effects. The design and therapeutic use of CA inhibitors as well as their mechanism of action are extensively studied. [1,2]

Two major groups of CA inhibitors are known: monovalent anions and aromatic and heterocyclic sulfonamides. [3,4] The CA inhibitors in current clinical use include such compounds as: acetazolamide (AAZ) (**1**), ethoxzolamide (EZA) (**2**), dichlorophenamide (**3**), methazolamide (**4**).

These compounds are used as diuretics, anticonvulsants, cerebral vasodilators, antiglaucoma and antisecretory agents, in the treatment of gastro-duodenal ulcers. [1,5,6]

The aim of this paper is to report a novel class of CA inhibitors: the metal complexes of heterocyclic sulfonamides, namely coordination compounds of Cu(II), Zn(II) and Ni(II) with sulfonamides **1** and **2**. These compounds were assayed also for their inhibitory action.

2. EXPERIMENTAL

Although sulfonamides are not prominent metal complexing agents [7] their coordinating ability may be increased by ionization, as sodium salts:

$$R-SO_2NH_2 + NaOH \rightarrow R-SO_2NH^-Na^+ + H_2O$$

---

* Dedicated to the memory of Mihai Elian.

** To whom correspondence should be addressed.

*** Present address: University of Bucharest, Dept. of Organic Chemistry, Bd. Republicii 13, Bucharest, Romania

Therefore, in order to dissolve and ionize the organic ligand, the hot methanolic suspensions of AAZ or EZA were treated with the corresponding amount of 1 M NaOH solution.

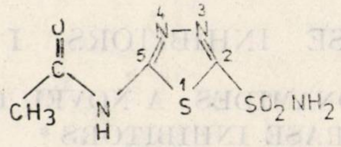

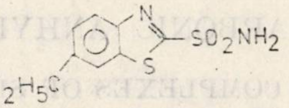

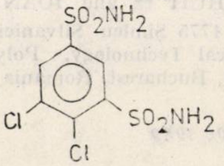

3

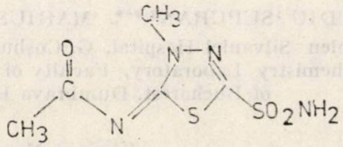

4

All complexes reported in this paper have been synthesized according to the following general procedure : methanolic solutions containing metal chloride ($CuCl_2 . 2 H_2O$, $NiCl_2 . 6 H_2O$ or $ZnCl_2$) and ionized heterocyclic sulfonamide (AAZ and EZA) were mixed with stirring in molar ratios 1 : 1 and 1 : 2. The resulting mixture was heated for 30 min on a water bath. The complexes precipitated from these solutions, were filtered off and dried in vacuum. During this work, the following coordination compounds were synthesized and characterized : $[Cu(AAZ)_2]$ (green-blue) ; $[Cu(AAZ)Cl]_2$ (green) ; $[Ni(AAZ)(OH)(H_2O)_2]_2 . 6 H_2O$ (blue) ; $[Zn(AAZ)_2]$(white) ; $[Cu(EZA)_2(H_2O)_2]$ (green) and $[Zn(EZA)_2]$ (white). In the above formulas, AAZ and EZA mean the corresponding anions. It is interesting to note that working in molar ratios $NiCl_2$: AAZ = 1 : 2 or 1 : 1, only the mentioned compound was obtained. The results of elemental chemical analysis are in satisfactory agreement with the proposed formulas.

The electronic spectra were recorded by diffuse reflectance technique using MgO as a reference material. Infrared spectra were recorded in KBr pellets. The thermogravimetric, TG, derivative thermogravimetric, DTG, differential thermal analysis, DTA, and temperature, T, curves have been recorded at heating rate $\beta = 10°/min$, using a MOM Budapest Q–1500 D derivatograph.

Assay for inhibitory activity of the prepared compounds was achieved by the method of Maren *et al.*[8]. The SEI (substrate — enzyme — inhibitor) procedure was used, at 4°C, under continuous flow of CO_2. Kinetic or thermodynamic data (K_I) were not determined, but the inhibitory power of the new compounds was compared with that of the parent sulfonamide. Stock solutions of 10^{-3} M inhibitor in DMSO were prepared and then diluted with deionized water. Bovine erythrocyte CA from Boehringer — Mannheim was the source of enzyme.

3. RESULTS AND DISCUSSION

According to the stoichiometry of the complex compounds synthesized by us, one may suppose that the anions of AAZ and EZA act as bidentate ligands. On the other hand, because the nitrogen atom of the SO_2NH^- group (a hard base in Pearson's theory) must surely interact with metal ions, the other donor atom of these ligands must be the neighbouring nitrogen atom (N—3) from the heterocycle, in agreement with the symbiotic behaviour of ligands. This interaction with the metal ions has no special steric requirements.

The IR spectra of all synthesized coordination compounds display the characteristic frequencies of the organic molecules acting as ligands.

For example, some selected IR bands found in the spectrum of $[Zn(AAZ)_2]$ are respectively : $\nu_{SO_2(as)} = 1350\ cm^{-1}$; $\nu_{SO_2(sim)} = 1120\ cm^{-1}$; $\nu_{amide\ I} = 1680\ cm^{-1}$; $\nu_{amide\ II} = 1550\ cm^{-1}$. The bands assigned to $\nu_{SO_2(as)}$ and $\nu_{SO_2(sim)}$ are slightly shifted at lower frequencies, comparatively with the free organic ligands.

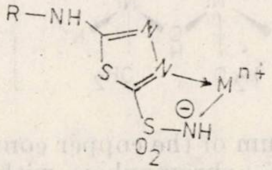

Clear stereochemical informations are obtained from the electronic spectra of two coordination compounds : $[Ni(AAZ)(OH)(H_2O)_2]_2 . 6\ H_2O$ and $[Cu(AAZ)_2]$. Indeed, the diffuse reflectance spectrum of the former is characteristic for nickel(II) ion in a (pseudo)-octahedral configuration (Fig. 1) :

ν_1 : $^3A_{2g} \rightarrow {}^3T_{2g}$ (1040 nm ; 9615 cm^{-1})

ν_2 : $^3A_{2g} \rightarrow {}^3T_{2g}$ (620 nm ; 18130 cm^{-1})

ν_3 : $^3A_{2g} \rightarrow {}^3T_{1g}$ (P) (385 nm ; 29970 cm^{-1})

$^3A_{2g} \rightarrow {}^1E_g$ (800 nm ; 12500 cm^{-1}; spin forbidden)

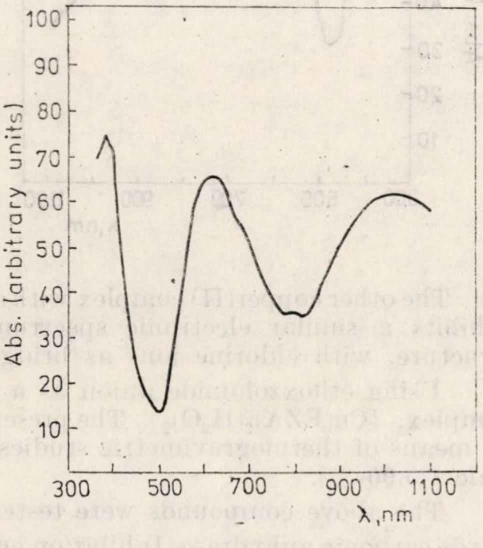

Fig. 1. — The electronic spectrum of the compound $[Ni(AAZ)(OH)(H_2O)_2]_2 . 6H_2O$.

The hexacoordination of nickel(II) ions is achieved most probably in a binuclear unit with two OH bridges.

Inequivalency of water molecules was proved by means of thermal analysis : the ten water molecules were evolved in two steps :

100—115 °C : 13,75% weight loss (calc. : 13.95 %) ; lattice water

170—240 °C : 9.60 % weight loss (calc. : 9.30 %) ; coordinated water :

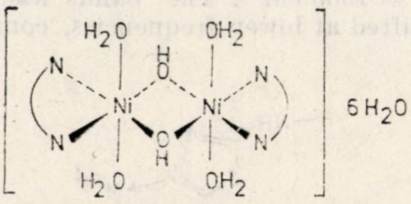

The electronic spectrum of the copper complex, $[Cu(AAZ)_2]$ (Fig. 2), is characteristic for a (CuN_4) chromophore with a compressed tetrahedral stereochemistry. [9]

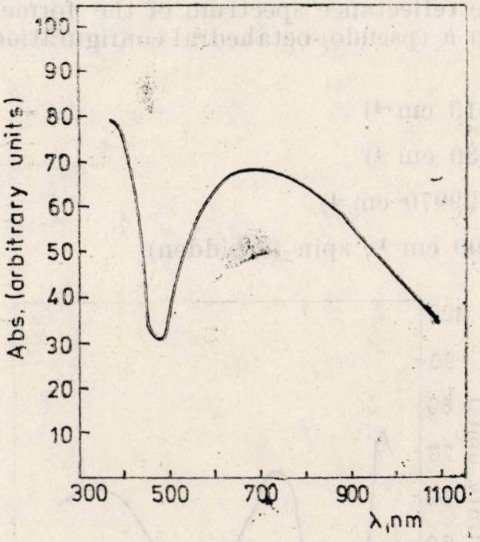

Fig. 2. — The electronic spectrum of the complex [Cu(AAZ)].

The other copper(II) complex with acetazolamide anion, $[Cu(AAZ)\text{-}Cl]_2$ exhibits a similar electronic spectrum and has probably a dinuclear structure, with chlorine ions as bridges.

Using ethoxzolamide anion as a ligand, we prepared a copper(II) complex, $[Cu(EZA)_2(H_2O)_2]$. The presence of water molecules was proved by means of thermogravimetric studies : weight loss (at 150° C) : 6.0 % (calc. : 5.90 %).

The above compounds were tested for their inhibitory activity towards carbonic anhydrase. Inhibition curves are presented in Fig. 3 and 4.

All the prepared compounds are highly active as enzyme inhibitors, the enzymic activity being completely suppressed at 10^{-6}M concentrations of inhibitor, in contrast to sulfonamides, where a reminiscent activity still persists.

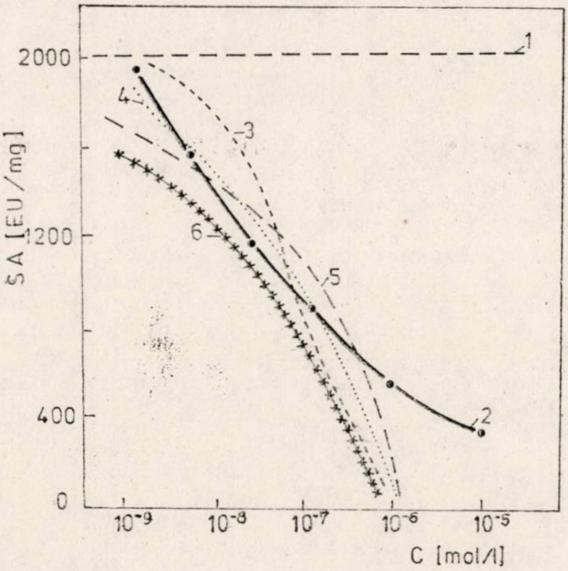

Fig. 3. — Inhibition curves of acetazolamide and its complexes (SA — specific activity vs. concentration) : 1 — uncatalyzed reaction : 2 — acetazolamide : 3 — $[Ni(AAZ)(OH)(H_2O)_2]_2 . 6H_2O$; 4 — $[Cu(AAZ)_2]$: 5 — $[Cu(AAZ)Cl]_2$; 6 — $[Zn(AAZ)_2]$. For sake of simplicity, the experimental points, corresponding at each concentration indicated on abscisa, are not represented.

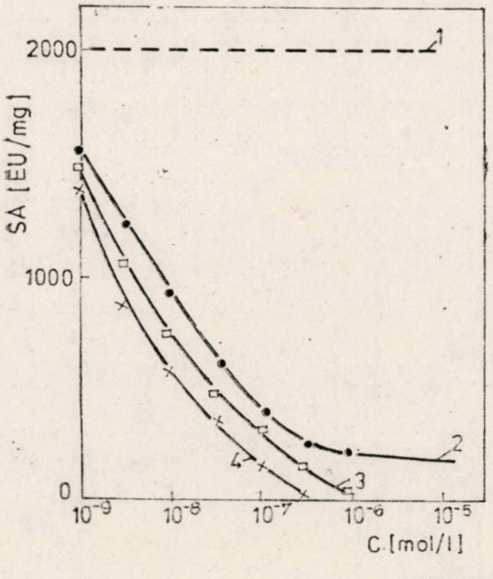

Fig. 4. — Inhibition curves of ethoxzolamide and its complexes ; specific activity vs. concentration of inhibitor : 1 — uncatalyzed reaction ; 2 — ethoxzolamide ; 3 — copper complex ; 4 — zinc complex.

REFERENCES

[1] S. Lindskog and P. J. Wistrand, "Inhibition of Carbonic Anhydrase", in "Design of Enzyme Inhibitors as Drugs", F. Sandler ed., Oxford Univ. Press, 1987.
[2] K. M. Mertz, R. Hoffmann and M. J. S. Dewar, *J. Amer. Chem. Soc.*, **111**, 4636 (1989).
[3] D. Keilin and T. Mann, *Biochem. J.*, **34**, 1163 (1940).
[4] T. Mann and D. Keilin, *Nature*, **146**, 164 (1940).
[5] T. H. Maren, *Physiol. Rev.*, **47**, 595 (1967).
[6] I. Pușcaș, *Ann. N. Y. Acad. Sci.*, **429**, 587 (1984).
[7] J. E. Coleman, *Ann. Rev. Pharmacol.*, **15**, 221 (1975).
[8] T. H. Maren, V. I. Ash and E.M. Bailey, *Bull. Johns Hopkins Hosp.*, **95**, 244 (1954).
[9] B. J. Hathaway, *J. Chem. Soc. Dalton*, **1972**, 1196.

Revue Roumaine de Chimie, 35, 3, 399–405 (1990)

CARBONIC ANHYDRASE INHIBITORS. II[1]

MEMBRANE-IMPERMEABLE DERIVATIVES OF 1, 3, 4-THIADIAZOLE-2-SULFONAMIDE *, **

CLAUDIU SUPURAN[a,***], ALEXANDRU T. BALABAN[b], MIRCEA D. GHEORGHIU[b]
ANA SCHIKETANZ[b], ANTONIE DINCULESCU[c] and IOAN PUȘCAȘ[a]
[a] Șimleu Silvaniei, Hospital, G. Coșbuc str. 29A, 4775 Șimleu Silvaniei, Sălaj, Romania
[b] Department of Organic Chemistry, Polytechnic Institute – TCH, 77206 Bucharest 16, Romania
[c] Chemical-Pharmaceutical Research Institute, Șos. Vitan 112, Bucharest, Romania

Received November 10, 1989

New derivatives of 1,3,4-thiadiazole-2-sulfonamide, possessing ammonium or pyridinium positively charged moieties in their molecules, were synthesized and assayed for inhibitory action on bovine carbonic anhydrase. These compounds are potential inhibitors of membrane-bound CA.

1. INTRODUCTION

Membrane-bound forms of carbonic anhydrase (CA), sometimes denoted as isozyme IV (CA IV), [2] were recently reported. [2,3] The actual physiological function of these forms is still elusive, but it seems that at least for kidneys and gastro-intestinal tract, they play a critical role in secretory processes. [4,5] Few data are available about selective inhibitors of CA isozymes. The scarcity of these data is even greater for CA IV.

CA IV-selective inhibitors were prepared by two approaches:

(i) covalent binding of heterocyclic/aromatic sulfonamides to macromolecules, such as dextran, [4,6] and (ii) attachment of a quaternary ammonium group to aromatic sulfonamides. Only one compound of this type was described, [6] i.e. the trimethylammonium derivative of homosulfanilamide (Fig. 1). These inhibitors do not penetrate cellular membranes. They were used to show that the active site of CA IV within the brush-border membrane of the renal tubules is located on the exterior, luminal side.

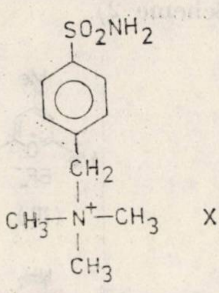

Fig. 1. – Trimethylammonium derivative of homosulfanilamide.

---

* Dedicated to the memory of Mihai Elian.

** Presented in part at the 6th Conference of Chemistry and Chemical Engineering, Bucharest, 13–14 October 1989, and at the 15th Session of Scientific Communications, Călimănești, 19–21 October 1989.

*** Present address: University of Bucharest, Dept. of Organic Chemistry, Bd. Republicii 13, Bucharest, Romania.

The second approach was used by us in the design of new membrane-impermeable CA inhibitors, derivatives of 1,3,4-thiadiazole-2-sulfonamide, reported in this paper.

The pyridinic nitrogen atom seemed to us a good candidate for introducing positive charges in a molecule. This could be achieved either by a mere protonation (even at physiological values of pH) or by N-alkylation. Compounds IIa—c were prepared upon this first assumption and IId-f upon the second one (Scheme 1). Well-known methods for acylation of amines were used to synthesize these compounds from 5-amino-1,3,4-thiadiazole-2-sulfonamide (I) and pyridine- or N-methylpyridinium-carboxylic acid acyl chlorides.

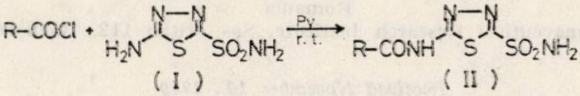

Compound	R	Yield (%)
IIa	2-pyridyl	68
IIb	3-pyridyl	83
IIc	4-pyridyl	72
IId	2-(N-methylpyridinium)	54
IIe	3-(N-methylpyridinium)	79
IIf	4-(N-methylpyridinium)	69

Scheme 1

Using amine I as a nucleophile and pyrylium salt III [7] or 1′-methylthiaminium salt V [8] as synthons, compounds IV and VI were prepared (Scheme 2).

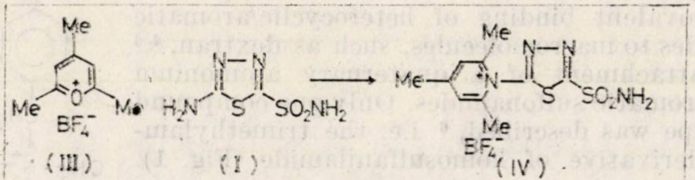

Compound	yield
IV	48
VI	62

Scheme 2

Compounds VIIIa, b were prepared by two alternative procedures (Scheme 3). Tertiary amines (triethylamine and pyridine) were subjected to quaternization with 5-halogenoacetamido-1,3,4-thiadiazole-2-sulfonamide (VII, X=Cl, Br), yielding directly the quaternary compounds VIII (route A). In the alternative procedure, quaternization was achieved with ethyl bromoacetate, followed by alkaline hydrolysis, treatment with $SOCl_2$, and acylation of amine I (route B).

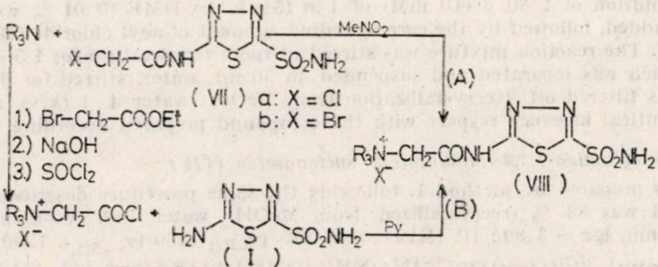

Compound	R_3N	X	route	yield(%)
VIIIa	Et_3N	Cl	A	72
VIIIa	Et_3N	Br	A	63
VIIIa	Et_3N	Cl	B	34
VIIIb	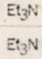	Cl	A	86
VIIIb		Cl	B	47

Scheme 3

The newly synthesized compounds were characterized by means of elemental chemical analysis, UV, IR and ^1H-NMR spectroscopy, and were assayed for inhibitory action.

2. EXPERIMENTAL

The melting points were determined on a heating-plate microscope and are not corrected. UV spectra were obtained in methanolic solution with a UV–VIS Specord spectrophotometer; IR spectra, in KBr pellets, with a Specord IR–71 spectrophotometer; and ^1H-NMR spectra were taken at 60 MHZ, on a Varian EM–360 L spectrometer. Chemical shifts are reported as parts per million relative to Me_4Si as internal standard. All compounds were analyzed (C, H, N) and values obtained were within ± 0.4% of the theoretical values. 5-Amino-1,3,4-thiadiazole-2-sulfonamide was prepared from acetazolamide by the method of Petrow[9]. 2,4,6-Trimethylpyrylium tetrafluoroborate[10] and 1^1-methylthiaminium bisperchlorate[11] were prepared by literature procedures. Cloroacetazolamide and bromoacetazolamide (VIIa, b) were prepared from 5-amino-1,3,4-thiadiazole-2-sulfonamide by literature procedures.[12] N-Methylpyridinium-carboxylic acids were prepared by methylation of the corresponding pyridine-carboxylic acids with methyl iodide and/or dimethyl sulfate. Pyridine-carboxylic acids, thionyl chloride, dimethyl sulfate, methyl iodide, tertiary amines, ethyl bromoacetate and solvents were from Merck and were used without further purification.

5-Picolinoylamido-1,3,4-thiadiazole-2-sulfonamide (IIa)

Method 1.

To a suspension of 1.80 g (10 mM) of I in 20 mL dry acetonitrile (0.01 % water), 1 mL (12.5 mM) dry pyridine was added under continuous stirring, maintaining the mixture at room temperature; 1.41 g (10 mM) picolinoyl chloride dissolved in 5mL acetonitrile were added dropwise. Stirring was continued for two hours at room temperature, after which the acylated amine was filtered off and washed with cold methanol on the funnel; 1 .78 g crude product IIa resulted. The filtrate was evaporated under reduced pressure and the yellow oil was treated with 5 mL water. After filtration, another portion (0 .28 g) of IIa resulted. Recrystallization from MeOH : water 4 : 1 (v/v) afforded 1 .94 g IIa (68 %) : mp 292° C ; UV (MeOH) : 268 nm, lgε=3 .99 ; IR (KBr) : 680, 730 (γ_{CH}), 1135 (υ_{s-SO_2}), 1310 (υ_{as-SO_2}), 1550 (δ_{NH}), 1665 (υ_{CONH}), 3070 (υ_{NH-}) cm^{-1};^{1}H-NMR (DMSO-d_6) : 8.4 (br s, 3H, SO_2NH_2+ CONH), 7 .9–9 .1 (m, 4H, ArH) ; Anal. $C_8H_7N_5O_3S_2$ requires : C, 33 .68 ; H, 2 .45 N, 24 .56. Found : C, 33 .31 ; H, 2 .63 ; N, 24 .18%.

Method 2.

To a solution of 1 .80 g (10 mM) of I in 15 mL dry DMF (0 .01 % water), 1 mL dry pyridine was added, followed by the corresponding amount of acyl chloride (10 mM) dissolved in 5 mL DMF. The reaction mixture was stirred at room temperature for 1.5 hours. A heavy oil formed which was separated and suspended in 50 mL water, stirred for 30 min, and the precipitate was filtered off. Recrystallization from MeOH : water 4 : 1 (v/v) afforded 1 .83 g IIa (64%) identical in every respect with the compound prepared according to Method 1.

5-Nicotinoylamido-1,3,4-thiadiazole-2- sulfonamide (IIb)

IIb was prepared by method 1, following the same procedure described for compound IIa. The yield was 83 % (recrystallized from MeOH: water 7 : 3 (v/v)), mp 269°C ; UV (MeOH) : 265 nm, lgε = 3 .89 ; IR (KBr) : 690, 815 (γ_{CH}), 1130 (ν_{s-SO_2}), 1290 (ν_{as-SO_2}), 1540 (δ_{NH}), 1160 (ν_{CONH}), 3070 (ν_{NH}) cm^{-1} ; ^{1}H–NMR (DMSO-d_6) : 8.5 (br s, 3H, SO_2NH_2 + CONH), 7.7–8.8 (m, 4H, ArH) ; Anal. $C_8H_7N_5O_3S_2$ requires : C, 33.68 ; H, 2.45 ; N, 24.56 ; Found : C, 33.47 ; H, 2.72 ; N, 24.30 %.

5-Isonicotinoylamido-1,3,4-thiadiazole-2-sulfonamide (IIc)

The same procedure was applied as for IIb. Compound IIc resulted with a yield of 72 % (recrystallized from MeOH : water 3 : 1 (v/v)) : mp 301 C ; UV (MeOH) : 265 nm, lgε = 4.02 ; IR (KBr) : 690, 820 (γ_{CH}), 1125 (ν_{s-SO_2}), 1300 (ν_{as-SO_2}), 1540 (δ_{NH}), 1650 (ν_{CONH}), 3070 (ν_{NH}) cm^{-1} ; ^{1}H–NMR (DMSO-d_6) : 8.5 (br s, 3H, SO_2NH_2 + CONH), 8 .0 – 9 .1 (m, 4H, AB, ArH) ; Anal. $C_8H_7N_5O_3S_2$ requires : C, 33 .68 ; H, 2 .45 ; N, 24 .56 ; Found : C, 33 .71 ; H, 2 .69 ; N, 22 .24 %.

5-(N-Methyl-pyridinium-2-carboxamido)-1, 3, 4-thiadiazole-2-sulfonamide methylsulfate (II d, A = $MeOSO_3$)

Both methods were applied for the synthesis of this compound as in the case of IIa. The yields were 54 % (method 1) and 32 % (method 2), respectively. The compound was recrystallized from MeOH. It melts at temperatures greater than 350°C. UV (MeOH) : 265 nm, lg ε=3 .79 ; IR (KBr) : 1130 (ν_{s-SO_2}), 1315 (ν_{as-SO_2}), 1545 (δ_{NH}), 1670 (ν_{CONH}), 2960 (ν_{as-CH_3}), 3070 (ν_{NH}) cm^{-1} ; ^{1}H–NMR(DMSO-d_6) : 4 .4 (s, 3H, CH_3), 8 .5 (br s, 3H, SO_2NH_2 + CONH), 8 .5 – 9 .8 (m, 4H, ArH) ; Anal. $C_{10}H_{13}N_5O_7S_3$ requires : C, 29.19 ; H, 3 .16 ; N, 17 .03 ; Found : C, 28 .89 ; H, 3 .54 ; N, 16 .67 %.

5-(N-Methyl-pyridinium-3-carboxamido) - 1, 3, 4-thiadiazole-2-sulfonamide methylsulfate (IIe, A = $MeOSO_3$)

The same procedure was applied as for IId. Yields were 79 % and 69 %, respectively. The compound was recrystallized from MeOH. It melts above 350°C. UV (MeOH) : 265 nm, lg ε=3 .90 ; IR (KBr) : 1130 (ν_{s-SO_2}), 1300 (ν_{as-SO_2}), 1540(δ_{NH}) 1665 (ν_{CONH}), 2965 (ν_{as-CH_3}), 3070 (ν_{NH}) cm^{-1} ; ^{1}H–NMR (DMSO-d_6) : 4 .5 (s, 3H, CH_3), 8 .8 (br s, 3H, SO_2NH_2 + CONH), 8 .1 – 9 .6 (m, 4H, ArH) ; Anal. $C_{10}H_{13}N_5O_7S_3$ requires : C, 29 .19 ; H, 3 .16 ; N, 17 .03 ; Found : C,29 .03 ; H, 2 .88 ; N, 17 .37.

5-(N-Methyl-pyridinium-4-carboxamido)-1,3,4-thiadiazole-2-sulfonamide methylsulfate (IIf, A = $MeOSO_3$)

The same procedure was applied as for IId. Yields were 69 % and 63 %, respectively (recrystallized from MeOH). The compound melts above 350° C. UV (MeOH) : 265 nm, lgε = =3 .94 ; IR (KBr) : 1130 (ν_{s-SO_2}), 1310 (ν_{as-SO_2}), 1540 (δ_{NH}), 1670 (ν_{CONH}), 2965 (ν_{as-CH_3}), 3070 (ν_{NH}) ; ^{1}H–NMR (DMSO-d_6) : 4 .5 (s, 3H, CH_3) ; 8.8 (br s, 3H, SO_2NH_2 + CONH), 7 .8 – 9 .2 (m, 4H, ArH) ; Anal. $C_{10}H_{13}N_5O_7S_3$ requires C, 29 .19 ; H, 3 .16 ; N, 17 .03 ; Found : C, 28 .98 ; H, 3 .47 ; N, 16 .57 %.

5-(2, 4, 6 -Trimethylpyridinium)-1,3,4-thiadiazole-2-sulfonamide tetrafluoroborate (IV)

1 .80 g of I (10 mM) were suspended in 40 mL absolute ethanol and 2 .0 g (10 mM) of 2,4,6-trimethylpyrilium tetrafluoroborate[10] were added. The mixture was heated at reflux temperature for 3 hours, treated with 0 .5 g activated charcoal (Norite) and refluxed for other 15 min, filtered and cooled in a refrigerator. White crystals of IV precipitated which were filtered off and recrystallized from isopropanol (1 .8 g, 48 %), mp 209 C, UV (MeOH) : 268 nm, lg ε = 3 .93 ; IR (KBr) : 605 and 1100 (very intense and broad bands, BF_4), 1320 (ν_{as-SO_2}), 3070 (ν_{NH}); ^1H-NMR (TFA) : 2 .65 (s, 3H, 4′ – CH_3), 2 .95 (s, 6H, 2′ – and 6′ – CH_3), 7 .70 (s,2H, ArH) ; Anal. $C_{10}H_{13}N_4S_2O_2^+BF_4^-$ requires : C, 27 .27 ; H, 2 .95 ; N, 12 .72 ; Found : C, 27 .62 ; H, 2 .39 ; N, 12 .94 %.

4′-Amino-5′-(2-sulfonamido-1,3,4-thiadiazolyl-5-aminomethyl)-1′,2′-dimethylpyrimidinium perchlorate (VI)

4 .80 g (10 mM) of 1′-methylthiaminium bisperchlorate (V) were suspended in 50 mL absolute MeOH and 3 .60 g (20 mM) of I were added. The mixture was heated at reflux temperature for 12 hours, cooled in a refrigerator and the white precipitate was filtered off. Recrystallization from MeOH afforded 2 .50 g of VI (62 %) : mp 221°C ; UV (MeOH) : 255 nm, lgε=4.29; IR (KBr): 625, 1100 (ClO_4^-), 1300(ν_{as-SO_2}), 2970 (ν_{as-CH_3}), 3300 (ν_{NH}); ^1H-NMR((DMSO-d_6) : 2 .8 (s, 3H, 2′-CH_3) 3 .9 (s, 3H, 1′–CH_3),5.4(s, 2H, CH_2), 8 .2 (s, 1H, NH), 8.8 (s, 2H, NH_2), 9 .3 (br s, 2H, SO_2NH_2), 9 .7 (s, 1H, ArH) ; Anal. $C_9H_{13}N_7O_2S_2^+ClO_4^-$ requires : C, 24 .97 ; H, 3 .18 ; N, 23 .99 ; Found : C, 24 .54 ; H, 3 .43 ; N, 24 .27 %.

4-(N,N,N-Triethylammonium-N-methylcarboxamido)-1,3,4-thiadiazole-2-sulfonamide, chloride (VIIIa, X = Cl)

Method 1 (route A)

1 .00 g (3 .9 mM) of 5-chloroacetamido-1,3,4-thiadiazole-2-sulfonamide (VIIa) suspended in 15 mL nitromethane and 2 .5 g (25 mM) of Et_3N were heated at reflux temperature for 10 hours. The precipitate was filtered off and recrystallized from MeOH (1 .79 g, 72 %), mp 228 °C. The same procedure was applied for the bromide (VIIIa, X = Br), using 5-bromoacetamido-1,3,4-thiadiazole-2-sulfonamide as starting material (63 % from MeOH, mp 249 C) ; UV (MeOH) : 265 nm, lgε=3 .74 ; IR (KBr) : 1140 (ν_{s-SO_2}), 1440 (N^+-CH_2), 1305 (ν_{as-SO_2}), 1540 (ν_{NH}), 1650 (ν_{CONH}), 3070 (ν_{NH}) ; ^1H-NMR (DMSO-d_6) : 1 .2 (t, 9H, 3 CH_3), 3 .1 (q, 6H, 3 CH_2 from ethyl), 5 .3 (br s, 2H, N^+-CH_2CO- ; quadrupole effect), 8 .3 (br, s, 3H, SO_2NH_2 + CONH) ; Anal. $C_{10}H_{20}N_5O_3S_2^+Cl^-$ requires : C, 33 .56 ; H, 5 .59 ; N, 19 .58 ; Found : C, 33 .13 ; H, 6 .01 ; N, 19 .20 %.

Method 2 (route B)

Ethyl bromoacetate and triethylamine were allowed to react without solvent, in equimolar amounts, at room temperature. The ester was hydrolysed with excess aqueous NaOH and the resulted solution was deionized (Dowex 8, $R_4N^+HO^-$ and Dowex 50, $8H^+$). After evaporation of water, the unpurified product was treated with a twofold excess of $SOCl_2$ and refluxed for 3 hours. Excess $SOCl_2$ was evaporated *in vacuo* and the acyl chloride was treated with the equivalent amount of I in dry acetonitrile, in the presence of pyridine (as in the case of IIa, method 1). Compound VIIIa, X = Cl, was isolated with an overall yield of 34 %, identical in every respect with the substance prepared by method 1.

5-(Pyridinium-N-methylcarboxamido)-1,3,4-thiadiazole-2-sulfonamide chloride (VIIIb, X = Cl)

Method 1 (route A)

The same procedure was used as in the case of VIIIa, using pyridine instead of Et_3N (86 % from MeOH) ; mp 238° C ; UV (MeOH) : 265 nm, lgε=3 .73 ; IR (KBr) : 1160 (ν_{s-SO_2}), 1320 (ν_{as-SO_2}), 1410 (N^+-CH_2), 1530 (δ_{NH}), 1640 (ν_{CONH}), 3060, 3300 (ν_{NH}) ; ^1H-NMR (DMSO-d_6) : 5 .9 (s, 2H, CH_2), 8 .4 (s, 3H, SO_2NH_2 + CONH), 8 .2 – 9 .2 (m, 5H, ArH) ; Anal. $C_9H_{10}O_3N_5S_2^+Cl^-$ requires : C, 32 .19 ; H, 2 .98 ; N, 20 .85 ; Found : C, 32 .04 ; H, 3 .36 ; N, 21 .18 %.

Method 2 (route B)

The same procedure was used as in the case of VIIIa, X = Cl, working with pyridine instead of Et_3N and ethyl bromoacetate. The overall yield was 47 % ; VIIIb obtained in this way was identical in every respect with substance prepared by method 1.

3. RESULTS AND DISCUSSION

All new compounds were tested for inhibitory action on bovine erythrocyte CA from Boehringer—Mannheim. This is a mixture of isozymes CA I + II. No pure isozymes were available so far. The sulfonamides were assayed at 4 °C by a changing pH indicator method [13] (Maren's method), which monitors the inhibition of CA catalyzed hydration of CO_2. The new compounds were tested in concentration ranges of 10^{-9}—10^{-6} M, in comparison with acetazolamide, the CA inhibitor mostly used. Inhibition curves are presented in fig. 2. For the uncatalyzed reaction, the specific activity (SA) is a constant (2000 EU/mg) at all concentrations of inhibitor. Addition of sulfonamide produces the gradual decrease of enzyme activity. For acetazolamide, this decrease starts to be significant at concentrations in the range 10^{-9}—10^{-8}M. The same was true for compounds IIa—c. Compounds IId—f, IV and VI were inactive at these concentrations. Compound VIIIb has a lower activity compared with acetazolamide; it begins to inhibit the enzyme strongly at 10^{-7}—10^{-6}M. The most active compound was VIIIa, but the differences in activity are not prominent compared to acetazolamide.

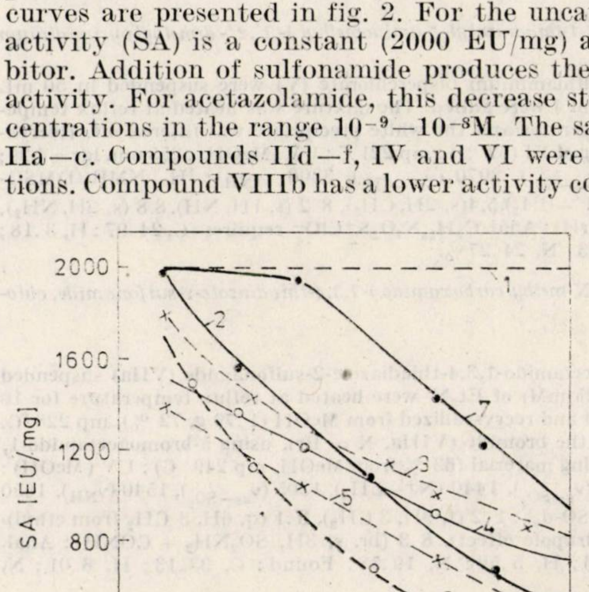

Fig. 2.—Inhibition curves for acetazolamide and the new compounds; S A (specific activity) *vs*, concentration; (1): uncatalyzed reaction; (2): acetazolamide; (3)—(5): IIa—c, respectively; (6), (7): VIIIa, b, respectively.

ACKNOWLEDGEMENT. Special thanks are addressed to biologist Olimpia Nagy for help with the enzymic assay and to Mr. Radu Slătineanu for his help with the graphical part of our paper.

REFERENCES

[1] Part I: C. Supuran, M. Andruh and I. Pușcaș, *Rev. Roumaine Chim.*, preceding paper.
[2] P. J. Wistrand, *Ann. N. Y. Acad. Sci.*, **429**, 195 (1984).
[3] P. J. Wistrand, *J. Med. Sci. (Uppsala), Suppl.*, **26**, 75 (1979).

[4] J. P. Tinker, R. Coluson and I. M. Weiner, *J. Pharmacol. Exp. Ther.*, **218**, 600 (1981).

[5] G. Lönnerholm, O. Selking and P. J. Wistrand, *Gastroenterology*, **88**, 1151 (1985).

[6] B. Karlmark, B. Agerup and P. J. Wistrand, *Acta Physiol., Scand.*, **106**, 145 (1979).

[7] A. T. Balaban, A. Dinculescu, G. N. Dorofeenko, G. W. Fischer, A. V. Koblik, V. V. Mezheritskii and W. Schroth, "Pyrylium Salts. Syntheses, Reaction and Physical Properties" in "Advances in Heterocyclic Chemistry", A. R. Katritzky Ed., Academic Press, New York, 1982.

[8] J. A. Zoltewicz, *Synthesis (Stuttgart)*,f**218** (980).

[9] V. Petrow, *J. Chem. Soc.*, 1958, 1508.

[10] A. T. Balaban and A. J. Boulton, *Org. Synth. Coll.* Vol. 5, 1112 (1973).

[11] J. A. Zoltewicz and T. D. Baugh, *Synthesis (Stuttgart)*,f**217** (1980).

[12] R. W. Young, K. H. Wood, J. A. Eichler, J. R. Vaughans and G. W. Anderson, *J. Amer. Chem. Soc.*, **78**, 4649 (1956).

[13] T. H. Maren, V. I. Ash and E. M. Bailey, *Bull. Johns Hopkins Hosp.*, **95**, 244 (1954).

[4] J. P. Tinker, R. Coulson and I. M. Weiner, *J. Pharmacol. Exp. Ther.*, **218**, 600 (1981).

[5] G. Lönnerholm, O. Selking and P. J. Wistrand, *Gastroenterology*, **88**, 1151 (1985).

[6] B. Karlmark, B. Agerup and P. J. Wistrand, *Acta Physiol. Scand.*, **106**, 145 (1979).

[7] A. T. Balaban, A. Dinculescu, G. N. Dorofeenko, G. W. Fischer, A. V. Koblik, V. V. Mezheritskii and W. Schroth, "Pyrylium Salts. Syntheses, Reactions and Physical Properties" in "Advances in Heterocyclic Chemistry", A. R. Katritzky Ed., Academic Press, New York, 1982.

[8] J. A. Zoltewicz, *Synthesis (Stuttgart)*, 218 (1980).

[9] V. Petrow, *J. Chem. Soc.*, 1958, 1508.

[10] A. T. Balaban and A. J. Boulton, *Org. Synth. Coll. Vol.* 5, 1112 (1973).

[11] J. A. Zoltewicz and T. D. Bench, *Synthesis (Stuttgart)*, 217 (1980).

[12] R. W. Young, K. H. Wood, J. A. Eichler, J. R. Vaughan and G. W. Anderson, *J. Amer. Chem. Soc.*, **78**, 4649 (1956).

[13] T. H. Maren, V. I. Ash and E. M. Bailey, Jr., *Bull. Johns Hopkins Hosp.*, **95**, 244 (1954).

Revue Roumaine de Chimie, 35, 3, 407–414 (1990)

SYNTHESIS AND EPR SPECTRA OF PERSISTENT AROXYLS. IV[1]

ORTHO, *ORTHO'*-DISUBSTITUTED PHENOLS POSSESSING IN THE *PARA*-POSITION A 2-BONDED-1,3-DICARBONYLIC (OR A FUNCTIONALLY RELATED) GROUP *

JEAN M. HERDAN,[a] VASILE DINOIU,[a] AURELIA MEGHEA,[a]
MIRCEA D. GHEORGHIU,[b] ANA SCHIKETANZ,[b] MARIA GIURGINCA[c]
and ALEXANDRU T. BALABAN[b]

[a] Institute of Technological Engineering, Research and Refinery Design, Ploiești, Romania
[b] Polytechnic Institute, Chair of Organic Chemistry, Splaiul Independenței 313, 77206 Bucharest, Romania
[c] Research Institute for Rubber and Plastics Processing, 79628 Bucharest, Romania

Received October 25, 1989

Two types of precursors of sterically hindered aroxyls were prepared: diethyl 3,5-di-t-butyl-4-hydroxyphenylmalonate II, and a dozen of 2-(3,5-dialkyl-4-hydroxybenzyl)-1,3-dicarboxylic derivatives IV derived from diethyl or dimethyl malonate, ethyl cyanoacetate, or acetylacetone, the two alkyl groups situated *ortho* to the hydroxy group are t-butyl and/or methyl substituents. ^{1}H-NMR and EPR assignments are discussed. The comparative behaviour of the reported phenols as antioxidants in rubber has been investigated.

INTRODUCTION

Two research groups have investigated the reaction of hindered phenolic Mannich bases or of their quaternary salts with 1,3-dicarbonylic compounds: several patents [2] described the reaction of quaternary bases of 3,5-disubstituted 4-hydroxybenzylic quaternary salts with acetylacetone in the presence of sodium hydride leading to mono- or bis-phenolic derivatives of acetylacetone: Schmidt and Bennet [3] described the reaction of dimethyl malonate with 3,5-di-t-butyl-4-hydroxy-N,N-dimethylbenzylamine, leading similarly to mono- or bis-phenolic derivatives.

Sterically hindered aroxyls and their phenolic precursors are important antioxidants for the chemical industry and some of these compounds are approved drugs. [4,5]

We report the preparation of new 2,6-di-t-butylphenols having in the 4-position a dialkyl malonate, an alkyl cyanoacetate, or a β-diketonic substituent; the *para*-phenolic position is connected with the median carbon of the 1,3-diketonic substituent either directly in compounds II, or through a methylene group in products IV. Such compounds can afford strong chelatic complexes with transition metals or with Main Group elements such as boron; metallic complexes may have practical applications, and theoretically they are also interesting because of the electronic interaction between the odd electrons in the organic ligands and in *d*-orbitals.

---

* Dedicated to the memory of Mihai Elian.

For comparison of the reactivity and for finding whether single electron transfer (SET) reaction are involved in condensations of β-diketonic systems with hydrazine or hydroxylamine derivatives, we report also the preparation of less hindered phenols possessing in 2 and 6 positions either two methyl groups, or a methyl and a t-butyl group. Our notation will employ capital letters: A for 2,6-di-t-butylphenoxy, B for 2-t-butyl-6-methylphenoxy, and C for 2,6-dimethylphenoxy groups. In order to facilitate ^1H-NMR assignments, we used both diethyl and dimethyl malonate. Small letters will discriminate the various substituents in *para*-position relatively to the hydroxy group.

SYNTHESIS

Two different approaches were employed, both of them starting from 2,6-disubstituted phenols (IA—IC). The first one involves nucleophilic substitution of halogen from α-bromomalonate by the 2,6-disubstituted phenoxide anion when the yield of II was 35%.

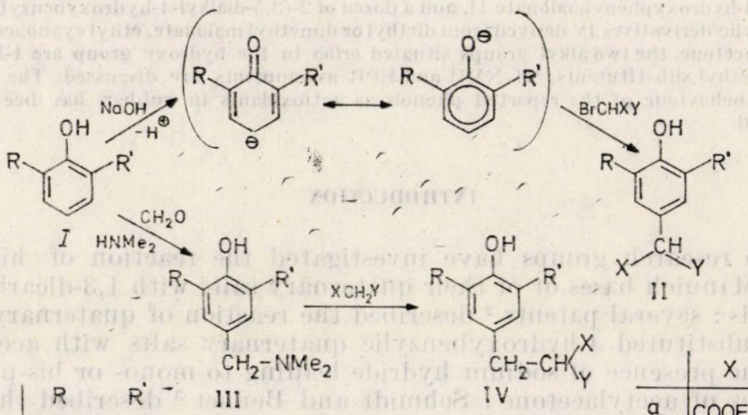

	R	R'
A	tBu	tBu
B	tBu	Me
C	Me	Me

	X	Y
a	COOEt	COOEt
b	COOEt	CN
c	COOMe	COOMe
d	COMe	COMe
e	$CONH_2$	CN

Better yields were obtained in the second approach which was more general and involved a Mannich reaction followed by condensation of the Mannich base III with the 1,3-dicarboxylic compound; the leaving group is dimethylamine and the yields of IV are usually above 50%.

Table 1 presents the structures and the yields of the compounds obtained by the second method, together with melting or boiling points. In can be observed that yields are good for cyanoacetates, low for 1,3-diketones and medium for dialkylmalonates.

Elemental analyses are indicated in Table 2.

Table 1

Physical data and yields for compounds IV

IV	R	R,	X	Y	Data (°C)[a]	Yield %
Aa	tBu	tBu	CO_2Et	CO_2Et	b.p. 192–5/2	52
Ab	tBu	tBu	CO_2Et	CN	m.p. 207–8/E	64
Ac	tBu	tBu	CO_2Me	CO_2Me	b.p. 180–3/3	57
Ad	tBu	tBu	COMe	COMe	m.p. 148–9/E	25
Ae	tBu	tBu	$CONH_2$	CN	m.p. 157–9/H	71
Ba	tBu	Me	CO_2Et	CO_2Et	b.p. 205–8/4	66
Bb	tBu	Me	CO_2Et	CN	b.p. 225–8/5	44
Bd	tBu	Me	COMe	COMe	b.p. 180–8/3	33
Ca	Me	Me	CO_2Et	CO_2Et	m.p. 190–2/E	41
Cb	Me	Me	CO_2Et	CN	m.p. 187–9/E	60
Cc	Me	Me	COMe	COMe	b.p. 160–9/2	39

[a] Melting points (when followed by capital letters indicating solvents for recrystallization : E, ethanol ; H, n-heptane) or boiling points (when followed by the pressure shown in Torr).

^{1}H–NMR SPECTRA OF PHENOLS

All phenols reported here were investigated by ^{1}H–NMR spectroscopy in $CDCl_3$ solution unless otherwise stated. The peaks and their assignment are presented in Table 3. For the 2-t-butyl-6-methyl-phenols IVB, the 3- and 5-protons appear distinct, with a small (doublet) splitting due to the *meta*-coupling constant (2.5 Hz).

Chemical shift non-equivalence of the methylene protons in compounds having asymmetric carbon atoms ($X \neq Y$), i.e. IVAb, IVAc, IVBb and IVCb complicates the precise location and assignment of the methylene and methine protons.

EPR SPECTRA OF AROXYLS IVA

On oxidation with lead tetraacetate in benzene or toluene solution, phenols IVAa–IVAe were converted into aroxyls VAa–VAe, respectively.

However, phenols II gave no EPR signal under these conditions probably owing to facile further oxidation to 4-quinonemethides VI. Phenols IVB and IVC with lower sterical shielding of the aroxyl centre than IVA give unstable aroxyls which at room temperature yield no detectable EPR signals.

Table2

Elemental analyses for II and IV

Comp.	R	R′	X	Y	Formula	C %		H %	
						Calc.	Found	Calc.	Found
II Aa	tBu	tBu	COOEt	COOEt	$C_{21}H_{32}O_5$	69.23	69.94	8.87	8.70
IV Aa	tBu	tBu	COOEt	COOEt	$C_{22}H_{34}O_5$	69.84	69.82	8.99	8.63
IV Ab	tBu	tBu	COOEt	CN	$C_{20}H_{29}NO_3$	72.50	73.07	8.76	8.71
IV Ac	tBu	tBu	CCOMe	COOMe	$C_{20}H_{30}O_5$	68.57	68.66	8.57	8.28
IV Ad	tBu	tBu	COMe	COMe	$C_{20}H_{30}O_5$	75.47	75.33	9.43	9.27
IV Ae *	tBu	tBu	CONH	CN	$C_{17}H_{24}N_2O_2$	—	—	—	—
IV Ba	tBu	tBu	COOEt	COOEt	$C_{19}H_{28}O_5$	73.91	73.92	8.69	8.40
IV Bb	tBu	Me	COOEt	CN	$C_{17}H_{23}NO_3$	70.58	71.02	7.96	7.99
IV Bd	tBu	Me	COMe	COMe	$C_{17}H_{24}O_3$	73.91	73.92	8.69	8.40
IV Ca	Me	Me	COOEt	COOEt	$C_{16}H_{22}O_5$	65.30	65.61	7.48	7.77
IV Cb	Me	Me	COOEt	CN	$C_{14}H_{17}NO_3$	68.01	68.11	6.88	6.61
IV Cd	Me	Me	COMe	COMe	$C_{14}H_{18}O_3$	71.79	72.18	4.70	4.51

* Calc. N, 9.21 ; found : 9.16%.

Table 3

^{1}H$-$NMR Peaks in $CDCl_3$

IV	R	R,	X	Y	2,6-Substituents		Aryl	4-Substituent				OH
					tBu	Me		CH$_3$	CH$_2$(Et)	CH	CH$_2$	
Aa	tBu	tBu	COOEt	COOEt	1.42	—	7.22	1.18	3.45	3.45	3.07	
Ab	,,	,,	COOEt	CN	1.43	—	7.07	0.90	3.92	*a*	3.08	
Ac	,,	,,	COOMe	COOMe	1.40	—	7.15	3.62	—	*a*		4.88
Ad	,,	,,	COMe	COMe	1.43	—	6.93	2.07	—	3.88	3.02	5.17
Ae^b	,,	,,	CONH$_2$	CN	1.45	—	7.07	—	—	3.45	3.15	5.13
Ba	tBu	Me	COOEt	COOEt	1.40	2.20	6.83 6.97	1.23	4.17	3.63	3.10	
Bb	,,	,,	COOEt	CN	1.43	2.23	6.83 6.95	1.30	4.23	*a*	*a*	4.75
Bd	,,	,,	COMe	COMe	1.43	2.23	6.77 6.93	2.10, 2.13	—	3.53	2.90	4.70
Ca^c	Me	Me	COOEt	COOEt	—	2.13	6.70	1.17	4.07	*a*	— 2.88	
Ca	,,	,,	COOEt	COOEt	—	2.17	6.73	1.20	4.12	3.40	3.03	
Cb	,,	,,	COOEt	CN	—	2.20	7.20	1.27	4.08	*a*	3.05	
Cd	,,	,,	COMe	COMe	—	2.17	6.73	2.10	—	*a*	2.70	

^{a} Overlapping bands

^{b} The NH$_2$ protons appear at 6.00 ppm

^{c} In $D_3C-SO-CD_3$ solution

Hyperfine coupling constants (hfc's) were determined from the EPR spectra. Table 4 presents these hfc's together with the g-values. The low values of the g-factors (2.0045–2.0048) prove that considerable spin delocalization is present over carbon and hydrogen atoms.

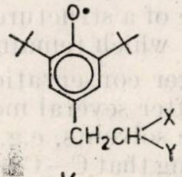

V

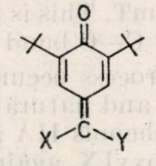

VI

Table 4

EPR Spectral parameters (a_H values in mT) for 2,6-di-t-butyl-aroxyls V

Comp.	X	Y	g	a_{CH_2}	a_H
VAa	CO_2Et	CO_2Et	2.0045	0.76	0.18
VAb	CO_2Et	CN	2.0048	0.44, 0.63	0.175
VAc	CO_2Me	CO_2Me	2.0045	0.80	0.17
VAd	COMe	COMe	2.0047	0.77	0.17
VAe	$CONH_2$	CN	2.0048	0.61	0.18

The highest spin density is at the *para*-methylene group (hfc's 0.4–0.8 mT); the *meta*-standing CH groups have normal hfc's (0.17–0.18 mT).

Interestingly, at the EPR time-scale the methylene protons in VAb are magnetically non-equivalent, being diasterotopic by attachment to an asymmetric carbon atom. No such non-equivalence could be detected for VAe, however, although here also an asymmetric carbon atom is present.

The lower value of the coupling constant for the methylene protons in VA than in the previously studied pyrazolyl-substituted aroxyls VII indicates for the latter a higher contribution of hyperconjugative limiting structures placing high spin densities on these protons : this is in agreement with the extended conjugation in such structures VII, which have $a_H = 1.1$ mT for the methylene protons. The related 4-benzyl-2,6-di-t-butyl-

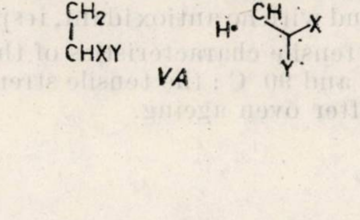

VA

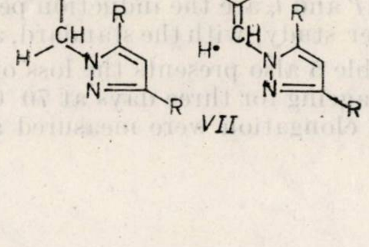

VII

phenoxyl VIII has an intermediate coupling constant for the benzylic protons, namely 0.87 mT. [6]

In time, at room temperature, the EPR spectra of radicals **VA** change after a few hours : the initial triplet of triplets is gradually replaced by an intense narrower multiplet, approximating a 1 : 4 : 6 : 4 : 1 quintet with spacing 0.185 mT. This is indicative of a structure devoid of benzylic protons, formed by C—C bond rupture, which remains to be elucidated.

A different process occurs on longer conservation of phenols II in the presence of air and natural light : after several months, one observes on dissolving the phenols IIA in organic solvents, e.g. benzene, the EPR spectrum of galvinoxyl X, again indicating that C—C bond fragmentations have taken place. A similar fragmentation was reported by us recently : [1] 24 hrs after the formation of phosphorus-containing aroxyls IX, the EPR spectrum of IX is replaced by another one with a doublet (a_H = = 0.57 mT) of quintets (four *meta*-protons with a_H = 0.13 mT). The latter EPR spectrum is identical with that of galvinoxyl X. [7]

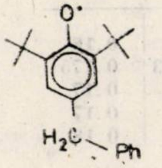

VIII

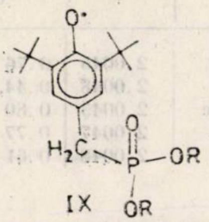

IX

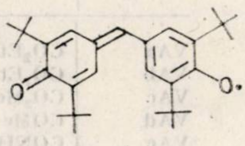

X

TESTS AS ANTIOXIDANTS FOR RUBBER

According to a previously published methodology, [10] the newly synthesized phenols were tested for their antioxidant activity for purified natural rubber. Samples were prepared from two parts of antioxidant for 100 parts of natural rubber.

The thermo-oxidative degradation was investigated and the induction period as well as the propagation period were determined (Table 5) by following the increase of the 1720 cm^{-1} IR absorption band of a rubber film maintained in air at 110 °C.

From the induction period, the relative activity A_r using as standard 2,6-di-t-butyl-4-methylphenol was calculated according to the formula

$$A_r = (t - t_0)/(t' - t_0)$$

where t, t' and t_0 are the induction periods of the rubber with the antioxidant under study, with the standard, and with no antioxidant, respectively.

Table 5 also presents the loss of tensile characteristics of the rubber on oven ageing for three days at 70 °C and 90 °C : the tensile strength and ultimate elongation were measured after oven ageing.

Table 5

Antioxidant activity of phenolic compounds II, IV for natural rubber

Comp.	R	R′	X	Y	Induction period (hrs)	Propagation period (hrs)	Relative Activity A_r	Relative loss on oven ageing (%)			
								72 hrs at 70°		72 hrs at 90°	
								Strength	Elongation	Strength	Elongation
—	No antioxidant				6	9	—	—	—	—	—
—	2,6–tBu_2-4-Me-phenol				18	5	1	18	21	37	42
IIAa	tBu	tBu	CO_2Et	CO_2Et	29	11	1.6	15	21	43	52
IVAa	tBu	tBu	CO_2Et	CO_2Et	36	11	2.0	7	18	23	33
IVAb	tBu	tBu	CO_2Et	CN	150	200	8.3	5	16	20	30
IVAd	tBu	tBu	COMe	COMe	204	144	18.9	6	10	25	30
IVBa	tBu	Me	CO_2Et	CO_2Et	28	7	1.6	15	21	40	47
IVBb	tBu	Me	CO_2Et	CN	16	11	0.9	18	14	39	42
IVBd	tBu	Me	COMe	COMe	18	16	1.0	12	20	32	41
IVCa	Me	Me	CO_2Et	CO_2Et	15	8	0.8	14	19	28	37
IVCb	Me	Me	CO_2Et	CN	9	11	0.5	8	14	28	28
IVCd	Me	Me	COMe	COMe	12	8	0.7	5	7	27	36

Judging from their highest relative activities, the two compounds IVAb and especially IVAd prove to be the best, surpassing the standard 10–20 times. The behaviour upon aging in these cases also shows minimal losses at 70 °C.

EXPERIMENTAL

Diethyl 3,5-di-t-butyl-4-hydroxyphenylmalonate, IIAa, (via the first method).

A solution of 2.44 g (61 mmol) sodium hydroxide in 2 ml water was added under argon atmosphere into a solution of 13 g (63 mmol) 2,6-di-t-butylphenol in 25 ml dimethylformamide (DMF). The reaction mixture was stirred for one hour at room temperature under argon, then about 12 ml of solvent was removed by distillation at 10–15 Torr (bp. 30–43° C). Then 14.34 g diethyl bromomalonate in 30 ml DMF was added and the mixture was stirred under argon for 18 hrs at 45–50° C. The reaction mixture was acidified with hydrochloric acid and diluted with water. The reaction product was extracted with diethyl ether. The extract was dried on Na_2SO_4, the solvent was removed under vacuum, and the product was then distilled.

IR Spectrum: 3645 cm^{-1} (OH), 1725 cm^{-1}(CO).

2-(3,5-Dialkyl-4-hydroxybenzyl)-1,3-*dicarbonylic compounds (IV),* via the second method.

To a solution of 30 mmol of 3,5-dialkyl-4-hydroxy-N,N-dimethyl-benzylamine in 100 ml DMF, 36 mmol of active methylene compound (1,3-diketone or malonic ester) were added and then, under argon, 42 mmol of powdered anhydrous potassium carbonate. The mixture was stirred under argon at 110–115° for 6–8 hrs. After cooling, the mixture was poured into 360 ml of 2N hydrochloric acid and the solution was extracted with diethyl ether. The ethereal extract was dried over sodium sulfate and fractionated at reduced pressure. In several cases (when the product is solid), further purification was achieved by recrystallization from ethanol or n-heptane.

REFERENCES

[1] Part III, J. Herdan, N. Negoiță, M. N. Grecu, M. D. Gheorghiu, and A. T. Balaban, *Rev. Roum. Chim.*, **34**, 1515 (1989).

[2] C. R. Everly and J. M. Roper (Ethyl Corp.), U. S. Pat. 4456770 (1984); 4456771 (1989); 4532356 (1985).

[3] A. Schmidt and H. Bennet, *Helv. Chim. Acta*, **59**, 522 (1976).

[4] V. V. Ershov, G. A. Nikiforov and A. A. Volodkin, "Prostranstvenno-zatrudrenye fenoly", Khimia, Moscow, 1972.

[5] Yu A. Shlyapnikov, S. G. Kiroshkin and A. P. Mar'in, "Antiokislitel'naya stabilizatsiya polimerov", Khimia, Moscow, V. D. Pokhodenko, L. S. Degtyarev, V. G. Kashetchko and V. S. Kutz, "Problemy khimii svobodnykh radikalov", Izd. Naukova Dumka, Kiev, 1984, p. 5–89; M. N. Emanuel and A. L. Buchachenko, "Khimiceskaya fizika molekulyarnogo razrusheniya i stabilizatsiya polimerov", Khimiya, Moscow, 1988; V. A. Roginskii, "Fenolnye antioxidanty", Nauka, Moscow, 1988.

[6] K. Scheffer, *Z. Elektrochem*, **65**, 439 (1961).

[7] G. M. Coppinger, *J. Am. Chem. Soc.*, **79**, 501 (1957); B. S. Joshi, *Chem. Ind.*, 525 (1957); P. D. Bartlett and T. Funahashi, *J. Am. Chem. Soc.*, **84**, 2593 (1962); the EPR spectrum is reproduced in refs. 8 and 9.

[8] G. R. Luckhurst, *Mol. Phys.*, **11**, 205 (1966).

[9] A. R. Forrester, J. M. Hay and R. H. Thomson, "Organic Chemistry of Stable Free Radicals", Academic Press, London, 1968, p. 282.

[10] G. Ivan and M. Giurginca, *Rev. Roum. Chim.*, **34**, 1351 (1989).

Revue Roumaine de Chimie, 35, 3 415–419 (1990)

^{1}H–NMR ASSIGNMENTS FOR 2,4-DIARYL-PYRYLIUM SALTS AND -PYRIDINES HAVING FUSED 5- OR 6-MEMBERED SATURATED RINGS BRIDGING 5,6-POSITIONS *

ANCA MARTON, URSULA BOLOGA, TEODOR-SILVIU BALABAN,
MIRCEA D. GHEORGHIU and ALEXANDRU T. BALABAN
Polytechnic Institute, Chair of Organic Chemistry, Splaiul Independenţei 313,
77206, Bucharest, Romania

Received October 28, 1989

The ^{1}H–NMR spectra of 2,4-diaryl-5,6,7,8-tetrahydrochromylium and 2,4-diaryl-5,6-trimethylenepyrylium perchlorates and of their α-deuterated isotopomers obtained by isotopic exchange with CH_3COOD were recorded allowing unambiguous assignments. Similar determinations and assignments were made for the corresponding pyridines obtained from the above pyrylium salts and ammonia; in addition, lanthanide-induced shifts were determined with $Eu(fod)_3$ in $CDCl_3$ for these pyridines.

INTRODUCTION

By diacetylation, methylenecyclohexane and methylenecyclopentane as well as their endocyclic isomers (1-methylcyclohexene and 1-methylcyclopentene) yield pyrylium salts having tri- and tetramethylene groups annelated to the pyrylium ring, and yielding fairly complicated ^{1}H–NMR spectra.[1–4] In the present paper we report the assignment for ^{1}H–NMR signals for the related 2,4-diaryl-analogues **4**, prepared from the 6- or 5-membered cyclanones **1** ($n = 5$ or 6) and chalcone **2**, followed by dehydration and dehydrogenation of the 1,5-diketones **3** resulted by Michael addition. Throughout this paper the anions of pyrylium cations will be perchlorate. Compounds **4** with $n = 6$ had been obtained earlier by Allen and coworkers,[5,6] and by Wizinger et al.[7], and both pyrylium salts **4**, $n = 5$ and 6 were used by Drexhage et al.[8] as starting materials for pyrylocyanines having electronic absorption bands in the infrared region.

In a previous paper,[9] it was shown that, when the dehydrogenation is carried out with t-butyl chloride and anhydrous aluminium chloride, the ketone **3** is t-butylated and then cyclized yielding 4-(p-t-butylphenyl)-derivatives **6** along with 4-(3,5-di-t-butylphenyl)-derivatives.

It will be reported in a separate paper[10] that this dehydrogenation method is superior to that using $Ph_3C^+ClO_4^-$ in acetonitrile for dehydrogenating alkyl-substituted 1,5-diketones because in that case (i) no aromatic t-butylations leading to side-products are possible, (ii) the yields albeit lower, are comparable, and (iii) the dehydrogenating agents are much more readily availabe and less expensive.

---

* Dedicated to the memory of Mihai Elian.

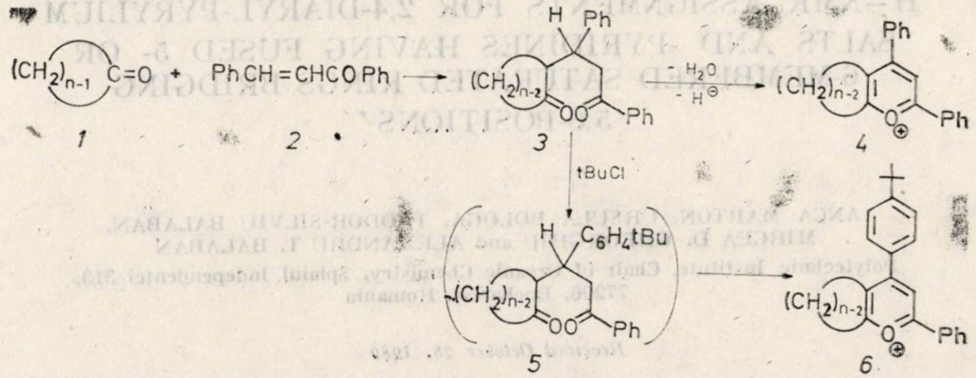
$(CH_2)_{n-1}$ C=O + PhCH=CHCOPh
H Ph
$(CH_2)_{n-2}$
O O Ph
$- H_2O$
$- H^\ominus$
Ph
$(CH_2)_{n-2}$
Ph
1
2
3
4
tBuCl
H C_6H_4tBu
$(CH_2)_{n-2}$
O O Ph
5
$(CH_2)_{n-2}$
Ph
6

The 2,4-diaryl-5,6,7,8-tetrahydrochromylium (5,6,7,8-tetrahydro-4-arylflavylium) salts **7** (i.e. **4** or **6**, with $n = 6$), and the related five-membered derivatives ($n = 5$) were subjected to two types of reactions: conversion into pyridine derivatives **8** under the action of ammonia, [4] and deuteration by isotopic exchange with AcOD.[11] It is known[11] that only α- and γ-methyl(ene) groups are deuterated under these conditions, yielding **9**. By subsequent reaction with ammonia at room temperature, the deuterated pyrylium salts afford deuterated pyridines **10** without losing their deuterium atoms.

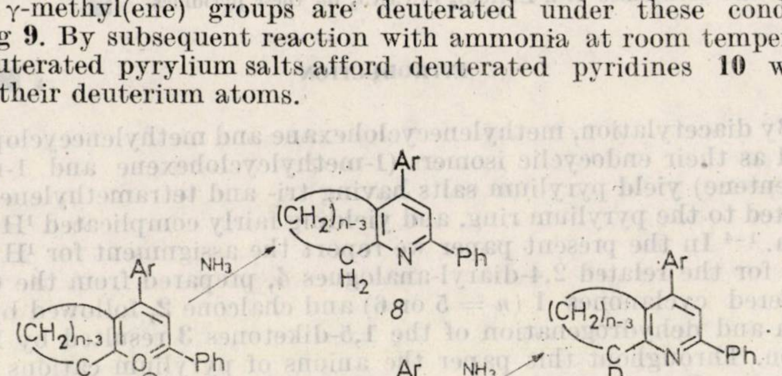
Ar
$(CH_2)_{n-3}$
C N Ph
H_2
8
NH_3
Ar
$(CH_2)_{n-3}$
C O Ph
H_2
7
AcOD
Ar
$(CH_2)_{n-3}$
C O Ph
D_2
9
NH_3
Ar
$(CH_2)_{n-3}$
C N Ph
D_2
10

In the previously mentioned paper, [9] the ^1H-NMR spectral assignments for the tetrahyroflavylium salts and the tetrahydroquinolines (**7** and **8**, respectively, $n = 6$) were based on the lower field at which the 8-methylene group resonated relatively to other methylene groups. However, the trimethylene groups in the 5-membered congeners (**7** and **8**, $n = 5$) give rise to overlapping multiplets, therefore here the assignments needed deuteration and lanthanide shift reagents.

^{1}H—NMR SPECTRAL ASSIGNMENTS

Table 1 presents ^{1}H—NMR chemical shifts of pyrylium salts **7** in trifluoroacetic acid (TFA) or in $CDCl_3$,and Table 2 corresponding data of pyridines **8** in $CDCl_3$. For the six-membered-annelated derivatives, the data are in agreement with previously reported spectra (in liquid sulphur dioxide for **7**, in carbon disulphide or $CDCl_3$ for **8**) and with preceding assignments; both the 5- and the 8-methylene groups appear as triplets in the ^{1}H—NMR spectra of tetrahydrochromylium salts **7** and tetrahydroquinolines **8** ($n = 6$), whereas their 6- and 7-methylene groups appear as an overlapping multiplet. For the pyrylium salts and pyridines annelated with a 5-membered ring ($n = 5$), the 5- and 7-methylene groups appear as triplets, whereas the 6-methylene group appears as a quintet.

Table 1

^{1}H—NMR Chemical shifts (δ, ppm) for pyrylium perchlorates **7** and **9**.

No.	n	Ar	Solvent	8—CH_2	7—CH_2	6—CH_2	5—CH_2	3—H	2—Ph(o)	Arom.
4	6	Ph	TFA	3.40t^a	2.10m	2.10m	3.00	8.02s	8.83m	7.60m
4	6	Ph	$CDCl_3$	3.03t^a	1.83m	1.83m	2.57t	7.95s	7.80m	7.35m
6	6	C_6H_4tBu	TFA	2.43t^a	2.13m	2.13m	3.10t	8.16s	8.05m	7.78
6	6	C_6H_4tBu	$CDCl_3$	3.08t^a	1.83m	1.83m	2.67t	7.93s	7.80m	7.33m
4	5	Ph	TFA	—	3.65t^a	2.58qnt	3.53t	8.43s	8.32m	7.83m

^{a} Disappears on deuteration (**7** → **9**).

Table 2

^{1}H—NMR Chemical shifts (δ, ppm) and molar induced shifts with $Eu(fod)_3$ (MIS, ppm, in brackets) for pyridines **8** and **10** in $CDCl_3$

Ar	n	8—CH_2	7—CH_2	6—CH_2	5—CH_2	3—H	2Ph(o)	Arom.
Ph	6	3.03t^a	1.83m	1.83m	2.63t	7.35s^c	7.95m	7.35m
Ph	6	(4.40)	(0.31)	(0.31)	(0.52)	(1.22)	(3.03)	(0.28)
C_6H_4tBu	6^b	3.08t^a	1.3m	1.83m	2.67t	7.33^s	7.93m	7.33m
C_6H_4tBu	6^b	(3.25)	(0.21)	(0.21)	(0.48)	(1.03)	(2.42)	(0.32)
Ph	5	—	3.17t^a	2.22m	3.05t	7.57s	7.97m	7.47m
Ph	5	—	(3.0)	(0.27)	(0.63)	(1.0)	(3.0)	(0.5)

^{a} Disappears on deuteration (**8** → **10**)
^{b} t-Butyl singlet at $\delta = 1.36$ ppm
^{c} Obscured by the other aryl protons

On deuteration, one observes the disappearance of the peaks due to the 8-methylene protons for $n = 6$, and correspondingly to the 7-methylene protons for $n = 5$, whereas the protons of the adjacent methylene group change their multiplicity, allowing unambiguous assignments.

For the pyridines **8** additional information is obtained from the molar induced shifts in $CDCl_3$ in the presence of the lanthanide shift reagent $Eu(fod)_3$ as seen in Table 2 : the largest MIS value corresponds to the protons (closest to the coordinating nitrogen heteroatom) which disappear on deuteration ($8-CH_2$ for $n = 6$, $7-CH_2$ for $n = 5$) ; the second largest MIS value corresponds to the two *ortho*-hydrogens on the 2-phenyl group, which appear as a multiplet (doublet of doublets) at very low field ; the third largest MIS value is to the $3-H$ on the pyridine ring, which is overlapping with the aromatic protons in the undoped spectrum, but appears as a sharp singlet upon addition of the LSR ; and the next largest MIS value corresponds to the $5-CH_2$ methylene protons, both for $n = 5$ and for $n = 6$.

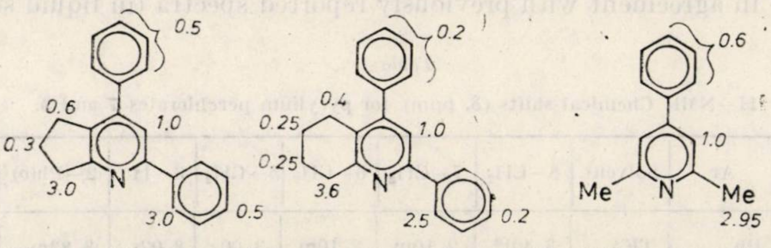

Fig. 1. — Comparison between molar induced shifts (MIS, ppm) with $Eu(fod)_3$ in $CDCl_3$ relative to the value of the value of the pyridinic proton in position 3, for the pyridines 8, $n=5$ and 6, and the 2,6-dimethyl-4-phenylpyridine described in ref. 12.

By comparison with MIS data (Fig. 1) for other substituted pyridines with both α-substituents being alkyl groups [12] the present induced shifts are lower, owing to the 2-phenyl group.

The present pyridines offer an interesting possibility for probing conformational change with LSR's. Both pyridines 4 and 5 have an α-CH_2 group which has two fixed hydrogen atoms pointing towards the complexed europium atom. In a mobile α-alkyl side chain (ethyl for instance), a mobile CH_2 group should lead to larger MIS values. Supporting this hypothesis (which will be tested in the near future) are the relatively larger MIS values for the pyridine annelated with the five-membered ring where the CH_2 protons are more remote from the nitrogen atom allowing the LSR to approach closer.

EXPERIMENTAL PART

^1H-NMR Spetra were recorded with Varian A—60A and EM—360L instruments using internal tetramethylsilane.

2,4-Diphenyl-5,6-trimethylenepyrylium perchlorate 4, $n = 5$. From 10 g cyclopentanone and 20 g chalcone in the presence of 20 ml piperidine, after 20 hrs at room temperature, filtration and recrystallization from ethanol, the saturated 1,5-diketone 3, $n = 5$ was obtained, m.p. 81 , 52% yield.

This diketone (4 g) was heated at 100° with 6.8 g triphenylmethyl perchlorate in 36 ml dry acetonitrile for 3.5 hrs. After cooling and filtration of the crystals, these were recrystallized from acetic acid. Yellow-orange crystals, m.p. 240° (dec.), yield 75%.

Deuteration. Acetic anhydride, freshly distilled (50 ml) was refluxed for 3 hrs with 10 ml deuterium oxide, yielding CH_3COOD. The pyrylium salt (0.5 g) was refluxed for 8 hrs with 1 ml CH_3COOD, filtered while warm, cooled, and diluted with diethyl ether.The deuterated pyrylium salt was filtered off and washed with diethyl ether.

Conversion into pyridine **8**, $n = 5$. The non-deuterated pyrylium salt (1 g) in 40 ml ethanol was refluxed for 20 min with 25 ml aqueous ammonia, diluted with water, and extracted with diethyl ether. The ethereal layer was shaken with 10% hydrochloric acid. The separated acid layer was extracted with ether and then made strongly alkaline. The precipitated pyridine was extracted with ether, the solvent evaporated, and the product was recrystallized from methanol. White crystals, m.p. 149°, yield 96%.

Synthesis of 4-aryl-5,6,7,8-tetrahydroflavylium perchlorates and of the corresponding pyridines. Analogous reactions starting with cyclohexanone and chalcone, followed by dehydrogenation with t-butyl chloride and anhydrous aluminium chloride were carried out as described in a preceding paper.[9] The deuteration was effected as indicated above.

REFERENCES

[1] A. T. Balaban and C. D. Nenitzescu, *J. Chem. Soc.*, **1961**, 3561.

[2] P. F. G. Praill and A. L. Whitear, *J. Chem. Soc.*, **1961**, 3573

[3] A. T. Balaban, W. Schroth and G. Fischer, *Adv. Heterocyclic Chem.*, **12**, 241 (1969).

[4] A. T. Balaban, A. Dinculescu, G. N. Dorofeenko, A. V. Koblik, G. W. Fischer, V. V. Mezheritskii and W. Schroth, "Pyrylium Salts. Syntheses, Reactions and Physical Properties", (Adv. Heterocyclic Chem., Suppl. Vol. 2, edited by A. R. Katritzky), Academic Press, New York, 1982.

[5] C. F. H. Allen and H. R. Sallans, *Canad. J. Research*, **9**, 574 (1933).

[6] C. F. H. Allen and W. E. Barker, *J. Am. Chem. Soc.*, **54**, 736 (1932).

[7] R. Wizinger and P. Ulrich, *Helv. Chim. Acta*, **39**, 221 (1956).

[8] A. Seilmeier, W. Kaiser, B. Sens and K. H. Drexhage, *Optics Lett.*, **8**, 205 (1983).

[9] A. T. Balaban, A. R. Katritzky and B. M. Semple, *Tetrahedron*, **23**, 4001 (1967).

[10] T.-S. Balaban and A. T. Balaban, to be published.

[11] A. T. Balaban, *J. Lebelled Comp. Radiopharm.*, **18**, 1621 (1981) and other references therein.

[12] T. S. Balaban, C. Uncuţa, M. D. Gheorghiu and A. T. Balaban, *Tetrahedron Lett.*, **26**, 4639 (1985).

ACKNOWLEDGEMENTS. Thanks are expressed to chem. eng. Corina Dimitrov and chem. eng. Daniela Istrate for experimental assistance.

Revue Roumaine de Chimie, 35, 3, 421–426 (1990)

SYNTHESIS OF SUBSTITUTED BENZOINS AND THE CORRESPONDING BIS-1,2-ENEDITHIOL COMPLEXES OF NICKEL, PLATINUM, AND PALLADIUM *

DANIELA CARMEN ONICIU[a], NICOLAE NEGOIŢĂ[b], MARILENA MORJAN[b],
MIRCEA D. GHEORGHIU[a] and ALEXANDRU T. BALABAN[a]
[a]Polytechnic Institute, Department of Organic Chemistry, Splaiul Independenţei 313, 77206 Bucharest, Romania
[b]Institute of Nuclear and Engineering Physics, Bucharest-Măgurele, Romania

Received November 3, 1989

The preparation, spectral properties, and characterization of non-symmetrically substituted benzoins 2 and of the corresponding bis-1,2-enedithiol complexes 4 of nickel, platinum and palladium are reported.

Until recently, bis-1,2-enedithiol complexes of transitional metals presented little interest, in spite of Schrauzer's efforts for elaborating convenient experimental conditions of synthesis and characterization.[1-3] Drexhage[4,5] and his co-workers have brought a new outlook in this field, by the synthesis of bis(4-dimethylamino-dithiobenzil)Ni(II), **1a**, which was found out to constitute an excellent saturable dye (Q-switch), with high performance in laser systems. The interest is mainly for dye lasers functioning in the near IR range, because of the characteristic absorption bands of these compounds in this region. By comparison with cyaninic dyes, compounds **1** have better thermal and photochemical stability.[6]

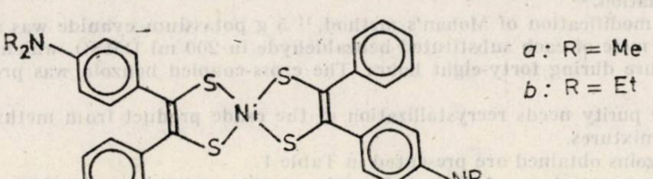

1

When one aromatic ring functions as electron donor and the other as electron acceptor, the conjugated electronic system is extended all over the ligand structure and the bathochromic shifts towards the near IR region are larger. The nature of the metal (nickel, platinum and palladium) has little influence on spectral parameters, but is significant for technological implications.[7]

---

* Dedicated to the memory of Mihai Elian.

The optimal synthetic strategy consists in the synthesis of the precursor benzoin **2**, followed by the synthesis of the thiophosphoric ester **3** generated by treatment of the benzoin **2** with phosphorus pentasulfide and finally its hydrolysis in the presence of metal chloride.[8]

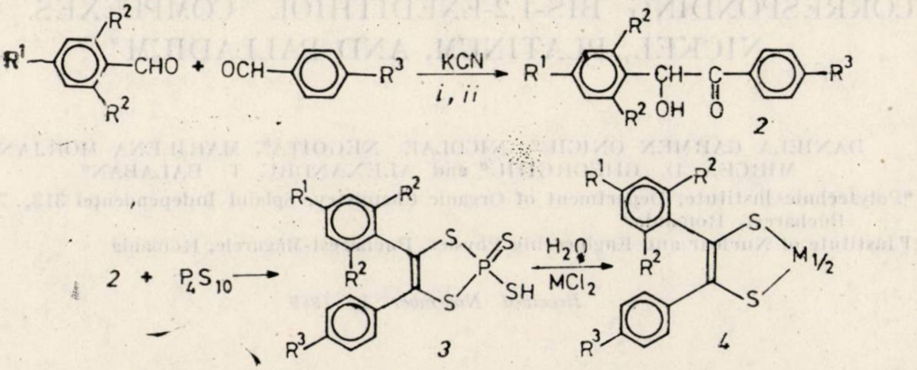

For increasing the range of new bis-1,2-enedithiol complexes one needs the synthetic availability of the corresponding benzoins with donor and acceptor substituents for such metallic complexes.

EXPERIMENTAL PART

Synthesis of substituted benzoins **2A** — **2G**. The synthesis was carried out by benzoinic condensation in the presence of potasium cyanide, as follows :[9]

i) 0.1 Moles of each substituted benzaldehyde in 50—100 ml refluxing ethanol (95 %) are treated with a solution of 5 g potassium cyanide in 10 ml water. The amount and concentration of the solvent must be sufficient for keeping the benzaldehydes dissolved. After two to four hours, the mixture was cooled and a first amount of cross-coupled benzoin was separated by filtration. A new amount of potassium cyanide in 10 ml water was added to the filtrate which was then refluxed for two more hours. On cooling the solution, a new amount of cross-coupled benzoin precipitated. The two combined fractions were purified by recrystallization.

After the synthesis of 4-metoxy-benzoin **2D**, the unreacted benzaldehydes were removed by steam-distillation.[10]

ii) As a modification of Mohan's method,[11] 5 g potassium cyanide was suspended in a solution of 0.1 mole of each substituted benzaldehyde in 200 ml DMSO, which was stirred at room temperature during forty-eight hours. The cross-coupled benzoin was precipitated with water.

A higher purity needs recrystallization of the crude product from methanol, ethanol or ethanol-water mixtures.

The benzoins obtained are presented in Table 1.

The purity control may be effected by tlc on Silica gel G 60, with elution system chloroform : ether (98 : 2).

Synthesis of bis- 1,2-enedithiol complex **4A** — **4E**. The reactions was carried out according to Drexhage and Mueller-Westerhoff's method[8]. Bis(dithiobenzil)nickel was synthesised by the following modified method : 0.1 mole substituted benzene, 0.15 mole phosphorus pentasulfide and 0.5 mole nickel acetate were refluxed during eight hours in 200 ml chloroform. To the reaction mixture cooled at 40°C, 50 ml water and 50 ml concentrated hydrochloric acid were added dropwise during two hours. The chloroform layer was dried over anhydrous calcium chloride, the solvent was evaporated, and the residue was purified by column chromatography on silica gel, using benzene as solvent. Higher purities were obtained by tlc on Silica gel G 60, elution system benzene : tetrachloromethhane (1 : 2).

The complexes **4A** — **4E** synthesized are presented in Table 2.

Attempts for preparing the complex corresponding to benzoin **2F** have failed.

Table 1

Substituted benzoins 2 synthesized by benzoinic condensation

Compd.	Structure	Method	m.p. (°C)	Yield %	Recryst. solvent
2A	$C_6H_5-CO-CHOH-C_6H_5$	ii	136[a]	98	
2 B	4-$Me_2N-C_6H_4-CO-CHOH-C_6H_5$	i	164[a]	70	methanol
2C	4-$Et_2N-C_6H_4-CO-CHOH-C_6H_5$	i,ii	111[b]	35	ethanol : water 3 : 1
2D	4-$MeO-C_6H_4-CO-CHOH-C_6H_5$	i	108[a]	40	ethanol : water 5 : 1
2E	4-$Me_2N-C_6H_4$-CO-CHOH-C_6H_4-Me-4′	i, ii	123[c]	i : 18 ii : 70	methanol
2F	$C_6H_5-CO-CHOH-C_6H_3$-2,6-Cl_2	i	139[d]	60	ethanol
2G	$C_6H_5-CO-CHOH-C_6H_4-NMe_2$-4′	ii	159[a]	85	ethanol : water 3 : 1

[a] In agreement with literature data.

[b] m.p. (lit. [11]) 106°C.

[c] Anal. Calcd. for $C_{17}H_{19}NO$: C_2, 76.40 ; H, 7.12 ; N, 5.24 ; found C, 76.32 ; H, 7.21 ; N, 5.36.

[d] Anal. Calcd. for $C_{14}H_{10}Cl_2O_2$: C, 59.81 ; H. 3.58 ; Cl, 25.22 ; found : C, 59.38 ; H, 3.41 ; Cl, 25.72.

Table 2

Bis-1,2-enedithiol complexes 4[a]

Comp.	Benzoin	M	m.p. (°C)	R_f[b]	% Ni	
					calcd.	found
4A	**2A**	Ni	293 (dec.)	0.61	—	—
4Ba=4G	**2B, 2C**	Ni	277 (dec.)	0.53	—	—
4Bb	**2B**	Pt	>300	0.66	—	—
4Bc	**2B**	Pd	>300	0.59	—	—
4C	**2C**	Ni	252 (dec.)	0.55	—	—
4D	**2D**	Ni	283 dec.)	0.56	9.73	9.89
4E	**2E**	Ni	265 (dec.)	0.51	8.93	8.89

[a] Capital letters discriminate structures of the bezoins ; lower case letters discriminate metals.

[b] Eluent tlc, benzene : tetrachloromethane (1 : 2).

DISCUSSION OF THE RESULTS

Interestingly, methods i) and ii) applied to the same mixture of benzaldehyde and *p*-dimethylamino-benzaldehyde gave two different isomeric benzoins **2B** and **2G**.

Spectral features of the non-symmetrically substituted benzoins are presented in Table 3.

IR Absorption spectra reveal for benzoins **2B** – **F** the absence of the free O–H stretching band, and the presence of a wide band characteristic for the associated O–H stretching, of mediu mintensity at 3400–3500 cm^{-1}, indicating an intramolecular chelation of the hydroxylic proton with the carbonyl group. Only benzoin **2G** presents a weak absorption band at 3600 cm^{-1}, characteristic for free O–H stretching vibration.

The carbonyl absorption band is shifted to lower wave-numbers (1640–1680 cm^{-1}), due to the conjugation with the aromatic nucleus, except for the benzoin **2F** (1700 cm^{-1}), probably owing to the chloro substituents, which cause non-planarity of the corresponding ring, suppressing thereby the conjugation.

In the ^{1}H–NMR spectra, the signal of the hydroxylic proton, confirmed by deuteration with D_2O, is situated at 4.60–5.00 ppm. The aromatic hydrogen atoms of the *para*-substituted rings present signals characteristic for an $AA'BB'$ system, with coupling constants $J = 6.5-10$ Hz, depending on the position and nature of the substituents and on the adjacent or non-adjacent position to the carbonyl group. The *ortho*-hydrogens relative to the carbonyl group resonate at lower fields (7.80–7.90 ppm, $J = 8-10$ Hz), while the *ortho*-hydrogens relative to electron-donor groups present signals at higher fields (7.20–7.40 ppm, $J = 8-10$ Hz). The aromatic hydrogen atoms in benzoin **2E** appear as three doublets centered at 6.63, 7.17 and 7.85 ppm. The structure of benzoin **2F** is confirmed by the ^{1}H–NMR spectrum : the unsubstituted ring is adjacent to the carbonyl group and its *ortho*-hydrogens resonate at 7.88 ppm ($J_{AB} = 6.5$ Hz, $J_{AR_1} = 2$ Hz), while the 2,6-dichloro-substituted ring is adjacent to the CHOH group ; its three hydrogens and three *meta*, *para*-phenyl hydrogens give rise to a multiplet at 7.10–7.45 ppm. The isomeric benzoin with the carbonyl adjacent to the 2,6-dichloro-substituted ring is not obtained during benzoinic condensation.

Spectral data of the bis-1,2-enedithiol complexes **4** are presented in Table 4.

IR Absorption spectra prove the structural similarities of these compounds ; the effect of the extended conjugation in the ligand induced by the dialkylamino and methoxy groups is displayed by the lower intensity of the C = C stretching band and by the shift of this band to lower wave-numbers than 1600 cm^{-1}, in agreement with literature data.[13]

Near IR absorption spectra suggest a correlation between the bathochromic shift of the absorption maximum and the nature of the substituents of the aromatic rings, when one ring acts as an electron donor, and the other as an electron acceptor.

This observation leads to the conclusion that one can design suitable benzoins, for introducing groups with antagonistic effects in the aromatic

Table 3

Spectral characteristics of substituted benzoins. Notation for ^1H-NMR spectral assignements :

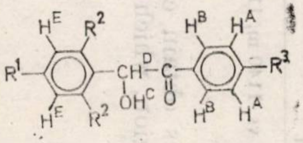

Compd.	^1H-NMR δ(ppm) $(CDCl_3)$[a]								IR, $\tilde{\nu}$ (cm^{-1}) $(CHCl_3)$
	R^1	R^2	R^3	H^A	H^B	H^C	H^D	H^E	
2B	7.30m 1H	7.30m 2H	2.97s 6H	6.57d 2H (10)	7.80d 2H (10)	4.73d 1H (6)	5.83d 1H (6)	7.39m 2H	3450m ; 1680s ; 1620vs ; 1240s ; 1060s
2C	7.36m 1H	7.36m 2H	1.11t 6H (7) 3.37q 4H (7)	6.57d 2H (9.5)	7.86d 2H(9.5)	4.87d 1H (6)	5.89d 1H(6)	7.30m 2H	3400m ; 1650 ; 1600vs ; 1260vs ; 1060vs
2D	7.33m 1H	7.33m 2H	3.04s 3H	6.57d 2H(10)	7.84d 2H(10)	4.83d 1H(6)	5.88d 1H(6)	7.33m 2H	3500m ; 1670vs ; 1600vs ; 1260vs ; 1040s
2E	2.33s 3H	7.17d 2H	3.06s 6H	6.63d 2H(9)	7.85d 2H(9)	4.78d 1H(6)	5.81d 1H(6)	7.17d 2H(3)	3370s ; 1650s ; 1590vs ; 1280vs ; 1050s
2F	7.32m 1H	—	7.88m 1H	7.88m 2H	7.88m 2H	4.97s 1H	6.47s 1H	7.32m 2H	300m ; 1700vs ; 1620vs ; 1600s ; 1280vs ; 1210vs
2G[b]	3.01s 6H	8.16d 2H (8)	7.43m 1H	7.43m 2H	7.43m 2H	—	6.17s 1H	7.55d 2H (8)	3620w ; 3400m : 1640s ; 1580vs ; 1280s ; 1050s.

[a] Coupling constants (in Hz) are enclosed in brackets.

[b] In the ^1H-NMR spectrum in $CDCl_3 : CF_3OOH$ 4 : 1, the O–*H* proton is masked by the solvent peak.

Table 4

Spectral characteristics of 1,2-enedithiol complexes **4**

Compd.	UV – Vis, λ_{max} (nm) in MeOH	Near IR, λ_{max} (nm) in CH_2Cl_2	IR, $\tilde{\nu}$ (cm^{-1}) in $HCCl_3$
4A	240, 270, 316, 417	866	1859 vs, 1136 s, 882s
4Ba=4G	244, 280, 385, 355, 460	1064	1355 vs, 1250 s, 1170 s, 1140 vs, 890 s
4Bb	244, 280, 285, 855, 460	950	1350 vs, 1180, s, 1140 s, 890 s
4Be	244, 280, 285, 355, 469	950	1350 vs, 1150 s, 1170 s, 870 s
4C	244, 270, 320, 360, 626, 800	1116	1345 vs, 1160 vs, 890 s
4D	244, 275, 290, 590, 800	900	1350 vs, 1170 s, 1130 s, 870 m
4E	244, 280, 290, 360, 480	1033	1350, vs, 1140 m, 1120 s, 890s

rings of bis-1,2-enedithiol complexes; one can thus obtain compounds having absorption in a wide range of the near IR region, which may have interesting applications as dye lasers or Q-switches.

REFERENCES

[1] G. N. Schrauzer and H. W. Finck, *Angew. Chem. Int. Ed. Engl.*, **3**, 143 (1964).
[2] G. N. Schrauzer, V. P. Mayweg and W. Heinrich, *Inorg. Chem.*, 4, 1615 (1965).
[3] G. N. Schrauzer and H. N. Rabinowitz, *J. Amer. Chem. Soc.*, **90**, 4297 (1968).
[4] K. H. Drexhage and U. T. Mueller-Westerhoff, *IEEE J. Quant. Electron. Q. E.*, **8**, 795 1972).
[5] K. H. Drexhage and G. A. Reynolds, *Opt. Commun.*, **10**, 18 (1974).
[6] A. Graczyk, E. Bialkowska and A. Konarzewsky, *Tetrahedron*, **38**, 2715 (1982).
[7] G. A. Reynolds and K. H. Drexhage, *J. Appl. Phys.*, **46**, 4852 (1975).
[8] K. H. Drexhage and U. T. Mueller-Westerhoff, U. S. Pat. 3.878, 478 (1975).
[9] W. S. Ide and J. S. Buck, *Organic Reactions*, **4**, 269 (1949).
[10] C. R. Kinney, *J. Amer. Chem. Soc.*, **51**, 1592 (1929).
[11] S. Mohan and J. S. Sandhu, *J. Indian Chem. Soc.*, **48**, 93 (1971).
[12] R. W. Bost and E. E. Jowell, *J. Amer. Chem. Soc.*, **70**, 903 (1948).
[13] G. N. Schrauzer and V. P. Mayweg, *J. Amer. Chem. Soc.*, **87**, 1488 (1965).

Revue Roumaine de Chimie, 35, 3, 427–435 (1990)

CRYSTAL AND MOLECULAR STRUCTURE OF THE 2-t-BUTYL-2-CYANOCYCLOBUTANONES RESULTED FROM THE CYCLOADDITION OF MOORE'S KETENE TO *endo*- AND *exo*-BENZOCYCLOBUTANONORBORNENES*

MIRCEA D. GHEORGHIU,**[a] LUMINITZA PÂRVULESCU,[a] K. M. TURDIBEKOV[b] and
YU. T. STRUCHKOV **[b]

[a] Department of Organic Chemistry, Polytechnic Institute—TCH, 76206 Bucharest 16, Romania
[b] Institute of Organoelement Compounds of the Academy of Sciences of the USSR, 28 Vavilov St., 117813 Moscow, USSR

Received November 20, 1989

The cyclobutanones **1** and **2**, obtained by cycloadditions of Moore's ketene (t-butylcyanoketene) to norbornene derivatives **3** and **4** respectively, have *exo*-configuration and the t-butyl group is pointing toward the methylene bridge. The four-membered ring is puckered in the cyclobutanone fragment and almost flat in the benzocyclobutano fragment. The cyclobutanone bond substituted at one side with the bulky t-Bu group, and at the other end with the norbornane, is allongated to 1.599 (cyclobutanone **1**) and 1.601 Å (cyclobutanone **2**). Bond angles of the t-Bu group and the adjacent cyclobutanone bonds are in the range of 120–128°. The stereochemistry of cyclobutanones **1** and **2**, proves that cycloaddition of Moore's ketene with norbornene derivatives occurs *via* the Woodward-Hoffmann $_{2}\pi_{s} + {}_{2}\pi_{a}$ reaction mode.

INTRODUCTION

Moore's ketene [1] was reported to react with norbornene[2] and norbornadiene [3], or with their annelated norbornenes with benzo-, *exo*- and *endo*-benzocyclobutano fragments [4] and related derivatives [5] leading to 2-t-butyl-2-cyanocyclobutanones. The analysis of $^{1}H-NMR$ spectra without [4a] or with shift reagents [4c] and of the $^{13}C-NMR$ spectra [4b] revealed a close structural resemblance among these cyclobutanones. Therefore we concluded that norbornene derivatives mentioned above had reacted with Moore's ketene following essentially the same reaction mode. Two basic results were secured by NMR methods. First, the configuration of the annelated cyclobutanone ring to the norbornene is *exo*. The ketene attack occurred *exo*-π facially upon the norbornene double bond. Second, the bulky t-Bu broup is pointing toward the methylene bridge from the norbornane skeleton. This outcome is strongly in favour of a Woodward-Hoffmann $_{2}\pi_{s} + {}_{2}\pi_{a}$ reaction mode[6] for the cycloaddition of Moore's ketene to norbornenes.

---

* Dedicated to the memory of Mihai Elian

** Correspondence authors

X-Ray analysis has been now completed and brings about definite molecular structure for both of the 2-t-butyl-2-cyanocyclobutanones resulted from norbornene derivatives and Moore's ketene. Since all the 2-t-butyl-2-cyanocyclobutanones obtained from norbornene derivatives and Moore's ketene are definitely structurally related, we have carried out X-ray structure determination for only two cyclobutanones considered as prototype. Thus, in compound **1**, the cyclobutanone fragment in annelated to *exo*-benzocyclobutanonorbornane skeleton, while in compound **2** the same four-membered ring is annelated to *endo*-benzocyclobutanonorbornane skeleton.

The interpretation of the X-ray experimental results was gratifying. They firmly support our previously proposed stereochemistry for the 2-butyl-2-cyanocyclobutanone annelated to norbornane skeleton.[4] Additionally, it is interesting to find out the geometrical parameters along which the steric crowding originating from the less favorable thermodynamic configuration of the t-Bu group, is in part alleviated.

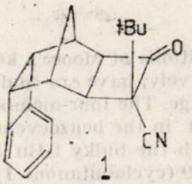

1

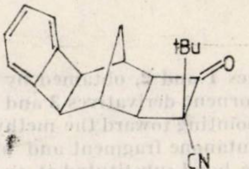

2

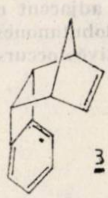

3

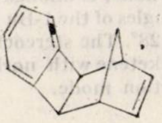

4

Finnally we would like to emphasize that our results regarding the stereochemistry of cyclobutanone obtained by cycloaddition of Moore's ketene to norbornene derivatives provide the second known *direct evidence* for the steric course of cycloadditions between an unsymmetrical ketene and a carbon-carbon double bond.[7-9] Unlike the results obtained by Ghosez *et al.*[10] in their study of cycloaddition of (carbomethoxy) chloroketene to cyclopentadiene, when unexpectedly the ester group, by X-ray measurements, was shown to be in *exo*-configuration, we put forward here as well as in our future contribution,[11] that for Moore's ketene cycloadditions, the Woodward-Hoffmann $_2\pi_s + {}_2\pi_a$ reaction mode[6] is fully operational. In other words, the two bulky groups, one from the ketenophile and the other from ketene, must be in *cis* configuration in the resulted cyclobutanone.

RESULTS AND DISCUSSION

A. The cyclobutanone ring

In both isomers the configuration of the cyclobutanone ring is *exo.* The attack of Moore's ketene occurred *exo-π* facially. Most electrophilic addition reactions at the double bond from the norbornene system have similar orientations.[12a] The underlying reason for such a high stereoselectivity is still debatable.[12b] The cyclobutanone ring in both isomers **1** and **2** is folded. The dihedral angle along C7–C9 * for **1** is 17.41°, 16.12° for **2A** and 17.42° for **2B** respectively. **

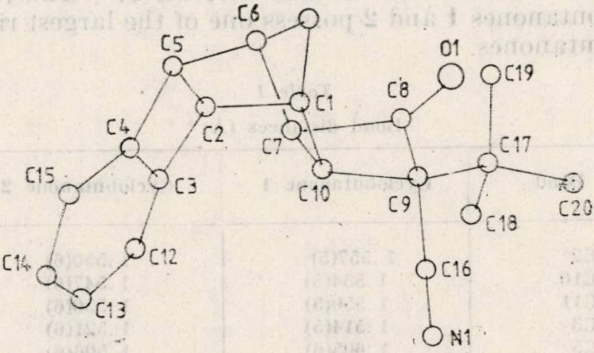

Fig. 1. — The structure of cyclobutanone **1**.

The C9–C10 bond has a remarkable length (see Table 1), 1.599 Å for compound **1** and 1.601 Å for compound **2**. *** This bound is flanked on one side by the bulky t-Bu ground and on the other side by the methine bridgehead. The latter is bound to the methylene bridge $-CH_2$-group, placed in a rather unfavorable geometrical position with respect to the t-Bu group. Unfortunately there is no structural information for comparison in the case of *exo* annelated cyclobutanone to norbornane skeleton. The only known reference deals with an *endo* annelated cyclobutanone to the norbornene ring.[13] In the case of the two cyclobutanones (the

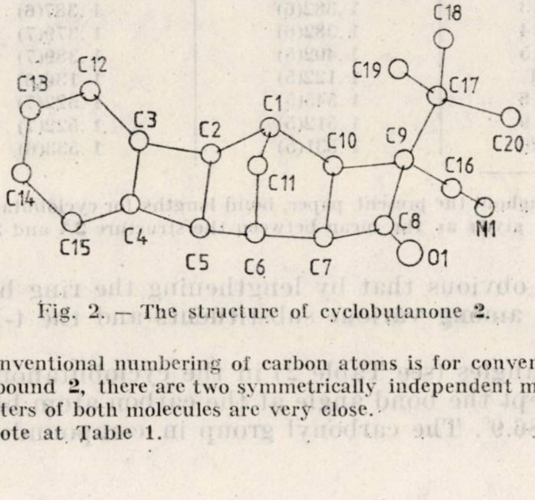

Fig. 2. — The structure of cyclobutanone **2**.

---

* The unconventional numbering of carbon atoms is for convenience.

** For compound **2**, there are two symmetrically independent molecules designed **2A** and **2B**. The parameters of both molecules are very close.

*** see footnote at Table 1.

compound has a dimeric structure) the lengths of the similar bonds are 1.558 Å and 1.561 Å. Now, examining other cyclobutanone systems, some of them less related structurally to our compounds, similar bonds are around 1.55 Å. [14] In highly strained cyclobutanones, embedded in polycyclic structures, similar bonds are 1.582 Å and 1.594 Å [15a] or 1.60 Å. [15b] The exceptional length of C9—C10 bond in **1** and **2** is very likely the result of the repulsion among the bulky t-Bu and the methylene bridge groups.

The common bond of the cyclobutanone fragment and of the norbornane system (Table 2) as well as the bonds involving the carbonyl group, from both compounds **1** and **2**, is slightly longer than that reported for the *endo*-cyclobutanone-norbornane derivative. [13] Thus, the 2-t-butyl-2-cyanocyclobutanones **1** and **2** possess one of the largest ring dimensions among cyclobutanones.

Table 1

Bond distances (Å) *

Bond	Cyclobutanone **1**	Cyclobutanone **2**
C1—C2	1 .557(5)	1 .550(6)
C1—C10	1 .534(5)	1 .547(6)
C1—C11	1 .550(5)	1 .550(6)
C2—C3	1 .514(5)	1 .521(6)
C2—C5	1 .605(6)	1 .506(6)
C3—C4	1 .386(5)	1 .383(6)
C3—C12	1 .374(5)	1 .382(6)
C4—C5	1 .520(5)	1 .520(5)
C4—C15	1 .371(5)	1 .379(6)
C5—C6	1 .551(5)	1 .534(6)
C6—C7	1 .526(5)	1 .535(6)
C6—C11	1 .545(6)	1 .539(6)
C7—C8	1 .540(5)	1 .531(6)
C7—C10	1 .583(5)	1 .578(6)
C8—C9	1 .586(5)	1 .579(6)
C8—01	1 .190(4)	1 .188(5)
C9—C10	1 .599(5)	1 .601(5)
C9—C16	1 .498(5)	1 .490(6)
C9—C17	1 .557(5)	1 .553(6)
C12—C13	1 .382(6)	1 .387(6)
C13—C14	1 .382(6)	1 .379(7)
C14—C15	1 .402(5)	1 .389(7)
C16—N1	1 .122(5)	1 .136(6)
C17—C18	1 .545(5)	1 .522(7)
C17—C19	1 .512(5)	1 .522(7)
C17—C20	1 .531(5)	1 .533(6)

---

* Throughout the present paper, bond lengths for cyclobutanone **2**, are given as the mean between the structure **2A** and **2B**.

It is quite obvious that by lengthening the ring bonds, the severe steric repulsions among various substituents and the t-Bu group are in part diminished.

The bond angles (see Table 2) in the cyclobutanone ring are quite close to 90°, except the bond angle at the carbon atom bearing the t—Bu group which is 86.9°. The carbonyl group in compounds **1** and **2** has no

"Concorde nose", as it was evidenced for some cyclobutanones.[14,15c] The sum of bond angles around this group is equal with 360°.

The magnitude of the bond angles involving the t-Bu group with adjacent cyclobutanone bonds are striking if one considers C9 as tetrahedral. Thus in the case of cyclobutanone **1**, the C10—C9—C17 bond angle is 125.3° and that of C8—C9—C17 is 122.4°. The same angles are 127.8° and 121.5° for **2A** and 126.7° and 122.2° for **2B**.

Table 2

Bond angles (grad)

	cyclobutanone **1**	cyclobutanone **2A**	cyclobutanone **2B**
C2C1C10	106 .2(3)	102 .3(3)	101 .5(3)
C2C1C11	98 .6(3)	102 .2(3)	101 .3(3)
C10C1C11	104 .9(3)	104 .6(3)	103 .9(3)
C1C2C3	123 .2(3)	118 .0(3)	117 .9(3)
C1C2C5	103 .7(3)	102 .8(3)	103 .4(3)
C3C2C5	85 .9(3)	85 .4(3)	85 .9(3)
C2C3C4	94 .3(3)	94 .5(3)	94 .1(3)
C2C3C12	144 .0(4)	143 .6(4)	142.6(4)
C4C3C12	121 .6(4)	121 .9(4)	123 .3(4)
C3C4C5	93 .9(3)	93 .9(3)	94 .3(3)
C3C4C15	121 .7(4)	122 .6(4)	121 .4(4)
C5C4C15	144 .3(4)	143 .5(4)	144 .3(4)
C2C5C4	85 .8(3)	86 .2(3)	85 .7(3)
C2C5C6	102 .0(3)	102 .4(3)	102 .6(3)
C4C5C6	122 .1(3)	116 .9(3)	117 .5(4)
C5C6C7	109 .2(3)	104 .8(3)	105 .5(3)
C5C6C11	100 .1(3)	103 .5(3)	102 .2(3)
C7C6C11	101 .4(3)	101 .7(3)	101 .1(3)
C6C7C8	114 .6(3)	116 .3(3)	116 .4(3)
C6C7C10	105 .1(3)	104 .5(3)	104 .8(3)
C8C7C10	89 .0(3)	88 .8(3)	88 .6(3)
C1C8C7	136 .0(3)	134 .9(4)	135 .2(4)
01C8C9	132 .1(3)	132 .1(4)	132 .0(4)
C7C8C9	91 .8(3)	92 .8(3)	92 .5(3)
C8C9C10	86 .9(3)	86 .4(3)	86 .0(3)
C8C9C16	104 .4(3)	105 .0(3)	105 .5(3)
C8C9C17	122 .4(3)	121 .5(3)	122 .2(3)
C10C9C16	104 .9(3)	104 .3(3)	103 .9(3)
C10C9C17	125 .3(3)	127 .8(3)	126 .7(3)
C16C9C17	109 .4(3)	108 .4(3)	109 .1(3)
C1C10C7	101 .7(3)	101 .3(3)	102 .6(3)
C1C10C9	121 .4(3)	122 .6(3)	122 .2(3)
C7C10C9	89 .8(3)	89 .8(3)	90 .4(3)
C1C11C6	95 .8(3)	95 .4(3)	96 .1(3)
C3C12C13	117 .4(4)	115 .8(4)	115 .4(4)
C12C13C14	121 .2(4)	121 .9(4)	121 .3(4)
C13C14C15	121 .3(4)	122 .4(4)	123 .4(5)
C4C15C14	116 .8(4)	115 .4(4)	115 .2(4)
N1C16C9	178 .0(4)	178 .6(5)	178 .2(4)
C9C17C18	108 .2(3)	108 .6(3)	108 .7(4)
C9C17C19	112 .5(3)	112 .3(3)	112 .2(4)
C9C17C20	109 .6(3)	108 .2(3)	108 .7(4)
C18C17C19	109 .4(3)	109 .4(3)	109 .2(4)
C18C17C120	109 .5(3)	110 .0(3)	110 .1(4)
C19C17C20	107 .3(3)	108 .3(3)	107 .9(4)

Such large values are unexpected for a tetrahedral carbon atom. They are large even for a trigonal carbon atom! Unfortunately there are few examples in the literature for comparison with our results.

A literature search revealed that such large bond angles are however not uncommon for alkyl substituents situated in a vicinal position to the carbonyl group. Thus in the only reported X-ray measurement for α-substituted cyclobutanone with t-Bu group,[16] namely *cis*-2,4-dibromo-2,4-di-t-butylcyclobutanone[17] the bond angles, quoted in the same order as above, are 123° and 120°. For another bulky substituent, CI_3C-CH_2- from 2-chloro-4-(2,2,2-trichloroethyl-3,3-dimethylcyclobutanone[15c] the same bond angles are 123° and 120°.

In the 3-aryl-2-t-butyl-2-cyanocyclobutanones (with aryl and t-Bu groups in *cis* configuration) the bond angle of the t-Bu group with the adjacent cyclobutanone substituted with aryl group is in the range of 122—123°. In the latter compounds the second bond angle is substantially lower and was evaluated in the range of 122—113°. It is interesting to note that when the aryl and the t-Bu groups are in *trans* configuration, both angles are reduced to 117.5° and 111.5° respectively.

With this information at hand, it is safe to conclude that as in compounds **1** and **2**, the t-Bu group has one of the largest known tilts, the supplementary angular deformation represents the second way by which steric repulsions are in part alleviated.

The dihedral angle C7C8C9C10/C6C7C10C1 is 118°. 2° for cyclobutanone **1**, 119.2° for **3**A and 119.6° for **3B**. Our previous numerical results obtained by multicenter approach model for induced shifts gave a dihedral angle with *ca.* 20° larger, and were therefore recognized as exaggerated.[4c] The X-ray determined angle for the *exo*-anhydride **5**[18] is 117°, which is a value very close to our results.

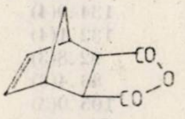

5

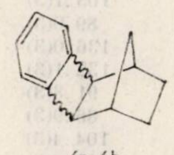

6a,6b

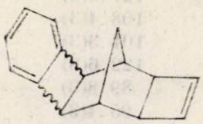

7a,7b

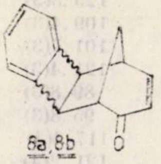

8a,8b

a: exo b: endo

This fact indicates that bond allongation, bond angle deformation and the puckering of the cyclobutanone ring suffice to remove the unfavorable steric repulsions between the methylene and t-Bu groups; there is no need to increase the dihedral angle between the cyclobutanone and norbornane fragment.

B. The cyclobutene ring

The cyclobutene rings, owing primarily to the annelation to the benzene ring, are almost planar. The dihedral angles along C3—C5 bond are 2.48° for **1**, 0.72° for **2A** and 1.24° for **2B**. Bond lengths are within normal ranges for what is expected for benzo-cyclobutenes structures.[19] The common bond with the norbornane skeleton is longer than the common bond of cyclobutanone ring with the norbornane skeleton. Molecular mechanics (MM2) calculations[20] carried out for related structures **6**, **7** and **8**, gave for the common bond shared by the *exo*- or *endo*-benzocyclobutano substituent and the five-membered ring from either the bicyclo (2.2.1)heptane or bicyclo (3.2.1) octane system, length between 1.597 and 1.611 Å. These theoretical results are nicely supporting the present findings (see Table 1).

The dihedral angle of the four-membered ring C2C3C4C5 and the norbornane C1C2C5C6 is 122.6 for **1**, 117.2° for **2A** and 117.5° for **2B**. The value quoted above for cyclobutanone **1** is quite close to that reported (126.5°) for the *cis*-2,3-dichloro-*ando*-benzocyclobutanonorbornane.[19b] No experimental data are available for comparison with our results in case of compound **2**.

C. The norbornane fragment

The norbornane fragment from the cyclobutanones **1** and **2** is, with few exceptions, very similar to the conformation of norbornane or its derivatives.[21] The conformation of the six-membered ring C1C2C5C6C7C10 is boat, the five-membered rings C1C2C5C6C11 and C6C7C10C1C11, respectively, are envelope like or slightly deformed envelope. According to the accepted nomenclature,[21] the conformation of the norbornane fragment in compounds **1** and **2A** could be considered as synchro twist (S(+, +)), while for **2B** it is contra twist (C(+, —)). The pseudorotational angle C2C1C6C5 is 0.3(6)° for compound **1**, 0.4(7)° for **2A**, and —0.3(7) for **2B**.

In the cyclobutanone **1**, atoms C3, C4, C8 and C9 are placed in respect to the norbornane C2, C5, C7, C10 plane at —1.49, —1.54, 0.87 and 0.55 Å. In compounds **2A** and **2B**, the four-membered rings are *exo-exo* oriented, as the C3, C4, C8 and C9 atoms are at (for **2A**) 0.69, 0.66, 0.77 and 0.47 Å, and (for **2B**) at 0.69, 0.67, 0.78 and 0.46 Å.

The methylene C1C11C6 bond angle is 95.8° for cyclobutanone **1**, 95.4° for **2A** and 96.1 for **2B**, quite close as magnitude to related structures.[18,21]

CONCLUSIONS

The molecular structure of the cyclobutanones obtained fro *exo*-(**3**) and *endo*-benzo-cyclobutanonorbornene (**4**) and Moore's ketene was determined by X-ray measurements. As expected, according to the Woodward-Hoffmann reaction mode ${}_2\pi_s + {}_2\pi_a$, the stereochemistry of the resulted cyclobutanones is characterized by the configuration of the bulky t-Bu group, as pointing toward the norbornane methylene bridge. Such crowded stereochemistry is in part lessened by (i) the allongation of the cyclobutanone bond carrying the bulky substituents, (ii) puckering o cyclobutanone ring, and (iii) increasing the bond angles of t-Bu grou with the adjacent cyclobutanone bonds to 123–126°.

EXPERIMENTAL PART

The cyclobutanones **1** and **2** were obtained by cycloaddition of Moore's ketene to *exo*-(**3**) and *endo*-bezocyclobutanonorborene (**4**), respectively. The reaction was carried out at reflux, in benzene solution. Moore's ketene was generated *in situ* by thermolysis of 2,5-diazido-3,6-di-t-butyl-1,4-benzoquinone. [1a,22]The ketene precursor was synthesized according to our methodology from hydroquinone.[1b,23] Column chromatography on silicagel, afforded pure samples of **1** and **2**. Crystals were grown by slow evaporation of solvent from solutions of **1** and **2** in benzene. Cell dimensions and intensities of reflections were recorded with a four-sector Helger — Watts diffractometer (λMoK_α, graphite monochromator, $\theta/2\theta$ scan technique, $2\theta \leqslant \leqslant 52°$ for **1** and 60° for **2**, respectively). Crystals of cyclobutanone **1** are orthorhombic, space group *Pbca*, $a = 9.1797(9)$, $b = 12.977(1)$, $c = 27.327(1)$ Å; $V = 3255.2$ Å^3; $C_{20}H_{21}HO$, $M_w = 291.2$; $D_c = 1.189$ g/cm^{-3}; $Z = 8$. Calculations were carried out using 1232 independent reflections with $I \geqslant 3\sigma$. Crystals of cyclobutanone **2** are triclinic, space group $P\bar{1}$. $a = = 10.787(1)$, $b = 12.606(1)$, $c = 12.871(1)$ Å; $\alpha = 84.941(6)$, $\beta = 86.240(6)$, $\gamma = 69.139(6)°$: $V = 1628.1$ Å^3; $C_{20}H_{21}NO$; $M_w = 291.2$; $D_c = 1.189$ g/cm^3; $Z = 4$. Calculations were carried out using 2646 independent reflections with $I \geqslant 2\sigma$. Structures were solved by direct methods. Block diagonal least squares refinements were solved initially in isotropic then in anisotropic approximation for nonhydrogen atoms. All hydrogen atoms for compound **2**, were located from difference synthesis, refined with fixed isotropic thermal parameter of 4Å^2. Hydrogens atoms in structure **1**, were not refined. Final residuals are $R = 0.057$ and $R_w = 0.034$ for compound **1** and $R = = 0.057$ and $R\ = 0.042$ for cyclobutanone **2**. All calculations were carried out on "Eclipse S1200" computer using INEXTL program. [23] Atomic coordinates for the cyclobutanone **1** and **2** have been deposited with the Director of the Cambridge Crystallographic Data Centre, University Chemical Lab., Lensfield Road, Cambridge CB2 1EW.

ACKNOWLEDGEMENT. M. G. and L. P. thanks Dr. Irina Shcherbakova (Institute of Physical Organic Chemistry, Rostov-on-Don University, USSR) for her interest and support for the present project. We are indebted to Drs. D. Belluš and B. Ernst (Ciba — Geigy AG, Basel Switzerland) for making available valuable information concerning cyclobutanones.

REFERENCES

[1] (a) H. W. Moore and W. Weyler, Jr., *J. Amer. Chem. Soc.*, **93**, 2812 (1971). The proposal to call t-butylcyanoketone as Moore's ketene was published in our paper :
(b) M. D. Gheorghiu, L. Pârvulescu, R. Ceclan, I. Manolescu, D. Constantinescu, C. Florea and M. Stănescu, *Rev. Roumaine Chim.*, **33**, 83 (1988).

[2] M. D. Gheorghiu, P. Filip, C. Drăghici and L. Pârvulescu, J. *Chem. Soc.*, *Chem. Commun.*, **1975**, 635.

[3] R. R. Brook and K. Hunt, *J. Chem. Soc.*, *Chem. Commun.*, **1974**, 989.

[4] (a) M. D. Gheorghiu, C. Drăghici and L. Pârvulescu, *Tetrahedron*, **33**, 3295 (1977) ; (b) M. D. Gheorghiu, M. Mihai, L. Pîrvulescu, A. Vaics and F. Niculescu, *Rev. Roumanie Chim.*, **32**, 979 (1987) ; (c) M. D. Gheorghiu, C. Drăghici, L. Pârvulescu and M. Elian, *Rev. Roumaine Chim.*, **34**, 1341 (1989).

[5] M. D. Gheorghiu, L. Pîrvulescu and C. Drăghici, *Rev. Roumanie Chim.*, **24**, 1005 (1979).

[6] R. B. Woodward and R. Hoffman, "The Conservation of Orbital Symmetry", Academic Press, New York, 1970, pag. 163. For recent challenge see : F. Bernardi, A. Bottoni, M. Olivucci, M. A. Robb, H. B. Schlegel and G. Tonechini, *J. Amer. Chem. Soc.* **110**, 5993 (1988).

[7] The references regarding X-ray structures of cyclobutanone resulted from cycloaddition of ketenes to carbon-carbon double bond, are provided by examples in which symmetrical ketene were employed, and thus the steric information was lost. Thus for (a) diphenyl-

ketene see : R. W. Holder, N. A. Graf, E. Duesler and J. C. Mors, *J. Amer. Chem. Soc.*, **105**, 2929 (1983); W. Friedrichsen, T. Debaerdemacker, A. Böttcher, S. Hahnemann and R. Schmidt, *Z. Naturforsch*, **38b**, 504 (1983); K. B. Becker, M. Hohermuth and G. Rihs, *Helv. Chim. Acta*, **65**, 235 (1982); (b) for dichloroketene see : T. Sasaki, T. Manabe and K. Hayakawa, *Tetrahedron Letters*, **22**, 2579 (1981); L. R. Nassimberi, A. G. Orpen, G. M. Sheldrick and J. C. van Niekerk, *Acta Cryst.*, **B33**, 3326 (1977); R. Hoge, J. Jager and K. Fischer, *Cryst. Struct. Comm.* **6**, 287 (1977);

[8] The allenes, in our view, are not to be expected to react by identical reaction mode as alkenes on diene. However, the structure of the methylenecyclobutanone resulted from the reaction of Moore's ketene with 1,3-diphenyl allene is instructive, therefore see : H. A. Bamphield, P. R. Brook, W. S. McDonald, *J. Chem. Soc., Chem. Commun.*, **1975**, 132 and W. S. McDonald, *Acta Cryst.* **B31**, 2504 (1975).

[9] Indirect evidence regarding the steric course of the cycloaddition Moore's ketene to 2-methyl-2-butene was provided by X-ray crystallography of the 4-chlorobenzoate of the resulted cyclobutanol from the reduction of cyclobutanone with $LiAlH_4$: P. R. Broock, A. M. Eldeele, H. Hunt and W. S. McDonald, *J. Chem. Soc., Chem. Commun.*, **1978**, 10.

[10] S. Goldstein, P. Vannes, C. Honge, A. M. Frisque-Hesbain, C. Wiaux-Zamar, L. Ghosez, G. Germain, J. P. Declercq, M. Van Meerssche and J. M. Arrieta, *J. Amer. Chem. Soc.*, **103**, 4616 (1981).

[11] M. D. Gheorghiu, M. Mihai, L. Pârvulescu, S. V. Sereda, K. M. Turdibekov and Yu. T. Struchkov, to be submitted.

[12] (a) T. G. Taylor, *Acc. Chem. Res.* **2**, 152 (1969);
(b) K. Ohno, T. Ishida, Y. Noutoh and Y. Izumi, *J. Amer. Chem. Soc.*, **107**, 8082 (1985); R. Gleiter and L. A. Paquette, *Acc. Chem. Res.* **16**, 328 (1983); J. Spanget-Larsen and R. Gleiter, *Tetrahedron Letters*, **24**, 2435 (1982); N. G. Rondan, M. N. Paddon-Row, P. Caramella, J. Mareda, P. H. Mueller and K. N. Houk, *J. Amer. Chem. Soc.*, **104**, 4974 (1982); S. Inagaki, H. Fujimoto and K. Fukui, *ibid.*, **98**, 4054 (1976).

[13] J. W. Bats, O. Bellinger and W. Reid, *Acta Cryst.*, C**40**, 184 (1984).

[14] For an excelent recent review on chemistry and structures of cyclobutanones see : D. Belluš and B. Ernst, *Angew. Chem. Int. Ed. Engl.* **27**, 797 (1988).

[15] (a) T. J. Greenhough and J. Trotler, *Acta Cryst* **B35**, 3084 (1979); (b) C. C. Biefeld and H. A. Eick, *Acta Cryst.* B **30**, 1172 (1974); (c) P. Martin, H. Greuter, G. Rihs, T. Winklen and Belluš, *Helv. Chim. Acta* **64**, 2571 (1981).

[16] We have deliberately not include in our discussion four-membered ring containing two trigonal carbon atoms. The methylenecyclobutanone obtained from Moore's ketene and 1,3-diphenylallene, for which X-ray measurements were carried out [8], has a molecular structure, in which very likely some geometrical parameters are highly dependent on the second trigonal center.

[17] C. Riche, *Acta Cryst*, B **30**, 587 (1974).

[18] R. Destro, G. Filipini, C. M. Gramaccioli and M. Simonetta, *Tetrahedron Lett*, **1969**, 3223.

[19] (a) For a review of benzocyclobutenes structure see : F. H. Allan, *Acta Cryst.* **B 37**, 900 (1981);
(b) The 2,3-dichloro-*endo* benzo-cyclobutanonorbornane X-ray structure is discussed by R. Baker and J. S. Wood., *J. Chem. Soc., Perkin Trans* 2, **1978**, 971.

[20] M. D. Gheorghiu, G. Surpăţeanu, A. Popescu, E. Olteanu, unpublished results. For preliminary results of MM2 calculations see for compounds **7** : M. D. Gheorghiu, E. Olteanu, L. Stănescu, M. Avram and G. Surpăţeanu, *Rev. Roumaine Chim.*, **34**, 1931 (1989); for compounds **8** see : M. D. Gheorghiu, A. Popescu and G. Surpăţeanu, *ibid.*, **34**, 481 (1989).

[21] C. Altona and M. Sundaralingam, *J. Amer. Chem. Soc.*, **92**, 1995 (1970).

[22] W. Weyler, Jr., W. G. Duncan, M. B. Liewen and H. W. Moore, *Org. Synth.* **55**, 32 (1976).

[23] M. D. Gheorghiu and M. Avram, *Org. Prep. Proc. Int.*, **6**, 231 (1974).

[24] R. S. Gerr, A. I. Yanovskii and Yu. T. Struchkov, *Kristallografiya*, **28**, 1029 (1983).

Revue Roumaine de Chimie, 35, 3, 437–444 (1990)

INTERACTIONS OF SUBSTITUTED FIVE-MEMBERED HETEROAROMATIC COMPOUNDS WITH ELECTRON ACCEPTORS. II[1]

INTERACTION OF 2-(*p*-BROMOPHENYLSULPHONYL)-PHENYL-5-ETHYLAMINO-1,3,4-THIADIAZOLE WITH TETRACYANOETHENE *

IOANA ŞARAMET,[a] CONSTANTIN DRĂGHICI[b] and MIRCEA D. BANCIU[c]

[a] Organic Chemistry Department, Faculty of Pharmacy, Traian Vuia Street 5, Bucharest, Romania

[b] Centre of Organic Chemistry, Spl. Independenţei 202B, Bucharest, Romania

[c] Organic Chemistry Department, The Polytechnic, TCH, Spl. Independenţei 313, Bucharest Romania

Received November 18, 1989

The title thiadiazole 3 affords on treatment with tetracyanoethene a green coloured charged-transfer complex with a dynamic behaviour which was followed by electronic spectroscopy. The final reaction product is the N-tricyanovinyl derivative 5, with potential biological activity. The reaction mechanism is discussed.

INTRODUCTION

In the preceding note [1] the formation of charge transfer complexes (CTC) between thiazoles **1** and **2** and tetracyanoethene (TCNE) was described.

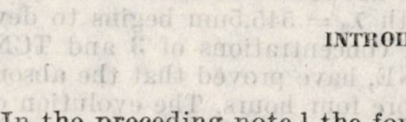

1

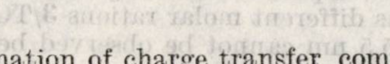

2

---

* Dedicated to the memory of Mihai Elian.

In this note we present the interactions which appear between 2(*p*-bromophenylsulphonyl)phenyl-5-ethylamino-1,3,4-thiadiazole (**3**) and TCNE.

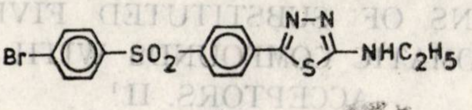

3

RESULTS

The thiadiazole **3**, m.p. 218 °C, was obtained [2] from the corresponding thiosemicarbazide **4** on cyclization with H_2SO_4.

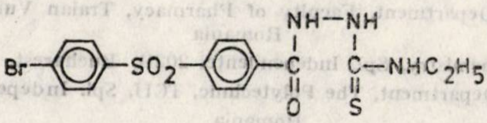

4

Treatment of thiadiazole **3** in CH_2Cl_2 solution at 20 °C with TCNE was accompanied by the instantaneous appearance of a green colour. In the electronic spectrum recorded immediately after mixing of the reactants two absorption bands with maxima at $\lambda_1 = 467$ nm and $\lambda_2 = 652$ nm, occur. These bands appearing neither in the electronic spectrum of **3** nor in that of TCNE should be attributed a to CT complex. Attempts to determine accurately the formation constant of the CTC using the Benesi-Hildebrand equation [3] failed due to the very fast modification of the spectra in time. Thus, both mentioned absorption bands increase in intensity within a few hours (Fig. 1). Interestingly, after about four hours at room temperature a new absorption maximum with $\lambda_3 = 545.5$nm begins to develop. Control experiments, using different concentrations of **3** and TCNE as well as different molar rations **3**/TCNE, have proved that the absorption at 545.5 nm cannot be observed before four hours. The evolution of the absorption maxima λ_1, λ_2, λ_3, characterized by their extinctions E_1, E_2 and E_3 respectively, was followed by recording the spectra at different time intervals. From graphical representation of extinctions *vs.* time (Fig. 2) it may be seen that the E_1 band increases continuously, whereas E_2 reaches a maximum then diminishes; at the same time the E_3 band increases practically in a linear fashion. Unfortunately, after 26 hrs at room temperature the reaction mixture begins to deposit a precipitate which hampers the further spectral analysis.

In order to elucidate the course of the reaction, some preparative determinations were also performed. In a preparative reaction performed at room temperature with CH_2Cl_2 as solvent, the modification of the colour was also clearly observed: from the initial green colour the solution became olive-coloured (after 48 hrs) then red-brown (after 72 hrs). A dark preci-

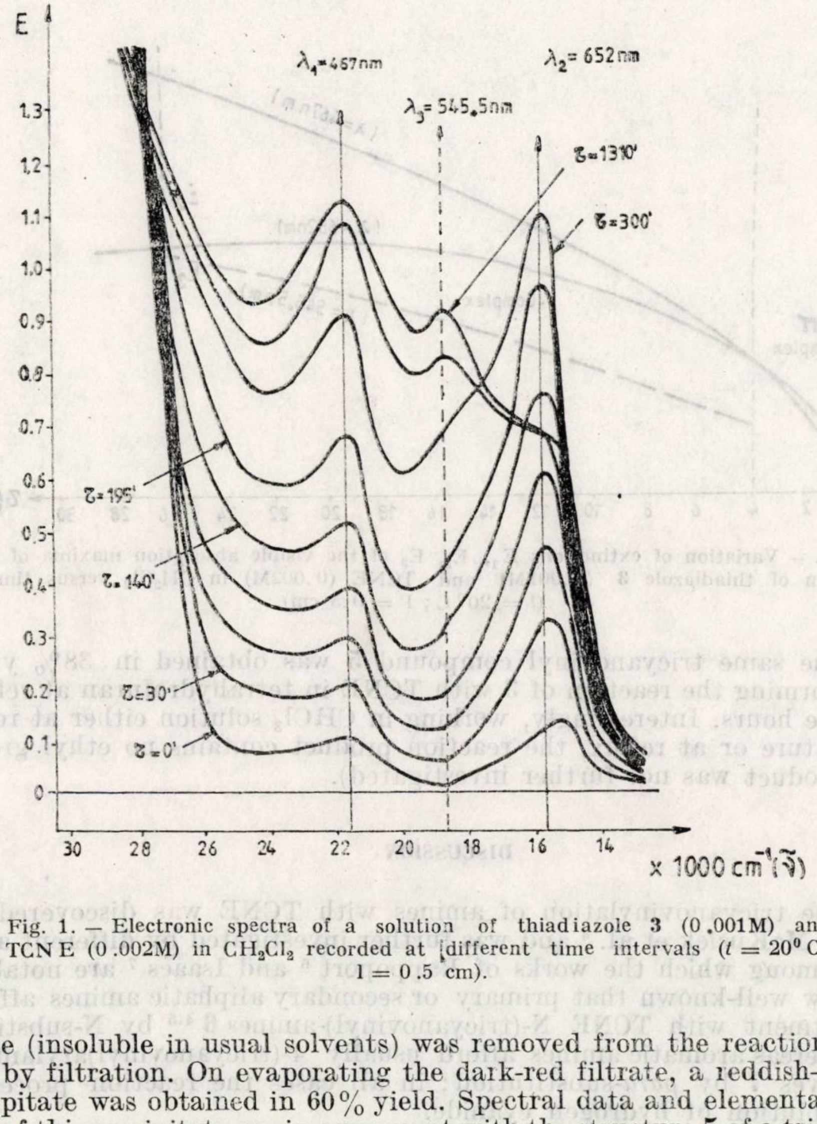

Fig. 1. — Electronic spectra of a solution of thiadiazole **3** (0.001M) and TCNE (0.002M) in CH_2Cl_2 recorded at different time intervals ($t = 20^0$ C; $l = 0.5$ cm).

pitate (insoluble in usual solvents) was removed from the reaction mixture by filtration. On evaporating the dark-red filtrate, a reddish-brown precipitate was obtained in 60% yield. Spectral data and elemental analysis of this precipitate are in agreement with the structure **5** of a tricyanovinyl derivative (see Experimental).

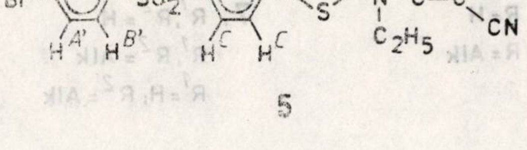

5

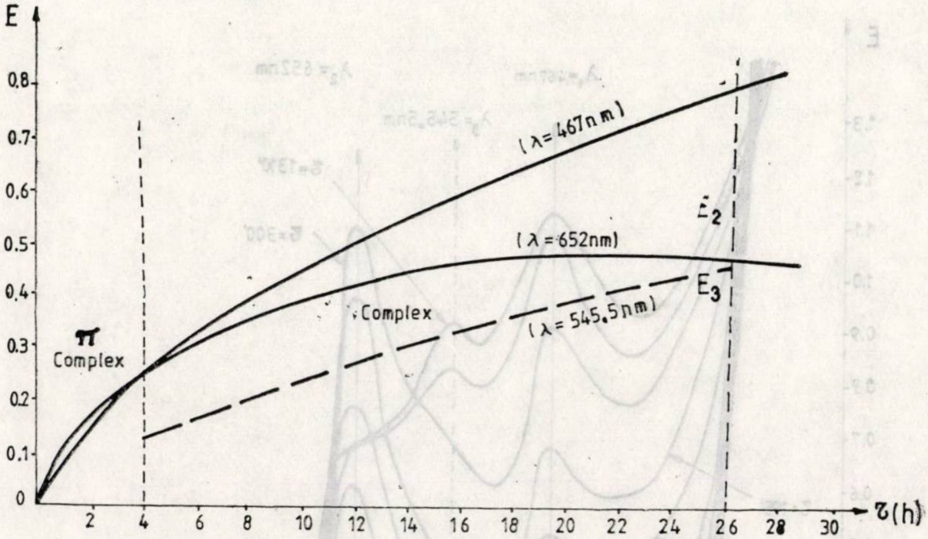

Fig. 2. — Variation of extinctions E_1, E_2, E_3 of the visible absorption maxima of a solution of thiadiazole **3** (0 .001M) and TCNE (0 .002M) in CH_2Cl_2 versus time ($t = 20^0$ C ; l = 0 .5 cm).

The same tricyanovinyl compound **5** was obtained in 38% yield on performing the reaction of **3** with TCNE in tetrahydrofuran at reflux for three hours. Interestingly, working in $CHCl_3$ solution either at room temperature or at reflux, the reaction product contains no ethyl group (this product was not further investigated).

DISCUSSION

The tricyanovinylation of amines with TCNE was discovered in 1958 by McKusick et al.[4] and was further investigated by different authors[5] among which the works of Rappoport[6] and Isaacs[7] are notable. It is now well-known that primary or secondary aliphatic amines afford on treatment with TCNE N-(tricyanovinyl)-amines **6**[4,5] by N-substitution, whereas aromatic amines afford usually 4-(tricyanovinyl)arylamine derivatives **7** by *para*-substitution ; in all cases the reaction proceeds with evolution of hydrogen cyanide.

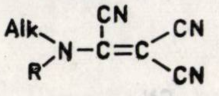

6; R = H
R = Alk

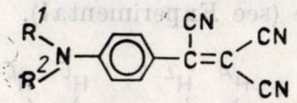

7; R¹, R² = H
R¹, R² = Alk
R¹ = H; R² = Alk

When an aromatic amine already bears a substituent in *para*-position, the reaction with TCNE occurs at the amino group producing tricyanovinylderivatives of the type **8**.[8]

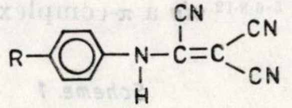

8; R = CH_3S
R = CH_3SO_2

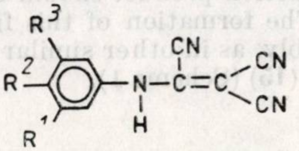

9: $R^1 = CF_3$; $R^2, R^3 = H$
$R^1, R^3 = H$; $R^2 = CF_3$
$R^1, R^3 = CF_3$; $R^2 = H$

Tricyanovinyl-amines have found a marked interest due to their optical-[9] and dyeing[4] properties (red colour). Very recently[10] the pharmacological qualities (anthelmintics, antibacterials, antimycotics, trichomonoacids) of tricyanovinyl derivatives **9**, obtained from the corresponding ring-substituted anilines were underlined.

Very few data seem to be known about the interactions between TCNE and secondary aryl-alkyl amines containing either a *para*-substituted phenyl ring or a heteroaromatic ring. However, formation of N-substituted tricyanovinyl derivative **10** from N-methyl-*p*-toluidine was mentioned.[4]

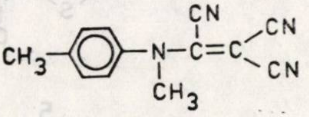

10

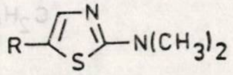

11; a) R = H; b) R = CH_3

A relatively recent investigation[11] describes the reaction of thiazoles **11** with TCNE: whereas the thiazole **11a** with a hydrogen atom in position 5 could undergo tricyanovinylation affording **12** (ring substitution) the thiazole **11b** ($R = CH_3$) gives rise to pentacyanopropenide thiazolium salt **13** as the sole product.

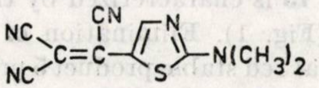

12

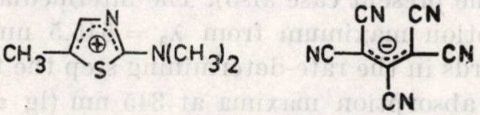

13

The presently investigated thiadiazole **3** may be considered as a secondary alkyl-aryl amine possessing a totally substituted aryl ring; the thiadiazolic ring bears no hydrogen atom and the remote phenyl groups have the *para*-positions blocked by substituents. Thus, it seems normal that the reaction product should be the N-substituted tricyanovinyl derivative **5**. The formation of this final stable reaction product **5** proceeds very probably, as in other similar cases, [5,6,8,12] *via* a π-complex (**14**) and a σ-complex (**15**) (Scheme 1).

Scheme 1

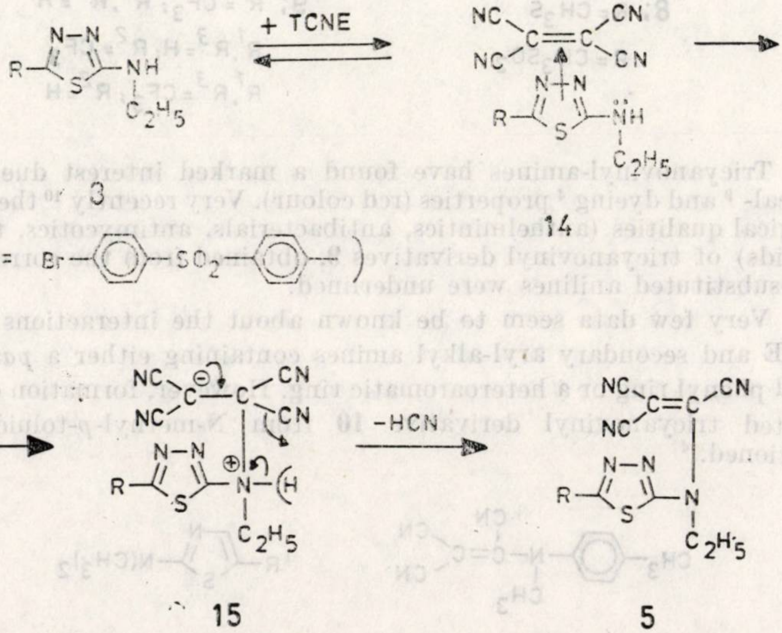

The green π complex **14** is formed very rapidly (from 0 to 4 hrs) and is characterized by absorption maxima at $\lambda_1 = 467$ nm and $\lambda_2 = 652$ nm. The rapid changes of the electronic spectrum (and of the colour of the reaction mixture) accompanies the transformation of the π-complex in another intermediate, most probably the σ-complex **15** (neutral species [13] or anion-radicals [7] were suggested in related cases as alternatives for the σ-complexes, and such types of intermediates could be operative in the present case also). The intermediate **15** is characterized by the absorption maximum from $\lambda_3 = 545.5$ nm (Fig. 1). Elimination of HCN affords in the rate-determining step the final red stable product **5** presenting absorption maxima at 345 nm ($\lg \varepsilon = 4.184$) and 485.5 nm ($\lg \varepsilon = 3.789$). It could be mentioned here that the compound **10** was characterized [4] by similar data : $\lambda_{max} = 335$ nm ($\varepsilon = 11900$).

An indirect proof for the above mechanism was brought by treatment of the N-acetylated thiadiazole **16** [2], (related with **3**) with TCNE in CH_2Cl_2 when no CTC was observed and no tricyanovinyl product was obtained.

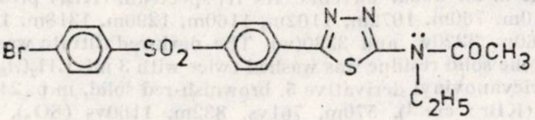

16

The absence of a tricyanovinyl product seems normal owing to the lack of removable hydrogen atoms (at aminic group or in *para*-position of an aryl group). The absence of CT-interactions between **16** and TCNE could be ascribed to the stronger electron-withdrawing effects of acetyl group (—I ; —E) which decreases the π-donor character of thiadiazole **16** (see also ref. [1]).

Finally, it could be added that the compound **5** (as well as related derivatives bearing different other substituents) could possess pharmacologic activities keeping in mind the above mentioned data for **9**, [10] and, on the other hand, the known biological effects of the thiazole ring [14a] and of the diphenylsulphone moiety. [14b]

In conclusion, this note presents a new example of the sparingly investigated interaction between TCNE and a secondary hetaryl-alkyl-amine (**3**) affording an N-substituted tricyanovinyl product **5** which may present biological activity. Formation of **5** proceeds *via* a coloured π-CT complex and a σ-complex (or its analog) which were evidenced spectrophotometrically. Further investigations in this area are in progress.

EXPERIMENTAL

The electronic spectra were recorded on a SPECORD UV—VIS (C. Zeiss-Jena) spectrophotometer using silica cells with $l = 0.5$ cm. IR spectra were run on a UR 20 (C. Zeiss-Jena) spectrophotometer. ^1H—NMR spectra were recorded on a VARIAN A-60A spectrometer with TMS as internal standard.

Reagents. The thiadiazole **3**, m.p. 218°C was obtained[2] by cyclization of the corresponding thiosemicarbazide in H_2SO_4 medium. Tetracyanoethene was recrystalized twice from chlorobenzene and showed a m.p. of 198.5—200°C. Dichloromethane was refluxed over P_4O_{10} and distilled.

Charge-transfer complex 14. The electronic spectrum of thiadiazole **3** and of TCNE present no absorption over 400 nm. When thiadiazole **3** and TCNE were simultaneously dissolved in CH_2Cl_2, the electronic spectrum of the green solution obtained presented two absorptions in the visible domain, at $\lambda_1 = 467$ nm and $\lambda_2 = 652$ nm (Fig. 1). Both absorption maxima change rapidly with the time (Fig. 1) hindering the accurate quantitative determinations of K-values after Benesi-Hildebrand relationship. [3] However the registration of the electronic spectrum of a typical mixture at different time intervals (Fig. 2) showed the modifications of the λ_1 and λ_2 absorption maxima beside the appearance of a new absorption maximum at $\lambda_3 = 545.5$ nm ; these changes are accompanied by the modification of the solution colour from green toward red-brown. After 26 hrs the reaction mixture begins to precipitate rendering impossible further spectroscopic determinations.

2(p-bromophenylsulphonyl)phenyl-5-ethyl-N-tricyanovinyl-1, 3, 4- thiadiazole (5). A solution of thiadiazole **3** (217 mg ; 0 .5 mmoles) and TCNE (72 m g ; 0.56 mmoles) in 25 mL anhydrous CH_2Cl_2 was prepared (green colour) and stored at room temperature for 72 hrs. The colour of the solution changes from green to olive then to reddish-brown, being accompanied by precipitation of a dark solid. Filtration of the reaction mixture afforded 80 mg black solid, m.p $>$ 350°, insoluble in all usual solvents. Its IR-spectrum (KBr) presents the following absorptions (cm^{-1}) : 610m, 760m, 1072m, 1102m, 1160m, 1290m, 1318m, 1490m, 1565m, 1650m, 2225m, 2980w, 3060w, 3220w, and 3330(w). The dark-red filtrate was evaporated *in vacuo* without heating and the solid residue was washed twice with 3 mL CH_2Cl_2 and filtered affording 160 mg (59.7%) of tricyanovinyl derivative **5**, brownish-red solid, m.p. 247—250°C.

IR spectrum (KBr ; cm^{-1}), 570m, 761vs, 832m, 1160vs (SO_2), 1290m, 1321vs (SO_2), 1350m, 1486s, 1609s(C=C), 2226m(CN), 2929w, 2972w and 3079w.

^1H-NMR spectrum ($CDCl_3$; δ ppm) : 1 .37 (t ; 3H ; J = 7 .5Hz ; CH_3) ; 3 .5 (q ; J = =7 .5 Hz ; 2H ; CH_2) ; 7 .75 (2H ; H^A ; AA′BB′ system ; J = 9 Hz) ; 7 .95 (2H ; H^B ; AA′BB′ system ; J = 9 Hz) ; 8 .05 (4H : H^C).

Electronic spectrum (ethanol ; λ_{max} ; lg ε_{max}) ; 244 (4.307) 258 .5 (4 .346) ; 345 (4 .184) ; 485 .5 (3 .789) ;

Reaction of thiadiazole **3** with TCNE performed in tetrahydrofurane for 3 hrs at reflux (after the general procedure of McKusick[4]) afforded the same tricyanovinyl product **5** in 38 % yield.

Working in $CHCl_3$ solution at 20° or at reflux, a new product was obtained (dark-red solid) whose ^1H-NMR spectrum indicated the loss of the ethyl group. This product was not further investigated.

REFERENCES

[1] Note I. I. Şaramet and M. Banciu, *Rev. Roumaine Chim.*, **30**, 559 (1985).

[2] I. Şaramet, Thesis, The Polytechnic, Bucharest, 1981.

[3] a) H. A. Benesi and J. H. Hildebrand, *J. Amer. Chem. Soc.*, **71**, 2703 (1949) ; b) R. L. Scott, *Req. Trav. Chim.*, **75**, 787 (1956).

[4] B. C. McKusick, R. E. Heckert, T. L. Cairns, D. D. Coffman and H. F. Mower, *J. Amer. Chem. Soc.*, **80**, 2806 (1958).

[5] See A. J. Fatiadi, *Synthesis*, **1986**, 249 and the literature cited therein.

[6] a) Z. Rappoport, *J. Chem. Soc.*, **1963**, 4498 ; b) Z. Rappaport and A. Horowitz, *J. Chem. Soc.*, **1964**, 1348 ; c) Z. Rappoport and E. Shohamy, *J. Chem. Soc.*, [B], **1969**, 77 ; d) Z. Rappoport and D. Ladkany, *J. Chem. Soc.*, [C], **1974**, 2595.

[7] N. S. Isaacs, *J. Chem. Soc.*, [B], **1966**, 1053.

[8] L. P. Gossen, E. A. Kruilikovskaya and V. N. Kumok, *Zh. Fiz. Khim.*, **51**, 277 (1977) ; **52**, 1817 (1978).

[9] A. Sasaki, J. Aihara and Y. Matsunaga, *Bull. Chem. Soc. Japan*, **47**, 2926 (1974).

[10] A. Kreutzenberger and S. Daus, *J. Fluorine Chem.*, **36**, 461 (1987).

[11] A. Medici, P. Pedrini, C. Venturoli and A. Dondoni, *J. Org. Chem.*, **46**, 2790 (1981).

[12] a) R. Foster and P. Hanson, *Tetrahedron*, **21**, 255 (1965) ; b) P. G. Farrell, J. Newton and R. F. M. White, *J. Chem. Soc.*, [B], **1967**, 637 ; c) J. E. Frey, R. D. Cole, E. C. Kitchen, L. M. Supernant and M. S. Sylwestrzak, *J. Amer. Chem. Soc.*, **107**, 784 (1985).

[13] P. G. Farell and J. Newton, *J. Chem. Soc.*, [B], **1970**, 1630.

[14] a) J. V. Metzger, "Comprehensive Heterocyclic Chemistry", vol. 6, part 4B ; A. R. Katritzky, W. Rees and K. T. Potts (editors) ; Pergamon, 1984, p. 328 ; b) E. Ciorănescu, "Medicamente de sinteză ", Ed. Tehnică, Bucharest, 1966, p. 634.

Revue Roumaine de Chimie, **35**, *3*, 445—452 (1990)

SOLVOLYSES IN SUBSTITUTED CYCLOPROPYLCARBINYLIC SYSTEMS. 8[1]

SOLVOLYSES OF 2-ARYL-1-CYCLOPROPYLETHANOLS AND THEIR 3,5-DINITROBENZOATES *

ALEXANDRU C. RĂZUŞ, FILIP CHIRALEU and ADRIAN I. IANCU
Centre of Organic Chemistry, Spl. Independenţei 202B, R-78100, Bucharest, Romania

Received July 15, 1989

In the solvolysis of several 2-aryl-1-cyclopropylethanols in the presence of perchloric acid, the following reaction products were identified : *cis*- and *trans*-1-cyclopropyl-2-phenylethene, 1-phenylpent-4-en-2-ol, 5-phenylpent-3-en-1-ol, and *trans*-2-benzylcyclobutan-1-ol. The kinetic and thermodynamic parameters supporting the proposed solvolysis reaction mechanism are presented.

INTRODUCTION

The neighbouring group participation in the ionization step of nucleophilic substitutions has been, and still is, a subject of interest. The estimation of the extent of neighbouring group participation is mainly based on kinetic and stereochemical data.

An interesting case is that in which two such neighbouring groups, whose individual behaviour is well established, give competing assistance at one and the same ionization centre. For instance, in the solvolysis of 2-norbornyl (or benzonorbornyl) compounds possessing a spiro-cyclopropanic ring in position 3, the relative reactivity *exo*/*endo* diminishes very much, indicating the leveling effect of the cyclopropylic substituent on the other influences in the molecule. [2]

The benzylcyclopropylcarbinylic system is another example in which both the cyclopropyl group and the phenyl group in β-position may give assistance at the ionization centre, and we decided to investigate this system.

---

* Dedicated to the memory of Mihai Elian.

RESULTS

1. Solvolysis of 1-cyclopropyl-2-phenylethanol 1a and its dinitrobenzoates

The solvolysis of the alcohol **1a** was performed in 0.5M perchloric acid in 50% aqueous dioxane. The composition of the solvolysis mixture was analyzed by gas-liquid chromatography. The reaction products were isolated by elution chromatography and by preparative glc. The identification of the reaction products was based on spectroscopic data (see experimental part).

The solvolysis of the alcohol **1a** gave *cis*- and *trans*-1-cyclopropyl-2-phenylethene (**2**-*cis* and **2**-*trans*, respectively), 1-phenylpent-4-en-2-ol **3** 5-phenylpent-3-en-1-ol **4**, and *trans*-2-benzyl-cyclobutan-1-ol **5** (Scheme 1)’

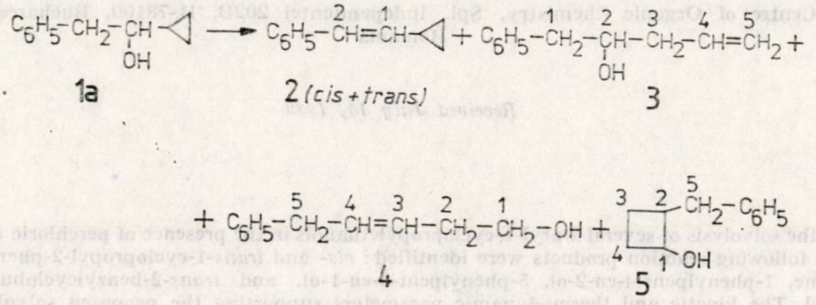

Scheme 1

The evolution of the reaction mixture composition up to three half-life times is presented in Figure 1.

In order to obtain more information on this system, the buffered and unbuffered solvolysis of 3,5-dinitrobenzenzoates of the alcohol **1a** (**1a**-DNB) were also performed. The buffered solvolysis was effected in 70% aqueous acetone, in the presence of 2,4,6-trimethylpyridine. In Table 1 are presented the results obtained in the solvolysis of 3,5-dinitrobenzoates in comparison with those obtained in the solvolysis of the alcohol **1a** in the presence of perchloric acid.

Table 1

The composition of the solvolytic mixture in the solvolysis of the alcohol **1a** and of its 3,5-dinitrobenzoate

Substrate	Time (hrs)	Temp. (°C)	Other conditions	**1a**	**2** *cis*	Composition (%)[a]			
						2 *trans*	**3**	**4**	**5**
1a[b]	6	65.6	—		6.1	19.0	11.2	21.2	31.7
1a[c]	8	70.0	—		3.8	10.6	7.6	48.3	20.6
1a—DNB	10	130.0	unbuffered	44.2	4.8	11.6	3.5	27.3	8.6
1a—DNB	10	130.0	buffered[d]	87.7	5.6	6.7	—	—	—

---

[a] up to 100%, high-boiling, unidentified components; [b] 59.0% conversion; [c] 90.6% conversion; [d] buffer: 2,4,6-trimethylpyridine.

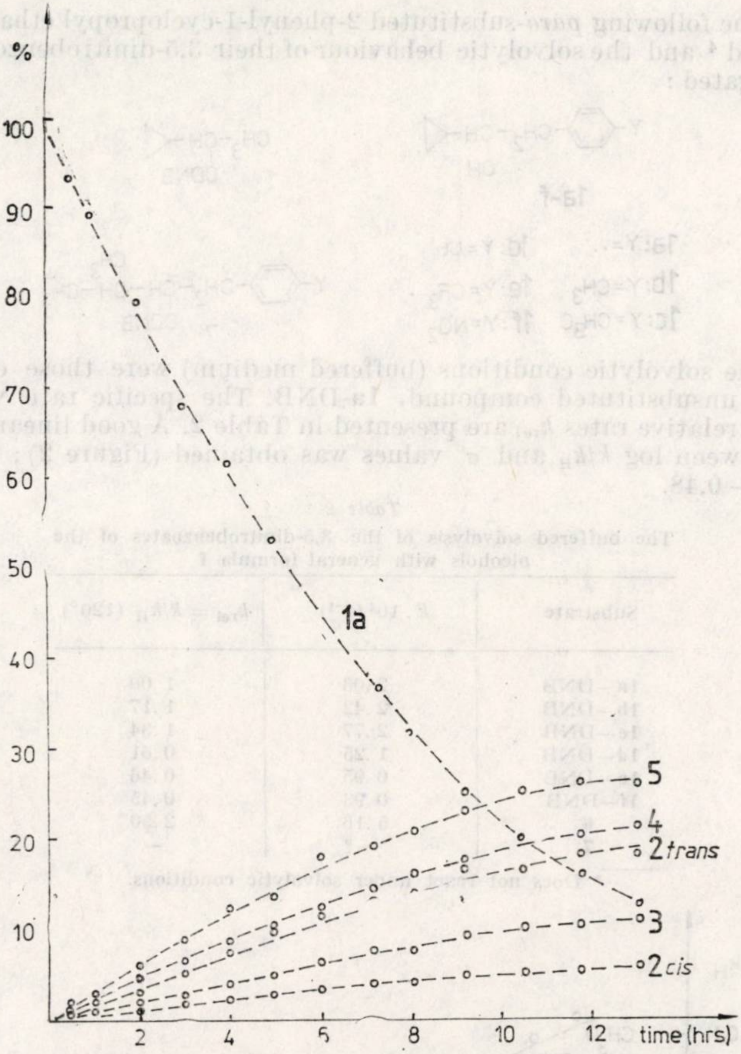

Fig. 1. — The evolution of the reaction mixture composition in the solvolysis of the alcohol **1a** at 65.6°C.

The activation parameters in the solvolysis of the 3,5-dinitrobenzoate **1a** were calculated from k values determined at 120° and 138°C ($2.06 \cdot 10^{-4}$ and $7.94 \cdot 10^{-4}$ s^{-1}, respectively). The following values were obtained : $\Delta H^{\neq} = 23.3$ kcal/mole and $\Delta S^{\neq} = -16.7$ e.u.

2. Kinetic study for 1-cyclopropyl-2-(*para*-substituted phenyl)-ethanols ; correlation parameters

The most conclusive evidence for the participation of the aromatic ring in the β-position to the reaction centre is obtained from the correlation of kinetic parameters.[3]

The following *para*-substituted 2-phenyl-1-cyclopropyl ethanols were prepared[4] and the solvolytic behaviour of their 3,5-dinitrobenzoates was investigated:

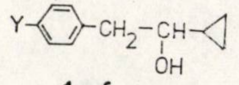

1a-f

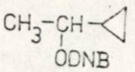

1a: Y=H
1b: Y=CH_3
1c: Y=CH_3O
1d: Y=Cl
1e: Y=CF_3
1f: Y=NO_2

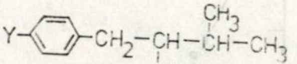

7

The solvolytic conditions (buffered medium) were those employed for the unsubstituted compound, **1a**-DNB. The specific rate values, k and the relative rates k_{rel} are presented in Table 2. A good linear correlation between log k/k_H and σ° values was obtained (Figure 2); the slope is $\rho = -0.48$.

Table 2

The buffered solvolysis of the 3,5-dinitrobenzoates of the alcohols with general formula **1**

Substrate	$k \cdot 10^4$ (s^{-1})	$k_{rel} = k/k_H$ (120°)
1a—DNB	2.06	1.00
1b—DNB	2.42	1.17
1c—DNB	2.77	1.34
1d—DNB	1.25	0.61
1e—DNB	0.95	0.46
1f—DNB	0.93	0.45
6	5.16	2.50
7	—*	—

* Does not react under solvolytic conditions.

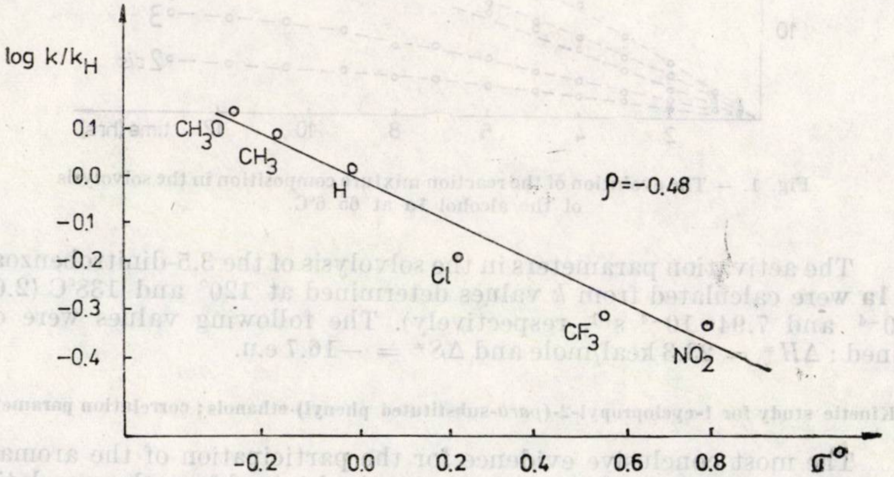

Fig. 2. — Plot of σ° vs. log k/k_H for the solvolysis of 2-aryl-1-cyclopropyl-3,5-dinitrobenzoates.

DISCUSSION

The investigated compounds presented the general solvolytic behaviour of cyclopropylcarbinylic systems. Under conditions preventing the reionization, such as those used in the buffered solvolysis of **1a**-DNB, solely the formation of the unrearranged alcohol **1a** was observed. This result is in agreement with previous observations attesting the fact that a charge-stabilizing group in the 1-position of the cyclopropylcarbinylic system leads to compounds with unrearranged skeleton under conditions of irreversibility of the reaction.[5]

In the solvolyses performed with perchloric acid or with 3,5-dinitrobenzoic acid (solvolysis in unbuffered medium), the nature of the products was similar with those usually obtained for the cyclopropylcarbinylic systems. However, an observation regarding the ratio between the obtained alcohols is to be underlined. The alcohol **4** is the "normal" product of the thermodynamically controlled solvolysis of the alcohol **1a**. One may assume that this alcohol is obtained by a nucleophilic attack at one of the methylenic carbon atoms of the cyclopropanic ring. However, this attack requires a rather high energy since the methylenic positions have lower charge densities than the trigonal carbon atom bearing the positive charge in the initially formed carbocation.

On the other hand, the isomeric alcohol **3** does not originate from the ion formed initially from the protonated alcohol **1a**. It is possible that this alcohol and the cyclobutanic alcohol **5** involve a common intermediate (presumably a puckered cyclobutanic one). This presumption is based on the fact that the ratio of the two alcohols **5 : 3** is almost the same (cca. 2.7) regardless of the reaction conditions.

Finally, the kinetic results confirm leveling effect of the cyclopropanic ring on the other neighbouring influences at the ionic centre. While 2-arylcarbinylic systems lacking cyclopropanic ring gave no Hammett correlation,[3] for our system a good Hammett-type correlation was observed. Obviously, the charge delocalization on the cyclopropanic ring is the main reason for this different behaviour.* This dissipation of the charge is reflected in a certain degree by the relatively low ρ value. There is still an influence of the aryl group, of inductive nature, reflected by the slower solvolysis rate of the alcohol **1a** compared with that of the alcohol **6** (see Table 2).

EXPERIMENTAL PART

Instrumentation

Melting points and boiling points are both uncorrected. The IR spectra were recorded with a Carl Zeiss Jena spectrometer. The ^{1}H-NMR spectra were recorded with a Varian A 60-A spectrometer, using TMS as internal standard. The analytical and preparative gas-liquid chromatographic separations were performed with a Willy Giede 18—3 apparatus, using a column 1 m × 4 mm filled with silanized Chromosorb W (60—80 mesh) coated with 13% ethyleneglycolsuccinate and 7% carbowax 20M.

---

* The comparison with a system lacking the cyclopropanic ring (**7**) gives a measure for the cyclopropanic neighbouring assistance (see Table 2).

Starting materials

The syntheses of the alcohols **1a**–**f** were reported.[4] The 1-cyclopropyl-2-(*para*-substituted phenyl)ethyl 3,5-dinitrobenzoates **1a**–**f**–DBN were prepared in the usual manner[6] from the corresponding alcohols **1a**–**f** and 3,5-dinitrobenzoyl chloride. In Tables 3 and 4 are presented the physical data, elemental analyses and ^{1}H–NMR spectral data of these esters.

1-Cyclopropylethyl 3,5-dinitrobenzoate **6** was prepared from 1-cyclopropylethanol[7] as crystalline compound with m.p. 87°C.

^{1}H–NMR ($CDCl_3$, δ, ppm) : 0 .30–0 .90 (m, 4H, cyclopropyl) ; 0 .90–1 .40 (m, 1H, cyclopropyl) ; 1 .53 (d, 3H, CH_3) ; 4 .74 (m, 1H, CH) ; 9 .20 (m, 3H, aromatics).

1-Phenyl-3-methyl-2-butyl 3,5-dinitrobenzoate **7** was prepared from 1-phenyl-3-methyl-2-butanol[8] ; this compound presents two allotropic forms, with m.p. 54° and 83°C.

^{1}H–NMR ($CDCl_3$, δ, ppm) : 1 .11 (d, 6H, $CHMe_2$) ; 2 .25 (m, 1H, $CHMe_2$) 3 .03 (d, 2H, CH_2) ; 5 .33 (m, 1H, CH) ; 7 .20 (s, 5H, 1–C_6H_5) ; 9 .10 (m, 3H, aromatic protons in dinitrophenyl).

Solvolysis of 1-cyclopropyl-2-phenylethanol 1a in acidic medium

A solution of 0 .2 g (1.23 mmoles) 1-cyclopropyl-2-phenylethanol **1a** in 18 mL purified dioxane-water mixture (5 : 4 in volume) was heated in a thermostate at the solvolysis temperature. To this solution 2 mL 5M perchloric acid, heated at the same temperature, was added and the mixture was kept in the thermostate under inert gas, for the desired reaction time. After cooling to room temperature, the reaction mixture was poured into 15 mL of saturated sodium bicarbonate solution and then extracted four times with 10 mL ethylic ether portions. The combined organic layers were washed with water, dried over magnesium sulfate and the solvent was distilled off under mild heating conditions, using a Vigreaux column. An oily product (0 .2g) was obtained.

Separation and identification of the solvolytic products of the alcohol 1a

The crude solvolytic mixture was analyzed by gas-liquid chromatography ; the result are presented in Table 1. The separation of the components was performed by preparative gas-liquid chromatography. Structure proofs are based on ^{1}H–NMR data for the reaction productss.

cis-1-Cyclopropyl-2-phenylethene (**2**-*cis*)

H^{1}–NMR (CCl_4, δ, ppm) : 0 .20–0 .95 (m, methylenic cyclopropylic groups) ; 1 .60–2 .20 (m, 1H, cyclopropylic methine group) ; 4 .98 (dd, 1H olefinic, 1–CH group, $J_{1,2}$=11.5 Hz, $J_{1,3}$ = 9 .5 Hz) ; 6 .29 (d, 1H olefinic, 2–CH group) ; 7 .00–7 .55 (s, 5H, aromatics).

trans-1-Cyclopropyl-2-phenylethene (**2**-*trans*)

^{1}H–NMR (CCl_4, δ, ppm) : 0 .36–1 .00 (m, methylenic cyclopropylic groups) ; 1 .20–1 .80 (m, 1H, cyclopropylic methine group) ; 5 .65 (dd, 1H olefinic, 1–CH group, $J_{1,2}$ = 15 .5 Hz, $J_{1,3}$ = 8 .0 Hz) ; 6 .37 (d, 1H olefinic, 2–CH group) ; 7 .16 (s, 5H, aromatics).

1-Phenylpent-4-en-2-ol (**3**)

^{1}H–NMR (CCl_4, δ, ppm) : 1 .99 (s, 1H, OH) ; 2 .16 (broad triplet, 2H, 3–CH_2 group, $J_{2,3}$ = 6 .0 Hz, $J_{3,4}$ = 7 .0 Hz) ; 2 .66(B part of an AB_2 system, 2H, 1–CH_2 group, $J_{1,2}$ =7 .0 Hz) ; 3 .75 (quintet, A part of an AB_2 system, 1H, 2–CH group, supplementarily coupled with 3–CH_2 methylenic protons) ; 5 .05(m, 2H olefinics, 5–CH_2 group) ; 5 .76 (m, 1H olefinic, 4–CH group) ; 7 .16(s, 5H, aromatics).

5-Phenylpent-3-en-1-ol (**4**)

^{1}H–NMR (CCl_4, δ, ppm) : 2 .21 (broad quartet, 2H, 2–CH_2 group, $J_{1,2}$ = 7 .0 Hz, $J_{2,3}$ = 6 .5 Hz) ; 3 .26 (d, 2H, 5–CH_2 group, $J_{4,5}$= 5 .0 Hz) ; 3 .53 (t, 2H, 1–CH_2 group) ; 5 .43 and 5 .63 (AB system, 2H olefinics, 3–CH and 4–CH groups, J_{AB} = 15 .0 Hz) ; 7 .13 (s, 5H, aromatics).

trans-2-Benzylcyclobutane-1-ol (**5**)

^{1}H–NMR (CCl_4, δ, ppm) : 1 .00–3 .00 (multiplet, 7H aliphatic + OH) ; 3 .88 (broad quartet, 1H, 1–CH group) ; 7 .23 (s, 5H, aromatics).

The normal ^{1}H–NMR spectrum of the alcohol **5** is not fully indicative for the structure. Recording the spectra in the presence of the lanthanide shift reagent $Eu(fod)_3$, the complex pattern in the range 1 .00–3 .00 ppm corresponding to eight protons is resolved ; the following assignments were made in the spectrum obtained for a molar ratio between $Eu(fod)_3$ and the alcohol **5** of 0 .25 : 9 .15 ppm (broad quartet, 1–CH), 8 .23 ppm (multiplet, 2 aromatic protons), 7 .63 ppm (multiplet, 3 aromatic protons), 6 .06 ppm (broad sextet, 1H, 2—CH), 5 .18 ppm (broad quintet, 1H, 4—CH, proton in *cis* relative position to the hydroxylic group) 4 .18 ppm (multiplet, 1H, 3—CH, proton in *cis* relative position to the hydroxylic group), 4 .10 and 4 .75 ppm (AB system for 5—CH_2 group, $J_{AB} = 14.0$ Hz), 2 .26—3 .36 ppm (multiplet, 2H, 3—CH and 4—CH, both protons in *trans* relative positionto the hydroxylic group).

The observed induced shifts suggest a relative *trans* orientation of the hydroxyl and benzyl groups in **5**. Indeed, for a relative *cis* orientation of the two groups, higher induced shifts would be expected for the methylenic protons in benzyl group than for the cyclobutanic hydrogen from 2—CH.

Unbuffered solvolysis of 1-cyclopropyl-2-phenylethyl 3,5-dinitrobenzoate (1a-DNB)

A solution of 2 .3 g (6 .5 mmoles) dinitrobenzoate of **1a** in 25 mL 70% aqueous acetone was sealed in a glass ampoule and heated at 130°C for 10 hours in a thermostate. After careful evaporation of the acetone, the liquid residue was extracted three times with 5 mL ethylic ether portions, the extract was washed with sodium bicarbonate solution, then with water, and was dried over magnesium sulfate. The oily residue obtained after careful evaporation of the solvent was analysed by gas-chromatography. The composition of the solvolysis mixture is presented in Table 1.

Buffered solvolysis of 1-cyclopropyl-2-phenylethyl 3,5-dinitrobenzoate (1a-DNB)

A solution of 2 .3 g (6 .5 mmoles) dinitrobenzoate of **1a** and 1 .5g (10 mmoles) 2,4,6-trimethylpyridine in 25 mL 70% aqueous acetone was sealed in a glass ampoule and heated at 130°C for 10 hours in a thermostate. After careful evaporation of the acetone, the aqueous residue was saturated with sodium chloride and extracted three times with 5 mL ethylic ether portions. The combined extracts were washed with cold 10% hydrochloric acid, then with saturated sodium bicarbonate solution and water, and were dried over magnesium sulfate. The oily residue obtained after careful evaporation of the solvent was analysed by gas-chromatography. The results are presented in Table 1.

Kinetic determinations

The ampoule technique was employed in the determination of the solvolysis rates of 1-cyclopropyl-2-(*para*-substitued phenyl)-ethyl 3,5-dinitrobenzoates (**1a**—**f**—DNB, **6** and **7**) in 70% aqueous acetone. The concentration of the ester was approximately 0 .005M and the molar ratio between the ester and the buffer (2,4,6-trimethylpyridine) was 1 : 2. The liberated

Table 3

Physical constants and elemental analysis for 1-cyclopropyl-2-(*para*-substitued phenyl)ethyl 3,5-dinitrobenzoates (**1a**—**f**—DNB)

Compound	Yield %	m.p. °C	Elemental analysis (%)							
			calculated				found			
			C	H	N	Cl	C	H	N	Cl
1a—DNB	53	95—96	60 .67	4 .53	7 .86	—	60 .87	4 .72	7 .61	—
1b—DNB	67	110—111	61 .61	4 .90	7 .57	—	61 .80	5 .08	7 .35	—
1c—DNB	42	105—106	59 .04	4 .70	7 .25	—	59 .10	4 .87	6 .91	—
1d—DNB	69	124	55 .32	3 .87	7 .17	9 .07	55 .10	4 .06	8 .80	7 .11
1e—DNB	50	115—116	—	—	—	—	—	—	—	—
1f—DNB	70	129—130	53 .87	3 .77	10 .47	—	53 .63	4 .06	10 .10	—

3,5-dinitrobenzoic acid was determined by potentiometric titration with 0.01M sodium hydroxide in 70% aqueous acetone. During the measurements, the alkaline solution was repeatedly checked with benzoic acid. All experiments were performed twice. The results obtained are presented in Table 2.

Table 4

^1H-NMR data for 1-cyclopropyl-2-(*para*-substituted phenyl)ethyl 3,5-dinitrobenzoates (**1a**–**f**–DNB)

Compound	^1H-NMR (CCl_4, δ, ppm)						
	cyclopropylic CH_2	cyclopropylic CH	CH_2	CH	CH_3	aromatic protons	aromatic protons (DNB)
1a–DNB	0.30–0.85 m	0.85–1.53 m	3.18 d	4.70 m	—	7.25 s	9.16 m
1b–DNB	0.25–0.80 m	0.80–1.43 m	3.11 d	4.70 m	2.25 s	7.05 s	9.13 m
1c–DNB	0.20–0.85 m	0.85–1.33 m	3.11 d	4.76 m	3.73 s	6.75; 7.16 m (A_2B_2)	9.10 m
1d–DNB	0.20–0.80 m	0.80–1.48 m	3.21 d	4.75 m	—	7.28 s	9.20 m
1e–DNB	0.20–0.85 m	0.85–1.40 m	3.26 d	4.81 m	—	7.40; 7.61 m (A_2B_2)	9.19 m
1f–DNB	0.25–0.80 m	0.80–1.56 m	3.37 d	4.86 m		7.55; 8.20 m (A_2B_2)	9.20 m

REFERENCES

[1] Part 7, A. C. Răzuş, M. D. Gheorghiu and E. Bartha, *Rev. Roumaine Chim.*, in press.

[2] C. E. Wilcox Jr. and R. G. Jesaitis, *Tetrahedron Lett.*, **1967**, 2567; D. Lenoir, P.v.R. Schleyer and I. Ipaktschi, *Ann.*, **750**, 28 (1971).

[3] C. J. Lancelot and P.v.R. Schleyer, in "Carbonium Ions", vol. III, G. A. Olah and P.v.R. Schleyer, Wiley Interscience, New York, 1971, chap. 27.

[4] A. C. Răzuş and A. I. Iancu, *Rev. Roumaine Chim.*, in press.

[5] T. A. Favorskaya, O. V. Sergievskaya and N. P. R. Ryzhova, *J. Gen. Chem. USSR*, **27**, 1018 (1957); C. G. Richey Jr. and J. M. Richey, *J. Amer. Chem. Soc.*, **88**, 4971 (1966).

[6] R. A. Sneen and A. L. Baron, *J. Amer. Chem. Soc.*, **83**, 614 (1961).

[7] K and K Laboratories of California, Inc., Hollywood, Calif., USA.

[8] D. M. Muir and A. J. Parker, *J. Org. Chem.*, **41**, 3201 (1976).

Revue Roumaine de Chimie, **35**, *3*, 453–457 (1990)

FRIEDEL-CRAFTS CHEMISTRY IN ALICYCLIC SYSTEMS. V[1]

REACTION OF CYCLOHEXYLIDENE- AND 1-CYCLOHEXENYLACETIC ACIDS WITH BENZENE IN THE PRESENCE OF $AlCl_3 \cdot CH_3NO_2$ AS THE CATALYST *

V. DRĂGUŢAN *, ILEANA DRĂGUŢAN, C. CONDEIU and ALICE-MARIE GLATZ
Centre of Organic Chemistry, 202B Spl. Independenţei, R-78100 Bucharest, Romania

Received June 18, 1989

Reaction of cyclohexylidene- and 1-cyclohexenylacetic acids with benzene in the presence of the $AlCl_3 \cdot CH_3NO_2$ complex at 40–45°C is studied. The observed catalyst activity and product distribution is compared with previous results obtained when using $AlCl_3$ as the catalyst. The mechanism and stereochemistry are discussed in terms of carbocationic pathways pointing out the particular role of the catalytic complex during the main reaction steps.

INTRODUCTION

Previous studies[2] showed that the reactions of cyclohexylideneacetic and 1-cyclohexenylacetic acids with benzene in the presence of $AlCl_3$ at 40–45 °C gave equilibrium mixtures of phenylated acids in which the phenyl group was found in all available substitution positions of the cyclohexene ring (2, 3 and 4 ; *trans*, *cis*- and *trans*- respectively). When the same reactions were carried out at 80 °C, mainly bicyclic ketones were obtained resulting by cyclialkylation of the corresponding phenylcyclohexylacetic acids. On the other hand, the reaction of the two alicyclic acids with benzene with various other Lewis acids[3] (e.g. $BF_3 \cdot Et_2O$, $AlCl_3 \cdot CH_3NO_2$, $FeCl_3$, $TiCl_4$, $SnCl_4$ or $ZnCl_2$) demonstrated that the position in which the phenyl group was located depended on the catalyst employed. These results were rationalized by a carbocationic mechanism involving 1,2- and 1,3-hydride ion shift and formation of intermediate lactoid species the process being accompanied by subsequent isomerization of the resulted phenylated products. At short reaction times the reaction showed to be under kinetic control and then thermodynamically controlled, the system being shifted to the equilibrium composition as a result of the acid catalyzed isomerization of the initially formed phenylcyclohexylacetic acids. In addition, the rate of the overall process proved to be dependent on the Brönsted and Lewis acidity of the catalytic system.

---

* Dedicated to the memory of Mihai Elian.

The present paper is devoted to the study of more detailed aspects of these reactions correlating results with the $AlCl_3 \cdot CH_3NO_2$ catalyst with previous observations.

RESULTS AND DISCUSSION

The reaction of cyclohexylidenacetic (**1**) and 1-cyclohexenylacetic (**2**) acids with benzene in the presence of the catalytic complex $AlCl_3 \cdot CH_3NO_2$ was carried out at 40–45 °C using a molar ratio acid : catalyst : benzene 1 : 1.5 : 20 ($AlCl_3 : CH_3NO_2 = 1-1.5$). The composition of the reaction products at various reaction times was determined by v.p.c. Both acid **1** and **2** gave the same reaction products : *cis*-2- (**3a**), *trans*-2- (**3b**), *cis*-3- (**4**) and *trans*-4-phenylcyclohexyl acetic (**5**) acids (Scheme 1) whilst the conversion and product composition were slightly different for **1** and **2** (Tables 1 and 2). Sharp differences were however observed as compared with previously reported results [2] with uncomplexed $AlCl_3$.

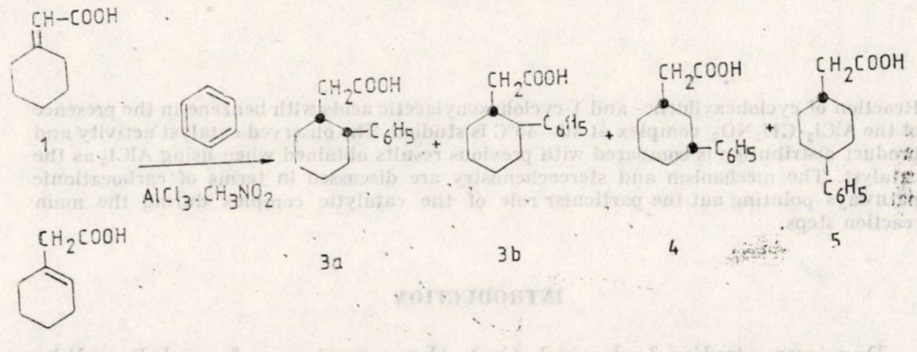

Scheme 1

Table 1

Reaction of cyclohexylideneacetic acid (*1*) with benzene in the presence of the $AlCl_3 \cdot CH_3NO_2$ catalyst[a]

Reaction time. min.	Conv., %	Product composition[b] %			
		3a	3b	4	5
1	18	3.0	10.0	2.1	2.6
5	32	2.0	19.0	4.6	6.1
15	35	1.1	22.0	5.5	6.8
60	40	0.5	18.5	7.0	10.5
240	55	0.4	16.8	14.0	23.8
600	79	0.3	4.3	23.4	51.0
1200	95	traces	1.1	30.0	63.0

[a] Molar ratio cyclohexylideneacetic acid : catalyst : benzene 1: 1.5 :20 ; [b] Small unidentified components were recorded too.

Table 2

Reaction of 1-cyclohexenylacetic acid (*2*) with benzene in the presence of the $AlCl_3 \cdot CH_3NO_2$ catalyst[a]

Reaction time, min.	Conv., %	Product composition[b], %			
		3a	**3b**	**4**	**5**
1	17.5	2.5	10.5	2.0	2.5
5	31.5	2.0	19.5	4.5	5.5
15	36.0	1.0	23.5	5.4	6.6
60	39.0	0.5	18.8	7.2	10.0
240	53.0	0.4	17.5	12.4	21.5
600	76.0	0.2	4.5	20.5	50.5
1200	92.0	0.1	1.5	28.0	62.0

[a]. Molar ratio 1-cyclohexenylacetic acid : catalyst : benzene 1 : 1.5 : 20, [b] Several small unidentified components were also recorded.

Thus, conversion of acid **1** to phenylcyclohexylacetic acids **3**—**5** varies in time within the range 18—95% and is much lower than that with $AlCl_3$ (Fig. 1). The product selectivity also varied substantially with the reaction progress: at short reaction time product *3b* was preponderant while in time products **4** and **5** became prevalent. It is noteworthy that with this catalyst both *cis*-2- (**3a**) and *trans*-2-phenylcyclohexylacetic (**3b**) acids were formed (with $AlCl_3$ only **3b**), along with *cis*-3- (**4**) and *trans*-4-phenylcyclohexylacetic (**5**) acids. In contrast to data [2] with $AlCl_3$, the equilibration of the reaction products was not attained even after prolonged reaction (20 hr).

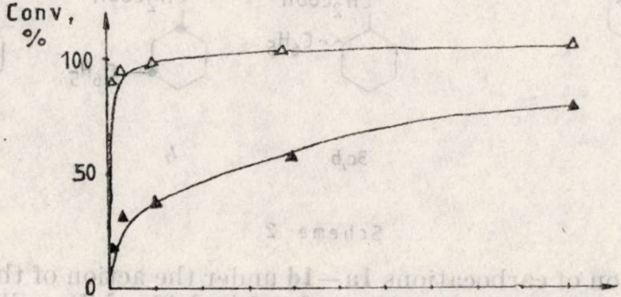

Fig. 1. — Time evolution of conversion of acid *1* with benzene in the presence of $AlCl_3$ (△) and $AlCl_3 \cdot CH_3NO_2$ (▲).

Analogous data were obtained in the reaction of 1-cyclohexenylacetic acid (**2**) with benzene working under the same conditions (see Table 2). Though the conversions are slightly lower with acid **1**, the net difference in activity between complexed and uncomplexed $AlCl_3$ is obvious (Fig. 2).

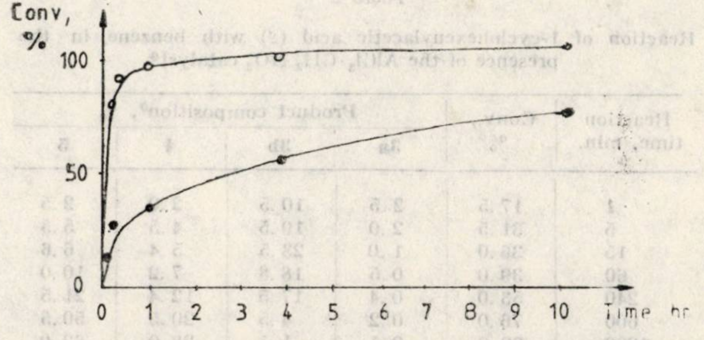

Fig. 2. — Time evolution of conversion of acid *2* with benzene in the presence of $AlCl_3$ (○) and $AlCl_3 \cdot CH_3NO_2$ (●).

The above results can be explained taking into account essentially the same mechanism earlier proposed for the $AlCl_3$ catalyzed reaction (Scheme 2). As generally accepted this is a carbocationic mechanism which

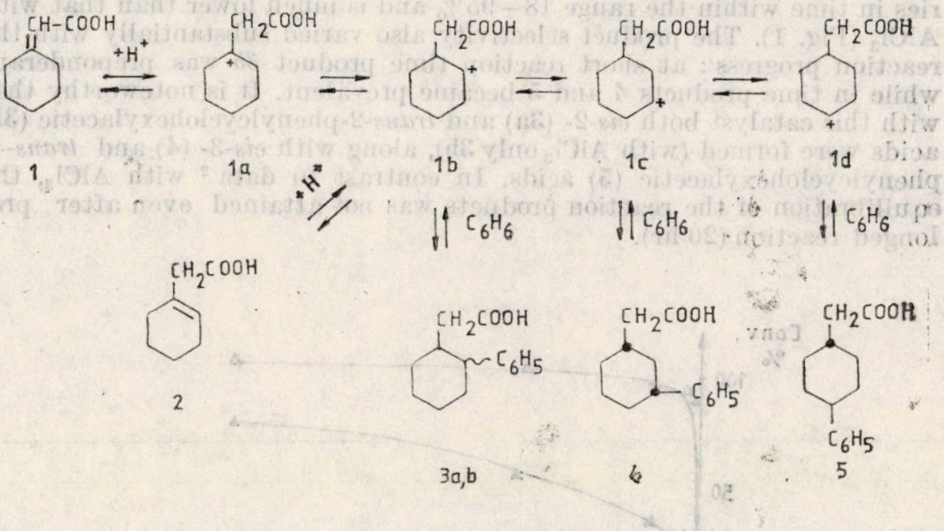

Scheme 2

implies generation of carbocations **1a**—**1d** under the action of the catalyst, rearrangements of these ions by 1,2- and 1,3-hydride shifts, alkylation of benzene by carbocations **1b**—**1d** and subsequent isomerization of the phenylated products.

In the presence of the catalytic complex $AlCl_3 \cdot CH_3NO_2$ the rate of each individual step is lower than that with $AlCl_3$ due to the reduced electrophilicity of the complexed active centres. The overall reduced rate suggests that the catalytic complex plays a significantly different role as a component of the intervening ion-pairs.

In contrast to the reaction catalyzed by $AlCl_3$, formation of both phenylated stereoisomers **3a** and **3b** indicates that the attack of benzene in the phenylation step occurs on both sides of the carbocation **1b** and the intervention of a lactoid species **1b′**, if any, is diminished (Scheme 3).

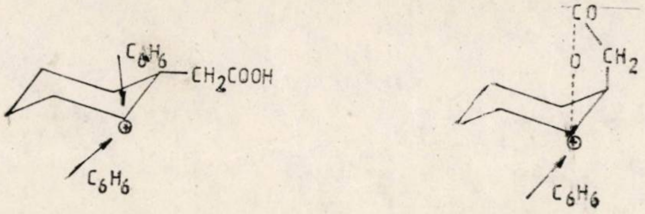

1b'

Scheme 3

Furthermore, the time evolution of product distribution in the presence of the catalytic complex $AlCl_3 \cdot CH_3NO_2$ implies a lower isomerization rate of the phenylcyclohexylacetic acids in this case as compared with the reaction catalyzed by $AlCl_3$.

EXPERIMENTAL

All melting points are uncorrected. V.p.c. analyses were carried out on a Willy Giede model 18 .3 gas chromatograph using a 3 m × 4 mm column packed with 10% ethyleneglycolsuccinate on Chromosorb W (60—80 mesh), column temperature 190°C. NMR spectra were recorded on a Varian A 60—A spectrometer using TMS as internal standard. IR spectra were recorded on UR—20 Carl Zeiss-Jena spectrophotometer.

Starting materials and autentic samples

Cyclohexylideneacetic acid (**1**) and 1-cyclohexenylacetic acid (**2**) were prepared using conventional methods. [4,5] For *cis*-2- (**3a**), *trans*-2- (**3b**), *cis*-3- (**4**) and *trans*-4-phenylcyclohexylacetic (**5**) acids the procedures described elsewhere [2] were followed. Benzene (Reactivul) was purified by distillation and dried over sodium wire, $AlCl_3$ (Merck-Schuchardt) of commercial grade was used without purification, nitromethane (Merck-Schuchardt) was purified by vacuum distillation.

Reaction of cyclohexylideneactic acid (1) and 1-cyclohexenylacetic acid (2) with benzene

The reactions of acids **1** and **2** with benzene in the presence of $AlCl_3 \cdot CH_3NO_2$ were performed at temperatures between 40 and 45°C using molar ratios acid : catalyst : benzene 1 : 1 .5 : 20 ($AlCl_3 : CH_3NO_2 = 1 - 1 .5$) according to the method described elsewhere [2]. The results obtained by v.p.c. are given in Tables 1 and 2.

REFERENCES

[1] Part. IV, V. Drăguţan, I. Drăguţan, C. Condeiu and A. M. Glatz, *Rev. Roumaine Chim.*, **34**, 977 (1989).
[2] V. Drăguţan, L. Stănescu and A. M. Glatz, *Rev. Roumaine Chim.*, **22**, 1045 (1977).
[3] V. Drăguţan, I. Drăguţan, F. Chiraleu and A. M. Glatz, *Rev. Roumaine Chim.*, **34**, 759 (1989).
[4] K. H. Wiberg and H. Hiatt, *J. Amer. Chem. Soc.*, **90**, 6495 (1968).
[5] R. L. Shriner, "Organic Reactions", Vol. 1, J. Wiley, New York, 1942, p. 1.

Revue Roumaine de Chimie, 35, 3, 459–466 (1990)

MESOIONIC OXAZOLONES. IV[1]

PROTONATION OF PLANAR AND NONPLANAR ACYLATED COMPOUNDS *

DAN RĂILEANU and HORIA PETRIDE
Centre of Organic Chemistry — ICECHIM
Spl. Independenţei 202 B, 78100 Bucharest 15, Romania

Received January 21, 1989

In perchloric acid solutions the nonplanar acylated mesoionic oxazolone 11a underwent protonation at the C_3 atom, while in the case of its planar analogs 12–13, the protonation occurred at the oxygen atom of the acyl group. In trifluoroacetic acid the protonation of the self-acylated compound 1 took place at the pyridinone oxygen, while only solvent effects could be observed in the ^1H-NMR spectra of 12–13.

No systematic study on the protonation of the stable acylated mesoionic oxazolones (acylated "münchnones") has been published as yet. The protonation of the self-acylated münchone **1** in trifluoroacetic acid (TFA) was described [2] by means of its ^1H-NMR spectrum as taking place at the C_3 atom to yield **2**. Using the same technique we were not able to confirm the existence of any absorption for the H_3 proton of **2**. Concerning the protonation of non-acylated mesoionic oxazolones very little is known at present. However, by the action of gaseous hydrobromic acid on an anhydrous solution of **3**, Huisgen *et al.* [3] isolated a straw coloured compound supposed to be **4** (protonation at C_4), but neither elemental analysis nor spectral data were given. The same type of cation (**4**) has been suggested as an intermediate of the Dakin-West reaction. [4,5]

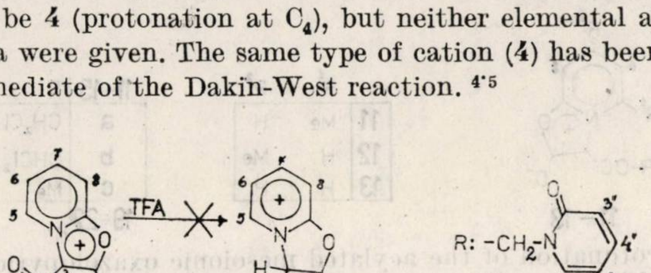

1 2

---

* Dedicated to the memory of Mihai Elian.

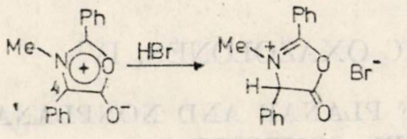

3 4

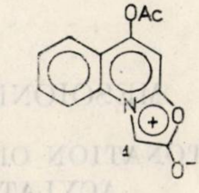

8

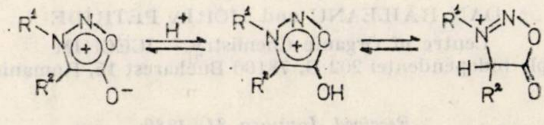

5 6 7

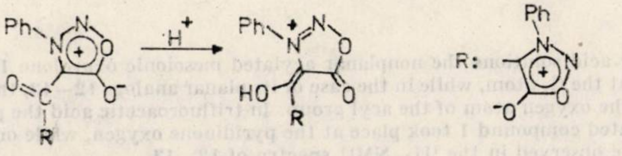

9 10

More data are available for the related sydnones. Thus, the sydnone **5** ($R^1 = Ph$; $R^2 = H$) in Magic Acid and at low temperature led to an oxygen-protonated form **6** ($R^1 = Ph$; $R^2 = H$)[6] while the derivative **5** ($R^1 = Ph$; $R^2 = D$)[7] was isolated from a D_2O/D_2SO_4 mixture at 100 °C, whose formation involves the keto-enol equilibria **5** $\rightleftharpoons$ **6** $\rightleftharpoons$ **7**. Quite analogously occurs the 1-deuteration of **8**.[8] The easy protonation at the lactonic *exo*-oxygen atom of the sydnone **5** ($R^1 = Me$; $R^2 = H$) to yield the cation **6** ($R^1 = Me$; $R^2 = H$) was confirmed by ^{13}C—, ^{15}N— and ^{17}O—NMR spectroscopy.[9,10] The acylated sydnone **9** displays a different behaviour in Magic Acid when protonation takes place at the acyl oxygen atom with formation of the cation **10**.[6]

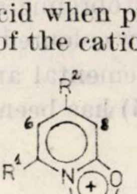

11–13

	R¹	R²
11	Me	H
12	H	Me
13	H	H

11–15	R
a	CH_2Cl
b	$CHCl_2$
c	Me

19-22

The protonation of the acylated mesoionic oxazolopyridinium compounds **11**—**13** seemed of interest to us so much the better as two distinct groups can be observed from a conformational point of view. As previously reported ,[1] the acyl group can be either coplanar to the rest of the molecule (**12**—**13** ; $R^1 = H$) or out-of-plane when hindered by the presence of a bulky substituent in the 5-position of the pyridine nucleus (**11** ; $R^1 = Me$). The perchloric acid was chosen as an acidic partner which is strong enough to ensure protonation and is also suitable for the spectral studies.

The spectral characteristics of the protonated forms were measured on the *in situ* generated species.

RESULTS AND DISCUSSSION

Preliminary experiments performed in the parallel on the planar and nonplanar münchnones **11**–**13** indicated that protonation occurs readily in $HClO_4/CH_2Cl_2$ and $HClO_4/Ac_2O$ mixtures and in a different way for each category of compounds. This was inferred, in the first place, from the IR spectral characteristics of **11a** and **12a** in anhydrous $HClO_4/CH_2Cl_2$ (Table 1); at the same time the IR spectra of the protonated forms of **11a** and **12a** differ considerably from one another. In addition, the same holds true for the ^1H–NMR spectra of **11a** and **12b** (Table 2) recorded in a $HClO_4/Ac_2O$ mixture. The attempts to isolate the protonated forms

Table 1

IR data[a] for **11a** and **12a**

Starting compd.	ν_{max} (cm^{-1}) in :	
	CH_2Cl_2 [b]	0.5 M $HClO_4/CH_2Cl_2$
11a	1633 s; 1645 sh; 1765 s; 1769 s	1647 s; 1761 m; 1863 s
12a	1612 s; 1648 w; 1771 s	1658 vs; 1780 (complex) w; 1808 m; 1841 s

[a] for assignments see text; substrate concentration: about 0.1 M;

[b] from ref.[1].

Table 2

^1H–NMR data for **11**–**13** in different solvents[a]

Starting compd.	Solvent	Chemical shifts (δ, ppm)[b]					
		H_2	R^1	H_6	H_8	R^2	R
11a	$CDCl_3$ [c]	—	2.78s	7.29d[d]		7.99	4.73s
	Ac_2O	—	2.70s	7.38d[d]		8.02	4.70s
	PAA [e]	7.10s	2.75s	7.83d[d]		8.77	5.07s
12a	TFA	—	9.73d	7.63d	7.60s	2.75s	4.88s
	PAA [e]	—	9.30d	7.72d	7.73s	2.82s	5.03s
12b	$CDCl_3$ [c]	—	9.75d	7.33d	7.30s	2.63s	7.20s
	PAA [e]	—	9.35d	7.75d	7.67s	f	7.67s
	TFA	—	9.76d	7.59d	7.53s	2.73s	7.33s
12c	$CDCl_3$ [c]	—	9.75d	7.18–7.37m		2.58s	2.53s
	Ac_2O	—	9.67d	7.20–7.40m		f	f
	PAA [c]	—	9.27d	7.56–7.70m		2.75s	2.80s
	TFA	—	9.61d	7.57–7.73m		2.75s	2.88s
13a	TFA	—	9.93d	7.80t	7.72d	8.32dd	4.85s
13d	TFA	—	9.95d	7.78t	7.72d	8.28dd	7.32s
13c	$CDCl_3$	—	10.10d	7.20–7.60m		7.93dd	2.53s
	TFA	—	9.67d	7.60–8.00m		8.47dd	2.92s

[a] for assignments of experimental spectra see text; **12a** and **13a**–**b** are insoluble in $CDCl_3$ or Ac_2O;

[b] vicinal coupling constants: $J_{5,6} = J_{6,7} = 7$ and $J_{7,8} = 9$ Hz;

[c] from ref.[1];

[d] apparent doublet with $J = 8$ Hz due to quasi-coincidental signals;[1]

[e] $HClO_4/Ac_2O$ mixture (5 : 1, v/v);

[f] under the solvent large peak.

failed, but aqueous treatment of the acidic solutions gave in the case of the planar substrates (i.e. **12a**—**b**) the unchanged starting compounds, while the nonplanar analog **11a** led to the ketone **15a.** The same compound **15a** resulted from a neutral hydrolysis of **11a.**[11] These observations substantiate the existence of two different protonated species corresponding to the planar and nonplanar acylated compounds studied in this paper.

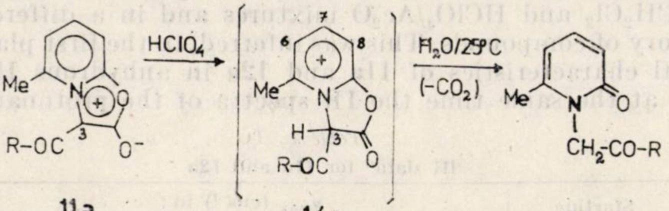

11a
nonplanar

14a

15a

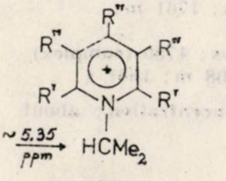

16

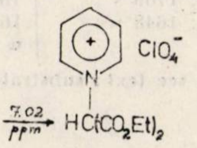

17

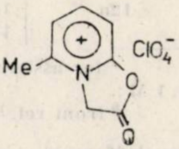

18

The most interesting feature of the ^{1}H—NMR spectrum of **11a** in $HClO_4/Ac_2O$, as compared to the spectra recorded in nonprotonating solvents ($CDCl_3$, Ac_2O), is the appearance of a new one-proton signal at δ7.1 ppm (Table 2). It was ascribed to the H_3 proton of **14a** which is being deshielded by three electron-withdrawing vicinal groups : a pyridinium nitrogen atom, a monochloroacetyl group and a lactonic carbonyl. This very low value can be rationalized in terms of the Shoolery rule if we use as a starting point the N-isopropylpyridinium compounds **16** (R′, R″ = H, Me) which display δ 5.35 ppm (averaged value) for β-H.[12] Adding the increments for the acyl (1.2) and the lactonic carbonyl (0.7) groups we obtain 7.2 ppm, which can be considered as a satisfactory agreement. At the same time, a good model compound for **14a** is the perchlorate **17**, which exhibits δ7.02 ppm for the corresponding proton.[13] Another consequence of the protonation is the deshielding of the ring protons H_6—H_8 with 0.5—0.8 ppm as being due to the formation of the pyridinium cation carrying a formally full positive charge. The model compounds **16** display quite similar chemical shifts for the ring protons.

These results were confirmed by the IR spectra in $HClO_4/CH_2Cl_2$ (Table 1). The most intense absorption bands of the protonated **11a** (1647 and 1863 cm^{-1}) are very similar to those of the perchlorate **18** (in KBr : $\nu_{ring} = 1651$ and $\nu_{CO} = 1860$ cm^{-1}).[14] A third band in the carbonyl region (1761 cm^{-1}) can be ascribed to the monochloroacetyl group of **14a**, by analogy with the monochloroacetone (1751 cm^{-1}). This is in accordance with protonation at C_3 for the bicyclic nonplanar münchnones of the type **11**.

The ${}^1H$—NMR spectra of the planar compounds **12b—c** in HCl_4/Ac_2O (Table 2) do not exhibit any signal corresponding to H_3 so that protonation at C_3 can be excluded. For the same compounds in nonprotonating solvents ($CDCl_3$ or Ac_2O), the high δ-value of H_5 cumulates the deshielding effects exerted by the positive pyridinium nitrogen atom and the neighbouring coplanar carbonyl group. [1] When the aprotic solvent was replaced by $HClO_4/Ac_2O$, an upfield shift of about 0.5 ppm could be observed for the same proton. This could be explained by the disappearance of the adjacent carbonyl group through enolization which is a consequence of the protonation at the acylic carbonylic group. Therefore, structure **19b—c** become plausible as protonated species of **12b—c**, respectively. At the same time, the IR spectrum of **12a** in $HClO_4/CH_2Cl_2$ (Table 1) displays two lactonic carbonyl bands at 1841 and 1808 cm^{-1}, indicating the presence of two protonated species, namely **19a** and **21a**, respectively. The lowering of the stretching frequency of the latter can be attributed to the intramolecular H-bonding. Such high wave numbers for five-membered lactonic carbonyl groups are encountered in related structures, i.e. **18** and **23** (in KBr : $\nu_{CO} = 1869$ cm^{-1}) [14]; supplementary conjugation lowers the frequency to 1810 cm^{-1}, as measured for **24**. [2] Nevertheless only one sharp singlet does arise for the CH_2Cl protons in the ${}^1H$—NMR spectra of protonated **12b—c** indicative of the existence of only one isomer. Therefore, the hypothesis can be advanced that in acetic anhydride the enolic hydroxyl is acetylated so that we are in the presence of only one single acetylated isomer with no more gain in energy due to the intramolecular H-bonding such as occuring in **21b—c**, whose presence can be accordingly excluded. In this

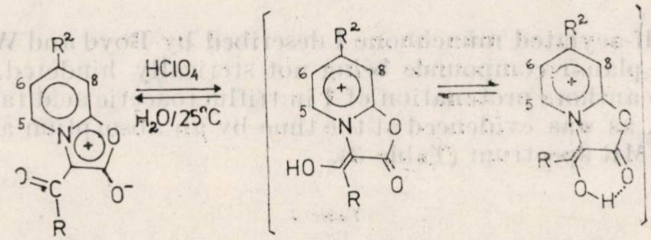

12-13

Z-planar

19-20

21-22

	R²	
12	Me	19;21
13	H	20;22

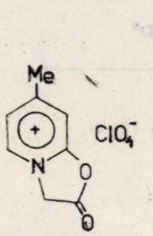

23

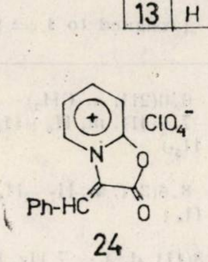

24

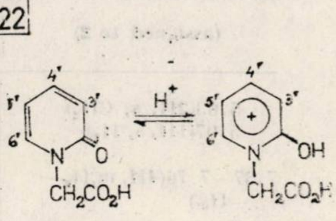

25

26

way the equilibrium **19** ⇌ **21** is shifted almost completely to the left, namely towards the more energetically favoured isomer.

These results imply that nonplanar acylated münchnones, for example **11a**, undergo protonation at the C_3 carbon atom, while in the case of their planar analogs (i.e. **12a**–**c** or **13a**–**c**) protonation takes place at the oxygen atom of their acyl group. The afore described behaviour towards water of these two different types of protonated species can be further substantiated by considering the hydrolysis of the related compounds **18** and **24**. At room temperature, the cation **18** easily undergoes hydrolysis to the pyridinoneacetic acid **25** (6′–Me), while **24** is very resistant to hydrolytic cleavage of its oxazolic ring being recovered unchanged.[11]

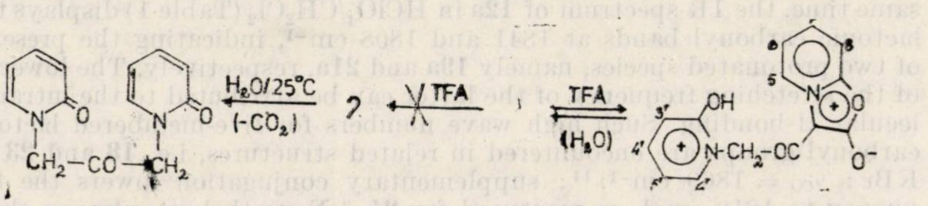

27

28

The self-acylated münchnone **1** described by Boyd and Wright[2] pertains to the planar compounds being not sterically hindered. According to the above authors protonation of **1** in trifluoroacetic acid takes place at the C_3 atom, as was evidenced at the time by an absorption at δ5.97 ppm in its ^1H–NMR spectrum (Table 3).

Table 3

^1H–NMR spectrum of **1** in TFA

Reported[2]	Found
(assigned to **2**)	(assigned to **1** ⇌ **28**)[a]
5.63(2H, s, CH_2)	6.0(2H, s, CH_2)
5.97(1H, s, H_3)	7.4–7.9(4H, m, $H_6+H_8+H_{3'}+H_{5'}$)
7.37–7.76(4H, m, $H_{3'}$–$H_{6'}$)	8.1–8.6(3H, m, $H_7+H_{4'}+H_{6'}$)
8.08–8.53(4H, m, H_5–H_8)	9.8(1H, d, J = 7 Hz, H_5)

[a] the OH function might be δ CF_3COO.

If the cation **2** would have been formed, the aqueous treatment of the acidic solution should have given the ketone **27**,[15] analogously to the described transformation of **14a** into **15a**. This is not actually the case, by dilution with water the trifluoroacetic acid solution of **1** giving the unchanged starting compound. Moreover, a closer examination of the ^1H-NMR spectrum of **1** in TFA obtained by us led to different conclusions (Table 3). Thus, the absorption at δ6.0 ppm corresponds to the CH_2 group and this unusually low-field values can be rationalized by the presence of an adjacent pyridinium ring which means that protonation takes place at the pyridinone oxygen atom (structure **28**). The singlet at δ5.63 ppm in the literature spectrum could be explained by the presence of an impurity, probably the uncyclized starting material, the pyridinoneacetic acid **25**. As a matter of fact we were able to find that the chemical shift of the CH_2—group in **25** fluctuates depending on concentration, which is to imply an equilibrium between the nonprotonated and protonated forms (**25**$\rightleftharpoons$**26**; see exp. part). Generally speaking, from the examination of the ^1H-NMR spectra in TFA of the planar compounds **12a—e** and **13a—e** (Table 2) it can be concluded that, in these conditions, no protonation of the mesoionic structure takes place and the slight modifications of the chemical shifts are due predominantly to solvent effects.

EXPERIMENTAL PART

IR spectra were recorded in KRS—5 cells (thallium bromide and iodide) with an UR—10 Carl Zeiss Jena spectrophotometer. ^1H-NMR spectra were performed with a Varian A—60A apparatus using TMS as a internal standard. The spectra were registered using freshly prepared solutions. The ^1H-NMR chemical shifts and coupling constants *J* are quoted in ppm (δ scale) and Hz, respectively.

The mesoionic compounds **11—13** were prepared according to described procedures.[1,2,14] The method of Plesch and Mathias [16] was followed to obtain anhydrous $HClO_4/CH_2Cl_2$ mixture.

2-Oxo-1(2H)pyridineacetic (**25**). It was obtained as described by Lawson and Miles. [17] No ^1H-NMR data are given in the literature. [2,17] As presented below, the CH_2 signal position fluctuates depending on concentration (within about 0.4 ppm) implying a **25**$\rightleftharpoons$**26** equilibrium (see text); the other chemical shifts are only slightly modified. **^1H-NMR** (TFA); 5.5 ± 0.2 (2H, s, CH_2); 7.2—7.7 (2H, m, $H_{3'}$ and $H_{5'}$); 8.0—8.5 (2H, m, $H_{4'}$ and $H_{6'}$).

The two multiplets may be rationalized as follows: 7.37 (quasi triplet, $J = 8$, $H_{5'}$); 7.48 (doublet, $J = 9$, $H_{3'}$); 8.13 (doublet, $J = 6$, $H_{6'}$) and 8.31 (quasi triplet, $J = 8$, $H_{4'}$).

Hydrolysis of the protonated forms of 11a, 112a-b and 1

About 2 mmoles of **11a** were dissolved in 0.1 M HCl_4/CH_2Cl_2 (30 mL) and the homogeneous solution was stirred twice with 30 mL of water for 10 min. The separated organic layer, after drying and evaporation of the solvent, gave a crystalline compound in 73% yield, proved to be identical to the ketone **15a**. [11]

Analogously, starting from **12a** (or **12b**) the unchanged starting compound was separated in 95% yield. A similar result was obtained for a $HClO_4/Ac_2O$ solution of **12a—b**).

A solution was made by dissolving **12a** (50 mg) in trifluoroacetic acid (1 mL). After one hour it was diluted with 10 mL water and extracted with CH_2Cl_2. Evaporation of the solvent gave back about 40 mg of the starting compound.

Similarly, the aqueous treatment of a trifluoroacetic acid solution of **1** led to a crystalline solid, identical to the starting compound.

This work has been inspired by the suggestions of the late Dr. Mihai Elian.

REFERENCES

[1] Part III: H. Petride and D. Răileanu, *Rev. Roumaine Chim.*, **34**, 1251 (1989).
[2] G. V. Boyd and P. H. Wright, *J. Chem. Soc. (C)*, **1970**, 1485.
[3] H. O. Bayer, R. Huisgen, R. Knorr and F. C. Schaefer, *Chem. Ber.*, **103**, 2581 (1970).

[4] R. Knorr and G. K. Staudinger, *Chem. Ber.*, **104**, 3621 (1971).

[5] N. L. Allinger, G. L. Wang and B. B. Dewhurst, *J. Org. Chem.*, **39**, 1730 (1974).

[6] G. A. Olah, D. P. Kelly and N. Suciu, *J. Amer. Chem. Soc.*, **92**, 3133 (1970).

[7] V. G. Yashunskii and V. F. Vasil'eva, *Doklady Akad. Nauk S.S.S.R.*, **130**, 350 (1960)

[8] Part I: E. Tighineanu, F. Chiraleu and D. Răileanu, *Tetrahedron*, **36**, 1385 (1980).

[9] L. Stefaniak, M. Witanowski and J. D. Roberts, *Spectrosc. Int. J.*, **2**, 178 (1983); *Chem. Abstr.*, **100**, 67718 (1984).

[10] L. Stefaniak, M. Witanowski, B. Kamienski and G. A. Webb, *Org. Magn. Reson*, **13**, 274 (1980).

[11] H. Petride and D. Răileanu, in preparation.

[12] C. Roussel, A. T. Balaban, U. Berg, M. Chanon, R. Gallo, G. Klatte, J. Memiaghe, J. Metzger, D. Oniciu and J. Pierrot-Sanders, *Tetrahedron*, **39**, 4209 (1983).

[13] C. A. Henrick, E. Ritchie and W. C. Taylor, *Aust. J. Chem.*, **20**, 2455 (1967).

[14] Part II: H. Petride and D. Răileanu, *Rev. Roumaine Chim.*, **33**, 729 (1988).

[15] several analogs cited in C. K. Brandsher and M. Zinn, *J. Heterocycl. Chem.*, **4**, 66 (1967).

[16] P. H. Plesch and E. Mathias, *Chem. Ind. (London)*, **1971**, 1043.

[17] A. Lawson and D. H. Miles, *J. Chem. Soc.*, **1959**, 2865.

Revue Roumaine de Chimie, 35, 3, 467–473 (1990)

SEPARATION OF AMINO ACIDS BY LIQUID MEMBRANES WITH MACROCYCLIC CARRIERS*

CONSTANTIN LUCA[a], LUCIA MUTIHAC[b] and TITUS CONSTANTINESCU[b]

[a] Department of Analytical Chemistry, Polytehnic Institute, Bucharest, Splaiul Independenţei, 313, Romania

[b] Institute of Physical Chemistry, Splaiul Independenţei, 202, Bucharest, Romania

Received November 23, 1989

The possibility of separating some α-amino acids (L-methionine, L-leucine, L-isoleucine, L-valine, L-phenylalanine and L-α-alanine) from a mixture was investigated; use has been made of a membrane with active transport assisted by a pH gradient : 18-crown-6 in 1,2 dichloroethane was used as selective carrier. The device employed affords efficient extraction (the yield ranged within 74.38–83.13% depending on the nature of the amino acid) in a relatively short time (6 h). The operational parameters of the process were estimated. The transport fluxes and separation yields were determined by amino acid analyzer method.

In a previous paper [1] the active transport of amino acids through liquid membranes with macrocyclic carriers and pH gradient was studied The results of this study have suggested the possibility of separating group of amino acids on liquid membranes.

The technique of separation through liquid membranes with macrocyclic carriers combines the selectivity of extraction with the activs transport of compounds.

In literature there are references to studies on transport thorugh membrane of some N-benzoyl amino acids as $-COO^-$ (as salts of alkali metals) [2–7] and on separation of racemic amines ($-NH_3^+$) with optically active carriers [8–13].

This paper presents the results of a study regarding separation of amino acids through a liquid membrane consisting of an organic liquid phase between two aqueous phases. In order that this process unfolds efficiently, use has been made of a device shown in Fig. 1. The source phase (I) contains the α-amino acids (mentioned in table 1) in aqueous solution and the picrate anion at pH = 2 ensured by HCl.

The organic phase (II) (which is the membrane) is a carrier (18-crown-6) solution in dicloroethane. The receiving phase (III) is an aqueous solution of LiOH at pH = 13.

---

* Dedicated to the memory of Mihai Elian.

The mechanism of α-amino acid transport in the membrane system studied was previously presented.[1] In this contribution this mechanism is considered in the conditions specified above.

EXPERIMENTAL

The macrocyclic polyether 18-crown-6 was of a higher purity than 98%, Merck-Schuchardt reagent. The other reagents were p.a. grade. The concentration of amino acids in the two aqueous phases were determined by "Carlo Erba 3A28M" amino acid analyzer; a digital MV—870 "Pracitronic" pH-meter with glass electrode and saturated calomel electrode calibrated with standard solutions of potassium biphthalate (pH = 4.01) and borax (pH = 9.18) was used.

The experiments were performed under stirring of phases at about 178 r.p.m.

RESULTS AND DISCUSSION

The 16 α-amino acids (mixtures) mentioned in Table 1 were studied; six of them (L-leucine, L-methionine- L-isoleucine, L-valine, L-phenylalanine and L-α-alanine) were extractible in 1,2-dichloroethane[14] under experimental conditions imposed to phases I and II. Separation of α-amino acids through the membrane system was carried out under stirring of phase in contact during 6 hours. The experimental results are listed in Table 1.

The influence of pH upon the transport of α-amino acids from acid aqueous phase to alkaline aqueous phase through the membrane containing the macrocyclic carrier was studied. The dependence of the α-amino acid extraction yield as a function of phase III pH is shown in Fig. 2.

Examination of data presented in Table 1 shows that the yields of extraction of α-amino acids extractible from acid aqueous phase (I) to alkaline aqueous phase (III) by means of membrane (II) range between 74.38—83.13% depending on the amino acid. These yields were obtained in a concentric tubular device in times which are short (6h) compared to those required by the classic U-shaped device (24 h)[1] which pleads for the efficiency of the former device.

The device employed (Fig. 1) consists of two concentric tubes; the inner one which contains phase I is provided with traps which also act as stirrer. Phases II and III are introduced in the outer tube.

Assuming that diffusion of the ion pairs is determined by the chemical potential ($\nabla \mu \neq 0$), that no chemical reaction occurs in the system ($A\rho = 0$, when $A\rho = \sum_k \partial_{k\rho}\mu_k$ is the chemical affinity and $\partial_{k\rho}$ the stoichiometric coefficient of ρ reaction) and that there are no temperature ($\nabla T =$

Table 1

Experimental data of a study on separation of some protonated α-amino acids through a liquid membrane (18-crown-6/1,2 dichloroethane)

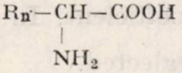

$$R_n-\underset{\displaystyle NH_2}{\underset{|}{CH}}-COOH$$

AMINO ACID	R_n		Initial concentration in phase I(mM)	Found in phase III after 6 h stirring	
	n	R		mM	%
L-Methionine	1	$-CH_2-CH_2-S-CH_3$	0.160	0.133	83.13
L-Isoleucine	2	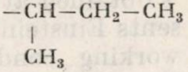 $-\underset{\displaystyle CH_3}{\underset{|}{CH}}-CH_2-CH_3$	0.160	0.130	81.25
L-Phenylalanine	3	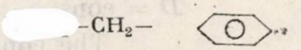	0.160	0.130	81.25
L-Leucine	4	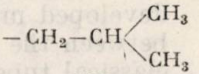	0.160	0.129	80.63
L-Valine	5	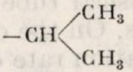	0.160	0.127	79.38
L-α-Alanine	6	$-CH_3$	0.160	0.119	74.38
Glycine	7	$-H$	0.160	0	0
L-Aspartic Acid	8	$-CH_2-COOH$	0.160	0	0
L-Glutamic Acid	9	$-CH_2-CH_2-COOH$	0.160	0	0
L-Serine	10	$-CH_2-OH$	0.160	0	0
L-Treonine	11	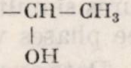 $-\underset{\displaystyle OH}{\underset{|}{CH}}-CH_3$	0.160	0	0
L-Proline	12	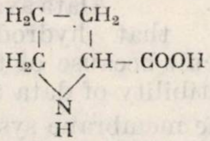	0.160	0	0
L-Lysine	13	$-CH_2-CH_2-CH_2-CH_2-NH_2$	0.160	0	0
L-Asparagine	14	$-CH_2-CO-NH_2$	0.160	0	0
L-Arginine	15	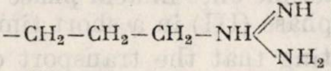	0.160	0	0
L-Histidine	16	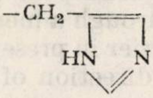	0.160	0	0

Phase I: Amino Acid ; [picric acid] = 1.60 mM ; HCl 0.05 N (pH = 2) ; 5 cm^3 ;
Membrane : [18-crown-6] = 10 mM/1,2 dichloroethane, 50 cm^3 ;
Phase III : LiOH 0.1N (pH = 13) ; 10 cm^3 ;

= 0) and viscosity ($\nabla \vec{v} = 0$) gradients, the flux of carried chemical species is proportional to the concentration gradient (Fick's law) :

$\vec{J} = -\rho D \nabla c$ where D stands for the difussion coeficient. In non-ideal solutions the diffusion coefficient is given by the equation :

$$D = BRT\left(1 + c\frac{\mathrm{d}\ln f}{\mathrm{d}c}\right)$$ where B is the mobility of transported species and f the activity coefficient. In ideal or dilute solutions the factor $c\frac{\mathrm{d}\ln f}{\mathrm{d}c} \ll 1$ may be neglected.

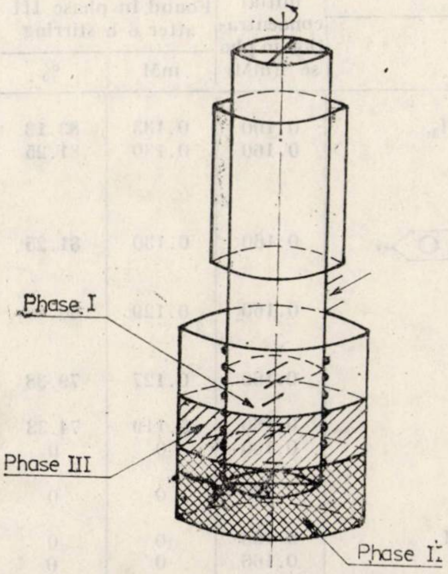

Fig. 1. — The device employed in separation of some amino acids through liquid membrane with macrocyclic carriers.

Thus the following equation :

$$D = BRT$$

s obtained at the limit which represents Einstein's law.[15] Under specific working conditions it results that $D = \text{const.}$

The concentric tubular device developed minimizes the distance d between the arms of the U shaped classical tube in which diffusion occurs. On the other hand the relative rotation rate of the concentric tubes induce convection currents in opposite direction of concentration gradient. Therefore the velocity of carrier species increases.

The device described above also ensures simultaneous stirring of the three phases without mixing then.

Data available in literature show that hydrodynamic characterization of liquid membranes is difficult bceause of the geometry of device employed and of the low reproductibility of data (about 15 %).[16]

The results obtained with the membrane system in Fig. 1 also suggested its utilisation in obtaining concentrates of amino acids in two aqueous phases : the non-extractible ones in acid phase (I) and the extractible ones in alkaline aqueous phase (III) in a short time.

It is also worth noting that the transport of α-amino acids from aqueous phase I to aqueous phase III through a membrane of 1,2 dichloroethane (phase II) with 18,crown-6 as carrier in presence of coupling partner (the picrate anion) takes place in the direction of pH gradient.

The dependence of extraction yield of some α-amino acids from phase I into phase III versus phase III pH is shown in Fig. 2. Examination of Fig. 2 shows that the extraction yields increase with the increase of pH of alkaline phase III.

The amino acid-macromolecular ligand-picrate anion complex carried from phase I to phase II is relatively stable and breaks only at high pH values ; then the amino acid anion species is formed again in phase III. On the other hand, these results prove that the inverse transport of amino acids as anions ($-COO^-$) in presence of picrate and macrocyclic lignand from phase III to phase I does not take place.

The experiments have suggested that under the working conditions adopted it is possible to classify α-amino acids into extractible and non-extractible ones [1,14]; this classification is based on the structural distinction between α-amino acids imposed by the more hydrophobic or hydrophylic character of chain R (Fig. 3.)

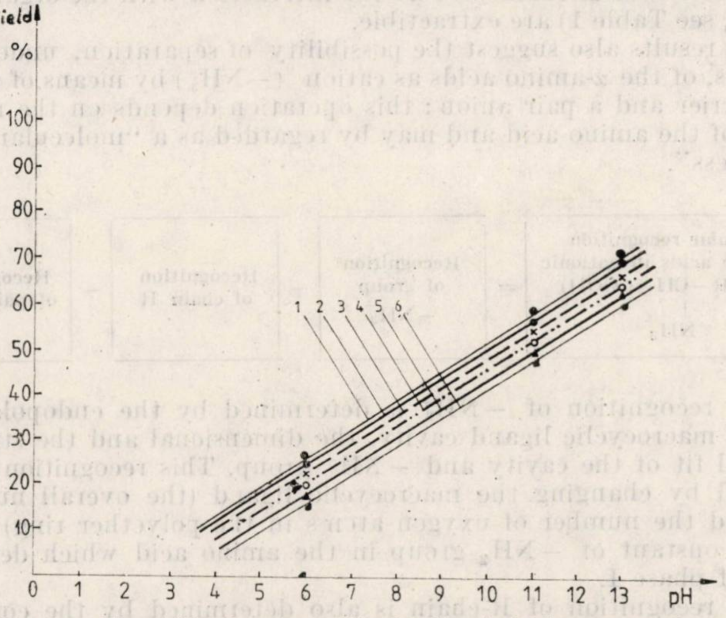

Fig. 2. — The yields of amino acid extraction in basic aqueous phase versus the pH: 1 — L-Methionine, 2 — L-Isoleucine, 3 — L-Leucine, 4 — Phenylalanine, 5 — L-Valine, 6 — L-α-Alanine.

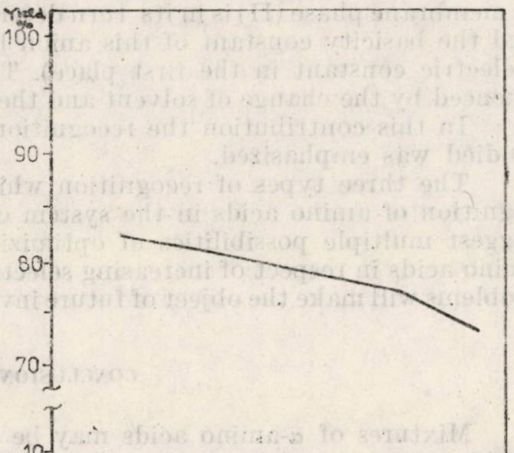

Fig. 3. — The dependence of amino acid extraction yields in basic aqueous phase on amino acid chains (see Table 1).

The plot of extraction yields versus the nature of chain R of α-amino acids under study shows that the α-amino acids whose R chain favours the interaction with water ($R_7 - R_{16}$, see Table 1) are not extractible while those whose R-chain favours the interaction with the organic phase ($R_1 - R_6$, see Table 1) are extractible.

The results also suggest the possibility of separation, under certain conditions, of the α-amino acids as cation ($-NH_3^+$) by means of a macrocyclic carrier and a pair anion; this operation depends on the nature of chain R of the amino acid and may by regarded as a "molecular recognition process".

Molecular recognition of amino acids in cationic form $(R-\underset{\displaystyle NH_3^+}{\underset{\vert}{CH}}-COOH)$	=	Recognition of group $-NH_3^+$	+	Recognition of chain R	+	Recognition of pair anion

The recognition of $-NH_3^+$ is determined by the endopolarophilic nature of macrocyclic ligand cavity, the dimensional and the structural-functional fit of the cavity and $-NH_3^+$ group. This recognition may be influenced by changing the macrocyclic ligand (the overall number of atoms and the number of oxygen atoms in the polyether ring) and the basicity constant of $-NH_2$ group in the amino acid which determines the pH of phase I.

The recognition of R-chain is also determined by the correlation between the nature of chain R and the solvent which makes up the membrane (the dielectric constant type, of solvent — R interactions). Thus, this recognition may be influenced by changing the solvent. A recognition of R-chain by the macrocyclic ligand itself must not be disregarded as well because various interactions may occur between the two entities.

The recognition of pair anion as component of the ion pair associated in membrane phase (II) is in its turn determined by the lipophilic character and the basicity constant of this anion by the nature of the solvent (its dielectric constant in the first place). This recognition may also be influenced by the change of solvent and the pH of aqueous phase I.

In this contribution the recognition of R-chain of the amino acids studied was emphasized.

The three types of recognition which add up in the molecular recognition of amino acids in the system of liquid membrane under study suggest multiple possibilities of optimizing the process of separation of amino acids in respect of increasing selectivity as well as the yields. These problems will make the object of future investigations.

CONCLUSIONS

Mixtures of α-amino acids may be separated as $-NH_3^+$ through a liquid membrane of 18-crown-6 in 1,2 dichloroethane in presence of picrate pair anion; separation is according to R-chain from the amino acid molecule so that a classification is possible: extractible (L-methionine, L-isoleucine, L-phenylalanine, L-valine and L-α-alanine) and non-extractible (glycine, L-aspartic acid, L-glutamic acid, L-serine, L-treonine, L-proline, L-lysine, L-asparagine, L-arginine and L-histidine) compounds.

The transport mechanism is actively assisted by the pH gradient (acid aqueous phase I, pH = 2, alkaline aqueous phase III, pH = 13) and is optimized by the geometry of the experimental device employed so that an efficient extraction is ensured (yield of about 74.38—83.13 %) depending on the amino acid extending over a relatively short time (6 h).

REFERENCES

[1] C. Luca, L. Mutihac, T. Constantinescu and A. Csuma, *Rev. Roumaine Chim.*, **34**, 11—12 (1989).
[2] J. P. Behr and J. M. Lehn, *J. Amer. Chem. Soc.*, **95**, 6108 (1973).
[3] H. Tsukube, *Tetrahedron Lett.* **22**, 3981 (1981).
[4] H. Tsukube, *J. Chem. Soc. Perkin Trans.*, **1**, 2359 (1982).
[5] K. Maruyama, H. Tsukube and T. Araki, *J. Amer. Chem. Soc.*, **104**, 5197 (1982).
[6] J. P. Behr, M. Kirck and J. M. Lehn, *J. Amer. Chem. Soc.*, **107**, 241 (1985).
[7] J. D. Lamb, J. J. Cristensen, J. L. Oscarson, B. L. Nilsen, B. W. Asay and R. M. Izatt, *J. Amer. Chem. Soc.*, **102**, 6820 (1980).
[8] D. J. Cram, "Applications of Biochemical Systems in Organic Chemistry", Part II, John-Wiley, New York, 815, 1976.
[9] M. Newcomb, J. L. Toner and D. J. Cram, *J. Amer. Chem. Soc.*, **101**, 4941 (1979).
[10] H. Tsukube, *Bull. Chem. Soc. Jpn.*, **57**, 2685 (1984).
[11] L. R. Sousa, D. H. Hoffman and D. J. Cram, *J. Amer. Chem. Soc.*, **96**, 7367 (1974).
[12] A. Kotyk and Janacek, "Cell Membrane Transport", Plenum Press, London, 1970.
[13] G. van Binst, "Design and Synthesis of Organic Molecules Based on Molecular Recognition", Springer-Verlag, Berlin, Heidelberg, New York, Tokyo, 1986.
[14] C. Luca, L. Mutihac and T. Constantinescu, *Rev. Chim. (București)*, **39**, 12 (1988).
[15] L. Georgescu, I. Petrea and D. Borșan, "Fizica stării lichide", Ed. Didactică și Pedagogică, Bucharest, 1982.
[16] T. M. Fyles, *J. Membrane Sci.*, **24**, 229 (1985).

Revue Roumaine de Chimie, 35, 3, 475–484 (1990)

THE ELECTRONIC STRUCTURE OF $[H_3SiNSiH_3]^{\ominus}$ ANION. A SIMPLE MOLECULAR ORBITAL TREATMENT *

IOAN SILAGHI-DUMITRESCU and IONEL HAIDUC
Department of Chemistry, University of Cluj-Napoca
R – 3400 Cluj-Napoca, Romania

Received December 4, 1989

The electronic structures of $[H_3SiNSiH_3]$-anions have been investigated by means of the simple Extended Huckel molecular orbital method. It was found that the SiNSi potential energy surface is very flat and these anions may have linear as well as bent structures. In the linear system, almost free rotation around the molecular axis is allowed, the actual conformation being determined by steric factors.

INTRODUCTION

Dicoordinate nitrogen containing $[R_3PNPR_3]^{\oplus}$ cations is known to exhibit a large variety of structures, including both linear and bent PNP moieties [1 and references therein]. The isoelectronic $[R_3\ SiNSiR_3]^{\ominus}$ anions have been not known until recently. [2,3]. The silicon analog of PPN cation, $[Ph_3SINSiPh_3]$ was found to be also bent [2] with a SiNSi angle of 154.9 and silicon-nitrogen bond lengths of 1.633–1.634 A. It would be of interest to investigate the electronic structure of these silylamide anions in order to discover the electronic effects (if there are any) which influence and determine their structures. To avoid steric hindrances due to large R substituents, molecular orbital calculations were performed on the parent $[H_3SiNSiH_3]^{\ominus}$ anion.

CALCULATION PROCEDURES

The molecular orbital computations were carried out at the Extended Huckel level, [4] using sp basis on nitrogen and silicon. Figure 1 shows the coordinate axes used throughout this paper.

---

* This paper is dedicated to the memory of Dr. Mihai Elian a great friend who contributed significantly to the type of reasoning used here.

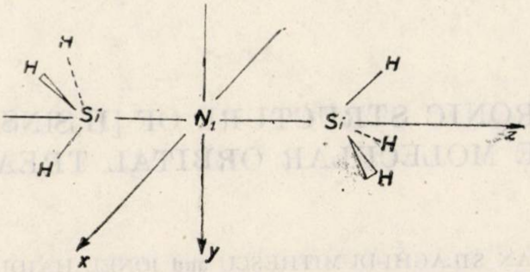

Fig. 1. — The coordinate system and location of atoms in H_3SiNSi_3.

As we were primarily interested in the qualitative features of the linear/bent $H_3SiNSiH_3$ system, only SiNSi angles were varied during calculations and no attempt was made to optimise the bond lengths or the other HSiSi or HSiH angles. All geometrical and orbital parametres are given in Appendix. Calculations were done on a SINCLAIR QL computer.

RESULTS AND DISCUSSION

A first question, which naturally arises when comparing SiNSi skeleton with the other isolectronic species, is whether a linear SiNSi system is possible. From classical point of view, the $[H_3SiNSiH_3]^{\ominus}$ anion may be described by the following (a — d) Lewis type structures :

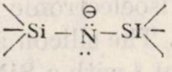
(a)

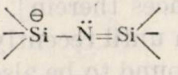
(b)

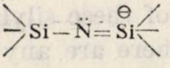
(c)

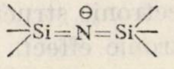
(d)

From these, (a) should be bent while (b — d) might be linear or bent depending on the ability of silicon to share the p electron pairs of the central nitrogen. A hint of what actually happens is given by the simple EH molecular orbital discussion of the system. Molecular orbitals may be described in terms of the initial atomic basis set, or in terms of fragment's orbitals involved. [5] For our system it is convenient to take two SiH fragments and to let them interact with the nitrogen valence orbitals. Molecular orbitals of AH units are well known, but for the sake of clarity and completeness we sketched them in Figure 2, as they came out from an Extended Huckel calculation.

From the five mo's shown of main interest is $2a_1$, well developed to the opposite side of ligands and thus prepared for bonding with the proper orbitals of nitrogen.

If now, two SiH_3 fragments are allowed to interact weakly, a set of little perturbed energy levels emerges. Their relative position and the approximate shape of the corresponding orbitals are pictured in Figure 3.

Note that only $2a_1$ of SiH_3 interact quite strongly and give $2a_{1g}$ and $2a_{2u}$ of $H_3Si\ldots SiH_3$ separated by an apreciable energy gap. Our $H_3Si\ldots SiH_3$ fragment transforms under the symmetry operators of D group as $3a_{1g} + 3a_{2u} + 2e_u + 2e_g$. On the other hand the orbitals of nitrogen transforms as $a_{1g}(s) + a_{2u}(p_z) + e_u(P_x, P_y)$. From the three a_{1g} of the $H_3Si\ldots SiH_3$ fragment, $3a_{1g}$ lies at high energy and do not mix with the nitrogen s orbital. What remains, leads to an interaction of three orbitals shown in figure 4. This diagram was constructed by mixing first $1a_{1g}$ with 2s which gives rise to (e) and (f):

Then the higher $2a_{1g}$ perturbes (f) in a bonding manner and gives the lower energy (g) and, also (h) located higher due to the very unfavorable phase of the orbitals entering it:

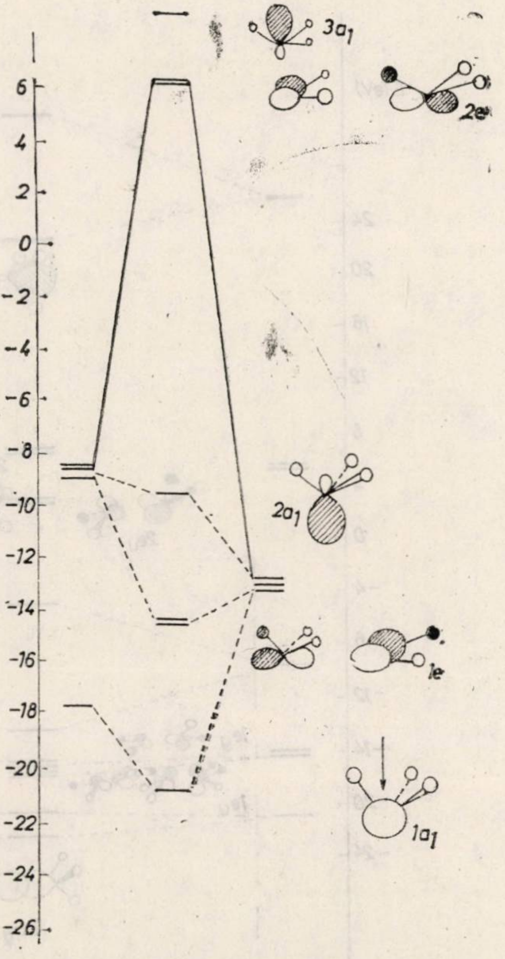

Fig. 2. — The molecular orbitals of SiH_3 fragment, oriented along the OZ axis. The high level $3a_1$ is out of scale.

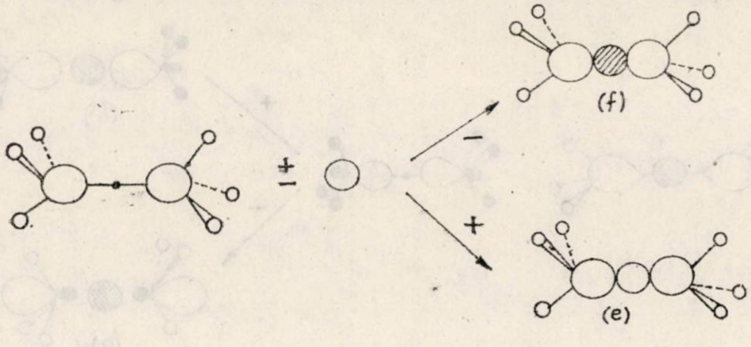

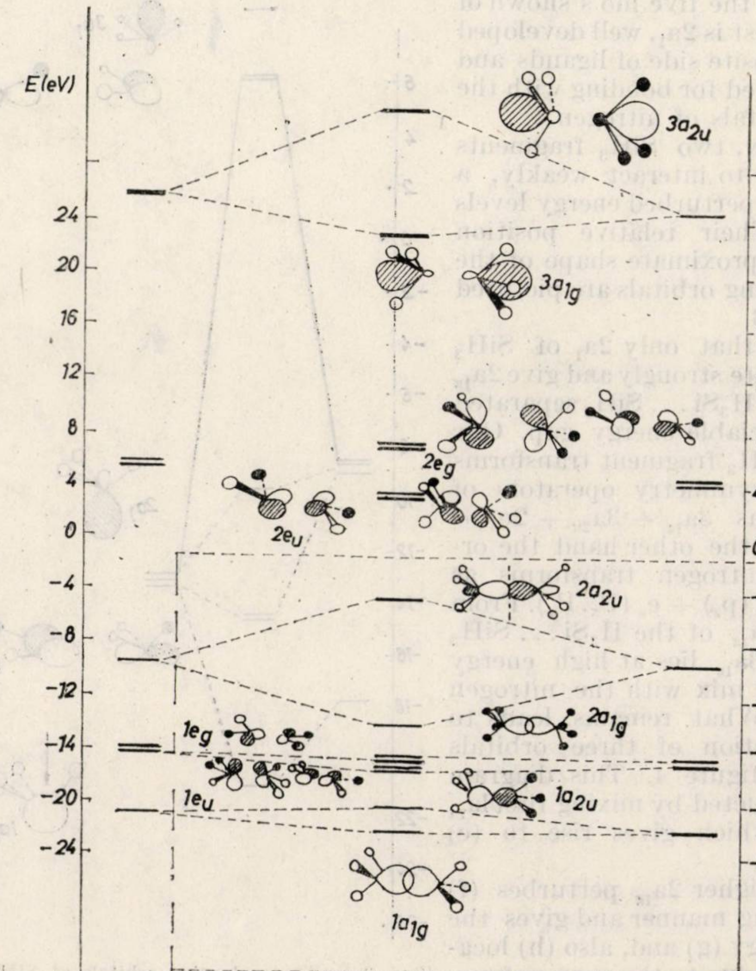
E(eV)
24
20
16
12
8
4
0
-4
-8
-12
-14
-20
-24
3a2u
3a1g
2eg
2eu
2a2u
2a1g
1eg
1eu
1a2u
1a1g
24
20
16
12
8
4
0
-4
-8
-12
-16
-20
-24

Fig. 3. — The result of weak interaction between two SiH_3 fragments.

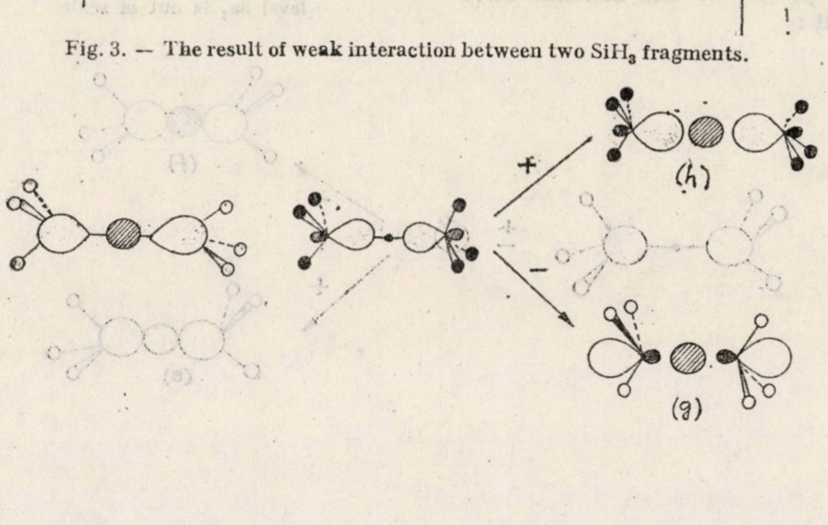

In a similar manner the interaction of a $_{2u}$ symmetry may be set up. The resulting diagram is given in figure 4.

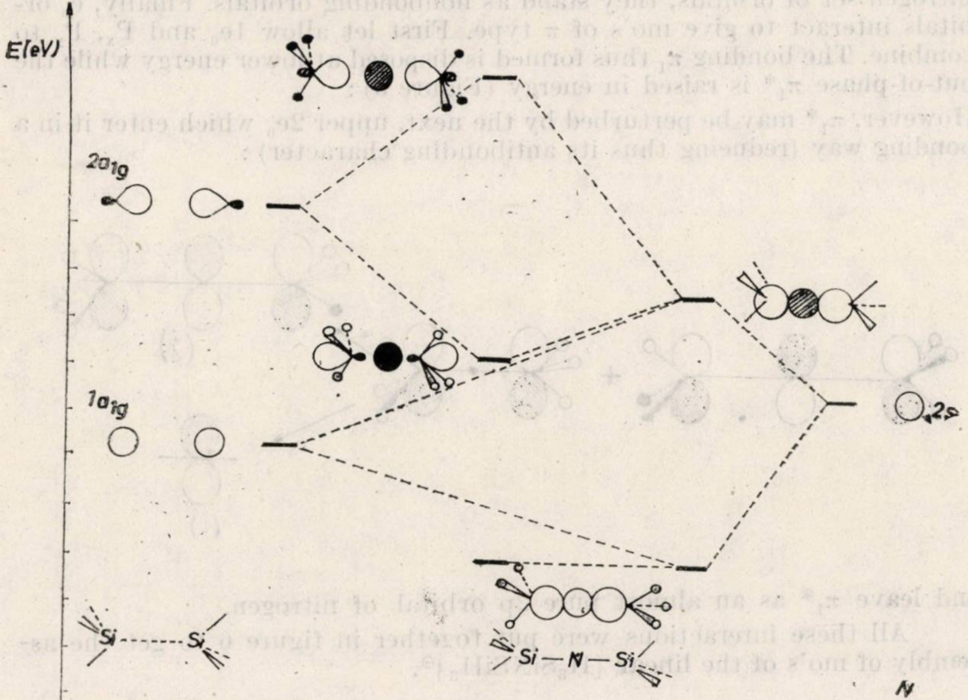
E(eV)
2a1g
1a1g
2p
Si
Si
Si — N — Si
N

Fig. 4. — Interactions between the orbitasls of a_{1g} symmetry.

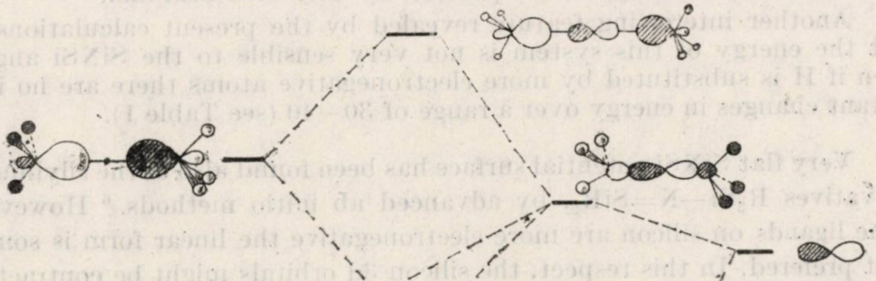

Fig. 5.— Three a_{2u} orbital interaction.

The e_g type orbitals of $H_3Si \ldots SiH_3$ have no counterpart in the nitrogen set of orbitals, they stand as nonbonding orbitals. Finally, e_u orbitals interact to give mo's of π type. First let allow $1e_u$ and P_x, P_y to combine. The bonding π_1 thus formed is disposed at lower energy while the out-of-phase π_1^* is raised in energy (Figure 5) :
However, π_1^* may be perturbed by the next, upper $2e_u$ which enter it in a bonding way (reducing thus its antibonding character) :

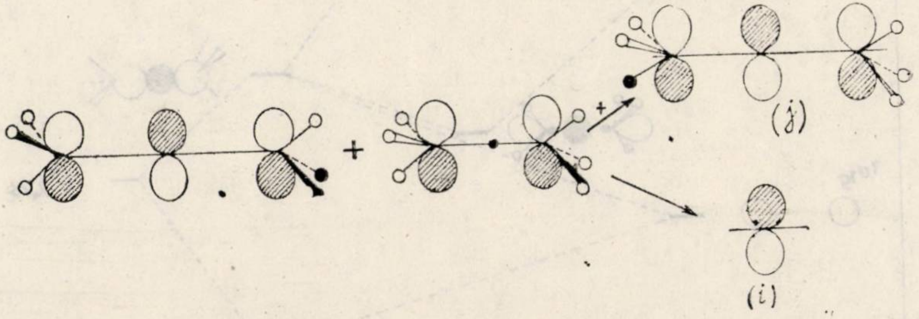

and leave π_1^* as an almost pure 2p orbital of nitrogen.

All these interactions were put together in figure 6 to get the assembly of mo's of the linear $[H_3SiNSiH_3]^{\ominus}$.

Due to the symmetry of these molecular orbitals, almost free rotation around the SiNSi axis is possible. Indeed, the eclipsed and staggered conformations of $[H_3SiNSiH_3]^-$ are separated by only 0.05 kcal/mol.

Another interesting feature revealed by the present calculations is that the energy of this system is not very sensible to the SiNSi angle. Even if H is substituted by more electronegative atoms there are no important changes in energy over a range of 30—40 (see Table 1).

Very flat SiNSi potential surface has been found also in the silylimine derivatives $R_3Si-N=SiR_2$, by advanced ab initio methods. [6] However, if the ligands on silicon are more electronegative the linear form is somewhat prefered. In this respect, the silicon 3d orbitals might be contracted by electronegative substituents and made favorable for overlapping with nitrogen $2p_x$ and $2p_I$ orbitals. [7] This influence of silicon 3d orbitals on the geometry is probably more complex than it seems at the first glance. Thus for certain SiNSi bond angle $Si \ldots Si$ 3d overlap become efficient and bent structures might be favored due to a subtle competition between direct $Si \ldots Si$ interaction and $Si=N$ bond formation.

No direct verification of this result is possible, but the structure of disiloxanes may support this idea. In Table 2 some of the SiOSi bond angles were compiled. As entries [1-6] show, the gradual reduction of the group electronegativities causes a stepwise decrease in the SiOSi bond angle, but all these values are still in the range predicted by our calculations (180–150). The case of t–Bu siloxane is a nice example of how steric effects control the geometry.

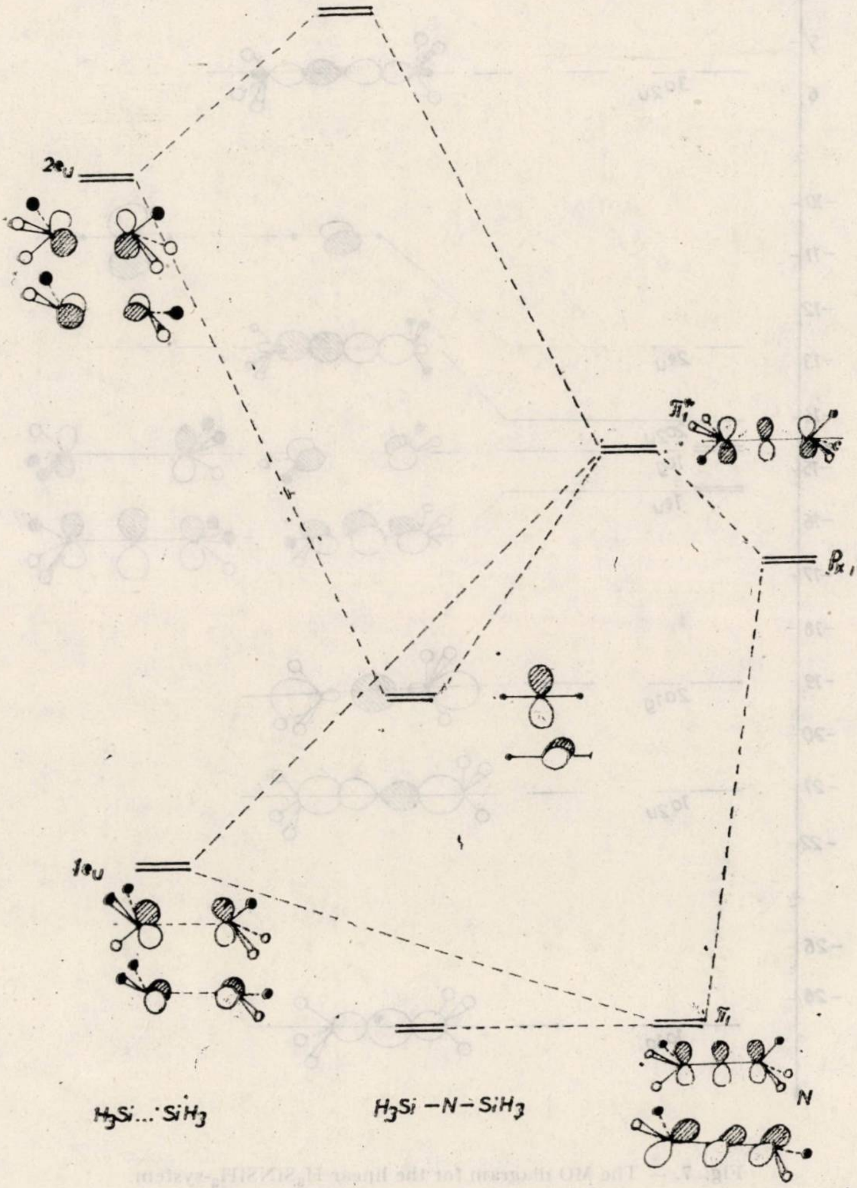
$2e_u$
π_1^*
P_x, P_y
$1e_u$
π_1
N
$H_3Si...SiH_3$
$H_3Si-N-SiH_3$

Fig. 6. — Three e_π type orbital interaction.

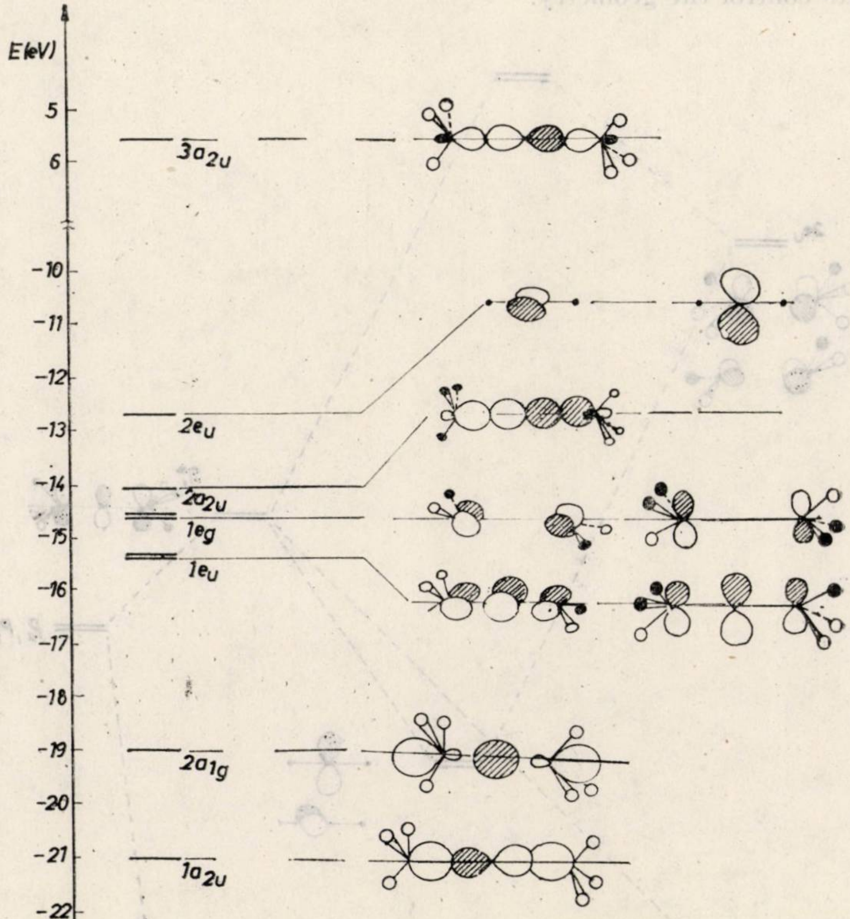
E(eV)
5
6
-10
-11
-12
-13
-14
-15
-16
-17
-18
-19
-20
-21
-22
-26
-28
$3a_{2u}$
$2e_u$
$2a_{2u}$
$1e_g$
$1e_u$
$2a_{1g}$
$1a_{2u}$
$1a_{1g}$

Fig. 7. — The MO diagram for the linear $H_3SiNSiH_3$-system.

Table 1

Total energy (kcal/mol) and orbital energies (eV) dependence on the SiNSi angle

MO no.	180	170	160	150
1	−28.645	−28.645	−28.647	−28.651
2	−20.857	−20.844	−20.806	−20.739
3	−18.818	−18.826	−18.851	−18.895
4	−15.154	−15.155	−15.158	−15.164
5	−15.154	−15.154	−15.151	−15.150
6	−14.644	−14.647	−14.654	−14.660
7	−14.644	−14.642	−14.637	−14.628
8	−14.097	−14.085	−14.049	−13.993
9	−12.852	−12.858	−12.876	−12.907
10	−12.852	−12.852	−12.854	−12.865
11	5.278	5.278	5.300	5.339
Total	−7730.37	−7730.39	−7729.32	−7727.40

Table 2

SiOSi angles in some disiloxane systems

$R_3SiOSiR_3$	∡ SiOSi (°)	Reference
$Ph_3SiOSiPh_3$	180	8
$Ph_3SiOSiHPh_2$	163.3	9
$Ph_3SiOSiMePh_2$	158.9	10
$Ph_2HSiOSiHPh_2$	160	11
$Ph_2MeSiOSiMePh_2$	140	12
$BzMe_2SiOSiMe_2Bz$	145.2	13
$Me_3SiOSiMe_3$	148.8	14
$H_3SiOSiH_3$	142.2	14
$Bu_3SiOSiBu_3$	180	15

$Me=CH_3$, $Bu = C(CH_3)_3$, $Ph = C_6H_5$,
$Bz = CH_2C_6H_5$.

APPENDIX

The EH calculations were performed at the following (fixed) bond lengths: SiN = 1.6 A, SiH = 1.45 A. All HSiH and HSiN angles were taken as tetrahedrally. The VOIP's and orbital exponents are as follows N−26.0 (s), −13.4 (p), 1.95 (); Si −17.93 (s), −8.99 (p), 1.383 (ξ); *H* − 13.6, 1.2 ().

REFERENCES

[1] I. Silaghi-Dumitrescu and I. Haiduc, *Rev. Roumaine Chim.*, **33**, 133 (1988).

[2] R. A. Bartlet and P. P. Power, *J. Amer. Chem. Soc.*, **109**, 6509 (1987).

[3] P. G. Williard, *Acta Cryst.*, **C44**, 270 (1988).

[4] R. Hoffman, *J. Chem. Phys.*, **39**, 1397 (1963).

[5] Many authors commonly use fragment orbitals to construct larger molecules. R. Hoffmans' papers are frequently quoted for this subject. For ex. see M. Elian and R. Hoffman, *Inorg. Chem.*, **14**, 1058 (1975).

[6] P. von Rague Schleyer and P. D. Stout, *J. Chem. Soc.*, *Chem. Commun.*, **1986**, 1373.

[7] Silicon 3d orbitals were invoked in describing the planar structure of trisilylamine ; B. Beagley and A. R. Courard, *Trans. Faraday Soc.*, **66**, 2740 (1970).

[8] C. D. Glidewell and D. C. Liles, *Acta Cryst.*, **B34**, 124 (1978).

[9] W. Wojnowski, B. Becker, K. Peters, E. M. Peters and H. G. von Sehnering, *Z. anorg. allg. Chem.*, **563**, 53 (1988).

[10] M. G. Voronkov, D. Iu. Nesterov, N. V. Alekseev and M. B. Loturev, *Dokl. Akad. Nauk. SSSR*, **256**, 1377 (1981).

[11] W. Wojnowski, K. Peters, E. M. Peters, T. Meyer and H. G. von Schnering, *Z. anorg. allg. Chem.*, **537**, 31 (1986).

[12] W. W. Becker, K. Peters, E. M. Peters and H. G. von Schnering, *Z. anorg. allg. Chem.*, **553**, 267 (1978).

[13] D. Wiese, U. Wannagat, U. Thewalt and T. Debeardamaeker, *Chem. Ber.*, **129**, 873 (1987).

[14] M. J. Barrow, E. A. V. Ebsworth and M. M. Harding, *Acta Cryst.*, **B35**, 2093 (1979).

[13] N. Wiberg, E. Kuhnel, K. Schurz, H. Borrman and A. Simon, *Z. Naturforsch.*, **43B**, 1075 (1988).

Revue Roumaine de Chimie, **35**, *3*, 485–487 (1990)

COMPTES RENDUS

"SYNTHESIS AND APPLICATIONS OF ISOTOPICALLY LABELLED COMPOUNDS 1988", **Proceedings of the 3rd International Symposium, Innsbruck, July 1988, (Editors : T. A. Baillie and J. R. Jones). Published by Elsevier, Amsterdam, 1989, hard cover, 860 pp., ISBN 0-444-87368-6, Price 295 US $**

The papers and posters presented at the Third International Symposium on Isotopically Labelled Compounds held in Austria on 17–21 July 1988 are presented in extenso in an excellently produced and bound heavy volume, surpassing in quality and quantity the two previous volumes of the first and second symposia in the same field held in Kansas City in 1982 and 1985.

About 150 scientists from 25 countries took part in the symposium. The volume contains the three plenary lectures, and most of the 70 oral communications and 73 posters.

The volume is divided according to the 15 topics of the sessions (minisymposia), each of the authors' contributions being limited to six pages, and then for the posters (four pages each).

The plenary lectures are the following : T. Cronholm, "Stable isotopes as metabolic tracers" ; G. Stöcklin, "Synthesis and applications of cyclotron-produced tracers" ; D. L. Hackey et al., "Stable isotopes in the study of lipid and lipoprotein metabolism".

The titles of minisymposia and the numbers of communications (in brackets) are : Synthesis and applications of organic compounds labelled with isotopic hydrogen (7) ; Applications of stable isotopes and NMR spectroscopy for *in vivo* studies (5) ; Radiation-induced reactions (4) ; Applications of stabilonuclidic isotopically-labelled compounds in clinical research (9) ; Isotopes in organic and bio-organic reaction mechanisms (5) ; New techniques in isotopic analysis (7) ; Synthesis and application of organic compounds labelled with iodine isotopes (2) ; Synthesis of isotopically-labelled compounds via organometallic chemistry (2) ; Synthesis and applications of organic compounds labelled with isotopic carbon, sulphur and other isotopes (6) ; Biotechnological methods for the stereoselective preparation of labelled compounds (2) ; The use of stabilonuclidic isotopically labelled compounds in studies of drug metabolism, disposition and toxicity (8) ; Synthesis and applications of organic compounds labelled with isotopic carbon (10) ; Synthesis and applications of labelled compounds in positron emission transaxial tomography (5) ; Applications of radioactively-labelled compounds to *in vitro* and *in vivo* research (4) ; Current trends and future prospects in the synthesis and applications of isotopically labelled compounds (2).

It may be seen even from the titles of the plenary lectures and of the first minisymposia that stable isotopes have gained in relative importanee, owing to their simple detection by mass spectrometric and NMR techniques, to their safe usage in infants and pregnant women, and to the perspective opened by NMR medical imaging or by magnetic resonance microscopy.

It will be impossible to highlight all interesting facts presented in the symposium and in the book, therefore the following selection will be highly subjective.

L. Pichat described the synthesis of tritiated biochemicals with high specific radioactivity : inhibitors of angiotensin-converting enzyme. F. J. Leeper and A. R. Battersby reported on chirally tritiated and deuteriated compounds in biosynthetic studies. G. T. Mc Conville described dilute and not so dilute impurities in tritium (showing how even 1 ppm levels of impurities can affect the Wilzbach-type exchange rate). E. Buncel, J. R. Jones et al. presented catalytic exchange reactions in biologically important heterocyclic compounds, in the presence of Ag(I) and Cu(II). F. M. Kaspersen et al. reported on ^{1}H, ^{2}H, ^{3}H and ^{13}C NMR spectroscopy in the analysis of compounds labelled with ^{2}H, ^{3}H, ^{13}C or ^{14}C.G.W. Kabalka lectured on isotope incorporation via organoboranes, describing how ^{123}I, ^{11}C, ^{13}N, ^{15}O or ^{2}H may be used with organoboranes. H. Gunther, H. Simon and H. L. Schmidt's communication concerns the use of biocatalysts for stereospecific labelling of organometallic compounds.

Among the posters, mention will be made of the following ones : J. J. Lockley, D. Hesk and J. R. Jones reported on the labelling of pharmaceutical agents by exchange with D_2O or HTO via rhodium(III)-catalysed isotope exchange with isotopic water and unlabelled drugs ; M. D. Gheorghiu, A. Schiketanz, A. Necula and A. T. Balaban reported on the ^{13}C- and ^{2}H-labelling of phenanthrene : catalytic automerization and NMR spectra ; V. P. Shevchenko, N. F. Myasoedov presented several tritiations of prostaglandins, and unsaturated lipids ; C. K. Myloaganam et al. showed how Ontario Hydro recovers ^{14}C from CANDU-type nuclear reactions, where it results via ^{14}N (n, p) ^{14}C or ^{17}O (n), ^{14}C reactions; over 50 kCi of ^{14}C is deposited in recoverable concrete containers, in order to protect the environment against contamination.

The state-of-the-art situation in the synthesis and applications of isotopically labelled compounds is excellently reflected in the present volume, which is a must for all libraries of institutions or universities in which stable or radioactive isotopes are being employed.

A. T. Balaban
Polytechnic Institute, Bucharest

MA TH/CHEM/COMP 1987" (editor R. C. Lacher), Studies in Physical and Theoretical Chemistry No. 54 (Proceedings of an International Course and Conference on the Interfaces between Mathematics, Chemistry and Computer Science, Dubrovnik, Yugoslavia, 22—26 June 1987), Elsevier Science Publishing Amsterdam and (for USA) Elsevier Science Publishing Company Inc., New York, 1988, 144.75 US $, 378 pp., ISBN 0-444-42930-1 (vol. 54 in the series "Studies in Physical and Theoretical Chemistry").

The international conference held in Dubrovnik in 1987 under the joint supervision of the Florida State University in Tallahassee and the Rugjer Bosković Institute in Zagreb was devoted to the interfaces between mathematics-chemistry-computer science, in an interdisciplinary spirit.

The areas scheduled to be covered are: 3-dimensional topology in molecular structure analysis; random walk models in chemistry; chemically inspired combinatorics and graph theory; discrete mathematics applications in quantum mechanics; expert systems in chemical computations; and macromolecules.

Among the 24 papers contained in this volume one can highlight the two papers by S. Edelson (on supercomputation and on expert systems in chemistry and chemical engineering), the two lectures on knot theory (one by J. Simon, the other by D. W. Sumners), N. Trinasjtić's paper ("On models and graphs"), M. Randić's lecture ("Molecular topographic descriptors"), and the joint paper of the last two authors, "On conjugated chains", which extends Randić's ideas on conjugated circuits.

M. Randell presented two papers on conformation spaces of molecular rings ending up with unsolved problems. W. A. Seitz, D. J. Klein and A. Graovac applied to regular polymer graphs transfer matrix methods which had been developed by W. A. Tzeits. Cluster expansion techniques were employed by T. G. Schmalz, T. Zivković and D. J. Klein for conjugated acyclic hydrocarbons. W. A. Seitz presented an application of Huang's asymmetrical Ising model to helix-coil transitions in polypeptides.

A series of papers are devoted to polymers: relationships between structure and mechanical properties for crystalline polymers (L. Mandelkern and A. J. Peacock); monomer sequence distributions in polyolefin copolymers obtained in the presence of Ziegler-Natta catalysts based on reactivity ratios of comonomers (K. W. Mc Laughlin); topological interlamellar connections in long-strand polymers (updating investigations presented earlier at MATH/CHEM/COMP—1986 by the editor of this volume, R. C. Lacher, who had organized also the previous meeting); description of topological entanglements in polymer systems (M. G. Brereton); aspects of random walks as applied to the structure of semicrystalline polymers, including loop entanglements and modelling by the "Gambler Ruin Problem" (J. L. Bryant); self-avoiding walks and spiral walks as models for linear or branched polymers (two papers by S. G. Whittington); random walks on lattice graphs, modelling branched polymers in moving solvents (D. Svrtan and D. Veljan). The latter author also presents a paper on enumeration of convex polyhedra and graphs.

V. Simeon and N. Paulić describe applications of factor analysis in chemistry, with emphasis on the principal-components model. The last paper, by W. Rhodes, is entitled "Dynamic properties of large molecular systems", discussing in detail spectral properties of helical biopolymers (polypeptides and polynucleotides) in order to explain the hypochromism of $\pi - \pi^*$ electronic absorption bands and the large increase in circular dichroism associated with this band.

The book is reproduced directly from authors' manuscripts and is therefore printer-error-free. In his foreword, G. Macesich, the director of the Center for Yugoslav-American Studies, Research and Exchanges (Florida State University at Tallahassee), presents the cooperative efforts of which the present volume is one example. The editor's preface states that the series of these MATH/CHEM/COMP conferences were initiated by professors D. Edelson, De Witt Sumners and by himself (Florida State University) as well as by Drs. A. Graovac and N. Trinajstić ("Rugjer Bosković" Institute, Zagreb).

The high quality of the research papers contained in this volume, and the selection of prestigious authors from the USA and Yugoslavia, who made major contributions to the development of the areas discussed in the present volume, make it highly recommended for all those interested in interfaces between mathematics, combinatorics, graph theory and chemistry or chemical engineering.

A. T. Balaban
Polytechnic Institute Bucharest

T. Eicher and H. J. Roth "Synthese, Gewinnung und Charakterisierung von Arzneistoffen", Georg Thieme Verlag, Stuttgart, 1986, 318 pp, flexicover, ISBN 3-13-692101-1.

In 1981, Professor T. Eicher (Chair of organic chemistry, University of Saarland in Saarbrücken), with L. F. Tietze as first author, published jointly a well-known laboratory handbook in the same publishing house, "Reaktionen und Synthesen im organisch-chemischen Praktikum", numbering almost 600 pages.

The present volume is about half as large, and is written for students of pharmaceutical chemistry, following a similar approach.

It should be mentioned that professor H. J. Roth (Pharmaceutical chair of the University Tübingen) is the author of four books on the synthesis and analysis of pharmaceuticals published by Georg-Thieme-Verlag during the last seven years.

The first chapter is a glossary including information on safety measures in the chemical laboratory. In the second chapter, standard assemblies of laboratory glassware are presented. with drawings, for all common procedures which will appear in the book.

Chapter 3 has 27 organic syntheses illustrating the most common reactions and classes of compounds and leading to useful intermediates for subsequent chapters. For each compound, its name, formula, molecular weight, and reaction scheme are presented, followed by indications on the standard assembly to be used, amounts of reagents and duration of the reaction, procedure(s) of separation and purification, yield, characteristic physico-chemical data for the characterisation of compounds. For all compounds, IR, ^1H-NMR and R_f (TLC) data are given, ending with selected literature references.

Then the next four chapters describe drug syntheses according to their main structural features: phenylalkylamines (Chapter 4: epinephrin, fendilin, tranylcypromin, pridinol); aralkyl compounds (Chapter 5: baclofen, phensuximid, cicloxylic acid, S—+)-naproxen; substituted and polycyclic aromatics (Chapter 6: phenacetin, paracetamol, ethenzamid, procaine, bumetanid, menadiol-diacetate, propranolol); sulfonamides (Chapter 7: sulfathiazole, sulfaguanidine); and heterocyclics (Chapter 8) subdivided into 5-membered heterocycles with one heteroatom (piracetam) or two heteroatoms (metamizol, ethomidate, phenytoin, tolazoline, clemizol), 6-membered heterocycles with one heteroatom (warfarin, ethianamid, nifedipin, amidoquin, pyrvinium iodide, cinchocaine) or two heteroatoms (trimethoprim, methaqualone, piroxicam), 7-membered heterocycles (diazepam, chlordiazepoxide) and polyheterocyclic systems (theophyllin, allopurinol, tetramisol both in racemic and in L-forms, —levamisol—).

The 9th and last chapter describes the isolation and synthesis of natural products; in its first part, one learns to isolate saccharides, casein, coffein, ergosterol, nicotine, theobromine, etc. In the second part one performs partial syntheses with the aid of natural products including such compounds as chenodeoxycholic acid, β-D-gentiobiose, 2-deoxy-D-ribose, aspartame.

In the last part several syntheses of natural products are described: α-terpineol, piperitone, phenylalanine, typtophan, coumarin, piperin. A subject index concludes the book.

For the orientation of students and teachers, each drug synthesis is marked according to its difficulty. Whenever possible, references to pharmacopeias (European, US, Britsh, German) are indicated. Comments and hints as to reaction mechanisms, safety measures used, etc. are included for each preparation. Special attention is paid to analytical methods.

The book is reproduced from a typewritten manuscript, and is produced in excellent graphic condition.

For all those involved in drug synthesis, i.e. students, and teaching staff, this book is an excellent source of information, offering an appetizing menu, with the guarantee of success in the pharmaceutical-chemical laboratory.

A. T. Balaban
Polytechnic Institute Bucharest

ORSZÁGOS MŰSZAKI INFORMÁCIÓS KÖZPONT ÉS KÖNYVTÁR 1883

NOTE POUR LES AUTEURS

La Revue Roumaine de Chimie publie des articles en anglais, français, russe, allemand ou espagnol. Les auteurs sont priés d'envoyer des articles et des comptes rendus inédits.

Les manuscrits seront dactylographiés à double interligne. La bibliographie, les tableaux et la légende des figures seront placés après le texte.

Si l'article fait partie d'une série numérotée, la partie précédente sera donnée comme première référence.

Chaque article sera précedé d'un résumé comprenant quinze lignes au maximum.

Les références bibliographiques dans le texte seront faites par des exposants sans parenthèses et paraîtront à la fin de l'ouvrage.

Les publications périodiques mentionnées dans la bibliographie seront présentés suivant les prescriptions internationales : le nom de l'auteur précédé de l'initiale du prénom, le titre du Périodique abrégé conformément à « Chemical Abstracts » et souligné par une ligné, le numéro du tome indiqué par des chiffres arabes et souligné par deux lignes, suivi de la première page de l'article ; à la fin, l'année de la parution sera placée entre parenthèses. Le numéro de la revue ne sera pas indiqué si les pages du volume sont numérotées consécutivement.

Les textes des livres ou traités inclueront : le nom des auteurs, précéde de l'initiale du prénom, le titre du livre entre guillemets et sans être souligné, le numéro du tome précédé par l'abréviation « vol. » (ou « Bd. »), le numéro de l'édition, les éditions (the publisher), la localité de la parution du livre, l'année de la parution et la page de la référence précédée par l'abréviation « p. » (ou « S. »).

Les brevets seront indiqués comme suit : l'auteur ou la firme, le pays et le numéro du brevet, la date et la revue *(Chem. Abstr.)* Par/ex. : M. Jones (to Union Carbide Co), Brit. Pat. 601 238, 2 Sept. 1959 ; ef. *Chem. Abstr.*, **24**, 12808 (1960).

Si la référence n'a pas été lue en original, on indiquera aussi la revue de références consultée.

Les diagrammes seront tracés à l'encre de Chine sur papier calque. Les tableaux et les figures (en nombre strictement nécessaire) ainsi que les courbes dans les figures seront numérotés par des chiffres arabes. Leur explication sera donnée dans la légende des figures. Priére de ne pas inscrire les mêmes données dans les tableaux et les figures. Chaque tableau aura un titre. On indiquera dans le texte la place approximative des tableaux et des figures. Les formules chimiques seront incluses dans le texte ; en outre, elle seront transcrites sur papier calque, à l'encre de Chine.

Les auteurs sont priés d'indiquer les caractères italiques (en soulignant les lettres au crayon), ainsi que tout autre caractère spécial ; les préfixes *ortho, meta, parc, cis, trans*, etc. seront soulignés pour indiquer leurs caractéres italiques et ne seront jamais écrits avec des majuscules.

Aucune correction à la main ne sera admise sur le manuscrit. Les corrections seront frappés à la machine. Les lettres grecques ou d'autres symboles spéciaux seron insérés à la main à l'encre clairement.

Le manuscrit sera signé par l'auteur.

Le titre-courant aura 50 lettres au maximum.

L'entière responsabilité du contenu des articles appartient aux auteurs.

Sur demande ou peut obtenir une note plus complète.

PRINTED IN ROMANIA

TRAVAUX PARUS AUX ÉDITIONS DE L'ACADÉMIE ROUMAINE

I. G. MURGULESCU, **Introducere în chimia fizică, Vol. I. Atomi, molecule, legătură chimică,** 1976, 560 p.

I. G.MURGULESCU, V. EM. SAHINI, **Introducere în chimia fizică, Vol. I. Structura şi proprietăţile moleculelor,**1979, 604 p.

I. G. MURGULESCU, E. SEGAL, **Introducere în chimia fizică, Vol.II. 1. Teoria-molecular-cinetică a materiei,** 1979, 1036 p.

I. G. MURGULESCU, TATIANA ONCESCU, E. SEGAL. **Introducere în chimia fizică. Vol. II. 2. Cinematică chimică şi cataliză,** 1981, 1024 p.

I. G. MURGULESCU, J. PĂUN, **Introducere în chimia fizică, Vol. I. 3. Nucleul atomic, reacţii nucleare, particule elementare,** 1982, 606 p.

I. G. MURGULESCU, RODICA, VÎLCU, **Introducere în chimia fizică, Vol. III. Termodinamica chimică,** 1982, 624 p.

I. G. MURGULESCU, O. M. RADOVICI, **Introducere în chimia fizică, vol. IV. Electrochimia,** 1986, 410 p.

CRISTOFOR I. SIMIONESCU, VALERIA GORDUZA, **Implicaţii biogenetice ale coloranţilor,** 1988, 208 p.

R. VÎLCU, M. LECA, **Termodinamica polimerilor prin cromatografie de gaze,** 1987, 238 p.

I. ZUGRĂVESCU, M. PETROVANU, **Cicloadiţii 3 + 2 dipolare,** 1987, 446 p.

RAUL MIHAIL, ION GROZEANU, **Estimarea secvenţională aplicată sistemelor chimice,** 1986, 406 p.

M. BREZEANU, L. PATRON, M. ANDRUH, **Combinaţii complexe polinucleare şi aplicaţiile lor,** 1986, 244 p.

A. T. BALABAN et al., **Labelled compounds and radiopharmaceuticals applied in nuclear medicine,** coedition avec John Wiley and Sons, 1986, 742 p.

D. PURDELA, **Nomenclatura chimiei organice — IUPAC,** 1986, 454 p.

PETRU BUDRUGEAC, **Probleme de chimie,** 1986, 280 p.

T. ONCESCU, S. G. IONESCU, **Conversie fotochimică şi stocare de energie,** 1985, 272 p.

V. DRĂGUŢAN, A. T. BALABAN, M. DIMONIE, **Olefin Metathesis and Ring-Opening Polymerization of Cyclo-Olefins,** coédition avec John Wiley and Sons, 1985, 544 p.

C. LITEANU, I. RÎCĂ, **Optimizarea proceselor analitice,** 1985, 360 p.

N. PETRESCU, **Chimia extracţiei cu solvenţi şi aplicaţii,** 1985, 242 p.

V. E. SAHINI, M. HILLERAND, **Chimie cuantică în exemple şi aplicaţii,** 1984, 378 p.

GH. MARCU, **Chimia compuşilor coordinativi,** 1984, 415 p.

E. CORDOŞ, G. MANOLIU, **Spectrometria de absorbţie şi fluorescenţă atomică,** 1984, 178 p.

C. BODEA, **Tratat de biochimie vegetală, p. II, t. 5,** 1984, 438 p.

N. ASANDEI, A. GRIGORIU, **Chimia şi structura fibrelor,** 1983, 395 p.

N. IONESCU, M. CĂLDĂRARU, **Oxidarea catalitică a olefinelor inferioare,** 1983, 178 p.

C. CAŞCAVAL, **Studiul polimerilor prin piroliză şi cromatografie de gaze,** 1983, 220 p.

C. I. SIMIONESCU, F. DANEŞ, **Originea vieţii,** 1983, 110 p.

C. BODEA, **Tratat de biochimie vegetală, p. II. t. IV,** 1982, 480 p.

I. GĂLĂŢEANU, **Procese şi metode radiochimice în energetica nucleară,** 1981, 234 p.

CR. SIMIONESCU, VALERIA GORDUZA, **Polimeri biocompatibili şi biologic activi,** 1980, 479 p.

ISSN 0035—3930

Universul c. 2001

42 428

Lei 40

F 1103

ACADÉMIE ROUMAINE

REVUE ROUMAINE DE CHIMIE

TOME 35
N° 4
Avril 1990

Rev. Roumaine Chim.

RRCHAX, 35, 4, p. 489–586 (1990), Bucarest

EDITURA ACADEMIEI ROMÂNE

ACADÉMIE ROUMAINE

COMITÉ DE RÉDACTION

Rédacteur en chef :

I. G. MURGULESCU, membre de l'Académie Roumaine

Rédacteurs en chef adjoints :

A. T. BALABAN et V. EM. SAHINI, membres de l'Académie Roumaine

Collège de rédaction :

EM. BRATU, ECATERINA CIORĂNESCU-NENITZESCU, CR. SIMIONESCU, P. SPACU, membres de l'Académie Roumaine ; M. ANDRUH, M. BANCIU, M. D. GHEORGHIU, I. HAIDUC, D. I. MARCHIDAN, G. NIAC et D. SĂNDULESCU

La Revue Roumaine de Chimie paraît 10 fois par an. Toute commande de l'étranger sera adressée à ROMPRESFILATELIA — sectorul Export-Import Presă, P. O. Box 12 — 201, télex 10376 prsfi r 78104 Bucarest, Calea Griviţei nr. 64 — 66, Roumanie

Les manuscrits, les livres et les revues proposés en échange, ainsi que toute correspondance seront envoyés à la rédaction :

REVUE ROUMAINE DE CHIMIE

125, Calea Victoriei, 79717 Bucarest, Roumanie, téléphone 50 76 80

EDITURA ACADEMIEI ROMÂNE
125, Calea Victoriei 79717, Bucarest, Roumanie, téléphone 50 76 80

REVUE ROUMAINE
DE
CHIMIE

Tome 35, N° 4 **Avril, 1990**

ORSZÁGOS MŰSZAKI INFORMÁCIÓS KÖNYVTÁR 1883

E. A. GOMAA, Y. A. ELEWADY and A. H. EL-ASKALANY, Mechanism of electroreduction of sodium nitroprusside (SNP) 491–494

EBI B. EDWARD INATIMI, Multi-element analysis by solvent extraction and high performance liquid chromatography of soil samples 495–502

FOUAD TAHA, A. M. EL-ROUDI, A. A. ABD EL GABER and F. M. ZAHRAN, Adsorption of cations on oxides 503–509

BARBARA BARSZCZ and JACEK KULIG, Studies on complexation of Co(II), Ni(II), Cu(II), Zn(II) and Cd(II) with 1-acetylimidazole in aqueous solution 511–521

ANTONIO ARROYO, Additivity of viscosity in binary and ternary aqueous-organic mixtures 523–533

MARIA BREZEANU, E. PINCOVSCHI, DANA MARINESCU and MARIUS ANDRUH, A new preparation method for μ_3-oxo-trinuclear chromium (III) formate 535–537

HARVIR SINGH and SURENDRA PAL SINGH TOMAR, Studies on viscosity of magnesium soaps of higher fatty acids in dilute aqueous solutions at different temperatures 539–544

T. O. OLAGBEMIRO and L. LAJIDE, Chemical components of the scent gland of the green vegetable bug: *Nezera viridula* 545–547

GEETA M. KULKARNI, MANOHAR V. KULKARNI, VEMANNA D. PATIL, D. B. SHRIDHAR and M. LAXMANA. Synthesis and anti-inflammatory activity of some new triheterocyclic thiazoles 549–554

P. S. MITTAL, N. KUMAR, K. K. GIRDHAR, A. D. TANEJA and J. S. TYAGI, Kinetic studies of tautomerisation and effect of temperature on enethiol contents of some carboxyalkyl-thiocarbamides 555–560

DANIELA CARMEN ONICIU, ANCA MARTON, TEODOR-SILVIU BALABAN, SORIN VLAD and ALEXANDRU T. BALABAN, Synthesis of 2,6-dimethyl-4-styrylpyrylium salts (from 2,4,6-trimethylpyrylium and donor-substituted benzaldehydes) and their conversion into pyridines 561–565

A. A. AFIFY, S. EL-NAGDY, M. A. SAYED and I. MOHEY, Synthesis and reactions of substituted benzoxazinones bearing a bulky group at position-2. Part I 567–575

H. M. LLANEZA, J. CORONA and J. M. BLANCO, Optimization by computer of the alkaline hydrolysis of isoamyl acetate 577–581

BOOK REVIEWS 583–585

Rev. Roumaine Chim. 35, 4, 489–586 (1990), Bucarest

Revue Roumaine de Chimie, **35**, *4*, 491–494 (1990)

MECHANISM OF ELECTROREDUCTION OF SODIUM NITROPRUSSIDE (SNP)

E. A. GOMAA*, Y. A. ELEWADY and A. H. EL-ASKALANY
Chemistry Department, Faculty of Science, Mansoura University, Mansoura, Egypt

Received November 21, 1987

The polarographic electroreduction of sodium nitroprusside (SNP) in 0.1 MNaF, KCl, KBr, Na_2SO_4 and Na_2SO_3 showed three reduction waves. On the other hand two waves are obtained on using 0.1 M NaI and $Na_2S_2O_3$ solutions. The three reduction waves in the former case are due to the formation of $[Fe(CN)_5\ NO]^{3-}$, $[Fe(CN)_5NO]^{4-}$ and $[Fe(CN)_5NHOH]^{2-}$ ions, respectively. The two waves in the latter case are also discussed.

The polarographic study of sodium nitroprusside (SNP) has been carried out by Kolthoff,[1] Joselskis[2] and Kumaret al.,[3,4] but the mechanism of reduction of SNP in the literature is not clearly explained for all the three reduction waves. Metrohm Polarecord E 506 and Polarography stand E 505 dc were used. Zhe pH values were adjusted by adding HCl and NaOH as desired. The capillary characteristics were m = 1.77 mg/s. and $t = 3.4$ s. A freshly prepared solution of sodium nitroprusside (Merck) was used. All the polarograms are recorded immediately after the preparation using Ag/AgCl/sat. KCl electrode as reference electrode.

The polarograms of 0.5 mM SNP in 0.1M KCl solution (Fig. 1) showed three reduction waves. The plot of log $(i_d - i)/i$ vs. E (in volts) gives a straight line for each of the three reduction waves with αn_a values of 0.845,0.0.786 and 0.325, respectively. This indicates the reversibility of the first two waves and the irreversibility of the third one. On plotting log i versus log h (mercury height relation), a straight line was obtained in each case. The slopes of the three lines were approximately 0.45, indicating that the electrode process is mainly diffusion controlled. The number of electrons consumed in the first and second waves was determined by applying the Stockes-Einstein relation,[5] which gave a value of one in each case. Hence, the first and second waves are due to

$$[Fe(CN)_5NO]^{2-} + e \rightleftharpoons [Fe(CN)_5NO]^{3-} \tag{1}$$

$$[Fe(CN)_5NO]^{3-} + e \rightleftharpoons [Fe(CN)_5NO]^{4-}. \tag{2}$$

Both $[Fe(CN)_5NO]^{3-}$ and $[Fe(CN)_5NO]^{4-}$ have been reported earlier in literature.[1–4].

---

* To whom correspondence should be sent. Present address : Teachers Training College, Salalah – P. O. Box 19905, Sultanate of Oman.

The limiting current value of the thid wave was twice that of each of the first two waves, indicating 2-electron reduction process. The half-wave potential for the first and second waves remains unchanged with increasing pH values, while the third wave shifts to more negative potentials. This indicates that the reduction process for the third wave involves hydrogen ion. The number of hydrogen ions consumed in the reduction process giving the third wave (Z_{H^+}) was calculated by using equation 3 and found to be 2.26.

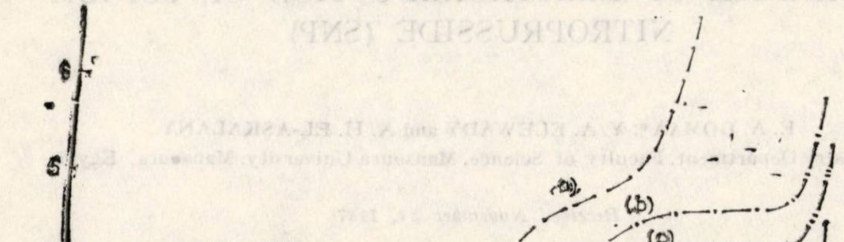

Fig. 1. — Polarograms of 0.5 mM sodium nitroprusside in 0.1 M KCl solution at different pH's.

$$\Delta E_{1/2}/\Delta \text{pH} = \frac{0.0591}{\alpha n_a \cdot Z_{H^+}} \qquad (3)$$

The αn_a in equation 3 is the mean value for the third wave obtained at different pH's. The reduction process for the third wave is :

$$[Fe(CN)_5NO]^{4-} + 2e + 2H^+ \rightarrow [Fe(CN)_5NHOH]^{2-} \qquad (4)$$

The same behaviour of the reduction of SNP in 0.1 M solutions of NaF, KBr, Na_2SO_4 and Na_2SO_3 was observed as in the case of KCl (see Figs 2 and 3). Thus three reduction waves for SNP are obtained by using these

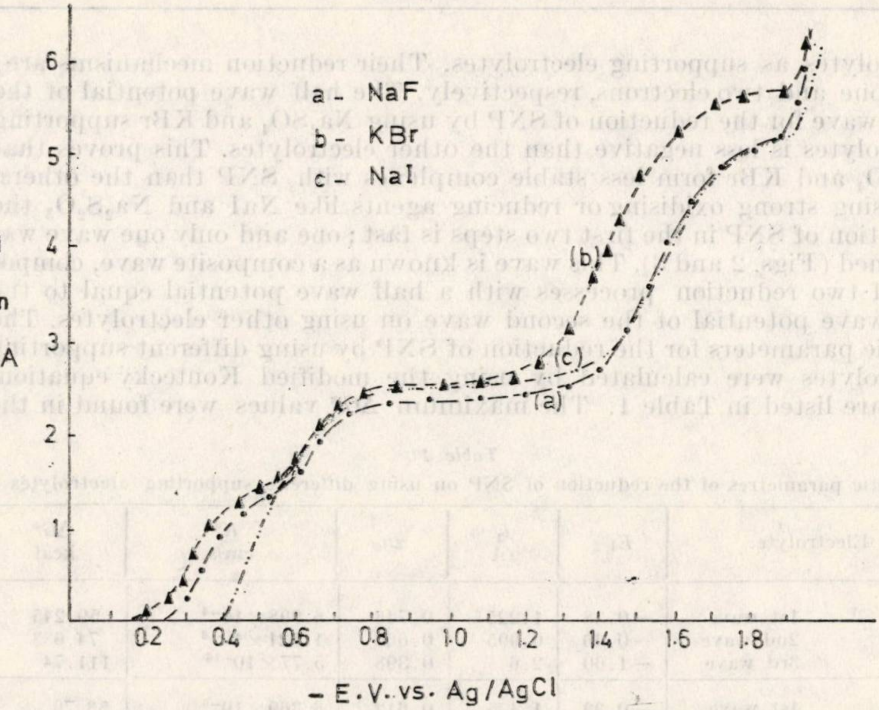

Fig. 2. — Polarograms of 0.5 m M sodium nitroprusside in 0.1M naF, KBr and NaI solutions.

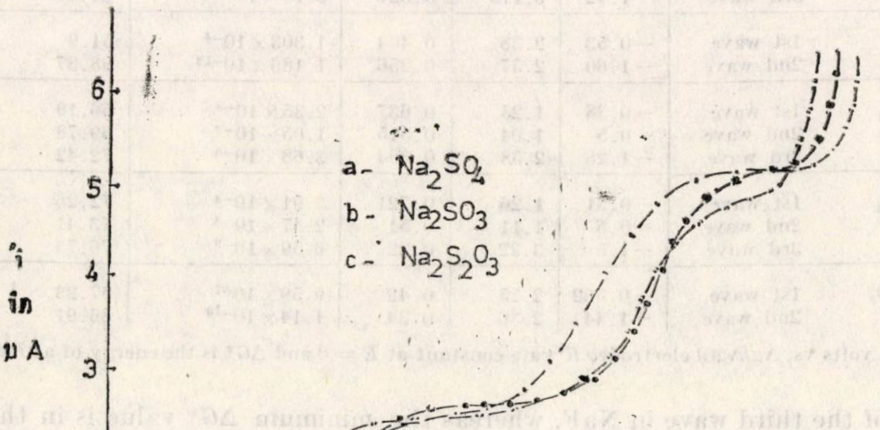

Fig. 3. — Polarograms of 0.5 mM sodium nitroprusside in 0.1 M Na_2SO_4, Na_2SO_3 and $Na_2S_2O_3$ solutions.

electrolytes as supporting electrolytes. Their reduction mechanisms are: one, one and two electrons, respectively. The half wave potential of the third wave for the reduction of SNP by using Na_2SO_4 and KBr supporting electrolytes is less negative than the other electrolytes. This proves that Na_2SO_4 and KBr form less stable complexes with SNP than the others. On using strong oxidising or reducing agents like NaI and $Na_2S_2O_3$ the reduction of SNP in the first two steps is fast; one and only one wave was obtained (Figs. 2 and 3). This wave is known as a composite wave, composed of two reduction processes with a half wave potential equal to the half wave potential of the second wave on using other electrolytes. The kinetic parameters for the reduction of SNP by using different supporting electrolytes were calculated by using the modified Koutecký equation[6] and are listed in Table 1. The maximum ΔG^* values were found in the case of the third wave in NaF, whereas the minimum ΔG^* value is in the case of the first reduction wave of SNP on using NaI as supporting electrolyte.

Table 1

Kinetic parametres of the reduction of SNP on using different supporting electrolytes

Electrolyte		$E_{1/2}$	i_1 μA	αn_a	K° cm/s.	ΔG^* kcal
NaF	1st wave	−0.38	1.225	0.746	6.998×10^{-6}	59.245
	2nd wave	−0.66	0.995	0.660	1.521×10^{-8}	74.633
	3rd wave	−1.60	2.6	0.398	5.77×10^{-15}	111.74
KBr	1st wave	−0.32	1.435	0.612	6.369×10^{-5}	53.70
	2nd wave	−0.64	1.215	0.758	5.225×10^{-9}	77.314
	3rd wave	−1.42	3.175	0.327	8.18×10^{-10}	81.97
NaI	1st wave	−0.53	2.38	0.404	1.303×10^{-4}	51.9
	2nd wave	−1.60	2.57	0.256	1.186×10^{-12}	98.37
Na_2SO_4	1st wave	−0.38	1.25	0.637	2.35×10^{-5}	56.19
	2nd wave	−0.5	1.04	0.515	1.05×10^{-7}	69.78
	3rd wave	−1.28	2.58	0.384	3.68×10^{-8}	72.42
Na_2SO_3	1st wave	−0.31	1.26	0.721	3.91×10^{-8}	72.26
	2nd wave	−0.5	1.11	0.51	2.47×10^{-8}	73.41
	3rd wave	−1.5	3.22	0.22	6.59×10^{-9}	76.73
$Na_2S_2O_3$	1st wave	−0.562	2.55	0.42	9.59×10^{-1}	67.23
	2nd wave	−1.44	2.36	0.34	1.14×10^{-10}	86.91

$E_{1/2}$ in volts vs. Ag/AgCl electrode, K° rate constant at $E = 0$ and ΔG^* is the energy of activation.[6]

REFERENCES

[1] I. M. Kolthoff and P. E. Toren, *J. Am. Chem. Soc.*, **76**, 1098 (1954).

[2] B. Joselskis and J. C. Edward, *Anal. Chem.*, **32**, 383 (1960).

[3] R. S. Kashyap P. N. Sharma and A. Kumar *Ind. J. Chem.*, **19A** 535 (1980).

[4] R. S. Kashyap P. N. Sharma and A. Kumar *Ind. J. Chem.*, **21A**, 543 (1982).

[5] I. M. Kolthoff and J. J. Lingane "Polarography", Vol. 1 (Interscience Publisher), New York, 1952.

Revue Roumaine de Chimie, 35, 4, 495–502 (1990)

MULTI-ELEMENT ANALYSIS BY SOLVENT EXTRACTION AND HIGH PERFORMANCE LIQUID CHROMATOGRAPHY OF SOIL SAMPLES

EBI B. EDWARD INATIMI

School of Science and Science Education, Abubakar Tafawa Balewa College, Ahmadu Bello University, PMB 0248, Bauchi Campus — Bauchi, Nigeria

Received November 21, 1987

The way of using high performance liquid chromatography (HPLC), after preliminary solvent extraction, for the complete separation of trace amounts of metal chelates prior to their non-selective determination is presented. A UV detector for the most intense absorbance peak of the reagent (used for the solvent extraction) was used as a universal detector for all the metal chelates at approximately the same sensitivity. The method of normal mode HPLC using diethyl dithiocarbamates was applied to the analysis of a series of soil samples. These were obtained as soil extracts in molar (1M) hydrochloric acid, prior to their extraction with a solution of diethyldithiocarbamate The results were compared with those of the analysis of the same samples by means of the atomic absorption spectroscopy (AAS) method.[3]

INTRODUCTION

As applied to soil investigation, the principal function of total trace elements analysis is connected with mineralogy and assists in determining the soil genesis and classification. It is also used in the study of long term changes in a soil. However, the determination of the total amount of an element will reveal its inadequacy.

In order to establish a fairly simple and routine multi-element method for monitoring trace elements in soil samples, HPLC, after preliminary solvent extraction was investigated for the complete separation of trace amounts of metal chelates prior to their nonselective determination. The overall selectivity of the organic reagents can be increased in this way up to the point at which they will be useful for the rapid routine figer-printing of groups of trace metals, and comparable to the use of derivative gas-liquid chromatography for organic compounds. If the separation is complete, an ultraviolet detector set to the most intense absorbance peak of the reagent itself can be used as a universal detector for all the metals at approximately the same sensitivity. A sulphur containing reagent, diethyldithiocarbamate (DDTC)[4] was chosen because of its high molar absorptivity and because it forms strong complexes with heavy trace metals, such as lead and mercury.

In this study HPLC was used in the absorption mode because metal chelates are typically very soluble in non-polar solvents such as chloroform. This high solubility has proved to be an advantage because, with the high distribution ratios of the complexes in such solvents, it was possible to use relatively small volumes for the extraction. This practice avoids the need for a slow evaporation step prior to direct injection of the aliquot on to the HPLC column.

The soil samples were initially dried (or ignited) and digested with a hydrofluoric-perchloric-nitric acid mixture and finally extracted with hydrochloric acid, before being extracted with the DDTC solution.

EXPERIMENTAL

Reagents

All reagents were of Analar grade unless stated otherwise.

Diethylammonium diethyldithiocarbamate (DDDTC) solution. Dissolve 0.50 ± 0.01 g of DDDTC in 100 ± 1 ml of dry chloroform (prepare freshly every week and store in a refrigerator after use).

Buffer solution. Dissolve 45.2 g ammonium chloride and 9.6 ml of concentrated ammonia solution (Sp.gr.0.880) in 1000 ml of water in a graduated flask. This solution should have a pH of 8.5. Dilute for 10 times before use.

Chloroform. Dry over a molecular sieve. **HPLC eluent.** Dry spectrograde benzene (Fisons Scientific Instruments, Loughborough, Great Britain) with a molecular sieve and degas before use.

Apparatus

The HPLC System chosen was the model PU4000 modular instrument (Pye Unicam, Cambridge, England) and the AAS instrument used was the GBC901 (GBC Scientific Equipments Pty Ltd. Australia).

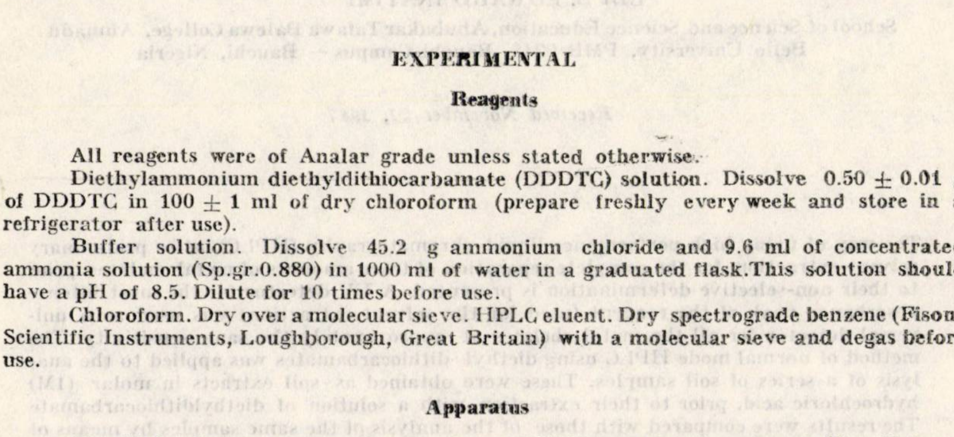
Sampling of Soil Samples
General Preparation Including, weighing, drying etc.
Extraction of Samples With Molar Hydrochloric Acid
Extraction with chelating agents e.g. DDDTC.
Injection of Appropriate Aliquot into Pre-conditioned HPLC column
Obtaining of HPLC chromatogram and evaluation of Results.

SUMMARY OF HPLC PROCEDURE FOR TRACE METAL ANALYSIS IN SOIL SAMPLES.

Samples tubes (20 × 50 mm) were used for the collection of organic phases after the solvent extraction of the samples. These tubes should be fitted with Snap-on polyethylene lids. Other apparatus consisted of 400 and 600 ml graduated borosilicate (pyrex) glass beakers and 500 and 1000 ml separating funnels fitted with ground-glass stoppers and taps (if possible Interflow polyethylene taps); 1ps silicone-treated phase separating paper (whatman labsales, springfield Mill, Maidstone, Great Britain) was used.

Procedure (including calibration)

Add an appropriate aliquot of the standard (see Note a below) or sample (Note b) solutions to a clean 600 ml graduated pyrex glass beaker and adjust the pH of the solution to about 8 with either 2M hydrochloric acid or 2M sodium hydroxide solution. Add an appropriate amount of buffer to maintain the pH of the metal solution at 8.5 ± 0.1 (Note c) (use a pH meter). Dilute the solution to 300 ± 1 ml in a beaker or large measuring cylinder.

Transfer the solutioninto a clean500-ml separating funnel, add 5.0 ± 0.05 ml of DDDTC (Note D) solution in chloroform with a clean pipette as required, stopper the funnel, shake it vigorously for 3 min ± 15 s and allow it to stand for 5 minutes ± 30 seconds.

Separate the organic from the aqueous phase by filtration through the pase separating paper into a sample tube and fit the lid (Note e). The HPLC stage must be completed during the same working day.

Inject 2 — 10 μl of this chloroform solution of the separated metal chelates on to an already equilibrated chromatographic column by the stopflow syringe mode of injection. Mark the injection point on the recorder trace.

Measure the peak heights and compare with calibration standards.

Blank determination. A blank must be run with each batch of determinations (e.g. up to 10 samples) using the same batch of reagents as for the samples and also the sample eluent for the HPLC run. Carry out the above steps again, but replace the standard or sample solution with distilled water and make up to mark as for samples.

Calibration. Stock standard solutions (Note a) are used for calibrations. Duplicate calibration standard should be run with each batch of determinations (e.g. up to 10 samples). Using an appropriate aliquot of the stock standard solution, carry out the steps. The linearity of the calibration graph should be checked from time to time, by plotting peak height against concentration of sample solution in the aqueous phase (the volume ratio, Vaq/Vo, used is 100, i.e. 500 ml of aqueous phase to 5 ml of organic phase).

Notes. (a) Stock standard solutions should be prepared by dissolving the appropriate metal or stoichiometric salt (Analar or 99.9% purity) at a concentration of 1000 ppm.

(b) Sample pre-treatment. The soil samples were sampled according to recommended procedures.[3,5] Accurately weight about 0.1 g of oven-dry, 0.15 mm soil into a platimum crucible and moisten with a drop or two of water. Add 5 cm^3 of hydrofluoric acid and 0.5 cm^3 of perchloric acid, nearly cover the crucible with its lid and heat on a sand-tray at 200°C until the liquid has evaporated. Any unoxidized organic matter deposited on the upper part of the crucible or its lid can be oxidized with the flame of a Meker Burner.[6]

After cooling, add 5 cm^3 of 6 m hydrochloric acid and half fill the crucible with water. Place the crucible in an electrothermal bunsen and gently boil the contents for 5 minutes. If this treatment does not completely dissolve the solids, evaporate to dryness and repeat theacid digestion. When the residue has been quite dissolved, transfer to a 100-cm^3 volumetric flask and dilute to volume.

(c) Do not use more than 100 ml of buffer solution, in order to avoid the introduction of errors.

(d) It was observed that some of the commercial diethyldithiocarbamic acids produce oxidation products that are liable to interfere in the determination of nickel and manganese dithiocarbamate, especially at lower levels. In order to remove these two interferents from the reagent, it is recommended that the reagent should be back-washed to remove oxidation products before being used for the preparation of metal complexes.

(e) All samples and standards should be processed to this stage before proceeding to the HPLC stage.

RESULTS AND DISCUSSION

The HPLC behaviours of the metal chelates of DDTC used in this work were studied on silica gel columns with spectrograde benzene as mobile phase. Typical HPLC conditions giving the best compromise between efficiency, speed and sensitivity of separation were: column, stainless steel (150 mm × 4.6 mm i.d.); packing Hypersil (5 um particles); eluting agent, spectrograde benzene; flow-rate, 1.25 – 1.50 ml min^{-1} at ambient temperature; detector, ultraviolet at a wavelength of 280 nm and with 0.05 a.u.f.s.d. With these chromatographic conditions, the limits of detection of the metals and the reproducibility are those given in this paper.

Figure 1 shows an example of the chromatogram obtained by using a standard mixture of transition metals, after separation as the DDTC complexes. The resolution between successive peaks is nearly complete in most instances and the complete profile can be recorded in about 8 minutes.

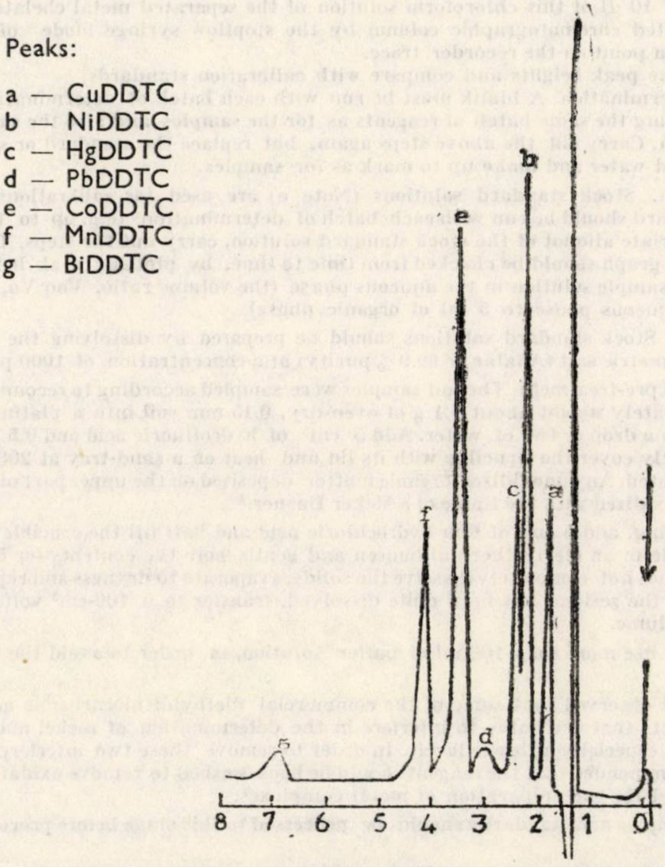

Fig. 1. — Standard trace metal sample (Extracted with DDDTC solution at pH 8.5).

Each peak of the chromatogram corresponds to about 100 ng of the metal, injected as the DDTC complex. The chromatogram proved reproducible with retention times, retention volumes and peak heights remaining constant to better than ± 5% (Coefficient of variation). Figure 2 shows calibration results for the peak heights of cobalt, copper, nickel, mercury, manganese and lead, extracted as the DDTC complexes. The number of theoretical plates in the 150-m column ranged from 520 for lead to 4,000 for manganese and most of the other first-row transition elements.

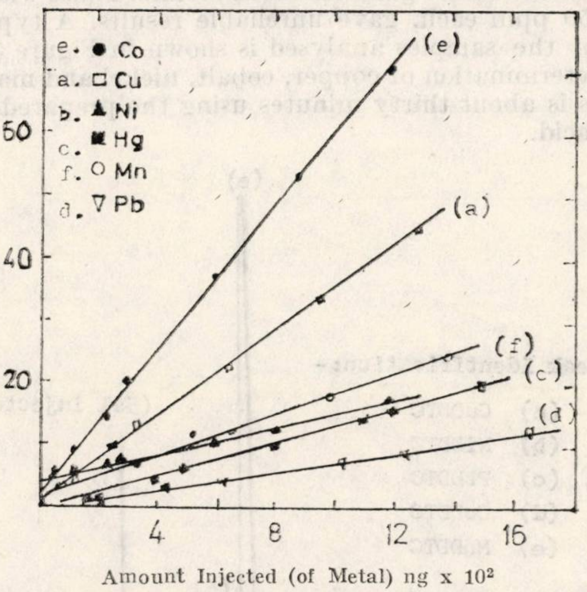

Fig. 2. — Dependence of peak height on the amount of metal injected for various metal-DDTC complexes.

Application to Soil Samples

The method of normal mode HPLC using diethyldithiocarbamate was applied to the analysis of soil samples from various sources including the Gezira Board, Sudan, Bauchi State Agricultural Development Programme (Bauchi State, Nigeria/World Bank Project), Nigeria and Dr. M. M. Thomson, Imperial College of Science and Technology, England. The samples were used as soil extracts in 1M hydrochloric acid.

5 ml of each appropriate extract of fifteen samples were treated in four batches by solvent extraction following the procedure described above. 1 ul of these organic extracts (5 ml) was eluted on the Hypersil column, using benzene as eluent. Each sample was run in replicate and, with each batch of samples, standards of known quantities of individual elements were also extracted and their HPLC chromatograms run along with the samples.

Peak identification was carried out by reference to the retention volume (V_R) of standard metal chelate peaks under similar conditions. This was subsequently confirmed by spiking the sample solution with a measured amount of a standard solution of the metal in question before the extraction step.

In some of the fifteen soil extracts examined in this study, it was found that the lead and zinc content was very high. This was as high as 600 to 900 ppm, and hence made the analysis of some trace metal difficult for a few of the samples.

However, the majority of the samples were found to contain low lead and zinc concentrations, hence do not interfere with the analysis of those samples. It was found that samples with up to 50 ppm each of lead and zinc in the soil extract gave excellent results. Those with lead and zinc levels above 50 ppm each, gave unreliable results. A typical chromatogram of one of the samples analysed is shown in Figure 3. The analysis time for the determination of copper, cobalt, nickel and manganese in one of the samples is about thirty minutes using the prepared soil extract in hydrochloric acid.

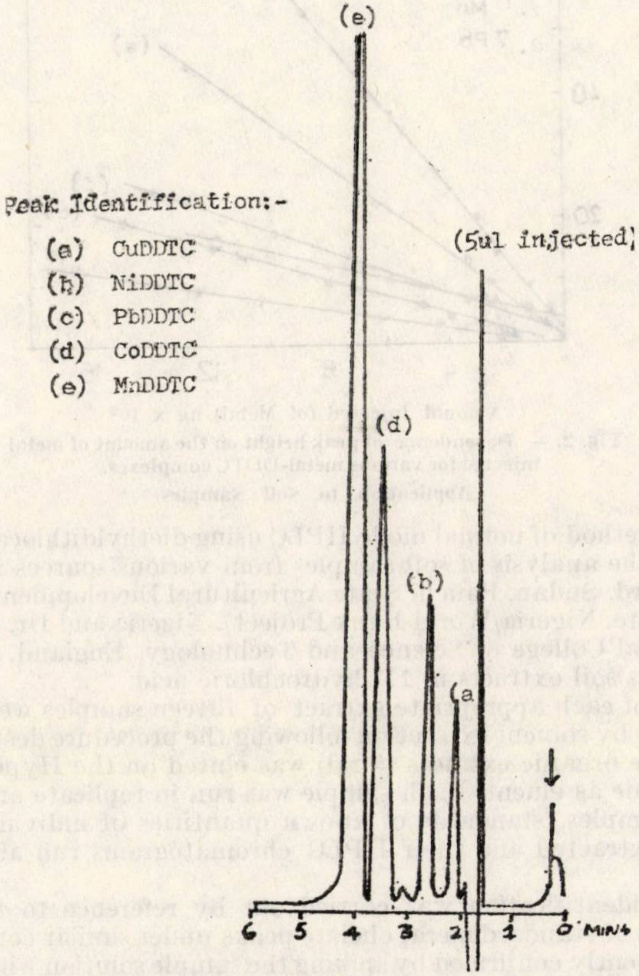

Fig. 3. — Typical soil sample (S.G.4) extracted at pH 8.5 with DDDTC solution in dry $CHCl_3$.

The results for the fifteen soil samples examined including the chromatographic conditions used are summarised in Table 1. The sample were also analysed by Atomic Absorption spectroscopy (AAS) method and the results were compared with those obtained by the HPLC method.

Table 1

Analysis of trace metals in soil samples. Column, Hypersil (5μm, 150×4.6 mm I.D.); Eluent, HPLC grade benzene; flowrate, 1.53 ml/min; pressure, 287 p.s.i. (19.5 bar); detector, UV, wavelength 285 nm at 0.01 a.u.f.s. Extraction was at a buffer pH of 8.5 with 0.5% (w/w) DDDTC in chloroform. 1μl sample injected as metal dithiocarbamates

Metal	Method	SAMPLE NO.														
		SG1	SG2	SG3	SG4	SG5	SN6	SN7	SN8	SN9	SN10	SK11	SK12	SK13	SK14	SK15
Copper/μgml^{-1}	Found by HPLC	0.08	0.3	0.3	1.15	0.3	0.2	—*	1.0	0.2	1.2	0.6	0.65	0.3	0.15	0.74
	Found by AAS	0.09	0.3	0.2	1.0	0.34	0.2	0.1	0.9	0.24	1.3	0.7	0.55	0.3	0.1	0.7
Nickel/μgml^{-1}	Found ny HPLC	—	0.6	0.3	0.4	0.46	2.5	0.3	1.1	0.8	—	—	0.3	0.1	—	—
	Found by AAS	0.07	0.5	0.2	0.4	0.56	2.6	0.2	1.0	0.4	0.6	0.3	0.3	0.16	0.04	40.1
Cobalt/μgml^{-1}	Found by HPLC	—	0.2	0.05	0.1	0.3	0.7	0.1	0.35	0.2	—	—	0.1	0.1	0.05	0.1
	Found by AAS	0.04	0.22	0.1	0.13	0.3	0.6	0.13	0.3	0.2	0.2	0.2	0.12	0.1	0.02	0.07
Manganese/μgml^{-1}	Found by HPLC	1.6	0.6	6.0	1.8	14.0	13.0	10.0	10.0	8.8	—	—	3.3	1.8	0.7	6.9
	Found by AAS	1.3	0.5	5.9	2.2	14.5	13.8	9.5	10.3	8.6	36.3	35.2	3.7	2.0	0.8	7.0

* Dashes indicate not detected

Samples SN10 and SK11 showed serious interference from lead and zinc possibly. However all other samples showed little or noi nterference effects during the determinations of the trace metals.

From the results shown in Table 1, it is observed that there is good agreement between the HPLC results and those obtained by the AAS method. Owing to interference by broad lead and zinc dithiocarbamate peaks the determination of manganese in particular in samples SE10 and SE11 respectively is affected adversely.

In conclusion the application of the method to the rapid analysis of soil samples extracts will be very useful particularly in developing countries where the careful characterization of soil samples for Agricultural usage is fast becoming a priority, as the dwindling food situation in such countries becomes more serious .This method owing to it sspeed of execution will be useful for adoption on a routine basis, especially for large sample throughout laboratories in developing countries, as the skills needed to apply the method are not too demanding.

ACKNOWLEDGEMENT. Grateful acknowledgement is hereby made to the Gezira Board in the Sudan, the Bauchi State, Ministry of Agriculture and Forestry Resources, Bauchi, Nigeria and Dr. M. Thompson, of Imperial College of Science and Technology, London, England, for generous gift of Soil Samples.

REFERENCES

[1] M. Schnitzer and S.I.M. Skinner, *Soil Science*, **102**, 361 (1966).
[2] M. Schnitzer, *Soil Sci. Soc. Amer. Proc.*, **33**, 75 (1969).
[3] W. J. Price, "Analytical Atomic Absorption Spectrometry", Heyden, London, 1972
[4] J. Stary, "The Solvent Extraction of Metal Chelates", Pergamon Press, Oxford, 1964.
[5] P. R. Hesse, "A Textbook of Soil Chemical Analysis", John Murray, London, 1971.
[6] M. L. Jacskon, "Soil Chemical Analysis", Constable, 1958.

Revue Roumaine de Chimie, 35, 4, 503–509 (1990)

ADSORPTION OF CATIONS ON OXIDES

FOUAD TAHA*, A. M. EL-ROUDI, A. A. ABD EL GABER and F. M. ZAHRAN
Chemistry Department, Faculty of Science, Minia University, Minia, Egypt

Received November 21, 1987

Over a wide range of pH, the electrokinetic potentials of eighteen oxides have been measured in solutions of KCl, $CaCl_2$ and $AlCl_3$. The adsorption of K^+, Ca^{++} ions on the oxides is physical in nature. The isoelectric points of all oxides in presence of 1 m mole/L of $AlCl_3$ solution are constant at 8.25 ± 0.25. That is an indication for the precipitation of $Al(OH)_3$ and complete surfaces coverage on the oxides by Al^{+3} ions. The non-indifferent electrolytes do not exhibit a certain behaviour, due to the different relative change in solubility and to the different formation of metal hydroxides which depend on the pH of the medium.

INTRODUCTION

Development of ion exchange technology using inorganic salts requires the characterisation of the nature of the adsorption forces acting between multivalent ions and oxide surfaces. This study has received considerable attention in recent years. [1-3]

Research workers concluded that the adsorption is considered to be specific if : 1) the isoelectric point (IEP) of the oxide in the test electrolyte is shifted relative to the IEP of the suspended oxide in water : 2) the IEP of the oxide depends on the concentration of electrolyte in solution or/and 3) in presence of the ions, charge reversal of the oxide surface occurs The adsorption is electrostatic in nature if any of these concepts is not applicable. The specific adsorption of anions on oxide-water interface is often thought to involve either ligand exchange for surface OH groups or a directed adsorption site adsorpate interaction that does not involve ligand exchange .[4] Nechaev and Sein [2] suggested that specific adsorption can take place on both charged and uncharged centers of the oxide surface depending on the conditions.

The present work throws some light on the adsorption of different cations K^+, Ca^{++} and Al^{+3} on various oxides, by measuring the electrokinetic potentials of these oxides in the chloride solutions of the salts over a wide range of pH 2 – 12. The effect of the non-indifferent electrolytes on the zero point charge of these oxides is also discussed.

*** Author for correspondence.**

EXPERIMENTAL

The oxides (natural or chemically pure (Table 1) were prepared by washing in bidistilled cled water several times until they were free of Cl^- ions, after which they were dried at 110°C The electrophoretic mobilities of particles were measured at 25°C using particle micro electrophoresis, Rank-Mark II instrument,[5,6] and the pH of the solutions was measured with a pH-meter, 710 A digital ionalizer. The zeta potential was calculated from the mobility data by means of the equation.

$$\xi = 14.3\ \nu/E \text{ m.v. at } 25°\text{C}$$

where ν represents the mobility of the particles, micron/s, and E the electric field strength $V.cm^{-1}$. No corrections were made for a retardation effect.[6] All chemicals used in this work were chemically pure.

RESULTS AND DISCUSSION

From the data depicted in figures 1 — 3, it can be seen that all studied oxides, except BeO, Cu_2O, PbO and La_2O_3 acquire a negative surface charge in bidistilled water. The pH of the solution depends on nature of the tested oxides (Table 1). The oxides of quadrivalent and hexavalent

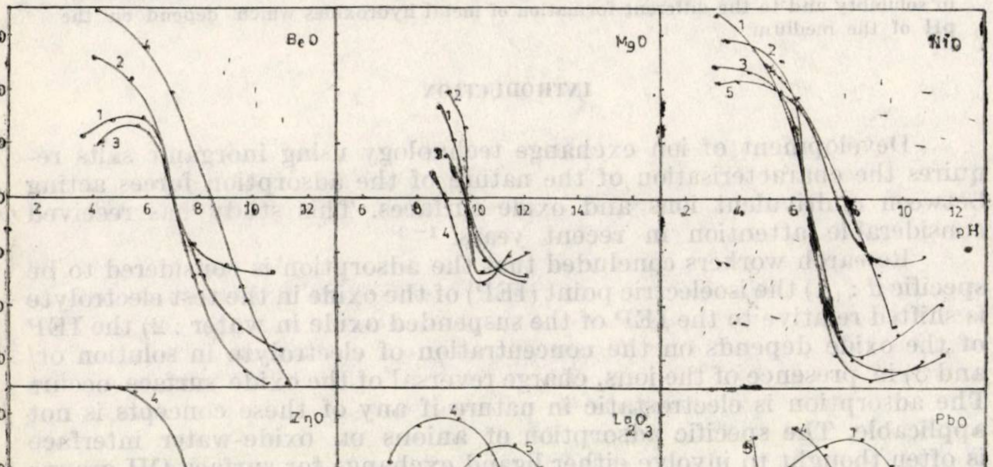

Fig. 1—3. — The effect of pH of the solution on ξ-potential of different oxides in presence of 1.0 1.0 m mol/1 salt : 1 — in absence of salts ; 2 — KCl ; 3 — $CaCl_2$; 4 — $AlCl_3$; 5 — in presence of non-indifferent electrolytes.

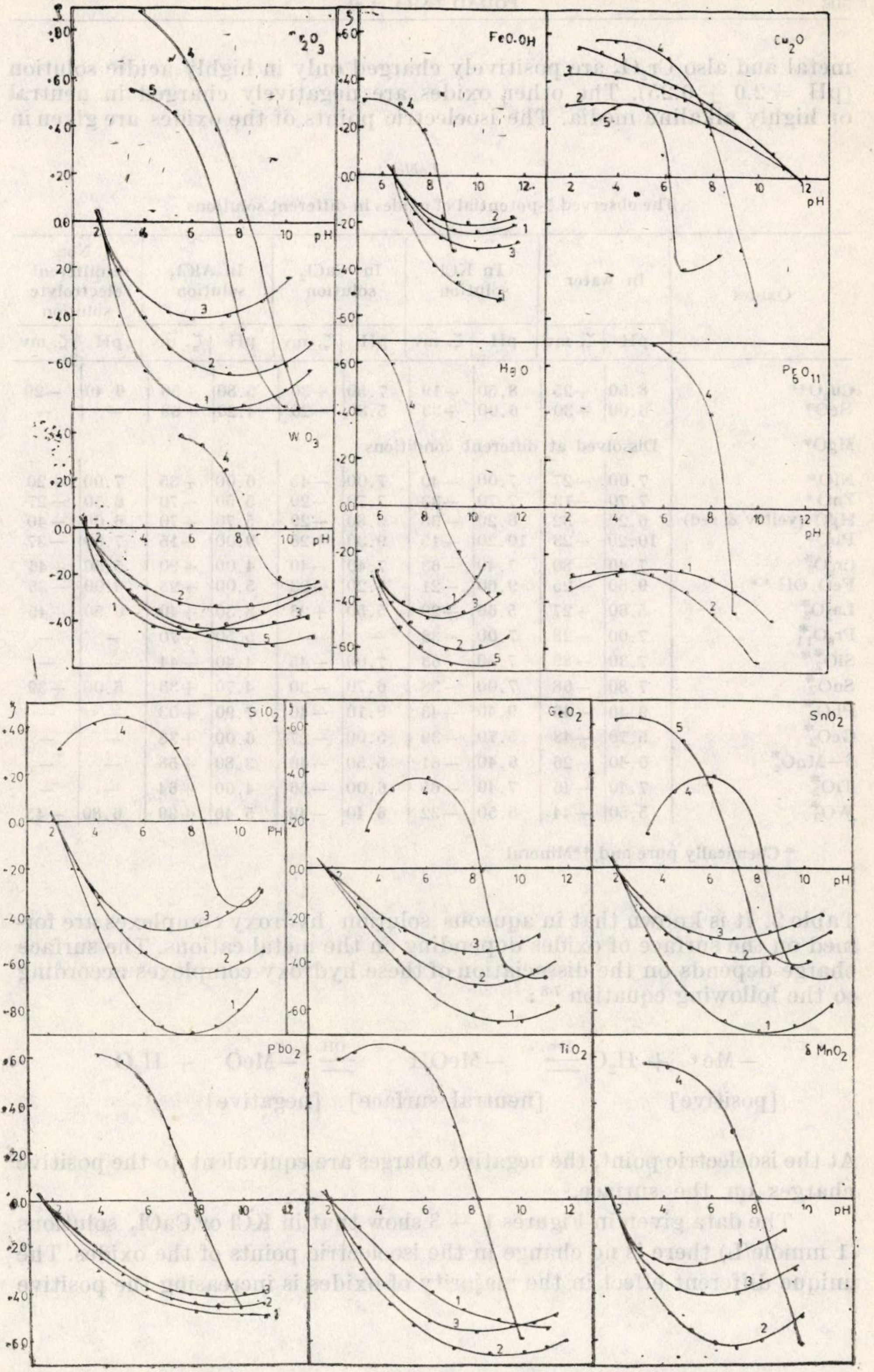
ζ
Fe2O3
FeO.OH
Cu2O
HgO
Pr6O11
WO3
SiO2
GeO2
SnO2
PbO2
TiO2
δ MnO2
+80
+60
+40
+20
0.0
-20
-40
-60
-80
2
4
6
8
10
12
pH
1
2
3
4
5

metal and also Cr_2O_3 are positively charged only in highly acidic solution ($pH = 2.0 \pm 0.25$). The other oxides are negatively charged in neutral or highly alkaline media. The isoelectric points of the oxides are given in

Table 1

The observed ζ-potential of oxides in different solutions

Oxides	In water		In KCl solution		In $CaCl_2$ solution		In $AlCl_3$ solution		Non indifferent electrolyte solution	
	pH	ζ, mv	pH	ζ, mv	pH	ζ, mv	pH	ζ, mv	pH	ζ, mv
Cu_2O**	8.50	+25	8.50	+19	7.50	+30	5.80	+50	6.40	−20
BeO*	6.00	+30	6.00	+33	5.80	+26	4.20	+69	—	—
MgO*	Dissolved at different conditions									
NiO*	7.00	−27	7.00	−40	7.00	−45	6.00	+35	7.00	+20
ZnO*	7.70	−13	7.70	−33	7.70	−20	5.50	+70	6.50	+27
HgO*(yellov & red)	6.20	−32	6.20	−38	5.80	−29	5.70	+70	6.00	−40
PbO*	10.20	+23	10.20	+15	9.30	+26	9.00	−15	7.00	−37
$Cr_2O_3^*$	7.40	−80	7.40	−63	7.40	−40	4.00	+90	5.50	+46
FeO.OH **	9.60	−25	9.60	−21	8.20	−23	5.00	+28	8.00	−35
$La_2O_3^*$	5.60	+27	5.60	+20	5.50	+26	3.30	+40	6.50	+45
$Pr_6O_{11}^*$	7.00	−28	7.00	−36	—	—	5.50	+70	—	—
SiO_2^{**}	7.30	−89	7.30	−63	7.00	−45	4.40	+44	—	—
SnO_2^*	7.80	−68	7.00	−38	6.70	−30	4.70	+33	6.00	+39
PbO_2^*	9.40	−46	9.40	−43	9.10	−40	7.90	+03	—	—
GeO_2^*	5.70	−48	5.70	−39	5.00	−27	6.00	+38	—	—
$\delta-MnO_2^*$	6.40	−26	6.40	−61	5.50	−40	3.80	+58	—	—
TiO_2^*	7.40	−46	7.40	−65	6.00	−56	4.00	+64	—	—
WO_3^*	5.50	−44	5.50	−32	6.40	−42	5.40	+39	6.80	−45

* Chemically pure and **Mineral

Table 2. It is known that in aqueous solution hydroxy complexes are formed on the surface of oxides depending on the metal cations. The surface charge depends on the dissociation of these hydroxy complexes according to the following equation [7,8]:

$$\underset{\text{[positive]}}{-Me^+ + H_2O} \overset{H^+}{\rightleftharpoons} \underset{\text{[neutral surface]}}{-MeOH} \overset{OH}{\rightleftharpoons} \underset{\text{[negative]}}{-MeO^- + H_2O}$$

At the isoelectric point, the negative charges are equivalent to the positive charges on the surface.[3]

The data given in Figures 1 — 3 show that in KCl or $CaCl_2$ solutions (1 mmole/L) there is no change in the isoelectric points of the oxides. The unique different effect in the majority of oxides is increasing the positive

Table 2

The observed isoelectric points of the investigated oxides in the different conditions

Oxides	IEP Values				
	In water	In KCl solution	In $CaCl_2$ solution	In $AlCl_3$ solution	Non indifferent electrolyte solution
Cu_2O	11.50	11.50	11.50	8.40	6.2($CuCl_2 \cdot 2H_2O$)
BeO	7.10	7.10	7.10	8.50	—
MgO	9.80	9.80	9.80	8.00	9.2($MgCl_2 \cdot 6H_2O$)
NiO	6.40	6.40	6.40	8.00	7.5($NiCl_2 \cdot 6H_2O$)
ZnO	6.90	6.90	6.90	8.30	8.4($ZnSO_4.6H_2O$)
HgO(yellow and red	Soluble at pH< 6 and gives negative ζ-Potentials at pH ~ 6−12			8.40	—
PbO	10.70	10.70	10.70	8.20	5.2($Pb(NO_3)_2$)
Cr_2O_3	2.25	2.25	2.25	8.40	7.1($Cr_2(SO_4)_3$)
FeO.OH	6.60	6.60	6.60	8.40	6.6($FeCl_3$)
La_2O_3	6.70	6.70	6.70	8.20	9.9($LaCl_3$)
Pr_6O_{11}	ζ-Potentials are —ve at all pH's		0.00	8.50	—
SiO_2	2.20	2.20	2.20	8.50	—
SnO_2	2.00	2.00	2.00	8.40	7.2($SmCl_2 \cdot 2H_2O$)
PbO_2	1.75	1.74	1.75	8.00	—
GeO_2	1.85	1.85	1.85	8.30	—
$\delta-MnO_2$	1.90	1.90	1.90	8.00	—
TiO_2	2.00	2.00	2.00	8.20	—
WO_3	1.95	1.95	1.85	8.40	1.95($Na_2WO_4.2H_2O$)

or decreasing the negative values of ζ-potential. This is presumably attributed to the physical adsorption of K^+ or Ca^{++} ions on the oxides surfaces and / or to the increasing in the ionic strength of the solution, which decreases the thickness of the double layer. The effect of Ca^{++} ions on the ζ-potential of oxides is higher than that of K^+ ions. The small effect of the divalent Ca^{++} ions on the electrokinetic potential of oxides may be due to the small concentration of these ions in the solution.

It is worth noting that in presence of Ca^{++} ions :

i) in PbO/$CaCl_2$ system the surface charge is zero at $pH > 10.0$. This indicates that at $pH > 10.0$ the adsorption of Ca^{++} ions is equivalent to that of OH^- ions.

ii) in ZnO/$CaCl_2$ system there is a small increase in the negative charge of the oxide surface at pH> IEP, but at *pH* < IEP, ZnO is soluble in $CaCl_2$ solution.

iii) in Pr_6O_{11}/$CaCl_2$ system, the surface charge is zero over a wide range of pH. This shows that the energy of Ca^{++} ions interaction with Pr_3O_{11} surface is so great that adsorption of the ions brings about an increase in degree of dissociation, at least for the nearest —M—OH groups .[2] Here, regardless of the pH, the negatively charged surface is neutralised by Ca^{++}, ions, and ζ-potential becomes zero.

The above-mentioned notes were clearly observed also from the effect of $CaCl_2$ on the turbidity of the sol solutions. This shows that the adsorption of Ca^{++} ions and the majority of the studied oxides except PbO, ZnO and Pr_6O_{11} is not specific in nature.

Curves 4 in Figures 1 — 3 illustrates the effect of addition of 1 mmole/L $AlCl_3$ to sol solutions on zeta potential of oxides. The isoelectric points of all oxides in $AlCl_3$ solution are constant and lie at pH 8.25 ± ± 0.25 (Table 2). This is in agreement with the previously reported value of IEP of $Al(PH)_3$.[9] This can be considered as a powerful indication for the precipitation and complete surface coverage of the oxides by $Al(OH)_3$.

In order to discuss the effect of $AlCl_3$ on the surface charges of oxides at different pH, the concentrations of aluminium hydroxy species at different pH must be calculated.

These calculations were made by assuming activity coefficients of unity and by utilizing the following equilibria :[10,11]

$$Al^{+++} + H_2O \rightleftharpoons AlOH^{++} + H^+ \tag{1}$$

$$K_1 = \frac{[AlOH^{++}]\,[H^+]}{[Al^{+++}]} = 1.4 \times 10^{-5}$$

$$Al(OH)_3\,(s) \rightleftharpoons Al^{3+} \times 3\ OH^- \tag{2}$$

$$K_2 = [Al^{3+}][OH^-]^3 = = 1.9 \times 10^{-33}$$

$$Al(OH)_3(s) \rightleftharpoons H_2AlO_3^- + H^+ \tag{3}$$

$$K_3 = [H_2AlO_3^-]\,[H^+] = 1.1 \times 10^{-15}$$

$$[Al^{3+}] + [AlOH^{++}] + [Al(OH)_3] + [H_2AlO_2^-] = 10^{-3}\ mol/l \tag{4}$$

The distribution of aluminium hydroxy complexes in solutions of different pH' s is given in Table 3. Table 3 shows that the positive charge on the surface of oxides in presence of $AlCl_3$ at pH < IEP is due to the adsorption

Table 3

Calculated concentrations of the various aluminium hydroxy species as a function of pH for an addition of 1 × 10^{-3} molar $AlCl_3$ to water

pH	Al^{+3}	$AlOH^{++}$	$Al(OH)_3(s)$	$H_3AlO_3^-$
4.0	8.8×10^{-4}	1.2×10^{-4}	0.0	0.0
5.0	1.9×10^{-6}	2.66×10^{-6}	9.95×10^{-4}	1.10×10^{-10}
6.0	1.9×10^{-9}	2.66×10^{-8}	1.00×10^{-3}	1.10×10^{-9}
7.0	1.9×10^{-12}	2.66×10^{-10}	1.00×10^{-3}	1.10×10^{-8}
8.0	1.9×10^{-15}	2.66×10^{-12}	1.00×10^{-3}	1.10×10^{-7}
8.2	4.8×10^{-16}	1.06×10^{-12}	1.00×10^{-3}	1.70×10^{-7}
8.4	1.2×10^{-16}	4.20×10^{-13}	1.00×10^{-3}	2.80×10^{-7}
8.6	3.0×10^{-17}	1.70×10^{-13}	1.00×10^{-3}	4.40×10^{-7}
8.8	7.6×10^{-18}	6.70×10^{-1}	1.00×10^{-3}	6.90×10^{-7}
9.0	1.9×10^{-18}	2.66×10^{-14}	1.00×10^{-3}	1.10×10^{-6}

of $AlOH^{++}$ and Al^{3+} ions and the negativity of the surface at $pH > IEP$ is due to the adsorption of $H_2AlO_3^-$ ions. At the isoelectric point the concentration of the positive ions on the surface is equal to that of negative ions, i.e.

$$[Al^{3+}] + [AlOH^{2+}] = [H_2AlO_3^-]$$

This shows that the major part of $H_2AlO_3^-$ ions on the surface goes into the solution.

In this investigation the effect of 1.0 m mol/L of nonindifferent electrolytes on the ζ-potential of the oxides is also studied. The results are illustrated in Figures 1 — 3, curve 5 and the new isoelectric points are tabulated in Table 2. The values of IEP obtained do not exhibit a definite direction; they may be increased (as in case of Cr_2O_3, ZnO, La_2O_3, NiO and SnO_2), decreased (as in case of Cu_2O and PbO) or not changed (as in case of WO_3, HgO, FeOOH). This behaviour can be attributed to the different extent of the relative change of the solubility of metal hydroxides $Me(OH)_n$ resulting from the excess existence of the same cation of oxide in its suspension.

In order to elucidate this phenomenon successively, it will be necessary in continuation of this work to carry out detailed studies with the simultaneous use of potentiometric titration technique.

REFERENCES

[1] S. M. Ahmed, "Oxides and Oxide Films", vol. 1, New York 1972, 319.

[2] E. A. Nechaev and V. N. Shein, *Kolloidnyi Zhurnal*, **41**, 361 (1979).

[3] G. A. Parks and P. L. De Bruyn, *J. Phys. Chem.*, **66**, 967 (1962).

[4] F. J. Hingston, R. J. Atkinson, A. M. Posner and J. P. Quirk, *Nature*, **215**, 1459 (1967).

[5] Fouad Taha, A. M. El-Roudi and M. B. Saleh, *Bull. Soc. Chim. Belg.*, **95**, 157, (1986).

[6] J. K. Critchley and S. R. Jewitt, *Trans. Inst. Min. Metall. Sec.* C, **88**, 57 (1979).

[7] S. M. Ahmed and D. Maksimov, *Can. J. Chem.*, **46**, 3841 (1968).

[8] S. M. Ahmed and D. Maksimov, *J. Colloid Interface Sci.*, **29**, 97, (1969).

[9] G. A. Parks, *Chem. Rev.*, **65**, 177 (1965).

[10] A. A. Abramov, S. B. Leonov, M. M. Sorakin, "Chemistry of Flotation Systems" M. Nedra 1982 (in Russian).

[11] C. M. Fuerstenau et al., "Transaction", Society of Mining Engineers, Dec. 1966, 321.

Revue Roumaine de Chimie, 35, 4, 511–521 (1990)

STUDIES ON COMPLEXATION OF Co(II), Ni(II), Cu(II), Zn(II) AND Cd(II) WITH 1-ACETYLIMIDAZOLE IN AQUEOUS SOLUTION

BARBARA BARSZCZ and JACEK KULIG
Institute of Chemistry, Pedagogical University,
25–020 Kielce, Poland

Received November 21, 1987

The formation of coordination compounds of 1-acetylimidazole with Co(II), Ni(II), Cu(II), Zn(II) and Cd(II) in aqueous solution has been studied by potentiometric and spectrophotometric methods. The composition and stability constants of the complexes were determined at a constant ionic strength, $I=0.5(KNO_3)$, at 25°C. The effect of substituents on the π-acceptor properties of the heterocyclic ring has been discussed.

INTRODUCTION

Our previous studies on coordination of the Co(II), Ni(II), Cu(II), Zn(II) and Cd(II) ions with heterocyclic ligands have shown that stability of the complexes was affected not only by the ligand basicity but also by the π-acceptor capacity of the ligands and the π-donor strength of the central ions. The contribution of the π-effect increases in going from a simple heterocyclic ring to molecules carrying more delocalised orbitals, such as acetylpyridine and 4-azobenzimidazole.

The purpose of this work was to determine equilibrium constants for the formation of the Co(II), Ni(II), Cu(II), Zn(II) and Cd(II) complexes of 1-acetylimidazole, the symmetry of the coordination sphere of the central ion and to estimate the contribution of the $\pi_{M\rightarrow L}$ effect to the metal-ligand bond. It was also of interest to evaluate the effect of the nature of the central ion on the strength of the $\pi_{M\rightarrow L}$ bond and the influence of the acetyl group on π-acceptor capacity of the heterocyclic ring.

EXPERIMENTAL

Reagents

1-Imidazolyl methyl ketone (Fluka A.G.), m.p. 93 – 96°C, was dried to constant weight and used without further purification. Solutions of the ligands of appropriate concentrations were prepared from weighed samples. The preparation of salt solutions and of nitric acid solutions was described.[1,2]

Equipmetn

Potentiometric measurements were carried out on a digital PHM-64 pH-meter (Radiometer, Copenhagen) using a GK 2401 C combination electrode.

The pH meter readings were checked against buffer solutions of pH 7.00 and 4.01 supplied by Radiometer.

The absorption spectra were taken with a Specord UV–VIS (Carl Zeiss, Jena) recording spectrophotometer using 1- and 2-cm quartz cuvettes.

Procedure

The complexation of Co(II), Ni(II), Cu(II), Zn(II) and Cd(II) with 1-acetylimidazole was studied by pH-metric titration at a fixed metal or ligand concentration. Particulars of this procedure were described elsewhere.[1,2] For each system studied, a few series of measurements were run at the central ion concentrations of 0.02, 0.03 and 0.05 mol × dm^{-3} as well as a few series of titrations with solutions of a fixed ligand concentration.

The dissociation constant of the acid form of the ligand was also determined potentiometrically using nitric acid as titrant.

Optical measurements were carried out with solutions of fixed metal concentration.

All measurements were run at 25 ± 0.1°C at a constant ionic strength (0.5, KNO_3).

RESULTS AND DISCUSSION

The dissociation constant of the protonated form of the ligand, K_a, was determined from pH-metric measurements. Over the free ligand concentration range 0.025 – 0.160 mol × dm^{-3} its value stabilised around 2.78×1^{-5}, whereas in the range 0.0 – 0.025 mol × dm^{-3} it dropped from 5.10×10^{-5} to $2.78\ 10^{-5}$.

On the basis of the pH measurements and the K_a values, the equilibrium ligand concentration, $[L]$, was found in solutions containing metal ions :

$$[L] = \frac{K_a(C_{HNO_3} - [H_3O^+])}{[H_3O^+]} \qquad (1)$$

To eliminate errors due to variation in the dissociation constant value, its value for particular ligand concentration, c_L, was taken from a plot of K_a against c_L. The calculated [L] values were then utilised for obtaining successive protonation constants $\bar{n}$ from the equation

$$\bar{n} = \frac{c_L - c_{HL^+} + [H_3O^+] - [L]}{c_M} \qquad (2)$$

where c_M is the analytical metal concentration.

These data enabled plotting of $\bar{n}$ against $-\log[L]$ for each cation (Fig. 1). The formation curves obtained in this way constituted a population of points for several concentrations of the metal ion. In each case, the shape of the curve is independent of the central ion concentration, thus indicating that only mononuclear species occur in solution. Further, the shape of the formation curves reveals that the complexation takes a similar course in each case.

The numerical values of the formation constants were found by the least-squares method.

Data of Table 1 show that 1-acetylimidazole forms less stable complexes with Co(II), Ni(II), Cu(II), Zn(II) and Cd(II) than those formed by both imidazole and 1-alkylimidazoles.

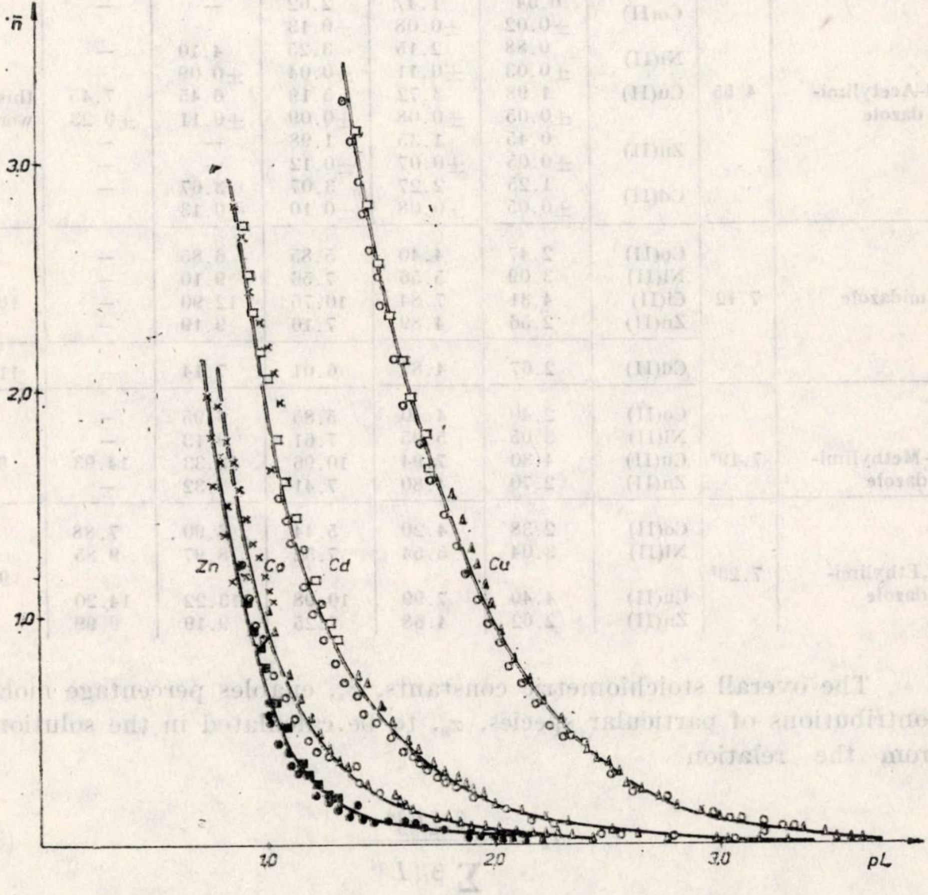

Fig. 1. — Formation curves of the Co(II), Cu(II), Zn(II) and Cd(II) complexes of 1-acetylimidazole at the following central ion concentrations : ○, ● — 20 mM ; □, ■ — 30mM ; △, ▲ = 50 mM ; x — results obtained at a fixed ligand concentration. The shape of the formation curve for the Ni(II) complexes resembles that for the Cd(II) ones.

The poorer stability can be attributed to the weak basicity of 1-acetylimidazole caused by inductive effect of the acetyl group. Our previous studies showed that the acetyl group in the pyridine ring lowered also the stability of the complexes.[34] The effect depends on the position of the acetyl group in the ring, 3-acetylpyridine complexes being less stable than their 4-acetylpyridine counterparts (Table 2).

Table 1

Stability constants of the imidazole and 1-substituted imidazole complexes at 25°C, ionic strength 0.5 (KNO_3)

Ligand	pK_a	$\log\beta_1$		$\log\beta_2$	$\log\beta_3$	$\log\beta_4$	$\log\beta_5$	Ref.
1-Acetylimidazole	4.55	Co(II)	0.54 ±0.02	1.47 ±0.08	2.62 ±0.13	—	—	this work
		Ni(II)	0.88 ±0.03	2.15 ±0.11	3.25 ±0.04	4.10 ±0.09	—	
		Cu(II)	1.98 ±0.05	3.72 ±0.08	5.19 ±0.09	6.45 ±0.11	7.45 ±0.23	
		Zn(II)	0.45 ±0.05	1.35 ±0.07	1.98 ±0.12	— —	— —	
		Cd(II)	1.25 ±0.05	2.27 ±0.08	3.07 ±0.10	3.67 ±0.13	—	
Imidazole	7.12	Co(II)	2.47	4.40	5.85	6.85	—	10
		Ni(II)	3.09	5.56	7.56	9.10	—	
		Ci(II)	4.31	7.84	10.76	12.90	—	
		Zn(II)	2.56	4.89	7.16	9.19	—	
		Cd(II)	2.67	4.87	6.01	7.14	—	11
1-Methylimidazole	7.19^{8}	Co(II)	2.40	4.40	5.85	6.95	—	8
		Ni(II)	3.05	5.95	7.61	9.13	—	
		Cu(II)	4.30	7.94	10.96	13.33	14.93	
		Zn(II)	2.70	4.80	7.41	9.32	—	
1,Ethylimidazole	7.23^{9}	Co(II)	2.38	4.20	5.44	6.90	7.88	9
		Ni(II)	3.04	5.54	7.52	8.97	9.85	
		Cu(II)	4.40	7.99	10.98	13.22	14.20	
		Zn(II)	2.62	4.68	7.25	9.19	9.99	

The overall stoichiometric constants, β_n, enables percentage molar contributions of particular species, α_n, to be calculated in the solutions from the relation

$$\alpha_n = \frac{\beta_n[L]^n}{\sum\limits_{i=0}^{N} \beta_i[L]^i} \tag{3}$$

where N is a maximum coordination number of the central ion.

The plots of α_n vs pH (Figs. 2 and 3) enable determination of the pH intervals over which particular successive complexes predominate. It is seen that the concentration of the free metal ions, α_0, sharply decreases as the ligand concentration, and at the same time the pH of solution increases. In no system considered, however, such a pH interval could be distinguished in which a particular type of the successive complex occurred exclusively.

Table 2

Stability constants of the pyridine and substituted pyridine complexes at 25°C, ionic strength 0.5(KNO_3)

Ligand	pK_a		$\log\beta_1$	$\log\beta_2$	$\log\beta_3$	$\log\beta_4$	Ref.
		Co(II)	1.15	1.70	1.40		
		Ni(II)	1.78	3.00	3.30	3.00	
Pyridine	5.21	Cu(II)	2.50	4.40	5.95		12
		Zn(II)	0.98	1.45	1.60	1.40	
		Cd(II)	1.42	1.96	2.40		
		Co(II)	0.86	1.51			
		Ni(II)	1.45	2.19			4
3-Acetylpyridine	3.48	Cu(II)	1.76	2.91	3.27		
		Zn(II)	0.65	1.40			
		Cd(II)	0.89	1.83			
		Co(II)	1.10	1.22	2.46		
		Ni(II)	1.58	2.85	3.81		
3-(N-acetyl-amino) pyridine	4.58	Cu(II)	2.16	3.96	5.38	6.43	13
		Zn(II)	1.00	1.68	2.02		
		Cd(II)	1.37	2.44	3.38		
		Co(II)	0.97	1.38			
		Ni(II)	1.50	2.43	2.79		
4-Acetylpyridine	3.70	Cu(II)	1.83	3.13	3.89	4.11	3
		Zn(II)	0.90	1.32			
		Cd(II)	1.15	1.87			

To evaluate the influence of other factors on the stability of 1-substituted imidazoles, substitution constants of protons by metal ions, $*\beta_1$, have been examined.

The $*\beta_1$ values refer to the equilibrium

$$M^{2+} + HL^{+} \rightleftharpoons ML^{2+} + H^{+} \tag{4}$$

and can be expressed by

$$*\beta_1 = \frac{[ML^{2+}][H^{+}]}{[M^{2+}][ML^{+}]} = \beta_1 \times K_a \tag{5}$$

Hence

$$\log*\beta_1 = \log\beta_1 - pK_a \tag{6}$$

Expression (6) shows that the $\log*\beta$ values characterize stability of metal complexes after elimination of the basicity of the ligand. Thus they enable the estimation of the contribution of $\pi_{M\rightarrow L}$ to the coordination link apart from the σ bond.

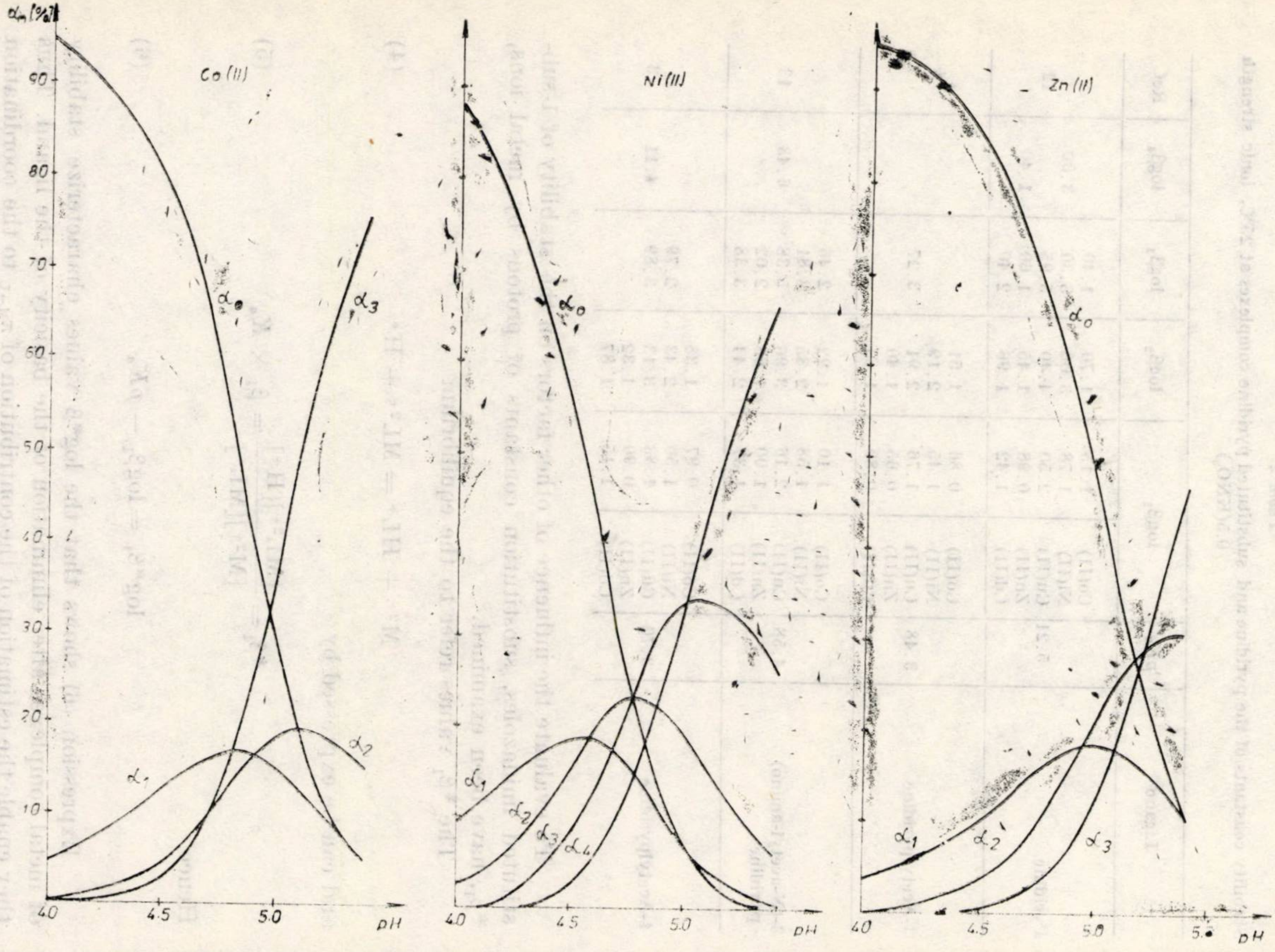

Fig. 2. — Molar contributions of particular Co(II), Ni(II) and Zn(II) complexes of 1-acetylimidazole as a function of the pH of solution.

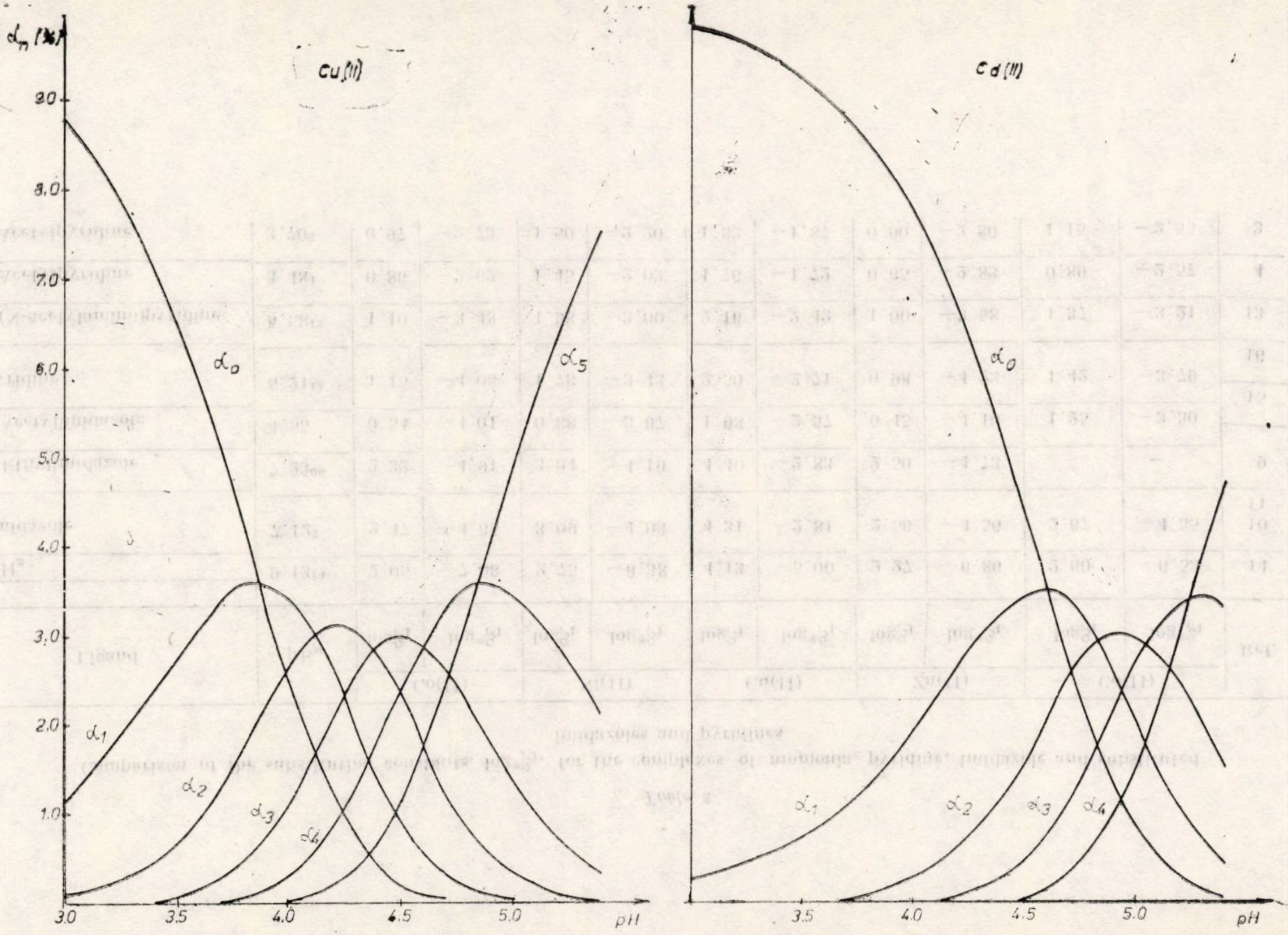

Fig. 3. — Molar contributions of particular Cu (II) and Cd(II) complexes of 1-acetylimidazole as a function of the pH of solution.

Table 3

Comparison of the substitution constants, $\log^*\beta_1$, for the complexes of ammonia, pyridine, imidazole and substituted imidazoles and pyridines

Ligand	pK_a	Co(II)		Ni(II)		Cu(II)		Zn(II)		Cd(II)		Ref.
		$\log\beta_1$	$\log^*\beta_1$	$\log\beta_1$	$\log^*\beta_1$	$\log\beta_1$	$\log^*\beta_1$	$\log\beta_1$	$\log^*\beta_1$	$\log\beta_1$	$\log^*\beta_1$	
NH_3	9.13[14]	2.05	−7.08	2.75	−6.38	4.13	−5.00	2.27	−6.86	2.60	−6.53	14
Imidazole	7.12[7]	2.47	−4.65	3.09	−4.03	4.31	−2.81	2.56	−4.56	2.67	−4.55	10 11
1-Ethylimidazole	7.23[09]	2.32	−4.91	3.04	−4.19	4.40	−2.83	2.50	−4.73	—	—	9
1-Acetylimidazole	4.55	0.54	−4.01	0.88	−3.67	1.98	−2.57	0.45	−4.10	1.25	−3.30	15
Pyridine	5.21[12]	1.15	−4.06	1.78	−3.43	2.50	−2.71	0.98	−4.23	1.42	−3.79	16
3-(N-acetylamino)pyridine	5.58[13]	1.10	−3.48	1.58	−3.00	2.16	−2.42	1.00	−3.58	1.37	−3.21	13
3-Acetylpyridine	3.48[4]	0.86	−2.62	1.45	−2.03	1.76	−1.72	0.65	−2.83	0.89	−2.57	4
4-Acetylpyridine	3.70[3]	0.97	−2.73	1.50	−2.20	1.83	−1.87	0.90	−2.80	1.15	−2.55	3

As it has been shown previously,[5,6] the higher the log$^*\beta_1$ values, the larger the contribution of the $\pi_{M\to L}$ component to the coordination linkage.

In Table 3 the log$^*\beta_1$ values are listed for the imidazole, pyridine and ammonia complexes. The molecule of ammonia does not exhibit π-acceptor properties. Hence, the stability of its complexes is determined by the strength of the $\sigma_{L\to M}$ bond only and consequently the complexes show low, negative log$^*\beta_1$ values.

A comparison of the log$^*\beta_1$ values (Table 3) reveals that both the pyridine and the imidazole rings exhibit π-acceptor properties, those of the 1,3-diazole being less pronounced than of pyridine. The π-acceptor properties of the imidazole ring depend on the nature of substituent. Substituents having positive inductive effects, i.e. increasing the electron density on the nitrogen atom of the ring (for instance, CH_3, C_2H_5) weaken the π-acceptor strength of the ligand. The 1-acetylimidazole complexes are slightly more stable than would be expected based on the ligand basicity only. The presence of the acetyl group with negative inductive effect enhances the π-acceptor properties of the azole. Consequently, in the Co(II), Ni(II), Cu(II), Zn(II) and Cd(II) complexes of 1-acetylimidazole the contribution of $\pi_{M\to L}$ is larger than in analogous complexes of imidazole and of 1-alkylimidazoles (Table 3).

The variation in the π-acceptor properties of the alkyl and acetyl derivatives of imidazole and pyridine in their complexes with Co(II), Ni(II), Cu(II) and Zn(II) is shown in Fig. 4 in which log$^*\beta_1$ values are plotted against the number of *d* electrons of the central ion. These graphs allow the substitution constants to be arranged in the following order :

3-Acpy > 4-Acpy > 3-NHAcpy $\approx$ 1-VinIz > py > 1-AcIz > Iz > 1-EtIz

It may be hypothesized that there is a similar rank order of the $\pi_{M\to L}$ components. Fig. 4 also shows that the weakest π-donors are the Co(II) and Zn(II) ions.

To determine the structure of the complexes in aqueous solution, absorption spectra were taken of the 1-acetylimidazole complexes with Co(II), Ni(II) and Cu(II) over the visible range. Both the shape and band positions show the compounds to be six-coordinate with an octahedral or pseudo-octahedral symmetry of the coordination sphere (Table 4). Hypsochromic shifts of the spectra are due to progressing interaction of the ligand fields due to substitution of the water molecules in the coordination sphere of the metal by the ligand molecules. The shape of the formation curves of the Co(II), Ni(II), Cu(II), Zn(II) and Cd(II) complexes of 1-acetylimidazole (Fig. 1) shows that the symmetry of the coordination sphere of all the metal ions should be identical or almost identical. It can thus be assumed that also Zn(II) and Cd(II) form six-coordinate compounds of pseudooctahedral symmetry.

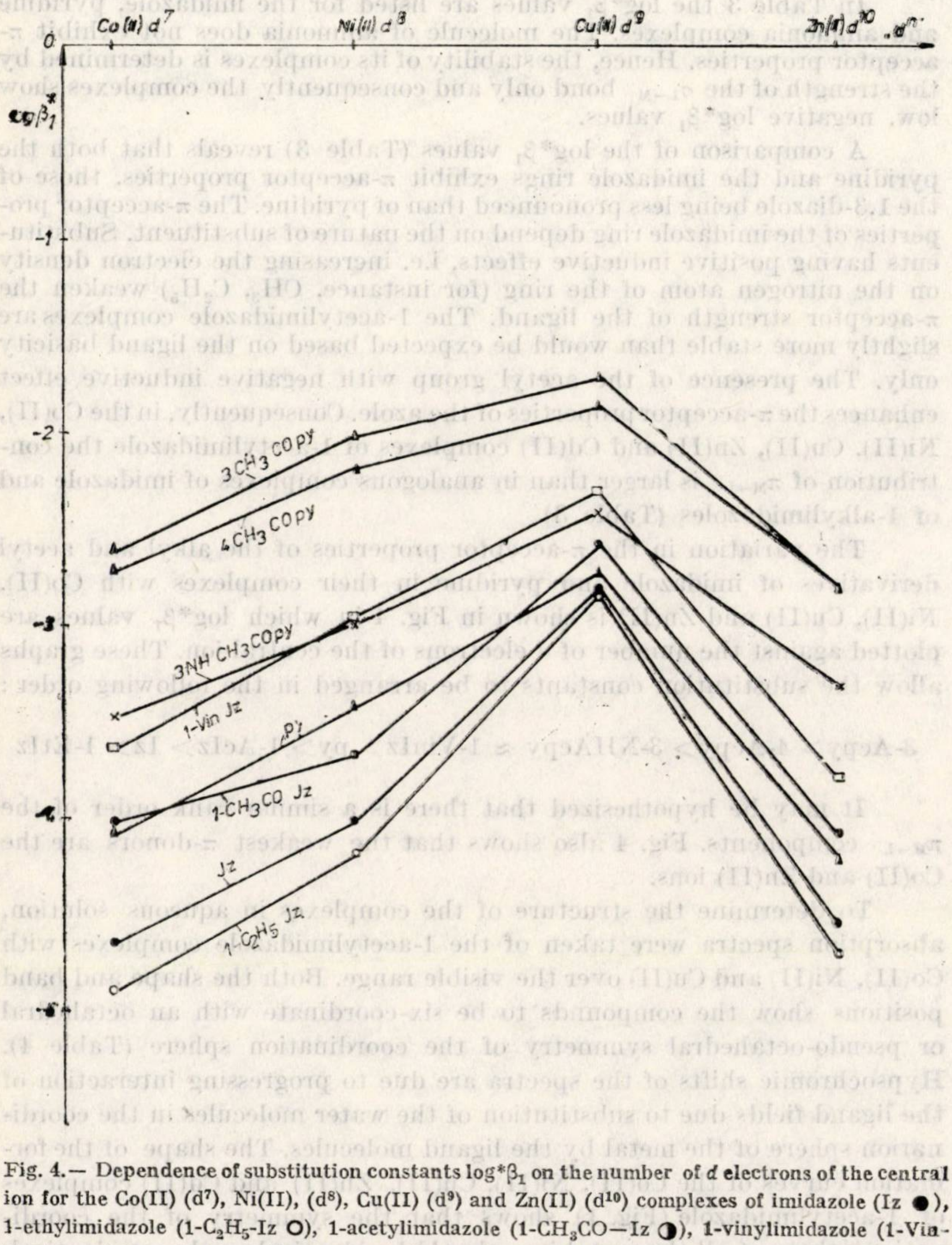

Fig. 4.— Dependence of substitution constants log*β_1 on the number of *d* electrons of the central ion for the Co(II) (d^7), Ni(II), (d^8), Cu(II) (d^9) and Zn(II) (d^{10}) complexes of imidazole (Iz ●), 1-ethylimidazole (1-C_2H_5-Iz ○), 1-acetylimidazole (1-CH_3CO—Iz ◑), 1-vinylimidazole (1-Vin-Iz□), pyridine (py▲), 3-(N-acetylamino) pyridine (3-$NHCOCH_3$py x), 3-acetyl-pyridine (3-CH_3COpy △) and 4-acetylpyridine (4-CH_3COPy▲).

Table 4

Position of the absorption bands of the Co(II), Ni(II) and Cu(II) complexes of 1-acetylimidazole in aqueous solution

Ligand	Observed electronic transitions Band positions are expressed in kK		
	Co(II)	Ni(II)	Cu(II)
	$^4T_{1g}(F) \rightarrow {}^4T_{1g}(P)$	$^3A_{2g}(F) \rightarrow {}^3T_{1g}(P)$	$^2E_g \rightarrow {}^2T_{2g}$
H_2O	19.4	25.3	12.6
1-Acetylimidazole	19.5	25.4	13.8

CONCLUSIONS

1. 1-Acetylimidazole forms mononuclear coordination compounds of pseudooctahedral symmetry of the coordination sphere with Co(II), Ni(II), Cu(II), Zn(II) and Cd(II).
2. The acetyl substituent lowers the basicity of imidazole, thus enhancing its π-acceptor strength. In the series of 1-substituted imidazoles the π-acceptor strength decreases in the following order:

   1-VinIz > 1-AcIz > Iz > 1-EtIz
3. Among the metal ions studied, the most pronounced π-donor character is exhibited by Cu(II) and Ni(II).

REFERENCES

[1] B. Lenarcik, J. Kulig and P. Leidler, *Roczniki Chem.*, **48**, 1151, (1974).

[2] B. Lenarcik B. Barszcz and J. Kulig, *ibid.*, **51**, 1315, (1977).

[3] B. Lenarcik and M. Rzepka *Polish J. Chem.*, **57**, 1149, (1983).

[4] E. Bezak-Mazur, B. Lenarcik and M. Rzepka *ibid.*, **60**, 399 (1986).

[5] M. Gabryszewski Thesis, Łódź, 1980

[6] M. Gabryszewski and B. Lenarcik *Polish J. Chem.*, **59**, 129, (1985).

[7] A. Chakravorty and F. A. Cotton, *J. Phys. Chem.*, **67**, 2978, (1963).

[8] B. Lenarcik and B. Barszcz *Roczniki Chem* **51**, 1849 (1977).

[9] B. Lenarcik B. Barszcz *Polish J. Chem.*, **53**, 963 (1979).

[10] E. V. Sklenskaya and M. Kh. Karapet yants *Russ. J. Inorg. Chem.*, **11**, 1102 (2061) (1961).

[11] G. Berthon, C. Luca, *Anal. Chim., Acta*, **51**, 239 (1970).

[12] J. Bjerrum, *Chem, Rev.*, **46**, 381, (1950).

[13] B. Lenarcik and M. Rzepka, *Polish J. Chem.*, **55**, 503, (1981).

[14] J. Bjerrum, "Metal Ammine Formation in Aqueous Solution", Copenhagen, 1957.

[15] J. Bjerrum, *Acta Chem. Scand.*, **27**, 970. (1973).

[16] C. Petitfaux *Ann. Chim. (Paris)* **8**, 33 (1973).

Revue Roumaine de Chimie, 35, 4, 523–533 (1990)

ADDITIVITY OF VISCOSITY IN BINARY AND TERNARY AQUEOUS-ORGANIC MIXTURES

ANTONIO ARROYO

Departament of Química Física, Colegio Universitario de Burgos, 09001 Burgos, Spain

Received November 21, 1987

Viscosities and densities for twenty binary and ternary liquid mixture systems have been measured as a function of composition at 25°C and ambient pressure. Systems were formed by the possible blends of polar liq. water, methanol, ethanol, 2-propanol and acetone. It is shown that viscosity calculated making use of mixture law agrees with experimental data within an average absolute error less than 5 %,

INTRODUCTION

The viscosity of liquid mixtures is of interest in many fields of research and industry : this datum is fundamental for the design of industrial equipments ; it plays an important role in biological processes ; it is a conditional factor of electrolytic properties of solvent mixtures because a low viscosity implies a low resistance to ionic transport, etc.

The present study has a twofold purpose : a) to measure experimentally the viscosities of binary and ternary mixtures formed by water (W), methanol (M), ethanol (E), 2-propanol (2P) and acetone (A) as a composition function, and b) to postulate a simple method for predicting the viscosity of polar liquid mixtures.

There has been a number of reviews and data compilations on viscosities of different binary and ternary solvent systems, but there is a greater number of systems whose viscosities are unknown. Various empirical or semiempirical equations for viscosity prediction in liquid mixtures as a composition function have been proposed,[1-4] ; these equations contain multiple adjustable parameters or equilibrium thermodynamic data, but this procedure is of little efficacy when mixture data are unavailable.

The method proposed here for mixture viscosity prediction is based on mixture law described by Stair[4] as an arithmetic mean

$$\bar{\eta}_{M(a)} = \left(\sum_i x_i \nu_{Mi} \right) \rho \qquad (1)$$

a geometric mean

$$\bar{\eta}_{M(g)} = \ln \rho + \sum_i x_i \ln \nu_{Mi} \qquad (2)$$

or a harmonic mean

$$\bar{\eta}_{M(h)} = \rho^{-1} \sum_i x_i \nu_{Mi}^{-1} \tag{3}$$

where η_M is mean mole viscosity, ρ is density of mixture, i denotes each pure component or molecular cluster stabilized by means of intermolecular bonds, x_i are mole fractions of components and ν_{Mi} are kinematic viscosities defined as

$$\nu_{Mi} = (\eta_i Mi)/\rho_i \tag{4}$$

The mixture absolute viscosity is predicted by

$$\eta = \bar{\eta}_M / \sum_i x_i Mi \tag{5}$$

where Mi is molar mass of i.

EXPERIMENTAL

Methanol, ethanol, 2-propanol and acetone (Fluka, analytical grade) were dried with 4 Å molecular sieve Merck and used without further purification. Water was distilled in glass.

Pure component densities, absolute viscosities and refractive indices were measured to ensure their purities, and results are reported in Table 1, along with literature values.

Table 1

Properties of pure solvents at 25°C

Solvent	Refr. index		ρ(g cm^{-3})		η(cp)	
	This work	Lit [6]	This work	Lit [6]	This work	Lit [6]
Water	1.3325	1.3325	0.9972	0.9970	0.8953	0.89024
Methanol	1.3263	1.3265	0.7866	0.7865	0.5526	0.5545
Ethanol	1.3590	1.3594	0.7855	0.7851	1.0812	1.0798
2-propanol	1.3747	1.3752	0.7813	0.7812	2.0158	2.0357(3)
Acetone	1.3556	1.3560	0.7846	0.7844	0.3025	0.3040

The mixtures were prepared gravimetrically weighing the components to 0.1 mg.

A thermostated Erma A-302-A abbe refractometer was used to measure the refractive index of pure solvents. Densities of pure components and their mixtures were measured using an Ostwald-Sprengel pycnometer which was calibrated with mercury. The experimental reproducibility is better than 2 part in 10^4. Viscosities were measured in an Amtec-Ubbelohde capillary viscometer with long flow times (60 — 500 s. in these experiments) in order to minimize the kinetic energy correction. Flow times were measured with a quartz timer which has a resolution of 0.01 s.

Viscosity was calculated by Hagen—Poiseuille equation for a capillary viscometer[7] in the form

$$\eta = A\rho t - B(\rho/t) \tag{6}$$

where t is the flow time. The constants A and B were determined plotting $(\eta/\rho t)$ versus $(1/t^2)$ and using literature data (Table 1) for the viscosity of pure components. The calculated kinetic energy corrections, $B(\rho/t)$, for our viscometer amounts to less than $2.10^{-4}\ \eta$ at 25°C, therefore this correction was ignored in calculating the binary and ternary mixture viscosities reported here.

Experimental determinations were performed, at least, in four replicates for each composition ; previously, pycnometer and viscometer were carefully rinsed with the new mixture. All measurements were made at 25 ± 0.03 °C by keeping pycnometer or viscometer in a suitable thermostatic bath.

RESULTS AND DISCUSSION

Measured mixture viscosities and densities are shown in Table 2 for binary systems and in Table 3 for ternary systems as a composition function. The average standard deviation determined from the replicate runs at each composition in binary mixtures was 0.02% for densities and 0.1% for viscosities, and in ternary mixtures was 0.02 % for densities and 0.4% for viscosities.

Figures 1 and 2 show the variation of viscosity with composition for binary mixtures. It may be seen that when water and organic solvents are mixed (Fig. 1) the curve passes through a well defined maximum at about 0.750 mole fraction of water for water + alcohol mixtures, and 0.875 mole fraction for water + acetone mixtures. The viscosity increases in water — organic mixed solvents may be explained as due to entanglement; that is clustering of an organic solvent molecule with the neighbouring solvent and water molecules. In case of nonaqueous binary mixture between these polar liquids (Fig. 2), all curves show the same pattern : the grafs of viscosity changes exhibit two nearly linear sections with point of inflection at about 0.5 mole fraction. These observations indicate a sort of interaction between the solvent molecules on mixing.

The viscosity data are in satisfactory agreement with volume and enthalpy excess results procured by other authors for water + alcohols[5,8,9], water + acetone[5,10], alcohol + alcohol and alcohol + acetone[5,11,12] which are also pointers to the molecular interactions. Enthalpy and volume excess are negative on water + organic solvent mixtures and show the same pattern as viscosity change, namely first increasing their absolute value, attaining maximum and then decreasing. However these data do not supply the calculation of intermolecular bond energies nor the structure on mixed solvents. No significant excess volume is observed on mixing two organic solvents but there is an increase of system enthalpy.

As viscosity of liquid is the internal friction which opposes the relative motion of adjacent layers causing resistance to liquid fluid, then viscosity value responds to the force necessary to overcome the molecular interactions of pure or clustered mixture liquid in the flow process. Therefore the knowledge of the liquid structure is fundamental to explain the viscosity values.

Disregarding the earliest model of structure of liquids, proposed by van der Waals[13] who considers liquids as dense gases, we assume the liquid structure as a disordered solid. Liquid differs from solid in that it has no rigidity and cannot maintain definite shape, but density of liquid is not very different from the one of solid, packing of molecules in liquid must be similar to that in solid. This assumption accords with the lattice and distribution function theories of liquid state,[14-19] and with the experimental

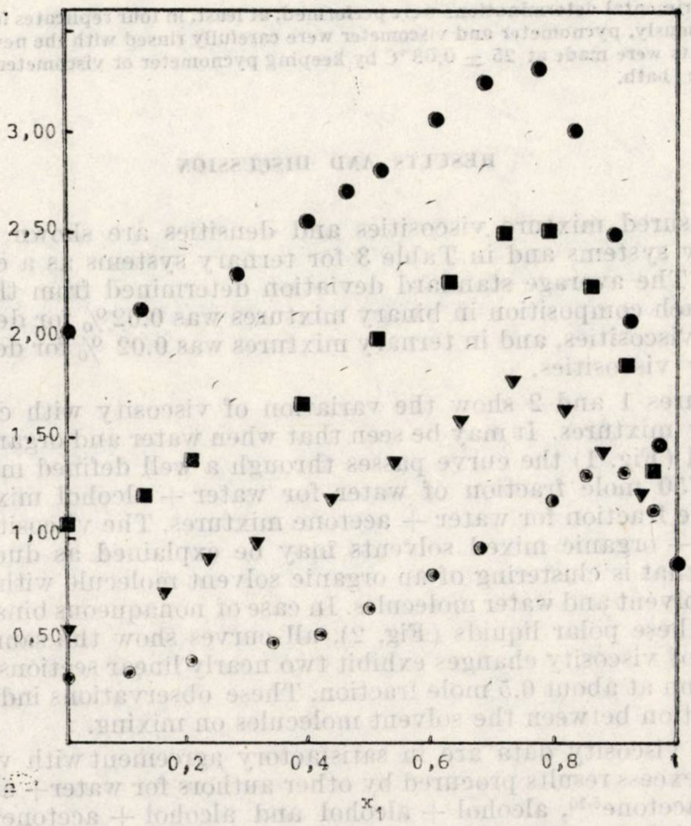

Fig.1. — Viscosity of water + organic binary mixtures. ▲ water + + methanol ; ■ water + ethanol ; ● water + 2-propanol, and ◉ water + acetone.

results from X-ray or neutron diffraction.[20-22] Like in solid, liquid space can be envisaged as partitioned into unit cells. Here we shall consider that : a) the molecules are uniformly distributed in three dimensional liquid space ; b) each specific molecule has four nearest neighbours, and c) a tetrahedral pentamer structure is compatible with X-ray and neutron scattering data [21,23].

Furthermore a liquid polar molecule produces an electrostatic field with determinate magnitude but continually changing in direction. Theoretically if two neighbour molecules with electrostatic fields identic in magnitude and opposite in direction are paired, the resultant electrostatic field is zero, but indeed a molecule is paired successively with every one of four nieghbour molecules. The results is, in the same manner, a null electrostatic field and moreover the foresaid unit cell in liquid structure is stabilized.

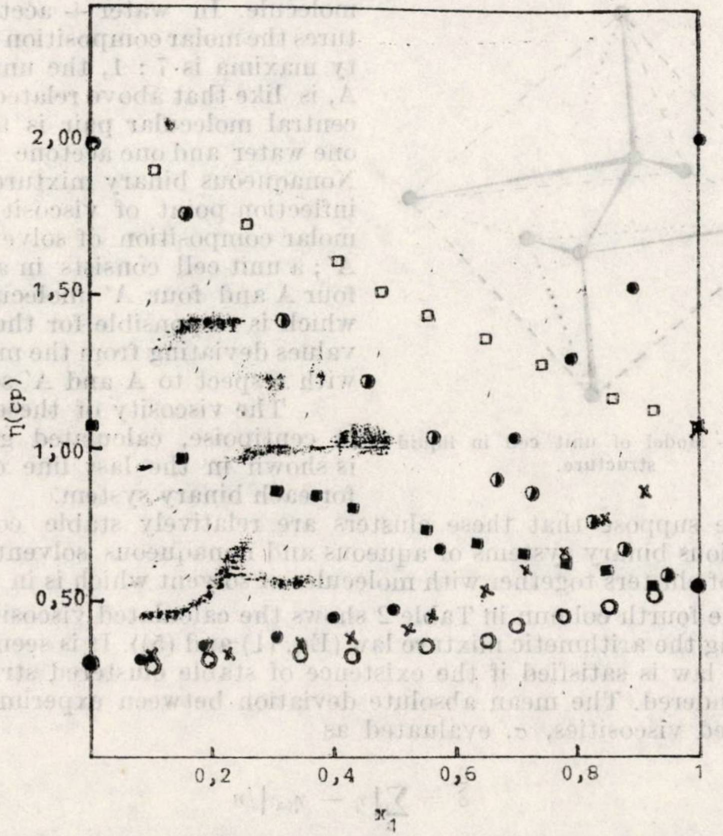

Fig. 2. — Viscosity of nonaqueous binary mixtures. ■ methanol + + ethanol; ◐ methanol + 2-propanol; ○ methanol + acetone; □ ethanol + 2 propanol; × ethanol + acetone and ● 2-propanol-acetone.

Figure 3 satisfies these conditions. The unit cell has six coordinated molecules around a molecular pair maintaining the tetrahedral pentamer structure. There are seven intermolecular bonds : one between the two molecules belonging to central molecular pair and three between each molecule in the central molecular pair and three neighbouring molecules. Moreover molecules in unit cell are so localized that the bonds are arranged in such manner that the cell is electrically neutral. When liquids are mixed a rearrangement of molecules occurs to stabilize the system and to restore the electrostatic neutrality in unit cell. This is accompanied by density, viscosity and heat changes that are directly measured.

At the same time, Figure 3 explains the peculiar variations with composition obtained in this work. In water + alcohol binary mixtures of viscosity maxima, the molar composition of system is 3 : 1 and we postulate that the unit cell consists in a cluster, W_6A_2, with two alcohol molecules bonded to form the central molecular pair and six water molecules coordinated, three on each alcohol molecule. In water + acetone mixtures the molar composition of viscosity maxima is 7 : 1, the unit cell, W_7A, is like that above related, but the central molecular pair is formed by one water and one acetone molecules. Nonaqueous binary mixtures show an inflection point of viscosity at 1 : 1 molar composition of solvents A and A′; a unit cell consists in a cluster of four A and four A′ molecules, $A_4A'_4$, which is responsible for the viscosity values deviating from the mixture law with respect to A and A′ solvents.

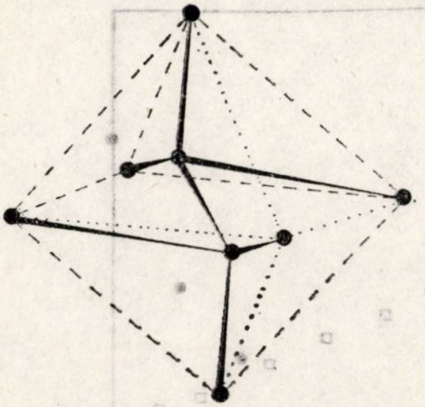

Fig. 3. — Model of unit cell in liquid structure.

The viscosity of these clusters, in centipoise, calculated graphically is shown in the last line of Table 2 for each binary system.

We suppose that these clusters are relatively stable compounds. The various binary systems of aqueous and nonaqueous solvent mixtures consist of clusters together with molecules of solvent which is in excess.

The fourth column in Table 2 shows the calculated viscosity values, η^{cal}, using the arithmetic mixture law (Eq. (1) and (5)). It is seen that the mixture law is satisfied if the existence of stable clustered structures is duly pondered. The mean absolute deviation between experimental and calculated viscosities, σ, evaluated as

$$\bar{\delta} = \sum_{n} |\eta - \eta_{cal}|/n \tag{7}$$

varies from 1.0% for ethanol + 2-propanol system at a maximum of 5.3% for water + acetone system (n is the number of experimental points for each binary mixture system).

The viscosity values calculated using equations (2) and (3) were carried up to 10% mean absolute deviations. These results are not tabulated.

In ternary mixtures we shall avoid possible ternary clustered structures and shall assume that these mixtures consist of two or three binary clusters together with the solvent which is in excess. Likewise, from results of the previous investigations[5,9-13] and the influence of clusters at viscosity observed in this work, we shall assume that the order of formation and stability of clustered structures is $W_6M_2 = W_6E_2 = W_6(2-P)_2 = W_7A > (2-P)_4A_4 > E_4A_4 > M_4A_4 > M_4(2-P)_4 > M_4E_4 > E_4(2-P)_4$. The fifth column in Table 3 shows the viscosity calculated values from the arith-

Table 2

Densities and experimental and calculated viscosities of binary mixtures at 25°C.

x_1	ρ	η	η_{cal}	x_1	ρ	η	η_{cal}
Water + Methanol				**Water + Ethanol**			
0.0000	0.7866	0.5526	0.5522	0.0000	0.7855	1.0812	1.0812
0.1615	0.8173	0.7420	0.7283	0.1305	0.7981	1.2136	1.2215
0.2332	0.8305	0.8124	0.8719	0.2213	0.8136	1.3732	1.3463
0.3078	0.8435	0.9770	0.9202	0.3901	0.8391	1.6740	1.6213
0.4328	0.8681	1.1983	1.1161	0.5229	0.8634	1.9713	1.9081
0.5425	0.8929	1.3842	1.3220	0.6303	0.8870	2.2681	2.2064
0.6401	0.9126	1.5953	1.5293	0.7189	0.9099	2.5039	2.5126
0.7272	0.9325	1.7802	1.7442	0.7932	0.9315	2.5030	2.4378
0.8058	0.9501	1.6463	1.6397	0.8565	0.9507	2.2523	2.0794
0.8768	0.9640	1.4361	1.3973	0.9109	0.9664	1.8571	1.6992
0.9412	0.9806	1.2257	1.1509	0.9584	0.9804	1.3352	1.3011
1.0000	0.9972	0.8953	0.8950	1.0000	0.9972	0.8953	0.8950
$x = 0.750$	$= 1.81$			$x = : .750$	$= 2.59$		
Water + 2-Propanol				*Water + Acetone*			
0.0000	0.7813	2.0158	2.0159	2.0159	0.7846	0.3025	0.3026
0.1220	0.7926	2.1173	2.1275	0.0987	0.7944	0.3420	0.3454
0.2704	0.8061	2.2980	2.2890	0.2027	0.8065	0.3950	0.3988
0.3885	0.8210	2.5554	2.4586	0.3389	0.8242	0.4873	0.4862
0.4547	0.8306	2.7252	2.5730	0.4112	0.8372	0.5614	0.5449
0.5130	0.8403	2.8254	2.6899	0.4963	0.8531	0.6675	0.6261
0.6109	0.8598	3.0863	2.9302	0.6047	0.8740	0.8205	0.7552
0.6901	0.8785	3.2665	3.1754	0.6816	0.8942	0.9547	0.8653
0.7833	0.9083	3.3054	3.2221	0.7973	0.9265	1.2051	1.1076
0.8334	0.9269	3.0121	2.8795	0.8447	0.9417	1.3281	1.2402
0.8956	0.9501	2.4865	2.3215	0.9113	0.9634	1.3162	1.2327
0.9303	0.9679	2.0843	1.9383	0.9574	0.9805	1.1505	1.0771
0.9678	0.9808	1.4497	1.4212	1.0000	0.9972	0.8953	0.8950
1.0000	0.9972	0.8953	0.8950				
$x = 0.750$	$= 3.40$			$x = 0.875$	$= 1.34$		
Methanol + Ethanol				*Methanol + 2 − Propanol*			
0.0000	0.7855	1.0812	1.0812	0.0000	0.7813	2.0158	2.0159
0.1486	0.7857	0.9853	1.0052	0.1507	0.7816	1.7964	1.7984
0.2963	0.7860	0.9005	0.9323	0.3173	0.7821	1.4414	1.5155
0.3705	0.7863	0.8746	0.8787	0.4488	0.7829	1.2276	1.2525
0.4334	0.7864	0.8243	0.9339	0.5543	0.7837	1.0732	1.0931
0.5496	0.7868	0.7626	0.7750	0.6671	0.7846	0.9208	0.9883
0.6354	0.7870	0.7205	0.7383	0.7334	0.7852	0.8791	0.8178
0.7035	0.7874	0.6891	0.7080	0.8196	0.7861	0.7685	0.8166
0.7756	0.7875	0.6553	0.6734	0.8760	0.7864	0.6985	0.7407
0.8486	0.7878	0.6228	0.6262	0.9461	0.7875	0.6044	0.6403
0.9252	0.7876	0.5879	0.5953	1.0000	0.7866	0.5526	0.5522
1.0000	0.7866	0.5526	0.5522				
$x= : .50$	$=0.79$			$x=0.50$	$=1.14$		

Table 2 (continued)

x_1	ρ	η	η_{cal}	x_1	ρ	η	η_{cal}
Methanol + Acetone				*Ethanol + 2-Propanol*			
0.0000	0.7846	0.3025	0.3026	0.0000	0.7813	2.0158	2.0159
0.1056	0.7860	0.3094	0.3176	0.0963	0.7814	1.9115	1.8746
0.1910	0.7871	0.3134	0.3213	0.2528	0.7816	1.7589	1.7739
0.3440	0.7891	0.3253	0.3302	0.3926	0.7826	1.6333	1.6252
0.4201	0.7897	0.3382	0.3347	0.4754	0.7827	1.5523	1.5350
0.5560	0.7907	0.3527	0.3580	0.5576	0.7832	1.4698	1.4638
0.6517	0.7913	0.3757	0.3909	0.6432	0.7835	1.3834	1.3931
0.7339	0.7913	0.4131	0.4248	0.7361	0.7840	1.2990	1.3211
0.8211	0.7910	0.4450	0.4602	0.8522	0.7844	1.2034	1.2206
0.8776	0.7904	0.4861	0.4868	0.9173	0.7848	1.1506	1.1606
0.9388	0.7880	0.5127	0.5171	1.0000	0.7855	1.0812	1.0812
1.0000	0.7866	0.5526	0.5522				
$x = 0.50$	$= 0.34$			$x = 0.50$	$= 1.51$		
Ethanol + Acetone				*2-Propanol + Acetone*			
0.0000	0.7846	0.3025	0.3026	0.0000	0.7846	0.3025	0.3026
0.0985	0.7847	0.3206	0.3247	0.0862	0.7830	0.3270	0.3284
0.2287	0.7849	0.3355	0.3460	0.2050	0.7814	0.3594	0.3839
0.3438	0.7851	0.3625	0.3640	0.3038	0.7806	0.3847	0.3932
0.4229	0.7853	0.3716	0.3770	0.4006	0.7799	0.4435	0.4217
0.5243	0.7854	0.4051	0.4974	0.4944	0.7795	0.4768	0.4494
0.5521	0.7856	0.4486	0.4539	0.5735	0.7792	0.6713	0.6835
0.6528	0.7859	0.5433	0.5822	0.7008	0.7792	1.0429	1.0838
0.7104	0.7859	0.6103	0.6581	0.7892	0.7795	1.2891	1.3603
0.8326	0.7857	0.7690	0.8257	0.8903	0.7805	1.5275	1.6756
0.9055	0.7857	0.8685	0.9328	1.0000	0.7813	2.0158	2.0159
1.0000	0.7855	1.0812	1.0812				
$x = 0.50$	$= 0.39$			$x = 0.50$	$= 0.45$		

Table 3

Densities and experimental and calculated viscosities of ternary mixtures at 25°C

x_1	x_2	ρ	η	η_{cal}	x_1	x_2	ρ	η	η_{cal}
Water+Methanol+Ethanol					*Water+Methanol+2-Propanol*				
0.245	0.244	0.8202	1.2353	1.2039	0.224	0.299	0.8169	1.6499	1.6582
0.556	0.144	0.8757	1.7090	1.7942	0.420	0.223	0.8483	1.9696	1.9935
0.745	0.083	0.9225	2.2473	2.3742	0.561	0.169	0.8747	2.3682	2.3060
0.879	0.042	0.9602	1.7607	1.8045	0.749	0.098	0.9212	2.9007	2.9212
0.921	0.026	0.9723	1.4304	1.1972	0.871	0.049	0.9590	2.1151	2.1896
0.963	0.012	0.9831	1.1313	1.1927	0.922	0.030	0.9715	1.6317	1.7526
0.230	0.456	0.8211	1.0634	1.0298	0.168	0.543	0.8116	1.2404	1.1996
0.534	0.276	0.8751	1.6159	1.5680	0.354	0.442	0.8496	1.5844	1.4905
0.727	0.161	0.9246	1.9636	2.0919	0.531	0.306	0.8780	1.8810	1.8423
0.861	0.082	0.9568	1.6513	1.7060	0.621	0.247	0.8904	2.0784	2.0590
0.914	0.051	0.9722	1.4326	1.4343	0.801	0.130	0.9443	2.2245	2.2673
0.959	0.024	0.9850	1.1462	1.1623	0.961	0.026	0.9856	1.2451	1.2744
0.213	0.639	0.8216	0.9482	0.8971	0.044	0.812	0.7988	0.8450	0.8284
0.511	0.397	0.8789	1.3833	1.3817	0.354	0.548	0.8530	1.3002	1.2356
0.709	0.236	0.9323	1.7039	1.8497	0.511	0.416	0.8779	1.5518	1.5081
0.581	0.121	0.9579	1.5496	1.6112	0.621	0.322	0.9033	1.7113	1.7570
0.907	0.076	0.9722	1.3292	1.3779	0.790	0.178	0.9432	1.8756	1.9640
0.956	0.025	0.9826	1.1104	1.1292	0.945	0.081	0.9720	1.3905	1.4575

Table 3 (continuede)

x_1	x_2	ρ	η	η_{cal}	x_1	x_2	ρ	η	η_{cal}
Water+Methanol+Acetone					*Water+Ethanol+2-Propanol*				
0.274	0.272	0.8211	0.5609	0.5801	0.067	0.283	0.7924	1.8350	1.7938
0.593	0.154	0.8806	0.9972	1.0311	0.239	0.231	0.8206	2.1265	2.0138
0.773	0.086	0.9229	1.3245	1.2837	0.462	0.163	0.8578	2.4062	2.3980
0.889	0.042	0.9611	1.3111	1.3186	0.549	0.136	0.8716	2.5958	2.5832
0.932	0.026	0.9726	1.2108	1.1749	0.721	0.085	0.9202	2.6100	2.7763
0.968	0.012	0.9868	1.0532	1.0353	0.846	0.047	0.9513	2.5657	2.6451
0.244	0.488	0.8216	0.6308	0.6020	0.168	0.471	0.8127	1.7587	1.6638
0.421	0.274	0.8441	0.8727	0.8492	0.389	0.347	0.8512	2.1641	2.0174
0.554	0.287	0.8767	1.0860	1.0058	0.512	0.271	0.8749	2.3928	2.3089
0.744	0.165	0.9224	1.3806	1.4435	0.625	0.212	0.8978	2.6523	2.6041
0.871	0.083	0.9573	1.3663	1.3815	0.870	0.073	0.9583	2.1748	2.2773
0.963	0.024	0.9840	1.0931	1.0552	0.942	0.033	0.9805	1.5133	1.6150
0.219	0.659	0.8209	0.7198	0.6857	0.254	0.595	0.8261	1.6655	1.5342
0.388	0.517	0.8533	0.9547	0.9263	0.354	0.514	0.8456	1.8935	1.7652
0.521	0.405	0.8809	1.1799	1.1545	0.635	0.295	0.9063	2.4659	2.4439
0.717	0.238	0.9243	1.5241	1.6063	0.707	0.234	0.9230	2.6824	2.7065
0.856	0.122	0.9568	1.3982	1.4480	0.840	0.127	0.9556	2.2368	2.3545
0.958	0.026	0.9832	1.1208	1.0767	0.901	0.079	0.9709	2.0302	2.1343
Water+Ethanol+Acetone					*Water+2-Propanol+Acetone*				
0.299	0.208	0.8213	0.5993	0.6005	0.091	0.221	0.8003	0.4653	0.4487
0.489	0.151	0.8521	0.8282	0.8513	0.194	0.196	0.8146	0.5654	0.5426
0.622	0.112	0.8794	1.0855	1.1030	0.431	0.138	0.8548	0.8667	0.8423
0.793	0.061	0.9273	1.4360	1.5020	0.650	0.085	0.8989	1.2078	1.3087
0.899	0.030	0.9610	1.3357	1.4147	0.819	0.044	0.9442	1.5605	1.6870
0.972	0.009	0.9861	1.1039	1.0667	0.971	0.007	0.9853	1.2015	1.2438
0.287	0.398	0.8203	0.7674	0.7538	0.231	0.378	0.8214	0.7683	0.7527
0.475	0.293	0.8516	1.1069	1.0497	0.404	0.293	0.8528	1.1392	1.0617
0.608	0.219	0.8785	1.3346	1.3721	0.553	0.220	0.8806	1.4585	1.4484
0.707	0.164	0.9045	1.9555	1.6985	0.672	0.161	0.9125	1.9540	1.9138
0.848	0.087	0.9452	1.7157	1.8075	0.851	0.073	0.9532	2.0215	2.0927
0.935	0.036	0.9722	1.2731	1.3459	0.917	0.041	0.9703	1.5539	1.6619
0.275	0.573	0.8203	1.0737	1.0848	0.138	0.641	0.8070	1.3990	1.3729
0.461	0.426	0.8497	1.3608	1.3947	0.375	0.465	0.8486	1.7584	1.7139
0.594	0.321	0.8786	1.6671	1.7041	0.511	0.364	0.8794	2.0245	1.9045
0.774	0.179	0.9224	2.0977	2.2398	0.702	0.221	0.9209	2.6233	2.5769
0.889	0.088	0.9584	1.6841	1.7380	0.878	0.090	0.9657	2.1627	2.2435
0.958	0.025	0.9845	1.0912	1.1736	0.956	0.027	0.9831	1.3839	1.4675
Methanol+Ethanol+2-Propanol					*Methanol+Ethanol+Acetone*				
0.303	0.235	0.7831	1.2460	1.2548	0.659	0.195	0.7895	0.5162	0.5134
0.295	0.416	0.7840	1.1167	1.1118	0.501	0.351	0.7884	0.5657	0.5867
0.254	0.591	0.7847	1.0399	1.0506	0.268	0.558	0.7873	0.6487	0.6642
0.526	0.185	0.7844	0.9702	0.9993	0.467	0.301	0.7889	0.4906	0.4914
0.514	0.285	0.7850	0.9151	0.9421	0.426	0.291	0.789	0.4643	0.4444
0.501	0.363	0.7854	0.8774	0.8929	0.311	0.378	0.7880	0.4728	0.4658
0.703	0.164	0.7860	0.7687	0.8231	0.320	0.179	0.7886	0.3809	0.3596
0.420	0.307	0.7843	1.0223	1.0399	0.536	0.266	0.7891	0.5222	0.5036
0.391	0.388	0.7846	1.0022	1.0214	0.409	0.379	0.7883	0.5564	0.5443
0.165	0.079	0.7814	1.5936	1.6925	0.810	0.134	0.7899	0.5444	0.5696
0.202	0.711	0.7847	1.0791	1.0339	0.184	0.734	9.7868	0.8308	0.8822
0.833	0.104	0.7857	0.7546	0.7039	0.184	0.143	0.7892	0.3342	0.3410

Table 3 (continued)

x_1	x_2	ρ	η	η_{cal}	x_1	x_2	ρ	η	η_{cal}
Methanol + 2-Propanol + Acetone					*Ethanol + Ethanol + Acetone*				
0.832	0.095	0.7869	0.4957	0.5167	0.248	0.553	0.7813	1.0876	1.1205
0.109	0.747	0.7939	1.2447	1.2532	0.466	0.339	0.7830	0.8990	0.9282
0.565	0.256	0.7864	0.4728	0.4691	0.621	0.181	0.7841	0.7545	0.7929
0.709	0.086	0.7861	0.4903	0.4693	0.248	0.369	0.7818	0.5704	0.5713
0.086	0.629	0.7839	0.9030	0.8644	0.383	0.293	0.7829	0.5758	0.5995
0.329	0.297	0.7859	0.4692	0.4540	0.456	0.193	0.7838	0.5600	0.5968
0.265	0.245	0.7841	0.4223	0.4048	0.261	0.167	0.7823	0.4204	0.3990
0.073	0.373	0.7834	0.4047	0.4232	0.340	0.377	0.7823	0.7411	0.7740
0.106	0.232	0.7839	0.3653	0.3828	0.439	0.269	0.7832	0.6594	0.6994
0.264	0.044	0.7828	0.3190	0.3334	0.135	0.794	0.7807	1.5362	1.6630
0.163	0.058	0.7832	0.3186	0.3308	0.826	0.084	0.7848	0.9157	0.9425
0.045	0.139	0.7840	0.3325	0.3483	0.121	0.089	0.7836	0.3409	0.3496
0.032	0.077	0.7942	0.3375	0.3283					
0.071	0.023	0.7844	0.3214	0.3139					

metic mixture law. Once more it is seen that equation (1) gives good results when the clusters are correctly used. The mean absolute deviation values vary from 3.1% for water + methanol + 2—propanol ternary system to 5.5% for ethanol + 2-propanol + acetone ternary system.

Therefore the arithmetic law mixture can be used for predicting the viscosity of binary and ternary polar liquid systems with acceptable accuracy when molar composition, density and viscosity of pure components and feasible clusters are known.

REFERENCES

[1] M. Tamura and M. Kurata, *Bull. Chem. Soc. Japan*, **25**, 32, (1952).

[2] F. W. Lima, *J. Phys. Chem.*, **56**, 1052, (1952).

[3] I. C. Wei and R. L. Rowley, *J. Chem. Eng. Data* **29**, 332, (1983); and *J. Chem. Eng. Data*, **29**, 336, (1983).

[4] R. M. Chiu and B. D. Chen, *J. Chin. Ins. Chem. Eng.*, **17**, 356, (1986).

R. A. Stair, *Can. J. Chem.*, **58**, 296, (1980).

[6] J. A. Riddick and W. B. Bunger, "Organic Solvents", Wiley and Sons, New York, 1970.

[7] F. Daniels, J. W. Williams, A. R. Alberty, P. Bender, C. D. Cornwell and J. E. Harriman, "Experimental Physical Chemistry", Mc Graw Hill, New York, 1969.

[8] S. G. Bruun and A. Hvidt, *Ber. Bunsenges Phys. Chem.*, *81*, 930 (1977).

[9] B. Marongiu, I. Ferino, R. Monaci, V. Solinas and J. Torrazas, *J. Mol. Liq.* **28**, 229 (1984).

[10] A. V. Benedetti, M. Cilense, D. R. Vollet and R. C. Montone, **66**, 219 (1983).

[11] I. Nagata and K. Tamura, *Fluid. Phase Equil.*, **15**, 67 (1893).

[12] S. J. Timmerman, "The Physicochemical Constants of Binary Systems", Interscience, New York, 1960.

[13] Van der Waals, *Doctoral Dissertation*, Leiden University, 1873

[14] J. E. Lennar Jones and A. F. Devonshire *Proc. Roy. Soc.*, **A—163**, 53; (1937); *Proc. Roy Sci.*, **A—169**, 317 (1938) and *Proc. Roy. Soc.*, **A—170**, 469, (1939).
[15] H. Eyring, J. O. Hirschfelder, *J. Phys. Chem.*, 1037, **41**, **249** and *J. Chem Phys*, **4**, 283, (1936).
[16] J. Frenkel, "Kinetic Theory of Liquids", Clarendon Press, Oxford, 1946.
[17] V. Verlet, *Phys Rew.*, **165**, 201, (1968).
[18] J. O. Hirchfelder, C. F. Curtiss, and R. B. Bird, "Molecular Theory of Gasses and Liquids", Wiley, New York, 1954.
[19] J. A. Barker "Lattice Theories of the Liquid State", Mac Millan, New York, 1963.
[20] C. G. Gray and K. E. Gubbins, "Theory of Molecular Fluids", Clarendon Press, Oxford, 1982, Vol. 1.
[21] L. Blum and A. H. Narten, *Adv. Chem Phys.*, **34**, 203, (1976).
[22] J. S. Rowlinson and F. L. Swinton "Liquid and Liquid Mixtures", Butterworths, London, 1982.
[23] P. Kruus, "Liquids and Solutions: Structure and Dynamics," Dekker, New York, 1977.

Revue Roumaine de Chimie, 35, 4, 535–537 (1990)

A NEW PREPARATION METHOD FOR μ_3-OXO-TRINUCLEAR CHROMIUM(III) FORMATE

MARIA BREZEANU, E. PINCOVSCHI, DANA MARINESCU and MARIUS ANDRUH

Inorganic Chemistry Laboratory, Faculty of Chemical Technology, Polytechnic Institute of Bucharest, str. Dumbrava Roşie, no. 23, Bucharest, Romania

Received July 2, 1989

A μ_3-oxo-trinuclear chromium(III) formate, $[Cr_3O(HCOO)_6\,(HCOOH)_3]HCOO \cdot 3H_2O$, was prepared by a new method, namely by reduction of potassium bichromate with formic acid. The compound was characterized by chemical analysis, infrared and electronic spectroscopy.

1. INTRODUCTION

The so-called "basic" acetates and formates of chromium(III) and iron(III) are the best known members of a family of complexes of general formula $[M_3O(RCOO)_6L_3]^+$, containing a central oxide ion in a triangular arrangement of metal ions, M^{3+}. Their structure was proved by means of magnetic measurements[1] and finally by X-ray diffraction [2,3]. In the last years, this class of coordination compounds was enriched by new members, namely mixed-valence compounds such as $[Fe^{II}Fe_2^{III}O(CH_3COO)_6L_3]$[4,5], $[Ru^{II}Ru_2^{III}O(CH_3COO)_6L_3]$[6,7], or mixed-metal complexes.[8,9] Some of these compounds are suitable as raw materials for mixed oxides.[10–12]

The usual way to prepare the μ_3-oxo-trinuclear chromium(III) formate starts from a chromium(III) salt[1] which is transformed into $Cr(OH)_3$, then the precipitate is dissolved in formic acid and refluxed for two hours.[13]

2. EXPERIMENTAL

5.98 g of potassium bichromate were dissolved in 40 mL water and then refluxed for 3 h with 11 mL solution of HCOOH 80 % (molar ratio 1 : 10). After cooling, the fibrous green crystals were filtered off and dried in vacuo over P_4O_{10}.

Analytical data : found : 23.1 %Cr ; 17.5 %C ; 2.8 %H ; calcd : 22.97 % Cr ; 17.67 % C ; 2.8 % H.

The electronic spectrum was recorded by diffuse reflectance technique using a SPECORD M40 (Carl Zeiss) spectrophotometer with MgO as a standard. The IR spectrum was recorded with a UR-10 (Carl Zeiss) spectrophotometer, as KBr pellets.

3. RESULTS AND DISCUSSION

In order to prove that the green compound obtained by the reduction of potassium bichromate with formic acid is a μ_3-oxo-trinuclear chromium formate, $[Cr_3O(HCOO)_6(HCOOH)_3]HCOO.n\ H_2O$, the electronic and IR spectra were recorded (Figs. 1 and 2).

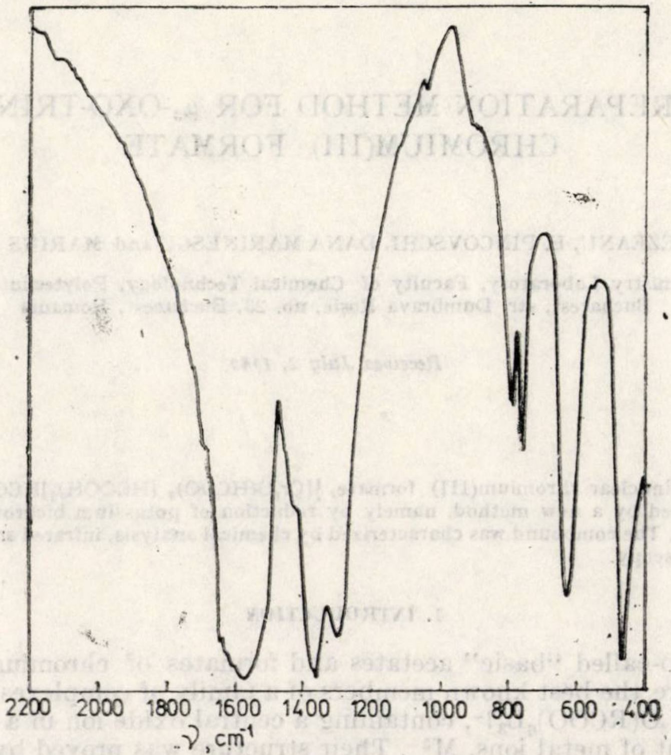

Fig.1.—The infrared spectrum of μ_3-oxo-trinuclear chromium (III) formate, $[Cr_3O(HCOO)_6(HCOOH)_3]HCOO.3H_2O$.

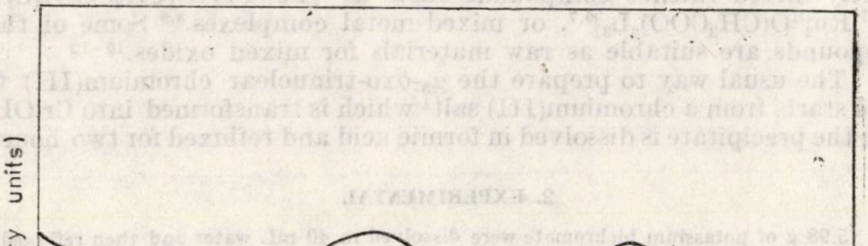

Fig. 2. — The diffuse reflectance spectrum of the μ_3-oxo-trinuclear chromium (III) formate.

The infrared spectrum (Fig. 1) was compared with those of other μ_3-oxo-trinuclear chromium formates.[13] The most characteristic band for a μ_3-oxo-trinuclear chromium complex is the band located at 630 cm^{-1} and assigned to ν_{asym} 0(Cr_3O) vibrational mode.[13] The strong absorptions at 1367 cm^{-1} and 1630 cm^{-1} are assigned to the bridging formate ligands (ν_{sym}(COO) and ν_{asym}(COO), respectively), while the bands located at 1300 cm^{-1} and 1570 cm^{-1} are assigned to the monodentate formate ions, coordinated in *trans* against the central oxide ion [13] (ν_{asym}(COO) and ν_{sym} (COO)). The other characteristic bands for the formate ions are respectively: 1040 cm^{-1} — weak (π(COO)), 760 cm^{-1} and 790 cm^{-1}(δ_{sym} (OCO)). The strong band located at 472 cm^{-1} is assigned to δ_{asym}(CH) mode.

The electronic spectrum, recorded in the range 30000 — 11000 cm^{-1}, is characteristic for the coordination compounds of chromium(III) in a (pseudo)octahedral environment (Fig. 2). The main absorptions, occurring at 16966 cm^{-1} (589 nm) and 22086 cm^{-1} (453 nm) are assigned to the spin allowed transitions $^4T_{2g} \leftarrow {}^4A_{2g}$ and $^4T_{1g} \leftarrow {}^4A_{2g}$. The shoulders observed in the 690 — 750 nm region, namely at 13800 cm^{-1} (725 nm) and 15126 cm^{-1} (661 nm), are assigned to transitions originating from different ground-state spin levels, allowed by an exchange coupling between the three chromium ions.[14] The band system between 365 and 330 nm (shoulders at 27966 and 29126 cm^{-1}) is assigned to double excitation of the energy doublet states, according to.[14]

REFERENCES

[1] A. Earnshaw, B. N. Figgis and J. Lewis, *J. Chem. Soc.* (A) **1966**, 1656.
[2] B. N. Figgis and G. B. Robertson, *Nature*, **205**, 694 (1965).
[3] S. C. Chang and G. A. Jeffrey, *Acta Cryst.*, **B26**, 673 (1970).
[4] D. Lupu and R. Ripan, *Rev. Roumaine Chim.*, **16**, 43 (1971).
[5] R. Grecu and D. Lupu, *Rev. Roumaine Chim.*, **16**, 1811 (1971).
[6] F. A. Cotton and J. G. Norman, *Inorg. Chim. Acta*, **6**, 411 (1972).
[7] T. J. Meyer, *Acc. Chem. Res.*, **11**, 94 (1978).
[8] A. B. Blake, A. Yavari and H. Kubicki, *J. Chem. Soc. Chem. Commun.*, **1981**, 796.
[9] A. B. Blake and A. Yavari, *J. Chem. Soc. Chem. Commun.*, **1982**, 1247.
[10] I. Ilie, M. Brezeanu and E. Segal, *Thermochim. Acta*, **94**, 393 (1985).
[11] L. Patron, A. Conţescu, G. Munteanu, M. Brezeanu and E. Segal, *Rev. Roumaine Chim.*, **31**, 811 (1986).
[12] M. Brezeanu, L. Patron and M. Andruh, "Polynuclear Coordination Compounds and Their Applications", Ed. Academiei, Bucharest, 1986 (in Romanian).
[13] M. K. Johnson, D. B. Powell and R. D. Cannon, *Spectrochim. Acta*, **37A**, 995 (1981).
[14] L. Dubicki and P. Day, *Inorg. Chem.*, **11**, 1868 (1972).

Revue Roumaine de Chimie, **35**, *4*, 539–544 (1990)

STUDIES ON VISCOSITY OF MAGNESIUM SOAPS OF HIGHER FATTY ACIDS IN DILUTE AQUEOUS SOLUTIONS AT DIFFERENT TEMPERATURES

HARVIR SINGH and SURENDRA PAL SINGH TOMAR*
Department of Chemistry, J. V. College, Baraut-250611, Meerut, India

Received November 21, 1987

The viscosity of magnesium soaps of higher fatty acids in water has been measured over a temperature range 35 — 50°C. The critical micelle concentrations are found to be independent of temperature, but decrease with increase in chain length of the soap. The equations of Vand and Moulik are applicable above CMC of the soaps. The parameters of the equations have been evaluated. These may be used to calculate the viscosity of soap solutions in the concentration range in which the equations hold good. The effect of temperature on viscous flow follows Arrhenius equation. The effect of soap concentration on viscosity of soap solution has also been discussed in the light of Eyring's equation and the thermodynamic parameters ΔH^*, ΔS^* and ΔG^* have been calculated.

INTRODUCTION

Viscosity measurements of magnesium soaps of lower fatty acids indicated the presence of soap micelles in water and methanol [1] at different temperatures. A number of studies have been made of viscosity of solutions of surfactants [2–8] to evaluate critical micelle concentration. The viscosity of magnesium soap solutions of higher fatty acids was measured in non-aqueous solvents at different temperatures. [9,10] Recent studies [11] of the conductivity of magnesium soaps of higher fatty acids in water indicated the presence of micelles. In order to obtain a better understanding, the viscosities of these soaps have been determined in aqueous solutions. The viscosity data have been interpreted in terms of various viscosity equations with a view to testing the validity of these equations and to finding out the nature of micelles formed under different conditions.

EXPERIMENTAL

Merck or B.D.H. reagent grade magnesium chloride. lauric, myristic, palmitic and stearic acids were used. The purity of the reagent was confirmed by determining their m.p. and b.p. The chemicals were purified and the soaps were prepared by the method described.[12]

---

* Present address: Surendra Pal Singh Tomar, Water Technology Centre, Indian Agricultural Research, Institute Pusa, New Delhi-110012, India

An Ostwald viscometer was used to determine the viscosity of soap solutions in a thermostatically controlled (0.05°C) bath. The densities were measured with an accuracy of ± 0.0001 g. with a dilatometer.

RESULTS AND DISCUSSION

The viscosity. η of soap solutions increases with increasing soap concentration. The plots (Fig. 1) of viscosity vs. concentration of the soap are characterised by an intersection of two straight lines at a definite concentration 7.0, 6.5, 6.0 & 5.0 $\times 10^{-5}$ M indicating the micelle formation for laurate, myristate, palmitate and stearate respectively at different temperatures. It appears that longer molecules impart greater viscosity at equal concentrations but the extrapolated values of viscosity for zero soap concentration are in good agreement with the corresponding experimental values at different temperatures and are independent of chain length of the soaps (Table 1). The soap molecules do not aggregate appreciably below critical micelle concentration.

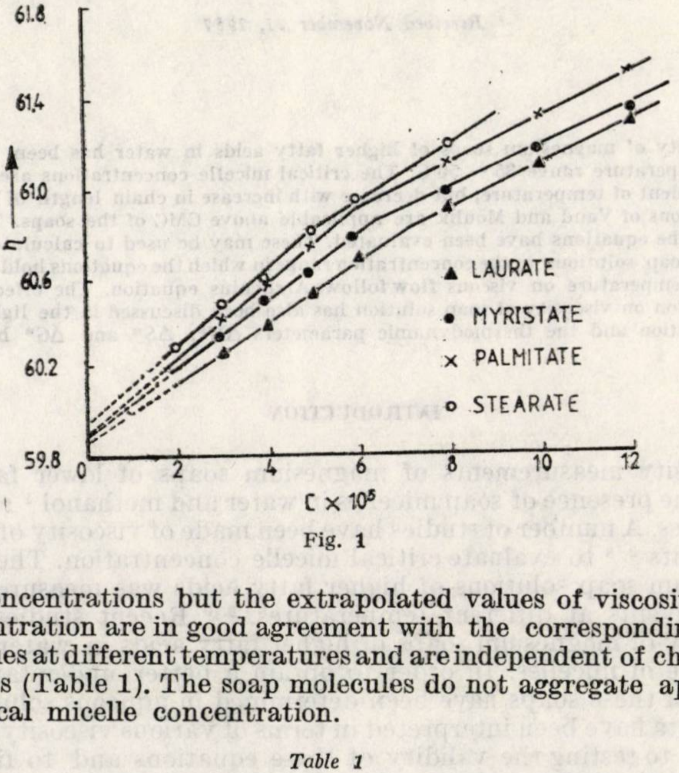

Fig. 1

Table 1

Extrapolated and experimental values of viscosity in poise of magnesium soap solutions for zero soap concentration at 35 — 50°C in water

Temperature in °C	Extrapolated ($\eta \times 10^4$)				Experimental $\eta \times 10^4$
	Laurate	Myristate	Palmitate	Stearate	
35	72.24	72.24	72.25	72.26	72.24
40	65.62	65.60	65.56	65.48	65.58
45	59.84	59 48	59.90	59.92	59.90
50	54.96	5	55.00	55.00	54.96

The plots (Figs. 2 and 3) of $1/C$ vs. $1/10g\eta/\eta_0$ for equation (i) and $(\eta/\eta_0)^2$ vs. C^2 for equation (ii) are found to be linear at 35 — 50°C over a limited range of concentration. Table 2 reveals that the following equations [13,14] are valid above CMC for magnesium soaps of higher fatty acids at different temperatures.

$$\text{Vand : } 1/C = (0.921/\overline{V})^{-1}.\ 1/\log(\eta/\eta_0) + Q\overline{V} \qquad \text{(i)}$$

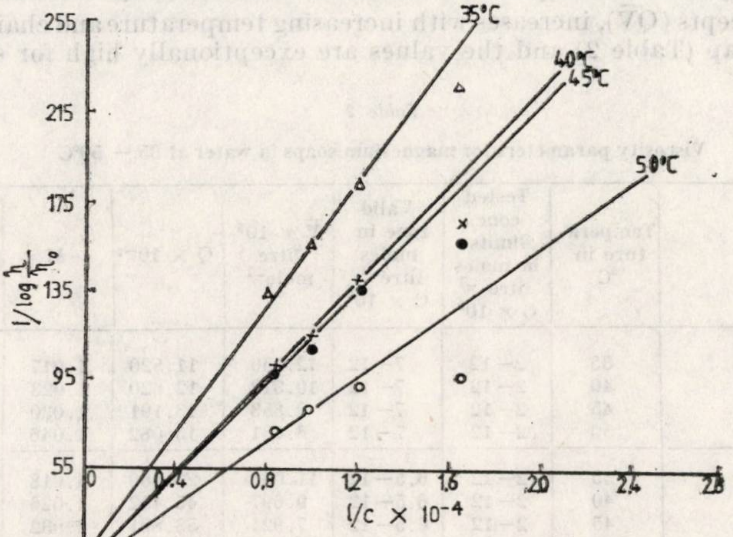

Fig. 2

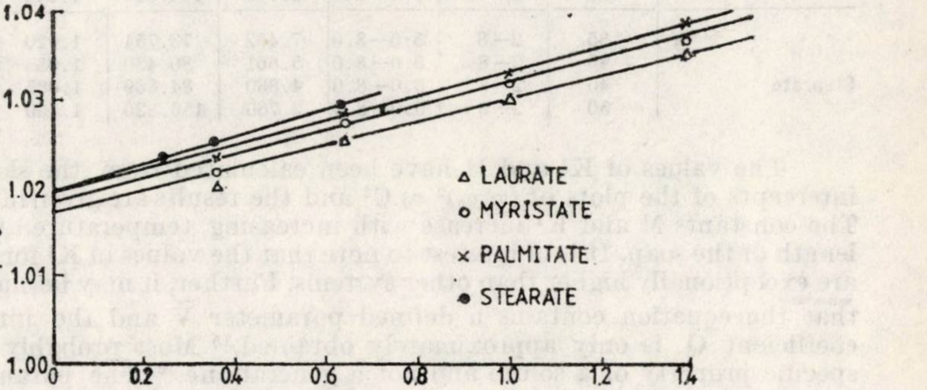

OP

Fig. 3

where Q and $\bar{V}$ are the interaction coefficient and molar volume of the solute in litre $mole^{-1}$ and C is the concentration in moles $litre^{-1}$.

$$\text{Moulik}: (\eta/\eta_0{}^2)^2 = M + K^1C^2 \quad \text{(ii)}$$

where M and K^1 are constants.

The values of molar volume $\bar{V}$ have been calculated from the slopes $(=\bar{V}/0.921)$ of the linear plots of $1/C$ *vs.* $1/\log(\eta/\eta_0)$ – and the results are given in table 2. The values of $\bar{V}$ decrease with increasing temperature and chain length of the soap. The interaction coefficient, Q, calculated from the intercepts $(Q\bar{V})$, increases with increasing temperature and chain length of the soap (Table 2) and the values are exceptionally high for stearate.

Table 2

Viscosity parameters for magnesium soaps in water at 35 – 50°C

Soap	Temperature in °C	Tested conc. limits in moles $litre^{-1}$ $C \times 10^5$	Valid zone in moles $litre^{-1}$ $C \times 10^5$	$\bar{V} \times 10^3$ litre $mole^{-1}$	$Q \times 10^{-2}$	M	$K^1 \times 10^{-4}$
Laurate	35	2–12	7–12	12.150	11.520	1.017	100.00
	40	2–12	7–12	10.312	12.620	1.023	135.02
	45	2–12	7–12	9.853	13.191	1.030	165.10
	50	2–12	7–12	6.631	15.082	1.046	170.01
Myristate	35	2–12	6.5–12	11.052	29.860	1.018	110.05
	40	2–12	6.5–12	9.697	45.452	1.026	145.03
	45	2–12	6.5–12	7.921	53.801	1.032	165.11
	50	2–12	6.5–12	2.912	80.501	1.047	172.04
Palmitate	35	2–10	6.0–10	10.315	31.020	1.019	125.01
	40	2–10	6.0–10	5.986	47.389	1.023	160.03
	45	2–10	6.0–10	5.802	56.790	1.033	175.05
	50	2–10	6.0–10	2.763	101.518	1.048	185.07
Stearate	35	2–8	5.0–8.0	7.462	73.751	1.020	150.12
	40	2–8	5.0–8.0	5.661	80.430	1.033	333.06
	45	2–8	5.0–8.0	4.880	84.889	1.035	333.01
	50	2–8	5.0–8.0	2.760	156.820	1.050	341.00

The values of K^1 and M have been calculated from the slopes and intercepts of the plots of $(\eta/\eta_0)^2$ *vs.*C^2 and the results are given in Table 2. The constants M and K^1 increase with increasing temperature and chain length of the soap. It is of interest to note that the values of K^1 for stearate are exceptionally higher than other systems. Further, it may be mentioned that the equation contains a defined parameter $\bar{V}$ and the interaction coefficient Q is only approximately obtained.[15] Most probably Q is a specific property of a solute and not a general one.[16] The parameters M and K^1 of Moulik's equation are not yet defined.

Relationships connecting viscosity and temperature were suggested empirically by Arrhenius,[17] Guzman [18] and theoretically by Andrade.[19]

The equation of Arrhenius

$$\eta = Ae^{E\varphi}/RT \tag{iii}$$

has been found to hold good for soap solutions. The term E_φ is defined as the energy required to transfer 1 g mole of the solute from one position of equilibrium to another and may be identified as activation energy of viscous flow. A is a constant. There is little doubt that it is in excellent agreement with experiment for many liquids. The plots of $\log\eta$ *vs.* $1/T$ are straight lines. The activation energy of viscous flow $E\varphi$ ($= H^*$ in Table 3) has been calculated from the slopes of the linear plots.

Table 3

Activation parameters for viscosity of Magnesium Laurate in water at 35 — 50°C

Conc. of soaps in moles litre^{-1}	ΔH^* kcals mole^{-1}	$-\Delta S^*$ cals. deg^{-1} mole^{-1}	ΔG^* at 35°C kcals mole^{-1}
3.0×10^{-5}M	3.670	40.970	16.288
4×	3.711	40.981	16.332
5×	3.760	41.000	16.388
6×	3.802	41.019	16.434
8×	3.851	41.040	16.490
10×	3.899	41.051	16.543
12×	3.950	41.080	16.593

The theory of absolute reaction rates was applied successfully to the problem of viscosity by Eyring and coworkers.[20-22] The temperature dependence of viscosity has been evaluated in terms of Eyring's equation.

$$\eta = \frac{hN}{V} \cdot e^{\Delta G^*/RT}$$
$$= \left(\frac{hN}{V} \cdot e^{-\Delta S^*/R}\right) e^{\Delta H^*/RT} \tag{iv}$$

The Arrhenius activation energy, $E\varphi$, has been taken as equal to ΔH^*, the Eyring energy of activation and the Arrhenius coefficient, A, have been equated with $\left(\frac{hN}{V}\right)e^{-\Delta S^*/R}$ to obtain ΔS^*, the entropy of activation. h and N are Planck's constant and Avogadro's number respectively, V is the molar volume of the solvent, R — is the gas constant in cals. dig. $^{-1}$ mole^{-1}, T is the absolute temperature and η is the viscosity in poise. The free energy of activation per mole, ΔG^* (Table 3) is then calculated at 35°C from Gibb's equation.

The activation energy of viscous flow, ΔH* increases as concentration increases. It measures the energy barrier to fluid motion and the increase in ΔH* with concentration indicates less fluidity and thus confirms structured solvent and micellar aggregation. The entropy of activation ΔS* (Table 3) also shows a little change with change in concentration and it decreases as concentration increases. This implies that the negative free energy of micellization is mainly the result of the entropy term in the water-soap system at very low concentrations. This conclusion is in agreement with the general concept that micelle formation in aqueous solutions is an entropy directed process and arises mainly from the break up of the "Frank-Evans icebergs" or "microcrystals" of the ordered water structure, even though the formation of aggregates by surfactant molecules is an entropy decreasing process. The free energy of activation ΔG* controls the rate of flow which is governed by slowest step in the fluid process. It increases as concentration increases. It is considered that non-linearity of free energy of activation for fluidity with the concentration of added solute becomes indicative of the formation of solute-solvent aggregate, as the principal Kinetic entity. Here it is observed that plots of ΔG* *vs.* C are linear above CMC. Therefore, the solvent-solute aggregation is not occurring but the aggregated soap molecules (micelles) remain in overall ordered surroundings.

ACKNOWLEDGEMENT. The authors express their thanks to Dr. R. P. Verma, Department of Chemistry, D. A. V. College, Muzaffar Nagar, INDIA for his keen interest in the work and to the college authorities for providing laboratory facilities. Financial assistance provided by University Grants Commission, New Delhi (INDIA) (grants No. 1481) is gratefully acknowledged.

REFERENCES

[1] R. P. Verma and K. Kumar, *J. Indian Chem. Soc.*, **L. IV**, 491 (1977).
[2] K. Hess, H. Kiessing and W. Philippoff, *Fette u. Seifen*, **48**, 377 (1941).
[3] K. A. Wright and H. V. Tartar, *J. Amer. Chem. Soc.*, **61**, 544 (1936).
[4] R. J. Vetter, *J. Phys. and colloid. Chem.*, **51**, 262 (1947).
[5] L. M. Kushner, B. C. Duncan and J. I. Hoffman, *J. Research matl. Bur. standards*, **49**, 85(1952).
[6] B. D. Flockhart and I. C. Graham, *J. Colloid Sci.*, **8**, 105 (1953).
[7] N. Sata and K. Tyuzyo, *Bull. Chem. Soc. Japan*, **26**, 177 (1953).
[8] K. Hess, W. Philippoff, and H. Kiessig. *Kolloid Z*, **88**, 40 (1939).
[9] A. N Bose and V. K. Dixit, *J. Amer Oil Chemists Soc.*, **34**, 386 (1957).
[10] A. N. Bose and V. K. Dixit, *Z. Physik Chem.* (Liepzig), **206**, 414 (1957) (Eng.)
[11] H. Singh and S.P.S., Tomar, *Bull. Chem. Soc. Japan* (Communicated).
[12] R. P. Verma and K. Kumar *Cellulose Chem. Technol.*, **9**, 23 (1975).
[13] V. Vand, *J. Phys. Colloid Chem.*, **52**, 277 (1948).
[14] S. P. Moulik, *J. Phys. Chem.*, **72**, 4682 (1968).
[15] "Intl. Encylo. Phys. Chem. and Chem. Phys." Pergamon Press, 1965, Topic 16, Vol. 3, P_4f.
[16] S. P. Moulik, *J. Indian Chem. Soc.*, **49**, 483 (1972).
[17] S. Arrhenius and Meddel, Vetenskapsaked, **3**, 20 (1916), Nobelins.
[18] J. de Guzman, *Anales Soc. espon., fis. quin.*, **11**, 353 (1913).
[19] E. N. dac. Andrade, *Phil. Mag.*, **17**, 497, 698 (1934).
[20] R. H.E. Well and H. Eyring, *Phil. Mag.*, **5**, 726 (1937).
[21] R. H. E—Well, *J. App. Phys.*, **9**, 252 (1938).
[22] J. Frenkel. *Z. Physik*, **35**, 652 (1926).

Revue Roumaine de Chimie, **35**, **4**, 545–547 (1990)

CHEMICAL COMPONENTS OF THE SCENT GLAND OF THE GREEN VEGETABLE BUG: *NEZERA VIRIDULA*

T. O. OLAGBEMIRO and L. LAJIDE
Chemistry Department, Abubakar Tafawa Balewa College, Ahmadu Bello University,
PMB 0248 Bauchi Campus, Bauchi, Nigeria

Received November 21, 1987

Using gas chromatography-mass spectrometry and comparisons with authentic samples, a series of saturated and unsaturated aliphatic hydrocarbons, aldehydes and esters have been found in the metathoracic scent glands of the Pentatomid green vegetable bug: *Nezera viridula* from Nigeria.

Currently, there is much interest in the expansion of knowledge on the composition of the scent volatiles produced by special glands of various insects. Waterhouse,[1] Blum,[2] Calam[3], Staddon[4] and Bazzini[5] did a great deal of work on insects secretions. A considerable number of active exocrine glands have been shown to co-exist with the ubiquitous metathoracic glands in adult Heteroptera. In fact, volatile compounds which have been associated with distinct pheromonal role have been recorded from the nymph and adults of this insect order particularly in the family Pentatomidae.

In this paper the identification of the chemical components of the metathoracic scent gland component of a pentatomid bug, *Nezera viridula* from Nigeria is being reported for the first time, although those from Australia and North America were previously reported.

RESULTS AND DISCUSSION

Gas chromatography and mass spectrometry of the 1% excised NaCl solution of the unruptured metathoracic scent glands of *Nezera viridula* followed by injection of authentic compounds as reference compounds revealed the presence of the compounds shown in Table 1.

Similar investigations on the *N. viridula* by Galby and Waterhouse,[6] Blum and Traynham [7] of the Australian and North American samples revealed some similarities and disparities in their chemical composition when compared with those from Nigeria. Tridecane (**2**) is the major metathoracic scent gland secretion in all the samples. The North American samples contained only trace amounts of dec-2-enal (4) while those of Nigeria and Australia contain 10.7% and 25% respectively. Similarly

Table 1

	Mol Formula	Structural formula	% Composition
1	$C_{12}H_{26}$	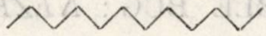	2.5
2	$C_{13}H_{28}$	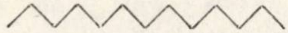	34.5
3	$C_6H_{10}O$	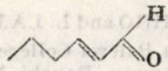	8.0[a]
4	$C_{10}H_{18}O$	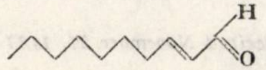	10.7[a]
5	$C_6H_8O_2$	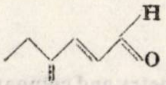	13.7[a]
6	$C_8H_{14}O_2$	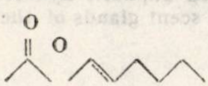	7.5[a]
7	$C_{10}H_{18}O_2$	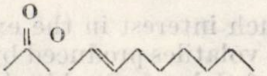	1.1[a]
8	$C_{12}H_{20}O_2$	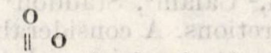	19.3[a]

(a) Bond geometry not determined

the North American *N. viridula* contains 33% of hept-2-3nal which was totally undetected in those of Nigeria and Australia. The latter contain only unsaturated aldehydes with even number of carbon atoms.

The biosynthetic implication of the presence of unsaturated aldehydes with odd or even number of carbon atoms in different geographical locations is a matter of conjecture. However, the presence of these compounds further adds to the array of chemicals used by insects for communication.

EXPERIMENTAL

Collection of *Nezera viridula*

The green vegetable bugs were collected during the rainy season on leafy vegetable gardens within the campuses of the Ahmadu Bello University and Bauchi Campus and Bayero University, Kano and were immediately stored in deep freezers.

Analysis

The metathoracic scent glands were excised under (1% NaCl) at room temperature, care being taken not to rupture the scent reservoir. Analyses of the scent materials were first performed using a Varian 1400 gas chromatograph (GC) equipped with a flame ionization detector. The 180 cm glass column (i.d. 2 mm) was packed with 3% OV 225 on 60 — 80 mesh gas chrom Q and was preceded by a 12 cm long precolumn (i.d. 4 mm). The entire gland suspended in a droplet of saline of prevent collapse, was introduced into the precolumn by the wire coil spoon technique[6]. The chromatograph oven temperature was programmed at 10°C/min from 80 to 200°C with nitrogen flow rate at 30 m/min. Chromatograms were numbered consecutively for purposes of identification and record storage. Comparison of retention times R_f of the scent volatiles with reference compounds were made by co-injection under the same GC conditions. Electron impact mass spectra were obtained using a Varian CH5D mass spectrometer linked to a 620i computer as described by Games et al.[9] The scent constituents were separated using a Varian 2700 gas chromatograph operating on line with the mass spectrometer. The gas chromatograph was equipped with a 180 cm (i.d. 2mm) glass column packed with 3% OV 225 in 100 — 120 mesh gas crhom Q. The oven precolumn was modified as above, and five-gland sample (metathoracic) was introduced, using the wire coil spoon technique. The mass spectra were recorded with an ionizing potential of 70 eV at an ion source temperature of 185°C. All authentic samples were obtained from Aldrich and BDH.

ACKNOWLEDGEMENT. We thank the International Foundation for Science for providing past funding for this work under Appl. Mv. AF/2089 grant No. F/882-1 and the use of mass spectra facilities at the University College, Cardiff.

REFERENCES

D. F. Waterhouse and A. R. Gilby, *J. Insect Physiol.*, **10**, 977 (1964).
[2] M. S. Blum, J. G. Traynham, J. B. Chridester and J. D. Boggus, *Science*, **132**, 1480 (1980).
[3] D. H. Gallam and G. C. Scott, *J. Insect Physiol.*, **15**, 1695 (1969).
[4] B. W. Staddon, *Adv. Insect Physiol.*, **14**, 351 (1979),
[5] V. M. Dazzini and M. Pavan, *Publ. Inst. Ent. Univ. Pavia.*, **5**, 1 (1979).
[6] A. R. Gilby and D. F. Waterhouse, *Proc. R. Soc. B*, **162**, 105 (1965).
[7] M. S. Blum and J. G. Traynham, *XI Int. Kongr. Ent. Vien.*, **3**, 48 (1960).
[8] B. W. Staddon, I. J. Everton and D. E. Games, *Comp. Biochem Physiol.*, **62B**, 259 (1979).
[9] D. E. Games and B. W. Staddon., *J. Insect. Physiol.*, **19**, 1527 (1973).

Revue Roumaine de Chimie, 35, 4, 549—554 (1990)

SYNTHESIS AND ANTI-INFLAMMATORY ACTIVITY OF SOME NEW TRIHETEROCYCLIC THIAZOLES

GEETA M. KULKARNI[a], MANOHAR V. KULKARNI*, VEMANNA D. PATIL[a,**]
D. B. SHRIDHAR[b] and M. LAXMANA[b]
[a]Department of Chemistry, Karnatak University, Dharwad-580 003, India
[b]Government College of Pharmacy, Bangalore, India

Received November 21, 1987

4-Aminomethylcarbostyrilhydrochloride (II) was treated with potassium thiocyanate in ethanol to get the corresponding thiourea (IIa), which in situ reacted with various 3-bromoacetyl coumarins (I) to give the triheterocyclic thiazoles (III). Spectral properties and anti-inflammatory activity of (I) and (III) are reported.

INTRODUCTION

Carbostyrile have been of immense importance due to their wide ranging biological properties. In recent years a number of carbostyril derivatives with diverse structural features have been patented for their anti-inflammatory, analgesic, anti-convulsant and anti-histaminic activities.[1–6]

Earlier work reported from this laboratory revealed that inflammation inhibiting property is associated with fused thiazolylcoumarins.[7] Structural variations, based on the probable biodegradative pathways of coumarin ring, have shown 2-aryl aminomethyl-4-coumarinylthiazoles [2] to be good anti-inflammatory agents, in a preliminary screening. Introduction of a second coumarin ring has also been found to enhance the activity and the tolerance level of these compounds in albino rats.[9] In view of the pharmacological property associated with carbostyril moiety it was thought of interest to synthesise some triheterocyclic systems incorporating carbostyril, coumarin and thiazole rings.

The present investigation, hence, reports the synthesis of 2-(4′-carbostyrilaminomethyl)-4-(3″-coumarinyl) thiazoles, and their anti-inflammatory activity.

---

* Present address: Department of Chemistry, Central College, Bangalore University, Bangalore-560 001.

** To whom the correspondence will be addressed.

CHEMISTRY

The sequence of reactions employed for the synthesis of title compounds is outlined in scheme 1. 3-Acetylcoumarins (Ia) were prepared by the reaction of salicylaldehydes with ethyl-acetoacetate in presence of piperidine at ice bath temperatures. These were brominated according to the method of Koelsch [10] to obtain the corresponding 3-bromoacetylcoumarins (I).[11]

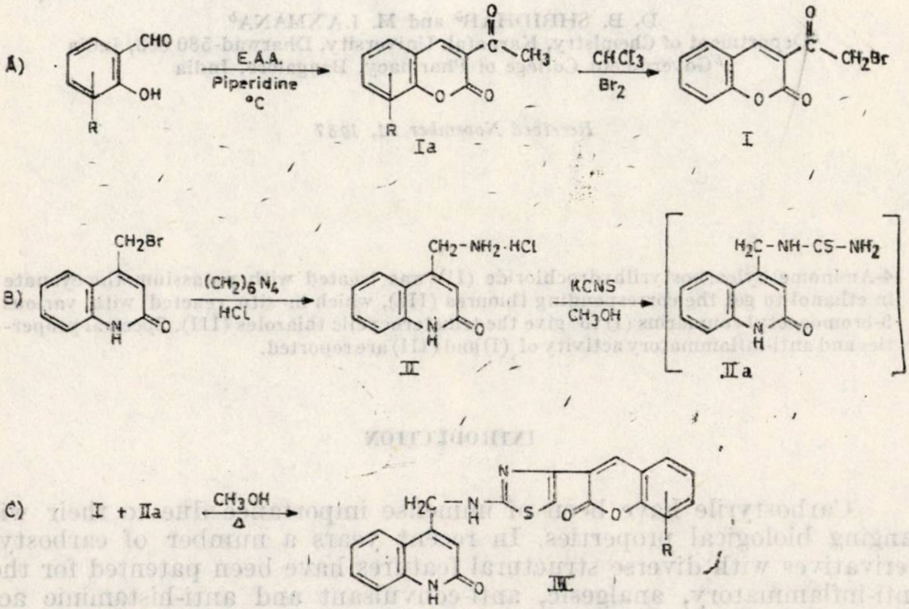

4-Bromomethylcarbostyril[12] was converted to 4-aminomethyl carbostyrilhydrochloride (II) by the acid hydrolysis of its hexamine adduct. Corresponding thiourea (IIa) was easily generated in situ by the reaction of II with potassium thiocyanate in dry methanol.

Title compounds (III) were obtained by the reaction of 3-bromoacetylcoumarins (I) and thiourea (IIa) which results in thoazole ring formation. In general, thiazoles were formed in refluxing methanol in about 3 — 4 hours in a free base form and no hydrobromides were isolated in accordance with literature.[13] Thiazole formation was indicated by a typical stable yellow colour of the reaction mixture. Thiazoles were generally found to be pale yellow or brownish solids and their structures agreed with the spectral and analytical data.

RESULTS AND DISCUSSION

3-bromoacetylcoumarins (I) showed two strong bands in the IR spectrum around 1730 cm^{-1} and 1680 cm^{-1} due to lactone carbonyl and coumarin-3-carbonyl stretching vibrations, respectively (Table 1). In the

^1H-NMR spectra ($CDCl_3$) 8-methoxy-3-bromoacetylcoumarin[11] showed the presence of methoxy protons at 4.0 ppm and of the CH_2 protons at 4.8 ppm. Aromatic protons were observed at 7.2 ppm, while the coumarin-4-proton was found to resonate at 8.7 ppm.

Table 1

IR spectral data of 3-bromoacetylcoumarins (I)

Compd.	R	C=O Lactone	C=O Ketine
Ia	6−Cl	1 740	1 695
Ib	6−Br	1 740	1 695
Ic	6,8−Br	1 740	1 700
Id	5,6−Benzo	1 725	1 705
Ie	8−OCH_3	1 725	1 690

The aminehydrochloride (II) exhibited strong bands at 3380 cm^{-1} and 1680 cm^{-1} due to NH and C = O stretching vibrations respectively.

The two strong bands in the IR spectra (Table 2) of triheterocyclic thiazoles (III) around 1680 cm^{-1} and 1720 cm^{-1} are due to amide and lactone carbonyl stretching vibrations respectively. The NH stretching

Table 2

IR spectral data of 2-(4′-carbostyril aminomethyl)-4−(3−coumarinyl) thiazoles (III)

Compd.	R	C=O Amide	C=O Lactone	N−H	C=N
IIIa	−H	1 675	1 720	3 340	1 610
IIIb	6″−Cl	1 680	1 735	3 390	1 610
IIIc	6″−Br	1 685	1 740	3 410	1 620
IIId	6″−8″−Br	1 685	1 750	3 370	1 620
IIIe	8″−OCH_3	1 690	1 720	3 400	1 620
IIIf	5″−6″−Benzo	1 670	1 720	3 400	1 615

Table 3

Analytical data of 2-(4′−carbostyril aminomethyl)−4−(3″−coumarinyl)− thiazoles (III)

Compd.	R	M.P. °C (d)	Yield %	Formula	Analysis % Required N	Analysis % Found N
IIIa	−H	170[a]	70	$C_{22}H_{15}N_3O_3S$	10.47	10.29
IIIb	6″−Cl	206[b]	40	$C_{22}H_{14}N_3O_3SCl$	9.64	9.54
IIIc	6″−Br	176[a]	40	$C_{22}H_{14}N_3O_3SBr$	8.75	8.64
IIId	6″, 8″−Br	210[a]	70	$C_{22}H_{13}N_3O_3SBr_2$	7.51	7.32
IIIe	8″−OCH_3	156[a]	70	$C_{23}H_{17}N_3O_4S$	9.74	9.52
IIIf	5″, 6″−Benzo	186[a]	80	$C_{26}H_{17}N_3O_3S$	9.31	9.14

[a] Acetic acid, [b] Ethanol.

band was observed as a broad hump around 3400 cm^{-1}. In the NMR spectra (TFA) (IIIa), the methylene protons appeared as a singlet at 4.6 ppm and the coumarin-4-proton was found to resonate at 8.6 ppm. Both the thiazole and the carbostyril C_3—H were found to merge in the aromatic multiplet centered around 7.6 ppm.

SCREENING RESULTS

Anti-inflammatory activity of some of the compounds reported herein has been evaluted by the rat paw edema method of Winter et al.[14] employing 3.5% formalin as the phlogistic agent. All the compounds were administered intraperitoneally as suspensions in 2% CMC, 30 minutes before the injection of the phlogistic agent, at dose level of 100 mg/kg body weight.

Phenyl butazone was employed as standard at a dose le vel of 150 mg/kg body weight. Groups of six albino rats were used in each experiment. Plain CMC (2%) served as the control. Inhibition of inflammation was measured at various time intervals (Table 4).

Table 4

Anti-inflammatory activity of compounds I and III

Compd.	R	% Inhibition of inflammation at the end of						
		0,5h	1h	2h	4h	8h	12h	24h
Ia	6—Cl	—	11.75	26.08	33.30	27.58	10.00	3.12
Ic	6,8—Br	—	11.78	17.38	37.50	24.13	13.34	3.12
Id	8—OCH_3	17.64	23.52	34.77	41.67	37.92	10.00	6.24
IIIa	—H	5.87	11.75	30.43	41.67	17.23	13.34	9.37
IIIc	6″—Br	—	11.75	34.77	37.50	20.69	16.67	9.37
IIId	6″—8″—Br	—	5.87	34.77	41.67	31.03	10.00	9.37
IIIe	8″—OCH_3	—	5.87	39.13	37.50	37.92	16.67	9.37
IIIf	5″,6″—Benzo	—	5.87	13.04	25.00	13.09	3.34	3.12
Phenylbutazone		5.87	17.64	43.47	50.00	27.58	13.34	12.49

Average weight of rats was in the range of 165—170 gms.
Standard error of mean in all the groups ranged from ±0.02 to ±0.04.

In the case of 3-bromoacetylcoumarins (I) the peak anti-inflammatory activity was observed at the end of four hours. 8-Methoxy substitution (Id) results in quick onset of action and considerable activity is retained at the end of twelve hours. 6.8-Dibromo compound (Ic) showed better activity compared to 6-chloro derivative (Ia).

Substituents in the coumarin ring have a marked influence on the anti-inflammatory activity of triheteroaryl thiazoles (III). The unsubstituted compound (IIIa) showed maximum activity at the fourth hour and was found to retain significant activity at the end of twelfth hour. Both 6,8-dibromo and 8-methoxy substituents favour the activity. 8-Methoxy triheteroaryl thiazole (IIIe) retains its peak action for a period of six hours and further shows comparable retention of activity with phenyl butazone at the end of twelfth hour. Introduction of a second aromatic moiety results in considerable loss of activity, which can be seen from the date of (IIIf). All the compounds retained about 80% activity in comparison with phenyl butazone at the end of twenty four hours. Structure activity relation studies indicate that 8-substitution favours the activity in compounds (I) and (III).

EXPERIMENTAL

All the melting points are taken in open capillaries and are uncorrected. IR (ν_{max} in cm^{-1}; KBr) and NMR (δ ppm, downfield from TMS) were recorded on a Perkin Elmer spectrometer and on a 90 MHz instrument respectively.

a) 4-Aminomethyl carbostyril hydrochloride (II)

A mixture of 4-bromomethylcarbostyril (4.8 g) and powdered, anhydrous hexamethylene tetramine (3.5 g) in superdry ethanol (50 mL) was refluxed on a water bath for 3 hours. Hexamine adduct thus obtained was filtered, treated with excess of hydrochloric acid (20 mL), dry ethanol (20 mL) and was refluxed again on a water bath for 2 hours and left overnight. The separated crystalline white solid was filtered and recrystallised from a mixture of ethanol and ether. M.p. 335°C (d) yield (80%), $C_{10}H_{11}N_2OCl$ required : C, 57.00 ; H, 5.22 ; N, 13.30 found : C, 56.84 ; H, 5.11 ; N, 13.15.

IR(KBr) : 1650(C = O)
3380(N–H)

b) 2-(4′–Carbostyril aminomethyl)–4–(3″–Coumarinyl)–Thiazoles (III)

In a typical experiment, a mixture of 4-aminomethyl-carbostyrilhydrochloride (0.63 g) and potassium thiocyanate (0.58 g) in ab. methanol (20 mL) was refluxed on a water bath for 3 hours. After cooling, separated potassium chloride was filtered off. To the mother liquor, 3-bromo acetyl coumarin (0.80 g) was added and refluxing was continued for further 4 hours. The reaction mixture was left overnight. Yellow crystals of thiazole were filtered and washed with excess of water.

Various Thiazolyl carbostyrils (III) thus prepared are listed with their spectral and analytical data in table 2 and 3 respectively.

ACKNOWLEDGEMENTS. The authors are thankful to U.G.C. New Delhi for the award of a fellowship to Mrs. G. M. Kulkarni, R.S.I.C. I.I.T Madras for the spectra and Head of the Chemistry Department, Karnatak University, Dharwad for providing laboratory facilities.

REFERENCES

[1] D. R. Brittain, E. D. Brown, W. Hepworth and G. J. Stacy, Ger. offen. 2, 611, 824 ; *Chem. Abstr.*, **86**, 16558z (1977).

[2] S. Yoshiazaki, S. Tamada and K. Nakagawa, Japan Kokai, 77, 83, 379 ; *Chem. Abstr.*, **88**, 6752k (1978).

[3] M. Tominaga, H. Tone and K. Nakagawa, Ger. offen. 2, 711, 719 ; *Chem. Abstr.*, **88**, 22663n (1978).

[4] G. E. Hardtmann, Ger. offen. 2, 706, 752 ; *Chem. Abstr.*, **88**, 6753m (1978).

[5] E. Muller, J. Nickl, J. Roch, B. Narr, W. Haarmann and J. M. Weisenberger, Can CA 1, 156, 657 : *Chem. Abstr.*, **101**, 7049k (1984).

[6] Otsuka Pharmaceutical Co. Ltd., Jpn. Kokai Koho JP. 59, 93 050 ; *Chem. Abstr.*, **101**, 191721x (1984).

[7] M. V. Kulkarni, V. D. Patil, S. Nanjappa and V. N. Biradar, *Arch. Pharm.* (Weinheim), **314**, 435 (1981).

[8] S. S. Hanmantgad, M. V. Kulkarni and V. D. Patil, *Nat. Acad. Sci. Lett.* (India), **7**, 77 (1984).

[9] S. S. Hanmantgad, Ph. D. Thesis, Karnatak University, Dharwad (India) (1983).

[10] C. F. Koelsch, *J. Amer. Chem. Soc.*, **72**, 2993 (1950).

[11] V. Rajeswer Rao and T. V. Padmanabha Rao, *Ind. J. Chem.*, **25B**, 413 (1986).

[12] D. J. Cook, R. E. Bowen and E. Daniels, *J. Org. Chem.* **26** 4949 (1961).

[13] A. K. Panigrahi and M. K. Raut, *J. Ind. Chem. Soc.* **48**, 665 (1971).

[14] C. A. Winter, E. A. Risley, and G. W. Nuss, *Proc. Soc. Exptl. Biol.* (*N. Y.*) **111**, 544 (1962).

Revue Roumaine de Chimie, 35, 4, 555—560 (1990)

KINETIC STUDIES OF TAUTOMERISATION AND EFFECT OF TEMPERATURE ON ENETHIOL CONTENTS OF SOME CARBOXYALKYL-THIOCARBAMIDES

P. S. MITTAL[a], N. KUMAR[a], K. K. GIRDHAR[b], A. D. TANEJA[c] and J. S. TYAGI[d]

[a] D. N. College, Hisar — 125001, India
[b] Dept. of Chemistry and Biochemistry H.A.U., Hisar, India
[c] HAU, Hisar—125004, India
[d] Meerut College, Meerut, India

Received December 7, 1987

A kinetic study of tautomerisation of carboxyalkylthiocarbamides I—XII is presented. The effect of temperature on enethiol content of compounds I—XII is also discussed.

INTRODUCTION

Although a few workers[1-3] have studied the effect of temperature on the enethiol contents of heterocyclic thiocarbamides, the literature reveals that practically little work has been reported on the kinetic study of tautomerisation of carboxy alkyl thiocarbamides, so it was thought desirable to make detalied kinetic studies of tautomerisation of the synthesized carboxy alkyl thiocarbamides.

EXPERIMENTAL

The chemicals used were of BDH AnalaR or E. Merck extra pure or GR quality. The compounds: N—methyl—N′—(1,5-dicarboxy propyl)—thiocarbamide (I), N—phenyl—N′—(1,5-dicarboxy propyl)—thiocarbamide (II), N—allyl—N′—(1,5-dicarboxy propyl)—thiocarbamide (III), N—methyl—N′—(1,4-dicarboxy ethyl)—thiocarbamide (IV), N—phenyl—N′ (1,4-dicarboxy ethyl)—thiocarbamide (V), N—allyl—N′—(1,4-dicarboxy ethyl)—thiocarbamide (VI), N—methyl—N′—(carboxy ethyl)—thiocarbamide (VII), N—phenyl—N′—(carboxy ethyl)—thiocarbamide (VIII), N—allyl—N′—(carboxy ethyl)—thiocarbamide (IX), Bis—N—methyl—N′—(carboxy ethyl thio)—thiocarbamide (X), Bis—N—phenyl—N′—(carboxy ethyl thio)—thiocarpamide (XI), Bis—N—allyl—N′—(carboxy ethyl thio)—thiocarbamide (XII) were prepared as described[4].

Indirect alkali titration technique was employed to determine the enethiol contents of the thiocarbamides.[5] To find out the effect of temperature and to study the kinetics of tautomerisation, standard solutions of thiocarbamides in ethanol were titrated at regular intervals of six hours each till the titre value became constant. Studies were made under different experimental conditions of temperature viz., 10, 20, 30, 40 and 50°C and the values of enthalpy change (ΔH), free energy change (ΔG) and entropy change (ΔS) were calculated by usual methods (Table 1). The rate of tautomerisation of the thiocarbamides was determined and the reaction was found to be a reversible first order reaction. The rate constant was calculated using the following equation for each thiocarbamide and the values are given in Table 2.

$$k_1 = \frac{2.303}{t}\,\frac{A_0 - A_e}{A_0}\,\log\frac{A_0 - A_e}{A - A_e}$$

where :

A_0 = concentration of compound at zero time

A_e = equilibrium concentration

A = Concentration at time 't'

k_1 = rate constant for the forward reaction

The reversible reaction can be represented as

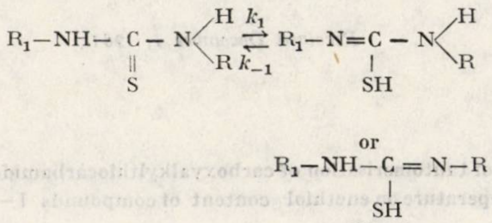

$$R_1{-}NH{-}\underset{\underset{S}{\|}}{C}{-}N\langle^{H}_{R} \underset{k_{-1}}{\overset{k_1}{\rightleftharpoons}} R_1{-}N{=}\underset{\underset{SH}{|}}{C}{-}N\langle^{H}_{R}$$

thione form

or

$$R_1{-}NH{-}\underset{\underset{SH}{|}}{C}{=}N{-}R$$

enethiol form

k_1 = rate constant for forward reaction

k_{-1} = rate constant for backward reaction

RESULTS AND DISCUSSION

The percent enethiol of different thiocarbamides in ethanol (Table 1) shows that in each category (similarly N-substituted compounds) the phenyl substituted thiocarbamide has the maximum thiol content whereas the methyl substituted has the minimum. It has been observed that the extent of thiol formation bears an inverse correlation to the electron donor properties of the substituent.[1,3,6] Methyl is an electron donor group and hence thiolises methyl substituted thiocarbamide to the least extent whereas phenyl being an electron withdrawing group thiolizes to the maximum extent. The percent enethiol in each category of compounds is found to be in the following order :

Phenyl substituted thiocarbamide > Allyl substituted thiocarbamide > Methyl substituted thiocarbamide

From Table 1 it is also observed that increase in temperature results in the increase in enethiol content of these thiocarbamides. K_{eq} and thermodynamic parameters were calculated using standard equations and are given in Table 1.

The rate of tautomerisation of these substituted thiocarbamides was determined in ethanol and the reaction was found to be reversible and first order.

Table 1

Effect of temperature on percentage enethiol and thermodynamic functions of carboxy alkyl-substituted thiocarbamides in ethanol

Compound No.	Temp °K	% Enethiol	K_{eq}	ΔG (kJmol^{-1})	ΔH (kJmol^{-1})	ΔS (JK^{-1} mol^{-1})
I	283.16	9.35	0.1031	5.35		
	293.16	10.61	0.1180	5.21		
	303.16	12.01	0.1360	5.01		
	313.16	13.69	0.1586	4.79	− 9.58	−48.07
	323.16	14.85	0.1743	4.67		
II	283.16	10.33	0.1152	5.09		
	293.16	12.07	0.1372	4.84		
	303.16	14.67	0.1713	4.44		
	313.16	16.00	0.1904	4.32	−11.71	−53.83
	323.16	17.50	0.2121	4.16		
III	283.16	9.03	0.0992	5.44		
	293.16	10.65	0.1191	5.18		
	303.16	13.01	0.1495	4.66		
	313.16	14.72	0.1726	4.57	−12.75	−58.32
	323.16	16.10	0.1918	4.44		
IV	283.16	9.35	0.1031	5.35		
	293.16	10.01	0.1111	5.36		
	303.16	12.60	0.1443	4.67		
	313.16	14.12	0.1644	4.70	−11.79	−55.40
	323.16	15.60	0.1848	4.54		
V	283.16	12.02	0.1366	4.69		
	293.16	13.36	0.1542	4.56		
	303.16	15.02	0.1764	4.37		
	313.16	16.64	0.1996	4.19	− 9.36	−45.40
	323.16	18.25	0.2230	4.03		
VI	283.16	12.02	0.1366	5.00		
	293.16	13.36	0.1542	4.80		
	303.16	15.00	0.1764	4.57		
	313.16	16.64	0.1996	4.41	−10.28	−49.25
	323.16	18.24	0.2230	4.26		
VII	283.16	10.67	0.1194	5.31		
	293.16	12.23	0.1393	5.10		
	303.16	14.00	0.1627	4.82		
	313.16	15.53	0.1838	4.71	−10.92	−52.26
	323.16	17.03	0.2052	4.53		
VIII	283.16	12.27	0.1462	4.51		
	293.16	14.00	0.1627	4.42		
	303.16	15.33	0.1810	4.31	− 5.79	−33.60
	313.16	16.00	0.1904	4.32		
	323.16	16.67	0.2000	4.32		
IX	283.16	11.90	0.1350	4.71		
	293.16	12.97	0.1490	4.64		
	303.16	14.20	0.1655	4.53		
	313.16	15.53	0.1838	4.41	− 7.56	−39.96
	323.16	16.70	0.2004	4.32		

Table 1 (continued)

Compound No.	Temp. °K	% Enethiol	K_{eq}	ΔG (kJmol^{-1})	ΔH (kJmol^{-1})	ΔS (JK^{-1}mol^{-1})
	283.16	13.30	0.1534	4.41		
X	293.16	14.28	0.1665	4.37		
	303.16	15.40	0.1820	4.29		
	313.16	16.57	0.1981	4.21	− 6.61	−35.98
	323.16	17.73	0.2179	4.09		
	283.16	16.45	0.1968	3.82		
XI	293.16	17.50	0.2121	3.78		
	303.16	18.72	0.2303	3.61		
	313.16	20.04	0.2506	3.60	− 6.17	−34.31
	323.16	21.40	0.2722	3.49		
	283.16	14.66	0.1717	4.15		
XII	293.16	15.63	0.1852	4.11		
	303.16	17.67	0.2000	4.05		
	313.16	17.73	0.2155	4.00	− 5.65	−31.21
	323.16	18.80	0.2315	3.93		

The values of first order rate constant (k_1) and rate constant for the reversible reaction (k_{-1}) are reported in Table 2. It can be seen from Table 2 that the variation of rate constant is due to the nature of the substituent in these thiocarbamides. The substituted thiocarbamides are divided into four sets depending upon the substituent. The variation of first order rate constant (k_1) in each set is in the following order :

Phenyl substituted thiocarbamide> Allyl> substituted thiocarbamide> Methyl substituted thiocarbamide.

Table 2

Specific rate constants, equilibrium constants thermodynamic functions of enethiolisation of carboxyalkyl-thiocarbamides.

Compd.	$k_1 \times 10^3$ (hr^{-1})	$k_{-1} \times 10^3$ (hr^{-1})	K_{eq}	ΔG (kJmol^{-1})	ΔH (kJmol^{-1})	S (JK^{-1}mol^{-1})	pK values dissociation of $-\underset{\mathrm{SH}}{\underset{\vert}{\mathrm{C}}}=$
I	2.0	14.7	0.1360	5.01	− 9.56	−48.07	11.50
II	2.5	14.6	0.1713	4.44	−11.71	−43.83	10.80
III	2.5	17.4	0.1495	4.66	−12.75	−58.32	11.39
IV	1.7	11.8	0.1443	4.67	−11.79	−55.40	11.81
V	2.3	13.0	0.1764	4.37	− 9.36	−45.40	11.11
VI	2.2	12.5	0.1764	4.57	−10.28	−49.25	11.75
VII	1.7	10.4	0.1627	4.82	−10.92	−52.26	11.70
VIII	2.3	12.7	0.1810	4.31	− 5.79	−33.60	10.99
IX	2.1	12.7	0.1655	4.53	− 7.56	−39.96	11.62
X	2.5	13.1	0.1820	4.29	− 6.61	−35.98	10.15
XI	2.9	12.6	0.2303	3.61	− 6.17	−34.31	9.50
XII	2.6	13.0	0.2000	4.05	− 5.65	−31.21	10.08

The comparison of the values of first order rate constant (k_1) for the forward reaction with k_{-1} for the backward reaction indicates that the equilibrium lies more towards the thione form than enethiol form of these substituted thiocarbamides. It is reported [1,3,6] that the extent of thiol formation depends upon the electron donor properties of the substituent. Hence the order of thiolisation expected is: phenyl> allyl> methyl.

From Table 2 it is clear that the values of first order rate constant are in agreement with the order of thiolisation of different thiocarbamides. The following mechanism has been suggested to explain the experimental observations :

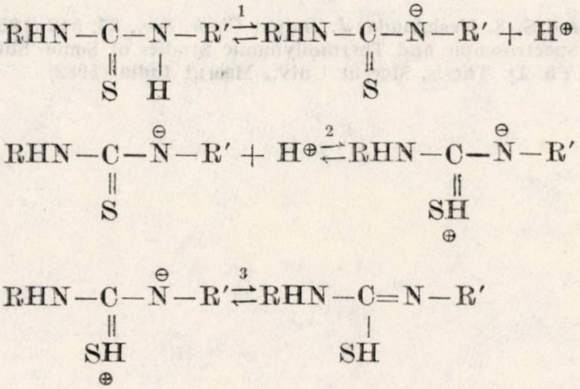

$$RHN-\underset{\overset{\|}{S}}{C}-\underset{\overset{|}{H}}{N}-R' \overset{1}{\rightleftharpoons} RHN-\underset{\overset{\|}{S}}{C}-\overset{\ominus}{N}-R' + H^{\oplus}$$

$$RHN-\underset{\overset{\|}{S}}{C}-\overset{\ominus}{N}-R' + H^{\oplus} \overset{2}{\rightleftharpoons} RHN-\underset{\overset{\|}{\underset{\oplus}{SH}}}{C}-\overset{\ominus}{N}-R'$$

$$RHN-\underset{\overset{\|}{\underset{\oplus}{SH}}}{C}-\overset{\ominus}{N}-R' \overset{3}{\rightleftharpoons} RHN-\underset{\overset{|}{SH}}{C}=N-R'$$

Rate of formation of $RHN-\underset{\overset{|}{SH}}{C}=N-R'$ can be represented as :

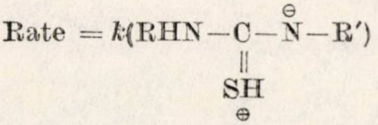

$$Rate = k(RHN-\underset{\overset{\|}{\underset{\oplus}{SH}}}{C}-\overset{\ominus}{N}-R')$$

The reaction is of the first order with respect to

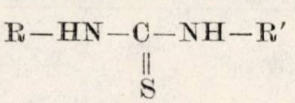

$$R-HN-\underset{\overset{\|}{S}}{C}-NH-R'$$

It is observed that the first order rate constant (k_1) depends upon the ionisation constants of these thiocarbamides. The higher the pK value due to dissociation of $-\underset{\overset{|}{SH}}{C}=$the lower should be the rate of thiolisation or enolisation and it can be observed from Table 2 that the rate constant generally decreases with the increase in pK values.

The values of free energy change and entropy change are the measure of the feasibility of the change of the system. The higher the value of free energy change, the lower will be the rate of thiolisation. It is observed from

Table 2 that the rate constant varies inversely with the values of free energy change in each set of the substituted thiocarbamide. Similarly, the higher value of entropy change stands for the lower value of rate constant.

REFERENCES

[1] C. S. G. Prasad, Ph. D. Thesis BITS, Pilani, India (1973).

[2] B. C. Kashyap, Ph. D. Thesis BITS, Pilani, India (1974).

[3] O. P. Khurana, Ph. D. Thesis, Meerut Univ., Meerut, India (1980).

[4] P. S. Mittal, J. S. Tyagi, N. Kumar and A. D. Taneja, *J. of Indian Chem. Soc.*, (Communicated).

[5] M. M. Bokadia and S. S. Neshpanda. *J. Indian Chem. Soc.*, **27**, 548 (1950).

[6] J. D. Gauba, "Spectroscopic and Thermodynamic Studies of Some Substituted Thiazolyl Thioureas" Ph. D. Thesis, Meerut Univ., Meerut India (1982).

Revue Roumaine de Chimie, 35, *4*, 561–565 (1990)

SYNTHESIS OF 2,6-DIMETHYL-4-STYRYLPYRYLIUM SALTS (FROM 2,4,6-TRIMETHYLPYRYLIUM AND DONOR-SUBSTITUTED BENZALDEHYDES) AND THEIR CONVERSION INTO PYRIDINES

DANIELA CARMEN ONICIU,[a] ANCA MARTON,[a] TEODOR-SILVIU BALABAN,[b] SORIN VLAD[a] and ALEXANDRU T. BALABAN[a]

[a] Polytechnic Institute, Organic Chemistry Department, Splaiul Independenței 313, 77206 Bucharest, Romania

[b] Centre of Organic Chemistry, Bucharest, Romania

Substituted *trans*-styrylpyrylium salts **5a**–**c** are obtained by condensation of the most active 4-methyl group of 2,4,6-trimethylpyrylium perchlorate with aromatic aldehydes; by treatment with ammonia, the corresponding *trans*-styrylpyridines **6a**–**c** are generated.

INTRODUCTION

Condensation reactions of alkyl groups in substituted pyrylium salts were reported for the first time by Dilthey and Fischer,[1] who treated 2-methyl-4,6-diphenylpyrylium and 4-methyl-2,6-diphenylpyrylium salts with aromatic aldehydes, for obtaining styrylpyrylium salts, such as **1** and **2**.

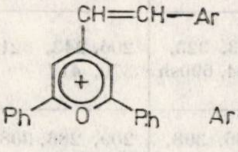

1

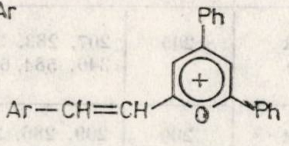

2

More recently,[2] electron-donating substituents attached to benzaldehydes were shown to facilitate such condensation reactions, probably by enhancement of the electrophilicity of the carbonyl group.

Other papers [3] which describe related condensation reactions evidence the greater reactivity of 4-methyl groups relative to the 2,6-methyl groups; this statement agrees with deuteration rates of 2,6-and 4-methyl groups,[4] which are higher for the latter groups.

The present paper reports the synthesis of three styrylpyrylium perchlorates **5a-c** and the corresponding styrylpyridines **6a-c**. Compounds **5a** and **6a** have been reported earlier.[5]

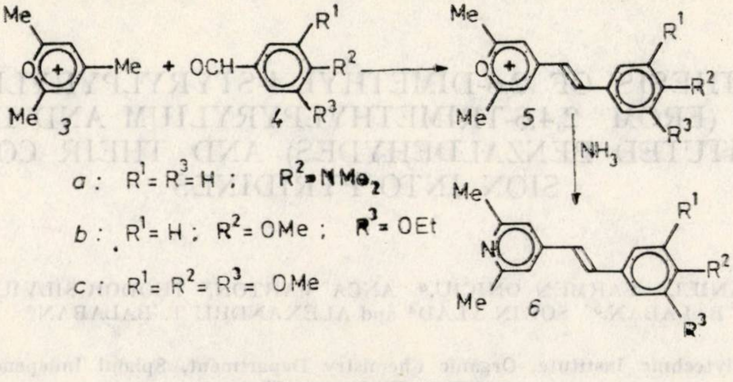

EXPERIMENTAL PART

Synthesis of 2,6-dimethyl-4-styrylpyrylium perchlorates. To a solution of 25 mmoles of 2,4,6-trimethylpyrylium perchlorate[6] in refluxing absolute methanol or glacial acetic acid were added dropwise 25 mmoles of freshly purified substituted benzaldehyde, during two hours. Heating was continued for about four hours. The reaction mixture was left to stand overnight, after which the condensation product crystallized. After filtration, products were recrystallized from ethanol or ethanol–ether acidified with perchloric acid.

The purity may be verified by tlc using as elution solvent ethyl acetate : acetic acid (3 : 2). Pyrylium salts **5a–c** were characterized according to Table 1.

Table 1

Data for styrylpyrylium perchlorates **5a – 5c**

Ref.	Compd.	Colour	m.p., °C	UV–VIS, λ, nm		IR, cm^{-1}, (KBr)
				MeOH	MeOH+HCl aq	
8	**5a**	dark blue	205	207, 283, 323, 346, 584, 690sh	206, 243, 321, 370, 417	1090 vs ; 1140 m ; 1280 s : 1550 s ; 1640 s.
a	**5b**	light red	200	209, 286, 308, 351, 469, 556 sh	209, 286, 308, 351, 469, 556, 556 sh	1020 s ; 1060 vs ; 1260 s ; 1590 s ; 1640 s.
b	**5c**	dark red		210, 217, 303, 444	210, 217, 303, 444	1020 s ; 1070 vs ; 1260 vs ; 1500 s ; 1690 s.

[a] Anal. Calcd. for $C_{18}H_{21}ClO_7$: C, 56.18 ; H, 5.50 ; found : C, 56.41 ; H, 5.92.
[b] Anal. Calcd. for $C_{18}H_{21}ClO_8$: C, 53.93 ; H, 5.27 ; found : C, 54.18 ; H, 5.34.

Synthesis of 2,6-dimethyl-4-styrylpyridines. 10 mmoles of 2,6-dimethyl-4-styrylpyrylium perchlorates **5a–c** were stirred with a large excess of aqueous ammonia, during two hours, in the presence of ether, and under cooling. The corresponding pyridine which is formed is collected in the ethereal layer, and is purified by extraction into dilute hydrochloric acid followed by alkalinization with sodium hydroxide.[7] The final ethereal layer was dried over sodium hydroxide ; the solvent was evaporated, leaving pyridines **6a–c** as crystalline compounds. They were further purified by tlc, using as elution systems mixtures of benzene : acetone. The pyridines **6a–c** are characterized according to Table 2.

Table 2

Data for styrylpyridines **6a**—**6c**

Ref.	Compd.	Colour	m.p., °C	R_f	IR, cm^{-1}(CHCl$_3$)
8	**6a**	dark yellow	156	0.5^c	1260 s ; 1570 s ; 1640 vs ; 1760 m.
a	**6b**	light yellow	109	0.4^d	1030 vs ; 1210 s ; 1570 s ; 1650 s ; 1740 m.
b	**6c**	light yellow	115	0.5^d	1260 vs ; 1400 s ; 1570 s ; 1640 s ; 1760 s.

[a] Anal. Calcd. for $C_{18}H_{21}NO_2$: C, 76.30 ; H, 7.47 ; N, 4.14 ; found : C, 75.92 ; H, 8.01 ; N, 4.58.

[b] Anal. Calcd. for $C_{18}H_{21}NO_3$: C, 72.22 ; H, 7.07 ; N, 4.68 ; found : C, 71.79 ;H, 7.28 ; N, 4.86.

[c] Eluent tlc benzene : acetone (5 : 1).

[d] Eluent tlc benzene : acetone (9 : 1).

DISCUSSION OF THE RESULTS

The electronic absorption spectra of the perchlorates **5a-c** consist in a few absorption bands specific for the vinylic and aromatic systems in the UV region and a long-wavelength band situated in the visible region for the conjugated chromophore system. The position of this last band is influenced by the electronic effect of the substituents which induce an extension of the delocalised system over the whole molecule.

Among all compounds reported in this paper, the *p*-dimethylaminostyryl-pyrylium salt **5a** is outstanding by its blue colour ; this is accounted for by electronic delocalization in which the *para*-quinonoid resonance structure **5aB** has a major contribution. The blue solutions of the pyrylium monocations **5a** with a *para*-dimethylamino group afford on acidification the corresponding dications **7a** presenting a strong hypsochromic effect : by acidifying methanolic solutions of compounds **5a**—**c** with con-

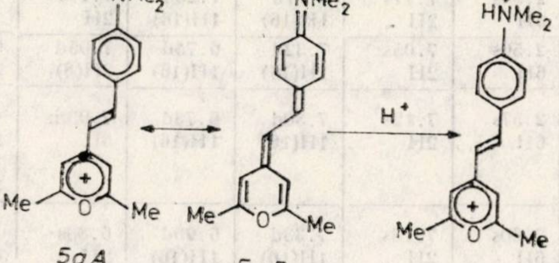

5aA 5aB 7a

centrated hydrochloric acid, one sees that significant modifications appear only in the electronic spectrum of **5a**, by the hypsochromic shift of the band due to conjugated system (at 17000 cm^{-1}) to lower wavelengths (27000 cm^{-1}). This may be explained by protonation of **5a** leading to dication **7a**. For compounds **5b** and **5c** no such modifications are observed in acid conditions.

The IR spectra of the perchlorates **5a**–**c** and pyridines **6a**–**c** confirm the structures proposed. Assignments are evident and in agreement with literature data :[8] the perchlorate bands at 625 and 1090 cm^{-1} ; the ether stretching vibrations $\bar{\nu}_{sym}$ at 1020 cm^{-1}, and $\bar{\nu}_{asym}$ at 1260 cm^{-1} ; the dimethylamino stretching bands $\bar{\nu}_{C-N\ aliph}$ at 1140 cm^{-1} and $\bar{\nu}_{C-N\ arom}$ at 1280 cm^{-1} and finally the vinylic and aromatic bands in the range 1500 – 1700 cm^{-1}.

The ^1H–NMR spectra confirm a *trans*-structure of the double bond, shown by the coupling constant $J = 16$ Hz of the vinylic hydrogens. The assignments for the new compounds are shown in Table 3.

Table 3

^1H–^{1}NMR spectra of styrylpyrylium perchlorates **5** (in trifluoroacetic acid) and styrylpyridines **6** (in $CDCl_3$)

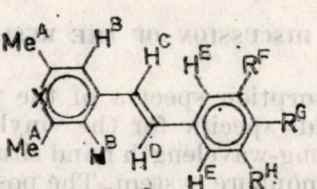

5 - 6

Compd.	X	H^A	H^B	H^C	H^D	H^E	H^F	H^G
5a	O+	2.93s 6H	7.93s 2H	8.23s 1H(16)	7.37d 1H(16)	8.07d 2H(8)	7.77d 2H(8)	3.56s 6H
5b	O+	2.97s 6H	7.91s 2H	8.38d 1H(16)	7.37d 1H(16)	7.80m 3H	4.50q 2H(7) 1.65t 3H(7)	4.18s 3H
5c	O+	2.83s 6H	7.77s 2H	8.17d 1H(16)	7.23d 1H(16)	7.17s 2H	4.00s 9H	
6a	N	2.56s 6H	7.05s 2H	7.32d 1H(16)	6.75d 1H(16)	7.05d 2H(8)	6.72d 2H(8)	2.98s 3H
6b	N	2.57s 6H	7.12s 2H	7.30d 1H(16)	6.78d 1H(16)	7.03m 3H	4.18q 2H(7) 1.51t 3H(7)	3.90s 3H
6c	N	2.60s 6H	7.13s 2H	7.33d 1H(16)	6.90d 1H(16)	6.83s 2H	4.00s 6H	3.95s 3H

[a] Coupling constants (in Hz) are enclosed in brackets.

The strong fluorescence of methanolic, ethanolic and ethereal solutions of styrylpyridines **6a—c**, as well as of methanolic and ethanolic solutions of styrylpyrylium perchlorates **5a—c**, is in agreement with data referring to other similar structures.[5]

The pyrylium derivatives may be tested as potential growth stimulating agents for plants and the structures of the corresponding pyridines suggest similarity to cholinesterase inhibitors.

ACKNOWLEDGEMENT. Thanks are expressed to chem. eng. Andrei Zlota for experimental assistance.

REFERENCES

[1] W. Dilthey and J. Fischer, *Ber. dtsch. chem. Ges.*, **57**, 1653 (1924).

[2] G. N. Dorofeenko, O. E. Shelepin, Z. N. Nazarova, V. N. Novikov and G. P. T. Khonova, *Zh. Obshch. Khim.*, **35**, 570 (1965).

[3] J. Kelemen and R. Wizinger, *Helv. Chim. Acta*, **45**, 1918 (1962).

[4] E. Gârd, I. Stănoiu, F. Chiraleu and A. T. Balaban, *Rev. Roum. Chim.*, **18**, 2571 (1973).

[5] M. Simalty, H. Strzelecka and H. Khedija, *Tetrahedron*, **27**, 3503 (1971).

[6] A. T. Balaban and C. D. Nenițzescu, Org. Synth., Coll. Vol. 5, 1106 (1973).

[7] A. T. Balaban and C. Toma, *Tetrahedron*, Suppl., **7**, 1 (1966).

[8] M. Avram and G. D. Mateescu, "Infrared Spectroscopy", Wiley-Interscience, New York, 1972.

Revue Roumaine de Chimie, 35, 4, 567–575 (1990)

SYNTHESIS AND REACTIONS OF SUBSTITUTED BENZOXAZINONES BEARING A BULKY GROUP AT POSITION-2. PART I

A. A. AFIFY, S. EL-NAGDY, M. A. SAYED and I. MOHEY

Chemistry Department, Faculty of Science, Ain Shams University,

Abbassia, Cairo, Egypt

Received October 31, 1987

2-(substituted)-4H-3,1-Benzoxazin-4-ones (II*a-c*) were synthesized by reaction of anthranilic acid with 2-phenyl-4-arylidene 5-(4)-oxazolones (I*a*–*c*). Aminolysis of II *a*, N-substituted benzamides (III*a-c*). Hydrazinolysis of IIa and *c* gave N-(substituted) anthranilic acid hydrazide derivatives (IV *a*–*f*), while ammonolysis of II *a* and *b* gave 2-(substituted)-3(4H)-quinazolin-4-ones (V*a* and *b*). Treatment of 4-quinazolone derivative (V*a*) with benzoyl chloride afforded 3N-benzoyl-2-substituted-3(4H)-quinazolin-4-one (VI). Compound (V*a*) reacts with a mixture of $PCl_5/POCl_3$ and gave 2-substituted-4-chloro quinazoline (VII). Mannich reaction on (V*b*) with different bases gave the Mannich bases 2-substituted-3N-substituted-4(3H) quinazolin-4-ones (XIV *a-c*). The reaction of 2-substituted-4-chloroquinazoline (VII) with acylhydrazides, sodium azide, alkylating agents and amino-acids yielded the corresponding quinazoline derivatives (VIII*a*–*c*), tetrazole derivative (IX), 2,4-disubstituted quinazolines (X*a*–*d*), and 2-substituted-4-substituted amino-quinazolines (XII*a* & *b*), respectively. Ring closure of XII*a* by acetic anhydride and sodium acetate gave the corresponding 5(4)-pyrazolone derivative (XIII).

The present investigation deals with synthesis and some reactions of some 2-(substituted)-4H–3,1-benzoxazin-4-ones (II*a*–*c*) bearing bulky substituents in position–2. We wished also to obtain some evidence to correlate the stability of the benzoxazinone nucleus with the bulk of substituents in position-2.

The compounds (II*a*–*c*) were prepared by treatment of anthranilic acid with 2-phenyl-4-arylidene-5(4)-oxazolones (I). The structure of compounds (II) was proved from their IR spectra, which exhibit absorption bands in region of 1750–1740, 1660–1640 (benzoxazino and amido – $>$C = O), and 3260–3220 cm^{-1} (amido NH).

It has been reported [1,2] that 2-substituted-4H-3,1-benzoxazin-4-ones react with amines or amino-acids to give *o*-(substituted)-N-substituted benzamide. The present investigation deals with aminolysis of II*a* with aniline, ethanolamine and/or glutamic acid in boiling methanol to give *o*-(benzamido-*p*-methoxystyryl)-N-substituted benzamide (III*a*–*c*). IR spectral data of III show bands at 1690, 1670–1645 (ν CO of carboxylic- and amidogroup) and 3314–3243 cm^{-1} (ν OH and/or ν NH).

Recently,[3] it has been shown that the reaction of 3,1-benzoxazin-4-ones with hydrazine hydrate produces the fission of the hetero-ring. Similarly, (II*a* and *c*) reacts with hydrazines, and the reaction proceeds *via* ring fission of the heterocyclic ring, with the formation of N-(substituted) anthranilic acid hydrazide derivatives (IV*a*–*f*). The IR spectra of compounds (IV) exhibit strong bands at 1670—1640, 3360—3220 cm^{-1} correlated with νCO and νNH respectively.

The ^1H-NMR spectrum of IV*b* (δ; DMSO) showed from low to high field the following signals : at 10.05 (broad, *s*, 2*H*, amido NH, amido of hydrazido group), 8.2—6.8 (*m*, 19*H*, Ar—*H* and olefinic proton), 3.7 (*s*, 1*H*, N*H*NHCO) and 2.95 (*s*, 3*H*, —OCH$_3$).

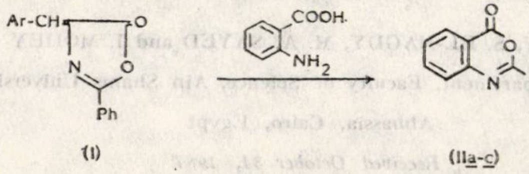
Ar-CH
O
N
O
Ph
COOH
NH2
O
N
O
C=CH-Ar
NHCOAr⁻

(I) (IIa-c)

a, Ar = $-C_6H_4.OCH_3$-p , Ar$^-$ = C_6H_5
b, Ar = $-C_6H_4.NO_2$-m , Ar$^-$ = C_6H_5
c, Ar = $-C_6H_4.OCH_3$-p , Ar$^-$ = $C_6H_4.Cl$-p

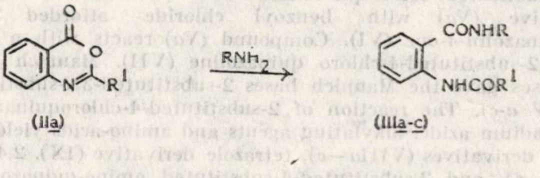
O
O
N
R1
RNH2
CONHR
NHCOR1

(IIa) (IIIa-c)

R^1 = $-\underset{\mid}{C}=CH.C_6H_4.OCH_3$-p
NHCOC$_6$H$_5$

a, R = $-C_6H_5$
b, R = $-CH_2CH_2OH$
c, R = $-CH(COOH).(CH_2)_2COOH$

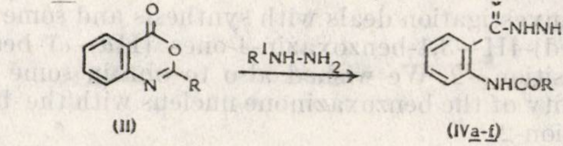
O
O
N
R
R1NH-NH2
O
C-NHNHR1
NHCOR

(II) (IVa-f)

	R	R^1
a,	$-\underset{\mid}{C}=CH.C_6H_4.OCH_3$-p NHCOC$_6H_5$	H
b,	$-C=\underset{\mid}{C}H.C_6H_4.OCH_3$-p NHCOC$_6H_5$	C$_6$H$_5$
c,	$-C=\underset{\mid}{C}H.C_6H_4.OCH_3$-p NHCOC$_6H_5$	C$_6$H$_4$.NO$_2$-p
d,	$-C=\underset{\mid}{C}H.C_6H_4.OCH_3$-p NHCOC$_6H_4$.Cl-o	COC$_6$H$_5$
e,	$-\underset{\mid}{C}=CH.C_6H_4.OCH_3$-p NHCOC$_6H_4$.Cl-o	-COC$_6$H$_4$.OH-o
f,	$-\underset{\mid}{C}=CH.C_6H_4.OCH_3$-p NHCOC.H..Cl-o	-COCH(CH$_3$)$_2$

Ammonolysis of II*a* and *b* with ammonia (furnished from ammonium acetate or formamide by fusion at 170°C) gave the corresponding 2-substituted-4(3H) quinazol-4-one derivatives (V*a* and *b*) as previously reported. IR spectral data of V*a* and *b* show stretching frequencies at 3443 – 3380, 3240—3121 and 1685—1670 cm^{-1} for ν OH, νNH and ν CO, respectively. Such IR data infer that quinazolinone (V) actually exists in a lactam-lactim toutomeric equilibrium, which was further confirmed chemically from the benzoylation and chlorination of V with benzoyl chloride and a mixture of $PCl_5/POCl_3$ respectively. Treatment of quinazol-4-one derivative (V*a*) with an excess of benzoyl chloride afforded 3N-benzoyl-2-substituted quinazol-4-one (VI). The IR spectrum of VI showed bands at 1675—1655 (broad, $>C=O$ of quinazolone nucleus, amido groups), 3400 cm^{-1} (NH) in the side chain in position-2. On the other hand, the reaction of V*a* with a mixture of $PCl_5/POCl_3$, gave 2-substituted-4-chloroquinazoline (VII). The IR spectrum of VII exhibits bands at 1670 ($>C=O$ of amido group), 1620 (νC = C, νC = N), and 3205 cm^{-1} (NH group of he side chain).

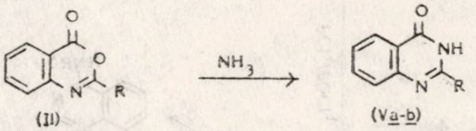

(II)

(V*a*-*b*)

a, $R = -\underset{\text{NHCOC}_6\text{H}_5}{\underset{|}{C}}{=}CH.C_6H_4.OCH_3\text{-}\underline{p}$

b, $R = -\underset{\text{NHCOC}_6\text{H}_5}{\underset{|}{C}}{=}CH.C_6H_4.NO_2\text{-}\underline{m}$

The reaction of 4-chloroquinazoline derivative (VII) with acylhydrazine, namely, isobutyroylhydrazine, benzoylhydrazine and/or salicyloylhydrazine in boiling butanol, gave the corresponding 2(substituted)-triazolo (2′-substituted [1,2-*a*]) quinazoline (VIII*a*—*c*). The IR spectra of VII*a*—*c* exhibit bands at 1670—1650, 1615—1595, 3285—3260 cm^{-1} correlated with νCO, νC=N or $\nu_{C=C}$ and ν_{NH} respectively.

Recently, it has been reported[4] that 2-substituted-4-chloroquinazoline derivatives react with NaN_3 to give 2-substituted-tetrazolo [1,2-*a*]-quinazoline derivatives. Similarly the reaction of 4-chloroquinazoline derivative (VII) with NaN_3 in DMF, gave 2-substituted tetrazole [1,2-*a*] quinazoline derivative (IX). The IR spectrum of IX shows bands at 1660, 1610 and 1020 cm^{-1} characteristic for amido $>C=O$, C=C and/or C = N and tetrazole nucleous respectively.

Also, we extended the investigation with active methylene compounds, alkoxides and amino-acids in order to obtain more precise information about the reactivity of 4-chloroquinazoline. The reaction of VII with active methylene, namely ethyl cyanoacetate, ethylacetoacetate, diethyl malonate and/or acetyl acetone in the presence of ($DMF/NaNH_2$), yielded the corresponding 2-substituted-4-alkyl quinazoline derivatives (X*a*—*d*).

The alkylation of VII with excess alkoxides, namely sodium methoxide and/or sodium ethoxide yielded 2-substituted-4-alkoxy quinazolines (XI*a* and *b*). The IR spectra of XI*a* and *b* show bands at 1665—1660 (amido $>$C=O), 1595 − 1590 (C=C and/or C=N), 1255−1250 (ether linkage) and 3250−3220 cm^{-1} (amido NH).

The IR spectral data of compounds (X*a*−*d*)

Compound	νCO	IR spectra (KBr), cm^{-1}		
		νC = C and/or C = N	νNH	νC≡N
X*a*	1735(ester) 1645(amido)	1608	3 173	2 215
X*b*	1738(ester) 1648(amido)	1 605	3 126	—
X*c*	1735(ester) 1650(amido)	1 610	3 185	—
X*d*	1646(amido)	1 605	3 457 (broad)	

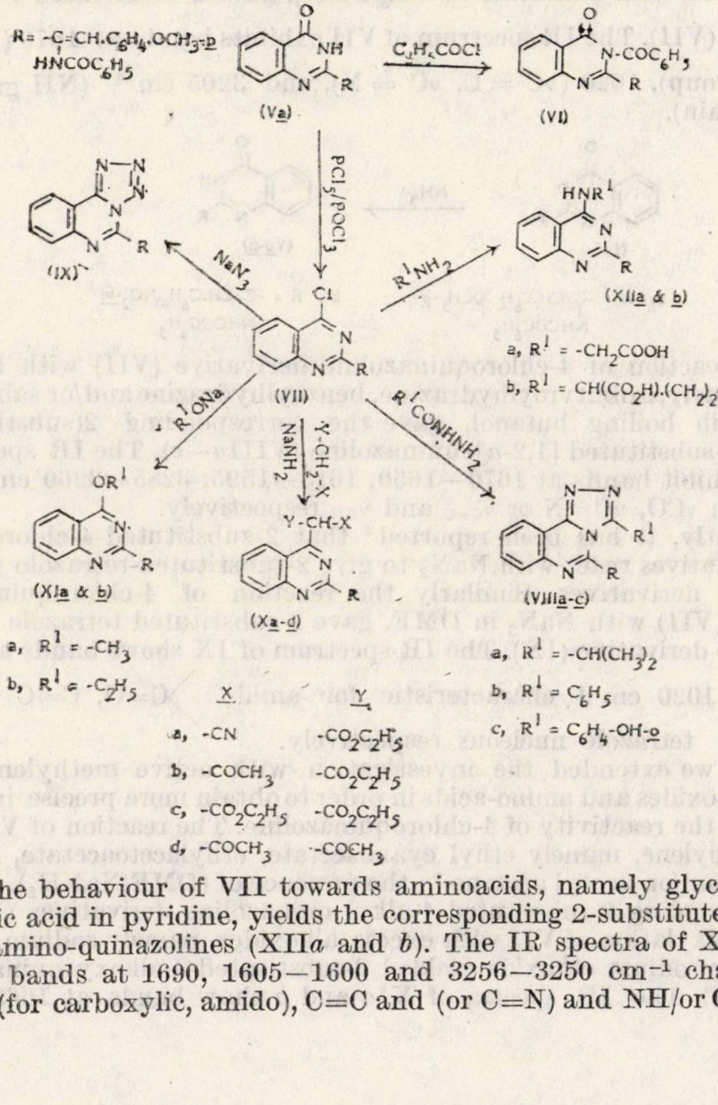
R= -C=CH.C6H4.OCH3-p
HNCOC6H5
NH
(Va)
C6H5COCl
N-COC6H5
(VI)
PCl5/POCl3
(IX)
NaN3
Cl
(VII)
R1NH2
HNR1
(XIIa & b)
a, R1 = -CH2COOH
b, R1 = CH(CO2H).(CH2)2COOH
R1ONa
NaH
Y-CH2-X
RCONHNH2
OR1
(XIa & b)
a, R1 = -CH3
b, R1 = -C2H5
Y-CH-X
(Xa-d)
R1
(VIIIa-c)
a, R1 = -CH(CH3)2
b, R1 = C6H5
c, R1 = C6H4-OH-o
X Y
a, -CN -CO2C2H5
b, -COCH3 -CO2C2H5
c, -CO2C2H5 -CO2C2H5
d, -COCH3 -COCH3

The behaviour of VII towards aminoacids, namely glycine, and/or glutamic acid in pyridine, yields the corresponding 2-substituted 4-substituted amino-quinazolines (XII*a* and *b*). The IR spectra of XII*a* and *b* exhibit bands at 1690, 1605−1600 and 3256−3250 cm^{-1} characteristic of νCO (for carboxylic, amido), C=C and (or C=N) and NH/or OH groups.

Refluxing of XII*a* with acetic anhydride and sodium acetate yields the corresponding 2-substituted-pyrazolono [1,2-*a*] quinazoline derivative (XIII). The IR spectrum of XIII shows bands at 1675, 1650, 3359 cm^{-1} correlated with ν_{CO} (pyrazolono and amido) and ν NH of amido groups, respectively.

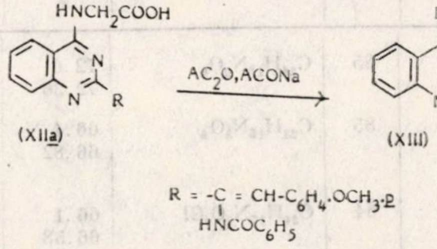
HNCH2COOH
N
N
R
AC2O,ACONa
N
N
O
N
R
(XIIa)
(XIII)
R = -C = CH-C6H4.OCH3-p
HNCOC6H5

Also 2-substituted quinazol-4-one (V*b*), reacts with formaldehyde and amides or imides, namely benzamide, phthalimide and/or succinimide in boiling ethyl alcohol to yield Mannich bases, 2-substituted-3N-substituted 3(4H),-quinazolin-4-ones (XIV *a*—*c*). The IR spectral data of XIV exhibit bands in the regions of 1665—1635, 3290—3140 (amido $>$C=O and NH groups) and 1605—1595 cm^{-1} (ν C = C and/or $\nu_{C=N}$ groups).

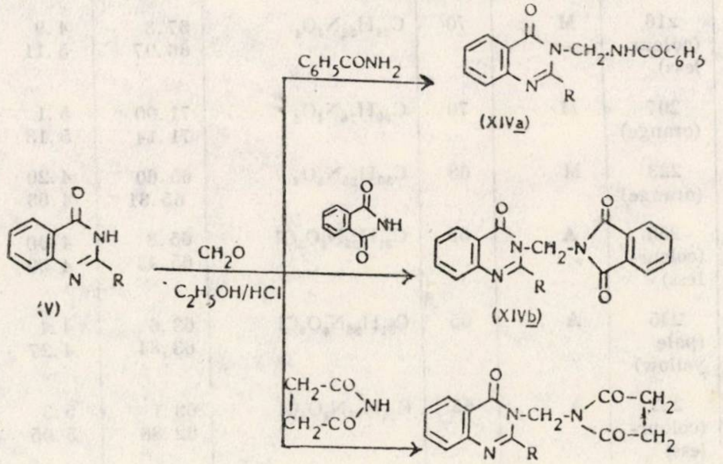
O
N-CH2.NHCOC6H5
C6H5CONH2
N
R
(XIVa)
O
NH
N
R
(V)
CH2O
C2H5OH/HCl
O
NH
O
O
N-CH2-N
N
R
O
O
(XIVb)
CH2-CO
NH
CH2-CO
O
N-CH2-N
CO-CH2
CO-CH2
N
R
(XIVc)
R = -C = CH.C6H4.NO2-m
HNCOC6H5

EXPERIMENTAL

All melting points are uncorrected.

The IR spectra were measured on a Unicam SP 200 G, Pye Unicam 641749 and Beckman 922623 spectrophotometers using KBr wafer technique. The ^{1}H—NMR spectrum was run on a Varian 60 MHz using TMS as internal standard.

Characterisation and physical data of all synthesised compounds are listed in Table 1.

Table 1

Characterisation and physical data of compounds (II – XIV)

Compound	M.P.°C (colour)	Solvent	Yield (%)	Molecular Formula	Analysis % Found/Calcd.		
					C	H	N
II*a*	185 (yellow)	A	85	$C_{24}H_{18}N_2O_4$	72.6 72.36	4.3 4.52	6.7 7.03
II*b*	255 (pale yellow)	A	85	$C_{23}H_{15}N_3O_5$	66.4 66.82	3.2 3.63	9.8 10.11
II*c*	210 (yellow)	A	84	$C_{24}H_{17}N_2O_4Cl$	66.1 66.58	4.1 3.93	6.7 6.4
III*a*	198 (colourless)	M	75	$C_{30}H_{25}N_3O_4$	73.4 73.31	5.2 5.09	8.7 8.55
III*b*	200 (colourless)	M	80	$C_{26}H_{25}N_3O_5$	67.6 67.9	5.7 5.4	8.9 9.1
III*c*	253 (yellow)	A	80	$C_{29}H_{27}N_3O_8$	64.1 63.85	5.2 4.95	7.4 7.07
IV*a*	216 (colourless)	M	70	$C_{24}H_{22}N_4O_4$	67.3 66.97	4.9 5.11	12.8 13.02
IV*b*	207 (orange)	M	70	$C_{30}H_{26}N_4O_4$	71.00 71.14	5.1 5.13	11.4 11.11
IV*c*	223 (orange)	M	68	$C_{30}H_{25}N_5O_6$	65.60 65.31	4.20 4.53	12.4 12.7
IV*d*	250 (colourless)	A	65	$C_{31}H_{25}N_4O_5Cl$	65.8 65.43	4.60 4.39	10.10 9.86
IV*e*	245 (pale yellow)	A	65	$C_{31}H_{25}N_4O_6Cl$	63.6 63.84	4.4 4.27	9.3 9.58
IV*i*	222 (colourless)	A	65	$C_{28}H_{25}N_4O_5Cl$	63.1 62.86	5.3 5.05	10.6 10.47
V*a*	> 280 (brown)	But,	50	$C_{24}H_{19}N_3O_3$	72.60 72.54	5.00 4.78	10.80 10.50
V*b*	230 (brown)	But.	50	$C_{23}H_{16}N_4O_4$	67.20 66.99	3.60 3.88	13.20 13.59
VI	170 (brown)	B	50	$C_{31}H_{23}N_3O_4$	74.6 74.25	4.10 4.59	8.00 8.38
VII	230 (pale red)	B	70	$C_{24}H_{18}N_3O_2Cl$	69.31 69.31	4.70 4.32	10.50 10.11
VIII*a*	> 280 (brown)	But.	60	$C_{28}H_{25}N_5O_2$	72.2 72.57	5.4 5.39	14.7 15.11

Table 1 (continued)

Compound	M.P.°C (colour)	Solvent	Yield (%)	Molecular Formula	Analysis % Found /Calcd.		
					C	H	N
VIII*b*	275 (deep brown)	But.	60	$C_{31}H_{23}N_5O_2$	74.2 74.84	4.20 4.62	13.8 14.08
VIII*c*	> 280 (pale brown)	But.	65	$C_{31}H_{23}N_5O_3$	72.10 72.51	4.6 4.48	13.3 13.64
IX	> 280 (pale yellow)	A	50	$C_{24}H_{18}N_6O_2$	67.8 68.24	4.4 4.26	19.3 19.90
X*a*	245 (brown)	B	65	$C_{29}H_{24}N_4O_4$	71.10 70.73	5.00 4.87	11.10 11.38
X*b*	> 280 (pale yellow)	B	65	$C_{30}H_{27}N_3O_5$	70.20 70.72	5.30 5.30	8.10 8.25
X*c*	> 280 (pale red)	B	65	$C_{31}H_{29}N_3O_6$	68.70 69.01	5.60 5.38	8.10 7.79
X*d*	97 (deep brown)	B	60	$C_{29}H_{25}N_3O_4$	72.30 72.65	5.10 5.21	9.10 8.76
XI*a*	> 280 (pale yellow)	P	50	$C_{25}H_{21}N_3O_3$	73.10 72.99	4.80 5.10	10.40 10.21
XI*b*	> 280 (brown)	P	55	$C_{26}H_{23}N_3O_3$	73.60 73.41	5.10 5.41	10.10 9.88
XII*a*	> 280 (colourless)	E	75	$C_{26}H_{22}B_4O_4$	69.1 68.72	4.70 4.84	12.10 12.23
XII*b*	> 280 (colourless)	E	70	$C_{29}H_{26}N_4O_6$	66.00 66.15	5.20 4.94	10.80 10.64
XIII	165 (yellow)	B	60	$C_{26}H_{20}N_4O_3$	70.90 71.55	4.70 4.58	13.10 12.84
XIV*a*	219 (yellow)	B	75	$C_{31}H_{23}N_5O_5$	68.6 68.25	5.00 4.62	12.6 12.84
XIV*b*	215 (pale yellow)	E	75	$C_{32}H_{21}N_5P_6$	67.6 67.25	3.30 3.67	12.1 12.25
XIV*c*	258 (pale yellow)	E	75	$C_{28}H_{21}N_5O_6$	64.7 64.24	3.90 4.01	13.00 13.38

A = Acetic acid ; B = benzene ; But. = Butanol ; E = Ethanol ;
M = Methanol ; P = Petrol (60 – 80°C).

Reaction of oxazolones (I*a*-*c*) with anthranilic acid : Formation of 2-(substituted)-4H-3, 1-benzoxazin-4-one derivatives (II*a*-*c*)

A mixture of oxazolones (1*a*—*c*) (0.05 mol) and anthranilic acid (0.035-mol) in boiling acetic acid was heated under reflux for 10 hr. The products obtained after cooling were filtered and recrystallised from a proper solvent to yield the corresponding benzoxazones (II*a*—*c*).

Action of primary amines on 2-(benzamido-p-methoxystyryl)-4H-3,1-benzoxazin-4-one (IIa) : Formation of o-(benzamido-p-methoxystyryl)-N-substituted benzamide (III *a*—*c*)

A solution of II*a* (0.01 mol) and primary amines (aniline, ethanolamine, or glutamic acid (0.01 mol) in 50 ml methanol was heated under reflux for 4 hr. The product was filtered and dried. Recrystallization of the solid product from a suitable solvent afforded (III*a*—*c*).

Action of hydrazines on 2-(substituted)-4H-3,1-benzoxazin-4-ones (IIa&c) : Formation of N-(substituted) anthranilic acid hydrazide derivatives (IV*a*—*f*)

A solution of benzoxazone (II) (0.01 mol) and hydrazines, namely hydrazine hydrate, phenyl hydrazine, *p*-nitropheyl hydrazine, benzoyl hydrazine, salicyloyl hydrazine or isobutyroyl hydrazine (0.03 mlol; in methanol (30 ml) or mixture of methanol/acetic acid (60 ml) (3V : IV) was heated under reflux for 4 hr. The product obtained after cooling was filtered and dried. Recrystallization of the solid product from a suitable solvent gave (IV*a*—*f*).

Action of ammonium acetate of formamide on (IIa & b) : Formation of 2-(substituted)-3(4H)-quinazol-4-one derivatives (V*a* & *b*)

Benzoxazone (II) (0.01 mol) and ammonium acetate or formamide (0.03 mol) in presence of anhydrous $ZnCl_2$ was fused in an oil-bath for 2 hr. The reaction mixture was poured into water, filtered and recrystallised from a suitable solvent to give the quinazolones(V*a* and *b*).

Action of benzoyl chloride on (Va) : Formation of 3N-benzoyl-2-substituted quinazol-4-one (VI)

A solution of V*a* (0.01 mol) in excess benzoyl chloride (30 ml) was heated under reflux for 2 hr. The product was poured into water, boiled and filtered while hot. The solid separated was recrystallised from benzene to give (VI).

Action of $PCl_5/POCl_3$ on (Va) : Formation of 2-(substituted)4-chloroquinazoline (VII)

A mixture of quinazolone (V*a*) (0.01 mol) and a mixture of $PCl_5/POCl_3$ (2 ml : 0.01 mol) were heated in an oil-bath at 170°C for 2 hr. After cooling, the product was washed with water, dried, and recrystallised from benzene to give (VII).

Action of acylhydrazine on (VII) : Formation of 2-(substituted) triazolo (2′-substituted) [(1,2-*a*)] quinazolines (VII*a*—*c*)

A mixture of VII (0.01 mol) and acyl hydrazine, namely isobutyroyl hydrazine, benzoyl hydrazine and/or salicyloyl hydrazine (0.01 mol) in boiling butanol (30 ml) was refluxed for 48 hr. The product obtained after concentration was recrystallised from an appropriate solvent to give the quinazoline derivatives (VIII*a*—*c*).

Action of sodium azide on (VII) : Formation of 2-(substituted) tetrazolo (1,2-*a*) quinazoline derivatives (IX)

A mixture of VII (0,01 mol) and NaN_3 (0.015 mol) in boiling dimethyl formamide (30 ml) was refluxed for 3 hr. After cooling, the product was washed with water and recrystallised from acetic acid to give the tetrazole derivative (IX).

Action of active methylene compounds on (VII) : Formation of 2-(substituted)- 4-alkyl quinazoline derivatives (X*a*—*d*)

A solution of 4-chloroquinazoline (VII) (0.01 mol) and active methylene compounds namely, ethyl cyanoacetate, ethyl acetoacetate, diethyl malonate or acetylacetone (0.01 mol) in presence of dimethyl formamide (50 ml) and sodamide (0.005 mol) was refluxed for 5 hr. After cooling, the product obtained was washed with water, filtered, dried and recrystallised from a suitable solvent to give (X*a*—*d*).

Action of alkoxides on (VII) : Formation of 2-(substituted)4-alkoxy quinazoline derivatives (XI*a* and *b*)

A mixture of (VII) (0.01 mol) and an excess of alkoxides, namely sodium methoxide or sodium ethoxide was heated under reflux for 6 hr. The product obtained was poured into dilute HCl, filtered, dried and recrystallised from a proper solvent to give (XI*a* and *b*).

Action of amino-acids on (VII) : Formation of 2-(substituted)-4N-substituted quinazolines (XII *a* and *b*)

A solution of VII (0.01 mol)and amino-acids, namely glycine, or L-glutamic acid(0.01mol) in boiling pyridine —H_2O (mixture 3V : IV was refluxed for 3 hr. The product obtained was poured into concentrated HCl, filtered, and recrystallised from a suitable solvent to give (XII*a* and *b*).

Action of acetic anhydride and sodium acetate on (XII*a*) : Formation of 2-(substituted) pyrazolone (1,2-*a*) quinazoline derivative (XIII)

A mixture of XII*a* (0.01 mol), acetic anhydride (1 mol) and dry sodium acetate (0.01 mol) was fused for 3 min. The reaction mixture was refluxed on a water bath for 2 hr. The solid obtained was washed with water, filtered, dried and recrystallised from benzene to give (XIII).

Reaction of Vb with benzamide, phthalimide or succinimide : Formation of Mannich bases, 2-(substituted)-3N-substituted-3(4H)-quinazol-4-ones (XIV*a*—*c*)

A mixture of quinazolinone (V*b*) (0.01 mol), formaldehyde (5 ml) and amides or imides, namely benzamide, phthalimide or succinimide in boiling ethanol (30 ml) and a few drops of concentrated HCl was refluxed for 3 hr. After cooling, a solid product was separated which was recrystallised from a proper solvent to give the corresponding Mannich bases (XIV*a*—*c*)

REFERENCES

[1] M. A. El-Hashash, A. M. Kaddah, M. El-Kady, and I. Ammer, *Pakistan J. Sci. Ind. Res.*, **25**, 104 (1982).

[2] M. A. El-Hashash, and M. A. Sayed, *Egypt. J. Chem.*, **21**, 115—31 (1980).

[3] M. M. Mohamed, A. A. El-Khamary, S. El-Nagdy, and S. W. Shoshaa, *Indian J. Chem.* **25B**, 207 — 211 (1986).

[4] A. Essawy, M. A. El-Hashash, and M. M. Mohamed, *Indian J. Chem.* **19B**, 663—666(1980).

Action of active methylene compounds on (VII): Formation of 2-(substituted)-4-alkyl quinazoline derivatives (Xa—d)

A solution of 4-chloroquinazoline (VII) (0.01 mol) and active methylene compounds, namely, ethyl cyanoacetate, ethyl acetoacetate, diethyl malonate or acetylacetone (0.01 mol) in presence of dimethyl formamide (30 ml) and sodamide (0.005 mol) was refluxed for 5 hr. After cooling, the product obtained was washed with water, filtered, dried and recrystallised from a suitable solvent to give (Xa—d).

Action of alkoxides on (VII): Formation of 2-(substituted)4-alkoxy quinazoline derivatives (XIa and b)

A mixture of (VII) (0.01 mol) and an excess of alkoxides, namely sodium methoxide or sodium ethoxide was heated under reflux for 8 hr. The product obtained was poured into dilute HCl, filtered, dried and recrystallised from a proper solvent to give (XIa and b).

Action of amino-acids on (VII): Formation of 2-(substituted)-4N-substituted quinazolines (XIIa and b)

A solution of VII (0.01 mol) and amino-acids, namely glycine, or L-glutamic acid (0.01 mol) in boiling pyridine —H_2O (mixture 3V : 1V) was refluxed for 3 hr. The product obtained was poured into concentrated HCl, filtered, and recrystallised from a suitable solvent to give (XIIa and b).

Action of acetic anhydride and sodium acetate on (XIIa): Formation of 2-(substituted) pyrazolone (1,2-a) quinazoline derivative (XIII)

A mixture of XIIa (0.01 mol), acetic anhydride (1 mol) and dry sodium acetate (0.01 mol) was fused for 5 min. The reaction mixture was refluxed on a water bath for 2 hr. The solid obtained was washed with water, filtered, dried and recrystallised from benzene to give (XIII).

Reaction of VI with benzamide, phthalimide or succinimide: Formation of Mannich bases, 2-(substituted)-3N-substituted-4(3H)-quinazol-4-ones (XIVa—c)

A mixture of quinazolinone (VI) (0.01 mol), formaldehyde (5 ml) and amides or imides, namely benzamide, phthalimide or succinimide in boiling ethanol (30 ml) and a few drops of concentrated HCl was refluxed for 3 hr. After cooling, a solid product was separated which was recrystallised from a proper solvent to give the corresponding Mannich bases (XIVa—c).

REFERENCES

[1] M. A. El-Hashash, A. M. Kaddah, M. [illegible] and [illegible], Pakistan J. Sci. Ind. Res., 25, 104 (1982).
[2] M. A. El-Hashash and M. A. Sayed, Egypt. J. Chem., 21, 115—21 (1980).
[3] M. M. Mohamed, A. A. [illegible], S. T. [illegible] and S. W. [illegible], Indian J. Chem. 25B, 209 — 211 (1986).
[4] A. Essawy, M. A. El-Hashash and M. M. Mohamed, Indian J. Chem. 19B, 663—666 (1980).

Revue Roumaine de Chimie, 35, 4, 577–581 (1990)

OPTIMIZATION BY COMPUTER OF THE ALKALINE HYDROLYSIS OF ISOAMYL ACETATE

H. M. LLANEZA, J. CORONA and J. M. BLANCO
S.T.S. Industrial Engineering, Dpt. of Chemistry, Asturias, Spain

Received December 28, 1987

The aim of this study is to obtain the maximum yield from the alkaline hydrolysis of isoamyl acetate in a batch reactor. This involves obtaining an initial sodium hydroxide concentration which will maximize the initial rate of hydrolysis for a given ester/aqueous solution of sodium hydroxide ratio specified in the experimental design. Furthermore, the sodium hydroxide concentration which will maximize the rate of hydrolysis also needs to be calculated at each stage of the process (calculations based on the quantity of unconverted ester observed); this will enable us to determine the concentration of sodium hydroxide necessary to obtain the maximum rate of reaction and thus the optimization of the overall process.

INTRODUCTION

In general, the rate of any particular homogeneous chemical reaction increases when the concentration of any of the reacting substances increases and when all the other variables are kept constant. This, however, is not the case of heterogeneous liquid-liquid reactions, in which, apart from the kinetic factors proper, other physicochemical and transport factors also intervene.

Such is the case of the alkaline hydrolysis of isoamyl acetate (ester hardly soluble in water) carried out in a batch reactor. At each stage in this reaction there is an optimum sodium hydroxide concentration for achieving maximum conversion assuming that all other variables remain constant.

The object of this study is to optimize the sodium hydroxide concentration so that the maximum conversion is achieved at any one given time.

Over the last decade, many investigators have used computer technology for treating kinetics data and for optimizing a great number of chemical reactions. Thus Frazer [1] uses computers in the kinetic treatment and optimization of the alkaline hydrolysis of nitrophenyl acetate. Tanner [2] uses computer programmes for the study and optimization of kinetic data in the hydrolysis of boric acid esters. Tucker [3] also makes use of computer technology in his study of the kinetics associated with the hydrolysis of nitrophenyl acetate. Rosenthal[4] develops a computer programme for analyzing the hydrolysis of esters catalyzed by acids and bases. Thomas and Costas [5] obtain optimum temperatures in their study of polymerization reactions carried out in a batch reactor. Chen et al. [6–7] carry out a study of the minimum final time for the polymerization of styrene in a batch reactor. The present study uses a third-degree polynomial regression programme to calculate the sodium hydroxide concentration necessary for maximizing the rate of reaction.

THEORETICAL CONSIDERATIONS

Statistical-mathematical approach to the problem :

Mathematically, the problem is resolved by least squares and by calculating the maximum for a two-variable function from values obtained in the experiment over 30 points.

A solution was initially attempted by simply calculating the maximum for the isotemporal regressions by means of a computer programme adequately designed ; this approach is highly efficient when a great number of points are available. However, this approach was not considered a satisfactory solution to the problem on account of certain typical deviations of importance encoutered therein.

It was decided, therefore, to use a programme which would calculate the coefficients of a polynomial with two variables. The polynomial of the second degree was rejected since it did not seem to conform to the characteristics of the function. The solution was, therefore, seen to be the polynomial of the third degree with the following structure :

$$z = F(x, y) = ax^3 + by^3 + cx^2y + dy^2x + ex^2 + fy^2 + gxy + \\ + hx + iy + j$$

where :

x = NaOH concentration in moles/l.

y = moles of unconverted ester.

z = rate of reaction in moles cm^{-3} s^{-1}

This system of non-linear equations was resolved by approximation methods with successive refinements by means of random-point generation in an adequate bidimensional field.

This system is sufficiently satisfactory as to warrant unnecessary the use of more accurate solutions such as that provided by a polynomial of the fourth degree.

EXPERIMENTAL

The materials, analytical methods and experimental procedure are described in.[8]

Several experiments have been carried out but we have selected only those experiments in which a fixed initial ester/NaOH aqueous solution ratio, temperature and stirring speed varying concentrations of sodium hydroxide in aqueous solution (Fig. 1).

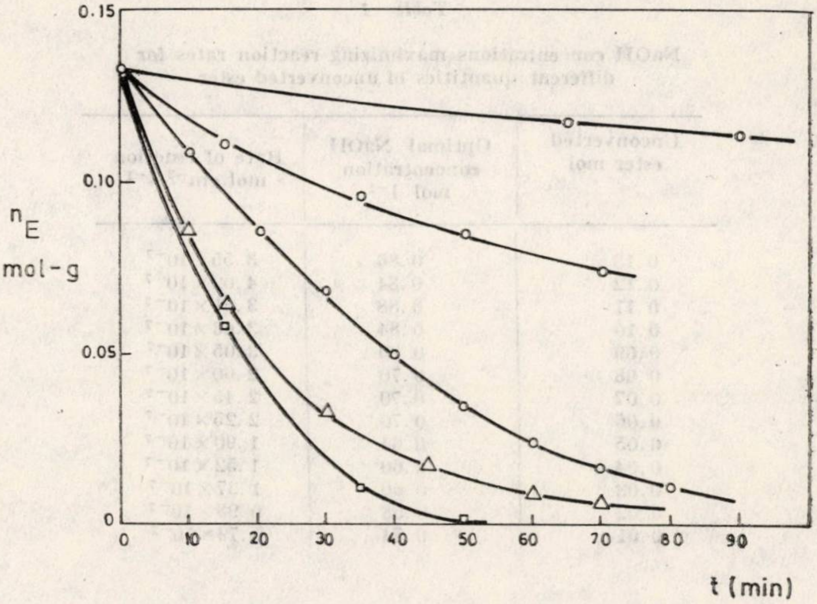

Fig. 1. — Effect of the initial NaOH concentration on the variation in time of the number of ester moles, at 25°C, 340 r.p.m., 20 cm^3/300 cm^3 initial ester/NaOH solution volume : △0.5 N NaOH ; □ 1.0 N NaOH ; ●2.0 N NaOH ; — ○ 3.0 N NaOH ; ◇ 5.0 N NaOH.

RESULTS AND DISCUSSION

The polynomial of the third degree determines the area represented in Fig. 2.

The maximum rate of reaction $z = 4.13 \times 10^{-7}$ mol. cm^{-3} s^{-1} corresponds to $x = 0.78$ mol/l ; $y = 0.118$ moles.

The area shown in Fig. 2 can now be given a series of cuts parallel to the X—Z plane. This obviously gives rise to a series of NaOH concentration-reaction rate curves in which the maximum corresponds to the optimum value of NaOH concentration necessary for obtaining the maximum conversion of the residual ester. This was done for 0.01 moles intervals of unconverted ester ; the thirteen values obtained are shown in Table 1.

It is seen therefore that the concentration of NaOH which produces the maximum rate of reaction can be controlled for a given quantity of unconverted ester.

Furthermore, the rates of reaction enable us to calculate the concentration of NaOH as a function of time, thus making the optimization process much easier. This possibility is reflected in Fig. 3.

It is seen that the process is completed in about 30 minutes.

Table 1

NaOH concentrations maximizing reaction rates for different quantities of unconverted ester

Unconverted ester mol	Optimal NaOH concentration mol l^{-1}	Rate of reaction mol cm^{-3} s^{-1}
0.13	0.86	3.55×10^{-7}
0.12	0.84	4.02×10^{-7}
0.11	0.88	3.91×10^{-7}
0.10	0.84	3.63×10^{-7}
0.09	0.80	3.05×10^{-7}
0.08	0.70	2.60×10^{-7}
0.07	0.70	2.45×10^{-7}
0.06	0.70	2.25×10^{-7}
0.05	0.64	1.90×10^{-7}
0.04	0.60	1.52×10^{-7}
0.03	0.60	1.37×10^{-7}
0.02	0.58	0.98×10^{-7}
0.01	0.54	0.79×10^{-7}

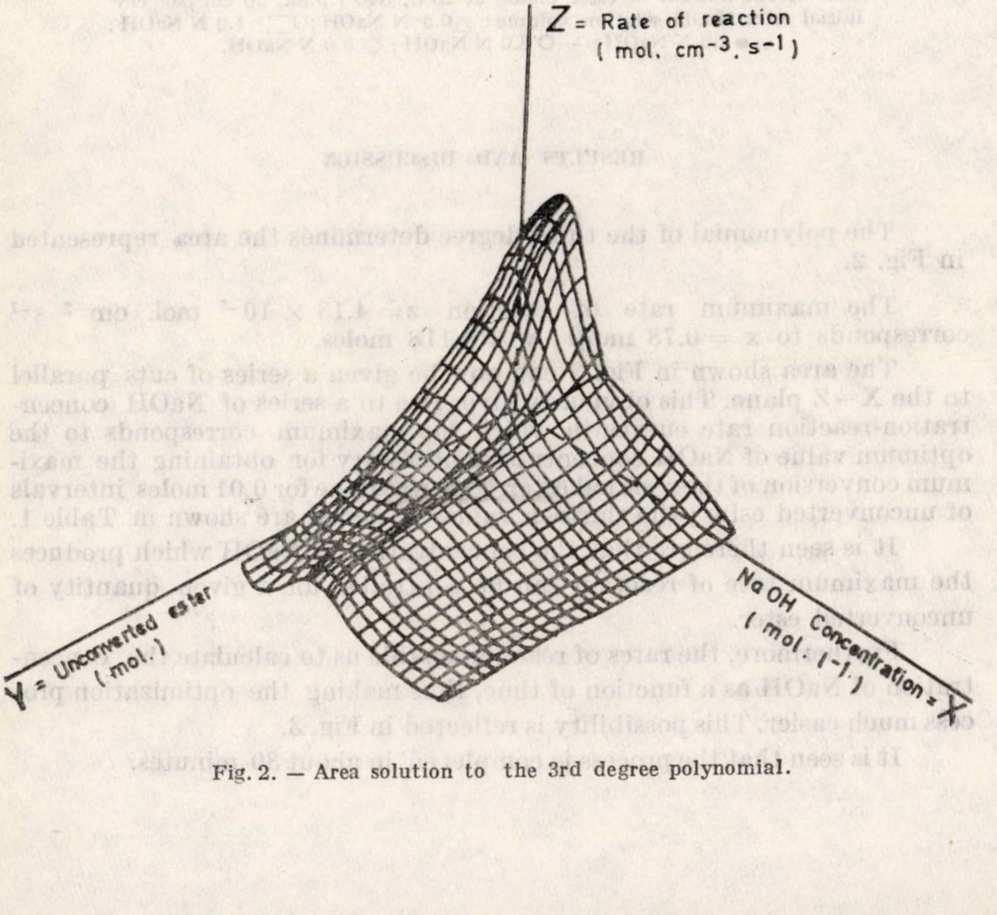

Fig. 2. — Area solution to the 3rd degree polynomial.

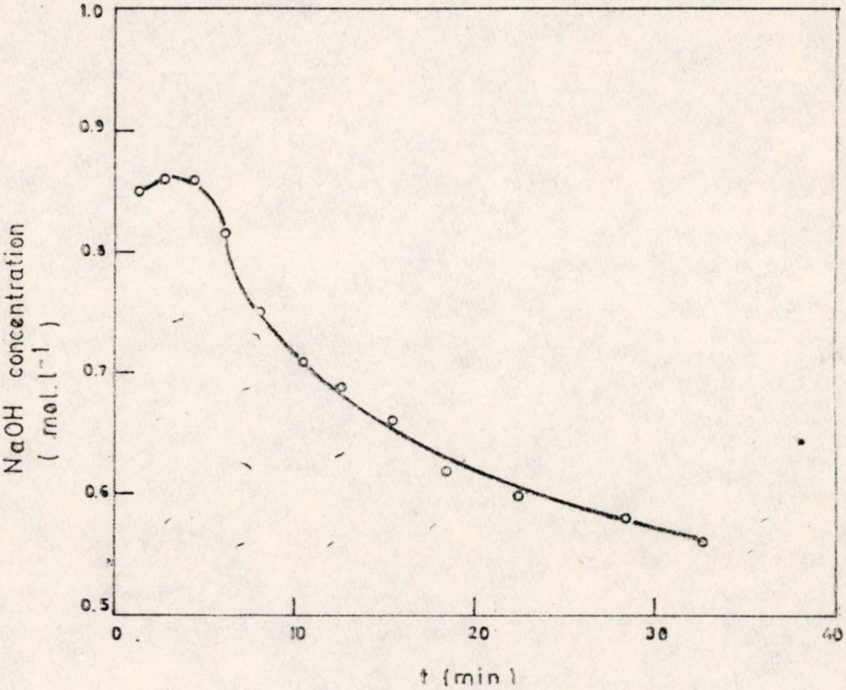

Fig. 3. — Optimum concentration of sodium hydroxide.

REFERENCES

[1] J. W. Frazer, *Anal. Chem*,. **52**, 1205 (1980).
[2] D. W. Tanner, *Diss Abst. B.*, **28**, 4079 (1968).
[3] I. G. Tucker, *Int. J. Pharm.*, **10**, 323 (1983).
[4] D. Rosenthal and D. Arnold, *J. Chem. Educ.*, **54**, 323 (1977).
[5] I. M. Thomas and K. Costas, *Can. J. Chem. Eng.*, **62**, 284 (1984).
[6] S. A. Chen and W. F. Jeng, *Chem. Eng. Sci.*, **33**, 735 (1978).
[7] S. A. Chen and N. W. Huang, *Chem. Eng. Sci.* **36**, 1295 (1981).
[8] H. M. Llaneza, *Afinidad*, **50**, 471 (1983).

Revue Roumaine de Chimie, **35**, *4*, 583–585 (1990)

COMPTES RENDUS

"Organic High Pressure Chemistry" (edited by W. J. Le Noble), Studies in Organic Chemistry No. 37, Elsevier Science Publishers, B. V. Amsterdam, and (for USA) Elsevier Science Publishing Comp. Inc. New York, 1988. Hard cover, 490 pp, ISBN 0-444-43023-7.

The present volume appeared soon after the publication of "Inorganic High Pressure Chemistry" edited by R. van Eldik (Elsevier, Amsterdam, 1986). Professor W. J. Le Noble has been active in the area of organic high pressure chemistry for more than 25 years and, like Bridgman in the twenties, Brower, Hamann, and the Zhulin-Gonikberg team since the fifties or Whalley since the sixties, has appreciably contributed to the development of the field. It is remarkable that the above chemists (except for Bridgman and Gonikberg) contribute with chapters to the present book.

The editor has written : (i) the introductory chapter indicating how pressures up to 80 kbar (8 GPa), influence chemical equilibria and reaction rates (expressed by "reaction volumes" and "activation volumes", respectively) and commenting the easy questions and the difficult questions (such as the dichotomy between high pressure effects on gases and liquids, where for the latter phase internal pressures amount to $10^2 - 10^3$ MPa) ; (ii) chapter 8, "Carbocationic Reactions" together with E. Whalley, indicating how pressure effects can provide information on reaction mechanisms, in particular distinguishing among uni- and bi-molecular mechanisms (in the sixties, research in Whalley's group at Ontario and in le Noble's group at the State University of New York was initially performed independently and in mutual ignorance) ; for instance the solvolyses of t-butyl and isopropyl halides have isothermal rate maxima around 1.7 and 4.5 GPa, respectively, indicating S_N1 mechanisms while methyl iodide has no such maximum up to 7 GPa indicating an S_N2 mechanism ; also for the non-classical ion problem high pressure gave conclusive results ; (iii) the final, 14th chapter on carbenes and related species : again, high-pressure experiments can prove the independent existence of unstable species (carbenes, cumulenylidenes, nitrenes) ; the conclusion is that at present high pressure chemistry has became almost a conventional tool in organic chemical laboratories both for synthetic and mechanistic problems.

Other chapters must be highlighted : O.Exner presents in the 2nd chapter empirical calculations of molar volumes, a problem which is important even for stable species where reaction volumes can be determined experimentally by dilatometry ; various systems of increments are presented and discussed critically : it is the reviewer's belief that topological indices might be useful too. The most senior of the authors, S. D. Hamann, reviews in chapter 3 chemical equilibria in liquids, classifying them as non-electrolytes (pure, dilute or concentrated solutions being further subdivisions) and electrolytes, where electrostriction effects outweigh other phenomena (again, dilute and concentrated solutions as well as zwitterions are discussed separately). Since *gauche* conformations have slightly lower volumes than *trans*-conformations, alkanes tend to become slightly more globular as the pressure rises. Similarly, *trans* to *cis* isomerizations of alkenes can be brought about by higher pressures.

Other chapter titles (authors in brackets) are : Proton tinnelling (Sasaki and Osugi), Stereoisomerizations (Asano), Pericyclic reactions (Jenner), Anionic reactions (Brower), Free radical reactions at high pressure (Zhulin), Organometallic chemistry (Rahm), Synthesis (Jurczak), Photophysics and photochemistry in the liquid phase at high pressure (Schmidt and Brauer), Bio-organic chemistry (Heremans).

The Diels-Alder and the Menshutkin reactions, discussed in detail in the chapters on pericyclic reactions and on synthesis are the typical reactions which respond favorably to high pressure, overcoming electronic or steric hindering factors which may prevent completely these reactions to occur at normal pressure.

The book is reproduced directly from authors' manuscripts : misprints are few (1.7 and 4.5 GPa on pp. 245 and 247, respectively, instead of 17 or 45 GPa ; isobutyl formate instead of isobutyl formamide on p. 266 ; chlorine substituent missing in chloroallene on p. 431 ; enough instead of inoff on p. 412).

The extensive coverage of the wide applications that high-pressure studies can offer at present to organic chemists interested in synthesis,mechanisms,or variations of physico-chemical properties, as well as the extensive literature coverage by the most prominent scientists who contributed, to the development of this field are compelling reasons for this book to be consulted by a wide range of chemists.

A. T. Balaban
Polytechnic Institute Bucharest

L. Sommer, "Analytical Absorption Spectrophotometry in the Visible and Ultraviolet. The Principles", Akadémiai Kiadó, Budapest, 1989, 311 pp. ISBN 963 05 4752 x.

Volume 8 of the series "Studies in Analytical Chemistry" written by L. Sommer, professor of analytical chemistry at "J. E. Purkyne" University in Brno, Czechoslovakia, deals with fundamentals of visible and ultraviolet spectrophotometry, its performances and analytical applications.

The books is organized in the following chapters :

1. Basis of spectrophotometry in the UV and VIS regions ;
2. Principles of instrumentation ;
3. Errors in spectrophotometry ;
4. Evaluation of the analyte concentration from spectrophotometric data ;
5. Optimization of spectrophotometric procedure ;
6. Some special approaches in spectrophotometry ;
7. Complexation and spectrophotometry ;
8. Some applications of UV and VIS spectrophotometry.

It is the special merit of the book to present, in a relatively small volume, almost all major basic and applied aspects of the field.

The accuracy of presentation, the logic sequence of chapters and the simple yet suggestive graphic illustrations are remarkable. All these qualities recommend Prof. L. Sommer's work as a rich source of updated information and a precious textbook.

Each chapter carries a rich list of thoroughly selected references and besides, in an appendix, are listed 39 highly prized books of UV and VIS spectrophotometry.

The book is useful to a wide range of specialists, from research chemists and physicists to students in chemistry, physics and related fields.

Constantin Luca
Department of Analytical Chemistry
Polytechnic Institute of Bucharest

E. Breuer, A. G. Aurich and A. Nielsen, "Nitrones, Nitronates and Nitroxides", edited by S. Patai and Z. Rappoport, Wiely-Interscience, Chichester, 1989. Hard cover, 435 pages, 61 £ ISBN 0 471 91700 5

Three chapters from the well-known book series "Chemistry of Functional Groups" edited by S. Patai and Z. Rappoport have been reprinted and updated by their authors with substantial new material. Thus, A. T. Nielsen's chapter "Nitronic acids and esters" from "The Chemistry of the Nitro and Nitroso Group", edited by H. Feuer in 1969, as well as E. Breuer's chapter "Nitrones and nitronic acid derivatives : their structure and their roles in synthesis" from "The Chemistry of Amino, Nitroso and Nitro Compounds", edited by S. Patai in 1982, have been updated in the third chapter (67 pages) of the present book by E. Breuer. The fourth chapter is a reprint of H. G. Aurich's "Nitroxides" originally published in the latter volume in 1982, and the fifth chapter is the update by the same author, "Appendix to Nitroxides" (28 pages).

Nitrones are N-oxides of Schiff bases, whereas nitronic acids are oxime-N-oxides, tautomers of primary or secondary nitro compounds ; correspondingly, nitronic esters are N-oxides of oxime ethers. Interestingly, the oxidation of oximes with Caro's acid or other oxidants is a useful route which has not been fully developed.

The chapter and the update follow exactly the same classification pattern, and the same section numbers are used ; the numbering of schemes, structures, and references runs continuously in the original chapters and the updating appendices.

The chapter on nitronic acids and esters (138 pages) describes the *aci*-nitro tautomerism, the preparation, properties and reactions of nitronic acids, and finally the derivatives of these nitronic acids : esters (in detail), salts, anhydrides (the cyclic anhydrides are known as furazans), mixed anhydrides with carboxylic acids (secondary nitronic acids afford stable mixed anhydrides, while those with primary nitronic acids tautomerize to hydroxamic acid esters), halides and amides.

The chapter on nitrones (105 pages) discusses their structure, spectra, E—Z (geometrical) isomerism, tautomerisms (to hydroxy-enamines, the Behrend rearrangement, and the ring-chain tautomerism), and the various reactions of nitrones and nitronic acid derivatives. Among the reactions, the review includes the Martynoff rearrangement to oxime O-ethers via iminoxy radicals, the rearrangements to oxaziridines or amides, olefin formation, oxidation, reduction 1,3-dipolar cycloaddition, reactions with heterocumulenes, electrophiles or nucleophiles, organometallic compounds, and free radicals. In the last reactions, nitrones act as radical traps.

Neither in the review, nor in the update, are synthesis of nitrones presented in detail because the topic had been recently reviewed fairly extensively.

The last chapter and its update, written by professor Aurich, reviews the important class of nitroxides which are stabilized free radicals : although their stabilization energy is considerable (about 30 kcal/mol), their persistence is variable. Ther formation by oxidation from amines, hydroxylamines, or aminyl radicals, as well as from nitroso derivatives or nitrones (by spin trapping or other reactions) is presented in detail. The investigations of nitroxides by physical methods which are reviewed include X-ray analysis, electron diffraction, electron paramagnetic resonance, NMR and ENDOR spectroscopy. Finally, the various reactions of nitroxides are presented : protonation and complex formation, addition of radicals to form O-substituted hydroxylamine derivatives, dimerization and disproportionation, reduction and oxidation, α-scission(retro-spin-trapping), β-scission (removal of β-hydrogen or halogen atoms leading to nitrones) ; a separate section presents reactions which do not involve directly the nitroxide group. A series of cited reviews on the application of nitroxides as spin labels in biochemical or biophysical studies evidences the increasing importance of this class of compounds.

With more than two thousand literature references, as well as detailed author and subject indexes, this book authored by recognized specialists in the field is an excellent and up-to-date source of information for all those interested in the chemistry and applications of these organic compounds containing functional group with nitrogen and oxygen.

A. T. Balaban
Polytechnic Institute Bucharest

NOTE POUR LES AUTEURS

Le Revue Roumaine de Chimie publie des articles en anglais, français, russe, allemand ou espagnol. Les auteurs sont priés d'envoyer des articles et des comptes rendus inédits.

Les manuscrits seront dactylographiés à double interligne. La bibliographie, les tableaux et la légende des figures seront placés après le texte.

Si l'article fait partie d'un série numérotée, la partie précédente sera donnée comme première référence.

Chaque article sera précédé d'un résumé comprenant quinze lignes au maximum.

Les références bibliographiques dans le texte seront faites par des exposants sans parenthèses et paraîtront à la fin de l'ouvrage.

Les publications périodiques mentionnées dans la bibliographie seront présentées suivan les prescriptions internationales : le nom de l'auteur précédé de l'initiale du prénom, le titre du périodique abrégé conformément à « Chemical Abstracts » et souligné par une ligne, le numéro du tome indiqué par des chiffres arabes et souligné par deux lignes, suivi de la première page de l'article ; à la fin, l'année de la parution sera placée entre parenthèses. Le numéro de la revue ne sera pas indiqué si les pages du volume sont numérotées consécutivement.

Les textes des livres ou traités inclueront : le nom des auteurs, l'initiale du prénom, le titre du livre entre guillements et sans être souligné, le numéro du tome précédé par l'abréviation « vol. » (ou « Bd. »), le numéro de l'édition, les éditions (the publisher), la localité de la parution du livre, l'année de la parution et la page de de la référence précédée(s) par l'abréviation « p. » (ou « S. »).

Les brevets seront indiqués comme suit : l'auteur ou la firme, le pays et le numéro du brevet, la date et la revue (*Chem. Abstr.*) Par ex. : M. Jones (to Union Carbide Co), Brit. Pat. 601 238, 2 Sept. 1959 ; *cf. Chem. Abstr.*, *54*, 12808 (1960).

Si la référence n'a pas été lue en original, on indiquera aussi la revue de référence consultée.

Les diagrammes seront tracés à l'encre de Chine sur papier calque. Les tableaux et les figures (en nombre strictement nécessaire) ainsi que es courbes dans les figures seront numérotés par des chiffres arabes. Leur explication sera donnée dans la légende des figures. Prière de ne pas inscrie les mêmes données dans les tableaux et les figures. Chaque tableau aura un titre. On indiquera dans le texte la place approximative des tableaux et des figures. Les formules chimiques seront incluses dans le texte ; en outre, elles seront transcrites sur papier calque, à l'encre de Chine.

Les auteurs sont priés d'indiquer les caractères italiques (en soulignant les lettres au crayon), ainsi que tout autre caractère spécial : les préfixes *ortho*, *meta*, *para*, *cis*, *trans*, etc. seront soulignés pour indiquer leurs caractères italiques et ne seront jamais écrits avec des majuscules.

Aucune correction à la main ne sera admise sur le manuscrit. Les corections seront tapées à la machine. Les lettres grecques ou d'autres symboles spéciaux seront insérés à la main à l'encre clairement.

Le manuscrit sera signé par l'auteur.

Le titre-courant aura 50 lettres au maximum.

L'entière responsabilité du contenu des articles appartient aux auteurs.

Sur demande on peut obtenir une note plus complète.

PRINTED IN ROMANIA

ORSZÁGOS MŰSZAKI INFORMÁCIÓS KÖZPONT ÉS KÖNYVTÁR
8833

TRAVAUX PARUS AUX ÉDITIONS DE L'ACADÉMIE ROUMAINE

I. G. MURGULESCU, **Introducere în chimia fizică, vol. I. 1. Atomi, molecule, legătură chimică,** 1976, 560 p.

I. G. MURGULESCU, V. EM. SAHINI, **Introducere în chimia fizică,** Vol. I, 2. **Structura și proprietățile moleculelor,** 1979, 604 p.

I. G. MURGULESCU, E. SEGAL, **Introducere în chimia fizică,** Vol. II. 1. **Teoria molecular-cinetică a materiei,** 1979, 1036 p.

I. G. MURGULESCU, TATIANA ONCESCU, E. SEGAL, **Introducere în chimia fizică,** Vol. II. 2. **Cinetică chimică și cataliză,** 1981, 1024 p.

I. G. MURGULESCU, J. PĂUN, **Introducere în chimia fizică,** Vol. I, 3. **Nucleul atomic, reacții nucleare, particule elementare,** 1982, 606 p.

I. G. MURGULESCU, RODICA VÎLCU, **Introducere în chimia fizică.** Vol. III. **Termodinamica chimică,** 1982, 624 p.

I. G. MURGULESCU, O. M. RADOVICI, **Introducere în chimia fizică,** Vol. IV. **Electrochimia,** 1986, 416 p.

R. VÎLCU, M. LECA, **Polymer Thermodynamics by Gas Chromatography,** coédition avec Elsevier, 1990, 204 p.

F. CUIBAN, A. X. XENIA, **Studiul structurii și sinteza peptidelor,** 1989, 282 p.

CRISTOFOR I. SIMIONESCU, VALERIA GORDUZA, **Implicații bioenergetice ale coloranților,** 1988, 208 p.

R. VÎLCU, M. LECA, **Termodinamica polimerilor prin cromatografie de gaze,** 1987, 238 p.

I. ZUGRĂVESCU, M. PETROVANU, **Cicloadiții 3 + 2 dipolare,** 1987, 446 p.

RAUL MIHAIL, ION GROZEANU, **Estimarea secvențială aplicată sistemelor chimice,** 1986, 406 p.

M. BREZEANU, I. PATRON, M. ANDRUH, **Combinații complexe polinucleare și aplicațiile lor,** 1986, 244 p.

A. T. BALABAN et al., **Labelled Compounds and Radiopharmaceuticals Applied in Nuclear Medicine,** coédition avec John Wiley and Sons, 1986, 742 p.

D, PURDELA, **Nomenclatura chimiei organice — IUPAC,** 1986, 451 p.

PETRU BUDRUGEAC, **Probleme de chimie,** 1986, 280 p.

T. ONCESCU, S. G. IONESCU, **Conversie fotochimică și stocare de energie,** 1985, 272 p.

V. DRĂGUȚAN, A. T. BALABAN, M. DIMONIE, **Olefin Metathesis and Ring-Opening Polymerization of Cyclo-Olefins,** coédition avec John Wiley and Sons, 1985, 544 p.

C. LITEANU, I. RÎCĂ, **Optimizarea proceselor analitice,** 1985, 360 p.

N. PETRESCU, **Chimia extracției cu solvenți și aplicații,** 1985, 212 p.

V. EM. SAHINI, M. HILLEBRAND, **Chimie cuantică în exemple și aplicații,** 1985, 382 p.

ISSN 0035–3930

Universul c. 2029

43 426

Lei 40

F1103

ACADÉMIE ROUMAINE

REVUE ROUMAINE DE CHIMIE

TOME 35
Nº 5
Mai 1990

Rev. Roumaine Chim.

RRCHAX, 35, 5, 587–690 (1990), Bucarest

EDITURA ACADEMIEI ROMÂNE

ACADÉMIE ROUMAINE

COMITÉ DE RÉDACTION

Rédacteur en chef :

I. G. MURGULESCU, membre de l'Académie Roumaine

Rédacteurs en chef adjoints :

A. T. BALABAN et V. EM. SAHINI, membres de l'Académie Roumaine

Collège de rédaction :

EM. BRATU, ECATERINA CIORĂNESCU-NENITZESCU, CR. SIMIONESCU, P. SPACU, membres de l'Académie Roumaine, M. ANDRUH, M. BANCIU, M. D. GHEORGHIU, I. HAIDUC, D. I. MARCHIDAN, G. NIAC et D. SĂNDULESCU

La Revue Roumaine de Chimie paraît 10 fois par an. Toute commande de l'étranger sera adressée à « ROMPRESFILATELIA » — sectorul Export-Import Presă, P.O. Box 12—201, télex 10376 prsfi r 78104 Bucarest, Calea Griviței nr. 64—66, Roumanie.

Les manuscrits, les livres et les revues proposés en échange, ainsi que toute correspondance seront envoyés à la rédaction :

REVUE ROUMAINE DE CHIMIE

125, Calea Victoriei, 79717 Bucarest, Roumanie, téléphone 50 76 80

EDITURA ACADEMIEI ROMÂNE
125, Calea Victoriei 79717, Bucarest, Roumanie, téléphone 50 76 80

REVUE ROUMAINE DE CHIMIE

Tome 35, N° 5 **Mai, 1990**

MARIA ZAHARESCU, CONSTANŢA PÎRLOG, MARIA CRIŞAN, MARINA SAHINI, ANA BRĂILEANU and N. DRĂGAN, Monolithic glasses prepared by non-traditional methods 589–593
TINCA ONOFREI, LUCIA ODOCHIAN and VIORICA DULMAN, Cu(II), Zn(II), Cd(II), Co(II) and Ni(II) sorption on *p*(benzylcellulose)-5-azo-8-hydroxyquinoline. Thermogravimetric characterization 595–599
M. CONTINEANU, SeO_2 radiolysis studied by EPR 601–606
ANDREI DĂNEŢ and KIM GWANG SIK, Complexing, extraction and determination of the $C_2H_5Hg^+$ ion with 1-(*p*-nitrophenyl), 3-(*p′*-azobenzene)-triazene 607–616
P. SPACU, LUMINIŢA PATRON, SILVIA PLOŞTINARU, ADRIANA CONŢESCU and N. STĂNICĂ, Coordination compounds as raw materials for mixed oxides. VI. Mixed coordination compounds of lanthanoides and Cr(III) as precursor of chromites 617–623
NEELAM VERMA and A. L. J. RAO, Determination of manganese N, N′-ethylene bis(dithiocarbamate) (Maneb) by a spectrophotometric method and its applications 625–630
A. ALBALAT, E. GÓMEZ, M. SARRET and E. VALLÉS, Contamination by chloride ions in electrod processes (in Spanish) 631–637
J. SUAREZ-VARELA, J. C. AVILA ROSÓN, L. GARCÍA REJÓN and T. GUARDIA CARRILLO, Complexes of 3,5-xylylamine-N, N-diacetic acid with various metal ions 639–648
MARGARETA TOMESCU, EUGEN SEGAL and STELIANA CREŢU, Thermal behaviour of acrylamide-maleic anhydride — styrene terpolymer . . 649–656
EMIL DUMITRIU and VASILE HULEA, Catalysis by polymers. VI. The epichlorohydrin esterification catalyzed by poly(N, N-dimethyl-*p*-vinylbenzyl-amine) 657–662
C. ANDREI, GEORGETA ANDREI, STANA PIŢĂ, OLIVIA PITPALAC and IOANA SONOC, Some aspects of linear low density polyethylene synthesis on $TiCl_4/MgCl_2$ catalysts 663–667
G. SURPĂŢEANU, M. CONSTANTINESCU, A. LABLACHE-COMBIER, P. GRANDCLAUDON, B. MOUCHEL and A. COUTURE, Theoretical and experimental study on the cycloaddition between 4-(*p*-tolyl) 1, 2, 4-triazolium(*p*-methoxy)phenacylide and ethyl cinnamate 669–674
A. COUTURE, A. LABLACHE-COMBIER, G. SURPĂŢEANU and M. CONSTANTINESCU, On the photocyclisation of 1-benzamido-2-(1-cyclohexenyl)cyclohexene 675–678
FATHY FAHIM ABDEL-LATIF, Synthesis of several new pyridinone derivatives 679–682
IOAN PUŞCAŞ, CLAUDIU SUPURAN and GHEORGHE MANOLE, Carbonic anhydrase inhibitors. III. Relations between chemical structure of inhibitors and activators 683–689

Rev. Roumaine Chim. **35**, *5*, 587–690 (1990), Bucarest

Revue Roumaine de Chimie, 35, 5, 589–593 (1990)

MONOLITHIC GLASSES PREPARED BY NON-TRADITIONAL METHODS

MARIA ZAHARESCU, CONSTANŢA PÎRLOG, MARIA CRIŞAN, MARINA SAHINI, ANA BRĂILEANU and N. DRĂGAN
ICECHIM — Center of Physical Chemistry, Spl. Independenţei 202, Bucharest, Romania

Received June 21, 1989

Dense silica glass (whose density is comparable to that of fused silica) and a SiO_2-TiO_2 glass stable at low temperature were prepared by hydrolysis of organo-metallic compounds with formation of gels which are subsequently thermally treated (sol-gel method). The structural changes occurring on polymerization at low temperature and followed by thermal treatment were pointed out by IR spectroscopy, thermal differential analysis, X-ray diffraction, electron microscopy and density measurements.

1. INTRODUCTION

In a previous work[1] we presented the results acquired in obtaining a silica porous glass by hydrolysis-polycondensation of tetraethyl orthosilicate followed by an adequate thermal treatment (sol-gel method). This glass contains micropores whose size varies within a narrow range (13.6–14.4 Å) and maintain throughout the whole temperature domain of thermal treatment (600–1000 °C). We have also obtained by the same method TiO_2-based vitreous coating materials.[2]

The present paper deals with the obtention of dense silica glasses and extends the studies to the SiO_2-TiO_2 binary system in the low concentration range (2 mol % TiO_2).

Studies concerning the obtention of glasses in this system by sol-gel method have been carried out by Kamiya and Sakka [3,4] for low TiO_2 concentrations (below 10 mole %) and recently, for higher TiO_2 concentrations (15–40 mole %) by Cheng and Wang[5], Yuan and Yao[6] and Shingyouchi et al.[7]

2. EXPERIMENTAL PART

The compositions of the studied solutions and the conditions of their hydrolysis are presented in Table 1. The added water was necessary in hydrolysis, the ethanol was used as diluant of the alcoholates while HCl and HNO_3 acted as catalysts. The hydrolysis reaction is allowed to proceed over rather long time ranges, under reflux and continuously stirring of the solution heated at 80 °C.

The polymerization was studied by measuring the viscosity at room temperature at 24 hours intervals, using the RVT Brookfield viscometer.

Table 1

Compositions of starting solutions (mole rations)
and the conditions of hydrolysis

Solution	$\frac{H_2O}{SiEt_4}$	$\frac{EtOH}{SiEt_4}$	$\frac{HCl}{SiEt_4}$	Conditions of hydrolysis	Gelling time
1	15.37	4.41	0.32	pH = 1–2 T = 80 °C Refluxing time : 1 h	11 days
2	15.00	8.03	0.27	,,	,,
	$\frac{H_2O}{Si_4Et+TiEt_4}$	$\frac{EtOH}{SiEt_4+TiEt_4}$	$\frac{HCl}{SiEt_4+TiEt_4}$		
3	13.75	7.11	0.25	pH = 2–3 T = 80 °C Refluxing time : 1 h	5 days
4	14.06	7.25	0.25	,,	,,

The gel-glass transition was conducted differently for each system, taking account of the DTA/TG results.

In order to prepare silica glass whose density was close to that of fused quartz use has been made of Klein's results, [8] which established an optimum heating rate of 2.5 °C min. in order to achieve maximum contraction and densification. This heating schedule was supplemented by annealing intervals at 250 °C, 650 °C and 950 °C, necessary for water removing, burning-out of organic residues in the gel and closing of interconnected pores in the gel structure respectively. The maximum temperature reached was 1000 °C.

The samples in the SiO_2-TiO_2 (98 : 2% mol) system underwent a larger thermal treatment, in order to remove organic residues and water, avoiding at the same time TiO_2 reduction and glass crystallization. The heating rate was 0.25 °C min, up to 900 °C, with 24 h plateaus at every 100 °C.

The dry gel and the glass resulted from the thermal treatment has been studied by the following methods :

- DTA using a MOM OD 103 Derivatograph between 20–1000 °C.
- IR spectroscopy, performed on a Carl Zeiss Jena Specord 75 IR Spectrophotometer.
- TEM, on a Tesla BM 540 transmission electron microscope, using Pt–C replices.
- X-ray diffraction on a HZG–3 diffractometer working with Cuk_α radiation.
- density measurements done in CCl_4 by the picnometer method.

3. RESULTS AND DISCUSSION

Sol-gel transition

The variation of viscosity vs. time is given in Figure 1. The polymerization process is slow for the SiO_2 sol. The viscosity presents a slow change at the early stages of the polymerization process then a deep increase when the gel structure is achieved.

For the SiO_2-TiO_2 sol the gelling process is continuous and rather fast.

Gel-glass transition

The density of the SiO_2 glass prepared as shown was 2.2010 g/cm^3.

The IR absorption spectra — Fig. 2. — show the formation of a structure analogous to that found in fused quartz by Tohge et al. [9]

X-ray diffraction pattern shows that only an amorphous phase is present. TEM suggests that the homogeneity of the gel-based glass is higher than that of fused quartz.

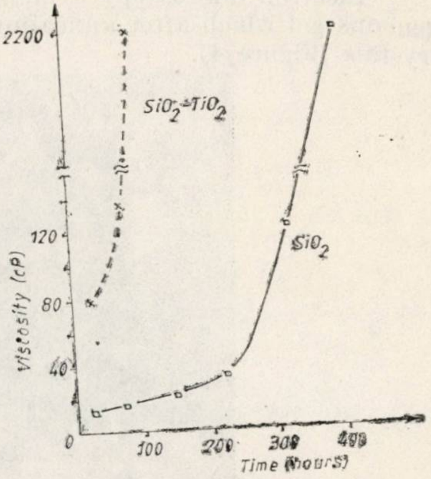

Fig. 1. — The viscosity variation vs time.

The IR spectra for the SiO_2-TiO_2 glass are given in Figure 3. The spectrum of the glass before thermal treatment exhibits, besides the bands due to Si—O—Si vibrations, peaks at 930 cm^{-1}, 1640 cm^{-1} and a large absorption between 3400—3700 cm^{-1}. Following thermal treatment the intensity of the band at 1640 cm^{-1} decreases, and the absorption between 3400—3700 cm^{-1} narrows and its intensity diminishes due to the impoverishment in OH^- and H_2O. The 930 cm^{-1} band does not vanish, as in the spectrum of SiO_2 glass, because Si—OH and tetracoordinated Ti—O vibrations overlap. [10,11] The band is sharper in the spectrum of the sample annealed at 500 °C. As the temperature rises, the intensity of the intertetrahedric Si—O—Si vibration band at 800 cm^{-1} increases. This behaviour points out the strengthening of the silicate lattice.

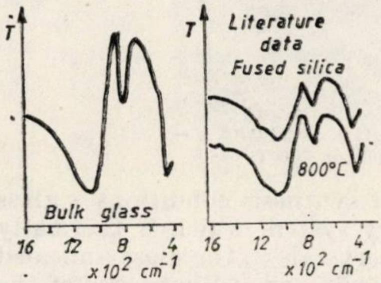

Fig. 2. — IR absorption spectra of SiO_2 glass.

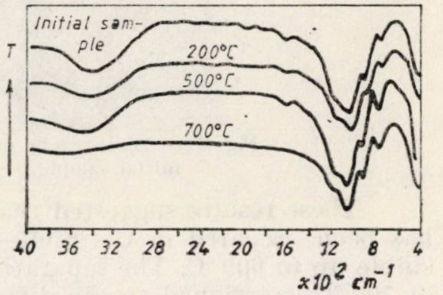

Fig. 3. — IR absorption spectra of SiO_2-TiO_2 glass.

The X-ray diffraction patterns show that the samples annealed up to 700 °C are amorphous. Over this temperature anatase is identified. The crystallisation of anatase by the thermal treatment of glasses in the SiO_2-TiO_2 binary system has also been observed by other authors. [5]

They established that the temperature at which this phase appears is lower as the TiO_2 content in glass is higher.

Electron microscopy evidences the formation of a relatively homogeneous gel which after annealing at 700 °C separates anatase microcrystals (Figure 4).

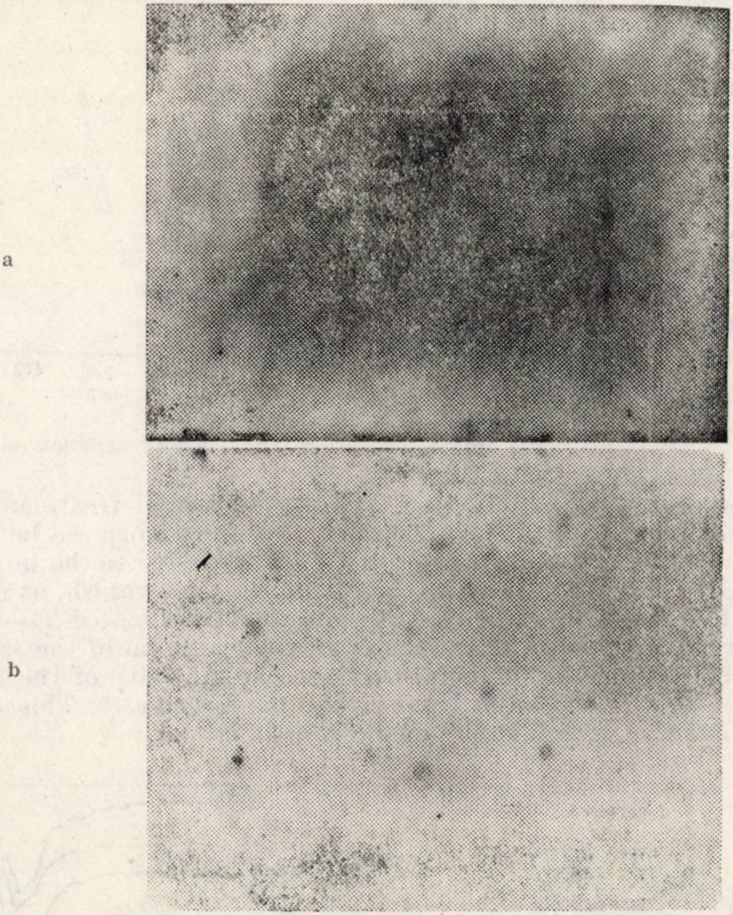

Fig. 4. — Micrographs of SiO_2-TiO_2 glass (×30.000) a — initial sample b — glass annealed at 700 °C.

These results suggested that under our synthesis conditions a glass has been prepared in the SiO_2-TiO_2 binary system which is thermally stable up to 600 °C. The separation of microcrystals in the glass annealed at 700 °C is assigned to the different hydrolysis and gelling rates of the two components, which probably lead to non-homogeneities in the bulk of the gel.

4. CONCLUSIONS

The sol-gel technique has been used in preparing a SiO_2 bulk glass whose density is close to that of fused quartz and a vitreous mass in the SiO_2-TiO_2 system, which was stable at low temperature (below 700 °C).

REFERENCES

[1] M. Zaharescu, C. Pârlog, M. Crişan and M. Sahini, *Rev. Roumaine Chim.*, **34**, 703 (1989).

[2] M. Zaharescu, C. Pârlog, M. Cişan, M. Sahini and D. Moraru, *Silikat Wechnik*, **37**, 165 (1986).

[3] K. Kamiya and S. Sakka, *Res. Rep. Fac. Eng. Mie Univ.*, **2**, 87 (1977).

[4] K. Kamiya and S. Sakka, *J. Materials Science*, **15**, 2937 (1980).

[1] J. Cheng and D. Wang, *J. Non. Cryst. Solids*, **100**, 288 (1988).

[6] K. Shingyouchi, A. Makishima, M. Tutumi, S. Takenouchi, *J. Non. Cryst. Solids*, **100**, 383 (1988).

[8] L. C. Klein, T. A. Gallo and G. J. Garvey, *J. Non. Cryst. Solids*, **63**, 23 (1984).

[9] N. Tohge, G. S. Moore and J. D. MacKensie, *J. Non Cryst. Solids*, **63**, 95 (1984).

[10] C. J. R. Gonzales-Oliver, P. F. James, H. Rawson, *J. Non. Cryst. Solids*, **48**, 129 (1982).

[11] Z. Deng, E. Breval, C. Pantano, *J. Non. Cryst. Solids*, **100**, 364 (1988).

Revue Roumaine de Chimie, 35, 5, 595–599 (1990)

Cu(II), Zn(II), Cd(II), Co(II) AND Ni(II) SORPTION ON *p*(BENZYLCELLULOSE)-5-AZO-8-HYDROXYQUINOLINE. THERMOGRAVIMETRIC CHARACTERIZATION

TINCA ONOFREI, LUCIA ODOCHIAN and VIORICA DULMAN
Faculty of Chemical Technology, Polytechnic Institute Jassy, Romania

Received November 19, 1988

p(Benzylcellulose)-5-azo-8-hydroxyquinoline has been analyzed thermogravimetrically under dynamic temperature conditions both before and after Cu(II), Zn(II), Cd(II), Co(II) and Ni(II) sorption. The results reached at evidenced a combined mechanism of physical and chemical sorption, chemosorption being prevalent for Cu(II), Zn(II), Co(II) and Ni(II) while for Cd(II) adsorption occurs preferentially.

Sorbents modified with functional-analytical groups show an increased selectivity for some metal ions and can be used for their concentration and separation. [1–2]

Several previous notes presented data concerning the synthesis of some celluloses modified with azo groups as well as the sorption and separation of different elements on such sorbents. [3–8]

In order to ellucidate the mechanism of Cu(II), Zn(II), Cd(II), Co(II) and Ni(II) sorption on *p*(benzylcellulose) 5-azo-8-hydroxyquinoline the sorbent was thermogravimetrically characterized under dynamic temperature conditions both before and after sorption.

EXPERIMENTAL

p(Benzylcellulose)-5-azo-8-hydroxyquinoline was synthetised from PAB-cellulose diazotized and coupled with 8-hydroxyquinoline. [9] Cu(II), Zn(II), Cd(II), Co(II) and Ni(II) sorption on this sorbent was carried out under static conditions. The equilibrium was achieved by stirring, for an hour, of about 0.5 g sorbent with 25 cm^3 of 10^{-2} M standard solution that contains the elements under the form of nitrates and chlorides.

The thermograms were registered by a MOM Budapest derivatograph under the following conditions : environment ; heating rate, 12 °C min ; maximum temperature, 600 °C ; sample mass, 18 mg (mixed with Al_2O_3 recently calcined at 1200 °C) ; sensitivity for DTG 1/10 and DTA 1/5.

RESULTS AND DISCUSSION

The tested samples are plotted in Table 1.

The thermograms show a specific thermal behaviour, as function of the sorpted metallic ion. The shape of DTG and DTA curves proves that the decomposition of samples 1, 2, 3 unfolds in two stages, the same holds true for the sorbent (Fig. 1) while the decomposition of samples 4

Table 1 . The tested samples

No. of sample	0	1	2	3	4	5
Sorpted element	Sorbent	Cu(II)	Zn(II)	Cd(II)	Co(II)	Ni(II)

Sorbent :

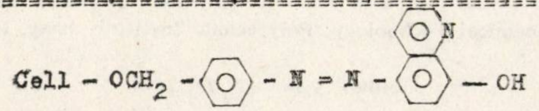

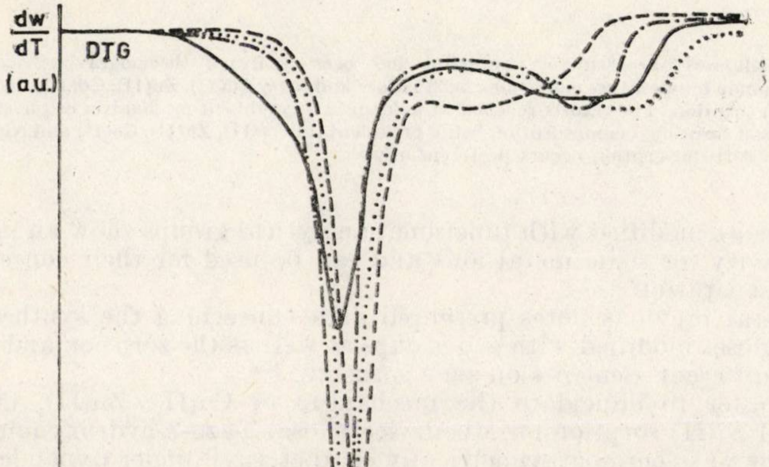

Fig. 1. —DTG and DTA curves for the decomposition of *p*(benzylcellulose)-5-azo-8-hydroxyquinoline : (—) before ; after sorption of (— — —) Cu(II), (—. —. —) Cd(II), (. . .) Zn(II) ;

and 5 takes place in three stages (Fig. 2), the first one being prevalent.

For all samples the stages of thermal decomposition are accompanied by exothermal reactions.

The thermostability of the samples was established on the basis of the specific temperatures (Table 2): the initial temperature (T_i), the temperature at maximum rate (T_m) and the final temperature of decomposition (T_f).

As a function of this criterion, the samples can be written in the following thermostability order

$$2 > 1 > 5 > 4 > 3 > 0$$

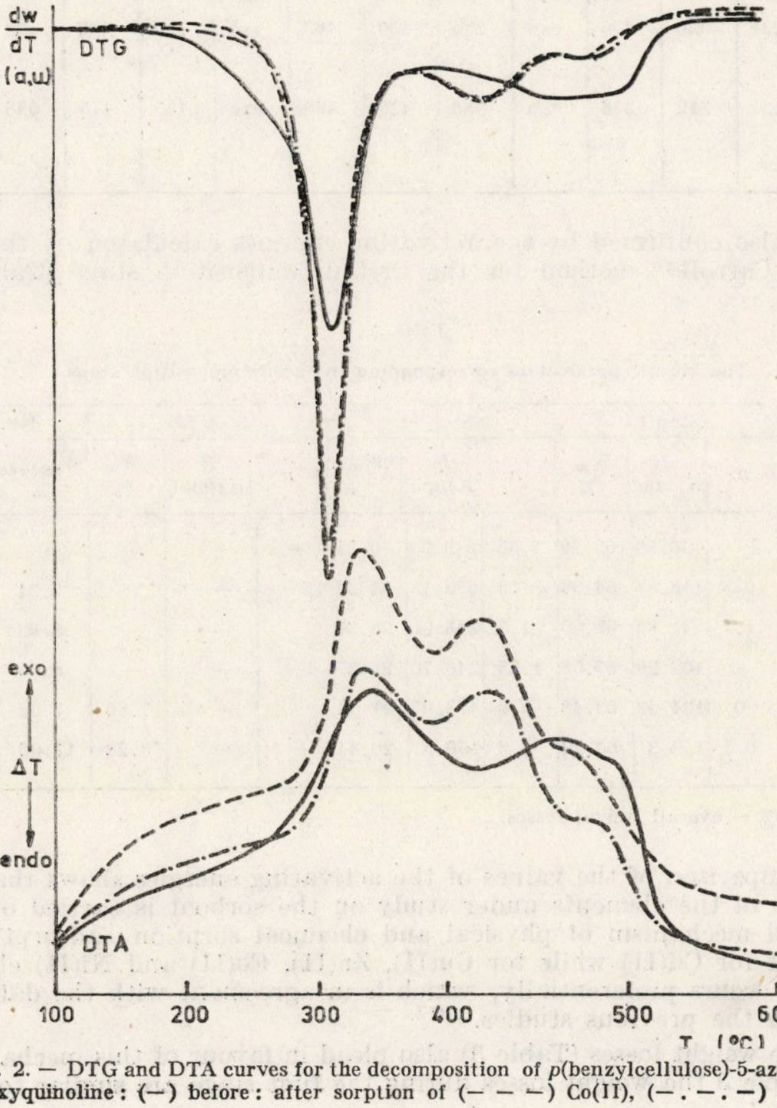

Fig. 2. — DTG and DTA curves for the decomposition of *p*(benzylcellulose)-5-azo-8-hydroxyquinoline: (—) before: after sorption of (— — —) Co(II), (— . — . —) Ni(II);

Table 2

The temperature characteristics of the samples

Sample	Step I °C				Step II °C				Step III °C			
	T_i	T_m	T_f		T_i	T_m	T_f		T_i	T_m	T_f	
0	184	314	375	exo	396	462	514	exo	—	—	—	—
1	238	320	376	exo	376	403	480	exo	—	—	—	—
2	240	312	384	exo	423	494	530	exo	—	—	—	—
3	220	320	391	exo	420	490	510	exo	—	—	—	—
4	224	320	376	exo	385	430	468	exo	480	493	528	Slighty exo
5	227	312	378	exo	386	425	460	exo	460	475	546	Slighty exo

that is also confirmed by the activating energies calculated by the Freeman — Carroll[10] method for the first decomposition stage (Table 3).

Table 3

The kinetic parameters corresponding to the decomposition steps

Sample	Step I			Step II			Step III			Residue	
	n	E Kj/mol	W_∞ %	n	E Kj/mol	W_∞ %	n	E Kj/mol	W_∞ %	$W_{residue}$ %	Nature
0	—	58.63	69.79	1.65	239.33	30.21	—	—	—	—	—
1	0.3	158.88	64.36	8.65	670.15	33.33	—	—	—	2.31	CuO
2	1.7	241.85	65.50	1.8	248.20	28.88	—	—	—	5.62	ZnO
3	—	102.29	67.58	1.55	240.70	26.37	—	—	—	6.05	CdO
4	0	134.02	63.48	5.6	478.67	21.34	—	—	7.86	7.32	CoO
5	0.5	153.3	60.22	8.8	150.5	20.44	—	—	8.28	11.06	NiO

W_∞% — overall weight losses.

Comparison of the values of the activating energies shows that the retention of the elements under study on the sorbent is carried out by combined mechanism of physical and chemical sorption: adsorption is prevalent for Cd(II) while for Cu(II), Zn(II), Co(II) and Ni(II) chemosorption occurs preferentially, which is in agreement with the data obtained in the previous studies.[9,11]

The weight losses (Table 3) also plead in favour of this mechanism. For sample 3 the weight losses during the first stage are similar to that of the sorbent which denotes a weak bond of Cd(II) with the modified cellulose. For the other elements the weight losses are different from those of the sorbent and one can notice a mechanism of thermal decomposition that is similar for samples 4 and 5, a fact also confirmed by the close values of the reaction order (Table 3).

CONCLUSIONS

The thermogravimetrical analysis (TG), the derivative thermogravimetry (DTG) and the differential thermal analysis (DTA) have shown that the Cu(II), Zn(II), Cd(II), Co(II) and Ni(II) sorption on *p*(benzylcellulose)-5-azo-8-hydroxyquinoline is carried out through a combined process of physical and chemical sorption, chemosorption being prevalent with the exception of Cd(II) for which adsorption takes place preferentially.

REFERENCES

[1] G. V. Myasoedova, O. P. Eliseeva and S. B. Savin, *Zhur Analit. Khim.*, **26**, 2172 (1971).
[2] G. V. Myasoedova and S. B. Savin, *Zhur Analit. Khim*, **37**, 499 (1982).
[3] S. Fişel, T. Ungurenaşu-Onofrei and I. Gabe, *Anal. St. Univ. "Al. I. Cuza" Iași*, **11**, 51 (1965)
[4] S. Fişel and T. Ungurenaşu-Onofrei, *Cell. Chem. Technol.*, **3**, 383 (1969).
[5] S. Fişel and T. Ungurenaşu-Onofrei, *3rd Anal. Chem. Conf. Budapest*, 99 (1970).
[6] T. Ungurenaşu-Onofrei and S. Fişel, *Proc. 3rd Nat. Anal. Chem. Conf. Brașov*, Romania, **4**, 61 (1971).
[7] T. Ungurenaşu-Onofrei and S. Fişel, *Chem. Analyt.*, **19**, 257, (1974).
[8] T. Ungurenaşu-Onofrei and S. Fişel, *Rev. Chim (Bucureşti)*, **24**, 926 (1973).
[9] T. Ungurenaşu-Onofrei, S. Fişel and Al. Cecal, *Bul. Inst. Politeh. Iași*, **27**, 25 (1981).
[10] E. S. Freeman and B. Carroll, *J. Phys. Chem.*, **62**, 394 (1958); *J. Polymer Sci.*, **54**, 299 (1961).
[11] T. Onofrei and V. Dulman, *Bul. Inst. Politeh. Iaşi* (in press).

[illegible] surface and [illegible] therefore a weak bond [illegible] [illegible]

CONCLUSIONS

[illegible] which adsorption [illegible]

REFERENCES

[illegible]

[11] T. [illegible] and V. [illegible] (in press).

Revue Roumaine de Chimie, 35, 5, 601–606 (1990)

SeO_2 RADIOLYSIS STUDIED BY EPR

M. CONTINEANU
Department of Physical Chemistry, The Polytechnic Radiation
Chemistry Laboratory, Blvd Republicii 13, Bucharest, Romania

Received December 20, 1988

The accumulation during the irradiation and kinetics of the disappearance with temperature of the SeO_2^- radicals formed at the γ-irradiation of polycrystalline SeO_2 has been studied. Spin densities on Se 4*s* and 4*p* orbitals as well as oxygen atoms were calculated. An adequate radiolysis mechanism has been proposed.

The radiolysis of Se oxycompounds has been the subject of a limited number of papers : Atkins [1] has made evident the formation of SeO_2^- and SeO_3^- radicals in Na_2SeO_3, K_2SeO_3 radiolysis. Cooke[2] has subsequently detected SeO_2^- radicals by EPR to the irradiation of a $NaHSeO_3$ single crystal.

Radiolysis of some Se oxycompounds studied by EPR has been done by Constantinescu [3,4] which suggested a possible reaction mechanism. Among the radical species occurring in Se oxyanions radiolysis, SeO_2^- ion radical turned out to be a resistant species at room temperature. Nevertheless, the previously mentioned papers did not report the radiolysis of the most simple Se oxycompound which would furnish a useful information concerning both the thermal behaviour of the formed radical and the corresponding radiolysis mechanism. For this reason, it appeared as interesting the radiolysis of the polycrystalline SeO_2 since it generates by irradiation a single radical species, namely SeO_2^- ion.

The present paper reports on the kinetical results of polycrystalline SeO_2 radiolysis, aiming at the spectral properties and thermal behaviour of SeO_2^- radical.

EXPERIMENTAL

SeO_2 samples used were supplied by Reanal. The polycrystalline SeO_2 was irradiated by γ rays from ^{60}Co source of 5.6 10^{12} Bq with a dose rate of 10^4 Gy/h.

Irradiations were also made using a 2 MeV electron beam produced from a Van de Graaff accelerator, β rays of a ^{90}Sr source having an activity of 18.5 × 10^5 Bq or UV light using a mercury lamp of 100 W.

EPR spectra of irradiated samples were recorded by means of an ART 5 instrument operating in the X band frequency at 100 kHz. All measurements were made at room temperature. The g factor was estimated using Mn^{2+} ions in CaO matrices. The reflactance spectra were recorded on a Pye-Unicam SP–1800 spectrograph equipped with a reflectance device. The non-irradiated polycrystalline SeO_2 sample was used as referance. Gas-chromatographic measurements were made on a Carlo Erba Cromatograph provided with a 6 A° molecular seave column and Argon as carrier gas.

RESULTS AND DISCUSSION

By γ-irradiation of polycrystalline SeO_2 samples, at room temperature asymmetrical EPR spectra were obtained, as illustrated in Figure 1.

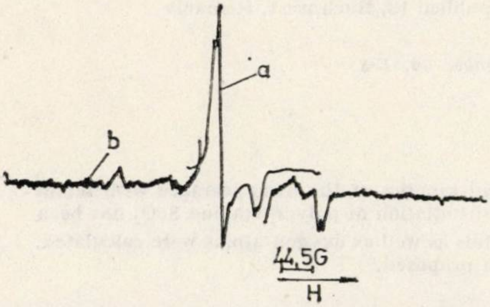

Fig. 1. — a) EPR spectrum of SeO_2 sample irradiated at room temperature with 3.10^5 Gy dose ; b) The same spectrum 10 X amplified

Intense EPR signals having subaxial symmetry were detected in all cases. If EPR measurements are accomplished at higher amplifications, the hyperfine structure of the signal becomes obvious, most likely due to the interaction between unpaired electron and the magnetic moment of the Se^{77} (natural abundence 7.6 %; $I = 1/2$). The hyperfine splittings and g values obtained from the experimental data are :

$$g_x = 1.9872,\ g_y = 2.0309,\ g_z = 1.9966.$$

$$A_x = 302\ \text{G},\ A_y = 140\ \text{G},\ A_z = 138.2\ \text{G},$$

The spectral data have allowed the calculation of spin densities on Se and O orbital. If the isotopic part of the hyperfine coupling experimentally determined $A_{iso} = 193.4$ G and the isotrope coupling constant [5] (Fermi contact term) $A_0 = 4810$ G for a 100 % occupance of Se 4s orbital are considered, the calculated spin density of Se 4s orbital in SeO_2^- radical assumes a value of 0.04.

If the anisotropic part of the hyperfine coupling calculated from the experimental data, $a_x = 108.6$ G; $a_y = -53.4$ C; $a_z = -55.2$ G and the theoretical values of unisotrope hyperfine interaction of an electron in $4p$ Se pure orbital, [5], $B_0 = 134$ G are considered, the spin density values for the uncoupled electron in Se $4p$ orbitals are : $C^2_{4p_z} = 0.409$, $C^2_{4p_x} = 0.0045$. In this case a value of 0.273 spin density results for p orbital of each oxygen atom.

The radical accumulation with the integral dose at room temperature is presented in figure 2.

As may be seen in figure 2, the signal intensity plotted versus the received dose, shows a linear dependence for short times, and reaches a steady value for longer times. Such a behaviour is typical in the case of two competitive processes taking place during irradiation : the radical formation and disappearance. In our measurements the steady value of the signal was reached for an irradiation time of 60 hrs (dose rate 10^4 Gy/h). Reflectance spectra were recorded for samples irradiated with different dose. Figure 3 shows the reflectance spectra obtained with SeO_2 nonirradiated (a) and irradiated (b) samples.

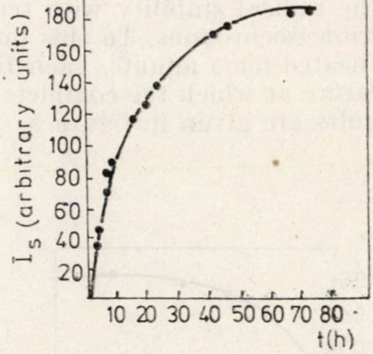

Fig. 2. — Intensity dependence of EPR signal function of integral dose for a γ-irradiated sample.

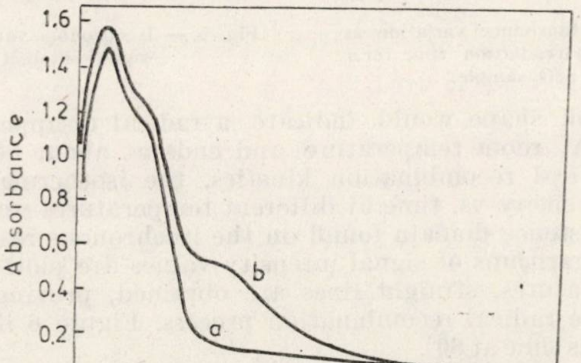

Fig. 3. — Reflectance spectrum of SeO_2 sample a) nonirradiated b) γ-irradiated.

As may be observed, the irradiated sample presents a characteristic absorption band with a maximum at 310 nm. This maximum has been assigned to be radical species formed by irradiation at room temperature.

The γ-irradiated $NaHSeO_3$ and Na_2SeO_3 samples present in their reflectance spectra a characteristic absorption maximum at 340 nm and 320 nm, respectively, attributed to the same paramagnetic species. [6]

The mentioned absorption maxima cannot be assigned to possible colour centres, because a previous optical bleaching of the γ-irradiated samples leaves their spectra unchanged. The appearance of a characteristic absorption maximum in the reflectance spectra for SeO_2^- ion-radical allows to follow the paramagnetic centre accumulation during irradiation. Figure 4 shows the absorption intensity measured at $\lambda = 310$ nm as a function of dose.

As may be seen, the absorbance follows the same variation as the EPR signal intensity (Figure 2), proving the radical origin of the absorption maxima.

The radical stability with temperature has been studied by means of reaction isochronous. To this purpose, the irradiated sample was gradually heated for 5 minutes each 10°, from the room temperature till the temperature at which the complete disappearance of radicals is observed. The results are given in figure 5.

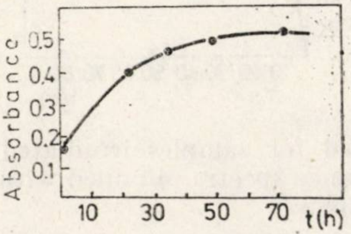

Fig. 4. — Absorbance variation at 310 nm with irradiation time for a SeO_2 sample.

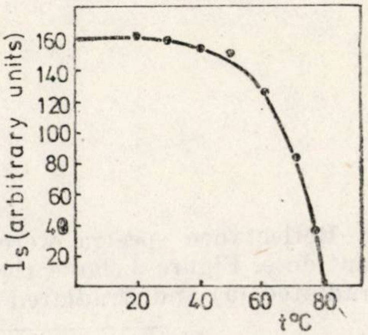

Fig. 5. — Isochronous variation of EPR signal intensity.

The graph shape would indicate a radical disappearance process which begins at room temperature and ends at about 80°. In order to study the radical recombination kinetics, the isothermal variation of EPR signal intensity vs. time at different temperatures was indicated by the radical existence domain found on the isochronous reaction.

If the logarithms of signal intensity values are plotted versus time for all temperatures, straight lines are obtained, proving a first order kinetics for the radical recombination process. Figure 6 illustrates lg I_s variation versus time at 80°.

The rate constant values have been estimated from the slopes of straight lines obtained with different temperatures. These values are summarized in table 1.

Table 1

Kinetic parameters estimated from SeO_2^- heating

t°C	T(K)	$\frac{1}{T}\,10^3$	$k\ 10^3$	lg $k + 3$
70	343	2.914	0.597	0.22
73	346	2.893	3.99	0.60
75	348	2.872	4.245	0.614
78	351	2.852	9.700	0.968
80	353	2.831	13.275	1.120

If lg k values are plotted against $1/T$, a straight line is obtained, as shown in figure 7.

From the straight line slope an activation energy of 78.34 kcal/mol has then been estimated.

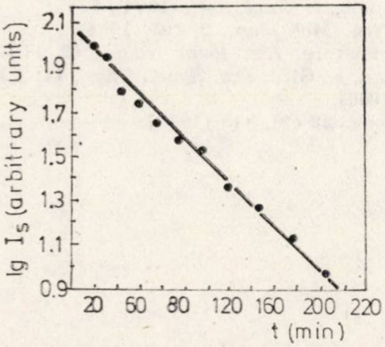

Fig. 6. — lg I_s variation as a function of time at 80°.

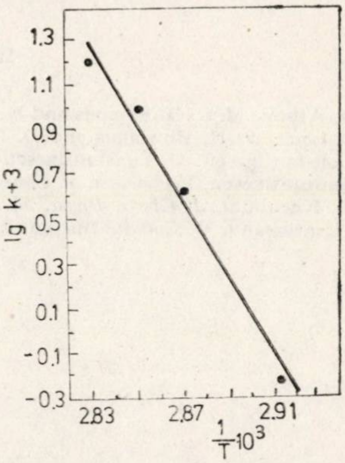

Fig. 7. — lg k variation against $1/T$.

CONCLUSIONS

The radiolysis processes which take place by SeO_2 irradiated are the following :

$$SeO_2 \rightsquigarrow SeO_2^+ + e^- \tag{1}$$

$$SeO_2 \rightsquigarrow SeO_2^* \tag{2}$$

$$SeO_2 + e^- \rightarrow SeO_2^- \tag{3}$$

The kinetic study followed by EPR shows the radical disappearance if the SeO_2 irradiated samples are heated. The SeO_2^- radicals disappear according to a first order reaction.

$$SeO_2^- \xrightarrow{t°} Se + O_2^-(O_2 + e^-) \tag{4}$$

O_2 formation by heating of irradiated samples has been chromatographically proved. To this purpose, the following experiment has been done. A γ-irradiated SeO_2 sample has been introduced into a tightly closed ampoule provided with a silicone rubber cork and heated at 80°. The gasses from ampoule chromatographically analyzed, show an increase of O_2 of about 25 %. The SeO_2^- radical disappearance has been studied by means of diffuse reflectance spectroscopy, the observed maxima at 310 nm being characteristic for the radical species. Their intensity diminishes with the heating time, a vertical shift of the whole spectrum due to the elementary red selenium formed in the chemical process[6] being also observed.

REFERENCES

[1] P. W. Atkins, M. C. R. Symons and H. J. Wardale, *J. Chem. Soc.*, (**1964**), 5215.
[2] R. J. Cook, J. R. Rowlands and D. H. Whiffen, *Mol. phys.*, **2**, 197 (1964).
[3] M. Constantinescu, O. Constantinescu and I. Pascaru, *Rev. Roum. Phys.*, **12**, 110 (1967).6).
[4] O. Constantinescu, I. Pascaru, M. Constantinescu, E. Gîrd, *Rev. Roum. Phys.*, **11**, 3 249 (196
[5] F. K. Kneubühl, *J. Chem. Phys.*, **33**, 1074 (1960).
[6] M. Contineanu, O. Constantinescu, *Rev. Chimie*, **28** (9), 845 (1977).

Revue Roumaine de Chimie, 35, 5, 607–616 (1990)

COMPLEXING, EXTRACTION AND DETERMINATION OF THE $C_2H_5Hg^+$ ION WITH 1-(*p*-NITROPHENYL), 3-(*p*′-AZOBENZENE)-TRIAZENE

ANDREI DĂNEŢ and KIM GWANG SIK

The Polytechnic Institute, Bucharest, Department of Analytical Chemistry, Splaiul Independenţei 313, Bucharest 77206, Romania

Received June 28, 1989

The values of the repartition constants were determined for the reagent, its complex with the ethyl-mercuric ion and for C_2H_5HgCl in the toluene-aqueous phase system which contains 20% methyl alcohol; they have the values of 2.4×10^4, 4.0×10^4 and 11.5, respectively. The reagent and the ethyl-mercury complex extracted in toluene have absorption maxima at 406 and 470 mm, respectively. The ethyl-mercury complex is practically extracted quantitatively within the pH range 7–9.5. The $HR/C_2H_5Hg^+$ combination ratio has the value of 1/1. The stability constant of the ethyl-mercury complex was determined by two methods obtaining the values of $10^{11.5}$ and $10^{11.4}$. The type bonding between $C_2H_5Hg^+$ and the reagent molecule was determined on the basis of the IR spectra. The thermal stability of the reagent and of the ethyl-mercuric complex was established on the basis of the TG, DTA and DTG curves. The reagent allows the determination of $C_2H_5Hg^+$ with a good selectivity, the molar absorptivity having the value of 3.21×10^4 l mol^{-1} cm^{-1}.

For several decades the very important pollutant effect of mercury on the environment has been evidenced.[1,2] This asks for analysis methods which would allow the determination of mercury in a wide variety of samples. A remarkable interest presents the differential determination of the mercury present as an organic form, because some of the organic compounds are characterized by a much higher toxicity than the inorganic ones.

The organomercuric compounds appear in the environment either due to the use of some organomercuric compounds in agriculture or industry, or due to the capacity of some micro-organisms to transform the mercury present under an organic form into organomercuric compounds.[3,4] The most used methods for the determination of mercury are the atomic absorption methods,[5–7] an interest presenting also those based on the use of the organic reagents.

The methods from the latter category, besides a good sensitivity and selectivity, have the advantage that they require a much simpler equipment than other methods of instrumental analysis.

From the great variety of organic reagents suggested for the determination of mercury,[5–7] the 1,3-diaryltriazenic derivatives have been studied in our laboratory, since they present a high selectivity in the reaction with mercury (II) and the organomercuric compounds.

On this basis, selective and sensitive methods have been suggested for the determination of Hg(II) in aqueous phase with 1-(*p*-nitrophenyl), 3-(*p* -natrium sulphonate)-triazene[8] or by extraction in organic solvents from a neutral or a very weakly alkaline medium of Hg(II) and $C_5H_6Hg(I)$ with 1,3-diphenyltriazene [9,10] and 1-(*p*-nitrophenyl), 3-(*p* -azobenzene)-triazene. [11,12]

These analysis methods present a neatly greater selectivity in comparison with the originally suggested method for the determination of mercury with 1-(*p*-nitrophenyl), 3-(*p* -azobenzene)-triazene, [13] in which the determinations are made in a basic medium of water-alcohol.

The sensitivity, but especially the high selectivity of these determination methods have suggested to us the study presented herein about the complexing and extraction equilibria with a view to establish the optimum conditions of determining ethyl-mercury with 1-(*p*-nitrophenyl), 3-(*p*'-azobenzene)-triazene.

EXPERIMENTAL PARTS

Apparatus and Reagents

The IR absorption spectra were recorded by means of the Specord UV VIS and 75 IR spectrometers and the absorbance determinations at a fixed wavelength were carried out by means of the VSU 2G spectrometer, all these apparatus coming from the Carl Zeiss, Jena firm (German Democratic Republic).

The pH measurements were made by the MV 85 apparatus (German Democratic Republic) and the thermograms were plotted by means of the J. Paulik, F. Paulik and L. Erdey system apparatus (Hungarian Republic). All the reagents used were analytically pure.

A 0.015% stock solution of 1-(*p*-nitrophenyl), 3-(*p*'-azobenzene)-triazene (Austranal) in methanol and an ethyl-mercuric chloride (Merck) solution (100 μg $C_2H_5Hg^+$/ml) in water were prepared. The solution of ethyl-mercuric chloride was obtained by dissolving first the weighed solid substance into 3—4 ml of acetone, followed by dilution with water. The solutions with necessary concentration were then obtained from these solutions by dilution.

THE WORKING PROCEDURE

For carrying out the complexing and extraction studies one proceeded as follows. In a 50 ml graduated cylinder, provided with a ground stopper, 2 ml of the 2*M* sodium acetate solution, the solution which contains the ethyl-mercuric chloride, distilled water, methanol and the reagent solution are introduced. The solution is stirred for homogenization and it is left to react for 10 minutes.

Then 5 ml of toluene are added and it is stirred vigorously for 1 minute. After phase separation, a sufficient quantity from the organic phase is taken out by means of a dry pipette, is introduced into the spectrophotometer cell and its absorbance is measured. In all cases cells of 1 cm thickness were used.

In order to plot the calibration curve and to determine the concentration of ethyl-mercury, one proceeded as above, but introducing 2 ml of reagent into all samples ; the absorbances were measured against a reference sample at 470 nm.

The ethyl-mercury complex with the considered reagent was prepared as follows : stoichiometric quantities of ethyl-mercuric chloride and of the reagent, corresponding to a ratio of 1/1, calculated in order to obtain 1 g of complex dissolved under heating in 10 ml and 100 ml, respectively, of acetone. Over the reagent warm solution the ethyl-mercuric chloride solution was introduced and then 10 g of solid $H_3CCOONa \cdot 3H_2O$, stirring until the complete dissolution of the latter. The solution is left cool down until, at the bottom of the glass a lightly coloured liquid phase is separated, which contains most of the sodium acetate dissolved into its crystallization water ; from acetone the formed complex precipitates and separates at the interface of the two phases. The solution was filtered on a crucible with G4 sintered glass, the precipitate was washed with hot water and then with a small quantity of acetone. It was dried in a drying oven at 105 °C. The solid complex obtained has a microcrystalline structure and is brick-red coloured. The yield is 80%.

The determination of the repartition constants of the reagent and of the ethyl-mercuric complex was made on the basis of their solubility into toluene and into an aqueous phase which has an identical composition to that used for the extraction studies. With that end in view, 50 ml of aqueous phase were brought into contact, into 100 ml separating funnels, with 10 ml of toluene and reagent or ethyl-mercuric complex taken in excess. The samples were stirred for 20 minutes. Then the phases were separated and filtered. From the aqueous phases saturated in the reagent or the complex these were extracted in a 2 and 10 times less volume of toluene respectively. The organic phases, which constitute saturated solutions of reagent or complex were diluted for 1000 and 300 times respectively. The absorbance measurements were made at the absorption maxima of the reagent and of the complex, respectively.

The repartition constants could be calculated from the absorbance values and taking into account the dilution.

The repartition constant of ethyl-mercuric chloride between toluene and an aqueous phase with the same composition as that from which the ethyl-mercury extraction had been made was determined in a similar way. Ethyl-mercury was transformed quantitatively into Hg(II) under the action of UV radiation, and then its concentration was determined on the basis of the method described in paper[17].

RESULTS AND DISCUSSION

Figure 1 presents the absorption spectrum of a 2.5×10^{-5} M solution of reagent extracted from toluene (curve 1) and of some solutions which contain the same amount of reagent and increasing quantities of ethyl-mercuric ions.

As can be seen from Fig. 1, the reagent presents an absorption maximum at 406 nm and the formed complex at 470 nm. The spectra have only one isosbestic point, which suggests the formation of a single complex. The difference between the absorbances of the complex and of the reagent is maximum at 470 nm.

Generally, the extraction studies have been made for a 20% (v/v) water-methanol medium. The variation of the methanol concentration between 10 and 50% does not determine a modification of the absorbance of the ethyl-mercuric complex extracted in the toluene. All the extractions were made for an aqueous phase which contains $0.4M$ sodium acetate, which prevents the pH decrease below the value of 8. The absorbance of the ethyl-mercuric complex extracted in toluene does not vary with the studied reagent in the pH range 7—9.5. All further determinations were carried out at pH 9. One minute of energetic stirring is sufficient for the complex extraction in toluene.

The absorbance of the complex is constant for more than 2 hours provided the organic extract is not submitted to a very strong light.

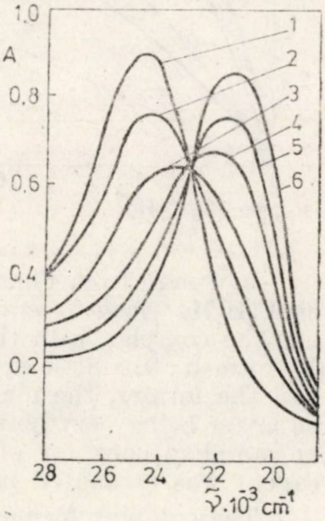

Fig. 1. — The absorption spectra of the reagent and of its complex with ethyl-mercury, extracted in toluene.(1)reagent, $2 \cdot 5 \times 10^{-5}M$; (2—6) the same concentration of reagent and increasing concentration of $C_2H_5Hg^+$, with the following $[HR]/[C_2H_5Hg^+]$ ratios: (2) 4/1, (3), 1/1, (4) 1/2, (5) 1/4, (6) 1/8.

The $C_2H_5Hg^+$/reagent combination ratio was determined by means of the continuous variations method, and it has the value of 1/1, in complete agreement with the ethyl-mercury coordinative properties.

In Fig. 2 are presented the curves obtained when applying the method of the continous variations [14] for isomolar solutions of ethyl-mercury and reagent.

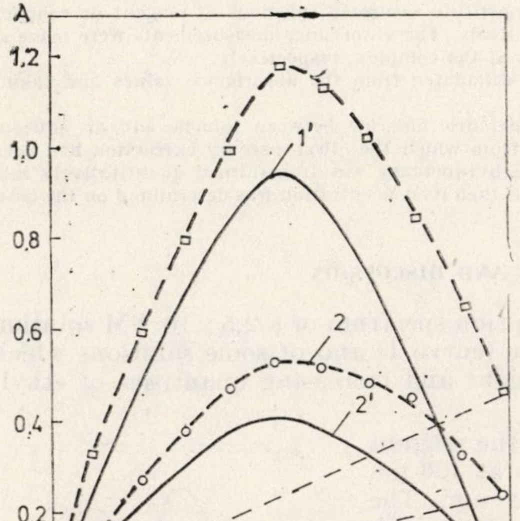

Fig. 2. — The curves obtained by applying the continuous variations method for isomolar solutions with total concentrations $[HR] + [C_2H_5Hg^+]$ equal to $8 \times 10^{-5} M$ (1) and $4 \times 10^{-5} M$ (2). The curves 1′ and 2′ represent the curves 1 and 2 corrected by subtracting the reagent absorption.

Although from Fig. 2 it results clearly that a complex is formed with the $C_2H_5Hg^+$/reagent combination ratio of 1/1, one can say, however, that the complex with the $C_2H_5Hg^+$/reagent combination ratio of 1/2 is also formed ; to a little extent, the latter has however a much less stability than the former, the maximum of the Job curves which correspond to the latter being very blurred. On the basis of the curves shown in Fig. 2 the stability constant of the ethyl-mercury complex with the studied reagent was estimated in the following way :

The complex formation in aqueous phase takes place according to the equilibrium

$$C_2H_5Hg^+ + R^- \rightleftarrows C_2H_5HgR \tag{1}$$

with the constant

$$K_{C_2H_5HgR} = \frac{[C_2H_5HgR]}{[C_2H_5Hg^+][R^-]} \tag{2}$$

Taking into account the repartition constants of the reagent and of the ethyl-mercury complex determined in this paper, the formation constant of the —NH— group from the triazenic group (—N=N—NH—) determined in paper [15] and the formation constants of ethyl-mercury hydroxocomplex determined in paper [16], one can write

$$K_{C_2H_5HgR} = \frac{[C_2H_5HgR]}{[C_2H_5Hg^+][R^-]} =$$

$$= \frac{[C_2H_5HgR]_0 P_{HR} K_{HR} [H^+]}{P_{C_2H_5HgR}[HR]_0} \left(\frac{1 + K_{C_2H_5HgOH}\ [HO^-]}{[C_2H_5Hg^+]_t - [C_2H_5HgR]_0} \right) \qquad (3)$$

where

$$P_{HR} = \frac{[HR]_0}{[HR]} = 2.4 \times 10^4$$

$$P_{C_2H_5HgR} = \frac{[C_2H_5HgR]_0}{[C_2H_5HgR]} = 4.0 \times 10^4$$

$$K_{HR} = \frac{[HR]}{[H^+][R^-]} = 10^{11.2}$$

$$K_{C_2H_5HgOH} = \frac{[C_2H_5HgOH]}{[C_2H_5Hg^+][OH^-]} = 10^{9.1}$$

The concentrations of the species in the organic phase bear the index O and those in the aqueous phase have no index. Knowing the concentration of ethyl-mercury ions initially introduced, $[C_2H_5Hg^+]$, the pH value which is 9, and determining $[C_2H_5HgR]_0$ at the maximum of the Job curves, the stability constant $K_{C_2H_5HgR}$ can be calculated by means of the relation (3), obtaining the values of $10^{11.45}$ and $10^{11.50}$ for the sum of the concentrations $[C_2H_5Hg^+] + [HR]$ of 4×10^{-5} and 8×10^{-5} *M*.

In Fig. 3 the influence of the Cl^- ions on the extraction of the ethyl-mercury complex with the studied reagent is presented.

In aqueous phase, the ethyl-mercury ion is present as the C_2H_5HgOH and C_2H_5HgCl species; the concentration of the C_2H_5HgR species can be considered as negligible due to the large repartition constant of the complex.

The C_2H_5HgCl species formed at high concentrations of Cl^- ions in the aqueous phase is distributed within the organic phase, the repartition constant having the value of 11.5.

As can be seen from Fig. 3, both in the absence and in the presence of 20% methyl alcohol in the aqueous phase, the curves which show the variation of the absorbance of the ethyl-mercury complex extracted in toluene as a function on the Cl^- ions are practically identical.

This leads to the conclusion that a content of methyl alcohol of up to 20% in the aqueous phase does not modify practically the value of the stability constants of the hydroxo- and chlorocomplexes of ethylmercury.

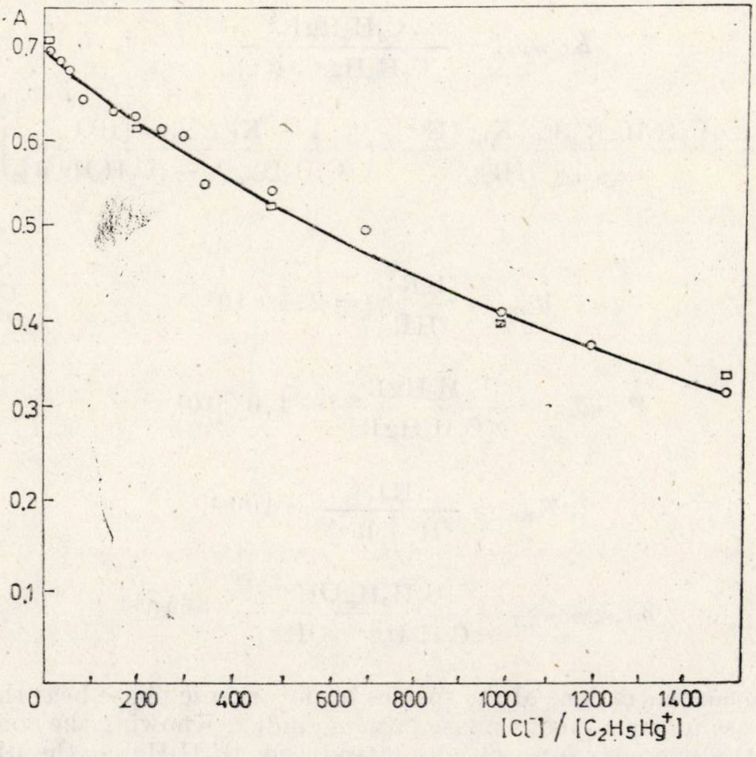

Fig. 3. — The variation of the absorbance of the ethyl-mercury complex extracted in toluene, as a function of the $[Cl^-]/[C_2H_5Hg^+]$ ratio. The initial value of $[C_2H_5Hg^+]$ in the aqueous phase $= 2.2 \times 10^{-5} M$; the initial value of [HR] in the organic phase $= 1.7 \times 10^{-4} M$. Equal volumes of both phases were used. In the presence of 20% methyl alcohol in the aqueous phase (○); in the absence of methyl alcohol (□).

Starting from the expression of the stability constant of the C_2H_5HgR complex one can write:

$$K_{C_2H_5HgR} =$$

$$= \frac{P_{HR} K_{HR} [H^+][C_2H_5HgR]_0}{P_{C_2H_5HgR}[HR]_0} \left(\frac{1 + 12.5 K_{C_2H_5HgCl}\,[Cl^-] + K_{C_2H_5HgOH}[OH^-]}{[C_2H_5Hg^+]_t - [C_2H_5HgR]_0} \right) \tag{4}$$

and, in another form

$$\frac{([C_2H_5Hg^+]_t - [C_2H_5HgR]_0)[HR]_0}{[C_2H_5HgR]_0} = \frac{P_{HR}K_{HR}[H^+]\cdot 12.5K_{C_2H_5HgCl}}{P_{C_2H_5HgR}\cdot K_{C_2H_5HgR}}\cdot$$

$$\cdot[Cl^-] + \frac{P_{HR}\cdot K_{HR}[H^+]}{P_{C_2H_5HgR}\cdot K_{C_2H_5HgR}}\cdot(1 + K_{C_2H_5HgOH}[OH^-]) \qquad (5)$$

Relation (5) is the equation of a straight line, which is shown in Fig. 4.

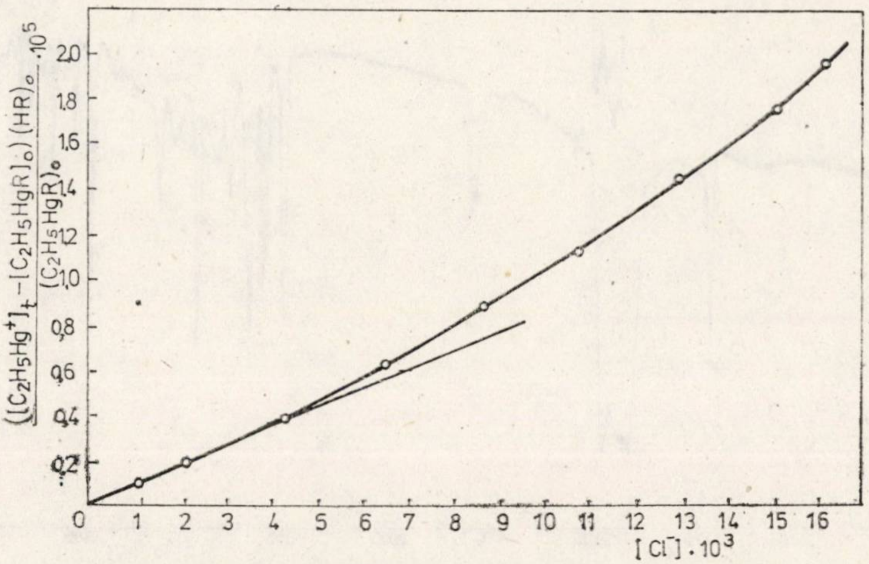

Fig. 4. — Graphic plot of equation (5).

On the basis of the data presented in Fig. 4 the conclusion can be drawn that at high concentrations of $[Cl^-]$ ions, the higher complexes $[C_2H_5HgCl_2]^-$ and $[C_2H_5HgCl_3]^{2-}$ are formed which makes relation (5) to be only valid at lower concentrations of Cl^- ions. These findings are in agreement with those noticed for the species C_2H_5HgSCN. [19]

From the slope of the straight line in Fig. 4, the values of $10^{11.40}$ was determined for the formation constant of C_2H_5HgR knowing the value of the constant $K_{C_2H_5HgCl} = 10^{5\ 32\ 20}$. In Fig. 5 the absorbance IR spectra are shown for the reagent and the ethyl-mercury complex obtained in a nujol mull.

From Fig. 5 one can see that in the spectrum of the complex, the bands at 3260 cm^{-1} and 1526 cm^{-1} which correspond to the deformation and valence vibrations of the —NH— group of the triazenic group [21] disappear. This is a clear indication that the complex formation takes place by substituting the hydrogen from the triazenic group by the $C_2H_5Hg^+$ ion, this fact explaining the combination ratio of 1/1 previously mentioned.

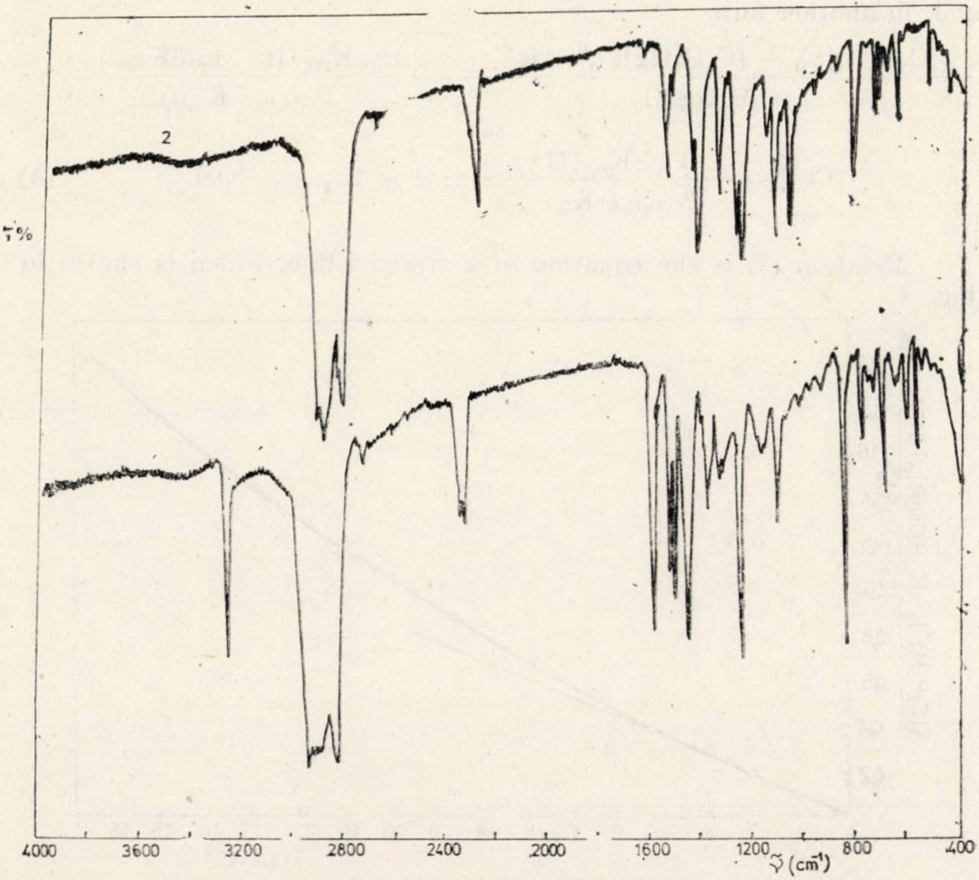

Fig. 5. — The IR absorption spectra of the reagent (1) and of the complex formed by the $C_2H_5Hg^+$ ion (2).

In Fig. 6 the TG, DTA and DTG curves are shown for the reagent (1) and its complex with ethyl-mercury (2). The complex is stable up to 190 °C, which allows the use of 1-(*p*-nitrophenyl), 3-(*p*′-azobenzene)-triazene for the gravimetric determination of ethyl-mercury.

A linear dependence is obtained between the absorbance of the ethyl-mercury complex extracted in toluene and the mercury concentration within the 0.25—8 μg $C_2H_5Hg^+$/ml range, the molar absorbance having the value of 3.21×10^4 l mol^{-1}cm^{-1}.

Taking into account the detailed study of interferences when determining the mercury with 1-(*p*-nitrophenyl), 3-(*p*′-azobenzene) triazene, presented in paper[11] we can draw the conclusion that the $C_2H_5Hg^+$ ion can be determined without interference for ion/$C_2H_5Hg^+$ rations equal to or greater than 1,000/1 for Li^+, Na^+, K^+, Fe^{3+}, Co^{2+}, Ni^{2+}, Be^{2+}, Mg^{2+}, Ca^{2+}, Sr^{2+}, Ba^{2+}, Zn^{2+}, Cd^{2+}, Ga^{3+}, In^{3+}, Tl^{3+}, Pb^{2+}, SO_4^{2-}, citrate and tartrate ; 500/1 for Cu^{2+}, Bi^{3+}, Cr^{3+}, Mn^{2+}, CrO_4^{2-} ; 100/1 for Rh^{3+}, Ir^{3+}, Pd^{2+}, Pt^{4+}.

The ions Hg^{2+}, Hg_2^{2+}, $C_6H_5Hg^+$, Br^-, SCN^-, CN^-, S^{2-} interfere, either by forming complexes with the reagent or by precipitating or complexing the ethyl-mercuric ion. The cations were introduced as nitrates, sulphates or acetates, and the anions as salts with alkali metals.

The interference of the Hg^{2+} and Hg_2^{2+} ions can be avoided if, first of all, these species are reduced to the elementary state with stannous chloride (the organomercuric compound being stable).[6,7]

CONCLUSIONS

The repartition constants were determined for the 1-(*p*-nitrophenyl), 3-(*p'*-azobenzene)-triazene, its complex with the $C_2H_5Hg^+$ ion, as well as for the H_5C_2HgCl in the toluene-aqueous phase system containing 20% (v/v) methyl alcohol.

The absorption spectra were plotted and the wavelengths determined for the absorption maxima of the reagent and of its complex with ethyl-mercuric ion extracted in toluene, and the pH range in which the extraction of the complex is maximum was established.

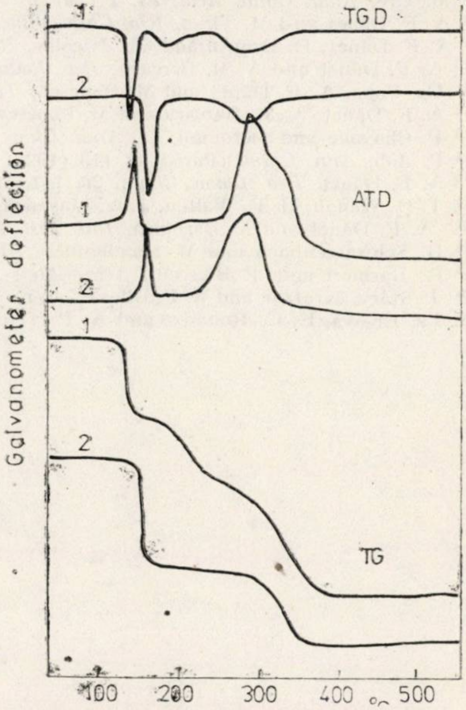

Fig. 6. — The TG, DTA and DTG curves for the reagent (1) and the complex of $C_2H_5Hg^+$.

By applying the method of the continuous variations, the $HR/C_2H_5Hg^+$ combination ratio was determined; it has the value of 1/1. From the obtained curves, the value of the stability constant of the complex has been estimated taking into account the competitive equilibria in the solution; it is $10^{11.5}$. The stability constant of the ethyl-mercury complex with the investigated reagent was also calculated on the basis of the competitive equilibria which appear when introducing the Cl^- ion into the aqueous phase, thus obtaining the value of $10^{11.4}$. On the basis of the absorption spectra of the reagent and of the ethyl-mercury complex, and taking into account the $HR/C_2H_5Hg^+$ combination ratio the way in which $C_2H_5Hg^+$ is bonded to the reagent molecule could be established.

The thermal stability range of the reagent and of its complex with the ethyl-mercury ion has been determined on the basis of the TG, DTA and DTG curves.

REFERENCES

[1] R. Hartung and B. D. Dinman, "Environmental Mercury Contamination", Ann Arbor Science Publishers Inc., 1972.
[2] P. A D'Itri and F. M. D'Itri, "Mercury Contamination : A Human Tragedy", Wiley, 1977.

[3] J. M. Wood, F. S. Kennedy and C. G. Rosen, *Nature*, **220**, 173 (1968).
[4] S. Jensen and A. Jernelov, *Nature*, **223**, 753 (1969).
[5] C. Luca, I. Tănase, A. F. Dăneţ and I. Ioneci, *Rev. in Analyt. Chem.*, **9**, 1 (1987).
[6] S. Chilov, *Talanta*, **32**, 205 (1975).
[7] M. Ure, *Anal. Chim. Acta*, **75**, 1 (1975).
[8] A. F. Dăneţ and M. Tiron, *Rev. Chim. (Bucharest)*, **30**, 376 (1979).
[9] A. F. Dăneţ, R. Dreptu and Gh. Nicolae, *Rev. Roum. Chim.*, **24**, 1229 (1979).
[10] A. F. Dăneţ and A. M. Bercaru, *Rev. Roum. Chim.*, **27**, 459 (1979).
[11] Gr. Popa, A. F. Dăneţ and M. Popescu, *Talanta*, **25**, 546 (1978).
[12] A. F. Dăneţ, A. M. Bercaru and M. Popescu, *Rev. Chim.* (Bucharest), **33**, 1133 (1982).
[13] P. Chavane and Geronimi, Cl. *Anal. Chim. Acta*, **19**, 442 (1958).
[14] P. Job, *Ann. Chim.* (Paris), **9**, 113 (1928).
[15] A. F. Dăneţ, *Rev. Roum. Chim.*, **26**, 141 (1981).
[16] T. D. Wangh, H. F. Walton, J. A. Liasmich, *J. Phys. Chem.*, **59**, 395 (1955).
[17] A. F. Dăneţ and A. Bărbuică, *Bul. Inst. Politeh. "Gh. Gh. Dej", Bucharest*, **42**, **47** (1980).
[18] G. Schwarzenbach and M. Schellenberg, *Hel. Chim. Acta*, **48**, 28 (1965).
[19] R. Barbieri and J. Bierrum, *Acta Chim. Scand.*, **19**, 469 (1965).
[20] J. Stary, Kratzer and J. Prasilova, *Anal. Chim. Acta*, **100**, 627 (1978).
[21] Tv. Erşova, E. C. Ruhadze and A. P. Terentiev, *Zh. Obsch. Khim.*, **39**, 59 (1969).

Revue Roumaine de Chimie, **35**, *5*, 617–623 (1990)

COORDINATION COMPOUNDS AS RAW MATERIALS FOR MIXED OXIDES. VI[1]

MIXED COORDINATION COMPOUNDS OF LANTHANOIDES AND Cr(III) AS PRECURSOR OF CHROMITES

P. SPACU, LUMINIŢA PATRON, SILVIA PLOŞTINARU, ADRIANA CONŢESCU and N. STĂNICĂ

Center of Physical Chemistry, Bucharest, Splaiul Independenţei 202, Romania

Received June 4, 1989

The polynuclear complex compounds obtained from Ln(III)–Cr(III) – gluconic acid (Gluc) system were studied in order to obtain $LnCrO_3$ oxides (Ln(III) = La – Tm). The complex compounds were characterized by elemental analysis, electronic and IR spectra, magnetic measurements and thermogravimetric analyses. The pure oxide phases have been put in evidence by X-ray diffraction and characterized by physico-chemical methods.

In some previous notes mixed oxides of perovskite structure, ABO_3, of lanthanoides with Co(III), Ni(III) and Fe(III) obtained by decomposition of polynuclear complex compounds were studied.[1,2]

This note deals with the obtention and characterization of lanthanoide chromites and of their precursors – the complex compounds containing Ln(III) and Cr(III).

These mixed oxides were mentioned first in 1960–1965 ; they were prepared by the ceramic classical method.[3] This method assumed a reaction in solid phase of the stoichiometric mixtures of Cr(III) and Ln(III) oxides.[4–6] Owing to the difficulties encountered in obtaining chromites by the ceramic method, their synthesis by nonconventional methods has been attempted recently by thermal decomposition of hydroxides or nitrates coprecipitates and oxalatochromate of lanthanoides).[7,8]

In this contribution the obtention of lanthanoide chromites by decomposition of polynuclear complex compounds was attempted. Because in the literature there is no mention of some complex compounds containing Cr(III) and Ln(III) we considered interesting the isolation and physico-chemical characterization of such complex species which are potential precursors of chromites.

Therefore the following system was studied :

Ln(III) – Cr(III) – Gluconic acid.

To isolate the mixed complex compounds a variant of Melson and Pickering's method[9] was employed as synthesis procedure. For a 1 : 1 ratio of the two metallic ions the following series of complex compounds was obtained :

$$LnCr(Gluc)_4 \cdot nH_2O$$

$$\text{where } Ln(III) = La - Lu\, ;\ n = 3-5.$$

The synthesized complex compounds were grey-blue powders, soluble in water and hardly soluble in most of the usual organic solvents.

All complex compounds were characterized by IR and electronic spectroscopy, magnetic determinations and differential thermal analysis.

Information regarding coordination of the ligand to the metallic ions was acquired from IR spectra of complex compounds in the range 400—4000 cm^{-1}; these spectra, were compared with similar data in literature on glucono — δ — lactone, natrium gluconate and simple gluconates of transition metals. The spectrum of glucono — δ — lactone shows a maximum at 1721 cm^{-1} assigned to $\nu_{C=O}$ which indicates the presence of free carbonyl group. Following the formation of these species the band at 1721 cm^{-1} disappears from IR spectrum of complex compounds whereas two bands appear; ν_{COO^-}-symmetrical at 1390 cm^{-1} and ν_{COO^-}-asymmetrical at 1590 cm^{-1} assigned to the coordinated COO^- group (Fig. 1).

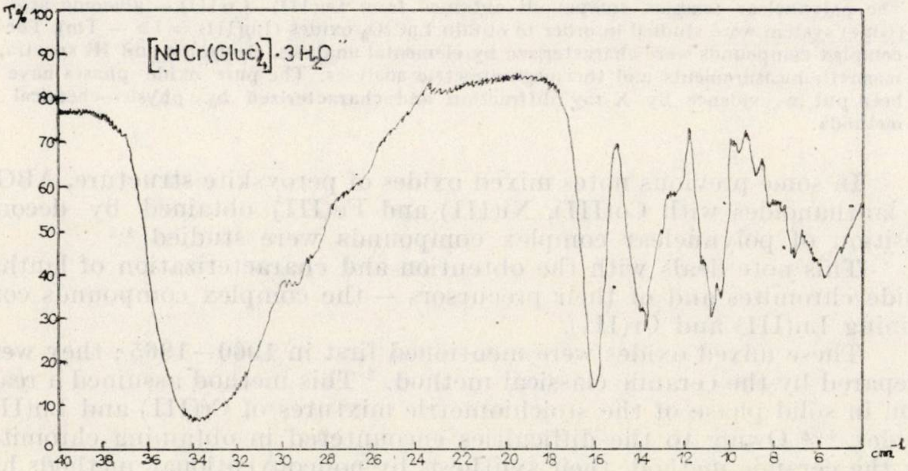

Fig. 1. — IR spectrum of $NdCr(Gluc)_4 \cdot 3H_2O$.

In the case of the polyhydroxycaboxylic ligands the coordination to the metallic ions is achieved most often by means of OH groups. The primary and secondary alcohool groups generate absorption bands associated to deformation of OH and C—O frequency lying within 1000—1400 cm^{-1}. Comparison of the spectrum recorded on complex compounds with that of natrium gluconate (in which the interaction between the metallic ion and alcohool groups is weakest) indicates a shift from 1090 cm^{-1} and 1060 cm^{-1} to lower values which, according to literature, correspond to the coordination of one or more secondary alcoholic groups.

The wide band at 3000—3600 cm^{-1} (maximum at 3400 cm^{-1}) in all IR spectra recorded is assigned to the formation of hydrogen bonds from water and/or alcohols.

The electronic spectra of mixed complex compounds were recorded in visible and were compared to electronic spectra of chromium gluconate, $Cr(gluc)_3 \cdot 6H_2O$.

The electronic spectra of mixed complex compounds containing Nd(III) and Er(III) were studied to establish to what extent the bands assigned to *f*—*f* transition in lanthanoide ions may be noted together with the *d*—*d* transitions of Cr(III) which are much wider and stronger.

To evidence the bands of lanthanoide ions, resolving of spectra was attempted by calculation and recording of the second order derivative of the spectrum. Thus, the bands characteristic to Cr(III) ion in an octahedral configuration and to Ln(III) ions were evidenced (Table 1).

Table 1

Electronic spectra of complex compounds

Complex compounds	Transition	Wavenumber (cm^{-1})
$NdCr(Gluc)_4 \cdot 3H_2O$	$^4A_{2g} \longrightarrow {}^4T_{1g}$	23.000
	$^4I_{9/2} \longrightarrow {}^4G_{9/2}$ (F)	20.960
	$^2G_{9/2}$	19.600
	$^4G_{7/2}$	19.040
	$*^4A_{2g} \longrightarrow {}^4T_{2g}$(P)	17.200
	$^4I_{9/2} \longrightarrow {}^4G_{5/2}$	17.240
	$^2H_{11/2}$	15.960
	$^4F_{9/2}$	14.400
	$*^4A_{2g} \longrightarrow {}^4T_{2g}$	13.600
	^2E_g	
	$^4I_{9/2} \longrightarrow {}^4F_{7/2}$	13.440
	$^4F_{5/2}$	12.480
	$^4F_{3/2}$	11.489
$ErCr(Gluc)_4 \cdot 3H_2O$	$^4I_{15/2} \longrightarrow {}^2G_{9/2}$	27.320
	$^4G_{11/2}$	26.360
	$^2H_{9/2}$	24.560
	$*^4A_{2g} \longrightarrow {}^4T_{1g}$ (F)	23.000
	$^4I_{15/2} \longrightarrow {}^4F_{5/2}$	22.120
	$^4F_{7/2}$	20.440
	$^2H_{11/2}$	19.120
	$^4S_{3/2}$	18.360
	$*^4A_{2g} \longrightarrow {}^4T_{2g}$ (P)	17.700
	$^4I_{15/2} \longrightarrow {}^4F_{9/2}$	15.240
	$*^4A_{2g} \longrightarrow \left\{ {}^4T_{2g} \right.$	13.800
	^2E_g	
	$^4I_{11/2} \longrightarrow {}^4I_{11/2}$	12.840
$Cr(Gluc)_3 \cdot 6H_2O$	$*^4A_{2g} \longrightarrow {}^4T_{1g}(F)$	23.000
	$\left\{ {}^4T_{2g} \right.$ (P)	17.886
	$^4T_{2g}$	14.126
	^2E_g	

* Bands characteristic to Cr(III) ion.

Determinations of magnetic susceptibility were carriep out on mixed complex compounds of Cr(III) and Nd(III) and on simple complex compounds of Cr(III) and Nd(III) (Table 2).

Table 2

Magnetic measurements of complex compounds

Complex compounds	$X_g \cdot 10^{-6}$ (cm^3/g)	μ(BM)
$Nd(Gluc)_2 \cdot 3H_2O$	7.517	3.80
$Cr(Gluc)_3 \cdot 6H_2O$	7.395	3.67
$NdCr(Gluc)_4 \cdot 3H_2O$	9.703	4.89

The aim of this contribution is the obtention of lanthanoide chromites and therefore the synthesized complex compounds were subjected to a thermogravimetric study intended to evidence the decomposition steps, their effects as a function of temperature and the optimum conditions for obtaining the oxidic phase.

The decomposition curves were recorded for Cr(III) gluconate, Nd(III) gluconate and mixed Cr(III) and Ln(III) complex gluconates (Ln(III)=La—Tm) and for mechanical mixture of chromium and neodimium gluconate of 1 : 1 ratio. Figure 2 shows the thermograms recorded for mixed complex compounds $NdCr(gluc)_4 \cdot 3H_2O$ and for the mechanicall mixture of the two simple complex compounds of 1 : 1 ratio. The overal loss is of 77% for mixed complex compounds which corresponds to a residue of 23% and a loss of 89.54% for the mechanical mixture which corresponds to a residue of 10.46%.

It is obvious that in a first step between 20—180° the complex compounds lose the three water molecules (5.51% calculated ; 5.25% experimental) while the mechanical mixture loses 8 water molecules (10.60% calculated ; 9.90% experimental).

The next steps between 110—700° correspond to the decomposition of anhydrous mixed complex compounds and to the evolution of resulted volatile products and formation of oxidic phases. The calculation of derivatograms has shown the step preceding the formation of $NdCrO_2(CO_3)$ and $Cr_2O_3 \cdot CO_2 + Nd_2O_3 \cdot CO_2$ for the complex gluconate of Nd(III) and Cr(III) and 1 : 1 mechanical mixture of gluconates respectively. The presence of this intermediate product of decomposition coincides with the results of the thermolysis of mixed oxalates of Ln(III) and Cr(III). [8]

The data in literature and our data on decomposition of complex gluconates of Fe(III) and Ln(III), [10] suggest the following schemes of decomposition of mixed complex compounds and the mechanical mixture

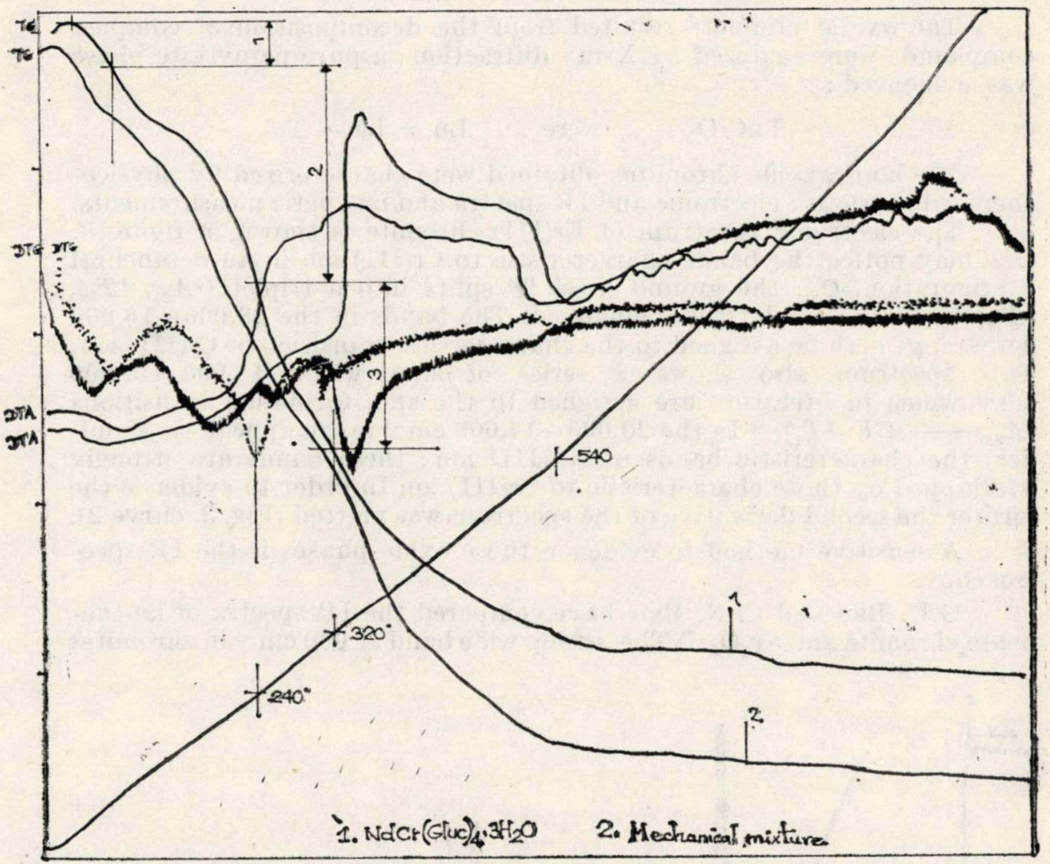

Fig. 2. — Thermal decomposition of :
1. $NdCr(Gluc)_4 \cdot 3H_2O$
2. physical mixture (1 : 1) gluconates.

of gluconates :

$$\text{I} \quad NdCr(Gluc)_4 \cdot 3H_2O \xrightarrow[25-110°]{\text{I}} NdCr(Gluc)_4 \xrightarrow[110-300°]{\text{II}} NdCr(CO_3)_3$$

$$\xrightarrow[300-540°]{\text{III}} NdCrO_2(CO_3) \xrightarrow[540-700°]{\text{IV}} NdCrO_3 + CO_2$$

$$\text{II} \quad Nd(Gluc)_3 \cdot 2H_2O + Cr(Gluc)_3 \cdot 6H_2O \xrightarrow[25-110°]{\text{I}} Nd(Gluc)_3 + Cr(Gluc)$$

$$\xrightarrow[110-540°]{\text{II}} Nd_2O_3 \cdot CO_2 + Cr_2O_3 \cdot CO_2 \xrightarrow[540-800°]{\text{III}} NdCrO_3 + 2CO_2$$

The oxidic products resulted from the decomposition of complex compounds were analyzed by X-ray diffraction ; a pure perovskite phase was evidenced :

$$LnCrO_3 \qquad \text{were} \qquad Ln = La - Tm$$

The lanthanoide chromites obtained were characterized by physicochemical methods : electronic and IR spectra and magnetic measurements.

The electronic spectrum of Er(III) chromite is shown in figure 3. One may notice the bands characteristic to Cr(III) ion in an octahedral configuration, O_h ; the ground level ^4F splits into a triplet ($^4A_{2g}$, $^4T_{2g}$, $^4T_{1g}$) while the level ^4P is unchanged. The bands in the 28,000–16,000 cm^{-1} range may be assigned to the characteristic transition of Cr(III)ion. This spectrum also shows a series of bands within 15,000–14,000 cm^{-1} which in literature are assigned to the spin forbidden transitions $^4A_{2g} \longrightarrow (^2E, {}^2T_1)$. [11] In the 20,000–14,000 cm^{-1} range appear (as shoulder) the characteristic bands of Nd(III) ion ; these bands are strongly overlapped by those characteristic to Cr(III) ion.In order to evidence the former the second derivative of the spectrum was plotted (Fig. 3, curve 2).

A sensitive method to evidence those oxide phases is the IR spectroscopy.

G.U. Rao and C. N. Rao have compared the IR spectra of lanthanoide chromite and Cr_2O_3. [11] The strong wide band at 600 cm^{-1} in chromites

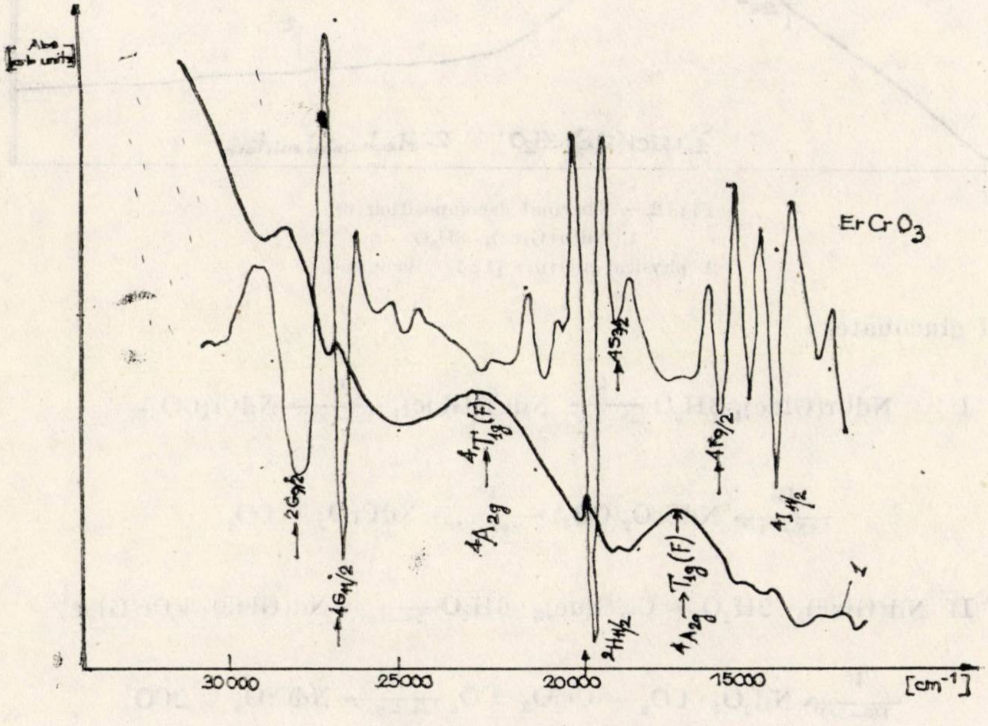

Fig. 3. – Electronic spectra of $ErCrO_3$.

was assigned to ν_{Cr-O} vibration (corresponding to the band at 640 cm^{-1} in Cr_2O_3). The fact that this band appears in chromites at lower wave numbers than in Cr_2O_3 may be assigned to the decrease of the degree of covalence of Cr—O bond in these oxides. Moreover, the authors noted a decrease of the wave number of these bands even in the series of lanthanoides (ν_{Cr-O} appears at 630 cm^{-1} in $LaCrO_3$ and at 580 cm^{-1} in $GdCrO_3$).

The spectra recorded with our orthochromites are similar to those obtained in the literature. The strong band at 600 cm^{-1} in these spectra was assigned to ν_{Cr-O}. Likewise one may note a small shift of this band from 600 cm^{-1} in $LaCrO_3$ to 580 cm^{-1} in $NdCrO_3$.

Ln(III) orthochromites represent a family of compounds which are paramagnetic at room temperature. The magnetic moments of some orthochromites, $LnCrO_3$ where Ln(III) = Pr, Er, Dy, containing Ln(III) with magnetic properties ($\mu_{Pr(III)} = 3.58$ MB ; $\mu_{Er(III)} = 9.59$ MB $\mu_{Dy(III)} = 10.63$ MB), where recorded. The values obtained (4.13 MB for $PrCrO_3$, 9.85 MB for $ErCrO_3$ and 10.85 MB for $DyCrO_3$) agree to those in the literature.[12]

REFERENCES

P. Spacu, S. Ploştinaru, L. Patron, A. Conţescu, D. Crişan and N. Stănică, *Rev. Roumaine Chim.*, **32**, 877 (1987).

[2] P. Spacu, S. Ploştinaru, L. Patron, A. Conţescu, D. Crişan and N. Stănică, *Rev. Roumaine Chim.*, **31**, 811 (1986).

[3] E. F. Bertaut and G. Buisson, *Bull. Soc. Chim. Fr.* (1965), 1132.

[4] C. D. Cerezova, *Dokl. Akad. Nauk. S.S.S.R.*, **254**, 1410 (1980).

[5] I. N. Pacuro, *Dokl. Akad. Nauk. S.S.S.R.*, **230**, 897 (1976).

[6] B. A. Dolgoplosk, *Dokl. Akad. Nauk. S.S.S.R.*, **216**, 807 (1974).

[7] P. Ganguly and K. K. Singh, *Rev. Chim. Min.*, **18**, 333 (1981).

[8] A. Ray and K. A. Nag, *J. Inorg. Nucl. Chem.*, **40**, 1501 (1978).

[9] G. A. Melson and W. F. Pickering, *Aust. J. Chem.*, **21**, 1205 (1968).

[10] P. Spacu, L. Patron, S. Ploştinaru, A. Conţescu, D. Crişan and N. Stănică, *Rev. Roumaine Chim.*, **34**, 323 (1989).

[11] G. S. Rao and C. N. R. Rao, *Appl. Spectroscop.*, **24**, 415 (1970).

[12] R. Aleonard and R. Pauthenet *C. R. Acad. Sci. Paris*, **262 B**, 799 (1966).

was assigned to [illegible] vibration (corresponding to the band at 640 cm⁻¹ in Cr_2O_3). The fact that this band appears in chromites at lower wave numbers than in Cr_2O_3 may be assigned to the decrease of the degree of covalence of Cr—O bond in these oxides. Moreover, the authors noted a decrease of the wave number of these bands even in the series of lanthanides ([illegible] appears at 630 cm⁻¹ in $LaCrO_3$ and at 580 cm⁻¹ in [illegible]CrO_3).

The spectra recorded with our orthochromites are similar to those obtained in the literature. The strong band at 600 cm⁻¹ in these spectra was assigned to ν_{Cr-O}. Likewise one may notice a small shift of this band from 600 cm⁻¹ in $LaCrO_3$ to 580 cm⁻¹ in $NdCrO_3$.

Ln(III) orthochromites represent a family of compounds which are paramagnetic at room temperature. The magnetic moments of some orthochromites, $LnCrO_3$ where Ln(III) = Pr, Nd, Dy, containing Ln(III) with magnetic properties [illegible] MB; [illegible] MB; [illegible] = 10.65 MB, were recorded. The values obtained ([illegible] MB for $PrCrO_3$, 5.83 MB for $NdCrO_3$ and 10.84 MB for $DyCrO_3$) agree to those in the literature.[12]

REFERENCES

[1] P. Spacu, S. Plostinaru, L. Patron, A. Contescu, D. Crisan and N. Stanica, Rev. Roumaine Chim., 32, [illegible] (1987).

[2] P. Spacu, S. Plostinaru, L. Patron, A. Contescu, D. Crisan and N. Stanica, Rev. Roumaine Chim., 31, [illegible] (1986).

[3] F. Bertaut and [illegible], Bull. Soc. Chim. Fr., (1964), 1142.

[4] [illegible], Dokl. Akad. Nauk SSSR, 204, 1410 (1972).

[5] [illegible], Dokl. Akad. Nauk SSSR, 228, 867 (1976).

[6] S. A. [illegible], Dokl. Akad. Nauk SSSR, 218, 867 (1974).

[7] P. [illegible] and R. S. Smith, Rev. Chim. Min., 10, 315 (1973).

[8] A. [illegible], J. Inorg. Nucl. Chem., 40, 1501 (1978).

[9] G. A. Nelson and W. L. Pickering, [illegible] Chem., 21, 1205 (1968).

[10] P. Spacu, L. Patron, S. Plostinaru, A. Contescu, D. Crisan and N. Stanica, Rev. Roumaine Chim., 34, 223 (1989).

[11] G. S. Rao and C. N. R. Rao, Appl. Spectrosc., 24, 436 (1970).

[12] R. Aleonard and R. Pauthenet, C. R. Acad. Sci. Paris, 262 B, 792 (1966).

Revue Roumaine de Chimie, 35, 5, 625–630 (1990)

DETERMINATION OF MANGANESE N,N'-ETHYLENE BIS (DITHIOCARBAMATE)(MANEB) BY A SPECTROPHOTOMETRIC METHOD AND ITS APPLICATIONS

NEELAM VERMA and A. L. J. RAO
Department of Chemistry, Punjabi University, Patiala—147002, India

Received October 12, 1987

A rapid, sensitive and simple spectrophotometric method for the determination of manganese N,N'-ethylenebis(dithiocarbamate) (maneb) in Dithane-45 and tomatoes has been developed. Maneb was transformed into a complex of N,N'-ethylenebis(dithiocarbamate) (EBDC) containing molybdenum. The complex was extracted into methyl isobutylketene (MIBK). The concentration of the complex in the solution was measured spectrophotometrically at 670 nm. Beer's law was obeyed in the concentration range 2–40 μg/ml. The recovery from fortified spiked tomato sample was 94 percent of maneb (added as a 0.01 percent alkaline solution). Maneb can be selectively determined in the presence of ziram, thiram and ferbam.

A program was undertaken to develop an analytical method for determining residue of maneb fungicide in tomatoes in view of increasing use of certain derivatives of dithiocarbamic acid as fungicides on vegetables. The use of certain derivatives of dithiocarbamic acid as fungicides is increasing because of the wide range of plant disease organism against which they are active and their low phytotoxicity. The most serious and persistent problem associated with the growing use of fungicides has been the microquantity of residues, which are left on food. This can create chronic damage to health as these items are consumed by men as a part of their normal dietary intake. Unless quantities of such fungicide residues are kept in close check, their persistent as well as cumulative action should be hazardous. So, precise and accurate analytical methods are useful for the determination of microquantities of fungicide residues remaining on crops after the application of these fungicidal agents. This paper represents briefly the spectrophotometric technique involved in a satisfactory analytical methods and the recovery and the efficiencies realised with this procedure and finally describes residue results obtained in maneb fungicide from tomatoes and purity of the commercially available Dithane N—45 (active ingredient maneb).

Most of the analytical methods in general use are based on the Clarke et al. method. [1] Dithiocarbamate fungicide residues, however, have been analysed [2–4] as the amount of carbon disulfide formed after adding hot mineral acid, spectrophotometrically. Hall[5] has reported on a collaborative study of the determination of maneb using modified versions of the methods of Clarke et al.[1] and Rosenthal et al.[3] The results obtained by both the methods were inconsistent. Maneb was determined also by a spectrophotometric method.[6] Maneb pesticide residues have been analysed by determining the released carbon disulfide spectrophotometrically.[7-9]

High performance liquid chromatography was used to determine dithiocarbamate fungicides in vegetable food stuffs.[10] Maneb was determined by titration with electrogenerated iodine.[11] However, all methods mentioned are time consuming. It was therefore of interest to develop a direct, simple, rapid and sensitive spectrophotometric method for the determination of maneb and use it for analysing maneb i.e. commercial Dithane M—45, and in tomatoes.

EXPERIMENTAL

Equipment : SP—20 spectronic spectrophotometer.

Reagents

Pure maneb was prepared by adding a solution of manganese salt to a solution of disodium ethylene-*b*is dithiocarbamate (Wilson laboratoires, Bombay). The precipitate was filtered off and dried over silica gel. The purity was checked by elemental analysis and by complexometric estimation of manganese after decomposition.[12] A 0.01 percent solution of maneb in 1.0 M sodium hydroxide was prepared[13] and added to tomato samples for recovery studies.[10] Sodium molybdate (2 percent w/v analytical reagent grade), sulfuric acid (analytical reagent grade), methyl isobutyl ketone (Merck analytical reagent grade), anhydrous calcium chloride (BDH analytical grade) were used. Alkali salts and metal salt solutions were prepared to study interferences. Ziram, thiram, zineb, ferbam and vapam (Wilson laboratories, Bombay) were used.

Procedure

To an aliquot containing 100 μg maneb in a beaker was added 1.0—1.5 ml of 2M H_2SO_4 and 2 mL of 2% sodium molybdate solution. The final volume was made to 5 mL with distilled water. The solution was boiled for 5 minutes, then cooled and again made to 5 mL with distilled water. The aqueous solution was transferred to a separatory funnel and the aqueous layer was shaken with 5 ml of methyl isobutyl ketone (MIBK) for one minute. Both phases were allowed to separate. The organic phase was transferred into a dry tube containing anhydrous calcium chloride. A portion of this dried solution was taken in a 1 cm cell and the absorbance was measured at 670 nm. A calibration curve was prepared under similar conditions.

RESULTS AND DISCUSSION

Absorption spectra : The absorption spectra of molybdenum ethylenebis-dithiocarbamate complex in MIBK against the reagent was recorded. The complex absorbed strongly at 670 nm where the reagent absorption was negligible at this wavelength.

Effect of H_2SO_4 : Extractions were carried out at different amounts of 2M H_2SO_4 keeping all other conditions constant. The absorption spectra in this concentration range studied were of similar nature indicating the formation of only one complex under these conditions. The absorption remained constant in concentration range of 1.0—1.5 ml of 2M H_2SO_4 (Table 1).

Optimizing the reaction conditions : 100 µg of maneb per 5 ml of the solution were examined. The amount of sodium molybdate solution was varied at constant H_2SO_4 (2M) concentration, and extractions were carried out by the general procedure. It was noted that the absorbance increased up to 2 ml of 2 % sodium molybdate solution (Table 2). The absorbance of the extract was constant when time of boiling was in the range 5 – 7 minutes. One minute shaking was sufficient and of all the solvents tried, the complex gave the maximum absorbance with MIBK (Table 3). The absorbance of the complex remained constant for 45 minutes and then started decreasing slightly.

Table 1

Effect of H_2SO_4 (2 percent) on extraction-of maneb. Maneb=100 µg, sodium molybdate = 2 ml

Amount of H_2SO_4(4N) taken for extraction (ml)	Absorbance at 670 nm
0.25	0.13
0,15	0.19
1.0	0.29
1.5	0.29
2.0	0.14

Table 2

Effect of sodium molybdate on the extraction of maneb. Maneb = 100 µg, 2M H_2SO_4 = 1.0 ml

Amount of sodium molybdate taken for extraction (ml)	Absorbance at 670 nm
0.5	0.18
1.0	0.23
1.5	0.26
2.0	0.29
2.5	0.29

Table 3

Effect of different solvents on the extraction of maneb under optimum conditions

Solvent taken for extraction	Absorbance at 670 nm
n-Butyl acetate	0.035
Amyl acetate	0.025
Diethyl ether	0.05
Butan-2-one	0.195
Ethyl acetate	0.20
Benzene	0.0
Chloroform	0.0
Carbon tetrachloride	0.0
Toluene	0.0
Hexane	0.0
Benzyl alcohol	0.0
Acetyl acetone	0.21
Isobutyl alcohol	0.215
Methyl isobutyl ketone	0.29

Beer's law and sensitivity : The absorbance with various concentrations of maneb was measured at 670 nm against a reagent blank under the optimum conditions described above. The absorbance varied linearly from 2−40 μg of maneb/ml of MIBK solution. Molar absorptivity and Sandell's sensitivity were calculated to be 3.84×10^3 mol^{-1} cm^{-1} and 0.069 μg/cm^2 respectively. Aliquots containing 100 μg of maneb gave a mean absorbance of 0.29 with a relative standard deviation of ±0.72%. Accuracy of the method was checked by preparing solutions containing different amounts of maneb and a fixed amount of H_2SO_4 (2M) and sodium molybdate solutions. The error was found within ±1%. The results are given in Table 4.

Table 4

Accuracy of the method

Sr No.	Amount of maneb present μg/5 ml	Maneb found μg/5 ml	% Error
1.	10	10.1	+1.0
2.	20	20.2	+1.0
3.	50	49.6	−0.8
4.	100	101.0	+1.0
5.	200	199.0	−0.5

Composition of the complex : The stoichiometry of the complex was studied by Job's menthod of continuous variation and the mole ratio method. 2 : 1 complex of molybdenum : maneb was found to be formed.

Effect of diverse ions : Among the anions examined, it was observed that 2 mg citrate, 3 mg bromide, 10 mg tartrate, 1 mg acetate, in 0.100 mg of maneb per 5 ml could be tolerated. Chloride, oxalate, nitrate, could be tolerated in lower amounts (0.180, 0.200, and 0.250 mg respectively in 0.100 μg of maneb per 5 ml of the solution respectively). Thio-sulphate, thiocyanate and EDTA interfered. Among common metal ions, 0.204 mg Pb(II), 0.108 mg Zn(II), 0.020 mg Bi(III), 0.241 mg Tl(I), 0.063 mg Cd(II) and 0.040 mg Mn(II) could be tolerated in 0.100 μg of maneb per 5 ml of solution.

Interference study of other pesticides :

Ziram, thiram and ferbam form a yellow coloured complex with sodium molybdate in presence of sulfuric acid in cold solution (absorption max. 420 nm), while maneb forms a blue coloured complex on boiling (with absorption at 670 nm). These compounds (thiram 5.0 mg, ziram 1.0 mg and ferbam 2.0 mg) did not interfere in the determination of 0.100 μg of maneb in 5 ml of the final solution. Being water soluble, nabam, and avapam could be removed by filtration. Zineb interfered in this method as it gives the same complex with sodium molybdate and solubility conditions are same as for maneb.

Applications : Maneb has its principal use as a vegetable fungicide. It appears to be slightly better than zineb for the late blight control in potatoes and is definitely to be preferred for the control of tomato anthracnose.[14]

Advantages of spectrophotometric method : Hall[5] has reported on a collaborative study of the determinations of dithiocarbamates, using modified versions of the methods of Clarke et a l.[1] and Rosenthal et al.[3] Results for maneb by both methods were inconsistent. The sensitivity of this method is better than that of the Lower,[15] Cullen[17] and Chmiel[8] methods. According to latter minimum 10 μg of CS_2 evolved can be determined, while according to others, a minímum of 20 μg CS_2 can be measured. But in present method, 10 μg of maneb (equivalent to 5.736 μg of CS_2) can be determined. Moreover, this method is direct, simple, selective and less time consuming.

Residual analysis of maneb in tomatoes :

The application of solvent stripping to maneb residues is complicated by their relative insolubility. Pyridine was successfully employed as a stripping agent, approximately 80% recovery was realised from pyridine solution.[15] Here acetonitrile is used as a solvent for extraction where 95% recovery is obtained. 20 g of tomatoes were finely crushed and were shaken with 100 ml acetonitrile for one hour. The mixture was filtered through filter paper and the residue in the funnel was washed with three 10 ml portions of acetonitrile. The extract was evaporated by a current of dry air at room temperature through the solution. The residue was dissolved in 5 ml of 1N NaOH solution. To 2 ml of this solution was added 1.5 ml of 4N H_2SO_4 and 2 ml of 2% sodium molybdate solution, and maneb was determined with the same general procedure.

The accuracy of the method was checked by recovery tests performed on an untreated sample and the results are presented in Table 5. Residual level of maneb pesticide tolerable in tomatoes is 0.5—4.0 ppm (16).

Table 5

Recovery of maneb from tomatoes

Tomatoes taken (gm)	Amount of maneb added (μg)	Amount of maneb found (μg)	Recovery (%)
20	10	9.0	90.0
20	20	18.0	90.0
20	40	37.0	92.50
20	60	56.0	93.30
20	80	75.0	93,75
20	200	189.0	94.5

Each reading is an everage of three experiments.

Determination of maneb in commercial sample :

Active ingradient maneb was determined from Dithane M—45 (Indofil chemicals) by the general procedure. The percent of maneb found was 72.84 by this method, whereas the actual value re ported was 73%

ACKNOWLEDGEMENTS. **The authors are grateful to Dr. P. K. Chattopadhyay, Reader in Forensic Science, Punjabi University, Patiala, for his suggestions. One of the authors (NV) is also thankful to Bureau of Police Research & Development, New Delhi for financial assistance.**

REFERENCES

[1] D. G. Clarke, H. Baum, E. L. Stanley and W. E. Hester, *Anal. Chem.*, **23**, 1842 (1951).

[2] R. Zaharadnik and P. Zuman, *Chem. Listy*, **52**, 231 (1958); *Coll. Czech. Chem. Comm.*, **24**, 11326 (1959).

[3] J. Rosenthal, R. L. Carlsen, and E. L. Stanley, *J. Assoc. Offic. Agr. Chemists*, **36**, 1170 (1963).

[4] W. K. Lowen, *J. Assoc. Offic. Agr. Chemists*, **36**, 484 (1953).

[5] C. H. Hall, *J. Assoc. Offic. Agr. Chemists*, **43**, 371 (1960).

[6] S. Petrescu. *Rev. Chim. (Bucharest)*, **17**, 687 (1966).

[7] Institute Superione di Sanita, *Boll. Chim. Unione Ital. Lab. Prov.*, Parte Sw, **6**, 619 (1980).

[8] Z. Chmiel, *Chem. Anal.*, **24**, 505 (1979).

[9] A. Thomas and J. E. Longbottom, *Govt. Rep. Announce*, Index (US), **82**, 1544 (1982).

[10] K. H. Gustafsson and C. H. Fahlgren, *J. Agric. Food. Chem.*, **31**, 461 (1983).

[11] D. Clyde, *D. J. Assoc. Off. Anal. Chem.*, **66**, 646 (1983).

[12] A. I. Vogel, "*A Textbook of Quantitative Inorganic Analysis*", 3rd ed., Longman, **434**, 1969)

[13] D. J. Hall, A. Townshend and P. Zuman, *Anal. Chim. Acta.*, **41**, 63 (1968).

[14] J. D. Wilson, *Ohio Agr. Expt. Sta. Res. Circ.*, 43 (1957).

[15] W. K. Lowen, *Anal. Chem.*, **23**, 1846 (1951).

[16] T. E. Cullen, *Analyt. Chem.*, **36**, 221 (1964).

Revue Roumaine de Chimie, **35**, *5*, 631–637 (1990)

CONTAMINACION POR IONES CLORURO EN PROCESOS ELECTRODICOS

A. ALBALAT, E. GÓMEZ, M. SARRET y E. VALLÉS
Departamento de Química física, Facultad de Química, Universidad de Barcelona, Martí i Franqués, 1, 08028 Barcelona, Spain

Recibido : el 18 de enero de 1988

Los procesos sobre electrodos de metales nobles (oro y platino) son especialmente sensibles a la presencia en la disolución de especies adsorbibles. Por ello se ha realizado un estudio voltamétrico sobre la influencia que pueden tener especies de reconocida fuerte adsorción como los haluros, especialmente los cloruros, cuando sus niveles de concentración pueden calificarse de contaminación.

A voltametric study was performed in order to discuss the influence of contamination of chloride ions on Au polycrystalline electrode. The possible sources of this contamination in usual experiments in electrochemistry kinetics were also analyzed. The method used consists of the study of the influence of controlled additions of chloride ions to the solution on the surface oxidation of gold electrode and on the oxidation of an organic compound on this electrode.

INTRODUCCIÓN

El estado superficial de un electrodo tiene una notable influencia sobre los procesos electródicos heterogéneos. [1,2] Es por ello que al utilizar las distintas técnicas electroquímicas, especialmente aquellas más sensibles, como pudieran ser voltametría o técnicas de medida de capacidad diferencial, es necesario definir cuidadosamente las condiciones de trabajo, evitando así resultados erróneos debidos a la presencia en la disolución de agentes contaminantes que adsorbidos sobre la superficie electródica modifiquen su estado superficial.

El objeto del presente trabajo es destacar la importancia de la posible contaminación causada por los iones haluro, en especial los cloruro, en un proceso redox sobre un electrodo policristalino de oro. El oro, aún no siendo de los electrodos más sensibles a la presencia de contaminación, como sería el caso del electrodo de platino, muestra significativas modificaciones en su comportamiento, ya, a bajas concentraciones de contaminante.

La contaminación de una disolución se da casi siempre por una deficiente manipulación en la preparación del montaje experimental. La contaminación por cloruros puede ser previsible como consecuencia, entre otras causas, de : a) la utilización como electrodos de referencia de ciertos electrodos que contienen disoluciones de cloruro, b) del empleo de algunas disoluciones de lavado, [3] y c) de una insuficiente calidad de los reactivos.

EXPERIMENTAL

Se ha utilizado un equipo formado por un potenciostato y un generador de señales Belport, utilizándose como registro X–Y un Philips modelo PM 8133.

Las disoluciones se han preparado con ácido sulfúrico y cloruro sódico Merck (ambos de calidad suprapur), las de ácido mesoxálico se preparan con ácido del 99 % de pureza (Aldrich), el agua utilizada proviene de un sistema Millipore-Milli Q[4], siendo desoxigenadas con nitrógeno de alta pureza.

El electrodo de trabajo es una esfera de oro policristalino del 99,998 % de pureza, obtenida por fusión de un hilo de 1 mm de diámetro y colocada en un soporte de teflon. La preparación superficial de este electrodo consiste en su calentamiento a la llama a elevada temperatura y su inmediata protección con agua Milli Q.[5] El contraelectrodo es una espiral de oro de la misma calidad.

El electrodo de referencia es un electrodo de mercurio/sulfato mercurioso (ESM), refiriéndose todos los potenciales a este electrodo. En algunas experiencias se ha utilizado un electrodo de calomelanos saturado de cloruro potásico.

Los voltamogramas se han registrado entre $-0{,}3$ y $1{,}0$ V a 50 mV/s en H_2SO_4 0,5 M, estando el margen de concentraciones para el cloruro entre $7 \cdot 10^{-7}$ M (cantidad que aporta el sulfúrico suprapur en las condiciones de trabajo) y 10^{-4} M aproximadamente. La concentración de las disoluciones de ácido mesoxálico et de $4 \cdot 10^{-3}$ M. Siendo la temperatura de trabajo de $18 \pm 0{,}2$ °C.

RESULTADOS

Para etablecer la influencia de la contaminación por iones cloruro se han escogido estudios voltamétricos de procesos electródicos conocidos, como son la propia oxidación de la superficie del electrodo de oro en medio sulfúrico 0,5 M y la oxidación sobre el oro de un compuesto orgánico, el ácido mesoxálico en el mismo medio.[6] Estudiándose estos procesos en presencia de cantidades controladas de cloruro, de orden de magnitud semejante al que podría ser consecuencia de una contaminación.

Los resultados obtenidos indican que el proceso de formación de óxidos de oro viene modificado por la presencia de cloruro a partir de una concentración del orden de $1 \cdot 10^{-6}$ M (Fig. 1), siendo la influencia de estos iones muy notable a concentraciones del orden de $1 \cdot 10^{-5}$ M de cloruro (Fig. 2). El primer pico de oxidación del oro es el más sensible, de forma que al aumentar la concentración de cloruro su intensidad disminuye, desplazándose la oxidación a potenciales más anódicos.

Por otra parte, se observa que incluso a concentraciones bajas de cloruro ($c < 2 \cdot 10^{-5}$ M), detenciones de potencial durante un tiempo controlado a potenciales correspondientes a proceso puramente capacitivo, provocan modificaciones notables del proceso de oxidación del oro (Fig. 3).

A estas bajas concentraciones de cloruro para las que su adsorción está controlada por difusión, se obtiene que al disminuir la velocidad de barrido del potencial, es mayor la deformación observada en el voltamograma correspondiente, es decir, al aumentar el tiempo en potenciales que favorecen la adsorción, la cantidad de cloruro adsorbido es lógicamente mayor. A concentraciones de cloruro superiores ($c > 2 \cdot 10^{-5}$ M) se detectan, además, nuevas reacciones, ampliamente descritas en la bibliografía que se interpretan como la formación de complejos clorurados de oro.[7,8]

Como la presencia de pequeñas cantidades de cloruro en disolución modifica ya la propia reacción de oxidación de la superficie del oro, cualquier proceso que tenga lugar sobre ella vendrá también modificado. Por

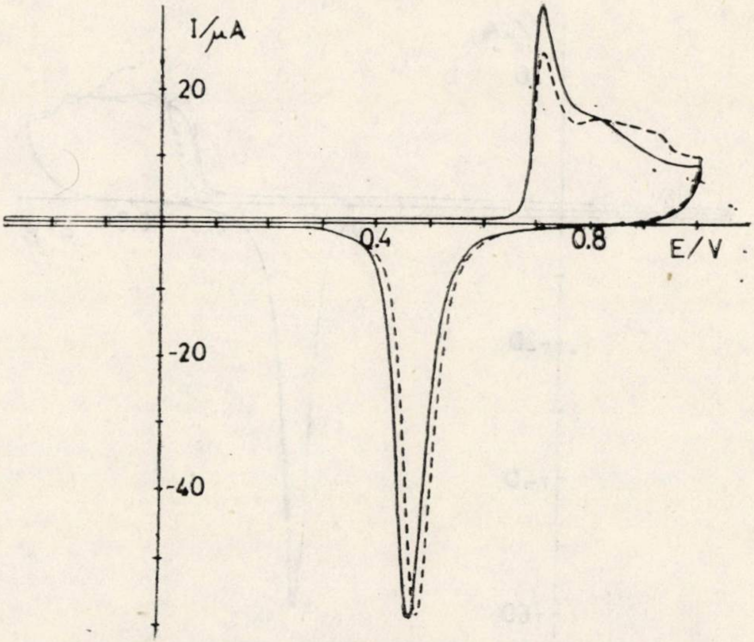

Fig. 1. — H_2SO_4 0,5 M. Voltamogramas para una concentración de Cl^- igual a la aportada por el H_2SO_4 Merck suprapur (———) y $4 \cdot 10^{-6}$ M (— — —). Área del electrodo 0,24 cm².

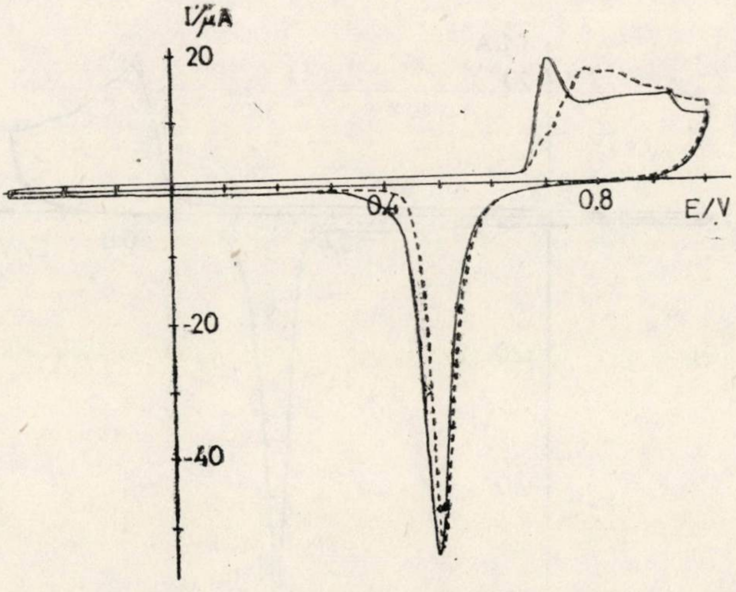

Fig. 2. — H_2SO_4 0,5 M + NaCl 10^{-5} M. Voltamogramas con (— — —) y sin (———) burbujeo de nitrógeno. Area del electrodo 0,24 cm².

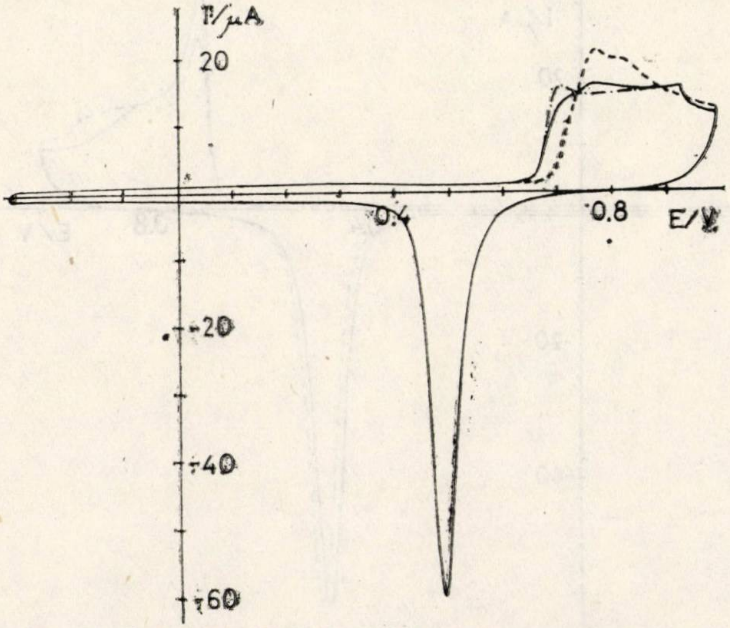

Fig. 3. – H_2SO_4 0,5 M + NaCl $2 \cdot 10^{-5}$ M. Voltamogramas registrados: (———) en barrido continuo: (— — —) parando 15" en 0,207 V y (—. —.—) parando 15" en –0,300 V. Area del electrodo 0,24 cm².

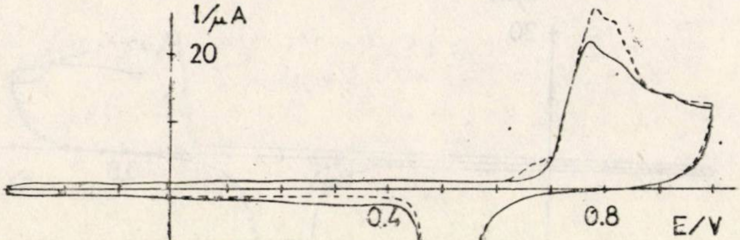

Fig. 4. – H_2SO_4 0,5 M + NaCl $4 \cdot 10^{-5}$ M. Voltamogramas con (– – –) y sin (———) burbujeo de nitrógeno. Area del electrodo 0,24 cm².

ello se ha estudiado la influencia que ejercen los iones cloruro sobre un proceso superficial, previamente estudiado,[6] como es la oxidación del ácido mesoxálico en medio ácido.

Se han estudiado disoluciones de ácido mesoxálico que contenían iones cloruro ($1 \cdot 10^{-6} \leqslant c \leqslant 1{,}6 \cdot 10^{-5}$ M).

Comparando los distintos voltamogramas obtenidos en estas condiciones se observa que el aumento de la concentración de cloruros en disolución se traduce en una deformación respecto al voltamograma original en ausencia de contaminación, que implica una disminución progresiva del pico de oxidación del ácido mesoxálico y un desplazamiento de su potencial de pico y en general del proceso hacia potenciales más anódicos (Fig. 5).

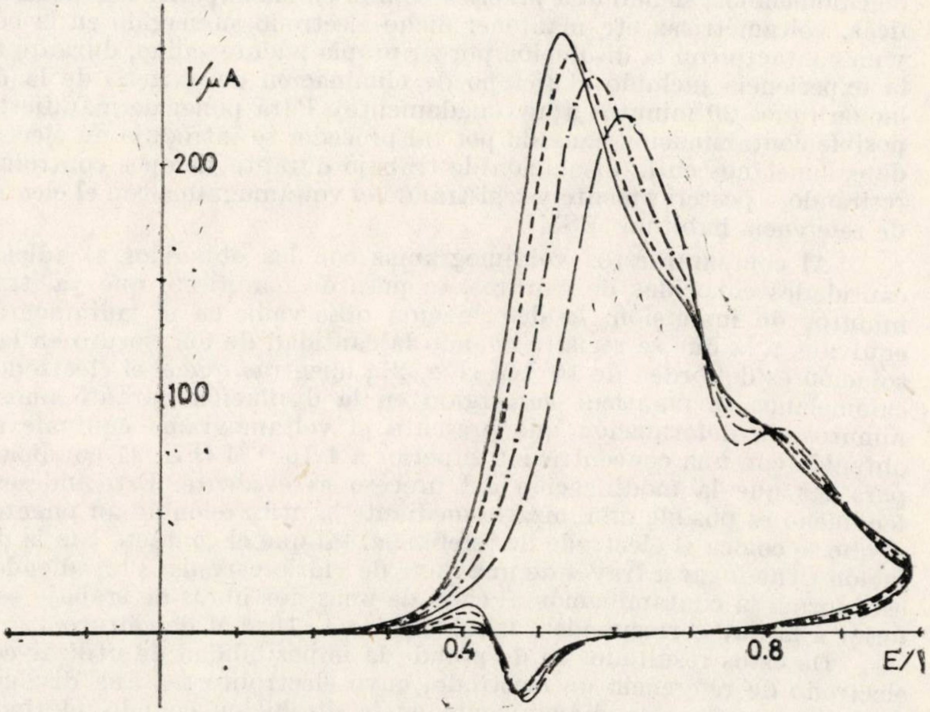

Fig. 5. — H_2SO_4 0,5 M + ácido mesoxálico $4 \cdot 10^{-3}$ M. Voltamogramas para diferente concentración de NaCl añadido: (———) 0; (— — —) $1{,}04 \cdot 10^{-6}$ M; (—. —. —.) $5.34 \cdot 10^{-6}$ M y (— —) $1{,}19 \cdot 10^{-5}$ M. Area del electrodo 0,19 cm^2.

El valor de la pendiente de Tafel del proceso, necesaria siempre que se pretenda establecer un posible mecanismo, pasa de su valor 60 mV/década[6] a valores más altos según va aumentando la concentración de cloruros. En la determinación de este valor y en el del resto de los parámetros cinéticos la presencia de contaminación puede conducir a un falseamiento de los resultados, debido a que estas magnitudes se determinan en estado estacionario, es decir, a velocidades de barrido muy bajas, de forma que la adsorción del cloruro y del contaminante en general es muy elevada.

DISCUSIÓN

Como se hace patente por los resultados experimentales obtenidos, es notable la influencia que la contaminación de la disolución por iones cloruro puede tener en estudios voltamétricos, ya que como se ha visto, a concentraciones muy pequeñas, inferiores en ocasiones a las suministradas por el propio reactivo, se tienen modificaciones notables del proceso.

En base a los resultados obtenidos analizaremos como puede influir la manipulación o utilización incorrecta y, por otra parte en muchos casos habitual, de técnicas o instrumentación no adecuada cuando se utilizan ciertas técnicas electroquímicas.

Uno de los electrodos de referencia más utilizados es el electrodo de calomelanos, siendo una práctica común en las experiencias polarográficas, voltamétricas, etc. mantener dicho electrodo sumergido en la célula y en contacto con la disolución por su propio puente salino, durante toda la experiencia incluido el tiempo de eliminación de oxígeno de la disolución (unos 20 minutos aproximadamente). Para poner de manifiesto la posible contaminación causada por tal proceder se introdujo un electrodo de calomelanos en la disolución de trabajo durante tiempos controlados, retirándose posteriormente y registrando el voltamograma con el electrodo de referencia habitual (ESM).

Al comparar estos voltamogramas con los obtenidos al adicionar cantidades conocidas de cloruros, se puso de manifiesto que ya, tras 5 minutos de inmersión, la deformación observada en el voltamograma equivale, a la que se registra cuando la cantidad de ión cloruro en la disolución es del orden de 10^{-5} M (Fig. 2); mientras que si el electrodo de calomelanos se mantiene sumergido en la disolución durante unos 30 minutos, la deformación que presenta el voltamograma equivale a la obtenida con una concentración superior a $4 \cdot 10^{-5}$ M (Fig. 4), condiciones para las que la modificación del proceso es evidente. Este indeseable fenómeno es posible minimizarlo mediante la utilización de un puente en el que se coloca el electrodo de referencia, tal que el contacto con la disolución tiene lugar a través de una llave de vidrio cerrada. Procediendo de esta forma la contaminación al cabo de unas dos horas de trabajo es inferior a la que corresponde a la adición de $4 \cdot 10^{-6}$ M de cloruro.

De estos resultados se desprende la imposibilidad de utilizar como electrodo de referencia un electrodo, cuyo electrolito sea una disolución de haluro, sumergido directamente en la disolución cuando el tipo de proceso que pretendemos estudiar es un previsible proceso superficial en especial si el electrodo utilizado es un metal noble. Sin embargo, la utilización de un puente de la características indicadas amplía notablemente las posibilidades de empleo de tales electrodos, puesto que en este tipo de trabajos el período de utilización de las disoluciones de trabajo es reducido.

Por otra parte, cuando la propia estructura del electrodo de oro utilizado hace imposible el tratamiento habitual de preparación superficial por fusión controlada, el tratamiento de limpieza alternativo de que se dispone requiere el uso del agua regia,[3] siendo estos casos más frecuentes en el caso de utilizar electrodos de disco rotatorio o disco-anillo. La eliminación de los residuos que pudiera dejar el agua regia, exige, no el lavado con agua Millipore, sino mantener al electrodo inmerso en un gran volumen de agua durante unas horas, o un tratamiento de lavado con vapor de agua.

Es por todo ello necesario extremar el cuidado tanto en la preparación de las disoluciones como en la manipulación de los electrodos, por lo que es recomendable antes de comenzar cualquier trabajo de tipo electroquímico comprobar el estado del sistema, lo cual fácilmente puede hacerse registrando el voltamograma correspondiente al blanco del electrodo en el medio de trabajo.

BIBLIOGRAFÍA

[1] A. C. Chialvo, W. E. Triaca, y A. J. Arvia, *J. Electroanal. Chem.*, **171**, 303 (1984).
[2] S. Motoo y N. Furoya, *J. Electroanal. Chem.*, **172**, 339 (1984).
[3] G. J. Brug, M. Sluyters-Rehbach, J. H. Sluyters y A. Hamelin, *J. Electroanal. Chem.*, **181**, 245 (1984).
[4] L. E. Lyons, G. C. Morris, D. H. Horton y J. G. Keyes, *J. Electroanal. Chem.*, **168**, 101, (1984).
[5] J. Clavilier, R. Faure, G. Guinet y R. Durand, *J. Electroanal. Chem.*, **107**, 205 (1980 // J. Clavilier y R. Parsons, 31st. ISE Meeting V I p. 280 (1980).
[6] J. M. Feliu, J. Claret, C. Muller, J. L. Vazquez y A. Aldaz, *J. Electroanal. Chem.*, **178**, 271 (1984).
[7] J. N. Gaur y G. M. Schmid, *J. Electroanal. Chem.*, **24**, 279 (1970).
[8] S. H. Cadle y S. Bruckenstein, *J. Electroanal. Chem.*, **48**, 325, (1973).

Revue Roumaine de Chimie, **35**, *5*, 639–648 (1990)

COMPLEJOS DEL ÁCIDO 3,5-XILILAMINO-NN-DIACÉTICO CON DIFERENTES IONES METÁLICOS

J. SUAREZ-VARELA *, J. C. AVILA ROSÓN **, L. GARCÍA REJÓN ***
y T. GUARDIA CARRILLO **

* Departamento de Química Inorgánica. Facultad de Ciencias. Universidad de Granada
** Departamento de Química Analítica. Facultad de Ciencias. Universidad de Granada
*** Departamento de Biología Animal. Facultad de Ciencias. Universidad de Granada

Recibido : el 17 de julio de 1988

Se ha obtenido el ácido 3,5-xililamino-NN-diacético así como los complejos sólidos que este ácido forma con los iones Cr(III), Mn(II), Fe(II), Ni(II), Zn(II) y Cd(II). Mediante el empleo de las técnicas termoanalíticas TG, DTG y CDB, se han estudiado los compuestos anteriormente citados, habiéndose aplicado asimismo la espectroscopía IR y la susceptibilidad magnética para establecer las estructuras moleculares de los diferentes complejos obtenidos.

3,5-Xylylamine-N-N-diacetic acid and its solid complexes with the metal ions Cr(III), Mn(II), Fe(II), Ni(II), Zn(II) and Cd(II) were obtained. The formed compounds have been studied by the TG, DTG and CDS techniques; likewise, for establishing the molecular structures of the isolated complexes, IR and magnetic measurements were used.

INTRODUCCIÓN

Los ácidos aminodiacéticos $R-N(CH_2-COOH)_2$ son excelentes agentes complejantes frente a cationes di y trivalentes, pudiendo considerarse como derivados de la glicina. La importancia de su estudio radica en sus posibles aplicaciones biológicas.

Estos ácidos son débiles, presentándose generalmente en forma de "Zwitterión", lo que da lugar a considerables diferencias entre sus dos constantes de disociación. Actúan como ligandos bidentados, tridentados o pentadentados, [1-15] ya que pueden enlazarse a los iones metálicos a través de los dos grupos carboxílicos presentes en su estructura o bien, a través de esos grupos y del nitrógeno amínico.

El propósito de este trabajo es comparar y discutir las propiedades térmicas determinadas por termogravimetría, termogravimetría diferencial y calorimetría diferencial de barrido, así como los datos aportados por la espectroscopía IR y la susceptibilidad magnética de los 3,5-xililaminodiacetatos de Cr(III), Mn(II), Fe(II), Ni(II), Zn(II) y Cd(II).

Teniendo en cuenta la totalidad de los resultados obtenidos se han sugerido posibles estructuras para estos complejos.

EXPERIMENTAL

El ácido 3,5-xililamino-NN-diacético ($3,5H_2$ —XADA), fué sintetizado siguiendo un método descrito previamente.[16] La obtención de los diferentes complejos aislados se realizó

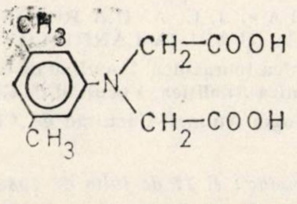

en la forma que se describe seguidamente. Se suspendieron 4,2 mmoles de $3,5H_2$-XADA en 20 ml de agua destilada y se añadieron gota a gota, agitando, una disolución de NaOH 2M hasta la total disolución del ácido. A continuación se procedió a añadir lentamente $4,2 \times 10^{-3}$ átomos-gramo del correspondiente ión metálico disueltos en 25 ml de agua destilada, produciéndose en todos los casos la precipitación instantánea de los complejos. Los sólidos así obtenidos se recogieron por filtración y se lavaron varias veces con agua fría, secándose posteriormente a vacio (sobre H_2SO_4) a temperatura ambiente.

El análisis elemental de estos compuestos se ha realizado en el laboratorio de microanálisis del Departamento de Química Bioorgánica (C.S.I.C.) de Barcelona. Los datos obtenidos se han recogido en la Tabla 1.

Tabla 1

Análisis elemental de las fases sólidas aisladas

	C(%)		H(%)		N(%)		Metal(%)		
COMPUESTO	Calc.	Enc.	Calc.	Enc.	Calc.	Enc.	Calc.	Enc.	COMPOSICION
Cr(3,5H—XADA) (3,5—XADA)·$3H_2O$	49'91	50'49	5'76	6'15	4'85	4'90	9'00	7'63	$CrC_{24}H_{33}N_2O_{11}$
Mn(3,5—XADA)· ·H_2O	46'77	46'23	4'91	5'02	4'54	4'47	17'82	16'94	$MnC_{12}H_{15}NO_5$
Fe(3,5-XADA)	49'52	48'52	4'50	4'80	4'81	4'99	19'19	18'03	$FeC_{12}H_{13}NO_4$
Ni(3,5-XADA)· ·$2H_2O$	43'68	42'53	5'19	5'28	4'24	4'09	17'79	16'68	$NiC_{12}H_{17}NO_6$
Zn(3,5-XADA)·H_2O	45'24	44'79	4'75	4'83	4'40	4'40	20'52	20'55	$ZnC_{12}H_{15}NO_5$
Cd(3,5-XADA)·H_2O	39'41	38'97	4'14	4'22	3'83	3'84	30'74	30'69	$CdC_{12}H_{15}NO_5$

Los espectros I.R. en la región 4.000—180 cm^{-1} se han realizado en un equipo Perkin-Elmer mod. 983G, utilizando KBr y polietileno como agentes dispersantes.

Los estudios térmicos del ácido $3,5H_2$-XADA y de sus complejos se realizaron en un equipo Mittler TA 3000, provisto de termobalanza Mettier TG—50 y calorímetro diferencial de barrido Mettler DSC—20. Para el registro de los diagramas termogravimétricos se operó con un flujo de aire de 100 ml. min^{-1}; velocidad de calentamiento de 5 °C · min^{-1} y pesos de muestra que oscilaban entre 4,72 y 17,10 mg. En la realización de la calorimetría diferencial de barrido se empleó atmósfera estática de aire y pesos de muestra comprendidos entre 0,55 y 1,51 mg; en este caso, la velocidad de calentamiento fué asimismo de 5 °C . min^{-1}.

Los difractogramas de los resíduos resultantes de los procesos pirolíticos de los complejos, se han realizado en un difractómetro Philips mod. PW 1710, provisto de un goniómetro Philips mod. PW 1050/81, estudiándose et intervalo comprendido entre 2 y 82°.

Las medidas magnéticas se han realizado empleando una magnetobalanza Bruker mod. B—M4, mediante el uso del método de Faraday.

RESULTADOS Y DISCUSIÓN

Los datos de análisis químico recogidos en la Tabla I indican una estequiometría metal/ligando igual a 1/1, excepto para el complejo de Cr(III), cuya estequiometría resulta 1/2.

Para estudiar la posible complejación de derivados de ácidos carboxílicos, es preciso designar correctamente las frecuencias $\nu_{as}(COO^-)$ y $\nu_s(COO^-)$, ya que está perfectamente establecido que el valor $\Delta = \nu_{as}(COO) - \nu_s(COO)$ es determinante del tipo de coordinación, o bien de las características iónicas de los compuestos. [17-21] Así, cuando Δ es mayor de 200 cm^{-1}, los compuestos en cuestión son complejos en los que cada anión carboxilato actúa como ligando monodentado. Valores de Δ comprendidos entre 171 y 164 cm^{-1} son los encontrados para acetatos alcalinos, siendo asimismo valores de Δ próximos a estos últimos los que se encuentran cuando los grupos carboxilato actúan en forma bidentada o en forma combinada, bidentada y puente.

En la Tabla 2 se han recogido algunas de las bandas más significativas de los espectros IR de los complejos aislados. De los valores de Δ hallados se puede sugerir que cada grupo carboxilato del $3,5H_2-XADA$ actúa como ligando monodentado en el complejo $Cr(3,5H-XADA)(3,5-XADA)\cdot 3H_2O$; mientras que en los complejos; $Mn(3,5-XADA)\cdot H_2O$, $Fe(3,5-XADA)$, $Ni(3,5-XADA)\cdot 2H_2O$, $Zn(3,5-XADA)\cdot H_2O$ y $Cd(3,5-XADA)\cdot H_2O$, cada ión carboxilato actúa como ligando bidentado, sin que se pueda descartar la posibilidad de formación de unión carboxilato puente. En estos complejos se observa además una disminución en la frecuencia de la banda correspondiente a ν (C—N), respecto a la posición de dicha banda en el espectro IR del ácido libre, que permite postular la existencia de un enlace N → M en todos los casos. En los espectros IR obtenidos empleando polietileno como medio de dispersión de las muestras, puede establecerse la presencia de agua de coordinación (Tabla 2).

En la Tabla 3 se han indicado los valores encontrados para los momentos magnéticos de los iones metálicos en estos compuestos. Tales valores sugieren, para el caso del complejo de Cr(III) la existencia de un enlace corto Cr—Cr. [22] Los valores de los momentos magnéticos para los demás iones corresponden a situaciones de elto espin. [22-24]

Tabla 2

Datos I.R. de los complejos aislados a partir del ácido 3,5-xililamino-NN-diacético

COMPUESTO	$\nu(OH)$	$\nu_{us}(COO^-)$	$\nu_s(COO^-)$	$\nu(C-N)$ alif.	$\nu(M-N)$	$\nu(M-OH_2)co$	$\nu(M-O)$	$\nu_{as}(COO^-) - \nu_s(COO^-)$
$3,5H_2-XADA$	3573	1600	1383	1189	—	—	—	—
$Cr(3,5H-XADA).(3,5-XADA) \cdot 3H_2O$	3000–3400	1601	1384	1196	498	—	307	217
$Mn(3,5\text{-}XADA) \cdot H_2O$	3503	1584	1422	1171	489	449	297	162
$Fe(3,5\text{-}XADA)$	3450	1589	1416	1177	490	—	287	173
$Ni(3,5\text{-}XADA) \cdot 2H_2O$	3000–3600	1592	1407	1178	565	—	339	185
$Zn(3,5\text{-}XADA) \cdot H_2O$	3520	1589	1416	1176	494	413	335	173
$Cd(3,5\text{-}XADA) \cdot H_2O$	3500	1585	1407	1176	560	490	303	178

Tabla 3

Valores de susceptibilidad y momentos magnéticos de los fases sólidas asiladas a 25 °C

COMPUESTO	$\chi \cdot 10^6$u.c.g.s.g^{-1}	$\chi_M 10^6$u.c.g.s.mol^{-1}	$\chi'_M 10^6$u.c.g.s.mol^{-1}	μ_{ef}
Cr(3,5H-XADA) (3,5-XADA) · · $3H_2O$	0′6895	398′183	718′183	1′31
Mn(3,5-XADA) · H_2O	44′7793	13.800′615	13.692′615	5′79
Fe(3,5-XADA)	36′953	10.756′540	10.906′540	5′12
Ni(3,5-XADA) · $2H_2O$	11′1256	3.671′053	3.844′053	3′04

Los diagramas térmicos del ácido $3,5H_2-$XADA vienen representados en la Gráfica 1 y los de los complejos de los iones Cr(III), Mn(II), Fe(II), Ni(II), Zn(II) y Cd(II) se dan en las Gráficas 2 y 3.

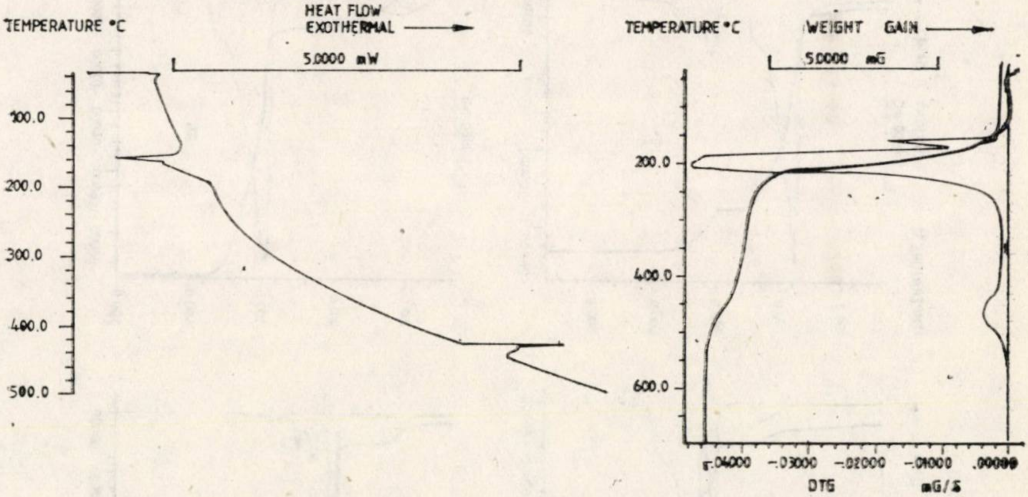

Gráfica 1. — Diagrama TG y CDB del ácido 3,5-xililamino-NN-diacético.

La curva TG del $3,5H_2-$XADA muestra que este ácido es estable térmicamente hasta los 120 °C, temperatura a la que comienza su descomposición pirolítica, terminando ésta alrededor de los 560 °C con la total eliminación de la muestra.

El diagrama de calorimetría diferencial de barrido del ácido $3,5H_2-$ —XADA muestra un efecto endotérmico centrado a 158 °C que corresponde al punto de fusión del compuesto. El valor de la entalpia de fusión calculada a partir del área de este efecto es de 41′4 KJ · mol^{-1}, descomponiéndose rápidamente el $3,5H_2$ fundido.

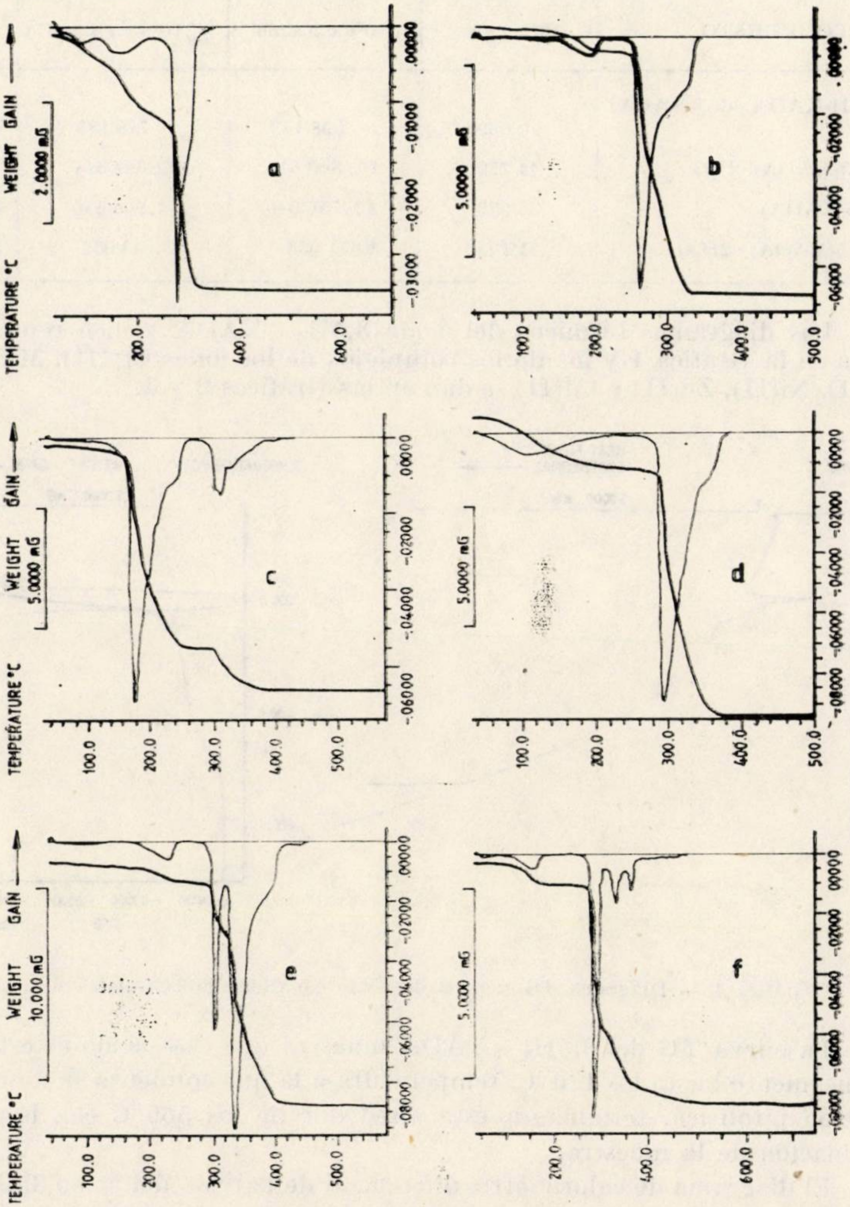

Gráfica 2. — Diagramas TG y DTG de los 3,5-xililamino-NN-diacetatos de ; Cr(III) [(a)] ; Mn(II)[(b)] ; Fe(II[(c)]) ; Ni(II) [(d)] ; Zn(II)[(e)] y Cd(II)[(f)].

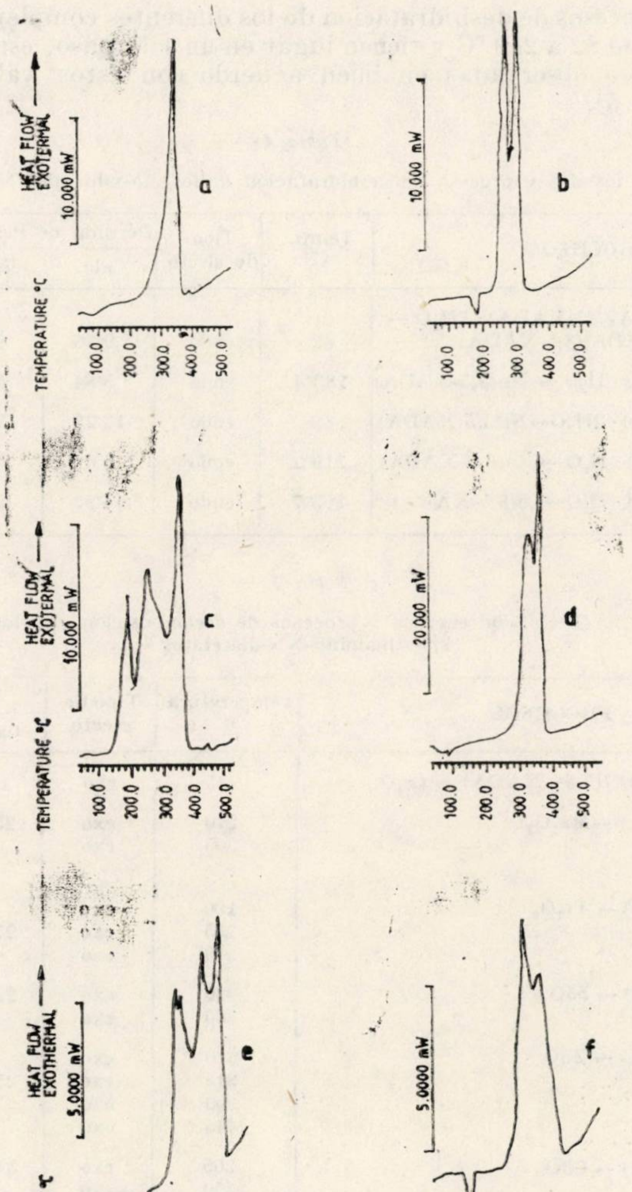

Gráfica 3. — Diagramas CDB de los 3,5-xililamino-NN-diacetatos de ; Cr(III)$^{(a)}$; Mn(II)$^{(b)}$; Fe(II)$^{(c)}$; Ni(II)$^{(d)}$; Zn(II)$^{(e)}$ y Cd(II)$^{(f)}$.

Los procesos de deshidratación de los diferentes complejos transcurre en el rango de 82 a 219 °C y tienen lugar en un solo paso, estando las pérdidas de peso observadas en buen acuerdo con estos valores teóricos (Tablas 4 y 5).

Tabla 4

Estabilidad térmica y proceso de deshidratación de los 3,5-xililamino-NN-diacetatos

PROCESOS	Temp. °C	Tipo de efecto	Pérdida de Peso (%)		Entalpia KJ/mol H_2O
			Calc.	Enc.	
$Cr(3,5H\text{-}XADA)(3,5\text{-}XADA) \cdot 3H_2O \rightarrow$ $\rightarrow Cr(3,5H\text{-}XADA)(3,5\text{-}XADA)$	82	endo	9'36	9'16	—
$Mn(3,5\text{-}XADA) \cdot H_2O \rightarrow Mn(3,5\text{-}XADA)$	183'4	endo	5'84	5'95	63'9
$Ni(3,5\text{-}XADA) \cdot 2H_2O \rightarrow Ni(3,5\text{-}XADA)$	88	endo	13'29	13'24	—
$Zn(3,5\text{-}XADA) \cdot H_2O \rightarrow Zn(3,5\text{-}XADA)$	219'2	endo	5'6 5	5'74	51'5
$Cd(3,5\text{-}XADA) \cdot H_2O \rightarrow Cd(3,5\text{-}XADA)$	153'7	endo	4'93	5'17	65'8

Tabla 5

Estabilidad térmica y procesos de decomposición de los 3,5-xililamino-NN-diacetatos

PROCESOS	Temperatura °C	Tipo de efecto	Resíduo (%)	
			Calc.	Enc.
$Cr(3,5H-XADA)(3,5-XADA) \rightarrow Cr_2O_3$	345	exo	13'16	11'15
$Mn(3,5\text{-}XADA) \rightarrow Mn_2O_3$	270	exo	25,23	24,34
	305	exo		
$Fe(3,5\text{-}XADA) \rightarrow Fe_2O_3$	190	exo		
	255	exo	27'43	25'78
	360	exo		
$Ni(3,5\text{-}XADA) \rightarrow NiO$	330	exo	22'64	21'22
	360	exo		
$Zn(3,5\text{-}XADA) \rightarrow ZnO$	310	exo		
	315	exo	25'38	25'58
	390	exo		
	445	exo		
$Cd(3,5\text{-}XADA) \rightarrow CdO$	305	exo	35'12	35'06
	350	exo		

El esperado comportamiento endotérmico de los procesos de deshidratación de estos complejos se ha observado en las respectivas curvas de calorimetría diferencial de barrido. Las entalpias de deshidratación calculadas se dan también en la Tabla 4, sugiriendo dichos valores la posibilidad de que exista coordinación entre una molécula de agua y el metal correspondiente en los complejos de Mn(II), Zn(II) y Cd(II). Los complejos de Cr(III) y Ni(II) parecen no poseer agua de coordinación debido a los bajos valores de sus temperaturas y entalpias de deshidratación.

Los compuestos anhidros suelen ser estables en un corto intervalo de temperatura y muestran una fuerte degradación pirolítica en una, dos o tres etapas que finalizan a temperaturas inferiores a 500 °C. En las curvas de calorimetría diferencial de barrido se aprecia que estos procesos de descomposición son los responsables de los efectos exotérmicos que aparecen indicados en la Tabla 5. La naturaleza de los resíduos de la descomposición pirolítica de los 3,5-xililaminodiacetatos se ha establecido a través de sus correspondientes diagramas de difracción de R–X,[25] Tabla 6.

Tabla 6

Datos de difracción para los resíduos pirolíticos a 650°C

Resíduo Cr(3,5H-XADA) (3,5-XADA) · $3H_2O$	Cr_2O_3 Eskolaita		Resíduo Mn(3,5-XADA) · H_2O	γ-Mn_2O_3		Resíduo Fe(3,5-XADA)	α-Fe_2O_3 Hematíes	
d_{obs}	hkl	$d_{estd.}$	d_{obs}	hkl	$d_{estd.}$	d_{obs}	hkl	$d_{estd.}$
3′625	012	3′633	4′910	101	4′92	4′649	111	4′669
2′648	100	2′666	3′092	112	3′08	2′872	220	2′860
2′470	110	2′480	2′867	020	2′88	2′440	311	2′438
2′158	113	2′176	2′757	103	2′76	2′017	400	2′021
1′826	024	1′8156	2′481	211	2′49	1′558	511	1′556
1′664	116	1′672	2′368	004	2′36	1′427	440	1′429
1′455	214	1′465	1′563	321	1′57			
1′429	300	1′4314	1′536	224	1′54			
1′297	1010	1′2961	1′445	314	1′44			
				040				

Tabla 6 (Continuación)

Resíduo Ni(3,5-XADA) · $\cdot 2H_2O$	NiO Bunsenita		Resíduo Zn(3,5-XADA) · H_2O	ZnO Zincita		Resíduo Cd(3,5-XADA) · H_2O	CdO	
d_{obs}	hkl	$d_{estd.}$	$d_{obs.}$	hkl	$d_{estd.}$	d_{obs}	hkl	$d_{estd.}$
2′427	111	2′410	2′822	100	2′816	2′727	111	2′712
2′099	200	2′088	2′612	002	2′602	2′356	200	2′349
1′478	220	1′476	2′484	101	2′476	1′655	220	1′661
1′263	311	1′259	1′915	102	1′912	1′419	311	1′416
1′204	222	1′206	1′630	110	1′626	1′356	222	1′355
			1′481	103	1′477	1′173	400	1′174
			1′406	200	1′407			
			1′381	112	1′379			
			1′360	201	1′359			

Del conjunto de información obtenida se pueden extraer las siguientes consideraciones estructurales:

a) El complejo $Cr(3{,}5H-XADA)(3{,}5-XADA)\cdot 3H_2O$ parece tener una coordinación octaédrica, actuando cada uno de los ligandos como trientado, utilizando un átomo de oxígeno de cada grupo carboxilato y el átomo de nitrógeno.

b) En los complejos $Fe(3{,}5-XADA)$ y $Ni(3{,}5-XADA)\cdot 2H_2O$, cada ligando puede actuar como pentadentado empleando los dos átomos de oxígeno de cada grupo carboxilato y el átomo de nitrógeno por lo que la estructura podría ser de pirámide de base cuadrada.

c) En el caso de los complejos $Mn(3{,}5-XADA)\cdot H_2O$, $Zn(3{,}5-XADA)$. H_2O y $Cd(3{,}5-XADA)\cdot H_2O$, cada grupo carboxilato parece actuar como bidentado con lo que el ligando en conjunto, actuaría como pentadentado, ocupando la molécula de agua una sexta posición de coordinación lo que conduciría a una geometría octaédrica distorsionada.

BIBLIOGRAFÍA

[1] V. P. Khramov, G. A. Aliev y L. M. Dvornikova, *Izv. Vyssh Uchebn Zaved. Khim. Tekhnol.*, **14**, 1960 (1971).

[2] F. Gonzalez Vilchez, M. C. Puerta Vizcaino y M. F. Gargallo Esteban, *Thermochim. Acta*, **42**, 295 (1980).

[3] M. Castillo Martos, F. Gonzalez Vilchez y E. Ramirez Carrasco, *Thermochim. Acta*, **60**, 131 (1983).

[4] J. M. Salas Peregrin, M. Roman Ceba, J. C. Avila Roson y J. Suarez-Varela, *Thermochim. Acta*, **80**, 115 (1984).

[5] J. M. Salas Peregrin, J. C. Avila Roson, M. Roman Ceba y J. Suarez-Varela, *Thermochim. Acta*, **89**, 151 (1985).

[6] V. V. Ramanujan, M. Rajalakshmi y B. Sivasankar, *Indian J. Chem.*, **20**A, 531 (1981).

[7] D. W. Coke, *Inorg. Chem.*, **5**, 1141 (1966).

[8] M. Mori, M. Shibata; E. Kyuno y F. Maruyama, *Bull. Chem. Soc. Jpn.*, **35**, 75 (1962).

[9] M. J. Rao, B. Selhuram y T. N. Rao, *Bull. Soc. Chem. Belg.*, **91**, 111 (1982).

[10] J. D. Joshi y P. K. Bhattachorya, *J. Indian Chem. Soc.*, **57**, 336 (1980).

[11] D. P. Graddon, *J. Inorg. Nucl. Chem.*, **22**, 85 (1961).

[12] P. Vieles y N. Israily, *Bull. Soc. Chem. Fr.*, **139** (1967).

[13] B. B. Smith y D. T. Sawyer, *Inorg. Chem.*, **7**, 2431 (1968).

[14] J. M. Salas Peregrin, M. Roman Ceba, J. C. Avila Roson y J. Suarez-Varela, *Thermochim. Acta*, **87**, 109 (1985).

[15] J. M. Salas Peregrin, E. Colacio Rodriguez, J. Suarez-Varela y J. C. Avila Roson, *Thermochim. Acta*, **90**, 201 (1985).

[16] F. Salinas, A. Guiraum y J. C. Avila Roson, *An. Quím.*, **78B**, 232 (1982).

[17] G. B. Deacon y R. J. Philips, *Coord. Chem. Rev.*, **33**, 227 (1980).

[18] K. Ito y H. J. Bernstein, *Can. J. Chem.*, **34**, 170 (1956).

[19] A. I. Grigor y V. N. Maksimov, *Russ. J. Inorg. Chem.*, **9**, 580 (1964).

[20] "Spectroscopic Properties of Inorganic and Organometallic Compounds; Specialist Periodical Reparts". Chem. Soc. London Vol. 1p.

[21] K. Nakamoto, "Infrared and Raman Spectra of Inorganic and Coordination Compounds", 3rd. Ed. p. 306. John-Willey N. Y., 1978.

[22] J. C. Bailar, "Comprehensive Inorganic Chemistry", Pergamon Press, Oxford, 1973.

[23] K. Burguer, "Coordination Chemistry; Experimental Methods", Butterwort, London p. 223, 1973.

[24] B. N. Figgis y J. Lewis, "The Magnetochemistry of Complex Compounds". Ed. Lewis and Wilkins. Prog. Inorg. Chem. Vol. 6. Interscience N. Y., 1964.

[25] Am. Soc. Test Mater (1970).

Revue Roumaine de Chimie, **35**, *5*, 649–656 (1990)

THERMAL BEHAVIOUR OF ACRYLAMIDE-MALEIC ANHYDRIDE – STYRENE TERPOLYMER

MARGARETA TOMESCU, EUGEN SEGAL and STELIANA CREȚU
Polytechnic Institute of Bucharest, Chair of Physical Chemistry and Electrochemical Technology, Bucharest, Romania

Received March 2, 1989

The paper contains a qualitative investigation of the thermal chemical changes undergone by some acrylamide — maleic anhydride — styrene copolymers, during their heating with a constant rate of temperature increase.

INTRODUCTION

Great importance has been attached to the study of chemical changes of polyacrylamide during heating. [1–4] The properties of such polymers change sharply as a result of thermal degradation. The amide groups can react with each ether, either intramolecularly or intermolecularly, similarly to the imidization catalysed by acids. [5] At highest temperature, chain scission has been put into evidence. In order to keep the thermal degradation under control the knowledge of this process appears to be very important.

This paper deals with the thermal destruction of the new copolymers, [6] acrylamide (AA)-maleic anhydride (MA)-styrene (S), with special emphasis on the monomers influence on the imidization process.

EXPERIMENTAL

Copolymers

The copolymers as well as the homopolymers used were prepared[6] in methyl — ethylketone solution, at 70°C using 0.1% azoisobutyronitrile. Polymerizations were carried out in an inert atmosphere, until the conversion reached 10%. The copolymer composition was determined by elemental analysis (C, H, N). For the determination of carboxylic group the potentiometric titration method was used.

Copolymers compositions are summarized in Table 1.

Table 1
Copolymers composition data

Copolymers code	Composition, wt %		
	AA	MA	S
1	55.13	42.51	2.36
2	15.72	51.68	32.60
3	3.90	31.65	64.45

Thermal analysis

The thermal curves were recorded by a MOM-Budapest, type Paulik-Paulik-Erdey, in air at a heating rate of 10°C/min. In all the experiments the sample weight was 0.1000 g.

For the identification of the gases evolved during heating a Perkin-Elmer chromatograph type 990, was used.

RESULTS AND DISCUSSIONS

The derivatograms recorded for polyacrylamide (PAA), polystyrene (PS) and AA – MA – S copolymers at different compositions are presented in Figures 1–5.

Polycrylamide

As seen in Figure 1, polyacrylamide undergoes a loss of 12 % water between 25 °C and 180 °C, followed at higher temperatures by softing (the polymer being characterized by a high hygroscopicity[8]), and imidization. The zero value of the decomposition rate which is recorded at 200 °C could be assigned to the cooling of the sample during its softing. The maximum imidization rate is recorded at 310 °C, this peak being characteristic for PAA pyrolysis.[3,4] Through intramolecular imidization one gets cyclic structures (I) whereas intermolecular imidization leads to network structures (II):

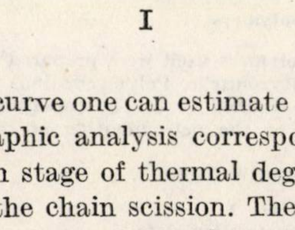

I

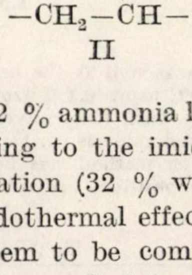

II

From the curve one can estimate a 12 % ammonia loss, as confirmed by chromatographic analysis corresponding to the imidization.

The fourth stage of thermal degradation (32 % weight loss) could be assigned to the chain scission. The endothermal effects corresponding to the breaking of the chemical bonds seem to be compensated by the exothermal ones due to the oxidation of the resulted fragments, as shown by the small peak on the DTA curve recorded at 420 °C. Gas chromatographic analysis allowed us to identify through the thermal degradation products until 600 °C, hydrocarbons with 2–4 carbon atoms, ammonia and CO_2.

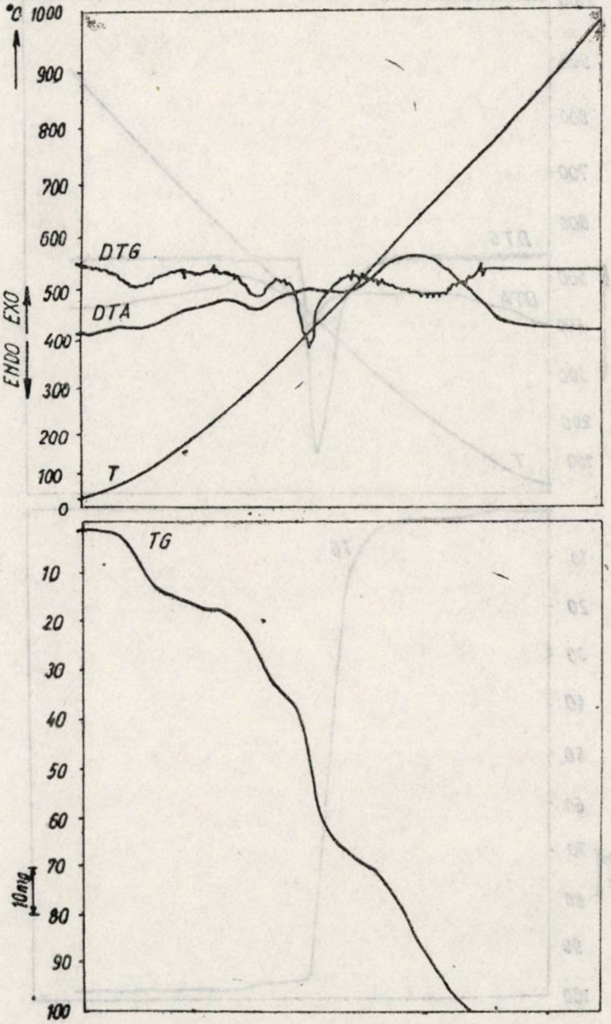

Fig. 1. — The derivatogram of PAA ; w = 0.1000 g (weight of sample).

The fifth stage of the degradation which occurs above 500 °C corresponds to the oxidation of the remaining fragments.

Polystyrene

The derivatogram of polystyrene given in Figure 2, shows a small loss of humidity, followed by depolymerization. The maximum depolymerization rate is recorded at 420 °C as shown by the DTG curve. An exothermal peak located at 560 °C is due to the oxidative degradation of the decomposition products.

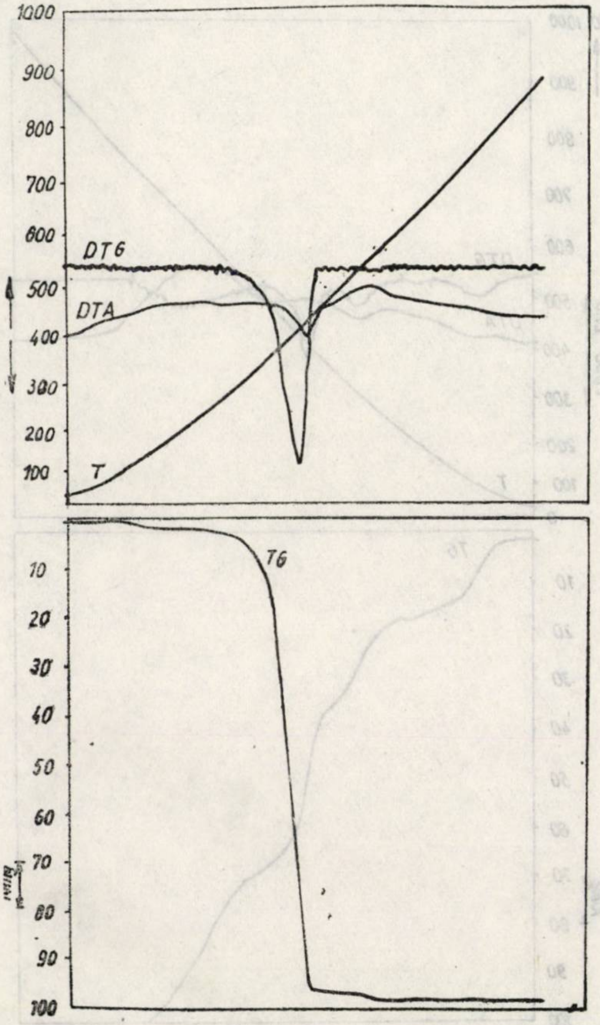

Fig. 2. — The derivatogram of PS; w = 0.1000 g.

AA-MA-S Copolymers

The thermal behaviour of these copolymers is different with respect to PAA and changes with the chemical composition.

The derivatogram of the copolymer 1 (Table 1) is given in Figure 3. The endothermal peak associated with intramolecular and intermolecular imidization is shifted from 300 °C (for PAA) to 250 °C. This shift can be assigned to the catalytic effect of MA units. Between 320 and 600 °C the share of the DTA curve suggests an important overlap between the endothermal effects corresponding to the chain scission and the exothermal ones due to the oxidation of the products. The thermal behaviour of the

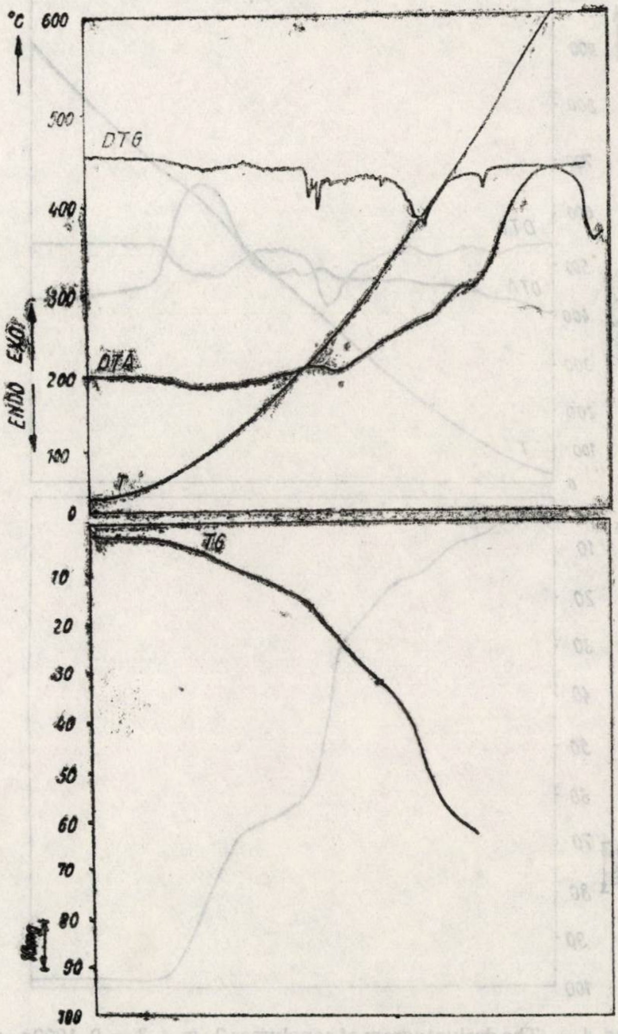

Fig. 3. — The derivatogram of copolymer 3 ; w = 0.1000 g.

copolymer is not influenced by its small content in styrene, the derivatogram of copolymer 1 being similar to the derivatogram of the binary copolymer AA—AM,[7] with quite the same composition (53.97% AA : 46.07%AM).

The derivatogram of copolymer 2 given in Figure 4 exhibits four main decomposition stages. The former two of them are due to the losses of water and ammonia. The intensity of the endothermal peak associated with imidization is smaller and the effect of MA units on its shift is higher. In this case, the maximum imidization rate is recorded at 202 °C. The latter two (the first one being splitted as shown by DTA curve) are exothermal, due to the reactions with molecular oxygen. The third stage

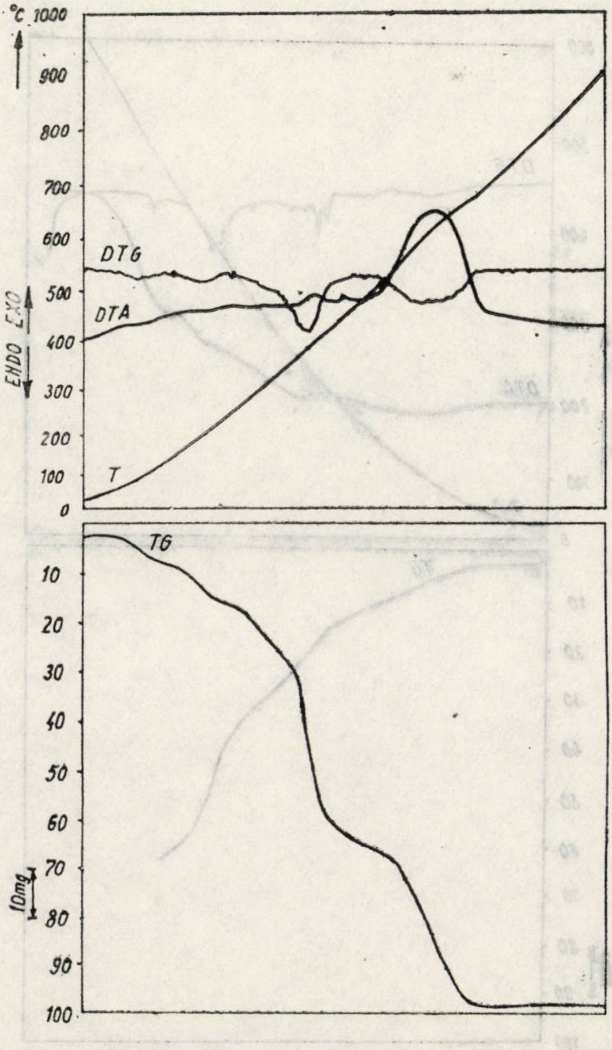

Fig. 4. — The derivatogram of copolymer 2 ; w = 3 = 0.1000g.

reflects probably some compensations between endothermal chain scission or styrene units depolymerization and exothermal oxidation.

The thermal decomposition curves from 25 °C to 600 °C four the copolymer 3 given in Figure 5 exhibit four stages in which losses of water, ammonia, styrene, carbon dioxide and hydrocarbons with 2—4 carbon atoms were put into evidence. [6]

The maximum imidization rate is recorded at 170 °C, the shift with respect to PAA being 140°. The reported shifts for the copolymers 1, 2 and 3 suggest the existence of an MA concentration corresponding to a minimal catalytic action.

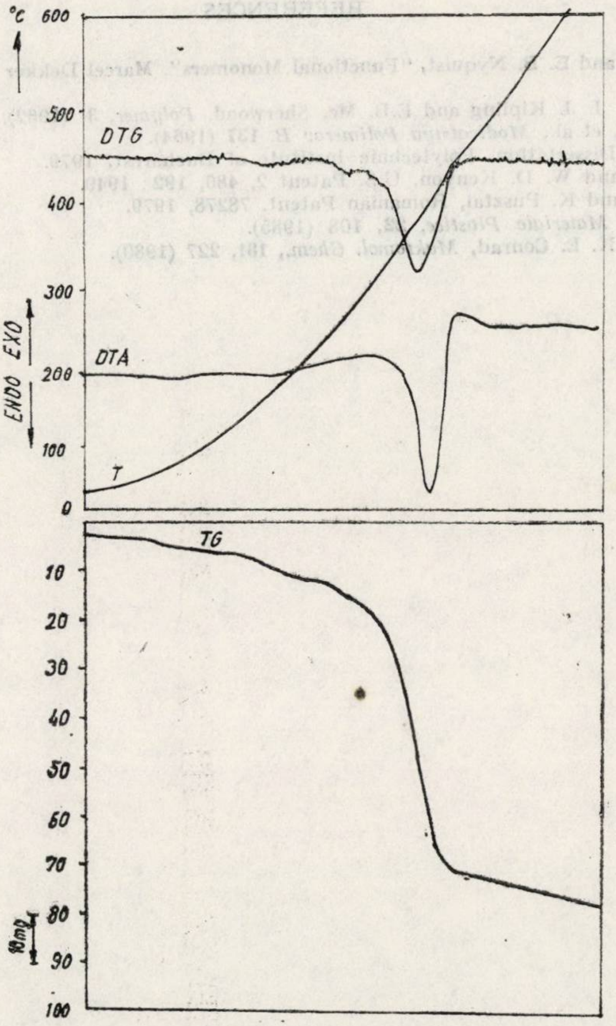

Fig. 5. — The derivatogram of copolymer 3 ; w = 0.1000 g.

CONCLUSIONS

(1) The thermooxidative destruction properties of the AA—MA—8 copolymers reflect their chemical composition, the thermal stability being changed according to the interactions between functional groups.

(2) The maleic anhydride units exhibit a catalytic influence on the imidization reaction of AA sequences in copolymers.

(3) The styrene units induce major changes in the thermal behaviour of copolymers, including depolymerization stages with loss of styrene.

REFERENCES

[1] R. H. Yokum and E. B. Nyquist, "Functional Monomers", Marcel Dekker Inc., New York, 1973.

[2] J. B. Gilbert, J. J. Kipling and E.B. Mc. Sherwood, *Polymer*, 3 (1962).

[3] S. R. Rafikov, et al., *Modicatsiya Polimerov B*, 137 (1964).

[4] C. A. Najab, Dissertation, Polytechnic Institute of Bucharest, 1979.

[5] L. H. Minsk and W. D. Kenyon, U.S. Patent 2, 486, 192 ; 1949.

[6] M. Tomescu and K. Pusztai, Romanian Patent. 78278, 1979.

[7] M. Tomescu, *Materiale Plastice*, **22,** 108 (1985).

[8] J. Klein and K. L. Conrad, *Makromol. Chem.*, **181,** 227 (1980).

Revue Roumaine de Chimie, 35, 5, 657–662 (1990)

CATALYSIS BY POLYMERS. VI[1]

THE EPICHLOROHYDRIN ESTERIFICATION CATALYZED BY POLY(N,N-DIMETHYL-p-VINYLBENZYL-AMINE)

EMIL DUMITRIU and VASILE HULEA
Department of Organic Chemical Technology, Faculty of Industrial Chemistry Bahlui Stinga 71
Jassy 6600, Romania

Received March 2, 1989

The catalytic properties of poly(N, N-dimethyl-p-vinyl-benzyl-amine) in the esterification reaction of epichlorohydrin have been investigated. The results indicated a very good catalytic activity of this polymer, in comparison with other basic polymers. Likewise, its activity is better than that of N,N-dimethylbenzylamine which was used as micromolecular model.

INTRODUCTION

Our previous studies concerning the esterification reaction of oxiranes with organic acids [1–5] have pointed out the influence of various factors on this process, an important role being attributed to the nature of catalyst. In relation to the catalyst nature, the activity of different types of functions, as well as the behaviour of catalytic functions, as a result of their concatenation on the macromolecular chains, were investigated. These studies have been extended by testing a new catalyst, namely poly(N, N-dimethyl-p-vinylbenzyl-amine) and a micromolecular model N, N-dimethyl-benzylamine.

EXPERIMENTAL

Reagents. Acrylic acid and epichlorohydrin were purified as previously described.[1]

Acetic acid was anhydrized with acetic anhydride, after which it was rectified. Propionic acid was distilled, b.p. = 141 · 3° C, $n_D^{20} = 1.885$. Benezene and N-N-dimethylformamide were purified by common methods.

Catalysts. N,N-Dimethylbenzylamine (Aldrich reagent) was distilled before use; b.p. = 183–184°/765 mm Hg, $d^{20} = 0.900$, $n^{20} = 1.50011$.

The polymer used as catalyst was synthesized as follows. The freshly distilled styrene was polymerized by the thechnique of suspension polymerization. The polymer beads were washed with deionized water then dried. The average viscosimetric molecular weight was $\overline{M}_v = 39{,}000$. The polystyrene was chloromethylated at 40°C using α-chloro-dimethylether, the polymer being removed from the reaction medium by precipitation with methanol. The purification was realised by several precipitations. The chlorine content, determined by the Schöniger method, stated a degree of 98.5% chloromethylation.

The chloromethylated polystyrene was aminated with dimethylamine in benzene solution. The reaction was carried out at 30–40°C for 10 hours. In order to avoid the quaternization, the molar ratio between amine and chloromethylated polymer was about 12 :1. Finally, the polymer was removed by precipitation with light petroleum. The degree of amination was proved from the nitrogen content determined by the micro-Kjeldhal method; the results showed a total transformation of the chloromethyl groups.

Esterification. The reaction of esterification was carried out on an installation which was previously described.[3] The initial concentration of reagents in solvent was about 5 moles/L and the weight of reaction mixture was about of 50 g. The experiments were carried out at 60°C and the extent of reaction was followed by the titration of unreacted acid. At certain intervals of time the samples were taken off from the reaction mixture (about 0.3 – 0.5 g) and the unreacted acid was titrated with 0.1 NaOH solution using a mixture of phenylphthaleine-bromothymol blue as indicator.

RESULTS AND DISCUSSION

The aim of this study consists in the analysis of the behaviour of acrylic acid-epichlorohydrin system in the esterification reaction catalyzed by poly(N,N-dimethyl-p-vinylbenzyl-amine). In order to reveal some specific features of the process, in the first stage N,N-dimethylbenzylamine was used as catalyst. In order to determine the kinetic model of the reaction, we have studied the influence of molar ratio of the reagents upon the evolution of reaction. Using various molar ratios of reagents it was observed that the reaction rate increases as the excess of epichlorohydrin was increased. Also, some experiments were carried out using various concentrations of catalyst ; the experimental data are shown in figure 1.

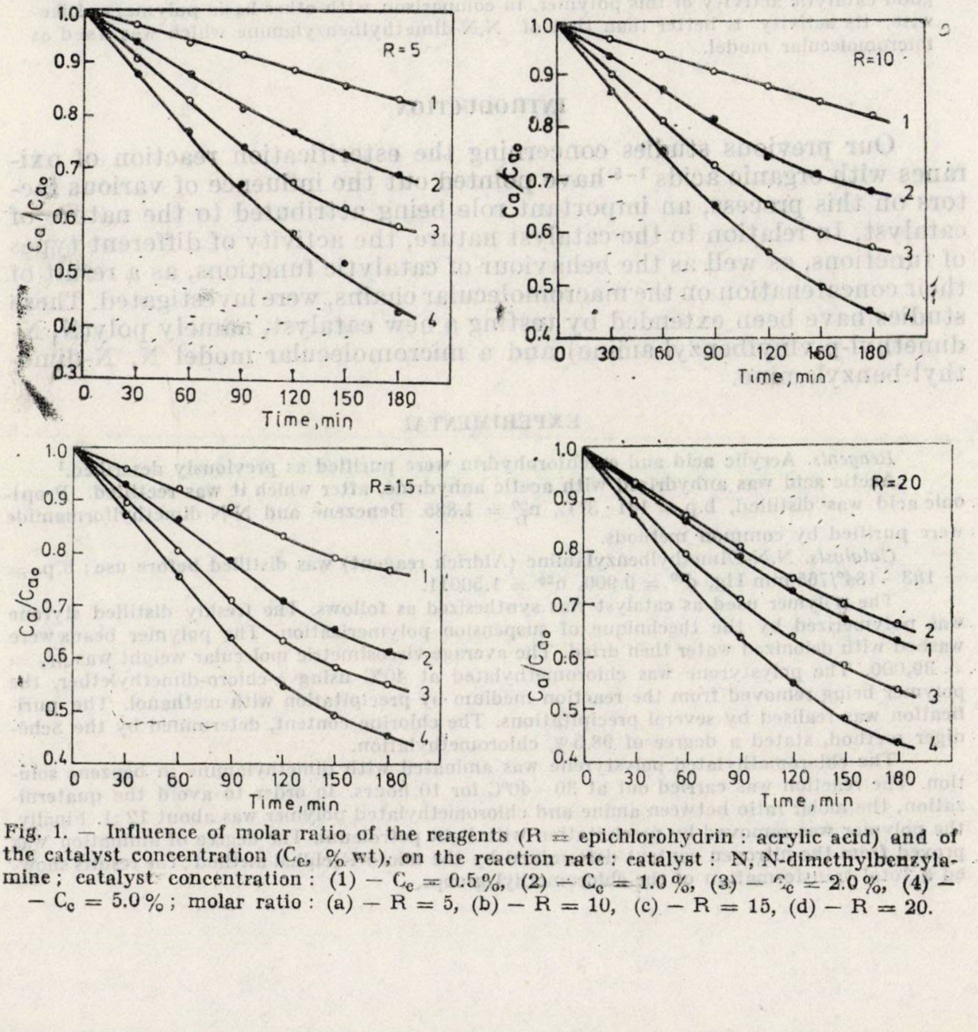

Fig. 1. — Influence of molar ratio of the reagents (R = epichlorohydrin : acrylic acid) and of the catalyst concentration (C_c, % wt), on the reaction rate : catalyst : N, N-dimethylbenzylamine ; catalyst concentration : (1) — $C_c = 0.5$ %, (2) — $C_c = 1.0$ %, (3) — $C_c = 2.0$ %, (4) — $C_c = 5.0$ % ; molar ratio : (a) — R = 5, (b) — R = 10, (c) — R = 15, (d) — R = 20.

These figures show that the relative concentration of the acid decreases more rapidly when the concentration of catalyst increases, but the following aspects must be underlined :

(i) — the tendency to homogenize the catalytic activity as the excess of epichlorohydrin is increased. More exactly, until 5 : 1 molar ratio of epichlorohydrin to acrylic acid there are noticeable differences between the slope of lines, but as far as the excess of epichlorohydrin increases these differences are diminished ;

(ii) — an anomalous behaviour of the curve corresponding to the catalyst concentration of 0.5 % (g) and a molar ratio epichlorohydrin : acrylic acid of 20 : 1.

The two observations led to the conclusion that the catalytic action of N,N-dimethylbenzylamine is determinant at low concentrations of oxiranes whereas at higher concentrations of epichlorohydrin the autocatalytic effect or solvent effect can smooth the catalytic activity of tertiary amine ; thus its concentration is not so important as the concentration of epichlorhydrin. These effects were already mentioned and studied by us. [4]

The role of epichlorohydrin in the esterification process can be better distinguished using organic acids weaker than acrylic acid (e.g. acetic acid or propionic acid). As shown in Figure 5 there is a direct correlation between the strength of acids and the reaction rate, but when the experiments were carried out in the abovementioned conditions, the tendency to homogenize the reaction rate appears more obvious in this case.

Moreover, the kinetic measurements offer a quantitative basis in the estimation of these phenomena. The kinetic parameters were determined using the technique of isolation, epichlorohydrin being in excess, and the relative rate constants (related to the acrylic acid) were obtained. The constants include in their values the concentration of oxirane and that of the catalyst.

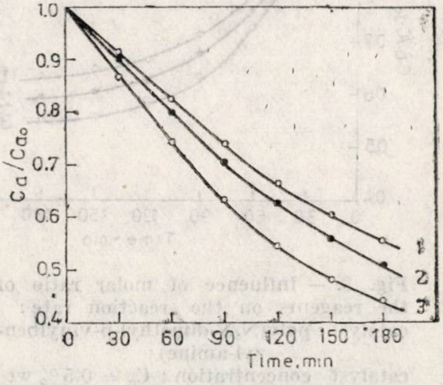

Fig. 2. — Effect of the acid nature on the reaction rate :
R = 20, C_c = 5.0 %, (1)—propionic acid, (2) — acetic acid, (3) — acrylic acid.

Table 1

Influence of catalyst concentration on the apparent rate constant ($k \times 10^5$, s^{-1}), in DMFA

R, mole/mole	Catalyst concentration, % wt			
	0.5	1.0	2.0	5.0
5	1.635	3.441	5.192	6.942
10	1.784	3.721	5.663	7.572
15	2.152	3.814	5.843	7.709
20	3.912	3.872	5.933	7.824

It must be mentioned that these data were obtained for the initial stage of reactions when one has stated that the partial order in relation to the acrylic acid is equal to unity. The validity of this kinetic model was proved in a previous paper. [1] But, as the extent of reaction is more advanced the deviation from the kinetic model is greater due to the autocatalytic and/or solvent effects. [4]

The second part of our study contains the aspects relating to the catalytic activity of poly(N,N-dimethyl-p-vinylbenzyl-amine). The experiments were carried out in N,N-dimethylformamide as solvent. It can also be observed that the reaction rate increases as the excess of epichlorohydrin is increased (Figure 3) but the most important aspect seems to be the upper catalytic activity of polymer comparatively with the catalytic activity of N,N-dimethylbenzylamine. At the same reaction conditions, i.e. the temperature of 60 °C, catalyst concentration of 0.5 (g) and molar ratio of 20 : 1 (epichlorohydrin : acrylic acid), the polymer shows a better catalytic activity than the micromolecular compounds. This behaviour is different in relation to the behaviour of poly(2-vinylpyridine), as has been shown in the previous paper. [1] A possible explanation consists, on the one hand, in the difference between the basicity of the two aminic functions. In the case of pyridine (or 2-vinylpyridine) the free electrons of nitrogen are into a strong interaction with the electrons of pyridine ring whereas the interaction between the free electrons of nitrogen and the aromatic ring is diminished due to the methylene group. On the other hand, these different catalytic activities can be explained by steric hindrance in relation to the access of the reacting molecules at the catalytic sites (at the atom of nitrogen; see Scheme I). This steric hindrance is more pronounced when the catalytic functions are concatenated into a macromolecular chain. Another aspects which must be mentioned, in relation to the catalytic activity of the tested polymer, consists in the fact that the catalytic activity of polymer decreases as the extent of reaction increases (Figure 4).

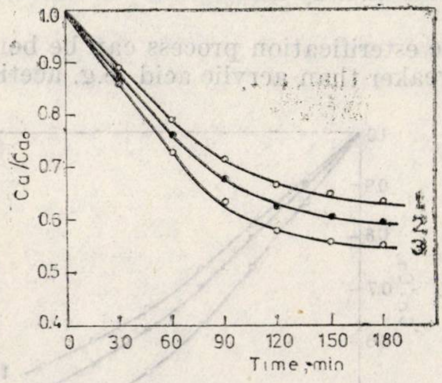

Fig. 3. — Influence of molar ratio of the reagents on the reaction rate: catalyst : poly(N,N-dimethyl-p-vinylbenzyl-amine); catalyst concentration : $C_c = 0.5\%$ wt ; (1) — R = 10, (2) — R = 15, (3) — R = 20.

Of course, the diminution of reacting species could be take into consideration, but it is also possible that the conformation of the macromolecular chain is responsible for this behaviour because the thermodynamic properties of the reaction medium are changed.

SCHEME I

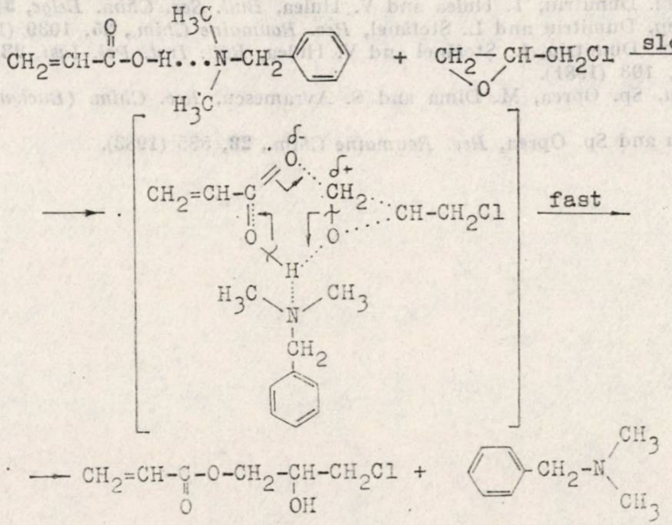

In order to verify this hypothesis we have introduced a sample of reaction mixture into a thermostated viscosimeter and the relative viscosity was measured at certain intervals of time. Also, at the same time the extent of reaction was determined. As can be observed from figure 5, there is a certain correlation between the change of viscosity and the diminution of catalytic activity of the polymer.

As a conclusion, we can underline the good catalytic activity of poly(N,N-dimethyl-p-vinylbenzyl-amine) which is better than that of poly(2-vinylpyridine) and than that of N,N-dimethylbenzylamine, too.

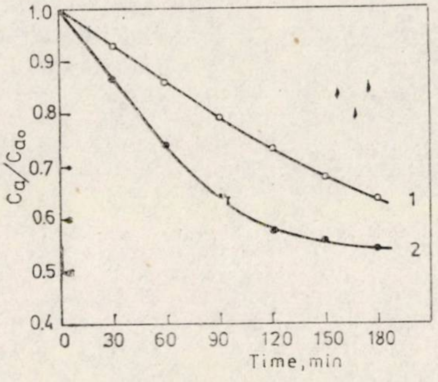

Fig. 4. — Effect of the catalyst nature on the reaction rate : R=20, $C_c = 0.5\%$wt, catalyst : (1) — N,N-dimethylbenzylamide, (2) — poly(N,N-dimethyl-p-vinylbenzyl-amine).

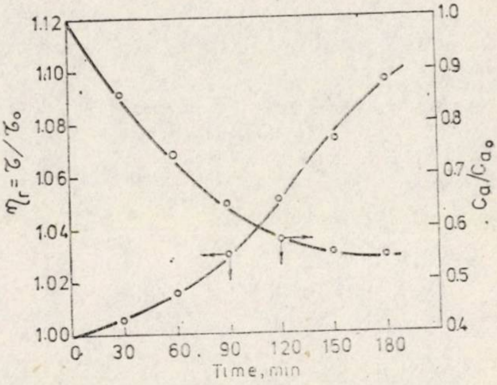

Fig. 5. — Variation of viscosity coefficient (ηr) and relative concentration vs. reaction time : R = 20, $C_c = 0.5\%$ wt, catalyst : poly(N,N-dimethyl-p-vinylbenzyl-amine).

REFERENCES

[1] Sp. Oprea, Em. Dumitriu, T. Hulea and V. Hulea, *Bull. Soc. Chim. Belge*, **94**, 7 (1985).

[2] Sp. Oprea, Em. Dumitriu and L. Ştefănel, *Rev. Roumaine Chim.*, **25**, 1039 (1980).

[3] Sp. Oprea, Em. Dumitriu, L. Ştefănel and V. Hulea, *Bull. Inst. Pol. Iaşi*, **28**, issue 3–4, Sect. II, 103 (1981).

[4] Em. Dumitriu, Sp. Oprea, M. Dima and S. Avramescu, *Rev. Chim.* (*Bucharest*), **32**, 225 (1981).

[5] Em. Dumitriu and Sp. Oprea, *Rev. Roumaine Chim.*, **28**, 535 (1983).

Revue Roumaine de Chimie, 35, 5, 663–667 (1990)

SOME ASPECTS OF LINEAR LOW DENSITY POLYETHYLENE SYNTHESIS ON $TiCl_4/MgCl_2$ CATALYSTS*

C. ANDREI, GEORGETA ANDREI, STANA PIȚĂ, OLIVIA PITPALAC and IOANA SONOC

Brazi Petrochemical Plant, Research Department, 2000 Ploiești, Romania

Received March 2, 1989

This paper presents various aspects of ethylene copolymerization with 1-hexene or 1-octene in order to obtain linear low density polyethylene (LLDPE), the copolymerization taking place in the presence of hydrogen (molecular weight regulator). Emphasis is placed upon the influence of the reaction temperature, upon the properties of the obtained polymers in the presence of a high activity catalyst system of $TiCl_4/MgCl_2-(i-C_4H_9)_3Al$.

INTRODUCTION

Recent developments concerning the improvement of catalyst systems and the low density polyethylene manufacturing technologies have led to the appearance of a new type of polyethylene, e.g. linear low density polyethylene (LLDPE) obtained by ethylene copolymerization with α-olefines at low temperatures and pressures.

From data published in technical literature we understand that this type of polyethylene, with better properties than conventional low density polyethylene (LDPE), can be obtained both in high pressure plants (bulk polymerization) and in low pressure plants (fluidised bed polymerization or liquid polymerization) in the presence of Ziegler-Natta type catalysts or modified Phillips catalysts. [1–3]

The most successful attempts to obtain LLDPE belong to Union Carbide Corporation. [4–5] According to this process, ethylene is polymerized in gaseous state in a fluidized bed reactor in the presence of high activity supported catalysts.

Great producing firms such as: Phillips Co., Dow Chem. Co., Du Pont of Canada, Montedison, Mitsui Petrochemical Industries and others, obtain LLDPE by adapting solution and suspension polymerization processes in the presence of Ziegler-Natta supported catalysts. [6–7]

This paper presents some aspects of ethylene copolymerization reaction with 1-hexene or 1-octene in the presence of a high activity catalyst system of the $TiCl_4/MgCl_2-(i-C_4H_9)_3Al$ type.

---

* Paper presented at the 3rd National Chemistry Congress, Bucharest, September 21–24, 1988.

EXPERIMENTAL

The copolymerization reaction of ethylene with α-olefine is carried out in n-hexane, in a reactor with a capacity of 2 l, at temperatures of 60°C to 130 °C and a pressure of 20 at.

An α-olefine is introduced to reduce the density of the obtained polymers.

Molecular weight control is ensured by introducing hydrogen in the reaction.

The polymers obtained with or without a comonomer have the following characteristics :

— flow index according to ASTM D 1238—73

— density according to ASTM D 1505—75

— viscosity average molecular weight ($\bar{M}v$) according to ASTM D 1601—61 and

— mechanical strength properties (yield tensile strength, ultimate tensile strength and elongation at break) according to ASTM D 638—76.

The obtained polyethylene morphology is studied by means of an ORTHOLUX — Leitz Optical microscope with a magnifying power of 940 times the initial value. The measurement is performed in polarized light.

RESULTS AND DISCUSSION

The high performances of LLDPE are due to its structure.

The essential difference between the three types of polyethylene HDPE, LDPE and LLDPE consists in the nature and the degree of branching.

While high density polyethylene (HDPE) is practically devoid of branches, low density polyethylene (LDPE) has a strongly branched structure in which long branches predominante.

LLDPE has only short branches whose number determine the values of crystallinity and density of the polymer. [7–8]

Short branches are obtained by introducing a comonomer in the polymer chain by way of an α-olefine (1-butene- 4-methyl-1-pentene, 1-hexene, 1-octene) introduced in the polymerization reaction. [9]

The degree of crystallinity is determined mainly by the nature and the quantity of the comonomer which is incorporated in the polyethylene chains. [10]

The choice of comonomer depends on the polymerization process and on the type of catalyst used, taking into account the fact that not all the types of catalysts have a high activity in the copolymerization reaction of ethylene, particularly with high α-olefines. [11]

The activity of the catalysts $TiCl_4/MgCl_2 - (i-C_4H_9)_3Al$ used in the ethylene copolymerization reaction at various reaction temperatures and properties of the obtained copolymers (ethylenel-hexene and ethylene-1-octene) are listed in tables 1 and 2.

The data listed in table 1 shown that the reaction temperature considerably influences the ethylene—1-hexene copolymers.

According to this, a rise in the reaction temperature leads to an increase flow index from 0.02 to 1.33 g/10 min. and respectively to a decrease of the viscosity average molecular weight from 226,700 to 79,580. The density of the polymers obtained at various reaction temperatures has not undergone severe changes.

The influence of the comonomer upon some properties of LLDPE is listed in table 2.

Table 1

Catalyst activity and properties of ethylene—1-hexene copolymers

Sample	Temperature, °C	Hydrogen partial pressure, at	Productivity, kg PE/gTi.h	Properties of copolymers					
				Flow index, g/10 min.	$\overline{M}v$	Density, g/cm³	Yield tensile strength, kgf/cm²	Ultimate tensile strength, kgf/cm²	Elongation at break, %
P_1	65	3.2	177	0.02	226,700	0.9335	174	438	635
P_2	80	2.5	125	0.22	120,600	0.9369	163	305	685
P_3	85	3.2	300	0.25	90,950	0.9340	191	336	810
P_4	95	3.7	434	1.31	68,420	0.9318	150	295	665
P_5	130	2.8	100	1.33	79,580	0.9337	130	320	600

Table 2

Properties of copolymers obtained in the copolymerization reaction of ethylene with 1-hexene or 1-octene

Sample	Comonomer	Temperature, °C	Hydrogen partial pressure, at	Properties of polymers			
				Melting point, °C	Flow index, g/10 min.	$\overline{M}v$	Density, g/cm³
P_6	22%, 1-hexene	130	3.0	125	1.30	80,000	0.9330
P_7	23%, 1-hexene	130	2.2	125	0.16	105,100	0.9343
P_8	25%, 1-octene	130	2.5	126.5	0.23	119,400	0.9278
P_9	31%, 1-octene	130	2.0	125	0.15	146,600	0.9226
P_{10}	—	130	2.8	132	0.80	93,480	0.9669

The data listed show that the properties of the obtained copolymers are determined by the nature and the quantity of comonomer used in the polymerization reaction.

In comparison with the polyethylene obtained without a comonomer, a major decrease in the copolymer density is observed; an increase of the comonomer concentration in the reaction accompanied by the lowering of the density is remarked as well.

By introducing a comonomer in the ethylene polymerization reaction, copolymers with a modified spherulite like structure are obtained (Fig. 1.a, b).

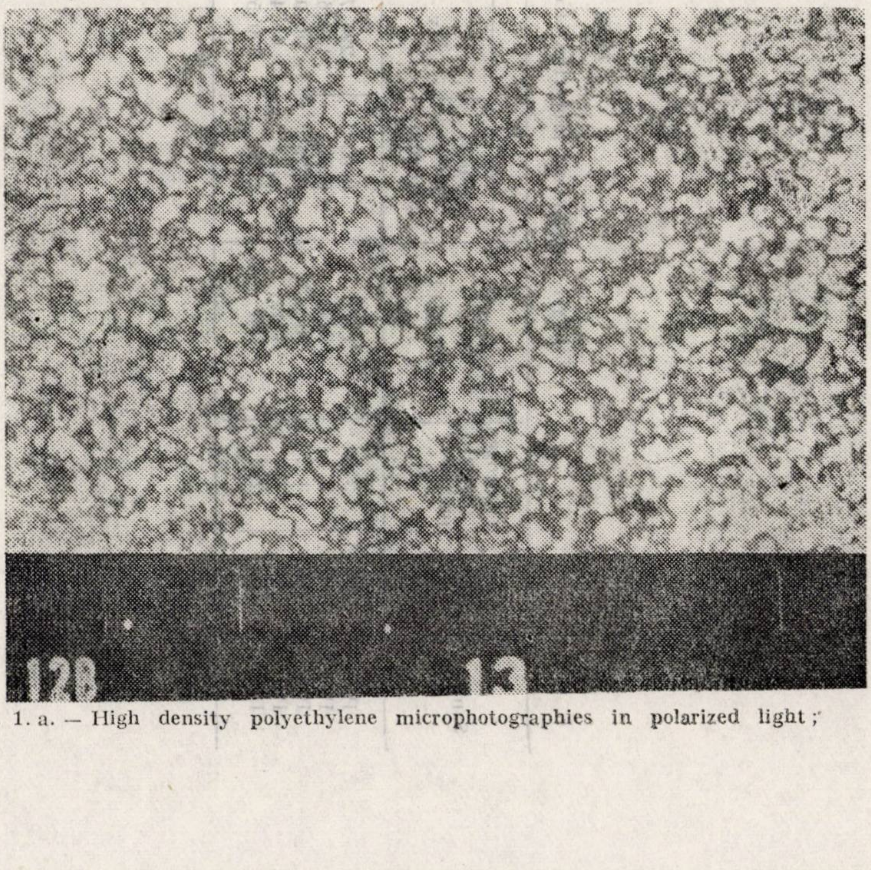

Fig. 1. a. — High density polyethylene microphotographies in polarized light;

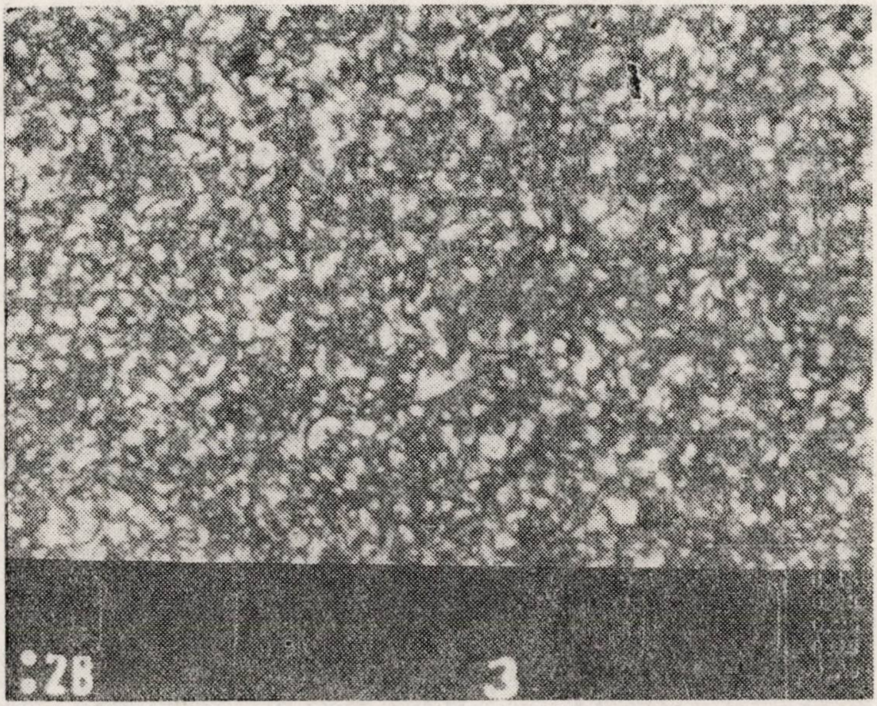

Fig. 1. b. — Ethylene—1-hexene copolymer microphotographies in polarized light.

The polyethylene obtained by the polymerization of ethylene without a comonomer has the well-grown spherulite structure and the polyethylene obtained by the copolymerization of ethylene in the presence of a comonomer (1-hexene) has the small and indistinct spherulite structure because the short-chain branching hinders the crystallization and the formation of spherulite.

REFERENCES

[1] V. Dobrescu and C. Andrei, "*Progrese în chimia şi tehnologia poliolefinelor*", Ed. Ştiinţifică şi Enciclopedică, Bucharest, 1987, p. 112.
[2] V. Dobrescu, G. Andrei, A. Câmpeanu and C. Andrei, *Rev. Roum. Chim.*, **33**, 399 (1988).
[3] T. Usomi, Y. Gotoh and S. Takayama, *Macromolecules*, **19**, 2722 (1986).
[4] S. M. Crimmin, *Hydrocarbon Processing*, **61**, 75 (1982).
[5] R. B. Seymour, *Pop. Plastics*, April, 39 (1986).
[6] * * * *Chem. Week*, Sept., **35**, 64 (1980).
[7] A. Furumiya, Y. Akana, Y. Ushida, T. Masuda and A. Nakajima, *Pure Appl. Chem.*, **57**, 824 (1985).
[8] * * * *Materie Plastiche ed Elastomeri*, July-Aug., 413 (1986).
[9] J. Seppala, *Polimery* (Warsaw), **29**, 457 (1984).
[10] M. M. Hert, *Inf. Chem.*, **220**, 171 (1981).
[11] J. N. Short, *Encycl. Chem. Technol.*, 3rd. Ed. **16**, 385 (1981).

Revue Roumaine de Chimie, 35, 5, 669–674 (1990)

THEORETICAL AND EXPERIMENTAL STUDY ON THE CYCLOADDITION BETWEEN 4-(p-TOLYL)1,2,4-TRIAZOLIUM(p-METHOXY)PHENACYLIDE AND ETHYL CINNAMATE

G. SURPĂŢEANU[a], M. CONSTANTINESCU[b], A. LABLACHE-COMBIER[b], P. GRANDCLAUDON[b], B. MOUCHEL[b] and A. COUTURE[b]
[a] Chemistry Department, Polytechnic Institute Iași, Splai Bahlui stg. 71, Iași 6600, Romania
[b] Laboratoire de Chimie Organic Physique, Bat. C3 Université des Sciences et Technique de Lille, Villeneuve d'Ascq Cedex 59655, France

Received October 20, 1989

A theoretical and experimental study on the cycloaddition reaction of 4-(p-tolyl)1,2,4-triazolium(p-methoxy)phenacylide and ethyl cinnamate has been performed. The structure of cycloaduct **7** was elucidated by elemental analysis, mass-spectra, IR-spectra, $^{13}C-NMR$(100.62 MHz). $^{1}H-NMR$(400.13 MHz) and 2D−NMR heteronuclear correlation of chemical shifts $^{13}C-^{1}H$ (Fig. 2). The interfrontier orbital diagram (Fig. 1) and experimental data point out that in this cycloaddition reaction the ylid carbon atom becomes bonded to C_1 carbon atom in ethyl cinnamate. A good agreement between theoretical and experimental data has been found.

In the previous papers [1,2] we have reported that some cycloimmonium ylides carbanion monosubstituted have been isolated and characterized as stereoisomers E and Z. Using the CNDO/2 method the barrier rotation energies of the 1, 2, 4-triazolium ylides of the type **1** have been calculated.

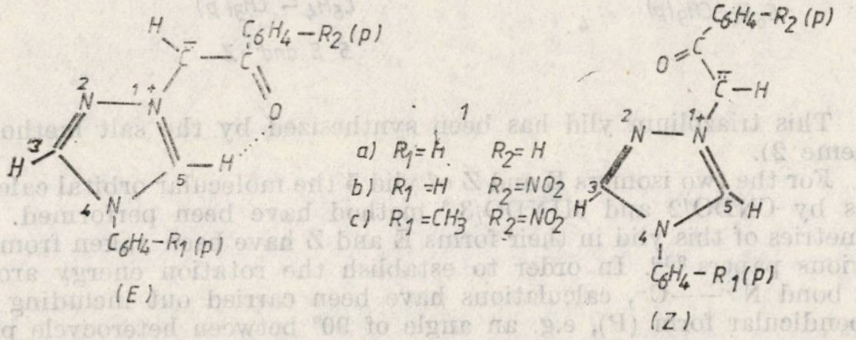

The structures were elucidated using $^{1}H-NMR$ (80Mz) and IR-spectra. The down field shifted proton H_5 has been assigned as two chemical shifts as singlet in the range $\delta = 10.80-11.51$ ppm and $\delta = 9.02-$

9.05 ppm respectively corresponding to E and Z forms. Also, for the proton bonded to ylid carbon atom, two chemical shifts have been assigned in the range $\delta = 7.04 - 7.17$ ppm belonging to both E and Z forms. Only a small difference in chemical shifts for the proton H_3 in both E and Z isomers was experimentally observed. IR-spectra of the triazolium ylides **1** (in KBr) are complex. In the isomers of the 1E type absorption bands $\nu_{C=O}$ are strongly shifted toward low frequency (1600 – 1640 cm^{-1}). On the other hand, in the isomers of the type 1Z, the same absorption bands are placed at about 1700 cm^{-1}. Only a hydrogen bond formation in the isomers 1E could explain the more deshielded H_5 proton and the low frequency of $\nu_{C=O}$.

The knowledge of the structures of isomers involved in cycloadditions as 1,3 dipoles allowed to establish the chemical ways by the construction of interfrontier orbital interaction diagrams.[3,4]

RESULTS AND DISCUSSION

In this paper we present an experimental and theoretical study on the cycloaddition between 4-(p-tolyl) 1, 2, 4-triazolium (p-methoxy) phenacylid **5** as 1,3 dipole and ethyl cinnamate as dipolarophile.

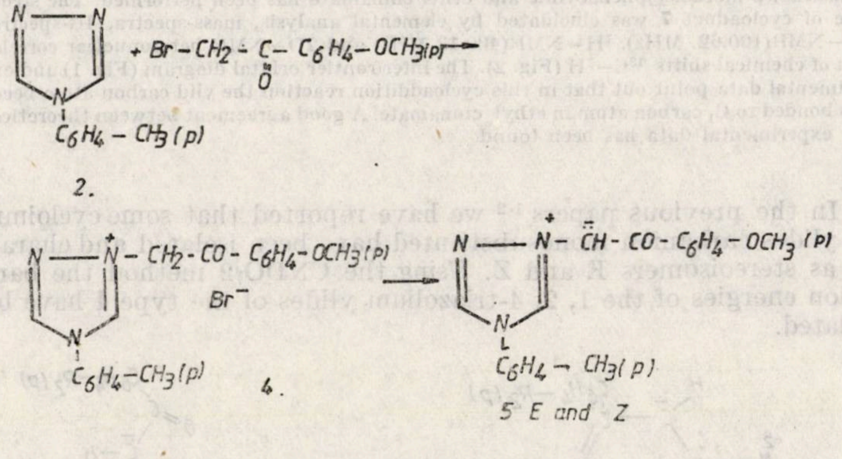
+ Br – CH2 – C – C6H4 – OCH3(p)
O
C6H4 – CH3 (p)
2.
N – CH2 – CO – C6H4 – OCH3 (p)
Br⁻
C6H4 – CH3 (p)
4.
N – CH – CO – C6H4 – OCH3 (p)
C6H4 – CH3 (p)
5 E and Z

This triazolium ylid has been synthesized by the salt method [5,6] (scheme 2).

For the two isomers E and Z of ylid 5 the molecular orbital calculations by CNDO/2 and MINDO/3 [8] method have been performed. The geometries of this ylid in their forms E and Z have been taken from the previous papers [9,10]. In order to establish the rotation energy around ylid bond $N^+ — C^-$, calculations have been carried out including the perpendicular form (P), e.g. an angle of 90° between heterocycle plane and the plane designed by ylid carbon and its neighbouring bonded atoms.

Table 1 gives results obtained using CNDO/2 method.

The 5E form is more stable than 5Z with 5 kcal/mol and the rotation barrier energy is of 19 kcal/mol. This means that there is no free rotation round ylid bond. In Table 2 the calculations using the MINDO/3 method are given.

Table 1

Total and frontier orbital energies, total atomic charges and coefficients of atomic orbitals, by CNDO/2 method

form	total energy eV and kcal/mol	frontier orbital total atomic charge	orbital energy e.V	Coefficients of atomic orbital of the atom :	
				C_i	C_5
	−5784.5	HOMO	−8.1934	−0.7142	0.3683
E	−133398	LUMO	2.1143	0.1002	0.4095
		Q		−0.2696	0.0254
P	−5783.7				
	−133393				
	−5784.3	HOMO	−8.0754	0.7086	−0.3751
Z	−133393	LUMO	1.9700	−0.1171	−0.4199
		Q		−0.2780	0.0152
				C_1	C_2
ethyl-cinammate		HOMO	−11.6629	0.4673	0.3329
		LUMO	1.1445	−0.4248	0.4717
		Q		−0.1118	0.0713

* P-perpendicular.

Table 2

Total and frontier orbital energies, total atomic charges and coefficients of atomic orbitals, by MINDO/3 method

form	heats of formation kcal/mol	frontier orbital total atomic charge	orbital energy e.V.	coefficients of atomic orbital of the atom :	
				C_1	C_5
		HOMO	−6.8100	−.7448	0.3561
E	62.99	LUMO	0.4671	−.0494	−0.2205
		Q		−0.4976	−0.1031
P	63.25				
		HOMO	−6.9121	−0.7418	0.3655
Z	65.61	LUMO	0.5230	0.	0.
		NLUMO	0.5720	−0.0084	−0.01109
		Q		−0.5184	−0.1093

* P-perpendicular.

We recall that the authors[8] of the MINDO/3 method defined the semiempiric parameter λ, which enters the internuclear repulsive term, as below:

$$\lambda = \exp\left(-\alpha_{AB} R_{AB}\right) \tag{1}$$

$$\lambda = \alpha_{AB} \exp\left(-R_{AB}\right) \tag{2}$$

The first definition (1) is generally valid, for the internuclear repulsive energies, the second one (2) is valid only for the repulsion between N—H and O—H atoms. α_{AB} is a characteristic parameter for all repulsions, statistically evaluated on a great and various number of molecular systems. Its value for the repulsion between O and H is of 0.4789. With this value, by the heats of formation it is a free rotation round ylide bond. Experimentally, the identification of the two isomers, **5E** and **5Z**, has been not observed. We have checked theoretically, using the CNDO/2 and MINDO/3 procedure methods the experimental data concerning free rotation round ylide bond in compound **5**. [11] At the MINDO/3 method level the **5E** form is still more stable with 2.62 kcal/mol than the **5Z** form.

The tri azolium ylid **5**, generated "in situ" in this salt **4**, reacted with ethylcinnamate. The structure of the cycloadduct **7** obtained in this synthesis has been established from chemical and spectral data.

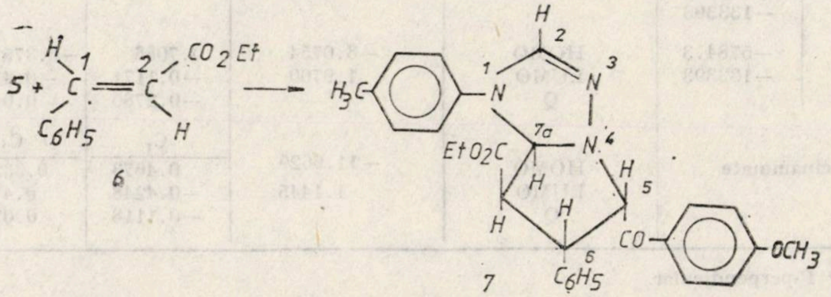

With theoretical data in Table 1 the frontier interorbital diagram was constructed.

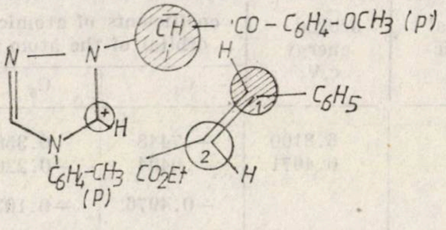

Fig. 1. — The frontier interorbital diagram between HOMO (ylid 5) — LUMO (ethylcynnamate). ● — ; ○+.

The ylid **5** in its **5E** form is more stable and the lowest difference in energy, of 9.337eV is between **HOMO** ylid **5E** and **LUMO** ester. Thus the ylid carbon atom C_1 is bonded with C_1 carbon atom from cinnamate.

Experimentally, this result is confirmed. In this cycloaddition reaction, four asymmetrical atoms, C_5, C_6, C_7 and C_{7a} are formed. Theoretically, sixteen isomers may be obtained. Their number can be reduced if we suppose that in the rigid bicyclic system the hydrogen H_{7a} is placed in an opposite position to the dihedral angle between the two fragments of heterocycles. If the cycloaddition is stereo and regioselective then one should evidence a "trans" coupling constant between the hydrogen H_6 and

H_7. Thus, finally there should be only four isomers. In this cycloaddition only one isomer, namely **7**, was isolated. Its structure was elucidated by $^{13}C-NMR$ (100.62 MHz), $^{1}H-NMR$ (400,13 MHz) and 2D$-$NMR heteronuclear correlation [12] of chemical shifts $^{13}C-^{1}H$ (fig. 2).

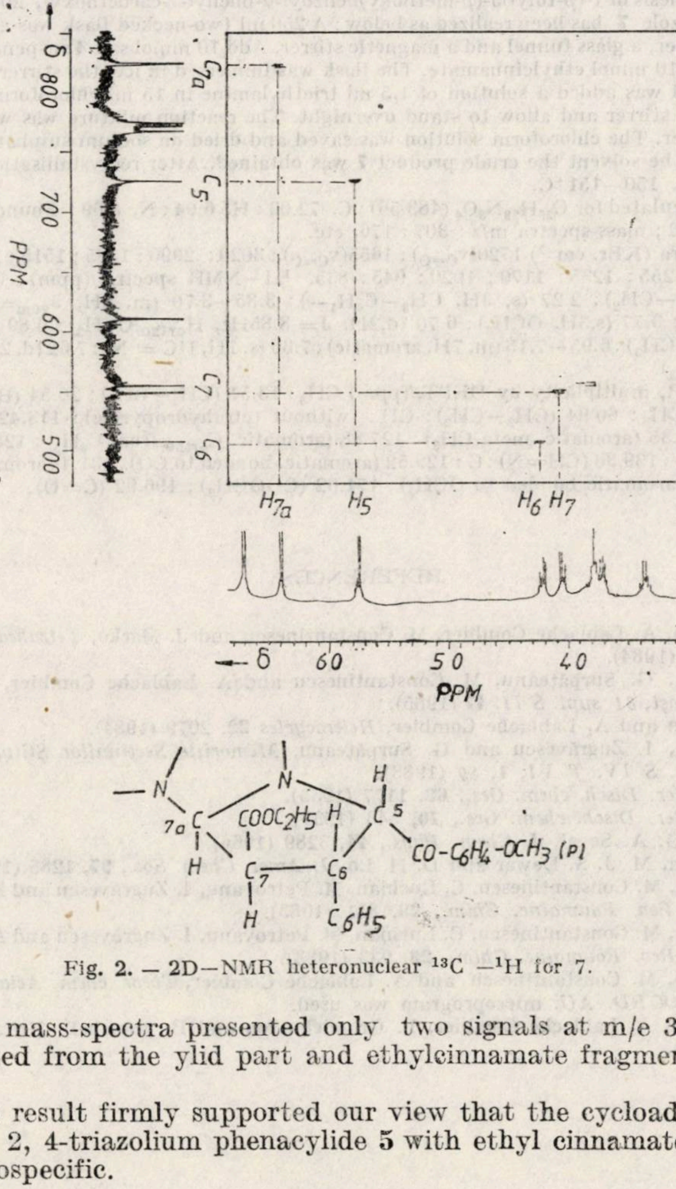
800
700
600
500
PPM
C_{7a}
C_5
C_7
C_6
H_{7a}
H_5
H_6 H_7
δ
60
50
40
PPM
N
N
H
$7a$ C
$COOC_2H_5$
H
C^5
$CO-C_6H_4-OCH_3$ (p)
H
C_7
C_6
H
C_6H_5

Fig. 2. — 2D$-$NMR heteronuclear ^{13}C $-^{1}H$ for **7**.

The mass-spectra presented only two signals at m/e 307 and m/e 176 resulted from the ylid part and ethylcinnamate fragment, respectively.

This result firmly supported our view that the cycloaddition reaction of 1, 2, 4-triazolium phenacylide **5** with ethyl cinnamate was regio- and stereospecific.

EXPERIMENTAL

The NMR-spectra were recorded with a Bruker AM$-$400, in $CDCl_3$ as solvent and TMS as internal standard. The 2D$-$NMR heteronuclear correlation $^{13}C-^{1}H$ of compounds **7** has been collected with the Bruker XHCOORD program. The multiplicity of the carbon atoms has been determined by a program DEPT. The IR-spectra and mass-spectra were recorded with a Perkin-Elmer-1310 and Ribemag 1010 Spectrometers respectively. The synthesis of 1-(*p*-methoxy)phenacyl-4-(*p*-tolyl)1,2,4-triazolium-bromide (4) has been achieved by the salt method described in a previous paper.[13]

The synthesis of 1-(*p*-tolyl)5-(*p*-methoxy)benzoyl-6-phenyl-7-carbethoxyl, 2b-tetrahydropyrolol 2,4-triazole **7** has been realized as below: A 250 ml two-necked flask was equiped with a reflux condenser, a glass funnel and a magnetic stirrer. Add 10 mmol salt **4** suspended in 50 ml chloroform and 10 mmol ethylcinnamate. The flask was immersed in ice, the stirrer was started and from funnel was added a solution of 1.5 ml triethylamine in 15 ml chloroform during 1.5 hours. Stop the stirrer and allow to stand overnight. The reaction mixture was washed twice with 30 ml water. The chloroform solution was saved and dried on sodium sulphate. After the evaporation of the solvent the crude product **7** was obtained. After recrystallisation from methanol has m.p. 150—151 °C.

Anal. calculated for $C_{29}H_{29}N_3O_4$ (483.56); C, 72.03; H, 6.04; N, 8.69; Found: C, 72.01; H, 6.01; N, 8.72; mass-spectra m/z: 307; 176, etc.

IR-Spectra (KBr, cm^{-1}) 1720($v_{C=O}$); 1655($v_{C=O}$); 3020; 2990; 1595; 1515; 1450; 1420; 1380; 1305; 1255; 1235; 1170; 1020; 945; 835. ^1H-NMR spectra,/(ppm): 0.89 (t, 3H, j = 7.0Hz, CH_3-CH_2); 2.27 (s, 3H, $CH_3-C_6H_4-$); 3.35—3.70 (m, 2H, J_{gem} = 10.7; J = = 7.0Hz, CH_2); 3.77 (s,3H, OCH_3); 6.70 (d,2H, J = 8.85Hz, H_{ortho}/OCH_3); 6.89 (d,2H, J = = 8.6Hz, H_{meta}/CH_3); 6.95—7.15 (m, 7H, aromatic); 7.36 (s, 1H, HC = N); 7.62 (d, 2H, J = 8.85 Hz, H_{meta}/OCH_3).

$^{13}C-NMR$, multiplicity by DEPT,/(ppm) CH_3: 13.51 (CH_2-CH_3); 20.54 ($BH_3-C_6H_4$); 55.36 (OCH_3); CH_2: 60.94 (CH_2-CH_3); CH: (without tetrahydropyrole): 113.42 (aromatic, ortho/CH_3); 115.35 (aromatic, meta/CH_3): 127.88 (aromatic, C_{ortho} from C_6H_5); 128.36 (aromatic, C_{meta}/OCH_3); 139.30 (CH=N); C: 129.52 (aromatic, bonded to CO); 131.4 (aromatic bonded to N_1); 163.42 (aromatic bonded to OCH_3); 171.02 ($COOCH_3$); 196.92 (C=O).

REFERENCES

[1] G. Surpăţeanu, A. Lablache Combier, M. Constantinescu and J. Marko, *Tetrahedron Letters*, **25**, 5751 (1984).

[2] M. Petrovanu, G. Surpăţeanu, M. Constantinescu and A. Lablache Combier, *Bull. Inst. Politeh. Iaşi*, *31. supl. S II*, **47** (1985).

[3] G. Surpăţeanu and A. Lablache Combier, *Heterocycles* **22**, 2079 (1984).

[4] M. Petrovanu, I. Zugrăvescu and G. Surpăţeanu, *Memoriile Secţiunilor Ştiinţifice Acad. Roumaine*, *S IV*, *T VI*, **1**, *89* (1983).

[5] F. Kronke, *Ber. Dtsch. chem. Ges.*, **68**, 1177 (1935).

[6] F. Kronke, *Ber. Dtsch. chem. Ges.*, **70**, 543 (1937).

[7] J. A. Pople, G. A. Segal, *J. Chem. Phys.*, **44**, 3289 (1966).

[8] R. C. Bingham, M. J. S. Dewar and D. H. Lo, *J. Amer. Chem. Soc.*, **97**, 1285 (1975).

[9] G. Surpăţeanu, M. Constantinescu, C. Luchian, M. Petrovanu, I. Zugrăvescu and A. Lablache Combier, *Rev. Roumaine. Chim.*, **28**, 831 (1983).

[10] G. Surpăţeanu, M. Constantinescu, C. Luchian, M. Petrovanu, I. Zugrăvescu and A. Lablache Combier, *Rev. Roumaine. Chim.*, **28**, 933 (1983).

[11] G. Surpăţeanu, M. Constantinescu and A. Lablache Combier, *Theor. chem. Acta* (in print).

[12] Bruker *XH COORD. AU.* microprogram was used.

[13] G. Surpăţeanu, A. Lablache Combier, P. Grandclaudon and B. Mouchel, *Heterocycles* **26**, 863 (1987).

Revue Roumaine de Chimie, 35, 5, 675–678 (1990)

ON THE PHOTOCYCLISATION OF 1-BENZAMIDO-2-(1-CYCLOHEXENYL)CYCLOHEXENE

A. COUTURE[a], A. LABLACHE-COMBIER [a], G. SURPĂŢEANU [b] and M. CONSTANTINESCU [b]

[a] Laboratoire de Chimie Organic Physique, Bat. C3
Université des Sciences et Technique de Lille, Villeneuve d'Ascq, Cedex 59655, France
[b] Chemistry Department, Polytechnical Institute Iaşi, Splai Bahlui stg. 71, Iaşi 6600, Romania

Received October 20, 1989

By irradiation of 1-benzamido 2-(1-cyclohexenyl) cyclohexene in a Rayonet PR–208 reactor in hexane 2-spirocyclohexyl 3-oxa-4-phenyl-5-azo [4.4.0] bicyclo 1(6),4 decadiene, **7** has been obtained. Using the MINDO/3 procedure method, molecular orbital calculations have been performed. Scheme 3, which takes in consideration an excited amido form **1A** is more probable for a satisfactory explanation of this photocyclisation.

In the previous papers [1,2] it is announced that the dienamides o the type **1a**, were converted, by irradiation, in the oxazines with a spiro-heterocyclic framework **2**. Irradiation was carried out in neutral solvent under nitrogen, in a Rayonet reactor (2537 and 3000 Å).

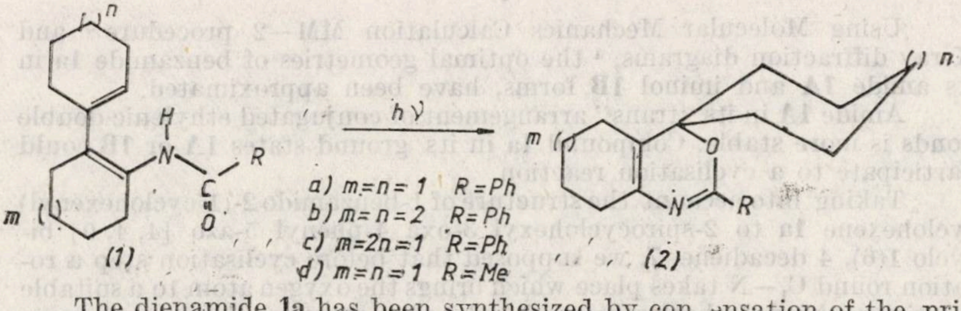

The dienamide **1a** has been synthesized by condensation of the primary amide **3** with 2–(1-cyclohexenyl)cyclohexanone, **4**, as below in the presence of p-toluolsulphonic acid via the carbinol-amide **5**:

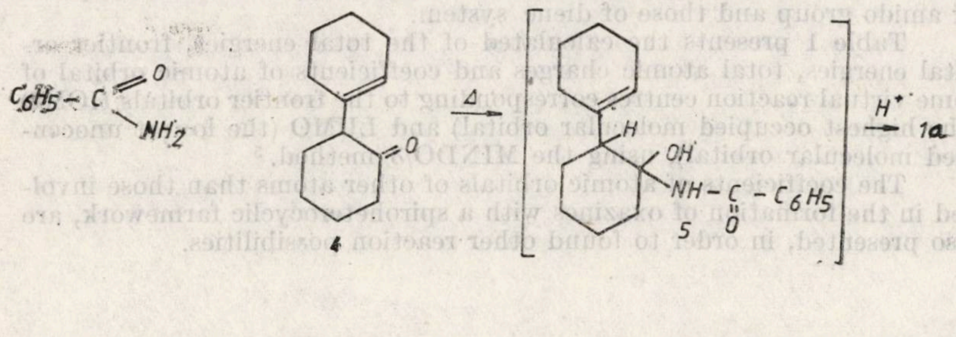

In this paper we present a study on the photocyclization of 1-benzamido 2-(1-cyclohexenyl) cyclohexene **1a** to 2-spirocyclohexyl 3-oxa 4-phenyl 5-azo [4,4,0] bicyclo 1(6),4 decadiene, **7**.

RESULTS AND DISCUSSION

Theoretically, several reaction mechanisms may be proposed in order to explain the photocyclization of dienamide **1a**. We retained two mechanisms, (a) one in which dienamide is involved as an amide structure, (b) the other is the one proposed in our previous paper[1] in which the dienamide reacts in its iminol form.

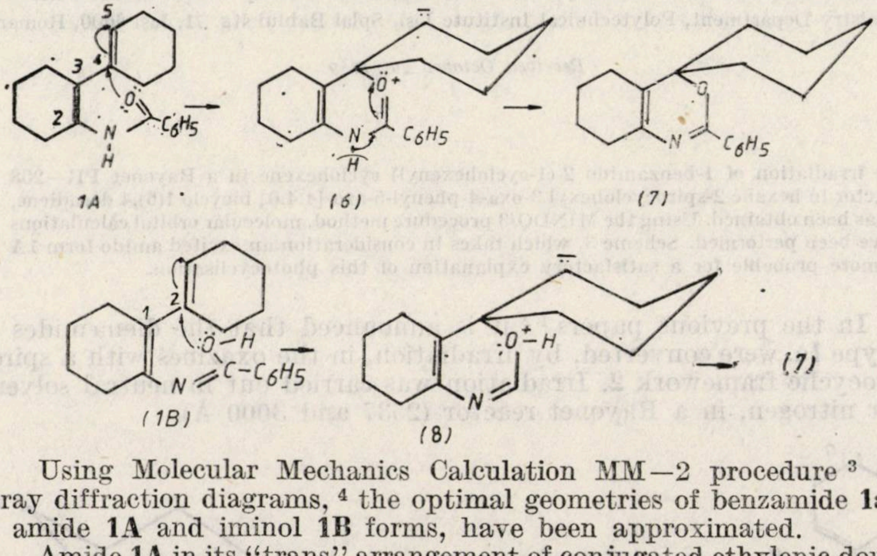

Using Molecular Mechanics Calculation MM—2 procedure[3] and X-ray diffraction diagrams,[4] the optimal geometries of benzamide **1a** in its amide **1A** and iminol **1B** forms, have been approximated.

Amide **1A** in its "trans" arrangement of conjugated ethylenic double bonds is more stable. Compound **1a** in its ground states **1A** or **1B** could participate to a cyclisation reaction.

Taking into account the structure of 1-benzamido 2-(1-cyclohexenyl) cyclohexene **1a** to 2-spirocyclohexyl 3-oxa 4-phenyl 5-azo [4, 4, 0] bicyclo 1(6), 4 decadiene, **7**, we supposed that before cyclisation step a rotation round C_1—N takes place which brings the oxygen atom to a suitable reactive position. In both schemes 3 and 4 after rotation, the oxygen atom as nucleophile reagent attacks the formaly noted C_4 atom of the double bond. This fact is achieved for a rotation angle of 135 °C between the plane of amido group and those of diene system.

Table 1 presents the calculated of the total energies, frontier orbital energies, total atomic charges and coefficients of atomic orbital of some virtual reaction centres corresponding to the frontier orbitals HOMO (the highest occupied molecular orbital) and LUMO (the lowest unoccupied molecular orbital), using the MINDO/3 method.[5]

The coefficients of atomic orbitals of other atoms than those involved in the formation of oxazines with a spiroheterocyclic farmework, are also presented, in order to found other reaction possibilities.

Table 1

The MO calculations of amide and iminol forms of dienamide 1A and 1B respectively by the MINDO/3 method

Amide **1A** Total energy −3234.62 eV = −74593.7 kcal/mol

HOMO −4.6018 eV

orbital	0	C_1	N	C_2	C_3	C_4	C_5
2s	−0.0208	−0.0084	−0.0570	0.0104	0.0117	−0.0219	0.0286
2px	−0.0250	0.0038	0.4076	−0.0825	0.0810	−0.0509	0.0421
2py	−0.0048	−0.0453	0.1918	−0.0269	0·0685	−0.0515	0.0698
2pz	−0.1353	0.0333	−0.3780	0.2876	0.3980	−0.1292	−0.3160

LUMO −2.5823 eV

orbital	0	C_1	N	C_2	C_3	C_4	C_5
2s	0.0583	−0.2412	0.3064	−0.1214	0.0539	0.0466	−0.0312
2px	0.1883	−0.3586	0.0140	0.0917	0.0241	−0.0051	−0.0258
2py	0.1035	−0.0217	0.0592	−0.1641	0.0571	0.0444	−0.0130
2pz	0.0648	0.1812	0.0871	−0.1597	0.1231	0.1233	−0.1950
charge	−1.2704	0.9153	−0.5227	0.1577	−0.0718	0.0253	−0.1150

Iminol **1B** Total energy −3234.49 eV = −74590.6 kcal/mol

HOMO −5.4752 eV

orbital	0	C_1	N	C_2	C_3	C_4	C_5
2s	0.0213	0.0246	−0.0075	−0.0046	−0.0402	0.0278	−0.0352
2px	0.0276	−0.0607	−0.5391	−0.0609	−0.0745	0.0301	−0.0331
2py	0.0888	−0.0553	−0.3351	0.0483	−0.1011	0.0496	−0.0599
2pz	0.0797	0.1217	0.4324	−0.1122	−0.3154	0.0093	0.1439

LUMO −0.3654 eV

orbital	0	C_1	N	C_2	C_3	C_4	C_5
2s	0.0131	0.0246	−0.0068	0.0019	0.0072	0.0311	−0.0253
2px	0.0183	−0.0970	0.0619	0.0028	−0.0047	−0.0170	−0.0187
2py	0.0315	−0.0612	0.0273	0.0088	0.0031	0.0423	−0.0234
2pz	0.0112	0.1244	−0.1227	−0.0297	0.0648	0.0234	−0.0691
charge	−0.7421	0.5688	−0.4496	0.2702	−0.1138	0.1178	−0.1058

Taking into account the data given in Table 1 the following resulted :

The dienamide **1a** in its amide form **1A** is more stable. The lowest difference in energy between the pair HOMO-LUMO is for omide form **1A**.

Briefly, in terms of second order perturbation theory[6] cyclisation is more probable in amide form as a result of the relatively high magnitude of the coefficients of atomic orbital of the atoms O and C_4 in LUMO. The square of the sum of the coefficients of atomic orbitals of oxygen (0.1712) and carbon C_4 (0.0481) as amide form is greater than those of the same atoms O (0.0055) and C_4 (0.0138) in iminol form. Thus, it may be concluded that the dienamide **1a** in its ground state by irradiation is excited in an intermediate form **1A**, which by cyclisation (scheme 3) is transformed into 1-benzamido 2-(1-cyclohexenyl) cyclohexene *1*a, to 2-spirocyclohexyl 3-oxa 4-phenyl 5-azo [4, 4, 0] bicyclol(6),4 decadiene **7**.

EXPERIMENTAL

Cyclisation of 1-benzamido 2-(1-cyclohexenyl) cyclohexène **1a** to 2-spirocyclohexyl 3-oxa 4-phenyl 5-azo [4,4,0] bicyclo 1(6),4 decadiene **7** is realised as follows : in a quartz reactor placed in the centre a photochemical reactor of the Rayonet PR—208 type, 250 ml solution ($5-10^{-3}$M) **1a** are added in hexane. The Rayonet-reactor is equipped with 8 lamps RUL 2537 Å and 3000 Å. The solution is continuously shaken by introduction of a current of argon all time of the irradiation (1.5 hours). The solvent is evaporated by distillation under low pressure and the crude product is chromatographied on the preparative plates of Kisel gel 60, HF—254+366.

By irradiation of 250 mg of dienamide **1a**, 195 mg of spirooxazine **Z** resulted (yield 78 %) mp 978 °C Anal. calculated for $C_{19}H_{23}NO$: C,81.10 ; H, 8.24 ; N,4.98 ; 0,5.69 ; Found : C, 80.93 ; H, 8.18 ; N, 4.85 ; H, 5.96. ^{1}HRMN (CDCl3, δ ppm) : 1.05—2.40 (18H, m, CH_2) ; 7.27.45 (3H, m, arom) 7.95—8.15 (2H, m, arom).

REFERENCES

[1] C. Bochu, A. Couture and A. Lablache-Combier, *Tetrahedron*, **44**, 1959 (1988).

[2] C. Bochu, A. Couture, P. Grandclaudon and A. Lablache-Combier, *J. Chem. Soc., Chem. Commun.*, 1986, 839.

[3] R. Jarret and M. Sounders, "MM2-Program" Yale University (1983).

[4] "Molecule Diagrams Catalogue", M, Section, B, Organic Compounds.

[5] R. C. Bingham, M. S. Dewar and D. H. Lo. ,*J. Amer. chem. Soc.*, **97**, 1285 (1975).

[6] G. Klopman, "Chemical Reactivity and Reaction Paths", John — Wiley, N. Y., 1974.

Revue Roumaine de Chimie, **35**, *5*, 679–682(1990)

SYNTHESIS OF SEVERAL NEW PYRIDINONE DERIVATIVES

FATHY FAHIM ABDEL-LATIF *

Chemistry Department, Faculty of Science, Minia University, Minia, A.R. Egypt

Received January 18, 1988

Several new pyridinone derivatives were obtained *via* the reaction of acrylonitrile derivates (Ia-e) with cyanoacetanilide and N-(2-pyridyl)cyanoacetamide (IIa, b), respectively.

Acrylonitrile and its derivatives are among the most commonly utilised reagents in heterocyclic synthesis $^{1-3}$. In continuation of our work aiming to explore the synthetic potentialities of acrylonitrile derivatives in heterocyclic synthesis, $^{4-6}$ I report here the results of my investigation on the reaction of acrylonitrile derivatives (Ia-e) with cyanoacetanilide (IIa), and N-(2-pyridyl) cyanoacetamide (IIb).

Thus it has been found that compounds (Ia-c) reacted with (IIa) in the presence and/or in the absence of piperidine to yield 1 : 1 adduct. The pyridinone structure (III) was established for the reaction product based on IR and ^{1}H–NMR spectra of the products (cf. Experimental). The formation of (III) is assumed to proceed *via* the addition of the active methylene group of (II) to the cyano group in (I) followed by cyclization by the addition of the amide nitrogen to the other cyano group. Alternately, addition of the amide nitrogen to the cyano group in (I) followed by cyclization by addition of the methylene group to the other cyano group would also lead to the formation of (III) (cf. scheme A).

Similarly, compound (Ia) reacts with (IIb) under the same reaction conditions to yield the pyridinone derivative (IIId). The assigned structure for compound (IIId) was based on grounds similar to those for (IIIa).

On the other hand, compound (Id) reacts with (IIa) in ethanol and in absence of piperidine to yield a product of molecular formula $C_{17}H_{11}N_3O_2S$. The aminopyridinone structure (IVa) was established for the reaction product based on its IR spectrum which reveals the presence of amino function at 3360–3050 cm^{-1}. Any other isomeric product will reveal a different pattern.

The formation of (IV) is assumed to proceed through the addition of the active methylene group of (II) to the cyano group in (I) followed by cyclization by loss of ethanol (c.f. scheme 1). In the same manner, compound (Ie) reacts with (IIa) under the same reaction conditions to yield the pyridinone derivative (IVb), while (Id) reacts with (IIb) in ethanolic piperidine solution to yield the acyclic product (V). The acy-

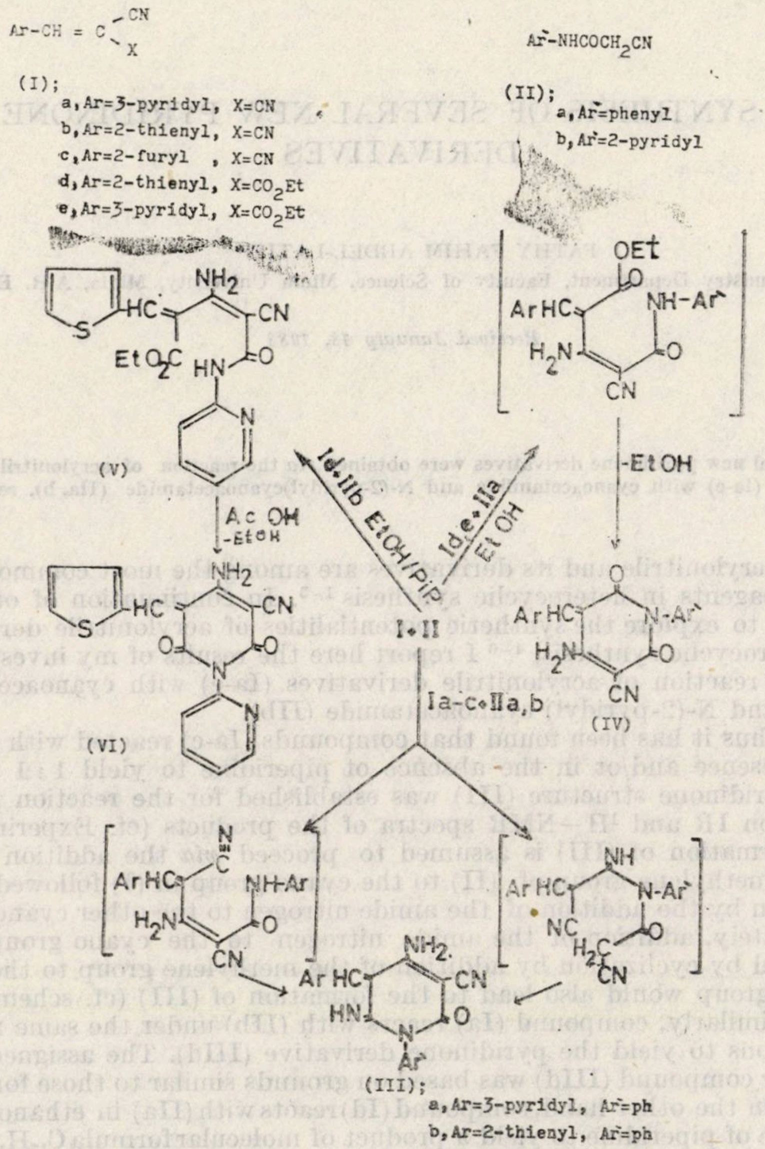
Ar-CH = C(CN)(X)
(I);
a, Ar=3-pyridyl, X=CN
b, Ar=2-thienyl, X=CN
c, Ar=2-furyl , X=CN
d, Ar=2-thienyl, X=CO2Et
e, Ar=3-pyridyl, X=CO2Et
Ar`-NHCOCH2CN
(II);
a, Ar`=phenyl
b, Ar`=2-pyridyl
(V)
Ac OH
-EtOH
(VI)
Ie+IIb EtOH/Pip
Id,e+IIa EtOH
I+II
Ia-c+IIa,b
-EtOH
(IV)
(III);
a, Ar=3-pyridyl, Ar`=ph
b, Ar=2-thienyl, Ar`=ph
c, Ar=2-furyl , Ar`=ph
d, Ar=3-pyridyl, Ar`=2-pyridyl

Scheme 1

clic adduct (V) could be cyclised into the pyridinone derivative (VI) on refluxing in acetic acid-ammonium acetate mixture.

EXPERIMENTAL

All melting points are uncorrected. IR spectra were recorded (KBr) with a Schimadzu 400 spectrophotometer. ^{1}H-NMR were measured on a Varian EM-390-90 MHz in DMSO using

Table 1

Characterisation of the newly synthesised compounds

Compound no.	m.p.(°C) solvent	yield %	Mol. formula	Analysis (calc/found) (%)				IR (KBr) υcm^{-1}	^{1}H-NMR (DMSO) δppm
				C	H	N	S		
IIIa[a]	280 DMF/H20	80	C18H13N5O	68.5 69.9	4.1 4.5	22.2 21 8		3400, 3150 (NH2, NH), 2200(CN), 1680–1660(CO, C=N)	3.4 s(, 3H, NH2, NH), 7.6–8.9 (m, 10H, ph, pyridinyl and CH)
IIIb[b]	195 EtOH	70	C17H12N4OS	63.7 64.0	3.7 3.9	17.5 17.5	10.0 9.8		
IIIc[b]	210 EtOH	50	C17H12N4O2	67.1 67.5	3.9 3.7	18.4 18.0			3.3 (s, 3H, NH2, NH) 6.9–8.5 (m, 9H, ph, furyl and CH)
IIIc[d]	280 DMF/H20	80	C17H12N6O	64.5 64.5	3.7 3.7	26.5 27.0			3.3 (s, 3H NH2, NH) 6.5–9.0 (m, 9H, pyridinyl and CH)
IVa[c]	195 EtOH	50	C17H11N3O2S	63.5 64.5	3.4 3.7	13.0 12.9	9.9 10.1	br 3360–3050 (NH2) 2200 (CN), 1690 ring CO	3.3 (s, 2H, NH2), 7 – 8.6 (m, 9H, ph, thienyl and CH)
IVb[a]	215 EtOH	70	C18H12N4O2	68.3 68.1	3.7 3.9	17.7 18.1			
V[d]	190 EtOH	70	C18H16N4O3S	58.6 59.1	4.3 4.7	15.2 15.0	8.6 9.0	br 3360–3060 (NH2, NH), 2200 (CN), br 1715–1670 (ester and ring CO)	1.1 (t, 3H, CH3), 3.2 (s, 2H, NH2), 4.3 (q, 2H, CH2), 7.3–8.7 (m, 8H, pyridinyl, thienyl and CH)
VI[c]	179 AcOH	40	C16H10N4O2S	59.6 59.9	3.1 3.1	17.3 16.9	9.9 9.6	br 3350–3150 (NH2), 2200 (CN), 1680–1660 ring (CO).	

[a] colourless crystals ; [b] brown crystals ; [c] yellow crystals ; [d] red crystals.

TMS as internal standard and chemical shifts are expressed as δppm. Analytical data were obtained from the analytical data unit at the Cairo University.

Reaction of (Ia-e) with (IIa, b)

General Procedure: To a solution of (Ia-e) (0.01 mol) in ethanol (50 mL), (IIa) or (IIb) was added in the presence and/or in the absence of piperidine (1 mL). The reaction mixture was heated under reflux for 4 h, then evaporated *in vacuo*. The solid product, so formed was collected by filtration, and crystallised from the proper solvent (c.f. Table 1).

Cyclisation of (V): To a solution of (V) (0.05 mol) in acetic acid (50 mL), ammonium acetate (0.04 mol) was added. The reaction mixture was boiled under reflux for 3 h. The solid so formed was collected by filtration, and crystallised from acetic acid.

REFERENCES

[1] M. H. Elnagdi, H. A. Elfahham and G. E. H. El-gemeie, *Heterocycles*, **20**, 519, 1982.

[2] H. Junek, P. Wibbmer, and B. Thierrichter, *Synthesis*, **1977**, 560.

[3] M. H. Elnagdi, *Tetrahedron*, **30**, 2791, (1974).

[4] A. M. Fahmy, M. Z. A. Badr, Y. S. Mohamed, and F. F. Abdel-Latif, *J. Heterocyclic Chem.* **21**, 1233 (1984).

[5] F. F. Adbel-Latif, A-K. M. N. Gohar, A. M. Fahmy, and M. Z. A. Badr, *Bull. Chem. Soc. Jpn*, **59**, 1235, (1986).

[6] F. F. Abdel-Latif, H. A. Regila, A-K. M. N. Gohar and Y. S. Mohamed, *Indian J. of Chem* **24B**, 775, (1985).

Revue Roumaine de Chimie, 35, 5, 683–689 (1990)

CARBONIC ANHYDRASE INHIBITORS. III[1]

RELATIONS BETWEEN CHEMICAL STRUCTURE OF INHIBITORS AND ACTIVATORS

IOAN PUŞCAŞ[a], CLAUDIU SUPURAN[a],* and GHEORGHE MANOLE[b]

[a]Hospital Şimleu Silvaniei, G. Coşbuc str. 29A, 4775 Şimleu Silvaniei, Romania
[b]Builder's Clinical Hospital, Bucharest, Romania

Received December 20, 1989

Close correlations were found between stereochemical/electronic requirements of sulfonamides, RSO_2NH_2 (carbonic anhydrase inhibitors) and substituted ethylamines, $R-CH_2-CH_2-NH_2$ (carbonic anhydrase activators). The nature of R is critical for both inhibition and activation of enzyme.

1. INTRODUCTION

Inhibition of carbonic anhydrase (CA) was extensively studied since the discovery of the first inhibitor, sulfanilamide, by Mann and Keilin. [2] Subsequently, a large number of inhibitors was prepared and some drugs were developed for use in clinical medicine as diuretics, antiglaucoma and antisecretory agents, in the treatment of gastro-duodenal ulcers. [3–5] In contrast, activation of this enzyme is rarely taken into account. It was only recently proved by Puşcaş et al. that histamine [6] and catecholamines [7] are CA activators, both *in vitro* and *in vivo*. This activation could be responsible for important physiological secretory processes. [6,12]

In this paper we report a generalization of the study of CA activators, and some correlations we found between the chemical structure of activators and inhibitors of this enzyme.

The following classes of compounds were tested for activatory/inhibitory action on CA : (i) aliphatic amines and their derivatives, and aliphatic sulfonamides, respectively ; (ii) aromatic amines and catecholamines, and aromatic sulfonamides, respectively, and (iii) heterocyclic amines, derivatives of ethylamine, and heterocyclic sulfonamides, respectively.

2. EXPERIMENTAL

Carbonic anhydrase inhibition/activation was determined by the method of Maren et al. [8] This is a changing pH indicator method which monitors the inhibition/activation of CA catalyzed hydration of CO_2. The assay was carried out at 4 °C in a special CO_2 bubbler cell. The concentration of enzyme in the system (E_0) was approximately $5 \cdot 10^{-9}$ M. The SEI (substrate — enzyme — inhibitor) technique was used; in the assay cell were added 0.3 mL deionized water, 0.4 mL phenol red indicator solution, 0.1 mL solution of the tested compound, approximately 2 EU of CA and 0.1 mL buffer solution (0.3 M Na_2CO_3 ; 0.2 M $NaHCO_3$). With a stopwatch was recorded the time to obtain a colour change (pH 7.2). Stock solutions of the tested compounds were prepared (10^{-3} M) in deionized water and successive dilutions were obtained thereafter. Erythrocyte bovine CA from Boehringer Mannheim was the source of enzyme. The provenience of the tested compounds was as follows : aliphatic amines and their derivatives, 2-phenyl-ethylamine, benzylamine, 2-pyridylethylamine, 5-methyl-histamine, serotonin and (R)-adrenaline were from Merck; histamine was from Fluka; sulfonamides, catecholamines, dopamine and ephedrine from Terapia — Cluj and the Drug Factory Bucharest; 2-(5-amino-1,3,4-thiadiazolyl)-ethylamine was prepared by literature procedures. [9]

---

* Correspondence author.
Present address: University of Bucharest, Dept. Organic Chemistry, Bd. Republicii 13, Bucharest 1, Romania

3. RESULTS AND DISCUSSION

Aliphatic sulfonamides do not inhibit the enzyme. [3a] We found that aliphatic amines and their derivatives with the general formula $R-CH_2-CH_2-NH_2$ have no effect on CA activation. The tested compounds are given in Table 1:

Table 1

$R-CH_2-CH_2-NH_2$

Structure	R	Compound
1	H	ethylamine
2	CH_3	*n*-propylamine
3	CH_3CH_2	*n*-butylamine
4	OH	ethanolamine
5 a	NH_2	ethylenediamine
5 b	SH	cysteamine

As was previously shown, [2,3] aromatic sulfonamides are strong CA inhibitors. As a counterpart for the activation of CA, the following aromatic amines, and their derivatives, were tested: benzylamine, 2-phenylethylamine, dopamine, ephedrine, adrenaline and one of its isomers (compound **10**) and noradrenaline (Table 2). With the exception of benzylamine, these compounds have the general formula:

$$R-CHR^1-CHR^2-NHR^3 \quad (I)$$

Benzylamine has no effect as CA activator. The other compounds (**6**—**11**) are enzyme activators, as may be seen in Fig. 1, where is represented concomitantly the inhibition of CA by sulfanilamide and *p*-toluene-sulfonamide. The presence of hydroxy groups at the aromatic and/or aliphatic fragment of the molecule enhances the potency of the given compound as enzyme activator. Substitution at the nitrogen atom with a methyl group (compounds **9** and **11**) seems to be without effect on the activatory power of these compounds.

Table 2

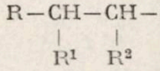

$$\underset{R^1}{R-CH}-\underset{R^2}{CH}-NH-R^3$$

(I)

No.	R	R¹	R²	R³	Compound
6	Ph	H	H	H	2-phenylethyl-amine
7	$3,4-(HO)_2C_6H_3$	H	H	H	dopamine
8	idem	OH	H	H	noradrenaline
9	idem	OH	H	CH_3	adrenaline ((R)-isomer)
10	idem	OH	CH_3	H	—
11	Ph	OH	CH_3	CH_3	ephedrine

Heterocyclic sulfonamides [3] and their metal complexes [10] are among the strongest CA inhibitors. Acetazolamide (5-acetylamino-1, 3, 4-thiadiazole-2-sulfonamide) and ethoxzolamide (6-ethoxy-benzothiazole-2-sulfonamide) among others, are extensively used in clinical medicine. In consequence, heterocyclic derivatives of ethylamine were tested as CA activators. The following compounds, with the general formula $R-CH_2-CH_2NH_2$, were tested (Table 3): 2-pyridyl-ethylamine, histamine, 5-methylhistamine, 2-(5-amino-1, 3, 4-thiadiazolyl)-ethylamine, and serotonin.

All these compounds activated the enzyme, as may be seen in Fig. 2, where is also represented the inhibition of CA by acetazolamide and ethoxzolamide. The strongest activation was achieved with histamine and the thiadiazole derivative, **15**. 5-Methylhistamine and 2-pyridylethylamine (**14** and **12**) are strong activators, but not as potent as the previous compounds. The weakest activator was serotonin (**16**).

One may suppose that some sterical and electronic factors are necessary to act in concert for an enzymatic activation to occur. It is obvious from Figs. 1 and 2 that heterocyclic derivatives of ethylamine are more potent activators of CA than the carbocyclic compounds. This is also the situation for CA inhibitors (heterocyclic vs. aromatic sulfonamides). The presence of a heteroatom in the radical R, both for sulfonamides RSO_2NH_2, and for amines with the formula (I), seems to assure a better interaction between the active site of the enzyme and the inhibitor/activator, whence the greater activity of such compounds. This happens also in the case of derivatives of 2-phenylethylamine, substituted at the benzene nucleus with hydroxy groups; compounds **7**—**10** are stronger activators than the parent, unsubstituted amine (**6**). But too bulky a substituent R), even heterocyclic, leads to a weak activator: serotonin (**16**) is approximately as potent as 2-phenylethylamine (**6**). This is different from inhibitors, where bicyclic sulfonamides (ethoxzolamide) are stronger inhibitors than mono(hetero)cyclic sulfonamides (acetazolamide or sulfani-

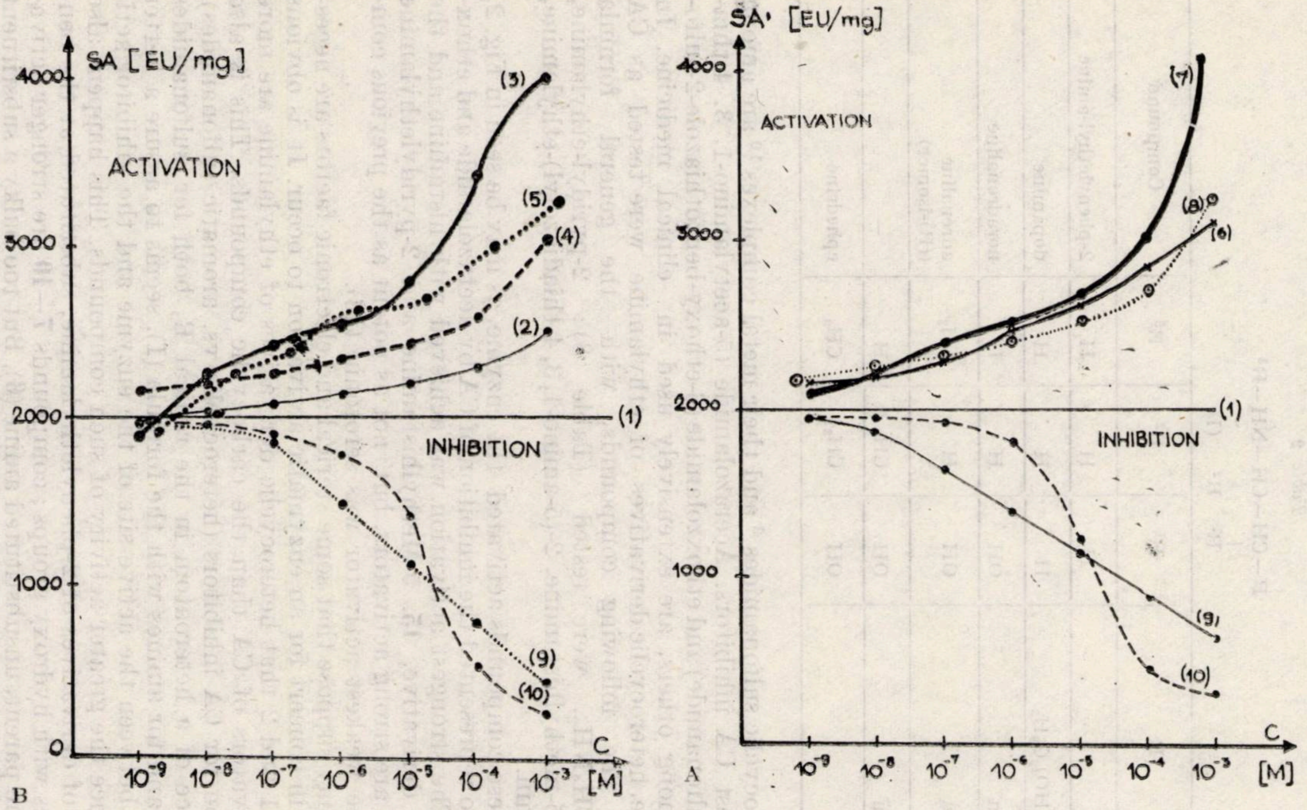

Fig. 1. — Activation/inhibition curves: aromatic amines and catecholamines/aromatic sulonamides; SA — specific activity (EU/mg) vs. concentration of activator/inhibitor (M): A. (1) uncatalyzed reaction; (2) phenylethylamine (**6**); (3) dopamine (**7**); (4) noradrenaline (**8**); (5)ephedrine (**11**); B. (6) racemic adrenaline (**9**) ;(7) (*R*)-adrenaline (**9**); (8) compound **10**; (9) *p*-toluene-sulfonamide; (10) sulfanilamide.

Table 3

$R-CH_2-CH_2-NH_2$

No.	R	Compound
12	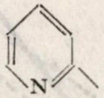	2-pyridylethylamine
13	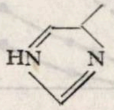	histamine
14	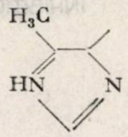	5-methylhistamine
15	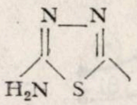	2-(5-amino-1,3,4-thiadiazolyl)-ethylamine
16	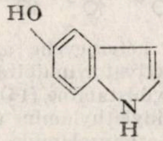	serotonin

lamide). The presence of methyl groups in the positions 1 or 2 (R^1 or R^2) or at the nitrogen atom (R^3) in the molecule of amines (I) seems to be without too great an effect on the activation potency of these compounds; **7**—**11** possess almost the same activity. The same is true when R^1 is OH. Finally, stereochemically pure adrenaline (R-enantiomer) is twice as active than the racemic adrenaline (curves 6 and 7 in Fig. 1B).

One may conclude that compounds with the general formula (I), where the nature of the substituents is as follows: R is an aromatic, hydroxy-substituted-aromatic, or heterocyclic radical; R^1 is H, OH or CH_3; R^2 and R^3 are H or CH_3, are CA activators.

The mechanism of action of these compounds is unknown, but we presume that they interact with the active site of the enzyme, intervening in the catalytic cycle. A recent paper of R. Hoffman and Dewar's groups,[11] using AM1 calculations focused on the mechanism of intramolecular proton transfer in the catalytic cycle of CA. It was shown that this is the determining step for the catalytic mechanism. We speculate that the CA activators interact with the active site of the enzyme and more precisely

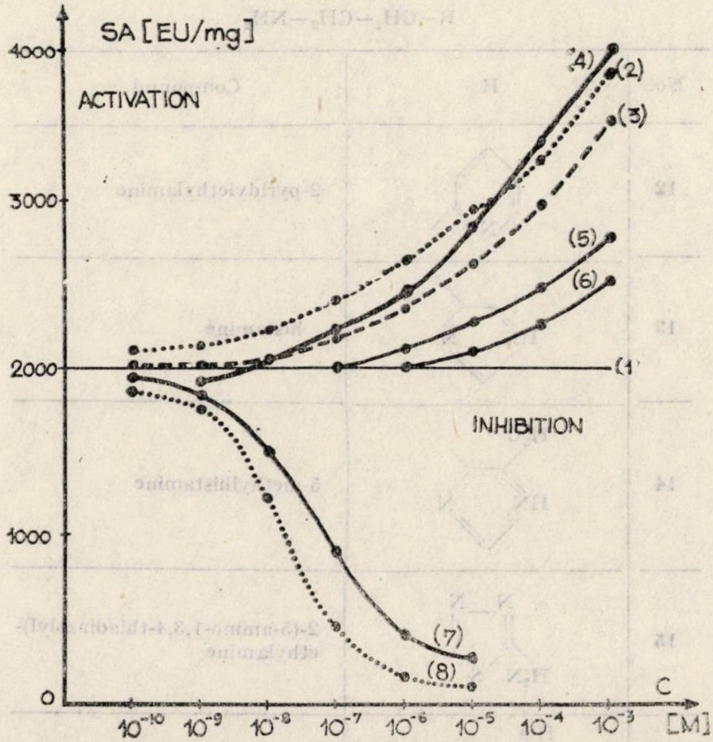

Fig. 2. — Activation/inhibition curves : heterocyclic amines/heterocyclic sulfonamides ; SA vs. concentration of activator/inhibitor. (1) uncatalyzed reaction ; (2) histamine (**13**) ; (3) 5-methylhistamine (**14**) ; (4) 2-amino-1,3,4-thiadiazolyl)ethylamine (**15**) ; (5) 2-pyridylethylamine (**12**) ; (6) serotonin (**16**) ; (7) acetazolamide ; (8) ethoxzolamide.

with the Zn^{2+} ion of it, and act at this point of the catalytic cycle, facilitating the proton transfer (if one considers the enzyme — activator complex as a "molecule", and consequently, this proton transfer as an intramolecular process). As in the case of the inhibition mechanism of CA, additional studies are needed to verify our hypothesis.

Note added in proof. At the suggestion of prof. Raja Khalifah (Univ. of Kansas), the activation experiments were carried out with a slight modification of the buffer, which contained Na_2CO_3 and $NaHCO_3$, as described in the experimental section, plus 10^{-3} MEDTA, disodium salt, in order to rule out the possibility that histamine or ohter amine of type (I) may complexate heavy ions, possibly present in traces in the assay system) which exert an inhibitory action on CA. The chelating agent added in a great excess supresses the possibility of artefacts due to such accidental contaminations. The results of experiments performed in these conditions were essentially similar with those described in this paper, suggesting once again that activation of CA is a phenomenom *per se,* and not an anterfact due to experimental irregularities.

ACKNOWLEDGEMENT. Special thanks are addressed to biol. Olimpia Nagy for help with the enzymatic determinations, and to Ms. Elena Petre for qualified secretarial assistance.

REFERENCES

[1] Part II, C. Supuran, A. T. Balaban, M. D. Gheorghiu, A. Schiketanz, A. Dinculescu and I. Puşcaş, *Rev. Roumanie Chim.*, **35**, 398 (1990).
[2] T. Mann and D. Keilin, *Nature*, **146**, 164 (1940).
[3] T. H. Maren, *Physiol. Rev.*, **47**,595 (1967).
[3a] T. H. Maren and C. E. Wiley, *J. Med. Chem.* **11**, 228 (1968).
[4] S. Lindskog and P. J. Wistrand, "Inhibitors of Carbonic Anhydrase", in "Design of Enzyme Inhibitors as Drugs", M. Sandler Ed., Oxford University Press, Oxford, 1987.
[5] I. Puşcaş, *Ann. N. Y. Acad. Sci.* **429**, 587 (1984).
[6] I. Puşcaş, G. Buzas, P. Contraşiu and P. Suranyi, *Rev. Roumaine Biochim.*, **16**, 317 (1979).
[7] I. Puşcaş, G. Buzas, A. Moldovan, A. Resnicek, D. Milaş, F. Perşa, R. Nemeş-Brateş and E. Kovacs, *Rev. Roumaine Biochim.* **22**, 225 (1985).
[8] T. H. Maren, V. I. Ash and E. M. Bailey Jr., *Bull. Johns Hopkins Hosp.*, **95**, 244 (1954).
[9] M. Ohta, *J. Pharm. Soc. Japan*, **72**, 1636 (1952).
[0] C. Supuran, M. Andruh and I. Puşcaş, *Rev. Roumaine Chim.*, **35**, 393 (1990).
[11] K. M. Merz, R. Hoffmann and M. J. S. Dewar, *J. Amer. Chem. Soc.*, **111**, 4636 (1989).
[12] I. Puşcaş, "Carbonic Anhydrase Inhibitors in the treatment of Gastric and Duodenal Ulcers", in "New Pharmacology of Ulcer Disease", S. Szabo and Gy. Moszik Eds., Elsevier, New York, 1987.

NOTE POUR LES AUTEURS

La Revue Roumaine de Chimie publie des articles en anglais, français, russe, allemand ou espagnol. Les auteurs sont priés d'envoyer des articles et des comptes rendus inédits.

Les manuscrits seront dactylographiés à double interligne. La bibliographie, les tableaux et la légende des figures seront placés après le texte.

Si l'article fait partie d'une série numérotée, la partie précédente sera donnée comme première référence.

Chaque article sera précédé d'un résumé comprenant quinze lignes au maximum.

Les références bibliographiques dans le texte seront faites par des exposants sans parenthèses et paraîtront à la fin de l'ouvrage.

Les publications périodiques mentionnées dans la bibliographie seront présentés suivant les prescriptions internationales : le nom de l'auteur précédé de l'initiale du prénom, le titre du périodique abrégé conformément à « Chemical Abstracts » et souligné par une ligne, le numéro du tome indiqué par des chiffres arabes et souligné par deux lignes, suivi de la première page de l'article ; à la fin, l'année de la parution sera placée entre parenthèses. Le numéro de la revue ne sera pas indiqué si les pages du volume sont numérotées consécutivement.

Les textes des livres ou traités inclueront : le nom des auteurs, précédé de l'initiale du prénom, le titre du livre entre guillemets et sans être souligné, le numéro du tome précédé par l'abréviation « vol. » (ou « Ed. »), le numéro de l'édition, les éditions (the publisher), la localité de la parution du livre, l'année de la parution et la page de la référence précédée (s) par l'abréviation « p. » (ou « S. »).

Les brevets seront indiqués comme suit : l'auteur ou la firme, le pays et le numéro du brevet, la date et la revue *(Chem. Abstr.)* Par/ex. : M. Jones (to Union Carbide Co), Brit. Pat. 601 238, 2 Sept. 1959 ; ef. *Chem. Abstr.*, **24**, 12808 (1960).

Si la référence n'a pas été lue en original, on indiquera aussi la revue de référence consultée.

Les diagrammes seront tracés à l'encre de Chine sur papier calque. Les tableaux et les figures (en nombre strictement nécessaire) ainsi que les courbes dans les figures seront numérotés par des chiffres arabes. Leur explication sera donnée dans la légende des figures. Prière de ne pas inscrire les mêmes données dans les tableaux et les figures. Chaque tableau aura un titre. On indiquera dans le texte la place approximative des tableaux et des figures. Les formules chimiques seront incluses dans le texte ; en outre, elle seront transcrites sur papier calque, à l'encre de Chine.

Les auteurs sont priés d'indiquer les caractères italiques (en soulignant les lettres au crayon), ainsi que tout autre caractère spécial ; les préfixes *ortho*, *meta*, *para*, *cis*, *trans*, etc. seront soulignés pour indiquer leurs caractères italiques et ne seront jamais écrits avec des majuscules.

Aucune correction à la main ne sera admise sur le manuscrit. Les corrections seront tapées à la machine. Les lettres grecques ou d'autres symboles spéciaux seron insérés à la main à l'encre clairement.

Le manuscrit sera signé par l'auteur.

Le titre-courant aura 50 lettres au maximum.

L'entière responsabilité du contenu des articles appartient aux auteurs.

Sur demande ou peut obtenir une note plus complète.

PRINTED IN ROMANIA

TRAVAUX PARUS AUX ÉDITIONS DE L'ACADÉMIE ROUMAINE

I. G. MURGULESCU, **Introducere în chimia fizică, vol. I, 1. Atomi, molecule, legătură chimică**, 1976, 560 p.

I. G. MURGULESCU, V. EM. SAHINI, **Introducere în chimia fizică, Vol. I, 2. Structura și proprietățile moleculelor**, 1979, 604 p.

I. G. MURGULESCU, E. SEGAL, **Introducere în chimia fizică, Vol. II. 1. Teoria molecular-cinetică a materiei**, 1979, 1036 p.

I. G. MURGULESCU, TATIANA ONCESCU, E. SEGAL, **Introducere în chimia fizică, Vol. II. 2. Cinetică chimică și cataliză**, 1981, 1024 p.

I. G. MURGULESCU, J. PĂUN, **Introducere în chimia fizică, Vol. I. 3. Nucleul atomic, reacții nucleare, particule elementare**, 1982, 606 p.

I. G. MURGULESCU, RODICA VÎLCU, **Introducere în chimia fizică. Vol. III. Termodinamica chimică**, 1982, 624 p.

I. G. MURGULESCU, O. M. RADOVICI, **Introducere în chimia fizică, Vol. IV. Electrochimia**, 1986, 416 p.

R. VÎLCU, M. LECA, **Polymer Thermodynamics by Gas Chromatography**, coedition avec Elsevier, 1990, 204 p.

F. CUIBAN, A. X. XENIA, **Studiul structurii și sinteza peptidelor**, 1989, 282 p.

CRISTOFOR I. SIMIONESCU, VALERIA GORDUZA, **Implicații bioenergetice ale coloranților**, 1988, 208 p.

R. VÎLCU, M. LECA, **Termodinamica polimerilor prin cromatografie de gaze**, 1987, 238 p.

I. ZUGRĂVESCU, M. PETROVANU, **Cicloadiții 3+2 dipolare**, 1987, 446 p.

RAUL MIHAIL, ION GROZEANU, **Estimarea secvențială aplicată sistemelor chimice**, 1986, 406 p.

M. BREZEANU, I. PATRON, M. ANDRUH, **Combinații complexe polinucleare și aplicațiile lor**, 1986, 244 p.

A. T. BALABAN et al., **Labelled Compounds and Radiopharmaceuticals Applied in Nuclear Medicine**, coédition avec John Wiley and Sons, 1986, 742 p.

D. PURDELA, **Nomenclatura chimiei organice — IUPAC**, 1986, 451 p.

PETRU BUDRUGEAC, **Probleme de chimie**, 1986, 280 p.

T. ONCESCU, S. G. IONESCU, **Conversie fotochimică și stocare de energie**, 1985, 272 p.

V. DRĂGUȚAN, A. T. BALABAN, M. DIMONIE, **Olefin Metathesis and Ring-Opening Polymerization of Cyclo-Olefins**, coédition avec John Wiley and Sons, 1985, 544 p.

C. LITEANU, I. RÎCĂ, **Optimizarea proceselor analitice**, 1985, 360 p.

N. PETRESCU, **Chimia extracției cu solvenți și aplicații**, 1985, 212 p.

1991 APR 0 5

ISSN 0035—3930

Universul c. 2072

43 426

Lei 40

F.1103

ACADÉMIE ROUMAINE

REVUE ROUMAINE DE CHIMIE

TOME 35

N° 6

Juin 1990

Rev. Roumaine Chim.

RRCHAX, 35, *6*, p. 691–800 (1990), Bucarest

EDITURA ACADEMIEI ROMÂNE

ACADÉMIE ROUMAINE

COMITÉ DE RÉDACTION

Rédacteur en chef :

I. G. MURGULESCU, membre de l'Académie Roumaine

Rédacteurs en chef adjoints :

A. T. BALABAN et V. EM. SAHINI, membres de l'Académie Roumaine.

Collège de rédaction :

EM. BRATU, ECATERINA CIORĂNESCU-NENITZESCU, P. SPACU, CR. SIMIONESCU, membres de l'Académie Roumaine ; M. ANDRUH, M. BANCIU, M. D. GHEORGHIU, I. HAIDUC, D. I. MARCHIDAN, G. NIAC et D. SĂNDULESCU

La Revue Roumaine de Chimie paraît 10 fois par an. Toute commande de l'étranger sera adressée à ROMPRESFILATELIA — sectorul Export-Import Presă, P. O. Box 12—201, télex 10376, prsfi r 78 104 Bucarest, Calea Griviţei nr. 64—66, Bucureşti, Roumanie

Les manuscrits, les livres et les revues proposés en échange, ainsi que toute correspondance seront envoyés à la rédaction

REVUE ROUMAINE DE CHIMIE

125, Calea Victoriei, 79717 Bucarest, Roumanie, téléphone 50 76 80

EDITURA ACADEMIEI ROMÂNE

125, Calea Victoriei, 79717 Bucarest, Roumanie, téléphone 50 76 80

REVUE ROUMAINE DE CHIMIE

Tome 35, N° 6 **Juin 1990**

F. G. BĂNICĂ, Voltammetric study of a catalytic electrode process with parallel complexation reaction. Reduction of nickel ion in the presence of nicotinamide 693–699

M. ABD EL MOTTALB and M. G. ABD EL WAHED, Electrical conductivity of some zincon complexes 701–706

P. L. LÓPEZ-DE-ALBA and A. VERGARA, Potentiometric determination of thorium (in Spanish) 707–711

MĂRIUCA GARTNER, NICOLAE STĂNICĂ and MIHAI VASS, Ellipsometric spectroscopy of pure and of oxygen and carbon monoxide-covered copper films 713–720

VASILE COCHECI, GHEORGHE PETCA and EUGEN GLÜCK, Studies concerning calcium carbonate scales formation and its prevention . II. Prevention by inhibitor addition 721–729

FLORICA ZĂLARU, ADALGIZA CIOBANU, ION BACIU and CARMEN PETREA, Coordination compounds of some “3d” metals with formylated derivatives of carvone and menthone 731–737

MIRCEA D. BANCIU, FILIP CHIRALEU and ANDREIA CIOBANU, Heterocycles with annelated dibenzocycloalkane skeletons. IV. Pyrazoles with annelated 7H-dibenzo[*c*,*e*]cycloheptene skeleton 739–745

HORIA PETRIDE, Mesoionic oxazolones. V. Ethanolysis and aminolysis of acylated compounds 747–755

VASUDEVA A. ADHIKARI and VIRUPAX V. BADIGER, Synthesis and biological activities of some new isoxazolo[5,4-d]pyrimidine derivatives . . . 757–765

I. GĂNESCU, CS. VÁRHELYI, I. ZSAKÓ und M. PREDA, New tetrathiocyanato-diamine chromates(III) with imidazole and benzimidazole (in German) 767–775

M. M. BADRAN, A. K. EL-ANSARI and S. EL-MELIGIE, Novel substituted-aminocoumarins as potential antimicrobial agents 777–783

AMIN A. AFIFY, A. A. EL-KHAMRY, A. Y. SOLIMAN, M. A. SAYED and E. A. KASSAB, Behaviour of 5,6-diphenyl-4-carbethoxy-2,3-dihydropyridazin-3-one, towards some different nucleophiles 785–789

TĂNASE VOLINTIRU, FRANCISC M. ALBERT, MARIA GIURGINCA and GHEORGHE IVAN, The effect of aromatic diamine + quinone-diimine couples in isoprene rubber 791–799

|Rev. Roumaine Chim.| **35**, *6*, 691–800 (1990), Bucarest

Revue Roumaine de Chimie, **35**, *6*, 693–699 (1990)

VOLTAMMETRIC STUDY OF A CATALYTIC ELECTRODE PROCESS WITH PARALLEL COMPLEXATION REACTION. REDUCTION OF NICKEL ION IN THE PRESENCE OF NICOTINAMIDE

F. G. BĂNICĂ

Polytechnic Institute of Bucharest, Dept. of Analytical Chemistry, Spl. Independenței 313,
Bucharest, Romania

Received November 20, 1989

The reduction of nickel ion on the static mercury-drop electrode in the presence of nicotinamide was studied by linear-scan voltammetry. Under these conditions the main nickel peak is preceded by a wave due to reduction of nickel ion catalyzed by nicotinamide ($E_{1/2} = -0.78$ V vs. SCE). The catalytic reduction is a steady-state process if the the scan-rate is low and the nickel ion is in excess. It was assumed that the complex NiL^{2+} ($L =$ nicotinamide) is the reducible species and the regeneration of this compound by a chemical reaction gives the electrode process the catalytic character. The kinetic equations founded on this mechanism are in fair accord with the experimental data and enable to calculate the equilibrium ($\log K_1 = 3.45$) and rate (about 1.2×10^4 mole^{-1} l s^{-1}) constants for the formation of NiL^{2+}.

Since the pioneering work of Mark and Reilley[1] the catalytic reduction of nickel or cobalt ion in presence of some ligands has deserved much attention. In this kind of electrode process, the actual depolarizer is a complex which forms only a minor part of the total metal-ion content. The reduction of this complex (at potentials less negative than the half-wave potential of the hydrated ion) delivers the free ligand which becomes able to bind another ion, thus regenerating the reducible species. As already pointed out[2], the rate of water exchange in the coordination sphere of the nickel ion is very low. Consequently, the formation of the reducible complex determines, to a high extent, the overall rate of the electrode process.

Despite the apparent simplicity of the reaction mechanism, some additional features hindered the development of a general theoretical treatment of the catalytic waves of nickel or cobalt. The main difficulties arise from the effects of the double-layer and the adsorption of the ligand-catalyst (see e.g. [3]). An additional complication is due to the variation of the adsorption coefficient with the potential. In this case, the catalytic wave assumes a peculiar, maximum-shaped feature.[4,5]

It is, therefore, important to find some systems where these complications are not present or, at least, are negligibly small. In this respect, an electrochemical technique with a time-scale lower than that of polarography appears to be promising, due to the minimization of the adsorption effects. This is why in this work the linear-scan voltammetry was used to study the catalytic reduction of nickel on the static mercury-drop electrode (SMDE) in the presence of nicotinamide (NA). Like pyridine, this compound gives a polarographic catalytic nickel prewave.[6] The reduction of NA does not interfere since at pH > 2 it occurs at potentials more negative than that of nickel ion reduction.[7] AC polarography failed to detect the adsorption of NA on the dropping mercury electrode.[8]

EXPERIMENTAL

NA (technical grade) was purified by recrystallization from ethanol. The purified product contains 99.5% NA (assessed by potentiometric titration). Other reagents used were of p.a. grade. A buffer system composed of CH_3COONa and Na_2HPO_4 (0.024 M both) was used as supporting electrolyte. The pH was adjusted with perchloric acid.

The SMDE (drop area, 2.5 mm^2) was built in our laboratory according to Novotny.[9] A saturated calomel electrode was used as reference and a platinum plate as auxiliary electrode. Conventional potentiostatic equipment was used to record the voltammograms at scan-rates < 0.1 Vs^{-1}. The experiments were run at 20°C.

RESULTS

The effect of NA on the reduction of nickel ion is shown in Fig. 1. While in absence of NA only the diffusion-controlled nickel peak is recorded (curve 1), the presence of NA induces a peculiar pattern at less negative potentials (curves 2 — 5). The shape of this pattern strongly resembles the irreversible cathodic wave recorded under steady-state conditions. This observation was confirmed by plotting $\ln[i/(i_l - i)]$ vs. E, as usually in DC polarography. The results of these plots are given in Table 1.

The limiting current is much higher than the current due to the simple reduction of a nickel-NA complex, even if it is assumed that the ligand is totally bound in this species. Thus, the catalytic character of the electrode process observed in presence of NA is clearly proved. Therefore, the voltammetric pattern recorded at potentials ranging between -0.6 and -0.9 V will be further termed as the catalytic nickel wave (CNW).

The occurrence of the steady-state during the catalytic reduction of nickel is also demonstrated by the cyclic voltammogram recorded in the region of the CNW (the inset in Fig. 1). The absence of important hysteresis on this record proves the fast regeneration of the reducible species.

The height of the main nickel peak is directly proportional to the square-root of the scan-rate. Conversely, the limiting current of the CNW

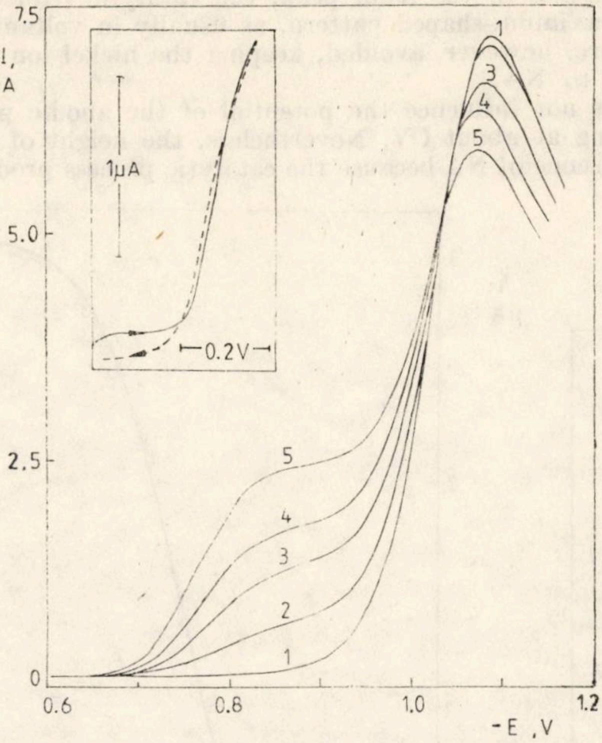

Fig. 1. — The catalytic effect of NA. pH = 6.50; Ni^{2+}, 4.5×10^{-4} M. NA, 10^{-5} M: (1) 0, (2) 2.4, (3) 6, (4) 9, (5) 15. Scan rate, 2 V/min. Inset: cyclic voltammogram recorded in the region of the CNW. Same solution as for the curve 3; scan rate, 4 V/min. Initial potential, −0.5 V.

Table 1

The parameters of the CNW obtained from the $\ln[i/(i_l - i)]$ vs. E plots. Same conditions as in Fig. 1

NA, 10^{-5} M	$-E_{1/2}$, V	αn	Correlation coefficient	Number of points
6	0.78 ± 0.01	0.94 ± 0.01	0.9990	19
9	0.77 ± 0.01	0.98 ± 0.01	0.9994	26
15	0.76 ± 0.05	1.10 ± 0.01	0.9996	26

is not dependent on this parameter (Fig. 2). This behaviour shows that the rate-determining step in the process giving the CNW is a chemical reaction.

The above observations are valid only as long as the limiting current of the CNW is small as compared to the main peak of nickel. If i_l is higher than one-half of the main peak, the catalytic reduction of nickel produces a maximum-shaped pattern, as usually in voltammetry. These conditions were, however, avoided, keeping the nickel ion in high excess as compared to NA.

NA does not influence the potential of the anodic peak of nickel amalgam, lying at about OV. Nevertheless, the height of this peak increases in presence of NA because the catalytic process produces an additional amount of nickel during the cathodic scan. The high difference between the cathodic and anodic peak potentials indicates the irreversible character of the electrochemical reaction.

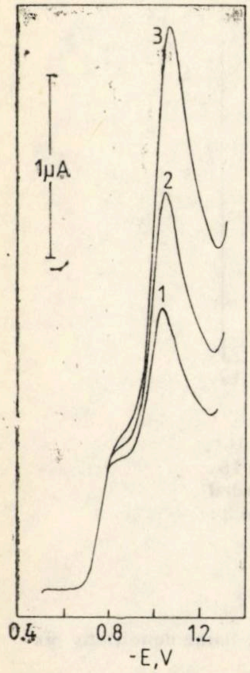

Fig. 2. — The influence of the scan rate. pH = 6.50; Ni^{2+}, 4.5×10^{-4} M; NA, 6×10^{-5} M. Scan rate, V/min.: (1) 1, (2) 2, (3) 4.

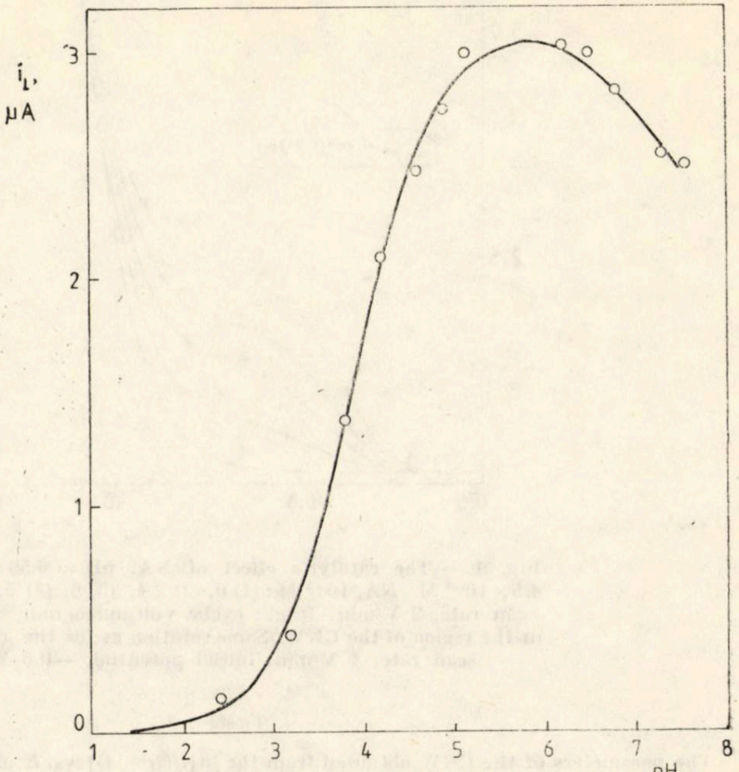

Fig. 3. — Effect of pH on the limiting catalytic current. Ni^{2+}, 6×10^{-4} M; NA, 1.2×10^{-4} M. Scan rate, 2 V/min.

The limiting current of the CNW is strongly dependent on the composition of the solution. Thus, at pH= 6.20, nickel ion concentration 1.2×10^{-3} M and NA concentration (*b*) ranging between 8×10^{-6} and 1.6×10^{-4} M, the following relationship was found by the method of the least squares:

$$i_l = 0.005 + 3.5 \times 10^4\ b \tag{1}$$

Here i_l is expressed in μA. The correlation coefficient (for 8 points) is 0.9996. Taking into account the negligible value of the intercept, it may be assumed that i_l is directly proportional to b.

i_l increases on the increase of nickel ion concentration, but the variation is non-linear. The effect of pH is shown in Fig. 3 and proves the influence of ligand protonation.

DISCUSSION

The CNW recorded under voltammetric conditions shows the characteristics of an irreversible electrode process with a parallel, rate-determining chemical reaction.[10] The reaction mechanism may be represented by the following steps :

$$HL^+ + Ni^{2+} \underset{k_2}{\overset{k_1}{\rightleftharpoons}} NiL^{2+} + H^+ \tag{I}$$

$$NiL^{2+} + 2e^- + H^+ \rightarrow Ni(Hg) + HL^+ \tag{II}$$

Here L represents the NA molecule and HL^+ is its conjugated acid ($pK_a = 3.35$[11]). The species reducible in the range of the CNW is assumed to be NiL^{2+} ($\log K_1 = 3.40$[12]). Because of the high excess of nickel used in this work, the formation of higher complexes may be neglected.

The above mechanism is analogous to those considered in[13] for the catalytic process with reversible electrode reaction and reversible reactant regeneration by a redox chemical reaction. In the nickel-NA system the regeneration of the reactant proceeds by complexation (I) whereas the reduction itself (II) is irreversible. The first characteristics do not modify the kinetic model of.[13] On the other hand, the results of this treatment are also valid for an irreversible electrode reaction, but only at the limit of high overvoltage, i.e. in the range of the limiting current. According to[13] we have :

$$i_l = n\,F\,A\,\{D(k_1[Ni^{2+}] + k_2[H^+])\}^{1/2}\,[NiL^{2+}]_0 \tag{2}$$

A is the electrode area, D is the diffusion coefficient of the reducible species, n and F have usual meanings and the subscript 0 denotes the equilibrium concentration. Due to its high excess, the concentration of the free nickel ion is taken as equal to the total concentration, a. The concentration of hydrogen ion is constant since the solution is buffered. The concentration of the reducible species is given by :

$$[NiL^{2+}]_0 = K_1\,K_a\,a\,b\,\{K_a(1 + K_1\,a) + [H^+]\}^{-1} \tag{3}$$

Since $k_1 k_2^{-1} = K_1 K_a$, it results :

$$k_1\,a + k_2[H^+] = k_1\,\{a + [H^+]\,(K_1\,K_a)^{-1}\} \tag{4}$$

Thus, the expression of the limiting current becomes :

$$i_l = nFA(K_1K_a)^{1/2}\, ab\{Dk_1(K_1K_a a + [\mathrm{H}^+])\}^{1/2}\{[\mathrm{H}^+] + K_a(1 + K_1 a)\}^{-1} \qquad (5)$$

As $K_1K_a a$ ranges between 10^{-4} and 10^{-3} M, at pH > 5 $[\mathrm{H}^+]$ is negligible as compared to other terms. Under these conditions the relationship (5) may be rearranged as follows:

$$a^{3/2}\, i_l^{-1} = (1 + K_1 a)\{nFAK_1\, b(Dk_1)^{1/2}\}^{-1} \qquad (6)$$

In good agreement with the experimental data (equation 1), equation (5) shows that the limiting current is directly proportional to the total ligand concentration, other parameters being constant.

According to equation (6), the plot of $a^{3/2}i_l^{-1}$ vs. a must be a straight line. This conclusion is confirmed by the experimental data. Thus, for 5 values of a ranging between 0.8 and 12×10^{-4} M (at pH $= 6.20$ and $b = 3.2 \times 10^{-5}$ M) it was found:

$$a^{3/2}i_l^{-1} = 7.71 \times 10^{-6} + 2.66 \times 10^{-2}\, a \qquad (7)$$

(i_l is in μA). The correlation coefficient is 0.9996. The ratio of the slope to the intercept of equation (7) gives the formation constant of the complex NiL^{2+}, i.e. $\log K_1 = 3.54$. This is in fair accord with the value found by spectrophotometry[12].

The rate constant k_1 may be estimated from the intercept of the line (7). To this end it is necessary to know the value of the diffusion coefficient. This was taken as equal to those of the free ligand, determined from the polarographic diffusion current of NA in acid medium (about 6×10^{-6} cm^2 s^{-1}). The value of the rate constant k_1 is, therefore, roughly estimated as 1.2×10^4 mole^{-1} ls.$^{-1}$. This value compares to that reported for the formation of the nickel-pyridine complex[14] (3.9×10^3 mole^{-1}ls^{-1}).

As shown by equation (5), the efect of pH is rather involved. However, several qualitative conclusions may be drawn. Thus, at pH < 2 we have $[\mathrm{H}^+] \gg K_a(1 + K_1 a)$ and $[\mathrm{H}^+] \gg K_1K_a\, a$. According to (5), under these conditions, i_l tends toward zero with the decrease of pH, in accord with the experimental data. At pH >5, equation (6) predicts that i_l becomes independent of pH. This conclusion is only partly confirmed by the experimental data. As shown in Fig. 3, at pH >6.5 the limiting current slowly decreases with the rise of pH. This is probably due to the partial hydrolysis of nickel ion.

Unlike cysteine, which influences the mechanism of both the anodic and cathodic reactions of nickel[15], NA has no effect on the anodic reaction. This behaviour may be related to the absence of surface activity of NA.

In conclusion, the kinetic equations founded on the reactions (I) and (II) fit very well the experimental data and enable to calculate the rate and equilibrium constants of the metal-ion complexation.

It is interesting to note that the combining ratio of the reducible complex (i.e. 1 : 1) is the same as in some catalytic systems with very different ligands as cysteinyl-dipeptides[5] or thiopyrimidine[16]. This suggests that the substitution of water by a single ligand molecule in the coordination sphere reduces so much the stability of the dipositive state of the metal that the fast reduction prevents the formation of higher complexes in the reaction layer. This conclusion may, probably, be restricted to the potential region of the limiting catalytic current.

From the analytical point of view, the CNW here described can be used to determine NA at concentrations ranging between 10^{-5} and 10^{-4}M, taking the advantage of the rapidity of voltammetry.

REFERENCES

1 H. B. Mark, jr. and C. N. Reilley, *J. Electroanalyt. Chem.*, **4**, 189 (1962).

2 J. Dandoy and L. Gierst, *J. Electroanalyt. Chem.*, **2**, 116 (1961).

3 H. B. Mark, jr., *Analyt. Chem.*, **35**, 195 (1963); idem, *ibid.*, **36**, 940 (1964); idem, *J. Electroanalyt. Chem.*, **7**, 276 (1964); idem, *ibid.*, **8**, 253 (1964); D. C. Olson, *Analyt. Chem.*, **39**, 1785 (1967); L. R. McCoy, H. B. Mark, jr. and L. Gierst, *J. Phys. Chem.*, **72**, 4637 (1968); L. R. McCoy and H. B. Mark, Jr. *J. Phys. Chem.*, **73**, 953 (1969); H. C. MacDonald, Jr. and H. B. Mark, Jr., *J. Phys. Chem.*, **74**, 3140 (1970); J. Čaja, H. C. MacDonald, Jr., E. Kirowa-Eisner, L. R. McCoy and H. B. Mark, Jr., *J. Phys. Chem.*, **76**, 1170 (1972).

4 J. Kůta, *Z. analyt. Chem.*, **216**, 243 (1966); A. Călușaru and V. Voicu, *J. Electroanalyt. Chem.*, **20**, 463 (1969); idem, *ibid.*, **32**, 427 (1971); F. G. Bănică and A. Călușaru, *J. Electroanalyt. Chem.*, **145**, 389 (1983).

5 F. G. Bănică, *Talanta*, **32**, 1145 (1985).

6 O. E. Ruvinskii, N. M. Uspenskaya and V. E. Godyatskii, *Elektrokhimiya*, 15, 1579 (1979).

7 G. Dryhurst, "Electrochemistry of Biological Molecules", Academic Press, New York, 1977, p. 473.

8 C. O. Schmakel, K. S. Santhanam and P. J. Elving, *J. Electrochem. Soc.*, **121**, 345 (1974).

9 L. Novotný, Proceedings of the J. Heyrovský Memorial Congress on Polarography, Prague, 1980, Vol. II, p. 129.

10 Z. Galus, "Fundamentals of Electrochemical Methods", Ellis Horwood, Chichester, 1976, p. 311.

11 H. H. G. Jellinck and M. G. Wayne, *J. Phys. Chem.*, **55**, 173 (1951).

12 P. Moore and R. G. Wilkins, *J. Chem. Soc.*, **1964**, 3455.

13 L. Rampazzo, *J. Electroanalyt. Chem.*, **14**, 117 (1967).

14 R. S. Bulmer, E. F. Caldin and A. W. Walton, *Trans. Faraday Soc.*, **67**, 3343 (1971).

15 E. Diacu and F. G. Bănică, *Bull. Soc. Chim. Belges*, **96**, 251 (1987).

16 J. M. López Fonseca, P. Sanz Pedrero and C. Gonzalez Posa, *J. Chim. Phys.*, **77**, 9 (1980).

In conclusion, the kinetic equations founded on the reactions (7) and (11) fit very well the experimental data and enable to calculate the rate and equilibrium constants of the particular [illegible].

It is interesting to note that the coordinating ratio of the reducible complex [illegible] 1 : 1 is the same as in some catalytic systems with very different [illegible], as [illegible] or [illegible]. It suggests that the [illegible] of [illegible] by a single ligand molecule in the coordination sphere [illegible] the [illegible] of the [illegible] state of the [illegible] but the last reduction [illegible] of [illegible] complexes in the reaction layer. This conclusion does, probably, be [illegible] to the principal reason of the limiting catalytic current.

From the analytical point of view, the [illegible] here described can be used to determine [illegible] at concentrations ranging between [illegible] and [illegible] [illegible] the [illegible] of the [illegible].

REFERENCES

[1] [illegible]
[2] [illegible]
[3] [illegible]
[4] [illegible]
[5] [illegible]
[6] [illegible]
[7] [illegible]
[8] [illegible]
[9] [illegible]
[10] [illegible]
[11] [illegible]
[12] [illegible]
[13] [illegible]
[14] [illegible]
[15] [illegible]
[16] [illegible]

Revue Roumaine de Chimie, 35, 6, 701—706 (1990)

ELECTRICAL CONDUCTIVITY OF SOME ZINCON COMPLEXES

M. ABD EL MOTTALB[a] and M. G. ABD EL WAHED[b,*]

[a] Faculty of Science, Al-Azhar University, Cairo, Egypt

[b] Faculty of Science, Zagazig University, Zagazig, Egypt

Received February 29, 1988

The electrical conductivity of zincon with different transition elements has been measured as a function of temperature. The result shows that the activation energy of the conduction process decreases with complexation. The Seebeck coefficients of the investigated complexes are positive. The results have been interpreted on the basis of the band theory.

INTRODUCTION

A considerable amount of works have been carried out on the electrical properties of organic compounds.[1-6] The conduction mechanism in organic materials is described either using the band picture or the hopping model. According to the band theory, the temperature dependence of conductivity is mainly due to variation of the charge carrier concentration with temperature, while in the hopping picture the change of mobility with temperature is attributed to the jumping or hopping from one organic molecule to the next.

Zincon (1-(2-hydroxy-5-sulphophenyl)-3-phenyl-5-(2-carboxy-phenyl)-formazan) is a well-known chelating agent. Some spectrophotometric studies have been reported on the complexation reactions of this ligand and various metal ions.[7] However, no work has been done on their electrical properties. The aim of the present paper is to investigate extensively the electrical properties of zincon and to study the effect of complexation on the resistivity of zincon.

EXPERIMENTAL

All the transition metal sulphates used were of AR grade. The solid complexes were prepared by mixing equi-molecular amounts of the ligand and metal salts in acetone. The mixture was stirred for about one hour then isolated by addition of ether and filtered immediately. Recrystallization of the solid complexes from acetone/ether was carried out and the solid was

---

[*] To whom all correspondence should be addressed.

then filtered off, washed and dried over P_2O_5. The structure of complexes was characterized on the basis of elemental analysis and IR spectral data.

The conductivity measurements were made on the discs having 8 mm diameter and 2 mm thickness in the absence of air. Other details of the experimental technique were the same as given earlier.[5]

RESULTS AND DISCUSSION

The conductivity is defined simply as the reciprocal of the resistivity and is related to the carrier mobility through the relation

$$\sigma = n\, e\, \mu$$

where n is the number of electrons/cm^3, e the charge per electron and μ the carrier mobility. According to the band theory of solids, n follows something like the Boltzmann distribution, exp $(-\Delta E/2kT)$, wherte ΔE is the energy gap. Thus as T increases n increases exponentially. For a semiconductor, the electron states are filled right up to the Brillouin zone boundaries, that is, up to the point where the Bragg condition for reflection produces standing waves. There is an energy gap at this boundary so that there are no available energy states just above it and, hence, no conduction. The conductivity is therefore governed by n rather than μ. Since n increases exponentially with temperature, so will the conductivity.

Table 1 lists the electrical resistivities ρ in ohm cm and the activation energies E in eV of various zincon complexes at 300 K. Experimentally, these activation energies can be obtained from the equation $\rho = \rho^\circ \exp(E/kT)$.

The plot of log ρ vs $1/T$ in Fig. 1 shows breaks for Zr, In, La, Ce and UO_2 complexes, but behaves linearly in the other complexes. The obtained transition temperatures are 582, 530, 558, 495 and 554 K, respectively. These phase transitions may be attributed to a change in the type of backing and a volume change. This change in the lattice would be expected to cause a change in the singlet-triplet separation energy. Therefore, the

Table 1

Resistivity ρ and activation energy E of zincon complexes at 400 K

Complex	ρ, ohm cm	E_1, eV	E_2, eV
Ligand	5.60×10^7	0.393	—
Fe-complex	2.65×10^7	0.323	—
Co-complex	1.57×10^7	0.366	—
Cu-complex	1.14×10^7	0.305	—
Zn-complex	8.63×10^6	0.323	—
Zr-complex	3.20×10^8	0.275	0.163
In-complex	6.30×10^9	0.275	0.154
La-complex	2.50×10^9	0.424	0.270
Ce-complex	1.55×10^9	0.550	0.154
UO_2-complex	1.51×10^8	0.262	0.190

relatively small activation energy value obtained above the transition temperature may be attributed to a change in the singlet-triplet separation energy.

The resistivities of investigated complexes lie in the range of typical semiconductor resistivities [8]. They follow the order La >Ce >Zr >UO_2 >

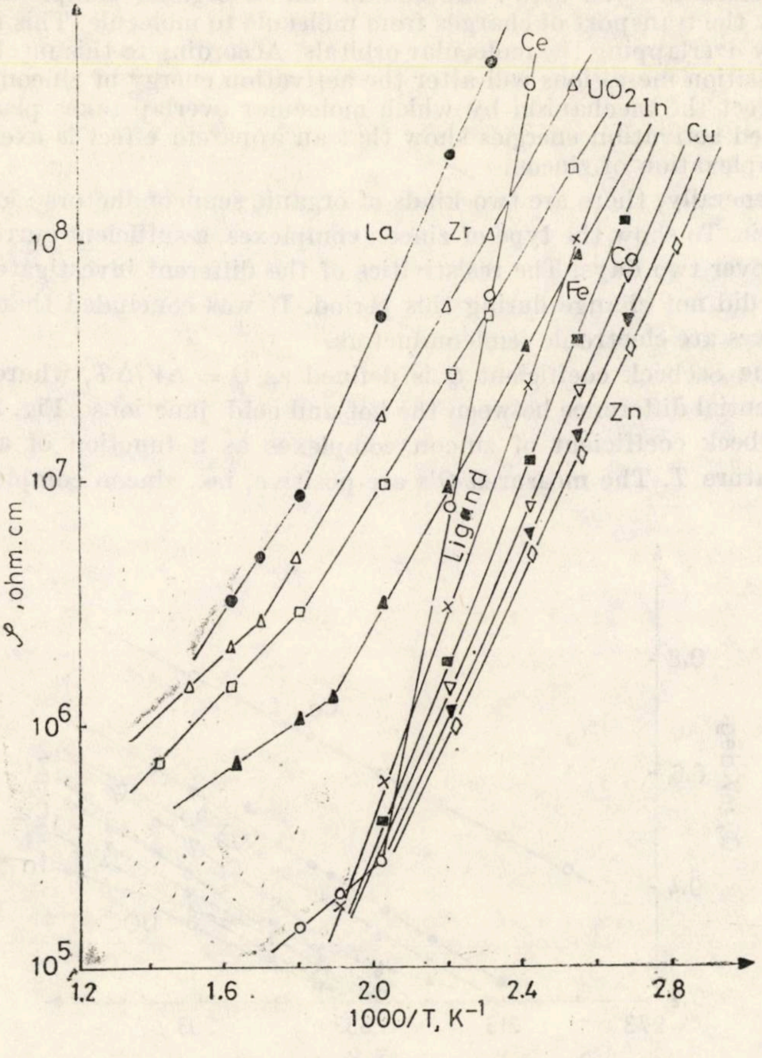

Fig. 1. — The resistivity of zincon complexes.

>In Fe >Co >Cu >Zn. It is clear that, increasing stability of the formed complexes leads to decrease the number of dislocted electrons and in other words increases the resistivity. These observations are in good agreement with the Irving-Williams sequence. [9] The stabilization of the complexes could be understood by considering that zincon molecule not only

induces a strong ligand to metal σ-bonding but also acts as a powerful π-acceptor. Such a metal to ligand π-bonding arising out of the d π- pπ interaction effectively reduces the electron density accumulated at the metal ion due to σ-bonding.

To explain the nature of conduction in zincon complexes, the following mechanism was used : the conduction in organic complexes takes place by the transport of charges from molecule to molecule. This is developed by overlapping the molecular orbitals. According to this mechanism, the transition metal ions will alter the activation energy of zincon only if they affect the mechanism by which molecular overlap takes place. The calculated activation energies show that an apparent effect is exerted by the complexation of zincon.

Generally, there are two kinds of organic semiconductors : ionic and electronic. To show the type of zincon complexes, a sufficient current was passed over two days. The resistivities of the different investigated compounds did not change during this period. It was concluded that zincon complexes are electronic semiconductors.

The Seebeck coefficient Q is defined as $Q = \Delta V / \Delta T$, where ΔV is the potential difference between the hot and cold junctions. Fig. 2 shows the Seebeck coefficient of zincon complexes as a function of absolute temperature T. The measured Q's are positive, i.e., zincon complexes ar

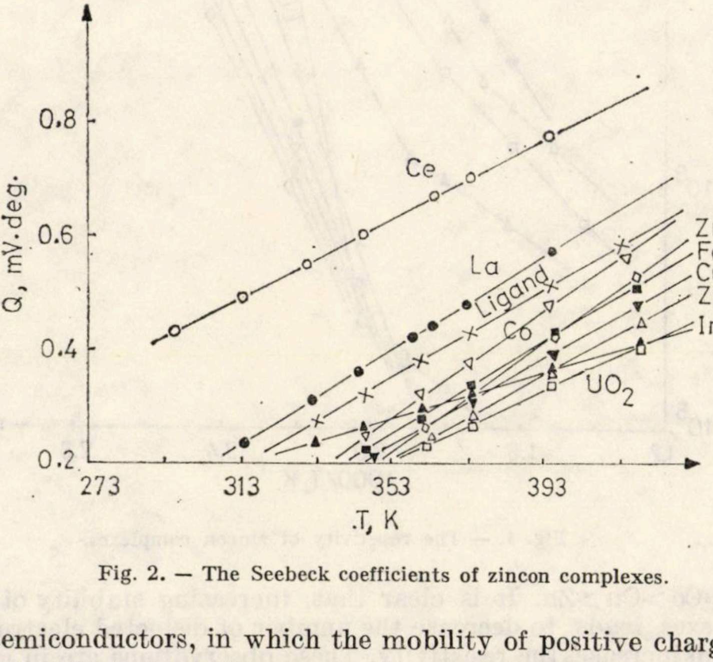

Fig. 2. — The Seebeck coefficients of zincon complexes.

intrinsic semiconductors, in which the mobility of positive charge carrier is greater than that of negative carrier. In other words, the equation of the curves is approximately Q = constant $-$ 28 log σ. This assumes also that these compounds are intrinsic semiconductors if the band theory is applicable.[10]

To determine the mobility of carriers μ and the density of states N, the concentration of electrons and holes n was calculated from the relation

$$n = 2\left(\frac{2\pi\, m^{+}\, kT}{h^{2}}\right)^{3/2} e^{-E/kT}$$

where m^{+} is the effective mass of charge carrier (taken here as the free electron mass), k , the Boltzmann constant and h the Planck constant. The density of states was given from the relation[11]:

$$n = N \exp\left(-(E_f - E_v)/kT\right)$$

where n is equal to $\sigma/e\ \mu$ and $(E_f - E_v) = Q\,T$. Table 2 illustrates the characteristic electrical data of zincon complexes ; one finds a density of states ranged from 10^{18} to 10^{19} cm^{-3}. Theoretically N gives 10^{19} cm^{-3} from the equation

$$N = 2\pi\, m^{+} k\, t^{3/2} / h^{2}$$

This is in a good agreement with the measured value.

The various theoretical interpretations of the mobility in electronic semiconductors that have been outlined in the present work give some indication of the increasing interest in explaining electronic conduction processes in solid complexes, but at the same time they clearly demonstrate that the present understanding is largely qualitative. Finally it should be emphasized that there are formal analogies between the path probability mechanism for ionic and electronic conduction.[12]

Table 2

Characteristic properties of zincon complexes

Complex	n (cm^{-3})	μ ($cm^2/V.s$)	Q ($mV/°C$)	N (cm^{-3})
Ligand	1.40×10^{9}	8.07×10^{-10}	0.54	1.28×10^{20}
Fe-complex	6.84×10^{14}	1.27×10^{-11}	0.45	6.04×10^{19}
Co-complex	4.05×10^{14}	7.51×10^{-12}	0.51	3.58×10^{19}
Cu-complex	2.94×10^{14}	5.45×10^{-12}	0.42	2.60×10^{19}
Zn-complex	2.23×10^{14}	4.13×10^{-12}	0.45	1.92×10^{19}
Zr-complex	8.26×10^{15}	1.53×10^{-10}	0.38	7.30×10^{20}
In-complex	1.63×10^{18}	3.01×10^{-11}	0.38	1.44×10^{20}
La-complex	6.25×10^{10}	3.60×10^{-5}	0.61	5.54×10^{18}
Ce-complex	2.19×10^{10}	1.00×10^{-5}	0.79	9.71×10^{18}
UO_2-complex	3.89×10^{15}	7.22×10^{-11}	0.36	3.44×10^{20}

REFERENCES

[1] A. Rembaum, A. M. Hermann, F. E. Stewart and F. Gutmann, *J. Phys. Chem.*, **75**, 513 (1969).

[2] I. F. Schegolev, *Phys. Stat. Sol.*, (A) **12**, 9 (1972).

[3] H. Afify, F. Abdel Kerim, H. Aly and A. Shabaka, *Z. Naturforsch.*, **33** a, 344 (1978).

[4] J. Martinsen, J. Stanton, R. Greene, J. Tanaka, B. Hoffman, and J. Ibers, *J. Am. Chem. Soc.*, **107**, 6915 (1985).

[5] M. G. Abd El Wahed and A. K. Abd El Kader, *J. Mat. Sci. Lett.*, **4**, 976 (1985).

[6] M. G. Abd El Wahed, M. Abdel Mottalb and A. K. Abd El Kader, *Thermochim. Acta*, to be accepted (1987).

[7] Y. Ahmed, M. Abdel Mottalb and A. Hassan, lst. Int. Conf. App. Sci., Zagazig, Egypt (1985).

[8] P. S. Kireev, "Semiconductor Physics", Mir Publishers, 1978.

[9] H. Irving and R. J. Williams, *J. Chem. Soc.*, 3192 (1953).

[10] V. Johnson and K. Lark-Horowitz, *Phys. Rev.*, **92**, 226 (1953).

[11] W. Shockley, "Electrons and Holes in Semiconductors", D. Van Nostrand Co., Inc., New York (1950).

[12] U. K. Shante and S. Kirkpatrick, *Adv. Phys.*, **20**, 325 (1971).

Revue Roumaine de Chimie, 35, 6, 707–711 (1990)

DETERMINACIÓN POTENCIOMÉTRICA DE TORIO

P. L. LÓPEZ-DE-ALBA y A. VERGARA

Universidad de Guanajuato, Instituto de Investigaciones Científicas, L. de Retana # 5,
Guanajuato, Gto., 36000 Mexico

Recibido : el 21 de Febrero de 1988

Un método electroanlítico rápido y preciso para la determinación de torio fue desarrollado. El método consiste en la valoración de una solución estandar de ortoarsenato dibásico de sodio con una solución de nitrato de torio, utilizando electrodos indicadores de quinhidrona-metálico, en combinación con el de — Ag/AgCl. Un marcado cambio en la F. e.m. es observado en el punto final, correspondiendo a la precipitación del $Th(HAsO_4)_2$. Las curvas tienen una forma regular. El máximo de dE/dV ocurre en el punto final y la precisión y reproducibilidad de los resultados electrométricos son buenos para bajas concentraciones de los reactivos (1×10^{-2} a 1×10^{-4} M). La valoración potenciométrica ofrece un método simple, rápido y exacto de determinación de torio.

A rapid and accurate electrometric method for the determination of thorium as orthoarsenate dibasic salts has been investigated. It consists in titration of a standard sodium dibasic orthoarsenate against a thorium nitrate solution, using a quinhydrone and a metallic indicator electrode respectively, in conjuction with Ag/AgCl. A marked change in e.m.f. is observed at the end-point corresponding to the precipitation of $Th(HAsO_4)_2$. The curves have a regular form, the pronounced maximum in dE/dV occurs at the end point, and the accuracy and reproducibility of electrometric results has been found to be excellent even at low concentrations (1×10^{-2} to 1×10^{-4} M) of the reactants. Potentiometric titrations offer a simple, rapid and accurate method for the determination of thorium.

INTRODUCCIÓN

Un reconocimiento de la literatura revela que existen varias referencias sobre el estudio de arsenatos de torio[1–4]; pero no existe ninguna referencia — considerando la determinación electroanalítica de torio como su ortoarsenatodibásico, aunque si existen algunos trabajos reportados aplicando alguna técnica electroanalítica.[5–9] En esta comunicación se presenta la continuación del estudio potenciométrico de la reacción del nitrato de torio con el ortoarsenato de sodio[10] adaptando esta reacción de precipitación al desarrollo de un método analítico para la determinación potenciométrica de torio.

EXPERIMENTAL

Los reactivos fueron Merck grado analítico ; nitrato de torio y ortoarsenato dibásico de sodio fueron usados y sus soluciones preparadas con agua desionizada libre de oxígeno. El electrodo de quinhidrona fue preparado mezclando soluciones decimomolares de — benzoquinona e hidroquinona en relación 1 : 1. La solución de Na_2HAsO_4 fue valorada como piroarsenato de magnesio y el torio como ThO_2 — vía su oxalato.[11]

El equipo utilizado para el estudio fue un potenciómetro construído en esta misma Institución. Diferentes concentraciones de reactivos fueron tomadas y una serie de titulaciones potenciométricas se corrieron en una celda tanto por el método directo como por el inverso. La solución de ortoarsenato dibásico de sodio fue adicionada por medio de una micro bureta a una solución de nitrato de torio presente en la celda con los electrodos y viceversa. La f.e.m. fue medida en el equipo antes mencionado — usando electrodos indicadores de aluminio/cobre quinhidrona, o bien, tungsteno-quinhidrona en combinación con el de Ag/AgCl. Siempre fueron tomadas alícuotas de 25 mL y adicionados a la celda junto con 10 mL de la solución de quinhidrona. Las soluciones a valorar fueron agitadas continuamente por un agitador magnético. En las curvas se graficó el E (observado) contra el volumen del titulante adicionado en mL. Para obtener el punto de equivalencia se aplicó el método de rectangulación o método geométrico.[12] Además, también se — determinó el punto de equivalencia por el máximo de dE/dV. Los resultados obtenidos se resumen en las Tablas 1 y 2. Las curvas típicas son ilustradas en las Figuras 1 y 2.

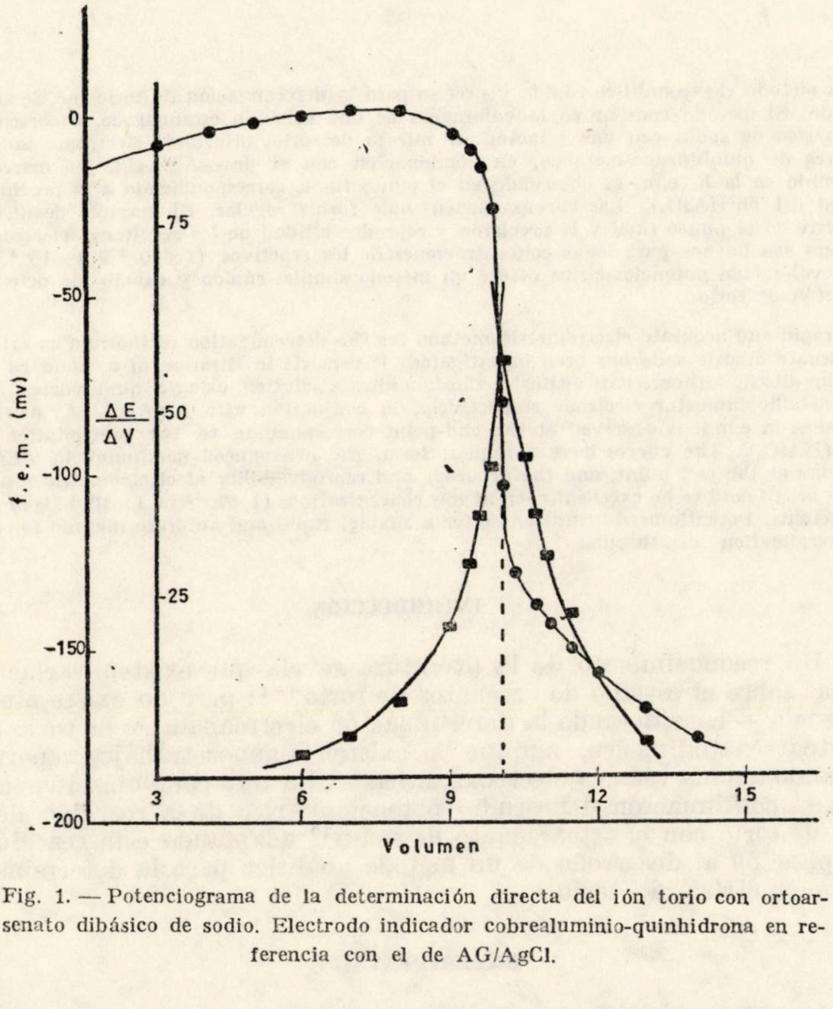

Fig. 1. — Potenciograma de la determinación directa del ión torio con ortoarsenato dibásico de sodio. Electrodo indicador cobrealuminio-quinhidrona en referencia con el de AG/AgCl.

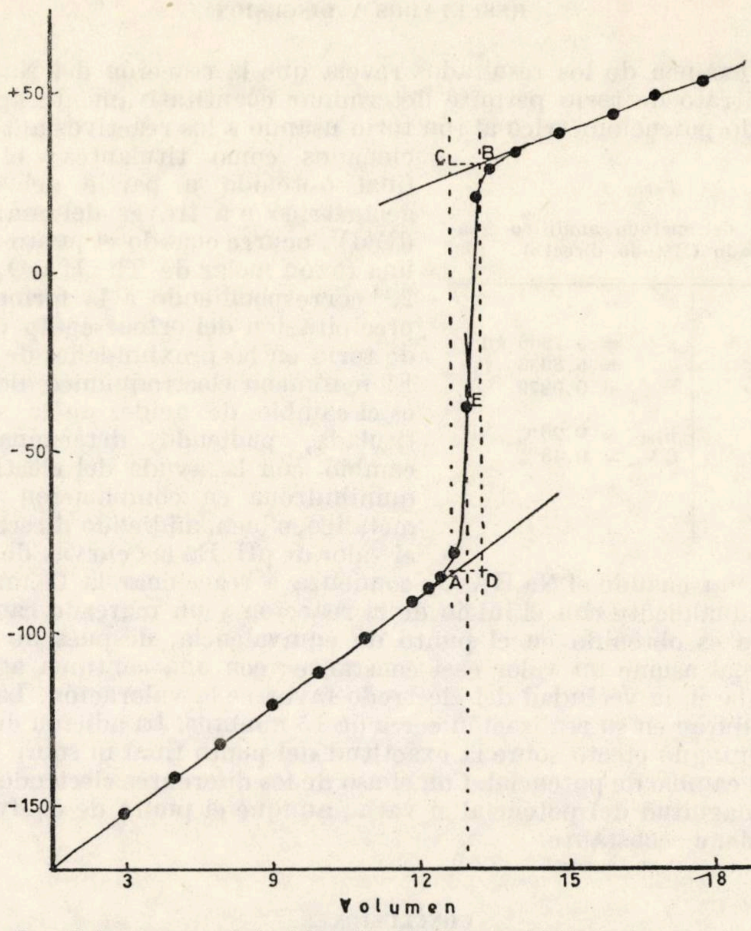

Fig. 2. — Potenciograma de la determinación inversa del ión torio con ortoarseniato dibásico de sodio. Electrodo indicador cobrealuminio-quinhidrona en Ref. Ag/AgCl.

Tabla 1

Determinación potenciométrica de Torio

TITULACIÓN DIRECTA			TITULACIÓN INVERSA		
Th_{exp} g/1	Th_{teo} g/1	error %	Th_{exp} g/1	Th_{teo} g/1	error %
26.4026	26.5322	+0.48	2.1397	2.1276	−0.56
14.9671	14.8226	−0.9	1.5536	1.5625	+0.56
6.3523	6.3834	+0.48	1.0387	1.0453	+0.63
3.0686	3.0712	+0.08	0.7608	0.7526	−1.33
1.1010	1.0919	−0.83	0.3567	0.3602	+6.97
0.8625	0.8707	+0.94	0.2127	0.2098	−1.38
0.5936	0.5893	−0.73	0.0989	0.0978	−1.12

RESULTADOS Y DISCUSIÓN

El examen de los resultados revela que la reacción del Na_2HAsO_4 con el nitrato de torio permite determinar cuantitativamente aplicando un método potenciométrico al ión torio usando a los reactivos antes mencionados como titulantes; el punto final obtenido a partir del método geométrico o a traves del máximo de dE/dV, ocurre cuando el punto está en una razón molar de Th : $HAsO_4$ de 1 : 2,[10] correspondiendo a la formación y precipitación del ortoarsenato dibásico de torio en las proximidades de pH 4.8. El fenómeno electroquímico detectado es el cambio de acidez de la solución titulada, pudiendo determinar este cambio con la ayuda del electrodo de quinihidrona en combinación con un métalico, o bien, midiendo directamente el valor de pH. En las curvas de valoración directa cuando el Na_2HAsO_4 comienza a reaccionar la f.e.m. disminuye gradualmente con el inicio de la reacción y un marcado cambio de pendiente es obtenido en el punto de equivalencia, después de lo cual el potencial asume un valor casi constante; con una continua agitación en la celda en la vecindad del electrodo favorece la valoración. Las valoraciones duran en su realización cerca de 15 minutos. La adición de etanol no tiene ningún efecto sobre la exactitud del punto final ni sobre la magnitud del cambio de potencial. Con el uso de los diferentes electrodos metálicos la magnitud del potencial si varía, aunque el punto de equivalencia se mantiene constante.

Tabla 2

Resultados del método analítico desarrollado (Método directo)

g/l	
5.7923	$\bar{x}$ = 5.7906 g/l
5.7846	μ = 5.8058
5.826	S = 0.0279
5.7996	
5.7902	E_{rel} = 0.26 %
5.8001	C.V. = 0.48 %
5.7721	
5.7829	
5.7916	

CONCLUSIONES

El método potenciométrico desarrollado es mucho más conveniente que los métodos corrientemente utilizados para la determinación de este metal; es simple, no requiere ni equipo sofisticado ni procedimientos complicados. Además, es rápido con una exactitud y precisión aceptables y los requerimientos químicos no son costosos.

AGRADECIMIENTOS. Se agradece a la Secretaria de Educación Pública de México el apoyo financiero para la realización de este trabajo y al Ing. Alvaro García T. las sugerencias hechas al mismo.

BIBLIOGRAFIA

[1] Atli Barberi, *Reale Accad. Maz. Lincei*, **19**, 462 (1910).

[2] Castel Pierre y C. R. Hebd, *Seances Acad Sci.*, **208**, 37 (1939).

[3] G. Le Flem, J. Lamic y P. Hagemuller, *Bull. Soc. Chim. France*, **6**, 183 (1966).

[4] S. Prasad, *Ciencia e Cultura*, **32,** 8 (1980).

[5] P. Sanchez Batanero et al, *Analusis*, **11,** 84 (1983).

[6] A. H. Castano et al., *Afinidad*, **37,** 369, (1980).

[7] F. H. Saint-Aubin et al., *Quim Anal.*, **31,** 6 (1977).

[8] P. S. Batanero et al, *Analusis*, **10,** 229 (1982).

[9] A. Harto et al, *Analusis*, **11,** 84 (1983).

[10] P. L. López-de-Alba et al., *Revue Roum. Chim.*, **32,** 387 (1987).

[11] A I. Vogel, "A Text Book of Quantitative Inorganic Analysis", Longmans, Green and Co., London, 1962.

[12] C. E. Meloan y R. M. Kiser, "Problems and Experiments in Instrumental Analysis", Ch. E. Merill Publishing Co., Columbus, Ohio, 1970.

Revue Roumaine de Chimie, **35**, *6*, 713–720 (1990)

ELLIPSOMETRIC SPECTROSCOPY OF PURE AND OF OXYGEN AND CARBON MONOXIDE-COVERED COPPER FILMS

MĂRIUCA GARTNER, NICOLAE STĂNICĂ and MIHAI VASS

ICECHIM – Center of Physical Chemistry, Spl. Independenţei 202, Bucharest, Romania 77208

Received May 9, 1989

Spectroscopic ellipsometric measurements (0.3–0.7 μm) have been performed on clean and on oxygen - and carbon monoxide-covered copper films in a high vacuum system. The complex dielectric functions of the clean surfaces were calculated from measurements at room temperature and used for indexing the interband transitions in the UV – VIS range. The adsorption of oxygen was investigated in the 10^{-6} – 10^{-5} torr range and at film temperatures ranging within 296–603 K.

The reaction of carbon monoxide with preadsorbed oxygen on the copper film was also investigated at 543 K. Another point of interest was the interaction of carbon monoxide with clean copper film at 77 K.

INTRODUCTION

Among the metals of the IB group, copper is the most intensively studied, undoubtedly due to the fact that it finds many applications in the heterogeneous catalysis. A good knowledge of its physico-chemical properties, derived from its energy structure as well as from its change following the adsorption and reaction of different gases on the surface can be very useful in the explanation of its catalytic action.

The adsorption of oxygen on copper was studied extensively in the visible range by ellipsometric method only for copper single crystals.[1–6] The studies of CO adsorption on copper films reported so far in the literature were performed mostly in the IR range, [7,8] Merkt and Wissmann [9] being the only ones who worked in the visible range.

The aim of this paper is to study the changes in the energy spectrum (as emphasized by the interband transitions) that occurs due to the adsorption of oxygen on polycrystalline copper films. These changes were studied by the method of ellipsometric spectroscopy. At the same time a suitable theoretical model of the oxygen/copper system was tested.

EXPERIMENTAL

The measurements were performed in high vacuum using an IFTAR+ (Romania) type ellipsometer. The experimental device and the procedure were described before.[10] The wavelengths ranged within 0.3 — 0.7 μm, at an angle of incidence Ø = 68.3 ± 0.5°.

The measuring cell [10] was provided with metallic bellows which allowed the displacement of the support. This made the alignment of the cell with respect to the ellipsometer much easier.

The ellipsometric measurements on clean metallic films were carried out in two zones, while those on the film with adsorbed gas in four zones, in order to increase the degree of measurement accuracy.

THE OPTICAL PROPERTIES OF CLEAN COPPER FILMS

(i) In order to check the experimental arrangements, we started by investigating clean uncovered copper films. The optical and dielectric constants were calculated from ellipsometric parameter Δ and ψ, measured on 0.08 μm thick films. (The numerical computation was performed using a suitable computer program). The optical constants are plotted in Fig. 1 as a function of wavelength.

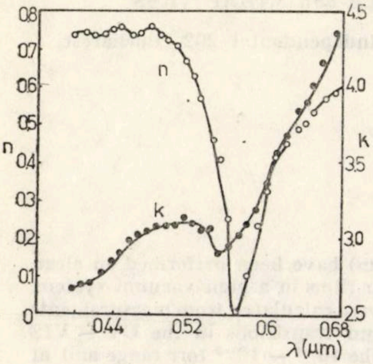

Fig. 1. — The optical constants (*n* and *k*) *vs* λ for clean and annealed copper film (○ — *n* ; ● — *k*).

(ii) The derivative of the imaginary part of the dielectric function with respect to the frequency (Fig. 2) identifies the interband transitions of clean copper.

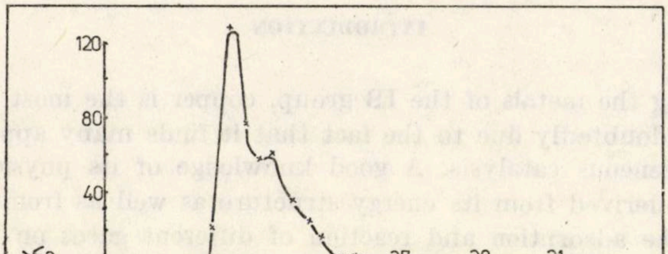

Fig. 2. — The derivative of the imaginary part of the dielectric function with respect to the frequency.

+IFTAR — Institute for Physics and Technology of Radiation Devices

They are located at 2.17 eV and 2.6 eV which is in fair agreement with the reflectometric values given by Ehrenreich[11] (for instance the L_3 Fermi surface transitions lies at 2.5 eV) and the theoretical ones given by Johnson and Christy[12] (2 eV and 2.58 eV respectively for the same transitions).

(iii) Besides the electronic transitions the optical mass (m_0) of the electron is also related to the complex dielectric function. According to Drude's theory[13] in the free electron region ($h\nu < 2.5$ eV) (using the approximation $\omega \gg 1/\tau$ for metals at near-infrared frequencies) the slope of $-\varepsilon_1 = f(\lambda^2)$ plot gives m_0 (Fig. 3).

Our value for copper is $1.49 \pm \pm 0.5$, the same as given by Johnson and Christy.[12]

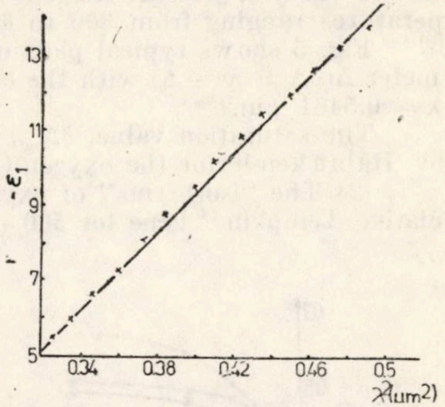

Fig. 3. — $-\varepsilon_1$ *vs* λ^2 in the near-infrared.

(iv) It is interesting to investigate not only the variations of dielectric constants, but also those of the quantity :

$$J(\omega) = (\hbar\omega)^2 \varepsilon_2(\omega)$$

which in the one-electron approximation is proportional to the associated density of states for transitions contributing to $\varepsilon_2(\omega)$

$$D(\omega) = \int_{B.Z} [2/(2\pi)^3 \delta[\hbar\omega_{if}(k) - \hbar\omega]\, d^3k$$

with $\hbar\omega_{if} = \hbar\omega_f - \hbar\omega_i$; i and f denoting the initial and final energy band, respectively.

Because of the simultaneous contributions of various transitions, the analysis of such a curve is difficult. However there are some facts which can be clearly distinguished :

— An extrapolation down to $J = 0$ gives the values of the onset of interband transitions $\hbar\omega_0 = 2.19$ eV for Cu.

— $J(\omega)$ is strictly parabolic in a range of 1eV above the onset

$$J(\omega) = \alpha(\hbar\omega - \hbar\omega_0)^{1/2}$$

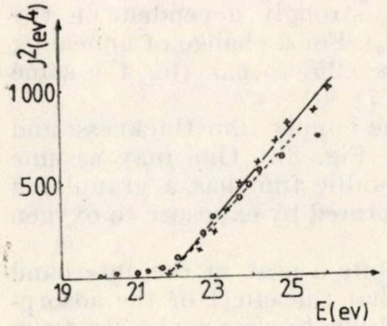

Fig. 4. — J^2 as a function of energy for films obtained by different annealing treatments (× — 25 min. at 373 K ; o — 15 min. at 353 K).

This behaviour was observed for many films with different structures. For all of them $\hbar\omega_0$ is the same, only the slope (α) of the experimental lines $J^2 = f(E)$ varies from one film to another according to its structure obtained by different annealing treatments (Fig. 4).

THE INTERACTION OF OXYGEN WITH CLEAN COPPER SURFACES

(1) Exposures to oxygen of clean annealed copper surfaces were carried out at a pressure range between $10^{-6} - 10^{-5}$ torr and at film temperatures ranging from 300 to 600 K.

Fig. 5 shows typical plots of the change in the ellipsometric parameter $\Delta(\delta\Delta = \overline{\Delta} - \Delta)$ with the oxygen exposure (N) for copper films at $\lambda = 0.5461$ μm.

The saturation value, $\delta\Delta_{sat}$, is temperature dependent as observed by Habraken [1,5] for the oxygen/Cu(100) but not for the oxygen/Cu(111).

(2) The "isotherms" of oxygen adsorption on copper are of dissociative Tempkin [14] type for $500 - 1 \times 10^4$ L as shown in Fig. 6.

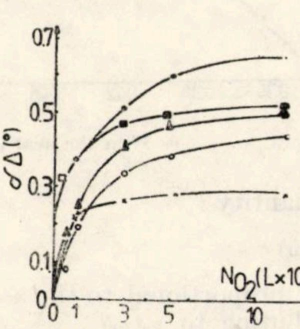

Fig. 5. — $\delta\Delta$ *vs* exposure to oxygen of clean and annealed copper film, for $\lambda = 0.5461$ μm (x — 296 K; ○ — 346 K; ▲ — 426 K; ■ — 488 K; ● — 603 K).

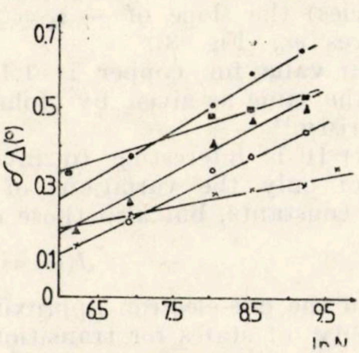

Fig. 6. — $\delta\Delta = f(N)$ for T : x — 296 K; ○ — 346 K; ▲ — 426 K; ■ — 488K; ● — 603 K; and $\lambda = 0.5461$ μm; Ø = 68.3°.

(3) The ellipsometric parameter $\delta\Delta_{sat}$, is strongly dependent on the annealing temperature of the copper film (T_a). For a change of annealing temperature of 110 K, $\delta\Delta_{sat}$ increases from 0.25° to 0.5° (for the same adsorption temperature $T = 296$ K) (Fig. 7).

(4) $\delta\Delta_{sat}$ is a decreasing function of the copper film thickness and reaches a constant value for $d = 0.04$ μm (Fig. 8). One may assume that for small thickness (0.017 μm) the metallic film has a granulated structure and that copper oxide islands are formed by exposure to oxygen as low as 1×10^3 L.

(5) A plot of $\delta\Delta_{sat} = f(\lambda)$ (Fig. 9) exhibits a peak at the interband transitions energy (2.6 eV) which suggests that the effect of the adsorption is mainly to intensify the transition and not to change the spectrum with respect to that of clean copper (as in case of CO/Au system [10]).

(6) Fig. 10 shows a plot of the change in the ellipsometric parameter ψ ($\delta\psi = \psi - \overline{\psi}$) during the oxygen exposure of copper films at 300 K and 346 K. Initially $\delta\psi$ decreases but afterwards it increases slowly as the oxide develops and grows.

The reason of this initial decrease in $\delta\psi$ seems to be the incorporation of oxygen into the copper lattice and the formation of a mixed layer of copper oxide islands in copper. (This "anomalous" behaviour is now considered typical for the initial stages of oxidation of most metal and semiconductor surfaces [15]).

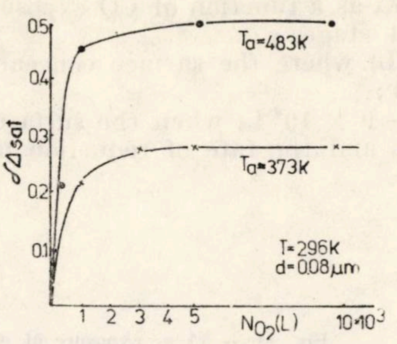

Fig. 7. — $\delta\Delta_{sat}$ *vs* exposure to oxygen of clean copper films annealed at 373 K – x; 483 K– ● (λ = 0.5461μm).

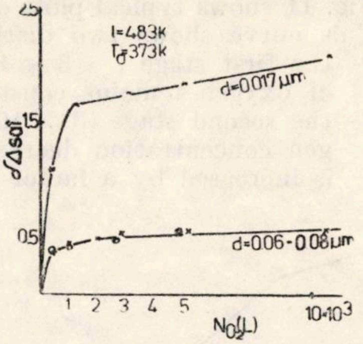

Fig. 8. — $\delta\Delta_{sat}$ *vs* exposure to oxygen of clean and annealed copper films of different thicknesses : * = 0.017 μm ; x – 0.06 μm ; O – 0.08 μm (λ = = 0.5461 μm).

In the case of copper oxidation, the magnitude of the initial decrease in δψ was dependent on the temperature of the oxidation. This is shown in Fig. 10. At room temperature only a small decrease was seen (δψ = = 0.01°). At 393 K the decrease in δψ is 0.3°.

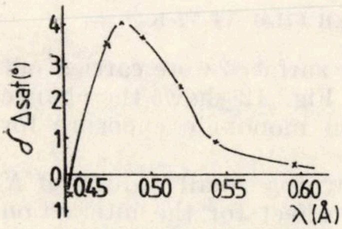

Fig. 9. — The variation of $\delta\Delta_{sat}$ with wavelength.

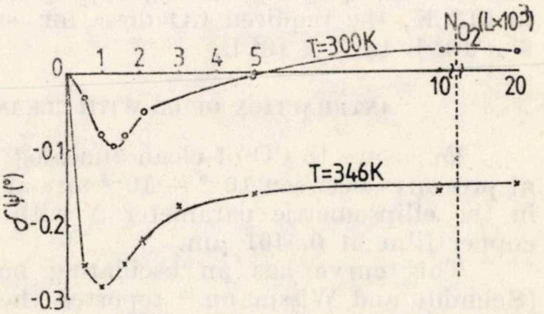

Fig. 10. — δψ *vs* N for *T*: O – 300 K ; x – 346 K (λ = 0.5461 μm, Ø = 68.3°).

This temperature behaviour could be explained by assuming that both the rate of oxygen incorporation and that of the oxide formation increase with temperature. If one may assume that at room temperature the rate of the oxide formation is lower, at about 373 K it becomes dominant.

THE REACTION OF CO WITH PREADSORBED OXYGEN

It is known that it is possible to reduce an oxidized surface by interaction with CO at temperatures higher or at least equal to the film oxidation temperature. Exposure to CO of a surface saturated with preadsorbed oxygen at $\delta\Delta_{sat} = 0.34°$ were carried out in the pressure range $5 \times 10^{-5} - 5 \times 10^{-4}$ torr at 543 K.

Fig. 11 shows typical plots of $\delta\Delta$ as a function of CO exposure. This curve shows two distinct stages:

- the first stage ($< 3 \times 10^4$ L) where the surface concentration of oxygen remains constant;
- the second stage ($3 \times 10^4 - 9 \times 10^4$ L) when the surface oxygen concentration decreases and the rate of reduction process is increased by a factor two.

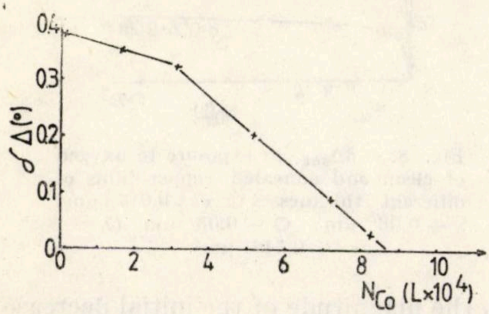

Fig. 11. — $\delta\Delta$ *vs* exposure of CO to a surface with preadsorbed oxygen ($\delta\Delta_{sat} = 0.34°$).

Upon increasing the reduction temperature, the preadsorbed oxygen can be completely removed at lower CO exposure. Habraken[1] showed, for example, that for Cu(111), by rising the temperature from 533 K to 613 K, the required CO dose for surface reduction decreases from 6×10^4 L to 3×10^4 L.

INTERACTION OF CO WITH CLEAN COPPER FILM AT 77 K

Exposure to CO of clean annealed copper surfaces were carried out at pressures between $10^{-6} - 10^{-5}$ torr at 77 K. Fig. 12 shows the change in the ellipsometric parameter Δ with carbon monoxide exposure for copper film at 0.5461 μm.

This curve has an oscillating behaviour for small values of N (Schmidt and Wissmann[16] reported the same effect for the interaction of oxygen with thin copper films at $\lambda = 1.152$ μm).

Fig. 12. — $\delta\Delta$ *vs* exposure to CO of clean copper film ($\lambda = 0.5461$ μm).

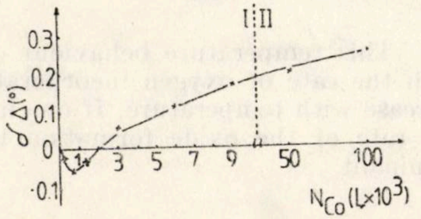

These results are in fairly good agreement with the observed changes in IR spectra[17] and in electron impact desorption[18] experiments of CO adsorbed on Cu, Ag, Au clean surfaces. These indicate a weak bond and a linear form of the CO adsorbed molecule at low temperature.

MODELS FOR THE ADSORBED LAYER

Attempting to explain the influence of the adsorbed gas on the metallic surface spectrum we have tried to assign several models proposed in the literature to the system oxygen/copper. We tried the one layer model, the double layer model, but a better fit was obtained with Bruggemanns effective medium model [19] (EMA). The layer which appears after adsorption is considered to be a mixture of both the clean metal and its oxide. For a two component medium (Cu, CuO) in which the effective component acts as a host, the EMA formula becomes :

$$f\,\frac{\varepsilon_1 - \langle\varepsilon\rangle}{\varepsilon_1 + 2\langle\varepsilon\rangle} + (1 - f)\,\frac{\varepsilon_2 - \langle\varepsilon\rangle}{\varepsilon_2 + 2\langle\varepsilon\rangle} = 0$$

where is the volume fraction of component number 1.

ε_1 — the dielectric constant of CuO available in the literature (Drobny and Pulfrey [20]) ;

ε_2 — the dielectric constant of clean copper measured immediately after the copper film was annealed ;

$\langle\varepsilon\rangle$ — the dielectric constant of the effective medium which is obtained by solving the equation for different values of f.

The value of $\langle\varepsilon\rangle$ as used to compute Δ^{calc}, $\psi^{calc} = f(\lambda)$ and to compare them with Δ^{exp}, $\psi^{exp} = f(\lambda)$ for $f = 0.1, \ldots\ldots 0.9$. These results (for $f = 0.2$) are shown in Fig. 13.

The calculated and experimental values of Δ are in good agreement (they differ by 0.1°), but the corresponding values of ψ are in a rather poor agreement for the whole range of f values (differences are as large as 0.7° in some points). This model is also far from the reality since it describes only isotropic, homogeneous media.

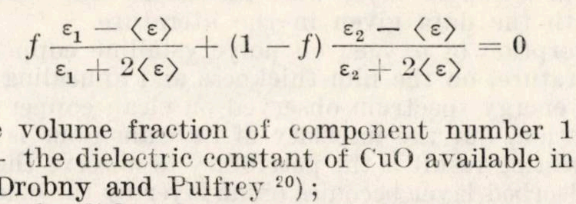

Fig. 13. — Ellipsometric parameters calculated for layers of mixtures of Cu and CuO (× — experimental values ; o — — calculated values for $f = 0.2$).

A more realistic model assumes rough and heterogeneous surfaces (EMA is only the first-order approximation of rough surface models). Aspnes [21] assumes a multilayer configuration on uniform substrate within which all layers, including the substrate, are treated as EMA mixtures, thus allowing for the calculation of the dielectric functions of a supported film. Based on this idea and making use of a complex computer program, Alterovitz [22] got very good results for the system SiO_2/a-Si.

We are trying to extend the Aspnes [21] model to the system CuO/Cu system. This work is in progress.

CONCLUSIONS

The dielectric constants, the optical transitions and optical mass of free electron in a copper layer were measured. The values are in good agreement with the data given in the literature.

The adsorption of oxygen on polycrystalline copper films depends on the temperature, on the film thickness and annealing temperature of the film. The energy spectrum observed on clean copper is not modified by the adsorption, but the intensity of its transitions is increased.

An interesting result is the possibility to observe the point in which the oxygen adsorbed layer becomes oxide layer by the change in the ellipsometric parameter ψ during the oxygen exposure.

The complete surface reduction of the preadsorbed oxygen layer by means of CO takes place either at higher CO adsorption temperatures or at higher CO pressures than the oxygen adsorption ones.

The adsorption of CO at 77 K on copper films is of the weak type, and for small exposures an oscillating behaviour of $\delta\Delta$ is observed.

Among the theoretical models which consider homogeneous and isotropic media, reasonable fit for our data was obtained with the effective medium model, but the results are not completely satisfactory.

REFERENCES

[1] F. H. P. M. Habraken, E. P. Kieffer and G. A. Bootsma, *Surf. Sci.*, **83**, 45 (1979).
[2] F. H. P. M. Habraken and G. A. Bootsma, *Surf. Sci.*, **87**, 333 (1979).
[3] F. H. P. M. Habraken, G. A. Bootsma, P. Hofmann, S. Hachicha and A. M. Bradshaw, *Surf. Sci.*, **88**, 285 (1979).
[4] F. H. P. M. Habraken, O. L. J Gijzeman and G. A. Bootsma, *Surf. Sci.*, **96**, 482 (1980).
[5] F. H. P. M. Habraken, C. M. A. M. Mesters and G. A. Bootsma, *Surf. Sci.*, **97**, 264 (1980).
[6] L. J. Hanekamp, W. Lisowski and G. A. Bootsma, *Surf. Sci.*, **118**, 18 (1982).
[7] M. J. Dignam and J. Fedyk, *Appl. Spectr. Rev.*, **14**, 249 (1978).
[8] M. Watanabe, *Surf. Sci.*, **138**, 95 (1984).
[9] U. Merkt and P. Wissmann, *Thin Solid Films*, **57**, 65 (1979).
[10] M. Gartner and M. Vass, *Rev. Raumaine Chim.*, **31**, 589 (1986).
[11] H. Ehrenreich and H. R. Philipp, *Phys. Rev.*, **128**, 1622 (1962).
[12] P. B. Johnson and R. W. Christy, *Phys. Rev.*, **6**, 4370 (1972).
[13] P. Drude, *Wied. Ann. Phys.*, **35**, 508 (1888).
[14] O. O. Hayward and B. M. W. Trapnell, "Chemisorption", London, Butterworths, p. 176, 1964.
[15] T. M. Christensen and J. M. Blakely, *J. Vac. Sci. Technol.*, **3**, 1607 (1985).
[16] R. Schmidt and P. Wissmann, *Surf. and Interface Analysis*, **12**, 407 (1988).
[17] M. A. Chesters, J. Pritchard and M. L. Sims, "Adsorption — Desorption Phenomena", Ed. Ricca, Academic Press, p. 277, 1972.
[18] A. Guţu, *Doctoral Thesis*, Univ. Bucureşti (1985).
[19] D. A. G. Bruggemann, *Ann. Physik*, **24**, 636 (1935).
[20] V. E. Drobny and D. L. Pulfrey, *Thin Solid Films*, **61**, 89 (1979).
[21] D. E. Aspnes and J. B. Theeten, *Phys. Rev. B*, **20**, 3292 (1979).
[22] S. A. Alterovitz, G. H. Bu-Abbud, J. A. Woollam and D. C. Liu, *Phys. Status Salidi*, **85**, 69 (1984).

Revue Roumaine de Chimie, 35, *6*, 721–729 (1990)

STUDIES CONCERNING CALCIUM CARBONATE SCALES FORMATION AND ITS PREVENTION. II *

PREVENTION BY INHIBITOR ADDITION

VASILE COCHECI, GHEORGHE PETCA and EUGEN GLÜCK

Faculty of Chemical Technology, Polytechnic Institute "Traian Vuia" Timişoara,
Bd. 30 Decembrie No. 2, Romania

Received November 16, 1989

On the basis of the kinetics of calcium carbonate precipitation from hyperthermal water a relationship for the calculation of sodium tripolyphosphate dosage, necessary for calcium carbonate scales inhibition, was stated under a great variety of conditions.

INTRODUCTION

Hyperthermal water exploitation conditions determine carbon dioxide desorption which leads to the supersaturation of water with calcium carbonate and finally to calcium carbonate deposits formation. They form in large quantities in well pipes of water or water-oil mixture, in pumps, degassing equipment, a.s.o., leading to productivity diminution and finally to equipment shut-down.[1]

Calcium carbonate scales formation from hyperthermal water can be avoided by several procedures such as degassing under pressure, acid addition, a.s.c.[2] The most common method however consists in the addition of scale inhibitors.[3,4] In literature a great number of inhibitors are reported : phosphates, polyphosphates, organophosphonates, polyacrylamides, polymethacrylates, a.s.c.[5-11] These chemicals, in low amounts, through a mechanism of absorption on the surface of the already formed crystals, reduce calcium carbonate crystallization rate till insignificant values. Although the mechanism and the inhibitor properties are described in a great number of papers, an expression for the calculation of inhibitor dosage as a function of water characteristics is not reported. Both for the prevention of scales formation and for corrosion processes, determined by the use of large amounts of inhibitors, it is necessary to know as exactly as possible the inhibitor dosage.

In the present work we propose an expression for the calculation of inhibitor dosage as a function of water characteristics and hyperthermal water exploitation conditions on the basis of calcium carbonate precipitation kinetics study. For this purpose, sodium tripolyphosphate was used as inhibitor.

EXPERIMENTAL

For experimental determinations the apparatus reported in a previous work[1] was used, which allows the realization of temperatures and various supersaturation degrees of calcium carbonate, for the whole route of hyperthermal water, reproducing properly the conditions from exploitation plants.

Sodium carbonate solution of desired concentration was introduced into the reaction vessel, which had a capacity of 2.5 dm^3. By bubbling an air-carbon dioxide mixture the carbonate was changed into dicarbonate, the degree of transformation being determined by the air/carbon dioxide ratio. After reaching the desired temperature and the equilibrium between the gaseous phase and solution, which was monitored by measuring pH, sodium tripolyphosphate solutions were added. After the homogenization of the mixture calcium carbonate crystals were added. For this purpose calcium carbonate A.R. MERCK was used. X-ray analysis showed that crystals consisted in calcite. After the homogenization of the suspension a 0.01 N calcium chloride solution was added under continuous stirring. Calcium carbonate crystals determined the heterogenous precipitation of calcium carbonate. Water samples were withdrawn at intervals and after rapid cooling were filtered. Calcium ion concentration was petermined by atomic absorption spectroscopy.

RESULTS AND DISCUSSION

Experimental conditions are presented in table 1. Plotting the variation of calcium ion concentration against time the variation curves presented in figure 1 were obtained. Reference to figure shows that the variation of calcium ion concentration in the presence of low amounts of sodium tripolyphosphate and in the absence of sodium tripolyphosphate differ from those obtained at average concentrations of sodium tripolyphosphate. Thus, at low sodium tripolyphosphate concentrations, calcium ion concentration decreases monotonously. At average concentration of sodium tripolyphosphate it is seen that sodium tripolyphosphate influences considerably the precipitation rate at the beginning of the process. After a while, however precipitation rate increases suddenly. When increasing sodium tripolyphosphate dosage, this increase in the rate was not observed during 15 minutes, as long as the experiment ran. The presence of the discontinuity on the precipitation curves, respectively the increase in reaction rate is due to either calcite or aragonite secondary nucleation,[22] or to sodium tripolyphosphate decomposition. A similar effect was observed in the presence of large amounts of magnesium ion, which inhibits calcite crystallization and favours aragonite formation.[22]

Experimental data thus obtained were correlated with Reddy's equation.[2]

$$\frac{[\mathrm{Ca}^{2+}]_t - [\mathrm{Ca}^{2+}]_e}{[\mathrm{Ca}^{2+}]_i - [\mathrm{Ca}^{2+}]_e} = kGf_D^2([\mathrm{Ca}^{2+}]_i - [\mathrm{Ca}^{2+}]_e)\,t \qquad (1)$$

obtaining a satisfactory linear correlation. The results are presented in figure 2. It is seen a decrease of the slopes of the lines, respectively of the rate constant, together with the increase of the sodium tripolyphosphate dosage. Plotting the slopes of the lines versus dosage, a good linear correlation of these data was obtained. By the extrapolation of the lines to slope equal to nough the sodium tripolyphosphate dosage results, for which

Table 1

Sodium tripolyphosphate dosage variation as a function of experimental conditions

Exp.	t °C	p_{CO_2} ata	$C_{HCO_3^-}$ $\frac{meq}{dm^3}$	C_{Ca_i} $\frac{mg}{dm^3}$	C_{Ca_e} $\frac{mg}{dm^3}$	NaTPP dosage $\frac{mg}{dm^3}$	Slope	Result. dosage $\frac{mg}{dm^3}$	Ref. to tab. 2
1	80	0.0645	26	19.5	0.8	0.05	1.05	0.133	I
2						0.075	0.9		
3						0.1	0.42		
4						0.12	0.16		
5						0.15	0		
6	80	0.0448	26	19.5	0.56	0.1	0.47	0.194	II
7						0.12	0.375		
8						0.15	0.2		
9						0.18	0.08		
10						0.22	0		
11	80	0.0234	26	19.5	0.29	0.15	0.46	0.380	III
12						0.2	0.36		
13						0.25	0.24		
14						0.3	0.17		
15						0.5	0		
16	80	0.1147	26	39	1.43	0	0.483	0.145	IV
17						0.075	0.264		
18						0.1	0.17		
19						0.12	0.086		
20						0.18	0		
21	80	0.0645	36.4	19.5	0.45	0.1	1.1	0.237	V
22						0.13	0.85		
23						0.16	0.62		
24						0.2	0.3		
25						0.25	0		
26	80	0.0645	26	12.45	0.8	0.04	0.56	0.0816	VI
27						0.05	0.44		
28						0.06	0.28		
29						0.08	0.025		
30						0.1	0		
31	70	0.097	26	20.75	1.96	0	0.79	0.064	VII
32						0.02	0.46		
33						0.03	0.325		
34						0.04	0.165		
35						0.08	0		
36	70	0.067	26	20.75	1.35	0	1	0.09	VIII
37						0.02	0.77		
38						0.05	0.42		
39						0.06	0.245		
40						0.12	0		
41	70	0.035	26	20.75	0.7	0	1.36	0.187	IX
42						0.05	1		
43						0.075	0.78		
44						0.1	0.56		
45						0.2	0		
46	90	0.035	26	20.75	0.28	0.15	2.16	0.372	X
47						0.2	1.57		
48						0.25	1.16		
49						0.3	0.71		
50						0.5	0		

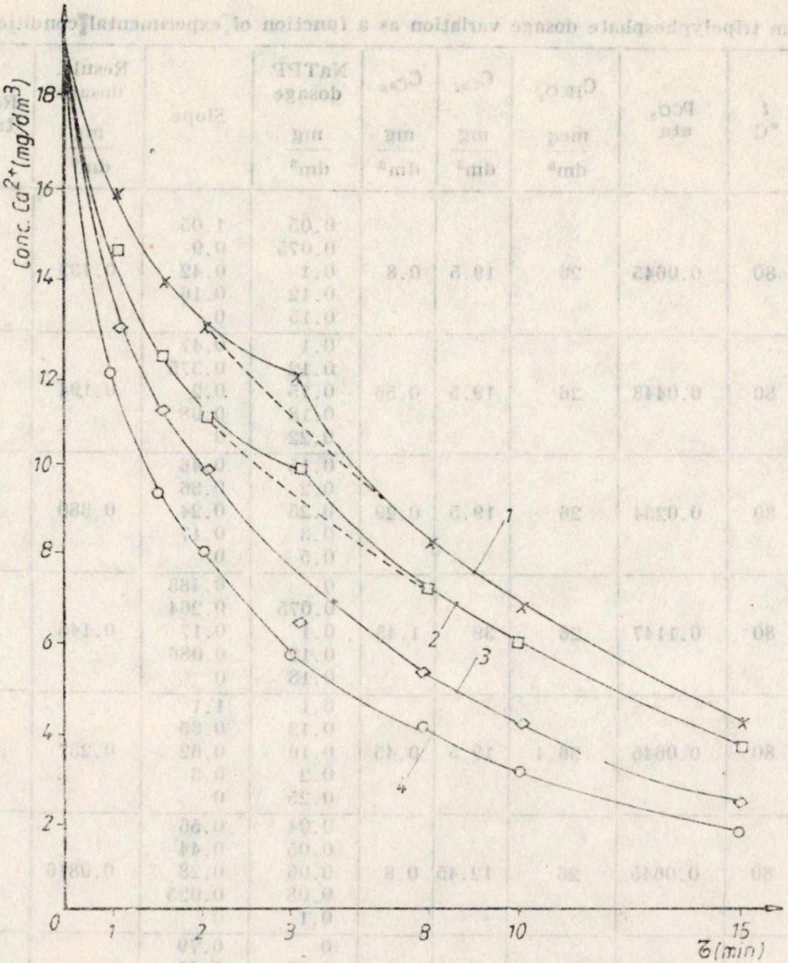

Fig. 1. — Calcium ion concentration curves as a function of time.
1 — Exp. 14 ; 2 — Exp. 13 ; 3 — Exp. 12 ; 4 — Exp. 11.

the rate constant is null, as it results from figure 3. Experimental attempts at higher dosages than the determined dosage confirmed the inhibition of calcium carbonate precipitation. The so determined dosage depends on the conditions of process proceeding.

Table 1 presents the data obtained for different partial pressures of carbon dioxide in gas. As was expected, dosage increases with the decrease in partial pressure of carbon dioxide. Plotting sodium tripolyphosphate dosage against 1/carbon dioxide partial pressure a linear correlation was obtained. By the extrapolation of the line, the partial pressure of carbon dioxide was determined for which sodium tripolyphosphate dosage is null. The partial pressure so obtained is in good agreement with the

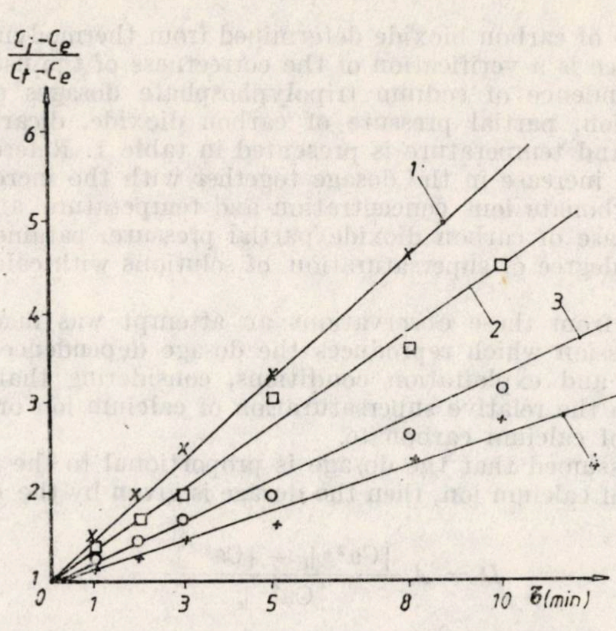

Fig. 2. — Variation of parameter $\frac{[Ca^{2+}]_i - [Ca^{2+}]_e}{[Ca^{2+}]_t - [Ca^{2+}]_e}$ against time. 1 — Exp. 11 ; 2 — Exp. 12 ; 3 — Exp. 13 ; 4 — Exp. 14

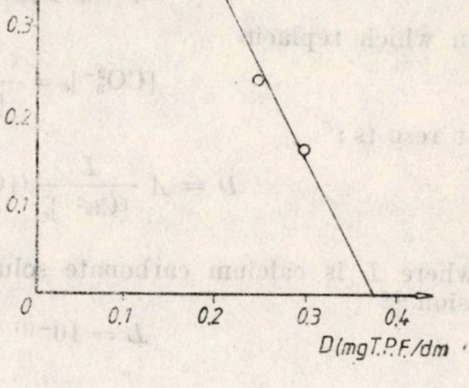

Fig. 3. — Slope variation as a function of sodium tripolyphosphate dosage.

partial pressure of carbon bioxide determined from thermodynamic data. This concordance is a verification of the correctness of the used method.

The dependence of sodium tripolyphosphate dosages on calcium ion concentration, partial pressure of carbon dioxide, dicarbonate ion concentration and temperature is presented in table 1. Reference to table 1 shows an increase in the dosage together with the increase of calcium and dicarbonate ions concentration and temperature and together with the decrease of carbon dioxide partial pressure, parameters which determine the degree of supersaturation of solutions with calcium carbonate.

Starting from these observations an attempt was made to establish an expression which reproduces the dosage dependence on water characteristics and exploitation conditions, considering that dosage is proportional to the relative supersaturation of calcium ion or to the supersaturation of calcium carbonate.

If it is assumed that the dosage is proportional to the relative supersaturation of calcium ion, then the dosage is given by the expression :

$$D = A\,\frac{[\mathrm{Ca}^{2+}]_i - [\mathrm{Ca}^{2+}]_e}{[\mathrm{Ca}^{2+}]_e} \tag{2}$$

On the basis of the experimental data presented in table 2, the value of coefficient A was established as being equal to 5.73 10^{-3} (mg/dm^3). Reference to table 2 shows that the deviation between the dosages experimentally determined and those calculated with the stated expression do not exceed 3.7% at 80°C, but the deviations exceed 10% at temperatures of 70°C and 90°C.

If it is assumed that the dosage is proportional to the supersaturation of calcium carbonate, then the dosage is given by the expression :

$$D = A f_D^2\,([\mathrm{Ca}^{2+}]_i\,[\mathrm{CO}_3^{2-}]_i - [\mathrm{Ca}^{2+}]_e\,[\mathrm{CO}_3^{2-}]_e)$$

As under the experimental conditions the concentration of carbonate ion was constant,[1] the expression becomes :

$$D = A[\mathrm{CO}_3^{2-}]_e f_D^2([\mathrm{Ca}^{2+}]_i - [\mathrm{Ca}^{2+}]_e)$$

in which replacin

$$[\mathrm{CO}_3^{2-}]_e = \frac{L}{[\mathrm{Ca}^{2+}]_e \cdot f_D^2}$$

it results :

$$D = A\,\frac{L}{[\mathrm{Ca}^{2+}]_e}\,([\mathrm{Ca}^{2+}]_i - [\mathrm{Ca}^{2+}]_e)$$

where L is calcium carbonate solubility product given by the expression :[13]

$$L = 10^{-(11.78-830/T-\lg 4.9)}$$

Table 2

Sodium tripolyphosphate experimental and calculated dosages and errors as a function of experimental conditions

Conditions from tab. 1	C_{Ca_i} mg/dm^3	C_{Ca_e} mg/dm^3	$C_{Ca_i} - C_{Ca_e}$ mg/dm^3	$\frac{C_{Ca_i} - C_{Ca_e}}{C_{Ca_e}}$	$L \frac{C_{Ca_i} - C_{Ca_e}}{C_{Ca_e}} \cdot 10^9$	Exp. dosage mg/dm^3	Dosage calc. with eq. 2 mg/dm^3	Error %	Dosage calc. with eq. 3 mg/dm^3	Error %
I	19.5	0.8	18.7	23.375	41.84	0.133	0.1337	+0.5	0.1334	+0.3
II	19.5	0.56	18.94	33.82	60.53	0.194	0.1938	−0.11	0.193	−0.45
III	19.5	0.29	19.21	66.24	118.56	0.380	0.3795	−0.13	0.378	−0.46
IV	39	1.43	37.57	26.27	47.02	0.145	0.1505	+3.7	0.15	+3.4
V	19.5	0.45	19.05	42.33	75.77	0.237	0.242	+2.1	0.241	+1.98
VI	12.45	0.8	11.65	14.56	26.06	0.0816	0.0834	+2.2	0.083	+1.88
VII	20.75	1.96	18.79	9.58	20.02	0.064	0.0549	−16.57	0.063	−1.56
VIII	20.75	1.35	19.4	14.37	30.03	0.09	0.0823	−9.3	0.095	+5.5
IX	20.75	0.7	20.05	28.64	59.85	0.187	0.164	−12.36	0.19	+2.11
X	20.75	0.28	20.47	73.10	114.25	0.372	0.418	+12.36	0.36	−2.0

Replacing, it results:

$$D = A \cdot 10^{-\left(11.78 - \frac{830}{T} - \lg 4.9\right)} \cdot \frac{[Ca^{2+}]_i - [Ca^{2+}]_e}{[Ca^{2+}]_e} \qquad 6(3)$$

In figure 4 are plotted the experimental data represented in table 2. From the figure it is seen a very good linear correlation according to expression 3. From the slope of the line the coefficient A from the expression 3, results as being equal to 3.19 $10^6 \frac{\text{mgdm}^3}{\text{mole}^2}$. As it results from the table, using expression 3 for the calculation of sodium tripolyphosphate dosage, the deviation from the experimental dosage does not exceed under all experimental conditions presented in table 2, the value of 5.5%. It results that equation 3 reproduces with a better precision the sodium tripolyphosphate dosage as a function of hyperthermal water characteristics and exploitation conditions.

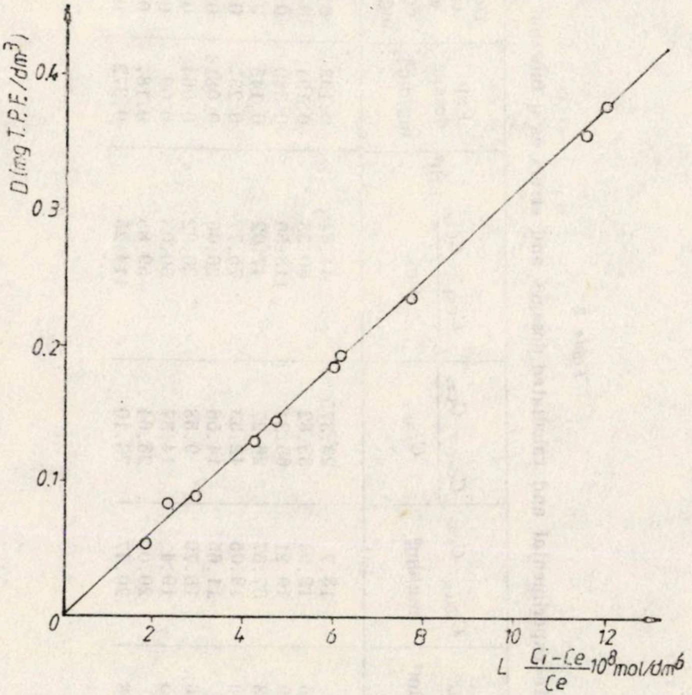

Fig. 4. — Variation of sodium tripolyphosphate dosage as a function of parameter $L \frac{[Ca^{2+}]_i - [Ca^{2+}]_e}{[Ca^{2+}]_e}$.

Expressions of the same form were also determined in case of other scale formation inhibitor reagents.

CONCLUSIONS

The kinetics of calcium carbonate precipitation under the conditions of hyperthermal water under a great variety of conditions and in the presence of sodium tripolyphosphate was studied. On the basis of the obtained results, the sodium tripolyphosphate dosage, necessary for calcium carbonate precipitation inhibition, was stated as a function of carbon dioxide partial pressure, dicarbonate and calcium ions concentration and temperature. It was stated that sodium tripolyphosphate dosage necessary for inhibition is proportional to the supersaturation degree of water, establishing an expression for the calculation of the dosage :

$$D = 3.19\ 10^6\ 10^{-\left(11.78 - \frac{830}{T} - \lg 4.9\right)} , \frac{[\mathrm{Ca}^{2+}]_i - [\mathrm{Ca}^{2+}]_e}{[\mathrm{Ca}^{2+}]_e}$$

Expressions of similar form were stated when using other inhibitors.

REFERENCES

[1] V. Cocheci, Gh. Petca and E. Glück, *Rev. Roumaine Chim.*

[2] V. Cocheci and Gh. Petca, Symposium "Probleme actuale ale protecției, tratării și epurării apelor în Republica Socialistă România", vol. II, Timișoara, 1984, p. 267.

[3] L. Iosifescu, G. Chițanu and A. Carpov, *Hidrotehnica*, **93**, 143 (1984).

[4] V. Cocheci and Gh. Petca, Symposium "Probleme actuale ale protecției, tratării și epurării apelor în Republica Socialistă România", vol. II, Timișoara, 1984, p. 263.

[5] A. Girou, R. Gardent, D. Dragone, G. Lecointre, J. Ropars and H. Roques, *Trib. Cebedeau*, **36**, no. 479, p. 409.

[6] M. M. Reddy and G. H. Nancollas, *Desalination*, **12**, 61 (1973).

[7] E. K. Giannimaras and P. G. Koutsoukos, *J. Calloid. Interface Sci.*, **116**, 423 (1987).

[8] J. B. Arots, *Mat. Perf.*, **19**, 28 (1980).

[9] K. G. Cooper, L. G. Hanlon, G. M. Smart and R. E. Talbot, *Desalination*, **31**, 257 (1979).

[10] M. H. Auerbach and M. S. Carruthers, *Desalination*, **31**, 279 (1979).

[11] B. L. Libutti, J. G. Knudsen and R. W. Mueller, *Mat. Perf.*, **23**, 47 (1984).

[12] G. H. Nancollas and K. Sawada, SPE Fifth International Symposium on Oilfield and Geothermal Chemistry, held in Stanford, California, May 28—30, 1980.

[13] H. N. S. Wiechers, P. Sturrock and G. v R. Marais, *Wat. res.*, **9**, 835 (1975).

Revue Roumaine de Chimie, **35**, *6*, 731–737 (1990)

COORDINATION COMPOUNDS OF SOME "3d" METALS WITH FORMYLATED DERIVATIVES OF CARVONE AND MENTHONE

FLORICA ZĂLARU, ADALGIZA CIOBANU, ION BACIU
and CARMEN PETREA

Faculty of Chemical Technology, Polytechnic Institute,
Bucharest, Romania

Received May 26, 1989

The paper reports on the coordination ability of carvone, menthone and formylated derivatives : formylcarvone and formylmenthone (A and B respectively), with the Cu(II), Co(II) and Ni(II) ions. Compounds of the type $MA_2 \cdot 2H_2O$ and $MB_2 \cdot 2H_2O$ were obtained by interaction of Ni(II) and Co(II) acetates, and in the case of Cu(II) only $CuB_4 \cdot 2H_2O$. The compounds were characterized by elemental chemical analysis, differential thermal analysis, electronic spectra, IR and ESR. The contribution of the ligands, in enolic tautomeric form, to coordination was evidenced. The biochemical tests showed, for the Co(II) compounds, a bacteriostatic activity against *Escherichia coli, Pseudomonas aeruginosa,* white *hemolytic staphylococcus.*

INTRODUCTION

The present interest in the study of the reactivities of some substances existing in plants (caraway, dill, mint) such as carvone, menthone and their derivatives might be explained by the numerous applications of these natural products and their derivatives (in medicine, industry of odorant products, additives in food industry).

Moreover, the investigations in the field of chemistry of chelates showed a higher antimicrobial activity than that of the free ligands.

The present study followed the coordination ability of carvone, formylcarvone, menthone and formylmenthone with some 3d metal ions (Co(II), Ni(II) and Cu(II)). The ligands are different by the nature and number of functional groups, and the formylated derivatives show a keto-enolic tautomerization that could influence the coordination ability,[1] evidencing their increased reaction.

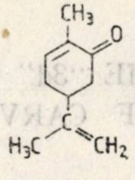
Carvone

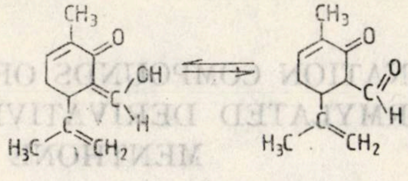
Formylcarvone

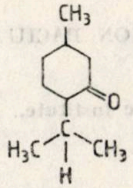
Menthone

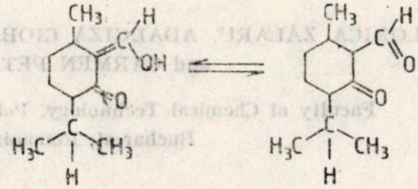
Formylmenthone

EXPERIMENTAL

Various molal ratios $MX_2 : L = 1 : 1$, $1 : 2$ and $1 : 4$, were used, where M(II) = Cu(II), Co(II), Ni(II) and X = CH_3COO^-, Cl^-, NO_3^-, 1/2 SO^{2-}. Ethanol, methanol and the methanol : water mixture = 9 : 1 were used as reaction medium. The compounds were obtained only by interaction of metallic acetates with formylcarvone and formylmenthone. The methanol-water mixture favoured the separation of complex compounds. Easy separation of the compounds and the better yields show a higher ability of complexation of formylmenthone.

The complexes were synthesized by the following general procedure: solutions containing ligands and metal acetate in a methanol-water mixture were mixed (molar ratio 2 : 1). The products were separated from the solutions as well formed crystals or microcrystalline powder. They were filtered off, washed with methanol and dried at room temperature.

The composition of the complexes, their colour and the results of elemental analysis are given in table 1.

The electronic spectra. Diffuse-reflectance spectra were recorded on VSU_2 Zeiss-Jena spectrophotometer within the 230 – 1100 nm range in dilution with MgO.

Thermodifferential analyses were carried out with Paulik-Paulik Erdey derivatograph Q–1500D MOM in a mixture with Al_2O_3 (m = 0.060, m = 0.050, STG = 500).

IR spectrum was recorded in the 700 – 4000cm^{-1} range by a Specord 71 Spectrophotometer. Samples were mounted in potassium bromide discs.

ESR spectra were recorded at room temperature on polycrystalline powders, on an ART-5-IFA Spectrograph. The Klystron frequency was 9060 MHz and the modulation of the magnetic field was 100 kc/s.

Metallic ions were determined gravimetrically after breakdown of the compounds with H_2O_2 and concentrated H_2SO_4.

RESULTS AND DISCUSSION

The isolated compounds were formulated on the basis of the elemental chemical analysis (Table 1). The presence of water in the complexes was confirmed by differential thermal analysis and by a broad and weak band at 3400 cm^{-2} in the IR spectrum, due to ν_{OH} in the coordination water.

Table 1

Analytical data

No.	Molar ratio M:L	Ligand	Compound	Colour	M % found	C found	H found	H_2O found
					calcd	calcd	calcd	calcd
1	1 : 2	A	$CoA_2 \cdot 2H_2O$	red-brown	14.05	55.1	7.35	10.08
					13.06	58.54	7.09	7.98
2			$NiA_2 \cdot 2H_2O$	green	14.16	54.2	7.7	
					13.06	58.54	7.09	
3		B	$CoB_2 \cdot 2H_2O$	red-brown	13.73	48.5	7.6	9.65
					12.74	51.5	8.55	7.84
4			$NiB_2 \cdot 2H_2O$	light green	13.09	59.2	7.8	
					12.75	57.55	8.55	
5			$CuB_4 \cdot 2H_2O$	green	6.99	54.2	7.6	
					7.67	63.9	9.18	

A = formylcarvone ; B = formylmenthone

Electronic spectra. Figures 1 and 2 show the electronic reflectance spectra, and Table 2 gives the absorption maxima ; their assignments are in agreement with the data in the literature.[2–10]

Analysis of these data shows the octahedral environment of the metallic ions. The Co(II) compounds, irrespective of the ligand, have a very similar electronic spectrum. The band ν_3 could overlap the band ν_2, whose tail stretches to 700 and 800 nm respectively. The spectra of the Ni(II) compounds show the three spin-allowed bands ν_1, ν_2 and ν_3, characteristic of the Ni(II) octahedral compounds.[2–5] The band ν_2 appears as a well-formed doublet. The structure of this band was interpreted

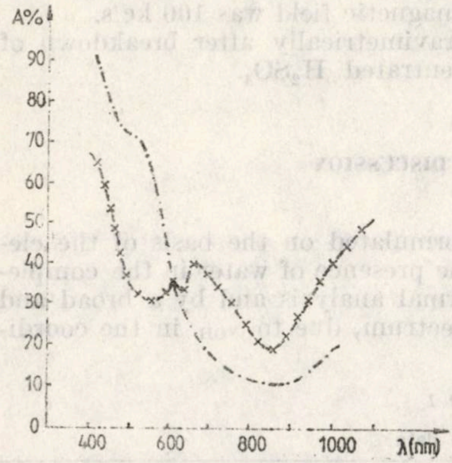

Fig. 1. — Electronic reflectance spectra of the compounds :

—·—·—·— $CoA_2 \cdot 2H_2O$

—×—×—×— $NiA_2 \cdot 2H_2O$

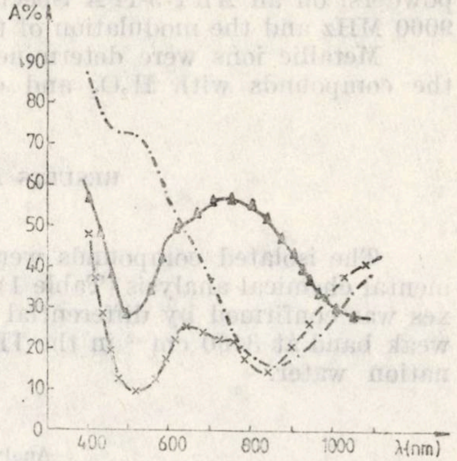

Fig. 2. — Electronic reflectance spectra of the compounds :

—·—·—·— $CoB_2 \cdot 2H_2O$

—×—×—×— $NiB_2 \cdot 2H_2O$

—▲—▲—▲— $CuB_4 \cdot 2H_2O$

Table 2

Visible absorption spectra

Compound	$^4T_{2g} \leftarrow {}^4T_{1g}$ υ_1	$^4A_{2g} \leftarrow {}^4T_{1g}$ υ_2		$^4T_{1g} \leftarrow {}^4T_{1g}$ υ_3	Ref.
$Co(H_2O)_6^{2+}$ $CoA_2.2H_2O$ $CoB_2.2H_2O$	1235 %1100 >1100	625		515.5 520 520	2
Compound	$^3T_{2g} \leftarrow {}^3A_{2g}$ υ_1	$^1E_g \leftarrow {}^3A_{2g}$	$^3T_{1g} \leftarrow {}^3A_{2g}$ υ_2	$^3T_{1g} \leftarrow {}^3A_2$ υ_3	Ref.
$Ni(H_2O)_6^{2+}$ $NiA_2.2H_2O$ $NiB_2.2H_2O$	1176 >1100 >1100	657.9 620 640	724.6 660 740	395	2

either as a spin-orbit coupling or as a spin-forbidden transition at the ^1E_g level.[2–5] The electronic spectrum of the $CuB_4 \cdot 2H_2O$ compound shows a broad band with λ_{max} centred at 720 nm and two shoulders at $\lambda = 650$ and $\lambda = 800$ nm. Such a spectrum is compatible with the hexacoordinated Cu(II) ion.[6–10]

ESR spectra : ESR spectrum of the $CuB_4 \cdot 2H_2O$ compound, recorded at room temperature on crystalline powders gives an isotropic signal with relatively little geometrical information.[7]

Infrared spectra. The infrared spectrum of the free ligands and the complex compounds has been reported in some detail and band assignments have been suggested (Tables 3 and 4).

Table 3

The main bands in the IR spectrum (cm^{-1})

L A	$CoA_2 \cdot 2H_2O$	$NiA_2 \cdot 2H_2O$	Assignments
3600			ν_{OH} nonassociated
	3400 vw broad	3400 w	ν_{OH} coordinated
2960	2980	2980	ν_{CH_3}, ν_{CH_2} asym. and sym.
2900	2935	2940	
2879	2880	2880 vw	
2810 vw			
1620 vs	1620 m	1630 m	
1640 sh	1570 vs		ν_{CO}
1450	1470	1590 1570 vs	
1420 m	1420 vs	1550	
1400	1380	1380 sh	
1370 m	1340 m	1335	
1300 vw	1270 vw	1270 vw	
1260	1235 m	1235	ν_{C-OH}
1200 vs	1200	1200	
1180	1180 w	1180 w	
1050 m	1070 w	1070 w	
	1050	1050	
900 s	910 w	910 w	γ_{CH_2}
700	700	700	

vw = very weak; vs = very strong; s = strong; m = medium sh = shoulder

The changes noticed in the spectrum of the complex compounds are similar and involve the ν_{CO} and ν_{C-OH} stretching bands (1690 cm^{-1}, respectively 1120 cm^{-1} in formylmenthone and 1620 cm^{-1} respectively 1200 cm^{-1} in formylcarvone). These changes could indicate the possibility of coordination to the metal via oxygen atoms. The ν_{C-OH} stretching band, that in ligands is very strong and structured in 5 or 4 peaks (Tables 4 and 3) has changed its positions, shapes and intensities. Likewise, the ν_{CO} stretching band is shifted or less intense. The broad and weak bands at 3400 cm^{-1} due to ν_{OH} stretching mode, and not met on the spectra of the free ligand, could show the presence of the coordination waters.

The presence of water is also confirmed by the thermodifferentia analysis.

These changes, correlated with the information obtained by the electronic spectra and elemental chemical analysis, may suggest that the ligands act bidentately in the case of Co(II) and Ni(II) by the oxygen donor atoms of the carbonyl group and the OH of the formyl group by its deprotonation, but only monodentately in the case of the $CuB_4 \cdot 2H_2O$ complex by the OH group deprotonation.

Table 4

The main bands in the IR spectrum (cm^{-1})

Ligand	$CoB_2 \cdot 2H_2O$	$NiB_2 \cdot 2H_2O$	$CuB_4 \cdot 2H_2O$	Assignments
3600				ν_{OH} nonassociated
	3400 w	3400 w	3400 w	ν_{OH} associated, broad band
2990	2970 m	2965 vs	2960 vs	
2880 vs	2890 w	2880 s	2870 s	ν_{CH_3}, ν_{CH_2} asym and sym.
1690 s	1690 m	1670 vw	1690 vw	$\nu_{C=O}$
1630—1590 (triplet)	1580 m	1600 1580 } vs	1590 1570 1530 } triplet vs	
1450 m	1420 1350 } br	1460—1420 1340 vs	1450 1430 triplet 1400 1370 vs	ν_{CH_2}
1260 m	1260 vw	1260 vw	1220 1200 } doublet	
1170 1120 1090 1070 1030 } vs	1230 1200 vw 1170 1120	1210 m 1170 w 1140 1120 vw	1170 w 1120 w 1150 1020	ν_{C-OH}
950		970 w		
930 w				
860	800 doublet vw		800	
700	680	705	700 689	γ_{CH_2}

This coordination mode might explain why the complex compounds are obtained only from the metallic acetates and glues from the chlorides, nitrates and sulphates of the respective metals. The acetate may favour the reaction, consuming the H^+ ions released during complexation.

CONCLUSIONS

By interacting the Co(II), Ni(II) and Cu(II) acetates with formylmenthone and formylcarvone, hexacoordinated complex compounds were obtained in all cases. No compounds were obtained for carvone and menthone or other salts of the metals (chlorides, nitrates, sulphates) than acetates. In the complex compounds of Co(II) and Ni(II) the ligands act bidentately by the O atoms and by the deprotonation of the OH group, making evident the participation of the ligands in the enolic tautomeric form and monodentately in the case of the $CuB_4 \cdot 2H_2O$ complex by deprotonation of the OH group.

REFERENCES

[1] E. W. Garbisch, *J. Amer. Chem. Soc.*, **85,** 1696 (1963).
[2] A. B. P. Lever, "Inorganic Electronic Spectroscopy", Elsevier, Amsterdam, 182, 1968.
[3] R. L. Carlin, *Transition Metal Chem.*, **1,** 1 (1965).
[4] R. L. Lintvedt, L. L. Borer, D. P. Murtha, J. M. Kuszaj and M. D. Glick, *Inorg. Chem.*, **13,** 18 (1974).
[5] J. T. Hashagen and J. P. Fackler Jr., *J. Amer. Chem. Soc.*, **87**, 2821 (1965).
[6] B. J. Hathaway, *J. Chem. Soc.*, **1972**, 1196.
[7] B. J. Hathaway and D. E. Billing, *Coordination Chem. Rev.*, **1970,** 143.
[8] B. J. Hathaway, *Structure and Bonding*, **57**, 85, 109 (1984).
[9] E. D. Mc. Kenzie, *J. Chem. Soc.*, A **1970,** 3095.
[10] M. Kato, H. B. Jonassen and J. C. Fanning, *Chem. Rev.*, **64,** 99 (1964).

Revue Roumaine de Chimie, 35, 6, 739–745 (1990)

HETEROCYCLES WITH ANNELATED DIBENZOCYCLOALKANE SKELETONS. IV[1]

PYRAZOLES WITH ANNELATED 7H-DIBENZO [*c,e*] CYCLOHEPTENE SKELETON

MIRCEA D. BANCIU,[a] FILIP CHIRALEU[b] and ANDREIA CIOBANU[a]
[a] Organic Chemistry Department, Polytechnic Institute, TCH, Splaiul Independenţei 313, 76206, Bucharest, Romania
[b] Centre of Organic Chemistry — ICECHIM, Splaiul Independenţei 202B, 78100, Bucharest, Romania

Received January 18, 1990

Reaction of 5-hydroxymethyl-5H-6,7-dihydrodibenzo[*a, c*]cyclohepten-6-one (5b) with hydrazine, phenylhydrazine and 2,4-dinitrophenylhydrazine affords the pyrazoles 6a-e which were characterized by IR, UV—VIS and ^{1}H—NMR spectroscopy. The reaction mechanism is discussed.

INTRODUCTION

In previous papers of this series we described the synthesis of heterocycles with dibenzobarrelene **1a-c**,[1,2] dibenzohomobarrelene **2a-c**[1,3] and dibenzobullvalene **3a,b**[4] skeletons.

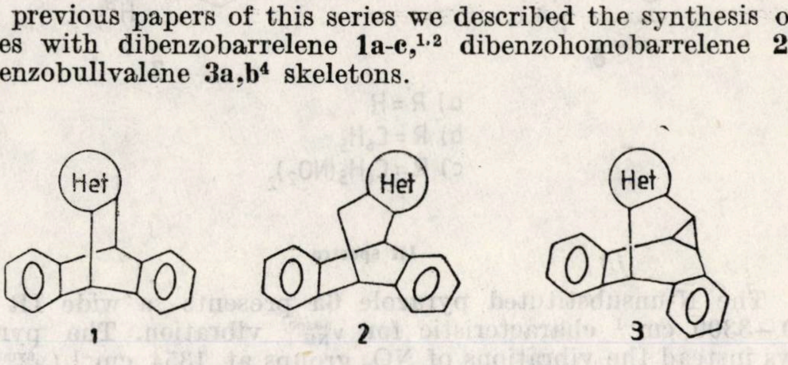

a) Het = pyrylium
b) Het = pyridinium
c) Het = pyrazole

In this short note the synthesis and characterization of some pyrazoles with annelated 7H-dibenzo[*c,e*]cycloheptene skeleton is presented.

RESULTS AND DISCUSSION

Synthesis

The key intermediate in the synthesis of the title pyrazoles was the known ketone **4**.[5] Condensation of this ketone with ethyl formate afforded the formyl derivative **5a** which was previously shown[6] to exist only in its tautomeric hydroxymethyleneketonic form **5b**.

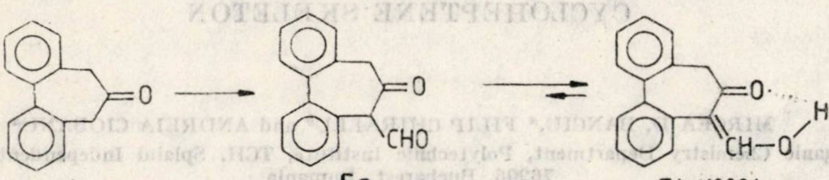

4 **5a** **5b** (100%)

In order to annelate a pyrazolic ring, the reaction of **5b** with hydrazine hydrate, phenylhydrazine or 2,4-dinitrophenylhydrazine was performed (in refluxing toluene in the presence of catalytic amounts of *p*-toluenesulfonic acid). The obtained solid pyrazoles were analyzed by means of IR, UV and ^{1}H-NMR spectra. The spectral data (vide infra) are in agreement with the structures **6a-c** and not with the isomeric ones **7a-c**.

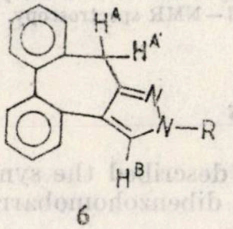

6

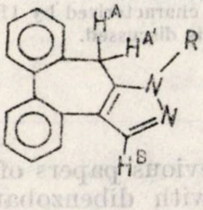

7

a) R = H
b) R = C_6H_5
c) R = $C_6H_3(NO_2)_2$

IR spectra

The N-unsubstituted pyrazole **6a** presents a wide IR band at 3000–3300 cm^{-1} characteristic for $\nu_{NH}^{assoc.}$ vibration. The pyrazole **6c** shows instead the vibrations of NO_2 groups at 1354 cm^{-1} ($\nu_{NO_2}^{sym}$) and at 1535 and 1545 cm^{-1} ($\nu_{NO_2}^{asym}$) as well as the γ_{CH} bands for 1,2,4-trisubstituted benzene at 835 and 870 cm^{-1}. The N-phenyl-substituted pyrazole **6b** presents two characteristic vibrations of a monosubstituted benzene at 690 and 757 cm^{-1}. Beside the above-mentioned bands all pyrazoles **6a-c** show the γ_{CH} band of *ortho*-disubstituted benzenes in the range of 742 – 747 cm^{-1}, the ν_{CH_2} band at 2915 – 2920 cm^{-1} and the ν_{CH}(aryl) ones at 3010 – 3060. All three pyrazoles **6a-c** present in the IR spectra a strong aromatic band : at 1598 cm^{-1} in **6a**, at 1595 cm^{-1} in **6b** and at 1606 cm^{-1} in **6c**. Other characteristic IR bands are shown in the Experimental part.

Electronic spectra

The electronic spectral data of pyrazoles **6a-c** are summarized in Table 1. All three pyrazoles present the shortest wavelength absorption maximum at 237 or 238 nm with lg ε-values above 4.44. The electronic spectra of pyrazoles **6a** and **6c** are similar excepting the longest wavelength absorption of dinitroderivative **6c** (345 nm) as well as its end absorptions in the visible domain conferring it a pale yellow colour. In opposition to both above spectra, the UV-spectrum of N-phenyl substituted pyrazole **6b** presents a strong absorption at 283 nm ($\lg\varepsilon = 4.47$). Examination of a Dreiding stereomodel of pyrazole **6b** reveals the conjugation between the phenyl group and pyrazole moiety (suggested by the coplanarity which may be attained between these rings). The extended conjugation in **6b** as compared with **6a** leads to the important bathochromic and hyperchromic shift of the second absorption maximum (from $\lambda = 258$ nm ; $\lg\varepsilon = 4.07$ in **6a** to $\lambda = 283$ nm ; $\lg\varepsilon = 4.47$ in **6b**).

Table 1

Electronic spectral data of pyrazoles **6a-c** (in methanol) ; $\lambda_{max}^{nm}(\lg\varepsilon_{max})$

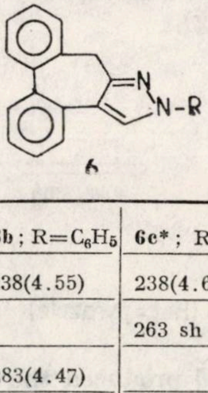

6

6a ; R=H	**6b** ; $R=C_6H_5$	**6c*** ; $R=C_6H_3(NO_2)_2$
237(4.44)	238(4.55)	238(4.67)
258(4.07)		263 sh (4.24)
	283(4.47)	
298(3.13)		296 sh (3.85)
		345 sh (3.67)
		end absorption up to 435 nm

* sh= shoulder

Introduction of two nitro groups in the N-phenyl substituent (such as in **6c**) causes a return to a spectrum very similar with that of **6a**; it seems that a steric inhibition of conjugation occurs in **6c**. Indeed the Dreiding model of **6c** suggests a strong steric hindrance between the *ortho*-nitro-substituent and the $\rangle$C—H group from the pyrazolic ring when this ring is coplanar with the adjacent benzenic one. A release of this hindrance could be achieved by rotation of the dinitrophenyl substituent around its bond with the pyrazole moiety; consequently, the conjugation between dinitrophenyl- and pyrazole ring is strongly reduced and the spectrum modified.

^{1}H-NMR spectra

The ^{1}H-NMR spectra of pyrazoles **6a-c** (see Experimental part) are in agreement with their structure. The eight aryl protons from the biphenyl moiety afford multiplets occurring at normal values of $\delta = 7 - 8.2$ ppm. The two methylene protons H^A, $H^{A'}$ from the seven-membered middle ring show at 20°C broad signals (apparently doublets) at $3.8 - 3.9$ ppm suggesting the mobile conformation of this ring (by slow rotation around the inter-ring biphenylic bond, leading to inversion of the seven membered ring).

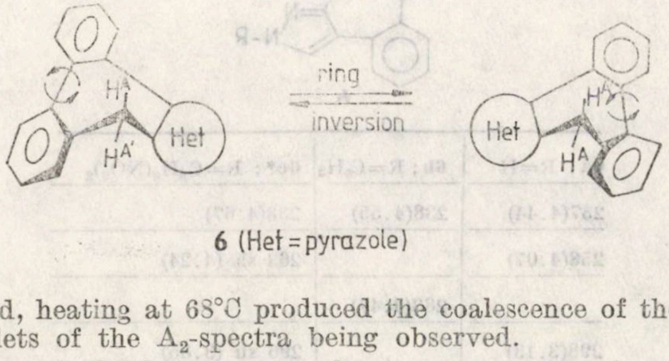

6 (Het = pyrazole)

Indeed, heating at 68°C produced the coalescence of these signals, sharp singlets of the A_2-spectra being observed.

The signal of H^B from pyrazole ring appears as sharp singlet at $\delta = 8.0$ ppm in **6a**, at 8.1 ppm in **6b** and at 8.75 ppm in **6c**. The important deshielding of this proton in **6c** could be ascribed mainly to the strong electron acceptor effects of the NO_2-groups favouring mesomeric structures of the type **6c**-A with a positive nitrogen atom (thus deshielding) adjacent to CH^B group. The N-H proton from **6a** could not be individually evidenced in the ^{1}H-NMR spectra run in d_6-acetone or d_6-DMSO being included in the HO-signal of water traces existing in these solvents (in anhydrous solvents such as CCl_4; $CDCl_3$; C_6D_6 the pyrazole **6a** is insoluble). In the pyrazole **6c** the protons H^C, H^D, H^E

from the dinitrophenyl moiety afford characteristic signals with the expected chemical shifts and coupling constants (see Experimental part).

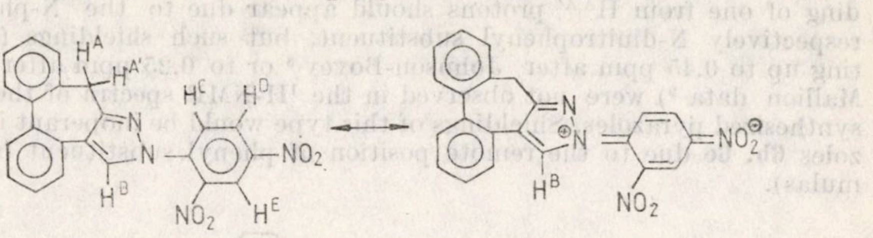
H^A
H^A'
H^C
H^D
N
N
NO2
H^B
NO2
H^E
N
⊕N
NO2⊖
H^B
NO2

6c **6c-A**

The structure of pyrazoles and the reaction mechanism

Formation of pyrazoles **6** from the dicarbonylic (hydroxymethyleneketonic) compound **5** proceeds most probably as in related cases [7,1] *via* the intermediate hydrazones which then undergo intramolecular cyclization. From the isomeric hydrazones of **5**, namely **8** and **9**, only the former seems to be formed and converted further to pyrazoles **6**. It should be reminded here that the compound **5** exists only as tautomer **5b**.[6]

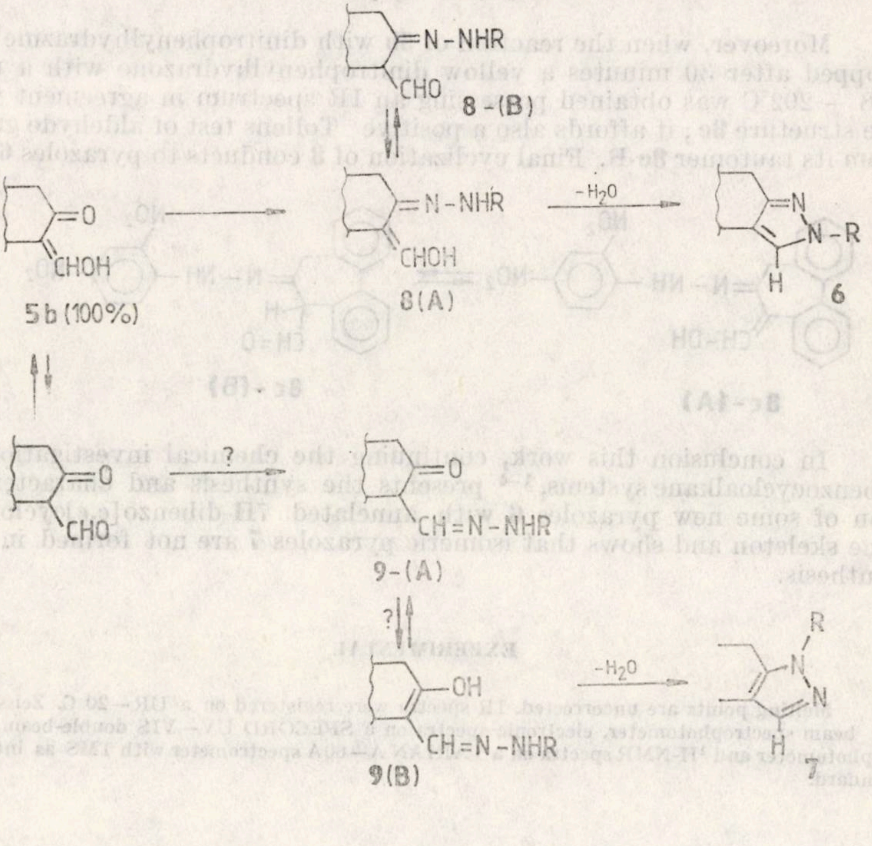
=N-NHR
CHO
8-(B)
=O
CHOH
5b (100%)
=N-NHR
CHOH
8(A)
-H2O
=N
N-R
H
6
=O
CHO
?
=O
CH=N-NHR
9-(A)
?
OH
CH=N-NHR
9(B)
-H2O
R
N
N
H
7

No isomeric pyrazole of the type **7** was obtained in the above described reactions. In such presumable pyrazoles **7b**, **7c** an important shielding of one from $H^{A,A'}$ protons should appear due to the N-phenyl or respectively N-dinitrophenyl substituent, but such shieldings (amounting up to 0.45 ppm after Johnson-Bovey [8] or to 0.25 ppm after Haigh-Mallion data [9]) were not observed in the ^1H-NMR spectra of the newly synthesized pyrazoles. Shieldings of this type would be inoperant in pyrazoles **6b**, **6c** due to the remote position of phenyl substituent (see formulas).

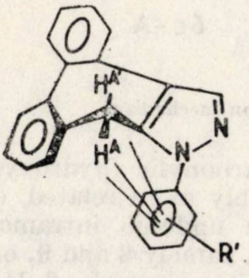

7b,c

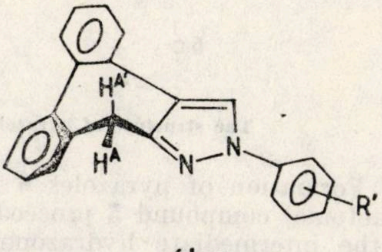

6b,c

$R'=C_6H_5;\ (NO_2)_2C_6H_3$

Moreover, when the reaction of **5b** with dinitrophenylhydrazine was stopped after 30 minutes a yellow dinitrophenylhydrazone with a m.p. 198 – 202°C was obtained possessing an IR spectrum in agreement with the structure **8c** ; it affords also a positive Tollens test of aldehyde group from its tautomer **8c**-B. Final cyclization of **8** conducts to pyrazoles **6.**

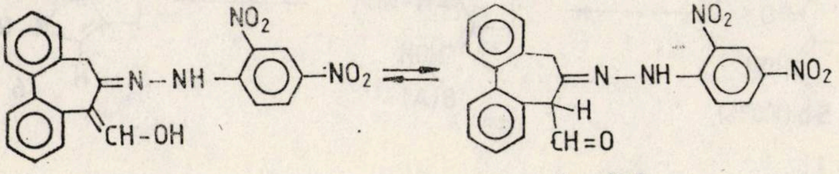

8c-(A) **8c-(B)**

In conclusion this work, continuing the chemical investigation of dibenzocycloalkane systems, [1–4] presents the synthesis and characterization of some new pyrazoles **6** with annelated 7H-dibenzo[*c*,*e*]cycloheptene skeleton and shows that isomeric pyrazoles **7** are not formed in the synthesis.

EXPERIMENTAL

Melting points are uncorrected. IR spectra were registered on a UR–20 C. Zeiss double beam spectrophotometer, electronic spectra on a SPECORD UV–VIS double-beam spectrophotometer and ^1H-NMR spectra on a VARIAN A–60A spectrometer with TMS as internal standard.

General procedure for synthesis of pyrazoles 6a-c

A mixture of equimolar quantities of hydroxymethylene-ketone **5b**^{6} and 80% hydrazine hydrate, freshly distilled phenylhydrazine or 2,4-dinitrophenylhydrazine in toluene (25 mL for 2 mmoles of **5b**) was heated in presence of catalytic amounts of *p*-toluenesulfonic acid. During 12 hrs of reflux small quantities of water were separated with an ASTM device. The obtained solutions were washed with water until pH = 7, dried over anhydrous MgSO$_4$, filtered and evaporated *in vacuo*. The solid residue was recrystallized twice from proper solvents affording pure pyrazoles **6a-c**. When the reaction of **5b** with 2,4-dinitrophenylhydrazine was stopped after 30 min the yellow dinitrophenylhydrazone **8c** was isolated (*vide infra*).

***7H-1′,2′*-Pyrazolo[*a*]dibenzo[*c,e*]cycloheptene (6a)**, white crystals m.p. 193—195°C (from ethanol); 80% yield.

IR spectrum (KBr; cm^{-1}): 465m, 505m, 620m, 730s, 742s, 750s, 763s, 778m, 789m, 820m, 955m, 1010m, 1145m, 1195m, 1330w, 1384w, 1430m, 1477m, 1510m, 1570m, 1598m-s, 2890m, 2905m, 2920m, 2950w, 3020w, 3060m, 3100m, 3000 — 3300 large.

UV spectrum (see text)

^{1}H-NMR spectrum (d$_6$-acetone; δppm): 3.80 (large signal; $_2$H^A + NH); 7.25 — 7.85 (m; 8Haryl); 8.0 (s; 1H^B).

***7H*-(*2′*-Phenyl)-*1′,2′*pyrazolo[*a*]dibenzo[*c,e*]cycloheptene (6b)** white crystals, m.p. 178 — 179°C (from ethanol); 82% yield.

IR spectrum (KBr; cm^{-1}): 480w, 498m, 510w, 575w, 592w, 670w, 690m, 747s, 757s, 770s, 792w, 807w, 900w, 952m, 1010w, 1043m, 1198m, 1403s, 1430w, 1488m, 1505m, 1577m, 1595s, 2915w, 2970m, 2990m, 3020w and 3045w.

UV spectrum (see text)

^{1}H-NMR spectrum (CDCl$_3$; δppm): 3.90 (large d; 2H^A); 7.0 — 7.9 (m; 13Haryl); 8.1(s; 1H^B).

***7H*-(2′-(2″,4″-Dinitrophenyl)-1′,2′-pyrazolo[*a*]dibenzo[*c,e*]cycloheptene (6c)**, yellow crystals, m.p. 228 — 231°C (from acetic acid); 70% yield.

IR spectrum (KBr; cm^{-1}): 480w, 502m, 630m, 662w, 710w, 716w, 747s, 767s, 782m, 835m 855w, 870w, 907m, 915s, 963m, 1018w, 1085w, 1100w, 1354s, 1404w, 1510m, 1535s, 1545s, 1606s, 2892w, 2920w, 3010w, 3058w and 3090w.

Electronic spectrum (see text)

^{1}H-NMR spectrum (trifluoroacetic acid; δppm): 3.85 (large d; 2H^A); 7.0 — 8.2 (m; 8Haryl); 8.38 (app d. 1H^C; J = 8.5 Hz); 8.75 (s; 1H^B); 9.18(q; 1H^D; J = 8.5; 2.5 Hz); 9.52 (app. d; 1H^E; J = 2.5 Hz).

2,4-Dinitrophenylhydrazone **8c** *of* **5b**, yellow solid, m.p. 198—202°C;

IR spectrum (KBr; cm^{-1}): 695m, 745m, 820m, 1010m, 1035m, 1115s, 1140s, 1320s, 1340s (NO$_2$); 1520s(NO$_2$); 1590s(C = C); 1612s(C=N); 2920w, 3090w, 3260w, 3320w(NH) and 2500 — 3300(OH) large.

REFERENCES

[1] Note III: M. D. Banciu, M. D. Stănescu and F. Chiraleu, *Rev. Roumaine Chim.*, **34**, 1921 (1989).

[2] M. Stănescu, M. Banciu and A. T. Balaban, *Rev. Roumaine Chim.*, **34**, 617 (1989).

[3] M. Banciu, A. T. Balaban, C. Drăghici and R. Vlad, *Rev. Roumaine Chim.*, **27**, 1037 (1982).

[4] M. Banciu, M. Stănescu, C. Florea, A. T. Balaban and E. Ciorănescu, *Rev. Roumaine Chim.*, **32**, 1161 (1987).

[5] B. Eistert and H. Minas, *Chem. Ber.*, **97**, 2479 (1964).

[6] M. Banciu, Phan-Le-Thuy and L. Stănescu, *Rev. Roumaine Chim.*, **24**, 957 (1979).

[7] G. R. Newkome and W. W. Paudler, "Contemporary Heterocyclic Chemistry", J. Wiley, New York, 1982.

[8] C. E. Johnson and F. A. Bovey, *J. Chem. Phys.*, **29**, 1012 (1958).

[9] C. W. Haigh and R. B. Mallion, *Org. Magn. Reson.*, **4**, 203 (1972).

Revue Roumaine de Chimie, **35**, *6*, 747–755 (1990)

MESOIONIC OXAZOLONES. V[1]

ETHANOLYSIS AND AMINOLYSIS OF ACYLATED COMPOUNDS

HORIA PETRIDE

Centre of Organic Chemistry
Spl. Independenţei 202 B, 78100 Bucharest 15, Romania

Received January 23, 1989

The nonplanar acylated mesoionic oxazolones 9–10 are several thousand times more reactive towards ethanol or aniline than their planar analogs 7–8. The nucleophiles attack the mesoionic ring at the C_2 atom. The tautomeric equilibrium of the ethanolysis product 11a is investigated. Methylation of 11a gives ylide 28a as by-product. The compounds 24a, 27a and 28a present in NMR spectra anisochronous CH_2Cl protons due to nonplanar grounds states.

Mesoionic oxazolones ("münchnones") are reactive compounds towards nucleophiles like water, alcohols or primary amines. Thus, it is known that the monocyclic derivative **1** undergoes reaction with methanol, *p*-toluidine or water to give the compounds **2a-c**, respectively.[2]

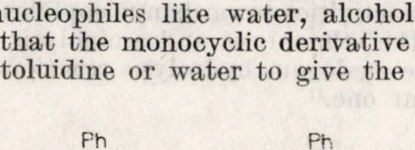

1

2a-c

2	Y
a	OMe
b	HN-C_6H_4-Me(p)
c	OH

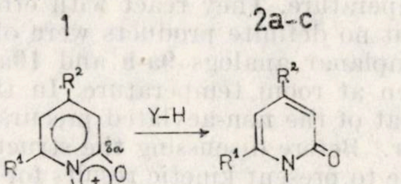

3a-b

4a-b

3-4	R	R²	Y
a	Me	H	OEt
b	H	H	HN-Ph

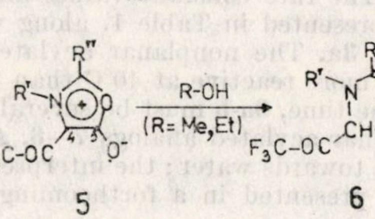

5

6

An analogous behaviour towards ethanol was presented by the 3-phenyl derivative of **1**.[3] In the same way, the bicyclic 3-unsubstituted compounds **3a-b**, generated *in situ*, yielded the derivatives **4a-b** in reaction with ethanol [4] or aniline.[5] Similarly, the acylated monocyclic münchnones **5** (R' = Me, Ph ; R'' = Ph, SEt) underwent alcoholysis to give the expected esters **6**.[6,7] Since the compound **6** (R' = R'' = Ph) gave an intensively coloured solution with ferric chloride,[2] one may assume that it is partly or totally enolised. Under forcing conditions the 3-acetyl derivative of **3b** was transformed by benzylamine into the amide **4** ($R^2 = R^2 = H$; $R = NHCH_2Ph$).[8]

Working with selectively ^{18}O-labelled **1**, Knorr [2] discovered that water molecule attacks the mesoionic ring at both 2 and 5 positions, the first pathway prevailing (70%). On the contrary, all alcoholysis and aminolysis reactions cited before implicate solely the nucleophilic attack at the carbon atom bounded to the exocyclic oxygen, namely C_5 for the monocyclic münchnones (i.e. **1**) and C_2 for their bicyclic analogs (i.e. **3**). Should the attack also occur in this case at C_2 (or C_{8a}, respectively), mixtures of reaction products would be obtained even working with ordinary-oxygen containing münchnones, which was not actually the case.

To gain more information about the reactivity towards nucleophiles and the position of the attack, a study on the acylated derivatives **7**–**10** was undertaken ; the experimental results obtained are presented in this paper. As reported previously,[10] the acyl group is coplanar with the mesoionic nucleus in **7a-b** and **8a-b**, but out of this plane in **9a-b** and **10a-b**. We expect different reactivities towards nucleophiles for these two types of compounds. Only the ethanolysis and aminolysis reactions will be exposed in this paper, the analogous hydrolysis reaction constituting the subject of a subsequent one.[11]

ETHANOLYSIS AND AMINOLYSIS

The planar acylated derivatives **7a-b** and **8a-b** are stable towards ethanol or aniline at room temperature. They react with ethanol at reflux and long reaction time, but no definite products were obtained.

On the contrary, the nonplanar analogs **9a-b** and **10a-b** undergo ethanolysis and aminolysis even at room temperature. In this respect, their behaviour is similar to that of the non-acylated precursors of type **3a** studied in a preceding paper.[4] Before discussing the structures of the reaction products, we would like to present kinetic results for ethanolysis of compounds **9a-b**.

The kinetic determinations were performed in acetonitrile : ethanol (1 : 1, v/v) mixture. The rate constant values and the activation parameters for **9a-b** are presented in Table 1, along with the corresponding values for compound **3a**. The nonplanar acylated derivatives **9a-b** are about 10 – 40 times more reactive at 40°C than their non-acylated precursor **3a**. At the same time, **9a-b** must be several thounsand times more reactive than the planar acylated analogs **7**–**8**. A similar order of reactivity has been found towards water ; the interpretation of the hydrolysis kinetic data will be presented in a forthcoming paper.[11]

The elemental analyses of the ethanolysis products indicate a formal addition of one ethanol molecule to the mesoionic substrate. The ^{1}H-NMR spectrum confirm the presence of an ethoxy residue; the remaining ethanolic hydrogen is now of enolic type, it being located over 12 ppm

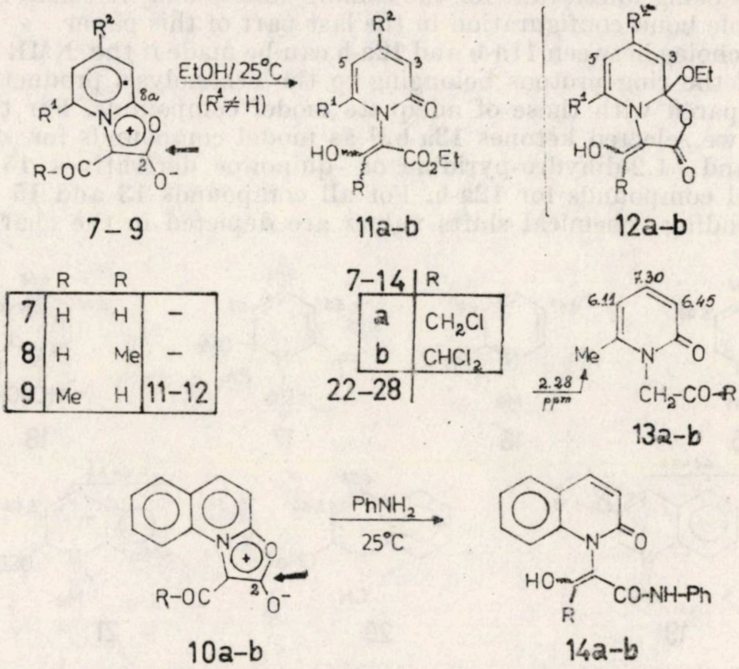
R²
R¹
8a
N
O
R-OC
2
O⁻
EtOH/25°C
(R¹≠H)
5
3
HO
CO₂Et
R
OEt
7–9
11a–b
12a–b
R R
7 H H –
8 H Me –
9 Me H 11–12
7–14 R
a CH₂Cl
b CHCl₂
22–28
7.30
6.11
6.45
Me
2.28 ppm
CH₂-CO-R
13a–b
PhNH₂
25°C
CO-NH-Ph
10a–b
14a–b

Table 1

Rate constants and activation parameters[a] for ethanolysis

Compd.	Temp., °C	$10^4 \cdot k$, s^{-1}	ΔH* kcal. M^{-1}	ΔS* e.u.	k_{rel}[b]
3a[c]	49.8	1.3			
	59.5	2.2	11.4	−41.3	(1)
	73.0	4.4			
9a	10.2	1.7			
	23.5	6.05	15.5	−20.9	39.4
	36.3	19.25			
3b	28.1	2.0			
	38.3	4.7	15.6	−23.6	8.6
	47.8	10.4			

[a] estimated errors : ΔH* ± 0.2 ; ΔS* ± 0.7.
[b] extrapolated at an intermediate temperature (40°C).
[c] from ref.[4].

in $CDCl_3$. Two structures for the ethanolysis products of **9 a-b**, namely **11a-b** and **12a-b**, may be written at a first sight. They originate from a nucleophilic attack at the atoms C_2 and C_{8a}, respectively, the two virtual electrophilic sites of a bicyclic münchnone, as discussed in introduction. The first formula contains a 2-pyridinone residue, while the last may be considered a 2-pyridinone ketal. All the structures have also a hydroxy-ethylidene radical whose configuration remains unprecised at this point, as being unrelevant for the coming discussion. We shall return to the double bond configuration in the last part of this paper.

A choice between **11a-b** and **12a-b** can be made if the NMR chemical shifts of the ring protons belonging to the ethanolysis products of **9a-b** are compared with those of adequate model compounds. For this comparison we selected ketones **13a-b**,[11] as model compounds for structures **11a-b**, and 1,2-dihydro-pyridine or -quinoline derivatives **15**—**21**,[12-16] as model compounds for **12a-b.** For all compounds **13** and **15**—**21**, the corresponding chemical shifts values are depicted in the charts. Comparing the chemical shifts of the ring protons in **11a**/**12a**, namely δ 6.47 (H_3), 7.30 (H_4) and 6.19 ppm (H_5), with the chemical shifts in the model compounds, we ascribed to this compound structure **11a** and not **12a.** The same holds true for the ethanolysis product of **9b**, which has the structure **11b.**

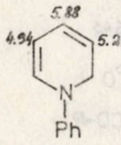

15

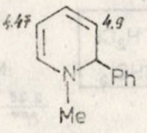

16

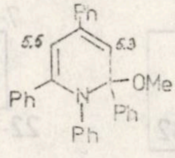

17

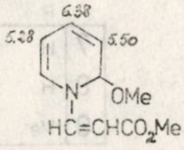

18

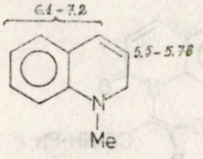

19

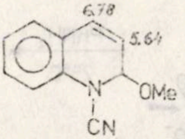

20

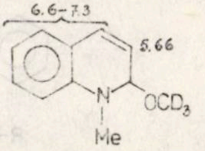

21

The formation of **11a-b** implies a regioselective nucleophilic attack at the C_2 atom in **9a-b.** This is in agreement with all alcoholysis data cited in the introduction of this paper.

The quinolinium derivatives **10a-b** react easily with aniline at room temperature. The elemental analyses and spectral data of the isolated reaction products fit the structures **14a-b**, namely enolic forms of β-keto-anilides. Here again, a regioselective nucleophilic attack at the C_2 atom of **10a-b** occurred.

STRUCTURE OF THE COMPOUND 11a

The ethanolysis product of the mesoionic oxazolone **9a** contains a 2-pyridinone ring linked to the enol form of a β-ketoacetic ester (structure **11a**). Taking into account the (E, Z)-isomerism of the ethylenic bond, two formulas may be written for **11a**, namely **22a** and **23a.** Both have an intramolecularly chelated enolic hydrogen, but different carbonyl partners. No evidence for the presence of the ketonic tautomer **25a** has been found in the NMR spectrum in $CDCl_3$.

Structure **22a** is similar to the enol **29**, a compound presenting anisochronous OCH_2 protons in the NMR spectrum in $CDCl_3$.[22] On the contrary, the ethanolysis product of **9a** presents in the same solvent a singlet for the CH_2Cl group and a normally splitted (quartet) signal for the OCH_2 group. This fact pleads for structure **23a**, which must contain the pyridinone ring nearly coplanar with the ethylenic moiety.

Table 2

^1H-NMR data for the compounds **11a**, **27a** and **28a**

Compound[a]	Solv.	Chemical shifts (δ, ppm)[b]						
		Me	H_5	H_4	H_3	$O-CH_2-CH_3$	CH_2Cl	OMe
23a	$CDCl_3$	2.22 (s)	6.19 (d; 7)	7.39 (dd: 7; 9)	6.47 (d; 9)	4.27; 1.25 (q; 7) (t; 7)	3.93 (s)	12.5[c]
	$(CD_3)_2CO$	2.27 (s)	6.27 (d; 7)	7.46 (dd: 7; 9)	6.40 (d; 9)	4.33; 1.22 (q; 7) (t; 7)	4.10 (s)	—
24a	$(CD_3)_2CO$	2.40 (s)	6.27 (d; 7)	7.46 (dd; 7;9)	6.40 (d;9)	4.26; 1.22 (q; 7) (t; 7)	4.94[d] (AB q)	—
	DMSO-d_6	2.12 (s)	6.20 (d; 7)	7.42 (dd; 7;9)	6.27 (d;9)	4.11; 1.13 (q; 7) (t; 7)	4.89 (AB q)	—
27a	$CDCl_3$	2.12 (s)	6.04 (d; 7)	7.26 (dd; 7; 9)	6.39 (d;9)	4.17; 1.20 (q; 7) (t; 7)	5.06[f] (AB q)	3.87 (s)
28a	$CDCl_3$	2.55 (s)	7.25 (d; 8)	8.08 (t; 8)	7.09[h] (d; 8)	4.09; 1.15 (q; 7) (t; 7)	4.75[g] (AB q)	4.07 (s)

[a] the compounds **23a** and **24a** are tautomers with general formula **11a** (see text);
[b] at room temperature, with TMS as internal standard; multiplicity and vicinal coupling constants (Hz) are shown in brackets;
[c] broad signal due to OH;
[d] $J_{AB} = 15$ Hz; $\nu_A = 5.05$ and $\nu_B = 4.82$ ppm; [e] $J_{AB} = 12.5$ Hz; $\nu_A = 5.09$ and $\nu_B = 4.69$ ppm; [f] $J_{AB} = 12.5$ Hz; $\nu_A = 5.73$ and $\nu_B = 4.39$ ppm;
[g] $J_{AB} = 12.5$ Hz; $\nu_A = 4.90$ and $\nu_B = 4.61$ ppm;
[h] the assignments for H_5 and H_3 may be inverted.

In more polar solvents, such as acetone or acetonitrile, compound **29** is in equilibrium with a solvent-bonded enolic form having magnetically equivalent methylene protons.[22] The opposite phenomenon was observed for **11a.** Thus, in DMSO-d_6 as solvent, the signal due to the CH_2Cl protons is splitted into an AB quartet and in acetone-d_6 both forms exist in a 3 : 1 ratio (form with equivalent CH_2Cl/form with non-equivalent CH_2Cl). The respective NMR data are presented in Table 2.

The anisochronism of the CH_2Cl protons might be due either to a chiral molecular axis (structure **24a**) or to the presence of an asymmetric carbon atom (structure **25a**). Although the formation of the ketonic tautomer **25a** would be favoured in more polar solvents, its existence seems doubtful because no signal attributable to the acidic CH proton has been found in acetone-d_6 or DMSO-d_6. Consequently, the magnetic non-equivalency of the CH_2Cl protons may be ascribed to the non-coplanarity of the pyridinone ring and the exocyclic ethylenic bond (structure **24a**).

The polar solvent competes with the pyridinone oxygen in the formation of the hydrogen bond and makes possible the deviation of the pyridinone ring from the molecular plane to alleviate the steric hindrance. Accordingly, the molecule becomes chiral.

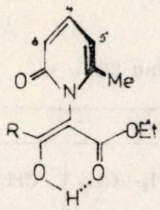

22a

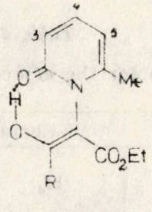

23a

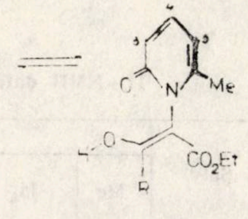

24a

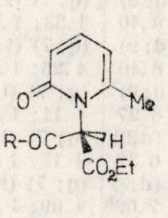

25a

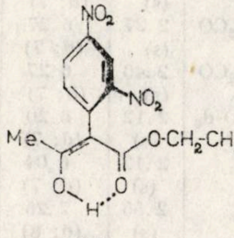

29

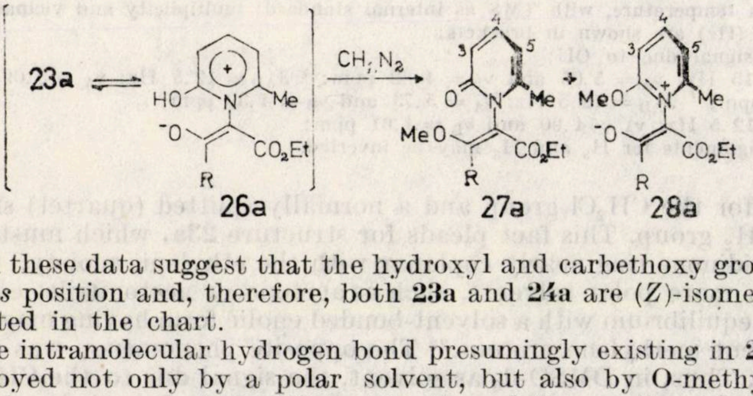

26a **27a** **28a**

All these data suggest that the hydroxyl and carbethoxy groups are in a *trans* position and, therefore, both **23a** and **24a** are (Z)-isomers, just as depicted in the chart.

The intramolecular hydrogen bond presumingly existing in **23a** can be destroyed not only by a polar solvent, but also by O-methylation. Indeed, the treatment of **11a** (**23a**) with ethereal diazomethane led to two isomeric products into a 3 : 1 ratio, both having anisochronous CH_2Cl protons.

The major methylation product is a colourless ether-soluble compound whose NMR features (Table 2) correspond to the formula **27a**. It contains a 2-pyridinone ring and a conjugated ester carbonyl group ($\nu_{CO}^{ester} = 1710$ cm^{-1}).

The minor methylation product is a yellow ether-unsoluble compound presenting in the NMR spectrum downfield shifted ring protons relatively to those of **27a** (Table 2). In addition, it does not show any IR carbonyl absorption band over 1660 cm^{-1}, indicating a more extended conjugation for its ester carbonyl group. In our opinion, all these features are consistent with the pyridinium ylide **28a** structure. Its NMR characteristics, including the anisochronism of the CH_2Cl protons, are similar to those of other pyridinium ylides synthesized by specific routes.[18]

The unexpected formation of **28a** implies the transient existence of the 2-hydroxy-pyridinium ylide **26a**, another tautomer of **23a**. This may be considered as an additional proof regarding the (*Z*)-configuration assigned to the ethylenic bond of **11a**. As a matter of fact, a nearly coplanar structure for **23a** renders more easily the hydrogen exchange between the two oxygen atoms.

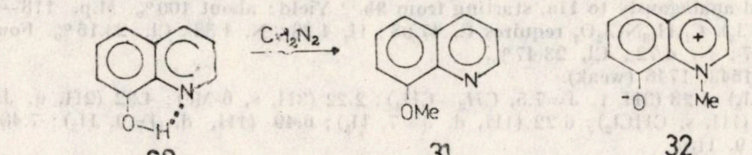

30 31 32

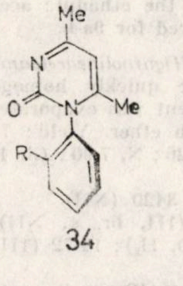

34

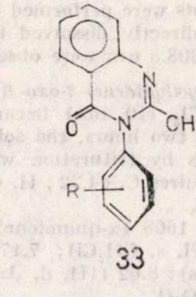

33

The behaviour of **11a** (**23a** ⇄ **24a** ⇄ **26a**) towards diazomethane is similar to that reported for oxine **30**. It is known[19] that **30** yields, in addition to the "normal" reaction product **31**, a second methylated compound, the zwitterionic derivative **32**.

Attempts were made to measure the energy barrier to rotation about the $N(sp^2) - C(sp^2)$ single bond of **11a** and **27a**. Unfortunately, **11a** was not stable in DMSO or nitrobenzene solutions above 90°C. However, no coalescence has been observed until this temperature, meaning that the barrier is higher than 18.5 kcal/mole (77 kJ/mole). The same trend was presented by **27a** in $CDCl_3$ solution until 55°C. A minimum value of 16.5 kcal/mole (69 KJ/mole) may be calculated for the rotational energy required for **27a**. Similar high barrier to rotation have been reported for the analogous compounds **33** and **34**.[20,21] For example, the lowest value has been quoted for **33** (R = 3-Br) containing an *ortho*-unsubstituted phenyl ring (18.9 kcal/mole at +94°C).[20]

EXPERIMENTAL PART

Melting points are uncorrected. IR spectra were recorded on a UR–10 Carl Zeiss spectrometer, ^{1}H-NMR spectra with a Varian A-60A apparatus and UV spectra on a Specord UV-VIS Carl Zeiss spectrophotometer. NMR chemical shifts and coupling constants, J, as well IR and UV absorption maxima are quoted in ppm (δ scale, internal TMS), Hz, cm^{-1} and nm, respectively.

Ethanolysis and aminolysis of 9 – 10

Ethyl (Z)-α-(2-chloro-1-hydroxyethylidene)-6-methyl-2-oxo-1(2H)pyridineacetate (**11a** ; **23a**, **24a**). A suspension of **9a** (1 mmole)[10] in n anhydrous ethanol (10 mL) was heated gently (40°C until the solid disappeared (10 min.) and the resulted homogeneous solution was left at room temperature overnight. Evaporation of the solvent *in vacuo* (max. bath temperature 40°C) gave **11a** in quantitative yield. M.p. 120–121°C (from $CCl_4/CHCl_3$) · $C_{12}H_{14}NClO_4$ requires C, 53.05 ; H, 5.19 ; N, 5.16 ; Cl, 13.05 %. Found C, 52.91 ; H, 5.31 ; N, 5.01 ; Cl, 13.37 %.
IR (CH_2Cl_2) : 1670, 1738 (weak).
UV (CH_2Cl_2) : 238 (log ε = 4.08), 255 (3.99 , 314.5 (3.81) ;
(MeCN : EtOH ; 1 :1 ; v/v) : 235 (4.04), 250 (3.94), 312.5 (3.85).

It gives a red-wine colour with alcoholic ferric chloride solution. Its ^1H-NMR spectrum corresponds to the equilibrium **23a** ↔ **24a** (Table 2 ; see text).

Ethyl (Z)-α-(2,2-dichloro-1-hydroxyethylidene)-6-methyl-2-oxo-1(2H)pyridineacetate (**11b**). It was prepared analogously to **11a**, starting from **9b**.[10] Yield : about 100 %. M.p. 118–119°C (from $CCl_4/CHCl_3$). $C_{12}H_{13}NCl_2O_4$ requires C, 47.08 ; H, 4.28 ; N, 4.58 ; Cl, 23.16 %. Found C 47.29 ; H, 4.07 ; N, 4.72 ; Cl, 23.47 %.
IR (CH_2Cl_2) : 1643, 1746 (weak).
^1H-NMR ($CDCl_3$) : 1.23 (3H, t, J=7.5, CH_3–CH_2) ; 2.22 (3H, s, 6-Me) ; 4.32 (2H, q, J=7.5, OCH_2) ; 6.03 (1H, s, $CHCl_2$) ; 6.22 (1H, d, J=7, H_5) ; 6.49 (1H, d, J=9, H_3) ; 7.40 (1H, dd, J=7 and 9, H_4).

Kinetic measurements were performed analogously to those for **3a**,[4] except for the fact that the substrates were directly dissolved in the ethanol : acetonitrile mixture. Isosbestic points at 237.5, 271 and 308.5 nm were observed for **9a-b**.

α-(2-Chloro-1-hydroxyethylidene)-2-oxo-1(2H)quinolineacetoanilide (**14a**). A suspension of **10a** (1 mmole)[10] in CH_2Cl_2 (10 mL) became quickly homogeneous after adding aniline (1 mmole). After standing two hours, the solvent was evaporated *in vacuo* and the residue solidified to white crystals by trituration with ether. Yield : 75 %. M.p. 304–306°C (from ethanol). $C_{19}H_{15}N_2ClO_3$ requires C, 64.32 ; H, 4.26 ; N, 7.90 ; Cl, 10.00 %. Found C, 64.60 ; H, 4.56 ; N, 4.56 ; Cl, 9.82 %.
IR (CH_2Cl_2) : 1598, 1642, 1668 (α-quinolone), 3420 (NH).
^1H-NMR ($CDCl_3$) : 3.88 (2H, s, CH_2Cl) ; 7.17 (1H, br. s, NH) ; 6.88 (1H, d, J=9, H_3) ; 7.2–7.9 (9H, m, aromatics) ; 8.02 (1H, d, J=9, H_4) ; 14.72 (1H, br. s, OH). Both NH and OH signals vanish with D_2O.

α-(2,2-Dichloro-1-hydroxyethylidene)-2-oxo-1(2H)quinolineacetoanilide (**14b**). It was prepared in nearly quantitative yield analogously to **14a**, starting from **10b**.[10] M.p. 282–285°C (from ethanol). $C_{12}H_{14}N_2Cl_2O_3$ requires C, 58.63 ; H, 3.63 ; N, 7.20 ; Cl, 18.22 %. Found C, 58.75 ; H, 3.85 ; N, 7.48 ; Cl, 18.53 %.
IR (KBr) : 1660 (α-quinolone), 3330 (NH).
^1H-NMR (acetone-d_6) : 6.13 (1H, s, $CHCl_2$) ; 6.68 (1H, d, J=9, H_3) ; 7.0–7.9 (10H, m, 9H aromatics + NH) ; 7.97 (1H, d, J=9, H_4).

Methylation of 11a

About 2 mmoles of **11a** were added to ethereal diazomethane (from 3.3 g of N-methyl-N-nitrosourea). After completion of the reaction (2–3 hrs.) the deposited brown-red solid (about 150 mg) was filtered off and several times recrystallized from benzene to afford pure yellow **28a** in 7 % yield. The ethereal filtrate was refluxed for 15 minutes with active charcoal and then filtered. The clear filtrate was evaporated to about 5 mL and petroleum ether (b.p. 30–40°C) was added until cloudiness. A viscous colourless oil (**27a**) was separated on cooling in 44 % yield.

Ethyl α-(1-chloro-2-methoxyethylidene)-6-methyl-2-oxo-1(2H)pyridineacetate (**27a**). Oil. $C_{13}H_{12}NClO_4$ requires C, 54.65 ; H, 5.64 ; N, 4.90 ; Cl, 12.41 %. Found C, 55.05 ; H, 5.33 ; N, 4.60 ; Cl, 12.75 %.
IR (CH_2Cl_2) : 1633, 1665, 1710.

Inner salt of 1-(3-chloro-1-ethoxycarbonyl-2-oxopropyl)-2-methoxy-6-methylpyridinium hydroxide (**28a**). M.p. 103–105°C. Found for $C_{13}H_{16}NClO_4$: C, 54.93 ; H 5.58 ; N, 5.16 ; Cl, 12.17 %.
IR (CH_2Cl_2) : 1632, 1660.

The ^2H-NMR spectra of **27a** and **28a** are presented in Table 2. The ratio between these two compounds was determined by evaporation of the ether from the crude heterogeneous mixture dissolving the resulted residue in $CDCl_3$ and recording its NMR spectrum. The integrals of the two 6-Me signals were measured.

REFERENCES

[1] Part IV : D. Răileanu and H. Petride, *Rev. Roumaine Chim.*, **35,** 459(1990)
[2] H. O. Bayer, R. Huisgen, R. Knorr and F. C. Schaefer, *Chem. Ber.*, **103,** 2581 (1970).
[3] H. Alper and M. Tanaka, *J. Amer. Chem. Sac.*, **101,** 4245 (1979).
[4] Part II : H. Petride and D. Răileanu, *Rev. Raumaine Chim.*, **33,** 729 (1988).
[5] G. V. Boyd and P. H. Wright, *J. Chem. Sac. (C)*, **1970,** 1485.
[6] G. Singh and S. Singh, *Tetrahedran Lett.*, **1964,** 3789.
[7] H. Gotthardt and F. Reiter, *Liebigs Ann. Chem.*, **1979,** 650 ; *Chem. Abstr.*, **91,** 56896 (1979).
[8] A. Lawson and D. H. Miles, *J. Chem. Soc.*, **1959,** 2865.
[9] R. Knorr, *Chem. Ber.*, **104,** 3633 (1971).
[10] Part III : H. Petride and D. Răileanu, *Rev. Roumaine Chim.*, **34,** 1251 (1989).
[11] H. Petride, in preparation.
[12] M. Saunders and E. H. Gould, *J. Org. Chem.*, **27,** 1439 (1962).
[13] L. M. Thiessen, J. A. Lepoivre and F. C. Alderweilreldt, *Tetrahedron Lett.*, **1974,** 59.
[14] R. Aveta, G. Doddi, N. Insam and F. Stegel, *J. Org. Chem.*, **45,** 5160 (1980).
[15] J. W. Bunting and W. G. Meathrel, *Can. J. Chem.*, **50,** 917 (1972).
[16] R. M. Acheson and J. McK. Woolhard, *J. Chem. Soc. (C)*, **1971,** 3296.
[17] G. E. Hall, D. Hughes, D. Rae and A. P. Rhodes, *Tetrahedron Lett.*, **1967,** 241.
[18] H. Petride, *Rev. Roum. Chim.*, **34,** 2057(1979).
[19] J. P. Phillips and R. W. Keown, *J. Amer. Chem. Soc.*, **73,** 5483 (1951).
[20] L. D. Colebrook and H. G. Giels, *Can. J. Chem.*, **53,** 3451 (1975).
[21] C. Kashima and A. Kato, *J. Chem. Soc. Perkin Trans.* 1, **1980,** 1599 .

Revue Roumaine de Chimie, **35**, *6*, 757–765 (1990)

SYNTHESIS AND BIOLOGICAL ACTIVITIES OF SOME NEW ISOXAZOLO[5,4-d]PYRIMIDINE DERIVATIVES

VASUDEVA A. ADHIKARI * and VIRUPAX V. BADIGER **
Department of Chemistry, Karnatak University, Dharwad-580 003, India

Received April 30, 1988

4,5-Dihydro-4-oxo-3,6-disubstituted isoxazolo[5,4-d]-pyrimidines (Ia-f) when refluxed with phosphorus oxychloride yielded 4-chloro-3,6-disubstituted isoxazolo-[5,4-d]pyrimidines (IIa-f) which on condensation with 2-aminoethanol and 3-amino-1-propanol gave 4-β-hydroxy-ethylamino-3,6-disubstituted isoxazolo[5,4-d]pyrimidines (IIIa-f) and 4-γ-hydroxypropylamino-3,6-disubstituted isoxazolo[5,4-d]pyrimidines (IV a-f) respectively. These intermediates, upon treatment with phosphorus oxychloride underwent smooth cyclisation with the formation of 2,3-dihydro-5,9-disubstituted isoxazolo[4,5-e]-imidazo[1,2-c]pyrimidines (Va-f) and 2,3,4-trihydro-6,10-disubstituted isoxazolo[4,5-e]-pyrimido[1,2-c]-pyrimidines (VI a-f). Structures of new compounds have been established by their spectral and elemental analyses. All the new compounds were subjected to *in vitro* antibacterial and antifungal screening using standard methods. Their structure-activity relationship has been studied.

INTRODUCTION

The biological activities of isoxazolo [5, 4-d] pyrimidine are little known and recently they have been shown to possess significant antibacterial[1,2] and analgesic[3] activities. Encouraged by the fact that imidazole and pyrimidine moieties are associated with a wide spectrum of physiological properties, we designed the synthesis of isoxazolo [4,5-e] imidazo [1,2-c] pyrimidines (Va-f) and isoxazolo [4,5-e] pyrimido [1,2-c] pyrimidines (VIa-f) wherein active imidazole and pyrimidine heterocycles are fused to potent isoxazolo [5,4-d] pyrimidine ring system. In view of the various pharmacological activities exhibited by a number of fused imidazo- and pyrimido [2,1-b] quinazolines,[4] [2,1-a] isoindoles,[5] [2,1-i] purines,[6] [2,1-b] benzimidazoles,[7] [1,2-a] phthalazines,[8] [1,2-b] benzothiazines[9] and [1,2-c] pyrazolopyrimidines,[10] we investigated the antimicrobial properties of all the new compounds IIIa-VIf by standard methods.

RESULTS

SYNTHESES

The reaction sequence leading to the formation of Va-f and VIa-f are outlined in Scheme 1.

The required 4,5-dihydro-4-oxo-3,6-disubstituted isoxazolo [5,4-d] pyrimidines (Ia-f) were synthesised from (un) substituted benzaldehydes

---

* **SDM College of Engg. & Tech., Dharwad-580 002, India.**

** **For correspondence**

Scheme 1.

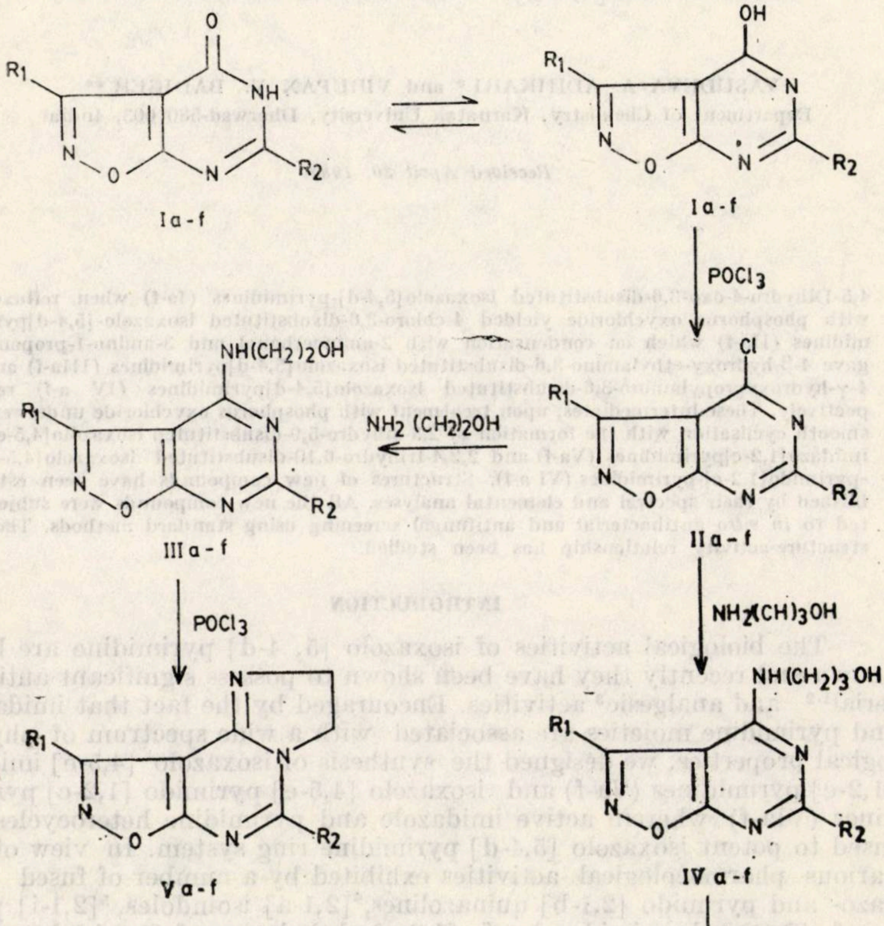
R1
NH
N
O
R2
Ia-f
OH
Ia-f
POCl3
Cl
IIa-f
NH2 (CH2)2OH
NH(CH2)2OH
IIIa-f
POCl3
Va-f
NH2(CH)3OH
NH(CH2)3OH
IVa-f
POCl3
VIa-f
R1 = C6H5,4-ClC6H4;
R2 = H, CH3, C2H5.

by reported procedures .[11-13] These were converted to 4-chloro-3,6-disubstituted isoxazolo [5,4-d]-pyrimidines (IIa-f) by refluxing them in excess of phosphorus oxychloride for 3-4 hrs. Since the chlorine atom in position-4 is highly reactive, the compounds IIa-f serve as valuable intermediates in the synthesis of IIIa-f and IVa-f by nucleophilic displacement reaction. Thus, 4-β-hydroxyethylamino or 4-γ-hydroxypropylamino-3,6-disubstituted isoxazolo [5,4-d] pyrimidines (IIIa-f and IVa-f) were readily obtained by refluxing IIa-f with 2-aminoethanol or 3-amino-1-propanol in absolute ethanol for 3-4 hrs. Further, the hydroxy compounds IIIa-f and IVa-f were conveniently cyclised to 2,3-dihydro-5,9-disubstituted isoxazolo[4,5-e]imidazo[1,2-c] pyrimidines (Va-f) and 2, 3, 4-trihydro-6,10-disubstituted isoxazolo[4,5-e]pyrimido[1,2-c]pyrimidines (VIa-f) by heating them with a little more than one equivalent of phosphorus oxychloride for 3—4 hrs. All the new compounds are almost colourless and were easily crystallizable to shining crystals. Their characterization data are summarized in Table 1. Structures of new compounds have been authentically established by their correct elemental analyses and spectral studies.

BIOLOGICAL ACTIVITY

Evaluation of antibacterial activity by disc diffusion method [14]

All the new compounds IIIa-VIf have been evaluated for *in vitro* antibacterial activity against five pathogenic microorganisms, viz., *Escherichia coli*, *Proteus vulgaris*, *Proteus aurigasa*, *Klebsiella pneumoniae* (all Gram-negative) and *Staphylococcus aureus* (Gram-positive) by disc diffusion method.[14] In this method, the sterilized nutrient agar (25 mL, pH = 7.2), while hot, was poured into the sterilized Petri dishes and allowed to cool to room temperature. The agar plates were inoculated with 18—24 hrs old culture by spreading uniformly with sterile swabs. Sterilized 10 mm discs, punched from Whatmann No. 1 filter paper, were impregnated with 0.1 mL (concentration : 200 μg) drug solution (prepared by dissolving 10 mg of the compound in 5 mL of DMF) and were placed in the Petri — dishes with sterile fine pointed forceps. The dishes were then incubated for 24 hrs at 37° and the zone of inhibition was measured in mm. In control, the filter paper discs saturated with pure DMF were used simultaneously. Sulfanilamide and phenol were used as standards. The results are subjectively graded and are presented in Table 2 along with the results obtained for standards.

Evaluation of antifungal activity by turbidity method [15]

The compounds IIIa-VIf were subjected to *in vitro* antifungal screening against three fungi, viz., *Aspergillus niger*, *Candida albicans* and *Aspergillus flavus* by turbidity method.[15] In the procedure, 0.1 mL of the test compound (200 μg in DMF) in 5 mL of sterilized fungi medium was treated with 3—4 drops of 48 hrs old culture in a sterilized test tube. The test tubes were then shaken well and incubated for 48 hrs at 37°. The extent of inhibition was determined by measuring the decrease in turbidity in terms of percentage of transmission at 660 mμ. Salicylic acid (5%) was used as standard and DMF as solvent control. The results are subjectively graded and are mentioned in Table 2 along with the results obtained for salicylic acid.

DISCUSSION

The formation of 4-β-hydroxyethylamino or γ-hydroxy-propylamino-3,6-disubstituted isoxazolo [5,4-d] pyrimidines (IIIa-f and IVa-f) from the corresponding 4-chloro-derivatives IIa-f was evidenced by their

Table 1

Characterization data of compounds IIIa – VIf

Compd.	R_1	R_2	Cryst. solvent.	M.P. °C	Yield %	Mol. formula	Analyses %		
							Calcd/Found		
							C	H	N
1	2	3	4	5	6	7	8	9	10
IIIa	C_6H_5	H	Benzene+ Pet. ether	141 – 42	78	$C_{13}H_{12}N_4O_2$	60.95 60.57	4.68 4.56	21.86 22.04
IIIb	C_6H_5	CH_3	Benzene	144 – 45	72	$C_{14}H_{14}N_4O_2$	62.24 62.03	5.18 4.98	20.72 20.58
IIIc	C_6H_5	C_2H_5	Ethanol	183 – 84	68	$C_{15}H_{16}N_4O_2$	63.39 63.66	5.63 5.87	19.70 19.98
IIId	4 – ClC_6H_4	H	Ethanol	181 – 82	74	$C_{13}H_{11}ClN_4O_2$	53.73 53.62	3.78 3.47	19.27 19.05
IIIe	4 – ClC_6H_4	CH_3	Benzene	204 – 05	76	$C_{14}H_{13}ClN_4O_2$	55.20 55.62	4.26 4.52	18.38 18.06
IIIf	4 – ClC_6H_4	C_2H_5	Ethanol	198 – 99	70	$C_{15}H_{15}ClN_4O_2$	56.54 56.78	4.70 4.92	17.57 17.37
IVa	C_6H_5	H	Benzene	129 – 30	72	$C_{14}H_{14}N_4O_2$	62.24 62.54	5.18 5.37	20.72 20.64
IVb	C_6H_5	CH_3	Benzene+ Pet. ether	132 – 33	67	$C_{15}H_{16}N_4O_2$	63.39 63.28	5.63 5.46	19.70 19.98
IVc	C_6H_5	C_2H_5	Benzene+ Pet. ether	122 – 23	70	$C_{16}H_{18}N_4O_2$	64.44 64.27	6.03 5.91	18.78 18.98

IVd	4-ClC$_6$H$_4$	H	Benzene	134-35	71	$C_{14}H_{13}ClN_4O_2$	55.20 55.37	4.26 4.17	18.38 18.64
IVe	4-ClC$_6$H$_4$	CH$_3$	Benzene	160-61	68	$C_{15}H_{15}ClN_4O_2$	56.54 56.33	4.70 4.98	17.57 17.78
IVf	4-ClC$_6$H$_4$	C$_2$H$_5$	Benzene+ Pet. ether	133-34	78	$C_{16}H_{17}ClN_4O_2$	57.77 57.52	5.11 5.27	16.83 16.57
Va	C$_6$H$_5$	H	Benzene	249-50	75	$C_{13}H_{10}N_4O$	65.56 65.75	4.19 4.08	23.51 23.74
Vb	C$_6$H$_5$	CH$_3$	Benzene+ Pet. ether	219-20	78	$C_{14}H_{12}N_4O$	66.68 66.57	4.75 4.92	22.20 22.03
Vc	C$_6$H$_5$	C$_2$H$_5$	Benzene	209-10	80	$C_{15}H_{14}N_4O$	67.68 67.52	5.26 5.07	21.04 21.28
Vd	4-ClC$_6$H$_4$	H	Benzene	261-62	72	$C_{13}H_2ClN_4O$	57.27 57.08	3.30 3.47	20.54 20.72
Ve	4-ClC$_6$H$_4$	CH$_3$	Benzene	247-48	78	$C_{14}H_{11}ClN_4O$	58.66 58.84	3.83 3.71	19.54 19.76
Vf	4-ClC$_6$H$_4$	C$_2$H$_5$	Benzene+ Pet. ether	202-03	71	$C_{15}H_{13}ClN_4O$	59.93 59.82	4.32 4.18	18.62 18.92
VIa	C$_6$H$_5$	H	Benzene+ Pet. ether	176-77	74	$C_{14}H_{12}N_4O$	66.68 66.55	4.75 4.92	22.20 22.02
VIb	C$_6$H$_5$	CH$_3$	Benzene+ Pet. ether	199-00	64	$C_{15}H_{14}N_4O$	67.68 67.83	5.26 5.42	21.04 20.88
VIc	C$_6$H$_5$	C$_2$H$_5$	Benzene+ Pet. ether	189-90	67	$C_{16}H_{16}N_4O$	68.58 68.32	5.71 5.86	19.98 20.12
VId	4-ClC$_6$H$_4$	H	Benzene	211-12	72	$C_{14}H_{11}ClN_4O$	58.66 58.46	3.83 3.98	19.54 19.42
VIe	4-ClC$_6$H$_4$	CH$_3$	Benzene+ Pet. ether	231-32	60	$C_{15}H_{13}ClN_4O$	59.93 60.12	4.32 4.22	18.62 18.85
VIf	4-ClC$_6$H$_4$	C$_2$H$_5$	Benzene+ Pet. ether	208-09	65	$C_{16}H_{15}ClN_4O$	61.07 61.32	4.76 4.61	17.79 17.96

Table 2

Biological activities of compounds IIIa—VIf

Compd.	Antibacterial activity* Zone of inhibition in mm after 24 hrs.					Antifungal activity‡ Percent transmission after 48 hrs		
	E.C.	P.V.	P.A.	K.P.	S.A.	A.N.	C.A.	A.F.
1	2	3	4	5	6	7	8	9
IIIa	—	—	+	—	+	++	++	++
IIIb	+	—	+	—	+	++	+++	+
IIIc	+	+++	—	++	+	+	++	+
IIId	+	+	—	+	+	+	++	++
IIIe	+	++	+	+	—	+	++	++
IIIf	+	++	+	++	—	+	++	+
IVa	+	+	+	++	+	+++	++	++
IVb	—	+	+	+	—	+	++	+
IVc	+	—	+	+	—	++	++	++
IVd	+	+	—	+	—	+	+++	+
IVe	+	—	+	+	++	++	+++	+
IVf	+	++	+	+	—	+	+++	+
Va	+	++	++	+	++	++	++	+
Vb	++	++	+	+	++	++	++	+
Vc	+	++	+	—	+	++	+++	+++
Vd	+	+	++	+	—	+++	+	+
Ve	+	+	—	+	++	+	++	—
Vf	+	++	—	++	++	++	++	++
VIa	+	+++	—	++	+	++	+++	++
VIb	+	—	+	+	+	++	++	+
VIc	+	+	++	++	+	++	++	++
VId	++	+	—	++	+	++	++	++
VIe	++	+	—	—	+	++	+++	++
VIf	+	+	++	+	++	++	++	+
S—1	+	++	+	+	+			
S—2	+	++	+	—	+			
S—3						+++	+++	+++

* Antibacterial activity : E.C. = *Escherichia coli* ; P.V. = *Proteus vulgaris*, K.P. = = *Klebsiella pneumoniae*, S.A. = *Staphylococcus aureus*. S—1 = Sulfanilamide ; S—2 = Phenol, zone of inhibition in mm after 24 hrs :14—16 = '—' No activity, 17—19='+' Positive activity, 20—22, ='++' Positive activity, 23—25 ='+++' Positive activity, 26—28 ='+++' Positive activity.

** Antifungal activity : A.N. = *Aspergillus niger*, C.A. = *Candida albicans*, A.F. = *Aspergillus flavus* ; S—3 = Salicylic acid.

Percent transmission at 660 mμ after 48 hrs : 1—25 = '—', No activity, 26—50 = = '+' Positive activity, 51—75 = '++' = Positive activity, 76—100 = '+++' Positive activity.

Concentration = 200 μg, Solvent control = DMF

IR spectra. The cyclization of IIa-f to fused imidazo compounds Va-f and IVa-f to fused pyrimido compounds VI-a-f was clearly indicated by the disappearance of peaks due to OH and NH groups at the region 3100 — 3500 cm^{-1} in their IR spectra and appearance of bathochromic shift of λ_{max} in their UV spectra. Structure of Vd was further confirmed by its ^{1}H—NMR spectrum which shows multiplets at δ3.25 ppm and 3.75 ppm due to two NCH_2 groups. Structure of Vd was authentically established by its Mass spectrum which shows molecular ion peak at m/z, 272. Spectral features of some representative compounds are given in detail in the experimental part.

From the results of antibacterial screening of test compounds it can be concluded that most of the compounds showed significant activity against all the five strains. Amongst them, compounds IIIc and VIa were found to be very active against *P. vulgaris*. It is observed that substitution by C_2H_5 group at position-6 of hydroyx compounds IIIa-IVf, appears to increase the activity in most of the cases, whereas replecement of β-hydroxyethylamino or γ-hydroxypropylamino group at position-4 does not alter the activity noticeably. It is interesting to note that cylisation of IIIa-IVf to Va-VIf has enhanced the activity to some extent. However, fused imidazo or pyrimido derivatives Va-VIf were found to exhibit more or less the same extent of antibacterial activity.

Results obtained for antifungal activity of hydroxy compounds IIIa-IVf revealed that the compounds were found to be more active against *C. albicans* when compared to their activity against *A. niger* and *A. flavus*. It is observed that in most of the cases the unsubstitution at position-6 of isoxazolo [5,4-d]-pyrimidine has enhanced the activity considerably, whereas replacement of β-hydroxyethylamino groups by γ-hydroxypropylamino group at position-4 did not show any appreciable change in the activity. The compounds, IIIb, IVd-f and IVa were found to be active against *C. albicans* and *A. niger* respectively. The cyclisation of hydroxy compounds III-IVf, to fused imidazo or pyrimido derivatives Va-VIf, has resulted in enhanced activity against *A. niger* and lowered activity against *C. albicans*. Amongst the various tested compounds Va-VIf, Vc, VIa, VIe and Vd showed the highest activity against *C. albicans* and *A. niger* respectively whereas Vc also showed better activity against *A. flavus*. It is noted that substitution of C_2H_5 group at position-5 or -6 has increased the activity in most of the cases. It can be readily concluded that fused pyrimido derivatives VIa-f exhibited higher antifungal activity when compared to the activity of fused imidazo derivatives Va-f against *C. albicans* and *A. flavus*, in particular.

EXPERIMENTAL

All mps are uncorrected and determined by the capillary method. The IR spectra were recorded on Perkin-Elmer 221 spectro-photometer using Nujol mull and the UV spectra were scanned on a Hitachi 150—20 spectrophotometer. The ^{1}H-NMR spectra were run on Varian EM-390, 90 MHz spectrometer using d_6-DMSO as solvent and TMS as internal standard. The mass spectra were recorded on Finnigan 4121, GC Mass spectrometer at 70eV (low resolution).

Preparation of 4-chloro-3,6-disubstituted isoxazolo[5,4-d]-pyrimidines

A mixture of Ia-f (8.3 g) and phosphorus oxychloride (83 mL) was refluxed for 3 hrs, cooled and evaporated to dryness under reduced pressure. The residual oil was triturated with a small quantity of benzene, evaporated to dryness and added to crushed ice and water. The solid that separated was filtered, washed with water, dried and crystallized using an appropriate solvent. Mps of IIa-f agreed with reported literature values. [11-13]

Preparation of 4-(β-hydroxyethylamino or γ-hydroxypropylamino)-3,6-disubstituted isoxazolo [5,4-d]pyrimidines(IIIa-IVf)

A solution of 0.61 g of 2-aminoethanol or 0.75 g of 3-amino-1-propanol (0.01 mole) in 10 mL of dry ethanol was added dropwise to a solution of 0.01 mole of IIa-f in 40 mL of dry ethanol with stirring. After refluxing the reaction mixture for 4 hrs, it was evaporated to small bulk and added to 200 g of crushed ice. The ice cold solution was rendered alkaline by adding 5% sodium carbonate solution to get colourless solid. It was separated, washed, dried and finally crystallized from a suitable solvent. The characterization data of IIIa-IVf are presented in Table 1.

IR spectrum of IIId : 3400 cm^{-1} (sharp, NH) ; 3257 cm^{-1} (broad, OH) ; 3030 cm^{-1} (weak CH_2) ; 1613 cm^{-1} (sharp, pyrimidine) ; 1580 cm^{-1} (sharp, aromatic) and 732 cm^{-1}(weak, C-Cl). UV spectrum of IIIe : $\lambda_{max}{}^{228}$ nm ; 245 nm and 288 nm. IR spectrum of IVd : 3400 cm^{-1}(very broad, NH and OH) ; 3049 cm^{-1}(weak, CH_2) ; 1618 cm^{-1}(sharp, pyrimidine) ; 1587 cm^{-1}(sharp, aromatic) and 740 cm^{-1}(weak, C-Cl). UV spectrum of IVe : λ_{max} 230 nm ; 245 nm and 290 nm.

Synthesis of 2,3-dihydro-5,9-disubstituted isoxazolo[4,5-e]-imidazo[1,2-e]pyrimidines (Va-f) and 2,3,4-trihydro-6,10-disubstituted isoxazolo[4,5-e]pyrimido(1,2-e)pyrimidines(IVa-f)

To 0.01 mole of IIIa-f or IVa-f, 10 mL of redistilled phosphorus oxychloride was added dropwise with continuous stirring at 0°. The resulting clear solution was stirred at room temperature for one hr and then at 100° for 3 hrs. It was then cooled and poured into 500 g of crushed ice with stirring. After keeping the solution overnight, it was filtered and alkalinized by adding NH_4OH solution. The white solid that separated was filtered, washed, dried and recrystallized from suitable solvent to get Va-VIf in good yield. The physical data of Va-VIf are summarized in Table 1.

IR spectrum of Vd : 3048 cm^{-1} (weak, CH_2) ; 1667 (sharp, pyrimidine) ; 1613 cm^{-1}, 1570 cm (weak, aromatic) and 730 cm^{-1} (weak, C—Cl). UV spectrum of Ve : λ_{max} 241 nm and 325 nm.

IR spectrum of VId : 3030 cm^{-1} (weak, CH_2) ; 1660 cm^{-1} (sharp, pyrimidine), 1615 cm^{-1} 1587 cm^{-1} (weak, aromatic) and 735 cm^{-1} (weak, C—Cl).

UV spectrum of VIe : λ_{max} 221 nm and 260 nm.

^1H—NMR spectrum of Vd : δ 8.1 ppm (singlet, 1H, CH at 5-position) ; δ 7—8 ppm (multiplet, 4H, phenyl) ; δ 3.75 ppm (multiplet, 2H, NCH_2) and δ 3.25 ppm (multiplet, 2H, NCH_2) Mass spectrum of Vd : m/z, 272 (M^+) : 75 ($C_6H_3^+$, base peak).

ACKNOWLEDGEMENTS. The authors are indebted to the head, RSIC, IIT, Madras for recording ^1H-NMR and Mass spectra and the Chairman, Chemistry Department, Karnatak University, for necessary laboratory facilities. Thanks are also due to V. P. Savalgi for his assistance in antimicrobial screening of the compounds.

REFERENCES

[1] A. Burch Homer, *US* 3, 770, 740 (06 Nov 1973) ***Chem. Abstr.***, **80**, 48033s (1974).

[2] Jpn. Kokai Koho, *JP* 5, 936, 383 (8, 436, 683, 28 Feb. 1984). ***Chem. Abstr.***, **101**, 110940 t (1984 .

[3] H. Yamanaka, Y. Sakamoto, A. Shiozawa and K. Adachi, Jpn. Kokai Koho, *JP* 7, **944,** 696, (09 Apr. 1979), *Chem. Abstr.*, **91,** 175 325r (1979).

[4] G. E. Hardtmann, *US*, 3, 919, 210 (11 Nov. 1975), *Chem. Abstr.*, **84,** 59548x (1976).

[5] T. S. Sulkowski, *US*, 3, 900, 494 (19 Aug. 1975), *Chem. Abstr.*, **84,** 4993h (1976).

[6] H. Grungl, W. Hayden and A. Plessing, *J. Heterocycl. Chem.*, **21** (2), 333 (1984).

[7] C. A. White and M. R. Black, US 3, 989, 709 (02 Nov. 1976), *Chem. Abstr.*, **86,** 72694c (1977).

[8] G. E. Hardtmann, *US*, 3, 704, 300 (28 Nov. 1972), *Chem. Abstr.*, **78,** 43504v (1973).

[9] K. Kubo, N. Ito, I. Soto, Y. Isomura and H. Honnia, *Jpn. Kokai Tokkyo Koho* 7, **922,** 399 (20 Feb. 1979) ; *Chem. Abstr.*, **91,** 5235u (1979).

[10] H. A. Dewald, *Eur. Pat. Appl. EP* 95, 289 (30 Nov. 1983), *Chem. Abstr.*, **100,** 139133x (1984).

[11] E. C. Taylor and E. E. Garcia, *J. Org. Chem.*, **29,** 2116 (1964).

[12] P. Rajagopalan and C. N. Talaty, *Tetrahedran*, **23,** 3541 (1967).

[13] V. A. Adhikari and V. V. Badiger, *Arch. Pharm.* in Press (1987).

[14] G. Czerkinsky, N. Diding and O. Ouchterbry, *Scan. J. Clin. Lab. Invest.*, **7,** 259 (1955) ; *Chem. Abstr.*, **50,** 7223e (1956).

[15] R. C. V. Robinson, T. N. Fercoit and Jr. H. M. Robinson, *Arch. Dermatol.*, **81,** 681 (1960).

Rev'ue Roumaine de Chimie, 35, 6, 767—775 (1990)

NEUE TETRATHIOCYANATO-DIAMIN-CHROMIATE MIT IMIDAZOL UND BENZIMIDAZOL

I. GĂNESCU *, CS. VÁRHELYI **, I. ZSAKÓ ** und M. PREDA *

* Lehratuhl für anorganische und analytische Chemie, Universität von Craiova, Craiova, Rumänien

* Fakultät der chemischen Technologie, „Babeş-Bolyai" Universität, Cluj-Napoca, Rumänien

Eingegangen am Dezember 7. 1987

Es wurde die Substitutionsreaktion von entwässertem $K_3[Cr(NCS)_2]$ mit Imidazol und Benzimidazol untersucht. Die Formeln der zwei neuen reineckeatanalogen Komplexanionen: $[Cr(NCS)_4(Imidazol)_2]^-$ und $[Cr(NCS)_4(Benzimidazol)_2]^-$ wurden auf präparativem Wege bestimmt. Es wurden 42 neue Salze mit den Chlorhydraten einiger heterocyclischer amine, Alkaloide, mit übergangsmetallionen und Kobalt(III)-amin-Basen dargestellt und charakterisiert. Die thermische Stabilität einiger Ammoniumsalze wurde auf derivatographischem Wege untersucht. Für die Klärung einiger Strukturfragen wurden auch spektrophotometrische Untersuchungen im UV und IR-Bereiche durchgeführt.

The substitution reaction of anhydrous $K_3[Cr(NCS)_6]$ with imidazole and benzimidazole was studied. The formulas of the new Reineckate analogous complex anions: $[Cr(NCS)_4(imidazole)_2]^-$ and $[Cr(NCS)_4(benzimidazole)_2]^-$ were established by preparation of 44 new salts by double decomposition reactions with the hydrochlorides of some heterocyclic N-bases, alkaloids, transition metal salts and cobalt(III)-amine bases. The thermal stability of some ammonium salts of this type was studied by derivatography. From UV and IR spectral data some structural problems were resolved and discussed.

EINLEITUNG

Von den Hexapseudohalogeno-chromiaten des Typs: $M_3[Cr(NCX)_6]$ $X = O$, S, Se, besitzt das $K_3[Cr(NCS)_6]$eine besondere Bedeutung in der präparativen und analytischen Chemie. Die $K_3[Cr(NCO)_6]$ und $K_3[Cr(NCSe)_2]$- Komplexsalze entstehen nur bei speziellen Experimentierbedingungen und haben eine kleine Beständigkeit, insbesondere in wässerigen, verdünnten alkoholischen Lösungen.[1,2] Das Tellurderivat: : $M_3[Cr(NCTe)_6]$wurde bis heute noch nicht hergestellt.[3]

Die von ROESSLER [4] entdeckte dreibasische Komplexsärue $H_3[Cr(NCS)_6]$ergibt mit Metallionen, Metall(II, III)-amin-basen und mit den Chlorhydraten organischer Aminen, Alkaloiden und Phosphinen in Wasser relativ schwer löslichen Niederschläge, die auch für analytische Zwecke verwendet wurden.[5–7]

Die nichtionogen gebundenen NCS-Gruppen im $K_3[Cr(NCS)_6]$kann man leicht mit neutralen ein- und zweizähnigen Komplexbildnern stufenweise verdrängen und damit eine Reihe von Komplexanionen oder Komplexkationen als auch Nichtelektrolyte erhalten.[8-10]

Eine Reihe von reineckesalzanalogen Verbindungen vom Typ: $Amin.H[Cr(NCS)_4(Amin)_2]$mit aromatischen Aminen wurden in unseren früheren Arbeiten beschrieben und die Kinetik der Solvolyse der $[Cr(NCS)_4(Amin)_2]^-$ — Komplexe in Wasser-Alkohol, bzw. Wasser-Aceton — Mischungen untersucht.[11-13]

Die ersten Tetrathiocyanato-diamin-chromaten mit heterocyclischen Aminen, wie Pyridin und 1,10-Phenanthrolin wurden von PFEIFFER und Mitarbeiter[14,15] beschrieben.

Wir haben beobachtet, daβ von den zahlreichen heterocyclischen Aminen auch das Imidazol und seine Derivate, wie 2-Methyl-Imidazol und Benzimidazol für diesem Zweck sehr geeignet sind.

Im Laufe der Substitutionsreaktion werden nur auch in diesem Falle nur zwei NCS- Reste im $[Cr(NCS)_6]^{3-}$ ausgetauscht:

$$K_3[Cr(NCS)_6] + 2\ Amin = K[Cr(NCS)_4(Amin)_2] + 2\ KCNS$$

EXPERIMENTELLER TEIL

Synthese der Komplexverbindungen

$NH_4[Cr(NCS)_4(Imidazol)_2]$ und $NH_4[Cr(NCS)_4(Benzimidazol)_2]$. In einem mit Korkstopfen versehenen Erlenmeyerkolben werden 0,1 Mol ontwässertes $K_3[Cr(NCS)_6]$ und 0,25 Mol Imidazol (bzw. 0,25 Mol Benzimidazol) innig vermischt und etwa 4—5 Studen auf dem Wasserbade unter mehrmaligem Umschütteln erhitzt, wodurch die anfangs blauviolette Farbe der Masse in eine rote übergeht. Nach Abkühlen wird das Produkt mit 10 %-iger Essigsäure behandelt um es von dem entstehendem KCNS und nichtreagiertem Amin zu befreien. Der breige Rückstand wird in 500—600 ml Methanol gelöst und in 1—1,5 l konz. wässrige NH_4Cl — Lösung tropfenweise zugefügt. Die Ammoniumsalze kristallisieren als rotviolette, mikrokristalline Massen aus. Die Niederschläge werden abgesaugt, mit Wasser gewaschen und an der Luft getrocknet. Ausbeute: 75—80 %

Analyse: Gef. Cr 11.77, S 2,912, N 28,59
aus $NH_4[Cr(NCS)_4(Imidazol)_2]$ (Mol. Gew. 438,6)
Ber. Cr 11,86, S 29,24, N 28,74
Gef. Cr 9,53, S 23,63, N 23,28
aus $NH_4[Cr(NCS)_4(Benzimidazol)_2]$ (M1. Gew. 538,7)
Ber. Cr 9,65, S 23,81, N 23,40

$Amin.\ H.\ [Cr(NCS)_4(Imidazol)_2]$ und $Amin.H[Cr(NCS)_4(Benzimidazol)_2]$. Je 20—25 mMol des betr. Amins werden mit 10 ml konz. Salzsäure behandelt und das Chlorhydrat in 80—100 ml Wasser gelöst und dazu werden 10 mMol Chrom(III)-Komplex in 50—60 Methanol-Butanol Mischung (5 : 1) gegeben. Nach 10—15 Minuten werden die ausgeschiedenen Kristalle abgesaugt, mit verd. Methanol (1 : 3) gewaschen und bei Raumtemperatur an der Luft getrocknet.

Derivate der $[Cr(NCS)_4(Amin)_2]^-$ mit Metallen und Metall(III)-aminen. Je 15—20 mMol MNO_3, bzw. je 10—15 mMol Kobalt(III)-aminsalze von verschiedenen Typ in 100 ml Wasser oder in verd. Methanol (1 : 3) werden mit je 5 mMol $NH_4[Cr(NCS)_4(Amin)_2]$ in 40—50 ml Methanol- Butanol Mischung (5 : 1) behandelt. Die ausgeschiedenen kristallinen Substanzen werden, wie oben, verarbeitet.

Analyse. Der Thiocyangehalt der Proben wurde gravimetrisch als $BaSO_4$, das Chrom jodometrisch, der Co+Cr Gehalt als Summe der $Co_3O_4 + Cr_2O_3$ bestimmt.

Thermische Analyse. Derivatogramme wurden mit einem MOM Derivatograph (Budapest) im Luftatmosphäre mit einer Aufheizungsgeschwindigkeit von 20 C/Min aufgenommen. Probemenge: 100 mg.

Spektrophotometrische Messungen. Elektronenspektren wurden mit einem SPECORD — Spektrophotometer in Methanol, die Ultrarotspektren in KBr- Preßlingen mit einem UR 20 Spektrophotometer (Carl Zeiss Jena) aufgenommen.

ERGEBNISSE UND DISKUSSION

Die erhaltenen reineckesalzähnlichen Verbindungen sind im Wasser sehr schwer löslich, lösen sich aber leicht in Aceton, Acetylaceton, Dimethylsulphoxid, Dimethylformamid, usw.

Die verdünnte Lösungen der $NH_4[Cr(NCS)_4(Imidazol)_2]$ und $NH_4(Cr(NCS)_4$ $(Benzimidazol)_2]$ in Methanol geben eine Reihe von Fällungsreaktionen mit Übergangsmetallionen, wie Cu(I), Ag(I), Au(I), Tl(I), mit anderen Schwermetallionen (Hg(II), Pb(II), Bi(III), mit den Chlorhydraten einiger heterocyclischer N-Basen und Alkaloiden, als auch mit Metall(III)-aminen von verschiedenem Typ (Hexamine, Monoacido--pentamine und Diacidotetramine des Kobalts(III) und Chroms(III)).

Eine Reihe, durch doppelte Umsetzung erhaltene neue Komplexsalze sind in Tabelle 1 bzw. Tabelle 2 Charakterisiert.

Tabelle 1

Neue Komplexsalze des Typs Amin. $H[Cr(NCS)_4(Amin)_2]$

Nr.	Formel	Ausb. (%)	Charakteristik	Analyse		
					ber.	gef.
1	Pyridin. HA	65	Rotviolette, dünne Plättchen	Cr	10,39	10,32
				S	25,62	25,43
				N	25,16	24,96
2	Pyridin. HB	62	Rotviolette kurze Prismen	Cr	8,65	8,53
				S	21,35	21,08
				N	20,97	20,69
3	γ-Picolin. HA	60	Rotviolette Nadeln	Cr	10,10	10,02
				S	24,92	24,83
				N	24,48	24,19
4	γ-Picolin. HB	64	Lange, hellrosa Nadeln	Cr	8,47	8,35
				S	20,88	20,59
				N	20,51	20,42
5	Triäthylamin. HA	67	Rosenfarbige mikrokryst. Masse	Cr	9,95	9,86
				S	24,53	24,41
				N	24,10	23,96
6	Triäthylamin. HB	63	Rosenfarbige, lange unregelmäss. Prismen	Cr	8,35	8,24
				S	20,59	20,36
				N	20,23	20,14
7	Tripropylamin. HA	66	Hellrosa, dunne Nadeln	Cr	9,20	9,14
				S	22,70	22,61
				N	22,30	22,08

Tabelle 1 (Fortsetzung)

8	Tripropylamin. HB	70	Kleine, hellrosa Nadeln	Cr S N	7,82 19,29 18,95	7,70 19,06 18,77
9	Tributylamin. HA	72	Aggregate aus hellrosa kurze Prismen	Cr S N	8,57 21,13 20,76	8,42 21,00 20,59
10	Trbutylamin. HB	73	Hellrote, unregelmässige, kleine Kristallen	Cr S N	7,35 18,14 17,82	7,26 18,10 17,69
11	Codein. HA	84	Rotviolette mikrokrist. Mase	Cr S N	7,21 17,79 17,47	7,14 17,62 17,30
12	Codein. HB	81	Rotviolette mikrokrist. Masse	Cr S N	6,33 15,62 15,34	6,20 15,40 15,11
13	Papaverin. HA	87	Rotviolette mikrokrist. Masse	Cr S N	6,83 16,85 16,56	6,75 16,72 16,31
14	Papaverin. HB	83	Rotviolette mikrokrist. Masse	Cr S N	6,04 14,91 14,65	6,00 14,83 14,39
15	Procain. HA	85	Rotviolette mikrokrist. Masse	Cr S N	7,90 19,50 19,15	7,84 19,33 19,02
16	Procain. HB	84	,, ,,	Cr S N	6,86 16,92 16,62	6,74 16,82 16,44
17	Spartein. HA	82	,, ,,	Cr S N	7,92 19,55 21,34	7,87 19,40 21,14
18	Spartein. HB	80	,, ,,	Cr S N	6,88 16,96 18,51	6,82 16,75 18,23
19	Pyramidon. HA	87	,, ,,	Cr S N	7,96 19,64 21,44	7,84 19,52 21,23
20	Pyramidon. HB	85	,, ,,	Cr S N	6,90 17,03 18,59	6,83 16,88 18,73

„HA" = $H[Cr(NCS)_4(Imidazol)_2]$ „HB" = $H[Cr(NCS)_4(Benzimidazol)_2]$

Tabelle 2

Neue Komplexsalze der $H[Cr(NCS)_4(Amin)_2]$ — Säuren mit Metallen und Metall-Aminen

Nr.	Formel	Ausb. (%)	Charakteristik	Analyse	
				ber.	gef.
1	Ag.A	92	Rotviolette mikrokrist.	Ag 20,41	20,33
			Masse	Cr 9,84	9,78
				S 24,27	24,11
2	Ag.B	94	„ „	Ag 17,16	17,00
				Cr 8,27	8,17
				S 20,40	20,23
3	Tl.A	88	„ „	Tl 32,70	32,38
				Cr 8,32	8,24
				S 20,52	20,40
4	Tl.B	87	„ „	Tl 28,19	28,01
				Cr 7,19	7,10
				S 17,69	17,51
5	Cu.A	90	Braunrote mikrokrist.	Cu 13,12	13,01
			Masse	Cr 10,74	10,58
				S 26,49	26,35
6	Cu.B	89	„ „	Cu 10,87	10,72
				Cr 8,90	8,81
				S 21,91	21,82
7	$Hg.A_2$	94	Rotviolette mikrokrist.	Hg 19,25	19,10
			Masse	Cr 9,98	9,92
				S 24,62	24,51
8	$Hg.B_2$	96	„ „	Hg 16,15	16,06
				Cr 8,37	8,26
				S 20,65	20,29
9	$Pd.A_2$	97	Dunkelbraune	Pd 11,23	11,09
			mikrokrist. Masse	Cr 10,97	10,86
				S 27,07	26,92
10	$Pd.B_2$	96	„ „	Pd 9,27	9,17
				Cr 9,06	9,00
				S 22,35	22,14
11	$[Co(DH)_2(m\text{-Xylidin})_2] \cdot A$	82	Rotbraune rhomb.	Co+Cr	
			Prismen	11,62	11,57
				S 13,41	13,20
12	$[Co(DH)_2(m\text{-Xylidin})_2] \cdot B$	84	Braune kurze	Co+Cr	
			Prismen	10,52	10,44
				S 12,20	12,06
13	$[Co(DH)_2(p\text{-Toluidin})_2] \cdot A$	83	Braune Nedeln	Co+Cr	
				11,98	11,86
				S 13,83	13,70
14	$[Co(DH)_2(p\text{-Toluidin})_2] \cdot B$	86	Braune, dünne	Co+Cr	
			hexagonale Platten	10,81	10,73
				S 12,46	12,29

Tabelle 2 (Fortsetzung)

15	$[Co(DH)_2(Pyridin)_2] \cdot A$	79	Rotbraune mikrokrist. Masse	Co + Cr	12,75	12,66
				S	14,72	14,59
16	$[Co(DH)_2(Pyridin)_2] \cdot B$	77	„ „	Co + Cr	11,43	11,40
				S	13,20	13,10
17	$[Co(DH)_2(NH_3)_2] \cdot A$	74	Hellrote mikrokrist. Masse	Co + Cr	14,87	14,80
				S	17,17	17,05
18	$[Co(DH)_2(NH_3)_2] \cdot B$	72	„ „	Co + Cr	13,11	13,06
				S	15,20	15,14
19	$[Co(ec)\ (Äthylamin)_2] \cdot A$	69	Rotbraune mikrokrist. Masse	Co + Cr	14,01	13,93
				S	16,16	16,14
20	$[Co(ec)\ (Äthylamin)_2] \cdot B$	72	„ „	Co + Cr	12,44	12,31
				S	14,35	14,22
21	$[Co(ec)(Propylamin)_2] \cdot A$	64	„ „	Co + Cr	13,53	13,44
				S	15,61	15,29
22	$[Co(ec)(Propylamin)_2] \cdot B$	62	„ „	Co + Cr	12,05	11,94
				S	13,91	13,28

„DH" — deprotoniertes Dimethylglyoxim : $C_4H_7N_2O_2$
„ec.H_2" — Äthylendiimino-bis-Acetylaceton

Diese Tetrathiocyanato-diamin-chromiate mit Alkaloiden, Metallen und Metall(III)-aminen sind unlöslich im Wasser, in verdünntem Methanol, bzw. Ethanol und in unpolaren Lösungsmitteln, wie Benzol, Toluol, CCl_4, $CHCl_3$, CS_2, usw. und lösen sich leicht in einigen polaren Lösungsmitteln.

Die obenerwähnten Salze zersetzen sich beim Erhitzen über 160—240°C ohne deutlichem Schmelzpunkt, unter Freiwerden von HCN, HCNS, CO, CO_2, NO, N_2 und Amine in nichtstöchiometrischen verhältnissen, in Function der Natur des Kations in äus erem Koordinationssphäre.

Der Rückstand bei 650—700 °C besteht aus Cr_2O_3, $Cr_2O_3 + M$, bzw. $Cr_2O_3 + M_2O$ (MO, M_2O_3) in Abhängigkeit von der Natur des Kations.

Derivatographische Messungen zeigen daβ im Falle der Ammoniumsalze in der ersten Phase der Thermolyse in einem endothermen Prozess die Basen der aüs eren Koordinationssphäre in Freiheit gesetzt werden, z.B.

$$NH_4[Cr(NCS)_4(Imidazol)_2] = NH_3 + H[Cr(NCS)_4(Imidazol)_2]$$

Die so entstandene freie Säure zerfällt sich dann in kurzer Zeit, eventuell augenblicklich, nach der Gleichung :

$$H[Cr(NCS)_4(Imidazol)_2] = Cr(NCS)_3 + NCNS + 2\ \text{Imidazol}$$

In fester Phase kann auch das Additionsprodukt $Cr(NCS)_3$. Imidazol als Abbauzwischenprodukt auftreten.

Wie aus den Abb. 1—2 hervorgeht, konnte die Bildung der freien Säuren $H[Cr(NCS)_4(Imidazol)_2]$und $H[Cr(NCS)_4(Benzimidazol)_2]$ mit Hilfe der Thermogramme nicht bestätigt werden (Die stöchiometrisch berechnete Säuremenge und der erste Knickpunkt der Thermogramme stehen nicht im Einklang).

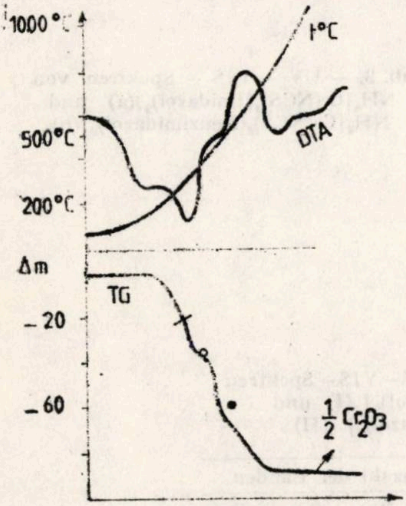

Abb. 1. — Derivatogramm von NH_4 $[Cr(NCS)_4$ $(Imidazol)_2]$
,,/" berechnete Menge von $H[Cr(NCS)_4$ $(Imidazol)_2]$
,,·" berechnete Menge von $Cr(NCS)_3$. Imidazol
,,0" berechnete Menge von $Cr(NCS)_3$
,,/" berechnete Menge von Cr_2O_3.

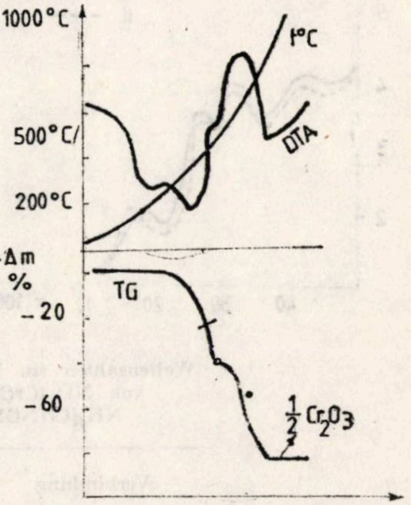

Abb. 2. — Derivatogramm von NH_4 $[Cr$ $(NCS)_4$ $(Benzimidazol)_2]$.

Der Inflexionspunkt der thermogravimetrischen Kurven um 320—360°C entspricht dem Additionsprodukte : $Cr(NCS)_3$. Imidazol, bzw. $Cr(NCS)_3$.Benzimidazol.

Die Bildung von $Cr(NCS)_3$ (um 400—450°C) bei diesem thermolytischen Vorgang ist weniger gut ausgeprägt als im Falle der Pyrolyse von Reineckeaten der N-Basen (Amin. $H.[Cr(NCS)_4(NH_3)_2]$).[16,17]

In den Elektronenspektren der neuen Komplexe zeigen sich vier Banden, wie im Falle anderer Reineckesalzanaloga mit aliphatischen und aromatischen Aminen[18] (Abb. 3.).

Die Wellenzahlen dieser Banden sind in Tabelle 3 wiedergegeben.

Die A- und B- Banden entsprechen einiger d — d Übergängen, nähmlich die A- Bande entspricht der $^{4\prime}T_{2g} \rightarrow {}^{4\prime}A_{2g}$ Übergang des oktaedrischen Komplexes $[Cr(NCS)_2]^{3-}$, und die Bande B der $^{4\prime}T_{1g} \rightarrow {}^{\prime 4}A_{2g}$ Übergang.[18] Die Spaltung dieser Banden im Ligandfeld von D_{4h} Symmetrie der Reineckesalzanaloga erweist sich nur als eine Asymmetrie der

Banden. Die C- und D-Banden entsprechen wahrscheinlich Ladungsüberführung Übergängen.

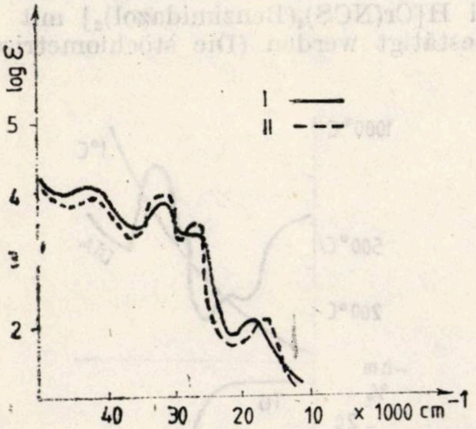

Abb. 3. — UV — VIS — Spektren von $NH_4[Cr(NCS)_4(Imidazol)_2]$(a) und $NH_4[Cr(NCS)_4(Benzimidazol)_2]$(b).

Tabelle 3

Wellenzahlen (in kK) der UV—VIS—Spektren von $NH_4[Cr(NCS)_4(Imidazol)_2]$ (I) und $NH_4[Cr(NCS)_4(Benzimidazol)_2]$ (II)

Verbindung	Wellenzahl der Banden			
	A	B	C	D
I	18,2	25,3	30,6	41,5
II	17,7	25,1	30,4	41,4

Der Einfluß der Amin-Liganden ist nur bei der Bande A deutlich. Das Vergleichen der Spektren dieser Verbindungen mit dem Spektrum des $K_3[Cr(NCS)_6]$zeigt, da der Austausch von zwei NCS-Gruppen im--$[Cr(NCS)_6]^{3-}$ mit heterocyclischen Aminen eine Verschiebung der Farbtönung von blauviolett nach rot verursacht.

Die Absorptionskurven folgen in allen Teilen dem Beerschen Gesetz in Methanol (Bedeutung aus analytischem Standpunkt).

Die wichtigsten Spektraldaten der Ultrarotspektren von $NH_4[Cr(NCS)_4(Imidazol)_2]$und $NH_4[Cr(NCS)_4(Benzimidazol)_2]$sind in Taelle 3 z usammengestellt.

Tabelle 4

Ur-Banden von $NH_4[Cr(NCS)_4(Imidazol)_2]$ (I), $NH_4[Cr(NCS)_4(Benzimidazol)_2]$ (II); $Ag[Cr(NCS)_4(Imidazol)_2]$ (III) $Hg[Cr(NCS)_4(Benzimidazol)_2]_2$ (IV)

Zuordnung der Schwingungsfrequenz	I	II	III	IV
$\nu_{C=N}$	2060—2075 (s)	2060—75 (s)	2066 (s) 2110 (s)	2070 (s) 2115 (s)
ν_{C-S}	785 (s) 765 (s)	685 (s) 760 (s)	780 (s) 760 (s)	770 (s) 750 (s)
δNCS	485 (s) 450 (m)	485 (s) 450 (m)	485 (s) 450 (m)	485 (s) 450 (m)

Die charakteristischen Frequenzen der koordinierten NCS-Gruppen zeigen, daß die Cr- Thiocyanat-Bindung in beiden Fällen durch das Stickstoffatom erfolgt.

Im Vergleich mit den Spektren der Isothiocyanato-Komplexen des Kobalts(III) : (z.B. $[Co(NH_3)_5NCS]Cl_2$, $[Co(en)_2(NCS)_2]Cl$, sind die Schwingungsfrequenzen der NCS- Gruppen in den Spektren der obenerwähnten Komplexen nach niedrigeren Wellenzahlen verschoben. Diese Verschiebung weist auf die Zunahme des kovalenten Charakters der M-NCS-Bindung von Co(III) nach Cr(III) hin.[19] Es ist bemerkenswert, daß in den Spektren der Silbersalze : $Ag[Cr(NCS)_4(Imidazol)_2]$ und $Ag[Cr(NCS)_4(Benzimidazol)_2]$ die Spaltung der $\nu_{C\equiv N}$-Bande aufritt. $\nu_{C\equiv N}$ 2110 (s) und 2060 cm^{-1} (s). Ein analoges Phänomenon wurde auch im Falle einiger $M[Cr(NCS)_4(NH_3)_2]$, $M_2[Pt(SCN)_6]$und $M_3[Cr(NCS)_6]$ (M = Ag, Hg, Pd) beobachtet. Diese Erscheinung spricht für eine M-SCN-Cr, M-NCS-Pt — Brückenbindung im Kristalligitter.[20]

LITERATUR

[1] K. Michelson, *Acta Chem. Scand.*, **17**, 1811 (1963).

[2] A. R. Bayley und W. T. Michelson, *J. Inorg. Nucl. Chem.*, **34**, 2935 (1972).

[3] E. Blasius, H. Augustin und V. Wenzel, *J. Chromatogr.*, **49**, 520 (1979); **50**, 319 (1970); **73**, 298 (1972).

[4] J. Roessler, *Liebigs Ann. Chem.*, **141**, 189 (1867).

[5] C. Mahr, *Z. anorg. Chem.*, **208**, 313 (1932).

[6] A. Scagliarini und B. Tartarini, *Gazz. chim. Ital.*, **53**, 617 (1923).

[7] R. Ripan, I. Gănescu und Cs. Várhelyi, *Rev. Roumaine Chim.*, **11**, 473, 717 (1966).

[8] A. Reinecke, *Liebigs Ann. Chem.*, **126**, 114 (1863).

[9] M. Bergmann, *J. Biol. Chem.*, **110**, 476 (1935).

[10] K. Issleib, Tzschach, *Z. anorg. Chem.*, **297**, 121 (1958).

[11] Cs. Várhelyi und I. Gănescu, *Monatsh. Chem.*, **98**, 472 (1967).

[12] I. Zsakó, Cs. Várhelyi, I. Gănescu und L. Zöldi, *Monatsh. Chem.*, **99**, 2235 (1968); **106**, 801 (1975).

[13] I. Zsakó, I. Gănescu, Cs. Varhelyi und G. Brînzan, *Z. physik. Chem. (Leipzig)*, **265**, 1001 (1984).

[14] P. Pfeiffer, *Ber. dtsch. chem. Ges.*, **34**, 4303 (1901).

[15] P. Pfeiffer und B. Werdelmann, *Z. anorg. Chem.*, **297**, 121 (1958).

[16] J. P. Krausz und J. Kovács, *Ann. Univ. Sci. Budapestinensis de R. Eötvös nom. Sect. Chim.*, **4**, 37 (1962).

[17] G. Boda, Cs. Várhelyi und Á. Mostis, *Stud. Univ. Babeş-Bolyai, Chem.*, **10** (2), 63 (1965).

[18] I. Zsakó, J. Sata, Cs. Várhelyi, *Acta Chim. Acad. Sci. Hung.*, **78**, 387 (1973).

[19] D. Forster und L. M. D. Goodgame, *J. Chem. Soc.*, **1965**, 262, 1286.

[20] J. Fujita, M. Kobayashi und K. Nakamoto, *J. Amer. Chem. Soc.*, **78**, 3295 (1956).

Die charakteristischen Frequenzen der koordinierten NCS-Gruppen zeigen, daß die Cr-Thiocyanat-Bindung in beiden Fällen durch das Stickstoffatom erfolgt.

Im Vergleich mit den Spektren der Isothiocyanato-Komplexen des Kobalts(III): (z.B. [Co(NH$_3$)$_5$NCS]Cl$_2$, [Co(en)$_2$(NCS)$_2$]Cl, sind die Schwingungsfrequenzen der NCS-Gruppen in den Spektren der oben erwähnten Komplexen nach niedrigeren Wellenzahlen verschoben. Diese Verschiebung weist auf die Zunahme des kovalenten Charakters der M–NCS-Bindung von Co(III) nach Cr(III) hin.[9] Es ist bemerkenswert, daß in den Spektren der Silbersalze: Ag[Cr(NCS)$_4$(imidazol)$_2$] und Ag[Cr(NCS)$_4$(benzimidazol)$_2$] die Spaltung der ν_{C-N}-Bande auftritt: ν_{C-N} = 2119 (s) und 2090 cm^{-1} (s). Ein analoge Erscheinung wurde auch im Reihe einiger M[Cr(NCS)$_4$(NH$_3$)$_2$], M$_3$[Cr(NCS)$_6$] und M$_3$[Cr(NCS)$_6$] (M = Ag, Hg, Pd) beobachtet. Diese Erscheinung spricht für eine M–SCN–Cr, M–NCS–Pt-Brückenbindung im Kristallgitter.[20]

LITERATUR

[1] K. Michelsen, Acta Chem. Scand. 17, 1811 (1963).
[2] A. H. Davies und W. T. Stephenson, J. Inorg. Nucl. Chem. 34, 2535 (1972).
[3] L. [illegible], H. Augustin und V. Wenzel, J. [illegible], 45, 335 (1970); 56, 319 (1970); 73, 293 (1973).
[4] J. [illegible], [illegible] 141, 185 (1967).
[5] O. [illegible], Z. anorg. Chem. 288, 313 (1956).
[6] A. [illegible] und [illegible], [illegible] 78, 617 (1964).
[7] R. [illegible], [illegible] und [illegible], [illegible] Chem. 11, 173, 17 (1990).
[8] A. [illegible], [illegible] Chem. 188, [illegible] (1949).
[9] M. [illegible], [illegible] Chem. 140, 478 (1932).
[10] K. [illegible], Z. anorg. Chem. 297, [illegible] (1958).
[11] G. [illegible] und J. [illegible], Monatsh. Chem. [illegible], 532 (1967).
[12] J. [illegible], [illegible] und [illegible], Monatsh. Chem. 93, 235 (1962); 166, [illegible] (1962).
[13] J. [illegible], [illegible] und O. [illegible], Z. anorg. Chem. (Leipzig) 268, 1001 (1956).
[14] P. Pfeiffer, Ber. dtsch. chem. Ges. 34, [illegible] (1901).
[15] P. Pfeiffer und R. [illegible], Z. anorg. Chem. 257, 121 (1948).
[16] J. P. [illegible] und J. Kovacs, [illegible] 4, 37 (1962).
[17] C. [illegible] und A. [illegible], [illegible] Chem. 10 (2), 61 (1966).
[18] I. [illegible], [illegible], Acta Chim. Acad. Sci. Hung. 78, 457 (1973).
[19] D. Forster und [illegible], J. Chem. Soc. 1965, 202, 1288.
[20] J. Fujita, M. Kobayashi und [illegible], J. Amer. Chem. Soc. 78, [illegible] (1956).

Revue Roumaine de Chimie, 35, *6*, 777–783 (1990)

NOVEL SUBSTITUTED-AMINOCOUMARINS AS POTENTIAL ANTIMICROBIAL AGENTS

M. M. BADRAN, A. K. EL-ANSARI and S. EL-MELIGIE
Organic Chemistry Department, Faculty of Pharmacy,
Cairo University, Egypt

Received February 8, 1988

The synthesis of a novel series of substituted-aminocoumarins (II), (III) and (IV) and the preliminary evaluation of their *in vitro* antimicrobial activity are described. The reaction of 4-hydroxycoumarin (I) with a number of primary or cyclic secondary amines affored the corresponding 4-amino-coumarin derivatives (II). Likewise, reacting the same substrate with different sulpha-drugs furnished the respective 4-[4-(N-substituted--sulphamoylphenyl)]-aminocoumarins (III). On the other hand, Mannich reaction of(I) with formaldehyde and certain amines yielded the desired 4-hydroxy 3-substituted-aminomethylcoumarins (IV). The antimicrobial screening has revealed that some of these novel compounds possess moderate activity against *Bacillus subtilis* and *Bacillus pumitis*.

INTRODUCTION

The potential antimicrobial activity of coumarin derivatives[1–3] continue to receive attention, and several substances containing this moiety, obtained either from natural or synthetic sources, are currently used in therapy.[4] Moreover, it is known that the antibiotic novobiocin[5] belongs to the 4-hydroxycoumarin series. This fact prompted many investigators to synthesise a number of N-alkyl or aryl-substitutes-3-aminocoumarins[6] as analogues of this antibiotic and evaluate their antimicrobial activities.

We report herein an attempt to develop new coumarin derivatives with broad antimicrobial action by the introduction of a substituted-amino group at positions-3 or-4 of the coumarin ring. Likewise, it was assumed that an introduction of a sulphamidoarylamino moiety at position 4-would produce new promising candidates for antibacterial agents.

RESULTS AND DISCUSSION

The synthesis of the title coumarin derivatives was accomplished by the route shown in Scheme 1.

4-Hydroxycoumarin (I), needed as a substrate in this study was prepared from 2-hydroxyacetophenone using the sodium/ethyl carbonate method of Boyd and Robertson.[7] Treatment of (I) with a molar equivalent of pyrrolidine, or morpholine in boiling benzene using a Dean-Stark water-separator gave the respective N-substituted derivatives (IIa and b). Also, fusion of the coumarin (I) with cyclohexylamine and a number of arylamines afforded the corresponding substituted-amino derivatives (II c–f). The structure of the compounds (II) was confirmed from diagnostic inspection of their IR and ^{1}H–NMR spectra. The IR spectra lack the stretching absorption characteristic of the 4-hydroxyl function, wheareas it indicates the presence of the lactone carbonyl absorptions at 1680 cm^{-1}. This value is consistent with coumarin derivatives.[8] The ^{1}H–NMR spectrum of (II c) revealed one proton signal at δ 5.46 for *CH* proton at position 3 in addition to the other required signals (Table 1).

Scheme 1

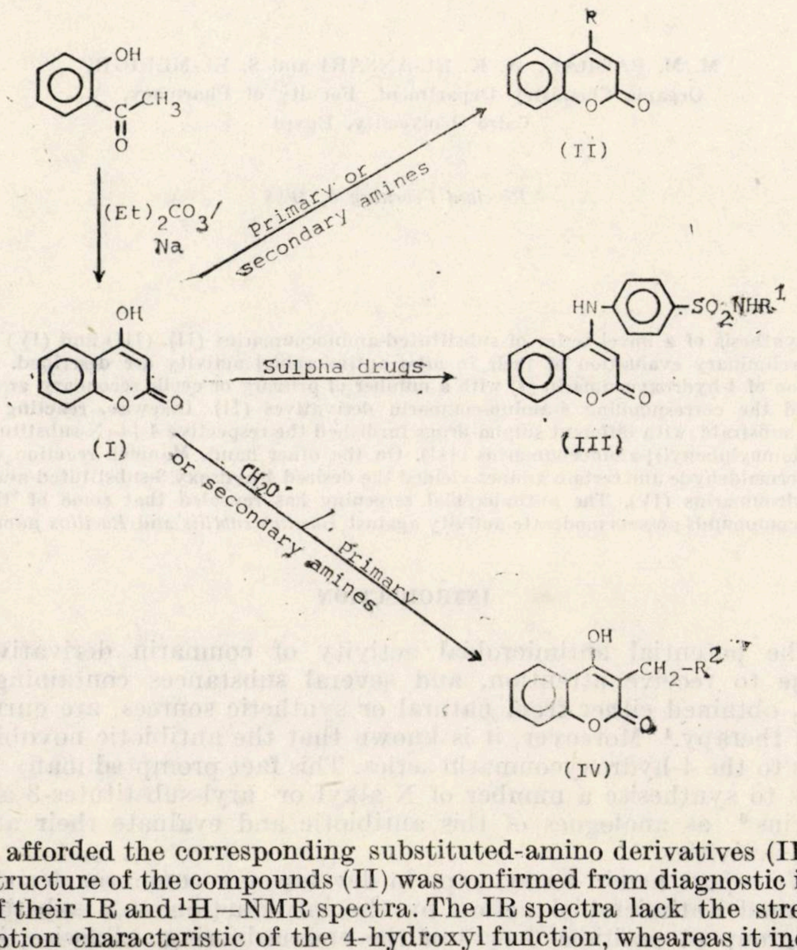

OH
CH_3
C
O
$(Et)_2CO_3/$
Na
OH
(I)
Primary or secondary amines
R
(II)
Sulpha drugs
HN
SO_2NHR^1
(III)
CH_2O Primary or secondary amines
OH
CH_2-R^2
(IV)

Likewise, condensation of the 4-hydroxycoumarin (I) with a group of sulpha-drugs gave the corresponding substituted aminocoumarin derivatives (III). The structure assigned for these products was confirmed by elemental analyses as well as by IR spectra, which displayed strong carbonyl absorption at 1680–1660 cm^{-1} and SO_2*NH* absorption at 3360–3320 cm^{-1}.

On the other hand, Mannich reaction of the same substrate (I) with formaldehyde and certain primary and secondary amines furnished the desired 4-hydroxy 3-substituted-aminomethylcoumarins (IV). However,

Table 1. 4-Substituted aminocoumarins (II)

No.	R	m.p °C	Yield %	Molecular formula		Analysis %	
						Calcd	Found
II_a^*	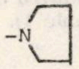	275	40	$C_{13}H_{13}NO_3$	C H N	72.5 6.0 6.0	72.3 5.7 6.1
II_b^*	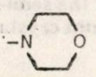	205	30	$C_{13}H_{13}NO_3$	C H N	67.5 5.6	67.2 6.0
II_c^{**}	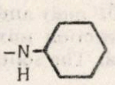	160	52	$C_{15}H_{16}NO_2$	C H N	74.3 6.6 5.7	74.0 6.8 5.5
II_d	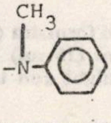	120	54	$C_{16}H_{13}NO_2$	C H N	76.4 5.1 5.5	76.9 5.2 5.2
II_e	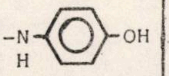	270	50	$C_{15}H_{11}NO_3$	C H N	71.1 4.3 5.5	71.5 4.3 5.5
II_f	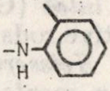	260		$C_{15}H_{11}NO_3$	C H N	71.1 4.3 5.5	71.5 4.3 5.5

* IR (cm^{-1}): 1680 (C=O lactone).

** ^1H-NMR (pyridine) δ 1.2–2.1 (m, 10H of cyclohexyl ring); 3.35 (hump, 1H $-\mathrm{N}-\underset{\mathrm{H}}{\mathrm{C}}\lt$); 5.46 (s, 1H at position 3); 7.1–8.6 (m, 11H aromatic and pyridine).

in case of piperazine, a bis-product was obtained (IVd). Supporting evidences for their structure were established on the basis of elemental analysis, IR and ^1H-NMR spectral data. The absence of the signal due to the proton at position 3 in the ^1H-NMR spectra, and the presence of absorption band at 3400–3350 cm^{-1} due to the 4-hydroxyl function in the IR spectra, are indicative to the assigned structure.

EXPERIMENTAL

Melting points were determined on a Griffin apparatus and are uncorrected. Elemental analyses were performed by the Microanalytical Center, Cairo University, Egypt. IR spectra were determined as KBr discs on a Pye Unicam sp 1100 or Shimadue 435 spectrophotometer. ^{1}H—NMR were scanned on a Varian 60 MHz and a Varian 90 MHz spectrometer.

4-Hydroxycoumarin was prepared as reported.[7]

4-Substituted-aminocoumarins (IIa—f) :

Method A : (II a and b)

To a suspension of 4-hydroxycoumarin (I), (0.01 mol) in dry benzene (30 mL), pyrrolidine or morpholine (0.01 mol) was added and the clear solution obtained was heated to reflux using a Dean-Stark water separator for 8 hours. The solvent was removed by distillation under reduced pressure and the product crystallised from methanol (Table 1).

Method B : (IIc-f)

A mixture of the coumarin (I), (0.01 mol) and the appropiate amine (0.01 mol) was fused at 100—130° for 3 hours. The reaction mixture was left to cool and the semi-solid mass obtained was triturated with ethanol. The solid so obtained was filtred and crystallized from ethanol (Table 1).

4-[4-(N-Substituted-Sulphamoylphenyl)] Aminocoumarins (IIIa-h) :

General method : A mixture of 4-hydroxycoumarin (I), (0.01 mol) and the appropriate sulpha-drug (0.01 mol) was fused at 150—160° for 2 hours. The reaction mixture was left to cool and the semi-solid cake obtained was triturated with ethanol. The solid so obtained was filtered and recrystallized from methanol (Table 2).

4-Hydroxyl-3-Substituted-aminomethylcoumarins (IV*a-f*) :

An ethanolic solution of the appropriate amine (0.015 mol) and formalin (1 mL ; 0.012mol) was added to a solution of the coumarin (I), (0.012 mol) in ethanol (15 ml) while stirring at room temperature for 3 hours. The reaction mixture was left overnight and the solid product separated was filtered and recrystallized from ethanol (Table 3).

Antimicrobial Activity

Compounds IIe, IIf, IIId, IIIe, IIIf, IIIg, IIIh, IVa, IVb and IVf were tested against *Staphylococcus aureus*, *Sarcina lutea* (Gram-positive cocci), *Bacillus subtilis*, *Bacillus pumitis* (Gram-positive rods), *Escherichia coli*, *Pseudomonas aeruginosa* (Gram-negative rods), *Neisseria sp* (Gram-negative cocci) and *Candida albicans*, *Trichophyton mentogrophytes* (as representative for fungi) by the disc-agar diffusion method.[10]

The compounds to be tested were dissolved in DMF (1000 μg/ml) in sterile Wasserman tubes. Sterile filter paper discs each containing 20 μl of the above solutions were placed over the surface of nutrient agar containing standardized inoculum from the test microorganisms. Plates were incubated at 37°C for 24 hours for bacterial isolates and at 27°C for 72 hours for fungal isolates. Zones of inhibition appeared after incubation are measured.

Results : The compounds which have shown appreciable activity are included in Table 4. Generally, none of the compounds tested was active against Gram-negative bacteria. Compounds IIIe, IVa and IVb showed reasonable activity against *Bacillus subtilis* and *Bacillus pumitis* (Gram-positive rods), wheareas compound IIIh showed activity against *Bacillus subtilis* only. All of the compounds tested are inactive against fungi.

Table 2. 4-[4-(N-Substituted-Sulphamoylphenyl)] amino-coumarins (III)

No.	R^1	m.p ^{o}C	Yield %	Molecular formula	Analysis %	
					Calcd	Found
III_a^{**}	H	192	48	$C_{15}H_{12}N_2O_4S$	C 56.9 H 3.7 N 8.8	57.1 4.0 8.4
III_b	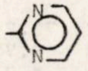	> 300	50	$C_{19}H_{14}N_4O_4S$	C 57.8 H 3.5 N 14.2	58.0 3.7 14.5
III_c	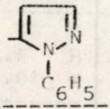	> 300	30	$C_{24}H_{18}N_4O_4S$	N 10.0	10.4
III_d^{*}	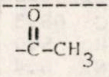 $-\overset{O}{\overset{\parallel}{C}}-CH_3$	> 300	40	$C_{17}H_{14}N_2O_5S$	C 56.9 H 3.9 N 7.8	57.4 4.3 8.3
III_e^{*}	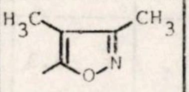	> 300	42	$C_{20}H_{17}N_3O_5S$	C 58.3 H 4.1 N 10.2	58.7 4.5 10.0
III_f	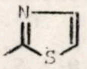	> 300	50	$C_{18}H_{13}N_3O_4S_2$	C 54.1 H 3.2 N 10.5	54.5 3.5 10.8
III_g^{*}	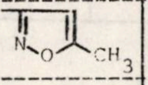	> 300	40	$C_{19}H_{15}N_3O_5S$	N 10.5	10.6
III_h	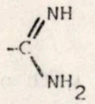	250	60	$C_{16}H_{14}N_4O_4S$	C 53.6 H 3.9 N 15.6	53.3 4.2 15.4

* IR (cm^{-1}):

(III_d) 1650 (C=O, lactone; 3350, 3250, two -NH groups)

(III_e) 1680 (C=O, lactone; 3350, 3250, two -NH groups)

(III_g) 1680 (C=O, lactone; 3320 -NH groups)

** ^1H-NMR (ppm) DMSO; δ 5.46 (s, 1H, proton at position 3), 7.2-8.2 (8 aromatic protons), 9.3 (1H -NH).

Table 3. 4-Hydroxy-3-Substituted aminomethylcoumarins (IV)

No.	R^2	m.p °C	Yield %	Molecular formula	Analysis% Calcd	
					Calcd	Found
IV$_a$**	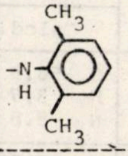	242	70	$C_{18}H_{17}NO_3$	C 73.2 H 5.7 N 4.7	73.5 5.7 5.1
IV$_b$	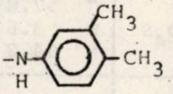	224	72	$C_{18}H_{17}NO_3$	C 73.2 H 5.7 N 4.7	73.0 5.5 4.3
IV$_c$	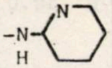	214	60	$C_{15}H_{12}N_2O_3$	C 67.1 H 4.4 N 10.4	67.2 4.7 10.0
IV$_d$***	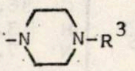	235	68@	$C_{24}H_{22}N_2O_6$	C 66.3 H 5.0 N 6.4	66.2 5.1 6.9
IV$_e$**	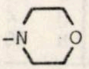	215	48	$C_{14}H_{15}NO_4$	N 5.3	5.0
IV$_f$*	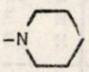	245	52	$C_{15}H_{17}NO_3$	C 69.4 H 6.5 N 5.4	69.0 6.1 5.2

R^3 =

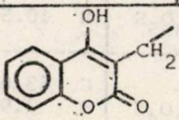

* This compound was previously prepared[9] with no data.

** IR (cm^{-1}):

(IV$_a$) 1680 (C=O lactone), 3350 (OH), 3280 (NH)

(IV$_e$) 1660 (C=O lactone), 3400 (OH)

*** ^{1}H-NMR (ppm) DMSO:

δ 2.9 (s, 16H, two piperazine rings); 3.6 (s, 4H, two $-\underline{CH_2}-N\langle$); 7.2-7.9 (m, 8H, aromatic protons).

@ Yield calculated with respect to molar quantity of (I).

Table 4. Antimicrobial Activity of Substituted-Aminocoumarins

Compd	Diamter of the inhibition zone in mm							
	E. coli	Ps. aeruginosa	S. aureus	S. lutea	B. subtilis	B. pumitis	C. albicans	Trichophyton mento-grophytes
III$_e$	–	–	–	–	13 mm	16 mm	–	–
III$_h$	–	–	–	–	12 mm	–	–	–
IV$_a$	–	–	–	–	15 mm	19 mm	–	–
IV$_b$	–	–	–	–	20 mm	18 mm	–	–

Stock culture, Microbiology Dept., Faculty of Pharmacy, Cairo University.

REFERENCES

[1] G.M. Cingolani, F. Gaultrieri, and M. Pigini, *J. Med. Chem.*, **12**, 531 (1969).

[2] K.S.R. Krishna Mohan Rao and N.V. Subba Rao, *Proc. Indian Acad. Sci., Sect. A.*, **67**, 42 (1968) ; *Chem. Abstr.*, **70**, 77840 (1969).

[3] B. Rao, C. Mouli, and Y.D. Reddy, *Ind J. Chem.*, **22** B, 176 (1983).

[4] F. C. De Schryver, (Katholieke Universiteit Lauren) PCT Int. Appl. Wo 84, 02, 133 (Cl C07D 491/052), 07 Jun., 1984, LU Appl, 84, 492, 29 Nov., 1982, 18 pp. ; *Chem. Abstr.*, **102**, 24610 (1985).

[5] E.A., Kaczka, F.J. Wolf, F.P. Rathe, and K.J. Folkers, *J. Amer. Chem. Soc.*, **73**, 6404 (1955).

[6] K.S.R. Krishna Mohan Rao, and N.V. Subba Rao, *Ind. J. Chem.*, **3**, 522 (1965).

[7] J. Boyd, A. Pobertson, *J. Chem. Soc.*, (1984) 174.

[8] F.M. Dean, "Naturally Occurring Oxygen Ring Compounds", Butterworths, London, (1963), p. 176, 248.

[9] V.L. Salelev, O.S. Artamonova, and V.S. Troitskaya, *Khim. Geterotsiki. Soedin*, **7**, 896 (1982) ; *Chem. Abstr.*, 97, 162763^{f} (1982).

[10] C.H. Collins "Microbiological Methods", Butterworths, London (1964), p. 92.

Revue Roumaine de Chimie, 35, 6, 785—789 (1990)

BEHAVIOUR OF 5,6-DIPHENYL-4-CARBETHOXY-2,3-DIHYDROPYRIDAZIN-3-ONE, TOWARDS SOME DIFFERENT NUCLEOPHILES

AMIN A. AFIFY, A. A. EL-KHAMRY, A. Y. SOLIMAN, M. A. SAYED
and E. A. KASSAB
Chemistry Department, Faculty of Science, Ain Shams University
Cairo, Egypt

Received February 29, 1988

The hitherto unknown 4-carbethoxy-5,6-diphenyl-2,3-dihydropyridazin-3-one (II) has been synthesised via cyclisation of diethyl-α-benzoylhydrazone-benzal malonate (I), which has been prepared on condensation of benzyl monohydrazone with diethyl malonate. Compound (II) reacted with primary amines, as well as secondary amines producing (III)a-g and/or (IV)a and b respectively. With some different Grignard reagents as carbon nucleophiles, (II) reacted affording (V) and b. Compound (II) also underwent hydroxymethylation on its reaction with formaldehyde to give (VI) and underwent complete Mannich reaction with formaldehyde and secondary amines providing (VII) a and b.

The present work is a continuation [1] of our comparative studies on some new prepared pyridazinone derivatives, with the aim of finding out the factors controlling their behaviour towards nucleophiles. The wide range of pharmacological properties of pyridatinone derivatives, [2,3,4] and also their use as agricultural fungicides made them worthy to be synthesized.

Condensation of benzyl monohydrazone with diethyl malonate in the presence of sodium ethoxide affords diethyl-α-benzoylhydrazone benzalmalonate (I) which underwent ring closure at long refluxation to give 4-carbethoxy-5,6-diphenyl-2,3-dihydropyridazin-3-one (II). The structure of either (I) or (II) was confirmed by i) correct analytical data; ii) the IR spectrum of (I) showed ν_{NH}, $\nu_{C=N}$, beside ν_{CO} of esters, while the IR spectrum of (II) displayed ν_{NH} and ν_{CO} both of amides and of esters (Table 1). Furthermore, on treatment of (I) with hydrazine hydrate, or phenylhydrazine the corresponding malonic acid hydrazides (VIII)a and b were produced. The structure of (VIII) was established from its elemental analysis, its IR spectrum which lacks absorption for ν_{CO} of esters (Table 1), and also from its PMR (in DMSO-d_6) which showed only a multiplet signal for Ar-*H* at δ 7.15. Compound (II) reacted with primary amines, namely, ethyl-, isopropyl-, cyclohexyl-, ethanol-, benzyl-amine, aniline and/or m-toluidine to give 4-(N-substituted) carbamido-2,3-dihydropyridazin-3-ones (III)a-g. Similarly, with secondary amines such as piperidine and/or morpholine (II) reacted producing 4-(piperidino- or morpholinocarbamido)-2,3-dihydropyridazin-3-one derivatives (IV)a and b. The structure of their (III) or (IV) was confirmed by the following : i) correct analytical data ; ii) their IR spectra which showed ν_{NH}, ν_{CO} of amides, $\nu_{C=N}$, in addition to ν_{OH} for (III)d (Table 1). The PMR for (III)g (in DMSO-d_6+ $CDCl_3$ mixture) showed signals at) δ 2.2 (S, 3*H* of Ar-*CH*$_3$), 6.4 and 7.3 (m, 14H of Ar—*H*). Also the NMR of (IV)a in (DMSO-d_6) showed signals at δ 1.5 (broad, *4H* of piperidine), 2.8 (broad *6H* of piperidine), 7.15 (10*H* of Ar—*H*).

Table 1

Characterization data of compounds prepared

Compd & yield		Molecular Formula & M.W.	Analysis Found/Req.			I.R.		
			C	H	N	NH, OH	CO	C=N
(I)	249—51	$C_{21}H_{22}N_2O_4$	69.11	5.94	7.43	3110	1730	1630
65		(366)	68.85	6.01	7.65	3195		1615
(II)	175—77	$C_{19}H_{16}N_2O_3$	71.54	4.85	8.43	3240	1720—1640	1630
65		(320)	71.25	5.00	8.75			
(III)	250—52	$C_{19}H_{17}N_3O_2$	71.72	5.51	13.40	3120	1660	1620
a, 85		(319)	71.47	5.32	13.16			
b, 85	256—8	$C_{20}H_{19}N_3O_2$	71.89	5.50	12.71	3180	1665	1630
		(333)	72.07	5.70	12.61			
c, 90	270—72	$C_{23}H_{23}N_3O_2$	73.56	6.32	11.51	3210	1680	1620
		(373)	73.99	6.16	11.26			
d, 90	246—48	$C_{19}H_{17}N_3O_3$	67.82	4.90	12.33	3350	1670	1635
		(335)	68.05	5.07	12.57	3100		
e, 80	255—56	$C_{24}H_{19}N_3O_2$	75.75	4.65	11.51	3020	1665	1615
		(381)	75.59	4.89	11.02			
f, 90	244—46	$C_{23}H_{17}N_3O_2$	74.95	4.22	11.71	3190	1670	1620
		(367)	75.20	4.63	11.44			
g, 75	255—57	$C_{24}H_{19}N_3O_2$	75.11	4.62	11.33	3200	1680	1630
		(381)	75.75	4.89	11.02			
IV	265—68	$C_{22}H_{21}N_3O_2$	73.20	5.52	11.33	3200	1675, 1680	1625
A, 70		(359)	73.53	5.84	11.69			
b, 75	259—61	$C_{21}H_{19}N_3O_3$	69.52	5.50	11.40	3160	1660—1670	1630
		(361)	69.80	5.26	11.63			
V	278—80	$C_{19}H_{16}N_2O_2$	75.40	5.00	9.51	3300	1670, 1680	1620
a 70		(304)	75.00	5.26	9.20			
b 70	275—76	$C_{24}H_{18}N_2O_3$	75.70	4.92	7.60	3450	166, 1675	1630
		(382)	75.39	4.71	7.32			
VI	234—35	$C_{20}H_{18}N_2O_4$	68.30	4.92	8.24	3500	1740, 1665	1610
60		(350)	68.57	5.14	8.00			
VII	243—44	$C_{28}H_{32}N_4O_2$	73.22	6.92	12.52	66	1660, 1650	1620
a 65		(456)	73.68	7.01	12.28			
b 70	220—22	$C_{26}H_{28}N_4O_4$	67.95	5.83	11.98	—	1686, 1665	1615
		(460)	67.82	6.08	12.17			
VIII	235—36	$C_{17}H_{18}N_2O_2$	63.35	5.97	26.51	3030	1660	1630
a 90		(328)	63.35	5.59	26.08			
b 90	240—45	$C_{29}H_{26}N_6O_2$	70.92	5.52	17.35	3330	1670	1610
		(490)	71.02	5.30	17.14			

* All compounds are colourless except (I) and (II) (yellow).

* All compounds are crystallisable from ethanol except (I) from toluene, (II) from benzene, and (VII) a and (VII) b from light petrol (60—80°).

Furthermore, with Grignard reagents as carbon nucleophiles, (II) reacted with ethylmagnesium iodide, as well as with p-anisylmagnesium bromide producing 4-acyl-5,6-diphenyl-2,3-dihydropyridazin-3-ones (V)a and b. The IR spectra data of (V)a and b (Table 1) revealed the presence of carbonyl groups for both ketones and amides, the fact that supports the proposed structure.

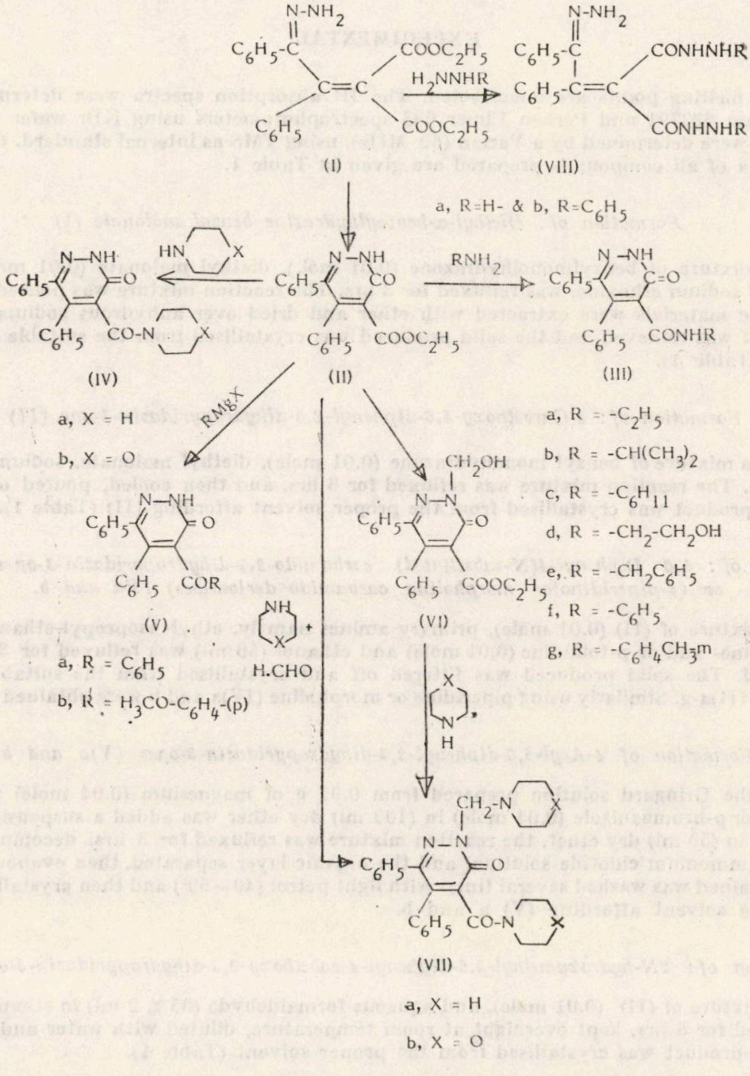
(I)
H2NNHR
(VIII)
a, R=H- & b, R=C6H5
(IV)
a, X = H
b, X = O
(II)
RNH2
(III)
RMgX
a, R = -C2H5
b, R = -CH(CH3)2
c, R = C6H11
d, R = -CH2-CH2OH
e, R = -CH2C6H5
f, R = -C6H5
g, R = -C6H4CH3-m
(V)
a, R = C2H5
b, R = H3CO-C6H4-(p)
H.CHO
(VI)
(VII)
a, X = H
b, X = O

Hydroxymethylation of (II) was achieved through its reaction with formaldehyde affording 2-N-hydroxymethyl-4-carbethoxy-5,6-diphenyl-2,3-dihydropyridazin-3-one (VI), whose IR spectrum exhibited ν_{OH}, ν_{CO} of esters, in addition to ν_{CO} of amides (Table 1). On the other hand, (II) treated with formaldehyde in presence of secondary amine such as piperidine or morpholine, behaves according to the Mannich pathway affording 2N-(piperidino or morpholino)-methylene-5,6-diphenyl-4N-(piperidino or morphilino)-carbamido-2,3-dihydropyridazin-3-ones(VII) a and b. The structure of (VII) was supported by : a) correct analytical data ; b) its IR spectrum which exhibited ν_{CO} of amides, while any absorption for ν_{CO} of esters is absent (Table 1) ; and c) they are easily obtained directly from (VI) on its treatment with piperidine or morpholine.

EXPERIMENTAL

All melting points are uncorrected. The IR absorption spectra were determined with Pye Unicam 633791 and Perken Elmer 683 spectrophotometers using KBr wafer technique. The NMR were determined by a Varian (60 MHz), using TMS as internal standard. Characterization data of all compounds prepared are given in Table 1.

Formation of: *Diethyl-α-benzoylhydrazine benzal malonate* (I)

A mixture of benzylmonolhydrazone (0.01 mol.), diethyl malonate (0.01 mole), and a solution of sodium ethoxide, was refluxed for 3 hrs. The reaction mixture was poured on water, the organic materials were extracted with ether and dried over anhydrous sodium sulphate, the solvent was removed and the solid produced was crystallised from the suitable solvent to give (I) (Table 1).

Formation of: *4-Carbethoxy-5,6-diphenyl-2,3-dihydropyridazin-3-one (II)*

To a mixture of benzyl monohydrazone (0.01 mole), diethyl malonate, sodium ethoxide was added. The reaction mixture was refluxed for 6 hrs, and then cooled, poured on ice/HCl. The solid product was crystallised from the proper solvent affording (II) (Table 1).

Formation of : 5,6 Diphenyl-4(N-substituted) carbamido-2,3-dihydropyridazin-3-ones (IIIa-g) or (4-piperidino/or morpholino carbamido derivatives) IVa and b.

A mixture of (II) (0.01 mole), primary amines namely, ethyl- isopropyl-ethanol-benzyl-amine aniline- and/or p-toluidine (0.01 mole) and ethanol (50 ml) was refluxed for 3 hrs, and then cooled. The solid produced was filtered off and crystallised from the suitable solvent producing (III)a-g. Similarly using piperidine or morpholine (IV)a and b were obtained (Table 1).

Formation of 4-Aryl-5,6-diphenyl-2,3-dihydropyridazin-3-ones (V)a and b

To the Gringard solution prepared from 0.97 g of magnesium (0.04 mole) and ethyl iodide and/or p-bromoanisole (0.04 mole) in (100 ml) dry ether was added a suspension of (II) (0.01 mole) in (50 ml) dry ether, the reaction mixture was refluxed for 3 hrs, decomposed with saturated ammonium chloride solution, and the organic layer separated, then evaporated. The residue obtained was washed several times with light petrol (40—60°) and then crystallised from the suitable solvent affording (V) a and b.

Formation of: *2N-hydroxymethyl-5,6-diphenyl-4-cabethoxy-2,3-dihydropyridazin-3-one (VI)*

A mixture of (II) (0.01 mole), and aqueous formaldehyde (35% 2 ml) in ethanol (20 ml) was refluxed for 6 hrs, kept overnight at room temperature, diluted with water and the separated solid product was crystallised from the proper solvent (Table 1).

Formation of 2-N(piperidino or morpholino) methylene-5,6-diphenyl-4-N-(piperidino or morpholino) carbamido-2,3-dihydropyridazin-3-ones (VII)a and *b.*

To a solution of (II) (0.01 mole) and piperidine or morpholine (0.02 mole) in methanol (20 ml), aqueous formaldehyde (35% 2 ml) was added. The reaction mixture was refluxed for

6 hrs, kept overnight at room temperature, diluted with water. The separated solid was crystallised from a suitable solvent affording (VII)a and b (Table 1).

Formation of the hydrazides (VIII)a and b

A solution of (I) (0.01 mole), hydrazine hydrate and/or phenylhydrazine (0.01 mole) in ethanol (50 ml), was allowed to stand at room temperature for 2 hrs. The solid separated was crystallised from the proper solvent to give (VIII) a and b.

REFERENCES

[1] Abdel Momen A. El-Khamry, Moamed E. Shaban and Mohamed M. Habshy, *Rev. Roum. Chim.* **31**, 387 (1966).

[2] A. Eshalier, M. Rodriguez, P. Duchene-Marullaz, J. Couguelet and P. Tronche, *Farmaco, Ed. Sci.* **40**, 200 (1985) (Eng.); *C.A.* **102**, 197721 (1985).

[3] Y. Lesher, B. Diekinson, William; U.S. US **4**,486,431 (Cl⁻ 424-250; A 61 K 31/50), 04 Dec. 1984, US Appl. 71,064, 30 Aug. 1979, 5pp. Cont. in part of U.S. Ser No. 225-024 abandand; *C.A.* **102**, 90141, (1985)

[4] V. K. Randy and A. K. Agarwal, *J. Indian Chem. Soc.* **56**, 707 (1979).

[5] Nippon Kayaku Cà. Ltd. Jpn. Kakai Tokkyo Koho JP, **59**,106,471 (84,106,71) (CI. CO 7D 337/14), 20 Ian. Appl. 82/216,797, 13 Dec. 1982, 3pp.; *C.A.* **102**, 6516 (1985).

[6] Inoue, Michiro, Ishikawa, Masayuki, Tsuchiya Takashi, Shimamoto, Tokio; Japan Kokai 7525, 580 (Cl CO 7D, A 61K) *C.A.* **83**, 136899, 179091, 179092 and 179093 (1975).

Revue Roumaine de Chimie, **35**, *6*, 791–799 (1990)

THE EFFECT OF AROMATIC DIAMINE + QUINONE-DIIMINE COUPLES IN ISOPRENE RUBBER*

TĂNASE VOLINTIRU[a], FRANCISC M. ALBERT[b], MARIA GIURGINCA[a]
and GHEORGHE IVAN[a]

[a]Research Institute for Rubber and Plastics Processing, R-79628 Bucharest, Romania
[b]National Institute of Chemistry, R-78126 Bucharest, Romania

Received March 2, 1989

The behaviour of some couples formed by aromatic diamines and quinone diimines in isoprene rubber matrix in conditions of accelerated thermo-oxidative and ozonizing degradation has been studied. The effect of couples was investigated using kinetical parameters obtained from the oxygen absorption and spectral measurements.

The aromatic diamines with antioxidant capability are implicated in the oxidative degradation process as hydrogen donors to peroxy radicals formed during oxidation of the polymer. [1] In final part of the induction step of the chain reaction, a significant amount of quinone diimine results [2–5]; the participation of quinone diimines in induction period is also advocated. [6] The quinone diimines possessing the base structures of the diaminic antioxidants are also known [7,8] to ensure antidegradant protection of rubbers. Because a diaminic antioxidant can co-exists with its corresponding quinone diimine in the same polymer system, the present paper reports on the investigation of the behaviour of some couples formed by diamines and their quinone diimines in an isoprene rubber matrix.

EXPERIMENTAL

The diamine antidegradants and their corresponding quinone diimines, used in the present study are presented in Table 1. The diamines were obtained, by crystallization, from commercial products; the quinone diimines were synthesized using a known method [7] and were checked by elemental analysis and UV and IR spectra.

The protecting capability of the diamine + quinone diimine couples in a matrix of purified natural rubber was investigated by the following tests: oxygen absorption at temperatures in the range from 80 to 120°C, and accumulation of oxygen bearing groups in thermo-oxidative degradation in air, following the absorption band in infrared spectrum at 1720 cm^{-1}.

The retention of the main physical properties of vulcanizates protected by various systems and aged at various temperatures was tested also, using a simplified recipe consisting

---

* Paper presented at 3rd National Congress of Chemistry, Bucharest 1988.

of (p—mass parts) : 100 p natural rubber, 5 p zinc oxide, 2 p stearic acid, 5 p mineral aromatic oil, 40 p HAF (high abrasion furnace) carbon black, 1 p cyclohexylbenzothiazolyl sulfenamide accelerator, 3 p sulfur, and 2 p protecting agent (diamine, quinone diimine, or their couples).

Table 1

Diamine antidegradants and their corresponding quinone diimines used in experiments

Abbreviation	Chemical structure	Mp (°C)
IPPD	N-isopropyl-N′-phenyl-p-phenylenediamine	79
DMBPPD	N(1,4-dimethylbutyl)-N′-phenyl-p-phenylenediamine	45
DPPD	N,N -diphenyl-p-phenylenediamine	150
QIPPD	quinone diimine of IPPD	55
QDMBPPD	quinone diimine of DMBPPD	45
QDPPD	quinone diimine of DPPD	135

For test of oxygen absorption, the cast films of protected elastomer were obtained in the diverticol of the Warburg apparatus ; for spectral measurements, the cast polymer films were prepared on the KBr windows.

RESULTS AND DISCUSSION

1. *Behaviour in oxygen medium of the elastomer containing protection couples.* From the plottings of oxygen amount absorbed during time at each temperature (Figures 1 and 2), induction periods, propagation periods, relative activity in induction period, and stability in propagation period are deduced. The *relative activity* was computed taking as reference the elastomer protected by diamine allone (IPPD or DPPD) using the relation :[6]

$$A_r = (t_x - t_0)/(t_s - t_0) \qquad (1)$$

where : t_x is the induction period (hours) for the elastomer protected by the diamine + quinone diimine couple ; t_s — induction period (hours) for the elastomer protected by corresponding diamine ; t_0 — induction period (hours) for the unprotected, purified elastomer.

The term *stability* (S_p) is adopted[6] for the slope of the curve after the completion of the induction period.

For the couples of antidegradants, a *co-operative index* can be computed using the known[9] equation :

$$\theta = t_{1+2}/(t_1 + t_2) \qquad (2)$$

where : t_{1+2} is the induction period for the elastomer protected by the couple of antidegradants at concentration $c_1 + c_2$; t_1 — induction period corresponding to the antidegradant 1 at concentration c_1 ; t_2 — induction period corresponding to the antidegradant 2 at concentration c_2.

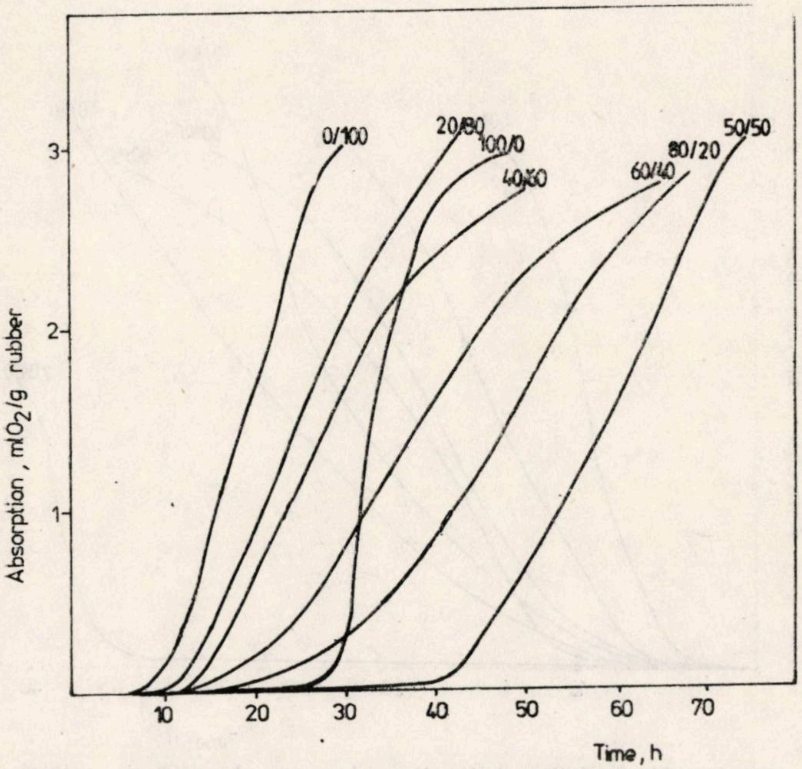

Fig. 1. — The evolution during time of oxygen absorption in natural rubber protected by various couples IPPD + QIPPD, at 100°C. IPPD/ /QIPPD ratio is noted on each curve.

The kinetic data presented in Table 2 emphasize some aspects concerning the antioxidant efficiency of the tested substances. The evaluation of the protecting capability of the both diamines, checked as single antioxidants, based on the induction period measurements, reveals a superior efficiency for IPPD in comparison with DPPD. Based on the same criterion, the induction period, for the systems IPPD + QIPPD the diamine appears more active than its corresponding quinone diimine, while for the systems DPPD + QPPD the situation is reversed.

For the elastomer protected by IPPD + QIPPD systems, the induction period diminishes with the decrease of IPPD amount in the system; a notable exception is the system containing equal amounts of components, for which the value of the co-operative index $\theta = 1.2$ reveals the existence of a synergistic effect.

The induction periods for the oxidation of natural rubber protected by DPPD + QPPD systems are lower in comparison with the levels recorded for the same elastomer protected by IPPD + QIPPD couples. All couples exhibit a protection capability superior to the reference (natural rubber containing DPPD allone) and this behaviour is particularly enhanced for the couple containing 20% DPPD + 80% QDPPD; for

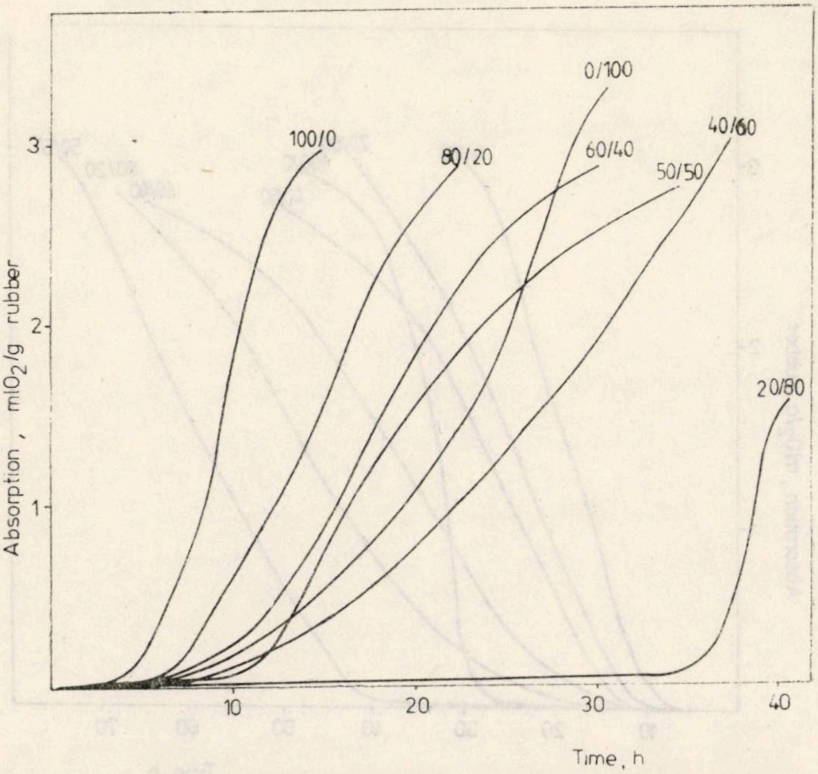

Fig. 2. — The evolution during time of oxygen absorption in natural rubber protected by various couples DPPD + QPPD, at 100°C. DPPD/ /QDPPD ratio is noted on each curve.

Table 2

Data concerning thermo-oxidative degradation in oxygen, based on oxygen absorption measurements using purified natural rubber protected by various systems

Protection system	Component ratio	Induction period (h) at temperatures (°C)		Relative activity, A_r, at temperatures (°C)		Stability, S_p, at temperatures (°C)	
		100	120	100	120	100	120
IPPD+QIPPD	100/0	26	10	1·0	1·0	·33	·40
	80/20	20	8	.8	.7	.08	.23
	60/40	16	7.5	.6	.7	.09	.23
	50/50	40	11	1.5	1.0	.09	.21
	40/60	12	3	.5	.5	.10	.14
	20/80	10	2.5	.4	.2	.11	.19
	0/100	8	2.5	.3	.2	.15	.23
DPPD+QDPPD	100/0	4	1	1.0	1.0	.40	.40
	80/20	6.5	2.5	1.6	2.5	.19	.60
	60/40	7.5	4.0	1.9	4.0	.18	.75
	50/50	10	5	2.6	5.0	.14	.60
	40/60	10	2.5	2.6	2.5	.20	.70
	20/80	35	8	9.7	8.0	.21	.78
	0/100	7.5	2	1.8	2.0	.14	.30

that case, the interaction parameter $\theta = 3.0$ at 100°C and $\theta = 2.7$ at 120°C emphasizes a high synergistic effect.

During the propagation period, the stability ensured by couples diamine + quinone diimine exhibits a marginal dependence on the ratio of the components for couples IPPD + QIPPD as well as for couples DPPD + QDPPD. The quinone diimine alone is able to improve stability of the elastomer, and is a rather surprising fact that QDPPD apears a little more efficient than QIPPD, while for couples of diamine + quinone diimine the systems IPPD + QIPPD are obviously superior to the systems DPPD+QDPPD.

Assuming that the overall thermo-oxidative process follows a first order kinetics,[10] the reaction rate constants of the degradation of protected natural rubber were deduced (Table 3) allowing to observe that the highest values are recorded for natural rubber protected by IPPD and the lowest values for the same elastomer containing the couple DPPD + QDPPD.

Table 3

Kinetic parameters computed for overall thermo-oxidative process, based on absorption measurements using purified natural rubber protected by various systems

Protection system *)	Reaction rate constant (h^{-1}) at temperatures (°C)	
	100	120
IPPD	.198	.466
DPPD	.075	.104
QIPPD	.104	.179
QDPPD	.048	.110
IPPD+QIPPD (60/40)	.080	.190
DPPD+QDPPD (50/50)	.045	.095

*) 2 mass parts per 100 mass parts of rubber

2. *Behaviour of the elastomer containing protection couples during thermo-oxidative degradation in air.* Cast films of purified natural rubber containing diamine + quinone diimine couples as antidegradants were submitted to thermo-oxidative degradation in hot air, following the evolution of oxygenated groups by recording the absorption at 1720 cm^{-1}. The kinetic curves were used to determine the process characteristics. For all protection couples, an efficiency comparable with diamine or at a higher level was observed during the induction period. That feature is expressed quantitatively by parameter A_r having values near or slightly higher than unit. For the co-operative factor θ, values near unit or slightly lower were deduced showing that the co-operation of the substances forming the antidegradant couple is near additivity. Table 4 contains only the information concerning the protection couples which exhibit the highest levels of the relative activity and, for comparison purpose, the behaviour of the elastomer protected by diamine or by the corresponding quinone diimine only are also presented.

Computation of the stability S_p during propagation step of the degradation of the elastomer protected by various couples revealed only marginal differences among the samples protected by different systems.

3. *Behaviour of the vulcanizates containing protection couples during accelerated ageing tests*. Vulcanizates based on a simplified recipe filled by active carbon black were tested by accelerated thermo-oxidative ageing (in oven) or in ozone-enriched atmosphere (in ozone testing cabinet). Protection of the vulcanizates was ensured by diamine and its quinone diimine alone or by their couple which exhibited the highest protection capability in previous experiments. The results of the tests are presented in Table 5 allowing to observe that the diamine alone and diamine + quinone diimine couples ensure a superior protection in comparison with the quinone diimine alone. The fact that the diamine + quinone diimine couples ensure an atioxidant protection at the level of the diamine allows the assertion that, in couples, the quinone diimine is able to preserve the antioxidant activity of the diamine itself.

Table 4

Data concerning thermo-oxidative degradation in air, computed from spectral measurements

Protection system	Component ratio	Induction period (h) at temperatures (°C)		Relative activity, A_r, at temperatures (°C)		Stability, S_p, at temperatures (°C)	
		100	120	100	120	100	120
IPPD + QIPPD	100/0	165	100	1.0	1.0	.010	.010
	60/40	185	120	1.1	1.2	.011	.012
	0/100	95	45	.6	.4	.009	.007
DPPD + QDPPD	100/0	150	75	1.0	1.0	.009	.009
	50/50	180	100	1.2	1.3	.007	.009
	0/100	80	45	.5	.6	.012	.013
DMBPPD + QDMBPPD	100/0	175	125	1.0	1.0	.008	.008
	50/50	190	125	1.0	1.0	.007	.008
	0/100	125	90	.7	.8	.010	.007

In ozonant destruction tests, the protection ensured by diamine + + quinone diimine couples is at the level of the diamine content, that means that quinone diimine does not own antiozonant activity.

The assembly of the experimental results shows that the most efficient co-operation is realized by DPPD + QDPPD couples, probably as a result of the extended conjugation present in the molecule of quinone diimine.

4. *Mechanism of participation of the quinone diimine in antioxidant protection*. During thermo-oxidative process, the aromatic diamines are able to react with peroxy radicals resulting in oxidation of the elastomer macromolecule, forming a complex which in its turn is transformed by the transfer of one proton or by reaction with a new peroxy radical :

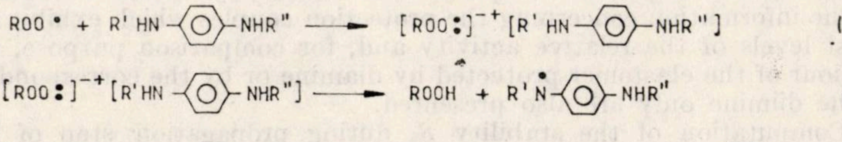
ROO• + R'HN–⟨◯⟩–NHR'' → [ROO:]⁻⁺[R'HN–⟨◯⟩–NHR'']
[ROO:]⁻⁺[R'HN–⟨◯⟩–NHR''] → ROOH + R'N•–⟨◯⟩–NHR''
[ROO:]⁻⁺[R'HN–⟨◯⟩–NHR''] + ROO• → 2ROOH + R'N=⟨⟩=NR''

(3)

(4)

(5)

Table 5

Behaviour by accelerated degradation of filled rubber vulcanizates protected by various antidegradants and antidegradant couples

Protection system	Component ratio	Loss of properties (%) after ageing 72 hours at 70°C		Loss of properties (%) after ageing 72 hours at 90°C		Ozone resistance, time (h) till appearance of cracks			
						In static conditions, 50 pphmO_3, 50°C		In dynamic conditions, 50 pphmO_3, 50°C	
		Tensile strength	Elongation at break	Tensile strength	Elongation at break	Initial	After ageing 72 h at 90°C	Initial	After ageing 72 h a 90°C
IPPD + QIPPD	100/0	9	15	25	30	40	42	50	48
	60/40	6	15	40	30	42	28	48	48
	0/100	10	32	37	33	3	3	2	2
DMBPPD + QDMBPPD	100/0	6	15	20	22	60	48	75	78
	50/50	5	14	18	26	48	42	48	42
	0/100	12	30	30	31	4	3	3	3
DPPD + QDPPD	100/0	14	33	33	39	20	12	18	12
	50/50	11	30	28	30	8	4	4	4
	0/100	25	39	50	42	2	2	2	2

The lower charge density on the nitrogen atoms in aromatic diamines enhances their capability to transfer protons to peroxy radicals and, consequently, their transformation in quinone diimines. [22] The quinone diimine is able to react with the elastomer macromolecule regenerating some amount of the initial diamine and/or grafting the diamine on the polymer blackbone : [22]

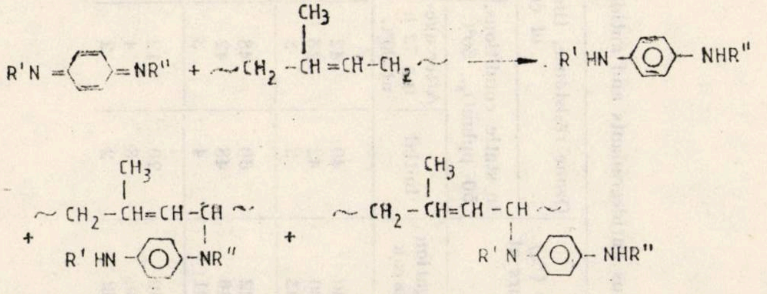

(6)

The ability of diamine antidegradant to form quinone diimines which in their turn regenerates the initial diamine or to form rubber-bound antidegradant by reaction with the macromolecules ensures an increase of the protecting capability by extension of the initiation step and by decreasing the degradation rate during the propagation step. The observed synergistic effect for some optimal couples diamine + quinone diimine supports the assertion concerning the co-operation of the members of the couple by regeneration of the diamine — the most efficient protecting component of the pair.

CONCLUSIONS

The presented data show that in circumstances of thermo-oxidative degradation in air or in pure oxygen, the quinone diimine co-operates with its corresponding diamine during initiation step and during propagation step of the degradation of the elastomer matrix extending the efficiency of the diamine by additive or synergistic effects. In vulcanized filled elastomer, the co-operation effect becomes less obvious, probably as a result of the interaction of the diamine and/or quinone diimine with the other components of the recipe.

REFERENCES

[1] J. R. Shelton, "Stabilization against Thermal Oxidation", Champ. 2 in "Polymer Stabilization" by L. Hawkins (Editor), Wiley, New York (1965). p. 29.

[2] J. Tsurugi, S. Murakami and K. Goda, *Rubber Chem. Technol.*, **44**, 857 (1971).

[3] J. Rotschová and J. Pospišil, *Chem. Ind.*, **1981**, p. 393.

[4] J. Rotschová and J. Pospišil, *J. Chromatography*, **211**, 199 (1981).

[5] J. Pospišil, "Aromatic Amine Antidegradants", Chap. 1 in "Developments in Polymer Stabilization", vol. 7 by G. Scott (Editor), Elsevier Applied Science, London 1984, p. 1.

[6] J. Rotschová and J. Pospišil, *Coll. Czech. Chem. Commun*, **47**, 2501 (1982).

[7] M. E. Cain, I. R. Gelling, G. T. Knight and P. M. Lewis, *Rubber Ind.*, **9**, 216 (1975).

[8] M. Giurginca, Thesis for Doctor Degree, National Institute of Chemistry, Bucharest, 1982.

[9] C. Latocha, W. Uhniat and W. Bucerowiak, *Polym. Degrad. Stabil.*, **7**, 189 (1984).

[10] D. W. van Krevelen, "Properties of Polymers", Elsevier, Amsterdam, p. 351, 1972.

[11] C. E. Boozer, G. S. Hammond, C. E. Hamilton and J.M. Sen, *J. American Chem. Soc.* **76**, 3851 (1955); **77**, 3238 (1956).

[12] J. R. Gelling and G. T. Knight, paper presented at International Rubber Conference, Brighten (England), 1977.

NOTE POUR LES AUTEURS

La Revue Roumanie de Chimie publie des articles en anglais, français, russe, allemand ou espagnol. Les auteurs sont priés d'envoyer des articles et comptes rendus inédits.

Les manuscrits seront dactylographiés à double interligne. La bibliographie, les tableaux et la légende des figures seront placés après le texte.

Si l'article fait partie d'une série numérotée, la partie précédente sera donnée comme première référence.

Chaque article sera précédé d'un résumé comprenant quinze lignes au maximum.

Les références bibliographiques dans le texte seront faites par des exposants sans parenthèses et paraîtront à la fin de l'ouvrage.

Les publications périodiques mentionnées dans la bibliographie seront présentées suivant les prescriptions internationales : le nom de l'auteur précédé de l'initiale du prénom, le titre du périodique abrégé conformément à « Chemical Abstracts » et souligné par une ligne, le numéro du tome indiqué par des chiffres arabes et souligné par deux lignes, suivi de la première page de l'article ; à la fin, l'année de la parution sera placée entre parenthèses. Le numéro de la revue ne sera pas indiqué si les pages du volume sont numérotées consécutivement.

Les textes des livres ou traités incluront : le nom des auteurs, l'initiale du prénom, le titre du livre entre guillemets et sans être souligné, le numéro du tome précédé par l'abréviation « vol. » (ou « Bd »), le numéro de l'édition, les éditions (the publisher), la localité de la parution du livre, l'année de la parution et la page de la référence précédée(s) par l'abreviation « p » (ou « S. »).

Les brevets seront indiqué comme suit : l'auteur ou la firme, le pays et le numéro du brevet, la date et la revue *(Chem. Abstr.)* Par ex : M. Jones (to Union Carbide Co,) Brit. Pat. 601 238, 2 Sept. 1959 ; cf. *Chem. Abstr.*, *54*, 12808 (1960).

Si la référence n'a pas été lue en original, on indiquera aussi la revue de référence consultée.

Les diagrammes seront tracés à l'encre de Chine sur papier calque. Les tableaux et les figures (en nombre strictement nécessaire) ainsi que les courbes dans les figures seront numérotés par des chiffres arabes. Leur explication sera donnée dans la légende des figures. Prière de ne pas inscrire les mêmes données dans les tableaux et les figures. Chaque tableau aura un titre. On indiquera dans le texte la place approximative des tableaux et des figures. Les formules chimiques seront incluses dans le texte ; en outre, elles seront transcrites sur papier calque, à l'encre de Chine.

Les auteurs sont priés d'indiquer les caractères italiques (en soulignant les lettres au crayon), ainsi que tout autre caractère spécial ; les préfixes *ortho*, *meta*, *para*, *cis*, *trans*, etc. seront soulignés pour indiquer leurs caractères italiques et ne seront jamais écrits avec des majuscules.

Aucune correction à la main ne sera admise sur le manuscrit. Les corrections seront tapées à la machine. Les lettres grecques ou d'autres symboles spéciaux seront insérés à la main à l'encre clairement.

Le manuscrit sera signé par l'auteur.

Le titre-courant aura 50 lettres au maximum.

L'entière responsabilité du contenu des articles appartient aux auteurs.

Sur demande on peut obtenir une note plus complète.

PRINTED IN ROMANIA

[illegible]

TRAVAUX PARUS AUX ÉDITIONS DE L'ACADÉMIE ROUMAINE

I. G. MURGULESCU, **Introducere în chimia fizică, Vol. I. 1. Atomi, molecule, legătură chimică**, 1976, 560 p.

I. G. MURGULESCU, V. EM. SAHINI, **Introducere în chimia fizică, Vol. I. 2. Structura şi proprietăţile moleculelor**, 1979, 604 p.

I. G. MURGULESCU, E. SEGAL, **Introducere în chimia fizică, Vol. II. 1. Teoria molecular-cinetică a materiei**, 1979, 1056 p.

I. G. MURGULESCU, TATIANA ONCESCU, E. SEGAL, **Introducere în chimia fizică, Vol. II. 2. Cinetică chimică şi cataliză**, 1981, 1024 p.

I. G. MURGULESCU, J. PĂUN, **Introducere în chimia fizică, Vol. I. 3. Nucleul atomic, reacţii nucleare, particule elementare**, 1982, 606 p.

I. G. MURGULESCU, RODICA VÎLCU, **Introducere în chimia fizică. Vol. III. Termodinamica chimică**, 1982, 624 p.

I. G. MURGULESCU, O. M. RADOVICI, **Introducere în chimia fizică. Vol. IV. Electrochimie**, 1986, 410 p.

R. VÎLCU, M. LECA, **Polymer Thermodynamics by Gas Chromatography**, coédition avec Elsevier, 1990, 204 p.

Fl. CUIBAN, ALFA-XENIA LUPEA, **Studiul structurii şi sinteza peptidelor**, 1989, 286 p

CRISTOFOR I. SIMIONESCU, VALERIA GORDUZA, **Implicaţii bioenergetice ale coloranţilor**, 1988, 208 p.

R. VÎLCU, M. LECA, **Termodinamica polimerilor prin cromatografie de gaze**, 1987, 238 p,

I. ZUGRĂVESCU, M. PETROVANU, **Cicloadiţii 3+2 dipolare**, 1987, 446 p.

RAUL MIHAIL, ION GROZEANU, **Estimarea secvenţială aplicată sistemelor chimice**, 1986, 406 p.

M. BREZEANU, I. PATRON, M. ANDRUH, **Combinaţii complexe polinucleare şi aplicaţiile lor**, 1986, 244 p.

A. T. BALABAN et al., **Labelled Compounds and Radiopharmaceuticals Applied in Nuclear Medicine**, coédition avec John Wiley and Sons, 1986, 742 p.

D. PURDELA, **Nomenclatura chimiei organice — IUPAC**, 1986, 451 p.

PETRU BUDRUGEAC, **Probleme de chimie**, 1986, 280 p.

T. ONCESCU, S. G. IONESCU, **Conversie fotochimică şi stocare de energie**, 1985, 272 p.

V. DRĂGUŢAN, A. T. BALABAN, M. DIMONIE, **Olefin Metathesis and Ring-Opening Polymerization of Cyclo-Olefins**, coédition avec John Wiley and Sons, 1985, 544 p.

C. LITEANU, I. RÎCĂ, **Optimizarea proceselor analitice**, 1985, 360 p.

N. PERESCU, **Chimia extracţiei cu solvenţi şi aplicaţii**, 1985, 212 p.

1991 APR 0 5

ISSN 0035—3930

I.P.„UNIVERSUL" c. 2134 | 43 426 | **Lei 40**

F 1103

ACADÉMIE ROUMAINE

REVUE ROUMAINE DE CHIMIE

TOME 35

Nos 7—9

Juillet—Septembre 1990

Rev. Roumaine Chim.

RRCHAX, 35, 7—9, p. 801—938 (1990), Bucarest

EDITURA ACADEMIEI ROMÂNE

ACADÉMIE ROUMAINE

COMITÉ DE RÉDACTION

Rédacteur en chef :

I. G. MURGULESCU, membre de l'Académie Roumaine

Rédacteurs en chef adjoints :

A. T. BALABAN et V. EM. SAHINI, membres de l'Académie Roumaine

Collège de rédaction :

EM. BRATU, ECATERINA CIORĂNESCU NENITZESCU, P. SPACU, CR. SIMIONESCU, GH. SUCIU, membres de l'Académie Roumaine; M. ANDRUH, M. BANCIU, M. D. GHEORGHIU, I. HAIDUC, D. I. MARCHIDAN, G. NIAC et D. SĂNDULESCU

La Revue Roumaine de Chimie paraît 10 fois par an. Toute commande de l'étranger sera adressée à ROMPRESFILATELIA — sectorul Export-Import Presă, P. O. Box 12—201, télex 10376, prsfir 78 104 Bucarest, Calea Griviţei nr. 64—66, Bucureşti, Roumanie

Les manuscrits, les livres et les revues proposés en échange, ainsi que toute correspondance seront envoyés à la rédaction :

REVUE ROUMAINE DE CHIMIE

125, Calea Victoriei, 79717 Bucarest, Roumanie, téléphone 50 76 80

EDITURA ACADEMIEI ROMÂNE

125, Calea Victoriei, 79717 Bucarest, Roumanie, téléphone 50 76 80

REVUE ROUMAINE DE CHIMIE

Tome 35, N°s 7–9 **Juillet–Septembre 1990**

The 3rd Symposium on Colloid and Surface Chemistry 803–804

RODICA STOICA and LUCIA GOLIAT, Surfactants in film-forming industry . . 805–814

J. CHARPIN, Separation of gases by diffusion and gaseous permeation. Application of gaseous permeation to the dehydration of natural gas 815–820

SHUJI SAITO, Critical surfactant concentration in the interaction between nonionic surfactants and polyacrylic acid. Effects of hydrophobic and polyoxyethylene moieties of surfactants 821–830

A. L. IEVLEV and V. V. TEPLYAKOV, Modern methods for determining the gas permeation and predicting the properties of dispersed polymer systems 831–842

E. CHIFU, J. ZSAKÓ, MARIA TOMOAIA-COTIȘEL and I. ALBU, Interfacial tension extrema at the adsorption from polycomponent systems 843–851

H. CĂLDĂRARU, AGNETA CARAGHEORGHEOPOL, A CĂLDĂRARU, M. DIMONIE, D.DONESCU, ILEANA DRĂGUȚAN and M.MARINESCU, Magnetic interaction between nitroxide spin probes and Cu(II) compounds as a method for characterization of penetrability in reversed micelles 853–858

LIVIU ONICIU, IOAN A. SILBERG, DAN A. LÖWY, MARIA JITARU, FLORENTINA CIOMOȘ, OVIDIU HOREA OPREA, BOGDAN C. TOMA and MARIANA TOMA, Effect of surfactants on the electroreduction of acrylonitrile 859–866

JÁNOS ZSAKÓ, MARIA TOMOAIA-COTIȘEL, EMIL CHIFU, IOSIF ALBU, AURORA MOCANU and PETRE T. FRANGOPOL, Protolytic equilibria in surface solutions of stearic acid, procaine and benzoic acid at the air/water interface 867–877

EMIL CHIFU, MARIA TOMOAIA-COTIȘEL, JÁNOS ZSAKÓ, IOSIF ALBU, AURORA MOCANU, PETRE T. FRANGOPOL, Penetration of procaine hydrochloride into stearic acid monolayers from underlying aqueous solutions 879–889

D. F. ANGHEL, I. MIRCIOAGĂ, D. R. ELLIS and E. A. DUFF, Phase behaviour of hydrocarbon-water mixtures in the presence of alkylpolyoxyethylene carboxylates 891–897

GHEORGHE NECHIFOR and GEORGETA POPESCU, Asymmetric membranes prepared by immersion-precipitation technique 899–908

MARIA ZAHARESCU, CONSTANȚA PÎRLOG, A. VASILESCU, D. CRIȘAN and ANA BRĂILEANU, Inorganic membranes obtained by the sol-gel method 909–914

ȘTEFAN KISS, MIHAIL DRĂGAN-BULARDA, DANIELA PAȘCA, HENRIETTE PINTEA, EVA ZBOROVSCHI, VASILE MUNTEAN and RADU CRIȘAN, Use of zeolite as an adsorbing surface for modelling systems analogous to therapeutic mud 915–918

Rev. Roumaine Chim. **35, 7–9, 801–938 (1990), Bucarest**

C. V. ZĂNOAGĂ, C. V. UGLEA, S. MATACHE and V. AVĂDĂNEI, Characterization of ion-exchange membranes used in electrooxidative processes 919–921

C. V. ZĂNOAGĂ, C. V. UGLEA and G. NECHIFOR, Redox aspects regarding the transfer of some heavy metals through semipermeable membranes 923–925

J. VODNÁR, E. KOLOZSI and N. MUREŞAN, Hydrodynamic and mathematic characterization of the Vodnár-type apparatuses, having pelliclizing (stripping) and recycling tubes 927–933

BOOK REVIEWS 935–938

Revue Roumaine de Chimie, **35**, 7–9, 803–804 (1990)

THE 3rd SYMPOSIUM ON COLLOID AND SURFACE CHEMISTRY

The 3rd Symposium on Colloid and Surface Chemistry was held in the University of Timişoara, September 12—14, 1989. It was organized by the Centre of Physical Chemistry, the Department of Detergents of the Chemical Research Institute-Bucharest, in cooperation with the University of Timişoara-Department of Economic Science and the Detergents Entreprise Timişoara, under the auspices of the Industrial Central for Dyestuffs, Lacquers and Detergents.

The proceedings were organized in four sections : interfacial phenomena, disperse systems, technological and biological membranes and colloidal surface-active substances in technological processes ; a poster session was also offered.

The participants were research scientists, engineers, university specialists in various fields involved in studies of phenomena specific to colloid chemistry. The contributions have evidenced the achievements of Romanian science in the fields of colloid and surface as well as their impact on technological development. Thus *Dr. Rodica Stoica*, Director of the Industrial Central for Dyestuffs, Lacquers and Detergents has presented in the first plenary lecture one of the most important utilizations of tensides : the industry of film-forming materials which include lacquer, ink, dye, adhesive and corrosion-protection. The other plenary lectures were presented by foreign honour invited guests :

Dr. Jean Charpin, Head of Department of Chemical-Physics of Materials of the Atomic Energy Authority Saclay-France, presented a general exposition of inorganic membranes for micro- and ultrafiltration explaining the concept of composite inorganic barrier and considering the various types of inorganic membranes presently known together with methods of characterization and the advantages they grant.

Dr. Allan Cadenhead, Professor of University of Buffalo, New York, senior researcher affiliated with NASA programs, has examined the nature of the various physical states in instable monomolecular states at air/water interface for a wide range of amphipatic mono- and dicomponent molecules ; special attention has been granted to liquid-extended and liquid-condensed states.

Dr. Shuji Saito, Director of the Research Department of Momotani Juntenkan — Japonia (for more than 100 years active in cosmetics industry) has gained notoriety with his works on the interaction of polymers with tensides. He has lectured on the solubilization properties of solutions of non-ionic surface active compounds in presence of a polymeric acid.

Dr. Alexander L. Ievlev from the Institute of Petrochemical Syntheses "A. Topchev" in Moscow, has concluded the series of plenary lectures presenting the methods of determining the gas permeation parameters and of predicting the properties of disperse polymeric systems.

In the four sections were presented 160 contributions issued by 300 authors; they referred to very disperse phenomena pertaining to colloid and surface chemistry. The poster session has included works specialized in a great deal of phenomena and processes specific to the same field; all of them were remarkable by the high scientific level and presentation. The congress has been attended with interest by the participants; the interdisciplinary discussions have evidenced the quality of contributions and the usefulness of the exchange of experience which is a sound basis for future cooperation.

This volume of the Revue presents some of the contributions which are representative for the sections which housed them; it is intended to emphasize the program of studies under way in research and higher education institutes.

ADVISORY BOARD

Revue Roumaine de Chimie, 35, 7–9 805–814(1990)

SURFACTANTS IN FILM-FORMING INDUSTRY

RODICA STOICA[a] and LUCIA GOLIAT[b]

[a] Industrial Central for Dyestuffs, Paints and Detergents
Bd. Chimiştilor 309, 74585 Bucharest, Romania
[b] Institute of Chemical Research, Detergents Department
Splaiul Independenţei 202, 79611 Bucharest, Romania

This contribution presents one of the applications of the surface-active agents, namely the film-forming materials, which include the paints, varnishes, inks, adhesives and anticorrosive protections industry, based on synthetic materials. The major applications of the surface-active agents in this area are: polymerization techniques for the respective binders, emulsion paints recipes, water-soluble primer compositions, preparation of pigments pastes for oil and organic solvent-based paints. The main species of surface-active agents, for each of the above-mentioned fields are described, in connection with their ionic character and chemical structure.

Modern industry supplies almost every item of common use with surface coating for two main purposes: to protect it from external attack and to make it look well.

Although some dictionaries define a paint as a mixture of a pigment and a suitable liquid to form adherent coating, a highly complex technology lies behind the common paint.

A paint consists of three main components: the binder, the pigment, the solvent and additives, but there are innumerable raw materials involved in the synthesis of these components.

The raw materials and intermediates used in the manufacturing of coating systems originate in nature (vegetable oils), in the petrochemical industry (phenolic resins, urea resins, melamine resins, polyurethane epoxy resins, acrylic polymers and inorganic and organic industry (pigments)). Modern paints contain additives of various kinds, such as: driers, wetting agents, emulsifiers, stabilizers, antiskinning, anticorrosive agents, thixotropic agents. If used correctly, the additives give valuable improvements in the coating systems and lower the production and processing cost.

Although there are numerous alternatives in formulating coatings, many additives are based on surfactants.

The wide variety of surfactants – anionic, nonionic, cationic, amphoter – as well as products based on surfactants have challanged the research to meet demands of new materials of higher quality and performance.

In Romania the surfactant industry produces chemicals with specific properties employed in many industries: fiber, textile, leather, paper coatings, petroleum, cosmetics, etc. As to surface coating Romania produces large amounts of synthetic resins, paints, varnishes and lacquers.

Table 1

Varnishes, paints, lacquers — world production between 1978 — 1989[1,4]

Production	1978	1989	1978	1989
	thousand tones		%	
World production	18397	20.700	100	100
G. Britain	838	816	4.6	3.9
France	804,9	826	4.4	4.0
West Germany	1290.3	1326,8	7.0	6.2
Italy	700	635	3.8	3.1
Netherland	214.7	212.3	1.2	1.0
Spain	303.4	285	1.6	1.4
Switzerland	72.6	112	0.4	0.5
Sweden	207.2	188.8	1.1	0.9
Japan	1500	1900	8.2	9.2
U.S.A	4682	5050	25.5	24.4
Bulgaria	89.5	129.2	0.5	0.6
Czechoslovakia	228.6	270.5	1.2	1.3
Democratic Republic of Germany	382.2	399	2.1	1.9
Yugoslavia	113.8	310	0.6	1.5
Poland	412.3	415.4	2.2	2.0
Romania	170	180	0.9	0.8
Hungary	126.6	120.1	0.7	0.6
Soviet Union	3098.8	3348	16.8	16.2
Other countries	1760	2200	9.5	10.5

Table 2

The raw materials and intermediates used in surface coating industry (Paints, Varnishes, Lacquers) in U.S.A.

Products	1983		1992	
	thousand tones	%	thousand tones	%
Total production	3979	100	3510	100
Synthetic Resins	998	25	1135	32
— Alkyd and polyesters	304	7.7	272	7.7
— Acrylic	207	5.2	272	7.7
— Vinyl	183	4.6	272	6.5
— Epoxy	65	1.6	91	2.6
— Polyurethan	56	1.4	91	2.6
— Other types	183	4.6	182	5.2
Pigments/Extenders	1180	30	1261	36
— Titanium dioxide	365	9	386	11
— Other pigments	198	5	216	6
Extenders	617	15	659	19
Solvents	1720	43	1022	29
— Hydrocarbons	920	23	450	13
— Esters, Alcohol, Ketones	777	20	545	15
— Other solvents	23	0.6	23	0.7
Additives	81	0.5	95	0.7
— Surfactants	20	0.5	27	0.7
— Thicking agents	25	0.6	31	0.9
— Plasticizer	17	0.4	10	0.4
— Siccatives	19	0.5	23	0.7

Today the advanced industry of coating products whose worlds production exceeds 30 bil. tones/year is remodelled taking account of ecological requirements. Thus, the coating systems have to be transformed from the conventional solvent-based products into other coating systems with high content of solids, powders and water-based coatings.

Table 2 lists the new raw materials and intermediates to be utilized in the future in the industry of coating products. The new type of coatings will save solvents and energy at lower cost.

Table 3 shows the same trends in Romania.

Table 3

The raw materials and intermediates used in surface coating industry (Paints, Varnishes, Lacquers) in Romania

Products	1983		1992	
	thousand tons	%	thousand tons	%
Total production	174.2	100	180	100
Synthetic resins	42,5	24,2	54	30
— Alkyd and polyesters	12.25	7.0	12.6	7
— Acrylic resins	17.5	10	23.4	13
— Vinylic resins	3.5	2	3.6	2
— Epoxy resins	1.7	1.0	4.8	2.7
— Polyurethan	2.1	1.2	3.9	2.2
— Other types	5.25	3	5.7	3.1
Pigments	49	28	54	30
— Titanium dioxide	21	12	25.2	14
— Other pigments	28	16	28.2	16
Extenders	28	16	34.2	19
Solvents	54.9	31.4	36	20
Additives	0.7	0.4	1.8	1

The properties of varnishes and lacquers are of considerable importance in all the industries which apply surface coatings. During the past years the technique of painting has been enriched by many new materials and a new method of application (cathodic, anodic protection, anaphoretic cathaphoretic deposition, electrostatic field).

ACRYLIC EMULSIONS

The development of acrylic polymer emulsions and their usage as base coatings require surfactants as emulsifiers.

The increasing acceptance of these products is due to their versatility and their properties : stability, durability and pigment binding characteristics.

In the coating systems are used copolymers of : ethyl acrylate-methyl methacrylate-hydroxyethyl methacrylate and acrylic acid.

In our country acrylic polymer and copolymer emulsions have already gained a commercial status being utilized in interior and exterior home and industrial coatings.

The acrylic emulsion products have been diversified by the development of thermosetting compositions, based on copolymers containing functionally substituted monomers, characterized by insolubility and high durability.

Thermosetting compositions can be obtained by self-curing reactions or by reactions with functional groups of other polymers or added substances.

The development of polymer emulsions in coating systems was correlated with the synthesis of new surfactants as emulsifier, antisetting and antifloating agents.

The emulsion polymerization process is complex because it involves seldom less than four ingredients (monomer, water, emulsifier, initiators) and various reaction conditions.

The role of emulsifier is complex and changes during the advancement of the reaction : — acceleration of polymerization,
— stabilization of emulsion product.

In the oil-in-water emulsions, which is the case of emulsion polymerization of acrylic and methacrylic monomers, the external phase is water containing salts, buffers and initiators saturated with emulsifier. The internal oil phase consists of micelles of the emulsifier and monomer droplets at the start of polymerization reaction ; in the final, the product consists of polymer particles on whose surface the emulsifier is adsorbed.The addition of a suitable surfactant in amounts above the critical micellar concentration, entails the formation of micelles-hydrated aggregates and, as a result, of a stable system.

The micelle comprises 50—100 surfactant molecules and can imbibe water and monomers.

The whole system is stabilised at the interface between water and micelles by an electrical double layer or by an associated atmosphere of water molecules.

When a monomer is present, the micelles are swelled by imbibing monomer, thus increasing the solubility of the latter. The extent of solubilization depends on monomer and emulsifier ; the polymer particle is dependent on the concentration and type of emulsifier.

The increase of polymerization due to the suitable emulsifier is caused by the development of polymerization in the micelles. Growth of the polymer chains within the micelles is very fast and is promoted by rapid diffusion of the monomer from the droplets into the growing micelles.

The polymerization without emulsifier takes place at a lower rate if mecanical homogenization or a monomer excess is ensured.

The emulsifier also plays the role of stabilizer for the end product, contributed to a good stability during storage at low temperature.

The emulsifier increases the resistance to mechanical shock during mill processing of the coating system.

The most suitable emulsifiers in polymerization are hydrophilic surfactants either anionic or nonionic. The cationic are not used because in many instances they exert adverse reactions against the initiators.

Despite their importance in the process of polymerization and for the final product, the surfactants are a source of weakness in the emulsion product. The hydrophilic nature of many emulsifiers provides a degree of water sensitivity in polymer films. The storage of many emulsions is also influenced by the type and amount of emulsifier. These adverse effects must be considered in selecting the emulsifier system.

The selection of a surfactant system requires a thorough investigation because establishing a relationship for the optimum chemical structure of emulsifiers is difficult.

The amount of surfactant used in polymerization is very important. The particle size of polymer emulsions is inversely proportional to the concentration of emulsifier. To obtain low particle size, rapid rate of reaction and good stability, 4–8% of emulsifier (based on monomer) is used. About 1–4% anionic surfactant or 2–6% nonionic surfactant are normally used to provide stable emulsion of fine particle size.

Table 4

Emulsifiers for acrylic emulsions [3]

Chemical structure	active matter	surface tension	c_K	foaming
	%	dyne/cm at 0.01 %	mol. /l	mm at 0′/5′
Nonionic surfactants				
— Alkylphenol polyethoxylated $n = 30 \ldots 40$	90–100	38...48	0.01...0.1	160/120... 130/120
— Fatty amides polyethoxylated $n = 15–20$	90	40	0.38	120/115
Anionic surfactants				
— Alkylphenolether sulfates	25–30	31	0.023	160/130
— Alkylphenolether sulfonates	20–25	31	0.1	160/140
— Alkylphosphates	80	28/(0,1%)	—	145/120
— Alkylesters sulfosuccinic salts	50–60	27 ,,	0.1	195/140

Table 4 lists some of surfactants utilized in polymerization of acrylic and methacrylic monomers.

ANIONIC SURFACTANTS

Examination of Table 4 shows that the most frequently employed anionic surfactants are: alkylaryl sulfonates, alkylphenoethoxysulfates, alkylphosphates and sulfosuccinates.

The viscosity and storage stability of finished emulsions stabilized by anionic surfactants may vary in time. This variation is related to the charge distribution of anionic surfactants to their sensitivity to electrolytes.

Mixture of anionic surfactants of different structures is recommended to improve storage stability.

NONIONIC SURFACTANTS

The nonionic surfactants are rarely utilized as emulsifiers for polymerization because they form micelles to a lesser extent than anionic surfactants. Their hydrophilic group is associated with water molecules around the aggregates resemble micelles and in this way, they act in stabilizing and isolating the polymerization sites and subsequent polymer particles, thus providing low particle diameters. The hydrated atmosphere around finished polymer particles contributes to the stability of the emulsion.

The most frequently employed nonionic surfactants for emulsion polymerization are the alkylphenol polyethoxylated ones containing 30–40 ethylenoxide groups per molecule and having HLB value between 15–18.

Nonionic surfactants stabilize the emulsions against electrolytes and freezing, owing to their structure and their mechanism of solubilization (by hydrogen bond or formation of a coordinative combination of polyoxonium hydroxides type).

Mixed anionic-nonionic systems are frequently used for the emulsion polymerization to obtain synergistic effects.

SURFACTANTS IN PIGMENT PROCESSING DISPERSING AND WETTING AGENTS

In coating systems, the pigments are of a great importance. Quality pigments, aside from their decorative effect are responsible for the durability of the film and protection.

The pigment dispersability and dispersion stability depend on the type of pigment, particle size, surface properties, wettability, oil absorption, agglomeration, flocculation, aggregation and vary from vehicle (binder) to vehicle. Most of these properties derive from the interaction of pigment-vehicle (binder).

The performance of a pigment in a coating system is influenced by the degree of dispersion and colour, gloss, strength and viscosity.

Practically, all coatings contain at least one surfactant. It may be added or is present in the pigment or in the binder.

If the surfactant acts specifically at a liquid/solid interface it is often called a wetting agent and when it assists the dispersion of a pigment is called dispersing agent. The same surfactant may serve both purposes.

In pigments processing, the surfactants are of great importance.

The action of the surfactants may be assigned to the adsorption of the polar groups on the polar surface of the pigment, leaving the nonpolar part of the surfactant, molecule available to associate with the binder. Thus, the affinity of the pigment for the binder is enhanced and wetting is improved.

The surfactants employed in pigment processing may act as follows :

— to facilitate wetting and dispersion of the pigment in the binder,

— to prevent settling of pigments (anti-settling agents),

— to alter the rheological properties of the coating system,

— to prevent colour changes due to flotation or flooding (in mixed pigments of different colours),
— to improve oil adsorption,
— to allow a higher pigment content in the mill base,
— to facilitate the mill process saving energy and thus lowering the cost,
— the hydrophobic film on the pigment surface reduces its hydrolysis in water-based coatings.

Although the action of the surfactants is specific, they are often used in mixture to obtain synergistic effect.

The electrical phenomena occurring at interface during the processing of pigments with surfactants play an important role in the understanding of flocculation and dispersion.

The dispersing agents act as protective colloids when they adsorb on the pigment particle and stabilize the dispersion by the repulsive effect of the electrical double layer. Owing to this action, it is very important to use an optimum amount of surfactants; the excess may produce flocculation.

There are three ways of obtaining suitable pigments for a given application: — drying and grinding the pigment after synthesis — to obtain powdery pigments.

— flushing, which is a process of stirring with oil (resin) a paste consisting of pigment dispersed in water, in order to remove the water (by decantation or evaporation) and form a paste of pigment dipersed in oil (resin). Presence of surfactants in the flushing process lowers the pigment/oil interface tension,

— lyophilization to obtain endophilic behavior in relation to a non-polar organic phase.

The surface treatment modifies the adhesion work and oil increasing the wettability of the pigment.

Anionic and cationic surfactants in flushing are used depending on the chemical structure of the pigment. The surfactants have to be soluble or dispersable in water and to be active in non-polar medium.

Lyophilization (changing the hydrophilic character of pigment in a lyophilic medium) is achieved by: — adding surfactants during precipitation of the pigment in aqueous solutions, — adding surfactants to solvents during milling.

The surfactants cover the surface of the pigment particles with a monomolecular layer (of 30...1000 $\times 10^{-6}$mm) whose polar groups are oriented towards the inner part of the particles and whose hydrocarbonate radicals towards the outer part, turning the hydrophilic character into lyophilic.

The surfactants used are specific to each pigment and belong to all groups: anionic, cationic and ampholytic surfactants.

Titanium dioxide is by far the most important white pigment used in coatings and it is produced in a great variety of types for different purposes.

To improve the compatibility of the pigments with the binder new surfactants were synthesized. These surfactants contain many carboxyl, oxydril or epoxy groups in their molecule, so that their chemical structure is more adequate to the binder. Owing to this structure, the pigment is

Table 5

Surfactants used in pigment processing [2]

Type of surfactant	Pigment	Effect
Anionic		
— Carboxylic acids	Titanium dioxide	Dispersion
— Soaps	Lead chromate	Anti-dust
	Zinc oxide	
— Polycarboxilic acids	Lead chromate	Dispersion
— Carboxymethyl cellulose	Iron oxides (red, yellow)	Wetting
— Maleates	Iron blues	Storage
— Alkylether sulfates	Zinc tetraoxychromate	stability
Nonionic		
(Polyethoxylated products):	Chromium oxides	Dispersion
— Fatty alcohol	Titanium dioxide	Storage
— Alkylphenol	Carbon black	stability
— Fatty amines	Barytes	
(Esters):		
— Sorbitol	Molybden red	Wetting
— Phthalic (dialkyl)	Phthalocyanines	Dispersion
— Ester-amides	Barium chromates	
(Hydrophilic polymers):		
— Polyacrylamide	Organic pigments	Providing
— Polyvinylalcohol	Lead chromates	transparency
Cationic — ampholites		
— Diamine(oleil-amino	Titanium dioxide	Dispersion
propylen amine)	Zinc chromate	Anti-settling
— Amino-polyalcohols	Iron oxide	
(polyvinylpyrolidone)	Titanium dioxide	
— Amino — imide	Lead silico-chromate	
— Lacithine	Zinc oxide	Stabilizing the colour
— Quaternary amonium	Molibdate lead chromate	
compounds	Organic pigments	Anti-dust
	Iron blue	
	Titanium dioxide	

compatible with the binder and milling process requires a shorter time. The final properties of the film are improved.

The additives that improve the coating systems are intended to:
— prevent skinning,
— improve flow and gloss especially in water-base coating,
— improve levelling,
— prevent pigment flooding and floating,
— clear varnish when a cloudiness is produced,
— ensure corrosions resistance especially on damp surfaces for example in underwater coatings,
— prevent the formation of a foam or to reduce foam persistence (antifoaming agent).

The amount recommended on the total formulation weight is 0.1—— 1.2%. The excess of additives used to prevent settling causes pigment flocculation which is seen by separation of the vehicle to the top of the coating.

The specific additives which prevent the pigments from flooding and floating are based on an acid salt of long chain amines with polycarboxylic acids. Frequently they are used combined with silicone resin.

Levelling agents are esters and ketones with high boiling point.

Anticloudiness agents are poly-amino-amides neutralised with phosphoric acid in a mixture of solvents.

Corrosion inhibitors are long chain diamines.

As anti-foaming agents are used the metallic soaps mixed with alcohols, mineral oil or silicon derivatives.

Additives with anti-foaming effect are used especially in water-based coatings. In solvent-based coating systems non-foaming products are used. If it is necessary, as anti-foaming agents siliconis products are used.

In water-based coating anti-foaming agents are used based on mineral oil mixed with alcohols, metallic soaps and emulsifiers to be compatible with the system.

Because the anti-foaming effect occurs at the surface of the coating film, the compatibility of the anti-foaming agent with the coating sys-

Table 6

Surfactants produced in Romania, utilized in surface coatings

Type of surfactants	Chemical structure
Anionics :	
— Soaps	$R-COO^{-}Me$ (Me = cation)
— Alkylarylsulfonates	$R-C_6H_4-SO_3Me$
— Alkylsulfates	$R(R^2)CH_2OSO_3Me$ ($R(R') = C_{12}-C_{14}$ $C_{16}-C_{18}$
— Alkylarylethoxy sulfates	$R(C_6H_4)-(O-CH_2-CH_2)_nOSO_3Me$ $n=6\ldots20$
— Alkylphosphates	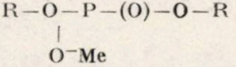 $R-O-\underset{O^{-}Me}{\underset{\vert}{P}}-(O)-O-R$ R = alkyl, aryl, alkylethoxy
— Mono(di) esters sulfosuccinate	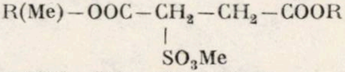 $R(Me)-OOC-CH_2-\underset{SO_3Me}{\underset{\vert}{CH_2}}-COOR$
— Maleates	$ROOC-CH=CH-COOR$
— Polycarboxylic acids	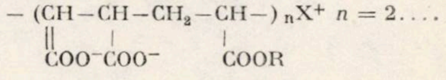 $-(\underset{COO^{-}}{\underset{\Vert}{CH}}-\underset{COO^{-}}{\underset{\vert}{CH}}-CH_2-\underset{COOR}{\underset{\vert}{CH}}-)_nX^{+}$ $n=2\ldots.$
Nonionics :	
— Polyethoxylated alkylphenol	$R-C_6H_4-O-(CH_2-CH_2-O)_nH$ $n=6\ldots40$
— Polyethoxylated fatty alcohols	$R-O-(CH_2-CH_2-O)_nH$ $n=3\ldots..$
— Polyethoxylated fatty acids	$R-COO-(CH_2-CH_2)O)_nH$ $n=3\ldots10$
— Polyethoxylated fatty amines	$R-NH-(CH_2-CH_2-O)_nH$ $n=3\ldots10$
— Polyethoxylated fatty amides	$R-CO-NH(CH_2-CH_2-O)_nH$ $n=3\ldots..$
Cationics :	
— Secondary (tertiary) amines	$R\ R'(R'')N(H)$
— Amido-amines	$R-CO-NH-(CH_2)_n-NH-(CH_2)-NH\ \ldots$
— Quaternary ammonium compounds	$R_1R_2R_2R_4)^{+}X^{-}$ X = anion

tem had to be limited. Ethylenoxide-propylenoxide nonionic surfactants or polypropylenglycols as emulsifiers in this case are used.

Bactericides and fungicides are used especially in coatings for food industry. The bactericides most often utilized are no surfactants.

The bactericides and fungicides belonging to surfactants are long-chain cationic agents and alkyl amino-acids as : alkyldimethyl ammonium chloride, dialkyl-dimethyl ammonium chloride, *o*-methylen dimethylbenzyl ammonium chloride.

Table 6 shows some of the surfactants produced in our country and used in coating systems.

The information presented is intended to show the present situation in Romania in the field of surfactants applied in coating systems.

Concerning trends in surface coating industry, the consumption of surfactants is expected to grow ; new products have to be synthesized ; a constant activity of technology improvement is necessary.

REFERENCES

[1] *Chemical Week*, 31 (1984). *Informations Chimie*, 270 (1986) ; *A W — Aussenwirtschaft* 40 (1984).

[2] *G. Wormald Pigment Colours for Paint, Paint Varn. Prod.*, 49(4), 33—44 March 1957 ; 49(5) 53—56 April 1957 ; 49(6), 43—48 May 1957.

[3] Farbe & Lack, 3(1985) ; 3, 7, 10 (1986) ; 1 (1987).

[4] European Chemical News Apr. (1987).

Revue Roumaine de Chimie, 35, 7–9, 815–820 (1990)

SEPARATION OF GASES BY DIFFUSION AND GASEOUS PERMEATION

APPLICATION OF GASEOUS PERMEATION TO THE DEHYDRATION OF NATURAL GAS

J. CHARPIN

Scientific Advisor

Institut de recherche et de développement
industriel, Centre d'Études Nucléaires de Saclay,
91191 Gif-sur-Yvette, CEDEX, France

The mechanisms of the transfer processes in the two principal gas or vapour separation techniques using membranes — gaseous diffusion and gaseous permeation — are compared. The possible applications of these techniques are discussed. An original application of the separation of gases by gaseous permeation is presented ; the dehydration of natural gas. The advantages of this method over the conventional glycol drying process are discussed. The method of approach for bringing a membrane process into operation is presented and details are given of the development of a permeation membrane suitable for the purification of gas from subterranean deposits.

GENERAL CONSIDERATIONS FOR THE SEPARATION OF GASES BY GASEOUS DIFFUSION AND SEPARATION

Elements common to gaseous diffusion and gaseous permeation

These two membrane techniques both use a pressure gradient across the membrane as the driving force. The flow is tangential : the feed gas is split into two flows of different composition, one which permeates the membrane and one which is retained upstream. There is never complete purification : this is an inherent feature of every membrane process : only an enrichment of the mixture in a given component is obtained.

The requirements for separative membranes concern, essentially :

— selectivity and permeability, which must be as high as possible : to obtain a high permeability the concept of a composite or asymmetric membrane has been developed, a thin separative layer is supported by a microporous substrate ;

— chemical and mechanical properties compatible with the process conditions ;

— costs competitive with other processes.

Gaseous diffusion

The best known application of the gaseous diffusion process is, of course, uranium isotope enrichment. The membrane is microporous and permeable with a composite structure and it may be organic or inorganic. The selectivity, which expresses the preferential flow of one component, obeys Graham's law. For a mixture of gases with masses M_1 and M_2, respectively, the selectivity, α, is given by :

$$\alpha = k \sqrt{M_1/M_2} = V_1/V_2 \qquad (1)$$

To have a value of k close to unity the pore radius, R, of the membrane must be smaller than the mean free path of the molecules. Usually, R has to have values of tens or hundreds of Angstroms.

Values for the gaseous diffusion of uranium isotopes and gas mixtures containing H_2 are compared in Table 1. It can be seen that the selectivities and the number of stages required are very different.

Table 1

A comparison of separation factors, number of stages and energy requirements in the gaseous diffusion of *U* isotopes and H_2 gas mixtures

	U Isotopes	H_2 Gas Mixture
α_{theor}	1.0043	2 to 5
$\alpha_{exp.}$	$\sim$1.002	1.3 to 2.5
No. of stages	1400	3 to 30 depending on mixture and deg. of purif.
Energy supply per kg feed	$\sim$2000 kWh	a few kwh

A few examples of the application of gaseous diffusion to the separation of gas mixtures can be considered :

Values of $\alpha > 3 - 4$ are required to obtain a competitive separation process : this is only possible with H_2 or He as a constituent, as in the following mixtures :

$$H_2/CO,\ H_2/N_2,\ \ H_2/CO - CO_2,$$
$$H_2/CH_4 - C_2H_6,\ \ He/NH_3,$$
$$He/\text{Natural gas or air.}$$

Some other separations are also possible for very special cases but are difficult (for example, at high temperatures) :

$$CO_2/CH_4,\ H_2S/CO_2,\ O_2/N_2$$

Gaseous permeation

In direct contrast to gaseous diffusion the membrane must be dense, without porosity and is exclusively organic. The selectivity is based on the differences in gas or vapour permeabilities through the polymers. The permeability depends both on the polymer and the gas. For a given polymer, the value of the permeability increases from ethane to water vapour.

The transfer process consists of three successive steps : gas dissolution at the high pressure interface of the membrane; gas diffusion through the polymer volume; gas desorption at the low pressure interface of the membrane.

The *permeability* coefficient, $P_i = D_i \times S_i$ (D_i = diffusion coefficient, S = solubility coefficient), depends on : chemical and physical properties of the gases and the polymers; temperature; pressure and gas concentrations.

The *selectivity* for a binary mixture is, then, given by:

$$\alpha = P_1/P_2 \tag{2}$$

The requirements for a gaseous permeation process are the following:

- to have a high feed flux;
- to limit the separation unit to a single stage;
- to operate at a very high pressure gradient (P up to 100 bars);
- to ensure stable operation (selectivity, flow rate);
- to have a modular and evolving system leading to large scale units.

Most of these requirements depend exclusively on the membrane properties. The critical properties of membranes used in gaseous permeation processes are governed by the following:

- the polymer must have a high intrinsic permeability;
- the selective layer must be very thin — 0.05 to 1 µm (the first H_2 separation units developed and put on the market by Monsanto use the thinnest membranes);
- the selectivity must be as high as possible — so as to have a single stage;
- for the membrane geometry, hollow fibres are currently used to ensure a high surface to volume ratio.

Principal fields of application for gaseous permeation

The principal fields of applications for gaseous permeation are in the following areas of separation:

— *separation of hydrocarbon gases* such as: deacidification H_2S — CO_2, dehydration, CO_2 separation (petroleum recuperation), CH_4 enrichment in biogases;

— *separation of air components*: O_2 enrichment of air (oxidations, fermentations, better combustion a.s.o.), N_2 production for inert atmospheres (agrifoods, industrial uses a.s.o.);

— H_2 *recuperation*: from NH_3 synthesis, from petroleum refinery units, from coal gasification;

— *others*: control of H_2/CO ratio in CH_4 synthesis, He recuperation from natural gas, Co_2 control in closed atmospheres, elimination of radioactive krypton and xenon from nuclear reactors.

The present market for permeation membranes and systems is essentially supplied by U.S.A. companies and, more recently, by Japanese firms (see Table 2).

DEVELOPMENT OF GAS PERMEATION MEMBRANES FOR THE DEHYDRATION OF NATURAL GAS

This research was sponsored by the European Economic Community, in the framework of a program involving the following firms or research centers:

Table 2

Present manufactures and applications of permeation membranes Essentially supplied by U.S. companies and, more recently, Japanese firms

COMPANY	COUNTRY	SYSTEM	MEMBRANE	APPLICATIONS
MONSANTO	USA	prism	polyxphenylene oxide,	CO_2/CH_4
		hollow fibers	polysulfone /silicone	Hydrogen
SEPAREX	USA	spiral modules	cellulose acetate	Hydrogen Biogas
DOW CHEMICAL	USA	hollow fibers	cellulose acetate polymethylpentene	CO separat. in petrol. recuperat. (CYNARA)
UOP	USA	spiral modules	polysulfone /silicone	Oxygen
GRACE ENVIROGENICS	USA	spiral modules	cellulose acetate	Deacidific. of hydrocarbon gases
BEND	USA			Air dehydration
AG TECHNOL.	USA	hollow fibers	polysulfone	Oxygen enrichment
DUPONT	USA	hollow fibers	polyamide polyimide	Deacidific. of hydrocarbon gase
UBE	Japan	hollow fibres	polyimide	Hydrogen

TOTAL/CFP, INSTITUT FRANÇAIS DU PETROLE, INSTITUT NATIONAL DE LA RECHERCHE APPLIQUEE, GAS UNIE, BRITISH GAS, COMMISSARIAT A L'ENERGIE ATOMIQUE.

The objective of this research is to study and develop membranes essentially, for the dehydration of raw natural gas in order to decrease the costs of operating gas fields not easily accessible such as those located offshore. This minimal dehydration reduces corrosion and the formation of hydrates in piping.

The usual method, drying with glycol, has several disadvantages, particularly in offshore operations. By comparison a membrane process looks very attractive :

— it is passive (pressure is the driving force),
— weight and dimensions are reduced,
— possibility of automation,
— modular system.

In spite of these potential advantages membrane processes are still not being used due to the lack of commercial membranes suitable for natural gas dehydration. Those available possess neither the required stability nor the ranges of permeability and selectivity.

Requirements for a membrane process for natural gas hydration

The process scheme has to be simple to avoid heavy and expensive equipment, such as compressors, heat exchangers and condensers. One stage permeation is imperative with a minimum of gas pretreatment. The membrane, of course, must have a good stability.

The permeabilities of the membrane to methane and water vapour must be adjusted to give a good compromise between the membrane area used, the weight and cost of the unit and the amount of gas lost.

The results of calculations carried out for a natural gas dehydration unit equipped with membranes of different characteristics are shown in Figure 1. The water content of the gas has to be reduced from about 600 ppm vol. (saturation at 70 bar, 30° C) to 145 ppm vol. A sweeping gas is used on the low pressure side of the membrane ($BP = 1.5$ bar) with a flow rate of 5 % of that of the feed gas. Obviously, a lower sweeping gas flow rate can be used. From these results it appears that membranes showing a high H_2O/CH_4 separation factor and a low methane permeability ($<10^{-6}$ cm^3 (STP)/cm$^2 \cdot$ s $\cdot$ cmHg) lead to low methane loss but to a very large membrane area. Conversely, a low H_2O/CH_4 separation factor (< 200) and a high methane permeability ($<10^{-4}$ cm^3 (STP)/cm$^2 \cdot$ s $\cdot$ cmHg) result in a small membrane area but high methane loss. From this first approach the following characteristics were defined for the membrane to be developed in the project :

CO_2/CH_4 separation factor > 50;
H_2S/CH_4 separation factor > 50;
H_2O/CH_4 separation factor > 200;
CH_4 permeability between 10^{-4} and 10^{-6} cm^3 (STP)/cm^2 (STP)/cm^2. s $\cdot$ cmHg;
good stability in presence of natural gas containing CO_2;
H_2S, water vapour and hydrocarbon vapours;
broad operating temperature range (20 to 80°C);
mechanical properties allowing a pressure difference of up to 100 bars;

Subsequently, taking the membrane manufacturing constraints encountered into account, *two target membranes* were defined more precisely :

— *membrane* M_1 ($GCH_4 = 5 \cdot 10^{-6}$ cm^3 (STP)/cm$^2 \cdot$ S $\cdot$ cmHg, α $H_2O/CH_4 = 300$, which can be used without a sweeping gas on the low pressure side

— *membrane* M_2 ($GCH_4 = 5 \cdot 10^{-6}$ cm^3 (STP)/cm$^2 \cdot$ s $\cdot$ cmHg, α $H_2O/CH_4 = 500$) for which the use of a sweeping gas on the low pressure side is generally necessary to obtain reasonable membrane areas.

With respect to the membrane facture, the methodology is the following :

— the first step is the selection of the polymer in the form of a dense film ;

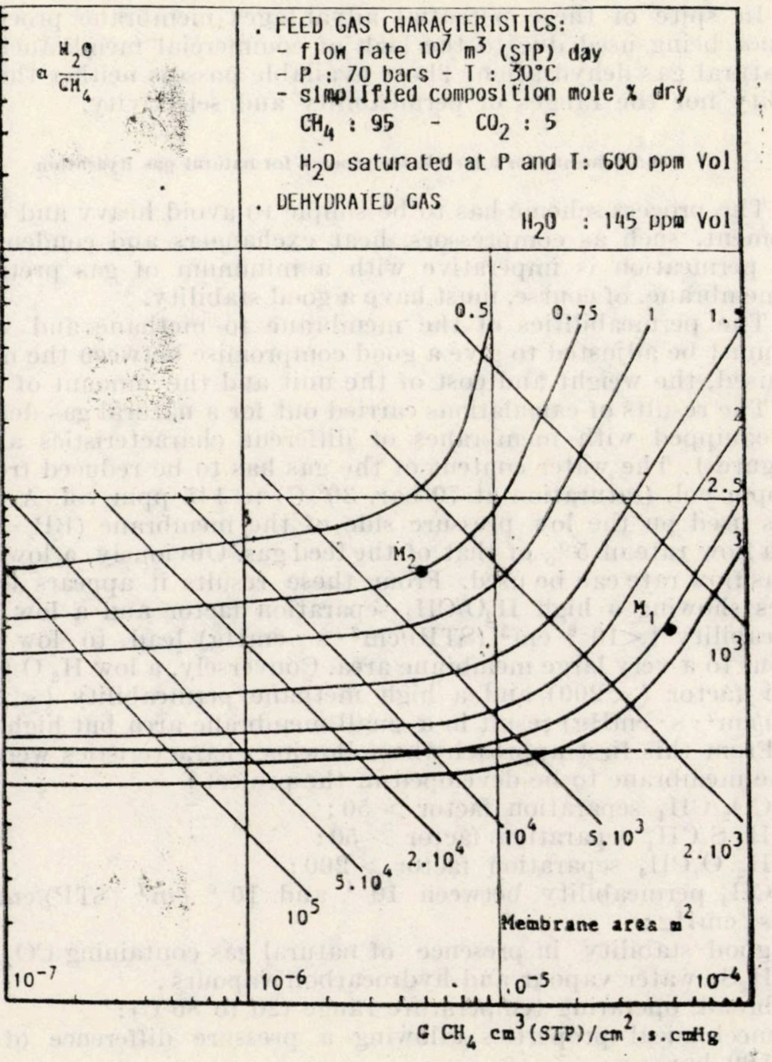

Fig. 1. — Characteristics of membranes. (Fournié F. and Agostini, J.P. (1984). A New Competitive Process for Offshore Gas Dehydration, 16th Annual Offshore Technology Conference, Houston, May 7–9,1984).

— the second, the development and fabrication of flat asymmetric membranes;

—finally, the manufacture of hollow fibers.

The polymer selected belongs to the family of polyamides, which possess adequate properties. Recently, hollow fibres close to the M_2 type have been produced. Their stability is good in the presence of simulated natural gas. At the end of 1989, a pilot plant with hollow fibers, with properties close to those of M_2, was tested at British Gas.

Revue Roumaine de Chimie, 35, 7–9, 821–830 (1990)

CRITICAL SURFACTANT CONCENTRATION IN THE INTERACTION BETWEEN NONIONIC SURFACTANTS AND POLYACRYLIC ACID. EFFECTS OF HYDROPHOBIC AND POLYOXYETHYLENE MOIETIES OF SURFACTANTS[1]

SHUJI SAITO
Momotani Juntenkan Ltd., Minatoku, Osaka 552, Japan

In the interaction between polyoxyethylene-type nonionic surfactants and polyacrylic acid (PAA), the binding or complex formation occurred abruptly at a certain surfactant concentration T_1 which was lower than the critical micelle concentration (CMC). In two series of surfactants, polyoxyethylene laurylethers and polyoxyethylene myristylethers T_1 was independent of the polyoxyethylene chain length and temperature but dependent on the hydrophobic moiety. The complexes are stabilized by a number of hydrogen bonds between polyoxyethylene parts of the surfactants and PAA and by cooperative hydrophobic interaction. The compositions of some complexes were estimated.

INTRODUCTION

In the interaction between anionic surfactants and some nonionic polymers in aqueous solution, the surfactant began to bind to the polymer abruptly in a cooperative manner at its certain concentration below the CMC. A similar trend has been observed in the binding of ionic surfactants to polyelectrolytes, polypeptides and proteins. [2–4] This critical concentration is denoted T_1, as proposed by Jones, because it is a transition point of the bound states of the surfactant on the polymer chain. [5]

Such a feature was common also to the interaction between nonionic surfactants of the polyoxyethylene type and polymeric carboxylic acids, in which, besides the hydrophobic attraction, hydrogen bonding between ether oxygens and carboxyl groups plays an indispensable role. [6,7,8] This critical surfactant concentration also was different from the CMC and denoted T_1, since the surfactant molecules above T_1 were supposed to associate like micelles locally on the polymer chain segments.

T_1 has been observed as a singular point in the dye solubilization or the viscosity relation of the surfactant-polyacrylic acid (PAA) mixtures as a function of surfactant concentration in the dilute region. [6,7,8] In the mixtures a water-soluble complex of both components was formed above the T_1, and at a low pH the complex became insoluble. At the low pH, there was a precipitation limit surfactant concentration (PLC) below which no surfactant was precipitated as complex with PAA. [8,9]. In some relevant conditions, T_1 was identified with the PLC at the low pH, and both T_1 and PLC were temperature-independent. [8]

In this report, T_1s of surfactants of the same hydrophobic moieties but with different polyoxyethylene chains in presence of PAA were stuied. Further data identifying T_1 with PLC at low pH were provided.

EXPERIMENTAL

Materials

Polyacrylic acid (PAA) with a molecular weight 1.5×10^5 was supplied from Wako Pure Chemical Ind., Osaka, as a 30% aqueous solution.[9] Polyoxyethylene (10 and 20 EO) octylphenyl ethers, $(EO)_{10}OP$ and $(EO)_{20}OP$, respectively, were the same as used before,[8] and polyoxyethylene (10 and 20 EO) nonylphenyl ethers, $(EO)_{10}NP$ and $(EO)_{20}NP$, respectively, were products of Tokyo Kasei Co., Tokyo. Polyoxyethylene (5, 10 & 15 EO) laurylethers, $(EO)_5C_{12}$, $(EO)_{10}C_{12}$, and $(EO)_{15}C_{12}$, respectively : polyoxyethylene (10&20EO) myristylethers, $(EO)_{10}C_{14}$ and $(EO)_{20}C_{14}$, respectively, were the products BL—NR and BM—NR series) of Nikko Chemicals Ind., Tokyo, and had a narrow distribution of the EO number without free PEO and a purity of alkyl groups above 96%. pHs of 1 mM solutions of these surfactants were about 5. Yellow OB, an oil-soluble dye, was the same as used before.[6]

Methods

1) The concentration of the alkylphenyl surfactants was determined by absorption at 275 nm with the relation of optical density $\times$ 0.753 mM with a Shimadzu Spectrophotometer UV—160 using a 1 cm cell.[8,11] Stock solution of a polyoxyethylene alkylether was prepared by dissolving a weighed amount of the dried surfactant.

2) The CMC of the surfactants and T_1 with PAA were determined by the Yellow OB solubilization method.[4] As supersaturated solubilized complex systems attained the equilibrium state very slowly, solubilization experiments were carried out at a regulated temperature. Aliquots were taken after being centrifuged for a short time. The amounts of solubilization thus determined were reproducible and consistent. PAA concentration around 10—30 mM, or pH around 3.4, gave a constant T_1 independent of PAA concentration.[6,8]

3) Precipitation of the alkylphenyl surfactants with PAA was determined as before.[8] pH 2 was appropriate precipitation of the surfactant-PAA complex.[8,9]

4) Reduced viscosity of surfactant-PAA mixtures was measured with an Ostwald viscometer.

5) Concentration of PAA was expressed in terms of its unit mole.

RESULTS AND DISCUSSION

1. CMC and T_1

Figures 1 — 6 illustrate the Yellow OB solubilization in solutions of various surfactants plotted against surfactant concentration in the absence and presence of 13.5 mM PAA at various temperatures. The solubilization increased linearly in the dilute surfactant region, and the cross-points in the absence and presence of PAA with the abscissa were marked as the CMC and T_1, respectively. In the C_{14} surfactants, in which the CMCs were very low, the corresponding $T_{1\mathrm{s}}$ included relatively bigger errors.

The CMC and T_1 of a series of the surfactants with the same hydrophobic moieties at various temperatures were summarized in Tables 1 and 2. Previous data on $(EO)_{10}OP$, $(EO)_{20}OP$ and $(EO_{20}NP_8$ were also included in Table 1. As found already,[6,8] T_1s of a surfactant at various temperatures coincided with each other despite widely different CMCs, and always lower than the respective CMC.

Furthermore, T_1s of the surfactants of the same hydrophobic moieties were constant, irrespective of the polyoxyethylene chain length and temperature, and T_1 was the lower for the more hydrophobic moiety. Thus, the local micellar aggregation of the surfactants on PAA is entirely of a hydrophobic cooperative nature including the hydrophobic part of the polymer. The fact that T_1s of these surfactants are independent of temperature despite a variety of hydrophobic as well as hydrophilic chains may rule out the possibility of a full compensation of endo- and exothermal effects involved in the binding processes, and rather suggests that the nonionic surfactants are bound to PAA so firmly by a number of hydrogen bonds

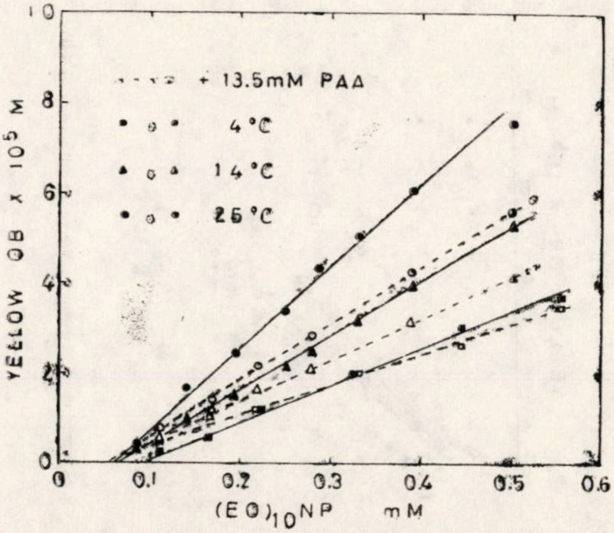

Fig. 1. — Solubilization of Yellow OB in $(EO)_{10}NP$ solutions without and with 13.5 mM PAA ar 4, 14 and 25 °C.

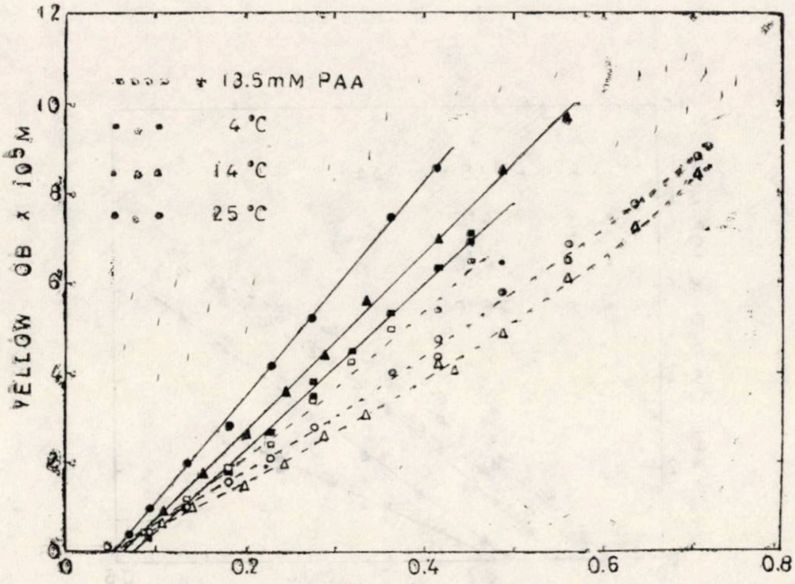

Fig. 2. — Solubilization of Yellow OB in $(EO)_5\ C_{12}$ solutions without and with 13.5 mM PAA at 4, 14 and 25°C.

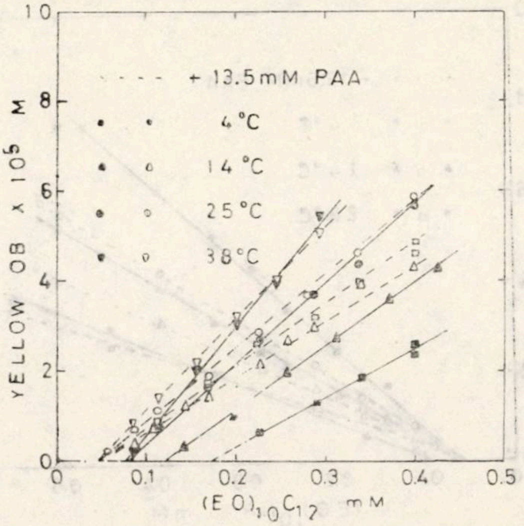

Fig. 3. — Solubilization of Yellow OB in $(EO)_{10}C_{12}$ solutions without and with 13.5 mM PPA at 4, 14,25 and 38°C.

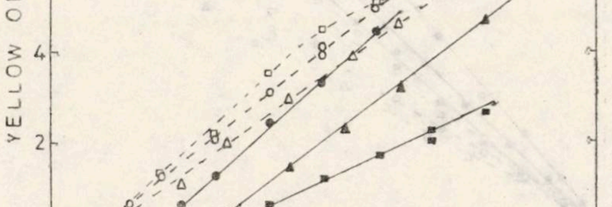

Fig. 4. — Solubilization of Yellow OB in $(EO)_{15}C_{12}$ solutions without and with 13.5 mM PAA at 4, 14 and 25°C.

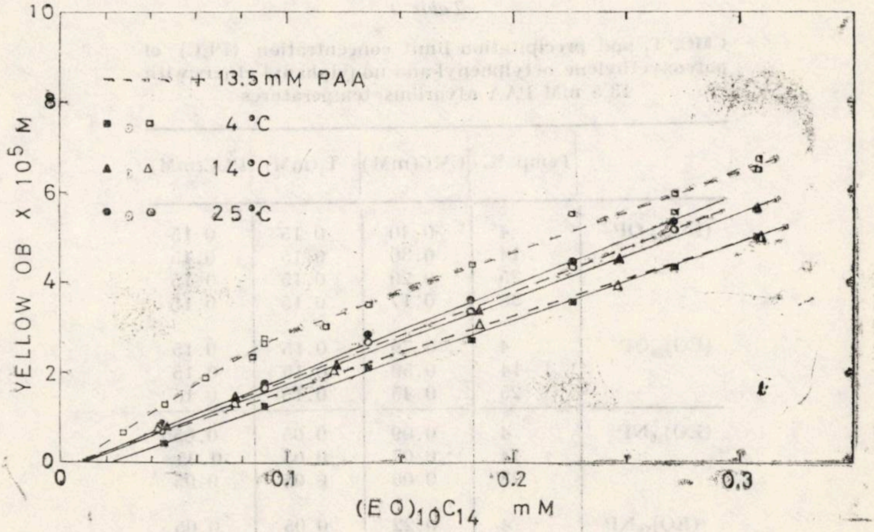

Fig. 5. — Solubilization of Yellow OB in $(EO)_{10}C_{14}$ solutions without and with 13.5 mM PAA at 4, 14 and 25°C.

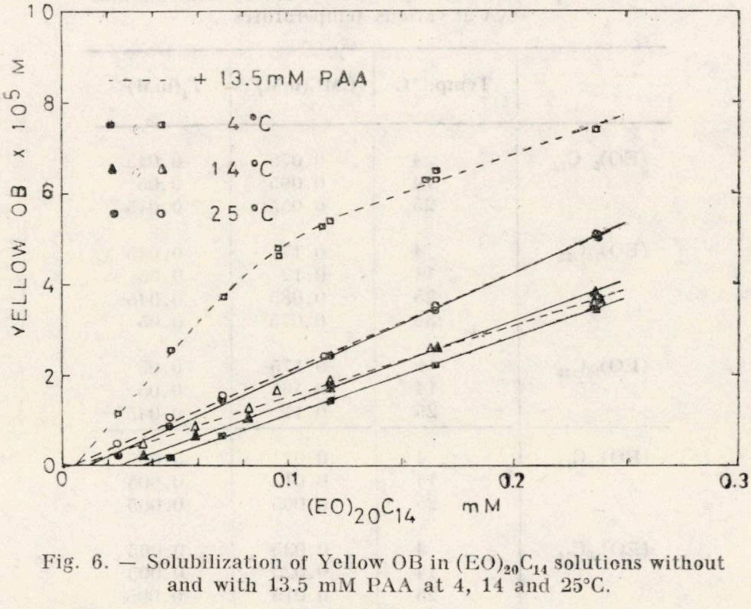

Fig. 6. — Solubilization of Yellow OB in $(EO)_{20}C_{14}$ solutions without and with 13.5 mM PAA at 4, 14 and 25°C.

and the strong cooperative hydrophobic attraction that the complex is stabilized against temperature change. [8] As mentioned below, microscopically some of the hydrogen bonds in the complex may be broken at low temperature, but macroscopically the composition is unchanged.

Table 1

CMC, T_1 and precipitation limit concentration (PLC) of polyoxyethylene octylphenyl and nonylphenyl ethers with 13.5 mM PAA atvarious temperatures

	Temp. °C	CMC(mM)	T_1(mM)	PLC(mM)
$(EO)_{10}$ OP	4	0.40	0.15	0.15
	14	0.30	0.15	0.15
	25	0.20	0.15	0.15
	38	0.17	0.15	0.15
$(EO)_{20}$OP	4	0,79	0.15	0.15
	14	0.59	0.15	0.15
	25	0.45	0.15	0.15
$(EO)_{10}$NP	4	0.09	0.05	0.055
	14	0.07	0.05	0.05
	25	0.06	0.05	0.05
$(EO)_{20}$NP	4	0.22	0.05	0.05
	14	0.13	0.04	0.04
	25	0.11	0.04	0.04

Table 2

CMC and T_1 of polyoxyethylene alkyl ethers with 13.5 mM PAA at various temperatures

	Temp. °C	CMC(mM)	T_1(mM)
$(EO)_5$ C_{12}	4	0.075	0.045
	14	0.065	0,05
	25	0.055	0.045
$(EO)_{10}C_{12}$	4	0.17	0.045
	14	0.12	0.05
	25	0.085	0.045
	38	0,075	0.05
$(EO)_{15}C_{12}$	4	0.175	0.05
	14	0.165	0,05
	25	0.11	0.045
$(EO)_{10}C_{14}$	4	0.02	0.005
	14	0.01	0.005
	25	0.005	0.005
$(EO)_{20}C_{14}$	4	0.035	0.005
	14	0.025	0.005
	25	0.015	0.005

Thus, as the surfactants anchor to a PAA chain through their polyoxyethylene parts, their movement as a whole is restricted, thereby facilitating micellar aggregation in the domain of PAA chain compared with the formation of the free micelle. This may explain that T_1 is always lower than the respective CMC. Such an aggregation may probably be smaller in size than the ordinary micelle, as in the cases of similar complex formation of ionic surfactants with various polymers.[3]

It is noted that, whereas the solubilization ability for Yellow OB of the micelles decreased with temperature drop, in some C_{12} and C_{14} surfactants, particularly in $(EO)_{20}C_{14}$ (Fig. 6), their PAA mixed solutions had higher solubilization abilities at 4°C than at room temperatures. Such a peculiar phenomenon has been found also in other surfactants with PAA, and will be discussed elsewhere.

2. Precipitation of Complex

$(EO)_{10}$ NP solutions each at a constant concentration and containing various PAA concentrations were precipitated at pH 2, and the supernatant surfactant concentrations were plotted against PAA concentration added at three temperatures in Figure 7. The surfactant concentration in the flat part of curve in the figure is denoted PLC, and included in Table 1 together with the values of other surfactants.[8] Thus, it is again confirmed that the PLC is independent of temperature within experimental error and agrees with the respective T_1, that the PLC depends

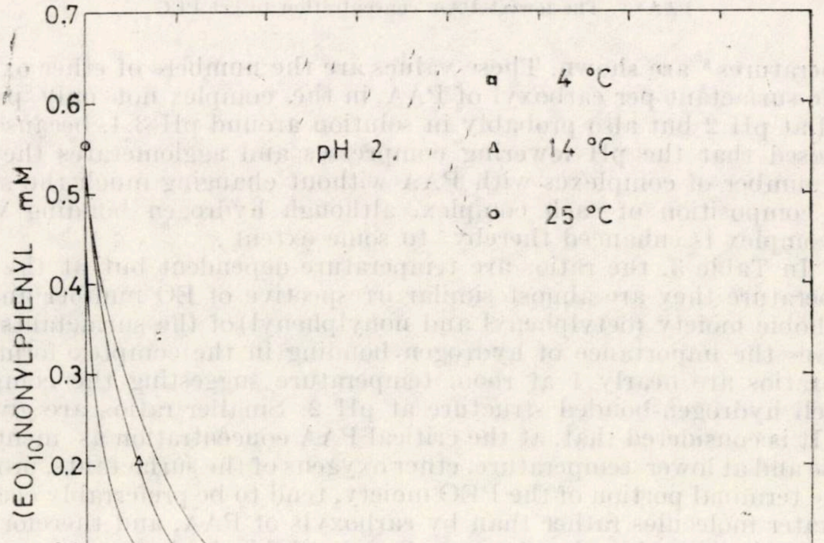

Fig. 7. — Concentration of supernatant $(EO)_{10}$NP in the precipitated systems from 0.55 mM surfactant plotted against PAA concentration at pH 2 at 4, 14. and 25°C. The difference from 0.55 mM is the amount of surfactant precipitated.

only on the hydrophobic part and not on the polyoxyethylene chain length of the surfactant, and that, therefore, the pH difference from 3.5 to 2 is insignificant in determining T_1.

The mole ratio of $(EO)_{10}NP$ precipitated to the lowest PAA concentration in the flat part of the curve in Figure 7 gives the composition of the complex, provided that all PAA added is confined in the precipitate at this critical PAA concentration. In Table 3 the ratios multiplied by the respective EO number of the four alkylphenyl surfactants at various temperatures[8] are shown. These values are the numbers of ether oxygens of the surfactant per carboxyl of PAA in the complex not only precipitated at pH 2 but also probably in solution around pH 3.4, because it is supposed that the pH lowering compresses and agglomerates the chain of a number of complexes with PAA without changing much the surfactant composition of each complex, although hydrogen bonding within the complex is enhanced thereby to some extent.

Table 3

Composition of nonionic surfactant-PAA complexes estimated from precipitation at various temperatures

Temp. °C	EO(C* − PLC)/PAA*			
	$(EO)_{10}OP$	$(EO)_{20}OP$	$(EO)_{10}NP$	$(EO)_{20}NP$
4	0.6	0.9	0.8	0.7
25	1	0.9	1.2	1.1
38	1.8			

C* Initial surfactant concentration
PLC Precipitation limit surfactant concentration
PAA* The lowest PAA concentration to get PLC

In Table 3, the ratios are temperature-dependent but at the same temperature they are almost similar irrespective of EO number and hydrophobic moiety (octylphenyl and nonylphenyl) of the surfactants. This stresses the importance of hydrogen bonding in the complex formation. The ratios are nearly 1 at room temperature suggesting the complexes of well hydrogen-bonded structure at pH 2. Smaller ratios are given at 4°C. It is considered that, at the critical PAA concentration as mentioned above and at lower temperature, ether oxygens of the surfactants, probably in the terminal portion of the PEO moiety, tend to be preferrably occupied by water molecules rather than by carboxyls of PAA, and therefore, the complex is more loosely structured and soluble at lower temperature. In the $(EO)_{10}OP$ complex at 38°C, ether oxygens are more dehydrated, and the complex is more compact, especially in its peripheral layer, and therefore, prone to be agglomerated with less PAA. However, when PAA concentration added is high enough, the overall composition of the complex becomes temperature-independent, as demonstrated in T_1 and PLC.

3. Complex in Solution

The reduced viscosity of 13.5 mM PAA solutions with surfactants was plotted against surfactant concentration added in Figure 8 (the left ordinate). With increasing surfactant concentration, the reduced viscosity decreased followed by levelling-off and a rise at high concentrations. The drop is attributed to the effect of hydrogen bonding of surfactant to PAA, and the rise is due to further surfactant binding by hydrophobic effect. T_1 is observed also in the viscosity curve at 0.15 mM for both $(EO)_{10}OP$ and $(EO)_{20}OP$.[2]

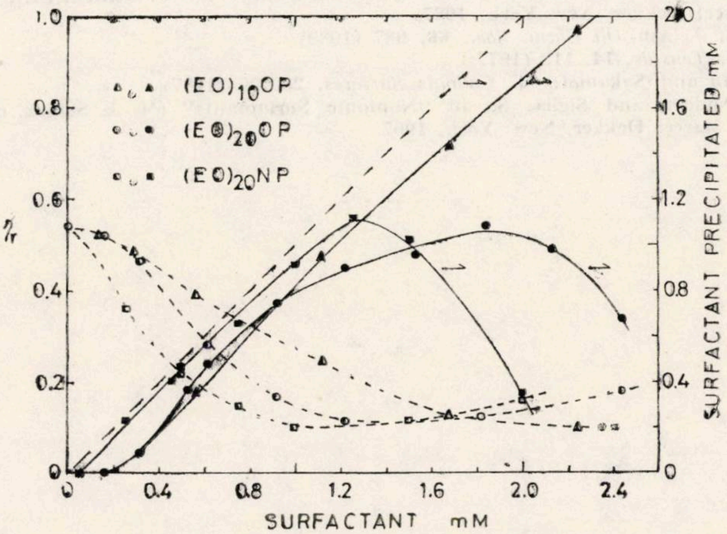

Fig. 8. — Reduced viscosity of 13.5 mM PAA solutions with surfactants (broken lines, the left ordinate) and the extent of surfactant precipitated with 13.5 mM PAA at pH 2 (solid lines, the right ordinate) plotted against surfactant concentration added at 25°C. The 45° line from the origin indicates the initial surfactant concentration before precipitation.

In parallel with the viscosity, the amount of precipitation of the surfactants from various concentrations with 13.5 mM PAA at pH 2 was measured, and was shown on the right ordinate in Figure 8. When the free surfactant concentration reached the CMC, the sediment began to disperse and the precipitation tended to diminish. In $(EO)_{20}OP$ and $(EO)_{20}NP$, the increase and decrease in the extent of precipitation and the transition zone in-between correspond to the drop, rise and the flat zone in the reduced viscosity curve, respectively. In $(EO)_{10}OP$, no viscosity rise was found in the surfactant concentration region measured, and the precipitation increased steadily. These results support that at the same temperature the compositions of the complexes in solution and in the precipitate at low pH are not much different, as mentioned above.

ACKNOWLEDGEMENTS. BL—NR and BM—NR series surfactants were given by Nikko Chemicals Ind. The Publication of this paper was permitted by Momotani Juntenkan Ltd.

REFERENCES

[1] Partially presented at the ACS 62nd Colloid and Surface Science Symposium in 19—22June, 1988 in State College, PA. USA, and at the 3rd Colloid and Surface Chemistry Sym-

posium in 11—14 September, 1989 in Timişoara, Romania, as a part of the plenary lecture.

[2] I. D. Robb, in "Anionic Surfactants. Physical Chemistry of Surfactant Action", (E. H. Lucassen-Reynders, ed.), Chapter 3, Marcel Dekker, New York, 1987.

[3] E. D. Goddard, *Colloids Surfaces*, **19**, 255, 301 (1986).

[4] R. Nagarajan, *Colloids Surfaces*, **13**, 1 (1985).

[5] M. N. Jones, *J. Colloid Interface Sci.*, **23**, 36 (1967).

[6] S. Saito, *Colloid Polymer Sci.*, **257**, 266 (1979).

[7] S. Saito, in "Nonionic Surfactants. Physical Chemistry" (M. J. Schick, ed.), Chapter 15, Marcel Dekker, New York, 1987.

[8] S. Saito, *J. Am. Oil Chem. Soc.*, **66**, 987 (1989).

[9] S. Saito, *Tenside*, **14**, 113 (1977).

[10] S. Saito and Sakamoto. T, *Colloids Surfaces*, **23**, 99 (1987).

[11] H. G. Nadeau and Sigiia, S., in "Nonionic Surfactants" (M. J. Schick, ed.), Chapter 26, Marcel Dekker, New York, 1967.

Revue Roumaine de Chimie, 35, 7–9, 831–842 (1990)

MODERN METHODS FOR DETERMINING THE GAS PERMEATION AND PREDICTING THE PROPERTIES OF DISPERSED POLYMER SYSTEMS

A. L. IEVLEV and V. V. TEPLYAKOV
"A. V. Topchiev" Institute of Petrochemical Synthesis, USSR Academy of Sciences, Leninski prospect, 29, 117912, GSP–1, Moscow, USSR

The methods for calculating the permeability coefficients based on the data of chromatographic analysis of steady-state membrane fluxes of concentration detector are discussed. Likewise, are considered some useful techniques and ways of interpretation of the obtained parameters for express prediction of the gas separation properties of the polymer based membrane. The models for the calculation of gas permeability parameters of the two-phase block-copolymers have been analyzed. It has been shown that the transfer of constant and inert gases through such polymers can be described with the use of the differential equation for gas diffusion along two interconnected routes in the framework of the dissociation diffusion model. A generalized empirical equation to estimate the gas separating properties of silicon-containing block-copolymers in the 0–100% range of changes in the volume content of the more permeable block is proposed on the basis of the properties of the polymeric medium components. Exemplified by siloxane-containing block-copolymers, the effect of a kind of dispersion on the selectivity and level of their permeability has been demonstrated. The proposed approach can be used for a preliminary selection of the polymeric materials and membrane-oriented compositions with the given parameters of the selective gas transport. All the abovementioned is realized as a software for measurement apparatus developed by the Institute of Petrochemical Synthesis of the USSR Academy of Sciences.

In the laboratory of synthesis of permselective polymers, the main field of our interests is a selective permeation of different gases through polymers, membranes and new materials for these aims. We investigate both known polymers and special synthesized polymers, copolymers and membranes on their bases. We give attention to silicon-containing carbochain polymers and copolymers. We deal with polyvinyltrymethylsilane and polydimethylsiloxane homopolymers (polyWTMS/ polyDMS), whose structure formulas are shown in figure 1. There are AB- and ABA-kind of silane-siloxane block-copolymers and $(AB)_n$ kind of arylate-silixane block-copolymers.

In the capacity of gases we use inert gases and permanent gases : H_2, O_2, N_2, methane, carbondioxide.

We shall try to elucidate our results for these block-copolymers and gases. It is known that we can describe the diffusion process by using Fick's equations (1,2). For example, in the simplest situation under some boundary and initial conditions (3), the gas flux through membrane is described by equations (4) and (5). It is possible to use the system of two equations (2) for describing of diffusion in two component polymer composition. This situation is complex. Anyway, we should measure and know coefficients of permeability, selectivity, diffusivity and solubility of gases for given copolymers as well as the temperature features. These coefficients are connected with equations (10), (11), (12).

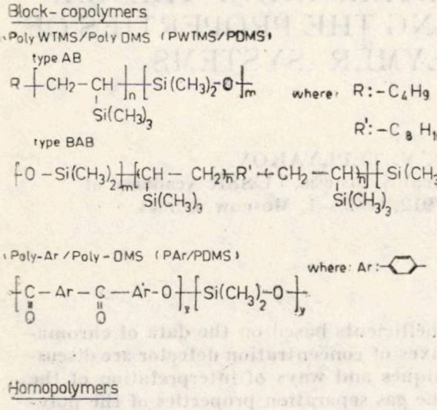
Block- copolymers
Poly WTMS/Poly DMS (PWTMS/PDMS)
type AB
where: R: -C4H9
R': -C8H10-
type BAB
Poly-Ar / Poly-DMS (PAr/PDMS)
where: Ar:
Homopolymers
Poly WTMS (PWTMS)
Poly DMS (PDMS)

Fig. 1. — The structure of the special polymers.

Only after this we can estimate the influence of chemical structure on permeselectivity properties of copolymer.

$$Q = -SD\left(\frac{\partial C}{\partial X}\right)_{X=H} \tag{1}$$

$$\frac{\partial C}{\partial t} = D\frac{\partial^2 C}{\partial X^2} \tag{2}$$

$$\begin{aligned} &C(X, 0) = f(X) \quad \text{(a)} \\ &\left.\begin{aligned} C(0, t) &= C_1 \\ C(H, t) &= C_2 \end{aligned}\right\} \text{(B)} \end{aligned} \tag{3}$$

$$\begin{aligned} Qt = {} & \frac{DS(C_2 - C_1)}{H} + \frac{2DS}{H}\sum_{n=1}^{\infty}[C_2(-1)^n - C_1]\exp\left\{-\frac{n^2\pi^2 Dt}{H^2}\right\} + \\ & + \frac{4DS}{H}C(0)\sum_{m=0}^{\infty}\exp\left\{-\frac{(2m+1)^2\pi^2 Dt}{H^2}\right\} \end{aligned} \tag{4}$$

$$Q_t = Q_\infty \left[(1-\alpha) + 2 \sum_{n=1}^{\infty} (-1)^{n+a} \exp\left\{ -\frac{n^2 \pi^2 Dt}{H^2} \right\} \right], \tag{5}$$

where $Q_\infty = \dfrac{DSC_0}{H}$

$$q_t = \frac{SD(C_2 - C_1)t}{H} - SH \sum_{n=1}^{\infty} \left(\frac{C_2}{6} + \frac{C_1}{3} \right) \exp\left\{ -\frac{n^2\pi^2 Dt}{H^2} \right\} + \tag{6}$$

$$+ \frac{S\,C(0)H}{2} \sum_{m=1}^{\infty} \left\{ 1 - \exp\left[-\frac{(2m+1)\,\pi^2 Dt}{H^2} \right] \right\}$$

$$q_t = C_0 DS \left[\frac{t}{H} - \frac{H}{6D} \sum_{n=1}^{\infty} \left\{ 1 - \frac{(-1)^n}{\pi^2} \exp\left[-\frac{n^2\pi^2 Dt}{H^2} \right] \right\} \right] \tag{7}$$

$$C = \sigma \cdot \Delta P \tag{8}$$

$$Q_\infty = D\sigma \frac{\Delta P}{H} S \tag{9}$$

$$P = D\sigma \tag{10}$$

$$P = \frac{Q_\infty \cdot H}{\Delta P \cdot S} \tag{11}$$

$$p = p_0 \exp\left(\frac{-E_P}{RT} \right)$$

$$D = D_0 \exp\left(\frac{-E_D}{RT} \right) \tag{12}$$

$$\sigma = \sigma_0 \exp\left(\frac{-\Delta H}{RT} \right)$$

For measuring the permeability parameters we use classical techniques (for example, Mac-Ben Balance), as well as modern techniques by using mass-spectroscopy, inverse gas chromatography, usual gas chromatography. Our methods for calculating the permeability coefficients are based on the data of gas chromatographic analysis of steady-state membrane fluxes. We can measure the quantity of gas after membrane (integral method); the flux of gas after membrane versus time (differential method); the derivative of the gas flux versus time (pulse method). We can get these kinetic curves and use the treatment by computer during the experiment. For example, it is very convenient to treat the kinetic curves by linearisation method. In this case the kinetic curves are transformed into linear dependences. We can estimate the coefficient of diffusivity from the slope in any part of kinetic curves.

For researches in gastransfer membrane processes, using an information measurement system based on the multichannel system (Fig. 2), it is possible to study the gas permeability of the different structure polymeric membranes. We used the gas-chromatographic method of permeability (Fig. 3).

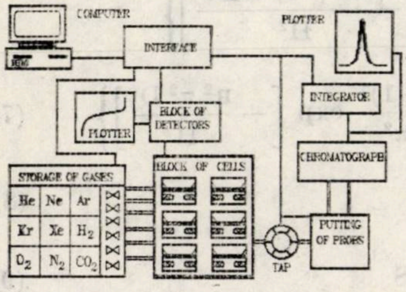
COMPUTER
IBM
INTERFACE
PLOTTER
PLOTTER
BLOCK OF DETECTORS
INTEGRATOR
CHROMATOGRAPH
STORAGE OF GASES
He
Ne
Ar
Kr
Xe
H_2
O_2
N_2
CO_2
BLOCK OF CELLS
TAP
PUTTING OF PROBS

Fig. 2. — Multichannel automatic apparatus for investigation of gas transport parameters.

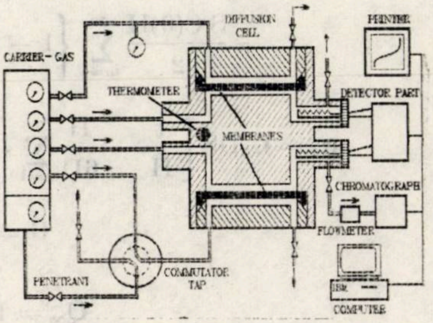
DIFFUSION CELL
PRINTER
CARRIER-GAS
THERMOMETER
DETECTOR PART
MEMBRANES
CHROMATOGRAPH
FLOWMETER
PENETRANT
COMMUTATOR TAP
IBM
COMPUTER

Fig. 3. — Gas-chromatographic method of permeability.

The software specially developed provides the calculation of the kinetic experiment in automatical conditions. We can use the express treatment of kinetic curves of permeability. The diffusivity coefficients can be estimated in terms of the classical model by using the linearisation and moment method. It is possible to have the treatment of nonusual kinetic curves by means of non-linear least square method. Linearisation was made with weights and moments methods. Figure 4 shows

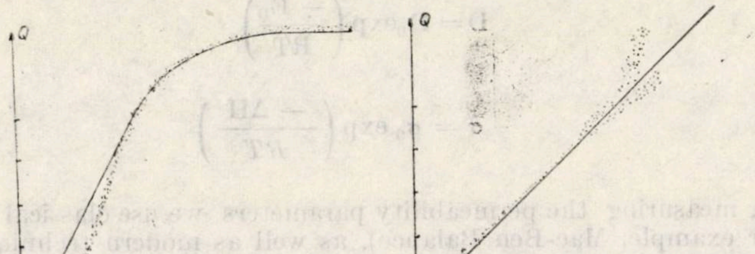

Fig. 4. — Method of satistical moments
D = 1.34E−07
Bad approximation by Fick's law
Linearization method
$D = 1.96E-07$.

the kinetic curves after treatment, by using the method of statistical moments and linearisation method. In the first case it is a bad approximation between the experimental and theoretical curves. The linearisation method gives better results.

We can verify the diffusion models: the diffusion with immobilisation model, the parallel diffusion model, the dissociation model (equations 13, 14, 15):

$$\left\{\begin{aligned} \frac{\partial C_1}{\partial t} &= D_1 \frac{\partial^2 C_1}{\partial x^2} - \lambda_1 \, (C_{2m} - C_2)\, C_1 + k_2 \, C_2 \\ \frac{\partial C_2}{\partial t} &= \lambda_1 (C_{2m} - C_2) C_1 - k_2 \, C_2 \end{aligned}\right. \qquad (13)$$

$$\left\{\begin{aligned} \frac{\partial C_1}{\partial t} &= D_1 \frac{\partial^2 C_1}{\partial x^2} - k_1 C_1 + k_2 C_2 \\ \frac{\partial C_2}{\partial t} &= D_2 \frac{\partial^2 C_2}{\partial x^2} + k_1 C_1 - k_2 C_2 \end{aligned}\right. \qquad (14)$$

with immobilization, where $D_2 = 0$

$$\left\{\begin{aligned} \frac{\partial C_1}{\partial t} &= D_1 \frac{\partial^2 C_1}{\partial x^2} - k_1 C_1 + k_2 \, C_2 \\ \frac{\partial C_2}{\partial t} &= k_1 \, C_1 - k_2 C_2 \end{aligned}\right. \qquad (15)$$

This treatment level includes analysis and prediction of permeability, diffusivity and solubility coefficients and their temperature parameter for a wide spectrum of gases.

Table 1 demonstrates the prediction of the parameters of gas transfer of PWTMS membrane based on minimum experimental data. When we have experimental values of the permeability of 4 gases, and the diffusivity of two gases in polymer, we can predict the values of permeability, diffusivity and solubility of 15 gases. We use our correlation dependences, which we found after computer treatment parameters of gas permeability published for the latest 30 years (Figs 5, 6). The best dependences for calculation of diffusion coefficients of gases are logarithm D versus d^2 (cross-section of gas molecule). As regards the solubility of gases we obtained the correlations logarithm σ versus force constant of potential 6 – 12 (ε/k). We use the empirical relation between permeability, diffusivity, solubility and selectivity of gas separation versus properties of gas molecules (molecular cross-section and force constant of gas molecules).

Table 1

Characteristic of the membrane : SILAR

Experimental data

gas	Permeability	Diffusivity	Solubility
He	1.400E−08	2.400E−05	5.833E−04
Ne			
Ar	1.700E−08		
Kr	3.000E−08	3.600E−06	8.333E−03
Xe			
Rn			
H2			
O2			
N2			
CO2			
CO			
CH4			
C2H6			
C3H8			
C4H1			

Predicted values

gas	Permeability	Diffusivity	Solubility
He	1.369E−08	2.419E−05	5.659E−04
Ne	1.030E−08	1.377E−05	7.480E−04
Ar	1.823E−08	5.389E−06	3.383E−03
Kr	2.862E−08	3.572E−06	8.012E−03
Xe	4.077E−08	2.088E−06	1.953E−02
Rn	6.211E−08	1.287E−06	4.827E−02
H2	2.169E−08	1.662E−05	1.305E−03
O2	1.773E−08	6.103E−06	2.905E−03
N2	8.743E−09	4.819E−06	1.814E−03
CO2	7.134E−08	4.977E−06	1.433E−02
CO	1.187E−08	4.819E−06	2.464E−03
CH4	2.162E−08	3.824E−06	5.653E−03
C2H6	5.975E−08	2.334E−06	2.561E−02
C3H8	9.600E−08	1.568E−06	6.123E−02
C4H1	2.352E−07	1.508E−06	.156

Error = 9.2 %

Another priority of our research is a simple method to estimate the properties of two-phase block-copolymer systems, such as steady-state permeability versus the structure of heterogeneous copolymers. The properties of composite materials can be estimated from knowledge of the properties of phases which make up the composite. Our purpose is not a new one. There are many papers on this subject in journals. In our study we used the equations of Fricke, Maxwell, Higuchi and Lichtenecker, when we have the lamination structure and the lamination is parallel to or normal versus the direction of the flow known (Appendix 1).

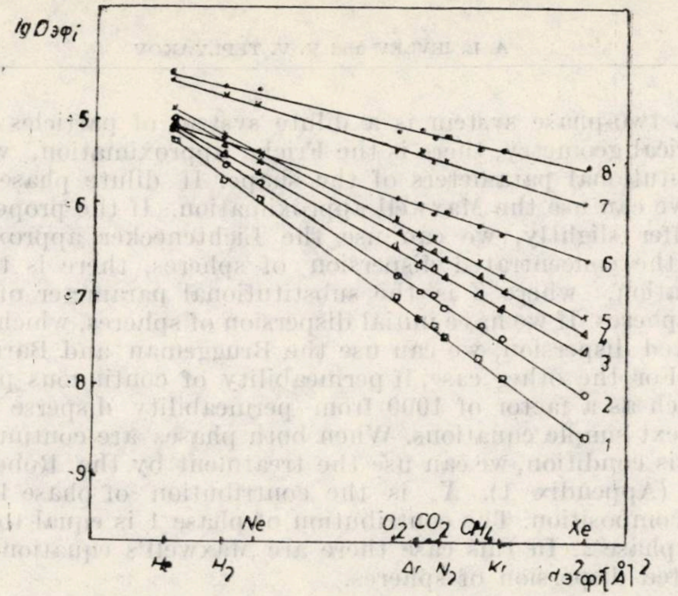

Fig. 5 — Plot of log D_{effi} vs. (d^2_{effi}) of gases: 1 — poly But/poly AN 61/39; 2 — poly But/poly AN 61/39; 2 — poly But/poly AN 68/32; 3 — poly But/poly AN 73/27; 4 — PWTMS/poly DMS 83/17; 5 — poly But/poly St 80/20; 6 — PWTMS/poly But 59/41; 7 — poly Ar/poly DMS; 8 — PWTMS/poly DMS 68/38.

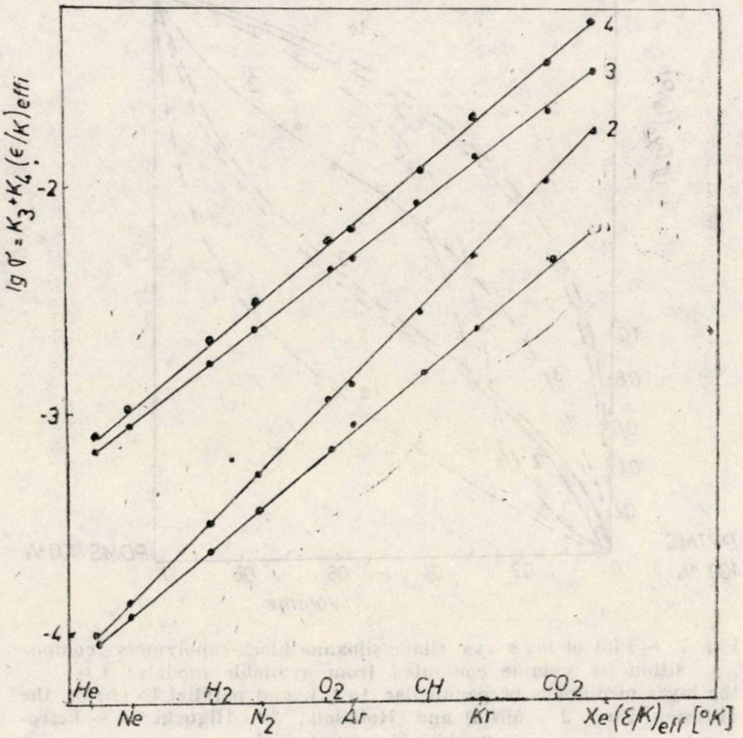

Fig. 6. — Plot of log σ vs. (ε/K) in gases: 1 — poly But/ poly St 80/20; 2 — poly But/poly AN 80/20; 3 — poly But/poly St 59/41; 4 — poly WTMS/poly DMS 83/17;

If a two-phase system is a dilute system of particles of more or less spherical geometry, there is the Fricke approximation, where A_i are the substitutional parameters of the shape. If dilute phase consists of spheres, we can use the Maxwell approximation. If the properties of two phases differ slightly, we can use the Lichtenecker approximation. If we have the concentrated dispersion of spheres, there is the Higuchi approximation, where Z is the substitutional parameter of interaction between spheres. If we have initial dispersion of spheres, which transforms the inverted dispersion, we can use the Bruggeman and Barrie approximations. For the other case, if permeability of continuous phase differs by as much as a factor of 1000 from permeability disperse phase, you can use next simple equations. When both phases are continuous or approach this condition, we can use the treatment by the Robeson approximation (Appendix 1). X_a is the contribution of phase 1 in permeability of composition. The contribution of phase 1 is equal to the contribution of phase 2. In this case there are Maxwell's equations for direct and inverted dispersion of spheres.

The dependence of diffusivity of XE on the silane-siloxane block-copolymers versus the volume composition calculated from available models, is shown in figure 7. All above mentioned should be taken into consideration (Appendix 2).

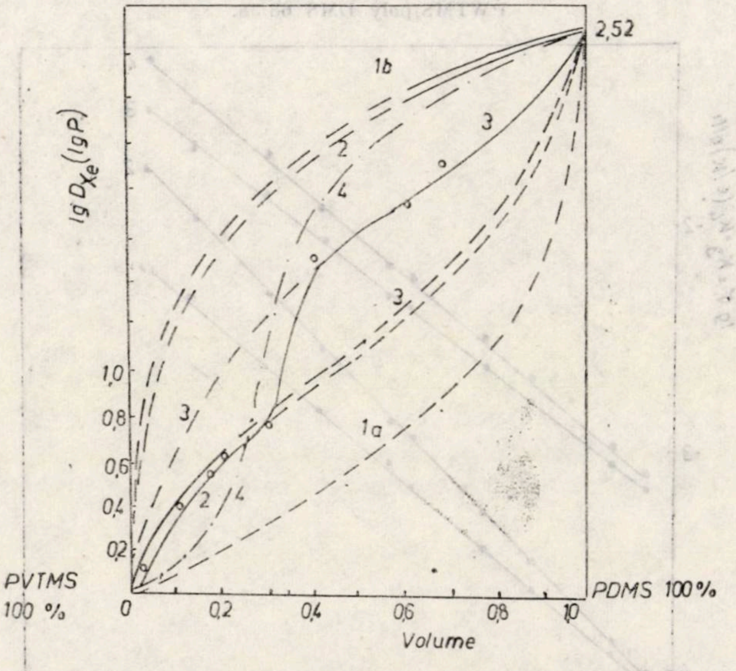

Fig. 7. — Plot of log σ vs. silane/siloxane block-copolymers composition by volume computed from available models: 1 — the layer medium is perpendicular to (a) and parallel to (b) of the diffusion flux; 2 — Mitoff and Robeson; 3 — Higuchi; 4 — Petropoulos; 0 — our models.

We used general Frick's equation for dispersion of spheroid-shaped particles, Higuchi's equation for concentrated dispersion of particles. The permeability coefficient can be expressed as a product of the diffusivity and solubility coefficients. The effective solubility coefficient is equal to the solubility coefficient of continuous phase. The continuous phase forms the surface of membrane and has constant general contribution of the solubility.

The general equation for calculation of diffusivity coefficient can be presented as the equation :

$$D_{eff} = f_a \frac{D_1 + \bar{\bar{K}} \dfrac{d}{1-d} D_2}{1 + \bar{\bar{K}} \dfrac{d}{1-d}} + (1 - f_a) \frac{D_2 + \bar{\bar{K}} \dfrac{d}{1-d} D_1}{1 + \bar{\bar{K}} \dfrac{d}{1-d}}$$

$$D_2 D_1 ; f_a = 1 - f_b ;$$

In this case, in the inversion region the contribution of f_a and f_b changes from zero to one since f_a plus f_b is equal to one.

The dependences of the contribution parameter in the gas inversion region can be approximated by the well-known function of normal distribution (Table 2).

Table 2

Parameters of function f_a in the region of phase inversion

$$f_a = 1/\Delta\Phi\sqrt{2\pi} \int_0^{\Phi} e^{-0.5(\Phi-\Phi_0)/\Delta\Phi_0} \, d\Phi$$

Sample of block-copolymer	Gas	Φo	ΔΦo
1. PVTMS–PDMS BCP	O_2	0.355±0.003	0.048±0.010
	Ar	0.359±0.004	0.043±0.015
	Kr	0.354±0.001	0.077±0.015
	Xe	0.356±0.001	0.077±0.018
	CO_2	0.328±0.002	0.050±0.033
2. Polysulfon–PDMS BCP	N_2	0.366±0.003	0.067±0.004
	O_2	0.349±0.004	0.074±0.004
3. Polycarbonat–PDMS BCP	O_2	0.336±0.006	0.084±0.006
		0.350±0.029	0.065±0.036

Computer analysis of numerous data of the gas permeability of block-copolymers has shown that the inversion point correlates with the volume composition of the block-copolymers. The parameters of this function are quite constant in various gases and copolymers.

The calculation of diffusion properties of block-copolymers based on the parameters of permeability of their constituent homopolymers can be rather realized on the computer (Table 3). A good correlation was obtained between experimental and calculated values of gas transfer parameters in block-copolymers.

Table 3

Experimental and calculated values of D_{eff} and P_{eff} of gases in silane-siloxane block-copolymers

Gas	$D_{calcul.}$	$D_{exper.}$	$P_{calcul.}$	$P_{exper.}$
	$(*10^7)$		$(*10^8)$	
1. PVTMS–PDMS BCP – 84.1/15.9 vol. %				
Ar	7.7	10.1	0.53	0.54
Kr	2.7	3.0	0.51	0.45
Xe	0.8	0.9	0.58	0.60
N_2	6.2	6.8	0.15	0.19
O_2	12.4	12.8	0.60	0.70
CH_4	4.8	4.5	0.43	0.50
CO_2	8.1	8.3	2.90	3.40
2. PVTMS–PDMS BCP – 32/68 vol. %				
Ar	62.8	60.7	3.1	2.7
Kr	30.4	25.7	3.8	4.6
Xe	18.8	21.3	7.5	6.3
N_2	53.9	48.6	1.4	1.4
O_2	76.6	69.1	3.4	2.9
CH_4	41.0	40.3	3.8	4.6
CO_2	61.0	59.0	15.9	12.4

The proposed methods of calculation of diffusion properties and their prediction by two-component block-copolymers can be used for a preliminary search for polymeric composition of membrane, when the parameters of the constituent homopolymers are known.

APPENDIX 1

The laminations are parallel or normal to the direction of flow:

$$P_{eff} = \Phi_1 P_1 + \Phi_2 P_2 \quad \text{(parallel)}$$

$$P_{eff} = P_1 P_2 / (\Phi_2 P_1 + \Phi_1 P_2) \quad \text{(normal)}$$

Fricke approximation : (diluted dispersion of spheres)

$$P_{\mathrm{eff}} = P_c + \frac{\Phi_d}{3(1-\Phi_d)} \sum_{i=1}^{3} \frac{P_d - P_{\mathrm{eff}}}{1 + (A_i/2)\,(P_d/P_c - 1)}$$

$(A_1 = A_2 = A\,;\ A_3 = 2 - 2A)$ (substitutional parameters of the shape)

When $A = = 2/3$:

Maxwell approximation :

$$P_{\mathrm{eff}} = P_c\,\frac{P_d + 2P_c - 2\Phi_d(P_c - P_d)}{P_d + 2P_c + \Phi_d\,(P_c - P_d)}$$

Lichtenecker approximation : (the properties of the two phases differ slightly)

$$P_{\mathrm{eff}} = P_c^{\Phi_c} \cdot P_d^{\Phi_d}, \quad \Phi_c = 1 - \Phi_d$$

Higuchi, Peterson approximation : (to the concentrated dispersion

$$P_{\mathrm{eff}} = P_c\,\frac{P_d + 2P_c - Z - \Phi_d\,(2P_c - 2P_d - Z)}{P_d + 2P_c - Z + \Phi_d\,(P_c - P_d + Z)}$$

where

$$Z = 0.78\ \ (P_d - P_c)^2/(2P_c + P_d)$$

Z – substitutional parameter of interaction

Bruggeman, Barrie approximations (from the dispersion of spheres – to the inverted dispersion of spheres)

$$P_{\mathrm{eff}} = P_c/\Phi_c \left(\frac{P_d - P_{\mathrm{eff}}}{P_d - P_c}\right)^3, \quad \Phi_c = 1 - \Phi_d$$

$$P_{\mathrm{eff}} = 1/2.\,3(\Phi_t\,P_c + \Phi_d P_d) - (P_d + P_c) + \frac{P_c\,P_d}{P_{\mathrm{eff}}}$$

Barrie, Bruggeman, Sax, Ottino approximations $(P_c \gg P_d)$:

$$P_{\mathrm{eff}} = P_c(\Phi_c)^{3/2}; \quad P_{\mathrm{eff}} = P_c\,\frac{1.61\ \Phi_c}{1.61 + 1.39\ \Phi_d}$$

$$P_{\mathrm{eff}} = P_c(1 - 3/2\ \Phi_d);$$

Appendix 1 (continued)

Robeson approximation: (two phase system — as that consisting of two continuous phases)

$$P_{\text{eff}} = X_a\, P_1\, \frac{P_2 + 2P_1 - 2\Phi_2(P_1 - P_2)}{P_2 + 2P_1 + \Phi_2(P_1 - P_2)} + X_b P_2\, \frac{P_1 + 2P_2 - 2\Phi_1(P_2 - P_1)}{P_1 + 2P_2 + \Phi_1\,(P_2 - P_1)}$$

$X_a + X_b = 1$, where (a) — phase 1 is continuous: $P_1 = P_c,\ P_2 = P_d$;

(b) — phase 2 is continuous: $P_2 = P_c,\ P_1 = P_d$;

$\Phi_1,\ \Phi_2$ — volume parts of phase 1 and phase 2.

APPENDIX 2

$$P_{\text{eff}} = P_c + \frac{\Phi_d}{3(1 - \Phi_d)} \sum_{i=1}^{3} \frac{P_d - P_{\text{eff}}}{1 - A_i/2 \left(\dfrac{P_d}{P_c} - 1 - \dfrac{Z}{P_c} \right)}$$

$$Z = 0.78\ (P_c - P_c)^2/\,(2P_c + P_d)$$

$$\bar{K} = 1/3 \sum_{i=1}^{3} [1 - A_i/2\,(P_d/P_c - 1 - Z/P_c)]^{-1}$$

$$P_{\text{eff}} = \frac{P_c + \bar{K}\, \dfrac{\Phi_d}{1 - \Phi_d}\, P_d}{1 + \bar{K}\, \dfrac{\Phi_d}{1 - \Phi_d}}$$

$$P_{\text{eff}} = D_{\text{eff}}\quad \sigma_{\text{eff}},\quad \sigma_{\text{eff}} = \sigma_{\text{contiauous phase}}$$

$$D_{\text{eff}} = \frac{D_c + \bar{\bar{K}}\, \dfrac{\Phi_d}{1 - \Phi_d}\, D_d}{1 + \bar{\bar{K}}\, \dfrac{\Phi_d}{1 - \Phi_d}}\,; \qquad D_{\text{eff}} = f_a D_{\text{eff}\cdot 1} + f_b\, D_{\text{eff}.2}$$

Revue Roumaine de Chimie, 35, 7–9, 843–851 (1990)

INTERFACIAL TENSION EXTREMA AT THE ADSORPTION FROM POLYCOMPONENT SYSTEMS

E. CHIFU, J. ZSAKÓ, MARIA TOMOAIA-COTIŞEL and I. ALBU
University of Cluj-Napoca, Physical Chemistry Department,
3400—Cluj-Napoca, Romania

Thermodynamical conditions of interfacial tension extrema are theoretically studied for two particular cases, viz. at gas/liquid interface if a chemical reaction occurs, and liquid/liquid (O/W) interface if the substance A dissolved in O reacts with B dissolved in W. It is shown that the extremum corresponds to a completely indifferent state of the system characterized by a similitude between the compositions of the interface and of the equilibrium liquid bulk phase/phases.

INTRODUCTION

According to literature data the interfacial tension at both air/liquid and liquid/liquid interfaces may exhibit extrema, minima or maxima, at certain compositions of the bulk phase/phases.

Generally, these extrema are assigned to the formation of addition compounds or molecular associations and it is presumed that the molar ratio of the components in the bulk phase/phases, at which the extremum of the interfacial tension appears, corresponds to the composition of the addition compound formed.

Mainly surface tension and interfacial tension minima have been reported,[1-7] but also maxima have been observed.[8,9]

In our previous papers the surface tension of aqueous solution of aluminium nitrate and mandelic[10] or lactic[11] acids was studied as a function of composition. The three minima or inflexion points observed e.g. at different overall concentrations always at the molar ratios lactic acid : Al equal to 1 :1, 2 :1 and 3 :1, respectively, were considered to indicate the formation of three complex species : AlL, AlL_2 and AlL_3.[11]

Similarly, the benzene/water interfacial tension has been found to exhibit minima[12-15] or maxima[16] at certain ratios ($m : n$) between the concentration of the substance B in benzene and of A in water and at the interface the formation of A_nB_m type complexes was postulated.

In the present paper an attempt is made to apply the methods used in[17] to study the conditions necessary for the appearance of surface tension extrema under isothermal, isobaric conditions.

We shall consider the following particular cases in which two bulk phases are separated by a single plane surface phase, viz. the :

1) G/W gas/liquid interface. Substances A and B, soluble in W, yield the product C, also soluble in W, according to the stoichiometric equation

$$\nu_A A + \nu_B B + \nu_C C = 0 \qquad (1)$$

A, B, and C are considered to be absent in the gaseous phase, i.e. their vapour pressure is practically equal to zero. In this case equilibrium of reaction (1) is established both in the bulk liquid phase and in the interface.

2) O/W liquid/liquid interface. A is soluble in O, insoluble in W, B is soluble in W and insoluble in O. In the interface phase occurs reaction (1).

In our study the Defay-Crisp phase rule for capillary systems with plane interfaces will be used. According to this rule (ref. 17, p. 77), the variance w is equal to

$$w = 2 + (c - r) - \varphi - (\varphi - s) \qquad (2)$$

where c stands for the number of components, r for the number of independent reactions, φ for the number of bulk phases, φ for the number of surface phases and s for the number of types of interfaces. In the above-considered cases there are two bulk phases, i.e. $\varphi = 2$ and they are separated by a single surface phase, i.e. $\psi = s = 1$. Consequently, eq. (2) becomes

$$w = c - r \qquad (3)$$

Under isothermal and isobaric conditions T and p being constant, the variance will be only

$$w_{Tp} = c - r - 2 \qquad (4)$$

In the surface phase, Gibbs' equation is valid, i.e.

$$d\sigma + \sum_{i=1}^{c} \Gamma_i d\,\mu_i = 0 \qquad (5)$$

where σ stands for the interfacial tension, Γ_i for the adsorption expressed in moles of i per unit surface and μ_i for the chemical potential of one mole of i.

In the case of bulk phases, the Gibbs-Duhem equations may be written for the chemical potentials:

$$\sum_{i=1}^{c} x_i d\,\mu_i = 0 \qquad (6)$$

where x_i stands for the molar fraction of component i in the bulk phase considered.

For each chemical reaction the condition of chemical equilibrium may be written as

$$\sum_{i=1}^{b} \nu_i d\mu_i = 0 \qquad (7)$$

where b stands for the number of substances participating in the chemical reaction considered.

RESULTS AND DISCUSSION

G/W gas/liquid interface

The number of components is $c = 5$, viz. the inert gas G. the solvent W, substances A, B and C. Number of reactions $r = 1$, viz. reaction (1). According to eq. (4), one has $w_{TP} = 2$. Eqs. (5)– (7) yield the following system :

$$\begin{aligned}
&d\sigma + \Gamma_G d\mu_G + \Gamma_W d\mu_W + \Gamma_A d\mu_A + \Gamma_B d\mu_B + \Gamma_C d\mu_C = 0\\
&x_G d\mu_G + x_W d\mu_W + x_A d\mu_A + x_B d\mu_B + x_C d\mu_C = 0\\
&x'_G d\mu_G + x'_W\, d\mu_W = 0\\
&\nu_A d\mu_A + \nu_B d\mu_B + \nu_C\, d\mu_C = 0
\end{aligned}$$

where x_i stand for the molar fractions of the components in the liquid bulk phase and x'_i for the molar fractions in the gaseous bulk phase.

Since the variance of the system is $w_{TP} = 2$, the conditions $d\sigma = 0$ will be fulfilled if all fourth order determinants of the matrix.

$$\begin{pmatrix}
\Gamma_G & \Gamma_W & \Gamma_A & \Gamma_B & \Gamma_C\\
x_G & x_W & x_A & x_B & x_C\\
x'_G & x'_W & 0 & 0 & 0\\
0 & 0 & \nu_A & \nu_B & \nu_C
\end{pmatrix} \tag{9}$$

are equal to zero.

With the columns of matrix (9) five fourth order determinants can be formed, which equalled to zero yield the following conditions :

$$\nu_A(\Gamma_B x''_W - \Gamma''_W x_B) + \nu_B(\Gamma''_W x_A - \Gamma_A x''_W) = 0 \tag{10}$$

$$\nu_A(\Gamma_C x''_W - \Gamma''_W x_C) + \nu_C(\Gamma''_W x_A - \Gamma_A x''_W) = 0 \tag{11}$$

$$\nu_B(\Gamma_C x''_W - \Gamma''_W x_C) + \nu_C(\Gamma''_W x_B - \Gamma_B x''_W) = 0 \tag{12}$$

$$\nu_A(\Gamma_B x_C - \Gamma_C x_B) + \nu_B(\Gamma_C\, x_A - \Gamma_A x_C) + \nu_C(\Gamma_A\, x_B - \Gamma_B x_A) = 0 \tag{13}$$

where x''_W and Γ''_W stand for

$$x''_W = x_W - \frac{x'_W}{x'_G}\, x_G \text{ and } \Gamma''_W = \Gamma_W - \frac{x'_W}{x'_G}\, \Gamma_G \tag{14}$$

Conditions (10) – (13) are not independent of each other. One can easily see e.g. that

$$(10) = \frac{\nu_B}{\nu_C}\ (11) - \frac{\nu_A}{\nu_C}\ (12)$$

On the other hand, by expressing Γ''_W/x''_W from eqs. (10) — (12) one obtains the following sequence of equalities :

$$\frac{\Gamma''_W}{x''_W} \equiv \frac{\Gamma_W-(x'_W/x'_G)\Gamma_C}{x_W-(x'_W/x'_G)x_C} = \frac{\nu_B\Gamma_A-\nu_A\Gamma_B}{\nu_Bx_A-\nu_Ax_B} = \frac{\nu_C\Gamma_A-\nu_A\Gamma_C}{\nu_Cx_A-\nu_Ax_C} = \frac{\nu_C\Gamma_B-\nu_B\Gamma_C}{\nu_Cx_B-\nu_Bx_C} \tag{15}$$

The above equalities yield eq. (13). Consequently, from eqs. (10) — (13) only two are independent from each other.

Since under experimental conditions the amounts of A and B are modified, it is convenient to choose μ_A and μ_B as independent variables. In this case the system of equations (8), by eliminating $d\mu_G$ between them may be written as :

$$\begin{aligned} d\sigma + \Gamma''_W d\mu_W + \Gamma_C d\mu_C &= -\Gamma_A d\mu_A - \Gamma_B d\mu_B \\ x''_W d\mu_W + x_C d\,\mu_C &= -x_A d\mu_A - x_B d\mu_B \qquad (8') \\ \nu_C d\mu_C &= -\nu_A d\mu_A - \nu_B d\,\mu_B \end{aligned}$$

or

$$\begin{vmatrix} 1 & \Gamma''_W & \Gamma_C \\ 0 & x''_W & x_C \\ 0 & 0 & \nu_C \end{vmatrix} d\sigma = -\begin{vmatrix} \Gamma_A & \Gamma''_W & \Gamma_C \\ x_A & x''_W & x_C \\ \nu_A & 0 & \nu_C \end{vmatrix} d\mu_A - \begin{vmatrix} \Gamma_B & \Gamma''_W & \Gamma_C \\ x_B & x''_W & x_C \\ \nu_B & 0 & \nu_C \end{vmatrix} d\mu_B \tag{8''}$$

Since the coefficient of $d\sigma$ is equal to $x''_W\nu_{/C}$, which can never be zero, the condition $d\sigma = 0$ will be fulfilled only if both right hand side determinants are equal to zero. These conditions yield eqs. (11) and (12). By eliminating between them the ratio Γ''_W/x''_W, one obtains the last equality (15) which may be written as :

$$\frac{x_A-(\nu_A/\nu_C)\,x_C}{x_B-(\nu_B/\nu_C)\,x_C} = \frac{\Gamma_A-(\nu_A/\nu_C)\Gamma_C}{\Gamma_B-(\nu_B/\nu_C)\Gamma} \tag{16}$$

It is easy to see that the left hand side of Eq. (16) represents the ratio between the overall amount of substance A, free and incorporated into the product C, and of substance B in the liquid bulk phase. The right hand side represents the same ratio for the interface. Therefore, eq. (16) may be written as

$$x^0_A/x^0_B = \Gamma^0_A/\Gamma^0_B \tag{16'}$$

The main conclusion is that at the surface tension extremum there is a resemblance between the composition of the bulk and of the surface phases.

We mention that by presuming eqs. (10)—(13) to be valid irrespective of the stoichiometry of reaction (1), i.e. of the numerical value of ν_A, ν_B and ν_C, one obtains

$$\frac{\Gamma''_W}{x''_W} = \frac{\Gamma_A}{x_A} = \frac{\Gamma_B}{x_B} = \frac{\Gamma_C}{x_C} \tag{17}$$

Eq. (17) is identical with Eq. (8.47) in [17] derived for systems in which no chemical reaction occurs. Eq. (17) claims the bulk and surface phases to have the same composition, at least with respect to components A, B and C, since in the case of G and W eq. (17) may be valid even if $\Gamma_W/x_W \neq \neq \Gamma_G/x_G$.

On the basis of the above discussions two possible hypotheses may be set forth :

1) Both presumptions : a) eqs. (10) — (13) are valid irrespective of the stoichiometry and b) no reaction occurs, are perfectly equivalent assumptions. Therefore, if a chemical reaction does occur, the validity of eq. (17) is not required, only eq. (15) will be valid. It is true that eq. (15) may be easily derived from eq. (17), but this means only that condition (17) is sufficient for the validity of (15), but it is not a necessary condition.

2) Presumptions a) and b) are not equivalent and if reaction (1) does occur, in eqs. (10) — (13) each expression multiplying a stoichiometric coefficient is equal to zero. Therefore, eq. (17) expresses a general property of systems exhibiting interfacial tension extrema, irrespective of the possibility of chemical reactions.

In order to choose between the above possibilities, we shall presume that hypothesis 1) is correct., i.e. eq. (15) may be valid even if eq. (17) is not. Let us presume that :

$$\Gamma_B/x_B = \beta \, \Gamma_A/x_A \text{ and } \Gamma_C/x_C = \gamma \, \Gamma_A/x_A \tag{18}$$

where β and γ differ from the unity. By combining eqs. (13) and (18) one obtains

$$\gamma = \frac{x_A}{x_C} \, \frac{\nu_C x_B - \nu_B x_C}{\nu_A x_B - \nu_B x_A} - \beta \, \frac{x_B}{x_C} \, \frac{\nu_C x_A - \nu_A x_C}{\nu_A x_B - \nu_B x_C} \tag{19}$$

Since ν_A and ν_B are negative numbers and ν_C is positive, the numerators of both terms in the right hand side of eq. (19) are always positive. If $x^0_A/x^0_B = \nu_A/\nu_B$, one has $\nu_A x_B = \nu_B x_A$ and in eq. (19) the denominator of both terms vanishes and eq. (19) becomes an $\infty - \infty$ type indetermination. In order to eliminate this indetermination, let us write eq. (19) in the following form :

$$\gamma = \frac{\nu_C x_A x_B (1 - \beta) - x_C(\nu_B x_A - \nu_A \beta \, x_B)}{x_C(\nu_A x_B - \nu_B x_C)} \tag{19'}$$

which is a 0/0 type indetermination. By using L'Hospital's rule, one obtains :

$$\lim_{\nu_A x_B \to \nu_B x_A} \gamma = 1 - \frac{\nu_C}{\nu_B} \, \frac{x_B}{x_C} (1 - \beta) \tag{20}$$

if the derivatives of the numerator and of the denominator of Eq. (19′) are calculated with respect to x_A and

$$\lim_{\nu_A x_B \to \nu_B x_A} \quad = \beta + \frac{\nu_C}{\nu_A}\frac{x_A}{x_B}(1 - \beta) \tag{21}$$

if derivation is performed with respect to x_B.

It is easy to see that eqs. (20) and (21) entail

$$\beta < 1 < \gamma < \beta \ \text{ for } \ \beta < 1$$
and
$$\gamma < 1 < \beta < \gamma \ \text{ for } \ \beta > 1$$

Consequently, the only possibility is to have $\beta = \gamma = 1$, which is in contradiction with our presumption that $\beta, \gamma \neq 1$. Therefore, hypothesis 1) cannot be correct. It follows the validity of hypothesis 2) and that the procedure, consisting of equalling to zero all expressions multiplying the stoichiometric coefficients in eqs. (10) – (13) is perfectly justified. Further, eq. (15) may be valid if, and only if also eq. (17) is respected. Therefore, the latter one is a generally valid relation for systems in which $d\sigma = 0$, both in the absence and in the presence of chemical reactions.

We mention the possibility of a simplified treatment of the above problems. By ignoring the component G and also the gaseous phase, one obtains $c = 4$ and $\varphi = 1$, eq. (2) yielding also $w_{Tp} = 2$ as above. In this case, instead of system (8), one obtains a system analogous with (8′) but having Γ_W and x_W instead of Γ_W'' and x_W'' respectively. Consequently, one can easily derive equations analogous with (10) – (12), (15) and (17), by substituting Γ_W and x_W for Γ_W'' and x_W'', respectively. Obviously, Eqs. (13) and (16) preserve their validity without any change.

O/W liquid/liquid interface

The number of components is $c = 5$, viz. O, W, A, B and C. Number of reactions $r = 1$, viz. reaction (1). According to eq. (4) one has $w_{Tp} = 2$, i.e. the system is also divariant as the previous one.

With respect to the solubilities : O and W are thought to be immiscible, A is presumed to be soluble in liquid O, but insoluble in W, reversely, B is thought to be soluble in W and insoluble in O. Under such conditions reaction(1) occurs in the interface. From thermodynamic point of view there are no completely immiscible liquids and completely insoluble substances. Consequently, we shall take into account the presence of all the components in each phase.

Eqs. (5) – (7) yield the following system :

$$\begin{aligned} d\sigma + \Gamma_0 d\mu_0 + \Gamma_W d\mu_W + \Gamma_A d\mu_A + \Gamma_B d\mu_B + \Gamma_C d\mu_C &= 0 \\ x_0' d\mu_0 + x_W' d\mu_W + x_A' d\mu_A + x_B' d\mu_B + x_C' d\mu_C &= 0 \\ x_0'' d\mu_0 + x_W'' d\mu_W + x_A'' d\mu_A + x_B'' d\mu_B + x_C'' d\mu_C &= 0 \\ \nu_A d\mu_A + \nu_B d\mu_B + \nu_C d\mu_C &= 0 \end{aligned} \tag{22}$$

where x'_i and x''_i stand for the molar fraction of the component *i* in the bulk phase in which the solvent is the liquid 0 and the liquid W, respectively.

By taking into account the above-mentioned solubility conditions it is obvious that :

$$x'_{\mathrm{W}} \ll x'_0,\ x''_0 \ll x^{\mathrm{W}}_{''},\ x''_{\mathrm{A}} \ll x'_{\mathrm{A}} \text{ and } x'_{\mathrm{B}} \ll x''_{\mathrm{B}} \tag{23}$$

Since the system is divariant and practically the amount of the components A and B, i.e. μ_{A} and μ_{B} are arbitrarily chosen, the system may be written as :

$$\begin{vmatrix} 1 & \Gamma_0 & \Gamma_{\mathrm{W}} & \Gamma_{\mathrm{C}} \\ 0 & x'_0 & x'_{\mathrm{W}} & x'_{\mathrm{C}} \\ 0 & x''_0 & x''_{\mathrm{W}} & x''_{\mathrm{C}} \\ 0 & 0 & 0 & \nu_{\mathrm{C}} \end{vmatrix} \mathrm{d}\sigma = - \begin{vmatrix} \Gamma_{\mathrm{A}} & \Gamma_0 & \Gamma_{\mathrm{W}} & \Gamma_{\mathrm{C}} \\ x'_{\mathrm{A}} & x'_0 & x'_{\mathrm{W}} & x'_{\mathrm{C}} \\ x''_{\mathrm{A}} & x''_0 & x''_{\mathrm{W}} & x''_{\mathrm{C}} \\ \nu_{\mathrm{A}} & 0 & 0 & \nu_{\mathrm{C}} \end{vmatrix} \mathrm{d}\mu_{\mathrm{A}} - \begin{vmatrix} \Gamma_{\mathrm{B}} & \Gamma_0 & \Gamma_{\mathrm{W}} & \Gamma_{\mathrm{C}} \\ x'_{\mathrm{B}} & x'_0 & x'_{\mathrm{W}} & x'_{\mathrm{C}} \\ x''_{\mathrm{B}} & x''_0 & x''_{\mathrm{W}} & x''_{\mathrm{C}} \\ \nu_{\mathrm{B}} & 0 & 0 & \nu_{\mathrm{C}} \end{vmatrix} \mathrm{d}\mu_{\mathrm{B}} \tag{24}$$

In (24) the coefficient of $\mathrm{d}\sigma$, i.e. $\nu_{\mathrm{C}}(x'_0 x''_{\mathrm{w}} - x_0 x'_{\mathrm{w}})$, according to (23) is always different from zero. Consequently, the condition to have $\mathrm{d}\sigma = 0$, irrespective of the value of $\mathrm{d}\mu_{\mathrm{A}}$ and $\mathrm{d}\mu_{\mathrm{B}}$, is that both determinants in the right hand side of eq. (24) to be equal to zero. One obtains :

$$\begin{aligned} &\nu_{\mathrm{A}}[\Gamma_0(x'_{\mathrm{W}}x''_{\mathrm{C}} - x'_{\mathrm{C}}x''_{\mathrm{W}}) + \Gamma_{\mathrm{W}}(x'_{\mathrm{C}}x''_0 - x'_0x''_{\mathrm{C}}) + \Gamma_{\mathrm{C}}(x'_0x''_{\mathrm{w}} - x'_{\mathrm{W}}x''_0)] = \\ &= \nu_{\mathrm{C}}[\Gamma_{\mathrm{A}}(x'_0x''_{\mathrm{W}} - x'_{\mathrm{W}}x''_0) + \Gamma_0(x'_{\mathrm{W}}x''_{\mathrm{A}} - x'_{\mathrm{A}}x''_{\mathrm{W}}) + \Gamma_{\mathrm{W}}(x'_{\mathrm{A}}x''_0 - x'_0x''_{\mathrm{A}})] \\ &\nu_{\mathrm{B}}[\Gamma_0(x'_{\mathrm{W}}x''_{\mathrm{C}} - x'_{\mathrm{C}}x''_{\mathrm{W}}) + \Gamma_{\mathrm{W}}(x'_{\mathrm{C}}x''_0 - x'_0x''_{\mathrm{C}}) + \Gamma_{\mathrm{C}}(x'_0x''_{\mathrm{W}} - x'_{\mathrm{W}}x''_0)] = \\ &= \nu_{\mathrm{C}}[\Gamma_{\mathrm{B}}(x'_0x''_{\mathrm{W}} - x'_{\mathrm{W}}x''_0) + \Gamma_0(x'_{\mathrm{W}}x''_{\mathrm{B}} - x'_{\mathrm{B}}x''_{\mathrm{W}}) + \Gamma_{\mathrm{W}}(x'_{\mathrm{B}}x''_0 - x'_0x''_{\mathrm{B}})] \end{aligned} \tag{25}$$

By taking into account the conclusions drawn from the discussion of the G/W interface, we can state that the system (25) must be valid irrespective of the value of ν_{A}, ν_{B} and ν_{C}. Consequently, all the expressions in square brackets in eqs. (25) must separately be equal to zero. Since in eqs. (25) the coefficients of ν_{A} and ν_{B} are the same, one obtains 3 conditions. By taking into account the inequalities (23), some simplifications may be made, viz. $x'_{\mathrm{W}}x''_0$ can be neglected before $x'_0x''_{\mathrm{W}}$, $x'_{\mathrm{A}}x''_{\mathrm{W}}$ before $x'_{\mathrm{A}}x''_{\mathrm{W}}$ and $x'_{\mathrm{B}}x''_{\mathrm{W}}$ before $x'_0x''_{\mathrm{B}}$. The above-mentioned 3 conditions take the following form :

$$\frac{\Gamma_{\mathrm{A}}}{x'_{\mathrm{A}}} \approx \frac{\Gamma_0}{x'_0} + \frac{\Gamma_{\mathrm{W}}}{x''_{\mathrm{W}}} \frac{x''_0 x'_{\mathrm{A}} - x''_{\mathrm{A}}x'_0}{x'_0x'_{\mathrm{A}}} \tag{26}$$

$$\frac{\Gamma_{\mathrm{B}}}{x''_{\mathrm{B}}} \approx \frac{\Gamma_{\mathrm{W}}}{x''_{\mathrm{W}}} + \frac{\Gamma_0}{x'_0} \frac{x'_{\mathrm{B}}x''_{\mathrm{W}} - x''_{\mathrm{B}}x'_{\mathrm{W}}}{x''_{\mathrm{B}}x''_{\mathrm{W}}} \tag{27}$$

$$\Gamma_{\mathrm{C}} \approx \frac{\Gamma_0}{x'_0}\left(x'_{\mathrm{C}} - x''_{\mathrm{C}}\frac{x'_{\mathrm{W}}}{x''_{\mathrm{W}}}\right) + \frac{\Gamma_{\mathrm{W}}}{x''_{\mathrm{W}}}\left(x''_{\mathrm{C}} - x'_{\mathrm{C}}\frac{x''_0}{x'_0}\right) \tag{28}$$

It is easy to see that the second term of the right hand side of both eqs. (26) and (27) can be neglected before the first term, since the denominator of the last fraction is practically equal to the molar fraction of a soluble compound (x'_A and x''_B, respectively), but the numerator is a difference between two products, containing both a vanishing factor (x''_0, x''_A, x'_W or x'_B, respectively). Consequently, one has a similitude between the composition of the interface and the bulk phases, viz.:

$$\frac{\Gamma_A}{x'_A} \approx \frac{\Gamma_C}{x'_C} \approx \frac{\Gamma_0}{x'_0} \text{ and } \frac{\Gamma_B}{x''_B} \approx \frac{\Gamma_W}{x''_W} \tag{29}$$

Concerning the product C, eq. (28) shows that if C is practically insoluble in both O and W, i.e. $x'_C, x''_C \ll x'_0, x''_W$, the second terms in both parentheses may be neglected before the first ones and one obtains

$$\Gamma_C \approx \frac{\Gamma_0}{x'_0} x'_C + \frac{\Gamma_W}{x''_W} x''_C \approx 0 \tag{28'}$$

i.e. reaction (1) practically does not occur at all.

Reaction (1) is possible only if C is soluble either in 0, or in W, or in both of them.

Let us presume that C is soluble in 0 and insoluble in W, i.e. $x''_C \ll \ll x'_C, x'_0, x''_W$. Under such conditions, eq. (28) becomes:

$$\Gamma_C \approx \frac{\Gamma_0}{x'_0} x'_C + \frac{\Gamma_W}{x''_W} \frac{x'_0 x''_C - x'_C x''_0}{x'_0} \tag{28''}$$

The second term in the right hand side of this equation may be neglected before the first one since the first factor of both products is of the same order of magnitude, but the second factor is not. x'_C has been presumed to have a finite value, whereas in the second factor of the second term the denominator is finite, but the numerator represents the difference between two vanishing products. It results that $\Gamma_C/x'_C \approx \Gamma_0/x'_0$ and eventually one obtains, instead of (29), the following conditions:

$$\frac{\Gamma_A}{x'_A} \approx \frac{\Gamma_C}{x'_C} \approx \frac{\Gamma_0}{x'_0} \text{ and } \frac{\Gamma_B}{x''_B} \approx \frac{\Gamma_W}{x''_W} \tag{30}$$

expressing even a more advanced similitude between the composition of the interface and the bulk phases than eqs. (29) do.

★

The above discussions show that the interfacial tension extremum implies a completely indifferent state of the system, as defined in[17a]. This state is characterized by a similitude between the composition of the interface and of the equilibrium liquid bulk phase/phases.

In the case of equilibria between bulk phases, among the indifferent states may exist states with uniform composition of the phases. [18] Uniform composition may be observed both in systems without chemical reactions (azeotrops) and in systems with chemical reactions. In the last case the composition of the phases corresponds to the composition of the addition compound formed.

Since the interface phase is a non-autonomous one,[17b] its composition can be the same as the composition of a bulk phase, only if it is situated between two bulk phases of uniform composition. In the case of the systems considered above, such a completely uniform composition is not possible, only with the G/W interface, and only in first approximation, by neglecting the presence of the gaseous phase and the presence of the component G in both the interface and in the liquid bulk phase.

Nevertheless, one may presume that the indifferent state characterized by the similitude between the composition of the interface and the liquid bulk phase/phases resembles the state of uniform composition in the case of equilibrium between bulk phases. Therefore, it seems to be reasonable to presume that if experimentally an interfacial tension extremum is observed, corresponding to a simple ratio $x_A^0/x_B^0 = a/b$, or $x'_A/x''_B = = a/b$, with a and b small integers, this might be assigned to the formation of an addition product, according to eq.(1) and even to have $a/b = \nu_A/\nu_B$.

REFERENCES

[1] E. Ferroni, G. Gabrielli and M. Ciarfuglia, *Ricerca sci.*, **25**, 539 (1955)

[2] E. Ferroni and G. Gabrielli, *Ann. Chim. (Rome)*, **45**, 715 (1955); *J. Phys. Chem.*, **60**, 1258 (1956)

[3] E. Ferroni, G. Gabrielli and E. Barbolani di Montanto, *Ann. Chim. (Rome)*, **46**, 459 (1956)

[4] N. Gagnioli, *Ann. Chim. (Rome)*, **48**, 839, 1122 (1958)

[5] G. Gabrielli, M. Marzocchi and S. Bartolini, *Ann. Chim. (Rome)*, **51**, 71 (1961)

[6] E. Chifu and G. Gabrielli, *Gazz. Chim. Ital.*, **98**, 1213 (1968)

[7] G. Gabrielli and M. Puggelli, *J. Colloid and Interface Sci.*, **33**, 484 (1970)

[8] H. J. Kazi and C. M. Desai, *Current Sci.*, **22**, 15 (1953); *J. Indian Chem. Soc.*, **30**, 287, 290, 421, 423, 424, 426 (1953); **31**, 163, 165, 633, 638, 640 (1954); **32**, 63 (1955)

[9] H. A. Heintz and D. N. Hume, *J. Phys. Chem.*, **61**, 462 (1957)

[10] E. Chifu, I. Albu and M. L. Huszár, *Studia Univ. Babeș-Bolyai, Chem.*, **16** (2), 15 (1971)

[11] E. Chifu and I. Albu, *Studia Univ. Babeș-Bolyai, Chem.*, **18**,(1), 81 (1973)

[12] E. Chifu, Z. Andrei and M. Tomoaia, *Ann. Chim. (Rome)*, **64**, 869 (1974)

[13] M. Tomoaia, Z. Andrei and E. Chifu, *Rev. Roumaine Chim.*, **18**, 1547 (1973)

[14] Z. Andrei and E. Chifu, *Studia Univ. Babeș-Bolyai, Chem.*, **21**, 10 (1976)

[15] E. Chifu and Z. Andrei, *Gazz. Chim. Ital.*, 107, 569 (1977)

[16] J. Demeter-Vodnár, M. Sălăjan, M. Tomoaia-Cotișel, J. Zsakó and E. Chifu, *Studia Univ. Babeș-Bolyai, Chem.*, **32** (1), 92 (1987)

[17] R. Defay, I. Prigogine, A. Bellemans and D. H. Everett, "Surface Tension and Adsorption" Longmans Green, London, 1966: a, p. 122; b, p. 56.

[18] I. Prigogine and R. Defay "Chemical Thermodynamics", Longmans Green, London, New York, Toronto, 1954.

In the case of equilibria between bulk phases, among the indifferent states may exist states with uniform composition of the phases.[18] Uniform composition may be observed both in systems without chemical reactions (azeotrops) and in systems with chemical reactions. In the last case the composition of the phases corresponds to the composition of the addition compound formed.

Since the interface phase is a non-autonomous one[17a] its composition can be the same as the composition of a bulk phase, only if it is situated between two bulk phases of uniform composition. In the case of the systems considered above, such a completely uniform composition is not possible, only with the G/W interface, and only in first approximation, by neglecting the presence of the gaseous phase and the presence of the component G in both the interface and in the liquid bulk phase.

Nevertheless, one may presume that the indifferent state characterized by the similitude between the composition of the interface and the liquid bulk phase phases resembles the state of uniform composition in the case of equilibrium between bulk phases. Therefore, it seems to be reasonable to presume that if experimentally an interfacial tension extremum is observed, corresponding to a simple ratio $x^s_A/x^s_B = a/b$, or $c^s_A/c^s_B = a/b$, with a and b small integers, this might be assigned to the formation of an addition product, according to eq. (1) and even to have $a/b = \nu_A/\nu_B$.

REFERENCES

[1] E. Ferroni, G. Gabrielli and M. Caerlugio, Ricerca sci., 25, 338 (1955)
[2] E. Ferroni and G. Gabrielli, Ann. Chim. (Rome), 45, 715 (1955); J. Phys. Chem., 60, 1258 (1956)
[3] E. Ferroni, G. Gabrielli and E. Bartholani di Montebello, Ann. Chim. (Rome), 48, 458 (1958)
[4] N. Gaguloff, Ann. Chim. (Rome), 48, 838, 1122 (1958)
[5] G. Gabrielli, M. Marzocchi and S. Bartolini, Ann. Chim. (Rome), 51, 71 (1961)
[6] E. Chifu and G. Gabrielli, Gazz. Chim. Ital., 98, 1219 (1968)
[7] G. Gabrielli and M. Puggelli, J. Colloid and Interface Sci., 32, 484 (1970)
[8] H. J. Keri and C. M. Desai, Current Sci., 22, 15 (1953); J. Indian Chem. Soc., 30, 287, 390, 421, 423, 424, 426 (1953); 31, 183, 195, 633, 638, 640 (1954); 32, 83 (1955)
[9] H. A. Hiemtz and D. N. Hume, J. Phys. Chem., 61, 382 (1957)
[10] E. Chifu, I. Albu and M. L. Ilussar, Studia Univ. Babeș-Bolyai, Chem., 16 (2), 14 (1971)
[11] E. Chifu and I. Albu, Studia Univ. Babeș-Bolyai, Chem., 18 (1), 61 (1973)
[12] E. Chifu, Z. Andrei and M. Tomoaia, Ann. Chim. (Rome), 64, 889 (1974)
[13] M. Tomoaia, Z. Andrei and E. Chifu, Rev. Roumaine Chim., 18, 1517 (1973)
[14] Z. Andrei and E. Chifu, Studia Univ. Babeș-Bolyai, Chem., 21, 10 (1976)
[15] E. Chifu and Z. Andrei, Gazz. Chim. Ital., 107, 569 (1977)
[16] J. Demeter-Vodnár, M. Salajan, M. Tomoaia-Cotișel, J. Zsakó and E. Chifu, Studia Univ. Babeș-Bolyai, Chem., 32 (1), 92 (1987)
[17] R. Defay, I. Prigogine, A. Bellemans and D. H. Everett, "Surface Tension and Adsorption", Longmans Green, London, 1966; a, p. 123; b, p. 36.
[18] I. Prigogine and R. Defay, "Chemical Thermodynamics", Longmans Green, London, New York, Toronto, 1954.

Revue Roumaine de Chimie, 35, 7—9, 853—858 (1990)

MAGNETIC INTERACTION BETWEEN NITROXIDE SPIN PROBES AND Cu(II) COMPOUNDS AS A METHOD FOR CHARACTERIZATION OF PENETRABILITY IN REVERSED MICELLES

H. CĂLDĂRARU[a], AGNETA CARAGHEORGHEOPOL[a], A. CĂLDĂRARU[b], M. DIMONIE[c], D. DONESCU[d], ILEANA DRĂGUȚAN[e] and M. MARINESCU[a]

[a] Romanian Academy, Institute of Physical Chemistry, Spl. Independenței 202, 77208 Bucharest, Romania;
[b] University of Bucharest, Department of Mathematics
[c] Polytechnic Institute — Bucharest;
[d] Research Institute for Plastic Materials, Bucharest;
Romanian Academy, Center of Organic Chemistry — Bucharest

The study by the spin probe technique of the reversed micelles formed in the cyclohexane/polyoxyethylene(4)nonylphenol/water system revealed that in the presence of a Cu(II) complex soluble only in cyclohexane, the ESR signal of the investigated nitroxide (confined only to the water-pool) loses its intensity without apparent broadening. The experimental results have been treated using Leigh's theoretical approach. This treatment led to quantitative data about the level of cyclohexane penetration through the surfactant chains of the micellar shell in terms of the amount of water in the aggregate.

Magnetic interaction between nitroxide spin probes and paramagnetic metal ions has been widely used for yielding useful information on systems of interest in biochemistry and biophysics.[1] The same interaction has gained interest in providing information about the location of the spin probe and implicitly on the structure of the micellar systems. [2] The nature of this interaction — either dipole-dipole or Heisenberg exchange — has been taken into account depending on the structure of the investigated system.[1]

The experimental results of Taylor's group [3] regarding the magnetic interaction between a spin probe (nitroxide) covalently bound to a protein and a Mn^{2+} ion in a specifically fixed position and the subsequent theoretical approach developed by Leigh[4] have been extensively exploited for measuring distances of interest in biological systems. The method measuring the radial distance between the spin probe (nitroxide) and the paramagnetic transition ion in a specific system is based on the experimental observation that the ESR signal of the spin probe loses its intensity without apparent broadening in the presence of the paramagnetic ion.

We have found the same behaviour when studying the aggregation pattern of reversed micelles (consisting of cyclohexane/polyoxyethylene(4) nonylphenol/water) by the spin probe technique in the presence of an "oil" only soluble Cu(II) complex. This observation has been further used for determining the "oil" (cyclohexane) penetrability in such aggregates and this work reports both the experimental observations and their treatment using Leigh's approach.

EXPERIMENTAL PART

Polyoxyethylene(4)nonylphenol (EO(4)NP) (commercial product) has been purified by repeated treatments with deionised water for removing the water soluble ethylene glycols. The final product has been dried in vacuum. Liquid chromatography analysis indicated an average number of 4.04 ethylene oxide units per molecule.

Cyclohexane has been dried on molecular sieves and then distilled. Deionized water freshly prepared has been used.

The water-only soluble nitroxide N,N,N-triethyl-N-(3-methylene-2,2,5,5-tetramethyl-2,5-dihydropyrrole-1-oxyl) ammonium bromide :

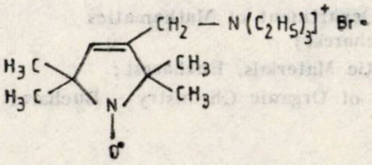

has been prepared as follows : to 0.2 g (0.858 mmol) of 3-bromomethyl-2,2,5,5,-tetramethyl' 2,5-dihydropyrrole-1-oxyl a five-fold molar excess of dry triethylamine was added and the red solution was heated for 2 hours at 80°C. The reaction mass has been triturated in ethyl ether and the resulting precipitate quickly filtered ; purification by crystallization from ethanol-ether afforded 0.13 g of the spin probe, light-brown crystals. m.p. 208—211°C (decomp.). IR spectrum (KBr pellet) : ν_{max} 1465, 2930, 2975 and 3050 cm^{-1}. Anal : Calc. for $C_{15}H_{30}N_2OBr$: C, 53.88 ; H, 9.04 ; N, 8.39 ; Br., 23.90. Found : C, 53.61 ; H, 8.78 ; N, 8.43 ; Br, 24.11.

The concentration of surfactant in cyclohexane has been 5.5×10^{-2} M. Various amounts of water were added to this solution and the resulting samples were mechanically stirred ; the concentration of water was measured by the Karl Fischer method. The resulting transparent solutions preserved their properties for months.

The spin probe (nitroxide) was added to the samples by the following procedure : the required amount of nitroxide in absolute ethanol was thoroughly evaporated in a volumetric flask and the sample was then added to give a concentration of the spin probe of 5×10^{-5} M ; the samples were shaken to assure the solubilization of the spin probe. Precautions have been taken for keeping both solution sample flasks and the ESR sample tubes tightly closed for preventing the constituent evaporation.

The cyclohexane soluble Cu(II) complex, CuX_2, where X = 1-methyl-2-carbethoxy-glyoxal-p-tolylanil-(1)-m-tolylhydrazone-(2) has the following formula :

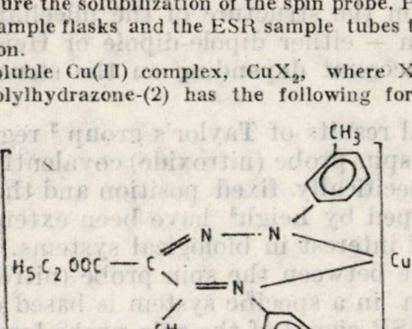

The ESR spectra were recorded at 25°C on a JES—3B(JEOL) spectrometer with 100 kHz field modulation using X-band frequency. Precautions on the microwave power and field modulation amplitude have been taken to avoid line broadening artifacts. The individual components of the nitrogen triplet were recorded with about 1G/min scan rate, each sample being measured 3—5 times for reproducibility. The parameters of the ESR spectra were measured in comparison with those of Fremy's salt ($a_N = 13.0$ G).

RESULTS AND DISCUSSION

The ESR spectrum of the spin probe in the investigated samples showed three symmetric lines, corresponding to unique location of the spin probe. Averaging between two locations is ruled out due to the insolubility of the spin probe in cyclohexane; in fact, we could not obtain its ESR spectrum in cyclohexane.

The ESR parameters (a_N and τ_c) of the spin probe in the investigated samples, as well as their water content (either in percentage or as molar water/surfactant ratio) are presented in Table 1; for comparison the values of the ESR parameters of the spin probe in water are given too.

The variation of a_N and τ_c with increasing of water content indicates the formation and increase of a water-pool in the micellar core.

The addition of CuX_2 complex, soluble only in cyclohexane, produces a decrease in the signal intensity of the spin probe, without apparent change in the line shape. This effect theoretically explained by Leigh [4] has been encountered by Taylor et al.[3,5] and Sarna et al.[6] for the paramagnetic metal ions (Mn^{2+}, Cu^{2+}, Gd^{3+}, other lanthanide ions) — radical interaction in systems of biological interests. Using Redfield theory, Leigh calculated the effect on the line shape of the A term of dipolar Hamiltonian for the paramagnetic ion — radical interaction. Under certain conditions, for a single ion — radical pair at a fixed distance he showed that the nitroxide radical line decreases in intensity with little apparent change in its shape. Sarna et al. [6] suggested that the same theory can be applied for circumstances somewhat different: a) more than one ion interacting with each radical, b) no single radial distance, c) no fixed orientation of the radial vector with respect to the nitroxide molecular coordinate system. Hyde and Rao [7] using the different approach of van Vleck's "method of moments" on the other terms (B, C, D, E and F) of the dipolar Hamiltonian calculated the saturation recovery and progressive saturation parameters for the case of

Table 1

The ESR parameters and $\bar{r}$, the calculated "distance of closest approach"

Sample	Water Content		a_N gauss	$\tau_c(10^{-10})$ s	$\bar{r}$ Å
	% H_2O	$[H_2O]/[EO(4)NP]$			
0	0.001	0.0	14.09[a]	a	—
1	0.07	0.55	15.09	5.4	13.6
2	0.33	2.55	15.48	2.7	22.5
3	0.88	6.91	15.68	1.4	33.4
Water			15.93	0.6	

[a] very weak spectrum

more than one paramagnetic ion interacting with the spin probe at varying radial distances. They concluded that the effects are dominated by the "distance of closest approach" between the radical and ion, extending this conclusion to the Leigh-type experiments [8].

Our experimental observations of apparent loss of intensity in the nitroxide radical spectra were treated theoretically within the frame of the above circumstances. These observations can be explained by assuming that the CuX_2, complex approaches the spin probe confined to the water-pool, penetrating between the surfactant chains of the aggregates. The distance between probe and Cu^{2+} ion is an approximate measure of the level of cyclohexane penetration.

For obtaining the quantitative information about the "distance of closest approach" using Leigh's theory[4], our experiments were performed as follows : the samples containing the spin probe were treated with CuX_2 complex until successive addition brought no decrease in the signal amplitude. In each case this spectrum was compared with a blank spectrum of the same sample with no CuX_2 in it. Typical examples of such spectra are given in Figure 1.

Within the frame of Leigh's theory each line of Lorentzian shape which makes up the spectrum is broadened by dipolar interaction with the paramagnetic ion, its line shape function being :

$$L(\theta, \varphi, H) = \frac{\delta H}{\delta H^2 + (H - H_0)^2} \tag{1}$$

where

$$\delta(H(\theta, \varphi) = C(1 - 3 \cos^2 \theta_r')^2 + \delta H_0 \tag{2}$$

and

$$\cos \theta_r' = \sin \theta_r \sin \theta \cos (\varphi_r - \varphi) + \cos \theta_r \cos \theta \tag{3}$$

and

$$C = \frac{g \beta \mu^2 T_{1k}}{\hbar^2 r^6} \tag{4}$$

Here (θ, φ) and (θ_r, φ_r) are the (azimuthal, polar) angles of the applied field H and of the radial vector (of r magnitude) between the spin probe and the paramagnetic ion respectively, θ_r' is the azimuthal angle between the radial vector and the H field direction, δH_0 is the linewidth in the absence of dipolar broadening ; μ is the effective magnetic moment of the paramagnetic ion, T_{1k} is its spin-lattice relaxation time. The broadened composite line shape is obtained by integrating over all possible orientations θ, φ in the expression :

$$L(H) = \int_0^{2\pi} \int_0^{\pi} L(\theta, \varphi, H) \sin\theta d\theta d\varphi \tag{5}$$

In our case of the isotropic radical motion within a relative confined volume (water-pool) characterized by no fixed orientation of the radial vector with respect to the nitroxide coordinate system and by no single radial distance, the definitions of θ_r and φ_r in eq. (3) are arbitrary [4] and r in eq. (4) becomes $\bar{r}$, the "distance of closest approach".

A computer program for solving the combined equations (1) — (5) has been developed on an IBM PC—XT computer, yielding the absorption line shape and its derivative.

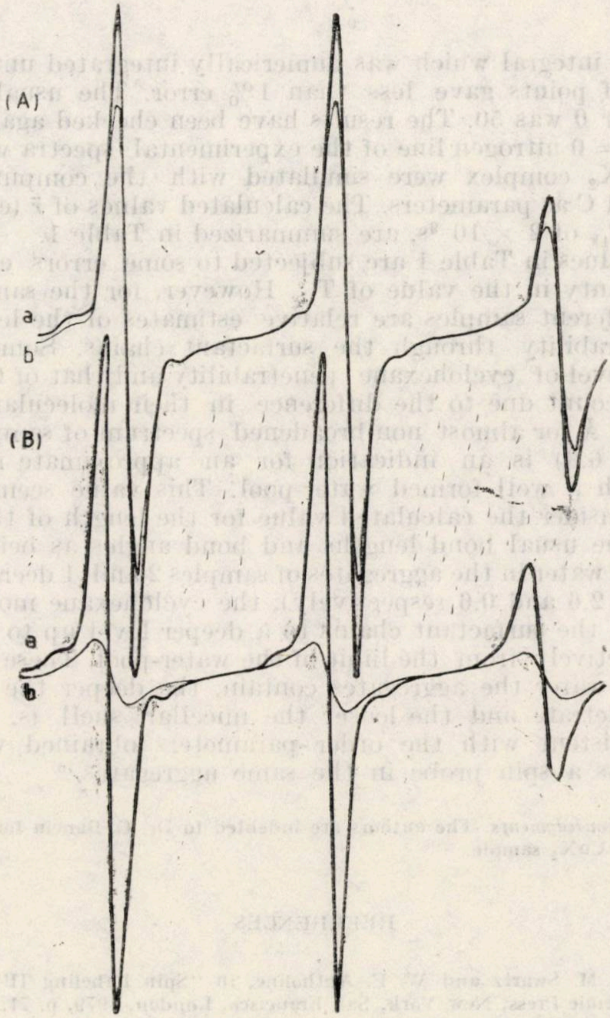

Fig. 1. — ESR spectra of the spin probe in (A) sample 2 (0.33 % H_2O) and (B) sample 1 (0.07 % H_2O) : a) without CuX_2 and b) with CuX_2.

A first program was written according to Leigh's original formula (5). The numerical integration of the two-variable integral required a considerable amount of time. As the θ_r value is arbitrary in our case, a second program was written using the particular $\theta_r = 0$ value. In this case formula (3) becomes :

$$\cos\theta_r' = \cos\theta$$

which does not depend on φ. So (5) becomes:

$$L(H) = 2\pi \int_0^\pi L(\theta, H) \sin\theta \, d\theta$$

a one-variable integral which was numerically integrated until increasing the number of points gave less than 1% error. The usual number of points used for θ was 50. The results have been checked against Leigh's.

The $m_I = 0$ nitrogen line of the experimental spectra without CuX_2 and with CuX_2 complex were simulated with the computer program, using δH_0 and C as parameters. The calculated values of $\bar{r}$ (eq. (4)), using a value[9] for T_{1k} of 2×10^{-9}s, are summarized in Table 1.

The $\bar{r}$ values in Table 1 are subjected to some errors chiefly due to some uncertainty in the value of T_{1k}. However, for the same T_{1k}, the $\bar{r}$ values for different samples are relative estimates of the level of cyclohexane penetrability through the surfactant chains. Some differences between the level of cyclohexane penetrability and that of CuX_2 may be taken into account due to the difference in their molecular size. The $\bar{r}$ value of ~ 33 Å for almost non-broadened spectrum of sample 3 ($[H_2O]/[EO(4)NP] = 6.9$) is an indication for an approximate radius of the aggregate with a well formed water-pool. This value seems reasonable good if we consider the calculated value for the length of the surfactant chain from the usual bond lengths and bond angles as being 30 Å. As the amount of water in the aggregates of samples 2 and 1 decreases ($[H_2O]/[EO(4)NP] = 2.6$ and 0.6 respectively), the cyclohexane molecules penetrate through the surfactant chains to a deeper level up to ~ 23 Å and ~ 14 Å respectively from the limit of the water-pool. These results show that the less water the aggregates contain, the deeper the cyclohexane molecules penetrate and the looser the micellar shell is. These data are also consistent with the order parameters obtained with 5-doxyl stearic acid as a spin probe in the same aggregates.[10]

Acknowledgments. The authors are indebted to Dr. C. Banciu for a generous gift of a CuX_2 sample.

REFERENCES

[1] J. S. Hyde, H. M. Swartz and W. E. Antholine, in "Spin Labeling II", ed. L. J. Berliner, Academic Press, New York, San Francisco, London, 1979, p. 71.

[2] J. Oakes, *Nature*, **231**, 38 (1971).

[3] J. S. Taylor, J. S. Leigh Jr. and M. Cohn, *Proc. Natl. Acad. Sci.* USA, **64**, 219 (1969).

[4] J. S. Leigh Jr., *J. Chem. Phys.*, **52**, 2608 (1970).

[5] M. Cohn, H. Diefenbach and J. S. Taylor, *J. Biol. Chem.*, **246**, 6037 (1971).

[6] T. Sarna, J. S. Hyde and H. M. Swartz, *Science*, **192**, 1132 (1976).

[7] J. S. Hyde and K. V. S. Rao, *J. Magn. Resonance*, **29**, 509 (1978).

[8] R. C. Sealy, C. C. Felix, J. S. Hyde and H. M. Swartz, in "Free Radicals in Biology", ed. W. A. Pryor, Academic Press, New York, London, Toronto, Sydney, San Francisco, 1980, p. 209.

[9] W. B. Lewis, M. Alei Jr. and L. O. Morgan, *J. Chem. Phys.*, **45**, 4003 (1965).

[10] H. Căldăraru, A. Caragheorgheopol, M. Dimonie, D. Donescu, I. Drăguţan and M. Marinescu, to be published.

Revue Roumaine de Chimie, **35**, *7–9*, 859–866 (1990)

EFFECT OF SURFACTANTS ON THE ELECTROREDUCTION OF ACRYLONITRILE

LIVIU ONICIU [a], IOAN A. SILBERG [b], DAN A. LÖWY [b], MARIA JITARU [b],
FLORENTINA CIOMOŞ[b], OVIDIU HOREA OPREA [b], BOGDAN C. TOMA[b]
and MARIANA TOMA[b]

[a] University of Cluj-Napoca, Department of Physical Chemistry, Cluj-Napoca, Romania
[b] ICECHIM – Institute of Chemical and Biochemical Energetics, Cluj-Napoca Research Group, Cluj-Napoca, Romania

Comparative experiments of acrylonitrile electroreduction on Pb *vs.* PbO_2 electrodes in neutral phosphate buffer, with – or without cationic surfactants demonstrated that the selectivity of the process is essentially under the control of the quality and quantity of the quaternary ammonium salt added. Thus, in the absence of surfactants, the process is directed towards the non-dimerizant electroreduction leading with high selectivity to propionitrile, whereas at levels of about ten times the critical micellar concentration the surfactant ensures a preponderant formation of the electrohydrodimerization products: adiponitrile and traces of methylglutaronitrile. At the same time, the phase transfer catalysis effect exerted by the surfactant entails, besides a favourable influence on the dimerizant electroreduction, an increased formation of water cyanoethylation products.

GLOSSARY

AcN	– acrylonitrile
PN	– propionitrile
AdN	– adiponitrile
MGN	– methylglutaronitrile
TCH	– 1,3,5 and 1,3,6-tricyanohexanes
HOPN	– β-hydroxypropionitrile
bCEE	– bis(cyanoethyl)ether
QAS	– quaternary ammonium salt
ATA^+Cl^-	– alkyltrimethylammonium chloride
$DDPA^+$ Cl^-	– diallyldipropylammonium chloride
$DDMA^+Cl^-$ – AA	– copolymer of diallyldimethylammonium chloride with acrylamide
CMC	– critical micellar concentration
NDE	– non-dimerizant electroreduction
EHD	– electrohydrodimerization
IHP	– inner Helmholtz plane
OHP	– outer Helmholtz plane

INTRODUCTION

Two competing processes occur when the homogeneous double bond of acrylonitrile (AcN) is electrochemically reduced: the well-known "Baizer reaction" – an electrohydrodimerization (EHD) resulting in adiponitrile (AdN) and methylglutaronitrile (MGN), and a less studied non-dimerizant electroreduction (NDE), leading to propionitrile (PN).

The early technologies of AdN electrosynthesis elaborated by Monsanto are strongly dependent on the pH value of the used electrolyte, an increase of pH from 5 — 10.3 favouring the NDE. [1] A more significant influence is exerted upon the selectivity of AcN electroreduction by the different species present in the electrolytic medium, especially those preponderantly adsorbed at the electrode surface, namely the surfactants. [2,3] Thus, a quaternary ammonium salt (QAS) facilitates the access of AcN at the cathode by lowering the lyophilic character of the interface.[4,5] Meanwhile, the cationic surfactant acts in the bulk phase too; its phase-transfer catalysis effect in EHD of AcN has been primarily mentioned by Oniciu *et al.* [6]

Recent experimental data, obtained by an NMR-investigation of aqueous solutions of AcN in the presence of relatively high concentrations (over ten folds the critical micellar concentration) of the used surfactant, brought direct evidences for the formation of AcN-quaternary ammonium salt cation complexes. [7]

In order to demonstrate the influence exerted by different cationic surfactants upon the selectivity of AcN electroreduction, experiments were carried out on Pb *vs.* PbO_2 electrodes, in neutral aqueous phosphate buffer solution, containing approximately ten times critical micellar concentrations (CMC) of four QAS. Blank experiments were effectuated without adding any surfactant.

There has been stated that both the selectivity and mechanism of the process are essentially controlled by the nature and the concentration of the surfactant. Thus, in the absence of QAS and at concentrations less than, or equal to CMC, an electroreduction leading mainly to PN occurs, while at concentrations above CMC, EHD processes are preponderant.

EXPERIMENTAL

The experimental set-up, consisting of an undivided pressfilter-type electrochemica reactor, fitted with monopolar electrodes, an on-line degassing vessel, in which anodic gases leave the system, a heat exchanger and a circulation pump, was previously described. [2] The electrode couple is connected to a stabilized direct current source. Cell voltage current intensity and temperature are monitored.

The neutral aqueous phosphate buffer supporting electrolyte, having a theoretical ionic strength of 1.19 (assuming full ionization), also contains a cationic surfactant : a symmetric or unsymmetric QAS with saturated or partially unsaturated alkyl chains. The behaviour of the following cationic surfactants was investigated :

- alkyltrimethylammonium chloride ($ATA^+ Cl^-$), manufactured by Intreprinderea de Detergenţi Timişoara. The surfactant is of technical grade ; it has the average molecular weight of 275.5 and contains approximately 60% C_{12} and 40% C_{14} alkyl chains
- diallyldipropylammonium chloride ($DDPA^+ Cl^-$), prepared by ICPAO — Mediaş,
- copolymer of diallyldimethylammonium chloride with acrylamide ($DDMA^+ Cl^-$ — AA) purchased from the "Petru Poni" Institute, Iaşi ;
- alkylbenzyldimethylammonium chloride, Intreprinderea de Detergenţi Timişoara.

RESULTS AND DISCUSSION

The products of AcN electroreduction obtained in 8 hours experiments under the above-mentioned conditions were analyzed by gas-chromatography with an M—9 type modular chromatograph (ITIM — Cluj-Napoca), according to a previously described method.[8] The concentration of the cationic surfactants in the aqueous phase was monitored by potentiometric titration, using an original liquid-membrane surfactant-selective electrode.[4] For multicomponent samples a new, heteropolyanionic titrant was used.[9]

Rigorous material balances of the electroreduction experiments were effectuated by taking into account of the individual and global solubilities of AcN and PN in the aqueous phosphate buffer medium[10]

The results of AcN electroreduction experiments, in the absence of cationic surfactants and at different concentration levels of saturated and unsaturated alkyl-chain QAS, are listed in *Table*. All results are recalculated for a current intensity of 10A. All data given in *Table* are average values of 3—5 experimental results.

NDE of AcN is the preponderant process (PN selectivity 91.5 ± 5%), in the absence of cationic surfactants; negligible quantities of impurities are formed (0.4 — 1.1%, w/w, of the transformed AcN), whereas dimerizant electroreduction (EHD) of AcN has a low contribution (3.3 to 12.1%, w/w, of the transformed AcN yields AdN).

A plausible explanation of the poor EHD under the mentioned conditions can be given considering the mechanism of the processes.[6,11] The splitting of the competing reactions occurs in the very moment, when the twice electronated and single protonated intermediary species (AcNH :⁻) is rejected from the surface of the cathode:

$$\underset{\text{AcN}}{CH_2=CH-CN} \xrightarrow{+e^-} \underset{\text{AcN}^-.}{/CH_2-CH-CN/^{\overline{\cdot}}} \xrightarrow[-HO^-]{+H_2O} \underset{\text{AcNH.}}{/CH_2-CH_2-CN/^{\cdot}} \xrightarrow{+e^-} \underset{\text{AcNH}^{\overline{:}}}{/CH_2-CH_2-CN/^{\overline{:}}} \qquad (1)$$

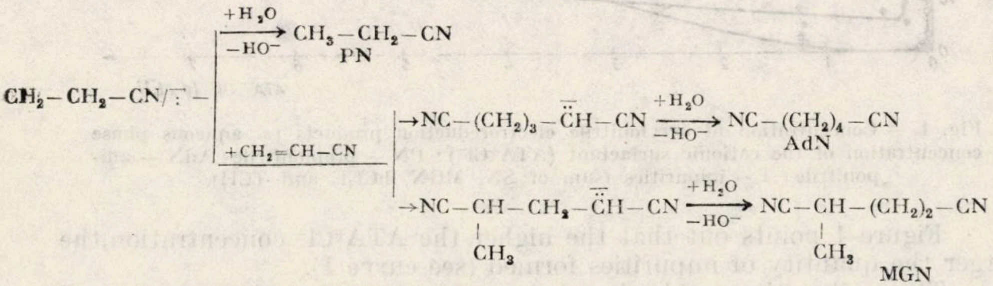

$$CH_2-CH_2-CN/^{\overline{:}}- \begin{cases} \xrightarrow[-HO^-]{+H_2O} \underset{\text{PN}}{CH_3-CH_2-CN} & (2) \\ \xrightarrow{+CH_2=CH-CN} \begin{cases} \to NC-(CH_2)_3-\overset{\overline{..}}{C}H-CN \xrightarrow[-HO^-]{+H_2O} \underset{\text{AdN}}{NC-(CH_2)_4-CN} & (3) \\ \to NC-\underset{CH_3}{\underset{|}{C}H}-CH_2-\overset{\overline{..}}{C}H-CN \xrightarrow[-HO^-]{+H_2O} \underset{\text{MGN}}{NC-\underset{CH_3}{\underset{|}{C}H}-(CH_2)_2-CN} & (4) \end{cases} \end{cases}$$

In our opinion the first three steps (sequence 1) take place in adsorbed form at the electrode surface,[6,12,13] while the competing processes: step (2) or sequence (3) occur in the bulk phase.[14]

In the absence of QAS, the Michael addition of the nucleophilic reactant AcNH⁻̣ to a neutral AcN molecule is hindered. This is why in experiments 1—4 in *Table*, NDE is predominant.

Though it diminishes to 65.1 ± 7%, NDE remains preponderant in examples 5 and 6, at ATA^+Cl^- concentrations approximately equal to and less than CMC.

The best selectivities of AdN formation are found at $ATA^+ Cl^-$ concentrations from CMC up to or depassing ten folds CMC (experiments

7 and 8), where the amount of EHD is from 60.5 to 86.7%. As seen in Figure 1 EHD reaches a maximum (92 ± 2%) at about six folds CMC of ATA^+Cl^-. This value corresponds to an initial amount of ten folds CMC (2.0 ± 0.2 $g.L^{-1}$) ATA^+Cl^- in the aqueous phase, [15] a concentration which, due to the partition after adding the organic phase, decreases to sixfolds CMC (about 1.2 $g.L^{-1}$). The kinetics of the partition was previously described [10]; 89.1% of the equilibrium is reached within 30 minutes and the partition is complete in 2 hours.

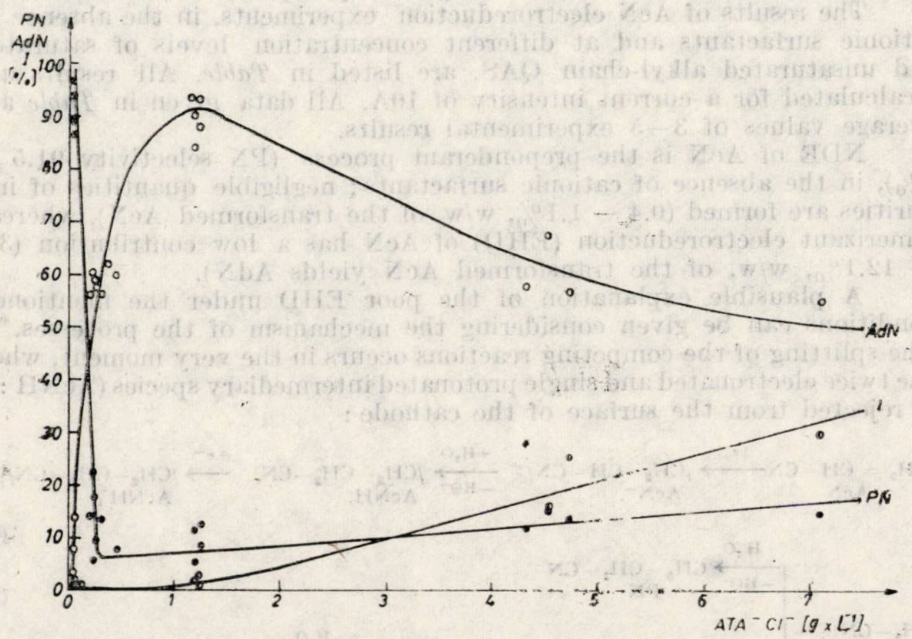

Fig. 1. — Concentration of acrylonitrile electroreduction products *vs.* aqueous phase concentration of the cationic surfactant (ATA^+Cl^-): PN — propionitrile; AdN — adiponitrile; I — impurities (sum of SN, MGN, bCEE and TCH).

Figure 1 points out that the higher the ATA^+Cl^- concentration, the larger the quantity of impurities formed (see curve I).

The explanation resides in a better phase transfer catalysis, ensured by the presence of cationic surfactants, which amplifies the chemical cyanoethylation reactions of water, leading to HOPN and bCEE. [16] For similar reasons, trimerizations to TCH are promoted too.

For a better understanding of the phenomena, let us consider Figure 2! In the absence of cationic surfactants, AcN molecules are adsorbed on a hydrated electrode surface (Fig. 2a). For a simpler representation, cations and anions of the phosphate buffer supporting electrolyte are neglected both in Fig. 2a and 2b.

After leaving the OHP, the reduced form ($AcNH_2^-$) might encounter in the bulk phase a proton-donator water molecule, an event resulting in the formation of PN. This process is far more probable than the conden-

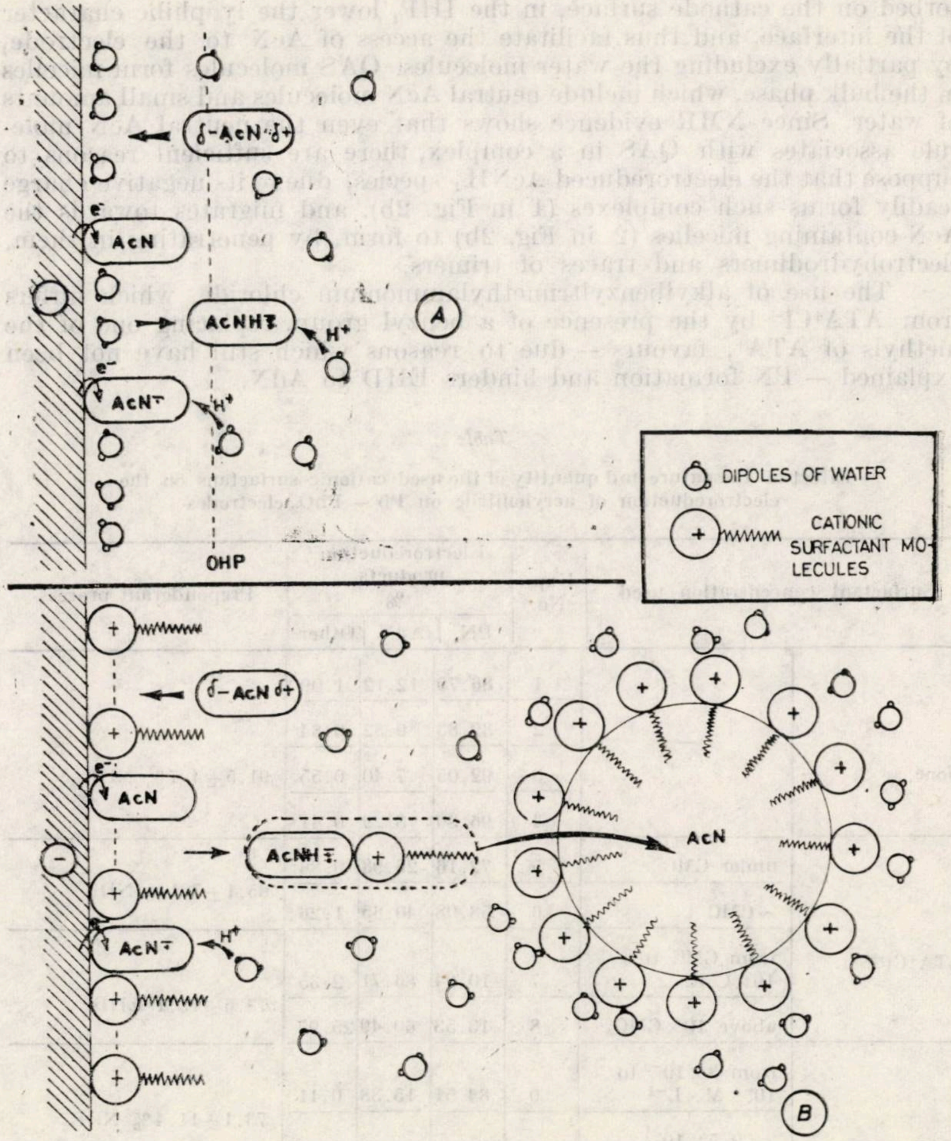
δ- AcN δ+
e⁻
AcN
AcNH·⁻
A
H⁺
e⁻
AcN⁻
H⁺
OHP
DIPOLES OF WATER
CATIONIC SURFACTANT MOLECULES
δ- AcN δ+
e⁻
AcN
⊖
AcNH·⁻
+
AcN
e⁻
AcN⁻
H⁺
B

Fig. 2. — Schematic representation of the cathode surface during acrylonitrile electroreduction. a) non-dimerizant electroreduction : hydrated electrode surface ; b) electrohydrodimerization : lyophilized cathode surface, by adsorbed cationic surfactant molecules. The electroreduced form, $AcNH_{\cdot}^{-}$, rejected from the cathode, migrates as an $AcNH^{-}$: — QAS complex (1) towards the AcN-containing micelle (2) in the bulk phase. The condensation process, resulting in hydrodimers, takes place inside the micelle.

sation of $AcNH_{\cdot}^{-}$ with a neutral AcN molecule to form AdN or MGN according to equation (3) and (4), respectively.

In the presence of QAS, a more complicated structure of the electrical double layer is to be assumed (Fig. 2b). The surfactant molecules, adsorbed on the cathode surface, in the IHP, lower the lyophilic character of the interface, and thus facilitate the access of AcN to the electrode, by partially excluding the water molecules. QAS molecules form micelles in the bulk phase, which include neutral AcN molecules and small amounts of water. Since NMR evidence shows that even the neutral AcN molecule associates with QAS in a complex, there are sufficient reasons to suppose that the electroreduced $AcNH_{\dot{2}}^{-}$ species, due to its negative charge readily forms such complexes (1 in Fig. 2b), and migrates towards the AcN-containing micelles (2 in Fig. 2b) to form, by penetrating in them, electrohydrodimers and traces of trimers.

The use of alkylbenzyltrimethylammonium chloride, which differs from ATA^+Cl^- by the presence of a benzyl group, replacing one of the methyls of ATA^+, favours — due to reasons which still have not been explained — PN formation and hinders EHD to AdN.

Table

Effect of the nature and quantity of the used cationic surfactans on the electroreduction of acrylonitrile on Pb — PbO_2 electrodes

Surfactant concentration used		Exp. No.	Electroreduction products %			Preponderant process
			PN	AdN	Other	
None	—	1	86.79	12.12	1.09	91.5±4.7% NDE
		2	89.83	9.32	0.84	
		3	92.05	7.40	0.55	
		4	96.30	3.29	0.41	
ATA^+Cl^-*	under CMC	5	72.16	26.98	0.86	65.1±7.1% NDE
	~CMC	6	58.08	40.65	1.26	
	from CMC to 10×CMC	7	10.94	86.71	2.35	73.6±13.1 EHD
	above 10×CMC	8	13.53	60.49	25.97	
$DDPA^+Cl^-$*	from 3×10^{-3} to 10^{-2} $M\times L^{-1}$	9	84.51	15.38	0.11	73.1±11.4% NDE
	$2-2.5\times10^{-1}$ $M\times L^{-1}$	10	61.72	36.85	1.42	
	$4-5.0\times10^{-2}$ $M\times L^{-1}$	11	27.67	70.12	2.21	78.4±8.3% EHD
		12	10.88	86.73	2.39	
$DDMA^+Cl^-$— — AA*	10 $g\times L^{-1}$	13	75.36	24.64	—	82.2±6.8% NDE
		14	88.95	11.05	—	

* See text

The influence exerted by different QAS-s upon the selectivity of NDE of AcN to PN had been previously investigated[5]. Preliminary investigations outlined that when working at concentrations less than, or equal to CMC, PN is formed with better selectivity in the presence of QAS-s having unsaturated alkyl chains : DDPA^{+}Cl^{-} or DDMA^{+}Cl^{-} — AA, than with ATA^{+}Cl^{-}.

Similar results are obtained by adding large quantities of DDMA^{+}Cl^{-} — AA : at concentrations of about 10 g $\times$ L^{-1}, NDE attains 82.2 $\pm$ $\pm$ 6.8%.

However, as shown in examples 11 and 12 of Table, at high concentration levels of DDPA Cl^{-} : $4.0-5.0 \times 10^{-1}$ M $\times$ L^{-1}, corresponding to approximately 1%, EHD occurs with good selectivity (up to 86.7 %).

We have to stress here that none of the industrialized AdN technologies uses unsaturated QAS-s[17].

CONCLUSIONS

Besides the widely used saturated short carbon-chain quaternary ammonium salts, like tetraethyl-, tributylethyl- and tetrabutylammonium sulfates, ethylsulfates or phosphates, several cationic surfactants are able to ensure the selctive EHD of AcN to AdN. Unlike literature data[3], the effectiveness of the examined QAS-s was not a function of the molecular size of the cation; concentration plays a much more important part. Consequently, the maintenance of well-defined QAS concentrations in order to control the selectivity of the EHD and to minimize side reactions, such as NDE to PN and cyanoethylations to HOPN and bCEE, is necessary; thus, an accurate monitoring of surfactant concentrations is indispensable.

In the absence of any surfactants, cathodic reduction of AcN leads to PN with very good selectivities.

REFERENCES

[1] M. M. Baizer, Fr. Pat. 82591 (1964).

[2] D. E. Danly, "Processes for Electrohydrodimerization of Acrylonitrile to Adiponitrile", Paper No. 1f, presented at the *AIChE 89th National Meeting*, August, 1980.

[3] W. V. Childs and H. C. Walters, *AIChE Syposium Series*, **185**, 75 : 19 (1979).

[4] L. Oniciu, D. A. Löwy, I. A. Silberg and D. F. Anghel, *Analysis*, **14**, 456 (1986).

[5] L. Oniciu, I. A. Silberg, D. A. Löwy, M. Jitaru and F. Ciomoş, *Studia Univ. Babeş-Bolyai Chemia*, **31**, 80 (1986).

[6] L. Oniciu, I. A. Silberg, I. Bâldea, F. Ciomoş, M. Jitaru, D. A. Löwy, O. H. Oprea and L. Radu, "Kinetics of Competing Reactions of Acrylonitrile Electroreduction to Adiponitrile and Propionitrile", *Proceedings of the 36th Meeting of ISE*, Salamanca, Spain, September 23—28, 1985, p. 13010.

[7] L. Oniciu *et al.*, to be published.

[8] D. A. Löwy, I. A. Silberg and L. Oniciu, *Rev. Chim.* (*Bucharest*), **36**, 354 (1985).

[9] A. Pătruţ and D. A. Löwy, *Rev. Chim.* (*Bucharest*), in press.

[10] L. Oniciu, D. A. Löwy, M. Jitaru, I. A. Silberg and B. C. Toma, *Rev. Roum. Chim.*, **32**, 701 (1987).

[11] L. Oniciu, D. A. Löwy and M. Jitaru, *Bull. Electrochem.*, **4**, 1041 (1988).

[12] L. Oniciu, M. Jitaru, D. A. Löwy, I. A. Silberg, B. C. Toma and I. Bâldea, "Kinetics and Mechanism of the Non-dimerizant Electroreduction of Acrylonitrile to Propioni-

trile", *Proceedings of the 38th Meeting of ISE*, Maastricht, The Netherlands, Sept. 1987, p. 285.

[13] L. Oniciu, D. A. Löwy, M. Jitaru, I. A. Silberg, B. C. Toma and I. Bâldea, *Rev. Chim. (Bucharest)*, **39**, 219 (1988).

[14] L. Oniciu, I. A. Silberg, I. Bâldea, F. Ciomoş, D. A. Löwy, M. Jitaru and O. H. Oprea, *Proceedings of the Second Symposium of Applied Electrochemistry*, Timişoara, 1985, Tome I, p. 201.

[15] L. Oniciu, I. A. Silberg, F. Ciomoş, M. Jitaru, P. Popescu, D. A. Löwy and O. H. Oprea, Romanian Pat. 88417, May 15 (1985).

[16] Oniciu, L., I. A. Silberg and F. Ciomoş, *Rev. Chim. (Bucharest)*, **36**, 406 (1985).

[17] R. Robert, R. P. Quellette and P. N. Chemisionoff, "Industrial Applications of Electroorganic Synthesis", Ann Arbor Science, Butterworth, p. 124.

Revue Roumaine de Chimie, 35, 7–9, 867–877(1990)

PROTOLYTIC EQUILIBRIA IN SURFACE SOLUTIONS OF STEARIC ACID, PROCAINE AND BENZOIC ACID AT THE AIR/WATER INTERFACE

JÁNOS ZSAKÓ[a], MARIA TOMOAIA-COTIŞEL[a], EMIL CHIFU[a], IOSIF ALBU[a], AURORA MOCANU[a] and PETRE T. FRANGOPOL[b]
[a] University of Cluj-Napoca, Physical Chemistry Department,
3400 Cluj-Napoca, Romania
[b] Institute of Physics and Nuclear Engineering, PO Box MG-6, R–76900,
Măgurele — Bucharest, Romania

Compression isotherms, i.e. surface pressure vs. molecular area curves of stearic acid monolayers, spread at the air/aqueous solution interfaces are recorded. The influence of benzoic acid and of procaine, dissolved in the subphase as well as of the subphase pH is studied. Benzoic acid and especially procaine have an expanding and fluidizing effect upon the monolayer of stearic acid. Procaine has also a stabilizing effect, indicated by increase of the collapse pressure of the monolayer. Surface characteristics are derived from the compression isotherms and state equations are established. Results are discussed in terms of penetration and subsequent expulsion of the subphase molecules during the compression of the monolayer, by taking into account the protolytic equilibria in which both the stearic acid and subphase molecules participate.

INTRODUCTION

Studies performed by using different experimental techniques showed some anesthetics to increase the fluidity of lipid bilayers, [1] to decrease the order in hydrocarbon chains, [2,3] to lower the temperature of the gel to liquid crystal phase transition, [4,5] to extend the surface area of both monolayer films maintained at constant surface pressure, [6,7] and of erythrocyte membranes, [6,8] and to increase the surface pressure of lipid films maintained at constant area. [9–12]

Although these experiments involve different physical parameters, presumably, the molecular origin of the effects observed is the same, viz. the weakening of the packing of lipids due to the anesthetic molecules inserted. [7]

The investigations concerning the mechanism of anesthesis, and the mechanism of the interactions between anesthetics and biomembranes revealed that there is a direct correlation (direct proportionality) between the efficiency of local anesthetics in blocking the nervous conduction and their penetration into the lipid monolayers. This penetration has been evidenced by the energies of interaction of anesthetics with phospholipid monolayers spread at the air/water interface. [11]

Similarly, there is a direct proportionality also between the efficiency of anesthetics and the following physico-chemical parameters: adsorption free energies of anesthetics at the air/water interface, their surface activity, partition coefficients of anesthetics between aqueous solutions and non-aqueous phase, from which eventually the standard free energies associated with the transfer of anesthetics from the aqueous to nonaqueous phases are estimated.

Nevertheless, concerning the mechanism of anesthesis, in the literature there are as many theories as theoretical researches.[13]

It was suggested that local anesthetics perform the blocking of nervous conduction by increasing the surface pressure of the nervous membrane, viz. by shutting the pores, through which ions are moving.[7] This interpretation is based on monolayer experiments performed at constant molecular areas. The efficiency of anesthetics in increasing the surface pressure was observed to be directly proportional to their relative anesthetic efficiency.[9]

The major part of these experiments was performed by using monolayer membranes of lipids.[7,10-12] The reason for using these model systems is the evidence of a direct correlation between the anesthetic efficiency and the oil/water partition coefficients of anesthetics.[11] Further, the monolayer represents the half of a lipid bilayer, the latter one determining the structure of the biomembrane. The study of monolayers allows us to obtain direct information, at the molecular level, concerning the conformation and packing of molecules having biological significance in natural biomembranes under conditions near to the "in vivo" ones. Monomolecular films provide a convenient structural framework for experimental research and allow a quantitative treatment of the physico-chemical interactions between the film forming molecules, between the latter ones and the various subphase components (drugs, electrolytes, soluble proteins etc.). Monolayers spread at the plane air/water interface are sufficiently stable and suitable for experimental research.

Therefore, in the present report the influence of procaine (P) upon stearic acid (SA) monolayers, spread at the air/water interface is studied. SA monolayers have been chosen as lipid membrane model since SA is a classical film forming substance, frequently used in monolayer studies, having one of the simplest structure.

During the compression of SA monolayers, at low surface pressures, their molecules undergo conformational transitions in the hydrocarbon chain. At higher surface pressures a liquid condensed to solid phase transition occurs in the monolayer, provided the subphase is acidic. The surface properties of SA monolayers depend on the subphase pH due to a protolytic equilibrium between the neutral SA molecules (AH) and the stearate anions (A^-). Therefore, on basic subphases the liquid condensed → solid phase transition is not observed and in the pH range comprised between about 4 and 8 the collapse pressure of SA monolayers exhibits an important increase.[14]

Procaine, similarly to many local anesthetics, is a tertiary amine and at the physiologic pH its neutral molecules are in equilibrium with the charged ones, viz. with procainium cations. The neutral species was found to penetrate into the hydrophobic core of the lipid bilayers. The charged species seems to have a specific action upon the membrane proteins, by blocking e.g. the sodium channels. In other cases the anesthetic modifies the structure of the lipid bilayer leading to the expansion of the membrane or to the modulation of the surface charges. At any rate, the structure of the charged species of most local anesthetics is very similar to the structure of hydrophobic ions known as able to be linked rather strongly to pure lipid membranes. [15] Consequently, the modification of the membrane surface due to the bonding of the local anesthetic in its charged form, might represent an additional mechanism for the regulation of electrophysiologic properties of membrane proteins, through the agency of the membrane surface potential.[16]

Besides its tertiary amine group, the procaine molecule, containing also a primary one, may exist as double charged cation in acidic media.

Since both the film forming material and the drug may participate in protolytic equilibria, in our investigations the influence of pH has also been studied. By taking into account the protective action of benzoic acid upon procaine in aqueous solutions of the latter used in various clinical treatments, the influence of the former has been tested as well.

Our previous studies indicate the penetration of P from the subphase into the SA monolayer. [17]

The formation of mixed monolayers implies specific intermolecular interactions between the SA molecules and the molecular species of the electrolytes. At high surface pressures these interactions might be evidenced by modifications of π, at low ones they may be judged on the base of state equations containing parameters which reflect these interactions Therefore an attempt is made to derive surface state equations for the monolayers studied, from the low π portion of the experimental compression isotherms.

MATERIALS AND METHOD

Stearic acid used was a Schuchardt commercial product, p.a., P was used as procaine hydrochloride, Hoechst commercial product of high purity, Benzoic acid (BzH) was a "Reactivul" commercial product p.a.

Monomolecular films of SA were spread at the air/water interface, at 22°C, by using benzene as spreading solvent. The surfactant solution was placed onto the subphase by means of a micropipette. It was left for 15–30 min. to allow evaporation of the spreading solvent and the monolayer obtained was compressed. The equilibrium between the monolayer and the subphase is established rapidly, allowing us to record a compression isotherm in 10 to 30 min. Compression speeds comprised between 0.005 and 0.025 nm^2/molecule. min ensured a good reproducibility. [14] The compression of the monolayers was performed discontinuously, by using the Wilhelmy method.

The subphase was twice distilled water in a first series of experiments, 10^{-2} M HCl solution in the second and phosphate buffer with pH = 8 in the third one.

The influence of P and of benzoic acid (BzH) was studied by solving these substances in the desired concentration, in the subphase before the spreading of the monolayer. As working concentration in the subphase $[P] = 10^{-3}$ M and $[BzH] = 10^{-3}$ M were chosen, since the effect of P was found not to increase significantly with its increasing concentration if $[P] > 10^{-3}$M. [17]

pH measurements were performed by using a glass electrode and an MV 84 type Clamann—Grahnert (Dresden) laboratory pH-meter.

RESULTS AND DISCUSSION

Molecular species involved

In order to have a clear image on the molecular state of the substances studied, in different working conditions, diagrams have been constructed, giving the fraction α of the different molecular species as a function of pH. In the case of SA, calculations have been performed by using the surface acidity constant reported earlier: $pK_a = 5.63$.[14] The acidity constant of BzH ($pK_a = 4.19$) and the acidity constant of the procainium cation PH^+ ($pK_a = 8.85$) were taken from the literature.[18] For the primary amine group of P one may presume that it has the same properties as in p-aminobenzoic acid. Since the latter has the basicity constant[18] $K_a = 1.7 \times 10^{-12}$, the acidity constant of the dication PH_2^{2+} was presumed to be $pK_a = 2.23$.

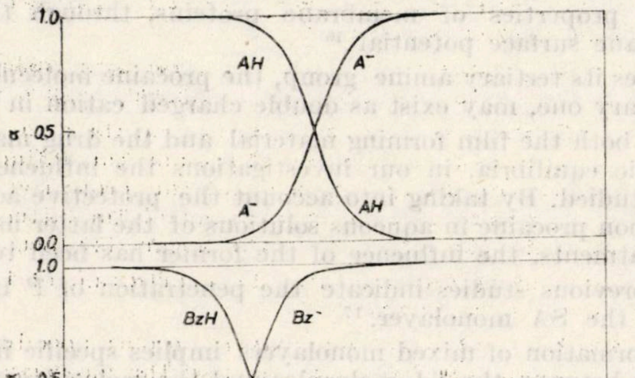

Fig. 1. — Fraction of different molecular species of SA, BzH and P as a function of pH.

The diagrams obtained are visualized in Fig. 1. From these curves one can see that SA is not ionized at all at pH = 2 (10^{-2} M solution of HCl). At pH = 3.5 (10^{-3}M solution of BzH) the fraction of neutral molecules AH is of about 0.99, i.e. only 1% of the SA molecules are ionized. At pH = 5.2 (10^{-3} Msolution of procaine hydrochloride SA is partially ionized, in a proportion of about 35%. On twice distilled water ($pH = 5.6$) SA is also partially ionized, in a proportion of about 48% while at $pH = 8$ it is practically completely ionized (over 99%).

BzH is practically completely unionized at $pH = 2$, completely ionized at $pH = 8$, at $pH = 3.5$ the neutral species is predominant and at $pH = 5.2$ the charged one.

P forms only monocations at $pH = 5.2$. At $pH = 3.5$ the dications are also present (5%), and their proportion attains over 60% at $pH = 2$. At $pH = 8$ the monocation is the predominant species but there are also neutral molecules, in a proportion of about 12%.

Since P is an ester, in aqueous solutions the possibility of its hydrolysis must also be considered. At $pH = 2$ this possibility is not likely, esters being hydrolysed in acidic media only by boiling. In basic solutions hydrolysis is much faster. By recording UV spectrum of a solution of P at $pH = 10$, one actually observes a variation in time, but the hydrolysis degree becomes equal to 3—4 % only in an hour. Consequently, at $pH = 8$, during the record of a compression isotherm, practically no hydrolysis can occur. In order to avoid completely the hydrolysis of P, at $pH = 8$ always freshly prepared P solutions were used.

Compression isotherms and monolayer characteristics

Compression isotherms of SA monolayers recorded on subphases with $pH = 2$ are presented in Fig. 2. Obviously, both P and BzH have an expanding effect, and P also increases the collapse pressure. Further, one observes that all curves exhibit two linear portions corresponding to the liquid condensed (LC) and to the solid (S) state of the monolayer, respectively.

From the compression isotherms the following surface characteristics have been derived :

A_0' — limiting molecular area for the LC state, obtained by the extrapolation to $\pi = 0$ of the first linear portion of the isotherm of intermediate surface pressure ;

A_0 — limiting molecular area for the S state, obtained by extrapolating the second linear portion of high surface pressure ;

A_c, π_c — collapse area and collapse pressure, representing the A and π values corresponding to the sudden slope change observed at high π values ;

$A_t, \pi_t =$ — molecular area and surface pressure corresponding to the LC → S phase transition ;

$(C_{s0}^{-1}) = A_0' \dfrac{\pi_t}{A_0' - A_t}$ — surface compressional modulus for the LC state ;

$(C_{s0}^{-1}) = A_0 \dfrac{\pi_c}{A_0 - A_c}$ — surface compressional modulus for the S state.

Monolayer characteristics derived from π vs. A curves presented in Fig. 2 are given in Table 1. As seen, both BzH and P have an expanding effect upon the SA monolayer, since in their presence the areas A_0', A_0 and A_t increase, and the compressibility of the film also increases as indicated by the decrease of compressional moduli$(C_{so}^{-1})'$ and C_{so}^{-1}. It is worth mentioning that A_c remains practically constant. These effects suggest the idea that the molecules of both BzH and P penetrate into the monolayer,

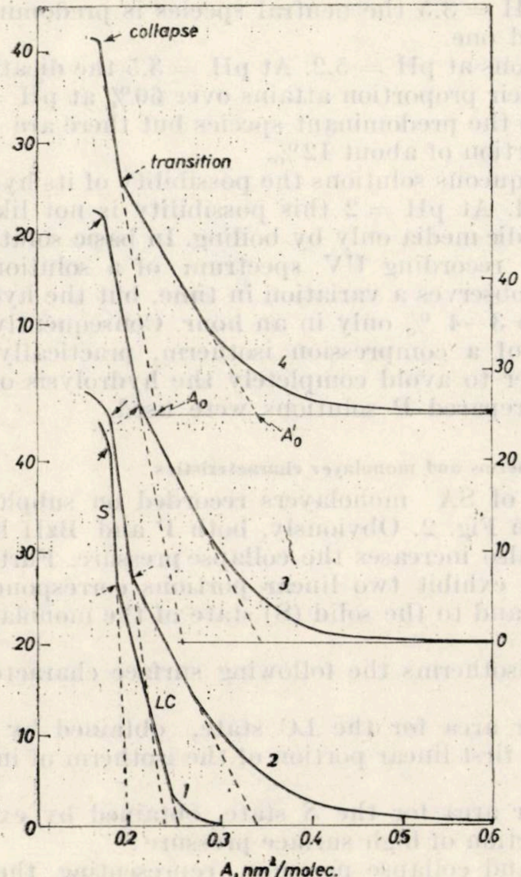

Fig. 2. — Compression isotherms of SA monolayers at pH = 2. Subphase: 1 — $HCl(10^{-2}M)$; 2 — $HCl(10^{-2}M) + P(10^{-3}M) + BzH(10^{-3}M)$; 3 — $HCl(10^{-2}M) + P(10^{-3}M)$; 4 — $HCl(10^{-2})M + BzH(10^{-3}M)$.

Table 1

Monolayer characteristics of SA at pH = 2

Subphase	HCl	HCl + + BzH	HCl + P	HCl+P+ + BzH
A'_0*	0.255	0.34	0.34	0.34
A_0*	0.20	0.23	0.26	0.24
A_c	0.18	0.18	0.175	0.18
A_t*	0.188	0.19	0.21	0.203
π_c**	40.8	41.0	47.0	45.0
π_t**	26.0	26.0	26.0	28.0
$(C_{so}^{-1})'$**	99.0	58.9	68.0	68.0
(C_{so}^{-1})**	408.0	157.2	143.8	180.0

* in nm²/molecule; ** in mN/m

the latter more easily than the former does, entailing expansion of the monolayer. Near to collapse these molecules seem to be expulsed from the monolayer into the subphase. This expulsion can be considered as a transformation of the mixed monolayer into a bilayer, the upper layer being the insoluble SA film, the lower one an adsorption film containing BzH and/or P.

It is further observed that the phase transition occurs practically at the same surface pressure, irrespective of the composition of the subphase. On the contrary, the collapse pressure remains unchanged in the presence of BzH, but it exhibits an important increase on subphases containing P. This indicates the stabilizing effect of P upon the SA monolayer, which might be due to specific ion-dipole interactions between the SA monolayer and an adjacent adsorption layer of procainium ions.

On the basis of the data presented in Table 1, BzH seems to diminish the effect of P, since the increase of A_0, A_t and π_c and of the surface compressibility caused by P in the presence of BzH is less than in its absence.

In order to obtain a clear image concerning the expanding effects, $\Delta\pi$ vs. A curves have been constructed; $\Delta\pi$ representing at the same molecular area the difference between the surface pressures in the presence of P and/or BzH and in their absence, i.e. curve 1 was subtracted from curves 2,3 and 4, respectively. These curves are given in Fig. 3 and they visualize the penetration and subsequent expulsion of the P and BzH molecules during the compression of the monolayer. The effect is less in the case of BzH and greater with P. In all cases the maximum of $\Delta\pi$ appears at about $A = 0.25$ nm²/molecule.

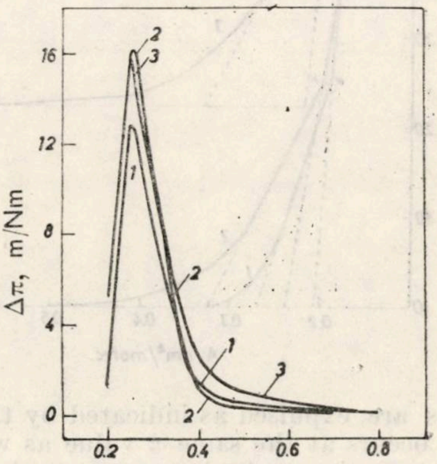

Fig. 3. — $\Delta\pi$ vs. A curves for SA monolayers. pH = 2. Subphase: 1 — BzH; 2 — P; 3 — P + BzH. All concentrations 10^{-3}M, each.

If the subphase does not contain HCl, the working pH is generated by P, BzH and by the CO_2 dissolved in the subphase water. The recorded compression isotherms are presented in Fig. 4 and the derived surface characteristics are given in Table 2. The general picture is the same as, in the previous case, BzH and especially P have an expanding effect, shown by the increase of A_0', A_0 and A_t, as well as by the decrease of surface compressional moduli. Near to the collapse the P and BzH molecules are expulsed as indicated by the low A_c values. The phase transition occurs at the same π value as with pH = 2. Concerning the π_c values, one must take into account that at pH = 3.5 the SA film is uncharged, but at pH = 5.2 and 5.6 it is partially charged and consequently exhibits a relatively high π_c value. In considering the stabilizing effect of P, the π_c values are to be compared in the case of BzH containing subphases with $\pi_c = 40.8$ mN/m of the uncharged film, reported above. At pH = 5.2 the collapse pressure of the SA monolayers is 42.9 mN/m. This is the value to which the π_c, observed on only pure P containing subphase, is to be compared. Similarly, by constructing the $\Delta\pi$ vs. A curves, presented in Fig. 5, curve 1 of Fig. 2 is to be subtracted from curves 2 and

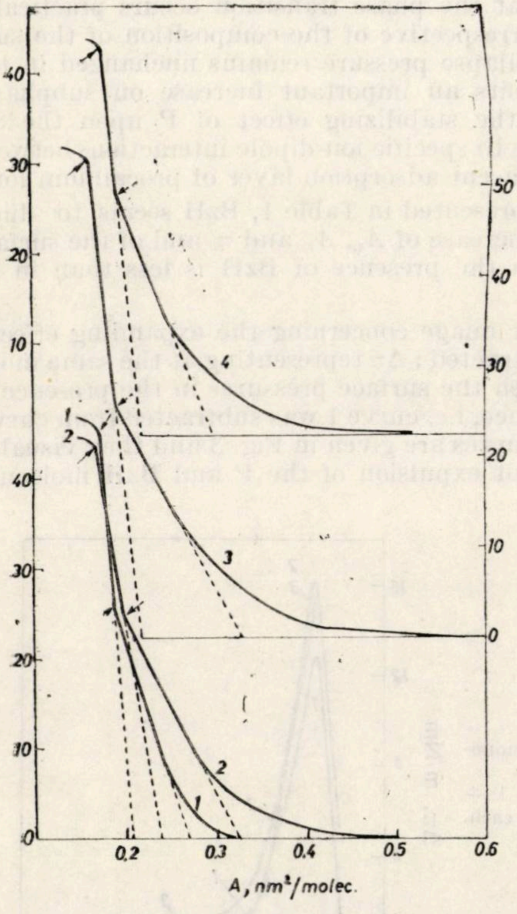

Fig. 4. — Compression isotherms of SA monolayers on subphases without HCl. Subphase: 1 — twice distilled water, pH = 5.6; 2 — P(10^{-3}M) + BzH(10^{-3}M) pH = 3.5; 3 — P(10^{-3}M), pH = 5.2; 4 — BzH (10^{-3}M), pH = 3.5.

4 given in Fig. 4, since the latter ones have been recorded at pH = 3.5, corresponding to completely uncharged SA monolayer, whereas curve 1 of Fig. 4 was obtained with partially charged SA film. The curves in Fig. 5 exhibit a clear maximum at about the same area of 0.25 nm^2 as with pH = 2. BzH seems also to diminish the effect of P in this case.

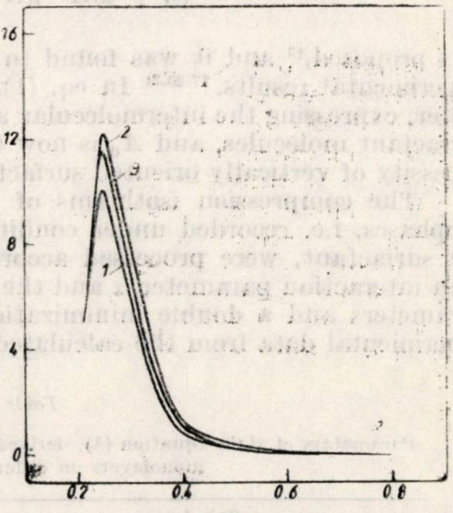

Fig. 5. — $\Delta\pi$ vs. A curves for SA monolayers in absence of HCl. Subphase: 1 — BzH(10^{-3}M); 2 — P(10^{-3}M); 3 — P(10^{-3}M) + BzH(10^{-3}M).

By using buffered subphases with pH = 8, the shape of the compression isotherms exhibits a fundamental change as compared to the previous curves. The phase transition disappears, π_c of the pure SA monolayer is higher, and the expanding effect of P is very important even at greater values of A.[17] All these effects are caused by the charged character of the monolayer formed of stearate anions. Since at pH = 8 BzH is completely ionized, its penetration into the negatively charged SA monolayer cannot be expected. Therefore, the influence of BzH upon the SA monolayer at pH = 8 was not studied in this paper.

Table 2

Monolayer characteristics of SA on subphases without HCl

Subphase	H_2O	BzH	P	P + BzH
pH	5.6	3.5	5.2	3.5
$A_0'^{*}$	0.27	0.30	0.33	0.33
A_0^{*}	0.21	0.22	0.22	0.24
A_c	0.175	0.18	0.165	0.17
A_t^{*}	0.19	0.20	0.20	0.195
π_c	45	43	53	44
π_t^{**}	26	27	26	26
$(C_{so}^{-1})^{**}$	87.8	63.9	66.0	63.6
$(C_{so}^{-1})^{**}$	279.0	172.0	212.0	150.9

* in nm^2/molecule; ** in mN/m

State equation of the uncharged SA monolayer

For cohering uncharged films, the state equation

$$(\pi + \alpha/A^{3/2})(A - A_0) = kT \quad (1)$$

was proposed,[19] and it was found to be in rather good agreement with experimental results.[17,20,21] In eq. (1), α stands for an interaction parameter, expressing the intermolecular attracting forces acting between the surfactant molecules, and A_0 is now the co-area, reflecting the own area necessity of vertically oriented surfactant molecules in monolayers.

The compression isotherms of SA monolayers spread onto acidic subphases, i.e. recorded under conditions not allowing the ionization of the surfactant, were processed according to eq. (1). For this purpose both interaction parameter α and the co-area A_0 were taken for adjusted parameters and a double minimization of the standard deviation Δ of experimental data from the calculated ones has been performed.[17]

Table 3

Parameters of state equation (1), derived from the compression isotherms of SA monolayers on different subphases

Subphase				A_0^* nm^2/molec.	$\alpha \times 10^{30}$ Nm^2	Δ_m mN/m
HCl	BzH	P	pH			
10^{-2}	0	0	2	0.1429	4.328	0.387
10^{-2}	10^{-3}	0	2	0.1906	4.497	0.143
10^{-2}	0	10^{-3}	2	0.2019	4.791	0.325
10^{-2}	10^{-3}	10^{-3}	2	0.1984	4.458	0.206
0	10^{-3}	0	3.5	0.1795	4.427	0.150
0	0	10^{-3}	5.2	0.1930	4.571	0.152
0	10^{-3}	10^{-3}	3.5	0.1870	4.487	0.130

* A_0 — means co-area

These calculations have been carried out for curves 1—4 in Fig. 2 and for curves 2—4 in Fig. 4, by using in all cases the portion corresponding to $\pi \leqslant 7$ mN/m. Results are summarized in Table 3, containing in the last column the minimum standard deviation Δ_m corresponding to the A_0 and α values given. As seen from Table 3, eq. (1) describes rather well the experimental compression isotherms, although Δ_m slightly exceeds the experimental errors in π measurements.

Both A_0 and α values are consistent with our above conclusions. The increase of the co-area in the presence of BzH and/or of P in the subphase, indicates the expanding effect of these substances, due to their penetration into the monolayer. The maximum effect is observed if the subphase contains P alone, and all the effects are a little higher, at pH = 2, than to less acidic subphases. The larger effect of P as compared to BzH seems to be reasonable. The BzH molecules are anchored into the aqueous phase by their carboxyl groups, the benzene ring remaining in the air phase. In the case of P, the molecules are anchored into the subphase by their protonated tertiary amine group and they are more strongly retained in the monolayer than the BzH molecules, since the hydrophobic moiety of the latter ones is more voluminous than that of the former ones.

The enhanced positive α values obtained with BzH and/or P containing subphases as compared to the pure SA monolayer are in, agreement with this general picture. The penetration of BzH into the monolayer entails the increase of intermolecular attractions, due both to the dipole-dipole interactions of the headgroups, and to the hydrophobic interactions of the air phase parts of the molecule. In the case of P, both the ion-dipole interactions between the headgroup and the hydrophobic interactions in the air phase may be expected to be stronger than with BzH. Therefore, the higher α values obtained in the presence of P, as compared to BzH, are in agreement with the above-mentioned expectations on the basis of molecular structure.

It is interesting to observe that the effects of BzH and P are not cumulated, but even the effect of P is diminished in the presence of BzH. This unexpected phenomenon suggests the idea that some specific interactions might operate presumably between the P and BzH molecules, hindering the penetration of P into the monolayer.

REFERENCES

[1] J. R. Trudell, W. L. Hubbell and E. N. Cohen, *Fed. Proc.*, **31**, 549 (1972).
[2] G. L. Turner and N. Oldfield, *Nature*, **277**, 669 (1979).
[3] Y. Boulanger, S. Schreier and I. C. P. Smith, *Biochemistry*, **20**, 6824 (1981).
[4] I. Ueda, C. Tashiro and K. Arakewa, *Anesthesiology*, **45**, 327 (1977).
[5] J. M. Vanderkooi, R. Landsberg, H. Selick and G. G. McDonald, *Biochim. Biophys. Acta*, **464**, 1 (1977).
[6] P. Seeman, *Pharmacol. Rev.*, **24** (4), 583 (1972).
[7] A. Seelig, *Biochim. Biophys. Acta*, **899**, 196 (1987).
[8] J. R. Trudell, *Biochim. Biophys. Acta*, **470**, 509 (1977).
[9] J. Chr. Skou, *J. Pharm. Pharmacol.*, **13**, 204 (1961).
[10] A. M. Shanes and N. L. Gerschfeld, *J. Gen. Physiol.*, **44**, 345 (1960).
[11] F. A. Villalonga, and E. W. Phillips, *J. Pharm. Sci.*, **68**, 314 (1979).
[12] F. A. Villalonga and E. W. Phillips, *J. Pharm. Sci.*, **69**, 102 (1980).
[13] I. C. P. Smith and K. W. Butler, in "Molecular and Cellular Mechanisms of Anesthetics", Eds. Roth, S. H. and Miller, K. W. Plenum Press, New York, 1986, pp. 309—318.
[14] M. Tomoaia-Cotișel, J. Zsakó, A. Mocanu, M. Lupea and E. Chifu, *J. Colloid Interface Sci.*, **117**, 464 (1987).
[15] C. Altenbach and J. Seelig, *Biochim. Biophys. Acta*, **818**, 410 (1985).
[16] E. K. Rooney and A. G. Lee, *Biochim. Biophys. Acta*, **732**, 428 (1983).
[17] M. Tomoaia-Cotișel, E. Chifu, A. Mocanu, J. Zsakó, M. Sălăjan and P. T. Frangopol, *Rev. Roum. Biochim.*, **25**, 227 (1988).
[18] Spravochnik Khimika, T. III, Goskhimizdat, Moscow, 1952, p. 496—511.
[19] J. Guastalla, *Cahiers phys.*, **10**, 30 (1942); *J. Chim. phys.*, **43**, 184 (1946).
[20] L. Ter Minassian-Saraga, *J. Chim. phys.*, **52**, 80 (1955).
[21] E. Chifu, J. Zsakò and M. Tomoaia-Cotișel, *J. Colloid Interface Sci.*, **95**, 346 (1983).

Revue Roumaine de Chimie, 35, 7–9, 879–889 (1990)

PENETRATION OF PROCAINE HYDROCHLORIDE INTO STEARIC ACID MONOLAYERS FROM UNDERLYING AQUEOUS SOLUTIONS

EMIL CHIFU[a], MARIA TOMOAIA-COTIŞEL[a], JÁNOS ZSAKÓ,[a] IOSIF ALBU,[a]
AURORA MOCANU,[a] PETRE T. FRANGOPOL[b]

[a] University of Cluj-Napoca, Physical Chemistry Department, 3400 Cluj-Napoca, Romania

[b] Institute of Physics and Nuclear Engineering, PO Box MG-6, R–76900, Măgurele – Bucharest, Romania

Penetration of procaine (P) dissolved in pure water into stearic acid (SA) monolayers spread at the air/water interface is studied by measuring surface tension of aqueous P solutions and by recording surface pressure vs. mean molecular area curves for SA monolayers spread onto P solutions of different concentrations. The amount of P in the interface is derived by means of Gibbs'equation applied to constant mean molecular area of SA. In the presence of the SA monolayer, enhanced adsorption of P is observed, which even increases at compressions of the monolayer, up to a maximum value. The penetrated P molecules are gradually squeezed out from the monolayer near to the collapse. Effects are similar, but a little larger than for systems in which the pH of the aqueous subphase is equal to 2.

INTRODUCTION

The adsorption of the soluble surfactant 2 dissolved in water (noted as component 1) at the air/water interface may exhibit an important increase if the insoluble surfactant 3 is spread onto the aqueous subphase. This enhanced adsorption is due to the interactions between the molecules of surfactants 2 and 3, both at their polar headgroups and hydrocarbon chains. The phenomenon is frequently called monolayer penetration,[1] since the spread pure monolayer can be thought to become a mixed one, containing also adsorbed molecules of species 2, penetrated into the monolayer from the subphase.

Penetration studies have been performed either by spreading the insoluble surfactant onto the subphase containing no soluble surfactant, followed by the injection of the latter into the subphase,[1,2] or by recording compression isotherms, i.e. mean molecular area A_3 of surfactant 3 vs. surface pressure π curves, the insoluble surfactant being spread onto a subphase containing already the soluble surfactant, the concentration of the latter being c_2.[3,4] By using the injection techniques, two main procedures are used, viz. either the surface pressure increase is recorded at constant mean molecular area A_3, or the measurements are performed at constant π and the area increase $\Delta A = A_3 - A_3^0$ due to the injection of 2 into the subphase is recorded (A_3^0 stands for the mean molecular area of 3 in the absence of 2 in the subphase, π having the same value).

Both techniques yield equilibrium π values as a function of mean molecular area A_3 and of molar concentration c_2 of the soluble surfactant in the bulk subphase.

The equilibrium between the bulk subphase and the mixed monolayer thermodynamically can be treated by using Gibbs'equation.[1,4]

Under isothermal conditions and for a constant A_3 value, Gibbs' equation has the following form :[4]

$$\Gamma_2' = \frac{1}{kT}\left(\frac{\partial \pi}{\partial \ln c_2}\right)_{T, A_3} \qquad (1)$$

Where Γ_2' stands for the number of soluble surfactant (2) molecules adsorbed per unit area of the "free" interface, i.e. not covered by insoluble surfactant molecules 3, k and T are Boltzmann's constant and absolute temperature, respectively.

The adsorption of 2 per unit area of the mixed monolayer (Γ_2) can be calculated from Γ_2' by taking into account the actual area necessity of the film forming molecules (3), i.e. the partial mean molecular area of 3, denoted as $\bar{A}_3$. One obtains:[1,4]

$$\Gamma_2 = \left(1 - \frac{\bar{A}^3}{A_3}\right)\Gamma_2' \qquad (2)$$

In view of approximating $\bar{A}_3$ several procedures have been proposed. One of them takes A_3^0 for $\bar{A}_3$[1]. Another derives $\bar{A}_3$ by an iterative procedure from A_{23} vs. x_2^M curves, where A_{23} stands for the mean molecular area of 2 and 3 in the mixed monolayer and x_2^M for the molar fraction of 2 in the monolayer, calculated by neglecting the number of moles of water (n_1) in the monolayer.[4] Since the molecules of 3 are anchored into the surface layer of the subphase through their polar headgroups, we proposed in our earlier paper[5] to take the collapse area (A_{3c}) of 3 for $\bar{A}^3$

Penetration studies revealed some common features of this phenomenon. Thus, penetration of dodecylsulphate into cholesterol monolayers[1], of hexadecyl-trimethylammonium bromide into octadecanol monolayers[3], of lysine, leucine, norleucine,[4] vinblastine sulphate,[6] dibucaine,[7] into lecithin monolayers and of procaine into stearic acid monolayer at pH = 2,[5] was found to increase with decreasing A_3 up to a maximum value and to decrease at low A_3 values corresponding to the expulsion of 2 from the mixed monolayer near to the collapse.

In the present paper penetration of procaine into stearic acid (SA) monolayers is studied, the SA monolayer being spread at the air/aqueous solution of procaine hydrochloride (P) interface and the subphase containing no other electrolyte besides P.

EXPERIMENTAL

Materials. Stearic acid (SA) used was a commercial product Schuchardt, of p.a. purity. Procaine (P) was used as procaine hydrochloride, commercial product Hoechst.

Methods. SA monolayers were spread at the air/aqueous solution interface at 22°C, by using benzene as spreading solvent. The surfactant solution was placed onto the subphase by means of a micropipette. It was left for 15—30 min for the evaporation of benzene and the monolayer obtained was compressed. The equilibrium between the monolayer and the subphase was established rapidly, allowing us to record a π vs. A_3 curve in 10 to 30 min. Compression speeds comprised between 0.005 and 0.025 nm^2/molec. min ensured a good reproducibility. [7,8] Compression of the monolayer was performed discontinuously, by using the Wilhelmy method. In all cases a number of 8 to 10 compression isotherms have been recorded under identical experimental conditions.

The subphase was redistilled water, containing varying amounts of P dissolved before spreading of the SA monolayer.

Surface tensions (σ) of P solutions not covered by SA monolayers were measured by using du Noüy's ring method at 20°C.

RESULTS AND DISCUSSION

Let us denote by σ_O, σ_P and σ_{SA} the surface tension of pure water, of aqueous P solution and of aqueous solution covered by a SA monolayer, respectively. The surface pressure will be defined in the absence of SA monolayer as $\pi_P = \sigma_O - \sigma_P$, in its presence as $\pi = \sigma_O - \sigma_{SA}$. The surface pressure directly measured by means of the Wilhelmy method at compression of the SA monolayer on subphases with P represents $\pi' = \sigma_P - \sigma_{SA}$. Consequently, the experimental π' value must be corrected for π_P. Therefore, one has $\pi = \pi' + \pi_P$.

Adsorption of P in the absence of SA

Surface tension of P solutions as a function of the P molar concentration c_2 is presented in Fig. 1. The use of the logarithmic concen-

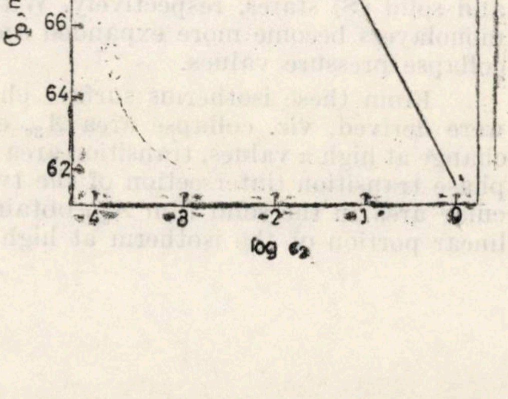

Fig. 1. — Surface tension of P solutions as a function of the P concentration (c_2).

tration scale allows us to graphically derive the adsorption of P (Γ_2^0) from the slope of the tangency of the curve given (see dashed line) in Fig. 1, by using Gibbs'equation :

$$\Gamma_2^0 = -\frac{1}{kT}\left(\frac{\partial \sigma_P}{\partial \ln c_2}\right)_T \qquad (3)$$

We mention that eq. (3) may also be obtained from eq. (1) for $A_3 \to \infty$, since in this case $\sigma_{SA} \to \sigma_P$ and $d\pi = -d\sigma_P$.

As seen from Fig. 1 the σ vs. log c_2 plot becomes linear at higher c_2 values indicating the saturation of the interface. The mean molecular area of P calculated from the slope of this linear portion is of 1.96 mm²/molecule, a little less as found earlier,[5] at pH = 2 (2.07 nm²). This value pleads for a horizontal, lying down orientation of P molecules (procainium cations) at the interface, since in this case the molecular model calculations show an area necessity of about 1.50 nm²/molecule.

It is worth mentioning that in the case of unbuffered solutions the P adsorption is much higher than at pH = 2, if subphases with the same P concentrations are compared. This is illustrated by Table 1. The large difference might be due to the protolytic equilibria in which participates P. At pH = 2 the amount of double protonated PH_2^{2+} cations approximately equals the amount of PH^+ monocations,[7] whereas in unbuffered solutions practically there are only PH^+ monocations, which are expected to have a higher surface activity as compared to the PH_2^{2+}dication.

Table 1

P adsorption ($\Gamma_2^0 \times 10^{-13}$, molec/cm²) at the air/water interface without SA monolayer obtained by means of eq. (3).

C_2, M	Subphase	
	pH = 2	unbuffered
10^{-3}	0.267	0.694
10^{-2}	0.908	2.616
10^{-1}	4.150	5.103
1	4.831	5.103

Compression isotherms and surface characteristics of SA monolayers

Compression isotherms of SA monolayers at several subphase P concentrations are visualized in Fig. 2. The general picture is similar to that reported earlier,[5] for pH = 2. One may observe that all isotherms contain two linear portions, corresponding to the liquid condensed (L. C.) and solid (S) states, respectively. With increasing P concentration the monolayers become more expanded and the isotherms exhibit increasing collapse pressure values.

From these isotherms surface characteristics of the SA monolayer were derived, viz. collapse area A_{3c} corresponding to the sudden slope change at high π values, transition area A_{3t} , corresponding to the L.C. → S phase transition (intersection of the two linear portions), limiting molecular area in the solid film A_{3o}, obtained by extrapolating to $\pi = 0$ the linear portion of the isotherm at high π values, limiting molecular area

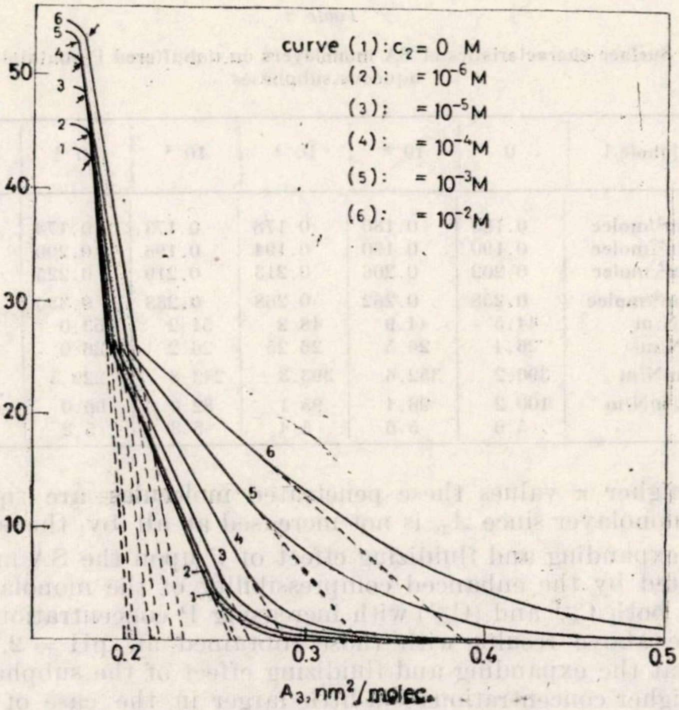

Fig. 2. — Compression isotherms of SA monolayers spread onto unbuffered aqueous P solutions at different P concentrations: c_2.

in the L.C. state A'_{3o}, obtained by extrapolating to $\pi = 0$ the linear portion of the isotherm obtained at intermediate π values, collapse pressure π_c, surface pressure at the phase transition π_t, surface compressional moduli C_{so}^{-1} and $(C_{so}^{-1})'$ of the S and of the L. C. film, respectively, defined as:

$$C_{so}^{-1} = -A_{3o}\left(\frac{d\pi}{d A_3}\right)_S = A_{3o}\frac{\pi_c}{A_{3o} - A_{3c}} ;$$

$$(C_{so}^{-1})' = -A'_{3o}\left(\frac{d\,\pi}{d\,A_3}\right)_{L.C.} = A_{3o}\frac{\pi_t}{A'_{3o} - A_{3t}}$$

Surface characteristics derived from the isotherms given in Fig. 2 are presented in Table 2.

As seen from this table, practically A_{3c} is not affected by the presence of P in the subphase, but all other characteristic area values, A_{3t}, A_{3o}, and A'_{3o}, increase with increasing P concentration. This means that P has an expanding effect upon the SA monolayer, as reported earlier, [7] which pleads for the penetration of P molecules between the SA ones in the monolayer.

Table 2

Surface characteristics of SA monolayers on unbuffered P containing aqueous subphases

[P] mole/l	0	10^{-6}	10^{-5}	10^{-4}	10^{-3}	10^{-2}
A_{3c}, nm^2/molec	0.180	0.180	0.178	0.173	0.173	0.178
A_{3t}, nm^2/molec	0.190	0.190	0.194	0.196	0.200	0.206
A_{3o}, nm^2/molec	0.202	0.206	0.213	0.219	0.225	0..233
A'_{3o}, nm^2/molec	0.258	0.262	0.268	0.288	0.330	0.390
π_c, mN/m	44.5	44.9	48.2	51.2	53.0	53.5
π_t, mN/m	26.4	26.5	26.25	26.2	26.0	26.25
C_{so}^{-1}, mN/m	390.2	352.6	393.3	243.8	229.3	226.6
$(C_{so}^{-1})'$, mN/m	100.2	96.4	95.1	82.0	66.0	55.6
pH	5.6	5.6	5.4	5.3	5.2	5.1

At higher π values these penetrated molecules are squeezed out from the monolayer since A_{3c} is not increased at all by the subphase P.

The expanding and fluidizing effect of P upon the SA monolayer is also reflected by the enhanced compressibility of the monolayer i.e. by decreasing both C_{so}^{-1} and $(C_{so}^{-1})'$with increasing P concentration. By comparing the above results with those obtained at pH = 2,[5] one may observe that the expanding and fluidizing effect of the subphase P especially at higher concentrations is a little larger in the case of unbuffered solutions as compared to subphases with pH = 2.

From the characteristic π values, practically π_t is not affected, similarly as at pH = 2, [5] but π_c varies very much, viz. it increases with increasing P concentration, indicating a stabilizing effect of the subphase Pupon the SA monolayer. This means that the P molecules expelled from the mixed monolayer, near to the collapse, must remain in an adjacent layer allowing a specific interaction, in vertical direction, between the P and SA molecules at air/water interface and leading to the increase of π_c of pure SA monolayer.

The π_c increase in unbuffered systems is more important than at pH = 2. It is worth mentioning that in the systems studied the subphase pH is not the same. It is generated by the atmospheric CO_2 and by the hydrolysis of the procainium salt, dissolved in the subphase and it varies in our experiments in the range comprised between 5.6 and about 5.1 (see Table 2). The surface acidity constant of SA corresponds to pKa = = 5.63. [8] Consequently, at pH = 2 the SA monolayer is completely uncharged. Conversely, under our experimental conditions it is partially charged. Due to a protolytic equilibrium at pH = 5.6, almost the half of the SA molecules is transformed into stearate anions. Ionization entails the increase of π_c of the SA monolayer. Therefore, the actual effect of P is a little larger than it results from Table 2. According to Table 2, π_c increases by 9 mN/m when c_2 increases from zero to 10^{-2} M. But for $c_2 = 10^{-2}$ M the pH is equal to about 5.1 and at this pH value π_c of the pure SA monolayer is only of about 42.6 mN/m, i.e. really π_c increases by 10.9 mN/m. This enhanced stabilizing effect of P might be due to the presence of the stearate anions in the monolayer which interact more strongly with procainium cations of the subjacent layer than the neutral SA molecules do.

Procaine penetration into the SA monolayer

The penetration of the soluble surfactant into the insoluble monolayer can be quantitatively characterized by the ratio between the number of soluble surfactant molecules (Γ_2) and of insoluble surfactant molecules (Γ_3) per unit area, [2] i. e. by the number of adsorbed P molecules per one SA molecule, which will be referred to as penetration number

$$n_P = \Gamma_2 / \Gamma_3 = \Gamma_2 A_3 \qquad (4)$$

A_3 can be easily obtained from the total area of the monolayer and from the amount of SA spread at the interface.

The amount of P penetrated into the SA monolayer can be estimated by using Gibbs'equation (1). For this purpose, from the compression isotherms given in Fig. 2, π values are derived which correspond to a given constant A_3 value. A plot of π vs. log c_2 is performed for different A_3 values. A set of such curves is presented in Fig. 3.

The general picture is similar as reported for the aminoacid penetration into lecithin monolayers, [4] and as found also for P penetration into SA monolayers at pH = 2. [5] With decreasing molecular areas A_3 the slope of the curves from Fig. 3 increases down to about 0.3 . . . 0.25 nm²/molec. and further it newly decreases.

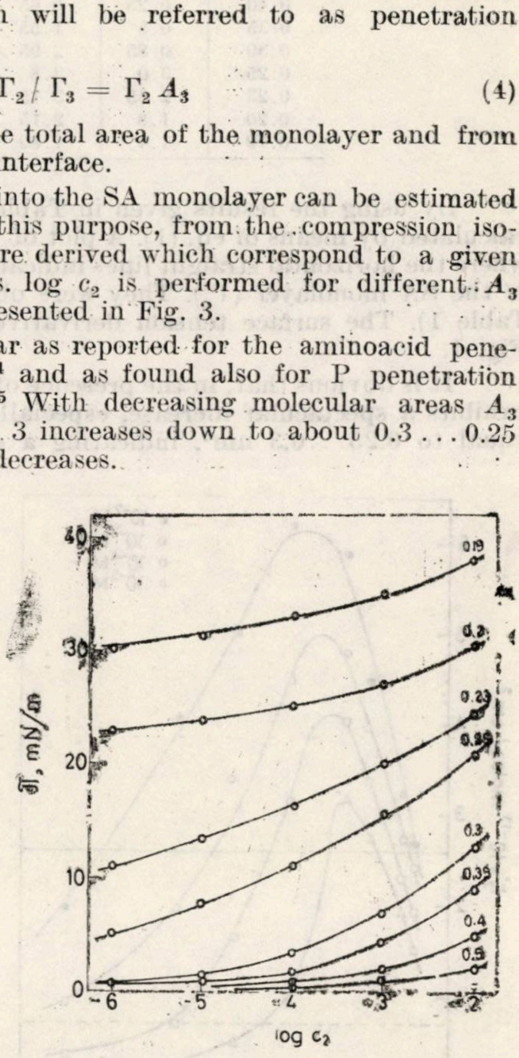

Fig. 3. — π vs. log c_2 curves for constant mean molecular areas (A_3) of SA. Figures near the curves indicate the value of A_3 expressed in nm²/molecule.

The curves given in Fig. 3 allowed us to graphically obtain the derivative $(\partial\pi/\partial \log c_2)_{T,A_3}$ for different c_2 and A_3 values. These values are summarized in Table 3.

Table 3

The derivative $(\partial\pi/\partial\log c_2)_{T,A_3}$ for mixed SA and P monolayers (π measured in mN/m, c_2 in mole/l) as a function of the subphase P concentration c_2 and mean molecular area A_3 of SA. Data taken from Fig. 3.

A_3 nm²/molec.	c_2, M			
	10^{-5}	10^{-4}	10^{-3}	10^{-2}
0.50	0.10	0.32	0.85	1.85
0.40	0.25	0.65	1.85	3.8
0.35	0.5	1.55	3.2	4.7
0.30	0.85	2.95	4.2	5.8
0.25	3.0	3.8	4.5	5.5
0.23	2.55	3.15	3.7	4.2
0.20	1.8	2.15	2.55	3.0
0.19	1.4	1.80	2.25	2.5

By using the results given in Table 3, the P adsorption Γ_2' can be calculated by means of eq. (1). A plot of Γ_2' vs. A_3 is visualised in Fig. 4 where the horizontal straight lines indicate the P adsorption in the absence of the SA monolayer (Γ_2^0). They were obtained by means of eq. (3), (see Table 1). The surface tension derivative was graphically obtained from Fig. 1.

It is obvious that, in the presence of SA monolayer, the P adsorption exhibits a spectacular increase, especially in the vicinity of the A_3 value equal to 0.25...0.3 nm², indicating a specific interaction between the

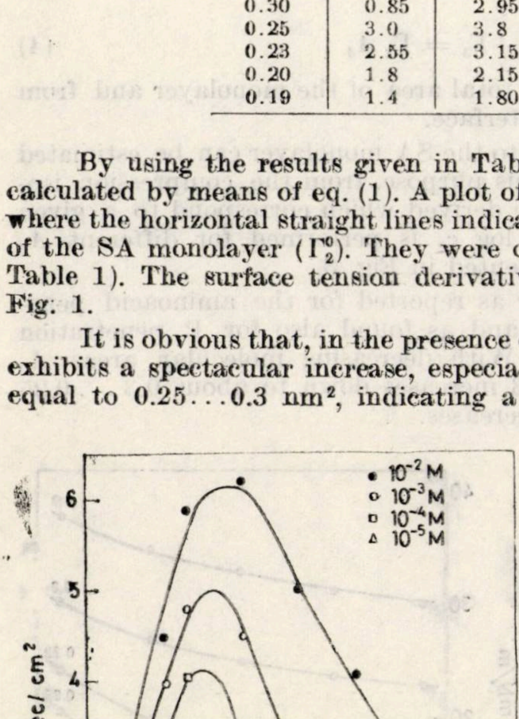

Fig. 4. — Padsorption per unit area of the "free" interface (Γ_2') as a function of c_2 and A_3, as calculated by means of eq.(1). Figures after the symbols of experimental points: subphase P concentration (c_2). Horizontal lines: P adsorption in the absence of the SA monolayer Γ_2^0 calculated by eq. (3) for $c_2 = 10^{-2}$ M (full line) and $c_2 = 10^{-3}$ M (dashed line).

insoluble surfactant (SA) molecules and the soluble surfactant (P) ones. On the other hand, the P adsorption depends very much on A_3, i.e. on the surface density of SA molecules. At compression of the monolayer Γ_2' increases and exhibits a maximum in the range $0.25 < A_3 < 0.3$ nm²/molec. and at further compression it decreases as expected on the basis of both Fig. 3 and our earlier findings concerning the surface pressure increments $\Delta\pi$ caused by the subphase P at a constant A_3 value; the $\Delta\pi$ vs. A_3 curve passes through a maximum even in the above-mentioned area range.[7]

The Γ_2 value necessary for the calculation of n_P by means of eq. (4), can be derived from Γ_2' by using eq. (2). By taking $\bar{A}_3 = A_{3c}$ as first approximation one obtains:

$$\Gamma_2 = \left(1 - \frac{A_{3c}}{A_3}\right)\Gamma_2' \tag{5}$$

The expression allowing us to derive penetration numbers directly from the experimental curves, presented in Fig. 3, can be obtained by combining eqs. (1), (4) and (5). One obtains:[5]

$$n_P = \frac{A_3 - A_{3c}}{k \cdot T}\left(\frac{\partial \pi}{\partial \ln c_2}\right)_{T,A_3} \tag{6}$$

For our calculations $A_{3c} = 0.18$ nm²/molec (see Table 2) was taken. The P adsorption per unit area of SA monolayer (Γ_2) calculated by means of eq. (5) is given in Fig. 5. As seen, it is much less than Γ_2' (Fig. 4), especially at low molecular areas, i.e. at high surface densities of the SA molecules. Nevertheless, especially at low c_2 values, there is a rather wide A_3 range where Γ_2 depasses much Γ_2^0 (see for example curve 10^{-3} M in P in Fig. 5 in comparison with the dashed one in Fig. 4). This is a clear evidence of the specific interactions between P and SA molecules, since the number of P molecules per unit area of the mixed monolayer is larger than this number in the adsorbed monolayer (in the absence of the SA film), although an important part of the interface is occupied by polar headgroups of SA molecules. Further, one observes that the maxima of the Γ_2 vs. A_3 curves (Fig. 5) are slightly shifted towards larger A_3 values, as compared to the analogous Γ_2' vs. A_3 curves (Fig. 4).

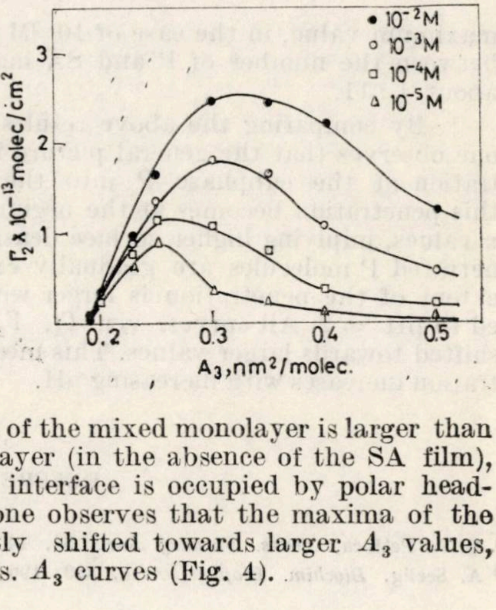

Fig. 5. — P adsorption per unit area of the SA monolayer (Γ_2) as a function of c_2 and A_3 as calculated by means of eq. (5). Symbols as in Fig. 4.

Penetration numbers were calculated by means of eq. (6) and are given in Fig. 6. In Fig. 6 *a* the n_P values are plotted vs. A_3, as Γ_2' and Γ_2 curves in Figs 4 and 5, respectively. In Fig. 6 *b* the plot is performed as a function of the surface pressure, measured in the presence of P in the subphase. As seen, n_P exhibits a maximum in the surface pressure range $5 < \pi < 10$ mN/m, but penetration numbers are not too large. Their maximum value, in the case of 10^{-2}M P solutions, corresponds to a ratio between the number of P and SA molecules in the monolayer equal to about 1 : 11.

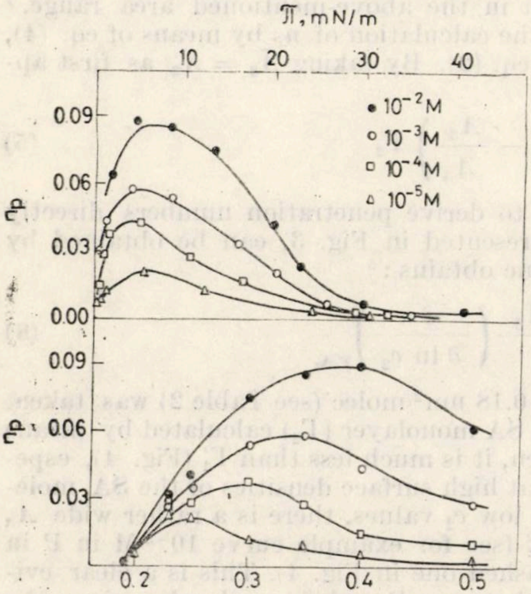

Fig. 6. — Penetration number (n_P) calculated by means of eq. (6) as a function of A_3 (*a*) and as a function of π(*b*). Symbols as in Fig. 4.

By comparing the above results with those obtained at pH = 2, [5] one observes that the general picture is the same, pleading for the penetration of the subphase P into the SA monolayers. At compression this penetration becomes at the beginning more important, but at larger π values, implying higher surface densities of the SA molecules, the penetrated P molecules are gradually expelled from the monolayer. The extent of the penetration is larger with unbuffered systems, as compared to pH = 2. All curves, viz. Γ_2', Γ_2 and n_P as a function of A_3 are shifted towards larger values. This means that the P adsorption and penetration increases with increasing pH.

REFERENCES

[1] B. A. Pethica, *Trans. Faraday Soc.*, **51**, 1402 (1955).

[2] A. Seelig, *Biochim. Biophys. Acta*, **899**, 196 (1987).

[3] M. A. McGregor and G. T. Barnes, *J. Colloid Interface Sci.*, **54**, 439 (1976).

[4] M. Nakagaki and E. Okamura, *Bull. Chem. Soc. Japan*, **55**, 1352, 3381 (1982); **56**, 1607 (1983).

[5] E. Chifu, M. Tomoaia-Cotişel, J. Zsakó, A. Mocanu and P. T. Frangopol, Seminars Biophysics, IAP Press, Bucharest 1990, vol. 6, p. 117.

[6] I. I. Panaitov, L. Ter-Minassian-Saraga and G. Albrecht, *Langmuir* **1**, 395 (1985).

[7] M. Tomoaia-Cotişel, E. Chifu, A. Mocanu, J. Zsakó, M. Sălăjan and P. T. Frangopol *Rev. Roum. Biochim.*, **25**, 227 (1988).

[8] M. Tomoaia-Cotişel, J. Zsakó, A. Mocanu, M. Lupea and E. Chifu, *J. Colloid Interface Sci.*, **117**, 464 (1987).

Revue Roumaine de Chimie, 35, 7—9, 891—897 (1990)

PHASE BEHAVIOUR OF HYDROCARBON-WATER MIXTURES IN THE PRESENCE OF ALKYLPOLYOXYETHYLENE CARBOXYLATES

D. F. ANGHEL, [a] I. MIRCIOAGĂ, [a] D. R. ELLIS [b] and E.A. DUFF[b]
[a] ICECHIM — Department of Physical Chemistry, Bucharest 79611, Romania
[b] ICI Chemicals and Polymer Ltd., PO Box No. 90, Wilton Centre, Middlesbrough, Cleveland TS6 8JE, United Kingdom

Sodium alkylpolyoxyethylene carboxylates such as Synperonic A3C(Na), A7C(Na), NP5C(Na), NP7C(Na, NP10C(Na) and Tridecanol 6.5C(Na) were used to obtain micellar solutions for enhanced petroleums recovery in reservoirs having high salinity of the connate water. Laboratory results with respect to phase equilibria in water-hydrocarbon-surfactant-cosurfactant-electrolyte mixtures are presented. The effects of petroleum, electrolyte, surfactant and cosurfactant are discussed. The results allow to obtain micellar solutions with high efficiency of oil recovery when the temperature, the petroleum composition and the brine concentration are given.

INTRODUCTION

Water and oil are practically immiscible liquids. However, their mutual solubility can be improved by means of a surfactant. Surfactants are organic compounds that have a hydrophilic head and an oleophilic hydrocarbon chain. As a result of this, they are able to partially dissolve in both water and oil. At the water/oil interface, they will concentrate with the hydrophilic heads anchored in the water, and the oleophilic tails dipped in the oil. If the surfactant is ionic an electrical double layer will appear at the interface due to ionic dissociation. Taking this effect into consideration, Shulman tried to obtain a stable emulsion by covering the oil droplets with a layer of ionic surfactant and dispersing these in water. The experiment failed due to the formation of a viscous gel. To destroy the gel, Shulman diluted it with a short-chain alcohol. Thus, he obtained a stable, slightly turbid homogeneous solution that was called a "microemulsion".[1]

During the past three decades much interest has been devoted to microemulsions. They have found application in the detergent, cosmetic and pharmaceutical industries, as special catalysts in the chemical industry, in biotechnology, in the field of medicine as blood plasma substitutes and in tertiary oil recovery processes.

Only about 30% of the oil-in-place is recovered during the primary and secondary stages of crude oil production. The purpose of tertiary oil recovery processes is to recover at least a part of the remaining 70% oil.

Microemulsion flooding as a tertiary oil recovery technique involves a decrease of capilary forces and an increase in the mobility of the oil bank.

At the same time, many oil fields are characterized by high salinities of the connate water. Divalent cations such as calcium and magnesium are among the most incompatible ions with surfactants such as petroleum sulfonates which are commonly used in microemulsion flooding. To overcome this, mixtures of anionic and nonionic surfactants or new surfactants such as ether-sulfates, ether-sulfonates and ether-carboxylates were proposed.

This work is devoted to the study of phase equilibria appearing in hydrocarbon-water systems in the presence of electrolytes and alkyl or alkylaryl polyoxyethylene carboxylates. Some of the systems do also contain short-chain alcohol cosurfactants.

EXPERIMENTAL

The surfactants used were Synperonic A3C(Na), A7C(Na), NP5C(Na), NP7C(Na), NP10C(Na) and Tridecanol 6.5C(Na). Synperonic is a Registred Trade Mark and is the property of ICI plc. They were supplied by Imperial Chemical Industries and were used as such. The A type Synperonics contain $C_{13} - C_{15}$ alkyl chains, whereas the NP types are nonylphenol based surfactants. Figures denote the ethoxylation degree, C denotes carboxymethylate and Na denotes sodium salt.

The oil phase was composed of pure hydrocarbons like n-hexane, cyclohexane, benzene and decane, and hydrocarbon mixtures like kerosene.

The cosurfactants used were n-propanol and isopropanol.

Sodium chloride and sodium chloride/calcium chloride (10 :1 mole ratio) solutions were the aqueous phase.

Phase behaviour determinations were made by equilibrating equal volumes of oil water in the presence of a constant amount of surfactant or surfactant-cosurfactant mixtures. The experiments were carried out at room temperature. The variable parameter was the salinity of the aqueous phase. The total volume of oil and water phase was 30 mL, and the amount of surfactant or surfactant-cosurfactants mixture used was 1 gramme. The measurements were carried out using graduated test tubes. After filling, the tubes were sealed, vigorously shaken and then left undisturbed to attain equilibrium. The equilibrium was reached when no change in the phase volumes was recorded in the measurements made on two successive days. The phase volume was determined with an accuracy of 0.2 mL (0.67 %). The solubility parameters of oil (V_o/V_s *i.e.* volume oil in middle phase : volume surfactant) and water (V_w/V_s *i.e.* volume water in middle phase : volume surfactant) were computed taking into account the volume of the excess phases. They are the amount of oil and water respectively solubilized in the microemulsion by the surfactant volume unit.

Interfacial tensions were measured with a spinninning-drop tensiometer.

RESULTS

Figure 1 shows the dependence of solubility parameters on salinity for the mixtures containing Synperonic A3C(Na). Middle-phase microemulsion appears only for benzene and cyclohexane. The surfactant is too polar to promote three-phase separation in mixtures containing hexane Synperonic A7C(Na) is even more polar. For this surfactant, only the system with benzene as oil phase shows middle-phase microemulsion (see Figure 2). The influence of calcium ions present in the aqueous phase behaviour of the system based on Synperonic A7C(Na) is shown

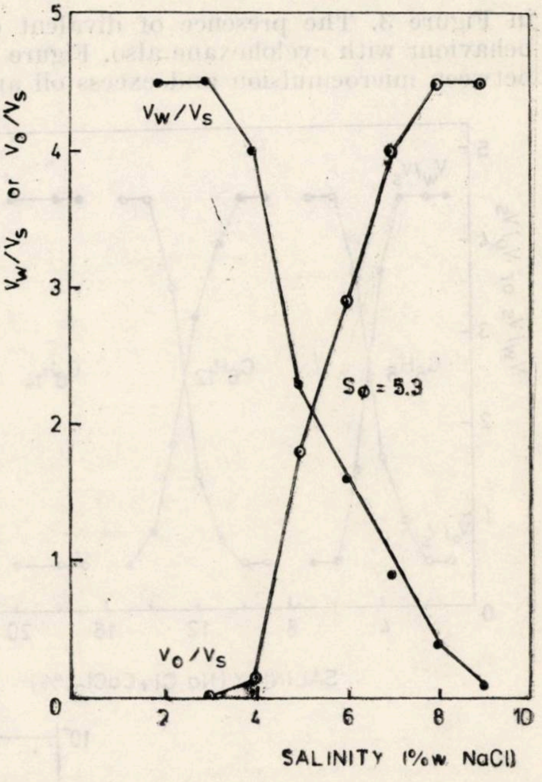

Fig. 1. — Plot of solubility parameters V_o/V_s and V_w/V_s versus salinity for a benzene aqueous NaCl solution in the presence of Synperonic A3C(Na) surfactant and *n*-propanol/isopropanol cosurfactant mixture. V_o/V_s = ratio of the volume of oil in the middle phase to the volume of surfactant present ; V_w/V_s = ratio of the volume of water in the middle phase to the volume of surfactant present ; SØ = optimal salinity from phase behaviour measurements.

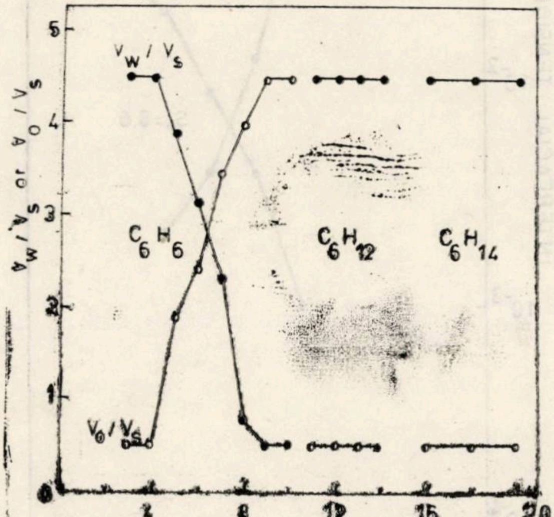

Fig. 2. — The effect of salinity on the solubility parameters for Synperonic A7C(Na). V_o/V_s and V_w/V_s as for Fig. 1

in Figure 3. The presence of divalent cations promotes normal phase behaviour with cyclohexane also. Figure 4 shows the interfacial tensions between microemulsion and excess oil and water phases. They were de-

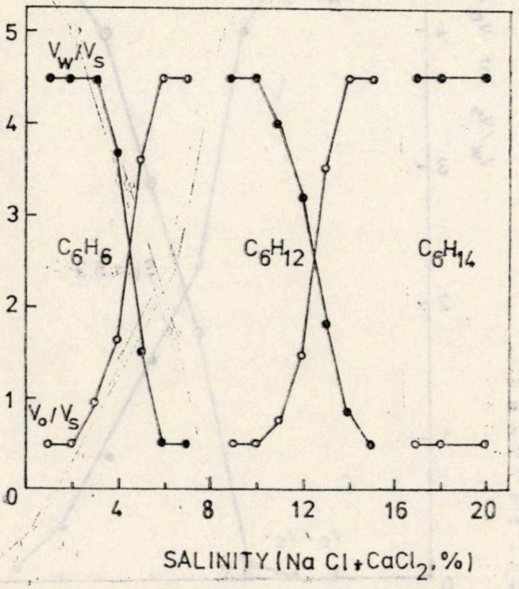

Fig. 3. — Plot of the effect of salinity (including Ca^{2+} ions) on the solubility parameters for Synperonic A7C(Na). V_o/V_s and V_w/V_s as for Fig. 1.

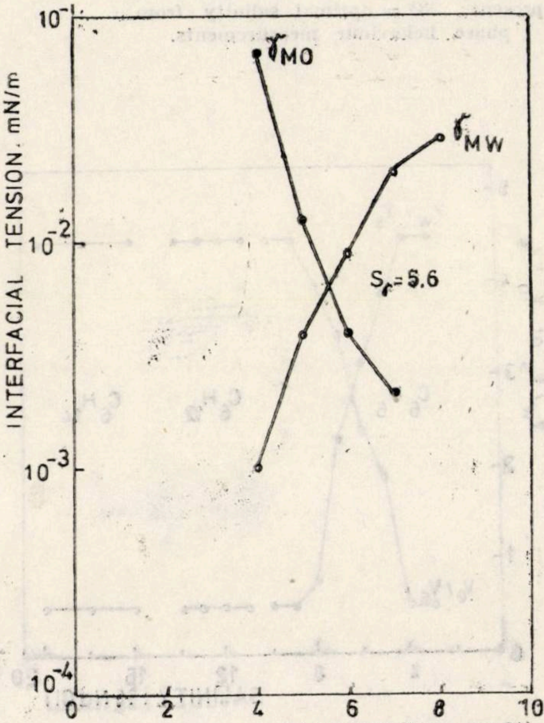

Fig. 4. — Interfacial tension between microemulsion and excess oil and water phases for a benzene-aqueous NaCl solution in the presence of Synperonic A3C(Na) surfactant and *n*-propanol/isopropanol cosurfactant mixture. γ_{MW} = interfacial tension between the microemulsion and excess water phase; $S\gamma$ = optimal salinity from interfacial tension measurements; γ_{MO} = interfacial tension between the microemulsion and excess oil phase.

termined for the benzene-aqueous sodium chloride solutions in the presence of Synperonic A3C(Na) surfactant and n-propanol — isopropanol cosurfactant mixture. Ultra-low values of the interfacial tension at the microemulsion/oil and microemulsion/water interfaces were recorded.

The optimal salinity values obtained from phase behaviour and interfacial tension measurements are presented in Table 1. The optimal salinity for phase behaviour agrees well with the value determined by interfacial tension measurements. Synperonic A7C (Na) is more hydrophilic than Synperonic A3C(Na) and has a higher salt tolerance. The presence of calcium ions in brine lowers the optimal salinity. In the case of benzene, the optimal salinity in the presence of calcium ions is 25 % lower than in NaCl only and thus confirms the observation that alkylpolyoxyethylene carboxylates have good resistance towards divalent cations.

Table 1

Optimal salinity from phase behaviour ($S\O$) and interfacial tension ($S\gamma$) measurements and lower (ε_l) and upper (ε_u) salinity critical end point for oil-water-surfactant-cosurfactant mixtures

Mixture	$S\O$/ (% NaCl)	S (%NaCl)	1 (% NaCl)	u (% NaCl)
Benzene-brine-Synperonic A3C(Na)-n-propanol-isopropanol	5.3	5.6	3.5	7.0
Cyclohexane-brine-Synperonic A3C(Na)-n-propanol-isopropanol	—	—	10.5	—
Benzene-brine-Synperonic A7C(Na)	6.0	—	4.5	8.5
Benzene-brine-Synperonic A7C(Na)	4.5*	—	2.5	5.5
Cyclohexane-brine-Synperonic A7C(Na)	12.6*	—	10..5	14.5

* The brine contains $NaCl-CaCl_2$ (10 :1 mole ratio) mixture.

None of the other surfactants used exhibited three phase behaviour in oil-brine mixtures irrespective of the nature of the oil, cosurfactant and electrolyte present in the water.

DISCUSSION

At constant temperature, mixtures of water, oil and surfactant or surfactant-cosurfactant may separate into three liquid phases: an aqueous lower phase, a surfactant-rich middle phase and an oil upper phase. In the middle phase, frequently referred to as microemulsion, one finds the highest mutual solubility between water and oil and a minimum interfacial tension between the aqueous and oil phases. This is why these systems have been widely considered for use in enhanced oil recovery. In the case of a particular reservoir, the temperature, the chemical nature of the oil and the salt concentration of the water are known. The challenge is to find the surfactant which is the most efficient in solubilizing these reservoir fluids at the given temperature.

If a lyotropic electrolyte is added into the water, the chemical potential of the aqueous phase will be changed. This kind of electrolyte makes the surfactant more hydrophobic thus increasing its solubility in the oil phase. Consequently, three-phase separation may occur.

Consider first a mixture of equal volumes of oil and water. The mixture will separate into two phases irrespective of the amount of the electrolyte added. At high electrolyte concentrations however three phases will be observed but one of them is solid salt and the system is not of interest. If a surfactant or a surfactant-cosurfactant mixture is added, and the salt content of the water is increased, the system will undergo the following changes :

— At low electrolyte levels the mixture will separate into two liquid phases, an aqueous surfactant-rich phase in equilibrium with an excess oil phase. This is the so-called Winsor I (O/W + O) type. 2 This notation is still in use although Knickerbocker *et al.* [3] proposed a more descriptive notation than ten years ago. They denoted a tow-phase system with the surfactant mainly dissolved in the lower phase with *2*.

— By increasing the electrolyte concentration the mixture will separate at one time into three liquid phases : a lower aqueous phase containing almost all the salt, a middle surfactant-rich phase, and an upper oil-rich phase. In the above notations they are denoted by Winsor type III (W + miceoemulsion + O), and Knickerbocker 3 respectively. The salt concentration at which the middle phase appears is the lower salinity critical end point (ε_l).

— With further increase of the salt concentration, the three phases will coexist within a salinity range that stretches up to upper salinity critical end point (ε_u), when middle phase merges with the upper phase. From now on, we will find again two phases but the surfactant is in the upper one. This is Winsor's type II (W/O + W) or Knickerbocker's $\bar{2}$.

The change in the system phases with respect to salinity is *2* → → 3 → $\bar{2}$. This sequence was recorded in only some of our systems (see Table 1). Except for the mixture based on cyclohexane and Synperonic A3C(Na), all the other systems have lower and upper salinity critical end points respectively. In these mixtures there is only one microemulsion region. With in this region, a continuous transition from O/W to a W/O droplet-type microemulsion is possible without passing through a multiphase region. It is highly probable that such a transition takes place via bicontinuous microemulsion. [4–6] In these systems, regions of oil and water, are interdispersed and their boundaries may fluctuate in time. Also both oil and water regions extend continuously throughout the microemulsion. However the boundaries between droplet type microemulsions and bicontinuous microemulsion will not coincide with the boundaries of the three phase region.

Recently, Jahn and Strey[7] proved by means of a special freeze fracture electron microscopy technique the existence of a bicontinuous structure in H_2O—*n*-octane—*n*-dodecylpentaethylene glycol system. For the system D_2O-*n*-decane—sodium bis(2-ethylhexyl)sulfosuccinate and H_2O—*n*-dodecane—didodecyldimethylammonium bromide a water in oil droplet structure was observed. Dilution with oil decreases the number of the droplets whereas their structure remains almost unchanged. The same droplet structure was found in a system containing cosurfactant (*i.e.* H_2O-n-dodecane-1-hexanol-potassium oleate). For the system with the nonionic surfactant a sponge-like structure for the bicontinuous microemulsion was proposed. Both structures are highly unstable. In the sponge-like structure the water and oil domains change their size and shape rapidly and the surfactant molecules change their position in the monolayer. In the droplet structure, droplets form and disappear continuously. Their shape may fluctuate and this will lead to some degree of local bicontinuity. Bicontinuous structures may therefore already exist in the two-phase regions, especially close to the three-phase boundary.

For a given amount of surfactant, the microemulsion will contain a fixed amount of water and oil. The surplus that cannot be absorbed by the structure is expelled. Thus, a lower aqueous bulk phase and an upper oil-rich bulk phase will form respectively. This behaviour is consistent with both sponge-like and droplet structure of the microemulsion.

As was previously stated, lyotropic electrolyte makes the surfactant more oleophilic. The higher the electrolyte concentration in the water the greater the tendency of the anionic surfactant to leave the aqueous phase. If the surfactant is too hydrophilic it cannot be forced to enter the oil phase even in the presence of a very high amount of salt. When such a surfactant is present in a mixture that exhibits middle phase microemulsion, increasing the electrolyte concentration will causes more water to be expelled from microemulsion. The volume of microemulsion will decrease but the microemulsion will not merge with the oil phase. This was the case of cyclohexane-brine-Synperonic A3C(Na)-n-propanol--isopropanol mixture, where only the *2* → 3 phase transition was recorded. Moreover, the majority of the systems studied by us did not undergo any phase transition. Upon increasing the electrolyte concentration no change in phase behaviour was observed. This is believed to have been due to the fact that the surfactants used were too hydrophilic.

The phase behaviour of the microemulsion systems studied here is typical for mixtures of a single-chain ionic surfactant and a short chain length alcohol as the cosurfactant. Among the alkyl and alkylaryl polyoxyethylene carboxylates used only Synperonic A3C(Na) and A7C(Na) proved to be suitable for surfactant flooding enhanced oil recovery. Although Synperonic NP5C(Na), NP7C(Na), NP10C(Na) and Tridecanol 6.5C(Na) did not give middle phase microemulsion here it is possible to find such microemulsions by changing the oils and the cosurfactants used. These surfactants deserve further attention because of their high salinity tolerances towards hard water.

REFERENCES

J. H. Shulman, W. M. Stoeckenius and L. M. Prince, *J. Phys. Chem.*, **63**, 1677 (1959).

[2] P. A. Winsor, *Trans. Faraday Soc.*, **44**, 376 (1948).

[3] B. M. Knickerbocker, C. V. Pesheck, L. E. Scriven and H. T. Davis, *J. Phys. Chem.*, **83**, 1984 (1979).

[4] L. E. Scriven, *Nature*, **263**, 123 (1976).

[5] L. E. Scriven, in ,,Micellization, Solubilization and Microemulsions", (K. L. Mittal, Ed.), Vol. 2, p. 877, Plenum, New York, 1977.

[6] P. G. DeGennes and C. Taupin, *J. Phys. Chem.*, **86**, 2294 (1982).

[7] W. John and R. Strey *J. Phys. Chem.*, **92**, 2294 (1988).

Revue Roumaine de Chimie, 35, 7—9, 899—908(1990)

ASYMMETRIC MEMBRANES PREPARED BY IMMERSION-PRECIPITATION TECHNIQUE

GHEORGHE NECHIFOR [a] and GEORGETA POPESCU [b]
[a] Polytechnic Institute of Bucharest, Romania
[b]Center of Physical Chemistry—ICECHIM,
Spl. Independenţei 202, Bucharest, Romania

The results of a study on the obtention of asymmetric membranes by phase inversion method are presented; the study has evidenced the generality of coagulation pathways theory developed by the Dutch membrane school. Simple structures were obtained by changing either the solvent or the coagulant in the polymer-solvent-nonsolvent system. In this study use has been made of polysulphone as reference polymer, dipolar aprotic solvents (DMF, NMP, DMAc, chloroform, cyclohexanone) and lower aliphatic alcohols ($C_1—C_4$) as nonsolvents. The structures of membranes were determined by scanning electron-microscopy. The influence of initial concentration of polymer solutions on membrane structure was also investigated.

INTRODUCTION

The successful applications of the Loeb and Sourirajan type membranes [1] has determined a tremendous development of membrane processes which imposed studies of methods and techniques of obtaining membranes in general and asymmetric membranes in special. [2–4] From among these methods phase inversion by precipitation immersion has been the most frequently studied method of obtaining asymmetric membranes.[5]

The obtention of membranes with preselected performances has been facilitated by the existence of reference studies as well as the development of the thermodynamics of polymer-solvent-nonsolvent ternary system.[6,7]

The results obtained by the Dutch membrane school have allowed Smolders to describe the possible pathways of coagulation when a polymer solution film contacts the coagulation agent (Fig. 1 a and b)

Basically, the coagulation pathways OA, OB, OC and ODE may be achieved by adequately selecting the variables of polymer-solvent-nonsolvent system.

In a previous paper we showed that one can obtain membranes of similar structure starting up with two different polymers (polysulphone or polyphenyl oxide) and choose the adequate solvent-nonsolvent system. [8]

This contribution presents the possibility of obtaining membranes with similar structures by changing the solvent (Fig. 2 a) and the nonsolvent (Fig. 2 b). The influence of polymer concentration upon membrane structure was also studied.

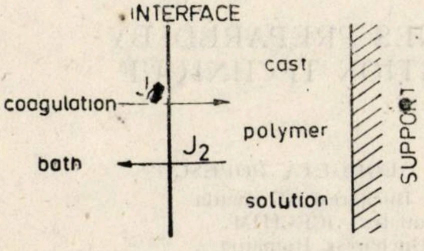

Fig. 1a. — Fluxes of non-solvent (J_1) and solvent (J_2) at the interface bath/cast polymer solution.

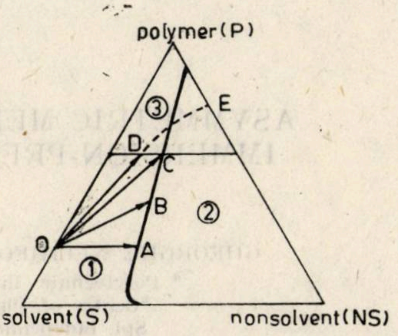

Fig. 1b. — Schematic phase diagram for a ternary system with a one-phase region 1, a two-phase region 2 and a gel region 3.

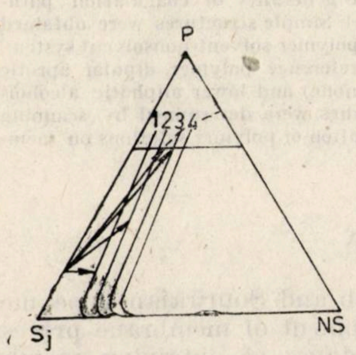

Fig. 2a. — Schematic phase diagram for a ternary system : polymer — solvent$_j$ — nonsolvent.

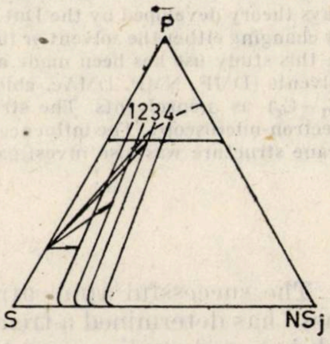

Fig. 2 b. — Schematic phase diagram for a ternary system : polymer — solvent — nonsolvent$_j$.

EXPERIMENTAL

The polymer : Udel type polysulphone (PSF) from the Institute of Macromolecular Chemistry "Petru Poni", Iassy : ; average molecular weight $\overline{M} = 35,000-45,000$ Dalton.

The solvents : dimethylformamide (DMF), N-methylpyrolidone (NMP), dimethylacetamide (DMAc), chloroform (CF), cyclohexanone (CH). The non-solvents : methanol (M), ethanol (E), propanol (P), butanol (B).

The preparation of casting solutions. Polysulphone was solved under continuous stirring at room temperature in the solvent to yield a solution of polymer concentration 10—25% (weight). The solution was filtered and degased.

The preparation of membranes. The degased solution was made into a film of constant thickness and was then immersed in nonsolvent. The membrane formed was washed and then dried at room temperature.

The determination of membrane structure. Specimens of the membranes obtained were fractured in liquid nitrogen, coated with platinum and examined at a Leitz REM 1600 T electron microscope.

RESULTS AND DISCUSSION

Continuing the experiments aiming at supporting Smolders and collab's theory of coagulation pathways described by the ternary diagram, the coagulant was modified. The micrographs were compared to those resulted from the modification of the solvent in the polymer-solvent-nonsolvent ternary system. Although the data do not allow a rigorous correlation of a certain coagulation pathway with a given structure they evidence the similitude of certain structures. Thus one can state that whenever similar structures are obtained the phenomena occurring in membranes are identical. Therefore the relation between the systems: polymer — solvent_j — nonsolvent ≡ polymer — solvent — nonsolvent_j, e.g. polysulphone — solvent_j — iso butanol ≡ polysulphone — cyclohexanone — nonsolvent_j, respectively, refer only to the phenomena which occur at phase inversion in the ternary system.

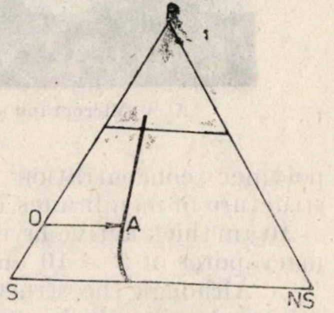

Fig. 3. — Schematic course of a coagulation path OA.

In the following the coagulation pathways are specified and the assignment in a classification of the structures resulted from the same pathway is argued:

a) *Pathway OA* (Fig. 3). The micrographs A_1 and A_2 were obtained in PSF —DMF — iso B and PSF — CH — M systems, respectively. According to this pathway, the fluxes of solvent (J_1) and nonsolvent through the polymer solution — nonsolvent interface are equal and important; therefore the coagulation is fast and the binodal curve is reached at a

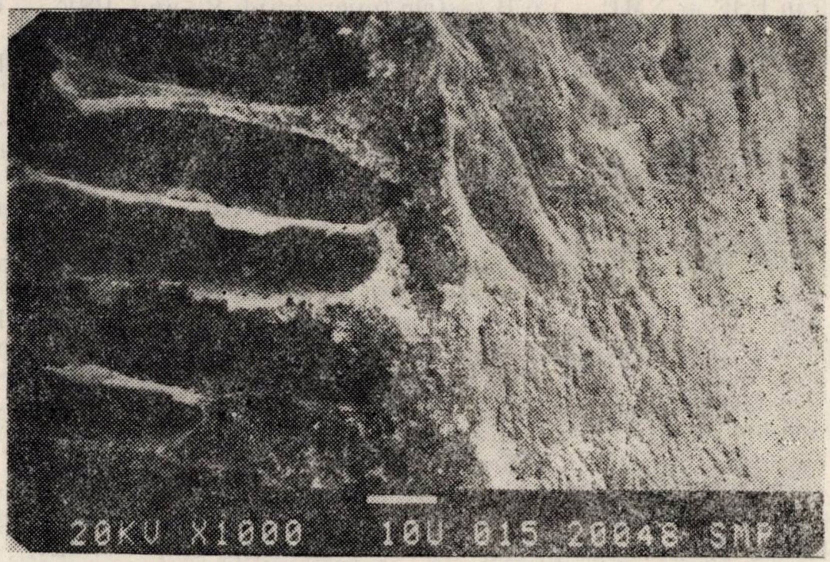

A_1 — Micrograph of membrane from system PSF — DMF — iso B.

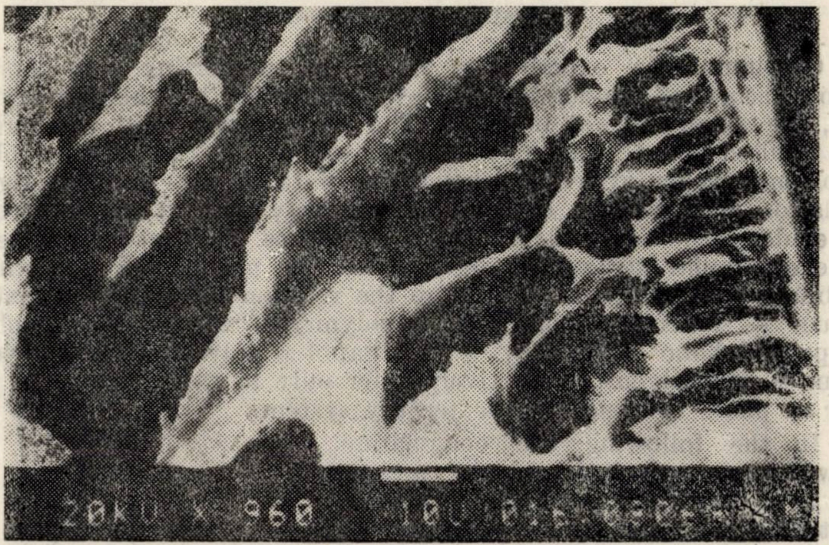

A_2 — Micrograph of membrane from system PSF — CH — M.

polymer concentration in the system equal to the initial one. The structure of membranes (micrograms A_1 and A_2) shows a compact 2 — — 10 μm thick active layer and a macroporous layer formed of cylindrical macropores of 5 — 10 μm diameter.

Although the structures evidenced are not identical, there are surprising details which suggest the similitude of the phenomena occurring in the two systems discussed.

b) Pathway OB (Fig. 4). The increase of the coagulation pathway length in PSF — NMP — iso B system (micrograph B_1) and PSF — CH— — E system (micrograph B_2) is more than formal and mirrors the increase of coagulation duration. The increase of coagulation duration is accounted for by the weaker interaction between solvent and nonsolvent and the stronger interaction between the polymer and the solvent. The micrographs A_1 and B_1 as well as B_1 and B_2 suggest that changing the solvent induces modifications of structure which are more important than those induced by changing the nonsolvent. In all these considerations the nonsolvent — solvent interaction is neglected. According to the micrographs B_1 and B_2 the membranes are more compact and their active layer is thinner.

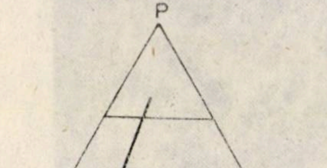

Fig. 4. — Schematic course of a coagulation path OB.

c) The pathway OC (Fig. 5). This pathway has fostered our study on structure — ternary system and structure — coagulation pathway correlation. The micrographs C_1 and C_2 obtained in PSF — DMAc — iso B and PSD — CH — P systems, respectively exhibit the transition from

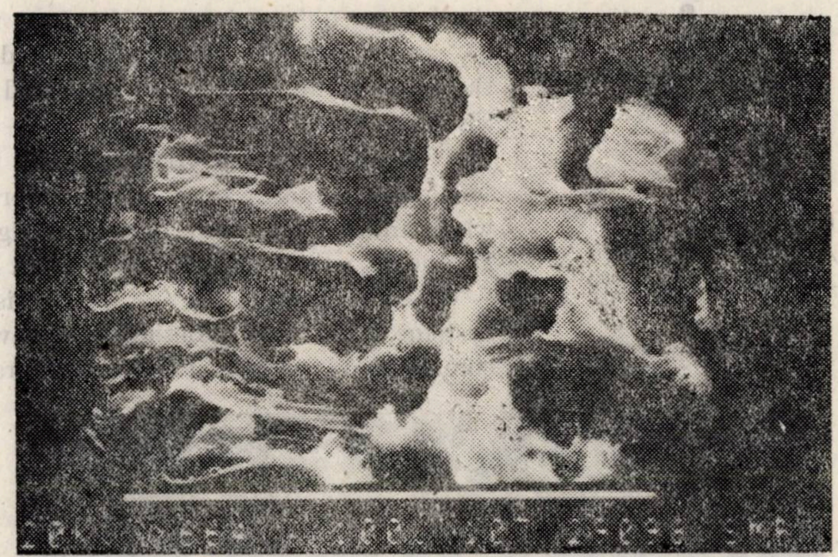

B_1 — Micrograph of membrane from system PSF — NMP — iso B.

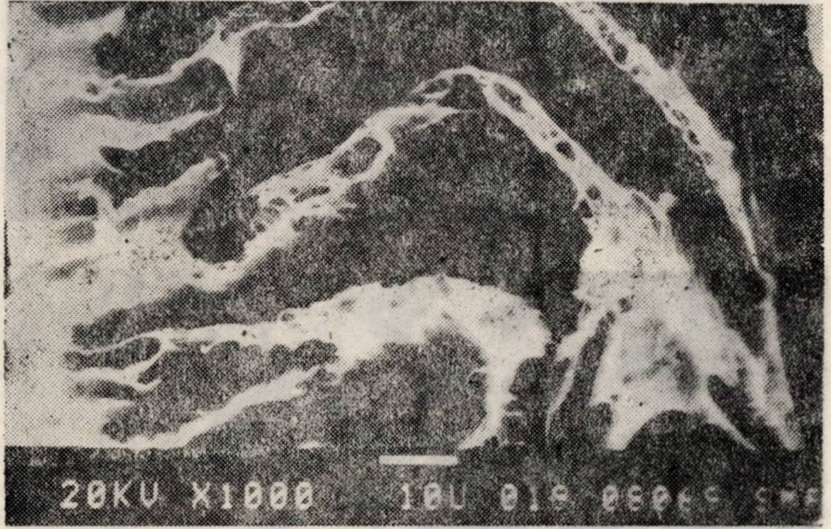

B_2 — Micrograph of membrane from system PSF — CH — E.

macropore-type structure to spongy structure which characterizes the direct transition from solution to gel state. The duration of coagulation increases significantly i.e. from fractions of a second to tens of seconds. The solvent — nonsolvent interaction is weak and dominated by polymer — solvent interaction which entails the formation of the gel which includes an important amount of solvent. One has to compare

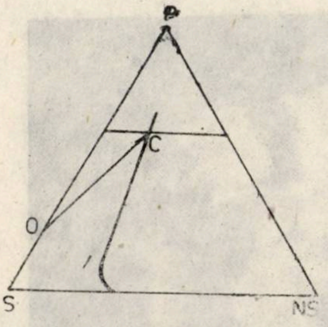

Fig. 5. — Schematic course of a coagulation path OC.

the images obtained in the fracture zone (C_1 and C_2). The micrographs evidence the compatibility of the structure and the thinning of the active layer.

d) The pathway ODE (Fig. 6). This coagulation pathway yields membranes whose micrographs may be seen in figures D_1 and D_2; they were obtained from PSF — CF — iso B and PSF — CH — iso B systems, respectively. Besides the previous comments syneresis these micrographs

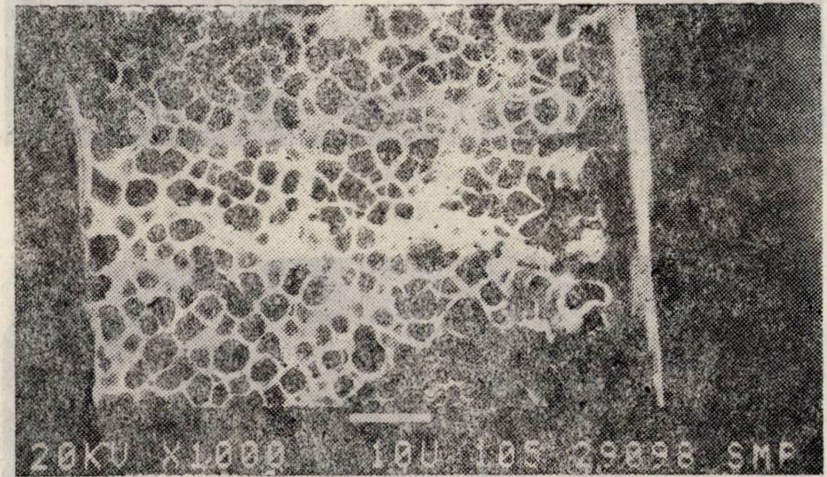

C_1 — Micrograph of membrane from system PSF — DMAc — iso B.

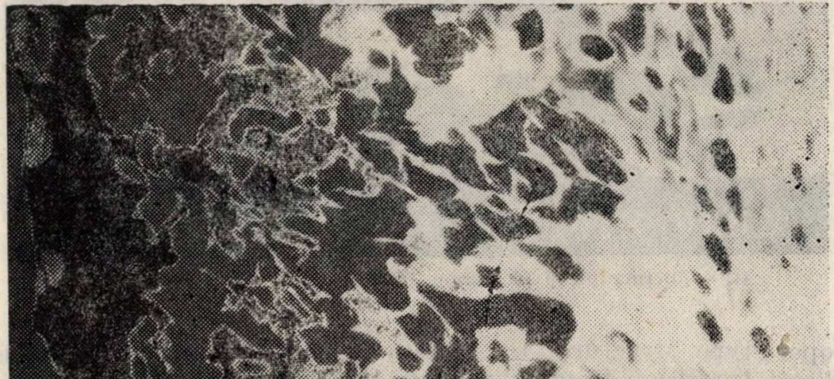

C_2 — Micrograph of membrane from system PSF — CH — P.

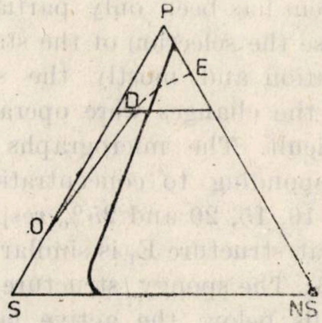

Fig. 6. — Schematic course of a coagulation path ODE.

exhibit the phenomenon (the arc DE); this phenomenon is evidenced by the compactness of the membrane in the spongy layer and the increase of the thickness and compactness of the active layer.

The aim of this contribution i.e. ensuring the reproducibility of structure according to the coagulation pathways in the ternary diagram through changes of polymer concentration in PSF — NMP —

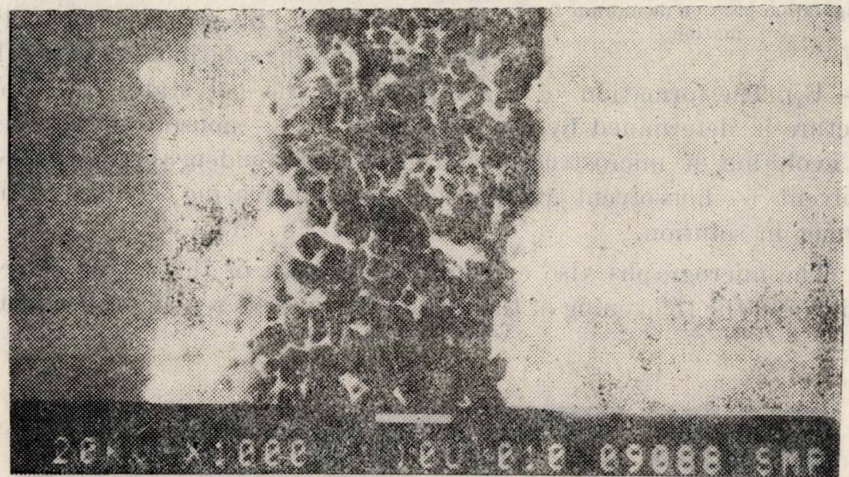

D_1 — Micrograph of membrane from system PSF — CF$_4$ — iso B.

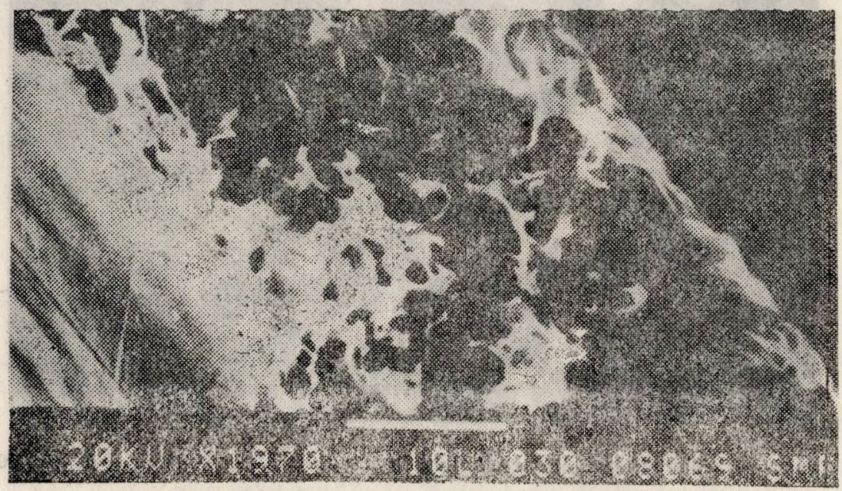

D_2 — Micrograph of membrane from PSF — CH — iso B.

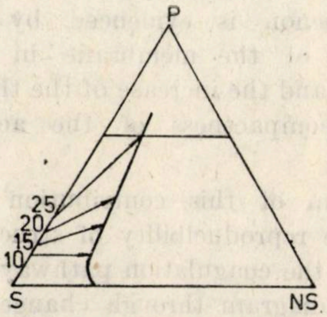

Fig. 7 — Influence of the concentration of the direction of the coagulation path on membrane formation.

E (Fig. 7) system has been only partially reached because the selection of the starting. concentration and mostly the system in which the changes were operated was very difficult. The micrographs E_1 — E_4 corresponding to concentrations (% weight) of 10, 15, 20 and 25% respectively show that structure E_1 is similar to A_2 and E_2 to B_2. The spongy structure of macropore walls below the active layer as well as the structure of this latter is assigned to the transition from sol to gel which is more intense as the polymer concentration in solution increases ($E_2 \rightarrow E_3 \rightarrow E_4$). The formation of macropores to the gel state with spongy structure is determined by the strong solvent — nonsolvent interaction. The evolution of microstructures from E_2 to E_4 evidences the diminishing of solvent — nonsolvent interaction with increasing concentration of polymer in solution.

The micrographs also evidence the growth of the active layer dispersion and the thickening of the membrane with increasing concentration.

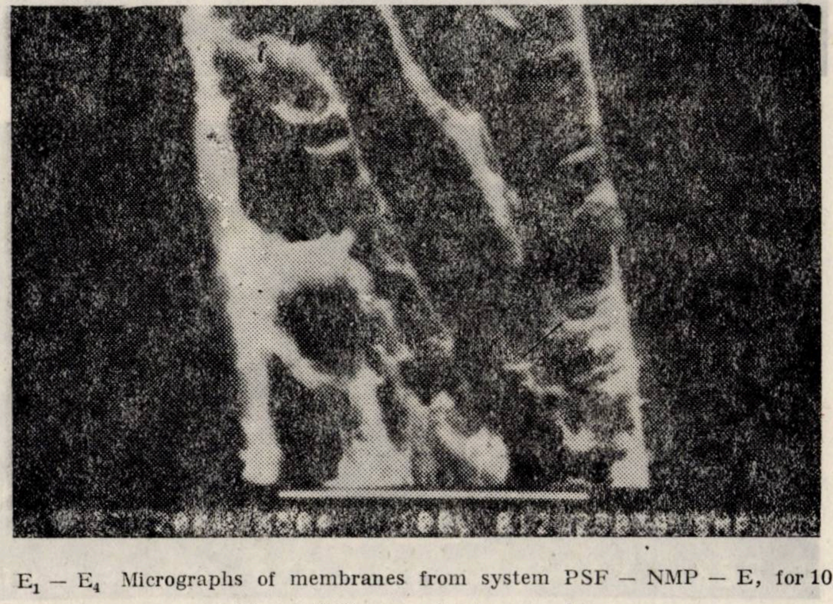

E_1 — E_4 Micrographs of membranes from system PSF — NMP — E, for 10, 15, 20 and 25% concentration of polymer.

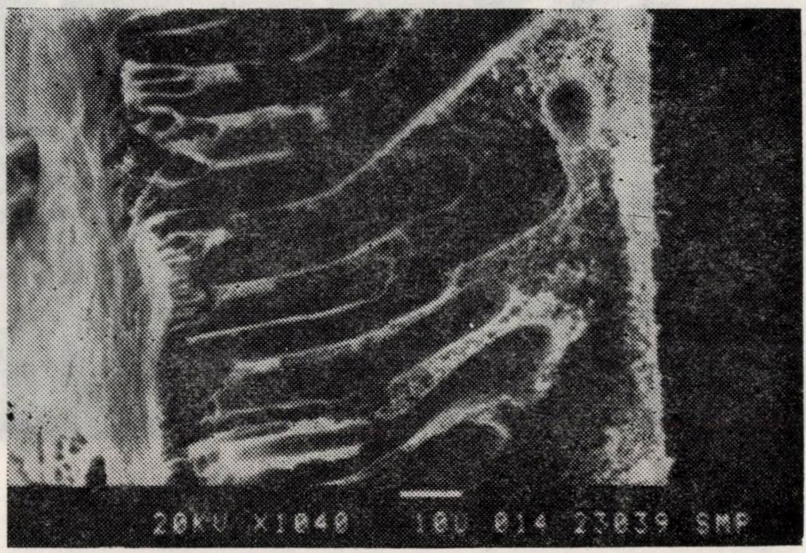
20KU X1040 10U 014 23039 SMP

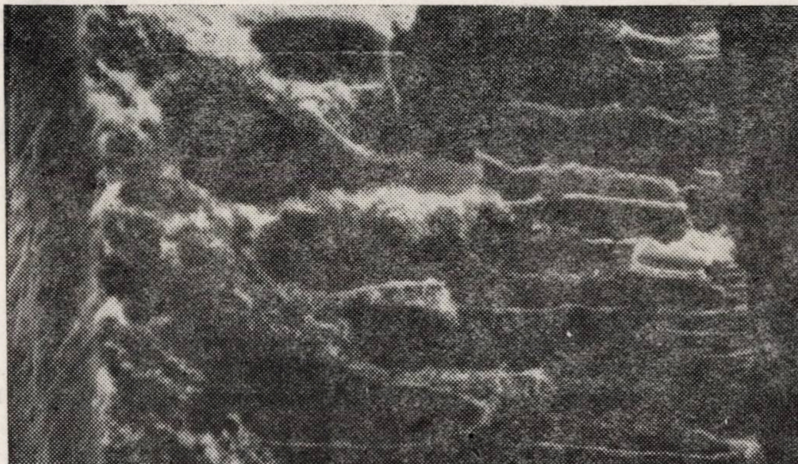
20KU X752 100U 018 23079 SMP

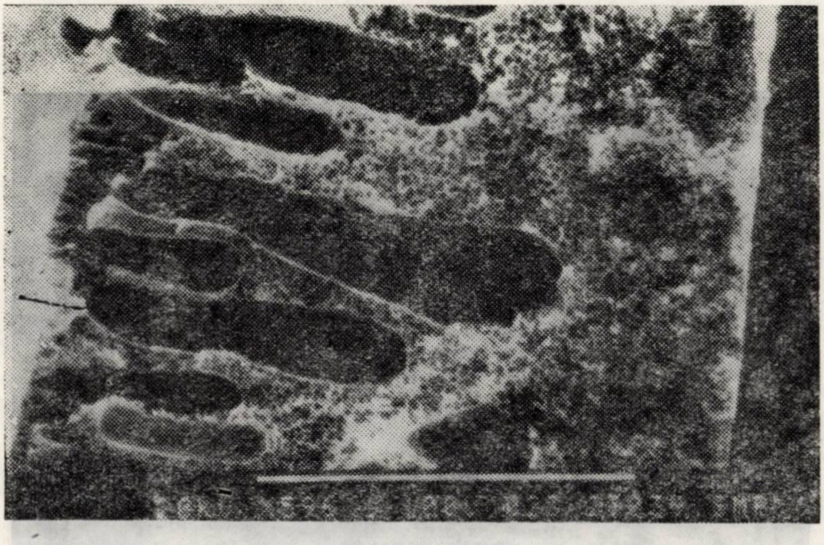

CONCLUSIONS

This study emphasizes the generality of coagulation pathway theory developed by the Dutch school of membranes, the possibility of obtaining membranes with similar structure from polymer — solvent$_J$ — nonsolvent or polymer — solvent — nonsolvent$_J$ systems and the importance of taking account of the polymer concentration.

It is possible to obtain membranes of similar structures from polymer — solvent — nonsolvent system by altering one of the parameters.

Controlling the membrane formation may be ensured through consideration of polymer — solvent, solvent — nonsolvent, nonsolvent — polymer interactions as well as of concentration, pressure and time.

The numerous interactions and parameters may be controlled efficiently by assigning them coefficients of relative importance and checking the assignments. All considerations require extensive experiments.

REFERENCES

[1] S. Loch and S. Sourirajan, *Advan. Chem. Ser.*, **38**, 117 (1962).

[2] S. Sourirajan, "Reverse Osmosis", Academic Press, New York, 1970.

[3] R. E. Kesting, ,,Synthetic Polymeric Membranes", McGraw-Hill, New York, 1971.

[4] H. K. Lonsdale, H. E. Podal Eds., "Reverse Osmosis Membrane Research", Plenum Press, New York, 1972.

[5] L. Broens, F. M. Altena, C. A. Smolders and D. M. Koenhen, *Desalination*, **32**, 33 (1980).

[6] J. G. Wijmans, J. P. B. Baaij and C. A. Smolders, *J. Membr. Sci.*, **14**, 263 (1983).

[7] A. J. Reuvers, J. W. A. van den Berg and C. A. Smolders, *J. Membr. Sci.*, **34**, 45 (1987).

[8] G. Nechifor, N. Luca, G. Popescu and M. Nechifor, *Rev. Roumaine Chim.*, **34**, 2046 (1989).

Revue Roumaine de Chimie, 35, 7–9, 909–914 (1990)

INORGANIC MEMBRANES OBTAINED BY THE SOL-GEL METHOD

MARIA ZAHARESCU, CONSTANȚA PÎRLOG, A. VASILESCU,
D. CRIȘAN and ANA BRĂILEANU
ICECHIM — Center of Physical Chemistry, Bucharest
Splaiul Independenței 202, Romania

Ceramic membranes (with predetermined texture) consisting of Al_2O_3 support and ultra-porous SiO_2 film were obtained ; the support as well as the film were prepared by sol-gel method. X-ray diffraction, specific surface, pore volume and pore size measurements were employed to determine the structural and textural properties of membranes. It was found out that while the structure and texture of the Al_2O_3 based support changes with the thermal treatment temperature, the SiO_2 film remains amorphous and with unaltered pore size up to 900°C.

1. INTRODUCTION

The ceramic membranes represent a distinct class of inorganic membranes.

Basically a ceramic membrane represents an ensemble consisting of a porous support which ensures mechanical strength and a micro- or ultra-porous film which achieves the separation. It is characterized by transfer selectivity as well as permeability to liquid or gaseous media in the presence of a pressure gradient. [1]

The materials used in ceramic membranes were refractory oxides (e.g. SiO_2, Al_2O_3, TiO_2, ZrO_2). They grant the membranes the following qualities :

— chemical inertness i.e. no corrosion during utilization in acid, basic and oxido-reducing media,

— mechanical strength which allows their surface to stand high pressure or pressure gradients,

— thermal resistance which affords utilization in separation processes at high temperatures ($T > 300°C$) which the usual membranes could not stand.

Al_2O_3 membranes currently enjoy the greatest attention the world over because of the qualities listed above and the multiple possibilities of preparing them. [2,3]

Although such companies as ALCOA, NORTON trade Al_2O_3 membranes for ultra- and micro-filtering one may affirm that the phenomena involved in preparation of these membranes are far from elucidated. [1,4]

From among the numerous alternatives of obtaining the porous Al_2O_3 support (ceramic, the ceramic with additives, [5] ceramic with powders resulted from coprecipitation and sol-gel[6–8]) the sol-gel method was selected which yields supports of controlled porosity, generally monodispersed. The same method was utilized to obtain SiO_2 ultraporous film.

2. EXPERIMENTAL

2.1. Obtaining of the porous support

The reagents employed were as follows :

- aluminium iso-propylate, $Al(i-OC_3H_7)_3$, as Al_2O_3 source ;
- nitric acid p.a. reagent (Reactivul) as catalyst ;
- distilled water, necessary in the hydrolysis process of $Al(i\text{-}OC_3H_7)_3$.

Composition of initial solution and synthesis condtions of obtaining Al_2O_3 support are listed in Table 1.

Table 1

Composition of initial solution and synthesis conditions of obtaining Al_2O_3 support

$Al(i-OC_3H_7)_3$ (mol)	H_2O (mol)	Catalyst HNO_3(mol)	Temperature (°C)	Time (minute)
1	100	0.07	80	30

The pseudobohemit sol resulted from the hydrolysis of Al $(i-Opr)_3$ was "aged" 7 days at 50°C to yield a translucent gel ; it was dried at 120°C and ground to a granulation lower than 60 μm.

Shaping of the powder was achieved by uniaxial pressing at 1600 daN/cm² to obtain discs 20, 30 and 50 mm in diameter.

The thermal treatment of pressed bodies was carried out according to the diagram in Figure 1.

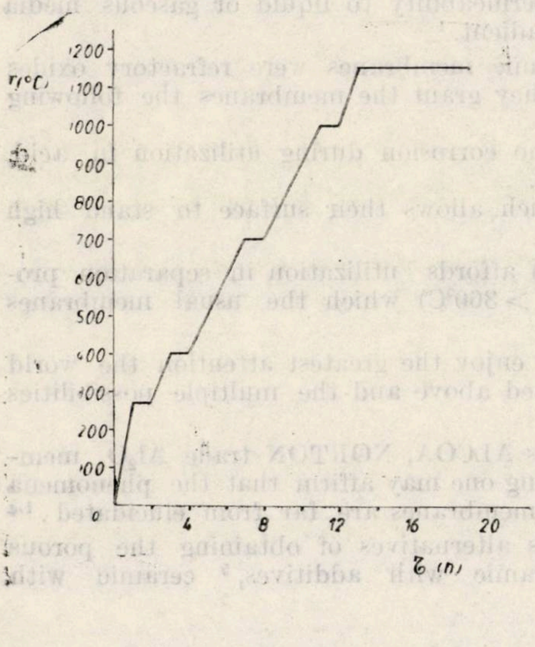

Fig. 1. — Thermal treatment diagram of pressed bodies.

The plateaus were established by DTA and are important to eliminate water (80 and 270°C) and organic rests (270° and 410°). The plateaus at higher temperature, 600, 1000 and 1150°C have been maintained in order to achieve powder sintering and convenient mechanical strength.

2.2. Obtention of ceramic membranes

To obtain the ceramic membrane on Al_2O_3 support (see section 2.1) the SiO_2 solution of composition shown in Table 2, previously polymerized to a viscosity of 2–6 cP was deposited on it. The deposition was achieved in two ways :

— by dip coating, in which the samples were immersed in solution at ambient temperature during 1–3 minutes and retracted with a constant speed of 6 cm/minute.

— by spinning i.e. droping of initial solution on a surface of the support which rotates with 3000 rot/minute.

Samples were dried in air and then subjected to thermal treatment at 500°C.

Table 2

Composition of initial solution and synthesis conditions of obtaining SiO_2 film

$Si(C_2H_5O)_4$ (mol)	H_2O (mol)	Solvent C_2H_5OH (mol)	Catalyst HCl	Temperature (°C)
1	4	4	2–3 drops	20

2.3. Characterization of ceramic membranes

The dry gels and the materials resulted from thermal treatment were studied by the following methods :

— DTA/TG, using a MOM OD–102 Derivatograph, between 20 and 1000°C, at a speed of 10°C/minute,

— X-ray diffraction on HZG–3 diffractometer, working with CoK_α radiation,

— BET adsorption of nitrogen gas at the temperature of liquid nitrogen

— adsorption-desorption isotherm for volume and size of pores determination.

3. RESULTS AND DISCUSSION

3.1. Al_2O_3 porous support

The sol-gel method consists of preparing oxidic gels in a sequence of hydrolysis-polycondensation reactions of some organometallic compounds of alcoholates, acetylacetonates, etc. type. The gels may be transformed by adequate thermal treatment at low temperature into glasses or crystallized materials.

In hydrolysis-polycondensation of $Al(i-OC_3H_7)_3$ results as a pseudobohemite gel according to the reaction :

$$n\,Al(i-OC_3H_7)_3 + 2n\,H_2O \xrightarrow{T > 80°C} nA\,10(OH) + 3n\,i-C_3H_7-OH$$

The results of structural and textural characterization of the gel resulted and of samples thermally treated at various temperatures are listed in Table 3.

Table 3

Structural and textural properties of the AlO(OH) gel and of samples thermally treated at various temperatures

Samples	Structure	BET surface area (m^2/g)	Dimension pores (Å)	Volume of pores (cm^3/g)
un-treated gel	AlO(OH)	325	—	—
gel treated at 600°C	$\gamma + \delta Al_2O_3$	150	40	0.4
gel treated at 1000°C	$\delta + \theta Al_2O_3$	4	164	0.52
gel treated at 1150°C	$\alpha\ Al_2O_3$	—	600	—

It was noted that at the beginning the gel is partially crystallized in a pseudobohemite structure. At 600°C the material consists of a mixture of gamma and delta alumina; at 1000°C gamma and theta alumina coexist while the material thermally treated at 1150°C consists only of alpha alumina.

Regarding the structure of pores it was found out that it changes as a function of thermal treatment temperature; with the rising of this temperature the number of pores per unit volume decreases and the size of pores increases from 40 Å at 600°C to 164 Å at 1000°C and 600 Å at 1150°C.

The change of the number and size of pores in Al_2O_3 membranes is related to the crystallization of the material over the temperature range mentioned and to polymorphous transformations undergone by aluminas at different thermal treatment temperatures. The relation existing between the polymorphous changes of alumina at various temperatures and the pore structure is confirmed in literature.[9,10]

The present results were confirmed by five syntheses followed by the thermal treatments mentioned; they showed that starting from aluminium iso-propylate as Al_2O_3 source one may obtain membrane supports of preselected porosity in reproducible conditions.

Taking account of the fact that the mechanical strength of the material increases with temperature of thermal treatment, the supports sintered at temperatures above 1000°C are recommended.

3.2. Al_2O_3 based ceramic membrane

The membrane was obtained by depositing a glassy SiO_2 film on the Al_2O_3 support in conditions specified in Table 2.

The structural and textural properties of thermally treated silica gels have previously been determined.[11]

X—Ray diffraction has confirmed that over the 20—900°C temperature range the gel does not crystallize and vitreous material results.

The changes in silica gel texture in the mentioned temperature range are listed in Table. 4.

Table 4

Texture properties of SiO_2 gel thermally treated in 20—900°C range

Thermal treatment temperature, (°C)	Volume of pores (0—150 Å) (cm^3/g)	Volume of micropores (0—15 Å) (cm^3/g)	Diameter pores Å	BET surface area (m^2/g)
20	0.35	0.33	14.4	481
600	0.35	0.34	13.6	522
800	0.30	0.29	13.7	451
900	0.26	0.25	14.3	385

The · SiO_2 gel and the vitreous material it yields are characterized by the formation of micropores whose diameters vary within a narrow range (13.6—14.4 Å); the thermal treatment does not influence the diameter of pores but lowers their number and consequently the specific surface of samples. This behaviour is correlated to the preservation of the vitreous character of samples all throughout the investigated temperature range.

The properties related to the utilisation of membranes consisting of a ultraporous SiO_2 film on Al_2O_3 support are determined by the ensemble of two components. The mechanical strength of membrane is ensured by Al_2O_3 while the separation properties by SiO_2 film.

The membranes are recommended for utilization in separation in liquid phase (proteins, clearing of wines) as well as in gas phase.

4. CONCLUSIONS

Ceramic membranes on porous Al_2O_3 support were obtained by thermal treatments at 600, 1000 and 1150°C of a pseudobohemit gel. A porous SiO_2 film was deposited on Al_2O_3 support followed by thermal treatment at 500°C to obtain a pore size of about 14 Å.

The porosity of Al_2O_3 support may be controlled by sol-gel method and by thermal treatment temperature.

The porosity of SiO_2 film remains unchanged over the temperature range investigated.

Utilization of sol-gel method allows the preparation of ceramic membranes with preselected specific properties which are suitable in specific separation processes.

REFERENCES

[1] H. Barnier, *L'Actualité Chimique*, **1988**, p. 131.
[2] A. Auriol and J. Gillot, FR Patent, April 26, 1985.
[3] T. Komoda, FR Patent, Octobre 17, 1986.
[4] H. P. Hsieh, R. R. Bhave and H. L. Fleming, *J. Membrane Sci.*, **39**, 221 (1988).
[5] K. Onuma, Y. Kageyama, H. Kobayashi, A. Matsuki, M. Suzuki and T. Kawakami, UK Patent Application, January 15, 1982.
[6] E. Matijevic, *Pure and Appl. Chem.*, **60**, 1479 (1988).
[7] R. Roy, *Science*, **238**, 1664 (1987).
[8] J. Livage, *L'Actualité Chimique*, **1989**, p. 29.
[9] B. E. Yoldas, *J. Mater, Sci.*, **10**, 1856 (1975).
[10] X. Yang, A. C. Pierre and D. R. Uhlmann, J. *Non. Cryst. Solids*, **100**, 371 (1988).
[11] M. Zaharescu, C. Pirlog, M. Crișan and M. Sahini, *Rev. Roumaine Chim.*, **34**, 703 (1989)

Revue Roumaine de Chimie, 35, 7–9, 915–918 (1990)

USE OF ZEOLITE AS AN ADSORBING SURFACE FOR MODELLING SYSTEMS ANALOGOUS TO THERAPEUTIC MUD

ȘTEFAN KISS[a], MIHAIL DRĂGAN-BULARDA[a], DANIELA PAȘCA[b],
HENRIETTE PINTEA[b], EVA ZBOROVSCHI[b], VASILE MUNTEAN[b]
and RADU CRIȘAN[b]

[a] Department of Biology, University of Cluj-Napoca, 3400 Cluj-Napoca, Romania

[b] Biological Research Centre, 3400 Cluj-Napoca, Romania

For modelling systems analogous to therapeutic mud, 18 experimental variants were prepared from zeolite or, comparatively, from kaolin as well as from powdered brown coal and air-dried peat, urea and KH_2PO_4. The mixtures were inoculated with halophilic microorganisms in the form of salt lake mud, then suspended in salt lake water and incubated under anaerobic or aerobic conditions by daylight or in the dark for 306 days. Zeolite and kaolin enhanced the microbial enzyme synthesis and/or accumulation of enzymes mostly in the variants which contained brown coal and were incubated under anaerobic conditions by daylight. The sediments of these variants manifested an enzymatic potential similar to that registered in the highly enzyme-active therapeutic muds from the Ocna Sibiului, Slănic-Prahova and Techirghiol salt lakes.

INTRODUCTION

In order to study the role of adsorbing surfaces in the synthesis and accumulation of enzymes in soil, the following materials were used for modelling systems analogous to soil : glass columns filled with a mixture of glass beads and cellulose, [1] perlite, [2] bentonite, kaolinite and colloidal-size clay-humic fraction separated from a silt loam soil. [3,4]

There are no literature data on the modelling of systems analogous to therapeutic mud as revealed by enzymological methods. We suggested such model systems based on the role played by microorganisms in mud genesis, [5] by clay minerals and humic substances in the accumulation of enzymes in soil [6] as well as on the experimental results of Ulyashova et al., [7,8] according to which zeolite used together with organic and mineral fertilizers stimulated the growth of microorganisms and led to increased phosphatase, proteinase and dehydrogenase activities of a podzolic soil and also to increased wheat yield.

In our model systems, zeolite (zeolitic tuff) and, comparatively, kaolin were used as surfaces adsorbing enzymes, powdered brown coal and air-dried peat served as C, urea as N and KH_2PO_4 as P and K sources for halophilic microorganisms inoculated in the form of salt lake mud. All these components of the model systems were suspended in paper-filtered salt lake water and incubated under anaerobic or aerobic conditions by daylight or in the dark.

EXPERIMENTAL

For preparing the experimental variants (see Table 1), glass columns were used. Zeolite or kaolin was applied in a single dose (250 g) like urea (1 g) and KH_2PO_4 (0.5 g). The amount of brown coal or air-dried peat was 500, 600 or 700 g. The mud was a sapropelic, unctuous one collected from the salt lake Băile located in Cojocna, Cluj county, and used at a rate of 50, 150 or 250 ml. The lake water originated from the same salt lake; its volume was 2000 or 7000 ml (for creating anaerobic conditions) or 600 ml (for aerobic conditions). Part of the experimental variants containing brown coal were incubated by daylight and the other part in the dark, under anaerobic or aerobic conditions. The variants containing peat were incubated in the dark, under anaerobic conditions. Incubation was carried out at room temperature and lasted 306 days.

Following incubation the mixtures were centrifuged (at 4000 rpm/30 min) and the sediments were submitted to determination of four enzyme activities (phosphatase, catalase and actual potential dehydrogenase) and three nonenzymatic catalytic activities (splitting of H_2O_2 and reduction of 2,3,5-triphenyltetrazolium chloride in reaction mixture without or with added glucose), by adopting methods of soil enzymology.[9, 10, 11] The activity values served for calculating the enzymatic indicator of sediment quality[12] in each experimental variant.

Table 1

Composition of experimental variants for modelling systems analogous to therapeutic mud

Exptl. variant	Zeolite (g)	Kaolin (g)	Brown coal (g)	Air-dried peat (g)	Urea (g)	KH_2PO_4 (g)	Salt lake mud (ml)	Salt lake water (ml)
1	250	—	500	—	1	0.5	250	2000
2	—	250	500	—	1	0.5	250	2000
3	250	—	600	—	1	0.5	150	2000
4	—	250	600	—	1	0.5	150	2000
5	250	—	700	—	1	0.5	50	2000
6	—	250	700	—	1	0.5	50	2000
7	250	—	—	500	1	0.5	250	7000
8	—	250	—	500	1	0.5	250	7000
9	250	—	—	600	1	0.5	150	7000
10	—	250	—	600	1	0.5	150	7000
11	250	—	—	700	1	0.5	50	7000
12	—	250	—	700	1	0.5	50	7000
13	250	—	500	—	1	0.5	250	600
14	—	250	500	—	1	0.5	250	600
15	250	—	600	—	1	0.5	150	600
16	—	250	600	—	1	0.5	150	600
17	250	—	700	—	1	0.5	50	600
18	—	250	700	—	1	0.5	50	600

RESULTS

Table 2 presents the enzymatic indicator of sediment quality in model systems analogous to therapeutic mud following their 306-day incubation. The values of this indicator, grouped in a decreasing order, made it possible to establish the position of each experimental variant depending on its composition and incubation conditions.

One can see from this table that the first two positions are occupied by experimental variants 1 and 2, *i.e.* these model systems containing kaolin or zeolite, brown coal, inoculated with 250 ml salt lake mud and incubated under anaerobic conditions by daylight are the most enzyme-

Table 2

Enzymatic indicator of sediment quality in zeolite — or kaolin-containing model systems analogous to therapeutic mud, following their 306-day incubation at room temperature

Position	Enzymatic indicator of sediment quality	No. of the experimental variant	Conditions of incubation *
1	533.7	2	An., L.
2	487.2	1	An., L.
3	263.8	3	An., L.,
4	245.3	1	An., D.
5	240.4	2	An., D.
6	233.7	8	An., D.
7	220.4	4	An., D.
8	200.4	3	An., D.
9	196.1	12	An., D.
10	191.3	10	An., D.
11	171.6	4	An., L.
12	163.2	5	An., D.
13	158.2	7	An., D.
14	158.2	6	An., D.
15	133.5	5	An., L.
16	131.9	11	An., D.
17	124.9	17	A., D.
18	121.8	6	An., L.
19	118.6	9	An., D.
20	110.4	15	A., D.
21	106.6	13	A., L.
22	106.3	18	A., L.
23	104.4	13	A., D.
24	90.9	14	A., L.
25	84.5	17	A., L.
26	82.1	14	A., D.
27	77.7	16	A., L.
28	75.2	16	A., D.
29	64.7	18	A., D.
30	59.7	15	A., L.

* An. = Anaerobic ; A. = Aerobic ; L. = By daylight ; D = In the dark.

active, enhancing to the largest extent the synthesis of enzymes by microorganisms and/or accumulation of enzymes by kaolin or zeolite. It should be mentioned that enzymatic indicators of the sediments of these two model systems are close to those registered in the therapeutic muds of the salt lakes in Ocna Sibiului, Slănic-Prahova and Techirghiol which hold the first places in the mud-quality based classification of salt lakes in Romania.[12] In other words, it was possible to create highly enzyme-active model systems analogous to therapeutic mud during a geologically very short period (306 days) by daylight.

When experimental variants 1 and 2 were incubated in the dark, enzyme synthesis and/or accumulation were less marked.

In experimental variants 3—6, also containing zeolite or kaolin and brown coal, but inoculated with smaller amounts of salt lake mud (150 or

50 ml) and incubated under anaerobic conditions by daylight or in the dark, the sediments were less enzyme-active.

In the experimental variants 7—12, containing peat and incubated under anaerobic conditions in the dark, enzyme synthesis and/or accumulation were mediocre, irrespective of the nature of adsorbing surface (zeolite or kaolin) and the amount of salt lake mud used for inoculation (250, 150 or 50 ml). This means that variants 1 and 2 containing brown coal are preferable to the variants with peat.

Sediments of the experimental variants 13—18, incubated under aerobic conditions by daylight or in the dark, were the less enzyme-active, irrespective of the amount of the inoculated salt lake mud. Since these variants had the same composition as the more active variants 1—6 incubated under anaerobic conditions, it is evident that anaerobiosis is more favourable than aerobiosis for enhancing enzyme synthesis and accumulation in the model systems analogous to therapeutic mud.

In general, zeolite as an adsorbing surface was as good as kaolin.

Other properties of the sediments separated from the model systems analogous to therapeutic mud are under study.

CONCLUSIONS

Of the 18 experimental variants for modelling systems analogous to therapeutic mud, the two most enzyme-active variants were prepared from kaolin or zeolite, brown coal, urea and KH_2PO_4, inoculated with salt lake mud, suspended in salt lake water and incubated under anaerobic conditions by daylight. The sediments of these variants manifested an enzymatic potential similar to that registered in the highly enzyme-active therapeutic muds from the salt lakes in Ocna Sibiului, Slănic-Prahova and Techirghiol.

REFERENCES

[1] M. K. Theodorou, M. J. Bazin and A. P. J. Trinci, *Trans. Brit. Mycol. Soc.*, **75**, 451 (1980).

[2] A. M. Grodzinskii, E. A. Golovko, S. A. Gorobets and L. I. Mazorchuk, *Dokl. Akad. Nauk Ukr. SSR, Ser. B*, No. 10, 69 (1983).

[3] C. F. A. Hope and R. G. Burns, *J. Gen. Microbiol.*, **131**, 1237 (1985).

[4] R. G. Burns, in P. M. Huang and M. Schnitzer (eds.), "Interactions of Soil Minerals with Natural Organics and Microbes", Soil Sci. Soc. Am., Madison, Wisconsin, 1986, p. 429.

[5] I. Ţuculescu, "Biodinamica lacului Techirghiol. Biocenozele şi geneza nămolului", Ed. Academiei, Bucharest, 1965.

[6] S. Kiss, M. Drăgan-Bularda and D. Rădulescu, *Adv. Agron.*, **27**, 25 (1975).

[7] R. M. Ulyashova, V. G. Dudchenko, G. A. Mazur and G. K. Medvid', "Mater. Vses. Simp. Mikroorganizmy kak Komponent Biogeotsenoza", Alma-Ata, 1982, p. 153.

[8] R. M. Ulyashova, "Tez. Dokl. Konf. Povyshenie Effektivnost Ispol'zovaniya Udobrenii i Plodorodiya Pochv Ukrainskoi SSR", Kharkov, 1985. p. 103.

[9] M. Krámer and G. Erdei, *Pochvovedenie*, No. 9, 99 (1959).

[10] H. Kappen, *Fühlings Landw. Ztg.*, **62**, 377 (1913).

[11] L. E. Casida, jr., D. A. Klein and T. Santoro, *Soil Sci.*, **98**, 371 (1964).

[12] S. Kiss, M. Drăgan-Bularda and D. Paşca, *Stud. Univ. Babeş-Bolyai, Biol.*, **31** (1), 3 (1986).

Revue Roumaine de Chimie, 35, 7–9, 919–921(1990)

CHARACTERIZATION OF ION-EXCHANGE MEMBRANES USED IN ELECTROOXIDATIVE PROCESSES

C. V. ZĂNOAGĂ[a], C. V. UGLEA[a], S. MATACHE[b] and V. AVĂDĂNEI[b]

[a] Center of Biological Research, Iassy, Calea 23 August 20 A, 6600, Romania
[b] Research Center for Chemical Fibers, Săvinești, Str. Uzinei 1, 5612, Romania

The paper discusses a new method of testing ion-exchange membranes, checked up on a membrane used in the process of electrooxidation of ammonium sulphate to ammonium persulphate. Knowing that, in such situations, the determining process is that of proton transfer through the membrane, the optimum redox (rH) conditions were sought for at the anolyte level, aiming at a maximum proton transport towards the catholyte, i.e for attaining a maximum oxidation rate of the anolyte. The process was modelled with two phases, separated by the tested membrane — the one simulating the catholyte containing sat./1000 of KCl and 0.67‰ of added quinhydrone (in view of obtaining a redox system that should permit acceptance or yielding of protons), while that simulating the anolyte offers the possibility of modifying the redox conditions, by means of a redoxtron, containing a solution of sat./1000 KCl. Experiments were performed for 4 hours: the catholyte — stirred permanently — was subjected to the influence of some rH values of the anolyte from one experiment to another and covering the whole domain of rH values. The optimum region of proton transfer towards the catholyte, materialized in the decrease of the catholyte's rH value, takes rH values $>$ 12 (optimum rH 33), values that should ensure maximization of the electrooxidation rate. The method dealt with in the paper offers new possibilities for characterizing membranes.

Electrooxidation of ammonium sulphate to ammonium persulphate employs — in view of increasing the reaction's yield — a membrane, separating the anodic space (where the process occurs) from the cathodic one. This membrane, made of a polymeric matrix, and playing a mechanical role, contains a vionyte ion exchanger permitting exclusively proton transfer (and for bidding that of the molecular species interested in the reaction).

The present paper aims at establishing a testing method for such types of ion exchanger membranes, examples being given with a concrete membrane, so that their screening should improve its composition.

MATERIAL AND METHOD

Taking into account the fact that the transfer of various chemical species [1] and of cations, [2] too, depends on the redox character — quantified as rH — of the phase towards which migration occurs, an experimental model — described elsewhere[1] — was employed, in which the donor phase — having constant redox conditions — is separated, through the test membrane, by the receiving phase, known as capable of varying/controlling the redox character, a series of experiments — differing through the rH values obtained in the donor phase — being thus performed.

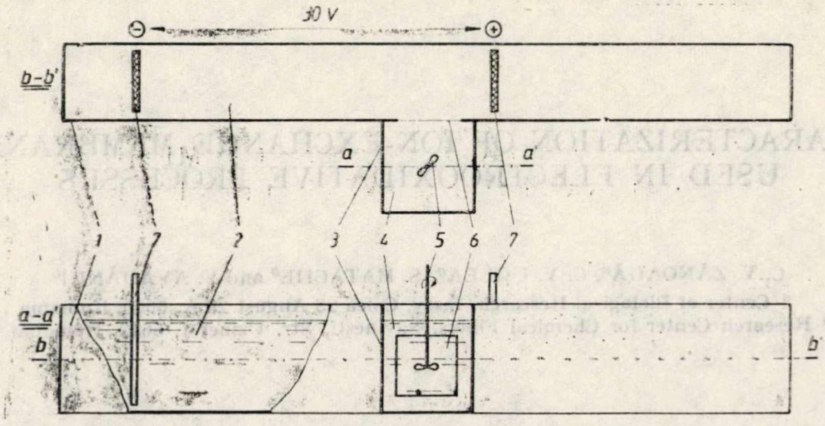

Fig. 1

The experimental device (Fig. 1) is made of a vat (3) equipped with a stirrer (5) including the donor phase (4) separated — through the tested membrane (6) — by the receiving phase (2), included in a redoxtron, consisting of a vat (1) with two inert electrodes (7), whose relative position towards the membrane region may be modified. In a previous paper[3] we have evidenced that application of a difference of potential between the two electrodes leads to a rH gradient ranging between 0 at the cathode and 42.4, respectively, at the anode. Under conditions of compositional and geometrical homogeneity of the electrolyte, the obtained rH gradient evidences a logarithmic aspect. Modification of the electrodes' position induces placement of the membrane in various positions — as against the electrodes — and, consequently, its arrangement in different redox conditions.

Concrete working conditions required a 16 cm^2 membrane surface, a 30 V voltage, the receptor phase made — as a a consequence of the redoxtron's operating requirements — of a saturated/1000 KCl solution ; for avoiding the presence of any concentration gradient, the donor phase has had the same composition. Addition of 0.67 ‰ quinhydrone in the donor phase was meant — on the one hand — at offering indications (by colour changing) upon the redox modifications occurring as a result of proton transfer, and — on the other hand — at constituting the donor/acceptor of the transferred protons.

Determination of the proton transfer rate was achieved by determining the rH of the donor phase, modified as a consequence of the proton transfer, by applying an electrometric method described elsewhere [4].

The duration of each experiment was of 4 hours, at a temperature of 20°C.

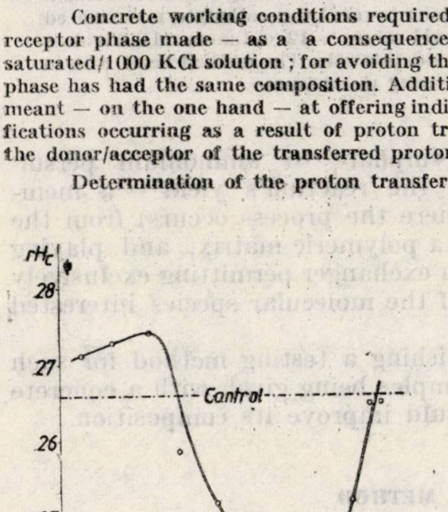

Fig. 2

RESULTS AND DISCUSSION

The obtained experimental results, plotted graphically in Fig. 2. evidence that, on modifying the redox character of the acceptor phase, a proton transfer occurs, beginning with the rH minimum value, i.e. 12 ; the maximum effect is to be observed at rH 33.

The reducing character of the protons explains both the lack of transfer at reducing rH values and the optimal transfer at an oxidative rH, on considering that — at membrane level — a redox neutralization process actually occurs.

CONCLUSIONS

All these observations draw the attention — in view of optimizing the process — upon the redox correction of the acceptor phase — in the case of the concrete technological process of anolyte oxidation, which results in maximization of the proton transfer and, consequently, in improving the current yield. The same situation may be reached at by selecting the ion-exchanger from the membrane composition, on having in view that the content of ion exchanger from the membrane cannot be "attacked" without modifying its mechanical caracteristics.

Conclusively, the method presented may be applied both for optimizing the membrane composition and the technological parameters, in other types of electrooxidation/reduction process, too.

REFERENCES

[1] C. V. Zănoagă, "The 14th Session of Scientific Communications, Rîmnicu Vîlcea, 13—15 Oct. 1988. Caiet selectiv", vol. IV, p. 17—20

[2] C. V. Zănoagă, C. V. Uglea and G. Nechifor, "The IIIrd Symposium on Colloid and Surface Chemistry, Timişoara, 11—14 Sept 1989. Abstracts", p. 93.

[3] C. V. Zănoagă, M. Zănoagă and C. V. Uglea, *Rev. Roum. Biochim.*, **24**, 357 (1987).

[4] C. V. Zănoagă, I. Neacşu, M. Zănoagă, *St. cerc. biochim.*, **31**, 53 (1988).

Revue Roumaine de Chimie, **35**, 7–9, 923–925 (1990)

REDOX ASPECTS REGARDING THE TRANSFER OF SOME HEAVY METALS THROUGH SEMIPERMEABLE MEMBRANES

C. V. ZĂNOAGĂ [a], C. V. UGLEA [a] and G. NECHIFOR [b]

[a] Center of Biological Research, Iassy, Calea 23 August 20 A, 6600, Romania
[b] ICECHIM – Center of Physical Chemistry, Bucharest, Splaiul Independenţei 202, 79611, Romania

A sulphonate semipermeable membrane was used for separating two phases, one of a 3% solution $CuSO_4 \cdot 5H_2O, ZnSO_4 . 7H_2O$ and $MnSO_4 . H_2O$, the latter made invariably of KCl sat/1000. The former phase was permanently stirred, while the latter was redox buffered, at various rH values, by means of a redoxtron, for 8 hours. The transfer of Cu, Zn and Mn, respectively, from the former towards the latter phase was observed as occurring specifically for each metal, the membrane being permeable only in some rH ranges, that may be connected with the valence of each ion. This situation makes possible the control of the transfer through the membrane so that adjustment of the rH value of the receiving phase ensures the transfer of the corresponding metal. This observation may be also applied to biological membranes where it could explain the selectivity of cation absorption, but also the operation of the Na^+ – K^+ pump, the redox conditions specific to the cell and its environment, inducing the transfer in opposite directions of the two cations.

The present paper aims at drawing the attention upon a less known parameter, observed as significantly influencing transmembrane transport and, more than that, its selectivity, namely, the redox character of donor phases, respectively the receivers involved in the transport.

The phenomenon has been already evidenced, our previous papers discussing the redox-type influence upon the direction of transmembrane transport of alkaline cations [1.2] or aminoacids[3,4] as well as of the intensity and specificity of transmembrane transport of glucose, urea and aminoacids, [5] both in the case of liquid [1–3] and semipermeable [4,5] membranes.

Having all these in view, we are now trying to extend such observations to transmembrane transport of the cations of some heavy metals through semipermeable membrane, more exactly, to evidence the dependence upon the redox character of the receiving phase of the specificity of the Cu, Zn and Mn transport, on employing a polysulphonic semipermeable membrane.

MATERIAL AND METHOD

The experiment performed made use of an experimental model, previously described, [56] involving separation through a semipermeable membrane (of the above-mentioned type) of a donor phase, containing successively, in the three experimetal series, a solution of 3% Cu SO

$\cdot$ $5H_2O$, $ZnSO_4 \cdot 7H_2O$ and $MnSO_4 \cdot H_2O$, respectively, constantly stirred and uncontrolled — — from a redox viewpoint — by another receiving phase, consisting of a saturated/1000 KCl solution, this time redox controlled/buffered by a redoxtron system. [5,6] Within each experimental series, the rH of the receiving phase has been varied in the 2.75 . .42.16 range, which means, practically, the whole definition domain of the rH (0 . . .42,4). Each time, the current passing through the redoxtron (i_r) has been determined, and found as being proportional to the electrical conductivity of the receiver phase, consequently, proportional to the amount of metallic cations passed through the membrane.

The obtained results have been graphically plotted as against the rH characterizing each experimental variant (Figures 1, 2 and 3, respectively).

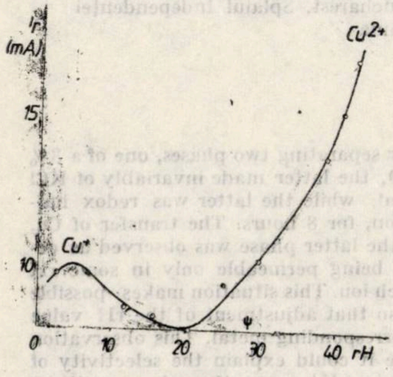

Fig. 1

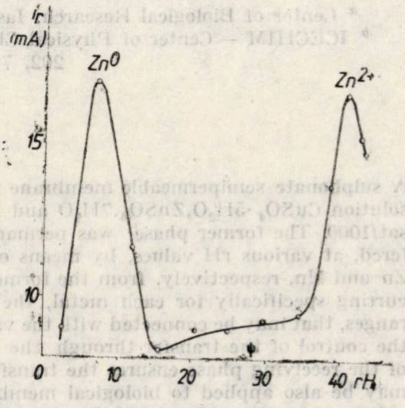

Fig. 2

RESULTS AND DISCUSSION

Analysis of the diagrams shows the existence of several rH domains ensuring the transfer of each cation, placed at an rH 5.5 and the oxidative extreme in the case of Copper, rH 7 and 40.5 with the Zinc and rH 15.7, 30.5 and 38.5, respectively, in the case of Manganese. Quite precisely, the obtained peaks may be related to the transport of cations to be found at various valencies, and determined by the rH of the receiving phase (Table 1). At the same time, no superposition of the peaks occurs,

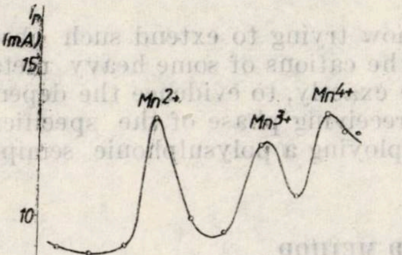

Fig. 3

Table 1

Metal	rH	Transferred ion
Cu	5.5 extreme OX	Cu^+ Cu^{2+}
Zn	7.0 40.5	Zn^0 Zn^{2+}
Mn	15.7 30.5 38.5	Mn^{2+} Mn^{3+} Mn^{4+}

which is indicative of the specificity of the transmembrane transport under conditions of the redox control of the receiving phase.

CONCLUSIONS

All these observations lead us to a first conclusion, according to which the redox control of the process may ensure the transport, at least preponderantly, of a given cation from a mixture, which may represent the starting point of new investigations, concerning recovery of heavy metals from residual solutions or poor minerals. At the same time, the redox-induced selectivity of transmembrane transport may be utilized as a criterion in membrane characterization.

Another conclusion drawn refers to the explanation to be given to the absorption selectivity by the living cell, that — similar to the receiving phase in the above-mentioned experiment — is capable of controlling the internal redox conditions; at the same time, the operating mechanism of the $Na^+ - K^+$ pump, that is, of the transfer — in opposite directions — of Na^+ and K^+ through the cell membrane, may be explained through the difference occurring between the intra- and, respectively, extracell rH, which induces the Na^+ transfer in one direction concomitantly being characteristic exclusively of the K transfer in an opposite direction.

REFERENCES

[1] C. V. Zănoagă and C. V. Uglea, *Bul. Soc. Nat. Biol. Cel.*, **12** (1987)

[2] C. V. Zănoagă and C. V. Uglea, *Bul. Soc. Nat. Biol. Cel.*, **15** (1988)

[3] C. V. Zănoagă and C. V. Uglea, "The 1st National Symposium of Membranology", Piatra-Neamţ, 24—27 May 1988, Abstracts, pp. 98—99.

[4] C. V. Zănoagă and C. V. Uglea, "Membranes and Membrane Separation Processes" (Proc. Int. symp., Sept 11—15, 1989), Ed. J. Ceynowa, N. Copernicus University, Toruń, 1989, pp. 323—325.

[5] C. V. Zănoagă, "The 14th Session of Scientific Communications", Rîmnicu Vîlcea, 13—15 Oct 1988. Caiet selectiv, vol. 4, p. 17—20

[6] C. V. Zănoagă, C. V. Uglea, S. Matache, V. Avădănei, *Rev. Roum. Chim.*, **35**, 919 (1990)

Revue Roumaine de Chimie, 35, 7–9, 927–933 (1990)

HYDRODYNAMIC AND MATHEMATIC CHARACTERIZATION OF THE VODNÁR-TYPE APPARATUSES, HAVING PELLICLIZING (STRIPPING) AND RECYCLING TUBES

J. VODNÁR, E. KOLOZSI and N. MUREȘAN

University of Cluj-Napoca, Faculty of Economic Sciences, Laboratory of Chemical Technology, 3400 Cluj-Napoca, Piața Șt. cel Mare No. 4, Romania

The present paper reports on a hydrodynamic and mathematic characterization of the Vodnár-type apparatuses. Compressed air and water were used as gaseous and liquid phases in the necessary measurements.

This paper describes the hydrodynamic and mathematic characterization of the Vodnár-type apparatuses, equipped with bubbling-pelliclizing stripping and recycling tubes, using small gas and liquid outlets. Self-induced mixing and recycling of the liquid phase are ensured. Compressed air and water used as gaseous and liquid phase, respectively, in the necessary measurements. The apparatus used is a "laboratory model" [1-3] built by Stiplex, provided with only one bubbling-stripping tube, the length of which ranges from 0.5 to 1.25 m, inner diameter from 0.008 to 0.034 m, while the inner diameter of the recycling tube was 0.006 m. The air outlet for a single bubbling-pelliclizing tube varied from 0.2 to 2.2 m^3/h and the water outlet between 0.1 and 2.2 l/h. The mathematic models deduced for the hydrodynamic and mathematic characterization of these apparatuses express the pressure drop (ΔP, [water mm column]), upon the Reynolds and Euler criteria, length (L_t, [m]) and inner diameter ($Ø_i$, [m]) of the bubbling-pelliclizing tubes, height of the liquid column in the recycling tube (H, [m]) and the intensity of the surface wetting (F, [kg liquid/$Ø_i \cdot \pi \cdot h$]).

During the use of these apparatuses equipped with bubbling-pelliclizing tubes or with spiral shaped tubes (serpentines), different technological necessities appear, concerning the gas and liquid outlets which must be used. To make possible the rational use of these apparatuses in different conditions of work, one must know their hydrodynamic and mathematic characterization.

EXPERIMENTAL

Method. Experiments were performed by means of a laboratory model apparatus described in two previous papers [2-3], with the difference that the apparatus used for these experiments was equipped with an internal recycling tube too, for the liquid phase. Most importance was granted to the pressure drop whose specific energy consumption necessary for the functioning of the apparatus, depends to a great extent on. There were used small gas ($0.2-2.2\ m^3/h$) and liquid ($0.1-2.2\ l/h$) outlets, to be perceptible the behaviour of these apparatuses in the conditions of work that were used. In similar conditions there are made many chemical reactions and physical industrial operations : chemical synthesis based on the utilisation of ketene, sulfur dioxide and trioxide (e.g. production of some detergents), chlorine, hydrogens ulfide, oxygen, ozone, ethylene and propylene oxides, gaseous olefins (e.g. for the alkylation) a.s.o. Compressed air and water were used as gaseous and liquid phase. The experimental procedure was the same as that described in some previous papers. [2-3]

RESULTS AND DISCUSSION

There were made about 8500 hydrodynamic measurements, using bubbling-pelliclizing (stripping) tubes having the following inner diameters ($Ø_i$) : 0.008 ; 0.01 ; 0.0146 ; 0.0179 ; 0.034 m. By every diameter were used tubes having the lengths : 0.55 ; 0.8 ; 1.0 and 1.25 m. With every length of tube were made measurements to know the pressure drop, using liquid outlets between 0.1 and 2.2 l/h (from 0.1 to 0.1 l/h) and gas outlets between $0.2-2.2\ m^3/h$ (from 0.2 to $0.2\ m^3/h$). For every liquid outlet value measurements were made with all bubbling-pelliclizing stripping tubes, having the mentioned lengths and diameters. All these categories of measurement were made by the following heights of recycling (H) : 0.28 ; 0.42 ; 0.5 ; 0.7 ; 0.82 and 0.93 m.

Based on the hydrodynamic measurements, electronic computation programs were made for the deduction of mathematic models which can be used to calculate the pressure drop by different values of Reynolds number (for gas and liquid : Re_g, Re_l), length (L_t[m]) and internal diameter ($\varnothing_i$ [m]) of bubbling.-pelliclizing (stripping) tubes, gas outlet (Q_g[m³/h]), liquid outlet (Q_l[l/h]), height of recycling (H, [m]) and by wetting intensity (F, [kg liquid/$Ø_i \cdot \pi \cdot h$]).

In the first part of computation two mathematic models were selected for the calculation of pressure drop (ΔP) which were solved on the Felix C-256 computer :

$$\Delta P = A \cdot Re_g/10 + B \cdot F + C \cdot H + D \tag{1}$$

$$\Delta P = A \cdot Re_g/10 + B \cdot \mathrm{Re}_l + C \cdot H + D \tag{2}$$

where ΔP is the pressure drop, [water mm column] ;

A, B, C, D — constants ;

Re_g — Reynolds number for gas (air) ;

Re_l — Reynolds number for liquid (water) ;

F — wetting intensity, [kg liquid/$Ø_i \cdot \pi \cdot$ h] ;

H — height of recycling (the height of the liquid column in the recycling tube), [m].

The numerical values of A, B, C and D constants are presented in table 1 for the model (1) and in table 2 for the model (2).

Many times, pressure drop must be calculated to different lengths of bubbling-stripping tubes, having the same internal diameters. For such computations we have stated the necessity of the separation of hydrodynamic measurements in two different categories. In the first category enter the experimental values where ΔP increases upon the Re_g and Q_g. These data are presented in table 3.

The adequate model for the calculation of ΔP values beside a single value of $Ø_i$ and all values of L_t (between 0.55 and 1.25 m) is noted by (3).

Table 1

The numerical values of the constants *A, B, C, D* for the mathematic model (1)

L_t, [m]	$Ø_i$, [m]	*A*	*B*	*C*	*D*
0.55	0.008	0.13481	0.19987	505.91919	62.19484
0.80	0.008	0.20930	0·14059	497.03816	105.61871
1.00	0.008	0.24837	0.15023	795.78311	−41.08696
1.25	0.008	0.23047	0.42819	533.24914	129.13393
0.55	0.01	0.12807	0.16778	238.85777	125.86587
0.80	0.01	0.17507	0.18506	248.35962	164.99948
1.00	0.01	0.26933	0.34334	337.64055	138.09038
1.25	0.01	0.31053	0.22992	389.59035	139.56048
0.55	0.0146	0.07507	0.17149	158.46778	135.63625
0.80	0.0146	0.05899	0.16499	155.67422	192.32682
1.00	0.0146	−0.00608	0.17807	158.83122	245.22679
1.15	0.0146	0.03117	0.24721	132.51083	286.52510
0.55	0.0179	−0.03430	0.21586	172.05902	152.87425
0.80	0.0179	−0.16305	0.14450	110.68740	253.86261
1.00	0.0179	−0.24609	0.22462	170.03034	273.04631
1.25	0.0179	−0.42879	0.20544	161.94017	367.73837
0.88	0.034	−1.78944	0.69366	98.77728	551.78852
1.06	0.034	−2.29539	0.76308	87.06385	679.58288
1.25	0.034	−1.97784	0.79414	108.42446	694.20516

Table 2

The numerical values of the constants *A, B, C, D* for the mathematic model (2)

L_t, [m]	$Ø_i$, [m]	*A*	*B*	*C*	*D*
0.55	0.008	0.13481	0.18078	505.91919	62.19484
0.80	0.008	0.20930	0.12716	497.03816	105.61871
1.00	0.008	0.24837	0.13588	795.78311	−41.08696
1.25	0.008	0.23047	0.38730	533.24914	129.13393
0.55	0.01	0.12807	0.15176	238.85777	125.86587
0.80	0.01	0.17507	0.16739	248.35962	164.99948
1.00	0.01	0.26933	0.31055	337.64055	138.09038
1.25	0.01	0.31053	0.20796	389.59035	139.56048
0.55	0.0146	0.07507	0.15511	158.46778	135.63625
0.80	0.0146	0.05899	0.14923	155.67422	192.32682
1.00	0.0146	−0.00608	0.16106	158.83122	245.22679
1.15	0.0146	0.03117	0.22360	132.51083	286.52510
0.55	0.0179	−0.03430	0.19525	172.05902	152.87425
0.80	0.0179	−0.16305	0.13070	110.68740	253.86261
1.00	0.0179	−0.24609	0.20317	170.03034	273.04631
1.25	0.0179	−0.42879	0.18582	161.94017	367.73837
0.88	0.034	−1.78944	0.62742	98.77728	551.78852
1.06	0.034	−2.29539	0.69020	87.06385	679.58288
1.25	0.034	−1.97784	0.71830	108.42446	694.20516

Table 3

Experimental data by which ΔP increases upon Re_g and Q_g

Ø$_i$, [m]	L_t, [m]	H, [m]	Q_g, [m^3/h]
0.008	0.55–1.25	0.2–0.9	0.2–2.2
0.01	0.55–1.25	0.2–0.93	0.2–2.2
0.0146	0.55	0.28	0.4–2.2
0.0146	0.55	0.42	0.6–2.2
0.0146	0.55	0.50	0.8–2.2
0.0146	0.80	0.41–0.7	0.6–2.2
0.0146	1.00	0.5 –0.9	0.6–2.2
0.0146	1.15	0.58	0.8–2.2
0.0146	1.15	0.70	0.6–2.2
0.0146	1.15	0.82	0.8–2.2
0.0179	0.55	0.27–0.52	0.6–2.2
0.0179	0.80	0.38–0.49	0.8–2.2
0.0179	0.80	0.60–0.73	1.2–2.2
0.0179	1.00	0.61–0.78	1.0–2.2
0.0179	1.25	0.60–0.90	1.0–2.2
0.034	0.88	0.45–0.64	2.0–2.2
0.034	0.88	0.80	1.8–2.2
0.034	1.06	0.49–0.85	2.0–2.2
0.034	1.25	0.76–0.85	2.0–2.2

$$\Delta P = k \cdot (Re_g)^a \cdot (L_t)^b \cdot (H)^c \cdot W_g^2 \cdot \rho_g \qquad (3)$$

where W_g is the linear speed of gas [m/s]; ρ_g — density of gas, [kg/m^3]; k, a, b, c — constants.

The mathematic model (3) was solved on a CORAL-4030 computer and so we obtained the numerical values of the constants k, a, b and c concerning the five inner diameters which were used. These data are presented in table 4.

Table 4

The values of the constants k, a, b and c for the mathematic model (3), when ΔP upon the Re_g and Q_g values increases

Ø$_i$, m	lg$k$	a	b	c
0.0080	7.88268	−1.90288	0.34332	0·65861
0.0100	7.91855	−1.89443	0.50014	0.42283
0.0146	8.07446	−1.88008	0.53365	0.28890
0.0179	8.19061	−1.86524	0.53586	0.25713
0.0340	9.05903	−1.92948	0.72992	0.08535

On the basis of constant values presented in table 4, has been calculated the value of these constants for some intermediary inner diameters (see table 5), using the Lagrange interpolation method. The calculation was made with a FORTRAN-77 program based on the Aiken algorithm.[4]

Table 5

The values of constants k, a, b and c calculated by FORTRAN-77 program, based on the Aiken algorithm

Ø$_i$, [m]	lg k	a	b	c
0.009	7.89642	−1.89811	0.43994	0.51913
0.012	7.97973	−1.88824	0.54541	0.32247
0.015	8.08926	−1.87860	0.53054	0.28705
0.019	8.22502	−1.85901	0.55887	0.22866
0.021	8.28180	−1.84666	0.63735	0.14370
0.025	98.38961	−1.82501	0.90668	−0.13051
0.029	8.55665	−1.82886	1.14135	−0.36102
0.032	8.79919	−1.87106	1.05235	−0.25731

In the second category enter the hydrodynamic measurements where ΔP decreases upon Re_g and Q_g. These data are presented in table 6.

Table 6

Experimental data by which ΔP decreases upon Re_g and Q_g

Ø$_i$, m	L_t, m	H, m	Q_g, m^3/h
0.0146	0.55	0.28	0.2−0.4
0.0146	0.55	0.42	0.2−0.6
0.0146	0.55	0.50	0.2−0.8
0.0146	0.80	0.41−0.7	0.2−0.6
0.0146	1.00	0.50−0.9	0.2−0.6
0.0146	1.15	0.58	0.2−0.8
0.0146	1.15	0.70	0.2−0.6
0.0146	1.15	0.82	0.2−0.8
0.9146	1.15	0.92	0.2−1.0
0.0179	0.55	0.27−0.52	0.2−0.6
0.0179	0.80	0.38−0.49	0.2−0.8
0.0179	0.80	0.60−0.73	0.2−1.2
0.0179	1.00	0.61−0.78	0.2−1.0
0.0179	1.25	0.60−0.90	0.2−1.0
0.034	0.88	0.45−0.64	0.2−2.0
0.034	0.88	0.80	0.2−1.8
0.034	1.06	0.49−0.85	0.2−2.0
0.034	1.25	0.76−0.83	0.2−2.0

For the experimental data presented in table 6 one may use the same mathematic model (3), to calculate the value of ΔP.

The numerical values of the constants k, a, b and c for the mentioned three inner diameters (see table 6). These data are presented in table 7.

Table 7

The values of the constants k, a, b and c for the mathematic model (3) when ΔP upon the Re_g and Q_g values, decreases

Ø$_i$, [m]	lg$k$	a	b	c
0.0146	9.03505	−2.19190	0.59644	0.36695
0.0179	9.42942	−2.26728	0.69173	0.29756
0.034	10.07481	−2.25785	0.83438	0.10571

On the basis of constant values k, a, b and c presented in table 7, the value of these constants for a few intermediary inner diameters (see table 8)has been calculated using the above-mentioned Lagrange interpolation metod.

Table 8

The values of constants k, a, b and c for some intermediary inner diameters, calculated by FORTRAN-77 program based on the Aiken algorithm (when ΔP upon R_{eg} and Q_g, decreases)

Ø$_i$, [m]	lg k	a	b	c
0·015	9.08760	−2.20244	0.60919	0.35799
0.019	9.54106	−2.28656	0.71850	0.27670
0.021	9.71867	−2.31413	0.76078	0.24169
0.025	9.97563	−2.34029	0.82057	0.18924
0.029	10.10158	−2.32780	0.84734	0.13923
0.032	10.11008	−2.29308	0.84735	0.11057

Using the mathematic model (3) one can calculate the value of ΔP which presents a deviation no more than 5%, in comparison with the measured values :

$$\frac{\Delta P \text{ calculated}}{\Delta P \text{ measured}} \in (0.95\,;\ 1.05).$$

If the calculation is made with some classical (simple) apparatuses (not with computers), highly exact results can be obtained when the logarithmic form of model (3) is used :

$$\lg(\Delta P/\rho_g \cdot V_g^2) = \lg\ k + a \cdot \lg Re_g + b \cdot \lg L_t + c \cdot \lg\ H \cdot = A$$

$$\Delta P = 10^A \cdot \rho_g \cdot V_g^2$$

REFERENCES

[1] J. Vodnár, Romanian Patent, No. 89508 (1985).
[2] I. Vodnár, *Rev. Chim.* (*Bucureşti*), **38**, 996 (1987).
[3] I. Vodnár, *Rev. Chim.* (*Bucureşti*), **39**, 719 (1988).
[4] B. V. Gnedenco, V. S. Koroliuc, V. S. Iushcienco, J. Szelezsán: "Bevezetés a Programozásba", vol. II, Müszaki Könyvkiadó, Budapest, 1964.

Revue Roumaine de Chimie, 35, *7—9*, 935—938 (1990)

COMPTES RENDUS

The book "Biological role of plant lipids", edited by Peter A. Biacs, Katalin Gruiz and Tibor Kremmer, includes contributions of the 8th International Symposium held in Budapest, between 25—28 July, 1988 by the Federation of Technical and Scientific Societies.

The symposium was attended by 180 participants involved in studies on plant lipids. Eleven plenary lectures, 75 communications and 70 posters were presented in two sections. The discussions have evidenced the remarkable progresses recorded in the field. The volume was dedicated to Prof. Hartmut K. Lichtenthaler, the Dean of Botany Department of Karlsruhe University. Prof. Lichtenthaler gathered together all research scientists in various fields related to the study of plant lipids and organized in 1976 in Karlsruhe the first international meeting in this field.

The contributions are organized in seven chapters. *Chapter 1* includes studies on lipid metabolism such as : desaturation of fatty acids of oleate and linoleate type synthesized from plants of horticultural interest, the biochemical characterization of oleic acid mutant from sunflower and its metabolism in pea roots. Studies on the biosynthesis of phosphate dylsulfocholine and deoxyceramidesulfonic acid in the diatom nitzschia alba, the biosynthesis of glycerolipides in plant mitochondria of galactolipides in chloroplasts, of triacylglycerols, hemoserine lipid as well as metabolization of the lipids deposited in germinating oilseeds or their composition in mature and germinated olive pollen or the metabolism of fatty acids oxygenated by leaves are also presented. Some mechanisms applied in the biosynthesis of lipids and of glycerolipids in microsomes, of enzymatic oxidation of unsaturated fatty acids and carotenoides are delt with in this chapter together with analytical studies on identification and determination of unsaturated fatty acids in plant extracts.

Chapter 2 reports studies on structural and functional organization of lipids. It presents the results of investigations on transmembrane distribution galactolipids, the structural-biological conformations of unsaturated fatty acids with specification of the part played by lipidic derivatives as phosphatidylglycerol in the photosynthesis membrane or the phase behaviour of membrane lipids. Protein-pigment association complexes were evidenced in photosynthetic membranes of phospholipids, interactions with specific glycolipids as well as the positional distribution of polyunsaturated fatty acids in phospholipids.

Use has been made of non-destructive experimental methods as photoacoustic spectroscopy, electron spin resonance or polarization fluorescence.

Chapter 3, specialized in the biosynthesis and function of prenyllipidis presents the results of studies on hydrogenation and cyclization reactions involved in the biosynthesis of carotenes and their conversion into lycopene, the biosynthesis of chromoplast monoterpenes as well as purification of enzymatic systems implied in the biosynthesis of diterpenes. The role of triterpenoids in epicuticular waxes and of diphenyl hexatrienes in vesicles containing plant sterols was emphasized.

Chapter 4 presents the carrier protein genetics of plant lipids. The phenomena which govern the lipidic metabolism, the pathways of molecular biology of plant proteins implied in the intracellular transport of phospholipids are studied in depth.

The immunochemical aspects of acyltransferases which catalyze the first steps of membrane lipid biosynthesis or isoforms of nonspecific lipid transfer protein are also considered. Special attention is given to the bioacids and their interaction with plant lipids.

Although *Chapter 5* is intended mainly for agronomists and mainly for agronomists and ecologists, it emphasizes the importance of herbicides upon the biochemistry of plants establishing correlations between their chemical structure and the alteration of plant lipid biosynthesis. The works issued by Lichtenthaler from Botanisches Institut, University of Karlsruhe are noteworthy.

The nutritional aspects of lipid biotechnology are discussed in *Chapter 6* which evidences that plant lipids are renewable sources for tenside industry. The results obtained by the Hungarian researchers on enzymatic modification of sun flower lecithin, the influence of metallic impurities of crude and edible vegetable oils, the biological role of soya lipids in nutrition or those regarding the role of lipids in adsorption of vitamines are remarkable.

The final *Chapter 7* presents problems related to the stability and response of membrane to stress factors, the strategy of membrane modification by catalytic hydrogenation and other results regarding the influence of surroundings.

The book "Biological role of plant lipids", amounting to 600 pages, distinguishes through the presentation of scientific novelty of the highest level which is outstandingly useful to specialists in the field, and through the remarkable graphics achieved by Akademiai Kiadó Budapest.

Georgeta Popescu
Center of Physical Chemistry
Bucharest

L. Kiss, "Kinetics of Electrochemical, Metal Dissolution", Akadémiai Kiadó — Budapest, 1988, 260 p.

The book "Kinetics of electrochemical metal dissolution" by L. Kiss was published as joint edition of Akadémiai Kiadó, Budapest, Hungary and Elsevier Science Publishers B. V., Amsterdam, The Netherlands.

It is in fact published by Elsevier Science Publishers as Vol. 47 in the series of "Studies in physical and theoretical chemistry".

Although the book does not cover the field of electrochemical metal dissolution entirely it deals mainly with the most important topics of this field.

The book provides a modern survey of the kinetics of electrochemical metal dissolution — anodic and spontaneous dissolutions — being divided into three main chapters. The thermodynamic aspects of the electrode processes are discussed in the first chapter. Multistep electrode processes taking place in several successive steps are reviewed in the second chapter. The theoretical analysis of spontaneous metal dissolution and that of electrochemical corrosion as well as the spontaneous processes occurring on metal electrodes are discussed in the third chapter.

In the first chapter, initially, the problems related to the equilibria of electrode reactions taking place at the electrodes are discussed in detail. It was explained that the potential of the electrode reaction ε_r depends on the activities of the species participating in the process, while at fixed electrode potential the equilibrium activities assumed will depend on the potential employed. The importance of the electrochemical equilibrium diagrams in recognizing the possibilities of different reactions proceeding in a heterogeneous electrochemical system under specified conditions was also emphasized in this chapter, showing that the electrochemical potential — pH diagrams are related to reversible conversions and are characteristic of the thermodynamics equilibria of the given processes.

The basic principles of the kinetics of electrode processes discussed in the second chapter represent the core of the book reviewing the kinetics of the complex processes taking place in consecutive and parallel reaction paths. In this way a gap was filled because no similar work relevant to stepwise mechanisms of electrode processes was previously published.

The kinetics of spontaneous electrode processes taking place in the presence of their own ions which have an important role in dissolution of metals, and the kinetics of corrosion brought about by effect of depolarizers are disscused in the last chapter.

In fact, this chapter covers all the problems of corrosion of metals describing all the factors which may affect the corrosion rate.

Each chapter includes an extensive use of figures, tables and an exhaustive bibliography.

The book reviews the kinetics of electrode processes, the first step in exploring a reaction mechanism. The author includes in the text his own results on the kinetic equations of multistep processes and on the application of rotating ring disc electrode.

Many specialists in electrochemical research and education, experts dealing with corrosion, electrochemical current sources, galvanotechniques, electrometallurgy and other electrochemical industrial processes can profit by the book.

N. D. Totir
Center of Physical Chemistry
Bucharest

F. Valach, J. Ondráček, M. Melnik, "Crystallographic Statistics in Chemical Physics", Springer-Verlag, Berlin, 1988, 185 pp., hard cover, DM 178, ISBN 3-540-18921-1.

Volume 12 in the series "Inorganic Chemistry Concepts" is devoted to an approach to statistical evaluation of internuclear distances in transition metal compounds. The development of crystal structure information systems as well as the increase of the volume of crystal structural data allow now a statistical treatment of internuclear distances, in order to search the most general rules and laws of structures in condensed matter.

The book introduces the concept of nonrigidity and asymmetry of the transition elements of central atoms in coordination compounds. This intrinsic bahaviour of central atoms in condensed matter is quantified by applying a statistical approach. The aim of this statistical endeavour is to obtain the purest possible information, rejecting noisy data derived from various physical methods. Averaging of extrinsic factors in crystal structures is tested by using variance analysis. One may note that the above-mentioned concept and applications of variance analysis, as an approximation for considering factors influencing properties of central atom in a crystal, are original and new.

The material is divided into five chapters:

— Statistics of interatomic distances (some statistical concepts and inferences; statistics of lengths of interatomic vectors);

— Factors influencing the dispersion of lengths of interatomic vectors;

— Statistics of crystallographic sites of central monoatomic entities (crystallographic sites; lattice complexes; matrix representations of symmetry point groups of crystallographic sites; occurrence of central monoatomic entities in sites of Weissenberg lattice complexes);

— Statistics of bond distances between central monoatomic entities and ligands.

The fifth chapter presents general conclusions.

The book includes also the necessary background of mathematics; 82 figures, drawn with care, as well as an up-to-day bibliography complete the volume.

Marius Andruh
Faculty of Chemistry
University of Bucharest

Shinichi Kawaguchi, "Variety in Coordination Modes of Ligands in Metal Complexes" (Inorganic Chemistry Concepts, vol. 11), Springer-Verlag, Berlin, 1988, 123 pp., hard cover, DM 128, ISBN 3-540-18305-1.

The book authored by Professor S. Kawaguchi mainly deals with a classical chapter of coordination chemistry, known since Werner's epoch, namely the linkage isomerism. However, an up-to-day bibliography emphasizes new aspects as well as new trends in this field, regarding the various coordinating abilities of some organic or inorganic ligands. On the other hand, the rapid growth of organo-metallic chemistry provides a rich variety of structures illuminating the different coordinating modes of an organic ligand. In the last two decades, structural organo-metallic chemistry has revealed the existence of new groups of compounds whose structures do not conform with conventional principles of the octet valence theory or stereochemistry; these are the so-called non-classically bonded compounds (see also: V. I. Minkin, R. M. Minyaev and Y. A. Zhdanov, "Non-classical Structures of Organic Compounds", Mir Publishers, Moscow, 1987). Transition metal complexes of alkenes, alkynes, arenes, an other unsaturated organic molecules involving the interaction of π electrons with metal orbitals represent the most important class of these nonclassical or non-Werner type coordination compounds.

Taking into account the present-day development of the coordination chemistry, Professor Kawaguchi's book printing is welcome and useful.

A brief introductory chapter presents a classification of ligands, encompassing both classical complexes and organo-metallic compounds. Some general aspects regarding the linkage isomerism are also discussed. Chapters 2 to 5 are devoted to the most important classes of coordination compounds with ligands having various coordinating abilities. The classification of these compounds follows the number of atoms composing the ligands: mono-, di-, tri-, tetra- and polyatomic ligands.

According to this classification, the second chapter deals with monoatomic ligands, especially the hybride ligand, H^-. Mononuclear complexes with terminal $M - H$ linkage as well as polynuclear systems containing $M(\mu - H)_nM$ bridges are discussed. Furthermore,

μ_2 (edge-bridging), μ_3(face-bridging) and encapsulated (interstitial) hydride ligands found in various metal clusters aroused a special structural interest.

Diatomic ligands taken up in the third chapter are carbon monoxide and dinitrogen, due to the important roles they play in the synthetic, biological or environmental chemistry. Since the discovery of the first dinitrogen complex, $[Ru(NH_3)_5(N_2)]^+$, in 1965, more than hundred N_2 complexes have been prepared, in order to achieve three important objectives: 1) synthesis of model clusters which should exhibit nitrogenase activity; 2) synthesis of transition-metal systems capable of reducing N_2 in solution, and 3) activation of N_2 through ligation to transition-metal atoms, leading to nitrogen hydrides and nitrogen-carbon bonds.

The stereochemistry of complex compounds discussed in chapters 2 and 3 is mainly non-classical. The fourth chapter is more orthodox, dealing with triatomic ligands, known since a very long time, especially ambidentate ligands such as: NO_2^-, NCS^-, $NCSe^-$, $NCTe^-$, N_3^-. Electronic and steric effects of ancillary ligands on the bonding mode of ambidentate ligands are emphasized. The author invokes also general principles, i.e. hard and soft acids and bases (Pearson) and the symbiotic behaviour of ligands (Jørgensen) in order to explain many experimental regularities.

Although known since long time, coordination compounds with β-dicarbonylic ligands are extensively studied up to our days, due to the rich variety of coordinative interactions that occur between a metal ion and the ligand. The last chapter summarizes the coordination modes established so far for β-dicarbonyl ligands as the molecule, monoanion and dianion, with special emphasis on the interconversions among them.

The book presents also some aspects regarding the reactivity of all mentioned classes of coordination compounds, e.g.:

— *trans*-influence of the hydride ligand, reactions of hydride-complexes with acids and bases, with halogens and organic halides, reductive elimination reactions;

— the catalytic activity of rhodium, cobalt and iridium complexes in hydrogenation of olefins;

— the use of organometallic compounds, especially metal carbonyl clusters, in the Fischer-Tropsch synthesis.

Applications of various experimental techniques (IR, ^{13}C (^1H) — NMR and mass spectroscopy, X-ray diffraction) in order to elucidate the binding mode of a ligand in metal-complexes are illustrated.

With 56 figures, which mainly illustrate X-ray structure of complex compounds, searching a rich university bibliography, volume 11 in the series "Inorganic Chemistry Concepts" is a useful guide for both inorganic and organic chemists.

Marius Andruh
Faculty of Chemistry
University of Bucharest

NOTE POUR LES AUTEURS

La Revue Roumaine de Chimie publie des articles en anglais, français, russe, allemand ou espagnol. Les auteurs sont priés d'envoyer des articles et des comptes rendus inédits.

Les manuscrits seront dactylographiès à double interligne. La bibliographie, les tableaux et la légende des figures seront placés après le texte.

Si l'article fait partie d'une série numérotée, la partie précédente sea donnée comme première référence.

Chaque article sera précédé d'un résumé comprenant quinze lignes au maximum.

Les références bibliographiques dans le texte seront faites par des exposants sans parenthèses et paraîtront à la fin de l'ouvrage.

Les publications périodiques méntionnées dans la bibliographie seront présentées suivant les prescriptions internationales : le nom de l'auteur précédé de l'initiale du prénom, le titre du périodique abrégé conformément à « Chemical Abstracts » et souligné par une ligne, le numéro du tome indiqué par des chiffres arabes et souligné par deux lignes, suivi de la première page de l'article : à la fin, l'année de la parution sera placée entre parenthèses. Le numéro de la revue ne sera pas indiqué si les pages du volume sont numérotées consécutivement.

Les textes des livres ou traités incluront : le nom des auteurs, précédé de l'initiale du prénom, le titre du livre entre guillemets et sans être souligné, le numéro du tome précédé par l'abréviation « vol. » (ou « Bd »), le numéro de l'édition, les éditions (the publisher), la localité de la parution du livre, l'année de la parution et la page de la référence précédée(s) par l'abréviation « p » (ou « S »).

Les brevets seront indiqués comme suit : l'auteur ou la firme, le pays et le numéro du brevet, la date de la revue (*Chem. Abstr.*) Par ex. : M. Jones (to Union Carbide Co.) Brit. Pat. 610 238, 2 Sept. 1959 : cf. *Chem. Abstr.*, 54, 12808 (1960).

Si la référence n'a pas été lue en original, on indiquera aussi la revue de références consultée.

Les diagrammes seront tracés à l'encre de Chine sur papier calque. Les tableaux et les figures (en nombre strictement nécessaire), ainsi que les courbes dans les figures seront numérotés par des chiffres arabes. Leur explication sera donnée dans la légende des figures. Prière de ne pas inscrire les mêmes données dans les tableaux et les figures. Chaque tableau aura un titre. On indiquera dans le texte la place approximative des tableaux et des figures. Les formules chimiques seront incluses dans le texte ; en outre, elle seront transcrites sur papier calque, à l'encre de Chine.

Les auteurs sont priés d'indiquer les caractères italiques (en soulignant les lettres au crayon), ainsi que tout autre caractère spécial : les préfixes *ortho*, *méta*, *para*, *cis*, *trans*, etc. seront soulignés pour indiquer leurs caractères italiques, et ne seront jamais écrits avec des majuscules.

Aucune correction à la main ne sera admise sur le manuscrit. Les corrections seront frappées à la machine. Les lettres grecques ou d'autres symboles spéciaux seront insérés à la main à l'encre clairement.

Le manuscrit sera signé par l'auteur.

Le titre courant aura 50 lettres au maximum.

L'entière responsabilité du contenu des articles appartient aux auteurs.

Sur demande on peut obtenir une note plus complète.

PRINTED IN ROMANIA

TRAVAUX PARUS AUX ÉDITIONS DE L'ACADÉMIE ROUMAINE

I. G. MURGULESCU, **Introducere în chimia fizică, Vol. I. 1. Atomi, molecule, legătură chimică**, 1976, 650 p.

I. G. MURGULESCU, V.EM. SAHINI, **Introducere în chimia fizică, Vol 2. 1. Structura şi proprietăţile moleculelor**, 1979,

I. G. MURGULESCU, E. SEGAL, **Introducere în chimia fizică, Vol. II. 1. Teoria molecular-cinetică a materiei**, 1979, 1036 p.

I. G. MURGULESCU, TATIANA ONCESCU, E. SEGAL, **Introducere în chimia fizică, Vol. II. 2. Cinetică chimică şi cataliză**, 1981, 1024 p.

I. G. MURGULESCU, J. PĂUN, **Introducere în chimia fizică, Vol. I. 3. Nucleul atomic, reacţii nucleare, particule elementare**, 1982, 606 p.

I. G. MURGULESCU, RODICA VÎLCU, **Introducere în chimia fizică. Vol. III. Termodinamica chimică**, 1982, 624 p.

I. G. MURGULESCU, O. M. RADOVICI, **Introducere în chimia fizică, Vol. VI. Electrochimica**, 604 p. 1986, 410 p.

R. VÎLCU, M. LECA, **Polymer Thermodynamics by Gas Chromatography**, coédition avec Elsevier, 1990, 204 p.

Fl. CUIBAN, Q—X. LUPEA, **Studiul structurii şi sinteza peptidelor**, 1989, 286 p.

R. VÎLCU, M. LECA, **Termodinamica polimerilor prin cromatografie de gaze, 1987, 238** p.

I. ZUGRĂVESCU, M. PETROVANU, **Cicloadiţii 3 + 2 dipolare, 1987, 446** p.

RAUL MIHAIL, ION GROZEANU, **Estimarea secvenţială aplicată sistemelor chimice**, 1986, 406 p.

M. BREZEANU, I.·PATRON, M. ANDRUH, **Combinaţii complexe polinucleare şi aplicaţiile lor**, 1986, 244 p.

A. T. BALABAN et al., **Labelled Compounds and Radiopharmaceuticals Applied in Nuclear Medicine**, coédition avec John Wiley and Sons, 1986, 742 p.

D. PURDELA, **Nomenclatura chimiei organice — IUPAC**, 1986, 451 p.

PETRU BUDRUGEAC, **Probleme de chimie**, 1986, 280 p.

T. ONCESCU, S. G. IONESCU, **Conversie fotochimică şi stocare de energie**, 1985, 272 p.

V. DRĂGUŢAN, A. T. BALABAN, M. DIMONIE, **Olefin Metathesis and Ring-Opening Polymerization of Cyclo-Olefins**, coédition avec John Wiley and Sons, 1985, 544 p.

C. LITEANU, I. RÎCĂ, **Optimizarea proceselor analitice**, 1985, 360 p.

N. PERESCU, **Chimia extracţiei cu solvenţi şi aplicaţii**, 1985, 212 p.

1991 APR 0 5

ISSN 0035—3930

I.P. Universul. c. 2198

43 426

Lei 80

F 1103

ACADÉMIE ROUMAINE

REVUE ROUMAINE DE CHIMIE

TOME 35
Nos 10–12
Octobre – Décembre 1990

Rev. Roumaine Chim.

RRCHAX, 35, *10–12*, p. 939–1060 (1990), Bucarest

EDITURA ACADEMIEI ROMÂNE

ACADÉMIE ROUMAINE

COMITÉ DE RÉDACTION

Rédacteur en chef :

I. G. MURGULESCU, membre de l'Académie Roumaine

Rédacteurs en chef adjoints :

A.T. BALABAN et V. EM. SAHINI, membres de l'Académie Roumaine

Collège de rédaction :

EM. BRATU, ECATERINA CIORĂNESCU-NENITZESCU, CR. SIMIONESCU, P. SPACU, GH. SUCIU, membres de l'Académie Roumaine; M. ANDRUH, M. BANCIU, M. D. GHEORGHIU, I. HAIDUC, D. I. MARCHIDAN, G. NIAC et D. SĂNDULESCU.

La Revue Roumaine de Chimie paraît 10 fois par an. Toute commande de l'étranger sera adressée à ROMPRESFILATELIA — sectorul Export-Import Presă, P. O. Box 12—201, télex 10376, prsfi r 78 104, 64—66, Calea Griviței, Bucarest, Roumanie.

Les manuscrits, les livres et les revues proposés en échange, ainsi que toute correspondance seront envoyés à la rédaction

REVUE ROUMAINE DE CHIMIE

125, Calea Victoriei, 79717 Bucarest, Roumanie, téléphone 50 76 80

EDITURA ACADEMIEI ROMÂNE

125, Calea Victoriei 79717 Bucarest, Roumanie, téléphone 50 76 80

REVUE ROUMAINE DE CHIMIE

Tome 35, Nos 10–12 **Octobre—Décembre, 1990**

SOLOMON STERNBERG, MIHAELA UNGUREANU, SORIN ROŞCA, DANIEL KRAITER, Electrochemical oxidation of carboxylic acids. III. Electrode processes in electrochemical oxidation of natrium monomethyl adipate on graphite . . . . 941— 950

RODICA VÎLCU, I. GĂINAR and G. ANIŢESCU, The second interaction virial coefficient of gas mixtures. III. Carbon dioxide + hydrogen mixture 951— 959

CRISTINA MANDRAVEL and LIGIA IONESCU, The influence of various factors on the optical activity of some essential aminoacids. Part II. . . . . 961— 965

MINODORA LECA, R. ŞERBAN and ANTOANETA VELICU, Dispersion of a cataphoretic resin in view of electrodepositicn . . . . 967— 972

VIORICA TRANDAFIR, MIOARA COSTEA and ELENA ROBU, Morphological characterization of collagen membranes for medical textile prostheses 973— 983

S. J. CYVIN, J. BRUNVOLL and I. GUTMAN, Annulenes and primitive coronoids: some topological properties and enumerations . . . . 985— 996

ALEXANDRU T. BALABAN, CORNEL CATANĂ, MARCIA DAWSON and ION NICULESCU-DUVĂZ, Applications of weighted topological index *J* for QSAR of carcinogenesis inhibitors (retinoic acid derivatives) . . . . 997—1003

MICHAELA-CARMEN BALABAN, TEODOR-SILVIU BALABAN, URSULA BOLOGA and ALEXANDRU T. BALABAN, Synthesis of novel furyl-substituted 3-cyano-2-pyridones . . . . 1005—1008

MIRCEA D. BANCIU, IOANA ŞARAMET and CONSTANTIN DRĂGHICI, Interactions of substituted five-membered heteroaromatic compounds with electron acceptors. III. Charge transfer complexes with tetracyanoethene and tricyanovinylation of some 3-mercapto-1,2,4,-triazoles . . . . 1009—1016

JEAN M. HERDAN, VASILE DINOIU, AURELIA MEGHEA, ANA SCHIKETANZ, MIRCEA D. GHEORGHIU and ALEXANDRU T. BALABAN, Synthesis and EPR spectra of persistent aroxyls. V. Aroxyls derived from chalcone and derivatives . . . . 1017—1024

E. TYAGI, S.S. VERMA, L. PRAKASH and R. L. MITAL, Heterocyclic compounds. Synthesis of some fluorinated 1,3,5-triazine derivatives . . . . . 1025—1029

STELIAN PETRESCU and RADU Z. TUDOSE, On the liquid-solid heat transfer with solid phase change (in French) . . . . 1031—1042

COMPTES RENDUS . . . . 1043—1044

INDEX DES AUTEURS . . . . 1045—1054

INDEX DES SUJETS . . . . 1055—1059

Rev. Roumaine de Chim. **35**, *10—12*, 939—1060 (1990), Bucarest

Revue Roumaine de Chimie, 35, *10–12*, 941–950 (1990)

ELECTROCHEMICAL OXIDATION OF CARBOXYLIC ACIDS. III*

ELECTRODE PROCESSES IN ELECTROCHEMICAL OXIDATION OF NATRIUM MONOMETHYL ADIPATE ON GRAPHITE

SOLOMON STERNBERG,[a, **] MIHAELA UNGUREANU,[a] SORIN ROȘCA,[b] DANIEL KRAITER[c]

[a] Laboratory for Applied Physical Chemistry, Faculty of Chemical Technology, Polytechnic Institute, 76206, Bucharest, Splaiul Independenței 313, Romania
[b] Department of Organic Chemistry, Polytechnic Institute, Bucharest, Romania
[c] "Victoria" Chemical Enterprise, Tîrgoviște, Romania

Received March 2, 1989

The present paper studies the electrode processes in electrochemical oxidation of natrium monomethyl adipate(I) on graphite that has been undertaken using the cyclic voltammetry method. The electrode processes occurring in the oxidation of natrium monomethyl adipate in methanolic solutions with low water content in the presence of free monomethyl adipate have been analysed. The influences of the anion concentration, of the acid concentration and of the scanning rate have been studied and the partial orders of reaction with respect to the anion and free acid concentrations have been calculated. A bielectronic oxidation process has been assumed to occur on graphite at values of the potential that are by approximately 1 V more electronegative than those corresponding to the oxidation on platinum.

INTRODUCTION

It is known that the oxidation processes of carboxylic acids may take place in two stages, i.e., monoelectronic oxidation, which leads to the formation of a radical type intermediary, and bielectronic oxidation, resulting in the formation of a carbocation type intermediary, according to the following pattern:

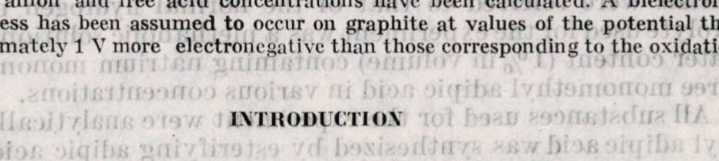

$$R-COO^- \xrightarrow{-e^-} R-COO\cdot \xrightarrow{-CO_2} R. \xrightarrow{-e^-} R^+$$

radical type stabilization products

cationic type stabilization products

It is also known that, at high values of the current density, platinum anodes favour monoelectronic oxidation and that, at low values of the current density, graphite anodes favour bielectronic oxidation.

---

* Part II, see ref. [7]

** Deceased on 19 January, 1990.

Due to the practical importance of dimethyl sebacate (which results from the dimerization of the radical formed in the first oxidation stage), the anodic oxidation of monomethyl adipate is a process that has been studied in detail.[1,2,3] The study has been performed using mainly electrodes made either of platinum or of another element from the platinum group because only by using these electrodes the highest yield of the dimerization process is obtained.

Preparatory electrolysis using graphite electrodes shows that, when these electrodes are used, the amount of dimethyl sebacate obtained is very small while the amount of products that may be interpreted as stabilization products resulting through the cationic channel and the amount of resulting resins are both increased.

The object of this paper is the study of electrode processes occurring in anodic oxidation of natrium monomethyl adipate on graphite using the cyclic voltammetry method. Based upon this study, explanations for the major differences that had been found between the resulting oxidation products on platinum and on graphite have been advanced.

THE EXPERIMENT

Potentiostatic measurements were performed in non-steady-state conditions using a potentiostatic device, that was presented in a previous paper.[4] The working electrode was a graphite disk ($S = 0.26$ cm^2), the counter electrode was a platinum mesh and the standard electrode was a saturated calomel electrode. The graphite electrode resurfacing was achieved by fine grinding using fine emery cloth before each measurement. All potentials were referred to that of the normal hydrogen electrode. The electrolyte used for the experiment was a methanolic solution with a reduced water content (1% in volume) containing natrium monomethyl adipate and free monomethyl adipic acid in various concentrations.

All substances used for the experiment were analytically pure. Monomethyl adipic acid was synthesized by esterifying adipic acid with methanol in acid medium and transesterifying the resulting dimethyl adipate with adipic acid.

Monomethyl adipic acid (MH) was purified by distillation and submitted to physico-chemical characterization procedures. Natrium monomethyl adipate (MNa) was obtained from natrium methoxide solutions in methanol and MH.

To stir the electrolyte a mechanical stirrer driven by a synchronous motor with 1500 rpm was used.

RESULTS AND DISCUSSION

The solid line in Figure 1 represents the first cyclovoltammogram obtained on graphite for $C_{\mathrm{MNa}} = 0.3$ M and $C_{\mathrm{MH}} = 0.5$M.

One may notice the existence of two characteristic oxidation regions. The first one, starting at about 1.3 V, is characterized by a rapid increase of the current with a maximum at about 1.9 V. It has been assumed that this process corresponds to a bielectronic oxidation of monomethyl adipate. The subsequent decrease of the current is probably due to the formation of a resins film that partially covers the surface of the electrode, since such a film had already been noticed during the preparatory electrolysis. [5] Beyond the potential of 2.6.V, a second oxidation region may be noticed, in which the increase of the current is slower. This region has been associated with the oxidation process that takes place through the resins film.

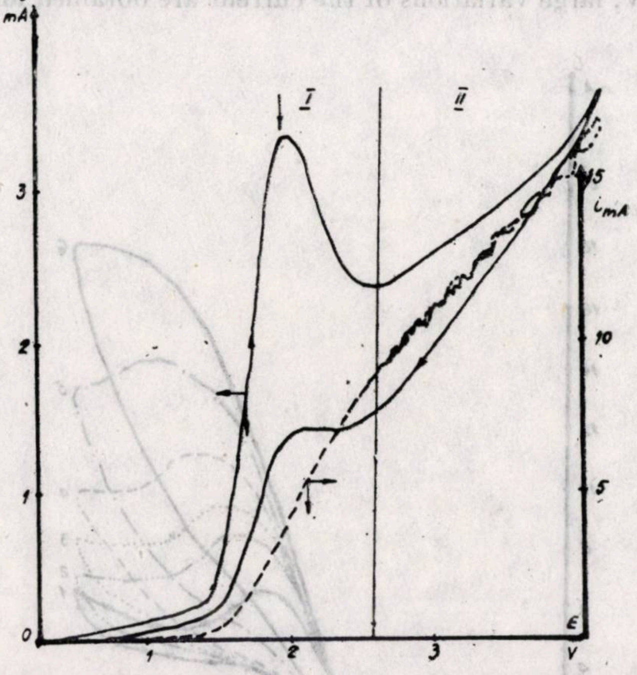

Fig. 1. — Cyclic voltammograms on graphite obtained with (— — — —) and without (————) stirring the electrolyte ; $c_{MNa} = 0.3$ M ; $c_{MH} = 0.5$ M ; v=8 mV/s.

During the anodic scanning gas bubbles were noticed to be generated on the surface of the electrode starting at about 1.9 V. The cyclovoltammogram also exhibits a marked hysteresis. In subsequent cycles the current decreases due to the covering of the surface of the electrode with gas bubbles. It has been noticed that by using mechanical stirring of the solution to remove the gas bubbles from the surface of the electrode, close values of the current are obtained in two successively recorded cyclovoltammograms. Based upon this observation, the surface of the electrode was degased each time before starting a new cycle.

The dotted line in Figure 1 represents the cyclovoltammogram obtained while stirring the electrolyte. The values of the current in this case were found to be about 5 times higher than those obtained in the cyclovoltammogram without stirring the electrolyte. Also the current does no longer decrease beyond 1.9 V (there is no maximum at 1.9 V) and this fact is due to the dispersion of the resins film. There is however a tendency for the current to reach a limitation starting at about 2.6 V. When the electrolyte is stirred, the cyclovoltammogram exhibits no hysteresis. Also, beyond 1.9 V, large variations of the current are obtained for very close values of the potential due to the generation and liberation of gas on the surface of the electrolyte.

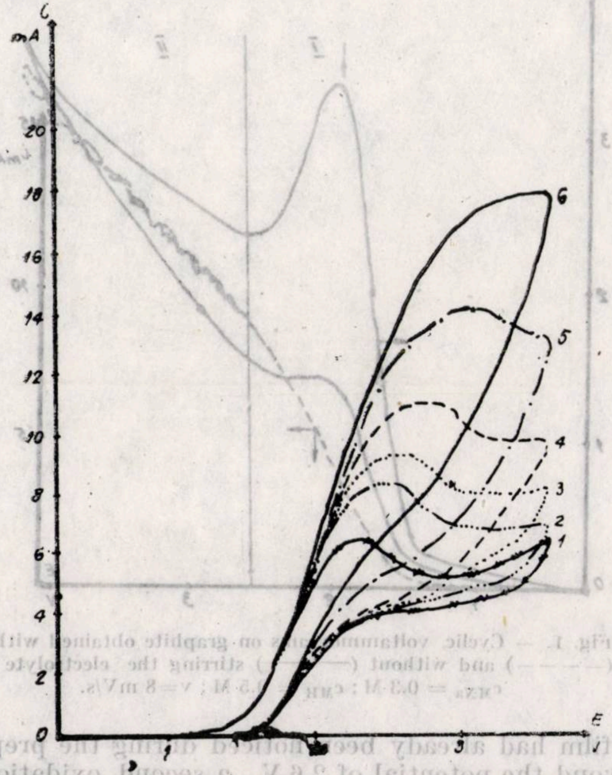

Fig. 2. — Cyclic voltammograms corresponding at different sweep rates (mV/s) : 8(1) ; 16(2) ; 24(3) ; 40(4) ; 80(5) ; 100(6) ; $C_{MNa} = 0.5M$; $C_{MH} = 1M$.

Figure 2 shows the influence of the scanning rate. One may notice that, as the scanning rate increases, a displacement of the maximum takes place from 1.9 V towards more electropositive values accompanied by the intensification of the anodic process and the accentuation of the hysteresis on the cathodic branch, these facts being in agreement with the assumption that a limitation of the oxidation process takes place due to the presence of the film.

Figure 3 presents the cyclovoltammograms obtained for anion concentrations varying from 0.1M to 0.5 M without stirring the electrolyte. A marked increase of the anodic current with the anion concentration may be noticed.

This increase of the current with the anion concentration may also be noticed when the electrolyte is stirred (Figure 4) accompanied in this case by a stronger tendency to present a limitation for low anion concentration.

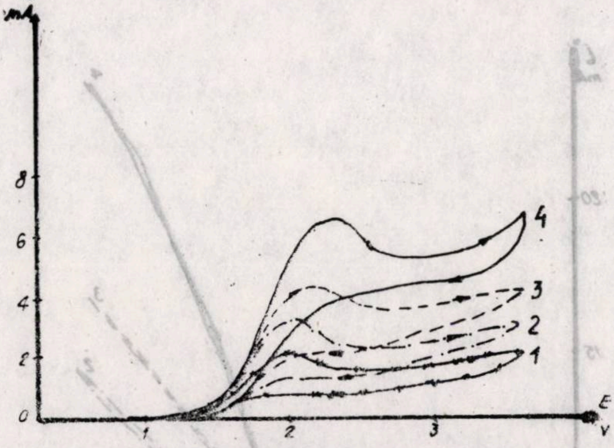

Fig. 3. — Influence of the anion concentration (cyclic voltammograms obtained without stirring the electrolyte) C_{MNa} : 0.1(1) ; 0.2(2) ; 0.3(3) ; 0.5(4) ; $C_{MH} = 1M$; $v = 8mV/s$.

The partial order of reaction with respect to the anion has been evaluated from the cyclovoltammograms obtained without stirring the electrolyte (Table 1). At potential values less than 1.8V, this is relatively constant and equal to 0.33. Between 2.8 V and 3 .4 V, this order is still less than unity but greater than 0.7.

Table 1

Evaluation of the partial order of reaction with respect to the anion concentration : $C_{MH} = 1M$; $v = 8$ mV/s

E	1.44	1.54	1.64	1.74	1.84	1.94	2.84	3.04	3.24	3.44
n	0.21	0.29	0.35	0.36	0.43	0.54	0.73	0.71	0.70	0.72

From the curves obtained when the electrolyte was stirred the partial order of reaction with respect tot the anion was to be constantly increasing (Table 2) varying between 0.47 and 0.71.

Table 2

Evaluation of the partial order of reaction with respect to the anion concentration (cyclovoltammograms obtained while stirring the electrolyte) ; $C_{MH} = 1M$; $v = 8mV/s$

E	1.54	1.64	1.74	1.84	1.94	2.04	2.14	2.24	2.34	2.44	2.54
n	0.47	0.37	0.52	0.51	0.52	0.55	0.57	0.60	0.63	0.66	0.67

The fact that the orders of reaction were found to be less than unity indicates that adsorption phenomena occur within the process.[6]

The influence of the acid concentration on the oxidation processes studied has also been considered. During the experiment the free acid concentrations ranged between 0.1 M and 1M. Figure 5 indicates that the maximum at 1.9 V is only slightly affected by the decrease of the acid concentration. The oxidation process through the resins film is however strongly influenced, a marked increase of the current occurring as the acid concentration decreases. Since the shape of the curve of cathodic scanning is gradually modified with the decrease of the acid concentration, the hysteresis is no longer the same. Thus, at the lowest value of the acid concentration, the return path is above the onward one, the values of the current being higher than those obtained for anodic scanning. This may be attributed to a reactivation of the process brought about by the cathodic scanning.

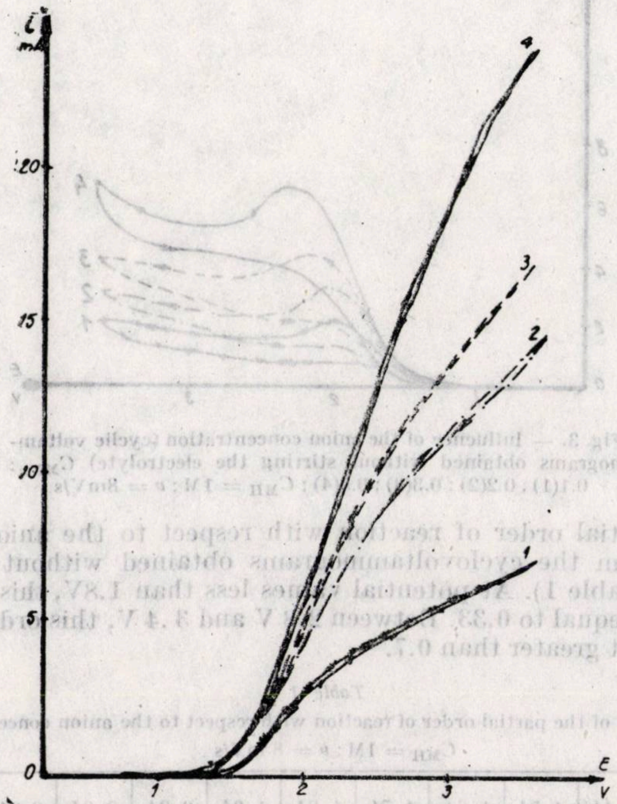

Fig. 4. — Influence of the anion concentration (cyclovoltammograms obtained while stirring the electrolyte) : C_{MNa} : 0.1(1) : 022(2) ; 0.3(3) ; 0.5(4) ; $C_{MH} = 1M$; $v = 8mV/s$.

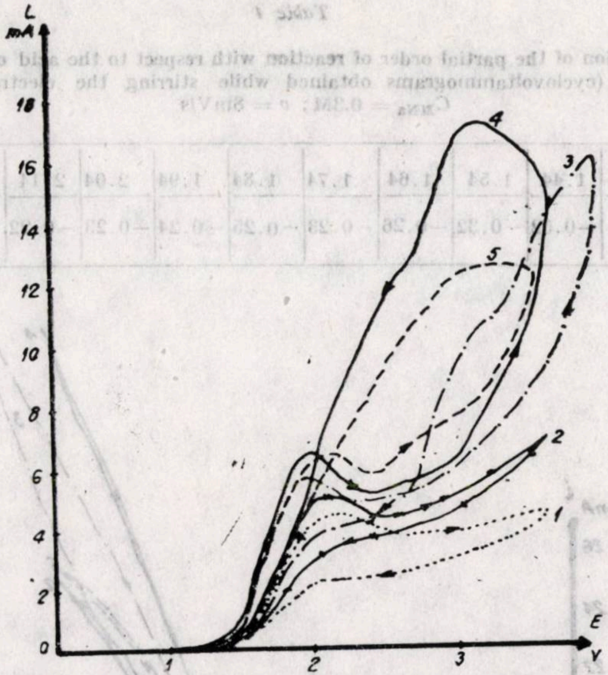

Fig. 5. — Influence of the acid concentration (cyclovoltammograms obtained without stirring the electrolyte) C_{MH} : 1(1) ; 0.5(2) ; 0.3(3) ; 0.1(4) ; 0. (5) M ; $C_{MNa} = 0.3M$; $v = 8$ mV/s.

Figure 6 shows the dependence of the cyclovoltammograms on the acid concentration when the electrolyte was stirred during the experiment. One may notice that, similarly to Figure 5, an increase of the current takes place as the acid concentration decreases. This fact may be explained by the competitive adsorption of the acid (electrochemically inactive species).

Tables 3 and 4 present the partial orders of reaction with respect to the acid corresponding to the cyclovoltammograms obtained with and without stirring the electrolyte. A negative order of reaction with respect to the acid has been obtained with an average value of about −0.3.

Table 3

Evaluation of the partial order of reaction with respect to the acid concentration : $C_{MNa} = 0.3M$; $v = 8$ mV/s

E	1.44	1.54	1.64	1.74	1.84	1.94
n	−0.20	−0.37	−0,35	−0.32	−0.27	−0.23

Table 4

Evaluation of the partial order of reaction with respect to the acid concentration (cyclovoltammograms obtained while stirring the electrolyte); $C_{MNa} = 0.3M$; $v = 8mV/s$

E	1.44	1.54	1.64	1.74	1.84	1.94	2.04	2.14	2.24
n	−0.52	−0.32	−0.26	−0.23	−0.25	−0.24	−0.23	−0.22	−0.23

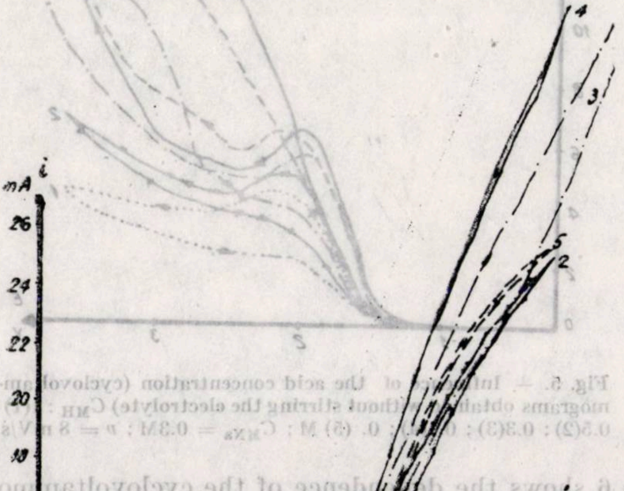

Fig. 6. — Influence of the acid concentration (cyclovoltammograms obtained while stirring the electrolyte) C_{MH} : 1(1) ; 0.5(2) ; 0.3(3) ; 0.1(4) M ; $C_{MNa} = 0.3$ M ; $v = 8$ mV/s.

CONCLUSIONS

Analysis of the results of the study of the process using the cyclic voltammetric method and their correlation with the results of the preparatory electrolysis shows that the oxidation process on graphite, characterized by a maximum at 1.9 V, is a bielectronic oxidation process of the monomethyl adipate anion. On graphite, the radical formed in the first stage of the oxidation remains adsorbed and subsequently undergoes a new transfer of an electron. This leads to the formation of the carbocationic intermediary which is rapidly desorbed and undergoes further stabilizing reactions, e.g., elimination of a proton and interaction with the solvent. These reactions may lead to electrochemical oligomerization products (resins) which conceal the surface of the electrode and thus determine the decrease of the current beyond the maximum and also its subsequent slow increase as a result of the oxidation that takes place through the resins film.

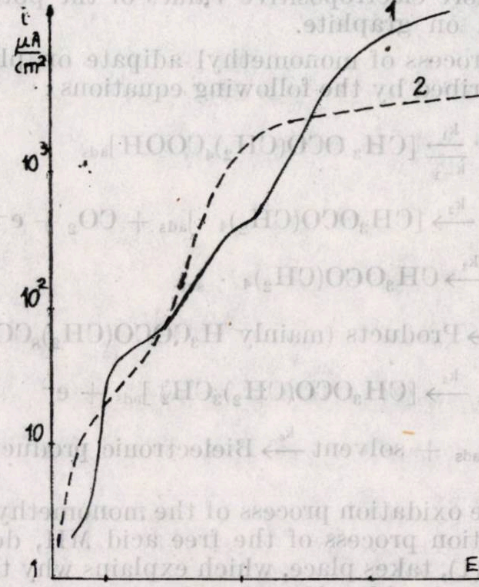

Fig. 7. — Steady-state current-potential curves on platinum (1) and on graphite (2) anodes ; $C_{MH} = 1$ M ; $C_{MNa} = 0.3$ M; Methanol with 1 % (vol.) water.

A comparative analysis of the behaviour of the monomethyl adipate anion in the oxidation process on platinum and on graphite (Figure 7) shows the essential differences occurring in two regions. Thus, within the region between 1.5 V and 2.3 V, the values of the currents obtained on platinum are much higher than those obtained on graphite. This behaviour may be explained by admitting the existence of two types of adsorption centres on the surface of the electrodes.[6] I — high energy adsorption centres and II — low energy adsorption centres. On the I centres the radical is strongly adsorbed and subsequently undergoes a new transfer of an electron, resulting in the formation of carbocation whose stabilization takes place afterwards. On the II centres a monoelectronic oxidation takes place. In the case of graphite electrodes adsorption centres of type I are predominant, while in the case of platinum electrodes adsorption centres of type II prevail , those of type I being obstructed by the formation of oxides. [7] That explains why monoelectronic oxidation on platinum occurs at more electropositive values of the potential than the bielectronic oxidation on graphite.

The oxidation process of monomethyl adipate on platinum and on graphite may be described by the following equations :

$$H_3COCO(CH_2)_4COOH \underset{k_{-1}}{\overset{k_1}{\rightleftharpoons}} [CH_3\,OCO(CH_2)_4COOH]_{ads} \qquad (1)$$

$$H_3COCO(CH_2)_4COO^- \xrightarrow{k_2} [CH_3OCO(CH_2)_4\cdot]_{ads} + CO_2 + e^- \qquad (2)$$

$$[CH_3OCO(CH_2)_4\cdot]_{ads} \xrightarrow{k_3} CH_3OCO(CH_2)_4\cdot{}_{sol} \qquad (3)$$

$$CH_3OCO(CH_2)_4\cdot{}_{sol} \xrightarrow{k_4} \text{Products (mainly } H_3COCO(CH_2)_8COOCH_3) \qquad (4)$$

$$[CH_3OCO(CH_2)_4\cdot]_{ads} \xrightarrow{k_5} [CH_3OCO(CH_2)_3CH_2^+]_{ads} + e^- \qquad (5)$$

$$[CH_3OCO(CH_2)_3CH_2^+]_{ads} + \text{solvent} \xrightarrow{k_6} \text{Bielectronic products} \qquad (6)$$

Parallel with the oxidation process of the monomethyl adipate anion a competitive adsorption process of the free acid MH, described by the equilibrium equation (1), takes place, which explains why the partial order of reaction with respect to the acid is negative.

REFERENCES

[1] E. P. Kovsman, S. N. Freidlin, G. A. Tarkhanov, "Electrochemical Synthesis of Monomers", Nauka, Moskva, 1980, p. 49.

[2] Yn. B. Vassiliev, E. P. Kovsman, G. N. Freidlin, *Electrochim. Acta*, **27**, *7*, 953 (1982).

[3] G. N. Freidlin, E. P. Kovsman, A. A. Adamov et al. in "Electrosintez Monomerov", Khimia, 1981, p. 37.

[4] S. Sternberg, Mihaela Ungureanu, S. Roşca, *Rev. Roum. Chim.*, **34**, *1*, 337 (1989).

[5] S. Sternberg, Mihaela Ungureanu, S. Roşca, *Rev. Roum. Chim.*, in press.

[6] Mihaela Ungureanu, S. Sternberg, to be published.

[7] S. Sternberg, Mihaela Ungureanu, S. Roşca, *Rev. Roum. Chim.*, 1990 .

Revue Roumaine de Chimie, 35, *10–12*, 951–959 (1990)

THE SECOND INTERACTION VIRIAL COEFFICIENT OF GAS MIXTURES. III[1,2]

CARBON DIOXIDE + HYDROGEN MIXTURE

RODICA VÎLCU, I. GĂINAR and G. ANIȚESCU
Polytechnic Institute, Physical Chemistry Department, Spl. Independenței 313, 77206
Bucharest, Romania

Received December 20, 1988

By means of a new genuine equipment based on the principle of volume variation accompanying the gas mixing, the excess volumes were obtained for the H_2-CO_2 system on a temperature range within 258–308 K and pressures up to 50 atmospheres. The experimental data thus obtained were used to calculate the second viral interaction coefficient (B_{12}). The B_{12} value was compared with that theoretically calculated using the Lennard-Jones potential and 11 combination mixing rules.

INTRODUCTION

In a series of papers[1,2], we reported data about the excess volumes for N_2+H_2, $Ar+H_2$ and $CH_4 + H_2$ systems at 293 and 298 K and pressures up to 80 atmospheres, using for this the method of volume variations associated to gas mixing. This method elaborated by Edwards and Roseveare[3] has been applied by various authors[4] to the lower range of pressures. The method has been later extended by a group of physicists of Kamerling Onnes Laboratory (Leyden)[2] for higher pressures.

Experimental data concerning the excess volumes for the system $CO_2 + H_2$ were used to calculate the second interaction viral coefficient B_{12}.

EXPERIMENTAL

The equipment described earlier[1,2] has allowed only the study of a small number of mixtures in the range of 0.3–0.6 molar fraction values, because the apparatus was provided with only three mixing cells.[1]

The new equipment contains six mixing cells with calibrated volumes equal to 50 cm^3, made from stainless steel and located in a 8 l Dewar flask (Fig. 1).

The liquid used for constant temperature bath, a mixture of ethyleneglycole + water, was recirculated by means of a Lauda cryostate, model K4R, with an electronic control on the platinum resistance thermometer. The temperature was set to within ± 0.02 °C

Connections between cells were made from stainless steel capillary tubes ($Ø_{int} = 0.2$ mm). Cell connections at the gas filling system were achieved by nine valves from stainless steel having very small dead volumes. As in previous paper[1,2], the gas mixing was performed by means of a mercury pump. The number of mixing operations dependent on temperature and working pressure was determined by the constant value of ΔP, pressure variation, associated to the mixing process. The small pressure variations were detected by means of a differential pressure transducer designed by us.[6]

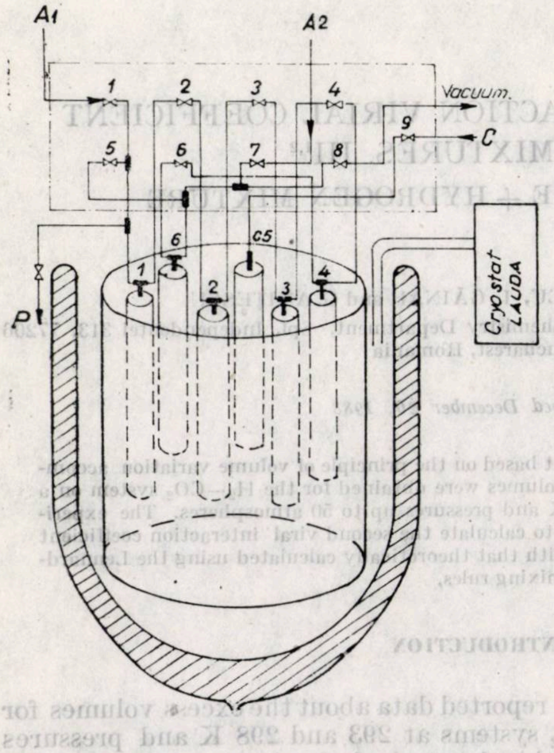

Fig. 1. — Experimental apparatus.

RESULTS AND DISCUSSIONS

The choice of the system $H_2 + CO_2$ is based on practical and theoretical reasons. This mixture is used to obtain the "synthesis gas", the thermodynamical behaviour of these two gases being very different : at temperatures and pressures at which the experimental measurements were made (258, 263, 273, 283, 293 and 308 K and 10, 15, 20, 30, 40 and 50 atmospheres respectively), hydrogen presents less obvious deviations from an ideal gas compared withCO_2 for which these values are near to the critical thermodynamic domain.

The values for the excess volumes in the mentioned range of temperatures and pressures are reported in tables 1, 2 and 3.

The values summarized in these tables are :

— x_2, the hydrogen molar fraction in the mixture with CO_2 ;

— Δn, the number of moles of gas mixture which must be removed from the system to obtain a value for the pressure after mixing which equals the initial one. For this purpose a quantity of gas concerning the excess pressure was removed from the system and collected in a constant temperature glass reservoir of about 2000 cm³. The pressure associated to this process takes such a small value compared with those of charging pressures (see P^E values) that it can be used to calculate Δn in the ideal gas approach ;

Table 1

Excess volumes of the $CO_2 + H_2$ mixture from experimental data at various pressures, temperatures and compositions

P (atm)	T (K)	x_{H_2}	$\Delta n \times 10^3$ (mol)	ΔP (torr)	P^E (torr)	V^E (cm³/mol)
10	258	0.431	2.58	91.63	21.88	44.67
	263	0.429	1.95	72.20	16.84	34.48
	273	0.433	1.73	71.81	15.47	33.41
	283	0.435	1.32	56.84	12.30	27.73
	298	0.440	1.24	55.08	12.14	29.43
	308	0.435	1.03	54.42	10.45	26.68
15	258	0.471	5.73	185.11	48.42	53.56
	263	0.468	3.75	126.35	32.33	35.56
	273	0.473	3.31	116.94	29.61	34.30
	283	0.478	2.30	98.50	21.38	26.08
	298	0.482	2.13	85.87	20.86	27.20
	308	0.485	1.72	72.42	17.40	23.63
20	258	0.211	9.95	230.37	83.97	42.73
		0.286	8.52	293.33	72.00	47.95
		0.445	10.64	301.11	89.81	51.17
		0.616	6.62	241.76	56.00	45.41
		0.707	6.99	208.80	59.07	37.00
20	263	0.214	7.08	194.83	60.97	32.01
		0.290	6.48	236.87	55.91	38.68
		0.449	8.41	246.24	72.39	42.35
		0.620	5.22	201.82	45.04	37.35
		0.710	5.46	172.19	47.06	32.51
20	273	0.219	5.20	156.26	46.55	26.44
		0.296	5.01	195.92	44.85	35.20
		0.457	6.50	203.85	58.11	36.21
		0.628	4.06	166.31	36.36	31.81
		0.717	4.42	149.49	39.61	28.64
20	283	0.226	4.27	133.10	39.65	27.42
		0.305	3.90	163.02	36.22	29.50
		0.467	4.98	166.12	46.16	32.74
		0.637	3.60	154.43	33.46	31.14
		0.724	3.82	132.23	35.44	25.17

Table 2

Excess volumes of the $CO_2 + H_2$ mixture from experimental data at 298 K and 20 atm

x_{H_2}	$\Delta n \times 10^3$ (mol)	ΔP (Torr)	P^E (torr)	V^E (cm³/mol)
0.180	4.14	108.22	40.54	18.17
0.234	3.36	105.51	32.86	22.93
0.314	2.97	115.67	29.00	27.48
0.370	4.78	139.34	48.39	29.77
0.478	4.34	140.68	42.37	21.12
0.569	5.40	143.23	49.54	30.01
0.647	2.93	120.56	28.64	28.82
0.733	3.27	110.72	31.96	24.40
0.779	3.49	98.86	34.20	20.78

Table 3

Excess volumes of the $CO_2 + H_2$ mixture from experimental data at 298 K and 10—50 atm.

P (atm)	x_{H_2}	$\Delta n \times 10^3$ (mol)	ΔP (torr)	P^E (torr)	V^E (cm^3/mol)
10	0.485	0.48	36.00	4.71	28.28
15	0.482	2.13	85.87	20.86	28.60
20	0.478	4.34	140.68	42.37	31.12
30	0.448	5.61	228.86	54.88	32.31
40	0.392	11.51	360.06	112.24	35.50
50	0.389	22.75	520.17	220.53	39.05

— ΔP represents the pressure variation, in mm Hg, resulting from the mixing process of the two gases.

The ΔP and P^E values must be determined with an accuracy of $1/10^5$ of the value of the filling pressure.

— V^E is the excess volume obtained from experimental data (Δn) and the quantities specific to the pure components ($V^0_{H_2}$, $V^0_{CO_2}$, n_{H_2}, n_{CO_2}), by means of the relationship :

$$V^E = \frac{\Delta n}{(n_{H_2} + n_{CO_2} - \Delta n)} (x_{H_2} \cdot V^0_{CO_2} + x_{CO_2} \cdot V^0_{CO_2}) \quad (1)$$

The quantities $V^0_{H_2}$, $V^0_{CO_2}$, n_{H_2} and n_{CO_2} were calculated using a computer program using the Beattie-Bridgemann equation of state.

Figure (2) presents the excess volumes, V^E, against the molar fractions. Such isothermes are described by parabolic curves their maxima being switched from the 0.5 molar fraction with the temperature decrease. These results are in good agreement with the theoretical predictions. Figures 3 and 4 show the pressure variations ΔP and P^E respectively, associated to the mixing process. One observes an obvious deviation of the effect at lower temperatures. At the maximal working temperature (308 K) the effect is obviously less sensitive, for pressures up to round 10 atm the dependence being nearly linear.

Figures 5 and 6 illustrate the ΔP and P^E variations as a function of working temperatures.

From the plot, $V^E = f(P)$, one obtains, by extrapolation at $P = 0$, the value $V^E(0)$, by means of which the B_{12} virial coefficient can be calculated.

$$B_{12} = \frac{V^E(0)}{2\,x_1 x_2} + \frac{B_{11} + B_{22}}{2} \quad (2)$$

B_{12} value calculated for the $CO_2 + H_2$ system at 25°C equal to $-$ 0.43 cm^3/mol are in good agreement with -1.1 cm^3/mol reported by M. Michels and J. A. Baerboom[4] using the same experimental method at low pressures.

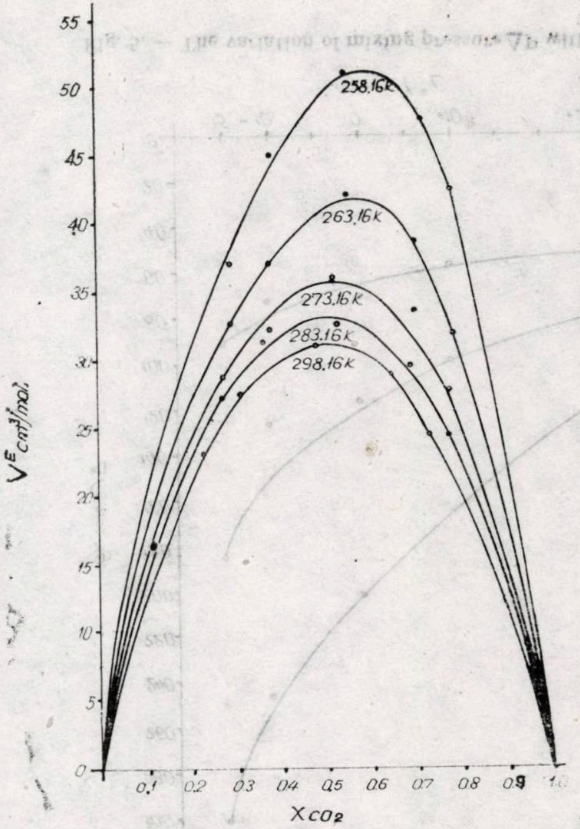

Fig. 2. — Excess volumes of the mixture as function of temperatures.

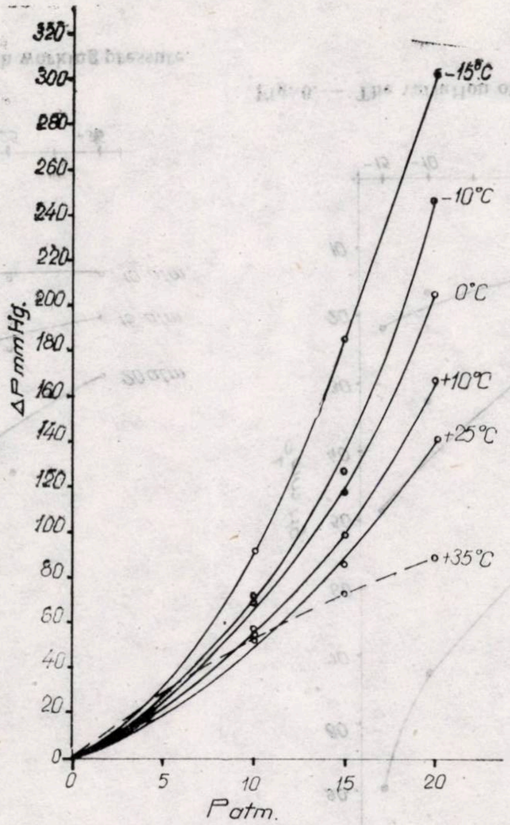

Fig. 3. — The temperature dependence of pressure variation of mixing ΔP.

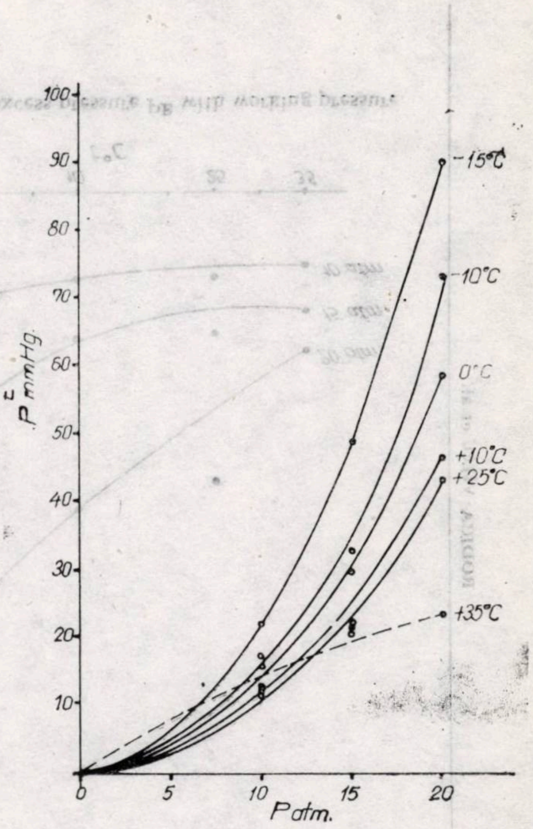

Fig. 4. — The temperature dependence of excess pressure pE.

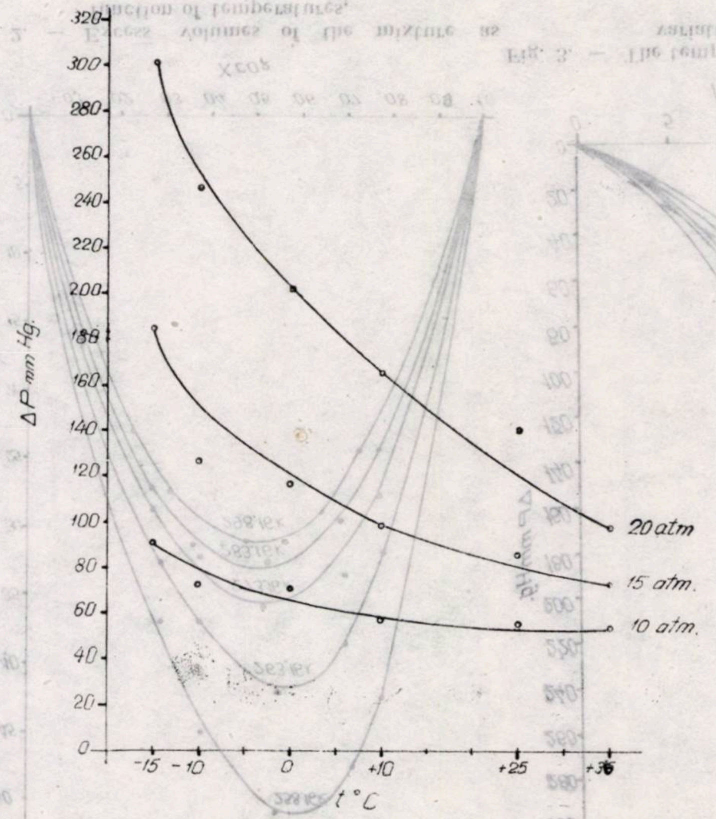

Fig. 5. — The variation of mixing pressure ΔP with working pressure.

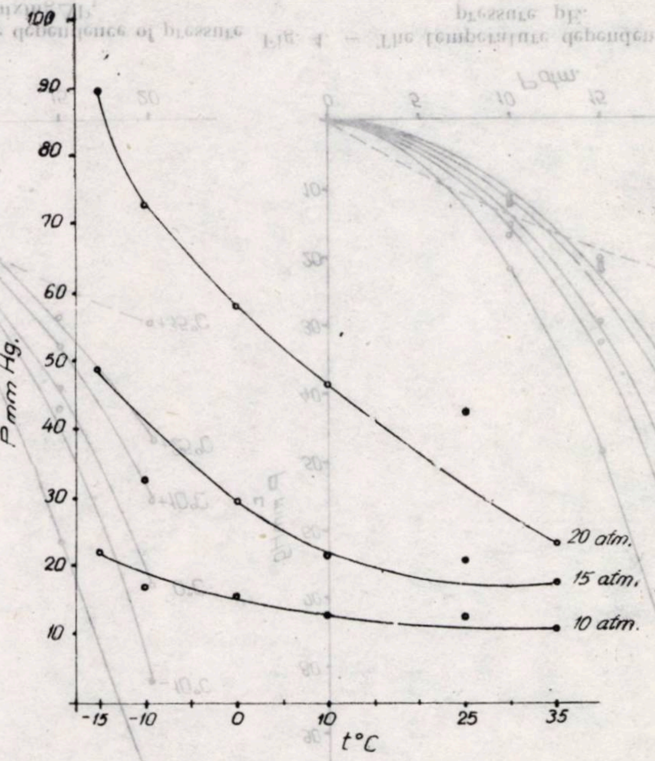

Fig. 6. — The variation of excess pressure P^E with working pressure.

For B_{12} calculation, the equation

$$B_{12} = 2\pi N \int_{0}^{\infty} (1 - e^{-\varphi_{12}/kT}) r^2 \, dr \tag{3}$$

was used. The integration of this equation for a Lennard-Jones[6,12] potential

$$\varphi_{12} = -4\varepsilon_{12} \left[\left(\frac{\sigma_{12}}{r} \right)^6 - \left(\frac{\sigma_{12}}{r} \right)^{12} \right] \tag{4}$$

leads to

$$B_{12} = \left(\frac{\sqrt{2}}{3} \right) \pi N \sigma_{12}^3 \left(\frac{4\varepsilon_{12}}{kT} \right)^{1/4} \cdot \left[\Gamma\left(\frac{3}{4} \right) - \right.$$
$$\left. - \frac{1}{4} \cdot \sum_{j=1}^{\infty} \left(\frac{4\varepsilon_{12}}{kT} \right)^{\frac{j}{2}} \cdot \Gamma\left(\frac{2j-1}{4} \right) \right] \tag{5}$$

where Γ is the "gamma function" and j is a summation integer. For a more detailed study of B_{12} dependence of ε_{12} and σ_{12}, the 11 combination rules, proposed by R. I. Good and C. J. Hope[7] are used. These rules are presented in table 4.

Equation (5) has been solved using a computer program. For each of the 11 combination rules, $B_{12}(T)$ was calculated for the six mentioned values of temperature. The values of the physical quantities used in calculation are presented in table 5 and the values so obtained for $B_{12}(T)$ are summarized in table 6.

There are very few data reported in the literature concerning theoretical calculation of B_{12} for $CO_2 + H_2$ system. The values of 3.0 cm³/mol[8] were calculated for 298 K using the sixth combination rule from table 4. The values of potential parameters used in calculation were unfortunately not indicated. If one takes into account that the intermolecular potential function is very sensitive to the choice of σ and ε parameters, we can consider our values obtained with combination rules 1, 2 and 6 as being correct, the other rules leading to quite different values.

To test our computer program, we have used the NBS data reported by M. E. Boyd[9]. In this paper, besides the classical term, quantum corrections of the Lennard-Jones ($m-6$) potential were made. Using the relations :

$$\begin{aligned} B^* &= B/b_0 \\ U^* &= U/\varepsilon \\ T^* &= kT/\varepsilon \\ R &= r/\sigma \\ \Lambda^* &= h/\sigma\,(2\mu\varepsilon)^{1/2} \end{aligned} \tag{6}$$

one may write

$$B^* = B^{*(0)} + \Lambda^{*(2)} \cdot B^{*(1)} + \Lambda^{*(4)} \cdot B^{*(2)} + \ldots$$

Table 4

The values of B_{12} obtained for some combining rules of ε_{12} and d_{12}

Rule number	d_{12}	ε_{12}
1	$(d_{11}\, d_{22})^{1/2}$	$(\varepsilon_{11}\, \varepsilon_{22})^{1/2}$
2	”	$\frac{(\varepsilon_{11}\, \varepsilon_{22})^{1/2}\, 2(I_1 I_2)^{1/2}}{(I_1 + I_2)}$
3	”	$\frac{2 \cdot \varepsilon_{11}\, \varepsilon_{22}}{(\varepsilon_{11} + \varepsilon_{22})}$
4	”	$\frac{2 \cdot \varepsilon_{11}\, \varepsilon_{22}\, \chi_1\, \chi_2\, (d_{11}\, d_{22})^3}{\chi_2^2\, d_{11}^6\, \varepsilon_{11} + \chi_1^2\, d_{22}^6\, \varepsilon_{22})}$
5	”	$\frac{2. \varepsilon_{11}\, \varepsilon_{22}\, \alpha_1\, \alpha_2\, (d_{11}\, d_{22})^3}{(\alpha_2^2\, d_{11}^6\, \varepsilon_{11} + \alpha_1^2\, d_{22}^6\, \varepsilon_{22})}$
6	$(d_{11} + d_{22}\, /2$	$(\varepsilon_{11}\, \varepsilon_{22})^{1/2}$
7	”	$\frac{(\varepsilon_{11}\, \varepsilon_{22})^{1/2}\, 2\, (I_1 I_2)^{1/2}\, 2^6\, (d_{11}\, d_{22})^3}{(I_1 + I_2)\, (d_{11} + d_{22})^6}$
8	”	$\frac{2\, \varepsilon_{11}\, \varepsilon_{22}}{(\varepsilon_{11} + \varepsilon_{22})}$
9	”	$\frac{(\varepsilon_{11}\, \varepsilon_{22})^{1/2}\, 2^6\, (d_{11}\, d_{22})^3}{(d_{11} + d_{22})^6}$
10	”	$\frac{2.\ \varepsilon_{11}\, \varepsilon_{22}\, \chi_1\, \chi_2\, (d_{11}\, d_{22})^3 \cdot 2^6\, (d_{11} d_{22})^3}{(\chi_2^2\, d_{11}^6\, \varepsilon_{11} + \chi_1^2\, d_{22}^6\, \varepsilon_{22})\, (d_{11} + d_{22})^6}$
11	”	$\frac{2.\ \varepsilon_{11}\, \varepsilon_{22}\, \alpha_1\, \alpha_2\, (d_{11}\, d_{22})^3\, 2^6\, (d_{11}\, d_{22})^3}{(\alpha_2^2\, d_{11}^6\, \varepsilon_{11} + \alpha_1^2\, d_{22}^6\, \varepsilon_{22})\, (d_{11} + d_{22})^6}$

Table 5

The potential parameters and some physical properties of pure H_2 and CO_2

Gas	I(eV)	$\alpha \times 10^{24}$(cm^3)	$\chi \times 10^{29}$(esu)	ε/k(K)	σ_0(Å)
H_2	13.60	0.79	0.66	29.20	2.87
CO_2	13.79	2.65	3.32	189.00	4.49

where the significance of the quantities $B^{(P)}$ calculated by Kihara is given in the cited paper[9].

For different T^* and in values, tables for $B^{*(0)}$, $B^{*(1)}$, $B^{*(2)}$ ... are presented.

In the case of the $CO_2 + H_2$ system, one obtains the following data for the potential (6—12) and (6—9) respectively :

$m = 12 \quad T^* = 4.014, \quad B^{*(0)} = 0.11541, \quad B_{12}\,(298) = 9.41$ cm^3/mol

Table 6

Theoretical values of B_{12} as a function of temperature for the 11 combination rules

T(K)	B_{12}					
	258	263	273	283	298	308
1	0.78	1.65	3.30	4.81	6.87	8.11
2	0.78	1.65	3.30	4.81	6.87	8.11
3	14.78	15.31	16.30	17.21	18.44	19.18
4	9.09	9.76	11.02	12.18	13.75	14.69
5	17.41	17.88	18.74	19.53	20.60	21.24
6	0.84	1.78	3.56	5.19	7.40	8.73
7	7.60	8.38	9.84	11.18	13.00	14.10
8	15.92	16.49	17.56	18.54	19.87	20.66
9	7.60	8.38	9.84	11.18	13.00	14.10
10	14.96	15.56	16.67	17.69	19.08	19.91
11	22.30	22.70	23.45	24.14	25.07	25.62

$m = 9 \quad T^* = 4.014, \quad B^{*(0)} = 0.10125, \; B_{12}(298) = 8.17$ cm^3/mol

The quantum corrections were neglected in these calculations, which for the system herein studied at 25° C, are insignificant.

REFERENCES

[1] R. Vîlcu and I. Găinar, Rev. Roum. Chim., 19, 1123 (1974).

[2] R. Vîlcu and I. Găinar, Rev. Roum. Chim., 22, 827 (1977).

[3] E. A. Eduards and W. E. Roseveare, J. Am. Chem. Soc., 64, 2816 (1942).

[4] A. Michels and A. J. H. Boerboom, Bull. Soc. Chim. Belg., 62, 119 (1953),

[5] P. Zandbergen, and J. J. M. Beenakker, Physica, 33, 343 (1967).

[6] R. Vîlcu and I. Găinar, Romanian Patent 89342 (1977).

[7] R. J. Good and C. J. Hope, J. Chem. Phys., 55, 111 (1971).

[8] J. O. Hirshfelder, C. F. Curtiss and R. B. Bird, "Molecular Theory of Gases and Liquids", Wiley, New York, 1954, p. 169.

[9] M. E. Boyd, J. Res. Nat. Bur. Stand., 75 A, 57 (1971).

Revue Roumaine de Chimie, **35**, *10–12*, 961–965 (1990)

THE INFLUENCE OF VARIOUS FACTORS ON THE OPTICAL ACTIVITY OF SOME ESSENTIAL AMINOACIDS. PART II

CRISTINA MANDRAVEL [a] and LIGIA IONESCU [b]

[a] Department of Physical Chemistry, Polytechnic Institute Bucharest, Bulevardul Republicii 13,

[b] Chemical and Pharmaceutical Research Institute, Calea Vitan 112, Bucharest, Romania

Received March 14, 1989

The dependence of the optical activity on the physical properties and/or other calculable structural features was investigated by spectropolarimetry for a series of aminoacids represented by the general formula R-CH(NH_2)-COOH. The structural properties taken into account include the molecular weight of the distinctive radical R, the position of the absorption bands in the UV-spectrum and the change density on asymmetric carbon atom and on different representative atoms in the R radical.

INTRODUCTION

Although the aminoacids have been intensively studied, modern research in this field is still of interest from two reasons : firstly, it ensures the development of selective methods for the enantiomer resolution[1–4] and secondly, it allows the understanding, on a modern theoretical basis, of the biomolecular chirality and of the empirical rules concerning the optical activity.[5–11]

The results of these investigations may be used in synthesis and formational study of stereospecific biopolymers.

Although the theory of the optical activity[7–10] has been developed, complete calculations have been restricted either to the simplest molecules or to regular structures with high symmetry and therefore, the interpretation of the optical rotatory properties resides at present in rather empirical regularities, which correlated optical activity to molecular structural parameters (Crum-Brown, Walden, Van't Hoff and Ciugaeff [11–14]).

The Ciugaeff rule, experimentally proved, shows that in a homolog series the increase of the molecular rotation with the increase of the molecular weight is limited to a member of the series and then remains practically constant.

RESULTS AND DISCUSSION

In the aminoacids series, studied by us[1], corresponding to the general formula $C_1R_2R_3R_4$ with $R_1 = H$, $R_2 = -NH_2$, $R_3 = -COOH$ the increase of the molecular weight is determined only by increasing molecular weight of the radical R_4, named distinctive radical. Radical R_4, in all studied aminoacids, contains a CH_2 group, alone with a heteroatom implicated in σ bond in cysteine, an imidazolic ring in histidine and a benzenic ring in tyrosine. The studied series does not represent a homologous series in the primary sense of the word, but a series for which molecular weight and structural changes have been localised in the radical R_4 (Fig. 1).

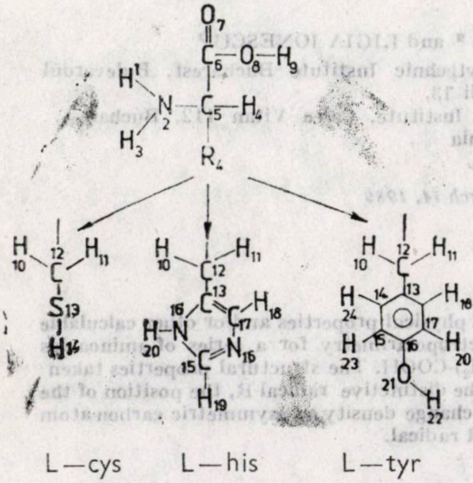

Fig. 1. — The numbering of the atomic centers in the series of aminoacids.

The differences in the structure of this radical would be reflected in molecular rotation, in the UV spectrum of the compound, in the charge density of the asymmetrical carbon atom and of different representative atoms of the distinctive radical. Therefore, it seems interesting to correlate the variation of rotatory specific power $/\alpha/_D^{20}$ and molecular rotation $/\Phi/_D^{20}$ in this series with the molecular weight of the distinctive radical, the position of the absorption bands in electronic spectrum, the density charge of the asymmetrical carbon atom (C_5) and on representative atoms (C_{12}, C_{13}) from the radical B_4.

Analysis of the experimental and calculated data, presented in Table 1 and Figure 2 outlines the following regularities :

The variation $/\Phi/_D^{20} = f(M_{R_4})$ or $/\alpha/_D^{20} = f(M_{R_4})$ (curve 1, Figure 2), which corresponds to the sense of Ciugaeff rule, reaches a maximum for L-histidine and then decreases for L-tyrosine (which by $\lambda = 589$ nm has the inversion temperature of optical rotatory power to 80°C[1]).

The magnitude of $/\alpha/_D^{20}$ or $/\Phi/_D^{20}$ as a function of λ increases steadly reflecting the increase of the number of the cromophpore-groups in the R_4 radical. The dependences $/\alpha/_D^{20} = f(q_{C_5})$ and $/\alpha/_D^{20} = f(q_{C_{12}})$ are presented in Fig. 2 (curves 2, respectively 3). They are quite similar, but positioned in dials II, III.

The plot of $/\alpha/_D^{20} = f(q_{C_{13}})$ (curve 4 Fig. 2) remembers the aspect of curve 1 and it is placed likewise in the dials I, IV. It seems that the atom centre C_{13} concentrated the structural differences of the R_4 radical in our series.

Table 1

The variation of the rotatory power with the different factors

The enantiomer	$[\alpha]_D^{20}$	$[\Phi]_D^{20}$	λ(nm)	$M_{R_4}^*$	q_{C_5}	$q_{C_{12}}$	$q_{C_{13}}$
L−cys	+6.3(8 %HCl 1N)	10.26	212	47(33)	−0.06122	−0.22758	$(\sigma) - 0.31744$
L−his	+9.3 (11 %HCl1N	13.32	215	81(67)	−0.01699	−0.28889	$(\sigma+\pi) + 0.80065$
L−tyr	−11.8(5 %HCl 1N)	−15.94	274	107(93)	−0.07113	−0.28843	$(\sigma+\pi) + 0.96150$

* The values of the R_4 molecular weight without — CH_2 group are given in brackets

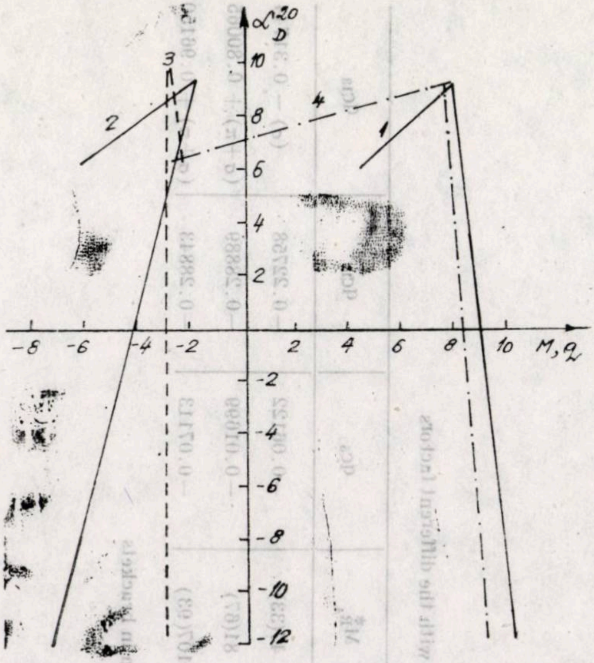

Fig. 2. — The variation of the optical strength with the weight of the R_4 radical and the charge densities

$1 - [\alpha]^{20}_{D} = f(M_{R_4})$; $2 - [\alpha]^{20}_{D} = f(q_{C_5})$:, $3 - [\alpha]^{20}_{D} = f(q_{C_{12}})$; $4 - [\alpha]^{20}_{D} = f(q_{C_{13}})$.

In conclusion, examination of the calculation and experimental data shows that in the investigated aminoacids the dependence of the optical specific rotation or molecular rotation on the charge density of the atom centre placed in a β-position versus the asymmetrical carbon atom is similar with the dependence of the same functions on the weight of the distinctive radical.

EXPERIMENTAL PART AND CALCULATIONS

The experimental technique was described elsewhere.[1]

The molecular rotation $/\Phi/^{20}_{D}$ was calculated using the relation :

$$/\Phi/^{20}_{D} = \frac{[\alpha]^{20}_{D} . M}{100}$$

where M is the molecular weight.

The parametrization for the calculation of σ- charge densities by Del Re method, as well as for the π HMO charge densities [15–16] were based on the analysis of the literature.

The computations were performed on the microcomputer TIM-S, using a program written in BASIC.

The numbering of the atoms used throughout the calculations is given in Fig. 1.

REFERENCES

[1] Part I, C. Mandravel and L. Anastasescu, *Rev. Roum. Chim.* **32,** 1045 (1987).

[2] S. V. Kyaghikh and T. V. Denidkina, *Mol. Biol.* **19,** 671 (1985).

[3] H. Yaeckele and L. Link, *J. Phys. Chem.* **88,** 1767 (1989).

[4] M. Juy, H. LanaThann and K. Lintner, *Int J. Dept. Prot. Res.* **22,** 437 (1983).

[5] W. J. Meiring, *Nature* **329,** 712 (1987).

[6] P. Drude, *Ann. Physik.* **48,** 536 (1893).

[7] W. Kuhn *Z. Phys, Chem.* **B4,** 14(1929).

[8] S. F. Boys, *Proc. Roa. Soc. A,* **144,** 655 (1934).

[9] R. Mallemann, *Trans. Farad. Soc.* **26,**281 (1931).

[10] Jig Nan Chiu, *J. Chim. Phys.* **52,** 3(1970).

[11] Crum– Brown, *Proc. Roy. Soc. Educ.* **17,** 181 (1891).

[12] P. Walden, *Z. Phys. Chem.* **17,** 245 (1895).

[13] L. A. Ciugaeff, *Ber* **31,** 360 (1898).

[14] I. G. Murgulescu and V. Em. Sahini, "Introducere în chimia fizică" vol. I,2, Ed. Academiei, 1978, p. 419.

[15] A. Stretwieser, "Molecular Orbital Theory for Organic Chemists" J. Wiley, New York, 1961, p. 103.

[16] V. E. Sahini and M. Hillebrand, "Chimie cuantică în exemple şi aplicaţii", Ed. Academiei, Bucharest 1985, p. 61, 200.

Revue Roumaine de Chimie, 35, *10–12*, 967–972 (1990)

DISPERSION OF A CATAPHORETIC RESIN IN VIEW OF ELECTRODEPOSITION*

MINODORA LECA [a], R. ŞERBAN [b] and ANTOANETA VELICU [b]
[a] Polytechnic Institute of Bucharest, Faculty of Chemical Technology, Department of Physical Chemistry, Blvd Republicii 13, Bucharest, Romania
[b] Research Center of Anticorrosive Protection Varnishes and Paints, Blvd Chimiştilor 309, Bucharest, Romania

Received November 6, 1989

The dispersion of an isopropanolic solution of a quaternary cationic copolymer in water as well as the manner some organic solvents, added in small amounts (2 to 3 per cent related to the whole volume of the system), influence the stability of the obtained dispersions were studied. The stability of the dispersions was correlated with film forming properties of the electrodeposited films.

Aqueous dispersions of polymers can be obtained by emulsion polymerization, dispersion of water insoluble polymer solutions in the presence of a suitable surfactant, dispersion of hydrophilic polymers in the absence of surfactants.

Now, the most employed method to obtain aqueous dispersions of film forming resins is the dispersion of concentrated resin solutions in the absence of surfactants, because they remain in the film and detract from water resistance.

A polymer is water dispersable when it contains hydrophilic groups, so that it is a polymeric surfactant which dissolves or disperses in water to provide micelle-like particles. The hydrophilic groups required for dispersion are very undesirable in a final film deposited from the dispersion, and must therefore be convertible during film formation or after deposition.

A cataphoretic resin can be dispersed into water only when the weight of the basic monomer is within 10 and 30 per cent. [1] A percentage under 10 does not ensure dispersion and a percentage above 40 makes the resin inadequate as a film-forming material.

The solvent is generally an alcohol or a glycol ether which has appreciable solubility in the resin and in water and serves several purposes : it reduces the viscosity of the polymer to facilitate dispersion, it influences the viscosity of the dispersion depending upon its distribution between the dispersed and continuous phases, it contributes to the stability of the dispersed polymer, serving as a weak volatile surfactant, it plasticizes the polymer to aid in film formation.

---

* Paper presented at the IIIrd Symposium on Colloid and Surface Chemistry, Timişoara, September 11–14, 1989, Romania

Thus, one of the most important problems, determining the stability of the systems as well as the qualities of the films, is the dispersion of the resin in water. The particle of the dispersed phase must have sizes and charges as uniform as possible to migrate with identical or very close velocities in electrical field and to build up a uniform film.

It was found[2] that other volatile organic solvents, also soluble in resin and in water, added in small quantities (2—3%), improve the solubility of the resin in water, facilitate the dispersion and increase the stability of dispersions, favouring in this way the film deposition control and its surface properties.

The paper continues the researches undertaken on a quaternary cataphoretic copolymer having tertiary amine groups partially neutralized as basic groups[3] and dwells on the influence of some organic solvents on the dispersion ability of concentrated isopropanolic resin solution, on the stability of the obtained dispersions and correlates the stability of dispersions with the properties of the electrodeposited films.

EXPERIMENTAL

The copolymer was obtained by solution method from the following comonomers: 2-hydroxyethyl methacrylate (30 per cent by weight), 2-dimethylaminoethyl methacrylate (20 %), butyl acrylate (25 %) and styren (25 %) in isopropanol as solvent and AIBN as initiator at a content of dry substance of 67 per cent.

The tertiary amine groups were neutralized, in proportion of 75 per cent, with 50 % acetic acid aqueous solution. The experiments were carried out on a pilot lot termed trak 125.

Some methods to disperse 67 % isopropanolic solution in water were used to obtain systems with 15 % resin required for electrodeposition but stability measurements were made only for the method applied industrially: the isopropanolic resin solution was poured under stirring to 1/3 of the required quantity of water, the stirring was maintained until the system looked homogenous, the rest of water was added and the stirring was maintained for another 5 minutes. Organic solvents as: dimethylformamide (DMF), diacetonealcohol (DAA), N-methylpirrolidone (NMP), n-nbutyl alcohol (n-BuOH), cyclohexanone (CH), methylethylketone (MEC), acetone (Ac) and some of thier binary mixtures were added in proportion of 2 per cent referred to the whole volume of the system.

The turbidities of the systems immediately after preparation and after 6, 10, 21 and 30 days were measured at $\lambda = 497$ nm using a spectrophotometer Specol with the following annexes: Ti standard — which measures the turbidity at a scattering angle of 0°, Ti for fluorescence — measuring the turbidity at 90° and TK which gives the turbidity at 45°. For annexes TK and Ti for fluorescence the turbidities were measured on the same amplification scale using the same cell.

The 15 % aqueous dispersions of trak 125, with 2 % organic solvents or binary mixtures of solvents, were electrodeposited on phosphatized steel sheets in industrial conditions: voltage — 100 V, deposition time — maximum 2'30" (until the current intensity became small enough and the electrodeposition ceased), temperature — 23...25°C, the cataphoretic bath had two anodes and one cathode and the distance anode-cathod was 8 cm. The films were cross-linked for 30' at 180°C. The electrodepositions were achieved after about 2 hours as well as after 11...14 days from preparation of the dispersions. Every time the plot current intensity in terms of time was recorded, from which the quantity of electricity at the maximum value of the intensity, Q_{Imax}, the total quantity of the electricity corresponding to the ultimate value of intensity, Q_{If} (to the minimum intensity) and current densities were calculated.

RESULTS AND DISCUSSION

In comparison to conventional film-forming resin organic solutions polymer aqueous dispersions, due to their colloidal nature, present the phenomena of sedimentation and viscosity changes. Sedimentation is related, as in any type of dispersion, to particle size : in general, if particles about 0.1 mμ or less in diameter are produced, the systems are stable.

Measurement of particle size of the dispersed polymers as well as the understanding of controlling factors are far to be understood.

Dispersion of hydropilic polymers in water results in potentially thermodynamically stable systems, approaching an equilibrium size which is stable, a slow process because of the high viscosity of the dispersed phase.

The methods used to determine the dimension of latex particles can be employed in essence to measure the dimension of the dispersed phase particles, but a problem arises in interpretation because the particle size is usually changed when the dispersion is modified for measurements. Optical particle size measurements are usually performed on samples which have been highly diluted with water, which alters both the solvent and neutralization balance, and therefore the extent of swelling. Samples examined by electron microscopy contain none of the volatile components, and are thus nonrepresentative of the particles present in the dispersion.

Despite these difficulties, comparisons can be made which provide a ranking of particle sizes which are valuable in quality control using, for example, the turbidimetric method which can be applied to concentrated systems.

The highest initial turbidities were registred for systems 5 and 8 and the lowest ones for systens 4, 3, 7 and 2 at all the measured scattering angles. Consequently n-BuOH and the mixture n-BuOH/DMF = 1/1 decrease the solubility of the resin in water, resulting in a greater number of dispersed phase particles and an increased turbidity. On the other hand NMP, DAA, the mixture CH/DAA = 1/1 and DMF increase slightly the solubility of the resin in water and the turbidities are smaller than for system 1, especially at a scattering angle of 0°.

It was also observed that the wavelengh at which the turbidity has maximum values is different for the above systems. Immediately after preparation the samples 1 and 7 have the maximum turbidity at a constant wavelength 493 and 518 nm, respectively, while all the other ones have the maximum between 495 and 535 nm. This demonstrates that the first two systems are practically monodisperse and the other one polydisperse and that the first system has the smallest particles.

As the systems become older the wavelengths of maximum turbidity increase, the ranges narrow tending to a point and the turbidities increase, which reflects the increasing and uniformization of particle dimensions After 30 days the turbidity has a maximum at the wavelengths 550, 556, 554 and 537 respectively for the systems 1, 2, 3 and 7.

The turbidity data were reevaluated calculating the Rayleigh scattering ratios and the dissymmetry factors, supposing a Rayleigh-type scattering.

The ratio between the intensity of the scattered light at an angle θ, I_θ, and the intensity of the incident light, I_0, is expressed by the Rayleigh scattering ratio, R_θ, given by the equation :[4]

$$R_\theta = r^2 I_\theta / I_0 \tag{1}$$

where r is the distance particle-observer. The turbidity τ is related to R_θ at the same angle by the relation :

$$\tau = 16 R_\theta / 3 \tag{2}$$

The dissymmetry of the light scattered by particles having diameters comparable with the wavelength of the incident light is estimated by the dissymmetry factor, z, which represents the ratio between the intensity of light scattered at two complementary angles, usually 45 and 135°, z_{45°, and is equal to the ratio of the two Rayleigh scattering ratios at the considered angles. The dissymmetry factor rises quickly when the dimension of the particles increases for spherical particles, more slowly for statistical coils and very slowly for cylindrical particles.

Being no possibility to determine the turbidities at a scattering angle of 135°, the dissymmetry factors for the complementary angles 0 and 90°, $z_0 0$, were calculated, as well as for the angles 45 and 90°, z_1. We consider z_1 values more accurate, both turbidities being measured at the same optical path and sensibility. These values are given in table 1.

Table 1

The dissymmetry factors z_1 for studied systems at 0, 6, 10, 21 and 30 days from the preparation

Sample	Additive	z_1				
		0	5	10	21	30
1	Reference	3.41	3.67	6.89	14.25	18.61
2	2% DMF	3.59	5.67	10.69	18.30	31.25
3	2% DAA	3.20	8.48	18.00	21.63	17.24
4	2% NMP	4.32	—	—	—	—
5	2% n-BuOH	83.57	—	—	—	—
6	2% CH	3.78	—	—	—	—
7	1% CH 1% DAA	4.13	11.33	19.72	16.24	11.09
8	1% n-BuOH 1% DMF	5.52				

The systems 4—6 and 8 are not stable in time. Sedimentation reducing uncontrollably the concentration of the dispersed phase, the measurements for these systems were not carried on, except the initial ones. They form adherent nonredispersable sediments.

Considering z_1 values it can be said that, immediately after preparation, the smallest particles are obtained with DAA as additive, followed by the reference system 1, DMF, CH and the mixture CH/DAA $= 1/1$ and the largest ones with n-BuOH. Consequently the first solvents increase the resin solubility, while the last one decrease it, giving larger particles.

When the stable systems maturate, dissymmetry factors rise showing that the particles grow big. The systems 1 and 2 are stable for 30 days; 3 is not stable over 21 days and 7 after 10 days. These make dissymmetry factors decrease because of the sedimentation. In contrast with instable systems their sediments are very easily redispersable.

It can be said that the most stable system is the refference one, but it gives nonsuitable films, followed by those containing DMF, DAA and CH/DAA = 1/1 mixture.

It is expected that the stable systems give the most uniform electrodeposited films, especially after maturation about 10 days.

The electrodeposition was achieved for the systems given in table 2 at about 2 hours from the preparation as well as after 11–14 days in conditions specified in the experimental part; it will be presented only in the measure in which it supports the stability data.

Systems containing 2% DMF or CH are the only ones which give acceptable films immediately after preparation. If the first system maintains its stability in time and its particles become more uniform, the second one sediments and the film is nonuniform.

Table 2

The additives used in proportion of 2%, Q_{Imax}, Q_{If} and film appearance

Sample	Additive	Time	Q_{Imax}, C	Q_{If}, C	Film appearance
1	—	A	5	15	Nonuniform
		B	5	21	Dissolves into water
2	i-PrOH	B	5	23	Nonuniform, pricks
		A	6	24	Nonuniform, shiny
3	n-BuOH	B	5	55	—,,— , coloured
		A	5	54	Almost uniform
4	CH	B	6	24	Orange peel effect
		A	5	51	Nonuniform, coloured
5	MEC	B	5	19	— ,, — , dissolves
6	Ac	A	5	16	— ,, —, drops
		B	5	17	— ,, — , dissolves
7	DAA	A	5	19	— ,, — , shiny
		B	3	17	Good
		A	5	17	Almost good
8	DMF	B	4	17	Good
		A	4	21	Nonuniform, coloured drops
9	NMP	B	4	17	— ,, — , pricks
	n-BuOH+	A	4	44	— ,, — , shiny
10	+ DAA	B	5	17	Almost uniform, coloured
		A	5	40	Nonuniform, shiny
11	CH + DAA	B	5	17	Good
	n-BuOH +	A	5	53	Nonuniform, shiny
12	+ Ac	B	5	17	— ,, — , coloured
		A	4	21	— ,, —
13	MEC + DAA	B	5	18	— ,, —
	n-BuOH+	A	4	50	— ,, —
14	+ DMF	B	5	13	Good
	n-BuOH +	A	4	50	Nonuniform
15	+ NMP	B	5	17	Good
	n-BuOH +	A	4	44	Nonuniform, shiny
16	+ CH	B	5	23	Orange peel effect
	DAA+	A	4	18	Nonuniform, shiny
17	+ DMF	B	5	15	Good

After 11—14 days of maturation the systems additivated with DAA, DMF and the mixtures CH/DAA, n-BuOH/DMF, n-BuOH/NMP, DAA/DMF give uniform films in accordance with stability data. On the other hand, n-BuOH, CH and their mixture gives orange peel effect. The other solvents and mixtures in table 2 practically do not alter the appearance of the films but change a little bit their thickness (Table 3).

Table 3

Mechanical properties of the electrodeposited films

Sample	System	Tihckesss, μ	Crosscut adhesion 1 mm	Persoz durity, s	Erichsen elasticity, mm	Conic mandrel flexibility
1	A	3	1	glides	3.2	—
2	B	2	1	290	3.5	—
4	A	1	1	300	3.2	—
6	B	1	1	312	3.0	—
	A	5	1	245	3.8	—
7	B	3	—	—		Good
8	A	4	1	250	3.5	—
	B	2	—	—	—	Good
9	A	5	1	300	2.8	—
	B	3	—	—	—	Good
10	B	9	1	glides	2.5	—
11	B	5	1	— ,, —	2.5	Good
12	B	5	1	297	1.5	—
14	B	2,5	1	310	2.8	—
15	B	7	1	302	1.5	—
	A	12	1	236	3.5	—
16	B	12	—	—	—	Good
	A	3	1	272	3.5	—
17	B	4	—	—	—	Good

The mechanical properties of the obtained films which correspond in respect to thickness and appearance are listed in table 3, preserving the numbering used in table 2. As can be seen from table 3, these systems have mechanical propertics as crosscut adhesion 1mm, Persoz durity, Erichsen elasticity and conic mandrel flexibility very good or good.

CONCLUSIONS

Some solvents or binary mixtures of solvents were find which increase the ability of the studied resin to disperse in water and which enhance the dispersion stability.

Maturation of these systems for about 10 days at room temperature results in uniform films with very good or good mechanical properties.

The thicknesses of the obtained films being too small, some other factors which can increase the film thickness must be studied.

REFERENCES

[1] N. Moga and M. Tudose, *Bul. tehnico-informativ CCPALV*, **10**, 77 (1985).

[2] A, L. Pallull, *Symposium on Electropainting for the Seventies*, London, Oct. 1969, paper 3.

[3] M. Leca, M. Olteanu, R. Şerban and N. Moga, *Materiale Plastice*, **24** (2), 91(1989).

[4] I. Măndru and M. Leca, "Chimia macromoleculelor şi coloizilor", Ed. Didactică şi Pedagogică, Bucharest 1977.

Revue Roumaine de Chimie, **35**, *10–12*, 973–983 (1990)

MORPHOLOGICAL CHARACTERIZATION OF COLLAGEN MEMBRANES FOR MEDICAL TEXTILE PROSTHESES*

VIORICA TRANDAFIR, MIOARA COSTEA and ELENA ROBU

Leather and Footwear Research Institute
Str. Bela Brainer 93, 74259 Bucharest, Romania

This paper presents ways of using fibrillar type I collagen from animal derma, as a material for impregnating the vascular prostheses ARTEX-POP D. POPA-DODU, manufactured by the Clinical Institute "Fundeni". The impregnating process means the layering of a film of fibrillar collagen on the outer part of the textile prosthese that will reduce the permeability and will increase the biocompatibility of the prosthese, since it enhances the process of building up the new tissue. The main characteristic that describes the morphological structure of the membranes resides in the pore distribution, as a function of pore dimensions, especially the pore radius or diameter. The samples of textile vascular prostheses and a textile net were compared to a natural membrane from cattle placenta. The tests made on dry membranes as well as on membranes swelled in distiled water at room temperature, for various periods of time (at 5 to 120 minutes) show that the membranes swelled for 30 and 60 minutes have much more small pores, a fact that provides the prosthese with minimal permeability to normal blood flow, reestablished intra- and post-operationally.

INTRODUCTION

Impregnation of the textile vascular prostheses ARTEX-POP D. POPA-DODU is meant to reduce the permeability of knitted textile prostheses eliminating blood leakage and preclotting of the textile prosthese intraoperationally, by means of accelerating the recovery of the new tissue.

The first attempts to use collagen in building up prostheses from Dracon are dated as back as 1960, when extruded collagen ducts were used. From then on, the research was continued and technologies to extract purer collagen were developed, attaining at present the level of marketing collagen impregnated vascular prostheses with zero permeability, absence of any infection an trombocitous aggregates at vascular wall/blood interface.[1–6] The specially prepared collage makes easy both the implant of the prosthese and its more rapid acceptance, in favour of the endothelization process.

The process of impregnation of textile prostheses may make use of biocompatible synthetic polymers such as : nonionic polymers (polyvinyl alcohol, polymethacrylic acid), or polymers with nitrogen (polyarylamide, polyvinylpirolidone).[7–10]

---

* Paper presented at the IIIrd Symposium on Colloid and Surface Chemistry, September 11–14, 1989, Timişoara, Romania

The main characteristic of the morphologic structure of the collagen membrane is the pore size distribution, namely the radius or the diameter of the pores. The zise, the shape and the distribution of pores can be experimentally determined by a set of methods such as the liquid permeation or gas absorption by means of absorption isomers, [11] optical microscopy,[12,13] the "bubble point" method, [14] filtration of colloids particles of known shape and size (proteines, latexes), [15] the measurement of constant air or water pressure flow, [16] the "Erbe" method of gas bubble, [17] porometric measurement with mercury. [18] This paper presents the results obtained using the latest method.

EXPERIMENTAL PROCEDURE

Porometric measurement with mercury is a destructive method to determine the size and distribution of pores using mercury penetration that works on the principle of liquids that do not wet the capillaries. It is well known the fact that having a wetting angle larger than 90° the liquid cannot spontaneously enter a capillary, a small pore respectively, due to the surface pressure , an opposition that can be broken by applying an outer pressure whose value is a function of pore size.

The relation between the pore size and the outer pressure is stated from the equilibrium condition, namely the equality between surface tension force of the liquid exerted on the contact surface area with a length equal to the circumference of the cylinder-like pore, and the force imposed by the outer pressure on the surface of the inner contacting circumference, as :

$$2\pi r \cos \emptyset = \pi r^2 p \qquad (1)$$

where : r represents the pore radius, p — the outer pressure and θ — the wetting angle of the liquid.

When mercury is used at a surface pressure of 480 dyn/cm and a wetting angle of 141.3°, supposing that all the pores are cylinder-like and opened, practically the following relation between the pore radius and the outer pressure may be used :

$$r = \frac{75.000}{p} \qquad (2)$$

where : $r =$ the pore radius (Å) and $p =$ the outer pressure (atm). Relation (2) is true only for pores with circular cross section. For pores with irregular shape this relation between their cross-section and their circumference is not proportional to the radius but, being a function of pore shape, it will result in lower values.

This method comprises other simplifying assumptions of the theory, namely : for the wetting angle that depends on the nature of the sample, a mean value is to be considered. For a diffraction with a radius X, wetting angle values of 135—142° for a large number of tests were obtained, 141.3° being the mean value considered. Also though the variation of surface pressure with temperature is not significant, that is (with mercury at 25°C) it has a value of 484.2 dyn/cm and with mercury at 50°C is of 472 dyn/cm, practically the mean value is considered to be of 480 dyn/cm.

The variable character of these values leads to errors and limits of the method that are to be found in each determination ; but since the nature of the material under consideration and the shape of the pores are constant for a given test, one can consider that the way of calculating the percentage distribution of the pore radii is relatively satisfactory. In other words accepting from the beginning the approximations, mercury based determination of pores is considered to be a method that permits gathering of data on open pore radius distribution within acceptable limits, thus conferring authority to this method.

Materials and methods. Two methods of depositing collagen gel were used to obtain a collagen membrane with low permeability on the surface of a textile prosthese : one layer only, thicker, free dried ; 5—6 thin consecutive layers, each free dried.

Denomination of tests. Natural membrane from placenta (type IV collagen) ; Pl — type I collagen based membrane of one layer only on net-like textile support (smooth surface, reinforced on the textile net); P2 — the same as P1, aldehyde cross-linked; P3 — type I collagen based membrane of one layer only on aldehyde cross-linked textile vascular prosthese (surface uniformly curving after the textile prosthese, with good adherence to the textile prosthese surface); P4 — type I collagen based membrane of 6 layers on the aldehyde cross-linked vascular prosthese (the surface the same as P3). To determine the size and distribution of pores a Carlo Erba porometer was used, to obtain values in the range 7.5—0.0037, at a pressure in the range 0—2000 atm.

The membranes were analysed when dry and after being swelled in distiled water for various periods of time: 5, 30, 50 and 120 minutes, at room temperature. The membrane P4 was tested to determine physico-mechanical properties: tear resistance, water absorption and permeability. Collagen impregnated textile vascular prostheses (the membrane on the outer surface of the prosthese) is used intraoperationally only after being previously swelled in physiological saline solution for 10—30 minute.

RESULTS AND CONCLUSIONS

The data in table 1 for the control membrane show a maximum percentage concentration of 80.9% for pores with radii between 1 and 0.007; the rest of ranges correspond to an initial pressure of 1 atm and of 4.7% pores with a radius of 7.5; the final pressure of 695 atm. corresponds to the same percent of pores with a radius of 0.01. A high value for the specific surface of pores of 19.72 m^2/g was obtained at high percentage concentration of pores.

For the same membrane the distribution of radii, the percentage concentration and the specific surface of pores is determined, after swelling in distiled water for various periods of time, as follows: after a 5-minute-swelling the highest percentage concentration of pores, 79%, is determined for a narrower range (0.008—0.007) as well as a threefold higher percentage of pores with big radii of 2.5 as compared to the dry control membrane and a specific surface of pores slightly diminished.

Increasing the swelling period of time, a significant decrease of pore concentration is registred in the range 1—0.008 (43 % after one hour swelling), while the concentration of big pores increases after a 2-hour-swelling, the morphology of the system coming to be completely changed.

An almost equal distribution of big pores with natural membrane from placenta is specific to the physiological function this membrane has: of mechanical protection and diffusional permeability where bounded and free water plays an important part.

As a biopolymer extracted in a nondenatured state the collagen under certain technologic conditions may form films with a structural morphology resembling that of the natural membranes. These membranes are used for dialysis and haemodialysis. Such a membrane is the P1, that resembles closely the natural membrane studied (Table 2). After one hour swelling the membrane Pl has the largest specific surface of pores (11.31 m^2/g) of all the membranes (Pl—P4), close to the value obtained for natural membranes (16.30 m^2/g). After a two-hour-swelling the percentage concentration of big pores (72%) is observed on a narrower range than in the case of the natural membrane.

Aldehyde crosslinking of collagen in membrane, P1, slightly modifies the distribution of pores. The membrane P2 showed high values of

Table 1

Mercury porometric measurement. Natural control membrane

State of the control membrane	Pore size distribution (μ)/ percentage concentration, %		Specific surface of pores m^2/g
Dried	7.5 μ 7.5 μ—1 μ 1—0.1 μ 1μ ———0.007μ 4.7% 9.5% 4.9% 80.9%	$\left.\begin{matrix} p_i = 1\text{atm} \\ n_i = 7.5\mu \end{matrix}\right\}$ 4.7% $\left.\begin{matrix} p_f = 659 \text{ atm} \\ n_f = 0.01\mu \end{matrix}\right\}$ 4.7%	19.72
Swelled for 5′	2.5μ 2.5μ ———————0.008μ 0.008μ — 1.3% 7.8% 79.2%	0.007μ $\left.\begin{matrix} p_i = 3\text{atm} \\ n_i = 2.5\mu \end{matrix}\right\}$ 13% $\left.\begin{matrix} p_f = 870 \text{ atm.} \\ n_f = 0.007\mu \end{matrix}\right\}$ 4.7%	17.07
Swelled for 30′	7.5μ ————— 1μ 1μ ———— 0.008μ 48.8% 51.2%	$\left.\begin{matrix} p_i = 1\text{atm} \\ r_i = 7.5\mu \end{matrix}\right\}$ 20% $\left.\begin{matrix} p_f = 906 \text{ atm} \\ r_f = 0.008\mu \end{matrix}\right\}$ 2.8%	13.863
Swelled for 1 h	3.7μ ———— 1μ 1μ —————— 0.008μ 56.9% 43.1%	$\left.\begin{matrix} p_i = 2\text{atm} \\ r_i = 3.7\mu \end{matrix}\right\}$ 2.9% $\left.\begin{matrix} p_f = 981 \text{ atm} \\ r_f = 0.008\mu \end{matrix}\right\}$ 5.8%	16.30
Swelled for 2 h	7.5μ 7.5μ — 2.5μ 2.5μ —————— 0.008μ 29.3% 15.9% 55.1%	$\left.\begin{matrix} p_i = 1\text{atm} \\ r_i = 7.5\mu \end{matrix}\right\}$ $\left.\begin{matrix} p_f = 896 \text{ atm} \\ r_f = 0.008\mu \end{matrix}\right\}$	9.129

Table 2

Mercury porometric measurement. Results. Collagen impregnated textile vascular prostheses. Symbol Pl

State of control membrane	Pore size distribution (μ)/percentage concentration %			Specific surface of pores m²/g
Dried	2.5μ 2.5 μ–0.1μ 0.1μ–0.01μ 0.01μ–0.006μ 4% 4% 56% 36%	$p_i = 3$atm $r_i = 2.5$ μ $p_f = 1302$ atm $r_f = 0.006$μ	4 % 4 %	8.07
Swelled for 5′	0.05 0.05–0.005μ 47% 53%	$p_i = 153$ atm $r_i = 0.05$μ $p_f = 1468$ atm $r_f = 0.005$β	47 % 1.5 %	4.72
Swelled for 30′	5μ 5–0.1μ 0.1–0.06 μ 2.8% 50.4% 46.8%	$p_i = 15$ atm $r_i = 5$μ $p_f = 125$ atm $r_f = 0.06$μ	2.8 % 2.8 %	3.921
Swelled for 1 h	0.03μ 0.03μ–0.009μ 5% 95%	$p_i = 247$ atm $r_i = 0.03$ μ $p_f = 844$ atm $r_f = 0.009$ μ	5 % 5 %	11.31
Swelled for 2 h	7.5μ 7.5μ–0.7μ 0.7μ–0.03μ 27.1% 0,6% 72.3%	$p_i = 1$ atm $r_i = 7.5$μ $p_f = 252$ atm $r_f = 0.03$μ	27.1 % 2.8 %	2.918

percentage concentration of 0.002—0.009 μ pores in about 60% dry state, a higher value, 88%, in the range 0.008—0.009μ after a 30-minute-swelling, corresponding to the specific surface of pores (Table 3).

Changing the textile support — the textile vascular prosthese in the case of membrane P3 — as well as strenghtening the cross linking with the aldehyde modify the morphological structure of this membrane of one layer. In all phases of swelling a decrease of percentage concentration of big pores is observed. A maximum concentration of about 91% for pores in the range 0.03—0.01 μ is observed after an hour swelling (Table 4).

The process of forming a multilayered collagen membrane (5—6 layers) as is the case of P4 membrane of the annular cylindric outer surface of the textile vascular prosthese ARTEX POP D. POPA-DODU modifies the morphological structure, namely simplifies it. Small radius pores prevail, having a narrow range of radius distribution, especially after swelling in distiled water for 30, 60 and 120 minutes, as follows (Table 5); 91% 0.01 μ radius pores (after a 30—minute-swelling); 96% 0.06—0.009μ radius pores after a 60-minute-swelling : 23% 0.02 μ radius pores and 77% 0.01—0.008 μ radius pores.

No big pores are present in the membranes P3 and P4 after a two-hour-swelling. The physico-mechanical properties of membrane P4 are shown in table 6. Although membrane P4 presents water absorption at a satisfactory level, after a 30-minute-swelling, its permeability to water under dynamic conditions is reduced : 3—4 g/h water permeating the prosthese.

The prosthese with a membrane P4 when tested on a blood pump presents a closeness to the permeability of blood. The collagen membrane formed on the outer side of the prosthese should be resistant to dissolution under "in vivo" conditions after implantation of the vascular prosthese. Therefore, a gradual yielding of the antibiotic drug already incorporated into the membrane, the risk of infection is eliminated.

The "in vivo" resistance of the collagenous membranes is tested "in vitro" in order to determine the time necessary for maceration in a 1% pepsin solution.

Aldehyde cross linking and multilayered membrane (P4) formation by succesive layering of collagen gel and free drying of each layer, prolongs the resorption time as follows : 12 h for P1, 22 h for P2 and P3, 58 h for P4.

We may *conclude* that the morphological characteristics of collagenous membranes (P4) formed the outer surface of the textile vascular prosthese ARTEX POP. D. POPA-DORU, imparts an almost zero permeability to blood and a good biocompatibility to these membranes favouring a rapid recovering of the newly formed tissue.

Table 3

Mercury porometric measurement. Results. Collagen impregnated textile vascular *p* prostheses. Symbol P2

State of control membrane	Pore size distribution (µ)/percentage concentration, %					Specific surface of pores m²/g
Dried			0.02µ	0.02 µ–0.009 µ	p_i = 412atm, r_i = 0.02µ } 38.8 %	18.48
			38 %	61.2 %	p_f = 819atm, r_f = 0.009µ } 5.5 %	
Swelled for 5′		0.1µ	0.1µ–0.01µ	0.01µ–0.008 µ	p_i = 53atm, r_i = 0.1µ } 3.8 %	5.32
		3.8 %	70 %	26.2 %	p_f = 964atm, r_f = 0.008µ } 3.8 %	
Swelled for 30′	2.5µ	2.5–1.6µ_____	0.008µ	0.008µ–0.009µ	p_i = 3atm, r_i = 2.5µ } 4.1 %	7.07
	4.1 %	4.1 %		91.8%	p_f = 808atm, r_f = 0.009µ } 4.1 %	
Swelled for 1 h			0.025µ	0.021–0.02µ	p_i =310 atm, r_i =0.025µ } 3 %	3.50
			3 %	97 %	p_f =345 atm, r_f =0.021µ } 12 %	
Swelled for 2 h	2.5µ	2.5µ____________0.01µ			p_i =3 atm, r_i =2.5µ } 5 %	9.36
	5 %	95 %			p_f =716 atm, r_f =0.01µ } 10 %	

Table 4

Mercury poreometric measurement. Results. Collagen impregnated textile vasular prostheses. Symbol P3

State of control membrane	Pore size distribution (µ)/percentage concentration, %					Specific surface of pores m²/g
Dryed	2.5µ	2.5µ−0.2µ	0.2µ−0.01µ	$p_i = 3$ atm $n_i = 2.5\mu$	4.1 %	8.36
	4.1 %	16.4 %	79.5 %	$p_f = 51$ atm $r_f = 0.01\mu$	4.1 %	
Swelled 5′	0.1µ	0.1µ−0.01µ	0.01µ−0.009µ	$p_i = 51$ atm $r_i = 0.1\mu$	3.9 %	8.84
	3.9 %	72 %	24.1 %	$p_f = 773$ atm $r_f = 0.009\mu$		
Swelled 30′	0.1µ	0.1µ−0.02µ	0.02−0.01µ	$p_i = 62$ atm $r_i = 0.1\lambda$	4.1 %	1.422
	4.1 %	41.7 %	54.2 %	$p_f = 758$ atm $r_f = 0.01\mu$	4.1 %	
Swelled 1h	0.1µ	0.1µ−0.01µ	0.01−µ−0.007µ	$p_i = 50$ atm $r_i = 0.1\mu$	3 %	10.29
	3 %	63.6 %	33.4 %	$p_f = 1022$ atm $r_f = 0.007\mu$	3 %	
Swelled 2h	0.1µ	0.1µ−0.01µ	0.01µ−0.007µ	$p_i = 50$ atm $r_i = 0.1\mu$	3 %	10.29
	3 %	63.6 %	33.4 %	$p_f = 1022$ atm $r_f = 0.007\mu$	3 %	

Table 5

Mercury poreometric measurement. Results. Collagen impregnated textile vascular prostheses. Symbol P4

State of control membrane	Pore size distribution (μ)/percentage concentration, %						Specific surface of pores m²/g
Dried	7.5μ	7.5μ–0.2μ	0.2μ–0.01μ		p_i =1 atm r_i =7.5 μ	41.1 %	9.88
	41.1 %	1.9 %	57 %		p_f =708 atm r_f =0.01μ	5.8 %	
Swelled for 5′	7.5μ	7.5μ–0.07μ	0.07μ–0.02μ		p_i =1 atm r_i =7.5μ	26.4 %	5.32
	26.4 %	3 %	70.6 %		p_f =408 atm r_f =0.02μ	6 %	
Swelled for 30′			0.01μ	0.01μ–0.009μ	p_i =745 atm r_i =0.01μ	91.4 %	1.35
			91.4 %	8.6 %	p_f =818 atm r_f =0.009μ	1.4 %	
Swelled for 1h			0.06μ	0.06μ–0.009μ	p_i =126 atm r_i =0.06μ	3.8 %	4.08
			3.8 %	96.2 %	p_f =869 atm r_f =0.009μ	3.8 %	
Swelled for 2h			0.02μ	0.01μ–0.008μ	p_i =410 atm r_i =0.02μ	22.7 %	4.54
			22.7 %	77.3 %	p_f =938 atm r_f =0.008μ	9 %	

Table 6

Physico-chemical properties of membrane P4

No.	Characteristics. The product analysed	Thickness	*Elongation* %	Tearing load 0.5 daN/mm²	Tensile *strength* daN/2cm	*Absorbtion* %				Permeability to water under dynamic conditions				
										Absorption			Quantity of permeated water g/h	
						1h	2h	4h	24h	1h	2h	3h	Isth	IIndh
Textile vascular prosthese (when dry) P4	a	1.16	—	10	8.0*	81.0	102.7	85.1	78.6					
	b	1.12	—	10	6.4*	94.2	113.9	98.4	92.2					
	average		—	10	7.2	87.6	108.3	91.7	85.4					
Prosthese swelled for 30′ in distiled water	a	1.42	—	10	6.0*					13.4	14.5	13.1	3.13	3.7
	b	1.46	—	10	5.0*					24.5	24.3	21.2	3.36	5.4
	average		—	10	5.5					18.9	19·4	17.1	3·24	4.5

* Note. The tensile strength value means the breaking of the collagen film.

REFERENCES

M. Chapil and M. Kraisicek, in "Modern Trends in Vascular Surgery", J. A. Gillispie (ed.), Butterwarths (1970).

[2] P. Menasche, P. Flaud, A. Huc and A. Piwnica, "Collagen Vascular Grafts", preliminary report life support, in *Systems*, **2**, 233 (1984).

[3] M. Chapil, R. L. Kronenthal and W. van Winkle jr., in "International Review of Connective Tissue Research", D.A. Hall and D. S. Jackson eds., Academic Press, New York, vol. 6, 1973.

[4] F. A. Kincl, L. A. Ciaccio and E. B. Henderson, *Archiv der Pharmazie*, **317**, 657 (1984).

[5] M. D. Smirnov, G. P. Samokhin, V. R. Muzykantov, G. L. Idelson, S. P. Domogatski and V. N. Smirnov, *Biochem. and Biophysical, Research Communications* **116**, 99 (1983).

[6] E. Bell, B. Ivarsson and C. Merril, *Proc. Natl. Acad. Sci. USA*, **76**, 1274 (1979).

[7] S. T. Li and E. P. Katz, *Biopolymers*, **15**, 1439 (1976).

[8] S. T. Li, E. Golub and E. P. Katz, *J. Mol. Biol.*, **98**, 853 (1975).

[9] * * * Patent France, 2558719, 1985.

[10] * * * Patent USA, 3512183, 1970.

[11] I. Cabasso, "Polymer Alloys", Plenum Press, New York, 1977.

[12] H. I. Preusse, *Kolloid Z. Z. Polymere*, **218**, 129 (1967).

[13] H. I. Preusse, *Kolloid Z. Z. Polymere*, **250**, 579 (1972).

[14] * * * ANSI/ASTM E 128– 61, F 316– 70.

[15] I. Mîndru and D. M. Cecăreanu, "Chimia coloizilor și suprafețelor", Ed. Tehnică Bucureşti, 1975.

[16] A. Kuhn, "Kolloid Chemisches Taschenbuch", Akad. Verlasges, 5th ed., Leipzig, 1960.

[17] M. M. Agrest, J. *Fizicescoi Himii*, **50**, 2425 (1976).

[18] E. Hanold and E. Skan, *Science*, **120**, 805 (1954).

Revue Roumaine de Chimie, 35, 10–12, 985–996 (1990)

ANNULENES AND PRIMITIVE CORONOIDS: SOME TOPOLOGICAL PROPERTIES AND ENUMERATIONS*

S. J. CYVIN, J. BRUNVOLL and I. GUTMAN[a]

Division of Physical Chemistry, The University of Trondheim,
N–7034 Trondheim–NTH, Norway

Received September 12, 1988

The previous topological studies of single-edge [$2p$]annulenes are viewed in a broader context by means of the association of these systems with benzenoids and primitive coronoids. The existing enumeration data of the considered [$2p$]annulenes are extended through $2p = 46$ by means of literature data, which were presented as pertaining to benzenoids. Extremal systems of the [$2p$]annulenes are discussed in details. They are defined by $h = h_{\min}(p)$ and $h = h_{\max}(p)$, where h is the number of hexagons of the hexagonal lattice in the interior of the annulene. Finally some recent analytical expressions for the numbers of hollow hexagons, a subclass of primitive coronoids, are adapted to an enumeration problem of [$2p$]annulenes.

INTRODUCTION AND DEFINITIONS

The present paper deals with annulene and coronoid systems as geometrical objects.[1-3] The systems have obvious chemical counterparts in hydrocarbon molecules. One therefore speaks about chemical graphs.

Among the [n]annulene systems (or shortly [n] annulenes) we shall only consider those which are cycles on a hexagonal lattice. In consequence, n should be restricted to the even numbers, say $2p$; more precisely: $n = 6, 10, 12, 14, 16, \ldots$ ($p = 3, 5, 6, 7, 8, \ldots$). Balaban[4-6] has given significant contributions to the topological properties of annulenes. In the most recent one[6] of the cited papers, in fact being one of the main references of the present work, he too considered [$2p$] annulenes which can be superimposed on the hexagonal lattice, but also allowed for overlapping edges. The systems of the last category are outside the scope of the present work. In the terminology of Balaban,[6] we only consider single-edge annulenes, but not the multiple-edge annulenes. In the following it is tacitly assumed throughout that the term "annulene" refers to an annulene in the restricted sense as defined above.

The chemistry of annulenes is a well-established and florishing branch within organic chemistry.[7-11]

---

* Part IV of the series "Enumeration and Classification of Coronoid Hydrocarbons". For Parts I–III, See Refs.[1-3]

[a] On leave from: Faculty of Science, University of Kragujevac, YU–34000, Kragujevac, Yugoslavia.

Coronoid[1] systems (or coronoids, also called coronaphenes[11]) are, loosely speaking, benzenoids[11] with a hole. More strictly, a coronoid is defined by two cycles on a hexagonal lattice, one inner perimeter completely embraced by an outer perimeter. The system should be planar and consists (like a benzenoid) of congruent regular hexagons. The benzenoid defined by the inner perimeter is referred to as the corona hole. It should consist of at least two hexagons. In the present work we shall only consider the class of primitive coronoids.[1] A primitive coronoid consists of a single chain of hexagons in a macrocyclic arrangement. In terms of the dualist graph[11] a primitive coronoid is a single cycle, which is not a triangle and not a hexagon.

Primitive coronoids have chemical counterparts among cycloarenes,[12-14] a new class of polycyclic aromatic hydrocarbons.

The present work started with a revisiting of the enumeration of annulenes. It was found that the numerical data of the pioneering work of Balaban[6] may be supplemented to a large extent. The supplements are in fact hidden in some material which has been published after the appearance of the Balaban paper. Some analytical descriptions of $[2p]$annulenes[6] are also commented and put into a larger context in relation to works published later.

The problem of enumeration and some topological properties of primitive coronoids are strongly related to the same problems for annulenes. In the present work we also try to build a link between these two areas.

In the attempts to combine the different areas as mentioned above we have made use of the following facts. Firstly, there is a one-to-one correspondence between an annulene and a benzenoid. Every annulene may serve as the perimeter for a benzenoid. This correspondence is obvious since both a benzenoid and an annulene are completely defined by a cycle on a hexagonal lattice. Secondly, a primitive coronoid may be associated with a $[2p]$annulene on identifying the latter with its inner perimeter. Kekulene,[12] for instance, is associated with [18]annulene. However, the converse is not true; a $[2p]$annulene cannot always serve as an inner perimeter of a primitive coronoid. This is not possible when the benzenoid associated with the annulene has a cove or fjord;[15] see also the next section. The corona holes of primitive coronoids are namely the benzenoids with at least two hexagons and without coves and fjords. This statement also brings up the last exception: benzene is recognized as an annulene and may as such be termed [6]annulene. However, benzene (one hexagon) cannot be a corona hole according to the strict definition of coronoids (see above). Nevertheless is it often expedient to consider coronene together with the real primitive coronoids. Then it is interpreted as a macrocycle of six hexagons around a hole of one hexagon. It is reasonable to call this system a quasi-coronoid. Then, in conclusion, we may associate benzene *alias* [6]annulene with the quasi-coronoid coronene.

ENUMERATION OF $[2p]$ANNULENES

When we speak about the enumeration of annulenes we refer to the numbers of the possible configurations of the annulenes.[6]

The annulene systems may be generated successively by increasing the size of the cycle in the way as described by Balaban,[6] who referred to the process as homologation. Here we shall formulate the generation of the annulenes in terms of the hexagons of the benzenoid associated with the annulenes. We are referring to the one-to-one correspondence mentioned above, where an annulene serves as the perimeter of the benzenoid associated with it. This approach will naturally lead us to the study of the particular $[2p]$annulenes, which Balaban[6] characterized as the least over-crowded single-edge configurations.

All (nonisomorphic) benzenoids with $h+1$ hexagons may be generated by adding one hexagon each time to all the benzenoids with h hexagons. Thus all benzenoids are built up successively from benzene. There are five types of the addition of one hexagon, depending on how many edges of the new hexagon coincide with the perimeter of the old benzenoid;

(i) one-contact addition; annelation to a free edge,
(ii) two-contact addition; fitting into a fissure;
(iii) three-contact addition; imbedding into a bay,
(iv) four-contact addition; filling a cove,
(v) five-contact addition; immersing into a fjord.

A free edge is an edge between two vertices of degree 2. Illustrations of the other features of the perimeter, viz. fissure, bay, cove and fjord, are given elsewhere.[15]

All the additions (i)—(v) are characterized by $h \to h+1$. The symbol h denotes as usual the number of hexagons of a benzenoid. The length of the perimeter, however, does not increase in the same pace. It will even decrease in two of the instances, viz. filling a cove and immersing into a fjord. The length of the perimeter, which is associated with a $[2p]$-annulene, is $2p$. Then we have specifically for the five types of addition:

(i) $p \to p+2$,
(ii) $p \to p+1$,
(iii) $p \to p$,
(iv) $p \to p-1$,
(v) $p \to p-2$.

These relations may be compressed into

$$p \to p - \varepsilon + 3$$

for the ε-contact addition.

Figure 1 shows all the ways in which the $[2p]$annulenes up to $p = 9$ can be generated from additions to the associated benzenoid. As expected this generation reproduces the forms depicted by Balaban.[6] In this paper also the 14 forms of [20]annulenes are displayed.

Since the paper of Balaban[6] was published several reports on computer-aided enumerations of benzenoids have appeared. The pioneering work by Balasubramanian et al.[16] was followed by a paper from the Düsseldorf -Zagreb group.[17] The latter work is of special interest in the present context because the enumerated benzenoids therein, actually up to $h = 10$, were classified according to the numbers of their internal vertices, say n_i. The number of external vertices (i. e. on the perimeter) is known to be (see, e.g. Cyvin and Gutman[15])

$$n_e = 4h - 2n_i + 2 \tag{1}$$

Now we identify the perimeter with a [$2p$]annulene, and hence $n_e = 2p$. The enumeration of [$2p$]annulenes is therefore equivalent to the enumeration of benzenoids with a given length of the perimeter. These benzenoids are of course distributed over a range of h values. It is therefore a problem to find out how far the Dűsseldorf-Zagreb numbers[17] give information about the numbers of [$2p$]annulenes. We need to know $h_{\max}$ for a given p. This problem was actually solved by Balaban[6] (see the next section). It is relevant to the Dűsseldorf-Zagreb numbers for $h < 10$ that $p = 11$ gives $h_{\max} = 10$ (but $p = 12$, $h_{\max} = 12$). Hence the formidable material of enumerated benzenoids[17] (38472 systems) gives information only about the numbers of [2p]annulenes up to the [22]annulene systems, one unit in p beyond the Balaban[6] enumeration.

In another enumeration of benzenoids Stojmenović et al.[18] oriented the procedure more specifically towards the length of the perimeter. From their material we are able to extract the numbers of [2p]annulenes up to the [46]annulene systems. These numbers are given in table 1.

Table 1

Numbers of [$2p$]annulenes, N

p	$n = 2p$	N	p	$n = 2p$	N
3	6	1	14	28	744
4	8	0	15	30	2291
5	10	1	16	32	6186
6	12	1	17	34	18714
7	14	3	18	36	53793
8	16	2	19	38	162565
9	18	12	20	40	482416
10	20	14	21	42	1467094
11	22	50	22	44	4436536
12	24	97	23	46	13594266
13	26	312			

EXTREMAL [$2p$] ANNULENES

It is of interest to investigate the lower and upper limits of h for [$2p$] annulenes where p has a given value. Here h is the number of hexagons of the interior of the annulene, i.e. of the benzenoid associated with it. In other words, $2p$ is the length of the perimeter of the benzenoid.

Harary and Harborth[19] studied the extremal properties of benzenoid and arrived at the formulas

$$2h + 1 + \left\{ \sqrt{12\,h - 3} \right\} \leqslant n \leqslant 4h + 2 \tag{2}$$

$$3h + \left\{\sqrt{12h - 3}\right\} \leqslant m \leqslant 5h + 1 \tag{3}$$

where $\{x\}$ denotes the smallest integer larger than or equal to x. The symbols n and m are used to identify the number of vertices and edges, respectively. The upper and lower bounds are the best possible, i.e. there exist extremal benzenoids where the signs of equality are realized. A simple deduction from the Harary and Harborth results for the number of internal vertices (n_i) reads

$$0 \leqslant n_i \leqslant 2h + 1 - \left\{\sqrt{12h-3}\right\} \tag{9}$$

Finally we have a similar relation for the number of external vertices (n_e), viz. [21]

$$2\left\{\sqrt{12h - 3}\right\} \leqslant n_e \leqslant 4h + 2 \tag{10}$$

This last equation is the one of special interest in the present context.

Since n_e pertains to the vertices on the perimeter, one has $n_e = 2p$, and consequently

$$\left\{\sqrt{12h - 2}\right\} \leqslant p \leqslant 2h + 1 \tag{11}$$

The extremal benzenoids with

$$p_{\max} = 2h + 1 \tag{12}$$

are easily accounted for. They are realized exactly by all catafusenes and compatible with

$$h_{\min} = \frac{1}{2}(p - 1); \quad p = 3, 5, 7, \ldots \tag{13 a}$$

For even p values one finds the formula

$$h_{\min} = \frac{1}{2}p; \quad p = 6, 8, 10, \ldots \tag{13 b}$$

The corresponding benzenoid systems are exactly those with one internal vertex each.

Having in mind the one-to-one correspondence between benzenoids and [$2p$]annulenes we realize that (12) and (13) also apply to the extremal annulenes with $h = h_{\min}$, where h is the number of hexagons of the hexagonal lattice in the interior of the annulene.

The maxima of h for a given p, on the other hand, are not so regular. First we have, of course,

$$p_{\min} = \left\{\sqrt{12\,h - 3}\right\} \tag{14}$$

Consequently the extremal benzenoids with $h = h_{\max}$ satisfy

$$p = \left\{\sqrt{12\,h_{\max} - 3}\right\} \tag{15}$$

In order to express $h_{\max}$ from the relation (15) note first that, bearing in mind the meaning of the symbol $\{x\}$,

$$p \geqslant \sqrt{12\, h_{\max} - 3} \tag{16}$$

On the other hand, since $h_{\max}$ is the greatest possible value of h,

$$p < \sqrt{12\,(h_{\max} + 1) - 3} \tag{17}$$

this implies

$$p^2 > 12h_{\max} - 3, \quad p^2 < 12h_{\max} + 9 \tag{18}$$

i.e.

$$\frac{p^2 - 9}{12} < h_{\max} \leqslant \frac{p^2 + 3}{12} \tag{19}$$

i.e.

$$\frac{p^2}{12} + \frac{1}{4} - 1 < h_{\max} \leqslant \frac{p^2}{12} + \frac{1}{4} \tag{20}$$

from which it is evident that

$$h_{\max} = \left[\frac{p^2}{12} + \frac{1}{4}\right] \tag{21}$$

where $[x]$ denotes the largest integer smaller than or equal to x.

It is noteworthy that already Balaban[6] gave the exact formulas for $h_{\max}$ as a function of p, referring to $[2p]$annulenes. He seems to be the first who studied the problem equivalent to the extremal benzenoids. His formulas for $h_{\max}(p)$ were published five years before the appearance of the frequently cited paper of Harary and Harborth.[19] We find it timely that the Balaban formulas are brought out of oblivion; they are given below in a slightly simplified form.

$$h_{\max}(6j - 3) = \frac{1}{12}(p^2 + 3) = 3j^2 - 3j + 1 \tag{22a}$$

$$h_{\max}(6 + \delta) = \frac{1}{12}(p^2 - \delta^2) = 3^2 + \delta; \quad \delta = -2, -1, 0, 1, 2 \tag{22b}$$

Here $j = 1, 2, 3, \ldots$, but $j > 1$ for $\delta = -2$. These equations are equivalent with (16), but they give the exact integer solutions without invoking the bracket symbol. The original Balaban formulas[6] emerge, apart from changes in the symbolism, by replacing j in (22) by $j + 1$.

Balaban[6] has also specified the six typical forms of extremal $[2p]$-annulenes with $h = h_{\max}$, which of course also account for the corresponding extremal benzenoids. There is exactly one system with $h = h_{\max}$ for a given p, and therefore also exactly one system with $p = p_{\max}$ for a given h. The representatives with $p = 3, 5, 6, 7, 8$ and 9 are found in Fig. 1. Balaban[6]

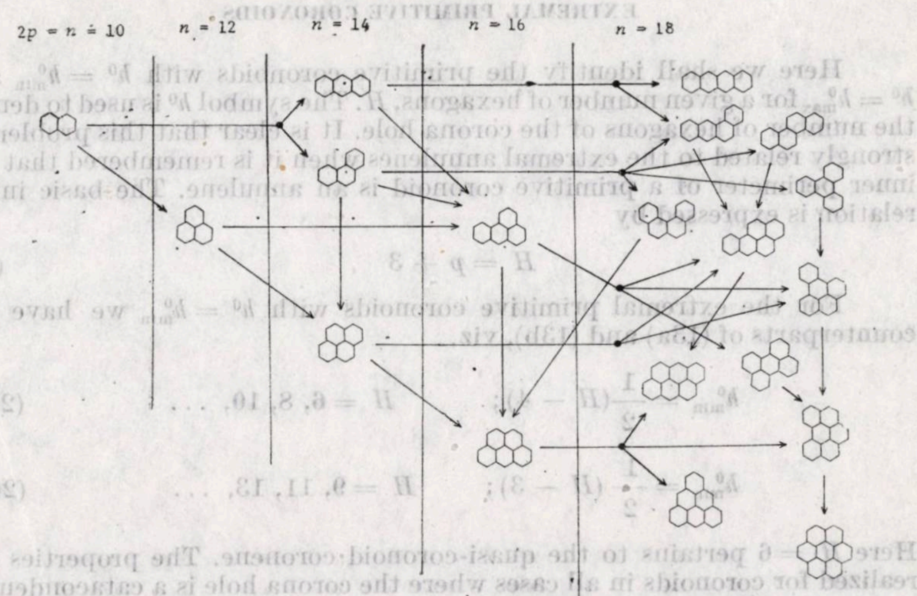

Fig. 1. — Generation of the $[2p]$ annulenes on the basis of their associated benzenoids.

has also depicted the systems for $p = 10, 11, 12, 13, 14$ and 15 ; therefore they need not be reproduced here. This author[6] referred to the extremal $[2p]$annulenes with $h = h_{\max}$ as the least overcrowded single-edge configurations.

It seems warranted to give some more details with regard to the relevance of the Balaban formulas (22) to the extremal benzenoids with $p = p_{\min}$, where $2p = n_e$. An elementary modification of (22a) reads

$$p = \sqrt{12h_{\max} - 3}\ ; \qquad p = 6j - 3 \tag{23a}$$

Consequently

$$p_{\min} = \sqrt{12\,h - 3}\ ; \quad h = 3j^2 - 3j + 1 \tag{24a}$$

This relation is compatible with (14), which was a consequence of the Harary-Harborth [19] relations. It is a special case where the square root attains integral values. All other cases are governed by eqn. (22b), from which one obtains

$$p = \sqrt{12\,h_{\max} + \delta^2}\ ; \qquad p = 6j + \delta \tag{23b}$$

and consequently

$$p_{\min} = \sqrt{12\,h + \delta^2}\ ; \quad h = 3j^2 + \delta j \tag{24b}$$

EXTREMAL PRIMITIVE CORONOIDS

Here we shall identify the primitive coronoids with $h^0 = h^0_{\min}$ and $h^0 = h^0_{\max}$ for a given number of hexagons, H. The symbol h^0 is used to denote the number of hexagons of the corona hole. It is clear that this problem is strongly related to the extremal annulenes when it is remembered that the inner perimeter of a primitive coronoid is an annulene. The basic interrelation is expressed by

$$H = p + 3 \tag{25}$$

For the extremal primitive coronoids with $h^0 = h^0_{\min}$ we have the counterparts of (13a) and (13b), viz.

$$h^0_{\min} = \frac{1}{2}(H - 4); \qquad H = 6, 8, 10, \ldots \tag{26 a}$$

$$h^0_{\min} = \frac{1}{2}(H - 3); \qquad H = 9, 11, 13, \ldots \tag{26 b}$$

Here $H = 6$ pertains to the quasi-coronoid coronene. The properties are realized for coronoids in all cases where the corona hole is a catacondensed benzenoid without coves or fjords.

For the extremal primitive coronoids with $h^2 = h^0_{\max}$ we have [22] in analogy with (21):

$$h^0_{\max} = \left[\frac{H^2}{12} - \frac{H}{2} + 1\right], \tag{27}$$

Also the Balaban formulas (22) may easily be adapted to the class of primitive coronoids.

The primitive coronoids with $h^0 = h^0_{\max}$ are associated with the appropriate annulenes in a one-to-one manner. The illustrations of Balaban[6] may therefore be transferred immediately to the coronoids. There is exactly one primitive coronoid with $h^0 = h^0_{\max}$ for each H. In Fig. 2 we have depicted the systems with $H = 12, 13, 14, 15, 16$ and 17.

ENUMERATION OF A SPECIAL CLASS OF [2p] ANNULENES

Balaban[6] pointed out that the enumeration problem of [2p]annulenes has not yet been solved analytically. This statement is still true today. However, an analytical solution has recently been found [23] for the number of hollow hexagons, [1] which is a subclass of the primitive coronoids. By virtue of the correlation between primitive coronoids and annulenes explained above this result is easily transferred to a special class of annulenes. One only has to make use of relation (26). In the following we report the new result for annulenes, which was deduced in the indicated way.

Consider the class of [2p]annulenes for which the associated benzenoid has exactly 6 free edges. A free edge is an edge between two vertices

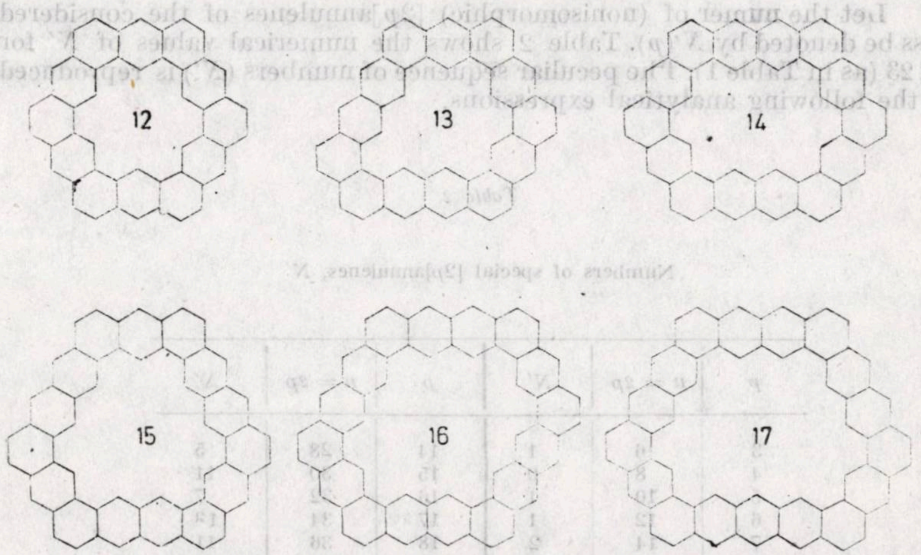

Fig. 2. — The primitive coronoids with $h^0 = \overset{0}{h}_{\max}$ for the inscribed H values.

of degree 2. All the extremal $[2p]$annulenes with $h = h_{\max}$ belong to this class. Actually all representatives for $p = 3$, 5, 6 and 8 ($h = 6$, 10, 12 and 16) of the considered class are the systems with $h = h_{\max}$. Figure 3 displays the members for $p = 7$, 9, 10, 11 and 12.

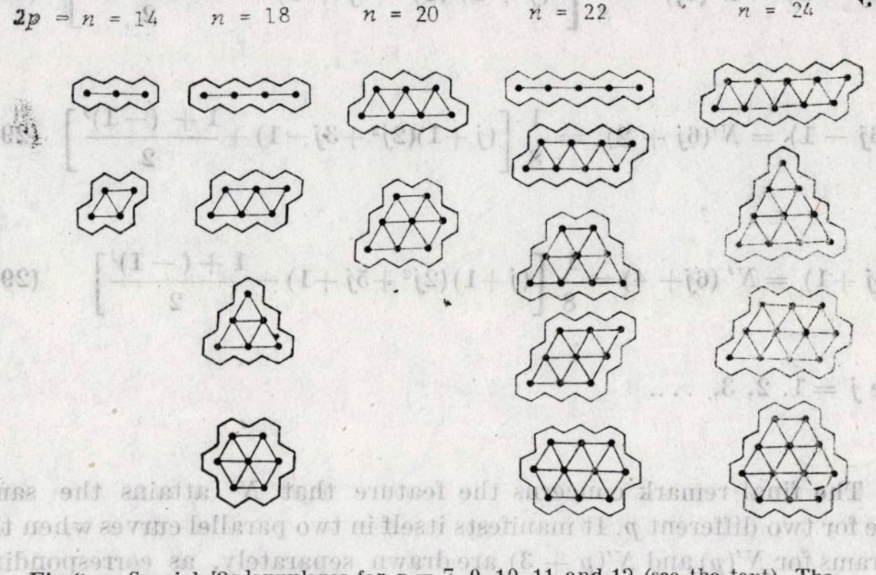

Fig. 3. — Special $[2p]$annulenes for $p = 7$, 9, 10, 11 and 12 (see the text). The systems at the bottom of each column are the annulenes with $h = h_{\max}$.

Let the **numer** of (nonisomorphic) $[2p]$annulenes of the considered class be denoted by $N'(p)$. Table 2 shows the numerical values of N' for $p \leqslant 23$ (as in Table 1). The peculiar sequence of numbers (N') is reproduced by the following analytical expressions.

Table 2

Numbers of special $[2p]$annulenes, N'

p	$n = 2p$	N'	p	$n = 2p$	N'
3	6	1	14	28	5
4	8	0	15	30	11
5	10	1	16	32	7
6	12	1	17	34	13
7	14	2	18	36	11
8	16	1	19	38	17
9	18	4	20	40	13
10	20	2	21	42	23
11	22	5	22	44	17
12	24	4	23	46	27
13	26	7			

$$N'(6j-3) = N'(6j) = \frac{1}{8}\left[(j+1)(2j^2+j+1) - \frac{1+(-1)^j}{2}\right] \quad (29\,\mathrm{a})$$

$$N'(6j-1) = N'(6j+2) = \frac{1}{8}\left[(j+1)(2j^2+3j-1) + \frac{1+(-1)^j}{2}\right] \quad (29\,\mathrm{b})$$

$$N'(6j+1) = N'(6j+4) = \frac{1}{8}\left[(j+1)(2j^2+5j+1) - \frac{1+(-1)^j}{2}\right] \quad (29\,\mathrm{c})$$

Here $j = 1.\ 2,\ 3,\ \ldots$.

The final remark concerns the feature that N' attains the same value for two different p. It manifests itself in two parallel curves when the diagrams for $N'(p)$ and $N'(p+3)$ are drawn separately, as corresponding to the left-hand side columns of (29); see Fig 4.

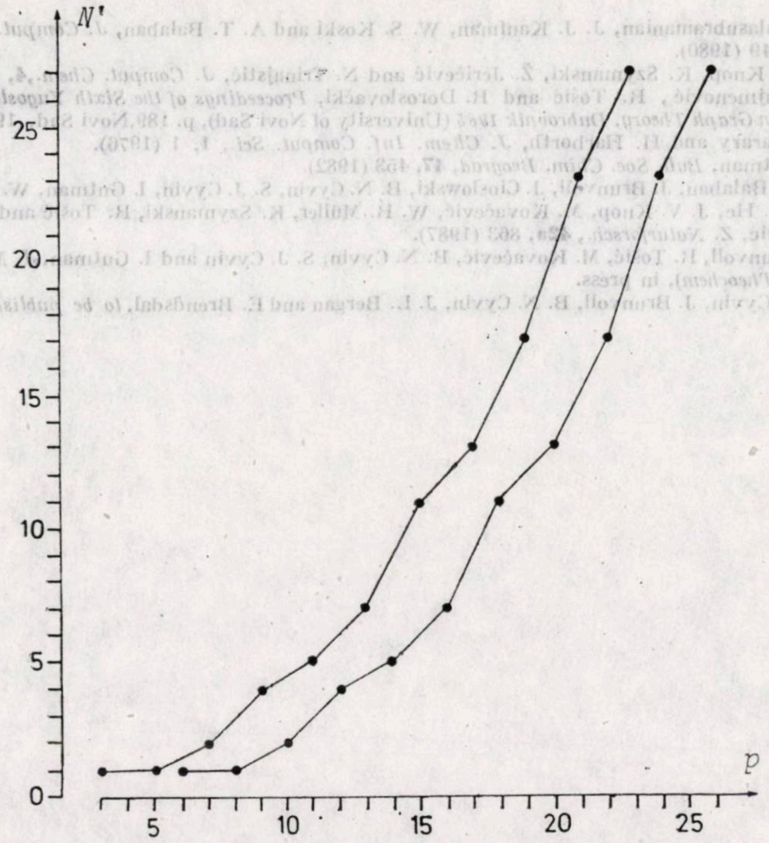

Fig. 4. — Graphical representation of $N'(p)$.

REFERENCES

[1] J. Brunvoll, B. N. Cyvin and S. J. Cyvin, *J. Chem. Inf. Comput. Sci.*, **27,** 14 (1987).

[2] S. J. Cyvin, B. N. Cyvin, J. Brunvoll and J. L. Bergan, *Coll. Sci. Papers Fac. Sci. Kragujevac*, **8,** 137 (1987).

[3] S. J. Cyvin, B. N. Cyvin and J. Brunvoll, *Chem. Phys. Letters*, **140,** 124 (1987).

[4] A. T. Balaban, *Rev. Roumaine Chim.*, **11,** 1097 (1966).

[5] A. T. Balaban, *Rev. Roumaine Chim.*, **15,** 463 (1970).

[6] A. T. Balaban, *Tetrahedron*, **27,** 6115 (1971).

[7] R. C. Haddon, V. R. Haddon and L. M. Jackman, "Topics in Current Chemistry", **16,** No. 2, Springer-Verlag, Berlin, 1971.

[8] F. Sondheimer, *Acc. Chem. Res.*, **5,** 81 (1972).

[9] F. Sondheimer, *Chimia*, **28,** 163 (1974).

[10] K. Müllen, *Chem. Rev.*, **84,** 603 (1984).

[11] A. T. Balaban and F. Harary, *Tetrahedron*, **24,** 2505 (1968).

[12] H. A. Staab and F. Diederich, *Chem. Ber.*, **116,** 3487 (1983).

[13] H. A. Staab and M. Sauer, *Liebigs Ann. Chem.*, **1984,** 742.

[14] D. J. H. Funhoff and H. A. Stabb, *Angew. Chem.*, **98,** 757 (1986).

[15] S. J. Cyvin and I. Gutman, "Kekulé Structures in Benzenoid Hydrocarbons" (*Lecture Notes in Chemistry,* **46**), Springer-Verlag, Berlin, 1988.

[16] K. Balasubramanian, J. J. Kaufman, W. S. Koski and A. T. Balaban, *J. Comput. Chem.*, **1**, 149 (1980).

[17] J. V. Knop, K. Szymanski, Ž. Jeričević and N. Trinajstić, *J. Comput. Chem.*, **4**, 23 (1983).

[18] I. Stojmenović , R. Tošić and R. Doroslovački, *Proceedings of the Sixth Yugoslav Seminar on Graph Theory, Dubrovnik 1985* (University of Novi Sad), p. 189, Novi Sad, 1986.

[19] F. Harary and H. Harborth, *J. Chem. Inf. Comput. Sci.*, **1**, 1 (1976).

[20] I. Gutman, *Bull. Soc. Chim. Beograd*, **47**, 453 (1982).

[21] A. T. Balaban, J. Brunvoll, J. Cioslowski, B. N. Cyvin, S. J. Cyvin, I. Gutman, W. C. He, W. J. He, J. V. Knop, M. Kovačević, W. R. Müller, K. Szymanski, R. Tošić and N. Trinajstić, *Z. Naturforsch.*, **42a**, 863 (1987).

[22] J. Brunvoll, R. Tošić, M. Kovačević, B. N. Cyvin, S. J. Cyvin and I. Gutman, *J. Mol. Struct. (Theochem)*, in press.

[23] S. J. Cyvin, J. Brunvoll, B. N. Cyvin, J. L. Bergan and E. Brendsdal, *to be published*.

Revue Roumaine de Chimie, 35, *10–12*, 997–1003 (1990)

APPLICATIONS OF WEIGHTED TOPOLOGICAL INDEX *J* FOR QSAR OF CARCINOGENESIS INHIBITORS (RETINOIC ACID DERIVATIVES)

ALEXANDRU T. BALABAN, [a] CORNEL CATANĂ, [b]
MARCIA DAWSON [c] and ION NICULESCU-DUVĂZ [d]

[a] Polytechnic Institute — TCH, Organic Chemistry Department, Splaiul Independenţei 313, 77206 Bucharest, Romania
[b] Institute for Chemical and Pharmaceutical Research, Bucharest
[c] Stanford Research Institute, USA
[d] Oncological Institute, Bucharest

Received February 15, 1990

For molecules containing heteroatoms, a new procedure for weighting the contribution of heteroatoms is presented, by multiplying the periodically varying relative Van der Waals radii with an adjustable parameter W_f in the calculation of topological index *JS*. As an application, several correlations with the antitumour activity of retinoic acid derivatives are represented.

INTRODUCTION ON TOPOLOGICAL INDICES AND THEIR APPLICATIONS IN QSAR

A topological index (TI) is a number obtained from a chemical structure by means of a topological (graph-theoretical) algorithm : starting from a set of topological invariants, one associates to each graph a numerical value of the TI translating thus chemical structures (discrete entities) into numbers which have a continuous range of variation exactly like the biological, physical or chemical properties of substances (these properties are measured and expressed also as numbers). There is no one-to-one correspondence between a graph and a TI because one cannot retrieve the graph from the TI ; rather, since more than one graph may have the same value of a given TI, these TI's are degenerate.

For quantitative structure-activity relationships (QSAR's) many TI's have been devised so far. Reviews on TI's [1–9] and on their biological applications [5,7,10] are available. Especially in the field of drug design, TI's (and especially Randić's molecular connectivity, [11] adapted for heteroatoms[5]) are widely employed, often in multiparametric correlations involving, in addition to the TI's, hydrophobicity, electronic, and/or steric parameters.

WEIGHTED TOPOLOGICAL INDEX J FOR MOLECULES CONTAINING HETEROATOMS

The average distance sum connectivity (J) is a topological index with low degeneracy,[12,13] defined with the aid of local vertex invariants which are termed distance sums s_i (sums of topological distances from vertex i to all other graph vertices):

$$J = \frac{q}{q - v + 2} \sum_{\text{edge } ij} (s_i s_j)^{-1/2} \qquad (1)$$

In formula (1), v is the total number of vertices (i.e. non-hydrogen atoms in the hydrogen-depleted molecular graph), and q is the number of edges (i.e. the lines representing covalent bonds between non-hydrogen atoms represented by graph vertices). The summation is extended to all edges between atoms i and j.

The TI J was derived so as to reflect graph branching : the more branched the graph, the higher the value of J. Most other TI's vary not only with molecular branching but also with the number v of vertices in the molecular graph. By contrast, J does not vary automatically with v. Ideed, J tends towards finite values for simple infinite graphs, e.g. J is $\pi = 3.14$ for a linear non-branched infinite alkane such as poly(ethene).[14] A computer program was devised for facilitating the calculation of J,[15] including the presence of multiple bonding.

Normally, J is to be used in multiparametric correlations having both J and v as independent variables (possibly other parameters too). Several criticisms [16,17] addressed to the "unsatisfactory" correlation ability of J are due to the fact that it was tested in monoparametric correlations for properties strongly influenced by the number of graph vertices. When v is used as an additional parameter along with J, this TI is found to possess excellent correlational ability.

For molecules containing heteroatoms, J was adapted to reflect the nature of the heteroatom either by taking into account the atomic number Z of the heteroatom,[18] or better, a periodically varying property vs. Z such as the Van der Waals radius (JS for sterical influence, or its electronegativity JE for electrical or electronegativity influence).[19] By means of a parametrized formula (2), a steric parameter Y_i is obtained :[*]

$$Y_i = 1.1191 + 0.0160\ Z_i - 0.0537\ G_i \qquad (2)$$

Z_i is the atomic number of the heteroatom and G_i is the number of the group in the short form of Mendeleev's Periodic System (for the new IUPAC system which has 18 groups in the s, p, and d blocks, G_i is the number of the group minus ten). The values of coefficients in eq. (2) have been selected so as to reflect relative Van der Waals radii of atoms, with the value of 1.00 for Y_i of carbon. One obtains $Y = 0.925$ for oxygen and 0.963 for nitrogen.

---

[*] In ref. [19] the coefficient -0.00537 should be replaced by -0.0537.

Alternatively, one might wish to calculate the steric differences between heteroatoms by considering Van der Waals volumes rather than Van der Waals radii (but we did not follow up this idea).

A formula similar to (2) exists for relative electronegatives, [19] but in the present case we did not use it.

In order to calculate JS, each distance sum s_i of a vertex i corresponding to a heteroatom is replaced by s'_i calculated with equation (3):

$$s'_i = W_f Y_i S_i \tag{3}$$

and then formula (1) is applied for computing JS, replacing s_i, s_j by s'_i, s'_j.

In the present paper we introduce a weighting factor W_f for attenuating or for enhancing the relative size of atoms. In ref. [19] the relative steric factors were used in eq. (3) without any weighting ($W_f = 1$).

For taking into account the presence of multiple bonds, two approaches have been considered: to treat each bond separately, or to include into the distance matrix the bond order (b) as follows: the topological distance between two adjacent atoms i, j connected by a multiple bond is:

$$1/b \tag{4}$$

(for single, double, triple, and aromatic bonds b is 1, 2, 3 and 1.5, respectively). This latter approach is adopted here, starting with formula (4), and following with (1) to (3).

In order to discriminate between groups (radicals) differing by the site of attachment such as propyl and isopropyl, the distance sums are calculated normally from the distance matrix, and then for the root vertex i corresponding to the attachment site of the radical, s_i is multiplied with 0.1. Subsequently one applies all formulas (1) — (3).

It will be seen that retinoids with formula I differ both in group R and in group R′. Calculations were performed both for the whole molecule I, and for group R with a correction for the nature of R′. The latter type of correlations gave better results and only these ones will be discussed further. The correction was performed by subtracting the value JS calculated for the whole retinoid molecule I for R′ = H from the corresponding value of R′ = Me/Et, and adding this difference to the JS value calculated only for group R′ (this difference is about 0.034).

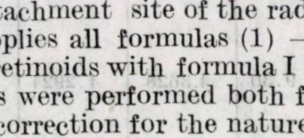

I

CORRELATIONS BETWEEN JS AND THE ANTITUMOUR ACTIVITY OF RETINOIC ACID DERIVATIVES

Experimental data are available [20] for the TOC assay inhibiting activity expressed as —log ED $_{50}$), for several retinoic acid derivatives possessing structure I, as seen in Table 1. The TOC assay (reversion of the

Table 1

Structures of retinoids I, TOC assay inhibiting activities, and *JS* values for various values of the weighting factor W_f

Comp.	R —	R'	$-\log ED_{50}$	W_f				
				0.35	0.5	0.65	1.00	3.00
1	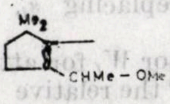	H	9.70	4.1825	4.0399	3.9681	3.8686	3.6939
2	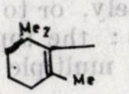	Me	9.52	—	4.2021	—	—	—
3	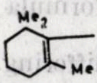	Et	9.30	—	4.2366	—	—	—
4	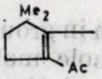	H	9.30	4.3628	4.2924	4.2482	4.1869	4·0792
5	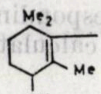	H	9.15	4.2891	4.2490	4.2073	4.1495	4.0479
6	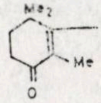	H	9.15	4.4820	4.4080	4.3615	4.2970	4.1806
7	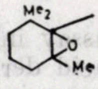	H	8.70	4.2212	3.9779	3.8250	3.6131	3.2409

Table 1 (continued)

Comp.	R —	R'	log ED_{50}	W_f 0.35	0.5	0.65	1.00	3.00
8	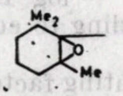	Me	8.52	4.2454	4.0021	3.8492	3.6373	3.2657
9	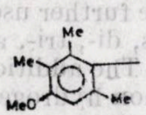	H	8.30	4.9498	4.8048	4.7136	4.5872	4.3652
10	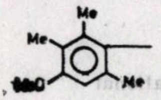	Et	7.70	5.0431	4.8381	4.8069	4.6805	4.4585
11	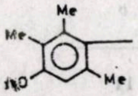	Et	7.70	5.1387	5.0536	5.0000	4.9159	4.7956
12	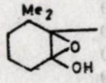	Me	6.70	5.3905	5.2479	4.9100	4.6530	4.3894
13	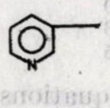	H	6.52	5.8849	5.6034	5.4263	5.1813	4.7506
14	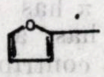	H	6.00	7.7984	7.0516	6.5821	5.9313	4.7881
Correlation coefficient r	—	—		0.8853	0.8898	0.8627	0.8145	0.6001

keratinization of hamster Tracheal cells in Organic Cells) is a test able to measure the intrinsic ability of retinoids to control the epithelial cell differentiaion. It is believed to have significant predictive value for the prevention of epithelial cancers ; ED_{50} is the dose (moles) of retinoids able to reverse the keratinization in 50% of the hamster tracheal cells.

The *JS* values for five different weighting factors W_f were calculated, and correlations with the antitumour activity ($y = -\log ED_{50}$) were studied. The correlations were monoparametric according to eq. (5) as it will be seen in Table 3.

From Table 1 it may be observed that the weighting factor $W_f = 1$ does not correspond to the highest correlation coefficient *r*. On the contrary, a higher correlation is found for $W_f = 0.5$, therefore these values of *JS* (according to formulas 1 through 3) with $W_f = 0.5$ are further used.

Next, in addition to monoparametric equations, di-, tri-, and tetraparametric correlations (6) — (12) have been studied. The additional parameters are *v* (number of vertices in group R, i.e. of non-hydrogen atoms), π (hydrophobicity parameter, calculated according to Hansch and Leo [21]), and an indicator variable δ (Kronecker delta) which distinguishes among retinoic acids having hydrogen bonds, and esters devoid of such bonds.

Table 2

Values of parameters employed in correlational equations

Comp.	*JS* (W_f=0.5)	π	δ	*v*
1	4.0399	−0.87	1	11
2	4.2021	0.30	0	9
3	4.2366	0.88	0	9
4	4.2924	−1.71	1	10
5	4.2490	−1.34	1	10
6	4.4080	−1.73	1	10
7	3.9779	−1.38	1	10
8	4.0021	−1.00	0	10
9	4.8048	−0.29	1	11
10	4.8981	0.59	0	11
11	5.0535	−0.06	0	10
12	5.2473	−2.04	0	10
13	5.6034	−2.46	1	6
14	7.0516	−2.36	1	5

From Table 3 which contains the correlational equations, it can be concluded that in this case the parameter *v* has the lowest coefficient, therefore it contributes in a very small measure to the correlation. In equations (7) and (8), the hydrophobicity parameter π has also a low coefficient, but in equations (11) and (12) it has a significant coefficient. The indicator variable δ has a significant contribution in all equations in which it appears (9) — (12). Among all biparametric equations, only (9) which includes δ gave a correlation coefficient above 0.9, unlike biparametric equations (6) and (7) which included *v* and π, respectively. Finally, in all equations (5) — (12) the topological index *JS* has significant coefficients.

Table 3

Correlational equations (5) — (12)

Correlation	r	*Eq.*
$y = -\log \mathrm{ED}_{50} = 14.3220 - 1.2749\ JS$	0.889	(5)
$y = 16.1070 - 1.4328\ JS - 0.1066\ \upsilon$	0.897	(6)
$y = 14.1465 - 1.2163\ JS + 0.1015\ \pi$	0.894	(7)
$y = 16.2315 - 1.3955\ JS - 0.1276\upsilon + 0.1367\pi$	0.904	(8)
$y = 14.2389 - 1.3021\ JS + 0.3689\delta$	0.904	(9)
$y = 15.5485 - 1.4176\ JS - 0.0776\upsilon + 0.3235$	0.907	(10)
$y = 13.5321 - 1.1324\ JS + 0.3650\ \pi + 0.8131\delta$	0.934	(11)
$y = 15.1263 - 1.2718\ JS - 0.0950\ \upsilon + 0.372\pi + 0.7617\delta$	0.938	(12)

In conclusion, by means of the topological index JS a series of equations were tested. Mono- and biparametric correlations (5) — (7) gave correlation coefficients $r = 0.889 - 0.897$. All tri- and tetraparametric correlations have correlation coefficients above 0.9, but only the last two ones, (11) and (12), including as significant variables δ and π have the best r values (0.93 to 0.94).

The above conclusions are supported by comparing Fischer's F factors and standard deviations (these latter data are situated between 0.5 and 0.6). for the $-\log \mathrm{ED}_{50}$ values which span the range of four orders of magnitude from 6 to 10.

REFERENCES

[1] A. T. Balaban, A. Chiriac, I. Moţoc and Z. Simon, "Steric Fit in QSAR", Lecture Notes in Chemistry No. 15, Springer, Berlin, 1980, chapter 3, p. 22.

[2] A. T. Balaban, I. Moţoc, D. Bonchev and D. Mekenyan, *Top. Curr. Chem.*, **114**, 21 (1983).

[3] N. Trinajstic, "Chemical Graph Theory", CRC Press, Boca Raton, vol. 2, chapter 4, p. 105.

[4] D. Bonchev, "Theoretic Information Indices for Characterization of Molecular Structures", Research Studies Press, Chichester, 1983.

[5] L. B. Kier and L. H. Hall, "Molecular Connectivity in Chemistry and Drug Research", Academic Press, New York, 1976; "Molecular Connectivity in Structure — Activity Analysis", Research Studies Press, Letchworth, 1986.

[6] D. H. Rouvray, *Sci. Amer.*, **254**, No. 9, 40 (1986).

[7] A. Sablijič and N. Trinajstić, *Acta Pharm. Jugosl.*, **31**, 189 (1989).

[8] P. J. Hansen and P. C. Jurs, *J. Chem. Educ.*, **65**, 574 (1988).

[9] M. I. Stankevich, I. V. Stankevich and N. S. Zefirov, *Usp. khim.*, **57**, 337 (1988).

[10] A. T. Balaban, I. Niculescu-Duvăz and Z. Simon, *Acta Pharm. Jugosl.*, **37**, 7 (1987).

[11] M. Randić, *J. Amer. Chem. Soc.*, **97**, 6609 (1975).

[12] A. T. Balaban, *Chem. Phys. Lett.*, **89**, 399 (1982); *Pure Appl. Chem.*, **55**, 199 (1983).

[13] A. T. Balaban and L. V. Quintas, *Math. Chem.*, **14**, 213 (1983).

[14] A. T. Balaban, N. Ionescu-Pallas and T. S. Balaban, *Math. Chem.*, **17**, 121 (1985).

[15] A. T. Balaban and P. Filip, *Math. Chem.*, **16**, 183 (1984).

[16] M. Razinger, J. R. Chrétien and J. E. Dubois, *J. Chem. Inf. Comput. Sci.*, **25**, 23 (1985).

[17] O. Mekenyan, D. Bonchev, A. Sabljić and N. Trinajstić, *Acta Pharm. Jugosl.*, **37**, 75 (1987).

[18] M. Barysz, G. Jashari, R. S. Lall, V. K. Srivastava and N. Trinajstić, in "Chemical Applications of Topology and Graph Theory", ed. R. B. King, Elsevier, Amsterdam, 1983, p. 222.

[19] A. T. Balaban, *Math. Chem.*, **21**, 115 (1986).

[20] D. L. Newton, W. R. Henderson and M. B. Sporn, *Cancer Res.*, **40**, 3413 (1980).

[21] C. Hansch and A. J. Leo, "Substituent Constants for Correlation Analysis in Chemistry and Biology", Wiley-Interscience, New York, 1979.

Revue Roumaine de Chimie, **35**, *10–12*, 1005–1008 (1990)

SYNTHESIS OF NOVEL FURYL-SUBSTITUTED 3-CYANO-2-PYRIDONES

MICHAELA-CARMEN BALABAN, [a] TEODOR-SILVIU BALABAN, [b]
URSULA BOLOGA [a] and ALEXANDRU T. BALABAN [a]

[a] Polytechnic Institute, Department of Organic Chemistry, Splaiul Independenţei 313, 77206 Bucharest, Romania

[b] Centre of Organic Chemistry, Splaiul Independenţei 202 B, 78100 Bucharest, Romania

Received February 15, 1990

Furyl analogues of chalcones (3,5-disubstituted-2-furyl styryl ketones, **4**) react smoothly with ethyl cyanoacetate and ammonium acetate to give 60–70% yields of the corresponding 4-aryl-3-cyano-6 (2-furyl)-2-pyridones, **5**, whose ^{1}H–NMR, IR and UV spectra are discussed.

Chalcones **1** (aryl styryl ketones or 1-aryl-3-aryl′-2-propene-1-ones) have been shown to react with ethyl cyanoacetate and ammonium acetate in absolute ethanol[1] or in n-butanol[2,3] yielding the corresponding 3-cyano-2-pyridones **2**.

In a recent paper,[2] several (2-thienyl)-substituted pyridones (**2**, Ar = 2-thienyl) were prepared and their antimicrobial activity was tested. Although these compounds were found to be inactive against *Staphyloccocus*, gram-negative *Bacillus sp.*, *Candida sp.*, and others, they may be precursors for novel heterocyclic systems by condensation of the cyano-pyridonic group. These new systems in which the 6-aryl group is replaced by a heterocyclic ring may possess increased biological activity.

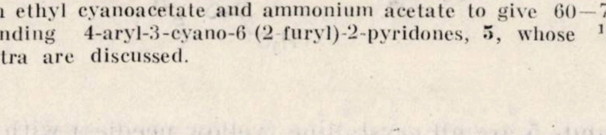

1

2

We report in the present paper the preparation of four new 3-cyano-2-pyridones **2** in which the 6-aryl group is replaced by a 3,5-disubstituted-2-furyl group.

Furyl analogues of chalcones **1**, namely 3,5-disubstituted-2-furyl styryl ketones **4** were prepared by known [4] methods, i.e. condensation of furyl methy ketones **3** with aromatic aldehydes.

On the other hand, the furyl methyl ketones **3** were prepared in good yields from the corresponding pyrylium salts by a modification of the previously reported oxidation. [5] The preparation of the furyl methyl ketones **3** will be reported separately.

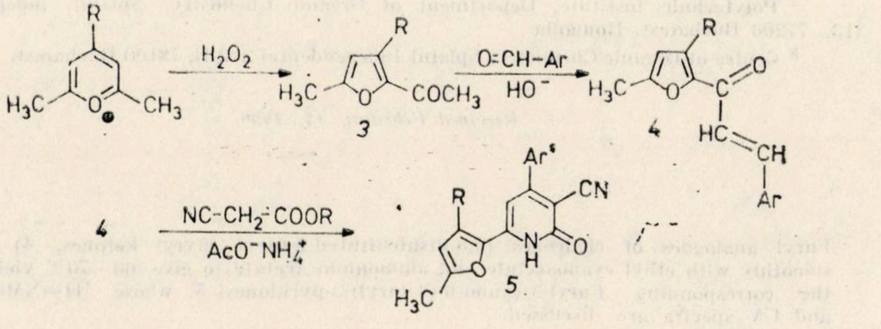

Compounds **5** are all crystalline (yellow needles) with high melting points (Table 1).

Table 1

Data for compounds **5**

No.	R	Ar′	Yield %	M. p. (°C)	Molecular formula	Analysis % N	
						found	required
5a	CH_3	C_6H_5	64	297–300	$C_{17}H_{14}N_2O_2$	9.59	9.65
5b	CH_3	p-$C_6H_4CH_3$	56	309–310	$C_{18}H_{16}N_2O_2$	9.50	9.33
5c	CH_3	p-$C_6H_4OCH_3$	71	305	$C_{18}H_{16}N_2O_3$	8.83	8.77
5d	C_6H_5	p-$C_6H_4OCH_3$	68	245–250	$C_{23}H_{18}N_2O_3$	7.06	7.32

Their ^{1}H-NMR spectra in trifluoroacetic acid show the 5-pyridonic and the 4-furylic protons as singlets, the former being more deshielded (7.2 ppm) than the latter (6.4 ppm) which is slightly broadened (at 60 MHz) owing to the allylic coupling with the 5-methyl group of the furan ring (Table 2).

The IR spectra in KBr pellets show for all compounds a medium-strong, sharp band at 2220 cm^{-1} due to the cyano group and strong bands at 1600 and 1650 cm^{-1} which can be assigned to the benzenic and pyridonic rings, respectively.

Table 2

^{1}H-NMR chemical shifts (δ, ppm) in trifluoroacetic acid for compounds 5

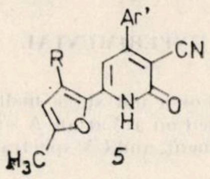

No.	R	Ar′	5-CH_3	R′	R	4—H	5—H	4—Ar	
5a	CH_3	C_6H_5	2.43	2.38	—	6.33	6.98	7.71 m	
5b	CH_3	p-$C_6H_4CH_3$	2.52^a	2.52^a	2.52^a	6.38	7.22	7.53d 7.75d	J=8 Hz
5c	CH_3	p-$C_6H_4OCH_3$	2.52^a	2.52^a	4.12	6.36	7.15	7.15d 7.80d	J = 8.5Hz
5d	C_6H_5	p-$C_6H_4OCH_3$	2.52	7.60m	4.00	6.46	6.97	7.10d 7.60d	J = 8 Hz

[a] On addition of C_6D_6 this signal splits into equal singlets.

We tried to verify the presence of an intramolecular hydrogen bond between the NH proton and the furan ring in conformation **5A**. To this end we synthesized the related 3-cyano-2-pyridone **6**, with a 6-*o*-hydroxyphenyl group which is more prone to intra- and intermolecular hydrogen bonding.

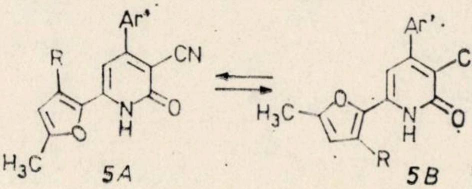

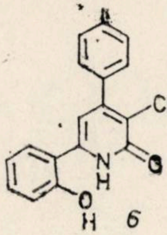

The low solubility of compounds **5** in protic or aprotic solvents prevented the study of their intramolecular hydrogen bonding which is not clear from the IR spectra in KBr pellets. An X-ray structural investigation may indicate if the hydrogen bonding in **5a**—**d** is important or not, if the conformation is **5A** or **5B**, and if the system **5** is coplanar.

The UV spectra in ethanol present a composite band at 395—405 nm which indicated conjugation not only with the 4-aryl group but also with the 6-furyl moiety. Other bands, somewhat less intense, appear at 220 nm and at 270—280 nm. The latter band presents a shoulder at 295 nm which is bathochromically shifted in the *p*-methoxy compound **5c** to 306 nm.

ACKNOWLEDGEMENTS. We thank Ms. Corina Muşat and Mr. Dan Daia for synthesizing some of the furyl analogues **4** of chalcone. Chemist M. Plăveţi is thanked for elemental analyses, and Mrs. V. Todan for the IR spectra.

EXPERIMENTAL

Melting points were determined on a hot stage melting point apparatus and are uncorrected. ^{1}H—NMR spectra were recorded on a Varian A—60A spectrometer; IR spectra were determined on a Zeiss UR—20 instrument, and UV spectra were run also on a Zeiss instrument.

3-Cyano-6-(3,5-dimethyl-2-furyl)-4-phenyl-1H-2-pyridone **5a**.
Typical procedure: 3-(3,5-dimethyl-2-furyl)-1-phenyl-1-propen-2-one (1.13 g, 5 mmol) was dissolved in n-butanol (15 ml) and ammonium acetate (3.08 g, 40 mmol) was suspended. After adding ethyl cyanoacetate (0.565 g, 5 mmol) the mixture was heated under reflux when it became clear and orange-red. Heating was continued for ten to twelwe hours. The reaction mixture was cooled in the refrigerator overnight; the crystals of **5a** (64% yield) were collected and recrystallized from boiling acetic acid.

3-Cyano-6-(2-hydroxyphenyl)-4-(4-methoxyphenyl)-1H-2-pyridone **6**.
The known [5] chalcone analog **1e**, 3-(2-hydroxyphenyl)-1-(4-methoxyphenyl)-1-propen-3-one (2.5 mmol) was condensed as above with ammonium acetate (20 mmol) and ethyl cyanoacetate (2.5 mmol) in boiling n-butanol (8 ml). The cyanopyridone **6** crystallized during the heating period. The mixture after refluxing for 10 hours was cooled, the crystals were collected and were recrystallized from acetic acid, m.p. 323°C. Found: N, 8.56%; $C_{18}H_{14}N_2O_3$ requires: N, 8.80%.

REFERENCES

[1] N. Latif, N. Mishniky and M. Gingis, *Indian. J. Chem.*, **20**, 147 (1981).

[2] K. M. Ghoneim, M. M. Badran, M. A. Shaaban and S. El-Meligie, *Egypt. J. Pharm. Sci.*, **29**, 553 (1988).

[3] A. Sammour, M. Abdallah and H. Zoorob, *J. Prakt. Chem.*, **317**, 387(1973).

[4] C. Weygand, F. Strobelt, *Chem, Ber.*, **68**, 1839 (1935).

[5] A. T. Balaban and C. D. Nenitzescu, *Chem. Ber.*, **1960**, 599; A. T. Balaban, *Org. Prep. Proc. Int.*, **1**, 63 (1969).

[6] St. v. Kostanecki and W. Szabranski, *Chem. Ber.*, **37**, 2534 (1904).

Revue Roumaine de Chimie, 35, *10–12*, 1009–1016 (1990)

INTERACTIONS OF SUBSTITUTED FIVE-MEMBERED HETEROAROMATIC COMPOUNDS WITH ELECTRON ACCEPTORS. III[1]

CHARGE TRANSFER COMPLEXES WITH TETRACYANOETHENE AND TRICYANOVINYLATION OF SOME 3-MERCAPTO-1,2,4-TRIAZOLES

MIRCEA D. BANCIU, [a] IOANA ŞARAMET [b] and CONSTANTIN DRĂGHICI [c]

[a] Organic Chemistry Department, The Polytechnic, TCH, Spl. Independenţei 313, Bucharest, Romania

[b] Organic Chemistry Department, Faculty of Pharmacy, Traian Vuia Street 6, Bucharest, Romania

[c] Center of Organic Chemistry, Romanian Academy, Bucharest

Received February 20, 1990

Coloured π-charge transfer complexes (CTC's) of substituted 3-mercapto-1,2,4,-triazoles 4 with tetracyanoethene were investigated by electronic spectroscopy. The stability constants (K_{CT}) and ε_{CT} of complexes, were determined and compared with those of related compounds. The π-complexes show a dynamic behaviour affording S-tricyanovinyl-derivatives of 4 as final stable compounds.

INTRODUCTION

In previous papers of this series [1,2] we described the interactions of substituted thiazoles **1** and thiadiazole **2** with tetracyanoethene (TCNE).

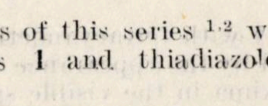

1

a) R = C_6H_5–
b) R = CH_3–

Whereas thiazoles **1**[2] afford relatively stable charge transfer complexes (CTC's) (**1a** complexing probably at the monosubstituted phenyl ring and **1b** at the thiazolic moiety, the thiadiazole **2**[1] indicated a more complicated behaviour. Thus, the initially formed CTC between **2** and tetracyanoethene (a π complex of thiadiazolic ring) is converted relatively fast into a stable red N-(tricyanovinyl)-derivative **3**, most probably *via* a σ-complex.[1]

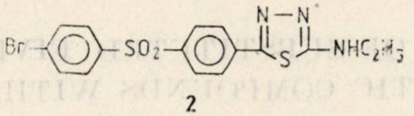

2

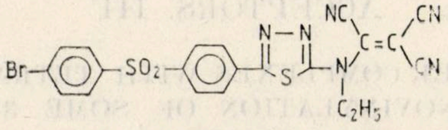

3

In order to extend the investigation of the interactions between five-membered heteroaromatics and electron acceptors, in this work we studied the behaviour of substituted 3-mercapto-1, 2, 4-triazoles **4** in the presence of TCNE.

RESULTS AND DISCUSSION

The triazoles **4a, b** were prepared[3] by cyclization of the corresponding thiosemicarbazides **5a, b** in NaOH medium.

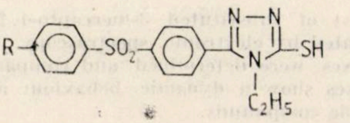

4

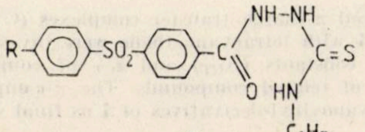

5

a) R = Br
b) R = Cl

a) R = Br
b) R = Cl

Treatment of triazoles **4** with tetracyanoethene in CH_2Cl_2 at room temperature was accompanied by the appearance of a violet colour and of characteristic absorption maxima in the visible spectra : $\lambda_{max} = 545.5$ nm for **4a**-TCNE and $\lambda_{max} = 543$ nm for **4b**-TCNE. These bands, which appear neither in the electronic spectra of **4a, b** nor in that of TCNE, must be attributed to CTC's. Variation of the molar ratios heterocycle/TCNE conducted to characteristic modifications of extinctions (see Experimental part). On the basis of experimental data the stability constants K_{CT} and molar extinction coefficients ε_{CT} for CTC were derived, as in our previous papers,[1 2] using Scott's[4] modification (eq. 1) of Benesi-Hildebrand equation[5]:

$$\frac{C_1 \cdot C_2 \cdot l}{E} = \frac{1}{K_{CT} \cdot \varepsilon_{CT}} + \frac{1}{\varepsilon_{CT}} \cdot C_1 \qquad \text{(eq.1)}$$

where C_1, C_2 are the molarities of reactants, E the absorbance of the complex and l (cm) the cell length.

The results are presented in Table 1 along with related literature data. The good linear correlations obtained for Scott's relationship suggest the 1 : 1 stoechiometry for both investigated CTC's.

Table 1

λ_{max}^{CT} (nm), K_{CT} and ε_{max}^{CT} for CTC of TCNE with aromatic donors

Aromatic donor	λ_{max}^{CT} (nm)	K_{CT} L . mol^{-1}	ε_{max}^{CT} L.mol^{-1} cm^{-1}	Ref.
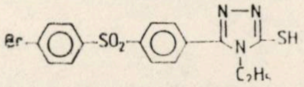 (4a)	545.5	4.49	1250	This work
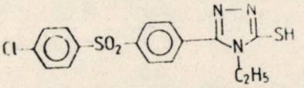 (4b)	543	3.15	1000	This work
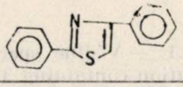	570	1.05	772	6
Pyridine	421	12.0	10500	7
Benzene	384	2.0	3570	7
Toluene	406	3.70	3330	7

The data from Table 1 indicate a good complexation of triazoles **4a, b** with TCNE, their K_{CT} values (4.49 and 3.15, respectively) being higher than those of 2,5-diphenylthiazole or of benzene but of the same magnitude order with that of toluene (3.70).[7] It seems that the known relatively strong aromatic character of the 1, 2, 4-triazolic ring equals in substituted compounds **4** that of toluene ; both the +I effect of C_2H_5-group and the +E effect of the - SH group in **4a, b** increase the electronic density in triazolic ring. Complexation at one of the disubstituted phenyl rings seems unprobable due to the strong electron withdrawing effect of SO_2 group. The slight difference between the K values of **4a** and **4b** could be ascribed to their different remote substituent (chlorine and bromine, respectively). The stronger —I effect of chlorine from **4b** decreases in a higher degree the electronic density in triazolic ring and consequently the K-value for CTC of **4b** becomes smaller than that of **4a**. The same remote substituent effect could influence the λ_{max}^{CT} of CTC of **4a, b** : the CT-band in the case of **4b** is slightly hypsochromically shifted in comparison with **4a**. The smaller ε_{max}^{CT} values observed for **4**-TCNE in comparison to toluene-TCNE could be ascribed, as in other cases, [2] to greater steric hindrance to complexation exhibited by mercaptotriazoles **4**.

It should be also added that the initially formed π-CTC's of **4a,b** with TCNE are unstable in time. Recording of the visible spectra at different time intervals shows characteristic modifications of the absorption maxima. A set of such visible spectra obtained using equimolar quantities of **4b** and TCNE in CH_2Cl_2 are presented in Fig. 1. A nearly similar behaviour was observed for **4a**-TCNE except the formation, after about three days, of a fine precipitate, which precludes a further good recording of the spectra.

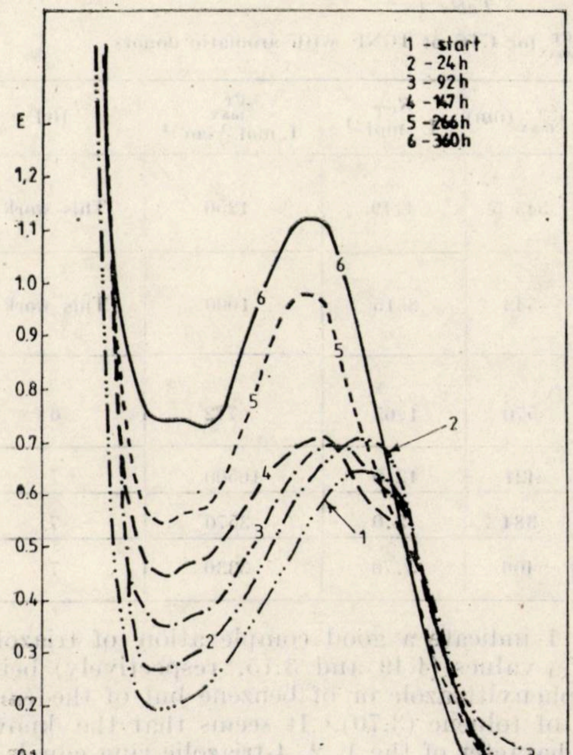

Fig.1. — Visible spectra of a solution containing triazole **4b** (1.3×10^{-2}M) and TCNE (1.3×10^{-2}M) in CH_2Cl_2 at different time intervals.

The above-mentioned changes are accompanied by a modification of the colour of both solutions toward reddish-brown.

In order to prove the formation of a stable reaction product between **4a, b** and TCNE some preparative reactions were performed in CH_2Cl_2 at reflux for 6 — 8 hrs. After the work-up of the reaction mixtures solid state, dark red products were obtained in both cases. For these products the structures of S-tricyanovinyl derivatives **6a, b** could be suggested on the basis of their spectral and elemental analysis.

Comparison of the IR spectra (in KBr) of the derivatives **6a, b** with those of their corresponding mercaptotriazoles **4a, b** shows clearly the disappearance of the ν_{SH} bands from 2561 and 2559 cm⁻¹ respectively, as well as the appearance of ν_{CN} bands at 2216 and 2264 cm⁻¹ in **6a**, and at 2218 and 2268 cm⁻¹ in **6b**. All the remainder IR absorptions (characteristic e.g. for $-SO_2-$; C_2H_5; substituted phenyl rings) are in agreement with the suggested structures.

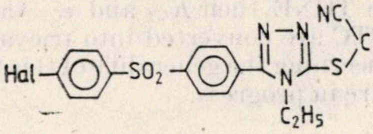

6

a) Hal = Br

b) Hal = Cl

The ^1H-NMR spectra of **6a, b** are very similar with those of the starting compounds **4a, b**, being at the same time in accord with the proposed structures.

The visible spectra are also in agreement with the structures of tricyanovinyl derivatives **6a, b**. Whereas TCNE and mercaptotriazoles **4a, b** present no absorption in the visible range, the products **6a, b** indicate characteristic absorptions for red compounds, namely at 421; 471 and 563 (sh) nm for **6a** and at 425.5; 487 and 571 (sh) nm for **6b**. The specific red colour of different tricyanovinylderivatives was repeatedly mentioned. [1,8,9]

On the basis of the present experimental results it seems that hetarylmercaptans may be also tricyanovinylated by TCNE in a fashion resembling the known reactions of amines [8,1] or of hydroxy-derivatives. [8] To our best knowledge no other example of S-tricyanovinylation was described. The mechanism of this reaction could be similar to that proposed for N-tricyanovinylation of amines (Scheme 1).

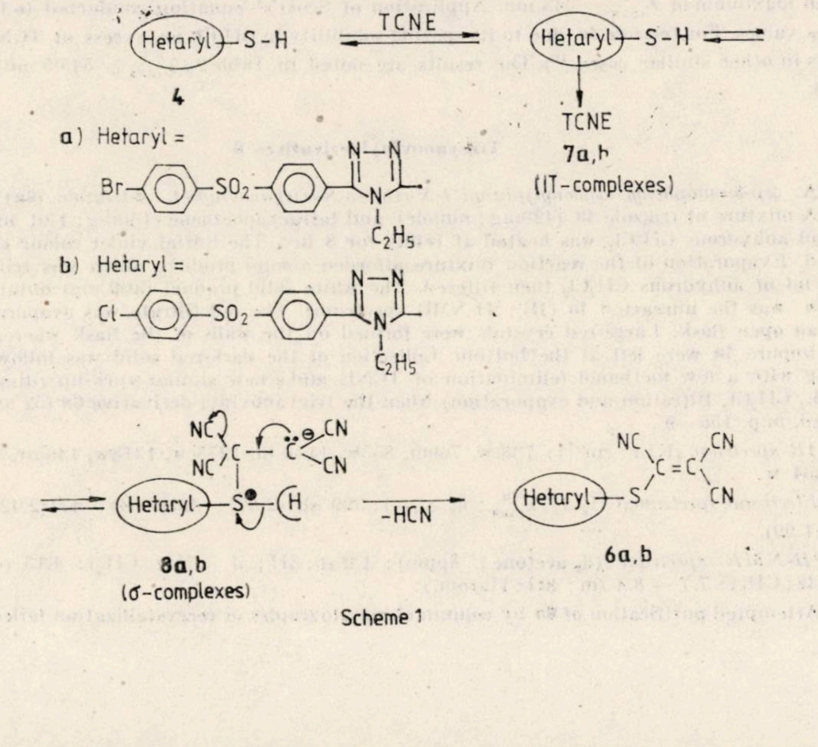

Scheme 1

Conversion of π-complexes **7a, b** into tricyanovinylderivatives **6a, b** could proceed *via* instable σ-complexes **8a, b**.

In conclusion this work has shown that substituted mercaptotriazoles **4** afford π-CTC with TCNE, their K_{CT} and ε_{CT} values being similar to those of toluene. The π-CTC are converted into tricyanovinyl derivatives. Further investigations concerning the generality of this S-tricyanovinylation as well as its mechanism are in progress.

EXPERIMENTAL

The electronic spectra were recorded on a SPECORD UV—VIS (C.Zeiss-Jena) spectrophotometer using silica cells with $l = 1$ cm. The IR spectra were registered on a UR20 (C.Zeiss-Jena) spectrophotometer and ^{1}H-NMR spectra on a VARIAN A 60—A spectrometer (TMS as internal standard).

Reagents. The triazoles **4a,b** were prepared and purified as described [3] by alkaline cyclization of the corresponding thiosemicarbazides **5a, b**.

Triazole **4a**, m.p. 273—4°C ;

IR - spectrum (KBr ; cm^{-1}) : 731 m, 762s, 830m, 848m, 1159s, 1281s, 1320m, 1351m, 1471m, 1566m and 2561w (ν_{SH}).

Triazole **4b**, m.p. 254—5°C

IR spectrum (KBr) ; cm^{-1}) : 750s, 772vs, 838s, 852s, 1161vs, 1275vs, 1321vs, 1360s, 1470m, 1562s and 2559w (ν_{SH}).

The triazoles **4a,b** present in the electronic spectra no absorption above 400 nm.

Tetracyanoethene (TCNE) was recrystallized twice from chlorobenzene ; m.p. 198.5 — — 200°C. Dichloromethane was refluxed over P_2O_5 and distilled.

Charge transfer complexes

Solutions of triazole **4b** in CH_2Cl_2 were prepared according to data from Table 2. Addition of a determined amount of TCNE produced the instantaneous appearance of a violet colour. Recording of the electronic spectrum permitted the determination of E_{max} for the absorption maximum of $\lambda^{CT}_{max} = 543$ nm. Application of Scott's[4] equation conducted to the K_{CT} and ε_{CT} values. For triazole **4a** due to its sparing solubility in CH_2Cl_2 an excess of TCNE was used (as in other similar cases. [10]) The results are noted in Table 2 ; $\lambda^{CT}_{max} = 545.5$ nm ; violet colour).

Tricyanovinylderivatives 6

A. *5(p-bromophenylsulphonyl)phenyl-4-N-ethyl-3-S-tricyanovinyl-1,2,4-triazole* (**6a**) :

A mixture of triazole **4a** (420mg ; mmole) and tetracyanoethene (130mg ; 1.01 mmoles) in 80 ml anhydrous CH_2Cl_2 was heated at reflux for 8 hrs. The initial violet colour changes into red. Evaporation of the reaction mixture afforded a solid product which was triturated with 3 ml of anhydrous CH_2Cl_2 then filtered. The white solid product (300 mg) obtained on filration was the unreacted **4a** (IR ; ^{1}H-NMR spectrum). The red filtrate was evaporated in air in an open flask. Large-red crystals were formed on the walls of the flask whereas traces of impure **4a** were left at the bottom. Collection of the dark-red solid was followed by washing with a few methanol (elimination of TCNE and a new similar work-up (dissolution in 2 mL, CH_2Cl_2 filtration and evaporation) when the tricyanovinyl derivative **6a** (52 mg) was obtained, m.p. 156—9°.

IR spectrum (KBr ; cm^{-1}) : 738 w, 769m, 855w, 1156 m, 1278 w, 1318w, 1465w, 2216w and 2264 w.

Electronic spectrum (CH_2Cl_2 ; λ^{nm}_{max} ; lg ε_{max}) : 399 sh (2.67) ; 421(2.64) ; 471(2.42) and 563sh (1.99).

^{1}H-NMR spectrum (d_6-acetone ; δppm) : 1.2.(t ; 3H ; J = 7Hz ; CH_3) ; 4.15 (q : 2H ; J = 7Hz ; CH_2) ; 7.7 — 8.4 (m ; 8H ; Harom.) ;

Attempted purification of **6a** by column chromatography or recrystallization failed.

Table 2

Charge-transfer complexes of triazoles 4 with TCNE (t = 20°C ; l = 1cm ; volume of samples 5 mL)

A. *Triazole* **4a** $\lambda_{\max} = 545.5$ nm

Triazole		TCNE		E	$\frac{C_1 \ C_2 \cdot l}{E}$
mg	mol/L (C_1)	mg	mol/L (C_2)		
5.3	0.0025	6.4	0.010	0.135	1.85×10^{-4}
5.3	0.0025	7.7	0.012	0.160	1.875×10^{-4}
5.3	0.0025	9.6	0.015	0.198	1.89×10^{-4}
5.3	0.0025	12.8	0.02	0.260	1.92×10^{-4}
5.3	0.0025	16.0	0.025	0.315	1.98×10^{-4}

B. *Triazole* **4b** $\lambda_{\max} = 543$ nm

Triazole		TCNE		E	$\frac{C_1 C_2 \cdot l}{E}$
mg	mol/L (C_1)	mg	mol/L (C_2)		
10.7	5.64×10^{-3}	4	6.25×10^{-3}	0.11	3.20×10^{-4}
14.0	7.38×10^{-3}	4	6.25×10^{-3}	0.142	3.24×10^{-4}
20.0	10.5×10^{-3}	4	6.25×10^{-3}	0.20	3.28×10^{-4}
22.0	11.6×10^{-3}	4	6.25×10^{-3}	0.22	3.29×10^{-4}
24.0	12.65×10^{-3}	4	6.25×10^{-3}	0.235	3.36×10^{-4}

B. *5(p-chlorophenylsulphonyl)phenyl-4-N-ethyl-3-S-tricyanovinyl- 1, 2, 4-triazole* (**6b**).

The compound **6b** was obtained from triazole **4b** in a similar way as **6a** (*vide supra*), m.p. 204°C.

IR spectrum (KBr ; cm^{-1}) : 772s, 850m, 1158vs, 1278s, 1319m, 1472m, 2218w and 2268 w.

Electronic spectrum (CH_2Cl_2 ; $\lambda_{\max}^{\mathrm{nm}}$; lg $\varepsilon_{\max}$: 425.5 (2.73); 487 (3.03); 571 (2.73)

^1H-NMR spectrum (d_6-acetone ; δppm) : 1.35 (t ; 3H ; J = 7Hz ; CH_3) ; 4.24 (q ; 2H ; J = 7Hz ; CH_2) ; 7.6–8.4 (m ; 8H ; Harom).

Found: N, 17.36%. Calcd. for $C_{21}H_{13}N_6O_2S_2Cl$, N, 17.48 %.

REFERENCES

1 Part II: I. Şaramet, C. Drăghici and M. Banciu, *Rev. Roumaine Chim.*, **35**, 437 (1990).
2 I. Şarament and M. Banciu, *Rev. Roumaine Chim.*, **30**, 559 (1985).
3 I. Şaramet, Ph. D. Thesis, The Polytechnic, Bucharest, 1981.
4 R. L. Scott, *Req. Trav. Chim.*, **75**, 787 (1956).
5 H. A. Benesi and J. H. Hildebrand, *J. Amer. Chem. Soc.*, **71**, 2703 (1949).
6 M. R. Mahmoud, A. M. El-Nady and H. M. A. Salman, *Bull. Soc. Chim. France*, **1989**, (3), 398.
7 R. E. Merrfield and W. D.Philips, *J. Amer. Chem. Soc.*, **80**, 2778 (1958).
8 A.J. Fatiadi, *Synthesis*, **1986**, 249.
9 B. C. McKusick, R.E. Heckert, T. L. Cairns, D. D. Coffman and H. F. Mower, *J. Amer. Chem. Soc.*, **80**, 2806 (1958).
10 Y. Takahashi, S. Sankararaman and J. K. Kochi, *J. Amer. Chem. Soc.*, **111**, 2954 (1989).

Revue Roumaine de Chimie, **35**, *10 – 12*, 1017–1024 (1990)

SYNTHESIS AND EPR SPECTRA OF PERSISTENT AROXYLS. V[1]

AROXYLS DERIVED FROM CHALCONE AND DERIVATIVES

JEAN M. HERDAN[a], VASILE DINOIU, [a] AURELIA MEGHEA, [b] ANA SCHIKETANZ,[c]
MIRCEA D. GHEORGHIU [c] and ALEXANDRU T. BALABAN [c,*]

[a] Institute of Research, Technological Engineering and Design for Refineries (ICITPR), 2000 Ploieşti, Romania
[b] Department of Physical Chemistry, Polytechnic Institute, Bucharest, Romania,
[c] Department of Organic Chemistry, Polytechnic Institute, Bucharest, Romania

Received March 2, 1990

Condensation of 3,5-di-t-butyl-4-hydroxybenzaldehyde (1) with *p*-substituted acetophenones yielded chalcone derivatives 2a – f; condensation of 3,5-di-t-butyl-4-hydroxyacetophenone (5) with *p*-substituted benzaldehydes afforded isomeric chalcone derivatives, 6a,6f. Condensation of 3 with 5 gave the bis-phenol 7. Oxidation of 2, 6 and 7 afforded aroxyls with characteristic EPR spectra. The UV–VIS spectra of chalcone derivatives 2, 6, and 7 in neutral and alkaline media, as well as their ^{1}H-NMR spectra are discussed.

INTRODUCTION

3,5-Di-t-butyl-4-hydroxybenzaldehyde **1** can be easily obtained from 2,6-di-t-butylphenol, t-butanol, and bromine.[2] By condensation with acetophenone and substituted acetophenones, various chalcone derivatives (aryl 3,5-di-t-butyl-4-hydroxystyryl ketones) **2a – f** have been prepared and are reported in the present paper together with their spectra and reactions.

Unlike the preparation of chalcone from benzaldehyde and acetophenone which occurs in alkaline medium,[3] in the present case basic catalysis (sodium hydroxide or hydride) is not effective, probably owing to the lack of reactivity of the aldehydic component which affords a delocalized anion **3**. However, in absolute ethanol in the presence of gaseous

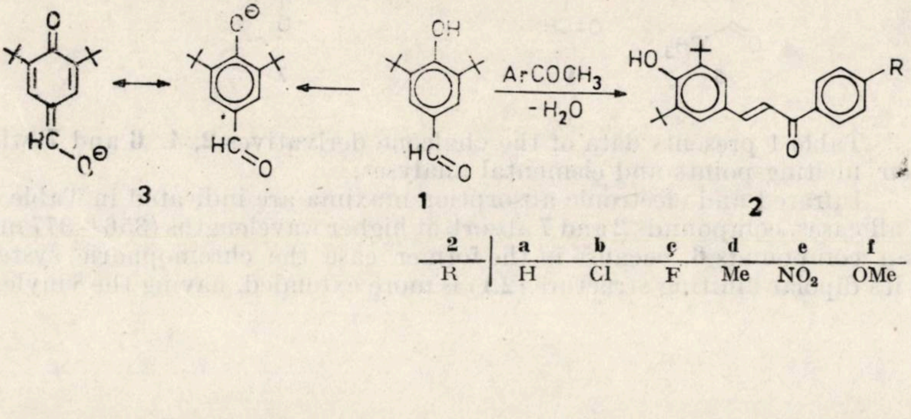

2	a	b	c	d	e	f
R	H	Cl	F	Me	NO$_2$	OMe

hydrogen chloride the condensation proceeds smoothly at room temperature.[4] The reaction mechanism **involves** electrophilic attack of the protonated aldehyde on the enolic form of the substituted acetophenone.[5]

From aldehyde **1** and propiophenone, an isomeric compound with **2d** was obtained analogously, but its ^{1}H-NMR and EPR spectra showed that it was a mixture of diastereoisomers **4A** and **4B**, therefore it was not further investigated (it had been hoped that substitution of one of the olefinic hydrogens would have helped in the ^{1}H-NMR and EPR assignments).

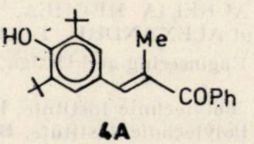

4A

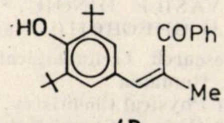

4B

An isomeric series of chalcone derivatives (3,5-di-t-butyl-4-hydroxyphenyl *p*-R-styryl ketones) **6** was obtained on starting from 3,5-di-t-butyl-4-hydroxyacetophenone **5** and substituted benzaldehydes,[6] under similar reaction conditions.

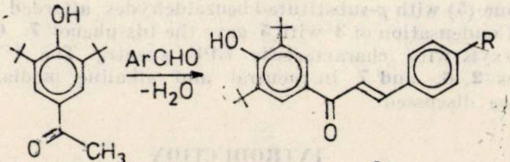

5 **6**

6	a	f
R	H	OMe

Finally, a bis-hydroxy-chalcone derivative **7** was prepared under the same reaction conditions from **1** and **5**.

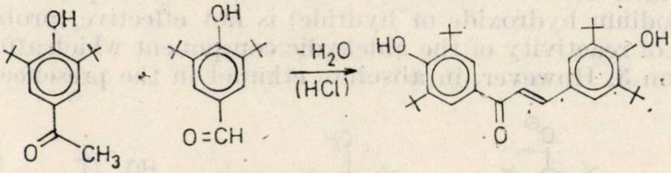

5 **1** **7**

Table 1 presents data of the chalcone derivatives **2**, **4**, **6** and **7** with their melting points and elemental analyses.

Infrared and electronic absorption maxima are indicated in Table 2. In all cases, compounds **2** and **7** absorb at higher wavelengths (356—377 nm) than compounds **6**, because in the former case the chromophoric system in its dipolar limiting structure (**2A**) is more extended, having the vinylene

Table 1

Melting points and elemental analyses

Comp.	R	Mp (°C)	Formula	C%		H%	
				Calc.	Found	Calc.	Found
2a	H	178—180	$C_{23}H_{28}O_2$	82.12	82.03	8.35	8.52
2b	Cl	123	$C_{23}H_{27}ClO_2$	74.49	75.23	7.28	7.31
2c	F	117—118	$C_{23}H_{27}FO_2$	77.96	78.12	7.62	7.71
2d	Me	145—147	$C_{24}H_{30}O_2$	82.24	82.45	8.62	8.77
2e	NO_2	172	$C_{24}H_{27}NO_4$	72.41	72.25	7.13	7.20
2f	OM	149—150	$C_{24}H_{30}O_3$	78.65	79.00	8.25	8.43
4	—	140—141	$C_{24}H_{30}O_2$	82.24	82.08	8.62	8.89
6a	H	176—177	$C_{23}H_{28}O_2$	82.12	82.21	8.35	8.52
6f	OMe	117—118	$C_{24}H_{30}O_3$	78.65	78.49	8.25	8.47
7	—	149	$C_{31}H_{44}O_3$	80.17	80.03	9.70	9.74

Table 2

Vibrational and electronic absorption maxima

Compound	R	IR in $CDCl_3$ (cm^{-1})	UV-VIS in EtoH (nm)	
			Neutral	NaoEt
2a	H	3640, 1665, 1630, 1600, 985	356, 254	520
2b	Cl	3635, 1665, 1630, 1600, 990	362, 259	—
2c	F	3630, 1660, 1630, 1600, 980	364, 257	—
2d	Me	3625, 1660, 1630, 1610, 980	357, 257	—
2e*	NO_2	3610, 1640, 1585, 980	377, 268	570
2f	OMe	3615, 1635, 1630, 1590, 955	357, 303, 247	520
6a	H	3620, 1660, 1640, 970	307, 227	404
6f	OMe	3630, 1650, 1620, 970	339, 294, 236	455
7	—	3635, 1660, 1630, 1600, 980	357, 294, 228	—

* IR Bands due to NO_2 groups : 1335, 1500 cm^{-1}

group between the acceptor carbonyl and the donor *p*-hydroxyphenyl group. Electron-attracting groups R in the Ar group exert a bathochromic effect in the electronic absorption spectra of compounds **2**, while electron-donating groups (methyl, methoxy) have practically no effect. On the other hand, in the electronic absorption spectra of compounds **6**, electron-donating substituents R in the Ar group exert a strong bathochromic effect, while electron-acceptor substituents have a strong hypsochromic effect.

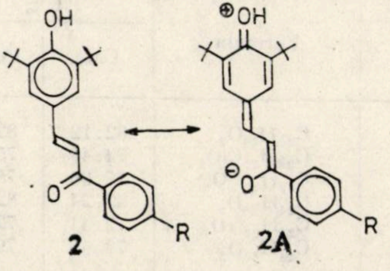

In alkaline medium (sodium ethoxide in ethanol) a new electronic absorption band appears at higher wavelengths, owing to the extended anionic chromophore.

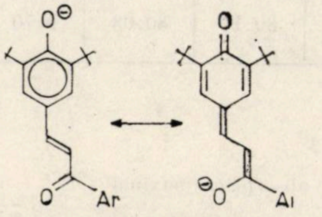

2-Anion

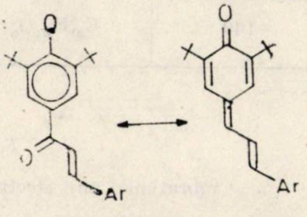

6-Anion

Whereas in the case of the anions derived from **2** the conjugated system between the two oxygen atoms is extensive (bathochromic shift about 160 nm on making the solution alkaline when R = H, and 200 nm when R = NO_2), the conjugated *para*-quinonoid system derived from **6** is smaller, and the corresponding bathochromic shift is likewise lower (only about 100 nm).

^{1}H-NMR SPECTRA

Chemical shifts and coupling constants in ^{1}H-NMR spectra are collected in Table 3. The multiplicity of the signals is indicated (singlet, doublet) in the headings of Table 3 ; for phenyl groups these multiplicities no longer apply.

The ^{1}H-NMR spectra confirm the structures of all compounds. In order to assign all the signals due to the *para*-substituted phenyl groups (AA′BB′ pairs of doublets with coupling constants 7.5–8.5 Hz) and the AB multiplet due to the *trans*-vinylene protons (coupling constants 15–17 Hz), it was necessary to determine all spectra in two solvents : $CDCl_3$ and C_6D_6. In the latter solvent aromatic solvent induced shifts (ASIS) cause a spreading of signals facilitating the assignment : the most

Table 3

^{1}H-NMR chemical shifts (δ, ppm) : multiplicities are indicated in brackets in the heading

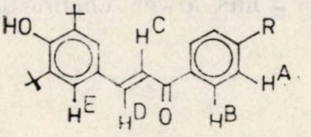

2

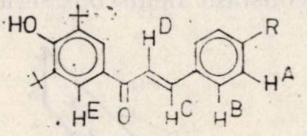

6

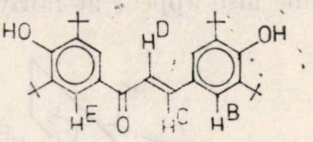

7

Comp.	R	Solvent	tBu (s)	R (s)	OH (s)	$H^A(d^a)$	$H^B(d^a)$	$H^C(d^b)$	$H^D(d^b)$	H^E(s)
2a	H	$CDCl_3$	1.50	—	5.43	7.4^c	$8.^c$	7.4^c	7.7^c	7.50
		C_6D_6	1.30	—	5.13	7.1^c	$7.^c$	7.37	8.03	7.37
2b	Cl	$CDCl_3$	1.50	—	5.57	7.43	7.97	7.30	7.73	7.43
		C_6D_6	1.30	—	5.23	7.03	7.70	7.23	8.00	7.37
2c	F	$CDCl_3$	1.50	—	5.57	7.13^d	8.00^e	7.13	7.50	7.47
		C_6D_6	1.30	—	5.27	6.70^d	7.85^e	7.32	8.07	7.43
2d	Me	$CDCl_3$	1.50	2.40	5.53	7.27	7.90	7.33	7.77	7.43
		C_6D_6	1.30	2.03	5.27	6.93	8.00	7.50	8.13	7.43
2e	NO_2	$CDCl_3$	1.50	—	5.63	8.33	8.06	7.20	7.77	7.43
		C_6D_6	1.33	—	5.27	7.73	7.57	7.20	8.03	7.43
2f	OMe	$CDCl_3$	1.50	3.90	5.57	7.00	8.07	7.40	7.83	7.50
		C_6D_6	1.37	3.70	5.27	6.73	8.03	7.43	8.03	7.47
6a	H	$CDCl_3$	1.50	—	5.73	7.2^a	7.2^c	7.76	7.50	7.93
		C_6D_6	1.33	—	5.46	7.2^c	7.2^c	8.10	7.57	8.20
6f	OMe	$CDCl_3$	1.50	3.83	5.73	6.93	7.57	7.77	7.33	7.90
		C_6D_6	1.37	3.23	5.50	7.00	7.33	8.13	7.57	8.27
7	—	$CDCl_3$	1.48, 1.50	—	5.50 5.67	—	7.47	7.70	7.30	7.90
		C_6D_6	1.37, 1.40	—	5.53 5.70	—	7.46	8.18	7.70	8.20

[a] $^3J_{AB} = 8$ Hz ; [b] $^3J_{CD} = 17$ Hz ; [c] Multiplet obscuring exact data ; [d] $^3J_{HF} = 9$ Hz ; [e] $^4J_{HF} = 6$ Hz

pronounced ASIS effects are observed in compounds **2** for the hydroxy, t-butyl, H^A and R-substituent protons (positive ASIS with $\delta_{C_6D_6} < \delta_{CDCl_3}$) as well as for the H^D protons (negative ASIS with $\delta_{C_6D_6} > \delta_{CDCl_3}$). By contrast, in the ^{1}H-NMR spectra of compounds **6**, the pronounced negative ASIS value characterizes protons H^C and H^E which are in close proximity to the carbonyl group. These effects are in agreement with known data for carbonylic compounds ;[7,8] as shown in Fig. 1 the geometry assumed for compounds **2** and **6** is similar to that determined by X-ray diffractometry in chalcone derivatives.[9]

A brief discussion of the ^{1}H-NMR assignments follows. The remarkable constancy of the tBu signals indicate that these groups are not perturbed by structural variations; the OH and H^E protons in the phenolic ring also appear at fairly constant fields but series **2** has lower chemical shifts than series **6** because the latter series has the carbonyl group directly bonded to the phenolic ring, hence the phenolic proton is expected to have enhanced acidity and all protons to be deshielded relative to the former series. The chemical shifts of H^A protons are lower than those of the H^B protons excepting the nitro-compound **2e**. In series **2**, chemical shifts of H^C are lower than of H^D, and vice-versa in series **6**.

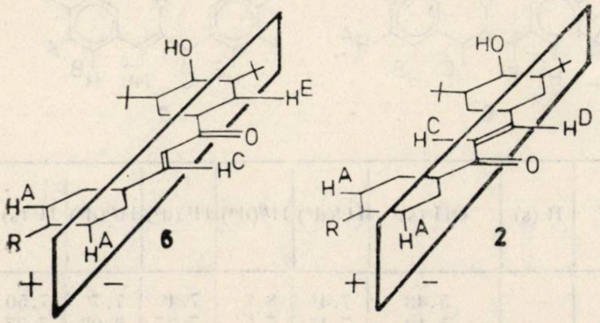

Fig. 1. — Regions for positive and negative ASIS in the ^{1}H-NMR spectra of compounds **2** and **6**.

Interestingly, in the presence of Eu(fod)$_3$ the highest molar induced shifts of **2f** are observed in decreasing order for $H^D > H^B > H^C$, i.e. the protons closest to the carbonyl oxygen which constitutes the coordination centre.

EPR SPECTRA

The EPR spectrum of the aroxyl formed from 3,5-di-t-butyl-4-hydroxystyryl *p*-fluorophenyl ketone by oxidation with lead dioxide (**2c**) shown in Fig. 2 presents a large doublet hyperfine splitting, a small

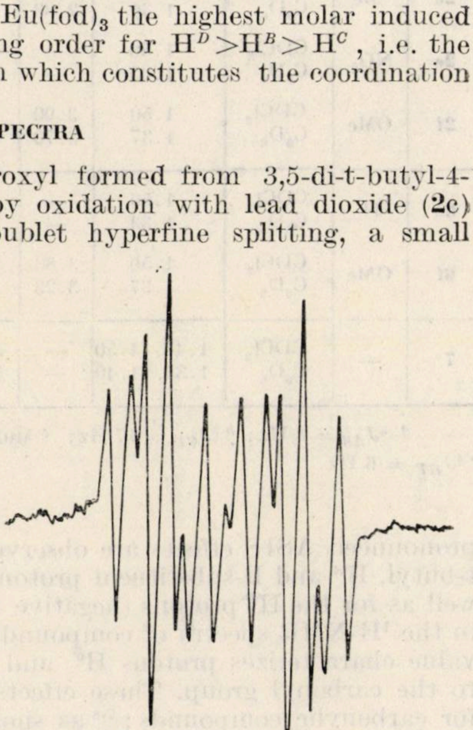

Fig. 2. — EPR spectrum of the aroxyl formed from compound **2c**.

doublet and an intermediate 1 : 2 : 1 triplet splitting ; the hyperfine coupling constants (hfc's) are 0.64, 0.125 and 0.17 mT, respectively.

The last hfc must be assigned to the two equivalent 2,6-protons, H^E, of the styryl residue. We assign the large hfc to the styryl proton, H^C, adjacent to the carbonyl group, taking into account the resonant formulas for the 2-aroxyl, while the small hfc is assigned to the other styryl proton, H^D, adjacent to the aroxyl ring. The g-factor is 2.0048. No hfc is observed for the aroyl nuclei.

The other compounds **2a**, **b**, **d**—**f** gave less well-resolved EPR spectra, but in all cases the trend was similar to the previous one.

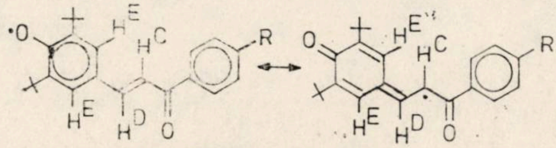

2-Aroxyl

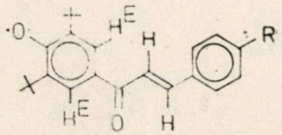

6-Aroxyl

The aroxyl formed by oxidation of 3,5,-di-t-butyl-4-hydroxyphenyl styryl ketone (**6a**) with lead tetraacetate has a simple EPR spectrum with a 1 : 2 : 1 triplet (H^E protons) having $a_H = 0.195$ mT ($g = 2.0051$). Thus, the spin density is confined to the aroxyl ring and has undetectable delocalization beyond the carbonyl group. The same was true for the previous aroxyls **2**, but there the spin density was distributed over the whole styryl residue.

ACKNOWLEDGEMENTS. Thanks are expressed for the UV—VIS determinations to Ms. Rodica Panait and for the IR spectra to Mr. Constantin Toma.

EXPERIMENTAL PART

The ^{1}H—NMR spectra were recorded with a 60 MHz Varian EM—360 L instrument. The ESR spectra were recorded with a Roumanian-made ART—5 spectrometer in the X-band frequency (9060 MHz) using Frémy's salt as standard.

Synthesis of chalcone derivatives **2**, **4**, **7**. Into 375 ml absolute ethanol, gaseous hydrogen chloride (prepared from 30 ml conc. hydrochloric acid and 45 ml conc. sulphuric acid) was dissolved, then 25 mmol each of 3,5-di-t-butyl-4-hydroxybenzaldehyde **1** and substituted acetophenones were added ; after 2 hrs' stirring at room temperature the mixture was left overnight.

Compound **2a** crystallized and was filtered off ; the other compounds were obtained by dilution with water. Purification was effected by recrystalization from ethanol. Reaction yields are in the range 75—80%.

Chalcone derivatives **6** were obtained analogously from 3,5-di-t-butyl-4-hydroxyacetophenone **5** and substituted benzaldehydes (25 mmol each) in 270 mi absolute ethanol into which the same amount of hydrogen chloride as above had been bubbled. The next day **6a** and **6f** were filtered off and recrystallized from ethanol. Yields were about 80%.

REFERENCES

[1] Part III, J.M.Herdan, N.Negoiță, M.N.Grecu, M.D. Gheorghiu and A. T. Balaban, *Rev. Roum. Chim.*, **34**, 1515(1989) ; Part IV, J. M. Herdan, V. Dinoiu, A. Meghea, M. D. Gheorghiu, A. Schiketanz, M. Giurginca and A. T. Balaban, *ibid.*, **35**, 407 (1990).

[2] T. H. Coffield, A. H. Filbey, G. C. Ecke and A. I. Kolka, *J. Amer. Chem. Soc.* **84**, 1625 (1962).

[3] L. A. Cohen and W. M. Jones, *J. Amer. Chem. Soc.*, **84**, 1625 (1962) and previous papers by L. A. Cohen et al.

[4] J. H. Adams, *J. Org. Chem.*, **32**, 3992 (1967).

[5] G. Sipos and F. Sirokman, *Nature*, **202**, 489 (1964).

[6] G. A. Nikiforov, K. M. Dyumaev, A. A. Volodkin and V. V. Ershov, *Izv. Akad. Nauk SSSR, Otdel. Khim. Nauk*, 1836 (1962).

[7] P. Laszlo, *Progress in NMR Spectroscopy*, **3**, 231 (1967).

[8] A. T. Balaban and M. D. Gheorghiu, *Rev. Roum. Chim.*, **23**, 1065 (1978).

[9] N. G. Furmanova, N. I. Sorokina, V. I. Andrianov, U. Bologa and A. T. Balaban, to be published (and references cited therein for five other chalcone derivatives with the same *trans*-geometry of the double bond and *s-cis* conformation of the $C = C - C = O$ system).

Revue Roumaine de Chimie, 35, *10–12*, 1025—1029 (1990)

HETEROCYCLIC COMPOUNDS

SYNTHESIS OF SOME FLUORINATED 1,3,5-TRIAZINE DERIVATIVES

E. TYAGI, S.S. VERMA, L. PRAKASH and R. L. MITAL *

*Department of Chemistry, University of Rajasthan, Jaipur-302004, India

Receiv' l January 24, 1988

2,4-Dichloro-6-(4-fluoroanilino) triazine (I), synthesized by the reaction of cyanuric chloride with 4-fluoroaniline, further reacted with 1 - trifluoromethyl-3-amino-4-chlorobenzene giving rise to 2-chloro-4-(2-chloro-5-trifluoromethylanilino)-6-(4-fluoroanilino)-1, 3, 5-triazine (II). Compound II was condensed with different aromatic amines yielding ten 2-(arylanilino)-6-(2-chloro-5-trifluoromethylanilino)-6-(4-fluoroanilino)-1, 3, 5-triazines (III_{a-j}).

INTRODUCTION AND RESULTS

The literature study revealed the synthesis,[1–4] of trisubstitued triazine derivatives, many of them with properties applicable in medicinal and agricultural fields. Their biological activities are : antimalarial[5], antiulcer, [6–7] antiviral, [8,9] antidiabetic, [9,10] antibacterial, [11] herbicidal, [12,13] antiarthritic, [14] and pesticidal. [15] In the hope of finding better therapeutic values some new fluorinated trisubstituted derivatives of 1, 3, 5-triazine have been synthesized in good yields (75—90 %). The first chlorine atom was replaced by *p*-fluoroaniline at 0—5°C giving rise to 2,4-dichloro-6-(4-fluoroanilino)-1, 3, 5-triazine (I). Compound I was further reacted with 1-trifluoromethyl-3-amino-4-chlorobenzene at 35—40°C, yielding 2-chloro-4-(2-chloro-5-trifluoro-methylanilino)-6-(4-fluoroanilino)-1, 3, 5-triazine

(II). Compound II was condensed with different arylamines at 85—90°C giving rise to ten different derivatives of type III (Scheme I).

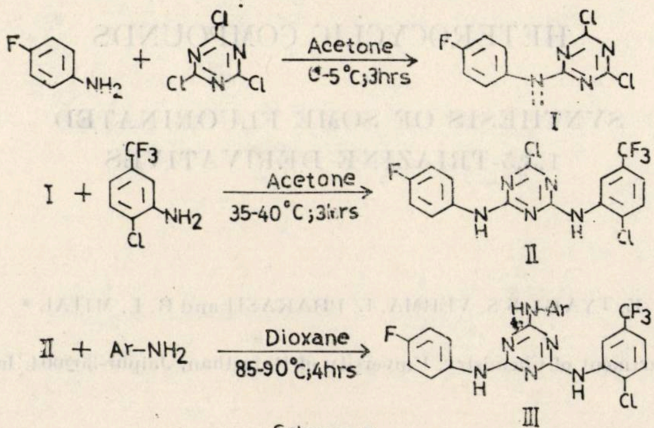

Scheme I

EXPERIMENTAL

IR spectra were recorded on a Perkin-Elmer 577 grating infrared spectrophotometer. ^{1}H and ^{19}F-NMR spectra were scanned on FX × 900 JEOL spectrometer (at 90 MHz).

Synthesis of 2,4-dichloro-6-(4-fluoroanilino)-1, 3, 5-triazine (1)

2, 4, 6-Trichloro-1, 3, 5-triazine (5.5 g; 0,03 mole) was dissolved in acetone (30 mL). To this the solution *p*-fluoroaniline (3.33 g; 0.03 mole) in acetone (20 ml) was added slowly and with stirring followed by the addition of aqueous NaOH (1.2 g; 0.03 mole, in 10 ml of water) in a dropwise manner. The reaction mixture was stirred for 3 hours at 0—5^{0}C. It was poured into the crushed ice and acidified with HCl. The product was filtered, washed, dried and recrystallized from ethanol, m.p. 216^{0}C; Yield 70%; Analysis % $C_9H_5Cl_2FN_4$ Required: C, 41,70; H, 1.93; N, 21.62. Found: C, 41.92; H, 2.13; N, 21.37. IR (KBr) ν_{max} cm^{-1}: 3380 (N—H str): 1250 (Ar-F str), 830 (C_3N_3 str), 795 (C—Cl str). ^{1}H-NMR d$_6$-DMSO δ ppm 10.29 (s, —NH); 7.22—8.35 (m, Ar—H); ^{19}F-NMR (d$_6$-DMSO) δ ppm — 113.405 (s, Ar-F).

Synthesis of 2-chloro-4-(2-chloro-5- trifluoromethylanilino)-6-(4-fluoroanilino)-1, 3, 5-triazine (II)

2, 4-Dichloro-6-(4-fluoroanilino)-1, 3, 5- triazine (I) 6.65 g; 0.025 mole) was dissolved in acetone (30 ml) then, 1-trifluoromethyl 3-amino-4-chlorobenzene-(4.9 g; 0.025 mole) was added with continuous stirring followed by the addition of aqueous NsaOH (1.0 g; 0,025 mole in 10 ml of water) in a dropwise manner. The reaction mixture was stirred for 3 hours at 35—40^{0}C. It was poured into the crushed ice and acidified with HCl. The product was filtered, washed, dried and recrystallized from ethanol, m.p. 173^{0}C; Yield 70%. Analysis % $C_{16}H_9Cl_2F_4H_5$ Required: C,45,93; H, 2.15; N, 16.75. Found: C,46.18; H, 2.27; N, 16.42. IR (KBr) ν_{max}cm^{-2} 3380 (N—H str), 1260 (Ar-F str), 1125 (CF_3 str), 820 (C_3N_3 str) 760 (C-Cl str). ^{1}H-NMR d$_6$-DMSO) δ ppm 9.81—10.42 (s, —NH), 6.68—8.62 (m, Ar—H); ^{1}F-NMR (d$_6$-DMSC) δppm — 55.370 (s, Ar-CF$_3$), —114.331 (s, Ar-F).

Table 1

Characterization and analytical data of compounds III (a—j)

No.	—Ar	Mol. Formula	mp..* (°C)	Yield (%)	Analysis % Required (Found)		
					C	H	N
3a	*p*-$COOHC_6H_4$	$C_{23}H_{15}ClF_4N_6O_2$	170	88	53.23(54.43)	2.89(3.10)	16.20(15.80)
3b	*m*-$COOHC_6H_4$	$C_{23}H_{15}ClF_4N_6O_2$	120	80	53.23(53.46)	2.89(3.09)	16.20(15.85)
3c	*m*-OHC_6H_4	$C_{22}H_{15}ClF_4N_6O$	163	90	53.82(54.16)	3.06(3.36)	17.13(17.51)
3d	*o*-$NO_2C_6H_4$	$C_{22}H_{14}ClF_4N_7O_2$	180	85	50.82(51.14)	2.69(2.91)	18.86(18.44)
3e	*p*-$NO_2C_6H_4$	$C_{22}H_{14}ClF_4N_7O_2$	200	90	50.82(51.12)	2.69(2.99)	18.86(18.56)
3f	*m* $CH_3C_6H_4$	$C_{23}H_{17}ClF_4N_6$	172	75	56.50(56.84)	3.48(3.68)	17.20(17.55)
3g	*o*-$OCH_3C_6H_4$	$C_{23}H_{17}ClF_4N_6O$	165	80	54.71(54.96)	3.37(3.13)	16.65(17.05)
3h	*o*-$OC_2H_5C_6H_4$	$C_{24}H_{19}ClF_4N_6O$	167	85	55.54(55.34)	3.66(3.82)	16.20(15.90)
3i	*m*-ClC_6H_4	$C_{22}H_{14}Cl_2F_4N_6$	160	80	51.87(51.65)	2.75(2.98)	16.50(16.15)
3j	α-$C_{10}H_7$	$C_{26}H_{17}ClF_4N_6$	115	75	59.49(59.81)	3.24(3.58)	16.02(16.42)

* Melting points are uncorrected.

Table 2

The IR, ^{1}H and ^{19}F- NMR spectral data of compounds III (a-j)

No.	—A	IR (KBr) ν_{max} cm^{-1}					^{1}H—NMR (d_6-DMSO) δ ppm for TMS			^{19}F — NMR δ ppm	
		—N— —H	A — F	CF^8	C^8N^8	C—Cl	—NH	Ar—H	—COOH —OH —CH^8 —OCH^8 —OCH^7CH^8	Ar—F	Ar—CF^8
3a	p-$COOHC_6H_4$	3380	1255	1120	820	800	9.21—9.61(m)	6.59—8.36(m)	9.74—10.0 (bs)	—117.749	—57.629
3b	m $COOHC_6H_4$	3400	1260	1110	830	800	8.73—9.74(m)	6.65—8.36(m)	11.08—11.41(bs)	—117.749	—57.687
3c	m-OHC_6H_4	3400	1260	1110	825	800	8.73—10.20(m)	6.32—8.40(m)	8.73—10.20(bs)	—117.922	—58.034
3d	o-$NO_2C_6H_4$	3400	1255	1115	830	805	8.10—8.38(m)	7.03—7.90(m)	—	—117.691	—57.687
3e	p-$NO_2C_6H_4$	3340	1240	1110	820	800	8.20—8.50(m)	6.53—8.10(m)	—	—117.749	—57.687
3f	m $CH_3C_6H_4$	3300	1260	1110	820	800	9.08—9.28(m)	6.68—8.36(m)	2.68(s)	—117.749	—57.629
3g	o-$OCH_3C_6H_4$	3400	1265	1110	830	800	7.93—8.01(m)	6.47—7.74(m)	4.79(s)	—117.749	—57.629
3h	o-$OC_2H_5C_6H_4$	3400	1265	1110	830	800	8.59—9.62(m)	6.27—8.08(m)	4.35(q) 1.55(t)	—117.749	—57.629
3i	m-ClC_6H_4	3400	1260	1110	820	800	8.75—9.08(m)	7.08—8.15(m)	—	—117.749	—57.687
3j	α-$C_{19}H_7$	3460	1255	1100	820	790	9.24—9.65(m)	6.67—8.82(m)	—	—116.648	—57.976

s = singlet, bs = broad singlet, t = triplet, q = quartet, m = multiplet.

Synthesis of 2-(arylanilino)-4-(2-chloro-5-trifluoromethylanilino) 6-(4-fluoroanilino)-1, 3, 5-triazine (III)

2-Chloro-4-(2-chloro-5-trifluoromethylanilino)-6-(4-fluoroanilino)-1, 3, 5-triazine (II) (00.1 mole) was dissolved in 1,4-dioxane (10 mL). The solution of different types of arylamines (00.1 mole) in dioxane (5 mL) and aqueous NaOH (0.01 mole in 5 mL of water) was added. The whole content was heated for 4 hours at 85—90°C. After cooling, it was poured into the crushed ice. The products were filtered, washed, dried and recrystallized from ethanol (Table 1).

SPECTRAL STUDIES
(Table 2)

The IR spectra were recorded by using KBr pellets. The C_3N_3 group frequency was obtained at 830—820 cm^{-1} whereas a broad band in the region 3460—3300 cm^{-1} corresponded to —NH stretching. The absorptions due to the Ar-F and $-CF_3$ linkages were observed in the region 1265—1240 cm^{-1} and 1100—1120 cm^{-1} respectively, and those due to the C—Cl linkage at 805—790 cm^{-1}. The ^1H—NMR spectra were recorded in d_6-DMSO using TMS as an internal standard. The chemical shifts are given in ppm downfield from tetramethylsilane. In trisubstituted compounds aromatic protons occurred as a multiplet in the region δ 6.27—8.82 ppm, whereas the — NH protons were assigned at δ 7.93—10.20 ppm. The integration ratios followed the ratio of chemically different types of protons present in the molecules. In the ^{19}F—NMR spectra, two characteristic signals observed in the range δ—57.629 to—58.034 ppm and δ — 116.648 to 117.922 ppm were assigned to the trifluoromethyl group and fluorine atom carried on the phenyl rings respectively. The ^{19}F—NMR spectra were recorded in d_6-DMSO and the values are relative to hexafluorobenzene used as an external standard.

ACKNOWLEDGEMENTS. We thank University Grants Commission, New Delhi, for providing financial support by awarding Research Fellowships (to E.T. and S.S.V.).

REFERENCES

[1] M. Kucharski and W. Mazurkiewicz, *Pol. PL*, **125**, 312 (1983).
[2] N. Bărbulescu, E. Bărbulescu, L. Ilie, M.G. Spiridon and V.Vasilescu, *Rom RO*, **85**, 390 (1984).
[3] A. Llobera, J. M. Saa and A. Peralta, *Synthesis*, **1**, 95 (1985).
[4] L. J. Stach and J. C. Pomes, Ger. Offen., **DE 3**, 330, 555 (1984).
[5] D. J. Knight and W. Peters, *Ann. Trop. Med. Parasitol.*, **74**, 393 (1980).
[6] A. Nomura, H. Nagasawa, M. Watanabe, H. Yamagata, H. Ninomiya, S. Akitsuki and H. Tamura, *Oyo. Yakuri*, **33**, 121 (1987).
[7] A. Ogino, S. Matsumura and T. Fujita, *J. Med. Chim.*, **23**, 437 (1980).
[8] M. E. Sanders, *U. S. US*, **4**, 576, 945 (1986).
[9] A. Kreutzberger and M. Loch, *Chem. Ztg.*, **110**, 295 (1986).
[10] O. Kristiansen, J. Drabek and V. Fluck, *Eur. Pat. Appl.*, EP **149**, 977 (1985).
[11] B. R. Parekh, N. C. Desai and K. A. Thaker, *J. Inst. Chem*, **57.**, 233 (1985).
[12] K. Morita, K. Ide, Y. Hayase, T. Takahashi and Y. Hayashi, *Agric. Biol. Chem.*, **51, 1339** (1987).
[13] O. F. Curtis, Jr., *Proc. Annu. Meet., Northeast. Weed Sci. Soc.*, **34**, 267 (1980).
[14] A. S. Tomcufcik and A. E. Sloboda, *Ger. Offen.*, **2**, 914, 051 (1979).
[51] M. Takahashi, M. Honda, Y. Murakami and Y. Iwane, *U. S.* **4**, 234, 582 (1980).

Revue Roumaine de Chimie, **35**, *10–12*, 1031–1042 (1990)

LE TRANSFERT DE CHALEUR LIQUIDE-SOLIDE À CHANGEMENT DE PHASE DU SOLIDE

STELIAN PETRESCU et RADU Z. TUDOSE
Institut Polytechnique de Iassy
Faculté de Technologie Chimie

Reçu le 14 mars, 1989

Dans le travail, en utilisant la technique du disque rotatif, on établit un modèle mathématique relatif au processus de fusion des solides. Ce modèle permet le calcul du coefficient individuel de transfert de chaleur. Le modèle mathématique se vèrifie en utilisant des disques de glace et comme liquide de l'eau. Les résultats obtenus montrent une bonne concordance entre les données expérimentales et théoriques en ce qui concerne les valeurs du coefficient individuel de transfert de chaleur.

This paper presents a mathematical model for heat transfer in the process of solid melting, using the rotating disk technique. This model enables the computation of the heat transfer individual coefficient in the melting process. The mathematical model is verified using ice disks which melt in water. The experimental results exhibit a good correspondence with the theoretical values on the heat transfer individual coefficient.

1. INTRODUCTION

Le transfert de chaleur liquide-solide à changement de phase du solide ainsi que le transfert de chaleur solide-liquide à changement de phase du liquide sont des phénomènes constituant la base du processus de fusion, respectivement de solidification, qui ont un grande application en technique. C'est pourquoi la littérature de specialité comprend de nombreux travaux traitant de ces phénomènes [4,6–9].

Dans ce travail, en utilisant la technique du disque rotatif, a été élaboré un modèle mathématique relatif au processus de fusion qui permet le calcul du coefficient individuel de transfert de chaleur. Ce modèle a été obtenu par deux méthodes différentes selon le système dans lequel se produit le processus de fusion : celui avec source intérieure de chaleur ou celui sans source intérieur de chaleur.

Ce modèle a été vérifié expérimentalement, utilisant comme solide des disques de glace et comme liquide de l'eau à 10°C, 12,5°C et 20°C.

2. MODELAGE MATHÉMATIQUE

Le processus du fusion d'un disque rotatif peut être décrit mathématiquement par les équations du transfert d'impulsion, par l'équation rhéologique, par l'équation de la continuité et par l'équation du bilan de l'énergie. Le système d'équations caractérisant l'hydrodynami que d'un disque rotatif a été resolu par Caramn et Cochran qui ont trouvé la solution suivante (relativement aux fluides newtoniens) [3].

$$V_r = r\cdot\omega\left(0{,}51\,\xi - \frac{\xi^2}{2} + \frac{0{,}616}{r}\cdot\xi^3 + \ldots\right) \tag{1}$$

$$V_\theta = r\cdot\omega\left(1 + 0{,}616\,\xi + \frac{0{,}51}{3}\,\xi^2 + \ldots\right) \tag{2}$$

$$V_2 = \sqrt{\nu\cdot\omega}\left(-\,0{,}51\,\xi^2 + \frac{1}{3}\,\xi^3 + \ldots\right) \tag{3}$$

où :

$$\xi = \sqrt{\frac{\omega}{\nu}}\cdot z$$

Dans ces conditions, l'équation de l'énergie[1,2,10],

$$\frac{\partial T}{\partial t} + V_r\frac{\partial T}{\partial r} + \frac{V_\theta}{r}\cdot\frac{\partial T}{\partial\theta} + V_z\frac{\partial T}{\partial z} = a\left[\frac{1}{r}\cdot\frac{\partial}{\partial r}\left(r\frac{\partial T}{\partial r}\right) + \right.$$

$$\left. + \frac{1}{r^2}\cdot\frac{\partial^2 T}{\partial\theta^2} + \frac{\partial^2 T}{\partial z^2}\right] + Sq \tag{4}$$

conjointement aux équations (1—3) décrit le processus de fusion d'un disque en mouvement de rotation, autour de son axe, dans un liquide à comportement newtonien, de la même nature que celle du matériel dont le disque est confectionné.

2.1. La méthode du modelage en cas d'existence d'une source de chaleur

Afin d'établir, en ce cas, le modèle mathématique du processus de fusion a été conçu un modèle physique de ce processus, représenté graphiquement dans la figure 1.

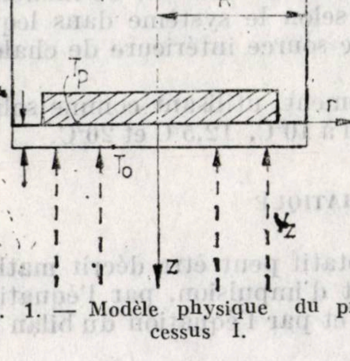

Fig. 1. — Modèle physique du processus I.

Conformément à ce modèle, le liquide se déplace vers la surface du disque suivant la direction z. La température du liquide (To) et celle de la surface du disque (Tp) restent constantes pendant le processus. Le transfert de chaleur se produit par le mécanisme conductif et convectif suivant uniquement la direction z. Grâce à la symétrie axiale $\frac{\partial T}{\partial\theta} = \frac{\partial^2 T}{\partial\theta^2} = 0$. Négligeant les effets d'extrémité et considérant le régime du processus stationnaire, l'équation de l'énergie devient :

$$\bar{V}_z \cdot \frac{\mathrm{d}T}{\mathrm{d}z} = a \cdot \frac{d^2T}{dz^2} + Sq \tag{5}$$

où, tenant compte que la soruce thermique $Sq = \frac{q_v}{\rho \cdot Cp}$, il résulte que :

$$\bar{V}_z \cdot \frac{dT}{dz} = a\, \frac{d^2T}{dz^2} + \frac{q_v}{\rho \cdot Cp} \tag{6}$$

où :

$$q_v = r_f \cdot \Delta H_f$$

En négligeant tous les autres termes de l'équation (3), excepté le remier, la composante axiale de la vitesse du liquide devient :

$$V_z = -\,0{,}51 \sqrt{\frac{\omega^3}{\nu}} \cdot z^2 \tag{7}$$

L'expression de la vitesse moyenne $\bar{V}_z$ est donnée par l'équation :

$$\bar{V}_z = -\,\frac{0{,}51}{\delta} \sqrt{\frac{\omega^3}{\nu}} \int_0^\delta z^2 dz = -\,0{,}17 \sqrt{\frac{\omega^3}{\nu}} \cdot \delta^2 \tag{8}$$

Substituant l'équation (8) en (6) et considérant l'expression de a ($= \lambda/\rho \cdot Cp$) il résulte :

$$\frac{d^2T}{dz^2} + \frac{0{,}17 \cdot \rho \cdot Cp}{\lambda} \sqrt{\frac{\omega^3}{\nu}}\, \delta^2 \cdot \frac{dT}{dz} - \frac{r_f \cdot \Delta H_f}{\lambda} = 0 \tag{9}$$

Si l'on introduit les notations :

$$a_1 = \frac{0{,}17 \cdot \rho \cdot Cp}{\lambda} \sqrt{\frac{\omega^3}{\nu}} \cdot \delta^2 \tag{10}$$

$$K = \frac{r_f \cdot \Delta H_f}{\lambda}$$

l'équation (9) se simplifie :

$$\frac{d^2T}{dz^2} + a_1 \frac{dT}{dz} + K = 0 \tag{11}$$

L'équation (11) aux conditions des limites suivantes,

$$z = 0,\ T = Tp$$

$$z = \delta,\ T = To \tag{12}$$

admet la solution :

$$T = \frac{To - Tp}{e^{-a_1 \cdot \delta} - 1} + Tp - \frac{To - Tp}{e^{-a_1 \cdot \delta} - 1} - \frac{K}{a_1} \cdot z \tag{13}$$

Le flux thermique spécifique transféré vers la surface du disque est donné par l'équation :

$$q = -\lambda \left. \frac{dT}{dz} \right|_{z=\delta} \tag{14}$$

Dérivant l'équation (13) par rapport à la variable z et remplaçant en (14), il résulte que :

$$q = -\lambda \cdot a_1 \frac{To - Tp}{e^{-a_1 \delta} - 1} \cdot e^{-a_1 \cdot \delta} + \frac{K}{a_1} \cdot \lambda \tag{15}$$

Egalisant l'équation (15) à l'équation (16),

$$q = \frac{\lambda}{\delta} \cdot \Delta T, \quad \Delta T = To - Tp, \tag{16}$$

développant dans la série Taylor la fonction $e^{-a_1 \cdot \delta}$, et retenant les deux premiers termes de la série, on obtient

$$a_1 \cdot \Delta T = \frac{K}{a_1}. \tag{17}$$

Etant donné que $q_v = \frac{q}{\delta} = \frac{V_f \cdot \Delta H_f}{\delta} = r_f \cdot \Delta H_f$, remplacant dans l'équation (17) et écrivant la notation :

$$a_1' = \frac{0{,}17 \cdot \rho \cdot Cp}{\lambda} \sqrt{\frac{\omega^3}{\nu}}$$

pour l'épaisseur de la couche thermique il résulte l'expression :

$$\delta = \sqrt[5]{\frac{V_f \cdot \Delta H_f}{a_1' \cdot \Delta T \cdot \lambda}} \tag{18}$$

Le coefficient individuel de transfert de chaleur peut être calculé par la relation :

$$\alpha = \frac{\lambda}{\delta} = \sqrt[5]{\frac{a_1' \cdot \Delta T \cdot \lambda}{V_f \cdot \Delta H_f}} \cdot \lambda \quad . \tag{19}$$

Si l'on substitue l'expression de a_1' dans l'équation (19), il résulte pour α, la relation suivante :

$$\alpha = 0{,}4922 \sqrt[5]{\frac{\rho^2 \cdot Cp^2 \cdot \lambda^4 \cdot \Delta T \cdot \omega^3}{V_f \cdot \Delta H_f \cdot \nu}} \tag{20}$$

où, remplaçant $V_f \cdot \Delta H_f = q$ par $\alpha \cdot \Delta T$ dans l'équation (20), on obtient :

$$\alpha = 0{,}5539 \sqrt[3]{\frac{\lambda^2 \cdot \rho \cdot Cp \cdot \omega^{1,5}}{\nu^{0,5}}} \tag{21}$$

2.2. La méthode de modelage en cas d'absence d'une source intérieure de chaleur

En ce cas on fait appel à un autre modèle physique du processus représenté dans la figure 2. Conformément au modèle physique, le liquide se déplace de manière radiale sur la surface du disque, le transfert de chaleur ayant lieu dans la couche thermique limite à proximité de la surface, grâce au mécanisme moléculaire suivant la direction z et grâce au mécanisme convectif suivant la direction r.

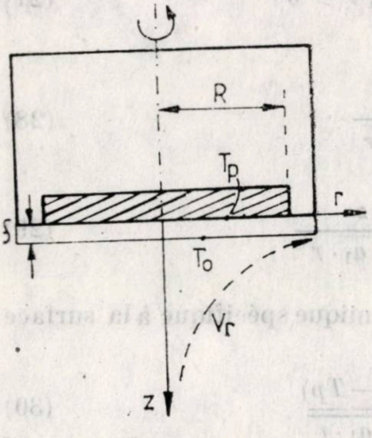

Fig. 2. — Modèle physique du processus II.

Négligeant les effets d'extrémité et considérant le régime stationnaire, l'équation de l'énergie acquiert la forme :

$$V_r \frac{\partial T}{\partial r} = \frac{a}{r} \cdot \frac{\partial T}{\partial r} + a \frac{\partial^2 T}{\partial z^2} \tag{22}$$

Etant donné que $a \ll r$,

$$\frac{a}{r} \simeq 0$$

et l'équation (22) devient :

$$\overline{V}_r \frac{\partial T}{\partial r} = a \frac{\partial^2 T}{\partial z^2} . \tag{23}$$

Si l'on introduit la variation non dimensionnelle pour la température,

$$u = \frac{To - T}{To - Tp} \tag{24}$$

il s'ensuit que,

$$\frac{\partial u}{\partial r} = a_1 \frac{\partial^2 u}{\partial z^2} \tag{25}$$

où :

$$a_1 = \frac{a}{\bar{V}_r} .$$

La vitesse moyenne $\bar{V}_r$ est obtenue par la médiation de la composante radiale de la vitesse du liquide dans l'intervalle $0 - \delta$.

Considérant uniquement le premier terme de l'équation (1), il résulte pour V_r, l'expression :

$$V_r = 0{,}1275\ \omega^{3/2}\ \nu^{-1/2} \cdot R \cdot \delta\ . \tag{26}$$

Les conditions à la limite en ce cas sont :

$$\begin{gathered} r \geqslant 0,\ T = To(u = 0),\ z > 0 \\ z = 0,\ T = Tp(u = 1),\ r > 0 \\ z = \infty,\ T = To(u = 0),\ r > 0 \end{gathered} \tag{27}$$

La solution de l'équation (25) est :

$$u = 1 - \frac{z}{\sqrt{\pi \cdot a_1 \cdot r}} \tag{28}$$

où :

$$\frac{T - To}{Tp - To} = 1 - \frac{z}{\sqrt{\pi \cdot a_1 \cdot r}} . \tag{29}$$

Sur la base de cette équation, le flux thermique spécifique à la surface du disque est :

$$q = - \lambda \left. \frac{\partial T}{\partial z} \right|_{z=0} = \frac{\lambda (To - Tp)}{\sqrt{\pi \cdot a_1 \cdot r}} . \tag{30}$$

Etant donné que q est variable par rapport au rayon, la médiation de q devient nécessaire :

$$\bar{q} = \frac{\lambda (To - Tp)}{R \cdot \sqrt{\pi \cdot a_1}} \cdot \int_0^R r^{-1/2}\, dr = \frac{2 \cdot \lambda (To - Tp)}{\sqrt{\pi \cdot a_1 \cdot R}} \tag{31}$$

Substituant a_1 et V_r dans l'équation (31), il résulte :

$$\bar{q} = \sqrt{\frac{4\cdot 0{,}1275\cdot \lambda\cdot \rho\cdot Cp\cdot \delta\cdot \omega^{1,5}(To - Tp)}{\pi\cdot \nu^{0,5}}}\,. \tag{32}$$

De l'équation (32) on obtient pour δ la relation :

$$\delta = \sqrt[3]{\frac{\pi\cdot \lambda\cdot \nu^{0,5}}{4\cdot 0{,}1275\cdot \rho\cdot Cp\cdot \omega^{1,5}}}\,. \tag{33}$$

Remplaçant l'expression pour l'épaisseur de la couche thermique limite dans l'équation $\alpha = \dfrac{\lambda}{\delta}$, il s'ensuit que :

$$\alpha = 0{,}5489 \sqrt{\frac{\lambda^2\cdot \rho\cdot Cp\cdot \omega^{1,5}}{\nu^{0,5}}}\,. \tag{34}$$

On peut donc constater que les deux équations obtenues pour α (21) et (34) diffèrent très peu et uniquement par la valeur du coefficient numérique qui peut être considéré approximativement 0,55. Par conséquent, l'équation pour le calcul du coefficient individuel de transfert de chaleur est :

$$\alpha = 0{,}55 \sqrt{\frac{\lambda^2\cdot \rho\cdot Cp\cdot \omega^{1,5}}{\nu^{0,5}}}\,. \tag{35}$$

3. LA DÉTERMINATION EXPÉRIMENTALE DU COEFFICIENT α. LA VÉRIFICATION DU MODÈLE MATHÉMATIQUE

La détermination expérimentale du coefficient individuel de transfert de chaleur implique en premier lieu la détermination de la vitesse de fusion. La vitesse de fusion est donnée par la relation :

$$V_f = \frac{\Delta m}{S\cdot \Delta t} \tag{36}$$

où : Δm est la variation de la masse du disque avant et après la fusion ;
S — la surface de contact du disque avec la phase liquide ;
Δt — la durée du contact du disque avec la phase liquide.

Connaissant la vitesse de fusion on peut calculer q respectivement α, sur la base des relations :

$$q = V_f\cdot \Delta H_f \tag{37}$$

$$\alpha = \frac{q}{To - Tp}. \tag{38}$$

Pour déterminer expérimentalement la vitesse de fusion on a utilisé l'installation de laboratoire (fig. 3).

Conformément à la figure 3, l'installation est constituée d'un dispositif pour produire le mouvement de rotation du disque (1) (d'un appareil Rhéotest de laboratoire), d'une pièce de couplage (2) entre le dispositif et le cylindre support (3) pour le disque (4), un vase cylindrique (5) où s'introduit le cylindre-support avec le disque.

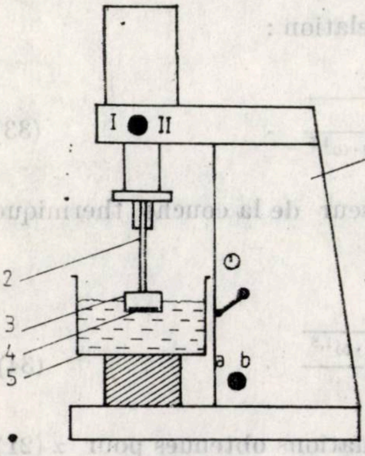

Fig. 3. — Installation expérimentale.

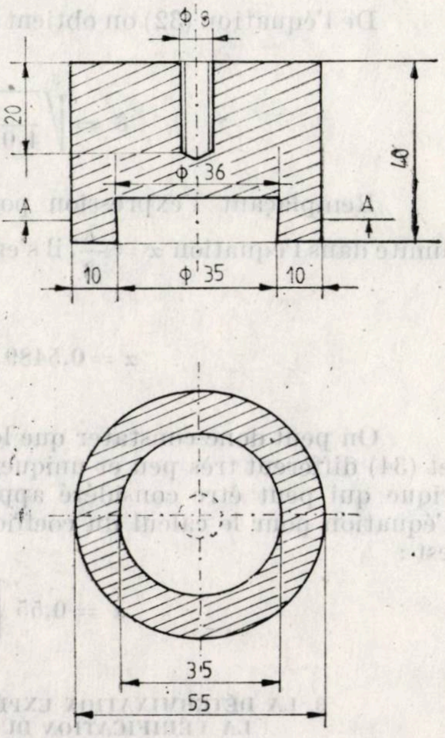

Fig. 4. — Cylindre-support pour les disques.

Le cylindre-support, en polyamide ($D = 55$ mm, $H = 40$ mm) est présenté en fig. 4. Il est prévu, du côté frontal, d'un creux peu conique des dimensions suivantes : $d_1 = 35$ mm ; $d_2 = 36$ mm ; $h = 10$ mm. La fixation du cylindre-support (3) à la pièce de couplage (2) se fait par vissage.

Expérimentalement on a utilisé des disques de glace et comme liquide de fusion de l'eau à des températures de 10°C, 12,5°C et 20°C, qui se sont maintenues constantes pendant les expérimentations. Le nombre de tours du disque a été réglé aux valeurs de 0,60 : 75 : 110 et 130 tours/min.

Les disques de glace ont été réalisés par la technique de congélation d'une quantité d'éau établie au préalable de telle manière que, pendant la congélation, le creux des cylindres-supports soit complètement rempli. Afin d'éviter l'apparition de fissures dans les disques de glace ou la formation de surfaces non uniformes des disques, la congélation s'est effectuée par étapes.

Les cylindres-supports à disques ont été ensuite pesés sur une balance analytique et assemblés successivement à l'installation. Avant cette opération ont été introduits dans le vase (5) 4,5 l d'eau distillée à une température préétablie maintenue constante par changement périodique. Puis, le vase (5) a été approché du cylindre-support pour que celui-ci soit immergé d'un tiers de sa hauteur. Immédiatement après on a commencé l'agitation et le chronométrage. Après un certain intervalle de temps, préétabli expérimentalement, l'agitation a été interrompue, le cylindre-support a été immédiatement démonté, séché avec du papier à filter, et pesé de nouveau sur la même balance analytique. De cette manière on a procédé pour les autres nombres de tours et les autres températures mentionnées plus haut. Utilisant ensuite la relation (36) ont été déterminés la vitesse de fusion, puis sur la base de l'équation (37) le flux technologique spécifiques. Les résultats obtenus sont représentés dans le tableau 1.

Tableau 4

Variation de la vitesse de fusion et du flux thermique spécifique

T(°C)	$10^2 \cdot V_f$[kg/m$^2\cdot$s]				$10^{-3}\cdot q$[W/m^2]			
n $\left[\frac{\text{tours}}{\text{min}}\right]$	5	10	12,5	20	5	10	12,5	20
0	0,447	0,981	1,555	2,541	1,496	3,281	5,281	8,499
60	1,443	3,627	5,658	8,733	4,828	12,134	18,929	29,213
75	1,569	3,779	5,939	1,294	5,249	12,642	19,866	37,781
110	1,729	4,662	7,362	13,248	5,784	15,593	24,628	44,314
130	1,869	5,413	8,714	16,379	6,252	18,106	29,150	54,787

L'équation (38) a permis le calcul du coefficient individuel de transfert de chaleur qui est représenté graphiquement dans le diagrame $\alpha - n$, fig. 5—7.

Pour la vérification du modèle mathématique établi, on a calculé α, utilisant l'équation (35) en prenant les propriétés physiques du liquide de la littérature[5] à la valeur moyenne de la couche limite thermique à la température du liquide et à la température de la paroi. Les valeurs obtenues sont représentées dans le même diagramme $\alpha - n$ aux valeurs expérimentales pour α-, respectivement dans les figures 5—7.

Les figures 5—7 montrent que le modèle mathématique se vérifie suffisamment dans l'intervalle de températures et de nombres de tours considérés. Les résultats obtenus montrent que, pour le calcul du coefficient individuel de transfert de chaleur pendant la fusion, les propriétés physiques du liquide seront considérées à la température de fusion (Tp) pour $T \leqslant 20$°C. Pour $T > 20$°C ces propriétés sont considérées à la température moyenne de la couche limite.

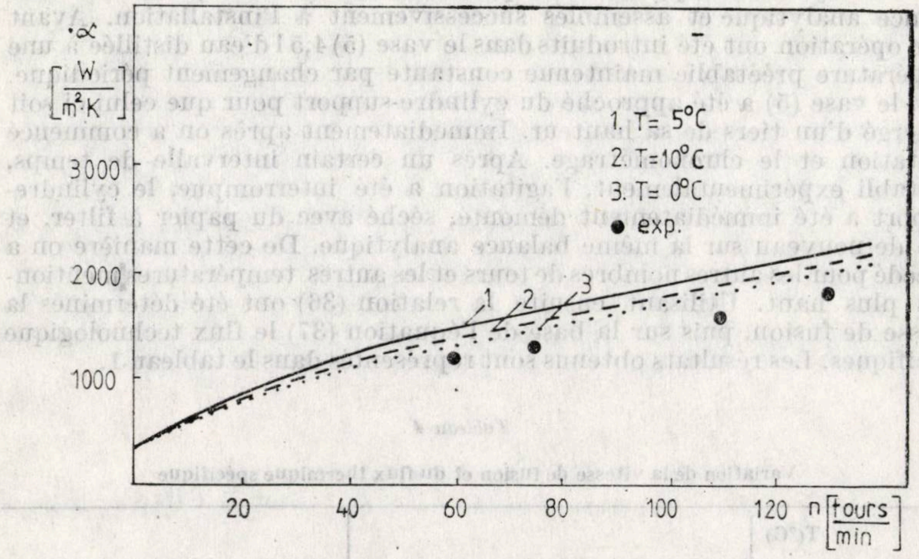

Fig. 5. — Dépendance α — n, *To* = 10°C.

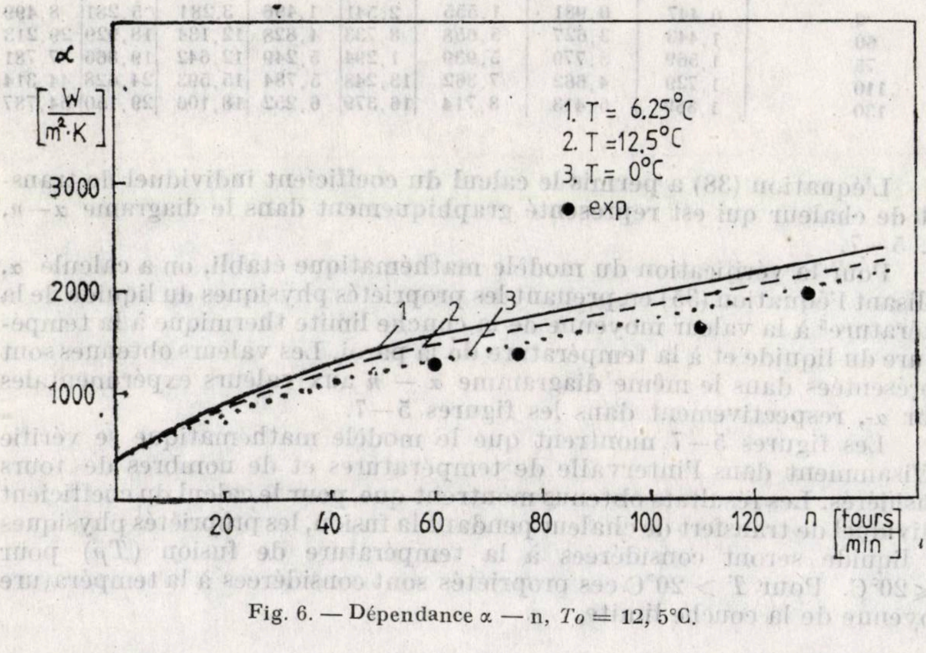

Fig. 6. — Dépendance α — n, *To* = 12, 5°C.

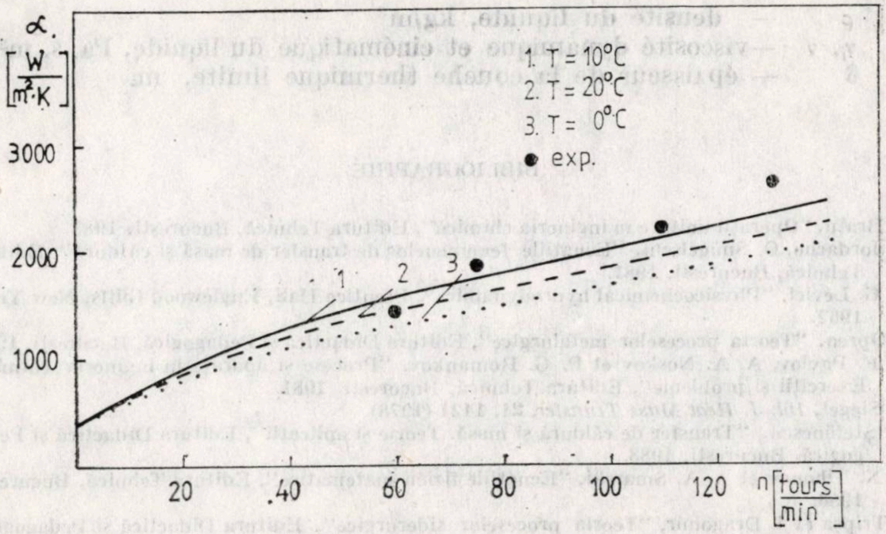

Fig. 7. — Dépendance α — n, $To = 20°C$.

4. CONCLUSIONS

Dans le présent travail on a établi un modèle mathématique pour le processus de fusion, utilisant la technique du disque rotatif, modèle qui permet le calcul du coefficient individuel de transfert de chaleur.

Pour obtenir ce modèle mathématique, deux méthodes différentes ont été utilisées : l'une pour le système avec source intérieure de chaleur, l'autre pour le système dépourvu de source intérieure de chaleur.

Comparant les valeurs du coefficient individuel de transfert de chaleur déterminées expérimentalement aux valeur calculées selon le modèle établi, on a constaté que le modèle se vérifie expérimentalement avec une précision considérable.

NOTES

V_r, V_θ, V_z — composantes radiale, tangente et axiale de la vitesse du liquide, m/s
ω — vitesse angulaire, s^{-1}
n — nombre de tours de disque, tours/min.
t — durée, s
ΔH_f — enthalpie de fusion, J/kg
a — diffusivité thermique du liquide, m^2/s
$\dot{r}_f$ — vitesse de fusion volumétrique, $kg/m^3.s$
V_f — vitesse de fusion, $kg/m^2.s$
q_v — flux thermique spécifiquement volumétrique, W/m^3
q — flux thermique spécifiquement, W/m^2
Cp — chaleur spécifique du liquide, $J/kg.K$

ρ — densité du liquide, kg/m^3

η, ν — viscosité dynamique et cinématique du liquide, Pa. s, m^2/s;

δ — épaisseur de la couche thermique limite, m.

BIBLIOGRAPHIE

[1] E. Bratu, "Operaţii unitare în ingineria chimică", Editura Tehnică, Bucureşti, 1983.

[2] O. Iordache, O. Smigelschi, "Ecuaţiile fenomenelor de transfer de masă şi căldură", Editura Tehnică, Bucureşti, 1981.

[3] V. G. Levici, "Physicochemical hydrodynamics", Prentice Hall, Englewood Cliffs, New York, 1962.

[4] F. Oprea, "Teoria proceselor metalurgice", Editura Didactică şi Pedagogică, Bucureşti, 1978.

[5] K. F. Pavlov, A. A. Noskov et P. G. Romankov, "Procese şi aparate în ingineria chimică. Exerciţii şi probleme", Editura Tehnică, Bucureşti, 1981.

[6] R. Siegel, *Int. J. Heat Mass Transfer*, **21**, 1421 (1978).

[7] D. Ştefănescu, "Transfer de căldură şi masă. Teorie şi aplicaţii", Editura Didactică şi Pedagogică, Bucureşti, 1983.

[8] A. N. Tihonov et A. A. Smarski, "Ecuaţiile fizicii matematice", Editura Tehnică, Bucureşti, 1956.

[9] J. Tripşa et I. Dragomir, "Teoria proceselor siderurgice", Editura Didactică şi Pedagogică, Bucureşti, 1972.

[10] R. Z. Tudose, T. Volintiru, N. Asandei, M. Lungu, E. Merică et Gh. Ivan, "Reologia compuşilor macromoleculari", vol. I, Editura Tehnică, Bucureşti, 1983.

Revue Roumaine de Chimie, **35**, *10 – 12*, 1043 – 1044 (1990)

COMPTES RENDUS

J.K.M. SANDERS and B. K. HUNTER, "MODERN NMR SPECTROSCOPY — A GUIDE FOR CHEMISTS", Oxford University Press, Oxford, 1988, 308 pp., flexicover, ISBN 0-19-855191-6.

As the two authors state in the introduction, this is a book for chemists, rather than for spectroscopists, taking into account the revolution produced in electronics, computers and spin physics, that led to bewildering advances in this techniques of investigating molecules in the last period. The book is a valuable guide for this type of scientists, providing them basic information in order to allow them a thorough exploitation of the different NMR techniques.

The first chapter deals with the one-pulse experiments. Continuous wave techniques are not approached, as they are actually no longer used, excepting for solid-state experiments. Basic principles of NMR are briefly reviewed, with just as much mathematics as needed to avoid incomprehensibility, but stressing on the physical aspects of the given equations. Fundamental notions like: magnetization and precession; the rotating frame of reference; free induction decay; Fourier transformation; relaxation; signal-to-noise ratio and sensitivity; resolution enhancement; as well as some practical aspects are further considered.

The brief, second chapter deals with spin decoupling experiments and difference spectroscopy, stressing again in the end on experimental approaches.

In the 3rd chapter are presented multiple-pulse techniques, pointing out the additional information which is provided by this type of experiments. Two methods are presented, which are used for the detection of the rates at which magnetization returns to equilibrium, after perturbing thes ystem by a pulse, i. e., inversion-recovery sequence — the most common method, and the spin-echoes and transverse relaxation. Thereafter, different sequences for combining pulses are presented, such as INEPT (Insensitive Nuclei Enhanced by Polarization Transfer), refocused INEPT, DANTE (Delays Alternating with Nutations for Tailored Excitation), and others.

The next chapter deals with 2-D techniques. Again the theoretical treatment is a fortunate mixture of pictorial vectors, population arguments and simplified mathematics. Heteronuclear shift correlations with different nuclei (^{13}C, ^{15}N or ^{31}P on one dimension and ^{1}H on the other) are first presented, followed by the description of such techniques as COSY (COrrelated Spectroscopy), SECSY (Spin-Echo Correlated Spectroscopy), and endly, the correlation through multiple-quantum coherence, INADEQUATE. Although the authors state that the approach they used, is somehow "inadequate for INADEQUATE", the description of this type of experiments is excellent, and the examples discussed further enhance the usefulness of such an approach.

Chapter 5 deals with the connections through bonds, for both homo- and heteronuclear one. The sequences previously described (COSY, INADEQUATE, etc.) are abundantly used to determine different structures, from classes of compounds as varied as coenzymes and coordination compounds, like Rh carbonyls, to derivatized sugars and organo-metallics.

Connections through space are approached in the 6th chapter, stressing upon the importance of NOE (Nuclear Overhauser Effect) which may provide a powerful tool for structure determinations. NOESY-type experiments and NOE difference spectroscopy are thereafter presented.

Chapter 7 deals with connections through chemical exchange; such phenomena and notions like: fast/slow chemical exchange; lifetimes and linewidths; the J-scale; the chemical shift anisotropy; the transfer of saturation, are presented, and thereafter, the use of NMR techniques for measuring slow reactions or investigating equilibrium processes.

The extensive 8th chapter deals with the different modes for editing NMR spectra or parts of them. The ways for broadband decoupling, solvent signals supression, suppression of broad lines and editing of sub-spectra are presented.

Chapter 9 deals with the solid-state NMR; the reasons why solids behave differently, and the technical problems that arise are shown, as well as examples of studies feasible with this technique.

The last chapter, the 10th, presents a case of history: sucrose octaacetate. One dimensionnal ^{1}H and ^{13}C, low and high frequency spectra are presented, as well as COSY experiments, ^{1}H — ^{13}C chemical shift correlations and NOE difference spectra. This is an excellent example for the richness of information which may be obtained with the aid of NMR.

The book ends with an appendix dealing with symmetry, non-equivalence and restricted rotation, and naturally, an index.

The book is free of printing errors, and the graphical presentation and the format (specific for OUP books) are very appropriate, making excellency a faint attribute for this important book.

Claudiu Supuran
University of Bucharest

Cecil R. Pace-Asciak, "Mass Spectra of Prostaglandin and Related Products", vol. 18 in "Advances in Prostaglandin, Thromboxane and Leukotriene Research" (formerly "Advances in Prostaglandin and Thromboxane Research"), B. Samuelsson and R. Paoletti Series Eds., Raven Press, New York, 1989, 565 pp., hardcover, ISBN 0-88167-474-5

Mass spectrometry played an essential role in the structural elucidation of the biologically active compounds implied in the polyunsaturated fatty acids (PUFA) cascade. This book stands as an impressive and valuable compendium of mass spectra (MS) of this type of compounds, containing more than 700 selected examples.

The first chapter represents a short review of the biochemical pathways leading to prostaglandins (PGs) and related oxygenated eicosanoids, as well as their metabolic degradation.

The second chapter, extending on more than 500 pages, comprises MS of an enormous range of compounds related to or implied in PUFA metabolism, starting with precursor fatty acids, lypoxygenase products, cytochrome P-450 monoxygenase products, as well as ω-oxidation producsts of fatty acids biotranformation, followed by leukotrienes (LTs), PGs and derivatized PGs, thromboxanes (TXs), cyclic ether fatty acids, and endly, metabolites of the different LTs, PGs and TXs. Under each spectra the information source(s) are cited (but a lot of spectra are unpublished results from the author's laboratory). The graphical presentation, for these figures and the entire book, is excellent; the editor states that a camera-ready copy was used as extensively as possible, and this is a reason why the book is printed error-free.

The third chapter, again a brief one, describes procedures of derivatisation for these classes of compounds, for GC-MS purposes; the different methods of derivatisation of carboxyl, keto and hydroxyl groups are summarized, and experimental examples provided in each case.

The last chapter, the fourth, is an alphabetical order of references of PGs literature. The book is completed with an excellent glossary and a list of abbreviations used in this research field.

For all those involved in PGs and related compounds research, this book is invaluable, but it would be beneficial to the non-expert too, by ways of clarity and excellence in presenting the state-of-the-art in the chemical-physical research of this important group of autacoids.

Claudiu Supuran
University of Bucharest

Revue Roumaine de Chimie, 35, *10–12*, 1045–1054 (1990)

INDEX DES AUTEURS

ABABI V. and N. BILBA, N. NAUM, GH. MIHAILA, Transformations of some hydrocarbons on zeolite catalysts 253

ABDEL-LATIF FATHY FAHIM, Synthesis of several new pyridinone derivatives

ADHIKARI A. VASUDEVA and VIRUPAX V. BADIGER, Synthesis and biological activities of some new isoxazolo [5,4-d] pyrimidine derivatives 757

AFIFY A.A., v. NAGDY S. EL 55

AFIFY A. A. and S. EL-NAGDY, M.A. SAYED, I. MOHEY, Synthesis and reactions of substituted benzoxazinones bearing a bulky group at position-2. Part I . . . 567

AFIFY A. AMIN and A. A. EL-KHAMRY, A. Y. SOLIMAN, M. A. SAYED, E. A. KASSAB, Behaviour of 5,6-diphenyl-4-carbethoxy-2,3-dihydropyridazin-3-one, towards some different nucleophiles 785

ALBALAT A., and E. GÓMEZ, M. SARRET, E. VALLÉS, Contamination by chloride ions in electrode processes (in Spanish) 631

ALBERT M. FRANCISC, voir VOLINTIRU T. 791

ALBU I., voir CHIFU E. 843

ALBU IOSIF, voir ZSAKÓ JÁNOS 867

ALBU IOSIF, voir CHIFU EMIL 879

ANDREI C. and GEORGETA ANDREI, STANA PITA, OLIVIA PITPALAC, IOANA SONOC, Some aspects of linear low density polyethylene synthesis on $TiCl_4/MgCl_2$ catalysts 663

ANDREI GEORGETA, voir C. ANDREI 663

ANDRUH MARIUS and N. STANICA, AURA MEGHEA, M. BERCU, Metal complexes with 4-benzoyl-pyridine. VI. New coordination compounds of copper (II) with 4-benzoyl-pyridine 3

ANDRUH MARIUS, voir SUPURAN CLAUDIU 393

ANDRUH MARIUS, voir BREZEANU MARIA 535

ANGELESCU EMILIAN, Professor dr. docent Ioan V. Nicolescu 143

ANGELESCU EMILIAN, voir NICOLESCU V. IOAN 145

ANGELESCU EMILIAN, voir NICOLESCU V. IOAN 173

ANGELESCU EMILIAN, voir NICOLESCU V. I. — 199

ANGELESCU EMILIAN and PAUL GURĂU, GEORGIANA POGONARU, GAVRIL MUSCA, GRIGORE POP, ECATERINA POP, Conversion of alkanes into gasoline on ZSM-5 zeolite catalysts 229

ANGHEL D.F. and I. MIRCIOAGA, D. R. ELLIS, E. A. DUFF, Phase behaviour of hydrocarbon-water mixtures in the presence of alkylpolyoxyethylene carboxylates 894

ANITESCU G., voir VÎLCU R. 951

ARROYO ANTONIO, Additivity of viscosity in binary and ternary aqueous-organic mixtures 523

AVADANEI V., voir ZANOAGA C.V. 919

AVILA ROSÓN J. C., voir SUAREZ-VARELA J. 639

AVRAMESCU FLORENTINA, voir NICOLESCU V. I. 193

BACIU ION, voir ZALARU FLORICA 731

BADIGER V. VIRUPAX, voir ADHIKARI A. VASUDEVA 757

BADRAN M. M. and A. K. EL-ANSARI, S. EL-MELIGIE, Novel substituted-aminocoumarins as potential antimicrobial agents 777

BALABAN T. ALEXANDRU, voir BRUNVOLL J. 85
— ,, — voir UNCUTA CORNELIA 323
— ,, — — ,, — GHEORGHIU D. MIRCEA 339
— ,, — — ,, — SCHIKETANZ IOSIF 345
— ,, — — ,, — DELEANU CĂLIN 349
— ,, — voir SUPURAN CLAUDIU 399
— ,, — voir HERDAN M. JEAN 407

BALABAN T. ALEXANDRU voir — ,,— Marton ANCA 415
— ,, — ONICIU DANIELA CARMEN 421
BALABAN T. ALEXANDRU and CORNEL CATANĂ, MARCIA DAWSON, ION NICULESCU-DUVAZ, Applications of weighted topological index *J* for QSAR of carcinogenesis inhibitors (retinoic acid derivatives) 997
BALABAN T. ALEXANDRU, voir ONICIU DANIELA CARMEN 561
— ,, — BALABAN MICHAELA-CARMEN 1005
— ,, — HERDAN M. JEAN 1017
BALABAN MICHAELA-CARMEN and THEODOR-SILVIU BALABAN, URSULA BOLOGA, ALEXANDRU T. BALABAN, Synthesis of novel furyl-substituted 3-cyano-2-pyridones 1005
BALABAN TEODOR-SILVIU, voir MARTON ANCA 415
,, — ONICIU DANIELA CARMEN 561
— ,, — BALABAN MICHAELA-CARMEN 1005
BANCIU ANCA, voir BANCIU D. MIRCEA 309
BANCIU D. MIRCEA and MIHAI ELIAN, ANCA BANCIU, CONSTANTIN DRĂGHICI, LIGIA STĂNESCU, PHAN LE THUNG, ECATERINA CIORANESCU, Carbonium ion reactions. XX. Synthesis and acetolysis of 8-chloromethyl-dibenzo [b,d]bicyclo [5.1.0]octa-2,4-diene 309
BANCIU D. MIRCEA, voir SARAMET IOANA 437
BANCIU D. MIRCEA and FILIP CHIRALEU, ANDREIA CIOBANU, Heterocycles with annelated dibenzocycloalkane skeletons. IV. Pyrazoles with annelated 7H-dibenzo [*c*, *e*] cycloheptene skeleton 739
BANCIU D. MIRCEA and IOANA SARAMET, CONSTANTIN DRĂGHICI, Interactions of substituted five-membered heteroaromatic compounds with electron acceptors. III. Charge transfer complexes with tetracyanoethene and tricyanovinylation of some 3-mercapto-1,2,4-triazoles 1009
BANICA G. F. and ELENA DIACU, Catalytic hydrogen prewave in cysteine or cystine-containing solutions. A polarographic and spectrophotometric study 9
BANICA G. F., Voltametric study of a catalytic electrode process with parallel complexation reactions. Reduction of nickel ion in the presence of nicotinamide 693
BARBULESCU V., voir NICOLESCU V. I. 193
BARSZCZ BARBARA and JACEK KULIG, Studies on complexation of Co (II), Ni(II), Cu(II), Zn(II) and Cd(II) with 1-acetylimidazole in aqueous solution 511
BASSIOUNY F. A. EL-, voir ISMAIL M. FEKRY 77
BEJAN CORNELIA, voir STOICA LIGIA 31
BERCU M., voir ANDRUH MARIUS 3
BILBA D., voir BILBA N. 263
BILBA N., voir LEONTE CORNELIA 41
BILBA N., voir ABABI V. 253
BILBA N. and G. STREDIE, D. BILBA, Ion-exchange of palladium in mordenite 263
BLANCO J. M., voir LLANEZA H.M 577
BOLOGA URSULA, voir MARTON ANCA 415
— ,, — BALABAN MICHAELA-CARMEN 1005
BOTEZ LIGIA, voir NICOLESCU V. I. 199
BRĂILEANU ANA, voir ZAHARESCU MARIA 589
— ,, — — ,, — 909
BRETAN V., voir STOICA LIGIA 31
BREZEANU MARIA and E. PINCOVSCHI, DANA MARINESCU, MARIUS ANDRUH, A new preparation method for μ_3-oxo-trinuclear chromium (III) formate 535
BRITCHI MIRELA, voir N. PETRESCU 97
BRUNVOLL J. and R. TOSIĆ, M. KOVACEVIĆ, A. T. BALABAN, I. GUTMAN, S. J. CYVIN, Enumeration of catacondensed benzenoid hydrocarbons and their numbers of Kekulé structures 85
BRUNVOLL J., voir CYVIN S. J. 985

CALDARARU A., voir CALDARARU H. 853
CALDARARU HORIA and AGNETA CARAGHEORGHEOPOL, A. CALDARARU, M. DIMONIE, D. DONESCU, ILEANA DRAGUTAN, N. MARINESCU, Magnetic interaction between nitroxide spin probes and Cu(II) compounds as a method for characterization of penetrability in reversed micelles 853
CALISTRU C., voir LEONTE CORNELIA 41

CARAGHEORGHEOPOL AGNETA, voir H. CALDARARU 853
CATANA CORNEL, voir BALABAN T. A. 997
CATUNEANU V. RODICA, voir STOICA LIGIA 31
CĂPĂŢ C., voir FILOTI G. 215
CĂPĂŢ C., voir FRUNZA LIGIA 221

CHARPIN J., Separation of gases by diffusion and gaseous permeation. Applications of gaseous permeation to the dehydration of natural gas 815
CHIFU EMIL and J. ZSAKÓ, MARIA TOMOAIA-COTISEL, I. ALBU, Interfacial tension extrema at the adsorption from polycomponent systems 843
CHIFU EMIL, voir ZSAKÓ JÁNOS 867
CHIFU EMIL and MARIA TOMOAIA-COTISEL, JÁNOS ZSAKÓ, IOSIF ALBU, AURORA MOCANU, PETRE T. FRANGOPOL, Penetration of procaine hydrochloride into stearic acid monolayers from underlying aqueous solutions 879
CHIRALEU FILIP, voir UNCUTA CORNELIA 323
— ,, — RAZUS C. ALEXANDRU 445
— ,, — BANCIU D. MIRCEA 739
CIOBANU ADALGIZA, voir ZALARU FL. 731
CIOBANU ANDREIA, voir BANCIU D. MIRCEA 739
CIOMOS FLORENTINA, voir ONICIU LIVIU 859
CIORĂNESCU ECATERINA, voir BANCIU D. MIRCEA 309
COCHECI VASILE and GH. PETCA, EUGEN GLÚCK, Studies concerning calcium carbonate scales formation and its preventiom. II. Prevention by inhibitor addition 721
CONDEIU C., voir DRĂGUTAN V. 453
CONSTANTINESCU M., voir SURPATEANU GH. 669
CONSTANTINESCU M., voir COUTURE A. 675
CONSTANTINESCU TITUS, voir LUCA CONSTANTIN 467
CONTINEANU M., SeO$_2$ radiolysis studied by EPR 601
CONTESCU, ADRIANA, voir SPACU P. 617
CORONA J., voir LLANEZA H. M. 577
COSTEA MIOARA, voir TRANDAFIR VIORICA 973
COUTURE A., voir SURPATEANU GH. 669
COUTURE A. and A. LABLACHE-COMBIER, GH. SURPATEANU, M. CONSTANTINESCU, On the photocyclisation of 1-benzamido-2-(1-cyclohexenyl) cyclohexene 675
CRETU STELIANA, voir TOMESCU MARGARETA 649
CRISAN D., voir FRUNZA LIGIA 221
CRISAN D., voir ZAHARESCU M. 909
CRISAN MARIA, voir ZAHARESCU MARIA 589
CRISAN RADU, voir KISS STEFAN 915
CRISTEA I., voir GOCAN S. 49
CYVIN S. J., voir BRUNVOLL J. 85
CYVIN S. J. and J. BRUNVOLL, I. GUTMAN, Annulenes and primitive coronoids: some topological properties and enumerations 985

DANET ANDREI and KIM GWANG SIK, Complexing, extraction and determination of the C$_2$H$_5$Ag$^+$ ion with 1-(p-nitrophenyl), 3-(p'-azobenzene)-triazene 607
DAWSON MARCIA, voir BALABAN T.A. 997
DELEANU CALIN, voir ELIAN MIHAI 299
DELEANU CALIN and ALEXANDRU T. BALABAN, Chemical graphs. Part 53. Benzo- and polybenzo-derivatives of valence isomers of [12]annulene 349
DIACU ELENA, voir BANICA G.F. 9
DIMONIE M., voir H. CALDARARU 853
DINCULESCU ANTONIE, voir SUPURAN CLAUDIU 399
DINOIU VASILE, voir HERDAN M. JEAN 407
DINOIU VASILE, voir HERDAN M. JEAN 1017
DONESCU D., voir CALDARARU H. 853
DRAGAN-BULARDA MIHAIL, voir KISS STEFAN 915
DRAGAN N., voir ZAHARESCU MARIA 589
DRAGHICI CONSTANTIN, voir BANCIU D. MIRCEA 309
— ,, — SARAMET IOANA 437
DRAGHICI CONSTANTIN, voir BANCIU D. MIRCEA 1009
DRAGUTAN ILEANA, voir DRAGUTAN V. 453

DRĂGUȚAN ILEANA CALDARARU H. 853
DRAGUTAN V. and ILEANA DRAGUTAN, C. CONDEIU, ALICE-MARIA GLATZ, Friedel-Crafts chemistry in alicyclic systems. V. Reaction of cyclohexylidine- and 1-cyclohexenylacetic acids with benzene in the presence of $AlCl_3$, CH_3NO_2 as the catalyst 453
DUFF E. A., voir ANGHEL D. F. 891
DULMAN VIORICA, voir ONOFREI TINCA 595
DUMITRIU EMIL and VASILE HULEA, Catalysis by polymers. VI. The epichlorohydrin esterification catalyzed by poly (N,N-dimethyl-p-vinylbenzyl-amine) 657

EL-ANSARI A. K., voir BADRAN M.M. 777
EL-ASKALANY A. H., voir GOMA E. A. 491
EL GABER A. A., voir FOUAD TAHA 503
EL-KHAMRY A. A., voir AFIFI A. AMIN 785
EL-MELIGIE S., voir BADRAN M. M. 777
ELMOTTALB M. ABD and G. ABD EL WAHED, Electrical conductivity of some zincon complexes 701
EL-NAGDY S., voir AFIFI A. A. 567
EL-ROUDI A. M., voir FOUAD ZAHA 503
EL WAHED G. ABD, voir EL MOTTALB M. ABD 701
ELEWADY Y. A., voir GOMAA E. A. 491
ELIAN MIHAI dr. (1937–1988) 279
ELIAN MIHAI, Conformational preference in substituted 5 *H*-dibenzo [*a*,*d*]-cycloheptenes: the influence of a carbon-bonded substituted in position 5 281
ELIAN MIHAI and CALIN DELEANU, SORIN ROSCA, From camphor to bis-[3-(trifluoroacetyl)camphorato] barium(II) in a one step synthesis 299
ELIAN MIHAI, voir BANCIU D. MIRCEA 309
ELLIS D. R., voir ANGHEL D. F. 891

FILOTI G. and VIORICA SPANU, I. UDREA, MARIANA UDREA, C. CAPAT, I. V. NICOLESCU, Mösbauer investigation of Fe-Cu-K catalysts for hydrocarbon synthesis 215
FRANGOPOL T. PETRE, voir ZSAKÓ JÁNOS 867
— „ — CHIFU EMIL 879
FRUNZA LIGIA and MARIANA UDREA, C. CAPAT, D. CRISAN, I. V. NICOLESCU, IR study of metal-suppport interactions in Ni/Al_2O_3 catalysts for CO hydrogenation 221

GAINAR I., voir VILCU R. 951
GANESCU I. and CS. VÁRHELYI, I. ZSAKÓ, M. PREDA, New tetrathiocyanatodiamine chromates (III) with imidazole and benzimidazole (in German) 767
GARCIA REJÓN L., voir SUAREZ-VARELA J. 639
GARTNER MARIUCA and N. STANICA, MIHAI VASS, Ellipsometric spectroscopy of pure and of oxygen and carbon monoxide-copper films 713
GHEORGHIU D. MIRCEA, voir UNCUTA CORNELIA 323
GHEORGHIU D. MIRCEA and IOSIF SCHIKETANZ, ANA SCHIKETANZ, ALEXANDRU T. BALABAN, ^{13}C-NMR spectral assignments for 2,5-diarylthiazoles 339
GHEORGHIU D. MIRCEA, voir SCHIKETANZ IOSIF 345
— „ — SUPURAN CLAUDIU 399
— „ — HERDAN M. JEAN 407
— „ — MARTON ANCA 415
— „ — ONICIU DANIELA CARMEN 421
GHEORGHIU D. MIRCEA and LUMINITZA PARVULESCU, K. M. TURDIBEKOV, Yu. T. STRUCHKOV, Crystal and molecular structure of the 2-t-butyl-2-cyanocyclobutanones resulted from the cycloaddition of Moore's ketene to *endo*- and *exo*-benzocyclobutanonorbornenes 427
GHEORGHIU D. MIRCEA, voir HERDAN M. JEAN 1017
GIRDHAR K.K., voir KUMAR N. 555
GIURGINCA MARIA, voir HERDAN M. JEAN 407
— „ — VOLINTIRU T. 791
GLATZ ALICE-MARIE, voir DRAGUTAN V. 453

GLÜCK EUGEN, voir COCHECI V. 721
GOCAN S., and LILIANA OLENIC, I. CRISTEA, Optimization of the mobile phase in thin layer chromatography for the sepraration of 4-benzylidene-1-pyrimidyl-5-pyrazolone dyes 49
GOLIAT LUCIA, voir STOICA RODICA 805
GOMAA E. A. and Y. A. ELEWADY, A. H. EL-ASKALANY, Mechanism of electroreduction of sodium nitroprusside (SNP) 491
GÓMEZ E., voir ALBALAT A. 631
GOTHÁRD A. FRANCISC, GHEORGHITA JINESCU, VICTORIA SAVESCU, Generalized correlation for vapor pressures of organic compounds 105
GRANDCLAUDON P., voir SURPATEANU G. 669
GUARDIA CARRILLO T., voir SUAREZ-VARELA J. 639
GURAU PAUL, voir ANGELESCU EMILIAN 229
GUTMAN I., voir BRUNVOLL J. 85
GUTMAN I., voir CYVIN S. J. 985
GWANG SIK KIM, voir DANET ANDREI 607

HAIDUC IONEL, voir SILAGHI-DUMITRESCU IOAN 475
HASHASH M. A. EL-, voir NAGDY S. EL- 55
HERDAN M. JEAN and VASILE DINOIU, AURELIA MEGHEA, MIRCEA D. GHEORGHIU, ANA SCHIKETANZ, MARIA GIURGINCA, ALEXANDRU T. BALABAN, Synthesis and EPR spectra of persistent aroxyls. IV. *Ortho*, *ortho*'-disubstituted phenols possessing in the *para*-position a 2-bonded-1,3-dicarbonylic (or a functionally related) group 407
HERDAN M. JEAN and DINOIU VASILE, AURELIA MEGHEA, ANA SCHIKETANZ, MIRCEA D. GHEORGHIU, A. T. BALABAN, Synthesis and EPR spectra of persistent aroxyls. V. Aroxyls derived from chalcone and derivatives 1017
HOFFMANN ROALD, Creation and discovery 305
HULEA VASILE, voir DUMITRIU EMIL 657

IANCU I. ADRIAN, voir RAZUS C. ALEXANDRU 445
IEVLEV A. L. and V. V. TEPLYAKOV, Modern methods for determining the gas permeation and predicting the properties of dispersed polymer systems 831
IFRIM LIVIA, voir LEONTE CORNELIA 41
INATIMI EBI B. EDWARD, Multi-element analysis by solvent extraction and high performance liquid chromatography of soil samples 495
IONESCU LIGIA, voir MANDRAVEL CRISTINA 961
ISMAIL M. FEKRY, FEKRIA S. SAYED, F. A., EL-BASSIOUNY, H. A. YOUNES, Reactions with N-aminophthalimide and some allied compounds 77
IVAN GH., voir VOLINTIRU T. 791

JINESCU GHEORGHIȚA, voir GOTHÁRD A. FRANCISC 105
JITARU MARIA, voir ONICIU LIVIU 859

KASSAB E. A., voir AFIFI A. AMIN 785
KISS STEFAN and MIHAIL DRAGAN-BULARDA, DANIELA PASCA, HENRIETTE PINTEA, EVA ZBOROVSCHI, VASILE MUNTEAN, RADU CRISAN, Use of zeolite as an adsorbing surface for modelling systems analogous to therapeutic mud 915
KOLOZSI E., voir VODNÁR J. 927
KOVAČEVIĆ M., voir BRUNVOLL J., 85
KULIG JACEK, voir BARSZCZ BARBARA 511
KULKARNI M. GEETA and MANOHAR V. KULKARNI, VERMANNA D. PATIL, D. B. SHRIDHAR, M. LAXMANA, Synthesis and anti-inflammatory activity of some new triheterocyclic thiazoles 549
KULKARNI V. MANOHAR, voir KUDKARNI M. GEETA 549
KUMAR NARINDER, voir MITTAL S. P. 23
KUMAR N., voir MITTAL P. S. 555
KRAITER DANIEL, voir STERNBERG S. 941

LABLACHE-COMBIER A., voir SURPATEANU G. 669
— ,, — COUTUREA. 675
LAJIDE L., voir OLAGBEMIRO T. O. 545

LAXMANA M., voir KULKARNI M. GEETA 549
LECA MINODORA and SERBAN R., ANTOANETA VELICU, Dispersion of a cataphoretic resin in view of electrodeposition 967
LEONTE CORNELIA, AL. SZÉP, N. BILBA, C. CALISTRU, LIVIA IFRIM, GH. MIHAILA, On thermal decomposition of dolomite 41
LINTES GH., voir SANDULESCU I. 207
LLANEZA H. M. and J. CORONA, J. M. BLANCO, Optimization by computer of the alkaline hydrolysis of isoamyl acetate 577
LÓPEZ-DE-ALBA P. L. and A. VERGARA, Potentiometric determination of thorium (in Spanish) 707
LÖWY A. DAN, voir ONICIU LIVIU 859
LUCA CONSTANTIN and LUCIA MUTIHAC, TITUS CONSTANTINESCU, Separation of amino acids by liquid membranes with macrocyclic carriers 467

MANDRAVEL CRISTINA and LIGIA IONESCU, The influence of various factors on the optical activity of some essential aminoacids. II 961
MANOLE GHEORGHE, voir PUSCAS IOAN 683
MARINESCU DANA, voir BREZEANU MARIA 535
MARINESCU M., voir CALDARARU H. 853
MARTON ANCA and URSULA BOLOGA, TEODOR-SILVIU BALABAN, MIRCEA D. GHEORGHIU, ALEXANDRU T. BALABAN, ^{1}H-NMR assignments for 2,4-diaryl-pyrylium salts and —pyridines having fused 5- or 6-membered saturated rings bridging 5,6-position 415
MARTON ANCA, voir ONICIU DANIELA CARMEN 561
MATACHE S., voir ZANOAGA C. V. 919
MEGHEA AURA, voir ANDRUH MARIUS 3
MEGHEA AURELIA, voir HERDAN M. JEAN 407
— ,, — — ,, — 1017
MIHAILA GHEORGHE, voir LEONTE CORNELIA 41
— ,, — ABABI V. 253
MIRCIOAGA I., voir ANGHEL D.F. 891
MITAL R. L., voir TYAGI E. 1025
MITTAL S. P. and NARINDER KUMAR, A. D. TANEJA, Spectral studies of some thiazolyl and pyrimidyl substituted thiocarbamides in different solvents . . . 23
MITTAL P. S. and N. KUMAR, K. K. GIRDHAR, A. D. TANEJA, J. S. TYAGI, Kinetic studies of tautomerisation and effect of temperature on enethiol contents of some carboxyalkyl-thiocarbamides 555
MOCANU AURORA, voir ZSAKÓ J. 867
— ,, — CHIFU EMIL 879
MOHEY I., voir AFIFI A. A. 567
MORJAN MARILENA, voir ONICIU D. C. 421
MOUCHEL B., voir SURPATEANU G. 669
MUNTEAN VASILE, voir KISS STEFAN 915
MUREȘAN N., voir VODNAR J. 927
MUSCA GAVRIL, voir ANGELESCU EMILIAN 229
MUTIHAC LUCIA, voir, LUCA CONSTANTIN 467

NAGDY S. EL-, M. A. EL-HASHASH, A. A. AFIFY, F. EL-SHAHED, Behaviour of benzoxazinone derivatives bearing a bulky group at position-2 toward some nitrogen and carbon nucleophiles. Part 2 55
NAUM N., voir ABABI V. 253
NECHIFOR G., voir ZANOAGA C. V. 923
NECHIFOR GHEORGHE and GEORGETA POPESCU, Asymmetric membranes prepared by immersion-precipitation technique 899
NEDELCU GH., voir NICOLESCU V. I. 185
NEGOITA NICOLAE, voir ONICIU DANIELA CARMEN 421
NICOLAU MARGARETA, voir STOICA LIGIA 31
NICOLESCU V. IOAN and VIORICA PARVULESCU, VASILE PARVULESCU, EMILIAN ANGELESCU, Preparation of the metallic supported catalysts from precursors with different immobilization capacities on γ-Al_2O_3 surface. I. γ-Al_2O_3 impregnation with a metallic species 145
NICOLESCU V. IOAN and VIORICA PARVULESCU, VASILE PARVULESCU, IOAN SANDULEȘCU, Preparation of the metallic suppported catalysts from

precursors with different immobilization capacities on γ-Al_2O_3 surface. II. Impregnation of the catalyst support Pd/γ-Al_2 O_3 with the second metallic component 161

NICOLESCU V. IOAN and VIORICA PARVULESCU, VASILE PARVULESCU, EMILIAN ANGELESCU, Preparation of the metallic supported catalysts from precursors with different immobilization capacities on γ-Al_2O_3 surface. III. The drying influence on the distribution of metallic components 173

NICOLESCU V. I. and GH. NEDELCU, A. ZSABO, Study of the electroconductivity of the Fe-Mg-O catalytic system used in the reaction of n-butenes oxidehydrogenations to butadiene 185

NICOLESCU V. I. and FLORENTINA AVRAMESCU, V. BĂRBULESCU, Catalyst for vapor-phase synthesis of isoprene from isobutene and formaldehyde . 193

NICOLESCU V. I. and LIGIA BOTEZ, EMILIAN ANGELESCU, Ethylene dimerisation catalyzed on coordinative compounds fixed on oxide supports 199

NICOLESCU V. I., voir SĂNDULESCU I. 207

—,,— FILOTI G. 215

—,,— LIGIA FRUNZĂ 221

NICULESCU-DUVĂZ ION, voir BALABAN T. A. 997

ODOCHIAN LUCIA, voir ONOFREI TINCA 595

OLAGBEMIRO T. O. and L. LAJIDE, Chemical components of the scent gland of the green vegetable bug: *Nezera viridula* 345

OLENIC LILIANA, voir GOCAN S. 49

ONICIU DANIELA CARMEN and NICOLAE NEGOIŢĂ, MARILENA MORJAN, MIRCEA D. GHEORGHIU, A. T. BALABAN, Synthesis of substituted benzoins and the corresponding bis-1,2-emedithiol complexes of nickel, platinum and palladium 421

ONICIU DANIELA CARMEN and ANCA MARTON, TEODOR-SILVIU BALABAN, SORIN VLAD, A. T. BALABAN, Synthesis of 2,6-dimethyl-4-styrylpyrylium salts (from 2,4,6-trimethylpyrylium and donor-substituted benzaldehydes) and their conversion into pyridines 561

ONICIU LIVIU and IOAN A. SILBERG, DAN A. LÖWY, MARIA JITARU, FLORENTINA CIOMOS, OVIDIU HOREA OPREA, BOGDAN C. TOMA, MARIANA TOMA, Effect of surfactants on the electroreduction of acrylonitrile 859

ONOFREI TINCA and LUCIA ODOCHIAN, VIORICA DULMAN, Cu(II), Zn(II), Cd(II), Co(II) and Ni(II) sorption on p(benzylcellulose)-5-azo-8-hydroxyquinoline. Thermogravimetric characterization 595

OPREA OVIDIU HOREA, voir ONICIU LIVIU 859

OYMAN ÜLKÜ, Dehydration of some 1-(2′-furyl)- and 1-(2-thienyl)-1-alkanols using cobalt (II) sulphate as catalyst 63

PATIL D. VEMANNA, voir KULKARNI M. GRETA 549

PATRON LUMINITA, voir SPACU P. 617

PASCA DANIELA, voir KISS STEFAN 915

PÂRVULESCU LUMINITZA, voir GHEORGHIU D. MIRCEA 427

PÂRVULESCU VASILE, voir NICOLESCU V. IOAN 145

—,,— —,,— 161

—,,— —,,— 173

PÂRVULESCU VIORICA, voir NICOLESCU V. IOAN 145

—,,— —,,— 161

—,,— —,,— 173

PETCA GHEORGHE, voir COCHECI V. 721

PETREA CARMEN, voir ZALARU FL. 731

PETRESCU MARIA, voir PETRESCU N. 97

PETRESCU N. and MARIA PETRESCU, MIRELA BRITCHI, Diffusion of vanadium in iron in surface coatings and calculation of diffusion coefficients . . . 97

PETRESCU STELIAN and RADU Z. TUDOSE, On the liquid-solid heat transfer with solid phase change (in French) 1031

PETRIDE HORIA, voir RAILEANU DAN 459

PETRIDE HORIA, Mesoionic oxazolones. V. Ethanolysis and aminolysis of acylated compounds 747

PINCOVSCHI E., voir BREZEANU MARIA 535
PINTEA HENRIETTE, voir KISS STEFAN 915
PITPALAC OLIVIA, voir ANDREI C. 663
PIȚĂ STANA, voir ANDREI C. 663
PÎRLOG CONSTANȚA, voir ZAHARESCU MARIA 589
—,,— —,,— 909
PLOSTINARU SILVIA, voir SPACU P. 617
POGONARU GEORGIANA, voir ANGELESCU EMILIAN 229
POP ECATERINA, voir ANGELESCU EMILIAN 229
POP GRIGORE, voir ANGELESCU EMILIAN 229
POPESCU GEORGETA, voir NECHIFOR GH. 899
POPESCU MARIA, Study on the reaction and composition of the Hg(II) complex with diazoaminobenzene 67
PRAKASH L., voir TYAGI E. 1025
PREDA M., voir GĂNESCU I. 767
PUȘCAȘ IOAN, voir SUPURAN CLAUDIU 393
—,,— —,,— 399
PUȘCAȘ IOAN, CLAUDIU SUPURAN, GHEORGHE MANOLE, Carbonic anhydrase inhibitors. III. Relations between chemical structure of inhibitors and activators 683

RAO A. L. J., voir VERMA NEELAM 625
RAILEANU DAN and HORIA PETRIDE, Mesoionic oxazolones. IV. Protonation of planar and nonplanar acylated compounds 459
RAZUS C. ALEXANDRU and FILIP CHIRALEU, ADRIAN I. IANCU, Solvolyses of 2-aryl-1-cyclopropylethanols and their 3,5-dinitrobenzoates 445
ROBU ELENA, voir TRANDAFIR VIORICA 973
ROȘCA SORIN, voir ELIAN MIHAI 299
ROȘCA SORIN, voir STERNBERG SOLOMON 941
RUSSU R., voir SĂNDULESCU I. 207

SAHINI MARINA, voir ZAHARESCU MARIA 589
SARRET M., voir ALBALAT A. 631
SAYED M. A., voir AFIFI A. A. 567
—,,— —,,— 785
SAYED S. FEKRIA, voir ISMAIL M. FEKRY 77
SANDULESCU IOAN, voir NICOLESCU V. I. 161
SANDULESCU I. and R. RUSSU, GH. LINTES, O. ȘERBAN, I. V. NICOLESCU, $Al_2O_3-SiO_2$ and HMgY acidity and reactivity in isomerization of 1-hexene and transalkylation of toluene 207
SAVESCU VICTORIA, voir COTHARD A. FRANCISC 105
SCHIKETANZ ANA, voir GHEORGHIU D. MIRCEA 339
SCHIKETANZ ANA, voir SCHIKETANZ IOSIF 345
—,,— SUPURAN CLAUDIU 399
—,,— HERDAN M. JEAN 407
—,,— —,,— 1017
SCHIKETANZ IOSIF, voir GHEORGHIU D. MIRCEA 339
SCHIKETANZ IOSIF and ANDREI ȘTEFĂNESCU, MIRCEA D. GHEORGHIU, ANA SCHIKETANZ, ALEXANDRU T. BALABAN Aminoketone, oxazole and thiazole syntheses. Part XII. 2,5-Diarythiazoles from thioazlactones and aromatic hydrocarbons 345
SEGAL EUGEN, voir TOMESCU MARGARETA 649
SHAHED F. EL-, voir NAGDY S. EL. 55
SHRIDHAR D. B., voir KULKARNI M. GRETA 545
SHUJI SAITO, Critical surfactant concentration in the interaction between nonionic surfactants and polyacrylic acid. Effects of hydrophobic and polyoxyethylene moieties of surfactants 821
SILAGHI-DUMITRESCU IOAN and IONEL HAIDUC, The electronic structure of $(H_3SiNSiH_3)$ anion. A simple molecular orbital treatment 475
SILBERG A. IOAN, voir ONICIU LIVIU 859
SINGH HARVIR and SURENDRA PAL SINGH TOMAR, Studies on viscosity of magnesium soaps of higher fatty acids in dilute aqueous solutions at different temperatures 539

SOLIMAN A. Y., voir AFIFI A. AMIN . . . 785
SONOC IOANA, voir ANDREI C. . . . 663
SPACU P. and LUMINIŢA PATRON, SILVIA PLOSTINARU, ADRIANA CONTESCU, N. STANICA, Coordination compounds as raw materials for mixed oxides. VI. Mixed coordination compounds of lanthanoides and Cr (III) as precursor of chromites . . . 617
SPANU VIORICA, voir FILOTI G. . . . 215
STANESCU LIGIA, voir BANCIU D. MIRCEA . . . 309
STANICĂ N., voir ANDRUH MARIUS . . . 3
—„— SPACU P. . . . 617
STANICA NICOLAE, voir GARTNER MARIUCA . . . 713
STERNBERG SOLOMON and MIHAELA UNGUREANU, SORIN ROSCA, DANIEL KRAITER, Electrochemical oxidation of carboxylic acids. III. Electrode processes in electrochemical oxidation of natrium monomethyl adipate on graphite . . . 941
STOICA LIGIA, RODICA V. CATUNEANU, CORNELIA BEJAN, MARGARETA NICOLAU, V. BRETAN, Recovery of metallic ions from waste waters by flotation . . . 31
STOICA RODICA and LUCIA GOLIAT, Surfactants in film-forming industry . . . 805
STREDIE G., voir BILBA N. . . . 263
STRUCHKOV T. YU., voir GHEORGHIU MIRCEA . . . 427
SUAREZ-VARELA J. and J. C. AVILA ROSÓN, L. GARCIA REJÓN. T. GUARDIA CARRILLO, Complexes of 3,5-xylylamine-N, N-diacetic acid with various metal ions . . . 639
SUPURAN CLAUDIU and MARIUS ANDRUH, IOAN PUSCAS, Carbonic anhydrase inhibitors. I. Metal complexes of sulfonamides: a novel class of carbonic anhydrase inhibitors . . . 393
SUPURAN CLAUDIU and A. T. BALABAN, MIRCEA D. GHEORGHIU, ANA SCHIKETANZ, ANTONIE DINCULESCU, IOAN PUŞCAŞ, Carbonic anhydrase inhibitors. II. Membrane-impermeable derivatives of 1,3,4-thiadiazole-2-sulfonamide . . . 399
SUPURAN CLAUDIU, voir PUSCAS IOAN . . . 683
SURENDRA PAL SINGH TOMAR, voir SINGH HARVIR . . . 539
SURPATEANU G. and M. CONSTANTINESCU, A. LABLACHE-COMBIER, P. GRANDCLAUDON, B. MOUCHEL, A. COUTURE, Theoretical and experimental study on the cycloaddition between 4-(p-tolyl)1,2,4-triazolium (p-methoxy)-phenacylide and ethyl cinnamate . . . 669
SURPATEANU G., voir COUTURE A. . . . 675
SZÉP AL., voir LEONTE CORNELIA . . . 41
SZABO A., voir NICOLESCU V. I. . . . 185
SZABO ALFRED, Characterization of MoO$_3$—Fe$_2$O$_3$ catalysts containing admixtures of metal oxides by the method of electroconductivity . . . 239
The 3rd Symposium on colloid and surface chemistry . . . 803

ŞARAMET IOANA and CONSTANTIN DRAGHICI, M. D. BANCIU, Interactions of substituted five-membered heteroaromatic compounds with electron acceptors. II. Interaction of 2-p-bromophenylsulphonyl-phenyl-5-ethylamino-1,3,4-thiadiazole with tetracyanoethene . . . 437
ŞARAMET IOANA, voir BANCIU D. MIRCEA . . . 1009
ŞERBAN O., voir SĂNDULESCU I. . . . 207
ŞERBAN R., voir LECA M. . . . 967
ŞTEFĂNESCU ANDREI, voir SCHIKETANZ IOSIF . . . 345

TAHA FOUAD and A. M. EL-ROUADI, A. A. ABD EL GABER, F. M. ZAHRAN, Adsorption of cations on oxides . . . 503
TANEJA D. A., voir MITTAL S. P. . . . 23
TANEJA A. D., voir MITTAL P. S. . . . 555
TEPLYAKOV V. V., voir IEVLEV A. L. . . . 831
LE THUY PHAN, voir BANCIU D. MIRCEA . . . 309
TOMA C. BOGDAN, voir ONICIU LIVIU . . . 859
TOMA MARIANA, voir ONICIU LIVIU . . . 859
TOMESCU MARGARETA and EUGEN SEGAL, STELIANA CREȚU, Thermal behaviour of acrylamide-maleic anhydride-styrene terpolymer . . . 649

TOMOAIA-COTISEL MARIA, voir CHIFU EMIL 843
—,,— ZSAKÓ J. 867
—,,— CHIFU EMIL 879
TOŠIĆ R., voir BRUNVOLL J. 85
TRANDAFIR VIORICA and MIOARA COSTEA, ELENA ROBU, Morphological characterization of collagen membranes for medical textile prosteses 973
TUDOSE Z. RADU, voir PETRESCU STELIAN 1031
TURDIBEKOV M. K., voir GHEORGHIU D. MIRCEA 427
TYAGI J. S., voir MITTAL P. S., ... 555
TYAGI E. and S. S. VERMA, L. PRAKASH, MITAL R. L., Heterocyclic compounds. Synthesis of some fluorinated 1,3,5-triazine derivatives 1025

UDREA I., voir FILOTI G. 215
—,,— FRUNZĂ LIGIA 221
UDREA MARIANA, voir FILOTI G. 215
—,,— FRUNZĂ LIGIA 221
UGLEA C. V., voir ZANOAGĂ C. V. 919
—,,— —,,— 923
UNCUȚĂ CORNELIA and FILIP CHIRALEU, MIRCEA D. GHEORGHIU, ALEXANDRU T. BALABAN, Reactions of pyrylium salts with nucleophiles. XV. Stereoisomers of polyarylpyridinium salts and their interconversion . . 323
UNGUREANU MIHAELA, voir STERNBERG SOLOMON 941

VALLÉS E., voir ALBALAT A., ... 631
VÁRHELYI CS., voir GANESCU I. 737
VASILESCU A., voir ZAHARESCU MARIA 909
VASS MIHAI, voir GARTNER MARIUCA 713
VELICU ANTOANETA, voir LECA M. 967
VERGARA A., voir LÓPEZ-DE-ALBA 707
VERMA NEELAM and A. L. J. RAO, Determination of manganese N, N′-ethylene bis(dithiocarbamate) (Maneb) by a spectrophotometric method and its applications 625
VERMA S. S., voir TYAGI E. 1025
VILCU RODICA and I. GAINAR, G. ANITESCU, The second interaction virial coefficient of gas mixtures. III. Carbon dioxide + hydrogen mixture 951
VLAD SORIN, voir ONICIU D. C. 561
VODNÁR J. and E. KOLOZSI, N. MUREȘAN, Hydrodynamic and mathematic characterization of the Vodnár-type apparatuses, having pelliclizing (stripping) and recycling tubes 927
VOLINTIRU T. and FRANCISC M. ALBERT, MARIA GIURGINCA, GH. IVAN, The effect of aromatic diamine + quinone-diimine couples in isoprene rubber . 791

YOUNES H. A., voir ISMAIL M. FEKRY 77

ZAHARESCU MARIA and CONSTANȚA PIRLOG, MARIA CRISAN, MARINA SAHINI, ANA BRAILEANU, N. DRAGAN, Monolithic glasses prepared by non-traditional methods 589
ZAHARESCU MARIA and CONSTANȚA PÎRLOG, A. VASILESCU, D. CRISAN, ANA BRAILEANU, Inorganic membranes obtained by the sol-gel method . 909
ZAHRAN F. M., voir FOUAD TAHA 503
ZALARU FLORICA and ADALGIZA CIOBANU, ION BACIU, CARMEN PETREA, Coordination compounds of some "3d" metals with formylated derivatives of carvone and menthone 731
ZANOAGA C. V. and C. V. UGLEA, S. MATACHE, V. AVADANEI, Characterization of ion-exchange membranes used in electrooxidative processes 919
ZANOAGA C. V. and C. V. UGLEA, G. NECHIFOR, Redox aspects regarding the transfer of some heavy metals through semipermeable membranes 923
ZBOROVSCHI EVA, voir KISS STEFAN 915
ZSAKÓ I., voir GANESCU I. 767
ZSAKÓ J., voir CHIFU EMIL 843
ZSAKÓ JÁNOS and M. TOMOAIA-COTISEL, E. CHIFU, I. ALBU, AURORA MOCANU, P. T. FRANGOPOL, Protolytic equilibria in surface solutions of stearic acid, procaine and benzoic acid at the air/water interface 867
ZSAKÓ J., voir CHIFU E. 879

Revue Roumaine de Chimie, **35**, *10 — 12*, 1055 — 1059 (1990)

INDEX DES SUJETS

Additivity of viscosity in binary and ternary aqueous organic mixtures. A. ARROYO 523

Adsorption of cations on oxides. F. TAHA, A. EL-ROUDI, A. A. ABD EL GABER and F. M. ZAHRAN 503

$Al_2O_3-SiO_2$ and HMgY acidity and reactivity in isomerization of 1-hexene and transalkylation of toluene. I. SANDULESCU, R. RUSSU, GH. LINTES, O. SERBAN and I. V. NICOLESCU 207

Aminoketone, oxazole and thiazole syntheses. Part XII. 2,5-diarythiazoles from thioazoactones and aromatic hydrocarbons. I. SCHIKETANZ, A. STEFANESCU, M. D. GHEORGHIU, A. SCHIKETANZ and A. T. BALABAN 345

Annulenes and primitive coronoids: some tipological properties and enumerations. S. J. CYVIN, J. BRUNVOLL and I. GUTMAN 985

Applications of weighted topological index *J* for QSAR of carcinogenesis inhibitors (retinoic acid derivatives) A. T. BALABAN, C. CATANA, M. DAWSON and I. NICULESCU-DUVAZ 997

Asymmetric membranes prepared by immersion-precipitation technique. GH. NECHIFOR and GEORGETA POPESCU 889

Behaviour of benzoxazinone derivatives bearing a bulky group at position-2 toward some nitrogen and carbon nucleophiles. II. S. EL. NAGDY, M. A. EL-HASHASH, A. A. AFIFI and EL-SAHED 49

Behaviour of 5,6-diphenyl-4-carbetoxy-2,3-dihydropyridazin-3-one, towards some different nucleophiles. A. A. AFIFY, A. A. EL-KHAMRY, A. Y. SOLIMAN, M. A. SAYED and E. A. KASSAB 785

Carbonic anhydrase inhibitors. I. Metal complexes of sulfonamides: a novel class of carbonic anhydrase inhibitors. C. SUPURAN, M. ANDRUH and I. PUSCAS 393

Carbonic andydrase inhibitors. II. Membrane-impermeable derivatives of 1,3,4-thiadiazole-2-sulfonamide. C. SUPURAN, A. T. BALABAN, M. D. GHEORGHIU, A. SCHIKETANZ, A. DINCULESCU and I. PUSCAS 399

Carbonic anhydrase inhibitors. III. Relations between chemical structure of inhibitors and activators. I. PUSCAS, CLAUDIU SUPURAN and GH. MANOLE 683

Carbonium ion reactions. XX. Synthesis and acetolysis of 8-chloromethyl-dibenzo [b,d]bicyclo [5.1.0]octa-2,4-diene. M. D. BANCIU, M. ELIAN, A. BANCIU, C. DRAGHICI, L. STANESCU, PHAN LE THUY and E. CIORANESCU 309

Catalyst for vapor-phase synthesis of isoprene from isobutene and formaldehyde. I. V. NICOLESCU, FL. AVRAMESCU and V. BARBULESCU 193

Catalysis by polymers. VI. The epichlorohydrin esterification catalyzed by poly(N,N-dimethyl-p-vinyl-benzyl-amine) F. DUMITRIU, V. HULEA and SP. OPREA 657

Catalytic hydrogen prewave in cysteine or cystine containing solutions. A polarographic and spectrophotometric study. F. G. BANICA and E. DIACU 9

Characterization of MoO_3-Fe_2O_3 catalysts containing admixtures of metal oxides by the method of electroconductivity. A. SZABO 239

Characterization of ion-exchange membranes used in electrooxidative processes. C. V. ZANOAGA, C. V. UGLEA, S. MATACHE and V. AVADANEI 919

Chemical components of the scent gland of the green vegetable bug: *Nezera viridula*. T. O. OLAGBEMIRO and L. LAJIDE 545

Chemical graphs. Part 53. Benzo- and polybenzo-derivatives of valence isomers of [12]annulene. C. DELEANU and A. T. BALABAN 349

^{13}C-NMR spectral assignments for 2,5 diarylthiazoles. M.D. GHEORGHIU, I. SCHIKETANZ, A. SCHIKETANZ and A.T. BALABAN 339

Complex to bis[3-(trifluoroacetyl)camphorato]barium (II) in a one step synthesis. M. ELIAN, C. DELEANU and S. ROSCA 299

Complexes of 3,5-xylyleamino-N,N-diacetic acid with various metal ions. J. SUAREZ-VARELA, J. C. AVILA ROSÓN, L. GARCIA REJÓN and T. GUARDIA CARRILLO 639
Complexing, extraction and determination of the $C_2H_5Hg^+$ ion with 1-(p-nitrophenyl), 3-(p′-azobenzene)-triazene. A. DANET and KIM GWANG SIK 607
Conformational preferences in substituted 5H-dibenzo(a,d)-cycloheptenes; the influence of a carbon bonded substituent in position 5. M. ELIAN 281
Contamination by chloride ions in electrode processes (in Spanish) A. ALBALAT, E. GÓMEZ, M. SARRET y E. VALLÉS 631
Conversion of alkanes into gasoline on ZSM-5 zeolite catalysts. E. ANGELESCU, P. GURAU, GEORGIANA POGONARU, G. MUSCA, GR. POP and ECATERINA POP 229
Coordination compounds as raw materials for mixed oxides. VI. Mixed coordination compounds of lanthanoids and Cr(III) — as precursor of chromites. P. SPACU, L. PATRON, S. PLOSTINARU, A. CONTESCU and N. STANICA 617
Coordination compounds of some "3d" metals with formylated derivatives of carvone and menthone. FL. ZALARU, A. CIOBANU, I. BACIU and CARMEN PETREA 731
Creation and discovery. R. HOFFMANN 305
Critical surfactant concentration in the interaction between non-ionic surfactants and polyacrylic acid. Effects of hydrophiobic and polyoxyethylene moieties of surfactants. SHUJI SAITO 821
Crystal and molecular structure of the 2-t-butyl-2-cynocyclobutanones resulted from the cycloaddition of Moore's ketene to endo- and exo-benzocyclobutanonorbornenes. M. D. GHEORGHIU, L. PARVULESCU, V. M. TURDIBEKOV and YU. T. STRUCHKOV 427
Cu(II), Zn(II), Cd(II), Co(II) and Ni(II) sorption on p(benzylcellulose)-5-azo-8-hydroxyquinoline. Thermogravimetric characterization. TINCA ONOFREI, LUCIA ODOCHIAN and VIORICA DULMAN 595

Dehydration of some 1-(2-furyl)- and 1-(2-thienyl)-1-alkanols using cobalt(II) sulphate as catalyst. Ü. OYMAN 63
Determination of manganese N,N′-ethylene bis-dithiocarbamate) (Maneb) by a spectrophotometric method and its applications. N. VERMA and A.L.J. RAO 625
Diffusion of vanadium in iron in surface coatings and calculation of diffusion coefficients. N. PETRESCU, M. PETRESCU and M. BRITCHI 97
Dispersion of a cataphoretic resin in view of electrodeposition. M. LECA, R. SERBAN and A. VELICU 967

Effect of surfactant on the electroreduction of acrylonitrile. L. ONICIU, I. A. SILBERG, DAN A. LÖWY, M. JITARU, FL. CIOMOS, O. H. OPREA, B. C. TOMA and M. TOMA 859
Effect of aromatic diamine + quinone-diimine couples in isoprene rubber. T. VOLINTIRU, F. A. ALBERT, M. GIURGINCA and GH. IVAN 791
Electrical conductivity of some zincon complex. M. ABD EL MOTTALB and M. G. ABD EL WAHED 701
Electrochemical oxidation of carboxylic acids. III. Electrode processes in electrochemical oxidation of natrium monomethyl adipate on graphite. S. STERNBERG, M. UNGUREANU, S. ROSCA and D. KRAITER 941
Electronic structure of $(H_3SiNSiH_3)^-$ anion. A simple molecular orbital treatment. I. SILAGHI-DUMITRESCU and I. HAIDUC 475
Ellipsometric spectroscopy of pure and of oxygen and carbon monoxide copper films. M. GARTNER, N. STANICA and M. VASS 713
Enumeration of catacondensed benzenoid hydrocarbons and their numbers of Kekule' structures. J. BRUNVOLL, R. TOSIĆ, M. KOVACEVIĆ, A. T. BALABAN, I. GUTMAN and S. J. CYVIN 85
Ethylene dimerisation catalyzed on coordinative compounds fixed on oxide supports. I. V. NICOLESCU, L. BOTEZ and E. ANGELESCU 199

Friedel-Crafts chemistry in alicyclic systems. V. Reaction of cyclohexylidene- and 1-cyclohexenylacetic acids with benzene in the presence of $AlCl_3$, CH_3NO_2 as the catalyst. V. DRAGUTAN, I. DRAGUTAN, C. CONDEIU and A. -M. GLATZ 453

Generalized correlation for vapor pressures of organic compounds. F. A. GOTHARD, G. JINESCU and V. SAVESCU 105

Heterocycles with annelated dibenzocycloalkane skeletons. IV. Pyrazoles with annelated 7H-dibenzo[c,e]cycloheptene skeleton. M. D. BANCIU, F. CHIRALEU and A. CIOBANU 739
Heterocyclic compounds. Synthesis of some fluorinated 1,3,5-triazine derivatives. E. TYAGI, S. S. VERMA, L. PRAKASH and R. L. MITAL 1025
^{1}H-NMR assignments for 2,4-diaryl-pyrilium salts and pyridines having fused 5- or 6-membered saturated rings bridging 5,6-positions. A. MARTON, U. BOLOGA T. S. BALABAN, M. D. GHEORGHIU and A. T. BALABAN 415
Hydrodynamic and mathematic characterization of the apparatuses of Vodnár type, having pelliclizing (stripping) and recycling tubes. J. VODNAR, E. KOLOZSI and N. MURESAN 927

Influence of various factors on the optical activity of some essential aminoacids. Part II. Cr. MANDRAVEL and L. IONESCU 683
Inorganic membranes obtained by the sol-gel method. M. ZAHARESCU, C. PIRLOG A. VASILESCU, D. CRISAN and A. BRAILEANU 909
Interfacial tension extrema at the adsorption from polycomponent systems. E. CHIFU, J. ZSAKÓ, M. TOMOAIA-COTISEL and I. ALBU 843
Interactions of substituted five-membered heteroaromatic compounds with electron acceptors. II. Interaction of 2-p-bromophenyl-sulphonyl-phenyl-5-ethylamino-1,3,4-thiadiazole with tetracyanoethane. I. SARAMET, C. DRAGHICI and M. D. BANCIU 437
Interactions of substituted five-membered heteroaromatic compounds with electron acceptors. III. Charge transfer complexes with tetracyanoethene and tricyanovinylation of some 3-mercapto-1,2,4-triazoles. M. D. BANCIU, I. SARAMET and C. DRAGHICI 1009
Ion-exchange of palladium in mordenite. N. BILBA, G. STREDIE, D. BILBA . . 263
IR study of metal-support interaction in Ni/Al_2O_3 catalysts for hydrogenation. L. FRUNZA, M. I. UDREA, C. CAPAT, D. CRISAN, I. V. NICOLESCU 221

Kinetic studies of tautomerization and effect of temperature on enethiol contents of some carboxyalkyl-thiocarbamides. P.S. MITTAL, N. KUMAR, K. K. GIRDHAR, A. D. TANEJA and Y. S. TYAG 555

Liquid-solid heat transfer with solid phase change (in French), S. PETRESCU and R. Z. TUDOSE 1031

Magnetic interaction between spin probes and Cu(II) compounds as a method for characterization of the penetrability of reversed micelles. H. CALDARARU, A. CARAGHEORGHEOPOL, A. CALDARARU, M. DIMONIE, D. DONESCU, I. DRAGUTAN and N. MARINESCU 853
Mechanism of electroreduction of sodium nitroprusside (SNP) E. A. GOMAA, Y. A. ELEWADY and A. H. EL-ASKALANY 491
Mesoionic oxazolones. IV. **Protonation of planar and nonplanar acylated compounds.** D. RAILEANU and H. PETRIDE 459
Mesoionic oxazolones. V. **Ethanolysis and aminolysis of acylated compounds. H.** PETRIDE 747
Metal complexes with 4-benzoyl-pyridine. VI. New coordination compounds of copper (II) with 4-benzoyl-pyridine. M. ANDRUH, N. STANICA, A. MEGHEA and M. BERCU 3
Modern methods for determining the gas permeation and predicting the properties of dispersed polymer systems. A. L. IEVLEV and V. V. TEPLYAKOV . . . 831
Monolithic classes prepared by non-traditional methods. M. ZAHARESCU, C. PIRLOG, M. CRISAN, M. SAHINI, A. BRAILEANU and **N.** DRAGAN . . . 589
Morphological characterization of collagen membranes for medical textile prostheses. V. TRANDAFIR, M. COSTEA and E. ROBU 973
Mössbauer investigation of Fe-Cu-K catalysts for hydrocarbon synthesis. G. FILOTI, V. SPANU, I. UDREA, M. UDREA, C. CAPAT and I. V. NICOLESCU . . . 215
Multi-element analysis by solvent extraction and HPLC of soil samples. E. B. ED. INATIMI 495

New preparation method for μ_3-oxo-trinuclear chromium (III) formate. M. BREZEANU, E. PINCOVSCHI, D. MARINESCU and M. ANDRUH 535

Novel substituted-aminocoumarins as potential antimicrobial agents. M. M. BADRAN, A. K. EL-ANSARI and EL-MELIGIE 777

Optimization by computer of the alkaline hydrolysis of isoamyl acetate. H. M. LLANEZA, J. CORONA and J. M. BLANCO 583
Optimization of the mobile phase in thin layer chromatography for the separation of 4-benzylidene-1-pyrimidyl-5-pyrazolone dyes. S. GOCAN, L. OLENIC and I. CRISTEA 49

Penetration of procaine hydrochloride into stearic acid monolayers from underlying aqueous solutions. E. CHIFU, M. TOMOAIA-COTISEL, J. ZSAKÓ, I. ALBU, A. MOCANU and P. T. FRANGOPOL 879
Phase behaviour of hydrocarbon-water mixtures in the presence of alkylpolyoxyethylene carboxylates. D. F. ANGHEL, I. MIRICIOAGA, D. R. ELLIS and E. A. DUFF 891
Photocyclisation of 1-benzamido-2-(1-cyclohexenyl)cyclohexene. A. COUTURE, A. LABLACHE-COMBIER, G. SURPATEANU and M. CONSTANTINESCU 675
Potentiometric determination of thorium (in Spanish) P. L. LÓPEZ-DE-ALBA and A. VERGARA 707
Preparation of the metallic supported catalysts from precursors with different immobilization capacities on γ-Al_2O_3 surface. I. γ-Al_2O_3 impregnation with a metallic I. V. NICOLESCU, V. PARVULESCU, V. PARVULESCU and E. ANGELESCU 145
Preparation of metallic supported catalysts from precursors with different immobilization capacities on the γ-Al_2O_3 surface. II. Impregnation of the catalyst support Pd/ Al_2O_3 with the second metallic component. I. V. NICOLESCU, VIORICA PARVULESCU, V. PARVULESCU and I. SANDULESCU 161
Preparation of metallic supported catalysts from precursors with different immobilization capacities upon γ-Al_2O_3 surface. III The drying influence upon the distribution of metallic components. I. V. NICOLESCU, VIORICA PÂRVULESCU and E. ANGELESCU 173
Protolytic equilibria in surface solutions of stearic acid, procaine and benzoic acid at the air/water interface. J. ZSAKO, M. TOMOAIA-COTISEL, E. CHIFU, I. ALBU, A. MOCANU and P. T. FRANGOPOL 867

Reactions of pyrylium salts with nucleophiles. XV. Stereoisomers of polyarylpyridinium salts and their interconversion. C. UNCUTA, F. CHIRALEU, M. D. GHEORGHIU and A. T. BALABAN 323
Reactions with N-aminophthalimide and some allied compounds. M. FEKRY ISMAIL, F. S. SAYED, F. A. EL-BASSIOUNY and H. A. YOUNES 77
Recovery of metallic ions from waste waters by flotation. L. STOICA, R. V. CATUNEANU, C. BEJAN, M. NICOLAU, V. BRETAN 31
Redox aspects regarding the transfer of some heavy metals through semipermeable membranes. C. V. ZANOAGA, C. V. UGLEA, G. NECHIFOR 923

SeO_2 radiolysis studies by EPR. M.CONTINEANU 601
Second interaction viral coefficient of gas mixtures. III. Carbon dioxide + hydrogen mixture. R. VILCU, I. GAINAR and G. ANITESCU 951
Separation of amino acids by liquid membranes with macrocyclic carriers. C. LUCA, L. MUTIHAC and T. CONSTANTINESCU 467
Separation of gases by diffusion and gaseous permeation. Application of gaseous permeation to the dehydration of natural gas. J. CHARPIN 815
Solvolyses in substituted cyclopropylcarbinylic systems. 8. Solvolyses of 2-aryl-1-cyclopropylethanols and their 3,5-dinitrobenzoates. A. C. RAZUS, F. CHIRALEU and A. I. IANCU 445
Some aspects of linear low density polyethylene synthesis on TiCl/$MgCl_2$ catalysts. C. ANDREI, G. ANDREI, S. PITA, O. PITPALAC and I. SONOC 663
Spectral studies of some thiazolyl and pyrimidyl substituted thiocarbamides in different solvents. P. S. MITTAL, N. KUMAR and A. D. TANEJA 23

Studies on complexation of Co(II), Ni(II), Cu(II), Zn(II) and Cd(II) with 1-acetylimidazole in aqueous solutions. B. BARSZCZ and J. KULIG 511

Studies concerning calcium carbonate scales formation and its prevention. II. Prevention by inhibitor addition. V. COCHECI, GH. PETCA and E. GLÜCK 511

Studies on viscosity of magnesium soaps of higher fatty acids in dilute aqueous solutions at different temperatures. H. SINGH and S. P. S. TOMAR . . 539

Study of the electroconductivity of the Fe-Mg-O catalytic system used in the reaction of n-butenes oxide-hydrogenation to butadiene. I. V. NICOLESCU, GH. NEDELCU and A. SZABO 185

Study on the reaction and composition of the Hg(II) complex with diazoaminobenzene. M. POPESCU 67

Surfactants in film-forming industry. R. STOICA and L. GOLIAT 805

Synthesis and anti-inflammatory activity of some new triheterocyclic thiazoles. G. M. KULKARNI, M. V. KULKARNI, V. D. PATIL, D. B. SHRIDHAR and M. LAXMANA 549

Synthesis and biological activities of some new isoxazolo [5,4-d]pyrimidine derivatives. V. A. ADHIKARI and V. V. BADIGER 757

Synthesis and EPR spectra of persistent aroxyls. IV. *Ortho, ortho'*- disubstituted phenols possessing in the *para*-position a 2-bonded-1,3-dicarbonylic (or a functionally related) group. J. M. HERDAN, V. DINOIU, A. MEGHEA, M. D. GHEORGHIU, A. SCHIKETANZ, M. GIURGINCA and A. T. BALABAN 407

Synthesis and EPR spectra of persistent aroxyls. V. Aroxyls derived from chalcone and derivatives, J. M. HERDAN, V. DINOIU, A. MEGHEA, A. SCHIKETANZ, M. D. GHEORGHIU and A. T. BALABAN 1017

Synthesis of 2,6-dimethyl-4-styrylpyrylium salts (from 2,4,6-trimethyl-pyrylium and donor-substituted benzaldehydes) and their conversion into pyridines. D. C. ONICIU, A. MARTON, T. S. BALABAN, S. VLAD and A. T. BALABAN 561

Synthesis and reactions of substituted benzoxazinones bearing a bulky group at position -2. Part I. A. A. AFIFY, S. EL-NAGDY, M. A. SAYED and L. MOHEY 567

Synthesis of several new pyridinone derivatives F. F. ABDEL-LATIF 679

Synthesis of substituted benzoins and the corresponding bis-1,2-enedithiol complexes of nickel, platinum and palladium. D. C. ONICIU, N. NEGOITA, M. MORJAN, M. D. GHEORGHIU and A. T. BALABAN 421

Synthesis of novel furyl-substituted 3-cyano-2-pyridones. M. — C. BALABAN, T. S. BALABAN, U. BOLOGA and A. T. BALABAN 1005

Tetrathiocyanato-diamine chromates (III) with imidazole and benzimidazole (in German). I. GANESCU, Cs. VÁRHELYI, I. SZAKÓ und M. PREDA . . . 767

Theoretical and experimental study on the cycloaddition between 4-(p-tolyl)1,2,4-triazolium (p-methoxy) phenacylide and ethyl cinamate. G. SURPATEANU, M. CONSTANTINESCU, A. LABLACHE-COMBIER, P. GRANDCLAUDON, B. MOUCHEL and A. COUTURE 669

Thermal behaviour of acrylamide-maleic anhydride — styrene terpolymer. M. TOMESCU, E. SEGAL and STELIANA CRETU 649

Thermal decomposition of dolomite. C. LEONTE, AL. SZEP, N. BILBA, C. CALISTRU, L. IFRIM and GH. MIHAILA 41

Transformations of some hydrocarbons on zeolite catalysts. V. ABABI, N. BILBA, N. NAUM and GH. MIHAILA 253

Use of zeolite as an adsorbing surface for modelling systems analogous to therapeutic mud. ST. KISS, M. DRAGAN—BULARDA, D. PASCA, H. PINTEA, E. ZBOROVSCHI, V. MINTEAN and R. CRISAN 915

Voltammetric study of a catalytic electrode process with parallel complexation reaction. Reduction of nickel ion in the presence of nicotinamide. F. G. BANICA 693

NOTE POUR LES AUTEURS

La revue Roumaine de Chimie publie des articles en anglais, français, russe, allemand ou espagnol. Les auteurs sont priés d'envoyer des articles et des comptes rendus inédits.

Les manuscrits seront dactylographiés à double interligne. La bibliographie, les tableaut et la légende des figures seront placés après le texte.

Si l'article fait partie d'une série numéritée, la partie précédente sera donnée comme première référence.

Chaque article sera précédé d'un résumé comprenant quinze lignes au maximum.

Les références bibliographiques dans le texte seront faites par des exposants sans parenthèses et paraitront à la fin de l'ouvrage.

Les publications périodiques mentionnées dans la bibliographie seront présentées suivant les prescriptions internationales : le nom de l'auteur précédé de l'initiale du prénom, le titre du périodique abrégé conformément à « Chemical Abstracts » et souligné par une ligne, le numéro du tome indiqué par des chiffres arabes et souligné par deux lignes, suivi de la première page de l'article ; à la fin, l'année de la parution sera placée entre parenthèses. Le numéro de la revue ne sera pas indiqué si les pages du volume sont numérotées consécutivement.

Les textes des livres ou traités inclueront : le nom des auteurs, l'initiale du prénom, le titre du livre entre guillemets et sans être souligné le numéro du tome précédé par l'abréviation « vol. » (ou « Bd. »), le numéro de l'édition (the publisher), la localité de la parution du livre, l'année de la parution et la page de la référence précédée(s) par l'abréviation « p. » (ou « S. »).

Les brevets seront indiqués comme suit : l'auteur ou la firme, le pays et le numéro du brevet, la date et la revue *(Chem. Abstr.)*. Par ex. : M. Jones (to Union Carbide Co), Brit. Pat. 601 238, 2 Sept. 1959 ; cf. *Chem. Abstr.*, **54**, 12808 (1980).

Si la référence n'a pas été lue en original, on indiquera aussi la revue de référence consultée.

Les diagrammes seront tracés à l'encre de Chine sur papier calque. Les tableaux et les figures (en nombre strictement nécessaire) ainsi que les courbes dans les figures seront numérotés par des chiffres arabes. Leur explication sera donnée dans la légende des figures. Prière de ne pas inscrire les mêmes données dans les tableaux et les figures. Chaque tableau aura un titre. On indiquera dans le texte la place approximative des tableaux et des figures. Les formules chimiques seront incluses dans le texte ; en outre elles seront transcrites sur papier calque, à l'encre de Chine.

Les auteurs sont priés d'indiquer les caractères italiques (en soulignant les lettres au crayon), ainsi que tout autre caractère spécial ; les préfixes *ortho, meta, para, cis, trans*, etc. seront soulignés pour indiquer leurs caractères italiques et ne seront jamais écrits avec des majuscules.

Aucune correction à la main ne sera admise sur le manuscrit. Les corrections seront tapées à la machine. Les lettres grecques ou d'autres symboles spéciaux seront insérés à la main à l'encre clairement.

Le manuscrit sera signé par l'auteur.

Le titre-courant aura 50 lettres au maximum.

L'entière responsabilité du contenu des articles appartient aux auteurs.

Sur demande on peut obtenir une note plus complète.

PRINTED IN ROMANIA

ORSZÁGOS MŰSZAKI INFORMÁCIÓS KÖZPONT ÉS KÖNYVTÁR
83

TRAVAUX PARUS AUX ÉDITIONS DE L'ACADÉMIE ROUMAINE

I. G. MURGULESCU, **Introducere în chimia fizică, vol. I. 1. Atomi, molecule, legătură chimică**, 1976, 560 p.
I. G. MURGULESCU, V. EM. SAHINI, **Introducere în chimia fizică, Vol. I. 2. Structura și proprietățile moleculelor**, 1979, 604 p.
I. G. MURGULESCU, E. SEGAL, **Introducere în chimia fizică, Vol. II. 1. Teoria molecular-cinetică a materiei**, 1979, 1036 p.
I. G. MURGULESCU, TATIANA ONCESCU, E. SEGAL, **Introducere în chimia fizică, Vol. II. 2. Cinetică chimică și cataliză**, 1981, 1024 p.
I. G. MURGULESCU, J. PĂUN, **Introducere în chimia fizică, Vol. I. 3. Nucleul atomic, reacții nucleare, particule elementare**, 1982, 606 p.
I. G. MURGULESCU, RODICA VÎLCU, **Introducere în chimia fizică. Vol. III. Termodinamica chimică**, 1982, 624 p.
I. G. MURGULESCU, O. M. RADOVICI, **Introducere în chimia fizică, vol. IV. Electrochimia**, 1986, 410 p.
C. ANDREI, I. DRĂGUȚAN, A. T. BALABAN, **Fotostabilizarea polimerilor cu amine impiedicate steric**, 1990, 240.
M. BREZEANU, E. CRISTUREANU, D. MARINESCU, A. ANTONIU, M. ANDRUH, **Chimia metalelor**, 1990.
R. VÎLCU, M. LECA, **Polymer Thermodynamics by Gas Chromatography**, coédition avec Elsevier, 1990, 204.
FL. CUIBAN, A. X. LUPEA, **Studiul structurii și sinteza peptidelor**, 1989, 286 p.
C. SIMIONESCU, V. GORDUZA, **Implicațiile bioenergetice ale coloranților**, 1988, 207 p.
R. VÎLCU, M. LECA, **Termodinamica polimerilor prin cromatografie de gaze**, 1987, 238 p
I. ZUGRĂVESCU, M. PETROVANU, **Cicloadiții 3+2 dipolare**, 1987, 446 p.
RAUL MIHAIL, ION GROZEANU, **Estimarea secvențială aplicată sistemelor chimice**, 1986, 406 p.
M. BREZEANU, I. PATRON, M. ANDRUH, **Combinații complexe polinucleare și aplicațiile lor**, 1986, 244 p.
A. T. BALABAN et al., **Labelled Compounds and Radiopharmaceuticals Applied in Nuclear Medicine**, coédition avec John Wiley and Sons, 1986, 742 p.
D. PURDELA, **Nomenclatura chimiei organice — IUPAC**, 1986, 451 p.
PETRU BUDRUGEAC, **Probleme de chimie**, 1986, 280 p.
T. ONCESCU, S. G. IONESCU, **Conversie fotochimică și stocare de energie**, 1985, 272 p.
V. DRĂGUȚAN, A. T. BALABAN, M. DIMONIE, **Olefin Metathesis and Ring-Opening Polymerization of Cyclo-Olefins**, coédition avec John Wiley and Sons, 1985, 544 p.
C. LITEANU, I. RÎCĂ, **Optimizarea proceselor analitice**, 1985, 360 p.
N. PETRESCU, **Chimia extracției cu solvenți și aplicații**, 1985, 212 p.

1991 JUN 0 4
1991
4
1991
4

ISSN 0035–3930

I. P. UNIVERSUL, c. 2219 | 43 426 | **Lei 80**